THE ISCHEMIC HEART

edited by:
SEIBU MOCHIZUKI
NOBUAKIRA TAKEDA
MAKOTO NAGANO
NARANJAN S. DHALLA

Kluwer Academic Publishers

THE ISCHEMIC HEART

PROGRESS IN EXPERIMENTAL CARDIOLOGY

Edited by Naranjan S. Dhalla, Ph.D., M.D. (Hon.), D.Sc. (Hon.)

1. S. Mochizuki, N. Takeda, M. Nagano, N. Dhalla (eds.): Volume 1: The Ischemic Heart, 1998. ISBN 0-7923-8105-X.

THE ISCHEMIC HEART

Edited by
SEIBU MOCHIZUKI, M.D., Ph.D.
Professor and Chairman
Department of Medicine
Aoto Hospital
Jikei University School of Medicine
Tokyo, Japan

NOBUAKIRA TAKEDA, M.D., Ph.D.
Associate Professor
Department of Internal Medicine
Aoto Hospital
Jikei University School of Medicine
Tokyo, Japan

MAKOTO NAGANO, M.D., Ph.D.
Professor Emeritus
Jikei University School of Medicine
Tokyo, Japan

NARANJAN S. DHALLA, Ph.D., M.D. (Hon.), D.Sc. (Hon.)
Distinguished Professor and Director
MRC Group in Experimental Cardiology
Institute of Cardiovascular Sciences
St. Boniface General Hospital Research Centre
Faculty of Medicine, University of Manitoba
Winnipeg, Canada

KLUWER ACADEMIC PUBLISHERS
BOSTON

Distributors for North America:
Kluwer Academic Publishers
101 Philip Drive
Assinippi Park
Norwell, Massachusetts 02061 USA

Distributors for all other countries:
Kluwer Academic Publishers Group
Distribution Centre
Post Office Box 322
3300 AH Dordrecht, THE NETHERLANDS

Library of Congress Cataloging-in-Publication Data

Printed on acid-free paper.

PRINTED IN THE UNITED STATES OF AMERICA

CONTENTS

This Page Intentionally Left Blank

CONTRIBUTING AUTHORS

Yoshifusa Aizawa
First Department of Internal Medicine
Niigata University School of Medicine
1-754 Asahi-machi
Niigata, 951
Japan

Motokuni Aoki
Department of Geriatric Medicine
Osaka University Medical School
Suita, Osaka, 565
Japan

Hirohisa Arata
Third Department of Internal Medicine
Showa University School of Medicine
1-5-8 Hatanodai, Shinagawa-ku
Tokyo, 142
Japan

Yoshihisa Arata
Third Department of Internal Medicine
Showa University School of Medicine
1-5-8 Hatanodai, Shinagawa-ku
Tokyo, 142
Japan

Hiroshi Asanuma
First Department of Medicine
Osaka University School of Medicine
2-2 Yamada-oka
Suita, Osaka, 565
Japan

Nobuhisa Awata
Department of Medicine
Osaka Medical Center for Cancer and Cardiovascular Diseases
1-3-3 Nakamichi, Higashinari-ku
Osaka, 537
Japan

Hong-Zhi Bai
First Department of Surgery
Institute for Cellular and Molecular Biology
Osaka University Medical School
2-2 Yamada-oka
Suita, Osaka, 565
Japan

Robert E. Beamish
Institute of Cardiovascular Sciences
St. Boniface General Hospital Research Centre
351 Tache Avenue
Winnipeg, MB R2H 2A6
Canada

Alexander S. Clanachan
Cardiovascular Disease Research Group
423 Heritage Medical Research Centre
Departments of Pediatrics and Pharmacology
Faculty of Medicine
University of Alberta
Edmonton, AB T6G 2S2
Canada

Federica del Monte
Cardiac Medicine
Imperial College School of Medicine at the National Heart & Lung Institute
Dovehouse Street
London, SW3 6LY
England, UK

Naranjan S. Dhalla
Institute of Cardiovascular Sciences
St. Boniface General Hospital Research Centre
351 Tache Avenue
Winnipeg, MB R2H 2A6
Canada

T. Dickfeld
Medizinische Klinik IV
Abteilung Für Kardiologie
Theodor-Stern-Kai 7
60596 Frankfurt am Main
Germany

P. Ferdinandy
Department of Biochemistry
Albert Szent-Györgyi Medical University
Kazinczy u.2
H-6720 Szeged
Hungary

Roberto Ferrari
Cattedra di Cardiologia
Universita' degli studi di Brescia
c/o Spedali Civili
P. le Spedali Civili, 1
25123 Brescia
Italy

Danielle Feuvray
Laboratoire de Physiologie Cellulaire
Université Paris XI, Bât 443
91405 Orsay Cedex 91405
France

Minako Fujishima
Department of Physiology
Tokai University
Isehara, 259-11
Japan

Takashi Fujiwara
Department of Thoracic & Cardiovascular Surgery
Kawasaki Medical School
577 Matsushima, Kurashiki
Okayama, 701-01
Japan

Yoshiaki Fukuhiro
Department of Thoracic & Cardiovascular Surgery
Kawasaki Medical School
577 Matsushima, Kurashiki
Okayama, 701-01
Japan

Hiroharu Funaya
First Department of Medicine
Osaka University School of Medicine
2-2 Yamada-oka
Suita, Osaka, 565
Japan

A. Martin Gerdes
Department of Anatomy and Structural Biology
University of South Dakota
414 E. Clark Street
Vermillion, SD 57069
USA

Eiichi Geshi
Third Department of Internal Medicine
Showa University School of Medicine
1-5-8 Hatanodai, Shinagawa-ku
Tokyo, 142
Japan

Masami Goto
Medical Engineering & Systems Cardiology
Kawasaki Medical School
577 Matsushima, Kurashiki
Okayama, 701-01
Japan

P. Grabisch
Medizinische Klinik IV
Abteilung für Kardiologie
Theodor-Stern-Kai 7
60596 Frankfurt am Main
Germany

Sian E. Harding
Cardiac Medicine
Imperial College School of Medicine at the National Heart & Lung Institute
Dovehouse Street
London, England SW3 6LY
United Kingdom

Hiroshi Hasegawa
Department of Geriatric Medicine
Keio University School of Medicine
35 Shinanomachi, Shinjuku-Ku
Tokyo, 160
Japan

Takaya Hasegawa
First Department of Medicine
Kinki University School of Medicine
Osakasayama
Osaka, 589
Japan

Kazuhiko Hashimura
Cardiovascular Division
Ishinkai Yao General Hospital
Osaka, 581
Japan

Hideharu Hayashi
Photon Medical Research Center
Hamamatsu University School of medicine
3600 Handa-cho
Hamamatsu 431-31
Japan

Yoko Hayashi
Department of Geriatric Medicine
Keio University School of Medicine
35 Shinanomachi, Shinjuku-Ku
Tokyo, 160
Japan

David J. Hearse
Cardiovascular Research
The Rayne Institute
St. Thomas' Hospital
London, England SE1 7EH
United Kingdom

I. Henke
Medizinische Klinik IV
Abteilung für Kardiologie
Theodor-Stern-Kai 7
60596 Frankfurt am Main
Germany

Jitsuo Higaki
Department of Geriatric Medicine
Osaka University Medical School
2-2 Yamada-oka
Suita, Osaka, 565
Japan

Kotaro Higuchi
First Department of Internal Medicine
Niigata University School of Medicine
1-754 Asahi-machi
Niigata, 951
Japan

Makie Higuchi
Department of Pharmacology
School of Medicine
University of the Ryukyus
Okinawa, 903-01
Japan

Kenichi Hongo
Department of Internal Medicine (4)
The Jikei University School of Medicine
3-25-8 Nishishinbashi, Minato-ku
Tokyo, 105
Japan

Masatsugu Hori
First Department of Medicine
Osaka University Medical School
2-2 Yamada-oka
Suita, Osaka, 565
Japan

Tomoyuki Hori
First Department of Internal Medicine
Niigata University School of Medicine
1-754 Asahi-machi
Niigata, 951
Japan

Katsuji Hoshi
Department of Pharmacology
Hokkaido College of Pharmacy
Otaru 047-02
Japan

Shiro Hoshida
First Department of Medicine
Osaka University Medical School
2-2 Yamada-oka
Suita, Osaka, 565
Japan

Kazuo Ichihara
Department of Pharmacology
Hokkaido College of Pharmacy
Otaru, 047-02
Japan

Toru Ida
First Department of Internal Medicine
Niigata University School of Medicine
1-754 Asahi-machi
Niigata, 951
Japan

Katsumiti Iijima
Third Department of Internal Medicine
Showa University School of Medicine
1-5-8 Hatanodai, Shingawa-ku
Tokyo, 142
Japan

Katumiti Iijima
Third Department of Internal Medicine
Showa University School of Medicine
1-5-8 Hatanodai, Shinagawa-ku
Tokyo, 142
Japan

Toshitaro Ikeda
Department of Molecular Physiology
National Cardiovascular Center Research Institute
Fujishiro-dai 5
Suita, Osaka, 565
Japan

Wataru Ikeda
Department of Medicine
Osaka Medical Center for Cancer and Cardiovascular Diseases
1-3-3 Nakamichi, Higashinari-ku
Osaka 537
Japan

Shoichi Imai
Department of Pharmacology
Niigata University School of Medicine
1-754 Asahi-machi
Niigata, 951
Japan

Hiroshi Inada
Department of Thoracic & Cardiovascular Surgery
Kawasaki Medical School
577 Matsushima, Kurashiki
Okayama, 701-01
Japan

Masahiko Inagaki
First Department of Medicine
Kinki University School of Medicine
Osakasayama
Osaka, 589
Japan

Hideyuki Ishida
Department of Physiology
Tokai University
Isehara, 259-11
Japan

Kinji Ishikawa
First Department of Medicine
Kinki University School of Medicine
Osakasayama
Osaka, 589
Japan

Haruhiko Ishioka
Third Department of Internal Medicine
Showa University School of Medicine
1-5-8 Hatanodai, Shinagawa-ku
Tokyo, 142
Japan

Mitsuaki Isobe
First Department of Internal Medicine
Shinshu University School of Medicine
3-1-1 Asahi
Matsumoto 390
Japan

Koichi Ito
First Department of Medicine
Osaka University School of Medicine
2-2 Yamada-oka
Suita, Osaka, 565
Japan

Seiji Itoh
Third Department of Internal Medicine
Showa University School of Medicine
1-5-8 Hatanodai, Shinagawa-ku
Tokyo, 142
Japan

Toshiyuki Itoi
Division of Pediatrics
Children's Research Hospital
Kyoto Prefectural University of Medicine
Kajiicho 465, Hirokoji, Kawaramachi
Kamigyoku, Kyoto, 602
Japan

Toshiki Iwata
Third Department of Internal Medicine
Showa University School of Medicine
1-5-8 Hatanodai, Shinagawa-ku
Tokyo, 142
Japan

Takehiko Izumi
Fourth Department of Internal Medicine
Aoto Hospital
Jikei University School of Medicine
6-41-2 Aoto, Katsushika-ku
Tokyo, 125
Japan

Tohru Izumi
Department of Internal Medicine and Cardiology
Kitasato University School of Medicine
1-15-1 Kitasato
Sagamihara, 228
Japan

Robert B. Jennings
Department of Pathology
Duke University Medical Center
P.O. Box 3712
Durham, NC 27710-0001
USA

Canwen Jiang
Department of Gene Transfer Research
Genzyme Corporation
Framingham, MA
USA

Keishi Kadoba
First Department of Surgery
Institute for Cellular and Molecular Biology
Osaka University Medical School
2-2 Yamada-oka
Suita, Osaka, 565
Japan

Koji Kagisaki
First Department of Surgery
Institute for Cellular and Molecular Biology
Osaka University Medical School
2-2 Yamada-oka
Suita, Osaka, 565
Japan

Fumihiko Kajiya
Medical Engineering & Systems Cardiology
Kawasaki Medical School
577 Matsushima, Kurashiki
Okayama, 701-01
Japan

Yasufumi Kaneda
First Department of Surgery
Institute for Cellular and Molecular Biology
Osaka University Medical School
2-2 Yamada-oka
Suita, Osaka, 565
Japan

Seiichiro Kano
Department of Pharmacology
Hokkaido College of Pharmacy
Otaru, 047-02
Japan

Takashi Katagiri
Third Department of Internal Medicine
Showa University School of Medicine
1-5-8 Hatanodai, Shinagawa-ku
Tokyo, 142
Japan

Yoji Kato
Cardiovascular Division
Ishinkai Yao General Hospital
Osaka, 581
Japan

Hideki Katoh
Third Department of Internal Medicine
Hamamatsu University School of Medicine
3600 Handa-cho
Hamamatsu, 431-31
Japan

Ryo Katori
First Department of Medicine
Kinki University School of Medicine
Osakasayma
Osaka, 589
Japan

Shinya Kawabata
Department of Internal Medicine and Cardiology
Kitasato University School of Medicine
1-15-1 Kitasato
Sagamihara, 228
Japan

Neelam Khaper
Institute of Cardiovascular Sciences
St. Boniface General Hospital Research Centre
351 Tache Avenue
Winnipeg, MB R2H 2A6
Canada

Yoshiyuki Kijima
Department of Cardiology
Higashi-osaka Municipal Hospital
2-3-1 Mikuriya Minami, Higashi-osaka
Osaka, 577
Japan

Akio Kimura
First Department of Medicine
Kinki University School of Medicine
Osakasayama
Osaka, 589
Japan

Hirofumi Kino
First Department of Medicine
Kinki University School of Medicine
Osakasayama
Osaka, 589
Japan

Adrienn Kis
Department of Pharmacology
Albert Szent-Györgyi Medical University
Dom ter 12
H-6701 Szeged
Hungary

Masafumi Kitakaze
First Department of Medicine
Osaka University School of Medicine
2-2 Yamadaoka
Suita, Osaka, 565
Japan

Koji Kitayama
First Department of Medicine
Kinki University School of Medicine
Osakasayama
Osaka, 589
Japan

Hideaki Kohri
Department of Pharmacology Section
Nutrition Research Institute
Otsuka Pharmaceutical Factory, Inc.,
Naruto, 772
Japan

Hironari Koka
First Department of Medicine
Kinki University School of Medicine
Osakasayama
Osaka, 589
Japan

Noburu Konno
Third Department of Internal Medicine
Showa university School of Medicine
1-5-8 Hatanodai, Shinagawa-ku
Tokyo, 142
Japan

Taku Konno
First Department of Internal Medicine
Niigata University School of Medicine
1-754 Asahi-machi
Niigata, 951
Japan

Bruce Kowaluk
Institute of Cardiovascular Sciences
St. Boniface General Hospital Research Centre
351 Tache Avenue
Winnipeg, MB R2H 2A6
Canada

Tsunehiko Kuzuya
First Department of Medicine
Osaka University Medical School
2-2 Yamada-oka
Suita, Osaka, 565
Japan

Gary D. Lopaschuk
Cardiovascular Disease Research Group
423 Heritage Medical Research Centre
Department of Pediatrics and Pharmacology
The University of Alberta
Edmonton, Alberta T6G 2S2
Canada

Kenneth T. MacLeod
Imperial College School of Medicine at National Heart & Lung Institute
Cardiac Medicine
Dovehouse Street
London, England SW3 6LY
United Kingdom

Hisao Masaki
Department of Thoracic & Cardiovascular Surgery
Kawasaki Medical School
577 Matsushima, Kurashiki
Okayama, 701-01
Japan

Takashi Masuda
Department of Internal Medicine and Cardiology
Kitasato University School of Medicine
1-15-1 Kitasato
Sagamihara, 228
Japan

Taku Matsubara
First Department of Internal Medicine
Niigata University School of Medicine
1-754 Asahi-machi
Niigata, 951
Japan

Hikaru Matsuda
First Department of Surgery
Institute for Cellular and Molecular Biology
Osaka Universty Medical School
2-2 Yamada-oka
Suita, Osaka, 565
Japan

Takashi Matsui
Massachusetts General Hospital Cardiovascular Research Center
Mailcode: 1494201
149 13th Street
Charlestown, MA 02129-2060
USA

Yasuhiko Matsu-ura
Cardiovascular Division
Ishinkai Yao General Hospital
Osaka, 581
Japan

Hidetsugu Matsushita
Department of Geriatric Medicine
Osaka University Medical School
2-2 Yamada-oka
Suita, Osaka, 565
Japan

Narihisa Matsuyama
Department of Internal Medicine and Cardiology
Kitasato University School of Medicine
1-15-1 Kitasato
Sagamihara, 228
Japan

Tetsuo Minamino
First Department of Medicine
Osaka University School of Medicine
2-2 Yamada-oka
Suita, Osaka, 565
Japan

Tetsuji Miura
Second Department of Internal Medicine
Sapporo Medical University School of Medicine
South-1 West-16, Chuo-ku
Sapporo, 060
Japan

Kanako Miyagi
Department of Pharmacology
School of Medicine
University of the Ryukyus
Okinawa 903-01
Japan

Masaru Miyataka
First Department of Medicine
Kinki University School of Medicine
Osakasayama
Osaka, 589
Japan

Seibu Mochizuki
Fourth Department of Internal Medicine
Aoto Hospital
Jikei University School of Medicine
6-14-2 Aoto, Katsushika-ku
Tokyo, 125
Japan

Seiichi Mochizuki
Medical Engineering & Systems Cardiology
Kawasaki Medical School
577 Matsushima, Kurashiki
Okayama, 701-01
Japan

Minhaz Uddin Mohammed
Department of Physiology
Tokai University
Isehara, 259-11
Japan

Isao Mori
Cardiovascular Division
Ishinkai Yao General Hospital
Osaka, 581
Japan

Ryuichi Morishita
Department of Geriatric Medicine
Osaka University Medical School
2-2 Yamada-oka
Suita, Osaka, 565
Japan

Ichiro Morita
Department of Thoracic & Cardiovascular Surgery
Kawasaki Medical School
577 Matsushima, Kurashiki
Okayama, 701-01
Japan

Taiji Murakami
Department of Thoracic & Cardiovascular Surgery
Kawasaki Medical School
577 Matsushima, Kurashiki
Okayama, 701-01
Japan

E. Mutschler
Pharmakologisches Institut für
Naturwissenschaftler
Johann Wolfgang Goethe-Universität
Frankfurt am Main
Germany

I. Nagy
First Department of Medicine
Albert Szent-Györgyi Medical University
H-6720 Szeged
Hungary

Shoji Nakai
First Department of Medicine
Kinki University School of Medicine
Osakasayama
Osaka, 589
Japan

Tohru Nakai
Department of Pharmacology
Hokkaido College of Pharmacy
Otaru, 047-02
Japan

Yasumitsu Nakai
First Department of Anatomy
Showa University School of Medicine
1-5-8 Hatanodai, Shinagawa-ku
Tokyo, 142
Japan

Takuro Nakamura
Third Department of Internal Medicine
Hamamatsu University School of Medicine
3600 Handa-cho
Hamamatsu, 431-31
Japan

Masaki Nakatani
Third Department of Internal Medicine
Showa University School of Medicine
1-5-8 Hatanodai, Shinagawa-ku
Tokyo, 142
Japan

Hiroe Nakazawa
Department of Physiology
Tokai University
Isehara, 259-11
Japan

Mikio Nakazawa
Department of Pharmacology
Niigata University School of Medicine
1-754 Asahi-machi
Niigata, 951
Japan

Masashi Nishida
First Department of Medicine
Osaka University Medical School
2-2 Yamada-oka
Suita, Osaka, 565
Japan

Kazuaki Nishio
Third Department of Internal Medicine
Showa University School of Medicine
1-5-8 Hatanodai, Shinagawa-ku
Tokyo, 142
Japan

Koichi Node
First Department of Medicine
Osaka University School of Medicine
2-2 Yamada-oka
Suita, Osaka, 565
Japan

Michiko Nojiri
Department of Pharmacology
Tokyo University of Pharmacy & Life Science
School of Pharmacy
1432-1 Horinouchi
Hachioji, Tokyo, 192-03
Japan

Iwao Ogawa
First Department of Medicine
Kinki University School of Medicine
Osakasayama
Osaka, 589
Japan

Toshio Ogihara
Department of Geriatric Medicine
Osaka University Medical School
2-2 Yamada-oka
Suita, Osaka, 565
Japan

Fumiko Okazaki
Fourth Department of Internal Medicine
Aoto Hospital
Jikei University School of Medicine
6-41-2 Aoto, Katsushika-ku
Tokyo, 125
Japan

Yasunaga Okazaki
Department of Surgery II
Kochi Medical School
Nankoku, 783
Japan

Hiroyuki Okumura
Fourth Department of Internal Medicine
Aoto Hospital
Jikei University School of Medicine
6-41-2 Aoto, Katsushika-ku
Tokyo, 125
Japan

Hans-Georg Olbrich
Medizinische Klinik IV
Abteilung für Kardiologie
Theodor-Stern-Kai 7
60596 Frankfurt am Main
Germany

Zenshiro Onouchi
Division of Pediatrics
Children's Research Hospital
Kyoto Prefectural University of Medicine
Kajiicho 465, Hirokoji, Kawaramachi
Kamigyoku, Kyoto, 602
Japan

Clive H. Orchard
Department of Physiology
University of Leeds
Leeds LS2 9JT
United Kingdom

Vince Palace
Institute of Cardiovascular Sciences
St. Boniface General Hospital Research Centre
351 Tache Avenue
Winnipeg, MB R2H 2A6
Canada

Wincenzo Panagia
Institute of Cardiovascular Sciences
St. Boniface General Hospital Research Centre
351 Tache Avenue
Winnipeg, MB R2H 2A6
Canada

Julius Gy Papp
Department of Pharmacology
Albert Szent-Györgyi Medical University
Dom ter 12
H-6701 Szeged
Hungary

James R. Parratt
Departments of Physiology and Pharmacology
University of Strathclyde
Glasgow, Scotland
United Kingdom

Sujata Persad
Institute of Cardiovascular Sciences
St. Boniface General Hospital Research Centre
351 Tache Avenue
Winnipeg, MB R2H 2A6
Canada

Philip A. Poole-Wilson
Department of Cardiac Medicine
Imperial College School of Medicine at the National Heart & Lung Institute
University of London
Dovehouse Street
London, England SW3 6LY
United Kingdom

Claudio Rigatto
Institute of Cardiovascular Sciences
St. Boniface General Hospital Research Centre
351 Tache Avenue
Winnipeg, MB R2H 2A6
Canada

Anthony Rosenzweig
Massachusetts General Hospital Cardiovascular Research Center
Mailcode: 1494201
149 13th Street
Charlestown, MA 02129-2060
USA

Matao Sakanashi
Department of Pharmacology
School of Medicine
University of the Ryukyus
Okinawa, 903-01
Japan

Hiroshi Sato
First Department of Medicine
Osaka University School of Medicine
2-2 Yamada-oka
Suita, Osaka, 565
Japan

Kiyotaka Sato
Department of Internal Medicine and Cardiology
Kitasato University School of Medicine
1-15-1 Kitasato
Sagamihara, 228
Japan

Hiroshi Satoh
Third Department of Internal Medicine
Hamamatsu University School of Medicine
3600 Handa-cho
Hamamatsu, 431-31
Japan

Kumi Satoh
Department of Pharmacology
Hokkaido College of Pharmacy
Otaru, 047-02
Japan

Yoshiki Sawa
First Department of Surgery
Osaka University
2-2 Yamada-oka
Suita, Osaka, 565
Japan

Shingo Seki
Department of Internal Medicine
Aoto Hospital
Jikei University School of Medicine
6-41-2 Aoto, Katsushika-ku
Tokyo, 125
Japan

Michael J. Shattock
Cardiovascular Research
The Rayne Institute
St. Thomas' Hospital
London, England SE1 7EH
United Kingdom

Nobuhiko Shibata
Department of Medicine
Osaka Medical Center for Cancer and Cardiovascular Diseases
1-3-3 Nakamichi, Higashinari-ku
Osaka, 537
Japan

Munekazu Shigekawa
Department of Molecular Physiology
National Cardiovascular Center Research Institute
Fujishiro-dai 5
Suita, Osaka, 565
Japan

Ken Shinmura
Department of Geriatric Medicine
Keio University School of Medicine
35 Shinanomachi, Shinjuku-ku
Tokyo, 160
Japan

Pawan K. Singal
Institute of Cardiovascular Sciences
St. Boniface General Hospital Research Centre
351 Tache Avenue
Winnipeg, MB R2H 2A6
Canada

Charles Steenbergen
Department of Pathology
Duke University Medical Center
P.O. Box 3712
Durham, NC 27710-0001
USA

Zhi Su
Department of Physiology
Tokai University
Isehara, 259-11
Japan

Yukako Suganuma
Department of Geriatric Medicine
Keio University School of Medicine
35 Shinanomachi, Shinjuku-ku
Tokyo, 160
Japan

Shiho Sugiyama
Third Department of Internal Medicine
Hamamatsu University School of Medicine
3600 Handa-cho
Hamamatsu, 431-31
Japan

Jun-ichi Suzuki
First Department of Internal Medicine
Shinshu University School of Medicine
3-1-1 Asahi
Matsumoto 390
Japan

Katsuo Suzuki
Second Department of Internal Medicine
Sapporo Medical University School of Medicine
South-1 West-16, Chuo-ku
Sapporo, 060
Japan

Keisuke Suzuki
Department of Medicine
Kitasato University School of Medicine
Kitasato
Japan

Ken Suzuki
First Department of Surgery
Institute for Cellular and Molecular Biology
Osaka University Medical School
2-2 Yamada-oka
Suita, Osaka, 565
Japan

László Szekeres
Institute of Pharmacology
Albert Szent-Györgyi Medical University
Kazinczy u.2
H-6720 Szeged
Hungary

Z. Szilvássy
First Department of Medicine
Albert Szent-Györgyi Medical University
Kazinczy u.2
H-6720 Szeged
Hungary

Michihiko Tada
Department of Medicine and Pathophysiology
Osaka University Medical School
2-2 Yamada-oka
Suita, Osaka, 565
Japan

Katsuhito Takahashi
Department of Medicine
Osaka Medical Center for Cancer and Cardiovascular Diseases
1-3-3 Nakamichi, Higashinari-ku
Osaka, 537
Japan

Satoshi Takeda
Fourth Department of Internal Medicine
Aoto Hospital, Jikei University School of Medicine
6-41-2 Aoto, Katsushika-ku
Tokyo, 125
Japan

Satoshi Takeo
Department of Pharmacology
Tokyo University of Pharmacy & Life Science
School of Pharmacy
1432-1 Horinouchi
Hachioji, Tokyo, 192-03
Japan

Yusuke Tamura
First Department of Internal Medicine
Niigata University School of Medicine
1-754 Asahi-machi
Niigata, 951
Japan

Masato Tani
Department of Geriatric Medicine
Keio University School of Medicine
35 Shinanomachi, Shinjuku-ku
Tokyo, 160
Japan

Ikuo Taniguchi
Fourth Department of Internal Medicine
Aoto Hospital
Jikei University School of Medicine
6-41-2 Aoto, Katsushika-ku
Tokyo, 125
Japan

Masayuki Taniguchi
Fourth Department of Internal Medicine
Aoto Hospital
Jikei University School of Medicine
6-41-2 Aoto, Katsushika-ku
Tokyo, 125
Japan

Kouichi Tanonaka
Department of Pharmacology
Tokyo University of Pharmacy & Life Science
School of Pharmacy
1432-1 Horinouchi
Hachioji, Tokyo, 192-03
Japan

Hajime Terada
Third Department of Internal Medicine
Hamamatsu University School of Medicine
3600 Handa-cho
Hamamatsu, 431-31
Japan

Shinji Teramachi
Division of Pediatrics
Children's Research Hospital
Kyoto Prefectural University of Medicine
Kajiicho 465, Hirokoji, Kawaramachi
Kamigyoku, Kyoto, 602
Japan

Cesare M.N. Terracciano
Imperial College School of Medicine at National Heart & Lung Institute
Cardiac Medicine
Dovehouse Street
London, England SW3 6LY
United Kingdom

Akihito Tsuchida
Second Department of Internal Medicine
Sapporo Medical University School of Medicine
South-1 West-16, Chuo-ku
Sapporo, 060
Japan

Ryuji Ueda
Third Department of Internal Medicine
Showa University School of Medicine
1-5-8, Hatanodai, Shinagawa-ku
Tokyo, 142
Japan

Tetsuya Ueda
Cardiovascular Division
Ishinkai Yao General Hospital
Osaka, 581
Japan

Yasunori Ueda
First Department of Medicine
Osaka University School of Medicine
2-2 Yamada-oka
Suita, Osaka, 565
Japan

Agnes Vegh
Department of Pharmacology
Albert-Szent-Györgyi Medical University
Dom ter 12
H-6701 Szeged
Hungary

Shigeo Wakabayashi
Department of Molecular Physiology
National Cardiovascular Center Research Institute
Fujishiro-dai 5
Suita, Osaka, 565
Japan

Ed White
Department of Physiology
University of Leeds
Leeds, LS2 9JT
United Kingdom

Ken-ichi Yabe
Department of Pharmacology
Tokyo University of Pharmacy & Life Science
School of Pharmacy
1432-1 Horinouchi
Hachioji, Tokyo, 192-03
Japan

Atsuko Yamamoto
Department of Pharmacology
Hokkaido College of Pharmacy
Otaru, 047-02
Japan

Shinichirou Yamamoto
Department of Internal Medicine and Cardiology
Kitasato University School of Medicine
1-15-1 Kitasato
Sagamihara, 228
Japan

Hisako Yamamura
Department of Medicine
Osaka Medical Center for Cancer and Cardiovascular Diseases
1-3-3 Nakamichi, Higashinari-ku
Osaka, 537
Japan

Nobushige Yamashita
First Department of Medicine
Osaka University Medical School
2-2 Yamada-oka
Suita, Osaka, 565
Japan

Masaru Yamazoe
First Department of Internal Medicine
Niigata University School of Medicine
1-754 Asahi-machi
Niigata, 951
Japan

Toshikuni Yanagishita
Third Department of Internal Medicine
Showa University School of Medicine
1-5-8 Hatanodai, Shinagawa-ku
Tokyo, 142
Japan

Takenori Yasuda
Cardiovascular Division
Ishinkai Yao General Hospital
Osaka, 581
Japan

Yutaka Yoshida
Department of Pharmacology
Niigata University School of Medicine
1-754 Asahi-machi
Niigata, 951
Japan

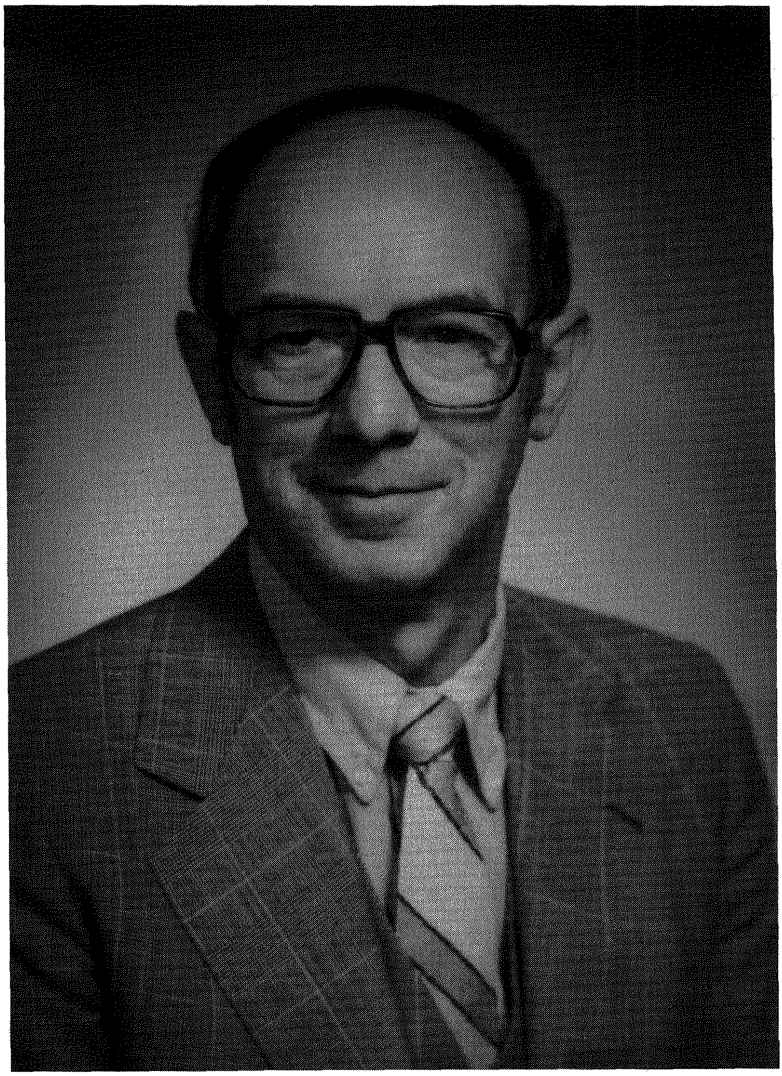

Robert B. Jennings, M.D.

This book is dedicated to Dr. Robert Jennings, James B. Duke Professor of Pathology at the Duke University Medical Center, for his pioneering work in the area of ischemia–reperfusion injury in the heart. His leadership in promoting cardiovascular research and the scientific basis for cardiology throughout the world in his capacity as President of the International Society for Heart Research (1978–1980) as well as Chairman of the Council of Cardiac Metabolism of the International Society and Federation of Cardiology (1986–1992) is acknowledged.

ROBERT B. JENNINGS: A MAN WITH A GREAT VISION AND COMMITMENT TO THE SERVICE OF CARDIOVASCULAR MEDICINE

Robert Burgess Jennings was born on December 14, 1926, in Baltimore and obtained his B.S., M.S., and M.D. degrees from Northwestern University in 1947, 1949 and 1950, respectively. He served in the Department of Pathology at the Northwestern University Medical School as Instructor (1953–1956), Assistant Professor (1956–1960), Associate Professor (1960–1963), Professor (1963–1969), and Professor and Chairman (1969–1975). In 1975, he moved to the Duke University Medical Center as Professor and Chairman of the Pathology Department, where he was appointed James B. Duke Professor of Pathology in 1980. At both Northwestern University and Duke University, he developed strong educational and research programs. He trained numerous fellows in cardiovascular pathology who are actively engaged in understanding the pathophysiology of heart disease.

Dr. Jennings is an excellent investigator in the field of cardiac pathology. As early as 1953, he set out to discover the cellular, metabolic, and molecular events that result in the death of ischemic cardiomyocytes. He observed dramatic changes in Na^+, K^+, and Ca^{2+} in the ischemic heart and showed release of cardiac enzymes such as glutamic oxaloacetic transaminase and lactic dehydrogenase upon occluding the coronary artery for a brief period. His well-thought-out and elegant experiments revealed a defect in the ability of the ischemic heart to metabolize glucose. Not only did he lay out the concept of reversible and irreversible ischemic injury to the heart but he also provided convincing evidence for the existence of these two phases of myocardial ischemia. Irreversibly damaged cardiomyocytes were reported by him to exhibit a very unusual form of necrosis in which the cells were swollen and

contained enormous contraction bands. Thus, his seminal experimental work on the temporary occlusion of the coronary artery for different durations laid the foundation for therapeutic effects of early reperfusion of the ischemic heart by thrombolysis, coronary bypass surgery, or angioplasty.

Dr. Robert Jennings is a man of great vision and extraordinary commitment to the promotion of cardiovascular science. It is no secret that he is known for his keen sense of direction and for the development of logic that enables others to follow his arguments on subjects ranging from science to philosophy. He challenges and inspires others to do great and difficult tasks. Nonetheless, he enjoys helping others to achieve their potential and demands excellence. During his Presidency of the International Society for Heart Research (1978–1980), he developed rules and regulations for improving the function of this Society. As Chairman of the Council of Cardiac Metabolism of the International Society and Federation of Cardiology (1986–1992), he promoted cardiovascular education throughout the world. In addition to the Peter Harris Award for Distinguished Investigators in the field of heart research and the Distinguished Achievement Award of the Society of Cardiovascular Pathology, he has been honored several times for his contributions in the field of ischemic heart disease. We believe that the dedication of *The Ischemic Heart* to Robert Jennings is a fitting tribute to this outstanding human being.

PREFACE

It is now well known that ischemic heart disease is a major health problem in the world. Over the past three decades, impressive progress in the fields of pathogenesis, prevention, and therapy of ischemic heart disease has resulted in a marked decline (from about 65% to 40%) in mortality in the Western world; however, the incidence of this devastating disease is on the rise in developing countries. It has become clear that several risk factors, such as high cholesterol, cigarette smoking, diabetes, hypertension, obesity, lack of exercise, and stress, promote the occurrence of ischemic heart disease as a consequence of both the formation of cholesterol plaque and/or thrombosis in the coronary arteries and the development of coronary spasm. These outcomes result in reduction of the blood supply to a given area of the myocardium, depending upon the site of occlusion in the coronary artery, and are associated with derangement of cardiac metabolism and cellular structure. Myocardial ischemia under acute conditions leads to the development of heart dysfunction and arrhythmias as a consequence of a shift in the intracellular concentration of cations as well as a deficiency of high-energy phosphate stores in the myocardium. Prolonged ischemia results in the development of myocardial infarction, and whenever the scar size is about or more than 30% of the ventricular wall, congestive heart failure occurs within two to five years. Thus, two basic problems are being investigated in the area of ischemic heart disease, namely, acute myocardial ischemia and myocardial infarction. While the biochemical changes in the heart due to acute myocardial ischemia are almost identified, a great deal of work regarding the sequence of events from angina and cardiac hypertrophy to congestive heart failure

due to myocardial infarction remains to be carried out in the future. In particular, it is noteworthy to point out that not only does a defect occur in the contractile machinery of the ischemic heart but also a loss of adrenergic support to the heart becomes evident during the development of congestive heart failure due to myocardial infarction.

Although restoration of blood supply to the ischemic myocardium by angioplasty, coronary bypass, and/or thrombolysis can be seen to produce beneficial effects, the outcome for the patient seems to depend upon the time taken to establish the coronary flow to the ischemic myocardium. In fact, another problem, namely, reperfusion injury, sets in if the blood flow is not restored within a certain critical time. Most of the research in this area has revealed that reperfusion of the ischemic heart results in the formation of oxyradicals and oxidants, and this oxidative stress appears to play an important role in the genesis of massive arrhythmias as well as additional ultrastructural damage, membrane defects, and contractile abnormalities. The exact mechanisms of ischemia–reperfusion injury have not been described; however, Ca^{2+}-handling abnormalities in cardiomyocytes have been identified as one of the major targets for preventing ischemia–reperfusion injury. In this regard, different β-adrenergic receptor blocking agents and Ca^{2+} antagonists have proven to be useful. In addition, brief episodes of ischemia—Ischemic Preconditioning—have also been shown to attenuate the effects of ischemia–reperfusion injury, but the mechanisms of the cardioprotective actions of ischemic preconditioning are poorly understood.

A symposium on "The Ischemic Heart" was organized in Tokyo on November 19–21, 1996, for an in-depth discussion of a wide variety of issues in the field of ischemic heart disease. For this book, selected speakers from this symposium were invited to contribute papers emphasizing their experiences on diverse issues in the area of ischemic heart disease. We have organized their contributions in two sections, namely, 1) Pathophysiologic Mechanisms of Ischemia–Reperfusion Injury, and 2) Preconditioning and Protection of Ischemia–Reperfusion Injury. It is our contention that the 45 chapters assembled for this book provide up-to-date information concerning the current concepts of ischemia–reperfusion injury, the sequence of events resulting in the loss of contractile dysfunction, the mechanisms of cardioprotection by several drugs, and the role of ischemic preconditioning in attenuating problems associated with ischemia–reperfusion injury. We believe this book will be helpful to both students and scientists as well as to clinical cardiologists and cardiovascular surgeons dealing with ischemic heart disease.

Seibu Mochizuki, Tokyo
Nobuakira Takeda, Tokyo
Makoto Nagano, Tokyo
Naranjan S. Dhalla, Winnipeg

ACKNOWLEDGMENTS

The conference on the Ischemic Heart was sponsored by the International Society and Federation of Cardiology, for which we are indeed grateful. The financial support for this meeting was kindly provided by several Japanese pharmaceutical industries. It would have been virtually impossible to organize this conference without the advice of Drs. Philip Poole-Wilson and Howard Morgan, who served as members of the International Advisory Board. The help of Ms. Susan Zettler in the preparation of this book is highly appreciated. Special thanks are due to Mr. Robert Holland and Ms. Melissa Ramondetta and their editorial staff at Kluwer Academic Publishers for their patience, interest, and hard work in assembling this volume.

This Page Intentionally Left Blank

THE ISCHEMIC HEART

Edited by
SEIBU MOCHIZUKI, M.D., Ph.D.
Professor and Chairman
Department of Medicine
Aoto Hospital
Jikei University School of Medicine
Tokyo, Japan

NOBUAKIRA TAKEDA, M.D., Ph.D.
Associate Professor
Department of Internal Medicine
Aoto Hospital
Jikei University School of Medicine
Tokyo, Japan

MAKOTO NAGANO, M.D., Ph.D.
Professor Emeritus
Jikei University School of Medicine
Tokyo, Japan

NARANJAN S. DHALLA, Ph.D., M.D. (Hon.), D.Sc. (Hon.)
Distinguished Professor and Director
MRC Group in Experimental Cardiology
Institute of Cardiovascular Sciences
St. Boniface General Hospital Research Centre
Faculty of Medicine, University of Manitoba
Winnipeg, Canada

KLUWER ACADEMIC PUBLISHERS, BOSTON

This Page Intentionally Left Blank

I. PATHOPHYSIOLOGIC MECHANISMS OF ISCHEMIA–REPERFUSION INJURY

This Page Intentionally Left Blank

FUNCTION OF CARDIAC MYOCYTES IN ISCHEMICHEART DISEASE: COMPARATIVE CHANGES IN RIGHT AND LEFT VENTRICULAR CELLS

SIAN E. HARDING, FEDERICA DEL MONTE, and PHILIP A. POOLE-WILSON

Imperial College School of Medicine at the National Heart & Lung Institute

Summary. The contraction and relaxation velocities of single myocytes isolated from failing and nonfailing left and right human ventricles have been compared in order to investigate the possible contribution of cellular changes to the diastolic dysfunction seen in vivo. Myocytes from the failing right ventricle (RV) showed slowed relaxation compared to those from nonfailing, and the change was quantitatively similar to that seen in the failing left ventricle (LV). Poor relaxation was observed in RV myocytes from patients with ischemic heart disease, idiopathic dilated cardiomyopathy, and congenital heart disease. Division of patients into groups with high and low pulmonary artery pressure (PAP) showed a significant relation between raised PAP and slow relaxation of RV myocytes. Cells from the high PAP group were also longer, but not wider, than those from the low PAP group. β-adrenoceptor desensitization was evident in RV myocytes from failing heart, but did not differ in magnitude between high and low PAP groups. As we have previously shown for the LV, diastolic dysfunction in the RV may be related to changes in myocyte function.

INTRODUCTION

Many of the characteristic functional changes in the failing human heart are the result of alterations in the muscle cells themselves. We have shown that single myocytes isolated from the left ventricles (LVs) of patients with ischemic heart disease (IHD) or idiopathic dilated cardiomyopathy (DCM) have a slow contraction and relaxation [1], show a reduced response to β-adrenoceptor agonists [2], and have lost the "positive staircase" with increasing frequency of stimulation [3]. Both qualitatively and quantitatively, these changes resemble those seen in vivo [4–8] or

S. Mochizuki, N. Takeda, M. Nagano and N. Dhalla (eds.). THE ISCHEMIC HEART.

in intact muscle strips from failing human hearts [9–12]. The myocyte alterations are not exclusive to one etiology of heart failure but seem to depend, in varying degrees, upon the severity and duration of the condition, hypertrophy of the ventricle, and the age of the patient [1,2]. LV myocyte size increases as the ventricle hypertrophies [1,13,14], but cell size per se does not influence function [1].

Right ventricular (RV) function in human heart failure, and its relation to dilation or hypertrophy, has been less well characterized. This is partly because the main determinant of a low cardiac output on exercise is usually LV function and also because the primary lesion can often be located to the LV, particularly for infarcted hearts. It is also more difficult to obtain accurate measurements of RV wall thickness and relaxation time. However, a recent study on a large number of subjects has shown that RV relaxation abnormalities are common in heart failure patients, with average RV isovolumic relaxation time almost double that of normal controls [15]. This finding was true not only for heart failure secondary to primary pulmonary hypertension, where an RV abnormality might be predicted, but for IHD and DCM patients also. Pulmonary artery systolic pressure showed a significant correlation with several parameters of RV diastolic function, such as deceleration time of the tricuspid E-wave [15].

In this chapter we give data on the relaxation velocity of myocytes from the right ventricle of failing human hearts. This study is largely retrospective, and we do not have accurate information on the wall thickness of the right ventricle. However, we have compared left and right ventricles from patients with IHD and DCM and have examined the change in cell size and the relation of the relaxation defect to raised pulmonary artery pressure (PAP). Our data support the hypothesis that poor RV relaxation is common in heart failure and suggest that at least part of the problem lies at the level of the cardiomyocyte.

METHODS

Myocyte preparation

Human left ventricular myocardial tissue was obtained from the free wall of explanted hearts at the time of transplantation (0.5–2 g). Tissue was transported to the laboratories in cold cardioplegic solution, with an average transport time of one hour, and was cut into chunks of approximately 1 mm^3 using an array of razor blades. The chunks were incubated for 12 minutes, with shaking, at 35°C in 25 mL of a low calcium medium of the following composition (mM): NaCl 120, KCl 5.4, $MgSO_4$ 5, pyruvate 5, glucose 20, taurine 20, HEPES 10, and nitrilotriacetic acid (NTA) 5, bubbled with 100% O_2. The pH was adjusted to 6.95, and the measured free [Ca^{2+}] was 1–3 μM. The medium was changed three times at three-minute intervals, and the chunks were stirred by bubbling with 100% O_2. The chunks were then drained and incubated for 45 minutes at the same temperature in low calcium medium with NTA omitted and 50 μM Ca^{2+} added and containing 4 U/mL Sigma type XXIV protease (pronase). The solution was shaken gently under an atmosphere of 100% O_2. Two further 45-minute digests were then carried out using collagenase

(Boehringer) at 400 IU/mL. The cell suspension was filtered at the end of each 45-minute period through 300-μm gauze to remove undigested tissue, and the myocytes were pelleted by gentle centrifugation (400 r/min). The pellet was resuspended in preoxygenated Krebs–Henseleit medium (mM): NaCl 119, KCl 4.7, $MgSO_4$ 0.94, KH_2PO_4 1.2, $NaHCO_3$ 25, glucose 11, containing 1 mM Ca^{2+} and equilibrated to pH 7.4. Rod-shaped myocytes were obtained from both collagenase digests. The proportion of rod-shaped cells was variable, occasionally reaching 50%–70% but usually below 5%. Right ventricular preparations, particularly those from the hearts of patients with ischemic cardiomyopathy, were notably and consistently better than those from the left ventricle in terms of yield and quality of myocytes.

Measurement of contraction

Myocytes were superfused with Krebs–Henseleit solution (1 mM Ca^{2+} added, equilibrated with 95% O_2, 5% CO_2, and warmed at 32°C) at a rate of 2 mL/min. Cells were electrically stimulated with a biphasic pulse (0.2 Hz, 50% above threshold) through platinum electrodes placed along the side of the bath. The contraction amplitude and the rates of contraction and relaxation were monitored using a video/length detection system with a scan rate of 50 Hz and a capture of 512 raster lines. Contraction amplitude (change in cell length or sarcomere length with each beat) was measured from a chart tracing of at least two minutes steady contraction. Contraction velocity (change in cell or sarcomere length μm/s) was measured from a simultaneous trace of the change in cell length between one field and the next, calibrated using a computer-generated moving line. Since the fastest part of the contraction or relaxation may not be captured on each beat, the averaged *maximum* velocities over the two minutes (60 beats) of steady contraction amplitude were taken by measuring an envelope of the differential tracing. To normalize for difference in length between cells, which increases the variability of the measurements, or for differences in amplitude, which will independently change velocity [16], data were expressed as the percentage of the total contraction that occurs in the 20-ms scan encompassing the fastest part of the beat. This approach has the added advantage of giving an immediate estimate of the reliability of the measurement.

For each myocyte, cell length (μm), sarcomere length (μm; number of sarcomeres [>30] crossing a defined area of the TV screen, measured with a ×100 objective), and stimulation threshold (mV) were measured. Prior to the experiment, a video hardcopy of the cell was taken to measure cell dimensions (area and perimeter) using a digitizing tablet with associated software (VIDS III, Analytical Measuring Systems, Cambridge, Massachusetts, USA). Myocytes were selected for study on the basis of five criteria: morphological appearance (rod shaped, no large blebs or areas of hypercontracture), sarcomere length greater than 1.70 μm, no spontaneous contractions when unstimulated in 1 mM Ca^{2+}, stable contraction amplitude and diastolic length at the basal stimulation rate of 0.2 Hz, and complete recovery after challenge

with maximally activating Ca^{2+} concentrations (see below). Cells that satisfied these criteria could be studied for up to 12 hours after the isolation procedure.

Concentration–response curves to calcium (1–25 mM) were constructed, with a maximum reached when there was no further increase in contraction amplitude or when toxic signs (large decreases in resting length, phasic contractions) were observed. Measurements of velocity and beat duration were made in the maximum Ca^{2+} concentration where stable amplitudes were obtained (6–20 mM). Concentration–response curves were only included in the analysis if the effect could be fully reversed on washout to exclude cells in which toxic signs were due to spontaneous cell death.

Materials

Salts were from BDH and were AnalaR grade except for KCl, taurine, and glucose, which were AristaR. BDH AnalaR water was used for low Ca^{2+} solutions and double-distilled deionized water (MilliQ) for others.

Statistical analysis

Results were analyzed using one-way ANOVA with Tukey's test for pairwise comparison of means. Data were obtained from 1–8 myocytes per preparation and averaged for each patient so that n values quoted represent patient numbers. Values are expressed as mean ± SEM.

RESULTS

Relaxation velocities of right and left ventricular myocytes from failing and nonfailing human ventricle are shown in figure 1; the failing group is divided into IHD and DCM. We performed the experiments under conditions (stimulation frequency 0.2 Hz) where differences in amplitude between failing and nonfailing myocytes were minimized [1,3]. Contraction amplitudes of myocytes (% cell shortening) did not differ significantly between LV and RV from either failing hearts (LV: 10.0 ± 0.9% (n = 24), RV: 10.0 ± 0.3% (n = 37)) or non-failing hearts (LV: 10.0 ± 0.6% (n = 18), RV: 7.7 ± 0.9% (n = 3)). Velocity was expressed as the fastest change between camera scans (20 ms), as a percentage of the total change: this expression gives a measure independent of contraction amplitude or cell length. As we have previously shown, LV relaxation velocity was reduced in myocytes from either IHD or DCM hearts compared to those from nonfailing hearts [1]. Although the number of nonfailing hearts from which RV myocytes were obtained was small, ANOVA showed that there was also a significant difference for RV between nonfailing, IHD, and DCM groups ($p = 0.025$). RV myocytes from patients with congenital heart disease also showed a slowing of relaxation, with a relaxation velocity of 11.3% ± 0.7% ($n = 7$) compared with 11.1% ± 0.3% in IHD and 17.3% ± 3.8% in nonfailing. There was no significant difference between RV and LV relaxation velocities in any of the failing or nonfailing groups.

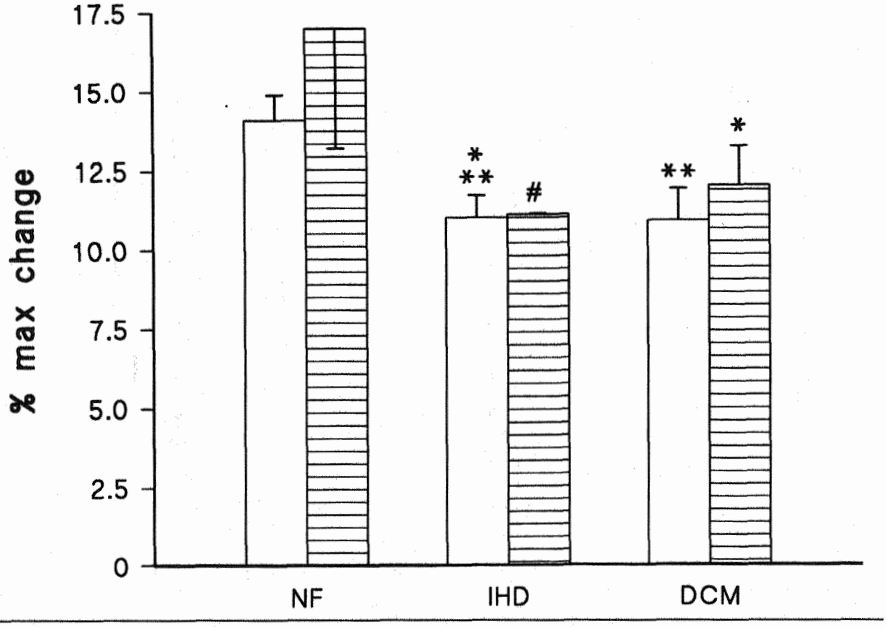

Figure 1. Relaxation velocity normalized for amplitude (% maximum change in single scan) for myocytes from the LV (open bars) and RV (lined bars) of nonfailing (NF; LV 18 patients, RV 3 patients), IHD (LV 20 patients, RV 30 patients), or DCM (LV 4 patients, RV 7 patients). Significantly different from LV nonfailing: *, $p < 0.05$, **, $p < 0.01$, ***, $p < 0.001$; from RV nonfailing: #, $p < 0.05$.

The RV myocytes from failing hearts only were divided according to pulmonary artery pressure (PAP), where this had been measured in the patients prior to transplant. Those patients with a diastolic PAP of 20 mmHg or higher were classified as high PAP: the mean diastolic PAPs in the two groups after division were 35.0 ± 4.3 ($n = 20$) and 13.8 ± 1.0 mmHg ($n = 11$). The respective systolic PAPs were 69.7 ± 8.6 and 36.2 ± 5.0 mmHg. Mean contraction amplitude and contraction and relaxation velocity for the two groups is shown in figure 2. There was little difference in contraction amplitude, but a significant slowing of both contraction and relaxation velocity ($p < 0.05$ for both) was seen in the high PAP group.

Cell length, area, and form factor (a measure of the circularity of the cell) were analyzed by PAP groups. RV myocytes from hearts that had experienced high PAP were significantly longer than those from the low PAP group (figure 3). The area was increased, but only in proportion to the change in length, showing that the cells had become longer but not wider. In confirmation, it was found that the form factor had decreased significantly in the high PAP group (0.41 ± 0.01 vs. 0.47 ± 0.02, $p < 0.05$), indicating an increase in the length: width ratio. Sarcomere length was not significantly different between the two groups (low PAP: 1.82 ± 0.02 μm; high PAP: 1.81 ± 0.02 μm).

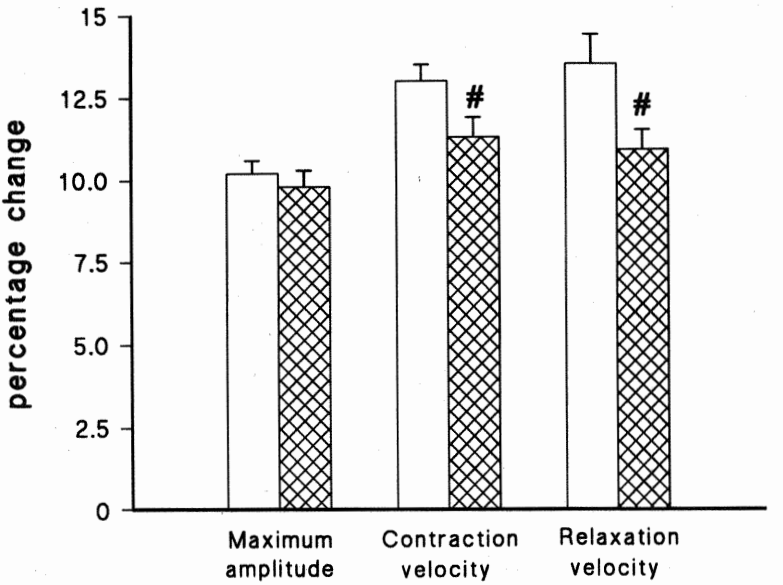

Figure 2. Maximum contraction amplitude (% cell shortening) and contraction and relaxation velocities for myocytes from RV of failing hearts, divided according to patient PAP. Low PAP group: $n = 11$, open bars; high PAP group: $n = 20$, cross-hatched bars. #, $p < 0.05$ compared to low PAP group.

RV myocytes from failing hearts, like those from the LV, exhibited β-adrenoceptor desensitization, but there was no difference between the low and high PAP groups. The isoproterenol: Ca^{2+} ratio (maximum response to isoproterenol compared to high Ca^{2+} in the same cell [2]) was 0.72 ± 0.05 in the low PAP group ($n = 10$) and 0.72 ± 0.06 ($n = 17$) in the high PAP group. This finding compares to 0.93 in RV myocytes from nonfailing hearts ($n = 2$), 0.98 ± 0.07 in LV myocytes from nonfailing hearts ($n = 14$), and 0.67 ± 0.03 in LV myocytes from failing hearts with IHD ($n = 14$).

DISCUSSION

This study demonstrates that RV myocytes from failing human hearts have a slower relaxation velocity than those from the nonfailing left or right ventricle. The deficit is similar in IHD and DCM and is also similar to LV myocytes from failing hearts. These data support the in vivo findings that poor RV relaxation is common in patients with heart failure of varying etiologies, and not only in those with primary pulmonary hypertension [15]. A quantitative comparison between in vivo and in vitro data is always problematic, and the myocyte results are limited by the small size of the nonfailing RV group, but some general conclusions may be drawn regarding the relative degree of change. In the intact RV, peak tricuspid E-wave velocity

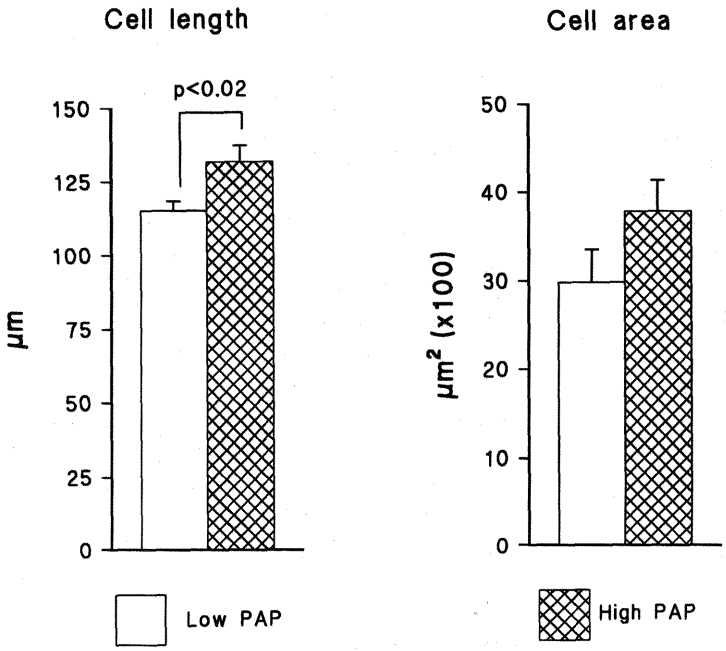

Figure 3. Cell length and area of RV myocytes from failing hearts of patients with low and high PAP.

decreased by up to 20% in the heart failure patients and the deceleration time of the transtricuspid E wave by up to 17% [15]. The peak relaxation velocity of the RV myocytes from failing hearts in the present study was decreased by 30% compared with nonfailing RV and by 20% compared with nonfailing LV. It is therefore possible that the slow relaxation of the myocytes contributes to the diastolic dysfunction seen in vivo.

For LV myocytes, poor relaxation was related to the wall thickness of the ventricle from which the cells were isolated [1]. Accurate measurements of RV wall thickness were not available for the majority of these patients, so the failing group was divided according to pulmonary artery pressure (PAP) as a measure of the stimulus to hypertrophy or dilation. Increasing PAP had been shown to correlate with a slowing in several of the parameters of RV relaxation in the in vivo study [15]. RV myocytes from the hearts of patients with high PAP had significantly slowed contraction and relaxation velocities compared with those from the low PAP group. Cell lengths in the high PAP group were also increased, indicating that some degree of hypertrophy or dilation had taken place. In the in vivo study, heart failure patients who had low PAP still had RV diastolic dysfunction compared to normal subjects, suggesting a further mechanism unrelated to pressure overload. RV myocytes from patients with low PAP (in the normal range) had relaxation velocity

values of 13%, compared to 14% in normal LV and 17% in normal RV. Once again, the small size of the normal RV group limits the analysis, but there may be a pressure-independent component to the impaired relaxation in the RV myocytes. This is similar to our findings in LV cells, where the decrease in relaxation velocity was significant in myocytes from failing thin-walled ventricles but significantly greater still in those from thick-walled ventricles [1].

Since length but not width of the RV myocytes was altered, it is more likely that there had been dilation in the RV rather than wall thickening. We have shown that LV myocyte area, not length, was enlarged in thick-walled ventricles but that an increase in cell length correlated with LV dilation [1]. The change in RV length in the high PAP group was modest (around 10%), in contrast to the large alterations seen in other studies [14,17]. Possible reasons for such discrepancies have been discussed [18].

The generality of the relaxation defect with respect to etiology and ventricle and the observation that there is a component unrelated to hypertrophy suggest that poor relaxation arises secondary to the disease process. One possible mechanism that has been explored is lowering of cyclic AMP levels following the well-known β-adrenoceptor desensitization in failing ventricle [10]. This study shows that reduced β-adrenoceptor responses are present in the RV myocytes, and we have previously shown that LV myocytes from patients with IHD, DCM, or mitral valve disease have similar degrees of desensitization [2]. β-adrenoceptor desensitization could slow relaxation in two ways. First, loss of the effect of catecholamines released from nerve endings in the failing heart would withdraw tonic lusitropic support in vivo, leading to slowed relaxation. Second, prolonged desensitization is accompanied by a reduction in basal cyclic AMP production in the absence of β-adrenoceptor stimulation [19–22]. If high basal cyclic AMP maintains relaxation speeds in the nonfailing ventricle, loss of this effect would lead to a slowing of velocity independent of β-adrenoceptor stimulation. Evidence for this second mechanism comes from our studies on single myocytes, where possible confounding effects of endogenous catecholamines are eliminated. Myocytes from failing LV show a much greater increase in relaxation velocity when cyclic AMP is raised than do myocytes from nonfailing LV. After maximum stimulation with β-agonists, there is no longer any significant difference between myocytes from failing and nonfailing LVs with respect to contraction and relaxation speeds [23].

In conclusion, a deficit in contraction and relaxation velocity has been shown in myocytes from the failing RV. The alteration was independent of etiology, related to increased PAP, and of a similar magnitude to that observed in LV myocytes. Poor relaxation of RV myocytes may contribute to the diastolic dysfunction seen clinically in failing RV.

REFERENCES

1. del Monte F, O'Gara P, Poole-Wilson PA, Yacoub MH, Harding SE. 1995. Cell geometry and contractile abnormalities of myocytes from failing human left ventricle. Cardiovasc Res 30:281–290.

2. Harding SE, Jones SM, O'Gara P, del Monte F, Vescovo G, Poole-Wilson PA. 1992. Isolated ventricular myocytes from failing and non-failing human heart; the relation of age and clinical status of patients to isoproterenol response. J Mol Cell Cardiol 24:549–564.
3. Davies CH, Davia K, Bennett JG, Pepper JR, Poole-Wilson PA, Harding SE. 1995. Reduced contraction and altered frequency response of isolated ventricular myocytes from patients with heart failure. Circulation 92:2540–2549.
4. Souffer R, Wohlgelernter D, Vita NA, Amuchestegui M, Sostman HD, Berger H, Zaret B. 1985. Intact systolic left ventricular function in clinical congestive heart failure. Am J Cardiol 55:1032–1036.
5. Litwin SE, Grossman W. 1993. Diastolic dysfunction as a cause of heart failure (review). J Am Coll Cardiol 22:49A–55A.
6. Fowler MB, Laser JA, Hopkins GL, Minobe W, Bristow MR. 1986. Assessment of the B-adrenergic receptor pathway in the intact failing human heart: progressive receptor down-regulation and subsensitivity to agonist response. Circulation 74:1290–1302.
7. Mulieri LA, Hasenfuss G, Leavitt BJ, Allen PD, Alpert NR. 1992. Altered myocardial force–frequency relation in human heart failure. Circulation 85:1743–1750.
8. Rihal CS, Nishimura RA, Hatle LK, Bailey KR, Tajik J. 1994. Systolic and diastolic dysfunction in patients with clinical diagnosis of dilated cardiomyopathy. Circulation 90:2772–2779.
9. Gwathmey JK, Copelas L, MacKinnon R, Schoen FJ, Feldman MD, Grossman W, Morgan JP. 1987. Abnormal intracellular calcium handling in myocardium from patients with end stage heart failure. Cardiovasc Res 61:70–76.
10. Bristow MR, Ginsburg R, Umans V, Fowler M, Minobe W, Rasmussen R, Zera P, Menlove R, Shah P, Jamieson S, Stinson EB. 1986. B1-and B2-adrenergic receptor subpopulations in nonfailing and failing human ventricular myocardium: coupling of both receptor subtypes to muscle contraction and selective B1-receptor down-regulation in heart failure. Circ Res 59:297–309.
11. Gwathmey JK, Slawsky MT, Hajjar RJ, Briggs GM, Morgan JP. 1990. Role of intracellular calcium handling in force–interval relationships of human ventricular myocardium. J Clin Invest 85:1599–1613.
12. Schwinger RHG, Bohm M, Muller-Ehmsen J, Uhlmann R, Schmidt U, Stablein A, Uberfuhr P, Kreuzer E, Reichart B, Eissner H-J, Erdmann E. 1993. Effect of inotropic stimulation on the negative force–frequency relationship in the failing human heart. Circulation 88:2267–2276.
13. Gerdes AM, Kellerman SE, Moore JA, Muffly KE, Clark LC, Reaves PY, Malec KB, McKeown PP, Schocken DD. 1992. Structural remodeling of cardiac myocytes in patients with ischemic cardiomyopathy. Circulation 86:426–430.
14. Beltrami CA, Finato N, Rocco M, Feruglio GA, Puricelli C, Cigola E, Quaini F, Sonnenblick EH, Olivetti G, Anversa P. 1994. Structural basis of end-stage failure in ischemic cardiomyopathy in humans. Circulation 89:151–163.
15. Yu CM, Sanderson JE, Chan S, Yeung L, Hung YT, Woo KS. 1996. Right ventricular diastolic dysfunction in heart failure. Circulation 93:1509–1514.
16. Harding SE, Vescovo G, Kirby M, Jones SM, Gurden J, Poole-Wilson PA. 1988. Contractile responses of isolated rat and rabbit myocytes to isoproterenol and calcium. J Mol Cell Cardiol 20:635–647.
17. Gerdes AM, Capasso JM. 1995. Structural remodelling and mechanical dysfunction of cardiac myocytes in heart failure. J Mol Cell Cardiol 27:849–856.
18. Poole-Wilson PA. 1995. The dimensions of human cardiac myocytes; confusion caused by methodology and pathology (comment). J Mol Cell Cardiol 27:863–865.
19. Danielsen W, van der Leyen H, Meyer W, Neumann J, Schmitz W, Scholz H, Starbatty J, Stein B, Doring V, Kalmar P. 1989. Basal and isoprenaline-stimulated cAMP content in failing versus nonfailing human cardiac preparations. J Cardiovasc Pharmacol 14:171–173.
20. von der Leyen H, Mende U, Meyer W, Neumann J, Nose M, Schmitz W, Scholz H, Starbatty J, Stein B, Wenzlaff H, Doring V, Kalmar P, Haverich A. 1991. Mechanism underlying the reduced positive inotropic effects of the phosphodiesterase III inhibitors pimobendan, adibendan and saterinone in failing as compared to nonfailing human cardiac muscle preparations. Naunyn-Schmiedebergs Arch Pharmacol 344:90–100.
21. Bohm M, Reiger B, Schwinger RHG, Erdmann E. 1994. cAMP concentrations, cAMP dependent protein kinase activity, and phospholamban in non-failing and failing myocardium. Cardiovasc Res 28:1713–1719.

22. Wynne DG, del Monte F, Harding SE. 1996. Cyclic AMP levels in ventricular myocytes from noradrenaline-treated guinea-pigs. Eur J Pharmacol 310:235–242.
23. Harding SE, Brown LA, del Monte F, Davies CH, O'Gara P, Vescovo G, Wynne DG, Poole-Wilson PA. 1996. Acceleration of contraction by β-adrenoceptor stimulation is greater in ventricular myocytes from failing than non-failing human hearts. Basic Res Cardiol 91(Suppl 2):53–56.

REMODELING OF CARDIAC MYOCYTES IN CHRONIC HEART DISEASE

A. MARTIN GERDES

University of South Dakota

Summary. Congestive heart failure is generally characterized by a dilated, relatively thin-walled ventricle. Isolated myocyte data obtained from failing explanted human hearts with and without ischemic disease indicate that alterations in cell shape may be largely, if not exclusively, responsible for this anatomical change. Specifically, myocyte length and length: width ratio are significantly increased. The increase in myocyte length: width ratio, the cellular analogue of chamber diameter: wall thickness, is clearly maladaptive, since this parameter is normally maintained within a very narrow range. Though cell lengthening appears to be the cause of chamber dilation, stunted or arrested growth of the myocyte transverse area may be the underlying cellular defect. Data from humans and animal experiments suggest that transverse growth may be arrested at a relatively normal level in nonhypertensives with heart failure. In hypertensives, the maladaptive increase in myocyte length may begin after transverse growth reaches an upper limit of approximately 350–400 μm^2. Understanding the molecular basis of maladaptive myocyte growth may lead to newer and more effective therapies in the treatment and prevention of heart failure.

INTRODUCTION

Chronic cardiovascular diseases such as ischemia and hypertension may lead to congestive heart failure. Although there is not general agreement on a comprehensive definition of heart failure, this clinical syndrome is typically characterized anatomically by cardiac hypertrophy and a dilated, relatively thin-walled ventricle [1]. Data from humans and experimental animals with chronic congestive heart failure have demonstrated a clear and consistent alteration in cardiac myocyte shape that appears to be maladaptive [2–5]. Irrespective of the underlying disease process

S. Mochizuki, N. Takeda, M. Nagano and N. Dhalla (eds.). THE ISCHEMIC HEART.

(e.g., chronic ischemia, hypertension, idiopathic dilated cardiomyopathy), ventricular dilation in heart failure is associated with a large increase in cardiac myocyte length due to series addition of sarcomeres [2–5]. The associated changes in myocyte cross-sectional area are not as obvious, though we believe that arrested or inadequate myocyte transverse growth may be an important early event leading to ventricular dilation and heart failure [6]. This chapter will review myocyte shape changes in cardiomegaly of various etiologies and compare myocyte remodeling in ischemic and nonischemic diseases leading to heart failure to determine if any specific alterations in cardiac myocyte shape can be attributed to ischemia. The discussion will focus largely on articles containing comprehensive data on myocyte shape (e.g., volume, length, cross-sectional area or width), since it is difficult to reach meaningful conclusions based on incomplete information (e.g., cell width or cross-sectional area only). This literature deals primarily with data collected from isolated cardiac myocytes, where cell boundaries and cardiac myocyte shape can be readily determined. The most consistent and best-documented approach to assess myocyte shape will be outlined briefly below.

DETERMINATION OF MYOCYTE SHAPE

It has been recognized for some time that myocyte length is difficult to measure from tissue sections due to the stair-step nature of the intercalated disc and the drawback of sampling from a finite plane of section [7,8]. Myocyte cross-sectional area, however, can be collected reliably from sections of whole tissue, provided that appropriate corrections are made for artifacts such as tissue compression, variation in sectioning angle, differences in contractile phase, and tissue processing artifacts [7]. In 1986, we demonstrated an excellent correlation between three methods for measuring myocyte size using whole-sectioned tissue and isolated myocytes [7]. These experiments were successful primarily because all known sources of error with the morphometric methods were eliminated or corrected for the first time. The most time-efficient and objective of these methods involves the measurement of isolated myocyte volume using a Coulter Channelyzer, measurement of cell length using a microscope, and calculation of myocyte cross-sectional area from volume/length. Application of these methods in the assessment of myocyte dimensions has provided a clear and consistent understanding of myocyte remodeling in volume and pressure overload-induced cardiac hypertrophy, cardiac atrophy, and heart failure (reviewed in [6,9]). A major advantage of this approach is that all data can be directly compared. For instance, comparison of data from normal rats, cats, hamsters, guinea pigs, hamsters, ferrets, and humans reported in several studies published over the past ten years indicates that average dimensions of left ventricular myocytes from each of these mammalian species are virtually the same [3,7,10–13]. While other methods may provide useful information, valid comparisons are often limited to experimental groups from the same study. This is particularly true when one makes comparisons of data produced in different laboratories using different techniques.

It should be pointed oute that the length of isolated myocytes can be readily measured using a microscope. This is not necessarily true, however, for myocyte diameter. Myocyte shape is highly variable but generally resembles that of an elliptical cylinder [12]. Since isolated myocytes tend to settle on their flat side when placed on a microscope slide, cell diameter measurements will tend to represent the major cross-sectional diameter. Furthermore, changes in the major and minor transverse diameters have been observed in cardiac hypertrophy and failure [12]. Consequently, one should exercise caution when estimating mean cell diameter by standard microscopy.

The question is often raised whether isolated myocyte preparations may yield a biased sampling of cells. To this author's knowledge, there are no convincing data to support this contention, but there are considerable data indicating that isolated myocytes accurately represent the tissue from which they came. For instance, myocyte size measurements collected from whole-sectioned myocardium and isolated myocytes obtained from animals of a similar size are identical if all known sources of error with the morphometric methods are considered [7]. Mean cell length of intact, undamaged isolated myocytes obtained from animals of a similar size but from cell preparations of variable quality (i.e., the percentage of undamaged rod-shaped cells ranged from 35% to 94%) is the same. Additionally, the percentage of binucleated myocytes, known to be about twice the size of mononucleated myocytes, is not altered in these preparations. Furthermore, we have consistently observed a proportional increase in myocyte volume and heart mass in models of cardiac hypertrophy known to have little or no fibrosis (e.g., physiological hypertrophy, hyperthyroidism, volume overloading due to a large aortocaval fistula) [9,14–17]. Collectively, these data provide convincing evidence that high-quality isolated myocyte preparations provide a sampling of cardiac myocyte size that is representative of the intact hearts from which they came. It is not known, however, if isolated myocyte preparations of poor quality (e.g., below 35% rod cells) provide an accurate sampling. In general,we do not use preparations containing less than approximately 50% undamaged rod cells.

CHANGES IN MYOCYTE SHAPE DURING GROWTH, HYPERTROPHY, AND ATROPHY

Grant et al. [18] and others [19] have indicated that changes in myocyte shape reflect the type of hemodynamic stress imposed during cardiac hypertrophy. Specifically, pressure overloading, which typically produces an increase in systolic wall stress and wall thickness with little or no change in ventricular volume during the compensatory phase of hypertrophy, leads to an increase in myocyte cross-sectional area only. This type of hypertrophy has been termed *concentric.* Alternately, increased volume load leads to a proportionate increase in chamber diameter and wall thickness (termed *eccentric* hypertrophy) that is reflected at the cellular level by an equal increase in myocyte length and diameter. Unfortunately, on the basis of an analysis of the literature published prior to 1985, it is difficult to reach the conclusion that changes in myocyte shape reflect gross anatomic alterations.

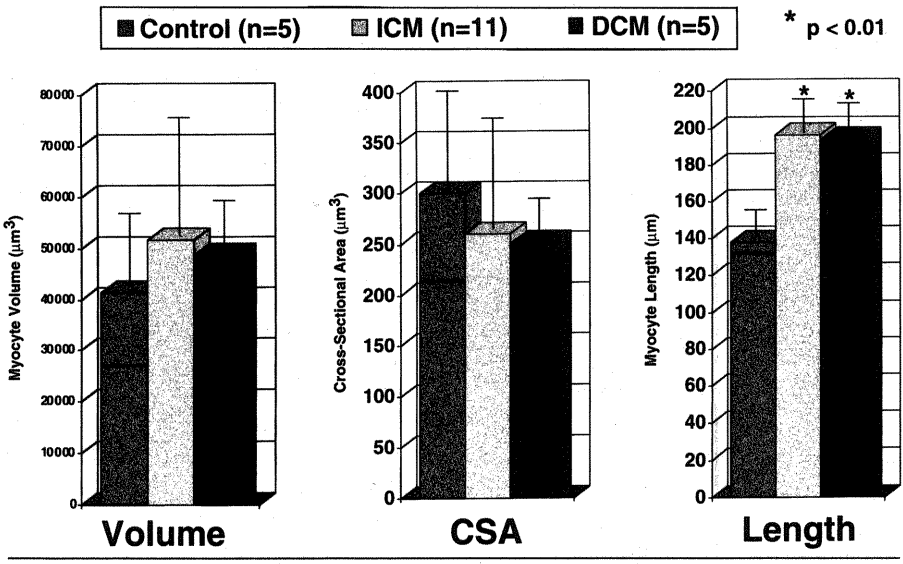

Figure 1. Changes in left ventricular myocyte shape in humans with heart failure due to ischemic cardiomyopathy (ICM) and idiopathic dilated cardiomyopathy (DCM). The control group contains three nonfailing hypertensives and two true controls. CSA: cross-sectional area. Solid horizontal line on control bars indicates mean values for the two true controls.

Over the past few years, alterations in cardiac myocyte shape have been evaluated in many models of hypertrophy using isolated myocytes and the Coulter Channelyzer approach. These studies have provided a clear and consistent picture of patterns of myocyte growth due to various loading conditions. Physiological growth [14], hyperthyroidism [15], or a large aortocaval fistula [16,17] each produce the same type of alteration in myocyte dimensions via increased volume loading, i.e., cell length and diameter increase proportionally. Stated another way, about two thirds of myocyte growth is due to increased cross-sectional area and one third is due to cell lengthening. Compensated hypertrophy due to pressure overload of various etiologies consistently produces an increase in myocyte cross-sectional area only [20–22]. Reduced left ventricular systolic pressure and cardiac atrophy due to hypothyroidism produced a reduction in myocyte cross-sectional area only [23]. Collectively, these data provide strong support for the theory that remodeling of myocyte shape mirrors known alterations in ventricular anatomy due to altered loading conditions. Isolated myocyte data from other labs has also demonstrated that ventricular dilation due to mitral regurgitation and rapid pacing is associated with an increase in myocyte length [24,25].

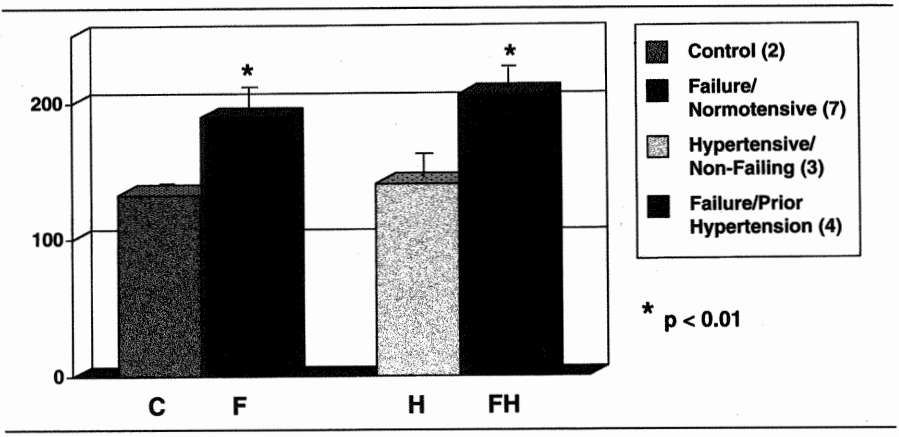

Figure 2. Changes in left ventricular myocyte length are compared between true controls and normotensive ICM patients and between nonfailing hypertensives and failing hypertensive from the ICM group. Values are expressed in μm.

CHANGES IN CARDIAC MYOCYTE SHAPE IN HUMANS WITH HEART FAILURE

Myocyte data were collected from left ventricular tissue obtained from the heart transplant program in Tampa, Florida [3,4]. High-quality isolated myocyte preparations (e.g., approximately 70% rod-shaped myocytes) were obtained from 11 patients with ischemic cardiomyopathy (ICM), five patients with idiopathic dilated cardiomyopathy (DCM), and five unsuitable donors. Of the 11 patients with ICM, seven were normotensive and four had a prior history of hypertension. Two of the unsuitable donors were "true" controls with no prior history of heart disease, while the other three unsuitable donors had a prior history of hypertension. Hearts from each of the unsuitable donors, however, were nondilated and nonfailing. Changes in cardiac myocyte shape in these three groups are summarized in figure 1. Myocyte length was increased significantly in patients with ICM and DCM. This outcome was due to the series addition of new sarcomeres, since sarcomere length was not altered. The evaluation of changes in myocyte cross-sectional area and volume is complicated by the presence of hypertension in some patients with and without failure. In general, however, heart failure due to either ICM or DCM produced a similar increase in myocyte length and the length: width ratio and no significant changes in cell diameter.

Although sample size is low, it is enlightening to examine cell shape data from subpopulations of the ICM and nonfailing groups based on the presence or absence of hypertension (figures 2 and 3). A similar increase in myocyte length is observed in heart failure with or without hypertension (figure 2). In normotensive failing and nonfailing patients, myocyte cross-sectional area is the same (figure 3). Myocyte cross-sectional area is also similar in hypertensive failing and nonfailing patients,

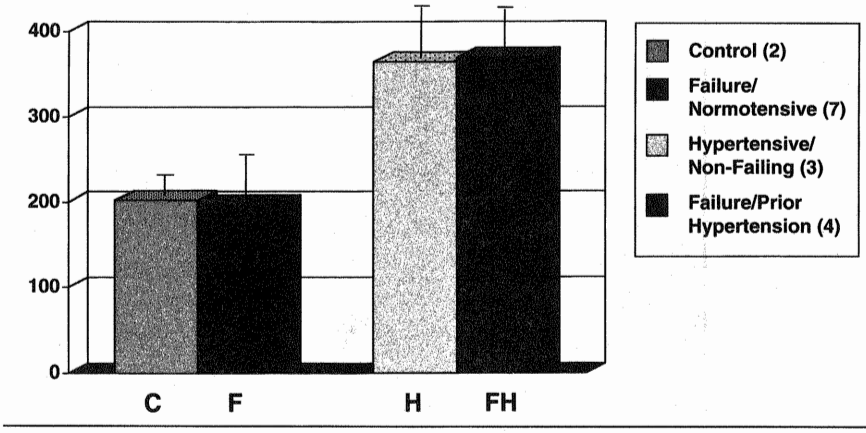

Figure 3. Changes in left ventricular myocyte cross-sectional area are compared between true controls and normotensive ICM patients and between nonfailing hypertensives and failing hypertensives from the ICM group. Values are expressed as μm^2.

although the values are much higher. Since systolic wall stress is likely to be elevated in these patients with heart failure, it appears that a known signal for the induction of myocyte cross-sectional growth is not creating the appropriate response. These data suggest that myocyte cross-sectional growth may become arrested while increased diastolic wall stress continues to cause an increase in myocyte length through series addition of sarcomeres. Since mechanisms for volume expansion are activated in the progression to failure, the process of cell lengthening in the absence of an increase in cell diameter (which would help to normalize wall stress) provides a positive feedback mechanism for additional myocyte lengthening and further deterioration of the chamber diameter: wall thickness ratio, leading to increased wall stress as calculated by the LaPlace equation.

MYOCYTE REMODELING IN ANIMAL MODELS OF HEART FAILURE

Obtaining adequate fresh tissue from human controls is an ongoing problem, although fresh myocardial tissue from humans with congestive heart failure is now readily available through transplant programs. Additionally, it is likely that critical early events that predispose the heart to failure are masked by a multitude of secondary changes that are present in tissues from patients with terminal heart failure. Consequently, there is a need for a relevant animal model of heart failure that will enable comprehensive temporal assessment of cellular and molecular events leading to failure. Transgenic mouse models of heart failure have been developed recently and offer much promise [26]. The small size of the mouse, however, leads to significant limitations in many experiments. The rapid pacing model of heart failure has also been very popular in recent years and offers the advantages of a larger animal model [25]. In this model, however, hearts dilate and fail but do not

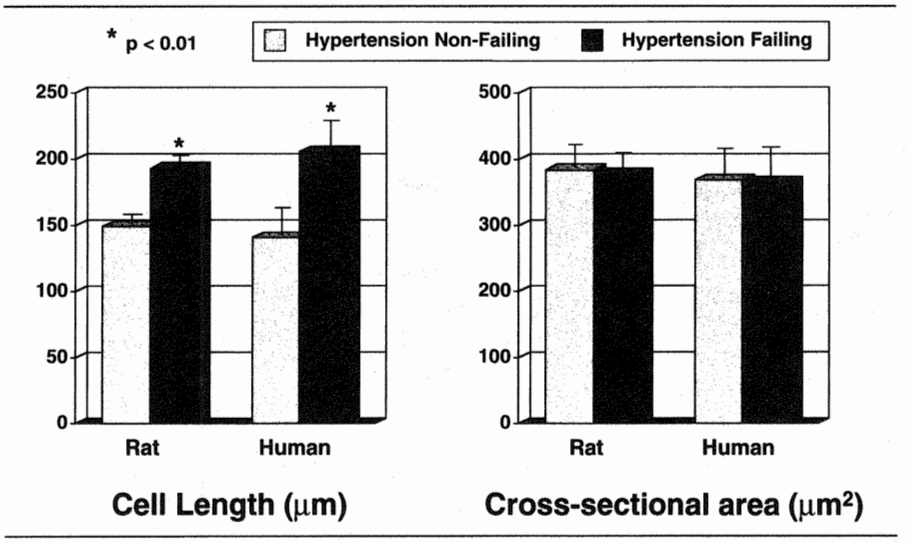

Figure 4. Changes in left ventricular myocyte length and cross-sectional area from hypertensive rats (SHHF) and humans with and without failure.

hypertrophy during the pacing period, while cardiac hypertrophy and improved function characterize the recovery period. Consequently, this model is an unusual one that differs from more common causes of failure that have a period of compensatory hypertrophy followed by ventricular dilation and failure.

Recently, we have been characterizing pathophysiological alterations in the Spontaneously Hypertensive Heart Failure (SHHF) rat [5]. This rat strain is designated SHHF/Mcc-*fa*^{cp} to indicate that the colony is maintained by Dr. McCune at Ohio State and may contain the *fa* and *cp* obesity genes, which are allelic [27]. Though our work has been almost exclusively with lean female SHHF rats to this point, animals homozygous for the *fa*^{cp} gene are obese. All animals, lean or obese, have hypertension and cardiac hypertrophy and eventually develop heart failure. As in the human population, male gender and obesity are significant risk factors that lead to earlier onset of heart failure. Lean females develop heart failure at approximately 24 months of age, while heart failure occurs in fatty males at about 10 months of age. In figure 4, left ventricular myocyte length and cross-sectional area from lean females with heart failure (approximately 24 months of age) and without heart failure (approximately 12 months of age) are compared to similar data from hypertensive patients with failure due to ICM and nonfailing unsuitable donors with hypertension. This increase in myocyte length is almost identical in rats and humans with heart failure. Additionally, myocyte cross-sectional area is elevated to a similar extent in rats and humans with and without failure. These data suggest that the SHHF rat is a valid model for humans with hypertension and heart failure.

Available information indicates that SHHF rats do not develop atherosclerotic lesions typical of the patients in the ICM group discussed above [27]. Thus, it

appears that the maladaptive change in cardiac myocyte shape in hypertension progressing to failure is the same irrespective of the presence (humans) or absence (rats) of ischemia. This conclusion may be hasty, however, since functional blood flow and blood flow reserve have not yet been assessed in the SHHF rat. It is possible that compressive forces due to elevated diastolic wall stress have led to a physiological impairment of blood flow independent of any anatomical lesions. Transmural changes in left ventricular myocyte shape or regional blood flow, however, have not been reported for the SHHF rat. Since the endomyocardium is known to be at greater risk to ischemia than the epimyocardium [28], more extensive maladaptive remodeling of myocyte shape in the endomyocardium would suggest an ischemic component. Additionally, ischemia cannot be excluded based on the absence of atherosclerotic lesions alone, since coronary vasospasms or other factors may cause functional ischemia. Obviously, further work is needed to clarify this point.

It is interesting to note that the highest values for myocyte cross-sectional area observed in our laboratory have consistently been in the 350–400 μm^2 range. This is true for left ventricular myocytes from failing and nonfailing rats and from humans with hypertension. Additionally, we noted a similar value for right ventricular myocytes in SHHF rats after the onset of LV failure [5]. It is possible that this value represents an upper limit for adaptive growth. Clearly, cardiac myocytes cannot continue to enlarge indefinitely. It is a fundamental limitation of cell growth that surface area for diffusion of metabolites and nutrients increases by a factor of radius squared, while cell volume increases by a factor of radius cubed. Surprisingly, cardiac myocytes are among the largest and most highly metabolic cells in the body. While an extremely high vascularization helps to maintain the energy needs of cardiac myocytes, it appears that the development of T tubules may enable cardiac myocytes to maintain a more favorable cell surface-to-volume relationship. Page and McCallister [29] demonstrated that during cardiac hypertrophy due to hyperthyroidism or hypertension, myocyte T-tubular surface area increases disproportionately, enabling myocytes to maintain a stable cell surface-to-volume ratio. The upper limit to this adaptive response, however, is not known at present.

SUMMARY AND FUTURE DIRECTIONS

Ventricular dilation in congestive heart failure is associated with a large increase in cardiac myocyte length. The absence of an appropriate increase in wall thickness, which would help to normalize wall stress, may be due to a stunted or arrested myocyte transverse growth response. A similar increase in the myocyte length: width ratio occurs in both normotensive and hypertensive individuals progressing to failure. Ischemic heart disease alone can lead to ventricular dilation, heart failure, and maladaptive remodeling of cardiac myocyte shape. Myocyte remodeling, however, is similar in patients with heart failure from DCM where coronary arteries are patent. Additionally, remodeling of cardiac myocyte shape in hypertension progressing to failure appears to be similar irrespective of the presence or absence of ischemic heart disease. Consequently, the specific role of chronic ischemia in the

remodeling of cardiac myocyte shape during the progression to heart failure is not clear at this time. On a positive note, however, we do know that cardiac myocytes have the ability to remove sarcomeres in series during the regression of chamber dilation due to hypertrophy [30].

Why is the myocyte cross-sectional area at or near normal in normotensive patients with heart failure? This finding appears to be the case in normotensive patients with either ICM or DCM. Clearly, myocytes have not exhausted their adaptive reserve for transverse growth. Excessive myocyte lengthening appears to be a major cause of ventricular dilation in either normotensive or hypertensive cases of heart failure. Is there a similar, final, common pathway leading to an increased myocyte length: width ratio in normotensive and hypertensive forms of heart failure? Should this maladaptive change in myocyte shape be viewed as excessive myocyte lengthening or as arrested transverse growth?

Finally, little is known about the molecular mechanisms of myocyte shape regulation. It is likely that myocyte cytoskeletal elements and perhaps intermyocyte collagen struts may be involved in the maladaptive change in cardiac myocyte shape associated with failure [31]. Cardiotrophin I, a member of the cytokine family, has been suggested as a candidate gene for myocyte lengthening [32]. Other factors believed to stimulate parallel addition of sarcomeres (e.g., myocyte transverse growth) are believed to work through the G-protein signal transduction pathway [32–34]. Additional work is needed to confirm this in vitro work in animal models and humans. Obviously, identification of specific signal transduction pathways leading to changes in myocyte shape could lead to major advances in the treatment of heart failure.

REFERENCES

1. Tan LB, Al-Timman JK, Marshall P, Cooke GA. 1996. Heart failure: can it be defined? Eur J Clin Pharmacol 49:S11–S18.
2. Zimmer HG, Gerdes AM, Lortet S, Mall G. 1990. Changes in heart function and cardiac cell size in rats with chronic myocardial infarctions. J Mol Cell Cardiol 22:1231–1243.
3. Gerdes AM, Kellerman SE, Moore JA, Clark LC, Reaves PY, Malec KB, Muffly KE, McKeown PP, Schocken DD. 1992. Structural remodeling of cardiac myocytes from patients with chronic ischemic heart disease. Circulation 86:426–430.
4. Gerdes AM, Kellerman SE, Schocken DD. 1995. Implications of cardiomyocyte remodeling in heart dysfunction. In Dhalla NS, Beamish RE, Takeda N, Nagano M (eds), The Failing Heart. New York: Raven Press, pp. 197–205.
5. Gerdes AM, Onodera T, Wang X, McCune SA. 1996. Myocyte remodeling during the progression to failure in rats with hypertension. Hypertension 28:609–614.
6. Gerdes AM, Capasso JM. 1995. Structural remodeling and mechanical dysfunction of cardiac myocytes in heart failure. J Mol Cell Cardiol 27:849–856.
7. Gerdes AM, Moore JA, Hines JM, Kirkland PA, Bishop SP. 1986. Regional differences in myocyte size in normal rat heart. Anat Rec 215:420–426.
8. Hatt P, Rakusan K, Gastineau P, LaPlace M, Cluzeaud F. 1979. Morphometry and ultrastructure of heart hypertrophy induced by chronic volume overload (aorto-caval fistula in the rat). J Mol Cell Cardiol 11:989–998.
9. Gerdes AM. 1992. The use of isolated myocytes to evaluate myocardial remodeling. Trends Cardiovasc Med 2:152–155.
10. Campbell SE, Gerdes AM, Smith TB. 1987. Comparison of regional differences in cardiac myocyte dimensions in rats, hamsters, and guinea pigs. Anat Rec 219:53–59.

11. Kozlovskis PL, Gerdes AM, Smets M, Moore JA, Koch G, Bassett AL, Myerburg RJ. 1991. Regional increase in myocyte volume after healing of myocardial infarction in cats. J Mol Cell Cardiol 23:1459–1466.
12. Gerdes AM, Kellerman SE, Malec KB, Schocken DD. 1994. Transverse shape characteristics of cardiac myocytes from rats and humans. Cardioscience 5:31–36.
13. Smith SH, Bishop SP. 1985. Regional myocyte size in compensated right ventricular hypertrophy in the ferret. J Mol Cell Cardiol 17:1005–1011.
14. Bai S, Campbell SE, Moore JA, Morales MC, Gerdes AM. 1990. Influence of aging, growth, and sex on cardiac myocyte size and number. Anat Rec 226:207–212.
15. Gerdes AM, Moore JA, Hines JM. 1987. Regional changes in myocyte size and number in propranolol-treated hyperthyroid rats. Lab Invest 57:708–713.
16. Liu Z, Hilbelink DR, Crockett WB, Gerdes AM. 1991. Regional changes in hemodynamics and cardiac myocyte size in rats with aortocaval fistulas. I. Developing and established hypertrophy. Circ Res 69:52–58.
17. Liu Z, Hilbelink DR, Gerdes AM. 1991. Regional changes in hemodynamics and cardiac myocyte size in rats with aortocaval fistulas. II. Long-term effects. Circ Res 69:59–65.
18. Grant C, Greene DG, Bunnell IL. 1965. Left ventricular enlargement and hypertrophy: a clinical and angiocardiographic study. Am J Med 39:895–904.
19. Grossman W, Jones D, McLaurin LP. 1975. Wall stress and patterns of hypertrophy in the human left ventricle. J Clin Invest 56:56–64.
20. Werchan PM, Gregory TJ, Summer WR, Gerdes AM, McDonough KH. 1989. Right ventricular performance following monocrotaline induced pulmonary hypertension. Am J Physiol 256:H1328–H1336.
21. Zierhut W, Zimmer HG, Gerdes AM. 1990. Influence of Ramipril on right ventricular hypertrophy induced by pulmonary artery stenosis in rats. J Cardiovasc Pharmacol 16:480–486.
22. Zierhut W, Zimmer HG, Gerdes AM. 1991. Effect of angiotensin converting enzyme inhibition on pressure-induced left ventricular hypertrophy in rats. Circ Res 69:609–617.
23. Liu Z, Gerdes AM. 1990. Influence of hypothyroidism and its reversal on hemodynamics and cardiac myocyte size in adult rats. J Mol Cell Cardiol 22:1339–1348.
24. Spinale FG, Ishihra K, Zile M, DeFryte G, Crawford FA, Carabello BA. 1993. Structural basis for changes in left ventricular function and geometry because of chronic mitral regurgitation and after correction of volume overload. J Thorac Cardiovasc Surg 106:1147–1157.
25. Spinale FG, Crawford FA Jr, Hewett KW, Carabello BA. 1991. Ventricular failure and cellular remodeling with chronic supraventricular tachycardia. J Thorac Cardiovasc Surg 102:874–882.
26. Chien KR. 1995. Cardiac muscle diseases in genetically engineered mice: evolution of molecular physiology. Am J Physiol 269:H755–H766.
27. McCune SA, Park S, Radin MJ, Jurin RR. 1995. The SHHF/Mcc-fa^{cp} rat model: a genetic model of congestive heart failure. In Singal PK, Beamish RE, Dhalla NS (eds), Subcellular Basis and Therapy of Heart Failure. Boston: Kluwer Academic Publishers, pp. 91–106.
28. Bache RJ, Vrobel TR, Ring WS, Emery RW, Anderson RW. 1981. Regional myocardial blood flow during exercise in dogs with chronic left ventricular hypertrophy. Circ Res 48:76–87.
29. Page E, McCallister LP. 1973. Quantitative electron microscopic description of heart muscle cells. Am J Cardiol 31:172–181.
30. Gerdes AM, Clark LC, Capasso JM. 1995. Regression of cardiac hypertrophy after closing an aortocaval fistula in rats. Am J Physiol 268:H2345–H2351.
31. Terracio L, Borg TK. 1988. Factors affecting cardiac myocyte shape. Heart Failure 4:114–124.
32. Wollert KC, Taga T, Saito M, Narazaki M, Kishimoto T, Glembotski CC, Vernallis AB, Heath JK, Pennica K, Wood WI, Chien KR. 1996. Cardiotrophin-1 activates a distinct form of cardiac muscle cell hypertrophy. J Biol Chem 271:9535–9545.
33. Lee HR, Henderson SA, Reynolds R, Dunnmon P, Yuan D, Chien KR. 1988. α_1-Adrenergic stimulation of cardiac gene transcription in neonatal rat myocardial cells. J Biol Chem 263:7352–7358.
34. Sadoshima J, Izumo S. 1993. Molecular characterization of Angiotensin II-induced hypertrophy of cardiac myocytes and hyperplasia of cardiac fibroblasts. Circ Res 73:413–423.

HIBERNATING MYOCARDIUM

ROBERTO FERRARI

Universita' degli Studi di Brescia

Summary. Left ventricular dysfunction is in most cases the consequence of myocardial ischemia. It may occur transiently during an attack of angina, and it is usually reversible. It may persist over hours or even days in patients after an episode of ischemia followed by reperfusion, leading to the condition known as *stunning*.

In patients with persistent limitation of coronary flow, left ventricular dysfunction may be present over months and years or indefinitely in subjects with fibrosis, scar formation, and remodeling after myocardial infarction. Chronic left ventricular dysfunction, however, does not mean permanent or irreversible cell damage. Hypoperfused myocytes can remain viable but akinetic. This type of dysfunction has been called *hibernating myocardium*.

Unfortunately, left ventricular dysfunction might also result from irreversible damage, leading to remodeling and heart failure.

The dysfunction due to hibernation can be partially or completely restored to normal by reperfusion. Thus, it is important to clinically recognize the hibernating myocardium.

In this chapter, we evaluate stunning, hibernation, and remodeling with respect to clinical decision making and, where possible, we refer to our own ongoing clinical experience.

INTRODUCTION

The differentiation of viable from nonviable myocardium in patients with coronary artery disease and left ventricular dysfunction is an issue of clinical relevance in this age of myocardial revascularization.

Impaired left ventricular function may occur transiently during an attack of angina and is usually reversible. It may persist over hours or even days in patients after an episode of ischemia followed by reperfusion, leading to the condition known as

S. Mochizuki, N. Takeda, M. Nagano and N. Dhalla (eds.). THE ISCHEMIC HEART.

stunning. In patients with persistent limitation of coronary flow, left ventricular dysfunction may be present over months or years, or indefinitely in subjects with fibrosis, scar formation, and remodeling after myocardial infarction. Severe ventricular dysfunction leads to the syndrome of heart failure, which is a progressive condition in which further damage to the heart may occur from increased afterload, fluid retention, and remodeling. However, chronic left ventricular dysfunction does not necessarily mean permanent or irreversible cell damage. Hypoperfused myocytes can remain viable but akinetic. This type of dysfunction has been called *hibernating myocardium* [1].

Thus, reversible dysfunction occurring in particular clinical circumstances and in selected experimental models has been named *stunning* and *hibernation*. These shortened terms are useful and help one understand the concept, but they may also give rise to confusion. Although in this chapter we will discuss hibernating myocardium, to avoid confusion it is essential to provide a clear definition of these terms.

VENTRICULAR DYSFUNCTION DUE TO MYOCARDIAL STUNNING

Stunning defines a transient left ventricular dysfunction that persists after reperfusion, despite the absence of irreversible damage and despite restoration of normal or near normal coronary flow [2]. This definition implies that 1) stunning is a transient, fully reversible abnormality, provided that sufficient time is allowed for recovery; 2) stunning is a mild, sublethal injury that must be kept apart from the irreversible damage occurring in myocardial infarction; and 3) stunned myocardium has a normal or near normal coronary flow. Thus, the hallmark of this condition is the presence of a flow–function *mismatch*, with normal flow but abnormal function. This condition is quite in contrast to the other forms of reversible myocardial dysfunction, such as ischemia and hibernation, in which depressed flow and function are matched.

A clear definition is certainly desirable and important, but its application to the clinical condition is often problematic. Diagnosis of stunning in patients would require demonstration of two major points: 1) the contractile abnormality is reversible with time; and 2) the dysfunctional myocardium has normal or near normal coronary flow [2]. This implies that it is possible to accurately measure regional myocardial function and blood flow in humans. The resolution of the available techniques (contrast ventriculography, radionuclide angiography, two-dimensional echocardiography, positron emission tomography), however, is not comparable to that obtainable with sonomicrometry and radioactive microspheres in experimental animals.

To fulfill the second point, the physician should allow sufficient time for the myocardium to recover before he or she makes a definitive diagnosis of stunning. This time requirement, in turn, suggests that, in general, myocardial stunning is a well-tolerated condition and that its diagnosis is important retrospectively for the better appreciation of the effects of reperfusion. But it does not imply a decision-making process for clinical management of the patient, basically because the myo-

cardium is already reperfused. It could be argued that in some high-risk situations, stunning can become dangerous. Therefore, stunning should be recognized and treated with positive inotropic interventions and/or agents that increase preload or decrease afterload [2]. Dramatic cases illustrating this point have been reported recently [3–5]. In clinical practice, stunning is dangerous when the degree and the extent of the left ventricular dysfunction is associated with a low-output syndrome. Under these circumstances, however, therapy with inotropic- and afterload-reducing agents is a common approach, independent of the diagnosis of stunning. Surgeons were probably aware of this phenomenon long before the definition of stunning, because they often successfully used calcium or positive inotropic agents to stimulate those hearts that were having difficulty recovering after reperfusion.

It has been suggested that recognition of stunning may be important in high-risk conditions (such as thrombolysis after acute myocardial infarction and reperfusion after cardiac surgery or transplantation) because the physician or the surgeon could try to prevent this condition from occurring [2]. Experimentally, stunning can be prevented by calcium antagonists administered before ischemia or by antioxidants given just before reflow [6]. At present, no controlled clinical data on the efficacy of these therapies are available. It is also essential to identify the high-risk conditions that need to be treated, in order to avoid unnecessary therapy in a vast population for the benefit of a few patients.

VENTRICULAR DYSFUNCTION DUE TO HIBERNATION

Hibernation presents itself as chronic left ventricular regional dysfunction. This condition arises from prolonged myocardial hypoperfusion in which myocytes remain viable but contraction is depressed. The dysfunction can be partially or completely restored to normal if the myocardial oxygen supply is favorably altered by improving blood flow with reperfusion and/or by reducing demand [1]. On imaging the heart, presents areas of left ventricular wall that may be hypokinetic, akinetic, or dyskinetic.

This definition implies that hibernation 1) is a chronic, reversible abnormality, provided that coronary flow is restored (in the case of ischemic heart disease) or that oxygen demand is reduced (in the case of chronic left ventricular overload); 2) represents a viable myocardium, showing residual contractile and coronary flow reserve that must be distinguished from the irreversibly damaged tissue present after myocardial infarction; and 3) has a moderately reduced coronary flow. Thus, the hallmark of this condition is a *matching* reduction in both flow and function.

The diagnosis of hibernation is clinically relevant because it has therapeutic implications, particularly in patients with coronary artery disease. In such patients, differentiation of viable from nonviable myocardium is important, since regional and global left ventricular function due to hibernation will improve after revascularization. This outcome is associated with improved survival [7].

If follows that the true clinical goal standard for hibernation is the improvement in systolic function of dysfunctional myocardial segments after revascularization.

Such a retrospective standard is, however, insufficient. An accurate prospective diagnosis of patients with potentially reversible left ventricular dysfunction is essential for the identification of ideal candidates for revascularization procedures. Thus, the hibernating myocardium poses a series of clinical and physiopathological issues. Clinically, the two fundamental issues are 1) how and with what accuracy this entity can be recogized and 2) how it should be best treated. From the physiopathological point of view, the most important issues are 1) which molecular mechanisms are involved in hibernation and 2) whether chronic ischemia exists.

PATHOPHYSIOLOGY OF HIBERNATION

The molecular factors responsible for hibernation and for the chronically depressed contractile function have not yet been defined. The hypothesized mechanism of a downregulated contractile performance matching the reduced energy supply is, in part, supported by experimental and clinical studies using positron emission tomography (PET). As in acute ischemia, during prolonged underperfusion, metabolism is shifted to predominant glucose utilization, with recruitment of glycolysis, in man, a mismatch of flow and glucose metabolism predicts recovery of mechanical function after revascularization. There are few data to support or disprove this theory of a perfect balance between reduced oxygen supply and contractile function so that myocardial injury is prevented [8], basically because there are neither adequate animal models for chronic persistent ischemia nor any clinical studies showing whether hibernating myocardium is truly a chronic condition.

If this mechanism were the only one responsible for hibernation, this condition should occur in every patient with reduction of coronary flow. Obviously, this is not the case. In addition, in clinical practice, hibernation is often present in patients with a history of acute ischemia, such as infarction or prolonged angina pain. This finding complicates not only the distinction between viable and nonviable myocardium but also the understanding of the pathophysiological mechanism underlying hibernation.

Different hypotheses have been suggested for the factor responsible for downregulation of contraction during hibernation. An early theory suggests that decrement in coronary perfusion pressure reduces sarcomere length because of distension in the adjacent coronary microvasculature; therefore, the extent of the contraction would be reduced by the Frank Starling mechanism. Several lines of evidence argue against this suggestion. Another theory considers that a reduction of energy stores might cause downregulation of contraction. ^{31}P-NMR studies in live animals, however, suggest that net ATP and CP stores are not depleted unless coronary flow is reduced to very low levels. Furthermore, it has been shown that in hibernating myocardium, ATP levels are normal [9].

We suggest that changes in intracellular pH, phosphate (Pi), and the myocardial NAD:NADH ratio are responsible for contractile and possibly metabolic downregulation in short-term hibernation in the experimental setting [10,11]. To mimic the clinical events, we used a model of short acute ischemia followed by

prolonged severe low-flow reperfusion (10% of initial coronary flow). Acute ischemia caused a drop of pH, an increase of Pi, a reduction of the NAD:NADH ratio, a 50% reduction in tissue content of ATP, and complete mechanical quiescence. Low-flow reperfusion was unable to restore normal pH, Pi, NAD:NADH ratio, and contraction. On the contrary, it resulted in a prolonged downregulation of myocardial contractility in the presence of aerobic metabolism, as demonstrated by the absence of lactate and CPK release, maintenance of mitochondrial function, and full recovery of tissue stores of ATP and CP. Reperfusion after as much as 4–6 hours of ischemia caused a near complete recovery of mechanical function. Most likely, the factors controlling contractile performance would then also be the factors regulating metabolic respiration. The primary regulators of respiration (PO_2, pH, Pi, cytosolic adenine nucleotides, and NAD^+) may all be involved, and their relative importance in regulating contraction and respiration is still a matter of discussion.

Doubts exist whether this new metabolic state (hibernation) should be considered a true ischemic condition. In strict terms, ischemia is a condition that exists when fractional uptake of oxygen is not sufficient to meet the rate of mitochondria oxidation, which, in the heart, is largely determined by the mechanical or physical activity of the myocytes [10]. It is likely that in hibernating myocardium, the residual flow is able to deliver enough oxygen to meet the reduced rate of mitochondrial oxidation. This concept will explain why the hibernating myocardium does not produce lactate (a typical marker of ischemia) and shows indirect signs of some metabolic activity. It also explains the full recovery after reperfusion and the retention of a contractile reserve. Thus, hibernation is not a state of chronic ischemia but instead represents a new metabolic state that is consequent to an ischemic condition but that is not actually ischemic. In strictly molecular terms, hibernation represents a chronic hypoperfusion of akinetic but aerobic myocytes.

A difficult concept to conceive, in clinical terms, is how the aforediscussed mechanisms or other, unknown ones could provide an exact balance between energy demand and supply for months to years. This outcome would probably require subcellular adaptative changes to occur, which are at present under investigation using a molecular biology approach to this fascinating problem.

ASSESSMENT OF REGIONAL LEFT VENTRICULAR VIABILITY AND CONTRACTILE RESERVE IN HIBERNATING MYOCARDIUM

In the past, viable myocardium was identified by coronary artery patency and preserved regional function. However, the inadequacy of an occluded coronary artery to predict nonviable myocardium in the presence of collateral circulation was soon recognized. Conversely, a patent coronary artery after thrombolysis is insufficient evidence that the dysfunctional myocardium perfused by this artery is viable.

Today, a number of methods are available to assess viability and contractile reserve in regions with hypokinetic or akinetic wall motion. These include cardiac imaging techniques that evaluate myocardial viability on the basis of myocardial

perfusion, cell membrane integrity, and metabolic activity and the infusion of a low-dose positive inotropic agent during echocardiography to evaluate contractile reserve.

These methods provide greater precision in the assessment of hibernation than can be achieved by analysis of coronary anatomy, regional function, or specific electrocardiographic changes. We will briefly review the values of the three most important techniques to assess hibernation. We will not address the single limits and advantages, nor the comparison of the results obtained by each technique, all of which have recently been discussed in detail elsewhere [12].

PET provides the capacity to quantitate regional blood flow noninvasively and to assess regional metabolic activity independent of flow. In addition, PET provides enhanced image resolution and routine correction for body attenuation. In this way, it overcomes the two major limitations of thallium imaging: poor resolution and photon attenuation.

Viable myocardium is identified by PET on the basis of enhanced or preserved metabolic activity in underperfused and dysfunctional myocardial regions. Usually, the metabolic shift from FFA to glucose is a marker of myocardial ischemia. These metabolic changes, however, may not apply to hibernating myocardium, in which a new state of perfusion–contraction coupling is achieved in the absence of ischemia. 18-F-fluorodeoxyglucose (FDG) has emerged as a marker of regional exogenous glucose utilization in hypoperfused regions. FDG is a glucose analogue that undergoes the same transport and phosphorylation of glucose but does not enter glycolysis or glycogen synthesis. An increase of FDG uptake in regions with reduced perfusion, the so-called *FDG–blood flow mismatch*, provides a metabolic signal for identifying viable myocardium.

Thallium myocardial imaging is an established and clinically important method to assess perfusion and sarcolemmal integrity and hence to detect myocardial viability. Regional thallium activity on redistribution images acquired either early (3–4 hours) or late (8–72 hours) after stress is commonly used to demonstrate the distribution of viable myocardial cells and the extent of myocardial fibrosis. Rest–redistribution is also successfully used to distinguish viable from nonviable myocardium. To this end, more recently, thallium reinjection after stress-redistribution imaging has also been proposed. All these protocols have advantages and disadvantages. Different opinions exist on which protocol should be used for the detection of hibernating myocardium. This decision obviously depends on the underlying clinical question and on the meaning of the term *hibernation*. In our experience, the clinical question in a patient with left ventricular dysfunction possibly due to hibernation is one of viability and not of inducible ischemia. Therefore, we use rest-redistribution thallium imaging to discriminate viable from nonviable myocardium [13].

Low-dose dobutamine infusion to enhance regional systolic contraction during two-dimensional echocardiography has been successfully used to identify viable versus necrotic myocardium during the first week following successful thrombolysis. Thus, this technique is able to unmask contractile reserve in stunned myocardium in which coronary flow has been restored. In patients with hibernating myocardium,

with reduction of coronary blood flow severe enough to produce sustained regional contractile dysfunction, the administration of a positive inotropic agent has been hampered by the risk of increasing myocardial demand in the setting of exhausted coronary flow reserve, thereby producing myocardial ischemia and persistent regional dysfunction. Despite this limitation, recent data suggest that low-dose dobutamine echocardiography is a safe and accurate method for assessing hibernating myocardium [14]. We have evaluated its role in identifying hibernation in 33 CAD patients with a positive thallium rest–redistribution test and persistent left ventricular dysfunction [15]. Reversible dysfunction was identified by functional improvement of akinetic areas immediately after surgical revascularization, detected by intraoperative epicardial echocardiography and both two weeks and three months later by means of transthoracic echocardiography. Infusion of dobutamine predicted reversible dysfunction in 178 of the 205 akinetic segments that recovered after surgery, with a sensitivity of 86.8% and identified 89 of the 109 segments that failed to recover, with a specificity of 81.6%.

In our study, echodobutamine predicted the immediate functional recovery after revascularization with higher accuracy than thallium rest redistribution. In contrast, scintigraphic imaging was better correlated than echodobutamine with long-term recovery of function [13]. This discrepancy stresses that the two tests have different clinical significance, since they explore two different aspects of the same issue: viability and contractile reserve of the akinetic myocytes. We believe that demonstration of viability provides the ultimate rationale for revascularization. Presence of contractile reserve provides information on the overall operative risk, thus overriding the additional concept that the global systolic ejection fraction is a crucial determinant of surgical risk. The global ejection fraction, in fact, can be related to different physiopathological mechanisms.

CLINICAL MANAGEMENT OF THE PATIENT WITH HIBERNATING MYOCARDIUM

The knowledge that a large portion of dysfunctional myocardium is viable rather than fibrotic is essential for the correct clinical management of the patient, since this knowledge justifies a revascularization procedure despite the presence of left ventricular dysfunction, often of severe entity.

In a decision-making process, however, it is our conviction that several steps should be fullfilled before myocardial revascularization is recommended. First, the symptomatic status of the patient is important. This status should not be limited to the presence of angina pectoris or of inducible ischemia but should also include the presence of signs of heart failure in the absence of other symptoms. Second, the coronary anatomy has to be suitable for revascularization either by open-heart surgery or angioplasty. Third, the extension and severity of the ventricular dysfunction has to justify an interventional procedure, the risk of which is not negligible. Fourth, the demonstration of viable myocardium by one or more of the possible imaging modalities is essential, particularly to predict long-term recovery after revascularization. Fifth, the demonstration of a contractile reserve by low-dose

dobutamine echocardiography is also important, since it confirms viability and provides further information on the surgical risk.

The available data suggest that when these criteria are all fulfilled, an improvement in ventricular function occurs after revascularization and translates into improved prognosis, confirming the concept that ventricular function is a critically important determinant of prognosis in coronary artery disease.

Revascularization of patients with end-stage ischemic cardiomyopathy and clinical manifestation of congestive heart failure rather than angina may also be considered an alternative to transplantation. Data regarding this possibility are scanty. In our study, one third of patients had dyspnea as the only symptom, a moderate to severe reduction of ejection fraction, and some of these patients were potential candidates for transplantation [15]. If we examine the existing literature on revascularization of severe ischemic cardiomyopathies and pool together the data, it seems that the perioperative mortality rate is between 15% and 20%, with 72%–75% survival at three years. There is a clear improvement of symptoms and of global ejection fraction. Demonstration of viability, however, is essential for a positive outcome. It is these cases, in which the differentiation of viable from nonviable myocardium and the stratification of operative risk are the overriding clinical concerns, that will justify further investigation in this fascinating field and that, hopefully, will improve our therapeutic possibilities.

ACKNOWLEDGMENT

This work was supported by the National Research Council (C.N.R) target project, "Prevention and Control Disease Factors" n. 91.00156 PF 41, and by a CNR target project, "Biotechnology and Bioinstrumentation." The authors thank Miss Roberta Bonetti for secretarial assistance in preparing the manuscript.

REFERENCES

1. Rahimtoola S. 1989. The hibernating myocardium. Am Heart J 117:211–221.
2. Bolli R. 1993. Myocardial stunning in man. Circulation 86:1671–1691.
3. Takahashi A, Ono Y, Shishido F, Uemura K, Kadowaki K, Kumagai T. 1990. PET evaluations of ischemic heart disease showing transient ST-T elevation: report of two cases. J Cardiol 20:241–248.
4. Kobayashi T, Imagawa H, Satoh H, Yoshino T, Fudemoto Y, Matsuwaka R. 1991. Biventricular assist support using centrifugal pump in cardiogenic shock following coronary bypass grafting: a case report of long survival. J Jpn Assoc Thorac Surg 39:924–929.
5. Shahian DM, St Ledger S, Kimmell W, Bogosian M, Abraham W, Johnson ME. 1990. Successful recovery of postischemic stunned myocardium using centrifugal left ventricular assist. J Cardiothorac Anesth 4:84–88.
6. Bolli R. 1990. Mechanism of myocardial "stunning." Circulation 82:723–738.
7. Eitzman D, Al-Aouar Z, Kanter HL, vom Dahl J, Kirsh M, Deeb GM, Schwaiger M. 1992. Clinical outcome of patients with advanced coronary artery disease after viability studies with positron emission tomography. J Am Coll Cardiol 20:559–565.
8. Ross J Jr. 1991. Myocardial perfusion–contraction matching: implications for coronary heart disease and hibernation. Circulation 83:1076–1082.
9. Schultz R, Guth BD, Pieper K, Martin C, Heusch G. 1992. Recruitment of an inotropic reserve in moderately ischemic myocardium at the expense of metabolic recovery: a model of short-term hibernation. Circ Res 70:1282–1295.
10. Ferrari R, Visioli O. 1991. Stunning: damaging or protective to the myocardium? Cardiovasc Drugs Ther 5:939–946.

11. Ferrari R, Cargnoni A, Curello S, Ceconi C, Volpini M, Visioli O. 1993. Metabolic adaptation of underperfused isolated rabbit heart: an insight into molecular mechanisms underlying hibernation. Circulation 88(4):1004.
12. Dilsizian V, Bonow R. 1993. Current diagnostic techniques of assessing myocardial viability in patients with hibernating and stunned myocardium. Circulation 87:1–20.
13. Giubbini R, Alfieri O, Ferrari R, Milan E, Rossini P, Lorusso R, Berra P, La Canna G. 1993. Thallium rest-redistribution and echo-dobutamine tests to predict functional improvement after bypass surgery in patients with left ventricular dysfunction. Circulation 88(4):2883.
14. Cigarroa CG, De Filippi CR, Brickner ME, Alvarez LG, Wait MA, Grayburn PA. 1993. Dobutamine stress echocardiography identifies hibernating myocardium and predicts recovery of left ventricular function after coronary revascularization. Circulation 88:430–436.
15. La Canna G, Alfieri O, Giubbini R, Gargano M, Ferrari R, Visioli O. 1994. Echocardiography during infusion of dobutamine for identification of reversible dysfunction in patients with chronic coronary artery disease. J Am Coll Cardiol 23:617–626.

This Page Intentionally Left Blank

LENGTH-DEPENDENT MODULATION OF CARDIAC MUSCLE CONTRACTILITY IN NORMOXIA, HYPOXIA, AND ACIDOSIS: POSSIBLE IMPLICATIONS FOR ISCHEMIA

KENICHI HONGO*, ED WHITE**, and CLIVE H. ORCHARD**

* *The Jikei University School of Medicine*

** *University of Leeds*

Summary. The results discussed in this chapter suggest that the stretch-dependent increase in cardiac contraction is inhibited during hypoxia and modulated during acidosis. In ischemia, both hypoxia and acidosis occur simultaneously, so the length-dependent changes in cardiac contractility during ischemia would be a function of the changes in both conditions. The increase in cardiac contractility observed following muscle stretch might be inhibited during ischemia, possibly by altered Ca^{2+} handling and a decreased Ca^{2+}sensitivity of the myofilaments. Thus, the contractile changes in the response to stretch observed in the present study during hypoxia and acidosis may modulate the contractile response of cardiac muscle to ischemia.

INTRODUCTION

The length-dependent control of cardiac contractility is known as the Frank-Starling law of the heart. An increase in diastolic filling produces more cardiac output and a decrease in diastolic filling causes less output. Until now, many investigators have tried to clarify the basic cellular mechanisms of this important phenomenon [1]. During ischemia, the contractile function of the heart is known to decrease. This decrease in contraction is due to failure of the action potential [2,3], intracellular acidosis [4,5], altered intracellular calcium handling [6,7], and the accumulation of metabolites [4]. Ischemic cardiac muscle may also contract under different mechanical conditions from normal tissue; weakly contracting ischemic muscle could be stretched and thus paradoxically lengthened by surrounding healthy tissue during contraction, so the length-dependent mechanism may offset the decrease in contrac-

S. Mochizuki, N. Takeda, M. Nagano and N. Dhalla (eds.). THE ISCHEMIC HEART.

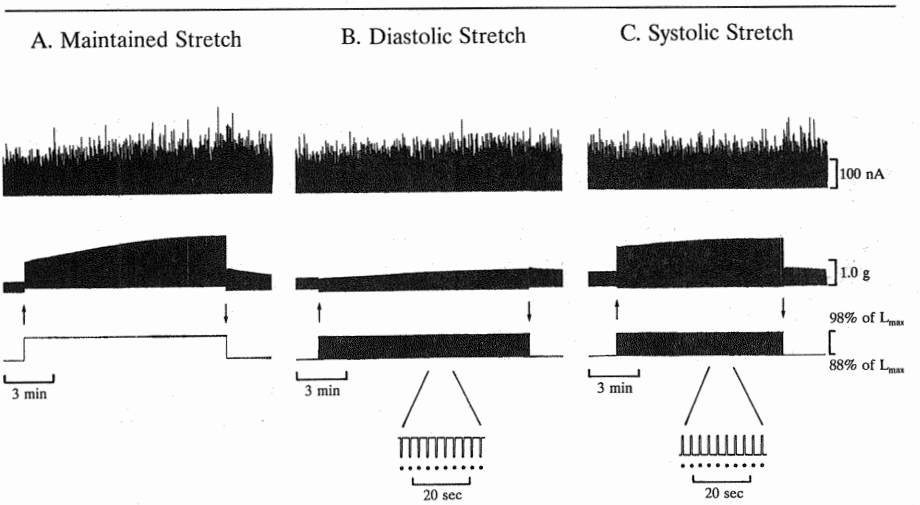

Figure 1. Effect of stretch on the Ca^{2+} transient and tension during normoxia: slow time base signals of the Ca^{2+} transient (upper traces), tension (middle traces), and muscle length (lower traces). (**A**) Maintained stretch. At the time indicated by an upward arrow, the muscle was stretched from 90% of L_{max} to L_{max} and was maintained at the longer length until tension reached a steady state. The muscle was released at the time indicated by a downward arrow. (**B**) Diastolic stretch. Muscle was stretched from 90% of L_{max} to L_{max} at the time only between contractions (diastolic period). Inset shows a faster time base trace of muscle length and the timing of electrical stimulations (•). For details, see text. (**C**) Systolic stretch. Muscle was stretched only the period during contraction (systolic period). Inset shows a faster time base trace of muscle length and the timing of electrical stimulations (•). For details, see test. Reproduced from Hongo et al. [11] with the permission of the American Physiological Society.

tion during ischemia. Despite the potential importance of length-dependent changes in cardiac muscle contractility during ischemia, there has been no study to investigate this issue. In this chapter, we investigate the length-dependent modulation of cardiac muscle contractility during hypoxia and acidosis, because these two conditions are known to be important in the response of the cardiac muscle contractility to ischemia [6,8,9].

METHODS

Thin papillary muscles were dissected from the right ventricle of ferret hearts and were mounted between a fixed hook and a lever system to monitor isometric tension and to change the length of the preparation. To measure the intracellular calcium concentration, aequorin was microinjected into the superficial cells of the preparation, and the photoluminescence of aequorin was monitored using a photomultiplier [10]. The preparation was superfused with bicarbonate Tyrode solution (composition in mmol/L: Na^+, 135; K^+, 5; Mg^{2+}, 1; Cl^-, 102; HCO_3^-, 20; HPO_4^{2-}, 1; SO_4^{2-}, 1; acetate, 20; glucose, 10; Ca^{2+}, 2; insulin, 5 U/L; equilibrated with 5% CO_2 + 95% O_2 to pH = 7.35 at 37°C). The preparation was electrically

stimulated with platinum electrodes, and the muscle length was adjusted to 90% of L_{max} (the length that produces maximal twitch tension). The preparation was then stretched to L_{max} in three different ways as follows [11]. In the *maintained stretch* protocol, the muscle was stretched from 90% of L_{max} to L_{max} and was maintained at this length until the tension reached a steady state (figure 1A). In the *diastolic stretch* protocol, the muscle was stretched only during the period between contractions (figure 1B). This protocol held the muscle at the greater length for 83% of each cycle (2.5 seconds in each 3-second interval). In the *systolic stretch* protocol, the muscle was stretched during the period of contraction (figure 1C) so that the muscle was held at the greater length for 17% of each cycle (0.5 seconds in each 3-second interval). To compare the relative changes in tension and the Ca^{2+} transient during these protocols, the magnitude of the changes in these signals during the stretch (slow phase; see below) were calculated as $[(X_s - X_1)/X_1] \times 100\%$, where X_s is the tension or the Ca^{2+} transient at the steady state after stretch and X_1 is the signal one minute after the stretch. Statistical analysis was made using a paired *t*-test. The averaged values were expressed as mean ± SEM.

RESULTS AND DISCUSSION

The effect of length changes on cardiac muscle contraction and the Ca^{2+} transient during normoxia

During maintained stretch, tension increased immediately after muscle stretch. This immediate increase in tension was followed by a slow increase in tension and in the Ca^{2+} transient over several minutes (figure 1A). During diastolic stretch, there was no immediate increase in tension; however, a slow increase in tension and in the Ca^{2+} transient was observed (figure 1B). During systolic stretch, there was an immediate increase in tension that was followed by a small, slow increase in tension and in the Ca^{2+} transient (figure 1C). During the immediate increase in contraction (maintained stretch and systolic stretch), the time course of contraction prolonged while the time course of the Ca^{2+} transient shortened, suggesting an increase in the affinity of calcium to the contractile element [10]. During the slow increase in contraction, the time courses of contraction and the Ca^{2+} transient were essentially unchanged, which suggests little change in the affinity of calcium to the myofilament. The amplitude of the Ca^{2+} transient was unaltered with the immediate increase in contraction (maintained stretch and systolic stretch); however, the slow increase in contraction was accompanied by a slow increase in the amplitude of the Ca^{2+} transient [10,12]. The relative slow changes in tension and in the Ca^{2+} transient were dependent on the type of stretch; the biggest occurred during maintained stretch and the smallest during systolic stretch (figure 2). Tension increased in amplitude, by 49.6% ± 7.7% during maintained stretch, 29.1% ± 6.1% during diastolic stretch, and 16.2% ± 2.6% during systolic stretch ($n = 11$). The Ca^{2+} transient increased by 36.0% ± 5.2% during maintained stretch, 20.5% ± 3.3% during diastolic stretch, and 15.5% ± 2.1% during systolic stretch ($n = 6$). Because the time of holding the preparation at the greater length during each cycle is

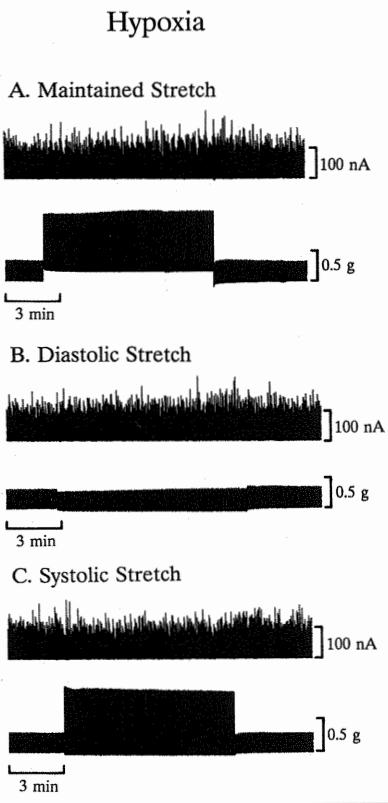

Figure 2. Effect of stretch on the Ca^{2+} transient and tension during hypoxia. Each panel shows slow time base signals of the Ca^{2+} transient (upper traces) and tension (lower traces). During hypoxia, the Ca^{2+} transient and tension reached a steady state within 15–20 minutes. The muscle was stretched from 90% of L_{max} to L_{max} in three ways: (**A**) maintained stretch; (**B**) diastolic stretch; and (**C**) systolic stretch. Reproduced from Hongo et al. [11] with the permission of the American Physiological Society.

different in the three stretch protocols, it seems likely that the longer the time spent at L_{max}, the greater the changes in tension and in the Ca^{2+} transient during the slow phase.

The effect of length changes on cardiac muscle contraction and the Ca^{2+} transient during hypoxia

To produce hypoxia, the bicarbonate Tyrode was equilibrated with 5% CO_2 + 95% N_2, which reduced the PO_2 of the solution to about 5 mmHg [7]. In hypoxia, tension decreased and reached a steady state within 15–20 minutes, while the Ca^{2+} transient decreased slightly [7]. During steady-state contractions, the preparation was stretched in the three ways described above. During a maintained stretch, tension more than doubled just after stretch, a result that was not significantly different from

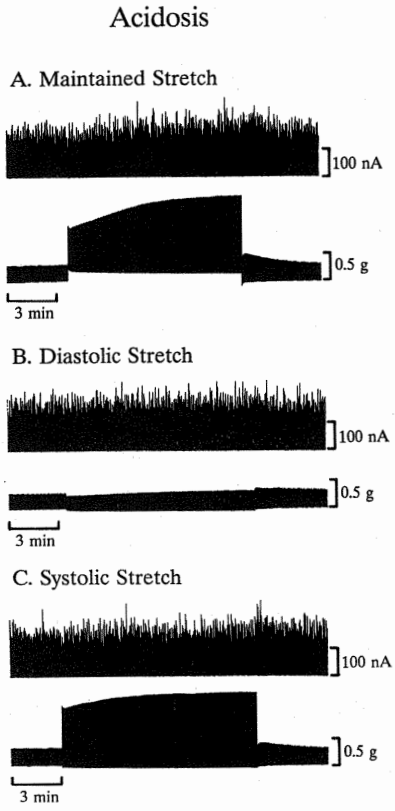

Figure 3. Effect of stretch on the Ca^{2+} transient and tension during acidosis. Each panel shows slow time base signals of the Ca^{2+} transient (upper traces) and tension (lower traces). After the Ca^{2+} transient and tension reached a steady state (20–30 minutes) during acidosis, the muscle was stretched from 90% of L_{max} to L_{max} in three ways: (**A**) maintained stretch; (**B**) diastolic stretch; and (**C**) systolic stretch. Reproduced from Hongo et al. [11] with the permission of the American Physiological Society.

that observed in normoxia (figure 3A). However, there was only a small increase in tension and in the Ca^{2+} transient in the slow phase, which was significantly smaller than that in normoxia (25.2% ± 5.5% for tension, $n = 11$; 19.2% ± 2.5% for the Ca^{2+} transient, $n = 6$) (figure 2). During diastolic stretch, the increase in tension and in the Ca^{2+} transient in the slow phase was also significantly smaller than in normoxia (13.9% ± 2.8% for tension, $n = 11$; 8.4% ± 2.9% for the Ca^{2+} transient, $n = 6$) (figures 2 and 3B). During systolic stretch, the immediate increase in tension was not significantly different from that in normoxia. However, the increase in tension and in the Ca^{2+} transient in the slow phase was significantly smaller than in normoxia (7.0% ± 2.4% for tension, $n = 11$; 5.2% ± 2.5% for the Ca^{2+} transient, $n = 6$) (figures 2C and 4). In summary, during hypoxia, the relative increase in

tension just after stretch was not significantly different from that in normoxia, whereas the relative slow increase in tension and in the Ca^{2+} transient was significantly smaller than in normoxia. Although hypoxia is known to decrease both maximal Ca^{2+} activated force and the Ca^{2+} sensitivity of the myofilaments, a decrease in maximal Ca^{2+} activated force is thought to be more important for the negative inotropic effect of hypoxia [13]. The increase in tension just after stretch is thought to be due to an increase in Ca^{2+} sensitivity of the myofilaments and a change in myofilament overlap [10,12]. This suggests that the relative increase in tension in the rapid phase was the same as in normoxia because of little change in the response of the myofilament Ca^{2+} sensitivity to a change in length. Because the slow increase in tension following stretch is due to a slow increase in the Ca^{2+} transient, the inhibition of the slow change in the Ca^{2+} transient appears to underlie the reduced slow change during hypoxia. In hypoxia, a number of Ca^{2+} handling processes are inhibited, including Ca^{2+} influx through the sarcolemma [2] and Ca^{2+} release from the sarcoplasmic reticulum [14]. Therefore, one of these processes might be involved in the slow response to stretch and might be affected by hypoxia.

The effect of length changes on cardiac muscle contraction and the Ca^{2+} transient during acidosis

To produce acidosis, the bicarbonate Tyrode was equilibrated with 15% CO_2 + 85% O_2, which decreased the pH of the solution from 7.35 to 6.90 [15]. In acidosis, tension rapidly decreased and then gradually recovered to reach a steady state within 20–30 minutes, while the Ca^{2+} transient increased slightly [15]. Under steady-state conditions during acidosis, the preparation was stretched in the three ways described above. During a maintained stretch, tension increased immediately after stretch; this increase was significantly bigger than that observed in normoxia. The slow increase in tension was accompanied by an increase in the amplitude of the Ca^{2+} transient (figure 3A). The changes in the slow phase were not significantly different from those in normoxia (50.8% ± 5.5% for tension, $n = 11$; 32.4% ± 8.5% for the Ca^{2+} transient, $n = 6$) (figure 4). During diastolic stretch, the slow increase in tension was significantly smaller than normal (19.8% ± 3.8%, $n = 11$), whereas the slow increase in the Ca^{2+} transient was not significantly different from normal (14.2% ± 2.3%, $n = 6$) (figures 3B and 4). During systolic stretch, the immediate increase in tension after stretch was significantly bigger than normal (figure 3C). The slow increase in tension was significantly bigger, although the slow increase in the Ca^{2+} transient was not significantly different from normal (22.6% ± 2.4% for tension, $n = 11$; 12.8% ± 3.5% for the Ca^{2+} transient, $n = 6$) (figure 4). In summary, the relative increase in tension just after stretch was significantly bigger than in normoxia, whereas the relative slow increase in tension was dependent on the type of stretch (see above). It is known that the length–tension curve shifts to the right during acidosis due to a decrease in the Ca^{2+} sensitivity of the myofilament [16]. If the shift of this curve produced by acidosis means that the length changes produced during acidosis occur on a flatter part of the length–tension curve than in normoxia, a smaller absolute tension response might be expected in acidosis [17]. However, since tension before

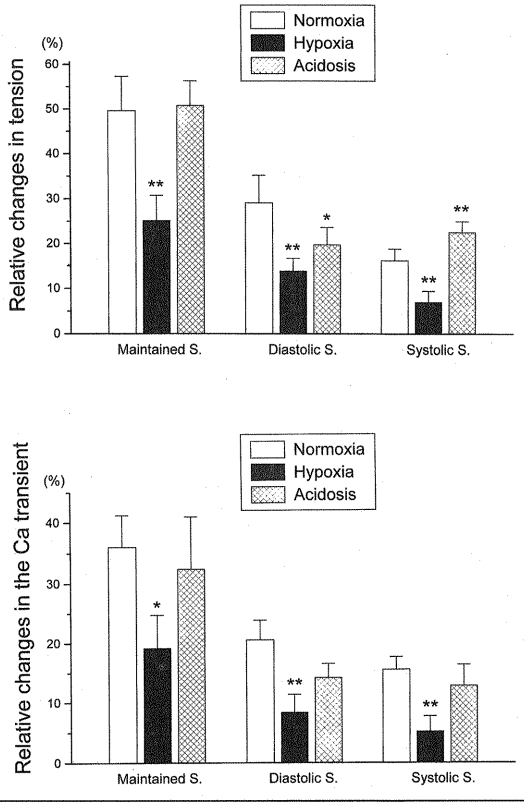

Figure 4. Relative changes in tension and the Ca^{2+} transient during the slow phase following stretch. The upper panel shows the averaged percentage increase in tension during the slow phase (n = 11). The lower panel shows the percentage increase in the Ca^{2+} transient during the slow phase (n = 6). The values were calculated as described in the Methods section (see text) and were expressed as mean ± SEM (error bar). The open bar shows normoxia, the closed bar shows hypoxia, and the hatched bar shows acidosis. For hypoxia and acidosis, asterisks show the results of a paired t-test in which each slow phase was compared to an equivalent slow phase during normoxia. No asterisk, $p > 0.05$; *, p between 0.05 and 0.01; **, $p > 0.01$.

the stretch is smaller during acidosis, the relative tension response might be larger in acidosis. The slow increase in tension during maintained stretch was not significantly different from normoxia; however, that in diastolic stretch was significantly smaller and that in systolic stretch was significantly bigger. Because these changes in tension were not accompanied by the concomitant changes in the Ca^{2+} transient, these differences seem to be due to a difference in the $[Ca^{2+}]_i$–tension relationship between normoxia and acidosis. The $[Ca^{2+}]_i$–tension relationship of cardiac muscle is dependent on sarcomere length [18], and acidosis may cause a parallel rightward shift of the $[Ca^{2+}]_i$–tension curve at different sarcomere lengths [17]. If the changes in $[Ca^{2+}]_i$ occurred at a flatter part of the $[Ca^{2+}]_i$–tension curve during diastolic

stretch and at a steep part of the curve during systolic stretch, a smaller change in tension during diastolic stretch and a larger change in tension during systolic stretch might occur.

REFERENCES

1. Lakatta EG. 1992. Length modulation of muscle performance. Frank-Starling law of the heart. In Fozzard HA (ed), The Heart and Cardiovascular System, 2nd ed. New York: Raven, pp. 1325–1351.
2. Lederer WJ, Nichols CG, Smith GL. 1989. The mechanism of early contractile failure of isolated rat ventricular myocytes subjected to complete metabolic inhibition. J Physiol 413:329–349.
3. Stern MD, Silverman HS, Houser SR, Josephson RA, Capogrossi MC, Nichols CG, Lederer WJ, Lakatta EG. 1988. Anoxic contractile failure in rat heart myocytes is caused by failure of intracellular calcium release due to alteration of the action potential. Proc Natl Acad Sci USA 85:6954–6958.
4. Allen DG, Morris PG, Orchard CH, Pirolo JS. 1985. A nuclear magnetic resonance study of metabolism in the ferret heart during hypoxia and inhibition of glycolysis. J Physiol 361:185–204.
5. Elliott AC, Smith GL, Eisner DA, Allen DG. 1992. Metabolic changes during ischaemia and their role in contractile failure in isolated ferret hearts. J Physiol 454:467–490.
6. Allen DG, Lee JA, Smith GL. 1989. The consequences of simulated ischaemia on intracellular Ca^{2+} and tension in isolated ferret ventricular muscle. J Physiol 410:297–323.
7. Allen DG, Orchard CH. 1983. Intracellular calcium concentration during hypoxia and metabolic inhibition in mammalian ventricular muscle. J Physiol 339:107–122.
8. Allen DG, Orchard CH. 1987. Myocardial contractile function during ischemia and hypoxia. Circ Res 60:153–168.
9. Orchard CH, Kentish JC. 1990. Effects of changes of pH on the contractile function of cardiac muscle. Am J Physiol 258 (Cell Physiol 27): C967–C981.
10. Allen DG, Kurihara S. 1982. The effects of muscle length on intracellular calcium transients in mammalian cardiac muscle. J Physiol 327:79–94.
11. Hongo K, White E, Orchard CH. 1995. The effect of stretch on contraction and the Ca^{2+} transient in ferret ventricular muscles during hypoxia and acidosis. Am J Physiol 269:C690–C697.
12. Allen DG, Nichols CG, Smith GL. 1988. The effects of changes in muscle length during diastole on the calcium transient in ferret ventricular muscle. J Physiol 406:359–370.
13. Marban E, Kusuoka H. 1987. Maximal Ca^{2+}-activated force and myofilaments Ca^{2+} sensitivity in intact mammalian hearts. J Gen Physiol 90:609–623.
14. Smith GL, Steele DS. 1992. Inorganic phosphate decreases the Ca^{2+} content of the sarcoplasmic reticulum in saponin-treated rat cardiac trabeculae. J Physiol 458:457–473.
15. Allen DG, Orchard CH. 1983. The effects of changes of pH on intracellular calcium transients in mammalian cardiac muscle. J Physiol 335:555–567.
16. Fabiato A, Fabiato F. 1978. Effects of pH on the myofilaments and the sarcoplasmic reticulum of skinned cells from cardiac and skeletal muscles. J Physiol 276:233–255.
17. Ricciardi L, Bucx JJJ, ter Keurs HEDJ. 1986. Effects of acidosis on force–sarcomere length and force–velocity relations of rat cardiac muscle. Cardiovasc Res 20:117–123.
18. Hibberd MG, Jewell BR. 1982. Calcium- and length-dependent force production in rat ventricular muscle. J Physiol 329:527–540.

ROLES OF SUPEROXIDE, NITRIC OXIDE, AND PEROXYNITRITE IN VARIOUS PATHOLOGICAL CONDITIONS

HIDEYUKI ISHIDA, MINHAZ UDDIN MOHAMMED, ZHI SU, MINAKO FUJISHIMA, and HIROE NAKAZAWA

Tokai University

Summary. It has become apparent that endothelial and inflammatory cells can produce both superoxide (O_2^-) and nitric oxide (NO). When O_2^- and NO coexist, they react to yield peroxynitrite ($ONOO^-$). $ONOO^-$ is a potent oxidant. This chapter reevaluates free radical-related injury with particular attention to the reaction of O_2^-, NO, and $ONOO^-$. Through ischemia–reperfusion study using isolated rat hearts, it is suggested that the cytotoxic molecule is $ONOO^-$. Similarly, in the study of activated leukocyte-induced cardiac myocyte injury, $ONOO^-$ appears to be responsible for the injury. However, in activated leukocyte-induced endothelial cell injury, the hydroxyl radical plays a significant role. The evidence to infer the formation of $ONOO^-$ was obtained from a study of patients with septic shock. In conclusion, cytotoxic molecules and the mechanism underlying cell damage appear to depend not only on the effector but also on the target cells, and it is very important to identify the actual cytotoxic molecule under an individual pathological condition.

INTRODUCTION

The extensive research work on oxyradicals during the last 20 years has clarified the importance of their roles in various pathophysiological conditions. We now know that virtually all aerobes produce superoxide (O_2^-) and other oxyradicals. With the discovery in 1987 by Palmer et al. [1] that a small gaseous radical, nitric oxide (NO), is an important physiological and pathological messenger in our bodies, the role of oxyradicals has become more important than ever, since most cells can produce not one but two radicals, namely, O_2^- and NO. The rapidly accumulating information related to NO has confirmed that NO is continuously released in both physiological

S. Mochizuki, N. Takeda, M. Nagano and N. Dhalla (eds.). THE ISCHEMIC HEART.

and pathological conditions. When O_2^- and NO coexist, they can react to yield peroxynitrite ($ONOO^-$). $ONOO^-$ is a potent oxidant [2] and has been shown to act as a pro-oxidant in various pathological conditions, including reperfusion injury of ischemic heart disease, acute lung injury, rheumatoid arthritis, inflammatory bowl disease, and acute gastric mucosal lesion. It is therefore necessary at this time to reevaluate oxyradical-related injury with particular attention to the reaction of O_2^- and NO and the detrimental effect of $ONOO^-$.

PUZZLING EFFECT OF SUPEROXIDE DISMUTASE (SOD)

In recent studies, we have obtained evidence showing that $ONOO^-$, rather than O_2^- or NO, may be the most likely candidate for the actual cytotoxic molecule in reperfusion injury [3]. If this is the case, the longstanding controversy regarding the role of O_2^- in producing the hydroxyl radical (OH·) in the iron-catalyzed Haber–Weiss reaction and Fenton reaction (see below) will be resolved. These reactions are as follows:

Haber-Weiss reaction: $O_2^- + H_2O_2 \rightarrow O_2 + OH^- + OH\cdot$, in the presence of Fe^{2+}

Fenton reaction: $H_2O_2 + Fe^{2+} \rightarrow OH\cdot + OH^- + Fe^{3+}$

Since it is well known that O_2^- has a limited reactivity toward biological molecules and that OH· is actually cytotoxic, it has been stated that O_2^- functions as a reducing agent in the Haber–Weiss reaction (reducing Fe^{3+} to Fe^{2+})—i.e., O_2^- increases the concentration of Fe^{2+} and promotes the formation of OH· in the presence of H_2O_2 by a Fenton reaction. However, this role of O_2^- may be irrelevant; other reducing agents such as ascorbate or glutathione are present in tissue in higher concentrations than O_2^-, and these agents can readily reduce Fe^{3+} to Fe^{2+} instead of O_2^-. In other words, OH· formation through the reaction of H_2O_2 and Fe^{2+} does not require the existence of O_2^-. Therefore, there is no logical reason why SOD can protect against O_2^--related injury, since SOD removes or scavenges O_2^- by dismutating it to H_2O_2, which in increased concentrations generates OH· in the presence of Fe^{2+} (figure 1, equation 1). This point has puzzled us for a long time. However, if $ONOO^-$ rather than H_2O_2-derived OH· is the actual cytotoxic molecule, the effect of SOD is readily explained, since the removal of O_2^- by SOD simply reduces the generation of $ONOO^-$ and thereby attenuates the injury (figure 1, equation 2). $ONOO^-$ itself is a potent oxidant that nitrates cellular constituents and has been shown to play an important role in tissue damage from rheumatic arthritis, acute lung injury, and myocyte injury [4–7]. Peroxynitrite is a surprisingly complex oxidant for a molecule with only four atoms (figure 2). The pK_a of $ONOO^-$ is about 6.8, and $ONOO^-$ has the weakest O–O bond strength. Thus, $ONOO^-$ can easily be protonated at normal pH to yield ONOOH, peroxynitrous acid. The weak O–O bond strength allows peroxynitrous acid to decompose spontaneously to form an oxidant with the reactivity of OH· [8,9]. That can react with the lipid bilayer of cell membrane just like an OH· molecule. This reaction in turn leads to the lipid peroxidation chain reaction and can attack DNA.

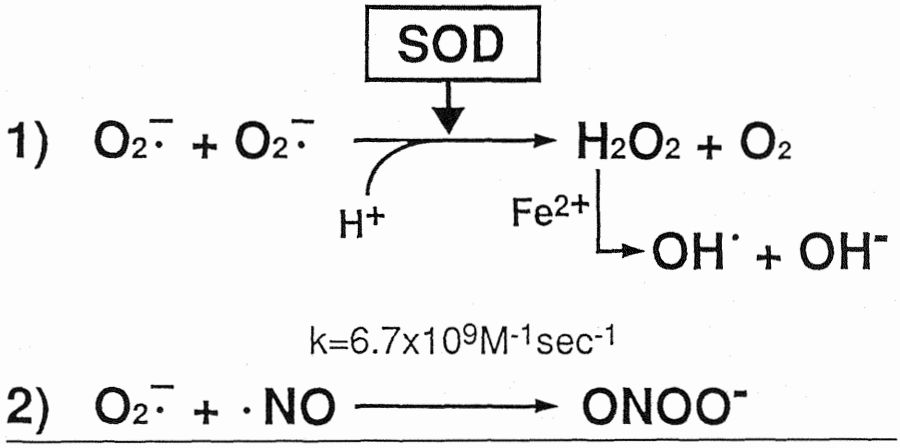

Figure 1. Puzzling aspects of the effect of superoxide dismutase (SOD). Dismutation of O_2 by SOD does not decrease OH· in equation 1, but removal of O_2^- by SOD in equation 2 results in a decrease in $ONOO^-$.

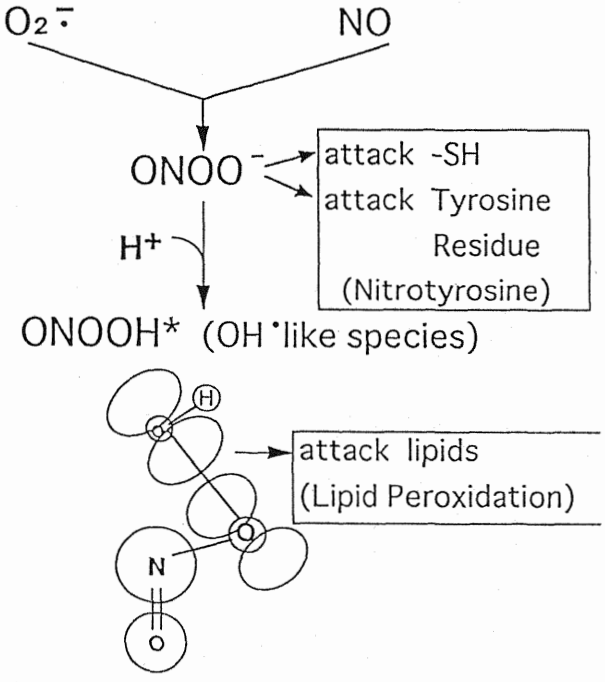

Figure 2. Peroxynitrite and peroxynitrous acid.

In the following section we will show that 1) SOD is effective in reducing ischemia–reperfusion injury in rat hearts, 2) human leukocytes can produce O_2^- NO and $ONOO^-$ upon activation with phorbol myritate acetate (PMA), 3) synthesized $ONOO^-$ produces dysfunction of cardiac myocytes, 4) endogenously produced $ONOO^-$ from activated human leukocytes appears to be the cytotoxic molecule for cardiac myocytes but not a major cytotoxic molecule for endothelial cells, and 5) some evidence suggests $ONOO^-$ formation in patients with septic shock.

EFFECT OF SOD IN ISCHEMIA REPERFUSION INJURY [10]

Isolated rats hearts were perfused retrogradely via the aortic root with modified Krebs–Henseleit buffer saturated with a gaseous mixture containing 95% O_2 and 5% CO_2 on a Langendorff apparatus under a continuous perfusion pressure of 120 cm of water. The temperature of the whole system was maintained at 36.5°C through the use of a water bath and a water jacket. A latex balloon was placed in the left ventricular cavity to measure the left ventricular developed pressure (LVDP), and coronary blood flow (CBF) was measured by an electromagnetic flow meter (Nihon Koden Co., Tokyo, Japan). To induce ischemia–reperfusion injury, the left coronary artery (LCA) was occluded for 60 minutes and perfused for another 60 minutes. Human recombinant SOD (rh-SOD) was perfused for the whole period of reperfusion starting five minutes prior to reperfusion. CBF and LVDP were continuously monitored, and the release of creatine phosphokinase (CPK) and rat heart endogenous-SOD (endoge-SOD) in coronary effluent were determined. At the end of experiment, LCA was religated and Evans blue was injected to delineate the risk area. The heart was sliced, and the necrotic area was determined by triphenyltetrazolium chloride (TTC) staining.

During ischemia, the CBF and LVDP values did not differ, but at the end of reperfusion both were significantly higher in rh-SOD-treated hearts than were the controls. CBF was 77% ± 1% and 67% ± 2% of preischemic values in the rh-SOD treated and control hearts, respectively, and LVDP was 77% ± 2% and 69% ± 1% of preischemic value in the rh-SOD treated and control hearts, respectively (figure 3). The risk area of the left ventricle showed no significant difference, indicating that a similar amount of tissue was jeopardized by the occlusion of LCA in rh-SOD-treated and control hearts (47% ± 2% and 48% ± 1%, respectively). However, when the necrotic area was expressed as a percentage of the area at risk, rh-SOD-treated hearts demonstrated a smaller area than did controls (15% ± 1% and 33% ± 1%, respectively). The total CPK release during the whole period of reperfusion was significantly lower in the rh-SOD treated hearts than in the controls (100 ± 2 and 116 ± 4 × 10^3 units/g wet weight of myocardium, respectively), and the total amounts of endoge-SOD release were 12 ± 1 and 14 ± 1 × 10^3 units/g wet weight of myocardium in rh-SOD-treated and control hearts, respectively. The peak release of CPK and endoge-SOD occurred at two minutes after the reperfusion, and then the release decreased rapidly, irrespective of the total amount of CPK and endoge-SOD released (figures 4A and 4B). The overall endoge-SOD

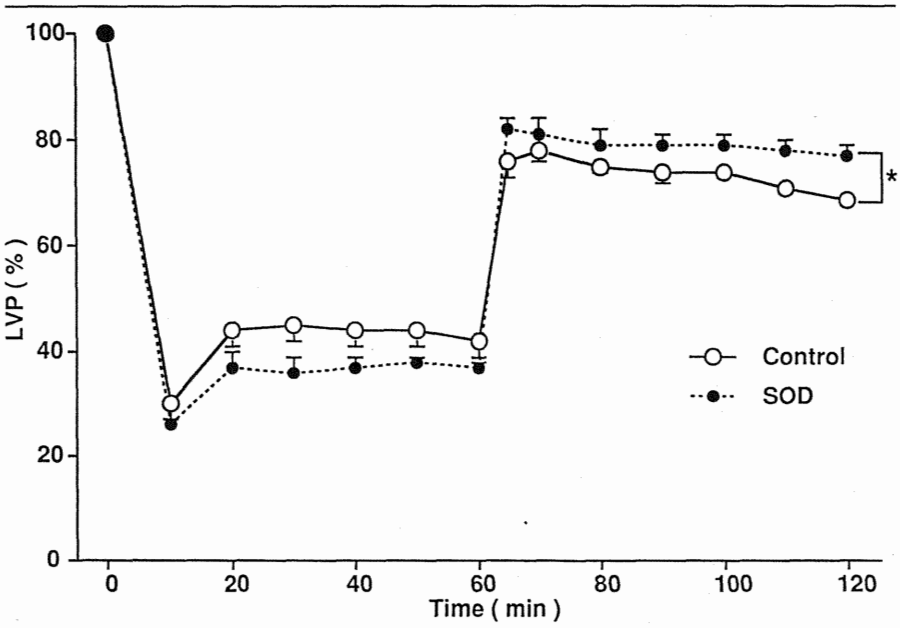

Figure 3. The time course of left ventricular developed pressure between rh-SOD-treated and control hearts. Results are expressed as the percentage of preischemic control (mean ± SEM). The asterisk denotes significant difference ($p < 0.05$).

release pattern during reperfusion did not differ from the CPK release pattern, indicating that the endoge-SOD leaks from plasma membrane and endoge-SOD release are merely a manifestation of myocyte damage.

These findings of a high CBF and LVDP, low CPK release, and small necrotic area in rh-SOD-treated hearts indicate that rh-SOD treatment at the initiation of reperfusion attenuates ischemia–reperfusion injury. In other words, O_2^- is a cytotoxic molecule in this model, since SOD removes O_2^-. The results favor equation 2 rather than equation 1 in figure 1.

PEROXYNITRITE FORMATION FROM ACTIVATED HUMAN LEUKOCYTES [11]

It is known that polymorphonuclear cells (PMNs) mediate the inflammatory process by producing O_2^- through the activation of NADPH oxidase. Moreover, the generation of NO by human PMNs has been demonstrated by several studies, although there are also several negative reports. Carreras et al. have shown that PMNs produce NO and abundant O_2^- in respiratory bursts, and they suggest that these two molecules can form $ONOO^-$ [12]. However, no studies have actually demonstrated the production of $ONOO^-$ from human PMNs; rat alveolar macrophages are the only cells from which $ONOO^-$ generation has been shown in a biological system [13]. In this chapter, we give our results, which demonstrate $ONOO^-$ production from human PMNs using the HPLC method by measuring

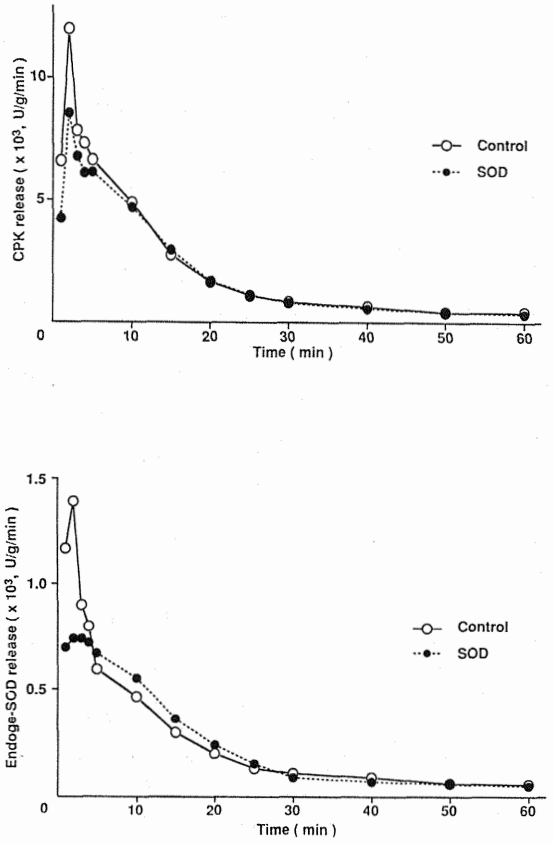

Figure 4. The time course of CPK (**A**) and endoge-SOD (**B**) release during reperfusion in the rh-SOD-treated and control hearts. The results are expressed as units/mL of coronary effluent/minutes, with normalization using wet heart weight.

nitration of 4-hydroxyphenylacetic acid (HPA) to 4-hydroxy-3-nitrophenylacetic acid (NO_2HPA) by $ONOO^-$.

Buffer based on Hanks balanced salt solution (HBSS) containing 137 mM NaCl, 5.4 mM KCl, 1.0 mM $MgCl_2$, 1.27 mM $CaCl_2$, 5.5 mM glucose, and 40 mM HEPES (HBSS-HEPES, pH 7.4 adjusted by NaOH) was used as an incubation medium. PMA was used as a stimulator for PMNs. The cytochrome *c* method and a chemiluminescence method with 2-methyl-6-(p-methoxyphenyl)-3,7-dihydroimidazol (1,2-α) pyrazine-3-one (MCLA) were used to measure O_2^- [14,15]. Nitric oxide production from PMNs was estimated by NO_2^- + NO_3^- content, which was measured with the Griess reaction on a flow-injection system equipped with a Cd/Cu column for nitrate reduction [16]. Peroxynitrite was synthesized using the quenched-flow method, and the concentration was deter-

mined with $\varepsilon_{302} = 1670 M^{-1}cm^{-1}$ [17]. Human recombinant CuZn SOD was used as a transition metal in a metal-catalyzed NO_2HPA measurement. Inactivation of SOD was achieved by treating SOD with phenylglyoxal and H_2O_2 [4] and eluted from a 10 × 1 cm Sephadex G25 (Pharmacia) column equilibrated with HBSS-HEPES buffer [4,14]. Rat alveolar macrophages were isolated with bronchoalveolar lavage as reported elsewhere [13], and human PMNs were isolated from heparinized fresh whole blood of healthy donors by gradient centrifugation (400 g for 30 minutes) using Mono-Poly resolving medium at room temperature. The PMN-enriched fraction was harvested into 50-mL centrifugation tubes and then washed with Ca^{2+}- and Mg^{2+}-free HBSS. After hypo-osmotic lysis of the contaminated erythrocytes, the PMNs were resuspended at an appropriate concentration in HBSS-HEPES. Peroxynitrite content was measured by the method reported by Ichiropoulos et al. [13], with slight modifications. The principle of measurement is based on the following: by the catalysis of transition-metal complexes such as SOD, $ONOO^-$ is converted to nitronium ion and nitrate phenolic compounds. HPA was used as a phenolic compound, and we estimated peroxynitrite content from the concentration of formed NO_2HPA, which is a nitrated product of HPA. Rat alveolar macrophages or human PMNs on 24-well dishes (10^7 cells in 500 μL of HBSS-HEPES) were stimulated with 1 μM PMA in the presence of 1 mM HPA with inactivated SOD (0.1 mg/mL) and incubated at 37°C for 2–4 hours. For human PMNs, 100 μM of ABAH, a myeloperoxidase inhibitor [18], was included through the Ultafree C3 LBC00 filter (0.45 μm pore size). The cellular supernatant was acidified with 10% H_3PO_4, and a final 20% acetonitrile was added. The sample was passed through a 0.45-μm filter before injection of 20 μL of samples. The HPLC apparatus consisted of two pumps (PU-980, JASCO), a UV/visual absorbance detector (UV-970, JASCO), and a 807IT integrator (JASCO) to construct the high-pressure gradient system. Analysis was carried out using a 4.6-mmϕ × 150-mm (C-18) reverse-phase column and 20%/80% acetonitrile/10% H_3PO_4 (pH 3.2) (v/v) as the mobile phase. The column was eluted with a linear gradient of 20% to 60% acetonitrile over 10 minutes at a flow rate of 1 mL/min. The separation method was developed using authentic HPA and NO_2HPA, which also served as internal controls. The NO_2HPA yield in this assay system was determined by mixing synthesized $ONOO^-$ (50 μM) with the corresponding reaction media.

A standard $ONOO^-$ assay showed that NO_2HPA can be determined down to *ca* 10 nM for μL samples (figure 5). This finding indicates that the detection limit is 0.2 pmol. $ONOO^-$ has a short half-life (less than two seconds) under physiological conditions, and its protonated form, ONOOH, can easily react with other molecules [17]; also, the yield of NO_2HPA is affected by the component of buffer solution. Therefore, the yield in a balanced salt buffer solution with 10 mM phosphate and 0.1 mg/mL SOD was 8%, as previously reported [13]. The yield was reduced to 3.4% in HBSS-HEPES, in which 40 mM HEPES was necessary for keeping the pH constant in the experiment in which PMNs may have reacted with $ONOO^-$. Thus, the produced $ONOO^-$ can be calculated using this recovery rate from the concentration of NO_2HPA.

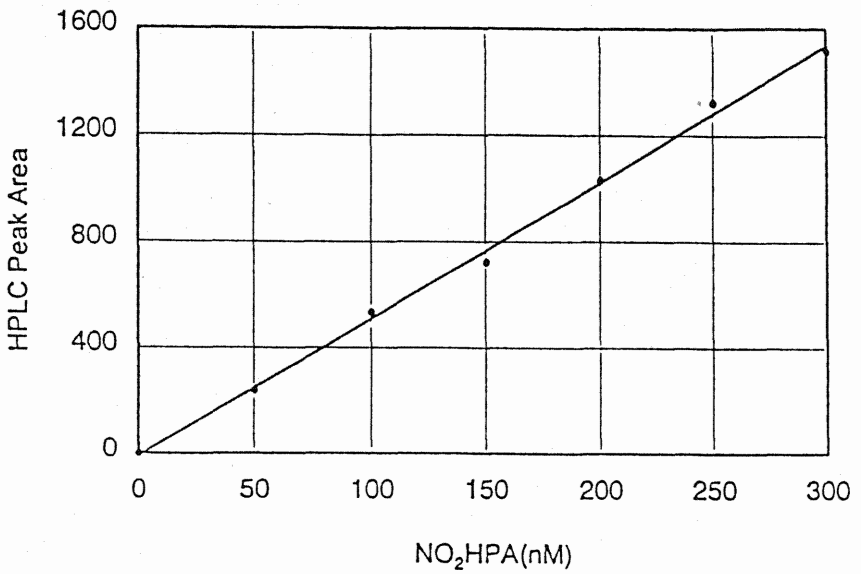

Figure 5. The correlation between peak area at 6.5 minutes and correlation of NO_2HPA for $ONOO^-$ assay. This method can determine 10 nM of NO_2HPA, which corresponds to *ca* 300 nM of $ONOO^-$ in HBSS-HEPES buffer.

To confirm that our system is valid for the determination of $ONOO^-$ generated in biological systems, $ONOO^-$ generation from rat alveolar macrophages was measured. A peak due to NO_2HPA (0.082 ± 0.003 pmL/10^6 cells/min) was observed in the supernatant of the alveolar macrophages at the retention time of 6.5 minutes. This value corresponds to 2.4 ± 0.1 pmol/10^6 cells/min of $ONOO^-$ production. The NO_2PHA formation was eliminated by the addition of 100 μM of L-NMMA, as reported elsewhere [13]. In contrast, the supernatant from human PMNs shows multiple unknown peaks and only a trivial peak of NO_2HPA at 6.5 minutes (figure 6). The reason for the production of multiple unknown peaks appears to be due to the myeloperoxidase, which can be released from the stimulated PMNs, since macrophages contain much less amount of myeloperoxidase. Myeloperoxidase converts H_2O_2 to OCl^-, and OCl^- can react with $ONOO^-$ when both are in protonated forms [19]. Thus, we used 100 μM of ABAH to inhibit myeloperoxidase. The addition of ABAH resulted in the reduction of unknown peaks and the enhancement of the NO_2HPA peak. To further confirm that NO_2HPA originated from the production of $ONOO^-$ by PMNs, 100 μM of L-NMMA was added in the presence of ABAH (figure 6). L-NMMA abolished the peak due to NO_2HPA, indicating that NO_2HPA was produced through $ONOO^-$ generation.

The time course of $ONOO^-$ generation was evaluated at hourly intervals, with the accumulation of NO_2HPA for four hours. Of the total $ONOO^-$ production,

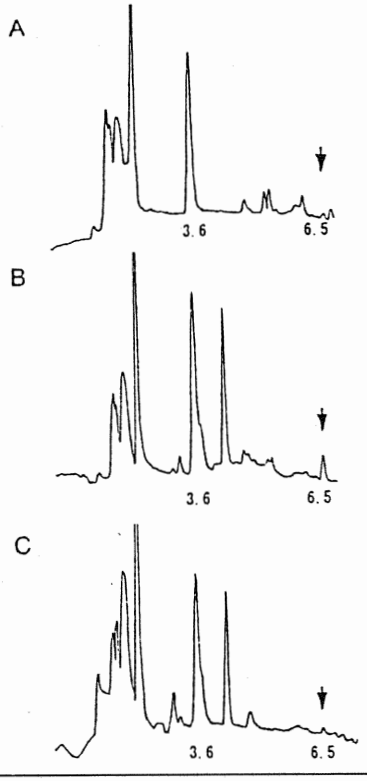

Figure 6. Peroxynitrite production from human PMNs. These chromatograms were obtained from the supernatant of PMN incubation medium after being stimulated with PMA for four hours. (**A**) Only a trace amount of NO_2HPA (with a peak at 6.5) was detected in the absence of a myeloperoxidase inhibitor. (**B**) Using a myeloperoxidase inhibitor, 4-ABAH (100 μM), the NO_2HPA peak emerged. (**C**) Nitric oxide synthase inhibitor (L-NMMA 100 μM) eliminated the production of NO_2HPA.

85% occurred within the first two hours, and $ONOO^-$ production ceased at four hours. Superoxide generation monitored with chemiluminescence showed a peak at 30 minutes after PMA stimulation and terminated within four hours, which is the same time profile as that of $ONOO^-$ production. Total NO_2HPA production was 0.489 ± 0.055 pmol/10^6 cells/hour ($n = 4$), which corresponded to 14.4 ± 1.6 pmol/10^6 cells/hour of $ONOO^-$ production, with a recovery rate of 3.4%. The total O_2^- generation determined with cytochrome *c* reduction was 150 nmol/10^6 cells/hour. Total $NO_2^- + NO_3^-$ content was 81 ± 16 pmol/10^6 cells/hour.

The total concentrations of $ONOO^-$, O_2^-, and $NO_2^- + NO_3^-$ indicate that *ca* 18% of nitric oxide released from PMNs is converted to $ONOO^-$ in a large excess of O_2^- production. This work showed that PMNs can produce $ONOO^-$ when activated. Thus, PMNs may be one of the sources of $ONOO^-$ in various inflammatory conditions in which a role of $ONOO^-$ is indicated.

EFFECT OF $ONOO^-$ IN CARDIAC MYOCYTES [20]

We used cardiac myocytes in monolayers prepared from mouse embryo hearts. The cardiac myocytes were placed on 25-mmϕ glass coverslips and incubated in humidified 5% CO_2–95% air at 37°C for two days. Morphological observation of the cells was performed using an inverted phase contrast microscope. The contractile state of the cells was assessed by the use of an optical video-motion-detector system (VMD200, NIC Co.Ltd., Japan), as described previously [20]. Intracellular Ca^{2+} ($[Ca^{2+}]_i$) and pH ($[pH]_i$) were monitored by the use of the fluorescent calcium indicator Calcium Green-1 and the pH indicator BCECF. $ONOO^-$ was synthesized in a quenched-flow reactor [11]: solutions of 0.6 M $NaNO_2$ and 0.6 M HCl/0.7 M H_2O_2 were mixed in a glass tube, with subsequent stabilization with 1.5 M NaOH. Excess H_2O_2 was removed by granular MnO_2. The concentration of $ONOO^-$ was determined spectrophotometrically at 302 nm (ε_{302} = 1670/M/cm) and diluted with HCl to the desired concentrations. When $ONOO^-$ was exposed to cardiac myocytes, the pH of the $ONOO^-$ solution was adjusted to 7.4 using a minimixing system that was closely attached to the inlet port of the chamber with cells. The final concentration of $ONOO^-$ in the chamber was determined by directly measuring an absorbance at 302 nm of the chamber. To exclude the influence of possible contaminants and decomposition products of $ONOO^-$, such as NO_2^- or NO_3^-, $ONOO^-$ was decomposed by incubating it for 30 minutes in HEPES-buffer physiological solution at pH 7.4, which was infused instead of the $ONOO^-$ solution.

As shown in figure 7, a simultaneous recording of cell motion and $[Ca^{2+}]_i$ during exposure to $ONOO^-$ demonstrates that perfusion of $ONOO^-$ (final concentration 0.2 mM) induced a decrease in cell motion within one minute that reached nearly complete arrest in diastole in two minutes. The decreased amplitude in cell motion coincided with an elevation in $[Ca^{2+}]_i$ during diastole. The onset of the diastolic arrest also occurred simultaneously with the onset of a persistent increase in $[Ca^{2+}]_i$ to higher than a peak systolic level. The diastolic arrest was sustained thereafter, even during the elevated $[Ca^{2+}]_i$ without oscillatory motion. In zero Ca–0.2 mM EGTA solution, $ONOO^-$ infusion did not produce the increase in $[Ca^{2+}]_i$ at all, indicating that the $[Ca^{2+}]_i$ elevation produced by $ONOO^-$ exposure is caused by Ca^{2+} influx through the plasma membrane and that the Ca^{2+} release from sarcoplasmic reticulum does not contribute to the rise in $[Ca^{2+}]_i$. Additional experiments with an L-type Ca^{2+} channel blocker showed that $ONOO^-$ infusion did not cause the increase in $[Ca^{2+}]_i$, although the amplitude of the $[Ca^{2+}]_i$ transient decreased in the presence of 50 μM of verapamil. The membrane fluidity measured by the diffusion coefficient at five minutes of exposure to 0.2 mM $ONOO^-$ did not change. Thiobarbiturate acid-reactive substance (TBARS) values of the cells that were determined at five minutes of exposure to $ONOO^-$ remained unchanged (from 0.17 ± 0.03 to 0.15 ± 0.02 nmol/mg protein, n = 5), suggesting that the damage of membrane lipids is not evident at this acute stage and that the lipid peroxidation of the cell membrane is less likely as the underlying mechanism for the increased entry of Ca^{2+}. This finding also supports the results of the experiment with the L-type Ca^{2+} channel blocker.

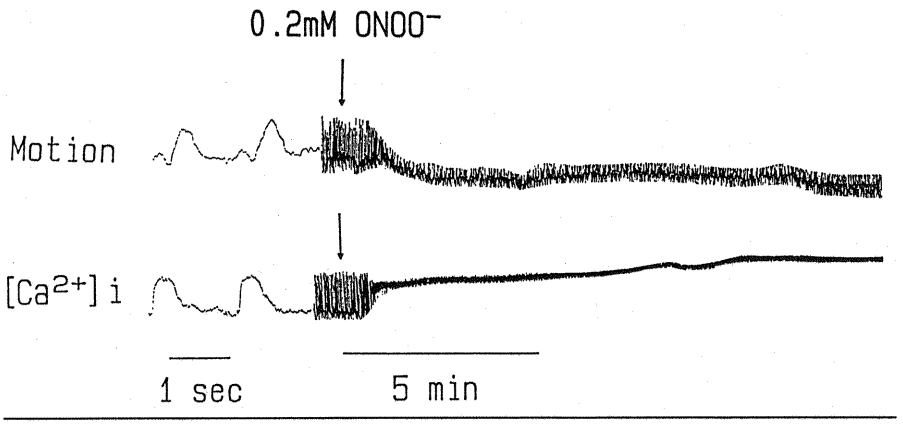

Figure 7. Effect of $ONOO^-$ on cell motion and $[Ca^{2+}]_i$. Upward shift in the motion depicts shortening or systole, and downward shift depicts a relax or diastole. Upward shift in $[Ca^{2+}]_i$ depicts an increase in $[Ca^{2+}]_i$. Representative tracings are shown from six experiments.

In this series of experiments, we were able to show the injurious effect of $ONOO^-$ on myocytes. Then we performed the next experiment to examine whether or not $ONOO^-$ is actually cytotoxic in biologically relevant situations of injury.

DIFFERENT ROLES OF $ONOO^-$ IN PMN-INDUCED CARDIAC MYOCYTE AND ENDOTHELIAL CELL INJURY

We used cardiac myocytes that had been isolated from fetal mouse ventricles by trypsinization and endothelial cells that had been obtained from fresh bovine aorta (BAECs). For the cardiac myocyte study, the experiments were performed immediately after the cells had adhered to 25-mmϕ glass coverslips. For the endothelial cell study, the experiments were performed using confluent cells after 6–12 passages. PMNs were isolated using the same method described in the previous section. PMNs were stimulated by PMA (1 μM). The generations of O_2^-, NO, and $ONOO^-$ from PMA-stimulated PMNs were measured by the chemiluminescence method and the Griess reaction, respectively, as was shown in the previous section [2,21]. Cardiac myocyte injury was evaluated by LDH release, and BAEC injury was evaluated by preincubated ^{51}Cr release. The coculture of cardiac myocytes and activated PMNs induced LDH release (21% ± 1% of total LDH at three hours). Treatment of L-NMMA and SOD significantly reduced LDH release (14% ± 1%, $p < 0.01$), but catalase and deferoxamine were not effective. In contrast to the results of cardiac myocytes, the ^{51}Cr release from BAECs cocultured with activated PMNs was potentiated by the treatment of L-NMMA. In the presence of an NO donor, ^{51}Cr release was attenuated. In the presence of an anti-CD18 mAb, which inhibited the adhesion molecule of PMNs, the ^{51}Cr release was inhibited to a nearly nonsignificant level. The anti-CD18 mAb-induced inhibition of ^{51}Cr release re-

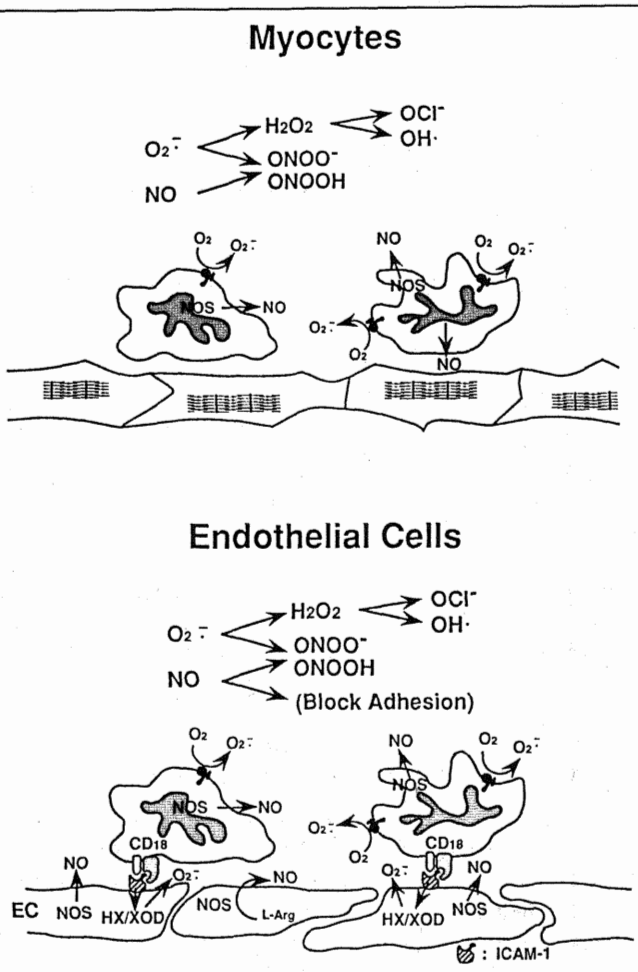

Figure 8. Interaction between PMNs and cardiac myocytes/BAECs.

mained at the same level even in the presence of L-NMMA. The plausible mechanism underlying the marked difference of the effect of NO on PMN-induced injury between cardiac myocytes and BAECs is illustrated in figure 8. As is clear, the interaction of myocytes and PMNs is not triggered by the adhesion molecules, i.e., adhesion molecules on the myocyte are not expressed prior to cytokine stimulation [5,22]. However, the interaction between BAECs and PMNs is largely dependent on adhesion molecules, since major adhesion molecules of CD11/CD18 are constitutively expressed on the surface of PMNs, and since the ligand of CD11/CD18, ICAM-1, is also expressed on the endothelial cell surface [23]. Another difference is that NO is continuously released from BAECs, and NO has an antiadhesion function in the BAEC and PMN system.

In this experiment, we showed that cytotoxic molecule and the mechanism underlying the cell damage appear to depend not only on the affector mechanism but also on the effector cells (tissue). Therefore, it is very important to identify the actual cytotoxic molecule (O_2^-, NO, or $ONOO^-$) in an individual pathological condition.

CLINICAL EVIDENCE OF PEROXYNITRITE FORMATION [24]

We evaluated the formation of nitrotyrosine in three patients with septic shock to show that $ONOO^-$ can actually be found in septic shock. Nitrotyrosine, which is a nitrated product of tyrosine in blood or tissue and whose presence infers $ONOO^-$ attack on tyrosine residues of protein and nonprotein origins, was selected as an indicator. The reason to select nitrotyrosine as an index for production of $ONOO^-$ is based on the fact that direct measurement of $ONOO^-$ in vivo is difficult because of its very short half-life [2]. We selected patients with chronic renal failure to increase the concentration of nitrotyrosine because nitrotyrosine was shown to be rapidly excreted in the urine [25]. Ten patients with chronic renal failure without sepsis (eight men and two women, mean age 52.9 ± 17.2 years) served as renal failure controls who were consecutively selected from routine hemodialysis sessions. Ten healthy volunteers served as healthy controls (six men and four women, mean age 36.7 ± 10.0 years). The three patients with chronic renal failure with septic shock were a 72-year-old women with sepsis induced by diverticulitis, a 68-year-old woman who developed sepsis during a course of cholangitis, and a 80-year-old woman with sepsis caused by ruptured cholangitis. All had been on standard hemodialysis treatment for more than six months (mean 63.96 ± 25.2 months) and showed the characteristic features of septic shock. Mean blood pressures were 82/48 mmHg, 78/40 mmHg, and 70/30 mmHg, respectively, despite intravenous volume replacement and infusion of dopamine. Residual renal function in septic and nonseptic renal failure patients was negligible, i.e., there was no urinary output. Blood was withdrawn in the morning without any restriction of meals in volunteers. In patients with renal failure, blood was withdrawn from the arterial (predialyzer) line before starting hemodialysis. Blood samples were centrifuged at 2000 rpm for five minutes. The plasmas were filtered through a 3000 Mr-cutoff filter to eliminate protein components. Nitrotyrosine was measured by a method described elsewhere, with slight modification [6]. Briefly, nitrotyrosine was separated using an HPLC C-18 reverse-phase column and measured with an ultraviolet detector set at 274 nm. The peak was identified on the basis of the retention time of authentic nitrotyrosine (the detection limit was 0.6 μM). The identity of the peak was also confirmed by treatment with excess $Na_2S_2O_4$, which reduces nitrotyrosine to aminotyrosine [26]. Nitrite + nitrate (NOx) in plasma was measured by the Griess reaction. Data are presented as mean and 95% confidence interval (CI). Unpaired two-tailed *t*-tests, assuming unequal variance, were used. In the plasma of healthy volunteers, nitrotyrosine was not detected and NOx was 28.7 ± 11.6 μM (figure 9). Renal failure patients without septic shock exhibited detectable nitrotyrosine (28.0 ±

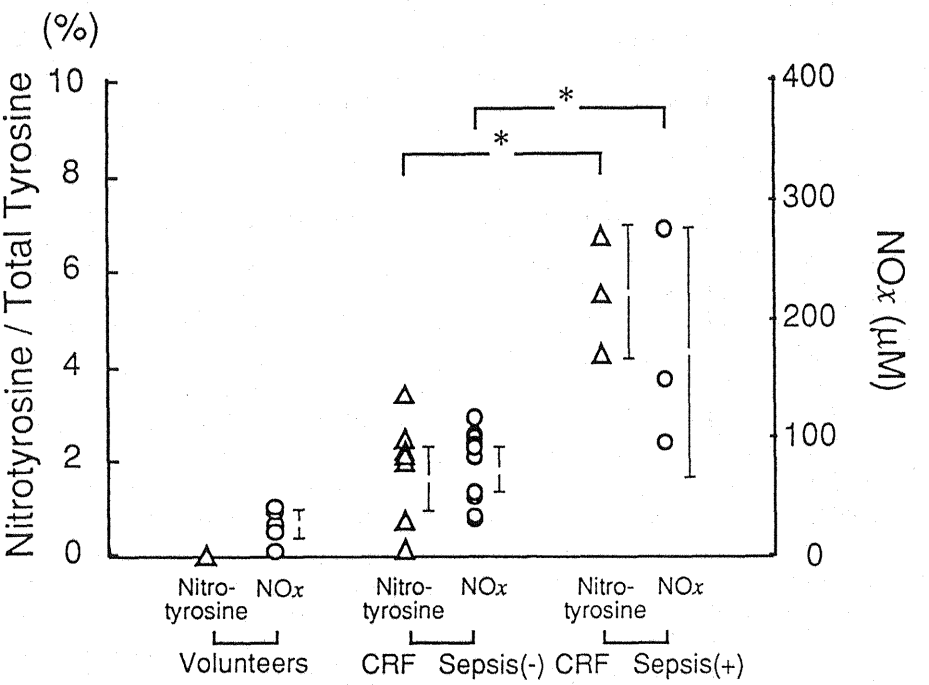

Figure 9. The increased level of plasma nitrotyrosine and nitrite–nitrate in chronic renal failure patients with septic shock.

12.3 μM, 1.6% ± 1.1% of total tyrosine) and had significantly higher NOx values (75.6 ± 19.1 μM, $p < 0.001$, 5.5% ± 1.2% of total tyrosine) than volunteers. In patients with septic shock, both nitrotyrosine and NOx were significantly elevated (nitrotyrosine: 118.2 ± 22.0 μM, 5.5% ± 1.2% of total tyrosine; NOx: 173.9 ± 104.7 μM) and NOx levels decreased to 43.0 ± 5.3 μM and 25.3 ± 11.9 μM, respectively, in blood withdrawn after the dialysis. These results show that plasma nitrotyrosine and NOx were increased in renal failure patients and that the increases were more marked in patients whose condition was complicated by septic shock. The higher nitrotyrosine levels in septic shock patients are highly indicative of the formation of peroxynitrite in septic shock.

In these five experiments performed in our laboratory, we attempted to identify the actual cytotoxic molecule in various pathophysiological conditions. However, many important issues remained to be clarified. The detailed chemical reactions of oxyradicals, including O_2^-, NO, and $ONOO^-$, in biological milieus will clarify the individual mechanisms underlying cell (tissue) injury in the near future.

REFERENCES

1. Palmer RMJ, Ferrige AG, Moncada S. 1987. Nitric oxide release accounts for the biological activity of endothelium-derived relaxing factor. Nature 327:524–526.
2. Huie RE, Padmaja S. 1993. The reaction of NO with superoxide. Free Rad Res Commun 18:195–199.
3. Fukuyama N, Ishida H, Ichimori K, Su, Z, Nakazawa H. 1995. Peroxynitrite in neutrophil-mediated cytotoxicity to myocardial cells (abstract). Endothelium 3(Suppl):S40.
4. Ichiropoulos H, Zhu L, Chen J, Tsai M, Martin JC, Smith CD, Beckman JS. 1992. Peroxinitrite-mediated tyrosine nitration catalyzed by superoxide dismutase. Arch Biochem Biophys 298:431–437.
5. Beckman JS, Ye YZ, Anderson PG, Chen J, Accavitti MA, Tarpey MM, White CR. 1994. Extensive nitration of protein tyrosine in human atherosclerosis detected by immunohistochemistry. Biol Chem Hoppe Seyler 375:81–88.
6. Kaur H, Halliwell B. 1994. Evidence for nitric oxide-mediated oxidative damage in chronic inflammation—nitrotyrosine in serum and synovial fluid from rheumatoid patients. FEBS Lett 350:9–12.
7. Wizemann TM, Gardner CR, Laskin JD, Quinoes S, Durham SK, Goller NL, Ohnishi T, Laskin DL. 1994. Production of nitric oxide and peroxynitrite in the lung during acute endotoxemia. J Leuk Biol 56:759–768.
8. Koppenol WH, Moreno JJ, Pryor WA, Ischiropoulos H, Beckman JS. 1992. Peroxynitrite: a cloaked oxidant from superoxide and nitric oxide. Chem Res Toxicol 5:534–842.
9. Pryor WA, Squadrito GL. 1995. The chemistry of peroxynitrite: a product from the reaction of nitric oxide with superoxide. Am J Physiol 268:L699–L722.
10. Minhaz U, Tanaka M, Tsukamoto H, Watanabe K, Koide S, Shohtsu A, Nakazawa H. 1996. Effect of MCI-186 on postischemic reperfusion injury in isolated rat heart. Free Rad Res 24(5):361–367.
11. Ishida H, Hirota Y, Nakazawa H. 1993. Effect of subskining concentrations of saponin on intracellular Ca^{2+} and plasma membrane fluidity in cultured cardiac cells. Biochim Biophys Acta 1145:58–62.
12. Carreras MC, Pargament GA, Catz SD, Poderoso JJ, Boveris A. 1994. Kinetics of nitric oxide and hydrogen peroxide production and formation of peroxynitrite during the respiratory burst of human neutrophils. FEBS Lett 341:65–68.
13. Ischiropolous H, Zhu L, Beckman JS. 1992. Peroxinitrite formation from macrophage-derived nitric oxide. Arch Biochem Biophys 298:446–451.
14. Pronai L, Nakazawa H, Ichimori K, Saigusa Y, Ohkubo T, Hiramatsu K, Arimori S, Feher J. 1992. Time course of superoxide generation by leukocytes—the MCLA chemiluminescence system. Inflammation 16:437–450.
15. Ludwig PW, Hunninghake DB, Hoidal JR. 1982. Increased leukocyte oxidative metabolism in hyperlipoproteinaemia. Lancet 2:348–350.
16. Green LC, Wagner DA, Glogowski J, Skipper PL, Wisnok JS, Tannenbaum SR. 1982. Analysis of nitrate, nitrite, and [^{15}N]nitrate in biological fluids. Anal Biochem 126:131–138.
17. Beckman JS, Beckman TW, Chen J, Marshall PA, Freeman BA. 1990. Apparent hydroxyl radical production by peroxynitrite: implications for endothelial injury from nitric oxide and superoxide. Proc. Natl Acad Sci USA 87:1620–1624.
18. Kettle AJ, Gedye CA, Hampton MB, Winterbourn CC. 1995. Inhibition of myeloperoxidase by benzoic acid hydrazides. Biochem J 308:559–563.
19. Floris R, Piersma SR, Yang G, Jones P, Wever R. 1993. Interaction of myeloperoxidase with peroxynitrate: a comparison with lactoperoxidase, horseradish peroxidase and catalase. Eur J Biochem 215:767–775.
20. Ishida H, Ichimori K, Hirota Y, Fukahori M, Nakazawa H. 1996. Peroxynitrite-induced cardiac myocyte injury. Free Rad Biol Med 20:343–350.
21. Fukuyama N, Ichimori K, Su Z, Ishida H, Nakazawa H. 1996. Peroxynitrite formation from activated human leukocytes. Biochem Biophys Res Commun 224:414–419.
22. Entman MK, Youker K, Shoji T, Kukielka G, Shappell SB, Taylor AA, Smith CW. 1992. Neutrophil induced oxidative injury of cardiac myocytes (a compartmented system requiring CD11b/CD18-ICAM-1 adherence). J Clin Invest 90:1335–1345.
23. Youker K, Smith CW, Anderson DC, Miller D, Michael LH, Rossen RD, Entman ML. 1992. Neutrophil adherence to isolated adult cardiac myocytes (induction by cardiac lymph collection during ischemia and reperfusion). J Clin Invest 89:602–609.

24. Fukuyama N, Takebayashi Y, Hida M, Ishida H, Ichimori K, Nakazawa H. 1997. Clinical evidence of peroxynitrite formation in chronic renal failure patients with septic shock. Free Rad Biol Med 22(5):771–774.
25. Oshima H, Brouet I, Bartsch H. 1990. Nitrotyrosine as a new marker for endogenous nitrosation and nitration of proteins. Fundam Chem Toxicol 28:647–652.
26. Sokolovsky M, Riordan JF, Vallee BL. 1967. Conversion of 3-nitrotyrosine to 3-aminotyrosine in peptides and proteins. Biochem Biophys Res Commun 27:20–25.

REAL-TIME MEASUREMENT OF NITRIC OXIDE IN CORONARY OUTFLOW DURING TRANSIENT MYOCARDIAL ISCHEMIA AND REPERFUSION

YOSHIAKI FUKUHIRO, SEIICHI MOCHIZUKI, MASAMI GOTO, TAKASHI FUJIWARA, TAIJI MURAKAMI, HIROSHI INADA, HISAO MASAKI, ICHIRO MORITA, and FUMIHIKO KAJIYA

Kawasaki Medical School

Summary. To examine the kinetics and determinants of the production and release of nitric oxide (NO) from a heart during transient myocardial ischemia and reperfusion, we directly measured NO in the coronary effluent from isolated beating rat hearts during reperfusion following transient myocardial ischemia using a newly developed NO microelectrode. Isolated rat hearts were perfused with an oxygenated Krebs–Henseleit buffered solution and were subjected to one-minute or ten-minute global ischemia followed by reperfusion at 100 cmH_2O. The time course of measured NO current during reperfusion showed a monophasic pattern in the case of one-minute ischemia but a biphasic pattern in the case of ten-minute ischemia. Immediately after the onset of reperfusion, coronary flow increased almost stepwise after one-minute ischemia and gradually after ten-minute ischemia. After one-minute ischemia, measured NO current first stayed at a relatively low level and then gradually increased (monophasic pattern). After ten-minute ischemia, following a transient peak, the measured NO current gradually increased (biphasic pattern). There was an excellent linear relationship between coronary flow rate and the calculated amount of NO during the second rise of NO release in the case of ten-minute ischemia. These data suggest that the time course of NO release from a heart during reperfusion is determined by the production of NO during ischemia, which is ischemic-duration dependent, and by the reperfusion-rate dependent mechanism.

INTRODUCTION

Nitric oxide (NO), which is known as endothelium-derived relaxing factor (EDRF), has been widely and extensively studied in a range of organ systems, including the heart [1]. Growing experimental evidence suggests that NO plays

S. Mochizuki, N. Takeda, M. Nagano and N. Dhalla (eds.). THE ISCHEMIC HEART.

important physiological roles in the regulation of coronary vascular tone [2] and myocardial contractility [3]. Recently, it has been suggested that endogenous NO contributes to the maintenance of coronary flow rate while it reduces the contractile function of the ischemic heart, thus improving the myocardial energy supply–expenditure balance [4,5]. It is conceivable that NO would also modify the coronary regulation during reperfusion following transient ischemia. However, there are still many uncertainties about the roles of NO in the regulation of coronary circulation during myocardial ischemia and reperfusion [4–7]. One of the major reasons for this limited understanding is the difficulty of direct real-time measurement of NO in the coronary circulation due to the high reactivity and short half-life of NO [2]. The time course and kinetics of production and the release of NO in the coronary circulation during myocardial ischemia and reperfusion are still unclear. Recently, several types of NO electrodes have been developed [8–10], and in vivo real-time measurement of NO has become possible [11,12]. Using a newly developed NO microelectrode, we have succeeded in real-time direct measurement of NO in the vascular media of isolated vessels and have confirmed the applicability of this measurement to the cardiovascular system [13]. In the work reported in this chapter, we observed the real-time change in NO released from an isolated beating rat heart using an NO electrode during myocardial ischemia and reperfusion.

METHODS

Wister strain male rats ($n = 10$) of 300–350 g were used in this study. Each rat was anesthetized with diethyl ether, and 200 IU heparin was injected into the femoral vein. Each heart was rapidly excised and was placed in an ice-cold solution of Krebs–Henseleit bicarbonate buffer (KHBB; Sigma Chemical Co., Missouri, USA) to produce cardiac arrest. The isolated heart was mounted on a perfusion apparatus by cannulating the aorta and was perfused in a nonrecirculating Langendorff mode with an oxygenated (95% O_2 and 5% CO_2) KHBB at a pressure of 100 cmH_2O. This perfusate was kept at 37 ± 0.5°C.

The coronary flow rate was measured using an electromagnetic flow meter (Model MFV-3100; Nihon Kohden, Tokyo, Japan), connected to a catheter inserted in the pulmonary artery. In this study, an NO-sensing microelectrode (100 μm in diameter, Model NOE-10W; Inter Medical, Nagoya, Japan) and an NO monitor (Model NO-501; Inter Medical) were used. This NO-sensing microelectrode consists of Pt-Ir alloy with three-layer coatings at the NO-detecting tip (figure 1). NO diffuses selectively through the coatings and is oxidized on the surface of a Pt-Ir electrode. The oxidation current of NO is measured as NO concentration (1 pA ≈ 1 nM NO). To measure NO concentration in the coronary effluent, the NO-sensing microelectrode was located in a small chamber that was connected to the catheter inserted into the pulmonary artery. This chamber was electromagnetically shielded in order to eliminate the effect of environmental electrical noise. After confirming a stable signal of NO current, each heart was subjected to either one minute or 10 minutes of cessation of perfusion. Following ischemia, hearts were reperfused with an oxygenated KHBB at a pressure of 100 cmH_2O.

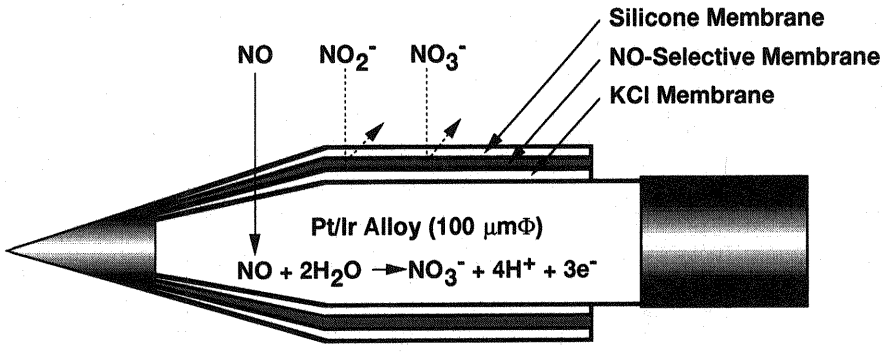

Figure 1. NO-sensing electrode.

RESULTS

Figure 2 shows the typical time course of coronary flow rate and NO after one-minute ischemia. Coronary flow rate increased immediately after the onset of reperfusion and reached a maximum level within 10 seconds after reperfusion. Coronary flow rate then decreased gradually and returned to a steady level (preischemic level) after two minutes of reperfusion. NO concentration simultaneously measured in the coronary effluent during reperfusion showed a monophasic pattern, in which NO current started increasing after approximately 30 seconds of reperfusion and reached a peak of approximately 20 pA after 100 seconds of reperfusion. Measured NO current then decreased gradually and was stabilized after four minutes of reperfusion. These patterns of coronary flow and NO current, i.e., a rapid increase in flow and a gradual monophasic change in NO current, were observed in all hearts studied (n = 5). In comparison with the preischemic levels, the maximum level of NO current was higher by about 10 pA.

Figure 3 shows the typical time course of coronary flow rate and NO current after 10-minute ischemia. In contrast to the rapid rise pattern of coronary flow following one-minute ischemia (figure 2), coronary flow after 10-minute ischemia increased gradually after the onset of reperfusion and reached a peak level from 4 to 5 minutes after reperfusion. The pattern of measured NO current in the coronary effluent during reperfusion was biphasic, which was different from that after one-minute ischemia (monophasic pattern; see figure 2). Measured NO current reached a transient peak at approximately 17 pA within 15 seconds from the onset of reperfusion and then decreased. After that, measured NO current started increasing again after approximately 90 seconds of reperfusion and reached a plateau at approximately 45 pA after four minutes of reperfusion. These patterns of coronary flow and NO current, i.e., a gradual increase in flow and a biphasic change in NO current, were observed in all the hearts studied (n = 5). The maximum level of NO current was higher by about 20 pA, compared with the preischemic levels.

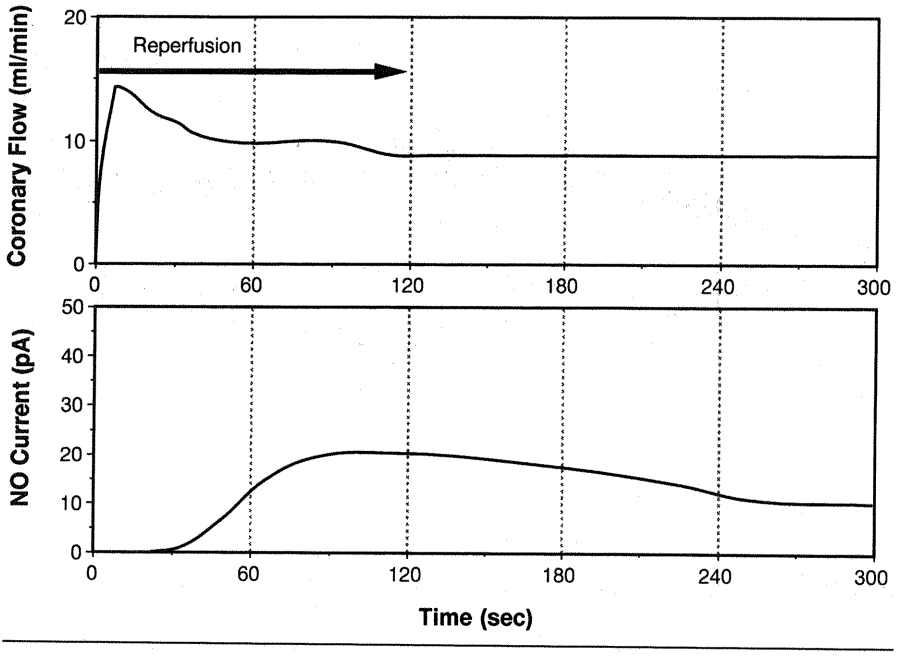

Figure 2. Time course of NO concentration and coronary flow rate after one-minute ischemia.

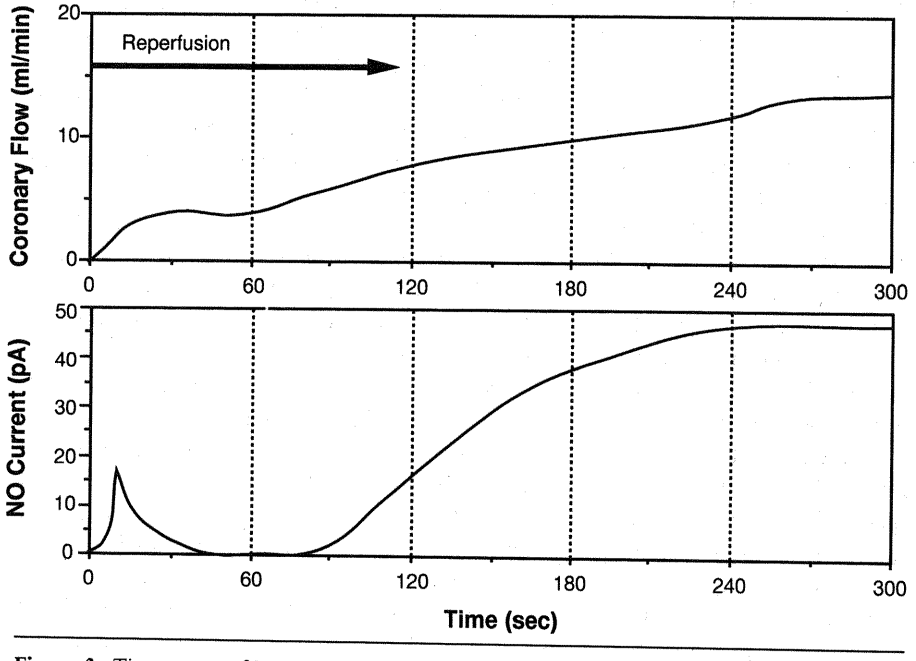

Figure 3. Time course of NO concentration and coronary flow rate after 10-minute ischemia.

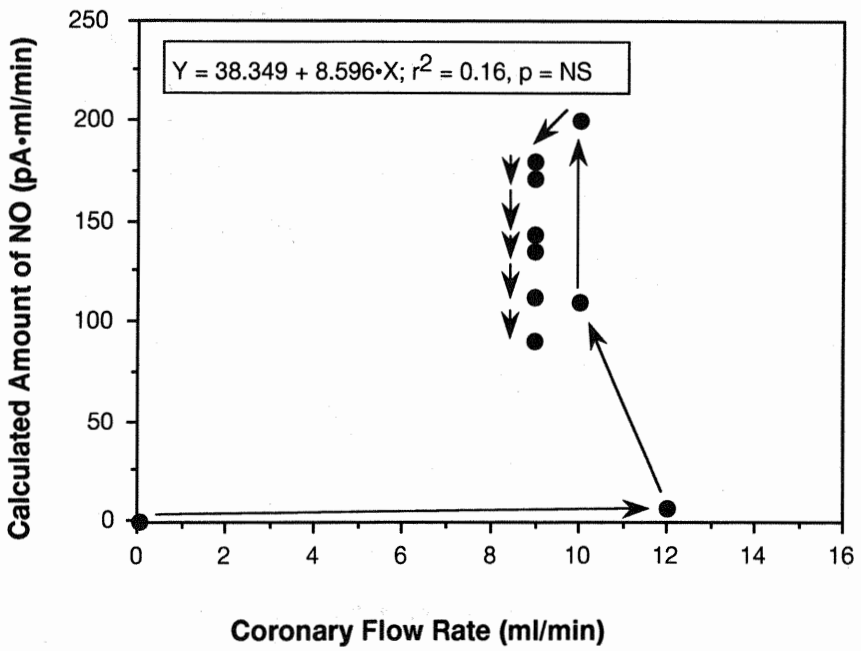

Figure 4. The relationship between the calculated amount of NO and coronary flow rate in the case of one-minute ischemia.

We analyzed the relationship between coronary flow rate and the calculated amount of NO, a product of coronary flow rate and measured NO current, both of which were measured every 30 seconds during reperfusion (figures 4 and 5). In the case of one-minute ischemia (figure 4), with an almost stepwise increase in coronary flow rate (see figure 2 above), the calculated amount of NO started to increase within 30 seconds after the beginning of reperfusion. While coronary flow rate stayed at a stable level (about 9 mL/min), the calculated amount of NO increased to a narrow range (about 100 pA · mL/min).

Figure 5 shows the relationship between coronary flow rate and the calculated amount of NO in every 30-second interval during the second rise (after 90 seconds) in the case of 10-minute ischemia. Coronary flow rate increased gradually and showed an excellent linear correlation ($Y = -497.885 + 83.402 \cdot X$; $r^2 = 0.94$, $p < 0.01$) with measured NO current. There was no linear relationships between coronary flow rate and the calculated amount of NO during the initial transient peak observed within one minute of reperfusion (p = NS).

DISCUSSION

In the study reported in this chapter, we successfully measured directly the NO released from an isolated beating heart on a real-time basis using an NO electrode

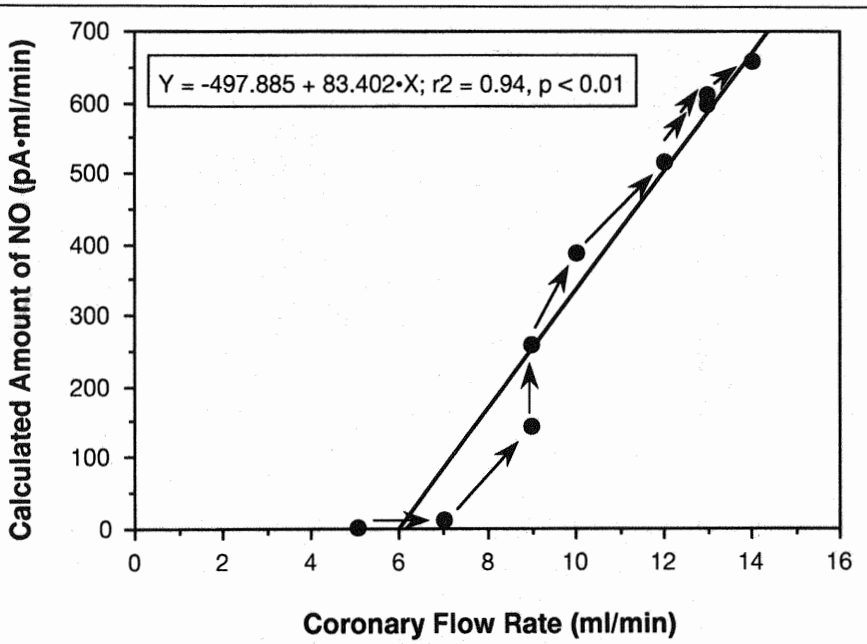

Figure 5. The relationship between the calculated amount of NO and coronary flow rate in the case of 10-minute ischemia.

and demonstrated that the time course of NO release during reperfusion following transient myocardial ischemia showed a monophasic pattern after one-minute ischemia but a biphasic pattern after 10-minute ischemia.

It has been reported that myocardial ischemia augments NO production in the heart. Node et al. [5,6] measured plasma nitrate and nitrite concentrations in a dog using the Griess method and observed that those plasma NO end products increased during ischemia. Zweier et al. [7] measured NO in an isolated rat heart using electron paramagnetic resonance and observed a strong triplet signal during ischemia as a function of the duration of ischemia. Accordingly, in the study reported here, the observed NO release from a heart following ischemia may be at least partly attributable to the production and accumulation of NO during ischemia. As a support for this explanation, the measured NO current level after the onset of reperfusion was higher in the case of longer (10-minute) ischemia (figure 3) than in that of shorter (one-minute) ischemia (figure 2).

It has been shown that NO production and release are enhanced by chemical factors, including acetylcholine, bradykinin, histamine, Ca^{2+} ionophores, inflammatory cytokines, etc. [14–18], and by flow-related wall shear stress [19–21]. During myocardial ischemia, some of the chemical factors such as bradykinin and histamine are released from the heart [22,23]. Thus, it is possible that NO was produced

during ischemia at least partly by these chemical factors, although these were not measured in the study reported here. Intracellular acidosis during ischemia may contribute to NO production: acidosis leads to an increase in the intracellular sodium via the Na–H exchanger, and this increased sodium leads to an increase in the intracellular Ca^{2+} influx via the Na–Ca^{2+} exchanger [24,25]. Previous studies [26–28] have suggested that NO production is increased with intracellular Ca^{2+}.

In the present study, the time courses of coronary flow after one-minute and 10-minute ischemia were different from each other—a rapid-rise pattern like that of reactive hyperemia after one-minute ischemia but a gradual-rise pattern after 10-minute ischemia. This difference in coronary flow rates may be at least partly attributable to the duration of ischemia. Prolonged ischemia could cause extended interstitial edema, and Heslinga et al. [29] suggested that coronary resistance increases due to interstitial edema. These different patterns of coronary flow rate during reperfusion may affect the flow-induced NO production during reperfusion. Kuchan and Frangos [21] reported that NO oxidation products released from the endothelial cells increase with increasing shear stress. Kanai et al. [19] measured NO directly using a porphyrinic microsensor and reported shear stress-induced NO release from cultured vascular endothelial cells. Furthermore, we measured NO directly in the vascular media of an isolated canine femoral artery using the microelectrode and observed a linear relationship between the perfusion flow rate and the measured NO current [13].

In the case of one-minute ischemia, measured NO current during reperfusion increased after a rapid increase in coronary flow rate. It is possible that coronary vascular endothelium may response quickly to the sudden change in wall shear stress and that NO may be released into coronary circulation [19,30]. In the case of 10-minute ischemia, since the coronary flow rate within one minute after the onset of reperfusion is lower than that in one-minute ischemia, the first transient peak following 10-minute ischemia is likely to reflect primarily the washout of accumulated NO during the longer ischemic period. On the other hand, the second rise of NO current (>1 min) is mainly attributable to the flow- (wall shear stress-) dependent NO production. In support of these explanations, we recognized a linear correlation between coronary flow rate and released NO during the second rise of NO in the case of 10-minute ischemia, but not in the initial peak of NO (<1 min; see figure 4). Accordingly, it is suggested that the effects of the washout of accumulated NO and the sudden change in the wall shear stress may appear separately in the time course of NO release after 10-minute ischemia but may overlap each other in the case of one-minute ischemia. However, we cannot neglect the possible contribution of shear stress-induced NO production to the biphasic pattern of NO release after 10-minute ischemia, since biphasic shear stress-induced NO production has been reported [31].

In conclusion, the production, release, and kinetics of NO during myocardial ischemia and reperfusion may be related to the duration of myocardial ischemia and perfusion rate (wall shear stress), although it has not been possible to evaluate these factors separately. Future investigations are thus still required.

ACKNOWLEDGMENTS

This study was supported by Grant-in-Aid 08671553 for Scientific Research (C) from the Ministry of Education, Science, and Culture, Japan, and by a research project grant (No. 8-203) from Kawasaki Medical School.

REFERENCES

1. Moncada S, Palmer RM, Higgs EA. 1991. Nitric oxide: physiology, pathophysiology, and pharmacology. Pharmacol Rev 43(2):109–142.
2. Kelm M, Schrader J. 1990. Control of coronary vascular tone by nitric oxide. Circ Res 66(6):1561–1575.
3. Hare JM, Colucci WS. 1995. Role of nitric oxide in the regulation of myocardial function. Prog Cardiovasc Dis 38(2):155–166.
4. Kelly RA, Balligant JL, Smith TW. 1996. Nitric oxide and cardiac function. Circ Res 79(3):363–380.
5. Node K, Kitakaze M, Kosaka H, Komamura K, Minamino T, Inoue M, Tada M, Hori M, Kamada T. 1996. Increased release of NO during ischemia reduces myocardial contractility and improves metabolic dysfunction. Circulation 93(2):356–364.
6. Node K, Kitakaze M, Kosaka H, Komamura K, Minamino T, Tada M, Inoue M, Hori M, Kamada T. 1995. Plasma nitric oxide end products are increased in the ischemic canine heart. Biochem Biophys Res Commun 211(2):370–374.
7. Zweier JL, Wang P, Kuppusamy P. 1995. Direct measurement of nitric oxide generation in the ischemic heart using electron paramagnetic resonance spectroscopy. J Biol Chem 270(1):304–307.
8. Malinski T, Taha Z. 1992. Nitric oxide release from a single cell measured *in situ* by a porphyrinic-based microsensor. Nature 358:676–678.
9. Shibuki K. 1990. An electrochemical microprobe for detecting nitric oxide release in brain tissue. Neurosci Res 9(1):69–76.
10. Ichimori K, Ishida H, Fukahori M, Nakazawa H, Murakami E. 1994. Practical nitric oxide measurement employing a nitric oxide-selective electrode. Rev Sci Instrum 65(8):2714–2718.
11. Tschudi MR, Mesaros S, Luscher TF, Malinski T. 1996. Direct in situ measurement of nitric oxide in mesenteric resistance arteries. Hypertension 27(1):32–35.
12. Vallance P, Patton S, Bhagat K, MacAllister R, Radomski M, Moncada S, Malinski T. 1995. Direct measurement of nitric oxide in human beings. Lancet 345:153–154.
13. Mochizuki S, Goto M, Hirano K, Fukuhiro Y, Kajiya F. 1996. Direct measurement of nitric oxide in arterial wall using newly developed nitric oxide microsensor. Biomed Eng 8(4):18–23.
14. Hecker M, Mulsch A, Bassenge E, Busse R. 1993. Vasoconstriction and increased flow: two principal mechanisms of shear stress-dependent endothelial autacoid release. Am J Physiol 265(3, Pt 2):H828–H833.
15. Cowan CL, Cohen RA. 1991. Two mechanisms mediate relaxation by bradykinin of pig coronary artery: NO-dependent and independent responses. Am J Physiol 261(3, Pt 2):H830–H835.
16. Masini E, Bianchi S, Mugnai L, Gambassi F, Lupini M, Pistelli A, Mannaioni PF. 1991. The effect of nitric oxide generators on ischemia reperfusion injury and histamine release in isolated perfused guinea-pig heart. Agents Actions 33(1–2):53–56.
17. Ungureanu LD, Balligand JL, Kelly RA, Smith TW. 1995. Myocardial contractile dysfunction in the systemic inflammatory response syndrome: role of a cytokine-inducible nitric oxide synthase in cardiac myocytes. J Mol Cell Cardiol 27(1):155–167.
18. Oddis CV, Finkel MS. 1995. Cytokine-stimulated nitric oxide production inhibits mitochondrial activity in cardiac myocytes. Biochem Biophys Res Commun 213(3):1002–1009.
19. Kanai AJ, Strauss HC, Truskey GA, Grews AL, Crunfeld S, Malinski T. 1995. Shear stress induces ATP-independent transient nitric oxide release from vascular endothelial cells, measured directly with a porphyrinic microsensor. Circ Res 77(2):284–293.
20. Korenaga R, Ando J, Tsuboi H, Yang W, Sakuma I, Toyo-oka T, Kamiya A. 1994. Laminar flow stimulates ATP- and shear stress-dependent nitric oxide production in cultured bovine endothelial cells. Biochem Biophys Res Commun 198(1):213–219.
21. Kuchan MJ, Frangos JA. 1994. Role of calcium and calmodulin in flow-induced nitric oxide production in endothelial cells. Am J Physiol 266(3, Pt 1):C628–C636.

22. Parratt JR, Vegh A, Papp JG. 1995. Bradykinin as an endogenous myocardial protective substance with particular reference to ischemic preconditioning—a brief review of the evidence. Can J Physiol Pharmacol 73(7):837–842.
23. Masini E, Giannella E, Bianchi S, Palmerani B, Pistelli A, Mannaioni PF. 1988. Histamine release in acute coronary occlusion–reperfusion in isolated guinea-pig heart. Agents Actions 23(3–4):266–269.
24. Tani M, Neely JR. 1989. Role of intracellular Na^+ in CA^{2+} overload and depressed recovery of ventricular function of reperfused ischemic rat hearts. Possible involvement of H^+/Na^+ and Na^+/Ca^{2+} exchange. Circ Res 65(4):1045–1056.
25. Marban E, Kitakaze M, Chacko VP, Pike MM. 1988. Ca^{2+} transients in perfused hearts revealed by gated ^{19}F NMR spectroscopy. Circ Res 63(3):673–678.
26. Fleming I, Busse R. 1995. Control and consequences of endothelial nitric oxide formation. Adv Pharmacol 34(187):187–206.
27. Busse R, Mulsch A. 1990. Calcium-dependent nitric oxide synthesis in endothelial cytosol is mediated by calmodulin. FEBS Lett 265(1–2):133–136.
28. Boulanger C, Schini VB, Moncada S, Vanhoutte PM. 1990. Stimulation of cyclic GMP production in cultured endothelial cells of the pig by bradykinin, adenosine diphosphate, calcium ionophore A23187 and nitric oxide. Br J Pharmacol 101(1):152–156.
29. Heslinga JW, Allaart CP, Westerhof N. 1996. Intramyocardial pressure measurements in the isolated perfused papillary muscle of rat heart. Eur J Morphol 34(1):55–62.
30. Corson MA, James NL, Latta SE, Nerem RM, Berk BC, Harrison DG. 1996. Phosphorylation of endothelial nitric oxide synthase in response to fluid shear stress. Circ Res 79(5):984–991.
31. Ayajiki K, Kindermann M, Hecker M, Fleming I, Busse R. 1996. Intracellular pH and tyrosine phosphorylation but not calcium determine shear stress-induced nitric oxide production in native endothelial cells. Circ Res 78(5):745–746.

This Page Intentionally Left Blank

PRODUCTION OF HYDROGEN PEROXIDE DURING HYPOXIA–REOXYGENATION IN ISOLATED MYOCYTES

RYUJI UEDA, NOBURU KONNO, MASAKI NAKATANI, TOSHIKI IWATA, YOSHIHISA ARATA, KATSUMITI IIJIMA, KAZUAKI NISHIO, EIICHI GESHI, TOSHIKUNI YANAGISHITA, TAKASHI KATAGIRI, and YASUMITSU NAKAI

Showa University School of Medicine

Summary. Active oxygen species, including hydrogen peroxide (H_2O_2), have been implicated in myocardial reperfusion injury. Recently, spin-trap agents and biochemical techniques applied to intact hearts have shown that H_2O_2 is generated by leukocytes, by endothelial cells, and by mitochondria in myocytes. In this study, we used electron microscopy and the cerium (Ce) method to histologically investigate H_2O_2 formation during hypoxia–reoxygenation and its toxic effects on myocardium. This Ce method involves the formation of an electron-dense precipitate when H_2O_2 reacts with cerium chloride ($CeCl_3$). Single myocytes were obtained from rat hearts by the collagenase method. Isolated myocytes were reoxygenated for 15 minutes after 30 minutes of hypoxia. Digitonin and $CeCl_3$ were added to make cell membranes permeable and to detect intracellular H_2O_2 by electron microscopy. In the control group, the ultrastructure was well preserved and no dense deposits were found in myocytes. However, in the hypoxia–reoxygenation group, precipitates, which were cerium–H_2O_2 reaction products, were found along swollen mitochondria. Moreover, in the hypoxia–reoxygenation group, cell viability was reduced to 72% of control. These results indicate that H_2O_2 is generated by mitochondria and that its relese into cytosol may lead to myocyte death during hypoxia–reperfusion.

INTRODUCTION

Free radicals have been implicated in myocardial reperfusion injury. Hydrogen peroxide (H_2O_2) serves as a precursor for highly reactive oxygen intermediates. Although H_2O_2 is a normal cellular metabolite, it can generate extremely reactive hydroxyl radicals through transition metal ion-catalyzed reactions. Under normal conditions, H_2O_2 is catalytically reduced to H_2O by either catalase or glutathione

S. Mochizuki, N. Takeda, M. Nagano and N. Dhalla (eds.). THE ISCHEMIC HEART.

peroxides as the cellular defense mechanisms. In such states as ischemia–reperfusion and hypoxia–reoxygenation, the activities of catalase and glutathione peroxide seem to be decreased, and the resulting increase in H_2O_2 and the hydroxyl radical (·OH), which originate from H_2O_2 by such chemical changes as the Fenton and Harbaer–Weiss reactions, causes, myocardial injury. Several studies have demonstrated histochemically that H_2O_2 is generated by leukocytes [1,2] and endothelial cells [3–5] and by mitochondria [6,7] in myocytes. Because cerium chloride ($CeCl_3$) reacts with H_2O_2 and forms insoluble precipitates, the cerium method is popular in cytochemical studies for detecting production of H_2O_2 [8]. However, Ce seems to have difficulty penetrating the cell membrane; hence, the detection of H_2O_2 formation in situ in myocytes is difficult with this technique. In the study reported here, we adopted a permeabilization technique that uses digitonin. When the dose and application time are appropriate, digitonin makes the plasma membrane permeable without affecting intracellular organelles. Using this technique, we histologically investigated both intracellular H_2O_2 formation during hypoxia–reoxygenation and its toxic effects on myocardium.

MATERIAL AND METHODS

Cell isolation

We prepared cardiac myocytes from male Wistar rats (200–300 g body weight) using collagenase, as decsribed previously [9]. Briefly, the hearts were excised after the rat had been anesthetized with an intraperitoneal injection of 70 mg/kg pentobarbital and were perfused retrogradely with well-oxygenated Krebs–Hensleit buffer for 40 minutes. Then the perfusate was changed to a medium consisting of Joklik's minimum, 60 mM taurine, and 5 mM N-2-hydroxyethyl-piperazine-N′-2-ethanesulfonic acid, pH 7.4. After five minutes of perfusion, 120 U/mL of collagenase and 12 μM $CaCl_2$ were added to the perfusion medium. Twenty minutes after the start of perfusion with collagenase, the ventricles were removed and minced with scissors. The minced heart muscle was incubated in the presence of 250 U/mL of collagenase and 1.5% bovine serum albumin for 30 minutes. For the last 20 minutes of incubation, the Ca concentration was increased to 50 μM. Then the suspension was filtered through a nylon mesh, and the myocytes were washed three times by gravity settling with a medium containing 1.0% albumin. Finally, the suspension medium was changed to a medium consisting of 250 mM sucrose, 1 mM ethylenediamine-N,N,N′,N′-tetra-acetic acid disodium salt, and 20 mM 3-N-morpholinopropanesulfonic acid at pH 7.2. The concentration of myocytes was adjusted to approximately 5×10^6 cells/mL.

Ultrastructural observation

The isolated myocytes, suspended in 0.25 M sucrose buffer, were incubated at room temperature. Some myocytes were aerated with 95% O_2 and 5% CO_2 gas for 45 minutes as a control group; others were incubated with bubbling 100% N_2 gas for 30 minutes and were then reoxygenated via aeration with 95% O_2 and 5% CO_2 gas

for 15 minutes as the hypoxia–reoxygenated group. After 45 minutes of incubation, digitonin and $CeCl_3$ were added to the incubation medium to final concentrations of 0.07 mg/mL and 0.5 mM, respectively. Immediately after the addition of digitonin and $CeCl_3$, the suspension was centrifuged at 3000× *g* for three minutes. The supernatant was discarded, and the pellet was fixed with 2.5% glutaraldehyde in 0.1 M of sodium-cacodylate (pH 7.4) at 4°C for two hours. After being rinsed in cacodylate overnight, the samples were postfixed in 1% osmium tetroxide in 0.1 M sodium cacodylate at 4°C for 60 minutes and then dehydrated with ethanol and propylene oxide. Samples were then embedded in an Epon–Araldite mixture. Silver–gold sections were prepared from fixed samples with an ultramicrotome and placed on copper grids. Most sections were counterstained with only uranyl acetate for eight minutes to allow visualization of cerium. Other samples were unstained and used for analytic electron microscopy.

Ultrathin uranyl acetate-stained sections were prepared from five to seven blocks of each sample; three to six grids were prepared from each block. At least 50 randomly selected myocytes were examined and photographed with an electron microscope, at an accelerating voltage of 75 keV.

Microbeam analysis

Unstained sections of fixed myocytes were carbon coated and subjected to electron microbeam analysis in an energy-dispersive x-ray detector to confirm that the electron-dense deposits observed in myocytes were composed of cerium. The microprobe conditions included 100 kV of accelerating voltage, a spot diameter of 30–50 nm, and 100–200 seconds counting time.

Statistical analysis

Results are expressed as mean ± SEM. Stastical analysis of data was performed with Student's *t*-test, and $p < 0.05$ was considered to indicate significance.

RESULTS

Cell viability

Figures 1 and 2 show light microscopic findings in the control and hypoxia–reoxygenation groups. The percentage of viable (rod-shaped), isolated myocytes in the control group (87 ± 1%; $n = 5$) was significantly higher than in the hypoxia–reoxygenation group (62 ± 1%; $n = 5$), a finding that suggests cellular injury occurs during hypoxia–reoxygenation.

Electron micrographs

Figure 3 and 4 show electron microscopic findings in the control group. The cell membranes of myocytes were slightly injured due to digitonin and $CeCl_3$. However, the structures inside single myocytes were nearly normal, and no dense deposits could be found.

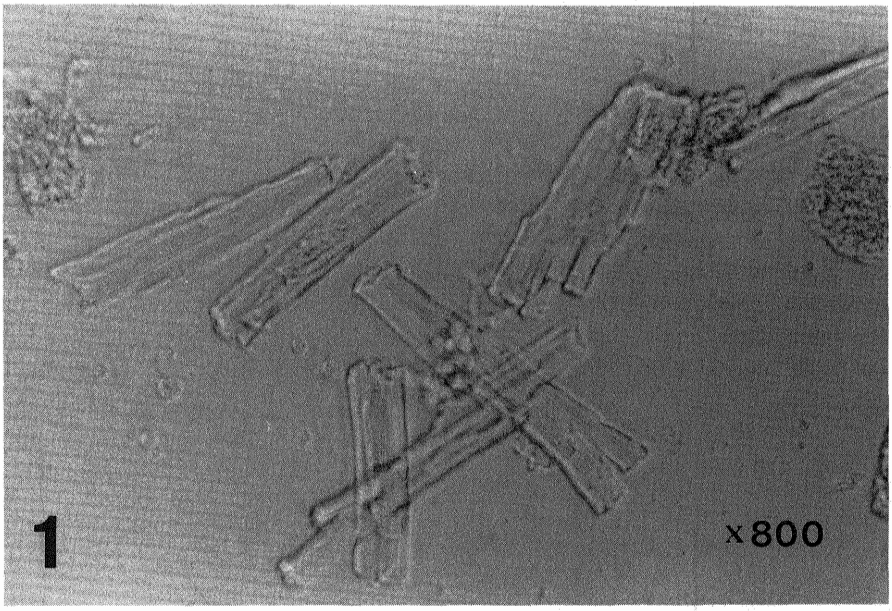

Figure 1. Light microscopic findings in the control group. The percentage of viable cells was 87% ± 1% (n = 5).

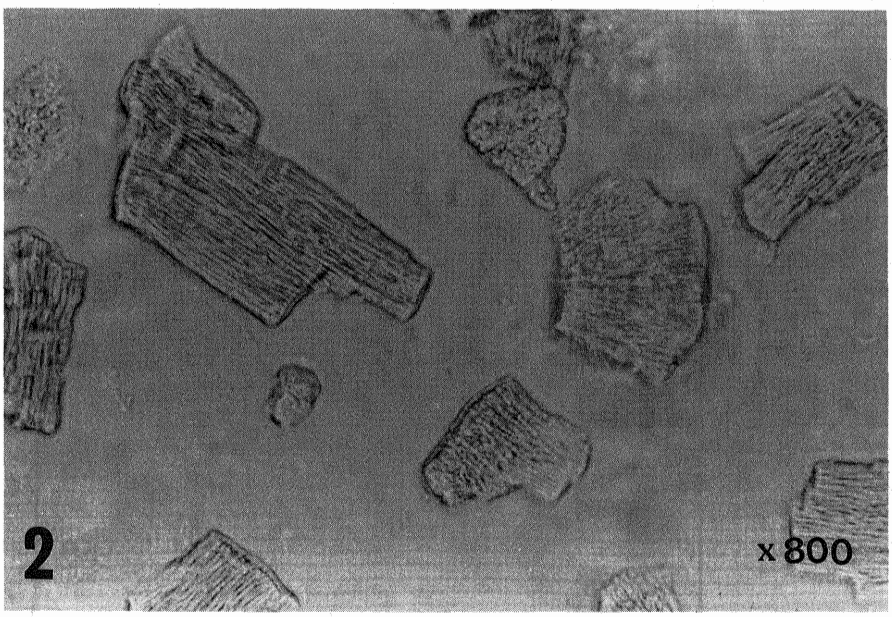

Figure 2. Light microscopic findings in the hypoxia–reoxygenation group. The percentage of viable cells was significantly decreased to 62% ± 1% (n = 5).

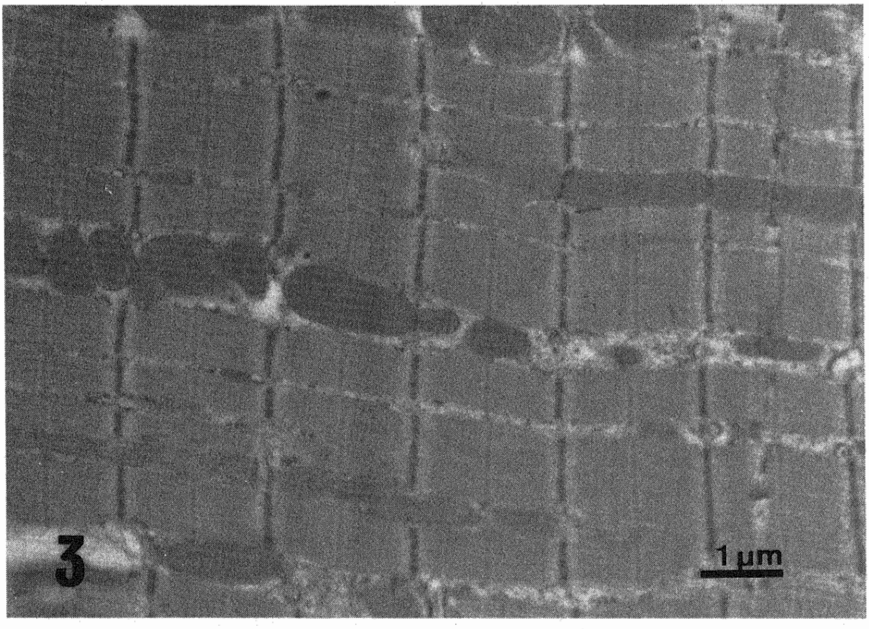

Figure 3. Electron microscopy findings of the rod-shaped cells in the control group. The ultrastructure of myocytes was nearly normal, and no dense deposits could be seen.

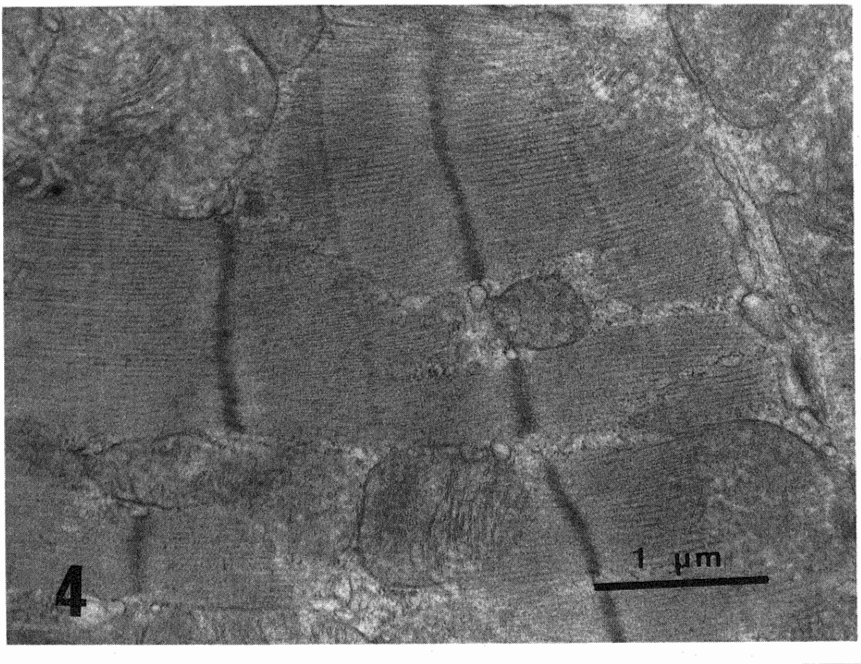

Figure 4. High-power electron micrograph of the control myocyte. The structure of mitocondria was nearly normal.

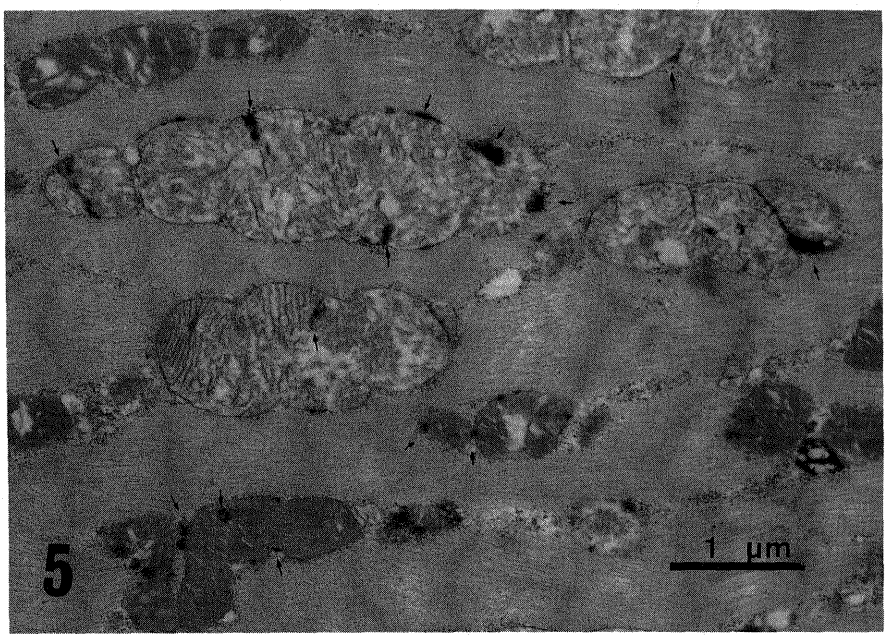

Figure 5. Electron microscopic findings in the hypoxia–reoxygenation group. Precipitates were seen along and inside mitochondria in nearly all rod-shaped cells (arrows).

Figures 5 and 6 show electron microscopic findings in the hypoxia–reoxygenation group. We found precipitates along and inside mitochondria in nearly all rod-shaped cells. However, we did not find precipitates at others sites, such as myofibrils. In many mitochondria, the matrix density was decreased and cristae were ruptured. Myofibrils were nearly normal.

Microanalysis x-ray

The results of electron microbeam analysis of precipitates are shown in figure 7. Because two peaks at 4.8 and 5.2keV corresponded to Ce [10], we suggest that these represent H_2O_2–Ce reaction products.

DISCUSSION

In this study, Ce–H_2O_2 reaction products were found along swollen mitochondria in isolated myocytes in the hypoxia–reoxygenated group. This finding suggests that H_2O_2 is released from injured mitochondria into the cytosol.

Reactive oxygen radicals have been postulated as one of the major causes of ischemia–reperfusion and hypoxia–reoxygenation injury, and H_2O_2 is one possible source of reactive oxygen intermediates. Mitochondria have been known to form H_2O_2 even under physiologic conditions [11]. However, H_2O_2 is catabolized imme-

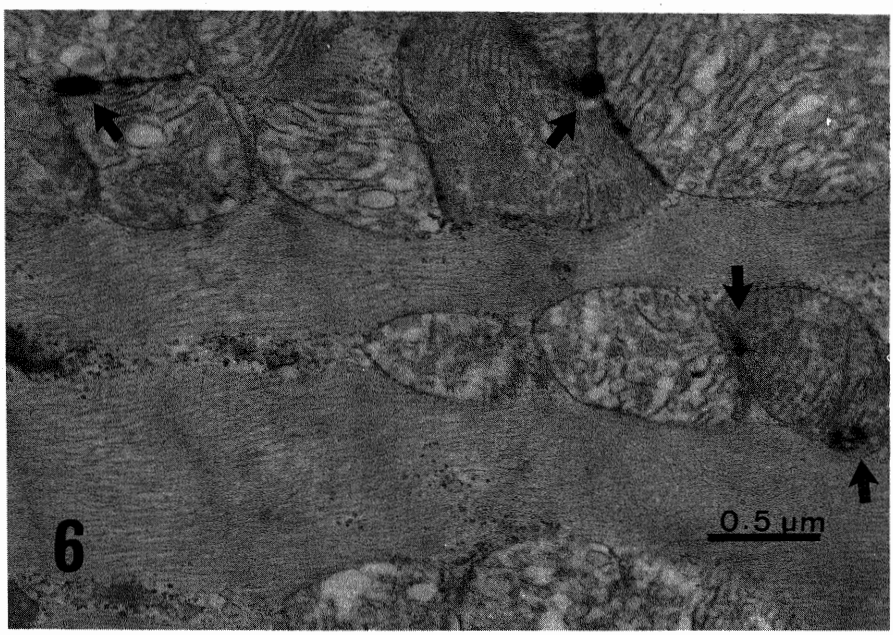

Figure 6. High-power electron micrograph of the rod-shaped cells subjected during 15 minute reoxygenation after 30 minutes hypoxia. There were many reaction products along and inside mitochondria (arrows), and in mitochondria the matrix density was decreased and cristae were ruptured.

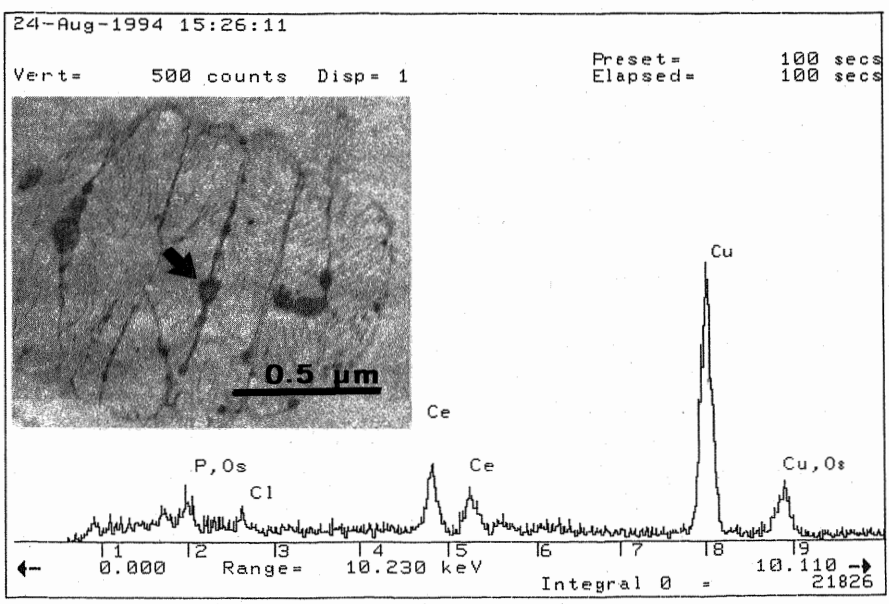

Figure 7. Results of x-ray microanalysis. The spectrum of an electron-dense deposit along a mitochondria in myocyte (arrow) exhibits cerium. The Os peaks, the P peak, and the Cl peak are artifacts of preparation. The Cu peak is intrinsic to the instrument.

diately by catalase and glutathione peroxidase under normal conditions. In ischemia–reperfusion, these enzymes, which are involved in cellular defense, seem less active, and the effect of reactive oxygen intermediates is increased.

The cerium method has often been used in histochemical studies to demonstrate H_2O_2 generation [7]. Brigg first used cerium for histochemistry and cytochemistry because of its electron density and its ability to trap H_2O_2 from leukocytes as a water-insoluble product of oxidase activity (most likely cerium perhydroxide [$Ce(OH)_2OOH$] [12]). This method has been used to demonstrate the positions of oxidase and phosphatase in leukocytes [13], macrophages [14], the thyroid [15], the lungs [16], and the heart [17–20]. Vandeplassche et al. [18] cut reperfused dog hearts after ischemia into pieces that were then fixed and incubated in a buffer containing $CeCl_3$ and NADH. They reported that H_2O_2 is generated by myocyte mitochondria by means of NADH-oxidase and increases in the ischemic state. Slezak [19] minced ischemia-reperfused rat hearts, which were then fixed and treated with $CeCl_3$ and various enzymes and inhibitors. After ischemia, H_2O_2–Ce-dependent precipitates were found at the sarcolemma and the abluminal side of endothelial cells; after reperfusion, they were also found in mitochondria and myofibrils.

These studies seem to suggest that the mitochondria are an important source of H_2O_2. However, in a preliminary study, we incubated minced heart muscles from ischemic and nonischemic regions with cerium but did not find Ce deposits in myocytes. Moreover, Shalfer [20] perfused rabbit hearts with a buffer containing $CeCl_3$ during reperfusion after ischemia and demonstrated Ce–H_2O_2-dependent products only at the luminal surface of endothelial cells. These findings suggest that cerium is unable to penetrate cell membranes under normal conditions. Therefore, demonstrating intracellular H_2O_2 may be impossible with a technique in which fixed samples are incubated with cerium.

In the study reported here, we used digitonin to make the sarcolemmal membrane permeable. Digitonin reacts with cholesterol within the membrane [21]. Because the cholesterol content of the sarcolemmal membrane is higher than that of other subcellular membranes, the function of organelles, such as mitochondria and the sarcoplasmic reticulum, is less affected. In the control group, fine structures were well preserved, a finding that suggests that digitonin did not seriously affect membranous organelles under our experimental conditions.

Konno showed that in permeabilized cells, the defense mechanisms against H_2O_2 were significantly impaired [22]; therefore, we cannot rule out the possibility that digitonin treatment decreases a cell's ability to catabolize H_2O_2 in the cytosol. However, because digitonin does not affect the mitochondria membrane, it does not affect the production of H_2O_2 by mitochondria or its release into the cytosol. Accordingly, the presence along mitochondria of dense deposits, which were confirmed by microbeam analysis to be composed of cerium, indicates that H_2O_2 is released from injured mitochondria in the hypoxia-reoxygenated state.

In conclusion, our findings suggest that the mitochondria produce H_2O_2 and release it into cytosol during hypoxia–reoxygenation. The increased level of H_2O_2 may injure myocytes and lead to their eventual deaths.

ACKNOWLEDGMENTS

The authors express their sincere thanks to Dr. Kazuhiro Debari, Dr. Seiji Shioda and Dr. Nobuko Naito, Showa University of Medicine, for their guidance and encouragement

REFERENCES

1. Briggs RT, Drath DB, Karnovsky MI, Karnovsky MJ. 1975. Localization of NADH oxidase on the surface of human polymorphonuclear leukocytes by a new cytochemical method. J Cell Biol 67:566–586.
2. Enger RL, Darlgren MD, Morris DD, Peterson MA, Schnid SGW. 1986. Role of leukocytes in response to acute myocardial ischemia and flow in dogs. Am J Physiol 251:H314–H322.
3. Jarasch ED, Bruder G, Heid HW. 1986. Significance of xanthine oxidase in capillary endothelial cells. Acta Physiol Scand 58:39–46.
4. Kim T, Kuzuya T, Hoshida S, Nishida M, Fuji H, Tada M. 1989. Reoxygenation induced endothelial cell injury provoked adhesion and diapedesis of neutrophila via arachidonate lipoxygenase metabolism. Circulation 80(4):II–400.
5. Camber DE, Park DA, Patterson G. 1985. Xanthine oxidase as a source of free radical damage in myocardial ischemia. J Mol Cell Cardiol 17:145–152.
6. Doroshow JH, Davies KJ. 1986. Redox cycling of anthracyclines by cardiac mitochondria. II. Formation of superoxide anion, hydrogen peroxide, and hydroxyl radical. J Biol Chem 261:3068–3074.
7. Zhang Y, Marcillat O, Giulvi C, Ernster L, Davies KJ. 1990. The oxidative inactivation of mitochondria electron transport chain components and ATPase. J Biol Chem 265:16330–16336.
8. Van-Noorden CJ, Frederiks W. 1993. Cerium methods for light and electron microscopical histochemistry. J Microsc 171:3–16.
9. Kaminishi T, Matsuoka T, Yanagishita T, Kako KJ. 1989. Increase vs. decrease of calcium uptake by isolated heart cells by H_2O_2 and HOCl. Am J Physiol 256:C598–607.
10. Bruijin WC, Schellen JPM, Buitenen JMH, Meulen J. 1980. X-ray microanalysis of colloidal-gold-labelled lysosomes in rat liver sinuoidal cells after incubation for acid phosphatase activity. Histochemistry 66:137–148.
11. Chance B, Sies H, Boveris A. 1979. Hydroperoxide metabolism in mammalian organs. Physiol Rev 59:527–605.
12. Briggs RT, Drath DB, Karnovsky MI, Karnovsky MJ. 1975. Localization of NADH oxidase on the surface of human polymorphonuclear leukocytes by a new cytochemical method. J Cell Biol 67:566–586.
13. Ohno YI, Hirai KI, Kanoh T, Uchino H, Ogawa K. 1982. Subcellular localization of H_2O_2 production in human neutrophils stimulated with particles and an effect of cytochalasin-B on the cells. Blood 60:253–260.
14. Kuroda M. 1986. Ultracytochemical localization of superoxide dismutase activity in rabbit alveolar macrophages: a comparative study using KO_2 or xanthine–xanthine oxidase as an O_2-generating system. Acta Histochem Cytochem 19:263–275.
15. Labato MA, Brigga RT. 1985. Cytochemical localization of hydrogen peroxide generating sites in the rat thyroid gland. Tissue Cell 17:889–900.
16. Warren JS, Kunkel RG, Simon RH, Johnson KJ, Ward PA. 1989. Ultrastructural cytochemical analysis of oxygen radical-mediated immunoglobulin A immune complex induced lung injury in the rat. Lab Invest 60:651–658.
17. Christie KN, Stoward PJ. 1982. The cytochemical reactivity of cerium ions with cardiac mucles. J Histochem Cytochem 15:656–672.
18. Vandeplassche G, Hermans C, Thone F, Borgers M. 1989. Mitochondrial hydrogen peroxide generation by NADH-oxidase activity following regional myocardial ischemia in the dog. J Mol Cell Cardiol 21:383–392.
19. Slezak J, Tribulova N, Pristacova J, Uhrik B, Khaper TTN, Kaul N, Singa PK. 1995. Hydrogen peroxide changs in ischemic and reperfused heart. Am J Pathol 147:772–781.
20. Shlafer M, Brosamer K, Forder JR, Simon RH, Ward PA, Grum CM. 1990. Cerium chloride as a histochemical marker of hydrogen peroxide in reperfused ischemic heart. J Mol Cell Cardiol 22:83–97.

21. Altschuld RA, Wenger WC, Lamka KG, Kindig OR, Capen CC, Mizuhira V, Vander HRS, Brierley GP. 1985. Structural and functional properties of adult rat heart myocytes lysed with digitonin. J Biol Chem 260:14325–14334.
22. Konno N, Kako KJ. 1992. Role of cellular defense against hydrogen peroxide-induced inhibition of myocyte respiration. Basic Res Cardiol 87:239–249.

OXYGEN FREE RADICALS ENHANCE ERGONOVINE-INDUCED CANINE CORONARY VASOCONSTRICTION

TAKU KONNO*, TAKU MATSUBARA*, SHOICHI IMAI*, MIKIO NAKAZAWA*, YUTAKA YOSHIDA*, TOMOYUKI HORI*, KEISUKE SUZUKI, TORU IDA*, KOTARO HIGUCHI*, YUSUKE TAMURA*, MASARU YAMAZOE*, and YOSHIFUSA AIZAWA***

* *Niigata University School of Medicine*
** *Kitasato University School of Medicine*

Summary. In order to examine the effects of oxygen free radicals on the ergonovine (EM)-induced coronary vasoconstriction in vivo, we administered EM (50 μg) into the ostium of the left coronary artery (LCA) and angiographically evaluated the change of diameter of the left anterior descending (LAD) and the left circumflex (LCX) coronary artery in eight dogs before and after selective administration of oxygen free radicals, generated by xanthine (X)-xanthine oxidase (XO) reaction, into the LCX. To investigate the participation of serotonin in EM-induced vasoconstriction, the concentrations of serotonin in the LCA and the coronary sinus (CS) were measured before and after administration of X − XO. The diameter of the LCX remained essentially unchanged after administration of X + XO. However, EM-induced constriction was greater in the LCX than in the LAD. The difference of serotonin (S) concentrations in the CS and in the ostium of the LCA [(S in CS) − (S in LCA)] gradually increased after administration of X + XO. Electron microscopy of endothelial surface revealed marked changes in the LCX, but such changes were not observed in the LAD. These results suggest that the enhancement of the EM-induced vasoconstriction of coronary artery by oxygen free radicals may probably be due to the morphological change and the rise in the S produced by oxidative injury.

INTRODUCTION

Coronary artery spasm plays in important role in the pathogenesis of ischemic heart disease, not only in variant angina but also in unstable angina, myocardial infarction, and sudden cardiac death [1–4]. However, the pathogenesis of coronary spasm is still unknown, and the elucidation of its mechanism remains an important clinical issue. Enhanced vasoconstriction to vasoactive stimuli has been noted in experimental

S. Mochizuki, N. Takeda, M. Nagano and N. Dhalla (eds.). THE ISCHEMIC HEART.

models with atherosclerotic blood vessels brought about by mechanical arterial injury [5–8]. In patients with variant angina, coronary vasoconstriction in response to provocative agents is also demonstrated at a site of organic stenosis or minimal atherosclerosis [9–11]. Thus, atherosclerotic change of coronary blood vessels may play an important role in coronary hyperconstriction.

Ergonovine maleate is the agent that has been used frequently to provocate coronary vasospasm in human [12] and experimental models [5,6,8]. Ergonovine-induced coronary hyperconstriction is thought to be mediated by activation of serotonergic receptors and a subsequent increase in calcium influx into vascular smooth muscle cells [13,14]. Serotonin is a spasm-provocating agent. It is released from platelets and plays a major part in the platelet-dependent coronary vasoconstriction after arterial injury [15]. Recently, we have reported an augmented response to ergonovine noted in canine coronary artery immediately after oxidative injury [16,17]. However, in that experimental condition, the ergonovine-induced coronary vasoconstriction was observed as diffuse coronary constriction because the solution containing oxygen radicals was infused into the ostium of the left coronary artery (LCA). The purpose of this study is to confirm that the increasing vasoconstrictor response to ergonovine with oxidative injury is a result of enhanced sensitivity to ergonovine brought about by oxygen radicals produced in locus quo and to examine the possible participation of serotonin in in vivo conditions. Thus, oxygen radicals are injected not into the ostium but into the branch of the LCA.

METHODS

Instrumentation

Eight mongrel dogs weighing 9 to 22 kg (15.4 ± 3.5 kg) were anesthetized with an intravenous administration of sodium pentobarbital (30 mg/kg). After intubation, the dogs were mechanically ventilated with room air. A 7.2-F catheter sheath was introduced into the abdominal aorta via the right femoral artery to measure the aortic pressure by means of a strain-gauge transducer (DT-4817, Spectramed Inc., Oxnard, California, USA). For the selective coronary angiography, a 5-F preshaped catheter (Judkins or Amplatz, Cordis Japan Inc., Japan) was advanced into the orifice of the LCA through the sheath under the guidance of fluoroscopy in the x-ray system. A 6-F preshaped catheter (Fansac, Clinical Supply Co. Ltd., Japan) was also placed at the coronary sinus (CS) via the left internal jugular vein for blood sampling. The electrocardiogram (limb leads I, II, and III) was monitored throughout the experiment. Heparin was administered intravenously at 200 IU/kg and then 1000 IU was added every hour by bolus.

Experimental protocol

To generate oxygen radicals, xanthine (X; 2 mM, Sigma, St. Louis, Missouri, USA) and xanthine oxidase (XO; 10 U/L, Sigma) were dissolved in the Krebs–Henseleit solution containing (in mM) NaCl 120.0, $NaHCO_3$ 25.5, KCl 4.7, KH_2PO_4 1.2, $MgSO_4$ 1.2, $CaCl_2$ 1.25, and glucose 11.0. This X − XO solution was oxygenated

with a mixture of 95% O_2 and 5% CO_2 (pH 7.4) for 60 minutes. We did not monitor the production of superoxide radicals in vivo in this experiment. However, the generation of superoxide radicals from X − XO had been confirmed in Krebs–Henseleit solution in a previous study [18]. Baseline electrocardiogram and aortic pressure were obtained after a stabilization period of 30 minutes and were recorded continuously throughout the experiment. A control left coronary arteriography was performed in the right anterior oblique projection by manually injecting 3–4 mL of the contrast medium (75.49% iohexol, Daiichi Pharmaceutical Co. Ltd., Tokyo, Japan). The position of the dog and the distance between the dog and the image intensifier were kept constant during the experiment in order to avoid the postural effects on magnification of the angiograms. Then, for selective infusion of the X − XO solution, a 2.5-F infusion catheter (Target Therapeutics Inc., Fremont, California, USA) was advanced into the proximal site of the left circumflex coronary artery (LCX) through the 5-F catheter. The position of the tip of the infusion catheter was determined by the injection of the contrast medium through the infusion catheter. Immediately after administration of 200 mL of the X − XO solution into the LCX through the infusion catheter, the infusion catheter was taken out, and the left coronary arteriography was performed in order to assess the direct effects of oxygen radicals. Next, we examined the effects of oxygen free radicals on the coronary vasoconstriction induced by ergonovine. The left coronary arteriograms were obtained immediately after intracoronary infusion of 50 μg ergonovine and 5, 10, 15, and 20 minutes thereafter. At the end of protocol, 1 mg of isosorbide dinitrate (ISDN; Eisai Co. Ltd., Tokyo, Japan) was administered intracoronarily, and left coronary arteriography was repeated in order to evaluate dilator response to ISDN.

Measurement of coronary diameter

Coronary diameter was measured with the use of an electronic caliper (Mitutoyo Co., Tokyo, Japan), and the absolute inner diameter (mm) of the coronary arteries was obtained from a reference diameter of the catheter. Luminal diameters of the left anterior descending coronary artery (LAD) and the LCX were measured at the same point using the readily identifiable branch of the coronary artery as a reference. The diameter of the LCX was measured at a point distal to the site at which the tip of the X − XO infusion catheter was placed. The responses to ergonovine and ISDN were expressed as the percentage of change of coronary luminal diameter compared with that in the control state.

Measurement of serotonin concentration

Blood samples were taken from the orifice of the LCA and from the CS, at the control state, after infusion of X − XO solution into the LCX, and 20 minutes thereafter. Serotonin concentration was measured by a high-performance liquid chromatography (HPLC). The differences of the serotonin concentration in the blood (ΔS) between the orifice of the LCA and the CS [ΔS = (serotonin in CS)

− (serotonin in LCA)] were used to assess the changes of serotonin content in coronary artery.

Histologic study

After the last coronary arteriography, the heart was excised and immersed in ice-cold Krebs–Henseleit solution. Small catheters were inserted into the LAD and the LCX, and these vessels were perfused with the fixative consisting of 2.5% glutaraldehyde and 3.7% formaldehyde in 0.1 M phosphate buffer (pH 7.4). When fixation was completed, the segments of the LAD and the LCX were removed and fixed for microscopic examination. Scanning electron microscopy was used to examine changes of the luminal surface of both left coronary arteries, and transmission electron microscopy was used to study changes in vascular endothelium.

Statistical analysis

All results were expressed as mean ± SE. The unpaired *t*-test was used to compare the percentage of coronary diameters of the LAD and the LCX at each experimental period. The sequential data were analyzed by analysis of variance (ANOVA) and Bonferroni's corrected *t*-test. A value of $p < 0.05$ was considered statistically significant.

RESULTS

In the control state, heart rate (HR) was 126.5 ± 7.0 bpm, systolic aortic pressure (SAP) was 159.5 ± 8.1 mmHg, and diastolic aortic pressure (DAP) was 96.5 ± 3.0 mmHg. During the experimental period, no significant changes were found in HR, SAP, and DAP, and there were no obvious changes in ST segment, T wave, or QRS complex on electrocardiograms.

Coronary diameters

Figure 1 shows coronary arteriograms at each period of protocol of one case. In control, the luminal diameter of the LAD was 1.94 ± 0.14 mm, and that of the LCX was 2.25 ± 0.16 mm. Ergonovine did not induce "spasm" as observed clinically in patients with vasospastic angina both in the LAD and in the LCX, but ergonovine-induced vasoconstriction was enhanced in the LCX (figure 1D). The changes in LAD and LCX diameters are shown in figure 2. There were no significant changes in the LCX diameter after administration of the X − XO solution into the proximal part of the LCX. Administration of ergonovine into the ostium of the LCA induced constriction of both coronary arteries, but the constriction was greater in the LCX than in the LAD. There were significant differences between responses to ergonovine in the LCX and in the LAD at 10 (−12.2% ± 3.2% vs −2.8% ± 0.9%, $p < 0.05$) and 15 (−10.9% ± 2.2% vs −4.5% ± 1.7%, $p < 0.01$) minutes after administration of ergonovine. With regard to the vasodilatator response to ISDN, there were no significant differences between LCX and LAD (+5.0% ± 1.0% vs +5.5% ± 0.9%).

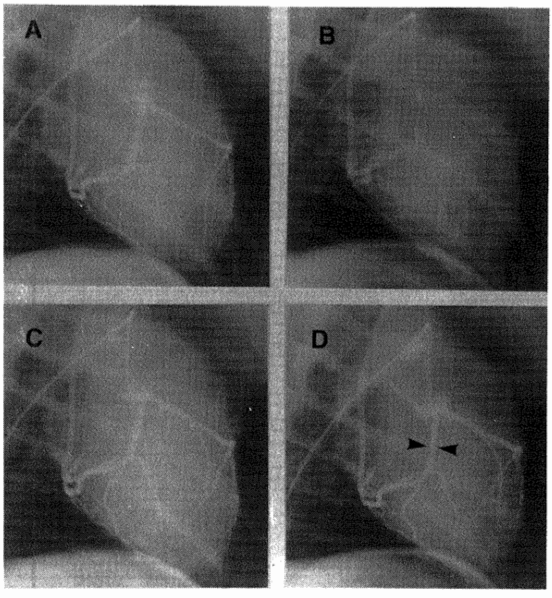

Figure 1. Coronary angiograms (CAGs) at each experimental period. Control CAG (**A**), superselective CAG of LCX through a infusion catheter (**B**), CAG after the administration of 200 mL of X − XO solution into the LCX (**C**), and 10 minutes after the administration of 50 μg of ergonovine into the LCA (**D**). Arrows in (D) indicate the position in which the ergonovine-induced vasoconstriction was enhanced by the administration of X − XO solution.

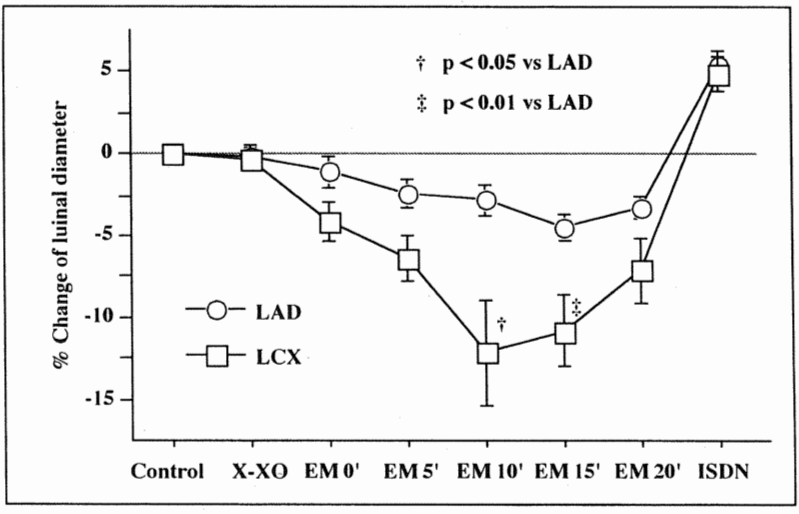

Figure 2. Plots show the changes in luminal diameter of the LAD (circles) and the LCX (square) vs. control. No significant changes were seen after the administration of X − XO into LCX, but ergonovine (EM)-induced vasoconstriction was enhanced significantly in the LCX 10 and 15 minutes after administration of 50 μg EM. After isosorbide dinitrate (ISDN) infusion, there were no significant differences between the diameters of the LAD and the LCX.

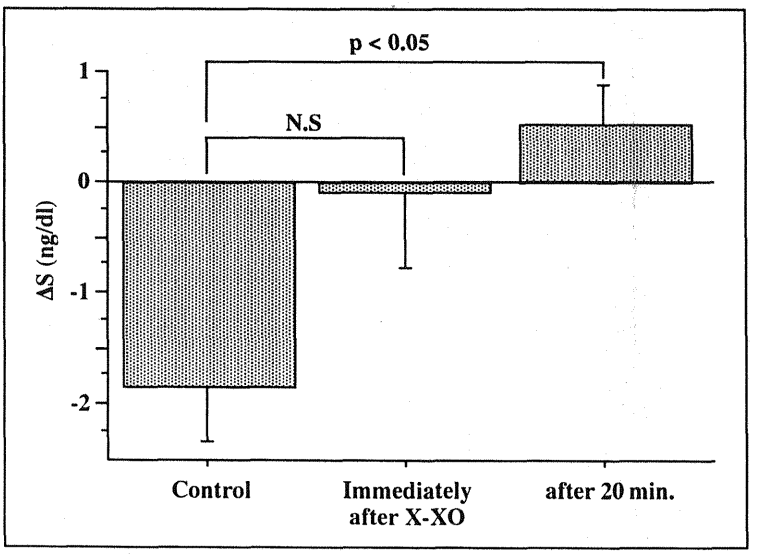

Figure 3. Change in serotonin concentration (S; ng/dL) after selective infusion of 200 mL X − XO solution into the LCX. ΔS = [(S in CS) − (S in LCA)]. ΔS was negative in control state, but turned positive 20 minutes after infusion of the X − XO solution.

Serotonin concentration

The differences in serotonin concentration (ΔS) between the orifice of the LCA and the CS are shown in figure 3. In the control state, the concentration of serotonin in the CS was lower than that in the LCA (ΔS; -1.8 ± 0.5 ng/dL). However, the concentration in the CS increased after the administration of the X − XO solution into the LCX, exceeding that in the LCA 20 minutes thereafter (ΔS; +0.5 ng/dL, $p < 0.05$ vs. control).

Histologic studies

In figure 4, the profiles of the endothelial surface of the LAD and the LCX as examined by scanning electron microscopy are shown. In the LAD without the administration of X − XO solution, the endothelial surface was normal and smooth (figure 4A and 4B); endothelial cells were arranged along the longitudinal axis parallel to the direction of blood flow, and nuclear bulges were seen (figure 4B). In the LCX with the administration of the X − XO solution, there were cracks and blebs (figure 4C and 4D), and ruptured blebs were seen as holes in surface. Figure 5 shows morphological changes observed by transmission electron microscopy. The LAD showed normal endothelial cells (figures 5A and 5B), while unruptured and ruptured blebs were see in endothelial cells of the LCX (figures 5C and 5D).

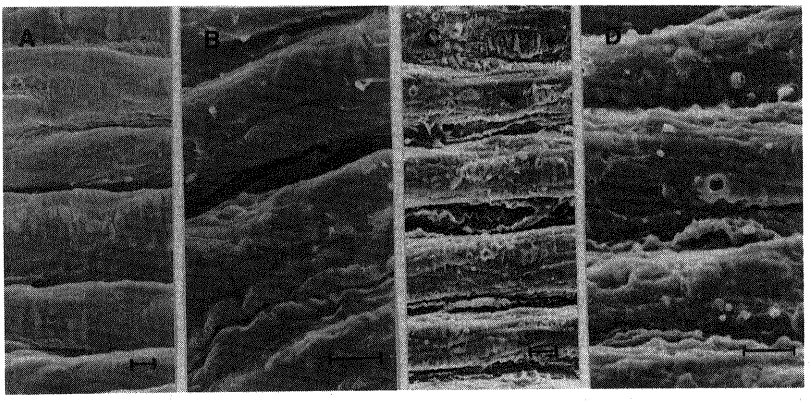

Figure 4. Scanning electron micrograph of coronary arterial endothelium. **(A, B)**; intact endothelial surface of the LAD; **(C, D)**: endothelial surface of the LCX that was injured by injection of X − XO solution containing oxygen radicals. Bars = 50 μm.

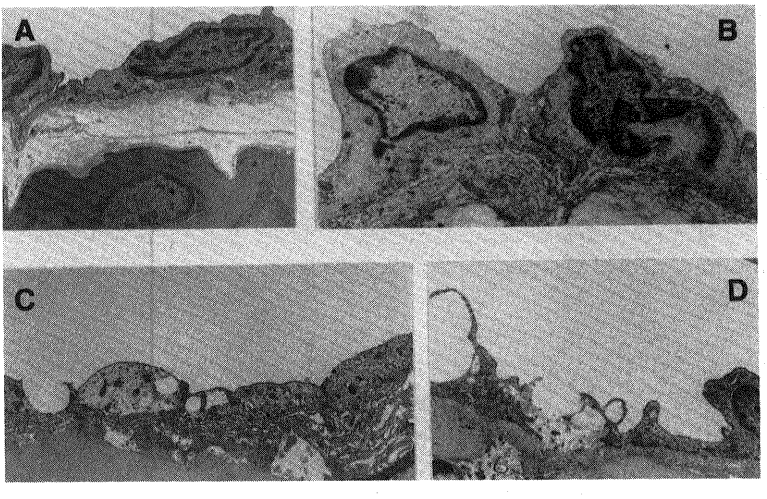

Figure 5. Transmission electron micrograph of the coronary artery. **(A, B)**: normal appearance of endothelial cells of LAD; **(C, D)**: injured endothelial cells of LCX in which X − XO solution was injected. Unruptured and ruptured blebs were seen.

DISCUSSION

The major findings of this study were the enhancement by oxygen free radicals of ergonovine-induced vasoconstriction of canine coronary artery in vivo, and the gradual increases in concentration of serotonin in the coronary artery after administration of oxygen free radicals. Oxygen radicals are considered to play an important role in the initiation of endothelial injury and the acceleration of atherosclerotic

process [19–21]. Moreover, in situ and in vitro studies have demonstrated that oxygen radicals modulate the vascular tone via direct action on vascular smooth muscle cells and via indirect mechanism connected with changes in endothelial function or biological activity of vasoactive mediators [22]. Our findings suggest the possibility that oxygen radicals may have a relation to the increased sensitivity to vasoactive mediators and the pathogenesis of coronary spasm.

Coronary spasm may result mostly from local hyperconstrictivity in the epicardial artery, which is considered to be related to the dysfunction of endothelium, hypersensitivity of vascular smooth muscle, or both [23]. It is well known that oxygen free radicals activate platelets by direct and indirect effects. It has been shown that coincubation of platelets with superoxide radicals enhances both serotonin secretion from platelets and platelet aggregation in vitro [24,25]. In the study reported here, the difference of the serotonin concentration between the CS and the orifice of the LCA diminished after intracoronary administration of oxygen free radicals, suggesting that oxygen radicals increased secretion and/or decreased absorption of serotonin in the coronary artery. Moreover, net serotonin secretion exceeded net serotonin absorption in the coronary artery 20 minutes thereafter. Because the activity of oxygen radicals decreases immediately, the changes in serotonin concentration may be responsible not only for the direct activation of platelets by oxygen radicals but also for the indirect activation of platelets caused by injured endothelium and/or decreased absorption of serotonin into injured endothelium.

The histological examination in the canine model in which balloon endothelial denudation was performed revealed intimal thickening with fibrous proliferation. Regenerated endothelium was observed in the denuded site [5,7,8,14]. In our study, cracks on the luminal endothelial surface and blebs formation were seen within endothelium exposed to oxygen free radicals. Although the primary target of oxygen radicals may be vascular endothelium, there is a possibility that oxygen radicals can modulate the reactivity of vascular smooth muscle by acting directly on the smooth muscle cells. Recent studies suggest that oxygen-derived free radicals have direct vascular effects, but the individual oxygen radicals have been considered to have different vascular effects and sometimes opposite effects, depending on experimental conditions [26–28]. Laurindo et al. [26] reported that the superoxide anion was involved in the genesis of vasoconstriction after coronary angioplasty in a canine in vivo experiment. However, we could not recognize the significant changes in the coronary artery diameter immediately after administration of X − XO solution.

Endothelium-derived relaxing factor is considered to be inactivated by reaction with the superoxide radical, presumably by formation of the nitrate ion ($NO + O_2^- \rightarrow NO_3^-$ [29]). Holtz and Griffith et al. showed that ergonovine induced a biphasic response to the coronary artery: small, transient dilatation, followed by developing constriction [30,31]. It was demonstrated that this initial dilator response was due to ergonovine-induced release of endothelium-derived relaxing factor and that the latter constricting response was mediated by stimulation of serotonin receptor.

Preparations with denuded endothelium showed disappearance of the initial dilator response and enhancement of the next constrictor response [31]. The endothelial damage produced by oxygen radicals in our experiment may be one of the causes that lead to enhancement of ergonovine-induced vasoconstriction.

CONCLUSION

This study provides in vivo evidence implicating oxygen free radicals in coronary artery constriction induced by ergonovine. The morphological change and the rise in the concentration of serotonin after oxidative injury may contribute to the potentiated responses to ergonovine. Oxygen radicals may play important roles in modulations of coronary vascular response in physiological or pathological conditions.

REFERENCES

1. Hills LD, Braunwald E. 1978. Coronary-artery spasm. N Engl J Med 299:695–702.
2. Maseri A, Severi S, De Nes M, L'Abbate A, Chierchia S, Marzilli M, Ballestra AM, Parodi O, Biagini A, Distante A. 1978. "Variant" angina: one aspect of a continuous spectrum of vasospastic myocardial ischemia. Am J Cardiol 42:1019–1035.
3. Yasue H, Omote S, Takazawa A, Nagao M. 1983. Coronary arterial spasm in ischemic heart disease and its pathogenesis: a review. Circ Res 52(Suppl):I-147–I-152.
4. Miller DD, Waters DD, Szlachcic J, Theroux P. 1982. Clinical characteristics associated with sudden death in patients with variant angina. Circulation 66:588–592.
5. Shimokawa H, Tomoike H, Nabeyama S, Yamamoto H, Araki H, Nakamura M, Ishii Y, Tanaka K. 1983. Coronary artery spasm induced in atherosclerotic miniature swine. Science 221:560–562.
6. Shimokawa H, Tomoike H, Nabeyama S, Yamamoto H, Ishii Y, Tanaka K, Nakamura M. 1985. Coronary artery spasm induced in miniature swine: angiographic evidence and relation to coronary atherosclerosis. Am Heart J 110:300-310.
7. Egashira K, Tomoike H, Yamamoto H, Yamada A, Hayashi Y, Nakamura M. 1986. Histamine-induced coronary spasm in regions of intimal thickening in miniature pigs: role of serum cholesterol and spontaneous or induced intimal thickening. Circulation 74:826–837.
8. Kawachi Y, Tomoike H, Maruoka Y, Kikuchi Y, Araki H, Ishii Y, Tanaka K, Nakamura M. 1984. Selective hypercontraction caused by ergonovine in the canine coronary artery under conditions of induced atherosclerosis. Circulation 69:441–450.
9. MacAlppine RN. 1980. Relation of coronary arterial spasm to site of organic stenosis. Am J Cardiol 46:143–153.
10. Mercuiro P, Kronzon I, Winer H. 1982. Spasm of a normal or minimally narrowed coronary artery in the presence of severe fixed stenosis of the remaining vessel: clinical and angiographic observations. Circulation 65:825–830.
11. Yamagishi M, Miyatake K, Tamai J, Nakatani S, Koyama J, Nissen SE. 1994. Intravascular ultrasound detection of atherosclerosis at the site of focal vasospasm in angiographically normal or minimally narrowed coronary segments. J Am Coll Cardiol 23:352–357.
12. Schroedar JS, Bolen JL, Quint RA, Clark DA, Hayden WG, Higgins CB, Wexler L. 1977. Provocation of coronary spasm with ergonovine maleate. Am J Cardiol 40:487–491.
13. Brazenor RM, Angus JA. 1981. Ergometrine contracts isolated canine coronary arteries by a serotonergic mechanism: no role for alpha adrenoceptors. J Pharmacol Exp Ther 218:530–536.
14. Egashira K, Tomoike H, Hayashi Y, Yamada A, Nakamura M, Takeshita A. 1992. Mechanism of ergonovine-induced hyperconstriction of the large epicardial coronary artery in conscious dogs a month after arterial injury. Circ Res 71:435–442.
15. Kuga T, Ohara Y, Hata H, Hirakawa Y, Tomoike H, Takeshita A. 1993. Inhibitory effects of heparin, aspirin and ketanserin on coronary artery vasoconstriction after arterial balloon injury in hypercholesterolemic miniature pigs. J Am Coll Cardiol 22:291–295.

16. Matsubara T, Nakazawa M, Yoshida Y, Imai S, Suzuki K, Izumi T, Shibata A. 1995. Hyperconstriction of canine coronary artery induced by ergonovine after oxidative injury. J Mol Cell Cardiol 27:A516.
17. Matsubara T, Nakazawa M, Yoshida Y, Imai S, Suzuki K, Hori T, Konno T, Higuchi K, Tamura Y, Yamazoe M, Ida T, Aizawa Y. 1997. Increasing vasoconstrictor response to ergonovine with oxidative injury in canine coronary artery. Coronary Artery Dis 8:1–7.
18. Matsubara T, Musat-Marcu S, Misra HP, Dhalla NS. 1995. Protective effect of vanadate on oxyradical-induced changes in isolated perfused heart. Mol Cell Biochem 153:79–85.
19. Kvietys PR, Inauen W, Bacon BR, Grisham MB. 1989. Xanthine oxidase induced injury to endothelium: role of intracellular iron and hydroxyl radical. Am J Physiol 257:H1640–H1646.
20. Steinberg D, Parthasarathy S, Carew TE, Khoo JC, Witztum JL. 1989. Modifications of low-density lipoprotein that increase its atherogenicity. N Engl J Med 320:915–924.
21. Steinbrecher UP. 1988. Role of superoxide in endothelial-cell modifications of low-density lipoproteins. Biochim Biphys Acta 959:20–30.
22. Rubanyi GM. 1988. Vascular effects of oxygen free radicals. Free Rad Biol Med 4:107–120.
23. Maseri A, Chierchia S. 1982. Coronary artery spasm: demonstration, definition, diagnosis and consequences. Prog Cardiovasc Dis 25:169–191.
24. Handin RI, Karabin R, Boxer GJ. 1977. Enhancement of platelet function by superoxide anion. J Clin Invest 59:959–965.
25. Salvemini D, de Nucci G, Sneddon JM, Vane JR. 1989. Superoxide anions enhance platelet adhesion and aggregation. Br J Pharmacol 97:1145–1150.
26. Laurindo FRM, da Luz PL, Uint L, Rocha TF, Jaeger RG, Lopes EA. 1991. Evidence for superoxide radical-dependent coronary vasospasm after angioplasty in intact dogs. Circulation 83:1705–1715.
27. Sasaki H, Okabe E. 1993. Modification by hydroxyl radicals of functional reactivity in rabbit lingual artery. Jpn J Pharmacol 62:305–314.
28. Sheehan DW, Giese EC, Gugingo SF, Russel JA. 1993. Characterization and mechanisms of H_2O_2-induced contraction of pulmonary arteries. Am J Physiol 264:H1542–H1547.
29. Gryglewski RJ, Palmer RMJ, Moncada S. 1986. Superoxide anion is involved in the breakdown of endothelium-derived vascular relaxing factor. Nature 320:454–456.
30. Holtz J, Held W, Sommer O, Kühne G, Bassenge E. 1982. Ergonovine-induced constriction of epicardial coronary arteries in conscious dogs: a-adrenoceptors are not involved. Basic Res Cardiol 77:278–291.
31. Griffith TM, Hughes ED, Lewis MJ, Henderson AH. 1984. Ergometrine induced arterial dilatation: an endothelium-mediated effect. J Mol Cell Cardiol 16:479–482.

STRUCTURE AND EXPRESSION OF CALPONIN IN ARTERIAL SMOOTH MUSCLE CELLS

HISAKO YAMAMURA, WATARU IKEDA, NOBUHIKO SHIBATA, NOBUHISA AWATA, and KATSUHITO TAKAHASHI

Osaka Medical Center for Cancer and Cardiovascular Diseases

Summary. The gene and cDNA clones encoding smooth muscle calponin (also called *basic calponin* or *calponin h1*) have been isolated and characterized. The NH_2-terminal region of calponin shares homology with a putative negative regulatory domain of the GDP–GTP exchanger for Rho-like GTP-binding proteins. Expression of the basic isoform of calponin is downmodulated in proliferating smooth muscle cells of atherosclerotic neointima and injured arterial media. Transfer of the recombinant human calponin gene into rabbit balloon-injured arteries or rat transgenic arteries in vivo increased calponin expression by smooth muscle cells and suppressed arterial myointimal hyperplasia. The cellular distribution of calponin has been shown to be dramatically changed upon stimulation with an agonist known to activate protein kinase C in vascular smooth muscle cells. In addition to regulation of the contraction–relaxation cycle of smooth muscle, the findings reviewed here suggest that calponin might also be involved in the control of adhesion, migration, and proliferation of smooth muscle cells.

INTRODUCTION

Calponin is an actin-, tropomyosin-, and calmodulin-binding protein [1–14] that is implicated in the auxiliary regulatory role of smooth muscle contraction [15–18]. The association of calponin with the actin filament results in the inhibition of actin-activated myosin MgATPase activity [6,19–28], which is mainly due to a decrease in the cycling rate of myosin ATPase [6,21,23]. Recent studies indicate that calponin inhibits the actin-activated myosin ATPase by blocking a strong myosin binding site on actin [28]. It has also been shown that calponin inhibits the rate of

S. Mochizuki, N. Takeda, M. Nagano and N. Dhalla (eds.). THE ISCHEMIC HEART.

dissociation of the high-affinity actomyosin complex and, consequently, increases maximum force production by smooth muscle myosin [27]. These observations suggest that calponin may be an integral component of the force producing myosin–actin cross-bridges in mammalian smooth muscle [27].

In this chapter, we describe recent findings on the structural and expressional characterization of vascular smooth muscle calponin.

CALPONIN STRUCTURE

Structural analysis of cDNAs encoding calponin isoforms has revealed the presence of three types of genes with distinct expressional regulation [29–34]. Each of the three calponin genes encodes distinct classes of isoforms categorized into acidic (pI 5–6), neutral (pI 7–8), and basic (pI 8–10) calponins on the basis of their isoelectric points (figure 1). The basic calponin gene (also called the *calponin-h1* gene [29]) encodes an originally isolated calponin isoform, which is predominantly specific to smooth muscle cells (SMCs). [5]. In addition, the α- (high molecular-) and β- (low molecular-) isoforms encoded by the SMC calponin gene have been found as products of alternative mRNA splicing in chicken smooth muscle tissues [5,33]. More recently, cDNA clones encoding a novel acidic calponin isoform with a deduced 330-amino-acid polypeptide have been isolated and shown to be expressed in both smooth muscle and extra-smooth muscle tissues of adult rats [30,35]. The neutral calponin is the equivalent of calponin-h2 [33], isolated from mouse uterus and porcine stomach smooth muscle tissues. In recent reports, we showed that a human equivalent of mouse calponin-h2 is also expressed in both smooth muscle and extra-smooth muscle tissues [31].

As noted in the sequence of chicken gizzard calponin [5], the amino acid sequences of mammalian calponins share homology with SM22α proteins [36] (44% identical and 69% conservative residues in a 186-amino-acid overlap between human basic calponin and human SM22α). SM22α is the equivalent of a product of the human gene, WS3-10, which is overexpressed in senescent human fibroblasts derived from Werner syndrome [37]. Inspection of the aligned sequences of calponin and SM22α indicates that, although incomplete, both the predicted human and chicken SM22α sequences contain a characteristic motif of the calponin repeat with 27 (human SM22) or 24 (chicken SM22) amino acids in length at their carboxyl-terminus. Twenty of the 25 positions in an overlap between the sequences of human and chicken SM22, and those of each calponin repeat, are well conserved. These form a signature consensus sequence, I(G/S)LQMG(T/S)NKGASQ-GMT-YG-RQ- (single-letter amino acid code); residues that contain more than three amino acids at the same position are marked by hyphens. Interestingly, as noted by Vancompernolle et al. [38], this consensus motif is strikingly similar to a consensus sequence in the repeats of the *unc*-87 gene product of *Caenorhabditis elegans* (a 357-amino-acid peptide with M_r 39759 [39,40]) that is located in the I-bands of the body wall skeletal muscle and is composed of seven repeats of the 41–53-amino-acid segment. The null mutants of the *unc*-87 gene (unc-87, st1005) show paralysis and

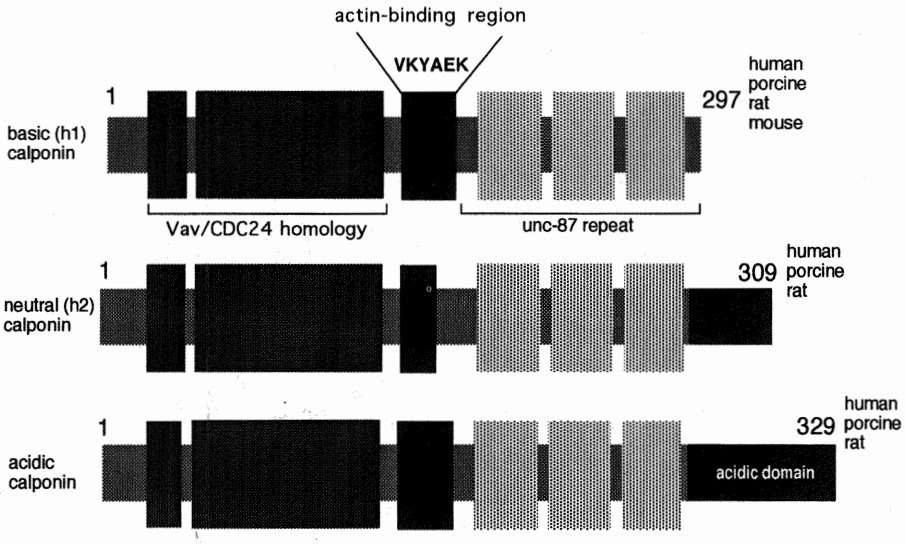

Figure 1. Schematic diagram of the domain structure of calponin isoforms and homologous proteins. Amino acid sequence in the actin-binding region [56] is conserved among human, porcine, rat, mouse, and chicken basic calponins.

disorganization of the thin filaments [39,40], suggesting that those proteins containing the characteristic motif of calponin's repeating structure may be members of an emerging new family of muscle and nonmuscle proteins involved in the regulation and organization of the actin filaments.

The NH_2-terminal half of the cloned aortic calponin molecules show extensive similarities to the NH_2-terminal region of the *vav* proto-oncogene product [41,42] (figure 2). Over the 89 NH_2-terminal amino acid residues of the *vav* proto-oncogene product (residues 32–121 of the human Vav sequence), there are 36% identity and 62% similarity to the mammalian calponin sequences [31]. The *vav* gene was originally identified as a locus that induced transformation of an NIH 3T3 mouse fibroblast by transfection of DNA extracted from a human esophageal carcinoma [41,42]. The *vav* proto-oncogene product, specifically expressed in hematopoietic cells, is an 845-amino-acid peptide (apparent M_r 95,000) with characteristic motifs reminiscent of a signaling protein [43,44] participating in the catalysis of guanine nucleotide exchange on the Rho-like GTP-binding protein: Dbl-homologous and Pleckstrin-homologous sequences, a cystein-rich sequence homologous to the zinc finger motif or the phorbol ester-binding domain of protein kinase C, and one SH2 and two SH3 domains (*src* homology region). Of particular interest is the finding that removal of the 67 NH_2-terminal residues of the Vav protein, which contains a region with the highest homology to calponin, is sufficient to activate the transforming potential of the *vav* proto-oncogene [41,42]. It is possible that a region homologous to calponin on the Vav sequence may function

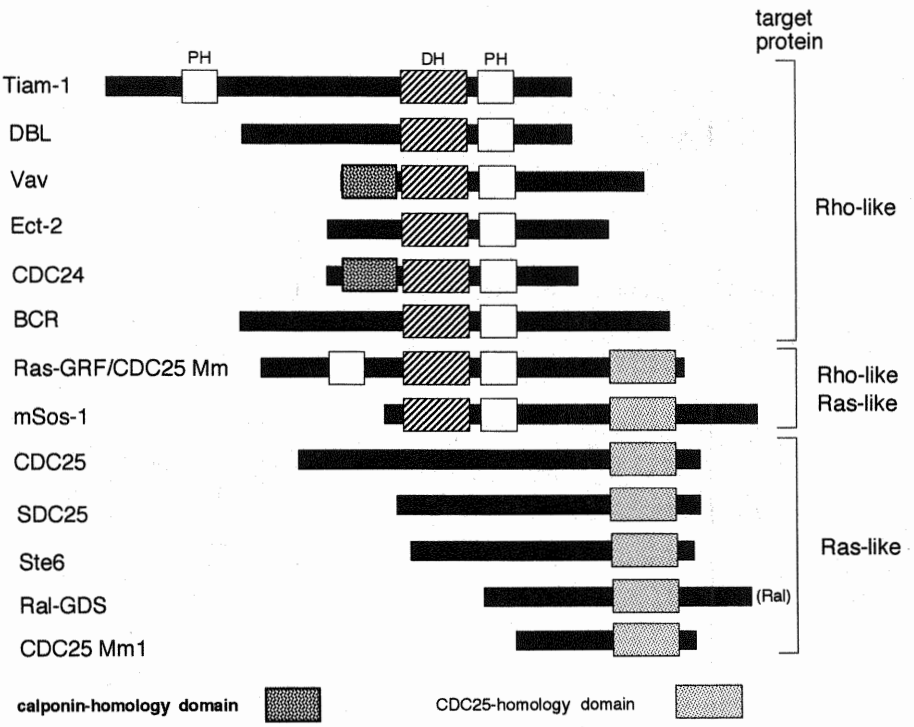

Figure 2. Schematic diagram of the domain structure of the Rho GDP–GTP exchange factors. DH, Dbl-homologous domain; PH, pleckstrin-homologous domain.

as a negative regulatory domain on the guanine nucleotide exchange activity by the Dbl- and Pleckstrin-homologous domain [41–43]. Furthermore, the NH_2-terminal portion of calponin is similar to that of CDC24 of budding yeast, an essential cell division cycle gene required for cytoskeletal organization at the site at which budding occurs [45]. Functional complementation studies as well as in vitro biochemical analysis indicate that CDC24 catalyzes the dissociation of GDP from CDC42, a yeast Rho-like protein, and thereby qualifies as a highly selective guanine nucleotide exchange factor for the Rho small GTP-binding protein [45]. Although cellular functions of the GDP–GTP exchange factors for Rho-like proteins in the smooth muscle regulation remain to be elucidated, the extensive sequence similarities between calponin and a putative negative regulatory domain of Vav or CDC24 proteins suggest that calponin might also be coupled to a cellular signaling pathway that inhibits the activities of the Rho-like GTP-binding proteins. Important in this connection is the finding that the GTP-bound form of Rho augments calcium sensitivity of the smooth muscle contractile apparatus [46]. It is also reported that

Tiam-1, a member of the GDP–GTP exchange protein family for Rho-like proteins is involved in inducing invasive properties of tumor cells [47]. Since invasion and proliferation of SMCs from arterial media to the intima are an underlying mechanism for atherogenesis or restenosis after balloon injury, it is interesting to study the expression of vascular smooth muscle calponin in normal and diseased arteries.

EXPRESSION OF VASCULAR SMOOTH MUSCLE CALPONIN IN NORMAL AND DISEASED ARTERIES

Basic calponin (h1) is normally expressed by differentiated SMCs. When cultured quiescent SMCs are stimulated by mitogen, calponin expression is rapidly downregulated at both mRNA and protein levels [7,11,48–50], and the extent of downregulation has been correlated with a proliferating SMC phenotype in vitro. Analysis of spatiotemporal distribution of calponin expression during avian embryonic development indicates that the calponin gene belongs to a group of late-differentiation determinants in smooth muscles [49]. These findings imply that downmodulation of the calponin gene could be a sensitive indicator for detecting phenotypic modulation of SMC in the diseased arteries. An anticalponin polyclonal antibody [48] and a basic calponin (h1)-specific cRNA were used as probes [51] to examine the expression of the calponin gene in atherosclerotic human arteries and balloon-injured rabbit carotid arteries. In the early stage of the atherosclerotic lesions with little or no intimal hyperplasia, most of the medial SMCs that express SMC-specific α-actin isoform at high levels also express immunoreactive calponin. SMCs that undergo proliferation and migration into the intima, however, express α-actin but not immunoreactive calponin. In human atherectomized lesions freshly excised from coronary and femoral arteries, calponin expression was downregulated in the majority of intimal α-actin-positive SMCs that underwent migration and proliferation [52].

Using a rabbit model of vascular injury, we found that the calponin expression in the medial SMCs was downregulated at an early time point (days 3–7) following balloon injury, concomitant with an increase in the number of proliferating SMCs. Subsequently, this change results in a significant increase of intimal thickening within two weeks. Six weeks after balloon angioplasty, SMC proliferation as well as calponin expression in both intimal and medial SMCs had returned to control levels.

By direct transfer of the human basic calponin (h1) gene into the cells and arteries of the live animals, we have shown that a constitutive calponin expression decreased the rate of migration and proliferation of a stimulated SMC. Liposome-mediated delivery of the recombinant human calponin gene into rabbit balloon-injured arteries in vivo increased calponin expression by SMCs and suppressed arterial myointimal hyperplasia [53]. Furthermore, we examined the potential of a full-length human basic calponin (h1) transgene to suppress SMC proliferation and neointima formation in the rat carotid artery model of restenosis [54]. Expression of the calponin cDNA was regulated by 2.5 kb of pCAGGS vector sequences, including cytomegalovirus enhancer and chicken β-actin promotor (figure 3). Transgenic

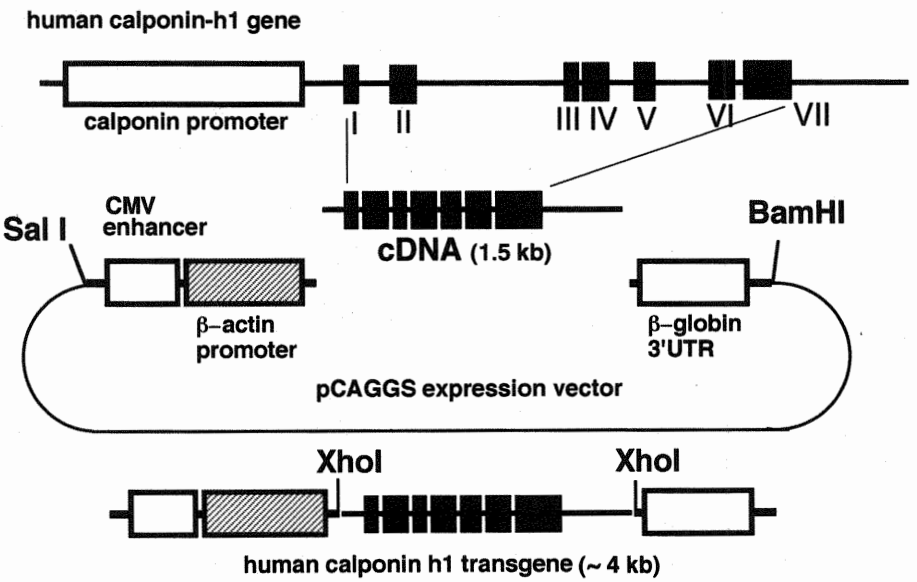

Figure 3. Construction of the human calponin (h1) transgene.

rats were generated by microinjection of the purified pCAGGS insert into zygotes from parents of stroke-prone spontaneously hypertensive (SHRSP/Izm) rats. Positive transgenic rats were identified by Southern blot analysis and PCR through the use of primers specific for the human basic calponin sequence. The transgene was preferentially expressed in muscle tissues, including vascular and cardiac muscles, as monitored by reverse transcription PCR as well as immunoblot analyses. Overexpression of calponin (1.5–5-fold) in vascular SMCs was assessed by RT-PCR and immunoblot analysis of whole-cell extracts of primary cultured carotid artery SMCs. The left carotid arteries of age- and blood pressure-matched adult SHRSP rats were injured by dilatation with three passages of a 2-F Fogarty catheter. Carotid arteries were removed 3, 14, or 28 days after balloon injury and were perfusion fixed in 2% paraformaldehyde, and the neointima-to-medial area ratio was determined for each animal. At three days after injury, calponin transgenic arteries showed a significant decrease in BrdU-stained medial cells relative to the wild-type arteries. At 14 days after injury, the transgenic arteries showed a significant decrease in the neointima: media ratio relative to injured control arteries. Suppression was sustained for 28 days. These results indicate the feasibility of calponin gene therapy for restenosis. The results indicate that calponin plays a role in the control of SMC proliferation and migration and suggest that a reduction of calponin in the arterial media may be responsible for the initiation of neointimal SMC hyperplasia. Genetic restoration of calponin in the artery wall may thus be of potential therapeutic value for cardiovascular disease.

INTRACELLULAR EXPRESSION OF CALPONIN IN CONTRACTILE VASCULAR SMOOTH MUSCLE CELLS

Morgan and her colleagues have used immunofluorescence and digital imaging microscopy to determine the cellular distribution of calponin in single vascular SMCs [14]. In resting cells, calponin is distributed throughout the cytosol, associated with filamentous actin structures. Upon stimulation with an agonist known to activate protein kinase C in these cells, however, Morgan et al. found that the calponin distribution changed from a primarily cytosolic one to one that is associated primarily with the surface cortex. Interestingly, this agonist-induced redistribution of calponin was not observed when the cell was stimulated with depolarization and was partially inhibited by the protein kinase C inhibitor calphostin. Furthermore, the redistribution of calponin overlapped in time with protein kinase C translocation and preceded contraction of the cells. Although the sites of relocalization for calponin are currently uncertain, these findings suggest two interesting possibilities: 1) the physiological function of calponin may be to mediate agonist-activated contraction via a protein kinase C-dependent pathway; 2) in addition to the inhibition of actomyosin ATPase activity, calponin might be involved in the regulation of the cortical actin cytoskeleton, e.g., by modulation of the cell surface signal transduction or cell–matrix and/or cell–cell adhesion properties [55].

REFERENCES

1. Takahashi K, Hiwada K, Kokubu T. 1986. Isolation and characterization of a 34,000-dalton calmodulin- and F-actin-binding protein from chicken gizzard smooth muscle. Biochem Biophys Res Commun 141:20–26.
2. Takahashi K, Hiwada K, Kokubu T. 1987. Occurrence of antigizzard p34K antibody cross-reactive components in bovine smooth muscles and non-smooth muscle tissues. Life Sci 41:291–296.
3. Takahashi K, Hiwada K, Kokubu T. 1988. Vascular smooth muscle calponin: a novel troponin T-like protein. Hypertension 11:620–626.
4. Takahashi K, Abe M, Hiwada K, Kokubu T. 1988. A novel troponin T-like protein (calponin) in vascular smooth muscle: interaction with tropomyosin paracrystals. J Hypertens 6:S40–S43.
5. Takahashi K, Nadal-Ginard B. 1991. Molecular cloning and sequence analysis of smooth muscle calponin. J Biol Chem 266: 13284–13288.
6. Nishida W, Abe M, Takahashi K, Hiwada K. 1990. Do thin filaments of smooth muscle contain calponin? A new method for the preparation. FEBS Lett 268:165–168.
7. Gimona M, Herzog M, Vandekerckhove J, Small JV. 1990. Smooth muscle specific expression of calponin. FEBS Lett 274:159–162.
8. Takeuchi K, Takahashi K, Abe M, Nishida W, Hiwada K, Nabeya T, Maruyama K. 1991. Co-localization of immunoreactive forms of calponin with actin cytoskeleton in platelets, fibroblasts, and vascular smooth muscle. J Biochem (Tokyo) 109:311–316.
9. Lehman W. 1991. Calponin and the composition of smooth muscle thin filaments. J Muscl Res Cell Motil 12:221–224.
10. Marston SB. 1991. Properties of calponin isolated from sheep aorta thin filaments. FEBS Lett 292:179–182.
11. Birukov KG, Stepanova OV, Nanaev AK, Shrinsky VP. 1991. Expression of calponin in rabbit and human aortic smooth muscle cells. Cell Tissue Res 31:16–21.
12. Walsh MP, Camichael JD, Kargacin GJ. 1993. Characterization and confocal imaging of calponin in gastrointestinal smooth muscle. Am J Physiol 265:C1371–C1378.
13. North AJ, Gimona M, Cross RA, Small JV. 1994. Calponin is localized in both the contractile apparatus and the cytoskeleton of smooth muscle cells. J Cell Sci 107:437–444.
14. Parker CA, Takahashi K, Tao T, Morgan KG. 1994. Agonist-induced redistribution of calponin in contractile vascular smooth muscle cells. Am J Physiol 267:C1262–C1270.

15. Itoh T, Suzuki S, Suzuki A, Nakamura F, Naka M, Tanaka T. 1994. Effects of exogenously applied calponin on Ca^{2+}-regulated force in skinned smooth muscle of the rabbit mesenteric artery. Pflugers Arch 427:301–308.
16. Jaworowski A, Anderson KI, Arner A, Engstrom M, Gimona M, Strasser P, Small JV. 1995. Calponin reduces shortening velocity in skinned taenia coli smooth muscle fibers. FEBS Lett 365:167–171.
17. Obara K, Szymanski PT, Tao T, Paul R. 1996. Effects of calponin on isometric force and shortening velocity in permeabilized taenia coli smooth muscle. Am J Physiol 270:C481–C487.
18. Horowitz A, Clement-chomienne O, Walsh MP, Tao T, Katsuyama H, Morgan KG. 1996. Effects of calponin on force generation by single smooth muscle cells. Am J Physiol 270:H1858–H1863.
19. Winder SJ, Walsh MP. 1990. Smooth muscle calponin: inhibition of actomyosin Mg-ATPase and regulation by phosphorylation. J Biol Chem 265:10148–10155.
20. Abe M, Takahashi K, Hiwada K. 1990. Effect of calponin on actin-activated myosin ATPase activity. J Biochem (Tokyo) 108:835–838.
21. Horiuchi KY, Chacko S. 1991. The mechanism for the inhibition of actin-activated ATPase of smooth muscle heavy meromyosin by calponin. Biochem Biophys Res Commun 176:1487–1493.
22. Makuch R, Birukov K, Shrinsky V, Dabrowska R. 1991. Functional interrelationship between calponin and caldesmon. Biochem J 280:33–38.
23. Miki M, Walsh MP, Hartshorne DJ. 1992. The mechanism of inhibition of the actin-activated myosin MgATPase by calponin. Biochem Biophys Res Commun 187:867–871.
24. Winder SJ, Sutherland C, Walsh MP. 1992. A comparison of the effects of calponin on smooth and skeletal muscle actomyosin systems in the presence and absence of caldesmon. Biochem J 288:733–739.
25. Shrinsky V, Birukov KG, Hettasch JM, Sellers JR. 1992. Inhibition of the relative movement of actin and myosin by caldesmon and calponin. J Biol Chem 267:15886–15892.
26. Gong B-J, Mabuchi K, Takahashi K, Nadal-Ginard B, Tao T. 1993. Characterization of wild type and mutant chicken gizzard alpha calponin expressed in E. Coli. J Biochem 114:453–456.
27. Haeberle JR. 1994. Calponin decreases the rate of cross-bridge cycling and increases maximum force production by smooth muscle myosin in an in vitro motility assay. J Biol Chem 269:12424–12431.
28. EL-Mezgueldi M, Marston SV. 1996. The effects of smooth muscle calponin on the strong and weak myosin binding sites of F-actin. J Biol Chem 271:28161–28167.
29. Strasser P, Gimona M, Moessler H, Herzog M, Small JV. 1993. Mammalian calponin: identification and expression of genetic variants. FEBS Lett 330:13–18.
30. Applegate D, Feng W, Green RS, Taubman MB. 1994. Cloning and expression of a novel acidic calponin isoform from rat aortic vascular smooth muscle. J Biol Chem 269:10683–10690.
31. Masuda H, Tanaka K, Takagi M, Ohgami K, Sakamaki T, Shibata N, Takahashi K. 1996. Molecular cloning and characterization of human non-smooth muscle calponin. J Biochem 120:415–424.
32. Samaha FF, Ip HS, Morrisey EE, Seltzer J, Tang Z, Solway J, Parmacek MS. 1996. Developmental pattern of expression and genomic organization of the calponin-h1 gene. A contractile smooth muscle cell marker. J Biol Chem 271:395–403.
33. Gao J, Hwang JM, Jin J-P. 1996. Complete nucleotide sequence, structural organization, and an alternatively spliced exon of mouse h1-calponin gene. Biochem Biophys Res Commun 218:292–297.
34. Miano JM, Olson EN. 1996. Expression of the smooth muscle cell calponin gene marks the early cardiac and smooth muscle cell lineages during mouse embryogenesis. J Biol Chem 271:7095–7103.
35. Trabelsi-Terzidis H, Fattoum A, Represa A, Dessi F, Ben-Ari Y. 1995. Expression of an acidic isoform of calponin in rat brain: Western blots on one- or two-dimensional gels and immunolocalization in cultured cells. Biochem J 306:211–215.
36. Lees-Miller JP, Heeley DH, Smillie LB, Kay CM. 1987. Isolation and characterization of an abundant and novel 22-kDa protein (SM22) from chicken gizzard smooth muscle. J Biol Chem 262:2988–2993.
37. Thweatt R, Lumpkin CK Jr, Goldstein S. 1992. A novel gene encoding a smooth muscle protein is overexpressed in senescent human fibroblasts. Biochem Biophys Res Commun 187:1–7.
38. Vancompernolle K, Gimona M, Herzog M, Van Damme J, Vandekerckhove J, Small V. 1990. Isolation and sequence of a tropomyosin-binding fragment of turkey gizzard calponin. FEBS Lett 274:146–150.
39. Goetink S, Waterston RH. 1994. The Caenorhabditis elegans UNC-87 protein is essential for maintenarce, but not assembly, of bodywall muscle. J Cell Biol 127:71–78.

40. Goetink S, Waterston RH. 1994. The Caenorhabditis elegans muscle-affecting gene unc-87 encodes a novel thin filament associated protein. J Cell Biol 127:79–93.
41. Katzav S, Cleveland JL, Heslop HE, Pulido D. 1991. Loss of the amino-terminal helix-loop-helix domain of the vav proto-oncogene activates its transforming potential. Mol Cell Biol 11:1912–1920.
42. Coppola J, Bryant S, Koda T, Conway D, Barbacid M. 1991. Mechanism of activation of the vav protooncogene. Cell Growth Differ 2:95–105.
43. Adams JM, Houston H, Allen J, Lints T, Harvey R. 1992. The hematopoietically expressed *vav* proto-oncogene shares homology with the *dbl* GDP–GTP exchange factor, the *bcr* gene and a yeast gene (CDC24) involved in cytoskeletal organization. Oncogene 7:611–618.
44. Matsuguchi T, Inhorn RC, Carlesso N, Xu G, Druker B, Griffin JD. ••. Tyrosine phosphorylation of $p95^{Vav}$ in myeloid cells is regulated by GM-CSF, IL-3 and Steel factor and is constitutively increased by $p210^{BCR/ABL}$. EMBO J 14:257–265.
45. Sloat BF, Adams A, Pringle JR. 1981. Roles of the CDC24 gene product in cellular morphogenesis during the Saccharomyces cervisiae cell cycle. J Cell Biol 89:395–405.
46. Hirata K, Kikuchi A, Sasaki T, Kuroda S, Kaibuchi K, Matsuura Y, Seki H, Saida K, Takai Y. 1992. Involvement of rho p21 in the GTP-enhanced calcium ion sensitivity of smooth muscle contraction. J Biol Chem 267:8719–8722.
47. Habets GGM, Scholtes EHM, Zuydgeest D, van der Kammen RA, Stam JC, Berns A, Collard JG. 1994. Identification of an invasion-inducing gene, Tiam-1, that encodes a protein with homology to GDP–GTP exchange for rho-like proteins. Cell 77:537–549.
48. Gimona M, Sparrow MP, Strasser P, Herzog M, Small JV. 1992. Calponin and SM22 isoforms in avian and mammalian smooth muscle: absence of phosphorylation in vivo. Eur J Biochem 205:1067–1075.
49. Duband J-L, Gimona M, Scatena M, Sartore S, Small JV. 1993. Calponin and SM22 as differentiation markers of smooth muscle: spatiotemporal distribution during avian embryonic development. Differentiation 55:1–11.
50. Shanahan CM, Weissberg PL, Metcalfe JC. 1993. Isolation of gene markers of differentiated and proliferating vascular smooth muscle cells. Circ Res 73:193–204.
51. Shanahan C, Cary NRB, Metcalf JC, Weissberg PL. 1994. High expression of genes for calcification-regulating proteins in human atherosclerotic plaques. J Clin Invest 93:2393–2402.
52. Negoro N, Fukui R, Tsuchikane E, Otsuji S, Kato O, Kobayashi T, Takagi M, Eshita Y, Nishida M, Kojima A, Takahashi K, Shibata N. 1994. Down expression of calponin in smooth muscle of coronary artery lesions identifies a group of lesions at high risk for restenosis after atherectomy: implications for human gene therapy by direct calponin gene transfer. Circulation 90:I-142.
53. Takahashi K, Fukui R, Kato O, Nakazawa S, Takagi M, Kinoshita I, Hiraishi T, Kojima A, Sato S, Eshita Y, Fujio Y, Kobayashi T, Shibata N. 1993. Percutaneous transluminal transfer of the human calponin gene for suppression of intimal hyperplasia following arterial balloon injury: a model for successful gene therapy for restenosis. Circulation 88: I–657.
54. Takahashi K, Miwa A, Takagi M, Kojima A, Eshita Y, Nara Y, Yamori Y, Hirabayashi M, Kato O, Awata N, Kobayashi T, Shibata N. 1995. Overexpression of calponin in transgenic rats inhibits intimal arterial smooth muscle cell hyperplasia in the carotid artery model of restenosis. Circulation 92:I–295.
55. Takahashi K, Takagi M, Ohgami K, Nakai M, Kojima A, Nadal-Ginard B, Shibata N. 1993. Inhibition of smooth muscle cell migration and proliferation caused by transfection of the human calponin gene is associated with enhanced cell matrix adhesion and reduced PDGF responsiveness. Circulation 88:I-174.
56. EL-Mezgueldi M, Strasser P, Fattoum A, Gimona M. 1996. Expressing functional domains of mouse calponin: involvement of the region around alanine 145 in the actomyosin ATPase inhibitory activity of calponin. Biochemistry 35:3654–3661.

This Page Intentionally Left Blank

STATUS OF β-ADRENOCEPTORS, G-PROTEINS, AND ADENYLYL CYCLASE IN ISCHEMIC HEART DISEASE

NARANJAN S. DHALLA*, SUJATA PERSAD*, VINCENZO PANAGIA*, SEIBU MOCHIZUKI, and ROBERT E. BEAMISH***

* *St. Boniface General Hospital Research Centre*
** *Jikei University School of Medicine*

Summary. It is now well known that the positive inotropic responses of ischemia-reperfused hearts to adrenergic stimulation are markedly attenuated; however, the mechanisms for this abnormality are not fully understood. Earlier studies have revealed an increase, a decrease, or no change in the β-adrenoceptor–adenylyl cyclase system in ischemic–reperfused hearts, but such conflicting results appear to be due to differences in the experimental model, times of inducing ischemia as well as reperfusion, and the methods employed for studying biochemical parameters. Recent studies have revealed that the alterations in the β-adrenergic receptor mechanisms in the ischemic heart were different from those in ischemic–reperfused hearts. The major problem in the ischemic heart appears to result from uncoupling of β-adrenoceptors with adenylyl cyclase, whereas the problem in the ischemic–reperfused heart seems to be in the decrease of β-adrenoceptor numbers, depression in the catalytic site of adenylyl cyclase, and a decrease in G_s-protein function. Nonetheless, ischemia–reperfusion-induced changes in the β-adrenoceptors and adenylyl cyclase system have been demonstrated to be prevented by the presence of superoxide dismutase plus catalase, a combination which is known to remove the actions of H_2O_2. Since H_2O_2 and oxyradicals were found to produce biphasic changes in the β-adrenergic signal transduction mechanism, it is likely that the observed changes in the ischemic and ischemic-reperfused hearts may be due to the accumulation of low vs. high concentrations of oxyradicals and oxidants such as H_2O_2. On the basis of this evidence, it is suggested that an increase in oxidative stress during both the ischemic and reperfusion phases may play an important role in the alteration of β-adrenergic receptors, the adenylyl cyclase and G_s-protein system, and the attenuation of the inotropic responses of the ischemic–reperfused hearts to catecholamines.

S. Mochizuki, N. Takeda, M. Nagano and N. Dhalla (eds.). THE ISCHEMIC HEART.

INTRODUCTION

Salvage of the ischemic myocardium has been the goal of numerous experimental and clinical cardiologists for many years. Of the various approaches, including the array of drugs that have been used to date [1–3], early restoration of myocardial blood flow is now generally accepted as the best means to achieve this goal. While reperfusion appears to be a prerequisite for tissue salvage, this process also carries with it a component that can prove deleterious to the ischemic myocardium. It is still a matter of debate whether the ischemic tissue is injured by the reperfusion itself or whether reperfusion simply causes cells already killed by ischemia to undergo sudden changes in appearance. There is also ample evidence to suggest that the cellular injury due to myocardial ischemia per se may occur through mechanisms that are different from those for reperfusion. Much of the current research is aimed at minimizing the risk:benefit ratio for procedures implemented to induce reperfusion and at elucidating the mechanisms responsible in promoting reperfusion injury and subsequently confirming the relevance of adjunctive therapy in potentiating salvage of the ischemic myocardium. Therefore, one of the fundamental issues in this regard is to establish the mechanisms responsible for the contractile abnormalities associated with myocardial ischemia and ischemia–reperfusion injury. It is understood that cardiac pump failure and changes in cardiac cell ultrastructure due to ischemia–reperfusion or hypoxia–reoxygenation involve a wide variety of complex pathological abnormalities, and the present information on these aspects is largely based on the beneficial effects of several pharmacological interventions. For example the beneficial effects of Ca^{2+} antagonists [4,5] have supported the role of intracellular Ca^{2+} overload, whereas those of both beta- and alpha-adrenergic blockers [6–9] point to the role of increased sympathetic activity [10] in the pathophysiology of ischemic heart disease. However, the involvement of prostaglandins and several other metabolic abnormalities during several stages of ischemic heart disease have also been identified [11,12].

In addition to producing dramatic reductions in high-energy stores such as adenosine triphosphate (ATP) and creatine phosphate (CP), myocardial ischemia has been shown to result in a large accumulation of free fatty acids (FFAs) and their acyl derivatives [13–17] as a consequence of changes in lipid metabolism. FFAs and their acyl derivatives have been shown to promote cardiac dysfunction [18,19] by depressing contractile force development [20]. The long-chain acyl derivatives of FFAs are also known to bind with membranes [21] and to change their properties [22,23]. Lysophospholipids that have accumulated in the ischemic heart [24–27] are known to induce arrhythmias [28–30]. Accumulation of other metabolites due to lack of washout also plays a large part in promoting the overall loss of normal functional capacity of the heart. In this regard, accumulation of protons derived from anaerobic glycolysis during ischemia is considered to exert inhibitory effects on contractile proteins [31,32]. On the other hand, acidosis due to the accumulation of both CO_2 and protons (decrease in pH) in the ischemic tissue [33] has been shown to be

beneficial as long as it is mild over a short period, however, it may be harmful when severe over a prolonged period [34]. Lactate accumulation, which is known to promote decreased contractility [35] and $NADH_2$ accumulation (due to impaired rate of mitochondrial metabolism), has been shown to promote intramitochondrial Ca^{2+} overload [36]. Over the years, however, it is becoming clear that the mechanisms of ischemic injury and reperfusion injury may be distinct, since no increase in intracellular Ca^{2+} occurs during ischemia, whereas intracellular Ca^{2+} overload is the hallmark of the ischemic–reperfused heart [37].

Although varying degrees of defects in different Ca^{2+} regulating systems located in the sarcolemmal (SL), sarcoplasmic reticular (SR), and mitochondrial membranes have been identified in the reperfused heart, the exact mechanisms of these membrane abnormalities are poorly understood [38–40]. A wide variety of SL defects, including changes in Na^+–K^+ ATPase, Na^+–Ca^{2+} exchange, Ca^{2+} pump, adenylyl cyclase, beta-adrenergic receptors, alpha-adrenergic receptors, and G-protein-mediated processes, in different models of heart disease [38–55], have been defined. Specifically, the β-adrenoceptor–G-protein–adenylyl cyclase system, which is known to play a major role in the regulation of heart function and metabolism, has been reported to be altered during both myocardial ischemia [56–59] and reperfusion [56,60–63]. However, reports of modifications incurred in the various components of the β-adrenergic pathway due to ischemia and reperfusion remain controversial [57,61–67]. These conflicting observations by different investigators appear to be due to the use of variable periods of ischemia as well as varying degrees of reperfusion in a variety of ex vivo and in vivo models in different species of animals. Furthermore, relatively little is known regarding the mechanism of changes in the β-adrenoceptor signal transduction system in the ischemic as well as in ischemic–reperfused hearts.

Oxygen-derived free radicals have been implicated as a major factor in the pathophysiology of ischemia–reperfusion injury in the myocardium [68–70]. These partially reduced forms of oxygen in ischemic–reperfused myocardium can be generated from a number of sources within the cardiomyocyte, including the mitochondrial respiratory chain [71], and by other extracellular and systemic sources such as arachidonic acid metabolism and catecholamine oxidation [69,72]. Different types of active oxygen species have been shown to produce electrical abnormalities [73,74], ultrastructural damage [75,76], intracellular Ca^{2+} overload [77], and cardiac dysfunction [78]. Also, various oxygen radical scavengers have been shown to exert beneficial effects on ischemia–reperfusion-induced changes in heart function and structure [79,80]. However, very little is known about the actions of oxyradical scavengers on the status of ischemia–reperfusion-induced alterations in signal transduction mechanisms such as β-adrenergic receptors, G-proteins, or adenylyl cyclase. Thus, in light of the importance of this cascade in myocardial functional regulation, this chapter will summarize the alterations effected upon the components of the β-adrenoceptor mechanisms during both myocardial ischemia and reperfusion as well as due to interaction with free radicals.

GENERATION OF FREE RADICALS DURING ISCHEMIA–REPERFUSION

It is now well known that free radicals are molecules that have an odd number of electrons. Because of their molecular configuration, free radicals are highly reactive and can cause cellular injury. Under normal physiological conditions, free radical reactions are critical for the operation of diverse biologic processes. Radical species are generated in vivo as byproducts of metabolism as well as under conditions such as exposure of organisms to ionizing radiation and drugs, which are capable of redox cycling, or to xenobiotics that can form free radical metabolites in situ. The occurrence of reactive oxygen species is therefore an attribute of normal aerobic life; the steady-state formation of these partially reduced forms of oxygen is balanced by a similar rate of their consumption by antioxidants such as superoxide dismutases and hydroperoxidases that may be enzymatic or nonenzymatic. *Oxidative stress* results from an imbalance in this oxyradical–antioxidant equilibrium in favor of the oxyradicals either due to their overproduction or as a consequence of reduced antioxidant reserve in the body.

Highly toxic oxygen radicals have been implicated in the pathogenesis of ischemia–reperfusion injury. Two popular theories of how reperfusion injury may occur are 1) the Ca^{2+} overload hypothesis and 2) the free radical hypothesis [8]. The former theory suggests that defects in the cellular capacity to regulate Ca^{2+}, established during ischemia, result in the accumulation of toxic levels of intracellular Ca^{2+} during reperfusion. The free radical theory is based on the understanding that supranormal quantities of reactive oxygen species, including superoxide anion ($O_2 \cdot^-$), hydrogen peroxide (H_2O_2), and hydroxyl radical ($\cdot OH$), are generated during reperfusion. Much of the support for this premise is due to many investigators (but not all [82]) who have found that free radical scavengers can reduce the injury in the isolated heart model. Subsequently, these reactive oxygen species are implicated in the induction of membrane defects that promote excessive Ca^{2+} entry into the cell, thus unifying both theories.

It has been proposed that different oxygen radicals formed upon reperfusion of the ischemic myocardium promote tissue necrosis, arrhythmias [83], myocardial stunning, and cellular damage [84–86]. The superoxide radicals, which serve a key role in this scheme, are thought to be cytotoxic, but their relatively short half life in biological systems limits their diffusion away from the site of generation. Superoxide radicals can be reduced further by SOD catalysis to form H_2O_2, which, although not a free radical species, is a potent oxidant. H_2O_2 is also membrane permeable and may traverse considerable distances in the cell and thus cause damage at sites distant from its origin [70]. H_2O_2 is also a precursor for the formation of $\cdot OH$ radicals that, although short lived, are extremely reactive with biological membranes to form carbon-centered alkoxy and peroxy radicals [70]. The involvement of free radicals during ischemia–reperfusion has been documented by the detection of bursts of oxygen radicals in coronary sinus blood as well as in systemic blood within minutes of reperfusion [87–90]. It has also been suggested that the breakdown of homeostatic mechanisms during hypoxia–ischemia can result in increased cytosolic

Ca^{2+}, activating a Ca^{2+}-dependent cytosolic protease that covalently modifies xanthine dehydrogenase, converting it to xanthine oxidase [68]. This enzyme catalyzes the univalent oxidation of purine substrates with the concomitant formation of $O_2 \cdot^-$ radicals, H_2O_2 [91,92], and perhaps singlet oxygen ($^1O_2$) [93]. Accumulation of these substrates during ischemia has been established by Jennings and Reimer [94], who reported that conversion of xanthine dehydrogenase to xanthine oxidase increased during the course of myocardial ischemia in dogs. Other studies showed damage to isolated organ systems by exogenous xanthine oxidase and purine substrate [75,95]. Allopurinol and oxypurinol, which are xanthine oxidase inhibitors, protected against oxidative damage in ischemia–reperfusion injury in cats [96], rats [97], and dogs [98]. However, studies done in man [99] and rabbits [100] indicate the failure of xanthine oxidase inhibitors to protect against ischemia–reperfusion injury; in fact, it has not been possible to detect measurable quantities of xanthine oxidase in human myocardium [101]. However, Yokoyama et al. [102] postulated that large amounts of xanthine oxidase may be produced in the liver following ischemia and initiated systemic production of free radicals. Once formed, the superoxide radicals promote the generation of an entire family of activated O_2 species formed by sequential reduction as follows:

$$O_2 + e^- \rightarrow O_2 \cdot^-$$

$$2O_2 \cdot^- + 2H \rightarrow H_2O_2 + O_2$$

$$O_2 \cdot^- + H_2O_2 \rightarrow {}^1O_2 + OH^- + \cdot OH$$

Other well-known biological sources of free radicals include activated neutrophils [103], direct donation of electrons from the reduced mitochondrial electron transport chain (NADH-dehydrogenase, ubiquinone-cytochrome b regions) to molecular oxygen [104], catecholamine oxidation [105], and cyclooxygenase and lipoxygenase enzymes (prostaglandins) [106].

Alterations of membrane lipids and proteins by free radicals are one of the critical and important factors in the evolution of ischemia–reperfusion damage. Cell membranes contain large amounts of polyunsaturated fatty acids complexed to phospholipids that, when peroxidized, result in loss of cellular integrity and function [107,108]. The alkoxy and peroxy radicals that are the intramembranal products of lipid peroxidation can further promote polymerization, peptide chain breakage, and altered amino acid structure of membranal proteins and enzymes. Proteins containing amino acids with sulfhydryl groups in their structure, such as tryptophan, tyrosine, phenylalanine, histidine, methionine, and cysteine, are most sensitive to modification of their structure [104], Functional alterations due to disruption of membrane integrity, leading to loss of activity of the membrane-bound enzymes, receptors, and ion channels, are some of the free radical-related effects that promote irreversible cellular destruction. Treatment of cardiac SR and SL membranes with oxygen free radicals has been shown to depress Ca^{2+} pump mechanisms, and these defects have been suggested to induce intracellular Ca^{2+} overload and heart dysfunc-

tion [70,109–112]. Depression in SL Na^+–K^+ ATPase and Na^+–Ca^{2+} exchange activity upon treatment of heart membranes with oxyradical-generating systems has been suggested to contribute towards the occurrence of intracellular Ca^{2+} overload [113,114]. Reeves et al. [115] reported a 10-fold increase in Na^+–Ca^{2+} exchange activity by reduced oxygen species in bovine cardiac sarcolemmal vesicles. The stimulation of activity required the presence of reducing agents ($O_2\cdot^-$) as well as oxidizing agents (H_2O_2) and probably resulted due to their influence on conformation of the exchanger through the modification of the thiol-disulphide groups in its structure. Kim and Akera [116] reported decreased Na^+–K^+ ATPase activity, depressed specific [^{3}H]-ouabain binding, and lowered sodium pump activity of the sarcolemma from ventricular muscle. These studies also revealed that scavengers of all species of activated oxygen ($O_2\cdot^-$, H_2O_2, ·OH, and $^1O_2$) had protective effects to various degrees. Perfusion of the isolated heart with an oxyradical-generating system have also been shown to degress both SL Na^+–Ca^{2+} exchange and Ca^{2+} pump activities during the development of contractile failure [117,118]. Although a decrease in the density of Ca^{2+} channels in the SL membrane [112] and in the sarcoplasmic reticulum [119] due to oxyradicals can be seen to result in the reduction of Ca^{2+} available for cardiac contraction, the contribution of depressed Ca^{2+}-stimulated ATPase of myofibrils [120] due to oxyradicals may also promote contractile abnormalities.

In the heart, contractile force development and/or heart rate are regulated by receptor systems acting via accumulation of intracellular cAMP (G_s-protein coupled), inhibition of cAMP formation (G_i-protein coupled), or independently of cAMP. Among all these receptors, the β-adrenoceptor–G_s protein–adenylyl cyclase–cAMP system is by far the most powerful contributor to the regulation of cardiac function. Since this pathway has also been shown to control the entry of Ca^{2+} into cardiomyocytes [40,121], alterations of this signal transduction pathway during ischemia–reperfusion and oxidative stress may promote significant increase in intracellular Ca^{2+} levels and subsequent cellular destruction and dysfunction. Thus, one of the aims of this chapter is to describe the characteristics and function of the components of this pathway and to define some of the alterations in these components under conditions of ischemia–reperfusion and oxidative stress.

It should be noted that the β-adrenergic receptor system is a multitransport system composed of five functional units:

1. A stimulatory receptor (β-adrenoceptor) that binds the stimulatory hormone or the neurotransmitter. The β-adrenergic receptor, like all known receptors that interact with guanine nucleotide binding proteins (G-proteins), is a transmembrane glycoprotein with seven putative membrane-spanning sequences.
2. The stimulatory G-proteins (G_s), which are coupled with adenylyl cyclase. Upon activation these initiate the production of cyclic AMP and thus regulate diverse metabolic functional events. The G_s-protein is composed of three subunits, namely, α_s, β, and γ; the α_s subunit possesses the GTP-binding site and is the target for cholera toxin catalyzed ADP-ribosylation by NAD^+, whereas the β and

γ subunits are tightly associated with each other. The G_s-proteins are located in the inner leaflet of the plasma membrane and are less hydrophobic than either the β-adrenoceptor or the catalytic unit of adenylyl cyclase.

3. The catalytic unit of adenylyl cyclase, which has a multitude of transmembrane spanning domains carrying its catalytic function at the cytoplasmic side of the membrane.
4. Inhibitory receptors that bind inhibitory neurotransmitters or inhibitory hormones and suppress the activity of adenylyl cyclase by transducing their signal via G_i-proteins.
5. The inhibitory GTP-binding protein (G_i). This protein, like G_s, is a heterotrimer composed of three subunits, namely, α_i, β, and γ; the βγ complex is highly similar to the one found in G_s.

β-ADRENERGIC RECEPTORS AND THEIR REGULATION

The β-adrenoceptors belong to the G-protein-coupled superfamily of receptors that have seven hydrophobic transmembrane-spanning regions and are proteins consisting of 402–560 amino acids [122]. Human β-adrenoceptors have been shown to consist of three subtypes, namely, β_1-, β_2-, and β_3-receptors, which are encoded by three distinct genes [123,124]. From structural studies carried out with these receptors, it is evident that the trans-membrane domain appears to be the site of agonist and antagonist binding, whereas the cytoplasmic domain is where G-protein interacts and the terminal -COOH tail appears to be where phosphorylation can take place. Comparison of the distribution of β-adrenergic receptors with marker enzymes of the sarcolemma, the sarcoplasmic reticulum, and the mitochondria has shown that β-adrenoceptors exist only in the SL membrane. This location renders them accessible to circulating catecholamines as well as to those released from sympathetic nerve terminals. It is now generally accepted that both β_1- and β_2-adrenoceptors coexist in the human heart; however, at present, there is no evidence for the existence of β_3-adrenoceptors in the human heart [125]. Some investigators have reported that the number of β-adrenoceptors in the normal human heart is quite evenly distributed in the right and left atrial as well as ventricular tissues; this has been demonstrated by radioligand binding studies (80–90 mol/mg protein in all four chambers of heart) [126,127], by quatitative autoradiographic studies [128], and in vivo by positron emission tomography studies [129]. On the other hand, work from other laboratories has suggested that the proportion of β_2-adrenoceptor is somewhat higher in the atria (approximately one third of the total β-adrenoceptor population) than in the ventricular myocardium (approximately 20% of the total β-adrenoceptor population) [126,127] and even higher in the atrioventricular conducing system (up to 50%) [130]. Although the β_1-adrenoceptors predominate in the human heart, especially in the ventricles, human cardiac adenylyl cyclase is preferentially stimulated by β_2-adrenoceptors [126,131,132]. This is in contrast to most other mammalian species (rabbit, cat, dog, rat), where the predominant type of β-adrenoceptor is the β_1-adrenoceptor, which is also responsible for the activation from these receptors of adenylyl cyclase by catecholamines [133].

The performance of the normal myocardium is not under the influence of the adrenergic system [134], which plays a major role under conditions of stress when sympathetic outflow is markedly increased. The number of receptors per unit area of sarcolemma (the receptor density) is not fixed but can rise (upregulation) or fall (downregulation) in response to certain physiological and pathophysiological circumstances. There is controversy surrounding the exact meaning of the term *downregulation* of receptors, and possibly the most correct explanation lies in the supposition that a decrease occurs in receptor numbers. Thus, downregulation of receptors would result from 1) internalization of receptors, 2) decreased rate of receptor synthesis, and 3) an increased rate of receptor degradation. Prolonged exposure of receptors to their agonists results in a time-dependent attenuation of responsiveness or refractoriness to continued stimulation by those agents. This phenomenon, termed *homologous desensitization* and exhibited by β-adrenoceptors, is thought to involve phosphorylation of the β-adrenoceptors [135] by a specific β-adrenergic receptor kinase (βARK) [136]. Once phosphorylated, the receptors are no longer able to couple to the G_s-protein [136] and the modified receptor becomes internalized. It should be mentioned that uncoupling of the β-adrenergic receptors and the G_s-protein after βARK-mediated phosphorylation requires the presence of another protein, β-arrestin [137]; the exact function of β-arrestin in this regard, however, is unclear. The internalized receptors are not necessarily degraded but may actually be stored in an intracellular "pool" to be eventually resensitized, by removal of the phosphate groups, and returned to the cell surface membrane. Another form of desensitization is called *heterologous desensitization*, which results from desensitization of the receptors by a cAMP-dependent kinase, and therefore can be triggered by a continued high rate of cAMP formation due to stimulation from not only β-receptors but also other receptors linked to adenylyl cyclase [138]. Not all receptors present at the surface membrane are in use at all times, since some of these "spare receptors" do not react to agonist stimulation. Thus, an altered number of receptors is not necessarily indicative of a corresponding alteration in the activity of the system. The human heart, however, contains only a few spare receptors for β-adrenoceptor-mediated positive inotropic effects, and nearly all the receptors present at the surface membrane at any one time are necessary to evoke maximal response to adrenergic stimulation [139]. It should be understood that even if the receptor density remains fixed, the activity of the receptors may be altered by molecular changes that regulate the affinity of the receptors for their agonists [140].

The *upregulation* of β-adrenergic receptors occurs under reduced exposure of cell to β-adrenoceptor agonists as achieved by denervation and treatment with β-adrenoceptor antagonists. Although the mechanisms involved in receptor upregulation are not well established, upregulation may occur due to reversal of all the parameters discussed in association with desensitization and downregulation. Acute exercise in rats was seen to induce rapid elevation of membrane-bound β-adrenoceptors accompanied by a reduction in the intracellular receptor "stores" [141], suggesting that externalization of intracellular receptors may be a mechanism. It should be mentioned that increments of β-adrenoceptor mRNA levels with 30–

60 minutes of incubation with adrenaline followed by an inhibition of β-adrenoceptor transcription after 24 hours of incubation has been demonstrated [142]. To this end, cAMP [142,143] and glucocorticoids [144] have been shown to regulate receptor gene transcription. Therefore, it appears that in the case of myocardial β-adrenergic receptors, both cycling of receptors between internal and external stores [145] as well as rapid changes in receptor protein synthesis [146] may provide means whereby the sensitivity of the heart to a given amount of β-stimulation can be modified.

ADENYLYL CYCLASE AND ITS REGULATION

Situated on the outer surface of the SL membrane, the β-adrenergic receptors couple to their intramembranal effector enzyme, adenylyl cyclase, when these are occupied by catecholamines such as norepinephrine and epinephrine. Although the regulation of adenylyl cyclase activity mainly involves stimulation by β-adrenergic agonists, this enzyme is known to serve as a final common effector that integrates and interprets convergent inputs from many other signal-generating pathways. The binding of agonist to an appropriate receptor causes activation of a stimulatory guanine nucleotide binding protein, G_s, which in turn stimulates adenylyl cyclase; the enzyme can also be inhibited by receptor–G_i protein pathways. To date, 10 species of adenylyl cyclase enzymes (isoenzymes) have been identified in different tissues. Pfeuffer and coworkers [146,147] were the first to purify the $G_{s\alpha}$- and Ca^{2+}-calmodulin-activated enzyme (type I adenylyl cyclase) using forskolin-affinity chromatography. Thereafter, Krupinski et al. [148] were able to derive a partial amino acid sequence and thus a full-length cDNA encoding of this type I adenylyl cyclase enzyme. Low-stringency homology probing and PCR techniques have since permitted molecular cloning of seven additional adenylyl-cyclase cDNAs as well as information regarding two partial sequences [149]. Structurally, the adenylyl cyclase enzyme is made up of a short amino terminal followed by six transmembrane spans, a large cytoplasmic domain of approximately 360–390 amino acids, and then a second set of six transmembrane spans followed by another large cytoplasmic domain of 255–330 amino acids [149]. Due to low levels of their expression in all tissues (0.001%–0.01% of membrane protein) and the unavailability of satisfactory antibodies, there is limited information available regarding the tissue distribution of adenylyl cyclase. It has been shown, however, that the isoforms of the enzyme present in the heart are types III to VII, with the greatest quantity being types V and VI [150,151]. Although the proposed molecular structure of adenylyl cyclase resembles the structure of certain ion channels and pore-forming molecules, there are no sequence similarities between these two classes of molecules [148]. Also, unlike the channel proteins, most of this enzyme protein has been reported to be located on the cytoplasmic side of the membrane [152], the presumed site of interaction with the G-protein α-subunit.

When an agonist occupies the G_s-coupled receptor, the complex thus formed catalyzes an exchange of GDP for GTP on the α-subunit of the G-protein. The

GTP-bound $G_{s\alpha}$ separates from the βγ-subunits of this heterotrimeric complex and thereafter interacts with adenylyl cyclase and activates the enzyme. Since the $G_{s\alpha}$-subunit possesses an intrinsic GTPase activity, the hydrolysis of $G_{s\alpha}$-bound GTP to GDP terminates the activation of adenylyl cyclase by $G_{s\alpha}$-GTP within seconds. $G_{s\alpha}$–GDP then reassociates with the βγ-subunit and awaits a new cycle of activation [153]. All mammalian species of adenylyl cyclase are thus far known to be stimulated directly by $G_{s\alpha}$. Type I and type VIII adenylyl cyclase are capable of integrating and interpreting signals that are received from G_s-linked receptors and from pathways that increase intracellular Ca^{2+} concentration [154,155]. The βγ-subunit complex, however, appears to be a potent inhibitor of the type I adenylyl cyclase, and its effect seems to be exerted directly on the enzyme [156]. It also seems that adenylyl cyclase type I is able to discriminate the source of the βγ-complex, since only high concentrations of βγ achieved by the activation of G_i or G_o are able to inhibit the enzyme significantly, while lower concentrations obtained by the activation of $G_{s\alpha}$ are unable to exert this effect [156]. This discrepancy is thought to be essential if dissociation of the G_s oligomer to yield $G_{s\alpha}$ and βγ is to successfully activate the enzyme. On the other hand, the βγ-subunit exerts striking stimulatory effects on type II and type IV adenylyl cyclase; these effects are dependent on coincidental activation by $G_{s\alpha}$ such that the system is designed to respond synergistically when two pathways are activated simultaneously [157]. Direct interaction of $G_{i\alpha}$ with adenylyl cyclase is by far the most well-known mechanism for the inhibition of adenylyl cyclase activity. Substantial (60%–80%) inhibition of cAMP synthesis has been reported for $G_{s\alpha}$- and forskolin-stimulated adenylyl cyclase activity by nanomolar to micromolar concentrations of different isoforms of $G_{i\alpha}$ ($G_{i\alpha1}$, $G_{i\alpha2}$, $G_{i\alpha3}$, and $G_{i2\alpha}$) [158,159]. Other regulators of adenylyl cyclase include Ca^{2+} and Ca^{2+}–calmodulin; both Ca^{2+} and calmodulin appear to have a stimulatory effect on adenylyl cyclase at approximately the 10–100 μM concentration range [160]. Finally, it has been reported that PKA is an inhibitor of adenylyl cyclase activity, whereas phosphorylation of the enzyme by PKC has a stimulatory effect on the activity [161].

G-PROTEINS AND THEIR REGULATION

The heterotrimeric guanine nucleotide-binding proteins (G-proteins) form the switchboard between a family of receptors and intracellular effector molecules [162]. Two types of G-proteins, namely, the stimulatory G-proteins (G_s) and the inhibitory G-proteins (G_i), are involved in the conveyance of signals from receptors to adenylyl cyclase. All G-proteins share a common structure, i.e., they are all made up of three subunits (α, β and γ); the α-subunit is thought to be the subunit responsible for the specific action of directly interacting and regulating the effector. The α-subunit of the G_s-proteins is of a molecular weight ranging from 39 to 52 kDa, while the α-subunit of G_i-proteins has a molecular weight of 40–41 kDa [162]. It should be pointed out that although a total of eight G_s-proteins have been purified, the cDNAs derived from a total of nine genes encoding the α-subunit have been cloned

and can be formally divided into four major classes derived from amino acid homology: α, α_i, α_q, and α_{12} [163]. All the isoforms of $G_{s\alpha}$-proteins are encoded by a single gene [164] and are produced as separate proteins by alternate splicing of the precursor mRNA transcript [165]. Members of all four classes have been detected in the myocardium [163]. Homologous cloning has revealed that there are at least four G_β and three G_γ genes; the 35-kDa G_β genes and the 8–10-kDa G_γ gene subunits appear to be tightly coupled as the $\beta\gamma$-complex. The α-subunit of G_s-protein is also a substrate for cholera-toxin-catalyzed ADP ribosylation, where NAD serves as the ADP-group donor [166]. Cholera-toxin-catalyzed ADP ribosylation locks the G_s-protein in the active state by virtue of the fact that it inhibits the GTPase activity of the protein. The ADP-ribosylation modifies an arginine residue located near the postulated GTP-binding region of the α-subunit. The G_i-protein is an inhibitory regulatory component of adenylyl cyclase when activated by muscarinic-cholinergic-, α_2-adrenergic-, adenosine-, somatostatin- and neuropeptide Y-receptors [167]. Three distinct isoforms of the $G_{i\alpha}$-subunit generated from three different genes are known to exist [168]; all three isoforms have been shown to be expressed in every tissue, although their specific mRNA expression varies [169]. In the heart, the predominant isoform is the $G_{i\alpha 2}$, although the others are also present [168]. As far as its inhibitory function is concerned, the mechanism seems to involve first a dissociation of the α_i-subunit from the $\beta\gamma$-complex, following which the $\beta\gamma$-subunit associates with and inhibits the activity of $G_{s\alpha}$-proteins. $G_{i\gamma}$ has not yet been demonstrated to have any direct inhibitory effect on the adenylyl cyclase activity [170]. Pertussis toxin catalyzes the ADP-ribosylation of the $G_{i\alpha}$-subunit in a manner similar to the cholera-toxin-catalyzed ADP-ribosylation of $G_{s\alpha}$ [171]. The result of ADP-ribosylation of $G_{i\alpha}$ is an increased affinity of this subunit for the $\beta\gamma$ complex, thereby promoting their reassociation. The physiological consequence of the outcome is the abolition of the inhibitory effect of G_i-proteins on the adenylyl cyclase enzyme.

It is thought that receptors bind the α-subunit of G-proteins at the carboxy terminal, and this interaction can be blocked by pertussis-toxin-induced ADP ribosylation of a cysteine residue located at the C-terminal of α_i and α_0 subunits as well as by mutagenesis of the C-terminal residues, and by antibodies raised against the C-terminal [172]. Furthermore, the C-terminal designates the specificity of receptor–G-protein interactions [173]. The N-terminals, on the other hand, are essential for binding to the $\beta\gamma$-subunit; binding of the $\beta\gamma$-subunit to the α-subunit is required for the receptor-stimulated exchange of GTP for GDP by the α-subunit [162]. The effector binding area of the α-subunit of G-proteins is also located at the C-terminal [173]. In the inactive state, G-proteins are bound to a GDP molecule at its nucleotide binding site. Upon interaction with an activated or occupied receptor, a conformational change occurs at the GDP binding site such that GDP is released and GTP gets preferentially bound. This exchange is considered to be the rate-limiting step in the activation process, and different isoforms of G-proteins exhibit different rates of exchange of GTP for GDP and thus get activated at different rates [174]. GTP binding is a Mg^{2+}-dependent process, with different G-proteins requir-

ing different Mg^{2+} concentrations for maximal guanine nucleotide-mediated activation [175]. The conformationally altered GTP-bound protein now splits into two compounds: the activated α-subunit and the βγ-complex. The α-subunit can now stimulate various effector molecules, including adenylyl cyclase and ion channels. Eventual hydrolysis of the GTP to GDP by the α-subunit itself increases its affinity for the βγ-complex, and the two portions reunite to produce the inactive G-protein ready for another cycle.

The role of the α_s-subunit of G-protein in β-adrenergic signaling includes activation of adenylyl cyclase and formation of cAMP and also direct activation of Ca^{2+} channels; both these effects are therefore considered to explain relaxant as well as positive inotropic actions of catecholamines on cardiac muscle. Gating of ion channels is another important function of G-proteins. G-proteins are thought to increase the opening probability of Ca^{2+} channels, but the mechanism of this effect is not known; such channels are called G-protein-gated channels [176]. In addition, G_s-protein has also been reported to mediate a direct (i.e., cAMP-independent) inhibition of Na^+ channels in rat neonatal ventricular myocytes [177]. Although the role of G-proteins in cardiovascular responses and in disease states is an area of intense research and although their altered status has been reported in a number of pathologies [178,179], modifications of these heterotrimeric proteins during ischemia reperfusion are not well established.

CARDIAC β-ADRENOCEPTOR–G-PROTEIN–ADENYLYL CYCLASE IN ACUTE MYOCARDIAL ISCHEMIA AND REPERFUSION

In acute myocardial ischemia, large amounts of catecholamines are liberated and, accordingly, receptor desensitization/downregulation is the expected end result. However, in reality, the opposite seems to occur. Myocardial ischemia in dogs, guinea pigs, and rats has been consistently associated with increased β-adrenoceptor number [57,63,64,67,180]. However, disparity exists as to the integrated activity and coupling of the increased β-receptor density to the G-protein–adenylyl cyclase complex and its physiological responsiveness. Although the mechanism for these increased adrenoceptor numbers in the face of elevated endogenous catecholamine levels is not understood, it may be associated with the depleted ATP levels in the myocardium leading to either enhanced externalization [180,181] or impaired internalization [57,182] of receptors. In isolated guinea pig hearts, global ischemia of 35–90 minutes increased β-adrenoceptor density and moreover stimulated adenylyl cyclase activity [180], indicating a sensitization of the β-adrenoceptor–adenylyl cyclase system. Studies done with an isolated rat heart model of global ischemia revealed an increase in β-receptor number immediately upon onset of ischemia, followed by an increased forskolin-stimulated adenylyl cyclase activity after 15 minutes of ischemia [57]. This outcome is indicative of an independent activation of the catalytic unit of the enzyme and suggestive of a dual sensitization of the β-receptor and adenylyl cyclase systems. Using the canine in vivo model of acute regional myocardial ischemia, it was found that β-adrenoceptor density increased within 30 minutes of regional ischemia in only those dogs that developed ventricular

fibrillation [183,184], while both β-adrenoceptor density and adenylyl cyclase remained unchanged in hearts without ventricular fibrillation [63,64,183]. In these studies, the β-adrenoceptor affinities remained unchanged; however, in other studies, the high-affinity receptors for isoproterenol have been reported to be either reduced [58,66] or unaffected [185]. In early ischemia (≤30 min), an enhancement of β-adrenoceptor stimulation is associated with an increase in adenylyl cyclase activity [57,180,182] as well as an impairment of the inhibitory adenylyl cyclase regulation, thereby suppressing the tonic inhibition of adenylyl cyclase [186]. However, unaltered adenylyl cyclase activity in early ischemia has also been reported [183]. It should be noted that while an increase in tissue levels of cAMP occurs within five minutes of ischemia, the activity of adenylate cyclase is increased only after 15 minutes of ischemia. This temporal disparity between cAMP content and adenylyl cyclase activity may be due to the dual sensitization of the β-receptor–adenylyl cyclase reported by Strasser et al. [57], whereby an initially increased β-receptor number may stimulate an unaltered adenylyl cyclase to produce greater quantities of cAMP, followed by activation of adenylyl cyclase at a later phase of ischemia that results in the same end point. Ischemia for a duration greater than 30 minutes but less than 60 minutes was reported to be associated with a persistent, increased number of β-adrenoceptors [57] but with reduced adenylyl cyclase activity [57,59,67,182] leading to decreased β-adrenoceptor responsiveness. In spite of the increased density of β-adrenoceptors in late ischemia, it was noted that the number of these β-adrenoceptors in the high-affinity coupled state was actually reduced [66]. The decreased adenylyl cyclase activity in late ischemia has been observed when the enzyme was stimulated in the presence of isoproterenol, Gpp(NH)p, of forskolin, as well as at the level of the catalytic subunit in the presence of Mn^{2+} [67]. It has been suggested that the enhancement of adenylyl cyclase in acute ischemia is linked to a simultaneously occurring activation of protein kinase C (PKC) [187], whereas the decrease in adenylyl cyclase during prolonged ischemia appears to be accompanied by and related to a decrease of G_s-protein activity [59,62,188]. Although a lack of consistency exists with regard to the observed alterations in the β-adrenoceptor pathway due to ischemia, relatively little is known about the status of this pathway in reperfused hearts. Although reperfusion of the ischemic myocardium maintains the increased β-adrenoceptor density [63], it reverses the depressed adenylyl cyclase activity [62].

The changes in the components of the signal transduction pathway are thought to have important implications during both ischemia and reperfusion. Although discrepancies in findings exist with regard to the ischemic myocardium, it has been suggested that there is an association between increased β-adrenergic receptor stimulation, cyclic AMP elevation, and the development of ventricular fibrillation in early ischemia of less than 30 minutes duration. It is hypothesized that since cAMP phosphorylates Ca^{2+} channels, enhanced quantities of this nucleotide may induce intracellular Ca^{2+} overload and precipitate the Ca^{2+}-mediated electrophysiological alterations that underlie ventricular fibrillation. On the other hand, the recovery of signal transduction with respect to increased β-adrenergic receptors and the adenylyl

cyclase enzyme during reperfusion is thought to have beneficial implications. Since adenylyl cyclase regulates Ca^{2+} fluxes across the SL and SR membranes, the alterations in the reperfused myocardium may represent mechanisms for the recovery of the ischemic–reperfused myocardium [189]. This explanation may help rationalize the ability of the stunned myocardium to respond to adrenergic stimulation. It should also be noted that in spite of the considerable effort that has been made for the understanding of alterations in the β-adrenoceptor pathway during ischemia, an enormous amount of discrepancy exists in the reports on this subject by various investigators. Although most of these studies have employed a variety of animal models, it is not known if similar changes occur in the human. Nonetheless, it is interesting to observe that one hour of cardiopulmonary bypass with cardioplegic cardiac arrest promoted marked desensitization of β-adrenoceptor-mediated right atrial adenylyl cyclase activation without affecting the right atrial β-adrenoceptor number in children with acyanotic congenital heart disease [190].

MECHANISMS RESPONSIBLE FOR ALTERATIONS IN THE β-ADRENOCEPTOR PATHWAY DURING ISCHEMIA–REPERFUSION

Various explanations have been provided for the increase in β-adrenoceptor density by ischemia. Several investigators have argued that β-adrenoceptors were redistributed from the intracellular vesicles to the membranes during ischemia [180,181,185,191,192]. On the other hand, it has been suggested that redistribution of β-adrenoceptors is due to impaired internalization, an effect attributed to ATP depletion [185,193]. However, Mukherjee et al. [64] have rejected the mechanism of receptor translocation as a possible explanation for an ischemia-induced increase in β-adrenoceptor density. An increase in protein synthesis, although attractive, is not a satisfactory explanation for the increase in receptor numbers because of the relatively short period of ischemia [64]. Likewise, the observed increase in receptor density may not be artefactual because no difference in membrane protein content was seen between control and ischemic hearts [64]. One explanation that has been gaining considerable recognition recently is that the effect of ischemia–reperfusion on β-adrenoceptors may be mediated via oxidative stress. In this regard, it should be noted that ischemia and reperfusion have been shown to be associated with oxidative stress, which has been observed to affect the β-adrenoceptor density [194]. On the other hand, oxygen-radical-generating systems were demonstrated to induce a decrease in maximal specific binding of ^{125}ICYP to membrane fractions from lungs, lymphocytes, or adipocytes [195,196]. More recently, it has been stated that relatively mild oxidative stress by H_2O_2 may increase the density of β-adrenoceptors in cardiac membranes, whereas higher concentrations of H_2O_2 decrease the density of the receptors without any alterations in their affinity [194]. However, in another study, mild oxidative stress produced by a variety of radical-generating systems decreased the affinity of ^{3}H-DHA binding to cardiac membranes and increased the maximal binding of ^{3}H-DHA [197]. Nonetheless, maximal binding of a hydrophilic ligand ^{3}HCGP-12177 was unaffected. This outcome has been interpreted to be indicative of oxygen-radical-induced alteration in membranes such that there is an

increase in the accessibility of β-receptors to hydrophobic but not hydrophilic ligands [197]. Extensive oxidative stress, however, decreased maximal binding to β-adrenoceptors for both hydrophilic and hydrophobic ligands [197]. Oxidative stress has also been shown to impair the overall β-adrenoceptor response in several organs. A reduced β-adrenergic response in airway smooth muscle has been observed due to both treatment with H_2O_2 [198] and oxygen free radicals produced by activated macrophages [199]. The positive inotropic response in cardiac muscle to catecholamines [200] and adrenergic relaxation of the small intestine [201] have been shown to be compromised by treatment with H_2O_2.

Similar to the divergent reports concerning the β-adrenoceptor status in ischemia and reperfusion, there is also no consensus with regard to the status of adenylyl cyclase activity and cAMP formation under the same conditions. Both decreases [58,62,66,67] and increases [180,185] in adenylyl cyclase activity due to ischemia have been reported. Will-Shahab et al. [202] reported that while the reduction in adenylyl cyclase in moderate ischemia was reversible, a more pronounced ischemia caused irreversible damage. It has been suggested that while reversible damage to adenylyl cyclase may be due to increased Ca^{2+} content of the heart, the irreversible damage may be due to oxidative stress [202]. However, one study indicated that adenylyl cyclase is the main target for oxidative stress, as seen in conditions such as ischemia–reperfusion [202] whereas Haenen et al. [203] suggested that the intermediary G-proteins are affected by oxidative stress. However, not much is known about the effect of ischemia–reperfusion or oxidative stress upon the coupling G-proteins in the β-adrenoceptor signal transduction pathway.

It is tempting to speculate that the effects of ischemia–reperfusion upon β-adrenoceptors–adenylyl cyclase is mediated via oxidative stress. If the reported effects during this condition are due to oxidative stress, this might to some extent explain the conflicting results obtained by various investigators. In this regard, it should be noted that peroxidation of membrane lipids due to oxidative stress has been reported to lower receptor density and alter plasma membrane viscosity, which affects receptor coupling [201]. Reactive oxygen species may also interact with thiol–disulphide groups in the protein components of the signal transduction system and may lead to altered receptor coupling. To this end, both β-adrenergic receptors [204] and adenylyl cyclase [205,206] have been shown to contain sulfhydryl groups that are essential for their function, and these are vulnerable targets for reactive oxygen species. G-proteins also contain essential sulfhydryl groups, the alkylation or oxidation of which can alter their ability to couple receptor signal to the effector—namely, adenylyl cyclase [205,207].

From the above discussion, it is evident that the functional responsiveness of the β-adrenoceptor–G protein–adenylyl cyclase system is altered during ischemia and reperfusion. However, upon studying the modifications of the components during these conditions, it is strikingly obvious that very little consistency exists in the findings by the various investigators, and several mechanisms have been proposed for these modifications. Ischemia–reperfusion has been shown to be associated with oxidative stress, which in turn is known to affect β-adrenoceptors and adenylyl

cyclase in various tissues. Intracellular targets for these reactive oxygen species appear to be both membrane lipids and proteins, especially the sulfhydryl groups and disulfide bridges of the proteins. However, relatively little is known about the effect of oxidative stress on β-adrenoceptors and adenylyl cyclase in the heart; moreover, the information available to date is divergent. In addition, almost nothing is known with regard to oxidative stress-induced alterations in G-proteins and their coupling activity.

CONCLUDING REMARKS

From the foregoing discussion, it is evident that early restoration of blood flow during acute myocardial ischemia is effective in reducing infarct size and improving ventricular function [208,209]. While reperfusion of the ischemic heart is generally thought to be a beneficial process, some detrimental effects, such as deterioration of contractile function and the ultrastructural damage known as reperfusion injury, have been observed when the ischemic myocardium is reperfused after a certain time [209–211]. In view of the important role played by β-adrenoceptors, G-proteins, and the adenylyl cyclase system in the regulation of heart function and metabolism, several investigators have reported that the β-adrenergic receptor mechanisms are altered during myocardial ischemia [56–59] as well as during coronary arterial reperfusion [56,60–63]. However, the effects of ischemia and reperfusion on various components of the β-adrenergic pathway remain controversial because increases, decreases, and no changes have been observed [57,61–67]. These conflicting results observed by different investigators appear to be due to the usage of variable periods of ischemia as well as varying degrees of reperfusion. In addition, reperfusion may be occurring simultaneously as a consequence of opening the collaterals under in vivo conditions. Nonetheless, relatively little is known regarding the mechanisms that change the β-adrenoceptor signal transduction system in the ischemic as well as ischemic–reperfused hearts.

Oxygen-derived free radicals have been implicated as a major factor in the pathophysiology of ischemia–reperfusion injury in the myocardium [68–70]. These partially reduced forms of oxygen in the ischemic–reperfused myocardium may be generated within the cardiomyocyte at the mitochondrial respiratory chain [71], or by other sources such as arachidonic acid metabolism and catecholamine oxidation [69,72]. Several investigators [75,212,213] have reported that exogenous free radicals produce functional and structural abnormalities in the heart. Treatment of cardiac SR and SL membranes with different oxyradical-generating systems has been shown to depress Ca^{2+} pump mechanisms, and these defects have been suggested to induce intracellular Ca^{2+} overload and subsequent heart dysfunction [70,109–112]. Depression in the SL Na^+–K^+ ATPase and Na^+–Ca^{2+} exchange activity upon treatment of heart membranes with oxyradical generating systems has also been suggested to contribute toward the occurrence of intracellular Ca^{2+} overload [113,114]. Perfusion of isolated hearts with an oxyradical-generating system has been shown to depress both the SL Na^+–Ca^{2+} exchange and Ca^{2+} pump activities during the development

of contractile failure [118,119]. Although a decrease in the density of Ca^{2+} channels in the SL membrane [112] and sarcoplasmic reticulum [119] due to oxyradicals can be seen to result in a reduction of Ca^{2+} available for cardiac contraction, the contribution of depressed Ca^{2+}-stimulated ATPase activity upon exposing myofibrils [120] to oxyradicals in promoting contractile abnormalities cannot be ruled out. Accordingly, it appears that heart dysfunction due to oxygen free radicals may be due to defects in both Ca^{2+} handling by cardiomyocytes and the interaction of Ca^{2+} with the contractile apparatus.

Since β-adrenoceptor mechanisms, including β_1- and β_2-adrenoceptors, G_s- and G_i-proteins, and adenylyl cyclase, are known to affect the entry of Ca^{2+} in cardiomyocytes and to play an important role in the regulation of heart function [40,121], some investigators have examined the effects of different oxyradical-generating systems on various components of this signal transduction pathway. For example, treatment of cardiac membranes with some oxyradical-generating systems increased the density but decreased the affinity of β-adrenoceptors [197], whereas treatment with H_2O_2, an active species of oxygen, decreased the affinity without any changes in the density of β-adrenoceptors [197,214]. On the other hand, treatment of heart membranes with H_2O_2 was reported to increase the density of β-adrenoceptor [194], whereas a loss in the number of β-adrenoceptors was seen upon treatment of cortical membranes with iron and ascorbic acid, a hydroxyl radical-generating system [203]. An increase or no change in the density of β-adrenoceptors in ventricular membranes has also been observed upon treatment with some oxidants [215,216]. Furthermore, it may be pointed out that no information regarding the effect of oxyradicals in oxidants on β_1- or β_2-adrenoceptors is available in the literature. It should be noted that a decrease in adenylyl cyclase activity was observed upon treating heart membranes with H_2O_2 and some oxidants by some investigators [40,215,216], whereas others [217] have reported an increase in the enzyme activity due to H_2O_2 in vascular smooth muscle cells. A transient increase followed by a decrease in the adenylyl cyclase activity was reported upon treatment of cardiac membranes with an iron–ascorbic acid system [218]. Although G-protein activities in heart membranes [214] and vascular smooth muscle cells [217] were unaltered due to oxyradical exposure, no detailed information in this regard is available with which to reach any meaningful conclusion.

Since relatively little is known about the role of oxygen free radicals in inducing changes in β-adrenergic receptor mechanisms due to reperfusion injury, and since conflicting information exists about this aspect in the ischemic heart, a series of experiments was undertaken in the study reported here to examine alterations in the various components of the β-adrenoceptor–G-protein–adenylyl cyclase in ischemic–reperfused hearts. Furthermore, experiments were carried out to investigate the effects of the superoxide dismutase (SOD) plus catalase (CAT) system, an excellent scavenger for the active species of oxygen [70], on various components of the β-adrenoceptor signal transduction pathway in ischemic–reperfused hearts. For this purpose, global ischemia–reperfusion injury was induced by occluding the coronary flow for 30 minutes followed by reperfusion for 60 minutes in isolated rat hearts

perfused in the absence or presence of SOD plus CAT. Ischemia–reperfusion-induced alterations in β-adrenoceptors, G-proteins, and adenylyl cyclase in cardiac membranes were found to be prevented by SOD plus CAT [219]. In addition, the depressed contractile activities as well as the attenuated inotropic responses of the ischemic–reperfused hearts to isoproterenol were corrected by SOD plus CAT, indicating the involvement of H_2O_2 in ischemia–reperfusion injury [219]. Perfusion of hearts with an oxyradical-generating system, xanthine plus xanthine oxidase, as well as with H_2O_2 was observed to alter β-adrenoceptor–adenylyl cyclase activities, which were prevented by SOD plus CAT [220,221]. In fact, the effect of xanthine plus xanthine oxidase on β-adrenergic-receptor-linked signal transduction was stimulated by H_2O_2 [222]. Because an increase in the production of H_2O_2 has been shown to occur in the ischemic–reperfused heart due to both dismutation of the superoxide radical and generation in the mitochondria [70,223–225], these recent experiments demonstrate that the attenuated inotropic responses of ischemia–reperfused hearts as well as altered β-adrenergic signal transduction mechanisms may be mainly due to the generation of H_2O_2 as a consequence of ischemia–reperfusion.

ACKNOWLEDGMENTS

The work reported in this chapter was supported by a grant from the Medical Research Council of Canada. Dr. V. Panagia was a senior scientist supported by the Medical Research Council of Canada.

REFERENCES

1. Becker LC, Ambrosio G. 1987. Myocardial consequences of reperfusion. Prog Cardiovasc Dis 30:23–44.
2. Braunwald E. 1989. Myocardial reperfusion, limitation of infarct size, reduction of left ventricular dysfunction and improved survival. Should the paradigm be expanded? Circulation 79:441–444.
3. Silverman NA, Levitsky S. 1987. Intraoperative myocardial protection in the context of coronary revascularization. Prog Cardiovasc Dis 29:413–428.
4. Urquhart J, Epstein SE, Patterson RE. 1985. Comparative effects of calcium-channel blocking agents on left ventricular function during acute ischemia in dogs with and without congestive heart failure. Am J Cardiol 55:10B–16B.
5. Cavero I, Boudot JP, Feuvray D. 1983. Diltiazem protects the isolated rabbit heart from the mechanical and ultrastructural damage produced by transient hypoxia, low flow ischemia and exposure to Ca^+-free medium. J Pharmacol Exp Ther 226:258–268.
6. Sharma AD, Saffitz JE, Lee BI, Sobel BE, Corr PB. 1983. Alpha adrenergic-mediated accumulation of calcium in reperfused myocardium. J Clin Invest 72:802–818.
7. Kitakaze M, Hori M, Sato H, Iwakura K, Gotoh K, Inoue M, Kitabatake A, Kamada T. 1991. Beneficial effects of α_1-adrenoceptor activity on myocardial stunning in dogs. Circ Res 68:1322–1332.
8. Nayler WG, Ferrari R, Williams A. 1980. Protective effect of pretreatment with verapamil, nifedipine and propranolol on mitochondrial function in the ischemic and reperfused myocardium. Am J Cardiol 46:242–248.
9. Ichihara K, Abiko Y. 1983. Effects of diltiazem and propranolol on irreversibility of ischemic cardiac function and metabolism in the isolated perfused rat heart. J Cardiovasc Pharmacol 5:745–751.
10. Jequier E, Perret C. 1970. Urinary excretion of catecholamines and their main metabolites after myocardial infarction: relationship to the clinical syndrome. Eur J Clin Invest 1:77–83.

11. Karmazyn M, Dhalla NS. 1984. Physiological and pathophysiological aspects of cardiac prostaglandins. Can J Physiol Pharmacol 61:1207–1212.
12. Beamish RE, Das PK, Karmazyn M, Dhalla NS. 1985. Prostaglandins and heart disease. Can J Cardiol 1:66–74.
13. Chien KR, Hans A, Sen A, Buja LM, Willerson JT. 1984. Accumulation of unesterified arachidonic acid in ischemic canine myocardium. Circ Res 54:313–316.
14. Idell-Wenger JA, Grotyohann LW, Neely JR. 1978. Coenzyme A and carnitine distribution in normal and ischemic hearts. J Biol Chem 253:4310–4318.
15. Shug AL, Folts JD, Thomsen JH, Folts JD, Bittar N, Klein MI, Koke JR, Huth PJ. 1978. Changes in tissue levels of carnitine and other metabolites during myocardial ischemia and anoxia. Arch Biochem Biophys 187:25–33.
16. Van der Vusse G, Roeman GT, Prinzen FW, Coumans WA, Reneman RS. 1982. Uptake and tissue content of fatty acids in dog myocardium under normoxic and ischemic conditions. Circ Res 50:538–541.
17. Lochner A, Kotze JC, Gevers W, Benade AJ. 1979. Substrate effects on mitochondrial function and tissue lipids in low flow hypoxia of isolated perfused rat hearts. Basic Res Cardiol 74:303–312.
18. Opie LH. 1979. Role of carnitine in fatty acid metabolism of normal and ischemic myocardium. Am Heart J 97:375–388.
19. Liedtke AJ. 1981. Alterations of carbohydrate and lipid metabolism in the acutely ischemic heart. Prog Cardiovasc Dis 23:321–326.
20. Stam H, Hubman WC. 1978. The role of endogenous catecholamines in the depressive effect of free fatty acids on isolated perfused rat hearts. Basic Res Cardiol 73:208–219.
21. Karnovsky MJ. 1979. Lipid domains in biological membranes: their structural and functional perturbations by free fatty acids and the regulation of receptor mobility. Am J Pathol 97:212–221.
22. Dhalla NS, Kolar F, Shah R, Ferrari R. 1991. Effects of some L-carnitine derivatives on heart membrane ATPases. Cardiovasc Drug Ther 5:25–30.
23. Spedding M, Mir AK. 1987. Direct activation of Ca^{2+}-channels by palmitoyl carnitine, a putative endogenous ligand. Br J Pharmacol 92:457–468.
24. Sobel BE, Corr PB, Robison AK, Goldstein RA, Witkowski FX, Klein MS. 1978. Accumulation of lysophosphoglycerate with arrhythmogenic properties in ischemic myocardium. J Clin Invest 62:546–553.
25. Woodley SL, Ikenouchi H, Barry WH. 1991. Lysophosphatidylcholine increases cytosolic calcium in ventricular myocytes by direct action of the sarcolemma. J Mol Cell Cardiol 23:671–680.
26. Prasad MR, Popescu LM, Moraru II, Liu XK, Maity S, Engelman RM. 1991. Role of phospholipase A_2 and C in myocardial ischemic–reperfusion injury. Am J Physiol 260:H877–H883.
27. Chien KR, Reeves JP, Buja LM, Bonte F, Parkey RW, Willerson JT. 1981. Phospholipid alterations in canine ischemic myocardium. Circ Res 48:711–719.
28. Nakaya H, Tohse N. 1986. Electrophysiological effects of acetyl glyceryl ester phosphorylcholine on cardiac tissue. Br J Pharmacol 89:749–757.
29. Giffin M, Arthur GS. 1988. Lysophosphatidic choline metabolism and cardiac arrhythmias. Can J Physiol Pharmacol 66:185–189.
30. Ferrara N, Abete P, Leosco D, Carcese P, Orlando M, DeCaprio L, Rengo F. 1990. Arrhythmogenic age related effects of lysophosphatidylcholine in the rat heart. Cardioscience 2:99–104.
31. Katz AM, Hecht HH. 1969. The early "pump" failure of the ischemic heart. Am J Med 47:497–502.
32. Kihara Y, Grossman W, Morgan JP. 1989. Direct measurement of changes in intracellular calcium transients during hypoxia, ischemia and reperfusion of the intact mammalian hearts. Circ Res 65:1029–1044.
33. Opie LH. 1976. Effects of anoxia and regional ischemia on metabolism of glucose and fatty acids. Relative rates of aerobic and anaerobic energy production during first 6 hours of experimental myocardial infarction. Circ Res 38(Suppl I):152.
34. Opie OHL, Brooks WW, Messer JV. 1973. Heart muscle viability during hypoxia: protective effect of acidosis. Science 180:1297–1298.
35. Tennant R. 1935. Factors concerned in the arrest of contraction in an ischemic myocardial area. Am J Physiol 113:677–682.
36. Lehninger AL, Reynafarre B, Vercesi A. 1978. Transport and accumulation of calcium in mitochondria. Ann NY Acad Sci 307:160–176.

37. Nayler WG, Poole-Wilson PA, Williams A. 1979. Hypoxia and calcium. J Mol Cell Cardiol 11:683–706.
38. Dhalla NS, Das PK, Sharma GP. 1978. Subcellular basis of cardiac contractile failure. J Mol Cell Cardiol 10:363–385.
39. Dhalla NS, Dixon IMC, Beamish RE. 1991. Biochemical basis of heart function and contractile failure. J Appl Cardiol 6:7–30.
40. Dhalla NS, Pierce GN, Panagia V, Singal PK, Beamish RE. 1982. Calcium movements in relation to heart function. Basic Res Cardiol 77:117–139.
41. Panagia V, Singh JN, Anand-Srivastava MB, Pierce GN, Jasmin G, Dhalla NS. 1984. Sarcolemmal alterations during the development of genetically determined cardiomyopathy. Cardiovasc Res 18:567–572.
42. Ganguly PK, Rice KM, Panagia V, Dhalla NS. 1984. Sarcolemmal phosphatidylethanolamine N-methylation in diabetic cardiomyopathy. Circ Res 55:504–512.
43. Daly MJ, Dhalla NS. 1985. Alterations in the cardiac adenylate cyclase in hypothyroid rat. Can J Cardiol 1:288–293.
44. Okumura K, Panagia V, Jasmin G, Dhalla NS. 1987. Sarcolemmal phospholipid N-methylation in genetically determined hamster cardiomyopathy. Biochem Biophys Res Commun 143:31–37.
45. Lefkowitz RJ, Caron MG, Stiles GL. 1984. Mechanisms of membrane receptor regulation. Biochemical, physiological and clinical insights derived from studies of the adrenergic receptors. N Engl J Med 310:1570–1579.
46. Denniss AR, Collucci WS, Allen PD, Marsh JD. 1989. Distribution and function of human ventricular beta adrenergic receptors in congestive heart failure. J Mol Cell Cardiol 21:651–660.
47. Gilson N, El Houda Bouanani N, Corsin A, Crozatier B. 1990. Left ventricular function and beta-adrenoceptors in rabbit failing heart. Am J Physiol 258:H634–H641.
48. Horn EM, Bilezikian JP. 1990. Mechanisms of abnormal transmembrane signalling of the β-adrenergic receptor in congestive heart failure. Circulation 82(Suppl I):I26–I34.
49. Bristow MR, Hershbergen RE, Port JD, Gilbert EM, Sandoval A, Rasmussen R, Cates AE, Feldman AM. 1990. β-adrenergic pathways in nonfailing and failing human ventricular myocardium. Circulation 82(Suppl I):I12–I25.
50. Newman J, Schmitz W, Scholz H, Von Meyerinck L, Döring V, Kalmár P. 1988. Increase in myocardial G_i-proteins in heart failure. Lancet 2:936–937.
51. Vago T, Beuilacqua M, Norbiato G, Baldi G, Chebat E, Bertora P, Baroldi G, Accinni R. 1989. Identification of α_1-adrenergic receptors on sarcolemma from normal subjects and patients with idiopathic dilated cardiomyopathy: characteristics and linkage to GTP-binding proteins. Circ Res 64:474–481.
52. Leier CV, Brikley PF, Cody RJ. 1990. Alpha-adrenergic component of the sympathetic nervous system in congestive heart failure. Circulation 82(Suppl II):68–76.
53. Daly MJ, Dhalla NS. 1987. Sarcolemmal Na^+-K^+ ATPase activity in hypothyroid rat heart. J Appl Cardiol 2:105–119.
54. Panagia V, Okumura K, Shah KR, Dhalla NS. 1987. Modification of sarcolemmal phosphatidylethanolamine N-methylation during heart hypertrophy. Am J Physiol 253:H8–H15.
55. Okumura K, Panagia V, Beamish RE, Dhalla NS. 1987. Biphasic changes in the sarcolemmal phosphatidylethanolamine N-methylation activity in catecholamine induced cardiomyopathy. J Mol Cell Cardiol 19:357–366.
56. Thandroyen FT, Muntz KH, Buja LM, Willerson JT. 1990. Alterations in β-adrenergic receptors, adenylate cyclase and cyclic AMP concentrations during acute myocardial ischemic and reperfusion. Circulation 82(Suppl II):30–37.
57. Strasser RH, Krimmer J, Braun-Dallaeus R, Marquetant R, Kübler W. 1990. Dual sensitization of the adrenergic system in early myocardial ischemic: independent regulation of the β-adrenergic receptors and the adenylyl cyclase. J Mol Cell Cardiol 22:1405–1423.
58. Freissmuth M, Schütz W, Weindlmayer-Göttel M, Zimfer M, Spiss CK. 1987. Effect of ischemia on canine myocardial β-adrenoceptor linked adenylate cyclase system. J Cardiovasc Pharmacol 10:568–574.
59. Sussani EE, Mandes WT, Knight DR, Vatner DE, Vatner SF, Homey CJ. 1989. One hour of myocardial ischemia decreases the activity of the stimulating guanine nucleotide regulatory protein G_s. Circ Res 65:1145–1150.

60. Kiuchi K, Shen Y-T, Vatner SF, Vatner DE. 1994. Mechanism mediating responsiveness to β-adrenergic stimulation after coronary reperfusion in conscious dogs. Am J Physiol 267:H1578–H1588.
61. Vatner DE, Kiuchi K, Mandes WT, Vatner SF. 1993. Effects of coronary arterial reperfusion on β-adrenergic receptor adenylyl cyclase coupling. Am J Physiol 264:H196–H204.
62. Karliner JS, Stevens MB, Honbo N, Hoffman JIE. 1989. Effects of acute ischemia in the dog on myocardial blood flow, beta receptors, and adenylate cyclase activity with or without beta blockade. J Clin Invest 83:474–481.
63. Mukherjee A, Bush LR, McCoy KE, Duke RJ, Hagler H, Buja LM, Willerson JT. 1982. Relationship between β-adrenergic receptor numbers and physiological responses during experimental canine myocardial ischemia. Circ Res 50:735–741.
64. Mukherjee A, Wang TM, Buja LM, Leftkowitz RJ, Willerson JT. 1979. Beta-adrenergic receptors and muscarinic cholinergic receptors in canine myocardium: effects of ischemia. J Clin Invest 64:1423–1428.
65. Drummond RW, Sordahl LA. 1981. Temporal changes in adenylyl cyclase activity in ischemic dog heart: evidence of functional subunit damage. J Mol Cell Cardiol 13:323–330.
66. Devos C, Bobberecht P, Nokin P, Wallbroeck M, Clinet M, Camus JC, Beaufort P, Schoenfeld P, Christophe J. 1985. Uncoupling between beta-adrenoceptor and adenylyl cyclase in the dog ischemic myocardium. Naunyn-Schmiedebergs Arch Pharmacol 331:71–75.
67. Vatner DE, Knight DR, Shen Y-T, Thomas JX, Homcy CJ, Vatner SF. 1988. One hour myocardial ischemia in conscious dogs increases β-adrenergic receptors but decreases adenylyl cyclase activity. J Mol Cell Cardiol 20:75–82.
68. McCord JM. 1985. Oxygen derived free radicals in post-ischemic tissue injury. N Engl J Med 312:159–163.
69. Kloner RA, Przykleuk K, Whittaker P. 1989. Deleterious effects of oxygen radicals in ischemia/reperfusion. Resolved and unresolved issues. Circulation 80:1115–1127.
70. Kukreja RC, Hess ML. 1992. The oxygen radical system: from equation through membrane protein interactions to cardiovascular injury and protection. Cardiovasc Res 26:641–655.
71. Zweier JL, Kappusamy P, Lutty GA. 1988. Measurement of endothelial cell free radical generation: evidence for a central mechanism of free radical injury in postischemic tissues. Proc Natl Acad Sci USA 85:4066–4150.
72. Jewett SL, Eddy LJ, Hochstein P. 1989. Is the autoxidation of catecholines involved in ischemia–reperfusion injury? Free Rad Biol Med 6:185–188.
73. Barrington PL, Meier CF. 1988. Abnormal electrical activity induced by free radical generating systems in isolated cardiocytes. J Mol Cell Cardiol 20:1163–1178.
74. Tarr M, Valenzeno DP. 1991. Modification of cardiac ion currents by photosensitizer generated reactive oxygen. J Mol Cell Cardiol 23:639–649.
75. Burton KP, McCord JM, Ghai G. 1984. Myocardial alterations due to free-radical generation. Am J Physiol 246:H776–H783.
76. Gupta M, Singal PK. 1989. Time course of structure, function and metabolic changes due to an exogenous source of oxygen metabolites. Can J Physiol Pharmacol 67:1549–1559.
77. Kaminishi K, Yanagishita T, Kako KJ. 1989. Oxidant injury to isolated heart cells. Can J Cardiol 5:168–174.
78. Prasad K, Kalra J. 1989. Effect of oxygen free radicals on cardiovascular function at organ and cellular levels. Am Heart J 117:1196–1202.
79. Jolly SR, Kane WJ, Bailie MB, Abrams GD, Lucchesi BR. 1984. Canine myocardial reperfusion injury: its reduction by the combined administration of superoxide dismutase and catalase. Circ Res 54:277–285.
80. Ambrosio G, Becker L. 1986. Reduction in experimental infarct size by recombinant human superoxide dismutase: insights into the pathophysiology of reperfusion injury. Circulation 74:1424–1433.
81. Hess ML, Manson NH. 1984. Molecular oxygen: friend and foe. J Mol Cell Cardiol 16:969–985.
82. Bolli R. 1991. Oxygen derived free radicals and myocardial reperfusion injury: an overview. Cardiovasc Drugs Ther 5:249–268.
83. Bernier M, Hearse DJ, Manning AS. 1986. Reperfusion induced arrhythmias and oxygen-derived free radicals: studies with "anti-free radical" interventions and a free radical generating system in the isolated perfused rat heart. Circ Res 58:331–340.

84. Faber NE, Vercellotti GM, Jacob HS, Peiper GM, Gross GJ. 1985. Evidence for a role of iron-catalyzed oxidants in functional and metabolic stunning in the canine heart. Circ Res 63:351–360.
85. Prezyklenk K, Kloner RA. 1986. Superoxide dismutase plus catalase improve contractile function in the canine model of the stunned myocardium. Circ Res 58:148–156.
86. Bolli R. 1988. Oxygen-derived free radicals and postischemic myocardial dysfunction ("stunned myocardium"). J Am Coll Cardiol 12:239–249.
87. Blasig IE, Lowe H, Ebert B. 1987. Radical trapping and lipid peroxidation during myocardial ischemic injury: radical scavenging by troxeratin in comparison to mannitol. Biomed Biochim Acta 46:5539–5544.
88. Bolli R, Patel BS, Jeroudi MO, Lai EK, McCay PB. 1988. Demonstration of free radical generation in "stunned" myocardium of intact dogs with the use of the spin trap alphaphenyl N-tert-butylnitrone. J Clin Invest 82:476-485.
89. Zweier JL, Kuppusamy P, Williams R, Rayburn BK, Smith D, Weisfeldt ML, Flaherty JL. 1989. Measurement and characterization of post ischemic free radical generation in the isolated perfused heart. J Biol Chem 264:18870–18895.
90. Mergner GW, Weglicki WB, Kramer JH. 1991. Postischemic free radical production in the venous blood of the regionally ischemic swine heart. Effect of diferoxamine. Circulation 84:2079–2090.
91. Granger DN, Rutill G, McCord JM. 1985. Superoxide radicals in feline intestinal ischemia. Gastroenterology 312:159–163.
92. Parks DA, Williams TK, Beckman JS. 1988. Conversion of xanthine dehydrogenase to oxidase in ischemic rat intestine: a reevaluation. Am J Physiol 254:G768–G774.
93. Duran N. 1982. Singlet oxygen in biological processes. In Adam W, Cilento G (eds), Chemical and Biological Generation of Excited States. New York: Academic Press, p. 345.
94. Jennings RB, Reimer KA. 1981. Letral myocardial ischemic injury. Am J Pathol 102:24–55.
95. Abdel-Elfattah AS, Jessen ME, Lekuen J, Doherty NE, Brunsting LA, Wechsler AS. 1989. Myocardial reperfusion injury. Role of myocardial hypoxanthine and xanthine in free radical-mediated reperfusion injury. Circulation 78(Suppl III):224–235.
96. Parks DA, Bulkley GB, Granger DN, Hamilton SR, McCord JM. 1982. Ischemic injury in the cat small intestine: role of superoxide radicals. Gastroenterology 82:9–15.
97. Grisham MB, Russel WJ, Roy RS, McCord JM. 1986. Reoxygenation injury in the isolated perfused working rat heart: roles of xanthine oxidase and transferrin. In Rofillio G (ed), Superoxide and Superoxide Dismutase in Chemistry, Biology and Medicine. Amsterdam: Elsevier, pp. 571–575.
98. Werns SW, Shea MJ, Mitsos SE. 1986. Reduction of the size of infarction by allopurinol in the ischemic–reperfused canine heart. Circulation 73:518–524.
99. Grum CM, Gallagher KP, Kirsh MM, Shlafer M. 1989. Absence of detectable xanthine oxidase in human myocardium. J Mol Cell Cardiol 21:263–267.
100. Al-Khalidi UAS, Chaglssian TH. 1965. The species distribution of xanthine oxidase. Biochem J 97:318–320.
101. Eddy LJ, Stewart JR, Jones HP, Engerson TD, McCord JM, Downey JM. 1987. Free radical-producing enzyme, xanthine oxidase, is undetectable in human hearts. Am J Physiol 22:H709–H711.
102. Yokoyama Y, Beckman JS, Beckman TK. 1990. Circulating xanthine oxidase: potential mediator of ischemic injury. Am J Physiol 258:G564–G570.
103. McCord JM. 1987. Oxygen-derived free radicals: a link between reperfusion injury and inflammation. Fed Proc 46:2402–2406.
104. Freeman B, Crapo JD. 1982. Biology of disease. Free radicals and tissue injury. Lab Invest 47:412–426.
105. Singal PK, Kapur N, Dhillon KS, Beamish RE, Dhalla NS. 1982. Role of free radicals in catecholamine-induced cardiomyopathy. Can J Physiol Pharmacol 60:1390–1397.
106. Kukreja RC, Kontos HA, Hess ML, Ellis EF. 1986. PGH synthase and lipoxygenase generate superoxide in the presence of NADH or NADPH. Circ Res 59:612–619.
107. Kellogg EW. 1975. Superoxide, hydrogen peroxide and singlet oxygen in lipid peroxidation by a xanthine oxidase system. J Biol Chem 250:8812–8817.
108. Mead JF. 1984. Free radical mechanisms in lipid peroxidation and prostaglandins. In Free Radicals in Molecular Biology and Disease. New York: Raven Press, pp. 53–65.
109. Rowe GT, Manson NH, Caplan M, Hess ML. 1983. Hydrogen peroxide and hydroxyl radical mediation of activated leukocyte depression of cardiac sarcoplasmic reticulum. Circ Res 53:584–591.

110. Okabe F, Hess ML, Oyama M, Ito H. 1983. Characterization of free radical-mediated damage of canine sarcoplasmic reticulum. Arch Biochem Biophys 225:164–177.
111. Kaneko M, Beamish RE, Dhalla NS. 1989. Depression of heart sarcolemmal Ca^{2+}-pump activity by oxygen free radicals. Am J Physiol 256:H368–H374.
112. Kaneko M, Lee S-L, Wolf CM, Dhalla NS. 1989. Reduction of calcium channel antagonist binding sites by oxygen free radicals in rat heart. J Mol Cell Cardiol 21:235–243.
113. Shao Q, Matsubara T, Bhatt SK, Dhalla NS. 1995. Inhibition of sarcolemmal Na^+–K^+ ATPase by oxyradical generating systems. Mol Cell Biochem 147:139–144.
114. Hata T, Kaneko M, Beamish RE, Dhalla NS. 1991. Influence of oxygen free radicals on heart sarcolemmal Na^+–Ca^{2+} exchange. Coronary Artery Dis 2:397–407.
115. Reeves JP, Baily CA, Hale CC. 1986. Redox modification of sodium calcium exchange activity in cardiac sarcolemmal vesicles. J Biol Chem 261:4948–4955.
116. Kim M-S, Akera T. 1987. O_2 free radicals: cause of ischemia–reperfusion injury to cardiac Na^+–K^+ ATPase. Am J Physiol 252:H252–H257.
117. Matsubara T, Dhalla NS. 1996. Effect of oxygen free radicals on cardiac contractile activity and sarcolemmal Na^+–Ca^{2+} exchange. J Cardiovasc Pharmacol Ther 1:211–218.
118. Matsubara T, Dhalla NS. 1996. Relationship between mechanical dysfunction and depression of sarcolemmal Ca^{2+}-pump activity in rat hearts perfused with oxygen free radicals. Mol Cell Biochem 160/161:179–185.
119. Holmberg SRM, Cumming DVE, Kusama Y, Hearse DJ, Poole-Wilson PA, Shattock MJ, Williams AJ. 1991. Reactive oxygen species modify the structure and function of cardiac sarcoplasmic reticulum calcium-release channel. Cardioscience 2:19–25.
120. Suzuki S, Kaneko M, Chapman DC, Dhalla NS. 1991. Alterations in cardiac contractile proteins due to oxygen free radicals. Biochim Biophys Acta 1074:95–100.
121. Tsien RW. 1977. Cyclic AMP and contractile activity in heart. Adv Cyclic Nucleotide Res 8:363–420.
122. Dohlman HG, Thorner J, Caron MG, Lefkowitz RJ. 1991. Model system for the study of seven-transmembrane-segment receptors. Annu Rev Biochem 60:653–688.
123. Chung F-Z, Lentes K-V, Gocayne J, Fitzgerald M, Robinson D, Kerlavage A, Fraser CM, Venter JC. 1987. Cloning and sequence of human brain β-adrenergic receptor. Evolutionary relationship to rodent and avian β-receptors and porcine muscarinic receptors. FEBS Lett 211:200–206.
124. Emorine LJ, Feve B, Pairault J, Briend-Sutren MM, Marullo S, Delavier-Klutchko C, Strosberg DA. 1991. Structural basis for functional diversity of β_1-, β_2- and β_3-adrenergic receptors. Biochem Pharmacol 41:853–859.
125. Kauman AJ. 1989. Is there a third heart β-adrenoceptor? Trends Pharmacol Sci 10:316–320.
126. Brodde O-E. 1991. β_1- and β_2-adrenoceptors in the human heart: properties, function and alterations in chronic heart failure. Pharmac Rev 43:203–242.
127. Steinfath M, Lavicky J, Schmitz W, Scholz H, Döring V, Kalmar P. 1992. Regional distribution of β_1- and β_2-adrenoceptors in the failing and nonfailing human hearts. Eur J Clin Pharmacol 42:607–612.
128. Elnatan J, Molenaar P, Rosenfeld F, Summers RJ. 1992. Autoradiographic determination of β-adrenoceptor density in human heart failure. J Mol Cell Cardiol 24(Suppl I):103.
129. De-Silva R, Rhodes CG, Lefroy D, Uren NG, Crake T, Boyd H, Choudhry L, Ueki J, Steel C, Waters S, Jones T, Hughes JMB, Camici PG. 1992. *In vivo* quantification of myocardial beta adrenoceptors in healthy male volunteers using [^{11}C]-(S)-CGP12177 and positron emission tomography (PFT). Eur Heart J 13:232.
130. Elnatan J, Molenaar P, Summers RJ. 1991. Density and distribution of β-adrenoceptor subtypes in human atrio-ventricular conducting system. Clin Exp Pharmacol Physiol (Suppl 18):16.
131. Bristow MR. 1989. Myocardial cell surface membrane receptors in heart failure. Heart Failure 5:47–50.
132. Kaumann AJ, Hall JA, Murray KJ, Wells FC, Brown MJ. 1989. A comparison of the effects of adrenaline and noradrenaline on human heart: the role of β_1- and β_2-adrenoceptors in the stimulation of adenylyl cyclase and contractile force. Eur Heart J 10:29–37.
133. Stiles GL, Caron MG, Lefkowitz RJ. 1974. β-adrenergic receptors: biochemical mechanisms of physiological regulation. Physiol Rev 64:661–743.
134. Spann JF, Sonnenblick EH, Cooper T, Chidsey LA, Willman VL, Braunwald E. 1966. Cardiac norepinephrine stores and the contractile state of the heart. Circ Res 19:317–325.
135. Levitzki A, Atlas D. 1981. A possible molecular mechanism for beta-receptor desensitization: experiments and hypotheses. Life Sci 28:661–672.

136. Benovic JL, Strasser RH, Caron MG, Lefkowitz RL. 1986. Beta-adrenergic receptor kinase: identification of a novel protein kinase that phosphorylates the agonist occupied form of the receptor. Proc Natl Acad Sci USA 83:2797–2801.
137. Strasser RH, Sibley DR, Lefkowitz RJ. 1986. A novel catecholamine activated adenosine cyclic 3′, 5′-phosphate independent pathway for β-adrenergic receptor phosphorylation in wild type and mutant S49 lymphoma cells: mechanism of homologous desensitization of adenylate cyclase. Biochemistry 25:1371–1377.
138. Sibley DR, Lefkowitz RJ. 1985. Molecular mechanism of receptor desensitization using the β-adrenergic receptor coupled adenylate cyclase as a model. Nature 317:124–129.
139. Brown L, Deighton NM, Bals S, Söhlmann W, Zerkowski H-R, Michel MC, Brodde O-E. 1992. Spare receptors for β-adrenoceptor mediated positive inotropic effects of catecholamines in the human heart. J Cardiovasc Pharmacol 19:222–232.
140. Yusuf S, Theodoropoulos S, Mathias CJ. 1987. Increased sensitivity of the adeneruated transplanted human heart to isoprenerline both before and after β-adrenergic blockade. Circulation 75:696–704.
141. Izawa T, Kombayashi T, Suda K, Kunisada Y, Shinoda S, Tsuboi M. 1989. An acute excercise induced translocation of β-adrenergic receptors in rat myocardium. J Biochem 105:110–113.
142. Collins S, Bouvier M, Bolanowski MA, Caron MG, Lefkowitz RJ. 1989. cAMP stimulates the β_2-adrenergic receptor gene in response to short term agonist exposure. Proc Natl Acad Sci USA 86:4853–4857.
143. Raymond JR, Hnatowich M, Lefkowitz RJ, Caron MG. 1990. Adrenergic receptors. Models for regulation of signal transduction processes. Hypertension 15:119–131.
144. Davies AO, Lefkowitz RJ. 1983. In vitro desensitization of beta-adrenergic receptors in human neutrophils. Attenuation by corticosteroids. J Clin Invest 71:565–571.
145. Brown MS, Anderson GW, Goldstein JL. 1983. Recycling receptors: the round-trip itinerary of immigrant membrane proteins. Cell 32:663–667.
146. Pfeuffer T, Metzger H. 1982. 7-0-Hemisuccinyl-deacetyl forskolin-sepharose: a novel affinity support for purification of adenylyl cyclase. FEBS Lett 146:369–375.
147. Pfeuffer T, Mollner S. 1985. Adenylate cyclase from bovine brain complex: purification and characterization of the catalytic unit. EMBO J 4:3675–3679.
148. Krupinski J, Coussen F, Bakalyar HA, Tang W-J, Feinstein PG. 1989. Adenylyl cyclase amino acid sequence: possible channel- or transporter-like structure. Science 244:1558–1564.
149. Sunahara RK, Ressauer CW, Gilman AG. 1996. Complexity and diversity of mammalian adenylyl cyclases. Annu Rev Pharmacol Toxicol 36:461–480.
150. Gao B, Gilman AG. 1991. Cloning and expression of a widely distributed (type IV) adenylyl cyclase. Proc Natl Acad Sci USA 88:10178–10182.
151. Hellevuo K, Yoshimura M, Mons N, Hoffman PL, Cooper DMF, Tabakoff B. 1995. The characterization of a novel human adenylyl cyclase which is present in brain and other tissues. J Biol Chem 270:11581–11589.
152. Schofield PR, Abbott A. 1989. Molecular pharmacology and drug action: structural information casts light on ligand binding. TIPS 10:207–212.
153. Helper JR, Gilman AG. 1992. G-proteins. Trends Biochem Sci 17:383–387.
154. Cali JJ, Zwaagstra JC, Mons N, Cooper DMF, Krupinski J. 1994. Type VIII adenylyl cyclase-A Ca^{2+}-calmodulin-stimulated enzyme expressed in discrete regions of rat brain. J Biol Chem 269:12190–12195.
155. Wayman GA, Impey S, Wu ZL, Kindsvogel W, Pritchard L, Storm DR. 1994. Synergistic activation of the type I adenylyl cyclase by Ca^{2+} and G_s-coupled receptors *in vivo*. J Biol Chem 269:25400–25405.
156. Taussig R, Quarmby LM, Gilman AG. 1993. Regulation of purified type I and type II adenylyl cyclases by G-protein, beta-gamma subunits. J Biol Chem 268:9–12.
157. Tang W-J, Gilman AG. 1991. Type specific regulation of adenylyl cyclase by G-protein βγ subunits. Science 254:1500–1503.
158. Taussig R, Iniguez-Lluhi J, Gilman AG. 1993. Inhibition of adenylyl cyclase by G_i. Science 261:218–221.
159. Taussig R, Tang W-J, Helper JR, Gilman AG. 1994. Distinct pattern of bidirectional regulation of mammalian adenylyl cyclase. J Biol Chem 269:6093–6100.
160. Premant RT, Jacobowitz O, Iyengar R. 1992. Lowered responsiveness of the catalyst of adenylyl cyclase to stimulation by G_s in heterologous desensitization: a role for cAMP dependent phosphorylation. Endocrinology 131:2774–2783.

161. Jacobowitz O, Iyengar R. 1994. Phorbol ester-induced stimulation and phosphorylation of adenylyl cyclase 2. Proc Natl Acad Sci USA 91:10630–10634.
162. Gilman AG. 1987. G-proteins: transducers of receptor generated signals. Annu Rev Biochem 56:615–649.
163. Neer EJ. 1995. Heterotrimeric G proteins: organizers of membrane signals. Cell 80:249–257.
164. Kozasa T, Itoh H, Tsukamoto T, Kaziro Y. 1988. Isolation and characterization of the human G_s gene. Proc Natl Acad Sci USA 85:2081–2085.
165. Bray P, Carter A, Simons C, Guo V, Puckett C, Kamholz C, Spiegel A, Nirenberg M. 1986. Human cDNA clones from species of $G_{s\alpha}$ signal transduction protein. Proc Natl Acad Sci USA 83:8893–8897.
166. Cassel D, Slinger Z. 1977. Mechanism of adenylate cyclase activation by cholera toxin: inhibition of GTP hydrolysis at the regulatory site. Proc Natl Acad Sci USA 74:3307–3311.
167. Birnbanmer L, Abramowitz J, Brown AM. 1990. Receptor effector coupling by G-proteins. Biochem Biophys Acta 1031:163–224.
168. Holmer SR, Sterens S, Homcy CJ. 1989. Tissue and species specific expression of inhibitory guanine nucleotide binding proteins. Cloning of a complementary DNA from canine heart. Circ Res 65:1136–1140.
169. Jones DT, Reed RR. 1987. Molecular cloning of five GTP binding protein cDNA species from rat olfactory neuroepithelium. J Biol Chem 262:14241–14249.
170. Katada T, Bokoch GM, Smigel MD, Ui M, Gilman AG. 1984. The inhibitory guanine nucleotide binding regulatory component of adenylate cyclase. Subunit dissociation and inhibition of adenylate cyclase in S49 lymphoma cyc- and wild type membranes. J Biol Chem 259:3586–3595.
171. Katada T, Ui M. 1982. Direct modification of the membrane adenylate cyclase system by islet activating protein due to ADP-ribosylation of a membrane protein. Proc Natl Acad Sci USA 79:3129–3133.
172. Neer EJ. 1994. G proteins: critical control points for transmembrane signals. Protein Sci 3:3–14.
173. Berlot CH, Bourne HR. 1992. Identification of effector-activating residues of G_s. Cell 68:911–922.
174. Graziano MP, Freismuth M, Gilman AG. 1989. Expression of $G_{s\alpha}$ in Escheria coli: purification and properties of two forms of the protein. J Biol Chem 264:409–418.
175. Codina J, Hilderbrand JD, Birnbaumer L, Secura RD. 1984. Effects of guanine nucleotide and Mg on human erythrocytes N_i and N_s, the regulatory components of adenylyl cyclase. J Biol Chem 259:11408–11418.
176. Brown AM, Birnbaumer L. 1988. Direct G-protein gating of ion channels. Am J Physiol 254:H401–H410.
177. Schubert B, Van Dongen AMJ, Kirsch GP, Brown AM. 1989. β-adrenergic inhibition of cardiac sodium channel by dual G-protein pathway. Science 245:516–519.
178. Insel PA, Ransnas LA. 1988. G proteins and cardiovascular disease. Circulation 78:1511–1513.
179. Neumann J, Schmitz W, Scholz H. 1988. Increase in myocardial G_i-proteins in heart failure. Lancet 2:936–937.
180. Maisel AS, Motulsky HJ, Insel PA. 1985. Externalization of β-adrenergic receptors promoted by myocardial ischemia. Science 230:83–186.
181. Maisel AS, Motulsky HJ, Ziegler MG, Insel PA. 1987. Ischemia- and agonist-induced changes in α- and β-adrenergic receptor traffic in guinea pig hearts. Am J Physiol 253:H1159–H1167.
182. Strasser RH, Marquetant R, Kübler W. 1990. Independent sensitization of β-adrenergic receptors and adenylate cyclase in acute myocardial ischemia. Br J Clin Pharmacol 30(Suppl I):275–365.
183. Thandroyen FT, Muntz KH, Ziman B, Buja LM, Willerson JT. 1988. Beta-adrenergic mechanisms in ischemic ventricular fibrillation (abstract). Circulation 78(Suppl II):461.
184. Ohyanagi M, Matsumori Y, Inasaki T. 1988. β-adrenergic receptors in ischemic and non-ischemic canine myocardium: relation to ventricular fibrillation and effects of pretreatment with propranolol and hexamethonium. J Cardiovasc Pharmacol 11:107–114.
185. Strasser RH, Krimmer J, Marquetant R. 1988. Regulation of β-adrenergic receptors: impaired desensitization in myocardial ischemia. J Cardiovasc Pharmacol 12:S15–S24.
186. Niroomand F, Bangert M, Beyer T, Rauch B. 1992. Reduced adenylyl cyclase inhibition by carbachol and GTP during acute myocardial ischemia. J Mol Cell Cardiol 24:471–475.
187. Strasser RH, Braun-Dallaeus R, Walendizik H, Marquetant R. 1992. α_1-Receptor-independent activation of protein kinase C in acute myocardial ischemia. Mechanisms for sensitization of adenylyl cyclase system. Circ Res 70:1304–1312.

188. Maisel AS, Ransnäs LA, Insel PA. 1990. β-adrenergic receptors and G_s-protein in myocardial ischemia and injury. Basic Res Cardiol 85:47–56.
189. Bolli R, Zhu WX, Myers ML, Hartley CJ, Roberts R. 1985. Beta-adrenergic stimulation reverses post-ischemic myocardial dysfunction without producing subsequent deterioration. Am J Cardiol 56:964–968.
190. Schranz D, Droege A, Broede A, Broderman G, Schäfer E, Oelert H, Brodde O-E. 1993. Uncoupling of human cardiac β-adrenoceptors during cardiopulmonary bypass with cardioplegic cardiac arrest. Circulation 87:422–426.
191. Maisel AS, Motulsky MG, Insel PA. 1986. Propranolol treatment externalizes β-adrenergic receptors in guinea pig myocardium and prevents further externalization by ischemia. Circ Res 60:108–112.
192. Drimal J, Knezl V, Magna D, Strizova K. 1987. External transport of β-adrenergic binding sites in ischemic myocardium. Gen Physiol Biophys 6:583–591.
193. Buja LM, Muntz KH, Rosenbaum T, Haghani Z, Buja DK, Sen A, Chien KR, Willerson JT. 1985. Characterization of a potentially reversible increase in isolated neonatal rat cardiac myocytes with impaired energy metabolism. Circ Res 57:640–645.
194. Haenen GRMM, van Dansik P, Vermeulen NPE, Timmerman H, Bast A. 1988. The effect of hydrogen peroxide on β-adrenoceptor function in the heart. Free Rad Res Commun 4:243–249.
195. Kramer K, Rademaker B, Rozendal WHM, Timmerman H, Bast A. 1986. Effect of lipid peroxidation on receptors. FEBS Lett 198:80–84.
196. Rejholcova M, Wilhelm J, Svoboda P. 1988. Lipid peroxidation inhibits norepinephrine-stimulated lipolysis in rat adipocytes. Reduction of β-adrenoceptor number. Biochem Biophys Res Commun 150:802–810.
197. Kaneko M, Chapman DC, Ganguly PK, Beamish RE, Dhalla NS. 1991. Modification of cardiac adrenergic receptors by oxygen free radicals. Am J Physiol 260:H821–H826.
198. Kramer K, Doelman CLA, Timmerman H, Bast A. 1987. A disbalance between β-adrenergic and muscarinic responses caused by hydrogen perxide in rat airways *in vitro*. Biochem Biohys Res Commun 145:357–362.
199. Engels F, Oosting RS, Nijkamp FP. 1985. Pulmonary macrophages induce deterioration of guinea pig tracheal β-adrenergic function through release of oxygen radicals. Eur J Pharmacol 11:143–144.
200. Bast A, Haenen GRMM. 1990. Receptor function in free radical mediated pathologies. In Classen V (ed), Trends in Drug Research. The Netherlands: Elsevier, pp. 273–286.
201. Van der Vliet A, Bast A. 1991. Hydrogen peroxide reduces beta-adrenoceptor function in the rat small intestine. Eur J Pharmacol 199:153–156.
202. Will-Shahab L, Schimke I, Haberland A, Küttner I. 1987. Responsiveness of cardiac adenylyl cyclase in the normal and ischemic myocardium: role of oxygen free radicals. Biomed Biochim Acta 46:S427–S432.
203. Heikkila RE. 1983. Ascorbate-induced lipid peroxidation and the binding of (^{3}H)-dihydroalprenalol. Eur J Pharmacol 93:79–85.
204. Stadel JM, Lefkowitz RJ. 1979. Multiple reactive sulfhydryl groups modulate the function of adenylate cyclase coupled β-adrenergic receptors. Mol Pharmacol 16:709–718.
205. Baba A, Lee E, Matsudo T, Kihara T, Iwata H. 1978. Reversible inhibition of adenylate cyclase activity of rat brain caudate nucleus by oxidized glutathione. Biochem Biophys Res Commun 85:1204–1210.
206. Skurat AV, Yurkova MS, Baranova LA, Gulyaev NN, Bulargina TV, Severin ES. 1985. Evidence for the existence of a sulfhydryl group in the adenylate cyclase active site. Biochem Int 10:451–461.
207. Korner M, Gilon C, Schramm M. 1982. Locking of hormone in the β-adrenergic receptor by attack on a sulfhydryl group in an associated component. J Biol Chem 257:3389–3396.
208. Koren G, Weiss AT, Hasin Y, Applebaum D, Welber S, Rosenman Y, Lotan C, Mossier M, Sapoznikov D, Luria MH, Gotsman MS. 1985. Prevention of myocardial damage in acute myocardial ischemia by early treatment with intravenous streptokinase. N Engl J Med 313:1384–1389.
209. Kloner GA, Ellis SG, Lange R, Braunwald E. 1983. Studies of experimental coronary artery reperfusion: effects on infarct size, myocardial function, biochemistry, ultrastructure, and microvascular damage. Circulation 68(Suppl I):I8–I15.
210. Sharma GP, Varley KG, Kim SW, Barwinsky J, Cohen M, Dhalla NS. 1975. Alterations in energy metabolism and ultrastructure upon reperfusion of the ischemic myocardium after coronary occlusion. Am J Cardiol 36:235–243.

211. Dhalla NS, Panagia V, Singal PK, Makino N, Dixon IMC, Eyolfson DA. 1988. Alterations in heart membrane calcium transport during the development of ischemia–reperfusion injury. J Mol Cell Cardiol 20(Suppl II):3–13.
212. Blaustein AS, Schine L, Brooks WW, Fenburg BL, Bing OHL. 1984. Influence of exogenously generated oxygen species on myocardial function. Am J Physiol 250:H595–H599.
213. Jackson CU, Mickelson JK, Pope TK, Rao PS, Lucchesi BR. 1986. O_2 free radical-mediated myocardial and vascular dysfunction. Am J Physiol 251:H1225–H1231.
214. Masuela H, Kaneko M, Hong RB, Ikegaya T, Hayashi H, Kobayashi A, Yamazaki N. 1993. Effects of hydrogen peroxide on stimulatory guanine nucleotide-binding protein in rat heart. Jpn Circ J 57:1007–1015.
215. Haenen GRMM, Veerman M, Bast A. 1990. Reduction of β-adrenoceptor function by oxidative stress in heart. Free Rad Biol Med 9:279–288.
216. Haenen GRMM, Plug HJM, Vermeulen NPE, Timmerman H, Bast A. 1989. Contribution of 4-hydroxy-2,3-trans-nonenal to the reduction of β-adrenoceptor function by oxidative stress. Life Sci 45:71–76.
217. Tan CM, Xenoyannis S, Feldman RD. 1995. Oxidant stress enhances adenylyl cyclase activation. Circ Res 77:710–717.
218. Schimke I, Haberland A, Will-Shahab L, Kuttner I, Papies B. 1992. *In vitro* effect of reactive O_2 species in the β-adrenoceptor–adenylyl cyclase system. Mol Cell Biochem 110:41–46.
219. Persad S, Takeda S, Panagia V, Dhalla NS. 1997. β-adrenoceptor-linked signal transduction in ischemic-reperfused heart and scavenging of oxyradicals. J Mol Cell Cardiol 29:545–558.
220. Persad S, Takeda S, Dhalla NS. 1997. Alterations in β-adrenoceptor mechanisms in hearts perfused with xanthine plus xanthine oxidase. J Cardiovasc Pharmacol Therapeut 2:115–124.
221. Persad S, Panagia V, Dhalla NS. In press. Role of H_2O_2 in changing β-adrenoceptor and adenylyl cyclase in ischemia-reperfused hearts. Mol Cell Biochem.
222. Persad S, Elimban V, Kaila J, Dhalla NS. 1997 Biphasic alterations in cardiac β-adrenoceptor signal transduction mechanism due to oxyradicals. J Pharmacol Exp Ther 282:1623–1631.
223. Kaul N, Siveski-Iliskovic N, Hill M, Slezak J, Singal PK. 1993. Free radicals and the heart. J Pharmacol Toxicol Meth 30:55–67.
224. Cochrane CG. 1991. Cellular injury by oxidants. Am J Med 91:235–305.
225. Slezak J, Tribulova N, Srivastava J, Uhrik B, Thomas T, Khaper N, Kaul N, Singal PK. 1995. Hydrogen peroxide changes in ischemic and reperfused heart. Am J Pathol 147:772–781.

This Page Intentionally Left Blank

OXYGEN CONSUMPTION AND MITOCHONDRIAL MEMBRANE POTENTIAL IN POSTISCHEMIC MYOCARDIUM

KAZUAKI NISHIO, NOBURU KONNO, YOSHIHISA ARATA, RYUJI UEDA, KATUMITI IIJIMA, TOSHIKI IWATA, and TAKASHI KATAGIRI

Showa University School of Medicine

Summary. Oxygen consumption may be disproportionately high relative to contractile function in postischemic reperfused myocardium. The study reported in this chapter investigated the mechanism of the dissociation between oxygen consumption and contractile function in postischemic reperfused myocardium using isolated rat hearts. Mitochondrial dysfunction secondary to increased calcium uptake has been implicated as an important mediator of reperfusion injury in the heart. In postischemic, isovolumic, antegrate-perfused rat hearts, the myocardial oxygen consumption rate (MVO_2) and contractile function were studied in relation to mitochondrial function. Left ventricular pressure, coronary blood flow, and oxygen consumption were determined. Mitochondrial respiration and the mitochondrial membrane potential were measured by polarography and flow cytometry, respectively. To examine the role of mitochondrial calcium uptake in ischemia reperfusion injury, isolated rat hearts perfused with ruthenium red, which inhibits calcium uptake by mitochondria, were compared to control perfused hearts. After stabilization, hearts were subjected to 60 minutes of no-flow ischemia, followed by 60 minutes of reperfusion. At 15 minutes after the onset of reperfusion, there was poor recovery of left ventricular developed pressure to 64% of the control level, but myocardial oxygen consumption was increased to 134% of control. The addition of 2.5 μM ruthenium red to the perfusate resulted in a decrease of myocardial oxygen consumption. The oxygen consumption rate in state 3 of mitochondria decreased similarly following reperfusion in control and ruthenium red hearts. The mitochondrial membrane potential was reduced to 89% (logarithmic scale) after 15 minutes of reperfusion and then returned to preischemic level. These data suggest that the dissociation between oxygen consumption and contractile function following early reperfusion is partly caused by the repair of intracellular damage resulting from calcium accumulation to mitochondria.

S. Mochizuki, N. Takeda, M. Nagano and N. Dhalla (eds.). THE ISCHEMIC HEART.

INTRODUCTION

In normal myocardium, there is a close relationship between contractile function and the oxidative metabolic rate [1,2]. Recently, several reports have indicated that this relation may be altered after postischemic reperfusion [3–5]. The mechanisms responsible for the dissociation between oxygen consumption and contractile function in the early period after reperfusion are incompletely understood. Periods of prolonged myocardial ischemia result in irreversible tissue damage and abnormalities of metabolic and mechanical function [6,7]. An important component of this injury may occur at the time of reperfusion and not during ischemia itself [6–8]. It seems possible that this reperfusion injury is brought about by mitochondrial calcium loading during reperfusion. Mitochondrial calcium loading causes important abnormalities of mitochondrial function, and mitochondrial damage may lead to uncoupling of oxidative phosphorylation [9]. These abnormalities of process include changes of transmembrane ion transport [10] and futile metabolic cycling [11]. Elevation of the cytosolic calcium concentration activates calcium transport systems at the inner mitochondrial membrane and at the sarcoplasmic reticulum, which may contribute to enhanced energy expanditure after reperfusion [10]. Ruthenium red is a polysaccharide stain that inhibits mitochondrial calcium accumulation without any changes in the cytosolic calcium concentration. The study reported here was designed to investigate the mechanism of the dissociation between oxygen consumption and contractile function in relation to mitochondrial calcium accumulation by using ruthenium red perfusion after reperfusion in rat hearts.

MATERIALS AND METHODS

Perfusion protocol

Male Wistar rats weighing 250–400 g were anesthetized by intraperitoneal injection of pentobarbital, and hearts were exercised and perfused in the Langendorff model at an aortic pressure of 100 cm H_2O with Krebs-Henseleit buffer consisting of 118 mM NaCl, 25 mM $NaHCO_3$, 4.5 mM KCl, 1.2 mM KH_2PO_4, 1.2 mM $MgSO_4$, 2.5 mM $CaCl_2$, and 11 mM glucose. The perfusion buffer was equilibrated with a mixture of O_2 (95%) and CO_2 (5%) at a temperature of 37°C and a pH of 7.4. A compliant latex balloon was inserted through the left atrium into the left ventricle to monitor myocardial function. The volume in the balloon was adjusted to set 50 μL. Hearts were paced at 250 beats per minute. There were three phases of perfusion in this experiment. The first phase consisted of a 45-minute control period allowing for experimental setup and the acquisition of baseline measurements. The second phase consisted of 60 minutes of global myocardial ischemia, during which time all perfusate flow to the heart was stopped. The third phase consisted of 60 minutes of reperfusion during which sequential collections of pulmonary artery effluent were made for determination of myocardial coronary flow. At the end of the experiment, the hearts were weighed. Myocardial oxygen consumption was calculated by multiplying the coronary arteriovenous difference of the oxygen

content divided by the myocardial blood flow. In the ruthenium red group, ruthenium red was added to the perfusion medium at the final concentration of 2.5 μM from the beginning of the first phase to the third phase.

Preparation of mitochondria

Mitochondria were prepared by a modification of the method of Sordahl et al. [12], utilizing crystalline protease (Nagarse, Nagase Co., Ltd). Heart muscle was chopped up with scissors and homogenized with a Polytron homogenizer for five seconds in nine volumes of a solution containing 0.25 M sucrose, 0.01 M glycoetherdiamine-tetraacetic acid (GEDTA), and 0.03 M tris-HCl (pH 7.2). Then the homogenate was centrifuged at 27,000× G for 10 minutes. Nagarse suspended in sucrose-GEDTA medium was added to the pellet at 1 mg/g tissue, followed by vortexing and incubation at 4°C for eight minutes. After incubation, 20 mL of a solution containing 0.18 M KCl, 0.01 M GEDTA, 0.5% (wt/vol) bovine serum albumin (BSA), and 0.03 M tris-HCl (pH 7.2) was added, mixed with a regular Teflon–glass homogenizer at 1000 rpm for three strokes, and then centrifuged at 500× G for five minutes. The supernatant was filtered through gauze and centrifuged twice at 12,000× G for 10 minutes, after which the pellet was suspended in a solution containing 0.18 M KCl, 0.5% (wt/vol) BSA, and 0.03 M tris-HCl (pH 7.2) at a final concentration of approximately 2 mg/min. The protein content was determined by Lowry's method [13] using BSA as a standard.

Mitochondrial respiration

Mitochondrial respiratory activity was determined with an oxygen electrode. The reaction medium contained 0.3 M mannitol, 5 mM $MgCl_2$, 30 mM KCl, and 10 mM KH_2PO_4 (pH 7.2) at 30°C, and succinate was used as a substrate.

Measurement of mitochondrial membrane potential

Mitochondrial membrane potential was measured flow-cytometrically according to Ronald's method [14] using rhodamine 123. For the flow-cytometric studies, mitochondria were suspended in a medium containing 0.3 M mannitol, 10 mM KCl, 5 mM $MgCl_2$, and 10 mM KH_2PO_4 at pH 7.2, as well as 1 mg/mL BSA where indicated. Mitochondria (125 μg protein/mL) were analyzed for their natural fluorescence and for their fluorescence after staining with aqueous rhodamine 123 (Sigma). For analysis of rhodamine 123 fluorescence, the excitation wave length was settled at 488 nm and 400 mW, while the final dye concentration was 5 nM. All measurements were made after a 30-minute incubation period in the presence of the dye, and 10,000 particles of mitochondria were assessed in each analysis. The potential was shown as fluorescence on a logarithmic scale. The mitichondrial membrane potential was expressed finally as the ratio between the fluorescence value, obtained from perfused heart mitochondria, and the value from control (not perfused) heart mitochondria.

Statistical analysis

Results are expressed as the mean ± SD. Statistical significance was evaluated by Student's *t*-test for paired or unpaired data, and *p* values (two-tailed) were calculated. *P* less than 0.05 was considered to be significant.

RESULTS

Hemodynamics

Figures 1A and 1B show left ventricular systolic pressure (LVSP) and myocardial oxygen consumption (MVO_2) in the control and ruthenium red groups. Values in the control group and ruthenium red group before ischemia were as follows: LVSP, 13.5 and 7.3 mmHg, respectively; and MVO_2, 1151 and 842 mmHg·mL/min/g, respectively. In the control group at 10 minutes after the beginning of reperfusion, MVO_2 was significantly increased to 135% ($p < 0.05$), but contractile function continued to decrease to 54% ($p < 0.05$), indicating the dissociation of contractility and oxygen consumption. In contrast, an increase of MVO_2 was not observed; on the contrary, MVO_2 decreased to 56% of its value before ischemia, while contractility decreased to 55% in ruthenium red group.

Figure 2 shows the changes of *dp/dt* after ischemia and reperfusion. When the heart became ischemic, *dp/dt* quickly fell to zero and then returned to the baseline after reperfusion similarly in both groups.

In our experimental model, the contraction was isovolemic and the beating rate was fixed by electrical pacing; thus, the ratio of oxygen consumption to left ventricular pressure is assumed to indicate the efficiency of the mechanical utilization of respiratory energy. Figure 3 shows the changes of MVO_2/LVSP as an index of contractile efficiency during ischemia–reperfusion. In the control group, MVO_2/LVSP increased significantly to 168% of the preischemic level (from 140 to 235 mL/min/g, $p < 0.05$) at 10 minutes after reperfusion, indicating the decrease of contractile efficiency, and after 30 minutes of reperfusion returned to the baseline. In the ruthenium red group, MVO_2/LVSP showed a decrease of 67% at 10 minutes after reperfusion and gradually increased during reperfusion. Coronary flow during the preischemic and reperfusion periods in the control and ruthenium red hearts is shown in figure 4. In the control group, coronary flow was transiently increased after 10 minutes of reperfusion (from 3.5 to 4.2 mL/min/g, $p < 0.05$), indicating the reactive hypermia, and returned to the baseline preischemic level. In the ruthenium red group, coronary flow was significantly decreased after the beginning of reperfusion, not showing the reactive hypermia.

Oxygen consumption rate in mitochondria

The mitochondrial oxygen consumption rate in state 3 is shown in figure 5. The values of the oxygen consumption rate in state 3 were 319 and 225 mμ Atoms O mg/protein/min in the control group and the ruthenium red group, respectively. After 15 minutes of reperfusion following 60 minutes of ischemia, the mitochondrial respiration had decreased to 71% and 49% in state 3 in the control

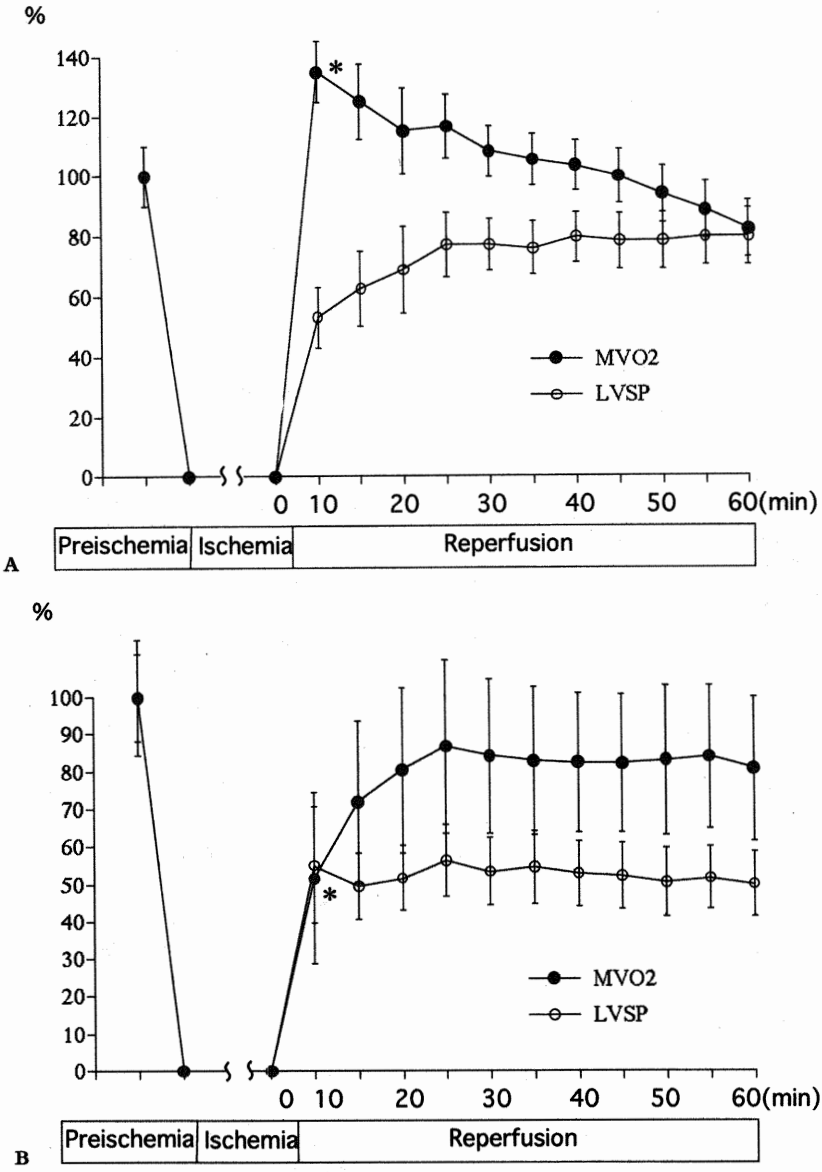

Figure 1. (**A**) Myocardial oxygen consumption (MVO_2) and left ventricular systolic pressure (LVSP) versus time. MVO_2 was significantly increased in postischemic myocardium despite the persistence of contractile dysfunction. (**B**) MVO_2 and LVSP in ruthenium red hearts versus time. An increase of MVO_2 was not observed in the early stage after reperfusion. *, $p < 0.05$ versus preischemia; **, $p < 0.01$ versus preischemia.

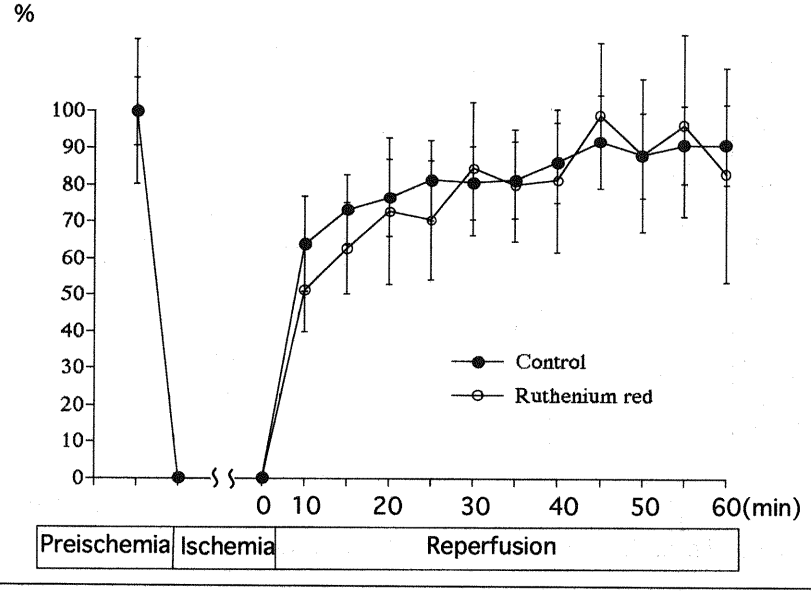

Figure 2. Myocardial contractility. Contractility was determined by the peak positive time derivative of developed pressure (*dp/dt*) versus time, and was similar in both groups.

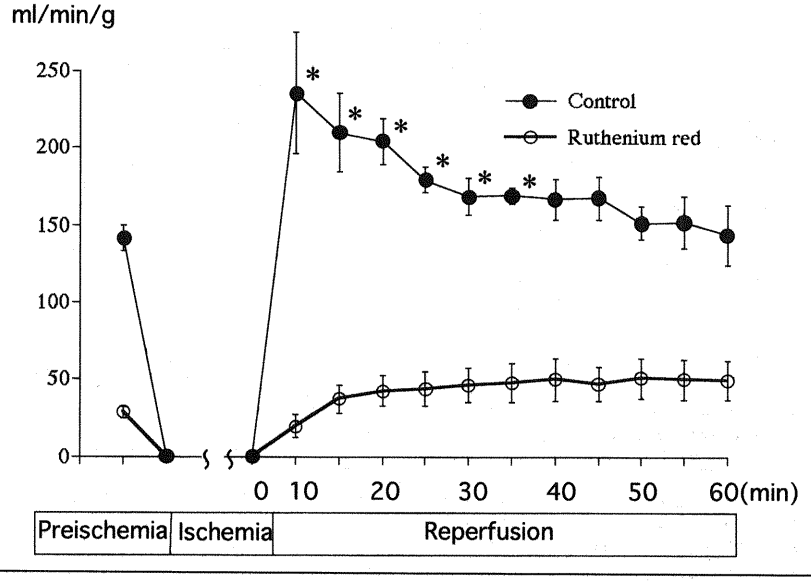

Figure 3. Myocardial oxygen consumption (MVO_2)/left ventricular systolic pressure (LVSP) versus time. MVO_2/g/LVSP was significantly increased in the control group in the early stage after reperfusion. In the ruthenium red group, no significant increase was observed in the early stage after reperfusion, but the ratio gradually increased during reperfusion. *, $p < 0.05$.

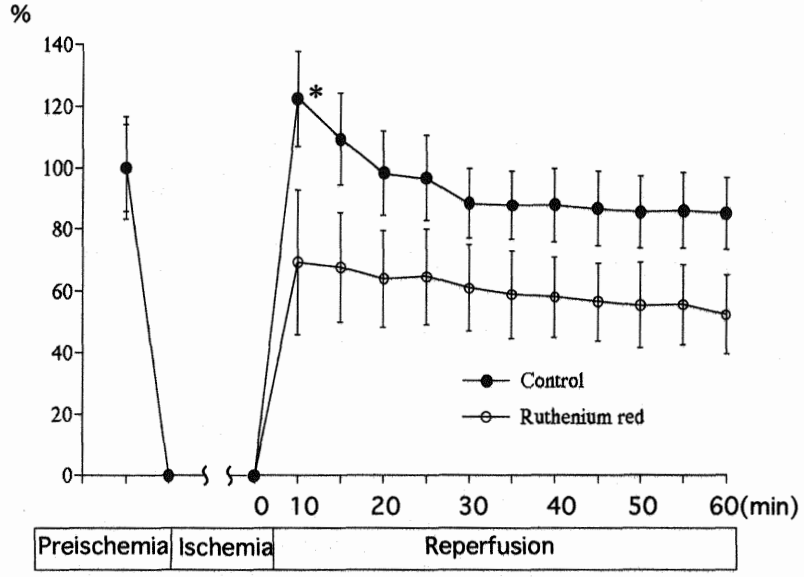

Figure 4. Coronary flow rate (mL/min/g) versus time. Coronary flow was significantly increased at 10 minutes after reperfusion, indicating reactive hypermia. In ruthenium red hearts, reactive hypermia was not observed. *, $p < 0.05$.

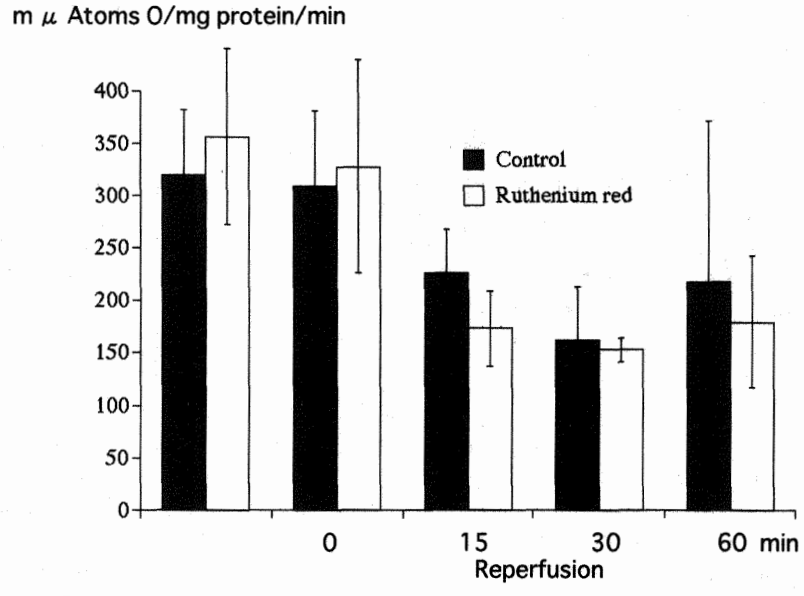

Figure 5. Oxygen consumption rate in state 3 mitochondria. Following ischemia and reperfusion, the oxygen consumption rate in state 3 decreased in both groups.

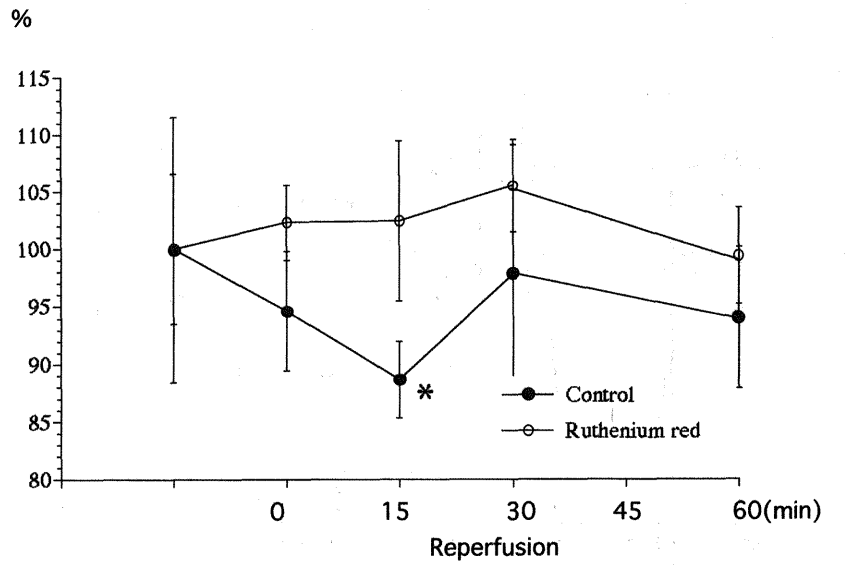

Figure 6. Mitochondrial membrane potential versus time. The membrane potential decreased transiently and then returned to the preischemic level in the control group. This reduction of membrane potential was not observed in the ruthenium red group. *, $p < 0.05$.

and the ruthenium red group, respectively. No significant difference was observed between two groups.

Mitochondrial membrane potential

The mitochondrial membrane potential during the preischemic period and after reperfusion in both the control and ruthenium red group is shown in figure 6. In the control group, the mitochondrial membrane potential was reduced to 89% of control ($p < 0.05$) at 15 minutes of reperfusion and returned to the baseline preischemic level. In contrast, in the ruthenium red group, no reduction of the mitochondrial membrane potential was observed after reperfusion.

DISCUSSION

Under physiological conditions, myocardial oxygen demand and supply are well balanced. However, many investigators have demonstrated the dissociation between myocardial oxygen consumption and the contractile function in postischemic reversible injured tissue as stunned myocardium [1–4]. Laxon et al. [4] reported in a study of awake dogs that three sequential 10-minute left anterior descending artery occlusions separated by 30-minute reperfusion periods resulted in progressive postischemic contractile dysfunction, but regional oxygen consumption was unchanged. Dean [15] and coworkers examined anesthetized dogs and found that regional

oxygen consumption was unchanged after 10-minute ischemia, although O_2 consumption markedly depressed after 120-minute ischemia. However, in experiments on the isolated perfused heart, relatively high myocardial oxygen consumption was found to be associated with depressions in regional contractility of irreversibly injured myocardium after prolonged ischemia. Benzi et al. [16] showed a dissociation between oxygen consumption and contractility after 60-minute ischemia in perfused rat hearts. The results of our study also demonstrated increased oxygen consumption in the early phase of reperfusion after 60 minutes of ischemia. In the isolated perfused heart model, global ischemia results in stoppage of rapid heart beating, even under electrical pacing. Therefore, the ischemia damage must be smaller than that in regional ischemic models.

In stunned myocardium, the mitochondrial respiratory function has been postulated to be unchanged [17–19]; thus, relatively high myocardial oxygen consumption in the postischemic tissue has not been considered in relation to mitochondrial respiration uncoupling. In contrast to these papers, our results demonstrated a significant decrease of mitochondrial respiration in the reperfused heart. Although mitochondrial respiration in the reperfused heart treated with ruthenium red, in which myocardial oxygen consumption did not increase, was shown to decrease, we can also state that the dissociation with oxygen consumption and contractile function in ischemic injured tissue is not secondary to mitochondrial uncoupling.

It is widely accepted that calcium contributes to cell injury in ischemia and reperfusion. Marban et al. [20] demonstrated that intracellular calcium increased significantly during 20 minutes of total global ischemia and reperfusion, resulting in a persistent elevation of calcium during the first five minutes. Calcium is transported across the inner membrane of the mitochondria by the uniport mechanism, driven by the interior negative potential [21]. The accumulation of calcium results in a reduction of mitochondrial calcium transport in order to compete with oxidative phosphorylation for respiratory energy [22]. Ruthenium red is a hexavalent polysaccaride stain that inhibits mitochondrial calcium transport without affecting the elevation of intracellular calcium [6], although the mechanism is not yet clarified [23]. Our results showed that ruthenium red improved cardiac efficiency. Cardiac efficiency was expressed as the rate of pressure work divided by the myocardial oxygen consumption shortly after reperfusion, suggesting that the dissociation between oxygen consumption and contractility was caused, at least partially, by the accumulation of calcium in the mitochondria. Calcium loading in the mitochondria may result in wasted respiratory energy by forcing the Ca^{2+}–H^+ antiport to release calcium to the matrix [24,25].

In the study reported in this chapter, at 20 to 60 minutes after the start of reperfusion, a progressive decrease of cardiac efficiency was observed in the ruthenium-red-treated group. Prolonged inhibition of calcium uptake by mitochondria may bring an increase of cytosolic calcium and result in an increase of ATP consumption by ion priming, e.g., via the Na^+–Ca^{2+} exchange system, or a decrease of calcium sensitivity in excitation–contraction coupling [26].

In conclusion, the results presented above indicate that the postischemic heart shows a dissociation between myocardial oxygen consumption and contractile function and that ruthenium red prevents this dissociation at an early stage after reperfusion. The dissociation is caused, at least partially, by the accumulation of calcium in the mitochondria.

ACKNOWLEDGMENTS

The authors are very grateful to Seiji Ito, M.D., Eiichi Geshi, M.D., and Kunihiko Fukuchi, M.D. for their kind guidance and encouragement of this work.

REFERENCES

1. Sarnoff SJ, Braunwald E, Welch GH Jr, Case RB, Stainsby WN, Macruz R. 1958. Hemodynamic determinants of oxygen consumption of the heart with special reference to tension-time index. Am J Physiol 192:148–156.
2. Neely JR, Liebermeister H, Battyersby EJ, Morgan HE. 1967. Effect of pressure development on oxygen consumption by isolated rat hearts. Am J Physiol 212:804–814.
3. Stahl LD, Weiss HR, Becker LC. 1988. Myocardial oxygen consumption, oxygen supply/demand heterogeneity, and microvascular patency in regionally stunned myocardium. Circulation 77:865–872.
4. Laxson DD, Homans DC, Dai X-Z, Sublett E, Bache RJ. 1989. Oxygen consumption and coronory reactivity in postischemic myocardium. Circ Res 64:9–20.
5. Schott RJ, Rohmann S, Braun ER, Schaper W. 1990. Ischemic preconditioning reduces infarct size in swine myocardium. Circ Res 66:1133–1142.
6. Peng CF, Kane JJ, Straub KD, Murphy ML. 1980. Improvement of mitochondrial energy production in ischemic myocardium by in vivo infusion of ruthenium red. J Cardiovasc Pharmacol 2:45–54.
7. Bourdillon PD, Poole-Wilson PA. 1981. Effects of ischemia and reperfusion on calcium exchange and mechanical function in isolated rabbit myocardium. Cardiovasc Res 15:121–130.
8. Bussen P. 1985. Suppression of cellular injury during the calcium paradox in rat heart by factors which reduce calcium uptake by mitochondria. Pflugers Arch 404:166–171.
9. Huang XQ, Liedtke AJ. 1989. Alterations in fatty acid oxidation in ischemic and reperfused myocardium. Mol Cell Biochem 88:145–153.
10. Kusuoka H, Koretune Y, Chacko VP, Weisfeldt ML, Marban E. 1990. Excitation–contraction coupling in postischemic myocardium: does failure of activator Ca^{2+} transients underlie stunning? Circ Res 66:1268–1276.
11. Trach V, Buschmans-Denkel E, Schaper W. 1986. Relation between lipolysis and glycolysis during ischemia in the isolated rat heart. Basic Res Cardiol 81:454–464.
12. Sordahl LA, Stewart ML. 1980. Mechanism(s) of altered mitochondrial calcium transport in acutely ischemic canine hearts. Circ Res 47:814–820.
13. Lowry OH, Rosenbrough NJ, Farr AL, Randall RJ. 1951. Protein measurement with the Folin phenol regent. J Biol Chem 193:265–275.
14. Ronald KE, Emaus RG, John JL. 1986. Rhodamine 123 as the transmembrane potential in isolated rat-liver mitochondria: spectral and metabolic properties. Biochim Biophys Acta 850:436–448.
15. Dean EN, Nicklas JM. 1990. The oxygen consumption paradox of "stunned myocardium" in dogs. Basic Res Cardiol 85:120–131.
16. Benzi RH, Lerch R. 1992. Dissociation between contractile function and oxidative metabolism in postischemic myocardium. Attenuation by ruthenium red administered during reperfusion. Circ Res 71:567–576.
17. Swain JL, Sabina RL, McHale PA, Greenfield JC Jr, Holmes EW. 1982. Prolonged myocardial nucleotide depletion after brief ischemia in the open-chest dog. Am J Physiol 242 (Heart Circ Physiol 11):H88–H826.
18. Zimmer SD, Michurski SP, From AHL, Foker JE, Ugrbil K. 1987. ^{31}P NMR studies of myocardial bioenergics in the post-ischemic myocardium. Proc Soc Magnetic Resonance Med 2:554.

19. Hoffmeister HM, Mauser M, Schaper W. 1986. Repeated short periods of regional myocardial ischemia: effect on local function and high energy phosphate levels. Basic Res Cardiol 81:358–372.
20. Marbon E, Kitakaze M, Koretsune Y, Yue DT, Chacko VP, Pike MM. 1990. Quantification of $[Ca^{2+}]_i$ in perfused hearts. Critical evaluation of the 5F-BAPTA and nuclear magnetic resonance method as applied to the study of ischemia and reperfusion. Circ Res 66:1255–1267.
21. Gunter TE, Peeifer DR. 1990. Mechanisms by which mitochondria transport calcium. Am J Physiol 258:C755–C786.
22. Versi A, Reynafarje B, Lehninger A. 1978. Stoichiometry of H^+ ejection and Ca^{2+} uptake couple to electron transport in rat heart mitochondria. J Biol Chem 253:6379–6385.
23. Ferrari R, di Lisa, Raddino R, Visioli O. 1982. The effects of ruthenium red on mitochondrial function during post-ischemic reperfusion. J Mol Cell Cardiol 14:737–740.
24. Richter C, Frei B. 1988. Ca^{2+} release from mitochondria induced by prooxidants. Frée Rad Biol Med 4:365–375.
25. Frei B, Richter C. 1988. Mono (ADP-ribosylation) in rat liver mitochondria. Biochem 27:529–535.
26. Kusuoka H, Porterfield JK, Weismann HF. 1987. Pathophysiology and pathogenesis of stunned myocardium. Depression–Ca^{2+} activity of contraction as a consequance of reperfusion-induced cellular calcium overload in ferret hearts. J Clin Invest 79:950–996.

This Page Intentionally Left Blank

PATHOPHYSIOLOGICAL BEHAVIOR OF THE MYOCARDIUM IN ACUTE ISCHEMIA AND REPERFUSION, WITH SPECIAL EMPHASIS ON THE SARCOPLASMIC RETICULUM

TAKASHI KATAGIRI, EIICHI GESHI, HIROHISA ARATA, HARUHIKO ISHIOKA, SEIJI ITOH, and NOBURU KONNO

Showa University School of Medicine

Summary. The myocardium under severe ischemia and reperfusion exhibits four types of different pathophysiologic behaviors: coagulation necrosis, stunning, ischemic preconditioning, and reperfusion injury. This chapter describes these changes in the postischemic myocardium in relation to the length of ischemia. Canine hearts were made ischemic by occluding the left anterior descending coronary artery (LAD), and the sarcoplasmic reticulum (SR) from the ischemia-reperfused myocardium was analyzed. In permanent occlusion of the LAD, Ca^{2+}–ATPase activity of the SR was reduced simultaneously with the degradation of the major ATPase protein in ischemia for 20 to 30 minutes. In the stunned myocardium, with occlusion of the LAD for 15 minutes and reperfusion, long-term reduction in the activity of the SR was noted simultaneously with a reduction in the percent of segment shortening, but without degradation of the ATPase protein of the SR. In the preconditioned myocardium, in which the LAD was occluded four times for five minutes each prior to LAD occlusion for 60 minutes and reperfusion, both ATPase activity and the SR ATPase protein were preserved. In reperfusion of the LAD after occlusion for 10 to 30 minutes, reduction in Ca^{2+}–ATPase activity and degradation of the ATPase protein occurred earlier, simultaneously with generation of free radicals, suggesting reperfusion injury. We conclude that pathophysiologic behaviors of the postischemic myocardium proceed in quite different ways depending upon the length of ischemia and will only be fully understood in the light of studies on ischemia and reperfusion of the heart muscle.

INTRODUCTION

Permanent severe ischemia for longer than 20 to 30 minutes induces *myocardial necrosis*, and the degradative processes have been discussed in many reports [1,2].

S. Mochizuki, N. Takeda, M. Nagano and N. Dhalla (eds.). THE ISCHEMIC HEART.

Short-term ischemia and subsequent reperfusion, which usually do not induce myocardial necrosis, have been noted to result in a rapid return to the preischemic state; however, it has been recognized that a short ischemic episode, even though it does not induce necrosis, brings about several characteristic phenomena called *stunning* [3], *ischemic preconditioning* [4], and *reperfusion injury* [5]. Stunning indicates contractile dysfunction of the postischemic myocardium, and ischemic preconditioning produces tolerance in the postischemic myocardium against forthcoming, more severe ischemia. These conditions induce little myocellular necrosis. In contrast, so-called reperfusion injury produces rather more severe myocardial damage, with the appearance predominantly of characteristic contraction band necrosis. The first two phenomena are usually observed with reperfusion after relatively short period of ischemia, e.g., 5–15 minutes, and the last occurs after 20–30 minutes of ischemia, just before ischemic myocardial necrosis begins.

In this chapter, we focus on the sarcoplasmic reticulum (SR) of the postischemic heart muscle, the site of excitation–contraction coupling, to study these four types of pathophysiologic behaviors in ischemia and reperfusion of the canine heart muscle.

MATERIALS AND METHODS

Animal experiment

Adult mongrel dogs weighing 12–25 kg were anesthetized with an injection of urethane at 450 mg/kg, α-chloralose at 45 mg/kg, and 10 mg diazepam. They were intubated and ventilated with room air with a Harvard respirator.

Coronary occlusion and reperfusion

Figure 1 shows the procedures of coronary occlusion and reperfusion in four experiments. For studies on permanent ischemia, the left anterior descending coronary artery (LAD) was occluded for 10 to 120 minutes. For studies on myocardial stunning, the LAD was occluded for a single 15-minute period and reperfused for 60 minutes to seven days. To elucidate the mechanism of myocardial stunning, superoxide dysmutase (SOD, a gift from Nippon Kayaku Pharmaceutical Co., Tokyo, Japan) was administered continuously throughout the experiment at 15,000 U/kg/min. For studies on ischemic preconditioning, the LAD was occluded for 5 minutes four separate times, with a 10-minute interval between each, and was then occluded again for 60 minutes and then released for 60 minutes. Throughout ischemia and reperfusion, 7.5 mg/kg of 8-phenyltheophylline (8-PT), 0.3 mg/kg of glibenclamide, and 20 ug/kg/min of nicorandil were given to elucidate the mechanism of preconditioning. For studies on reperfusion injury, the LAD was occluded for 10, 20, and 30 minutes, followed by reperfusion for 60 minutes. The ischemic portion of the heart muscle was excised and cut at the center of the wall into subendocardial (Endo) and subepicardial (Epi) muscles. A part of the posterior muscle was treated in the same manner as a nonischemic control.

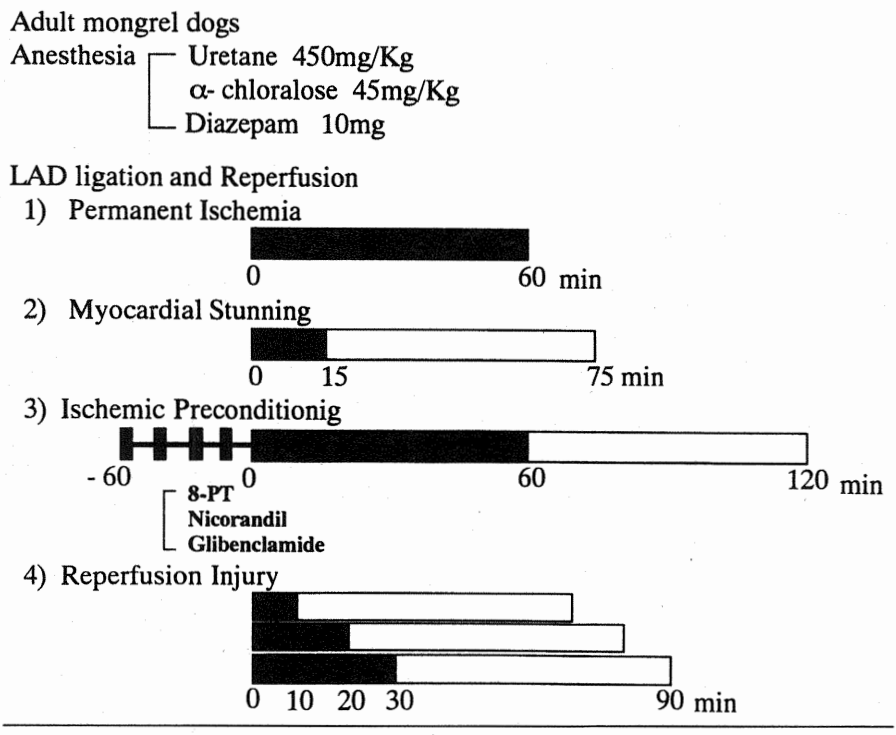

Figure 1. Experimental procedures. The protocol of the left anterior descending coronary artery (LAD) occlusion and reperfusion in four series of experiments is shown.

Hemodynamic measurements

Throughout the experimental procedures, basic hemodynamic parameters, such as left ventricular pressure (LVP), left ventricular end-diastolic pressure (LVEDP), left ventricular developed pressure (LV *dp/dt*), and cardiac output (CO), were measured through pig tail and Swan-Ganz catheters. Percent segment shortening (%SS) was measured by ultrasonic crystals (Nihon Kohden Co., Tokyo, Japan) inserted into the nonischemic and ischemic left ventricular walls. Blood flow of the LAD was measured by the ultrasonic doppler method (Triton Technology Inc., San Diego, California, USA) at a point just below the occlusion, and regional myocardial blood flow was measured by the H_2 gas clearance method (Unique Medical Co., Tokyo, Japan).

Preparation of sarcoplasmic reticulum

Sarcoplasmic reticulum (SR) was prepared as a light microsome fraction of the myocardial homogenate by the method of Konno et al. [6]. Myocardial specimens

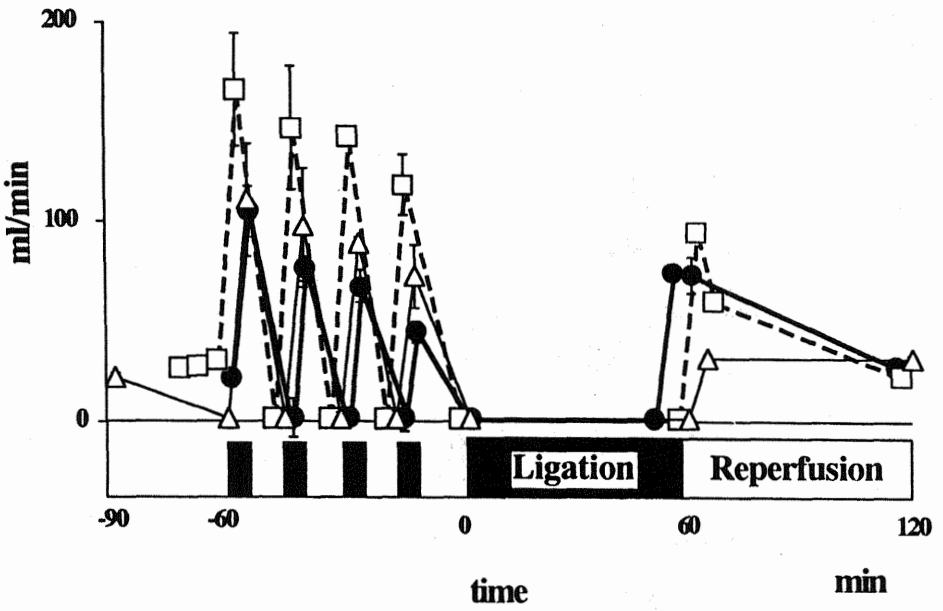

Figure 2. Blood flow of LAD in the experiment on ischemic preconditioning. Reactive hyperemia was reduced successively with each occlusion of the LAD for 5 minutes. But the flow was not affected by the administration of 8-phenyltheophylline and nicorandil. Closed circles show LAD flow of the preconditioned dogs; open squares show 8-PT-treated dogs; and open triangles indicate dogs treated with nicorandil. * $p < 0.05$; ** $p < 0.01$.

were homogenized with a Polytron homogenizer with 0.01 M $NaHCO_3$ and were spun at 12,000× G for 30 minutes twice, and the supernatant was ultracentrifuged at 120,000× G for 30 minutes twice. The final precipitate was regarded as SR. Ca^{2+}-stimulated ATPase activity was determined [6], and the SR-composing proteins were analyzed by SDS polyacrylamide gel electrophoresis.

Electron spin resonance (*ESR*)

For the study of reperfusion injury the spin-trapping agent α-phenyl N-tert-butyl nitrone (PBN) was injected intravenously [7], and circulating blood was taken from the right atrium during ischemia and reperfusion. The blood samples were applied directly to ESR (RE-1X, JEOL, Tokyo, Japan), and the ESR signal was recorded with Mn^{2+} as a standard.

Statistics

Statistical analysis was done with Student's *t*-test, and *p* values of less than 5% were regarded as significant.

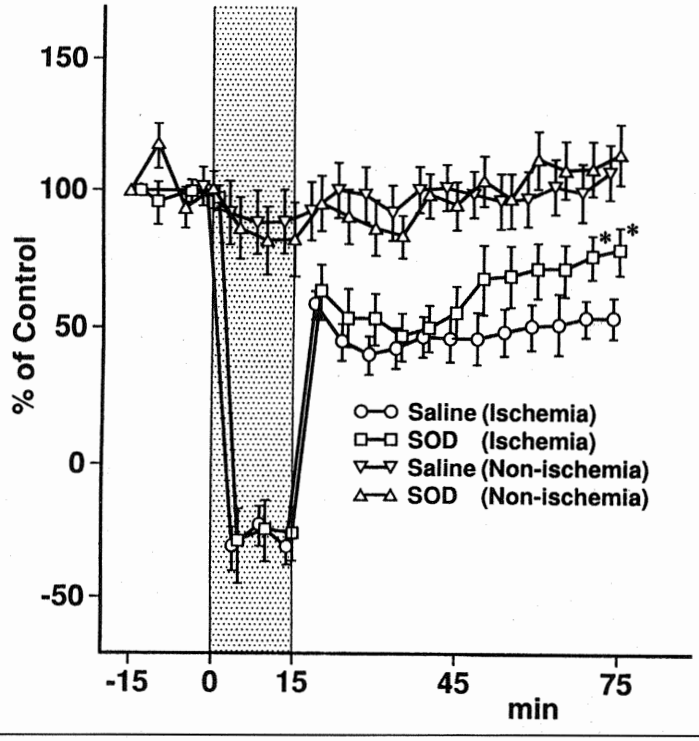

Figure 3. Segment shortening in stunned myocardium. After coronary occlusion for 15 minutes, %SS of the ischemic myocardium was reduced to about 50%, showing stunning. Pretreatment with superoxide dismutase partially improved this outcome. $\star$ $p < 0.05$ against control values.

RESULTS

Hemodynamics and coronary blood flow

In all four studies, hemodynamic parameters such as heart rate, LVP, LV *dp/dt*, and CO did not change significantly throughout the experimental procedures. Both coronary and regional blood flow diminished to near zero by occlusion of the LAD, but returned to the control level following the overshoot phenomenon of about 300% immediately after reperfusion, which indicated reactive hyperemia. In the experiment for preconditioning, reactive hyperemia had become smaller due to repetition of the LAD occlusion and reperfusion, as shown in figure 2.

Percent segment shortening (%SS)

In the studies on myocardial stunning, %SS was reduced to 50% during 15 minutes of LAD occlusion, which indicated dyskinesis. This reduced %SS recovered to only about 40% of that of the nonischemic heart muscle in the period from immediately after reflow to 60 minutes, which indicated stunning, and then recovered gradually

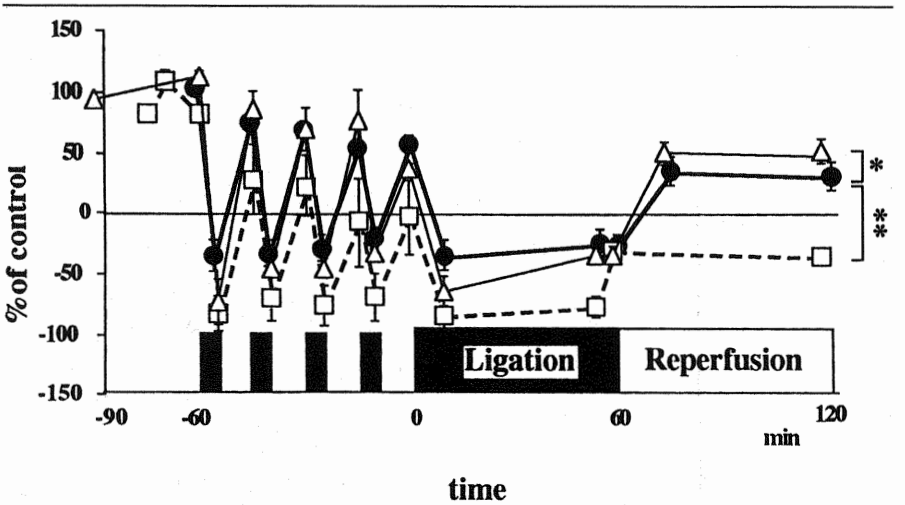

Figure 4. Segment shortening of the preconditioned heart muscle. %SS was preserved in the preconditioned myocardium. Treatment with nicorandil, a K channel opener, augmented the effect of preconditioning, but the administration of 8-phenyltheophylline (8-PT) abolished the effect. Closed circles show the preconditioned myocardium; open squares show the administration of 8-PT; and open triangles indicate the administration of nicorandil.

from 24 hours to seven days after reperfusion, as shown in figure 3. With SOD treatment, %SS after LAD reperfusion recovered to about 70%–80% of the nonischemic portion.

In the experiments for ischemic preconditioning, %SS decreased to about −50% in a manner similar to the study of myocardial stunning, indicating severe dyskinesis during the repeated short-term ischemia. During the following long-term coronary occlusion, this phenomenon was more intensified, showing a decrease of −100% in the control group. However, in the preconditioned group, %SS was maintained at akinetic level through the long-term ischemia, and after the release of coronary occlusion, the wall movement returned to about 50% of the baseline level, as shown in figure 4. After pretreatments with 8-PT and glibenclamide, %SS of the preconditioned heart muscle did not recover in the same manner as heart muscle without preconditioning. And with the administration of nicorandil, %SS was preserved at the same level as that of the nonischemic heart muscle, as shown in figure 4.

Ca^{2+}-stimulated ATPase activities of SR

Figure 5 shows Ca^{2+}–ATPase activity of the SR from heart muscle in permanent ischemia. The activity was reduced significantly, to about 35% of that of the nonischemic heart muscle—in Endo significantly at 20 to 30 minutes after LAD occlusion, and in Epi at 30 to 60 minutes [6]. In the study of myocardial stunning, Ca^{2+}–ATPase activity of SR from the postischemic myocardium was reduced significantly in a manner similar to heart muscle in permanent ischemia after

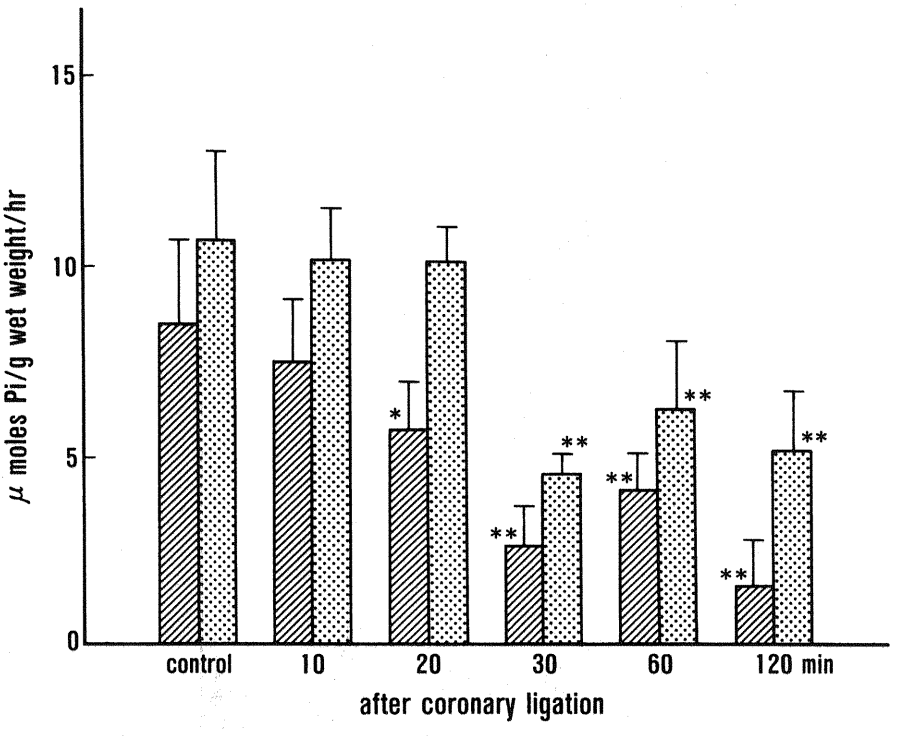

Figure 5. Ca^{2+}–ATPase activity of the sarcoplasmic reticulum from the subendocardial and subepicardial muscles in permanent ischemia. Hatched bars indicate activity from the subendocardial muscle; dotted bars indicate activity from the subepicardium. * $p < 0.05$, ** $p < 0.01$ against the activity of the control.

reperfusion (figure 6A). Treatment with SOD preserved Ca^{2+}–ATPase activity at about 70% of that in nonischemic mycoardium, simultaneously with recovery of %SS. And in ischemic preconditioning, this activity was reduced in a manner similar to that of permanent ischemia without preconditioning; the ATPase activity remained at a level of more than 80% of that of the SR from nonischemic heart muscle, showing the effect of preconditioning. This preservation phenomenon was intensified by treatment with nicorandil, an ATP-sensitive K-channel opener, but was abolished completely with the addition of 8-phenyltheophylline and of glibenclamide, as shown in figure 6B. In the studies on reperfusion injury, reduction in Ca^{2+}–ATPase activity was noted earlier in the ischemic period than in permanent ischemia, as shown in figure 6C.

SDS gel electrophoresis of SR proteins

In SDS gel electrophoresis, SR proteins were separated into the major ATPase protein (110kDa), several acidic proteins (30–70kDa), and proteolipids (around

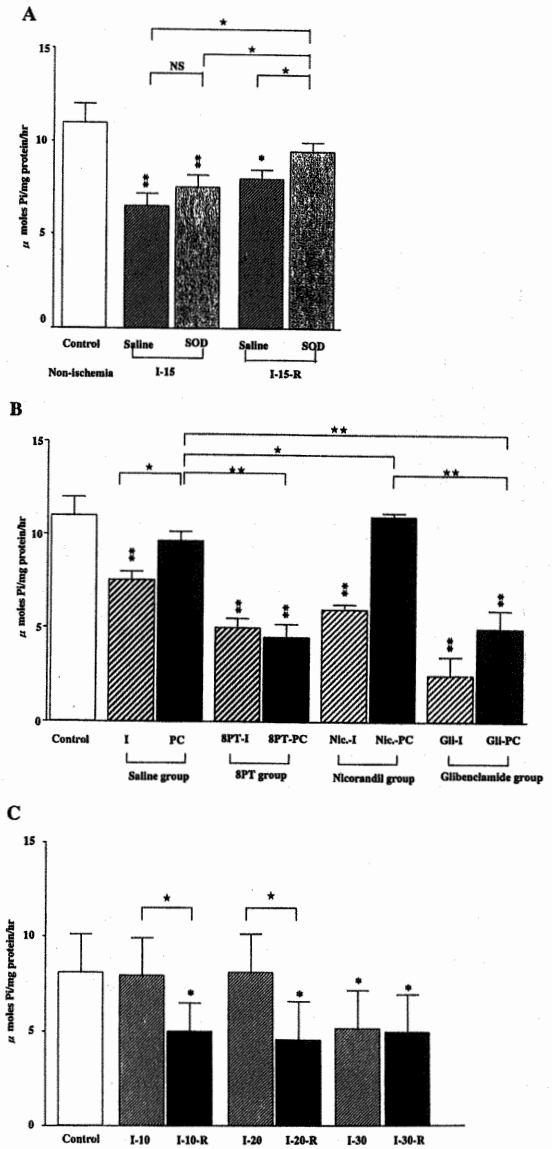

Figure 6. Ca^{2+}-dependent ATPase activities of SR from the subendocardial muscle. (**A**) Stunned myocardium; (**B**) ischemic preconditioning; (**C**) reperfusion injury. $\star$ $p < 0.05$, and $\star\star$ $p < 0.01$ against the activity of the control.

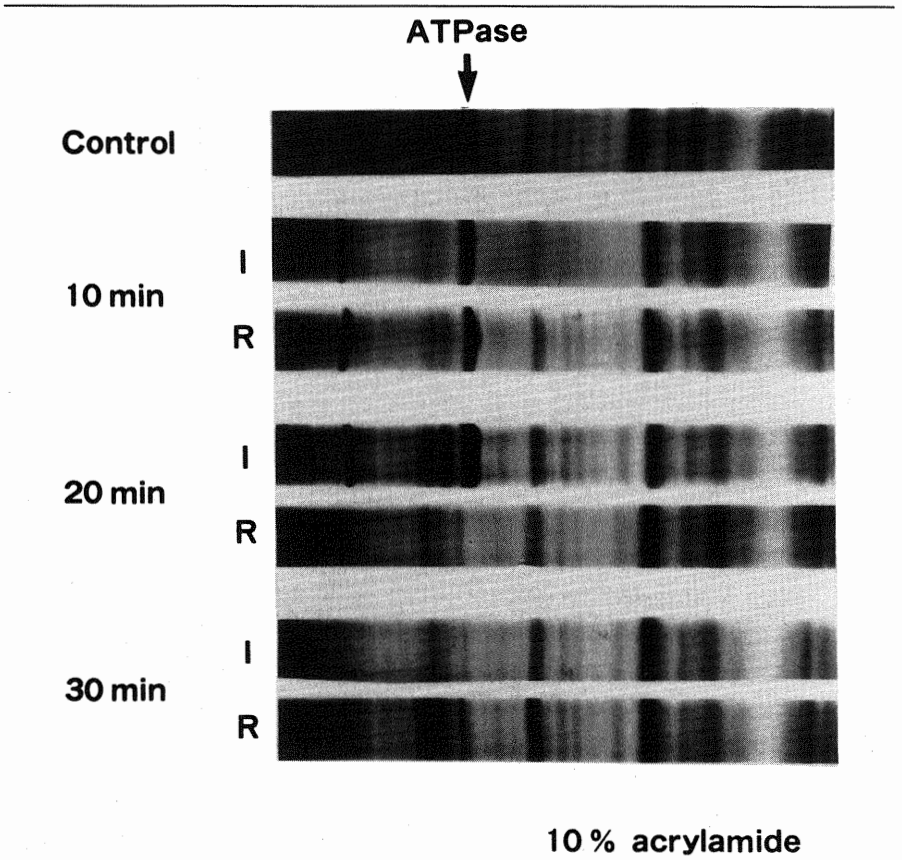

Figure 7. SDS gel electrophoresis of the proteins of the sarcoplasmic reticulum. In permanent ischemia (I), the major ATPase protein was degradated in ischemia for 30 minutes. In LAD occlusion with subsequent reperfusion (R), the band of the ATPase protein was decreased earlier, in ischemia (and reperfusion) for 20 minutes, indicating reperfusion injury. Reprinted from [8], with permission of the authors.

18 kDa) [6,8], as shown in figure 7. The major ATPase protein occupied about 40% of the total SR proteins. In permanent ischemia, a reduction in the major ATPase protein band was noted in Endo in ischemia for 20 to 30 minutes, indicating the degradation of the most important and largest protein among the SR-composing proteins, which indicates the necrotic changes accompanying degradation of the SR membrane. In the experiment on myocardial stunning, the composition of the SR proteins did not change at all. In the studies on ischemic preconditioning, the major ATPase protein band was degradated in a manner similar to permanent ischemia without preconditioning, but it was preserved well in the preconditioned hearts. With pretreatment using 8-PT and glibenclamide, the major ATPase protein band was reduced in a manner similar to that without preconditioning, but it was

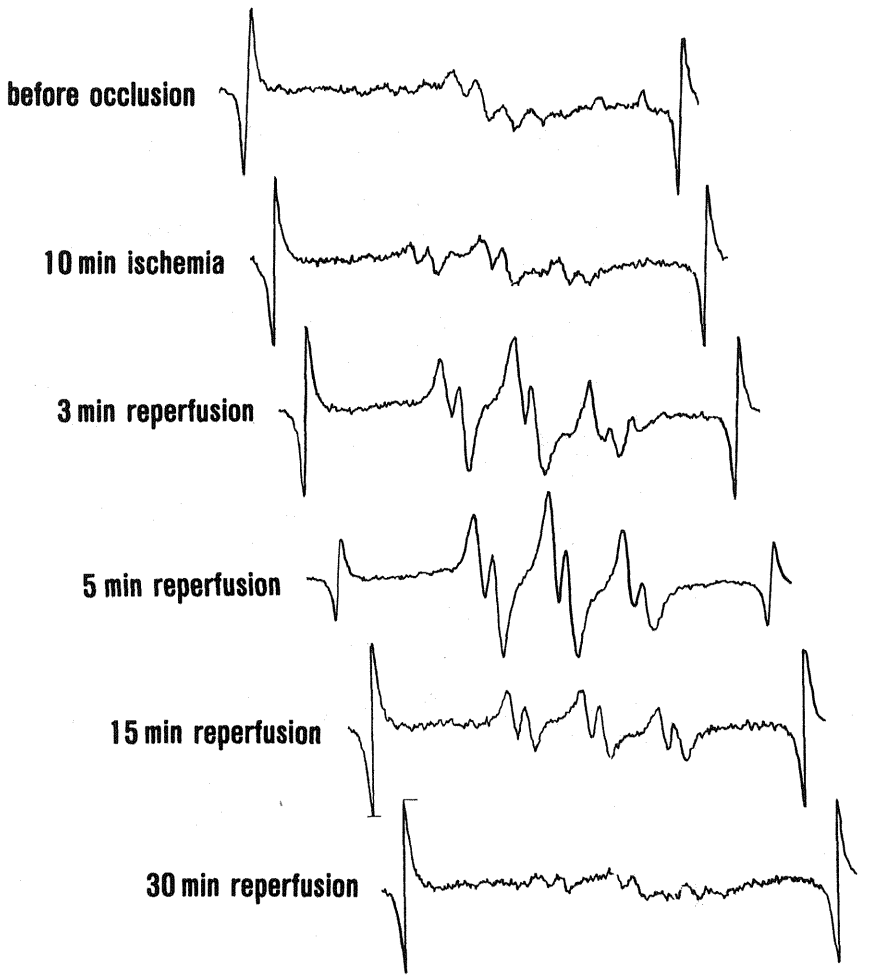

Figure 8. Free radicals from right atrial blood in coronary occlusion and reperfusion. Free radicals, were detected with the spin-trapping agent α-phenyl N-tert-butyl nitrone (PBN). Signals from free radicals, likely to be carbon-centered radicals generated by oxygen-derived free radicals, increased dramatically in ischemia for 10 minutes and reperfusion for 3–5 minutes.

preserved plentifully with administration of nicorandil. In reperfusion injury, the major ATPase protein was degradated earlier, in ischemia for 10 to 20 minutes (figure 7). The composition of the major ATPase protein corresponded well to Ca^{2+}–ATPase activity and to %SS in all the experiments.

ESR signals in ischemia–reperfusion studies

Figure 8 shows ESR signals from the circulating blood in coronary occlusion and reperfusion. During ischemia, the ESR signal was hardly detected in the circulating

blood, but it increased swiftly and markedly after reperfusion. The peak of the signal was observed at around 15 minutes after coronary reperfusion; the pattern of the signal suggests carbon-centered free radicals.

DISCUSSION

It has long been believed that the myocardium insulted by acute severe ischemia may return rapidly to the preischemic state with establishment of a sufficient amount of coronary reflow. The critical point of no return was determined in the classic paper of Jennings et al. [2] to be 22 minutes in the canine heart. But experimental and clinical studies have revealed that the postischemic myocardium, even after a short period of ischemia, does not return fully to the preischemic state. Ischemia–reperfused nonnecrotic heart muscle exhibits contractile dysfunction, becomes tolerant of forthcoming more severe ischemia, and sometimes reaches the most severe, necrotic state even though coronary reflow is fully accomplished. These phenomena are termed *myocardial stunning* [3], *ischemic preconditioning* [4], and *reperfusion injury* [5]. It is important to elucidate the chronological pathophysiology of these quite different but sequential phenomena. We used the sarcoplasmic reticulum (SR) as an indication of ischemic injury, because the microorgans of the SR are very sensitive to ischemia, even though the SR is quite anaerobic.

In permanent ischemia, the Ca^{2+}-dependent ATPase activities of the SR were decreased after even 20 to 30 minutes of ischemia in Endo; at this time, myocardial necrosis is just occurring [6]. Degradation of the major ATPase protein was accompanied by a reduction in Ca^{2+}-dependent ATPase activity. This finding means that the decrease in ATPase activity is caused by the degradation of the ATPase protein itself and thus indicates the degradation of the SR membrane, which in turn is strongly related to necrosis of the ischemic myocardial tissue [6]. In the stunned myocardium, the Ca^{2+}–ATPase activity was decreased, with a reduction in the percent of segment shortening, but the major ATPase protein did not decrease. In the study reported in this chapter, we did not show mitochondrial respiratory activity in stunned myocardium, but the respiratory activity was also reduced in the stunned state [9]. In stunned myocardium, the contractile systems, both the energy-consuming and energy-producing systems, are damaged. To explain the mechanism of myocardial stunning, three hypotheses have been proposed, namely the effect of oxygen-derived free radicals generated with reflow, Ca^{2+} overload, and impairment of excitation–contraction coupling [10]. Given the improved results after treatment with SOD, it is conceivable that oxygen free radicals generated at the time of reperfusion reacted with membranous microorgans such as the SR and mitochondria and damaged their active site reversibly. The short period of ischemia and reperfusion that brings about myocardial stunning may lead to ischemic preconditioning. As to the mechanism of ischemic preconditioning, stunning—a lowered metabolic state—was at first suggested, but this hypothesis was discarded because the duration of stunning (hours to days) was longer than the effective period of preconditioning (several 10-minute periods) [11]. Currently, activation of the adenosine-A1 receptor and the ATP-sensitive K^+ channel and the resulting

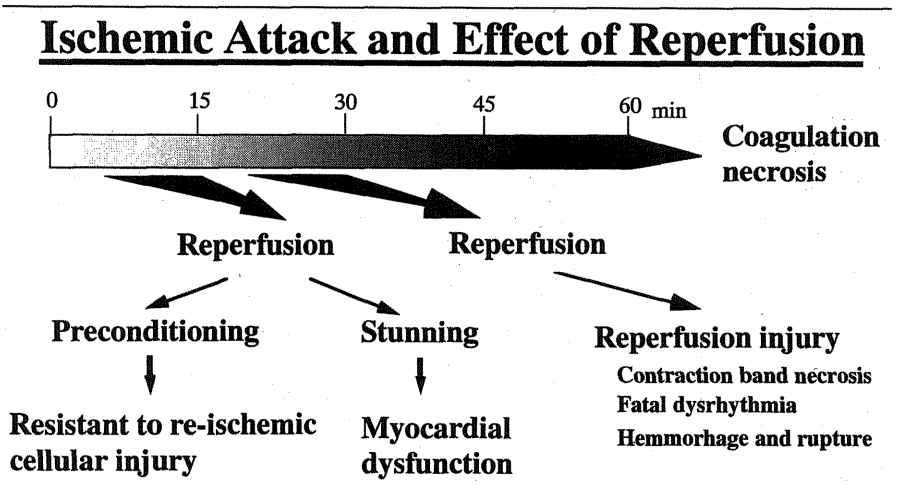

Figure 9. Schematic illustration of coronary obstraction and reperfusion. Prolongation of the period of ischemia gives rise to quite different pathophysiologic phenomena with reperfusion.

suppression of inflow of extracellular Ca^{2+} are believed to be the mechanism of ischemic preconditioning [12,13]. Our studies also support this hypothesis, since treatments with 8-phenyltheophylline, a blocker of the adenosine-A1 receptor, and glibenclamide, an ATP-sensitive K^+ channel blocker, abolished the effect of preconditioning, and the administration of nicorandil, a K+ channel opener, reinforced the effect of preconditioning.

In the experiment concerning reperfusion injury, free radicals generated via reperfusion appear to cause the damage [8,14]. As shown in figure 8, free radicals, likely to be carbon-centered radicals, were detected by ESR through the administration of spin-trapping agent, PBN. In addition, lipid peroxidation of membrane-composing phospholipids and the subsequent excess inflow of extracellular Ca^{2+} might have induced degradation of the major ATPase protein of the SR [8].

The four types of pathophysiological behaviors—stunning, ischemic preconditioning, reperfusion injury, and coagulation necrosis in permanent ischemia—occur successively in the ischemic heart muscle at a velocity of minutes in the length of ischemia. Only a few additional minutes of ischemia bring a quite different pathophysiological phenomenon, as shown in figure 9. These chronological pathophysiologic changes in the ischemic muscle need to be fully understood in studies of ischemia–reperfusion of the heart muscle.

ACKNOWLEDGMENTS

The work reported in this chapter was in part supported by grants from the Ministry of Education, Science and Culture of Japan for 1992, 1994, 1995, and 1996, and by Grants-in-Aid from the Vehicle Association of Japan for 1992, 1993, and 1994.

The authors wish to express sincere thanks to Drs. Toshikuni Yanagishita, Hiroshi Suzuki, and Shinji Koba of Showa University School of Medicine for their collaboration.

REFERENCES

1. Blumgart HL, Gilligan DR, Schlesinger MJ. 1941. Experimental studies on the effect of temporary occlusion of coronary arteries. II. The production of myocardial infarction. Am Heart J 22:374–389.
2. Jennings RB, Ganote CE. 1974. Structural changes in myocardium during acute ischemia. Circ Res 34, 35(Suppl III):III-1456–III-168.
3. Braunwald E, Kloner RA. 1982. The stunned myocardium: prolonged, postischemic ventricular dysfunction. Circulation 66:1146–1149.
4. Murry CE, Jennings RB, Reimer KA. 1986. Preconditioning with ischemia: a delay of lethal injury in ischemic myocardium. Circulation 74:1124–1136.
5. Braunwald E, Kloner RA. 1985. Myocardial reperfusion: a double edged sword? J Clin Invest 76:1713–1719.
6. Konno N, Yanagishita T, Geshi E, Katagiri T. 1987. Degradation of the cardiac sarcoplasmic reticulum in acute myocardial ischemia. Jpn Circ J 51:411–420.
7. Bolli R, Patel BS, Jeroudi MO, Lai EK, McCay PB. 1988. Demonstration of free radical generation in "stunned" myocardium of intact dogs with the use of the spin trap α-phenyl N-tert-butyl nitrone. J Clin Invest 82:476–485.
8. Itoh S, Yanagishita T, Mukae S, Konno N, Katagiri T. 1992. Study on reperfusion injury on sarcoplasmic reticulum in acute myocardial ischemia. Jpn Circ J 56:411–420.
9. Arata H, Geshi E, Ishioka H, Katagiri T. 1995. Alterations in sarcoplasmic reticulum and mitochondrial functions in stunned myocardium: relation between regional myocardial function and biochemical analyses. Showa Univ J Med Sci 7:83–94.
10. Bolli R. 1990. Mechanism of myocardial "stunning." Circulation 82:723–738.
11. Murry CE, Richard VJ. 1991. Myocardial protection is lost before contractile function recovers from ischemic preconditioning. Am J Physiol 260:H796–H804.
12. Liu GS, Thronton J, Van Winkle DM, Stanley AWH, Olsson RA, Downey JM. 1991. Protection against infarction afforded by preconditioning is mediated by A1 adenosine receptors in rabbit heart. Circulation 84:350–356.
13. Murry CE, Jennings RB, Reimer KA. 1991. New insights into potential mechanisms of ischemic preconditioning. Circulation 84:442–445.
14. McCord JM. 1985. Oxygen-derived free radicals in postischemic tissue injury. N Engl J Med 312:159–163.

This Page Intentionally Left Blank

Ca^{2+} ION SHIFTS IN VIVO IN REVERSIBLE AND IRREVERSIBLE ISCHEMIC INJURY

ROBERT B. JENNINGS and CHARLES STEENBERGEN

Duke University Medical Center

Summary. The changes in ion content and H_2O detectable in vivo in the intact canine heart in reversible and irreversible ischemic injury are described, with emphasis on the role Ca^{2+} movements may play in causing ischemic injury. Changes in extracellular ion concentrations and pH revealed by ion-specific electrodes in ischemia are reviewed, as are the contributions of nuclear magnetic resonance measurements of ionized Ca^{2+} to our understanding of Ca^{2+} ion homeostasis in ischemia.

During the reversible phase of ischemic injury in vivo, there is little evidence of significant failure of ion pumps. Nevertheless, substantial shifts in ions and water occur while the myocardium is ischemic. Moreover, after reperfusion with arterial blood, living reversibly injured myocytes exhibit altered volume regulation that persists for minutes to hours. Increases in intracellular Ca^{2+} ion are small (i.e., μM) during the reversible phase and are much larger (i.e., mM) during the irreversible phase of ischemic injury, at which time the so-called calcium overload is clearly present. It is not known whether the overload is an epiphenomenon or a primary cause of lethal injury in ischemia and reperfusion.

INTRODUCTION

Our understanding of the effect of ischemia on cell volume regulation in in vivo ischemia is incomplete. Much of this understanding actually has been derived from results of in vitro studies on a variety of cellular systems, such as isolated myocytes [1,2], myocytes in tissue culture [3], erythrocytes [4], myocardial tissue slices [5], and isolated perfused hearts [6,7], that have been suspended in, perfused with, or superfused with a variety of hypoxic or anoxic crystalloidal solutions.

S. Mochizuki, N. Takeda, M. Nagano and N. Dhalla (eds.). THE ISCHEMIC HEART.

Our current concepts of how cell volume is controlled were derived from studies in simpler systems, and the results have been applied to the whole heart with considerable efficiency. However, it has been difficult or impossible to establish that the events known to occur in vitro actually occur in ischemic reversibly injured myocytes in vivo. The absent or depressed flow of in vivo ischemia imposes constraints on the use of impermeant extracellular markers to measure intracellular volume because a constant extracellular concentration of the marker cannot be ensured when there is no arterial flow. As a consequence, ion changes in the intracellular and extracellular compartments cannot be estimated by direct measurement of total tissue electrolyte contents and plasma electrolyte concentrations. Also, many of the transport ATPases and ion exchangers work at such high rates of speed at 37°C in vivo [3] that changes that may have occurred in living myocytes during an episode of ischemia are altered rapidly by reperfusion because of the speed with which ion gradients are restored after the tissue is reperfused with oxygenated arterial blood.

In this chapter, we shall review the changes in ions and H_2O detectable by direct measurement in reversible and irreversible ischemic injury in intact myocardium, concentrating on the in vivo canine heart, paying particular attention to changes in cations and anions known to be concentrated in the intracellular space and focusing on the role of Ca^{2+} movements between compartments in ischemic injury. Also, we shall review the contribution of ion-specific electrodes to our understanding of electrolyte shifts in ischemia, as well as the contribution of various indicators and nuclear magnetic resonance (NMR) techniques to the analysis of alterations in Ca^{2+} homeostasis in ischemia.

BIOLOGY OF ISCHEMIA

Sudden proximal occlusion of the circumflex branch of the left coronary artery in the open-chest anesthetized dog heart results in an instantaneous reduction in the volume of arterial flow to the myocardium supplied by that vessel. In 98% of canine hearts, circumflex artery occlusion reduces arterial flow to the subendocardial myocardium of the affected bed to 0%–7% of control [8]. A reduction of 7% or less of arterial flow is termed *severe* ischemia. In most dog hearts, collateral vessels provide a higher level of arterial blood flow to the mid- and subepicardial myocardium than to the subendocardial myocardium. The result is a *transmural gradient of ischemia*, with the inner layer receiving the least and the outer layer the most arterial blood flow. In roughly 10% of canine hearts, because of the absence of collaterals, there is virtually no flow throughout the ischemic bed [8]. The focus of the following discussion is on the changes occurring in severely ischemic myocardium.

The small quantities of collateral arterial flow noted in the subendocardial myocardium originate from interarterial connections on the surface of the heart between branches of the circumflex and the anterior descending arteries. These range from 20 to 200 microns in diameter. The larger connections are noted in hearts with large volumes of collateral flow, while hearts with very low collateral flows exhibit scattered, small connections [9,10].

The reduced or absent arterial flow of ischemia results in deficient supplies of O_2 to support aerobic metabolism. As a result, aerobic metabolism ceases about 8–10 seconds after coronary occlusion [11]. Anaerobic glycolysis (AG) supervenes as the only source of new high-energy phosphate (~P) production. Because of the lack of O_2 to support mitochondrial metabolism of substrates to CO_2 and H_2O and the lack of flow to wash end products out of the ischemic bed and into the systemic circulation, lactate, the end product of glycolysis, and H^+ both accumulate [11,12]. Because consumption of ~P continues in the ischemic myocytes in excess of what is produced by anaerobic glycolysis, much of the ~P reserve in the form of creatine phosphate is depleted in 30 to 60 seconds, and adenine nucleotide pool degradation begins [13].

Elimination of the ischemic insult by successful reperfusion with arterial blood allows one to test whether myocytes are alive or dead. If they survive, when reperfused, the injury is *reversible*. Reversibly injured myocytes clearly have been damaged by ischemia, but the damage is nonlethal. On the other hand, the injury is *irreversible* if myocytes are not salvaged by reperfusion but rather disintegrate and are replaced with fibrous tissue [8,14]. In the zone of severe ischemia in the canine heart, all myocytes survive 15 minutes of severe ischemia, while most myocytes in this zone are dead after exposure to 40–60 minutes of severe ischemia [8].

Microelectrode measurements of electrolyte activity during ischemia have demonstrated changes in electrolyte distribution between the intracellular and extracellular space during ischemia [15], but the precise contribution of water and electrolyte fluxes cannot be quantitated by direct analysis of total tissue contents until diffusion into and out of the zone of ischemia has had time to occur. This diffusion allows the interstitial fluid electrolytes to equilibrate with plasma, permitting estimation of intracellular concentrations by subtraction of the extracellular contribution from the total tissue measurements.

ELECTRON MICROSCOPIC CHANGES OF REVERSIBLE AND IRREVERSIBLE ISCHEMIC INJURY

Routine light microscopic techniques reveal no detectable difference in the morphology of myocytes late in the reversible or early in the irreversible phase of injury [16]. However, compared to control nonischemic left ventricle, there are striking changes in the fine structure of the reversibly injured tissue, which can be demonstrated by electron microscopy (figure 1) [17]. The affected myocytes are swollen, contain less glycogen, and exhibit some peripheral aggregation of nuclear chromatin, stretched myofibrils, and occasionally swollen mitochondria. The sarcolemma, which is disrupted in irreversible injury, remains structurally intact. On the other hand, irreversibly injured myocytes exhibit all the changes seen in reversible injury as well as superstretched myofibrils, swollen mitochondria with disorganized cristae, numerous amorphous matrix densities, and foci of disruption of the plasmalemma of the sarcolemma (figures 2 and 3) [12].

The disruption of the sarcolemma is considered to be the lethal event from which the ischemic myocytes cannot recover [12]. It is of interest that these changes,

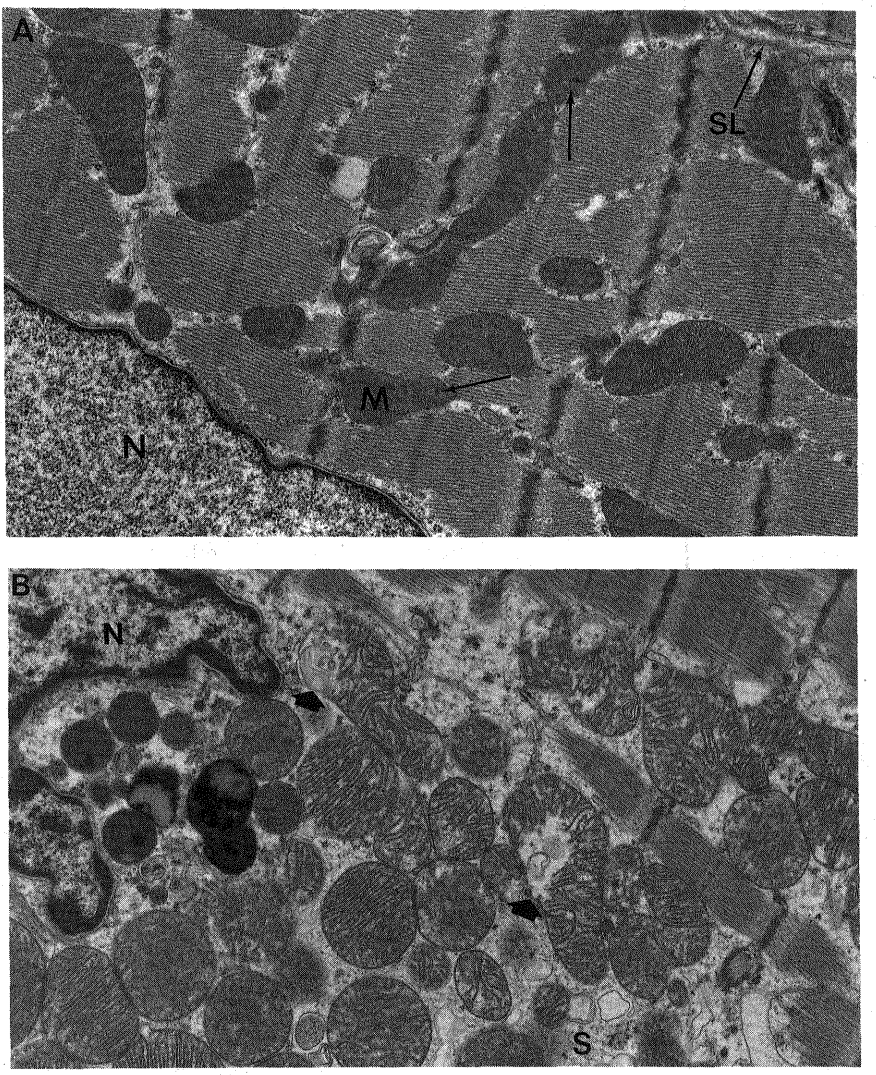

Figure 1. Fifteen minutes of ischemia in the canine heart. The typical structural changes induced by 15 minutes of severe ischemia are shown in (**B**) and should be contrasted to a representative nonischemic myocyte of the same heart (**A**). Note that the chromatin of the nucleus (N) is peripherally aggregated in the ischemic tissue. Also, the sarcoplasm (S) of the damaged myocyte is clearer and more abundant than the control; moreover, it contains less glycogen. The cristae of the mitochondria (M) are packed densely in control; the matrix is scanty and contains occasional tiny matrix granules (arrows), whereas the ischemic tissue shows an increased matrix space in some mitochondria, as well as focal swelling (thick arrows). Although not illustrated in the ischemic tissue, the sarcolemma (SL) was indistinguishable from control. The ATP of the ischemic tissue in this heart was reduced by 67% to 1.85 mmol/g wet. Glutaraldehyde osmium fixation. Magnification X 15,750. Reproduced with permission from [17].

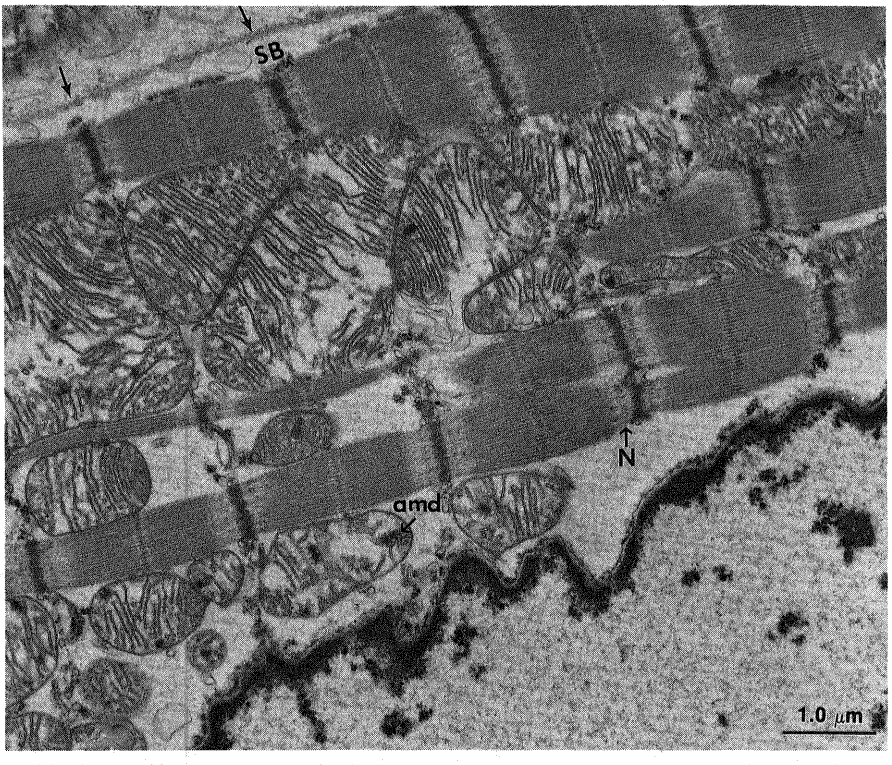

Figure 2. This myocyte of the subendocardial myocardium of the canine heart shows the changes characteristic of irreversible ischemic injury. This tissue was fixed after 40 minutes of continuous ischemia in the canine heart. The chromatin of the nucleus (lower right corner) is markedly aggregated peripherally. The myocyte is swollen, and the volume of the sarcoplasm is increased. Also, it contains very little glycogen. All mitochondria are enlarged and have an increased matrix space in which amorphous matrix densities (amd) are common. The myofibrils are markedly stretched and show N bands (N) in the I band regions. The sarcolemma is lifted off the underlying myofibrils to form subsarcolemmal blebs (SB). The plasmalemma of the sarcolemma overlying such blebs is focally disrupted (arrows) and in the sarcolemma shown in this micrograph has almost disappeared. (Magnification X 18,800; reduced by 67%). Reproduced with permission from [22].

which are obvious after only 30 minutes of severe ischemia, progress but at a very slow rate; they are little changed by 24 hours of ischemia, except that the sarcolemmal disruption is more widespread and more severe [18].

WATER AND ELECTROLYTES IN LATE REVERSIBLE AND EARLY IRREVERSIBLE ISCHEMIC INJURY

Measurement of total tissue contents of electrolytes and H_2O in samples of tissue removed late in the reversible and early in the irreversible phase of ischemic injury shows no significant differences between control and ischemic tissue [19]. The findings in tissue samples exposed to 10 or 40 minutes of severe ischemia in the

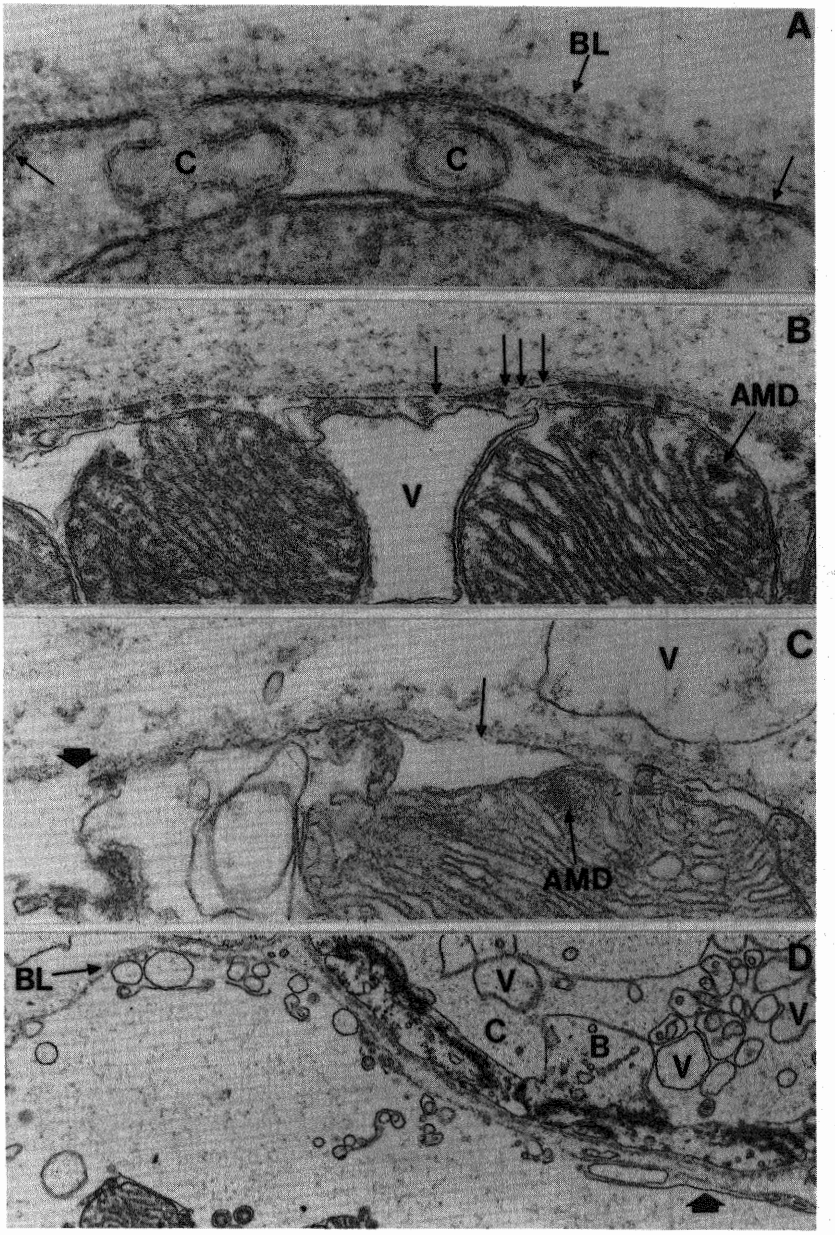
A
BL
C
C
B
AMD
V
C
V
AMD
D
BL
V
C
B
V
V

Table 1. Electrolytes in ischemic canine left ventricle after episodes of reversible (10 min) or irreversible (40 min) ischemia[a]

	TTW mL/100 g dry	Na^+	K^+	Mg^{2+}	Ca^{2+}
		mmol/100 g dry			
Control[b]	369.91 ±2.04	15.4 ±0.60	37.6 ±0.6	4.6 ±0.08	0.39 ±0.02
Reversible[c] injury 10'I	372.2 ±7.22	15.4 ±1.52	37.7 ±0.44	4.50 ±0.34	0.37 ±0.01
Irreversible[c] injury 40'I	365.3 ±3.20	15.9 ±0.68	37.0 ±0.68	4.40 ±0.02	0.43 ±0.05
10'I & 20'R[d]	398.2 ±2.27	16.14[e] ±0.39	44.1[f] ±0.53	4.4 ±0.11	0.397 ±0.03

[a] Data from table 1 of [22].
[b] Control group is nonischemic tissue from the seven hearts in the 10'I + 20'R group. These controls are representative of tissue electrolytes and water in the canine left ventricle.
[c] Reversible ischemic injury was induced by 10' ischemia caused by proximal occlusion of the circumflex artery of the open-chest anesthetized dog heart. Irreversible injury was induced by 40 minutes of ischemia. All tissue studied was severely ischemic, i.e., it exhibited flows of less than 0.07 mL arterial blood/min/g wet heart.
[d] Electrolytes and water in tissue reversibly injured by 10' ischemia (10'I) followed by 20' reperfusion (20'R). The statistical significance for comparisons between control and damaged tissue from the same hearts was determined using a two-tailed paired *t*-test.
[e] $p < 0.05$.
[f] $p < 0.005$.

canine heart are shown in table 1. The 10-minute and 40-minute samples are representative of reversible and early irreversible injury. As noted earlier, the failure to find changes in ions or water is due to greatly slowed diffusion into and out of areas with little or no arterial flow. Studies of total tissue K^+ *content* as well as total tissue water (TTW) in severely ischemic myocardium showed that decreases in K^+ were detectable but were not marked until several hours of ischemia had passed

Figure 3. Various views of the sarcolemma from control (**A**) and irreversibly injured myocytes (**B, C, and D**). These were obtained from the subendocardial myocardium of severely ischemic canine left ventricle. The tissue was fixed in glutaraldehyde buffered with 0.1 M cacodylate (approximately 600–650 milliosmolar) followed by postosmification. (**A**) is representative of the sarcolemma of control nonischemic myocardium. It consists of a plasmalemma and a fuzzy coat of glycoprotein, the basal lamina (BL). The plasmalemma has the typical trilaminar structure (arrow) of a cell membrane. Two caveoli (C) are shown as well (**B**) is representative of an area of sarcolemmal disruption (arrows) found in an irreversibly injured myocyte after 30 minutes of severe ischemia. A swollen mitochondrial vacuole beneath the outer membrane of the mitochondria is labeled (V). (**C**) is a representative view of a subsarcolemmal bleb found after 40 minutes of severe ischemia. Over the bleb is a large break in the plasmalemma at the thick arrow and a smaller break at the little arrow. Amorphous matrix densities (AMD) are present in the mitochondria shown in (B) and (C). (D) shows a large subsarcolemmal bleb found after 120 minutes of ischemia. The basal lamina (BL) still is generally intact, but the plasmalemma is thrown up into circular profiles underneath it. A capillary showing the endothelial blebs (B) and vacuoles (V) characteristic of advanced ischemic injury is also present in (D). Reproduced with permission from [12].

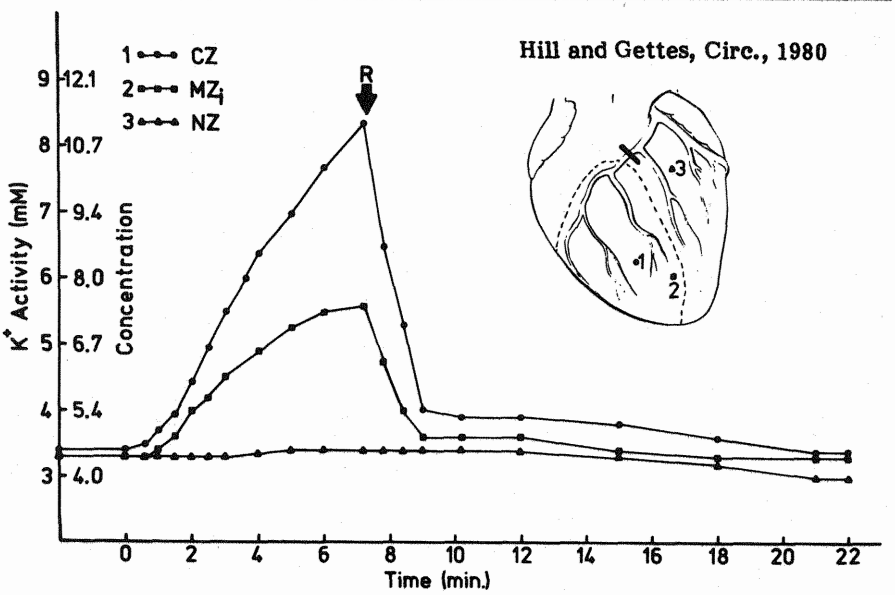

Figure 4. The redistribution of tissue K^+ from the intracellular to the extracellular space that begins within 30 seconds of the onset of ischemia is shown in this figure from Hill and Gettes [15]. They measured the change in $[K^+]_E$ in the central zone (CZ) of a large area of ischemia in the pig heart with a K electrode. The $[K^+]_E$ rose from 3.5 to 8.5 during 10 minutes of ischemia. The $[K^+]_E$ concentration decreased quickly within a few seconds after the onset of reperfusion. The marginal zone (MZ_i) shows less marked changes because it contains a mixture of ischemic and non-ischemic myocytes plus the fact that this region is much closer to well-perfused tissue. Reproduced with permission from [15].

[20]. At this time, the tissue was quite edematous, and tissue $[K^+]$ was approaching that of the extracellular fluid. These late changes in ions occurred as a consequence of diffusion of ions and water into and out of the area of injury. Since the tissue exhibited marked alterations in structure by electron microscopy after 60 minutes of ischemia, while analysis of the tissue demonstrated no changes in electrolytes and water, it seemed likely that changes in electrolyte and H_2O balance undoubtedly had occurred even though they could not be quantitated directly [21]. Furthermore, extraordinary changes in tissue electrolytes and water occurred when this tissue was reperfused with arterial blood [17,21–27].

Ino-specific electrodes and ion changes during ischemia and reperfusion

Even though the total tissue K^+ content remains constant during ischemia, dramatic shifts in K^+ have been demonstrated by Hill and Gettes [15] using K^+-sensitive electrodes implanted in the subendocardial myocardium in the center of an area of regional ischemia in the pig heart to measure extracellular K concentration ($[K^+]_E$).

H^+ ion electrodes also were implanted, and $[K^+]_E$ and $[pH]_E$ were monitored continuously in this area of total ischemia. The results were striking. Although direct chemical analysis (table 1) showed no changes in total tissue K^+ content following 10 or 60 minutes of severe ischemia, there clearly was redistribution of K^+ in the ischemic tissue. Moreover, the changes in $[K^+]_E$ developed quickly (figure 4); within 60 seconds of the onset of ischemia, $[K^+]_E$ rises significantly, essentially doubling after 8–10 minutes of ischemia. $[K^+]_E$ then plateaus at this level for the next 10 minutes before beginning to rise again [15]. The second rise in $[K^+]_E$ has been attributed to irreversible injury [28]. When all the myocytes are dead and have lost the ability to maintain ion gradients, $[K^+]_E$ theoretically would be 108 mmol/L (total tissue K^+/TTW). The longer the tissue is ischemic, the greater the proportion of dead cells. Assuming myocyte death occurs on the same time scale in the pig as in the dog, the second rise in $[K^+]_E$ is consistent with the appearance of irreversible injury. However, endothelial cells, pericytes, and fibroblasts, all of which contribute to total tissue K^+, survive for longer periods during ischemia than myocytes, and therefore the rise in $[K^+]_E$ does not reach its theoretical limit.

Effect of reperfusion

Reperfusion of the ischemic tissue with arterial blood results in rapid restoration of both $[K^+]_E$ and $[H^+]_E$ to the control range [29] (figure 4). The decrease in $[K^+]_E$ occurs secondary to K^+ uptake by the damaged myocytes as well as K^+ washout from the interstitium to the systemic circulation. The lactate produced during ischemia either is metabolized to CO_2 and H_2O or is washed out to the systemic circulation by the arterial blood reperfusing the tissue. Intracellular and extracellular pH also is restored quickly to control levels [30].

Effect of reperfusion with arterial blood on water and electrolytes of irreversibly injured tissue

Reperfusion of irreversibly injured tissue in zones of severe ischemia induced dramatic changes in morphology, electrolytes, and water [31]. Tissue irreversibly injured by 40 minutes of ischemia and then exposed to 2, 5, 10, and 20 minutes of reflow swelled quickly and markedly (figure 5). Water increased by 21% after only two minutes of reflow and, after 20 minutes of reflow, had increased to 35%. In addition, tissue K^+ and Mg^{2+} decreased markedly, while Na^+ and Cl^- increased. These changes in electrolytes and H_2O were associated with marked changes in ultrastructure [32,33]. The tissue developed large contraction bands and great swelling. This appearance is shown in figure 6. Sarcolemmal disruption was even more marked than it had been prior to reperfusion, presumably because of the increased cell water of the swollen myocytes.

Changes in Ca^{2+}

One of the striking features of evolving contraction band necrosis was the accumulation of large quantities of Ca^{2+} in the areas of injury. This increase occurred

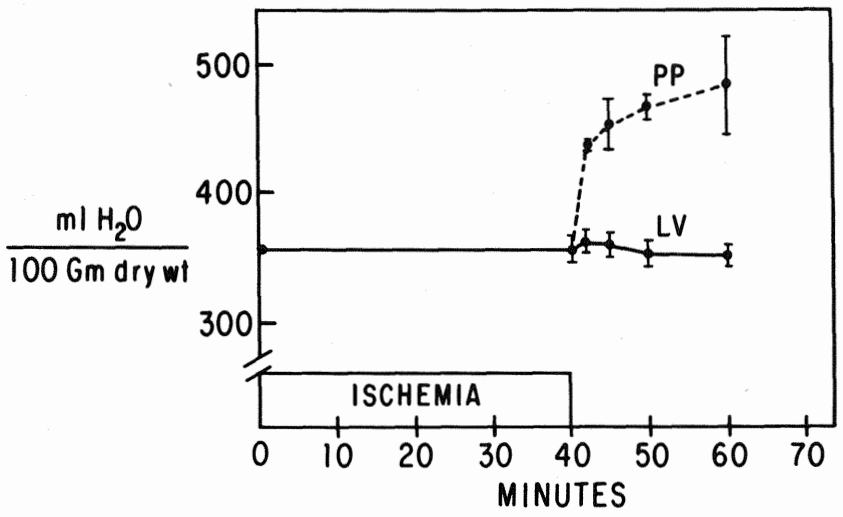

Figure 5. The changes in total tissue water (TTW) that result when tissue containing large numbers of myocytes irreversibly injured by 40 minutes of ischemia is reperfused with arterial blood are shown here. Groups of ischemic hearts, labeled PP, were reperfused for 2, 5, 10, and 20 minutes after having been irreversibly injured by 40 minutes of ischemia. Note that the TTW increased by 21% after only two minutes of reperfusion and slowly increased thereafter, reaching levels as high as 500 mL H_2O/100 g dry weight. This increase in water was associated with a marked decrease in K^+ and Mg^{2+} and a rise in Na^+, Ca^{2+}, and Cl^-. Contraction band necrosis was detected after only two minutes of reperfusion. The earliest time of its appearance is unknown, but it most likely first develops during the first minute of reperfusion [32]. Reproduced with permission from [31].

quickly and resulted in a tenfold increase in Ca^{2+} content as compared with control myocardium (figure 7) [31]. Virtually all the increased Ca^{2+} originated from the plasma reperfusing the area of ischemia [27]. Moreover, much of this increased Ca^{2+} was in the mitochondria, where it accumulated in the form of calcium phosphate (hydroxyapatite) (see insert, figure 6) [26]. Active mitochondrial metabolism is required to accumulate the calcium phosphate. This metabolism took place in preference to oxidative phosphorylation and thereby potentiated injury in the sense that energy is required to maintain viability and available aerobic energy was being shortcircuited to ion accumulation [34], although if the cells were already lethally injured and the calcium influx was due to sarcolemmal disruption, the effects of calcium uptake on energy production would be moot. However, marked Ca^{2+} accumulation clearly reduces or eliminates mitochondrial function in the reperfused tissue and therefore could be a lethal event. This represents a form of so-called *calcium overload*. Later, Kloner et al. [35] showed that mitochondrial Ca^{2+} accumulation did not occur in tissue successfully reperfused after 90 minutes

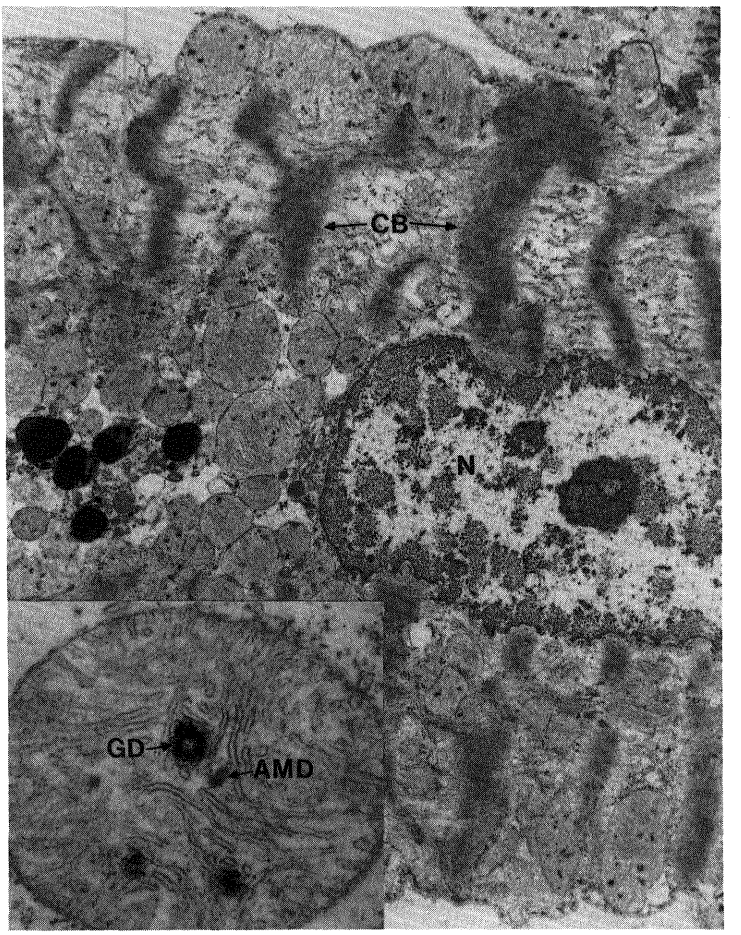

Figure 6. Ultrastructural features of contraction-band necrosis induced by 40 minutes of in vivo ischemia and 20 minutes of reperfusion. Numerous dense myofibrillar contraction bands (CB) are obvious. Peripheral condensation of nuclear chromatin (N) also is apparent, and mitochondria appear swollen and contain both amorphous and granular matrix densities. The insert on the lower left shows a higher-power view of characteristic granular densities of calcium phosphate found in the mitochondria of these cells. Both amorphous (AMD) and granular densities (GD) are present. Osmium fixation. X14,000; inset X45,000. Reproduced with permission from [57].

of ischemia even though the tissue still developed contraction band necrosis, presumably because integrated mitochondrial function was not possible after 90 minutes of ischemia.

The hypothetical explanation of the formation of contraction bands is uncontrolled entry of Ca^{2+} into the sarcoplasmic space. Most of this entry is assumed to

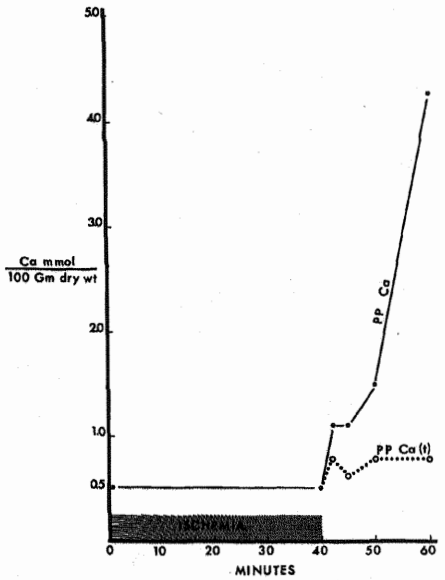

Figure 7. The massive increase in tissue Ca^{2+} that develops in tissue irreversibly injured by ischemia when it is reperfused with arterial blood is graphed here. The increase in Ca^{2+} accompanied the increase in TTW shown in figure 5, but the increased plasma water itself provided very little Ca^{2+} (see PPCa(+) for the Ca^{2+} contributed by the plasma water). Much of the Ca^{2+} was accumulated in the mitochondria in the form of hydroxyapatite (see insert, figure 6). These changes only develop early in the phase of irreversible injury, i.e., when the mitochondria still have some capacity to generate a proton gradient. Reperfusion after 90 minutes of ischemic injury is not accompanied by mitochondrial accumulation of calcium phosphate. Reproduced with permission from [31].

occur through the plasmalemmal defects, but in intact myocytes, the process of Na^+–H^+ and Na^+–Ca^{2+} exchange also could contribute both to myocyte swelling and to the increased sarcoplasmic Ca^{2+} [36].

Significance of Ca^{2+} entry: the Ca^{2+} overload hypothesis

In aerobic rat hearts given large doses of catecholamines, scattered small islands of contraction band necrosis appear shortly after the drug is administered. Moreover, the necrosis can be prevented by blocking beta receptors with propranolol or by blocking Ca^{2+} entry with verapamil [37–39]. These observations on Ca^{2+} entry in catecholamine poisoning plus our observation on Ca^{2+} entry in reperfused irreversibly injured tissue and others [40] led to the hypothesis that *excessive Ca^{2+} entry might be a lethal event in cellular injury.* In the case of ischemia, it has been impossible to prove that massive Ca^{2+} entry (overload) through intact cell membranes causes cell death because of the concurrent development of plasmalemmal defects through

which calcium overload could occur. In the latter instance, overload is secondary to the defective plasmalemma and is not the primary event causing lethality. Many years of effort have led us to conclude that Ca^{2+} entry is clearly deleterious, but we have not been able to establish whether it is an epiphenomenon or actually causes cell death in ischemia and reperfusion. Furthermore, a small proportion of dead myocytes within an area of primarily reversible injury could produce a disproportionate rise in total tissue calcium, even though there might be no change in calcium in the vast majority of intact myocytes.

Effect of reperfusion with arterial blood on water and electrolytes of tissue late in the phase of reversible injury

As shown in figure 1, myocyte architecture is well preserved late in the reversible phase of ischemic injury (15 minutes of severe ischemia in the in vivo canine heart); mitochondrial swelling occurs in widely scattered mitochondria, but the mitochondria remain intact and free of amorphous matrix densities. Moreover, no defects in the plasmalemma of the sarcolemma are detectable in this tissue. In addition, 20% of the adenine nucleotide pool is still present within the myocytes [17]. Since the injury is defined as reversible, reperfusion clearly has prevented the death of myocytes damaged by ischemia and destined to die in the absence of reflow. Although these myocytes resume function and aerobic metabolism when they are reperfused, they are injured. *Stunning* is the most obvious functional sign of this injury [41,42]. However, they also are *preconditioned*, which makes them less susceptible to injury during a subsequent episode of ischemia, and they contain excess Mg^{2+}, Pi, and glucose [43] and exhibit a creatine phosphate overshoot [44].

On the basis that the Ca^{2+} overload seen in irreversible injury might be in the process of development during the late phase of reversible injury, we assessed various features of water and electrolyte balance as well as alterations in ultrastructure occurring during ischemia and reperfusion late in the reversible phase of ischemic injury. Reversible injury was induced by exposing the canine heart to 15 minutes of severe ischemia followed by reperfusion with arterial blood. The tissue was sampled at 0, 0.5, 3, 20, 60, 240, and 1440 minutes [17].

Water and electrolytes during reperfusion

Figure 8 shows the changes in TTW, K^+, Na^+, and Mg^{2+} that occurred during reflow. The TTW was increased significantly after three minutes of reflow, as was Na^+ and K^+. Mg^{2+} was unchanged. Total tissue Na^+ content gradually began to return towards control after 20 minutes. K^+ still was increased at four hours and was increased, but not significantly, at 24 hours. Moreover, the tissue still was edematous 24 hours after the onset of reperfusion.

We assume that most of the increase in TTW is due to an increase in cell water. Although, the increased blood volume associated with reactive hyperemia might contribute to the increase noted during the first three minutes of reperfusion, it probably is not a significant feature at later times because hyperemia no longer is

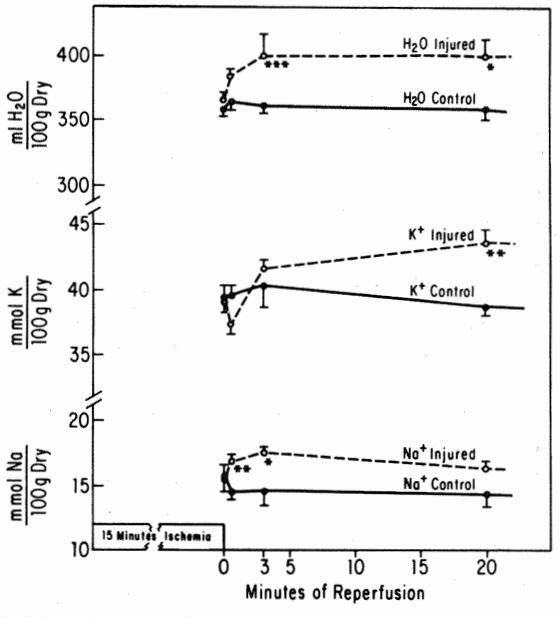

Figure 8. The effects of various periods of reperfusion on TTW, Na^+, and K^+ in damaged myocardium (late reversible phase) and control myocardium are plotted as a function of the period of reperfusion. As expected, because of the very low collateral flow in the PP, there was no change in TTW, Na^+, or K^+ at the end of 15 minutes of sustained ischemia [31]. After reperfusion, both Na^+ and H_2O increased promptly and remained elevated. However, after 30 seconds of reperfusion, the K^+ of the damaged tissue was slightly lower than control (not significant). Thereafter, tissue K^+ rose to much higher levels than control. At 20 minutes, the injured tissue had restored its normal ultrastructure and adenylate charge but still showed a marked increase in K^+ and smaller increases in Na^+ and H_2O. In other studies [58], these changes were still present after 60 minutes but not after 1440 minutes of reperfusion. Similar changes develop in tissue reversibly injured by 10 minutes of ischemia and then reperfused (see table 1). Reproduced with permission from [17].

present after 20 minutes of reperfusion, i.e., at the time when the electrolyte and H_2O changes are maximal. The increase in K^+ in mmol/100 g of tissue is considered to be secondary to this increase in cell water, since the Na–K ATPase drives K^+ into the cell to reestablish the K gradient.

Changes in Ca^{2+}

To test whether shifts in Ca^{2+} occurred in the badly damaged living myocytes when they were reperfused with arterial blood, we labeled the plasma Ca pool with ^{45}Ca by injecting it intravenously immediately after occluding the circumflex artery. If calcium uptake were occurring during ischemia or occurred during reperfusion, we should be able to detect it during the early phase of reperfusion by providing an infinite supply of plasma Ca^{2+} labeled with ^{45}Ca in the reperfusing blood. Thus,

Table 2. ^{45}Ca activity in damaged and control left ventricular myocardium after 15 minutes of ischemia followed by three minutes of reperfusion

	Plasma-free tissue Ca^{2+}									
	^{45}Ca dpm/g wet / ^{45}Ca dpm/mL plasma		mmol Ca^{2+}/100 g dry		TTW (mL/100 g dry)		Myocardial plasma content (mL/100 g dry)		ATP (umol/g wet)	
Tissue site	Injured	Control	Injured	Control	Injured	Control	Injured	Control	Injured	Control
Subendocardial	0.302 ±0.012	0.272 ±0.022	0.379	0.313	402.0 ±6.2[a]	360.2 ±2.6	20.2 ±3.5	18.5 ±2.8	2.81 ±0.23[a]	5.22 ±0.25
Midmyocardial	0.294 ±0.002	0.293 ±0.008	0.358	0.339	387.0 ±14.0	363.0 ±4.9	22.3 ±4.4	14.4 ±0.5	3.63 ±0.10[a]	
Subepicardial	0.298 ±0.009	0.285 ±0.017	0.344	0.331	361.3 ±8.6	364.0 ±1.0	18.1 ±1.8	21.2 ±2.8	4.10 ±0.29[a]	

[a] $p < 0.01$.

Data from three dog hearts. All samples are free of endocardium and epicardium. The subendocardial samples are from the posterior and anterior papillary muscles. The midmyocardial and subepicardial samples are from the inner and outer half of the free wall of the left ventricle under each papillary muscle. The ^{45}Ca results have been corrected for the ^{45}Ca contributed by the plasma. TTW, total tissue water. All results are given as mean ± SEM. Footnote a indicates the probability that the means are different by a two-tailed nonpaired *t*-test. The water and ATP data show a transmural gradient of injury, with the subendocardial layer being the most injured and the mid- and subepicardial layers demonstrating progressively less injury. However, ^{45}Ca was not accumulated at any site in the damaged tissue. Plasma content was slightly increased in the ischemic–reperfused tissue as compared with control, but this change was not significant after three minutes of reperfusion. Plasma-free tissue Ca^{2+} was converted from units of tissue dpm per g wet weight divided by plasma dpm/mL to mmol/100 g dry using a plasma calcium of 2.5 mM and the appropriate TTW for wet weight to dry weight conversion. Inclusion of plasma calcium would increase tissue calcium by approximately 0.05 mmol/100 g dry.

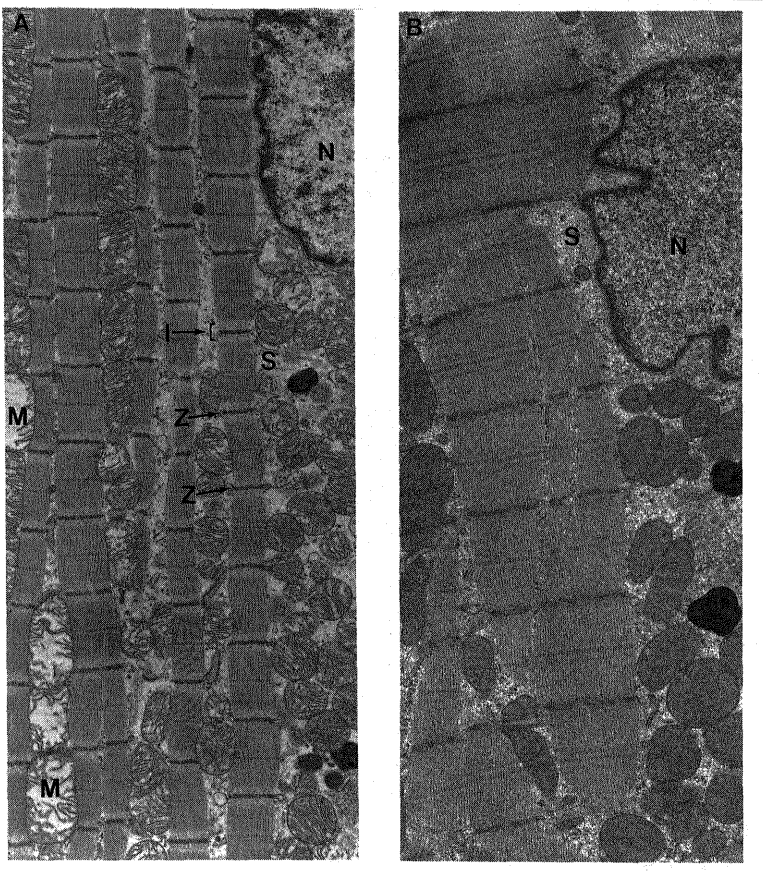

Figure 9. Late reversible injury induced by 15 minutes of ischemia in the canine heart followed by three minutes of perfusion. Marked swelling was noted in some mitochondria after this brief period of reperfusion; those labeled M are representative of the badly swollen variety. The remaining mitochondria were less markedly involved. The chromatin of the nucleus (N) still is aggregated peripherally. The sarcoplasm (S) is less dense and contains little granular glycogen. The myofibrils are relaxed; they demonstrate large I bands, in contrast to the myocytes of control, which are contracted. The damage shown in (**A**) is as marked as we observed after a brief period of arterial reperfusion. Three of the five dogs studied showed this degree of change. (**B**) is from the nonischemic AP of the same dog and is presented as a control to compare to (**A**). The appearance is similar to control tissue presented in figure 1A. Glutaraldehyde fixation with postosmication. A: 7750X; B: 10,075X. Reproduced with permission from [17].

an increase in Ca^{2+} entry would result in an increase in total tissue Ca^{2+} or in the proportion of ^{45}Ca in the tissue. As shown in table 2, no change in Ca activity was noted. These results indicate that an increase in tissue Ca^{2+} is not detectable during reperfusion of tissue late in the reversible phase of ischemic injury. Since an enormous amount of Ca^{2+} enters irreversibly injured myocytes [31], the period of

ischemia used in this experimental protocol cannot be extended because of the risk of killing scattered myocytes. If any cell death with its associated massive Ca^{2+} overload occurred in the tissue, it would overwhelm any changes that might occur in the intact myocytes.

Ultrastructural changes

After three minutes of reperfusion, the mitochondrial changes in the reversibly injured reperfused tissue are more severe; all mitochondria are more swollen than they were prior to the onset of reperfusion. However, these changes are transient and are no longer detectable after 20 minutes or 24 hours of reperfusion (figure 9). However, a rare mitochondrion is disrupted totally. This is the only structural monument to the injury induced by the ischemic episode. The remaining mitochondria appear intact and are indistinguishable from controls [17].

Assessment of electrolyte and water balance in tissue injured in vivo using tissue slices

Since electrolyte and water changes occurring during ischemia are difficult to detect in vivo and since reperfusion studies suggested that electrolyte and water balance is altered early in ischemia, we developed an in vitro technique to assess cell volume regulation in tissues injured by ischemia in vivo. The in vitro analysis was performed on thin, free-hand tissue slices prepared from tissue injured by regional ischemia in vivo. The function of slices of damaged heart was compared to the function of slices prepared from control tissue of the same heart. The slices were incubated in continuously oxygenated or nitrogen-equilibrated Krebs Ringer's phosphate media at pH 7.2. Slices of control tissue maintained their ultrastructure, water content, and ion gradients. Following an initial release of K^+ during preparation of the slices, the tissue accumulated K^+ (figure 10). Na^+ content remained low. In addition, CP was synthesized, and tissue ADP and AMP were low (data not shown). However, about 50% of the adenine nucleotide pool was lost during preparation of the slice.

Tissue excised during the reversible phase of injury functioned as well as control tissue, while tissue early in the irreversible phase of injury could maintain neither cell volume nor ion gradients. In addition, the use of inulin to estimate the extracellular space (inulin is a neutral molecule with a molecular weight of 5000 that is excluded from the intracellular space) permitted an assessment of sarcolemmal integrity by estimating the inulin diffusable space (IDS). IDS measurements showed large increases in this space in irreversibly injured tissue and no change in the IDS in reversibly injured tissue. This finding provided functional confirmation of the defects in the plasmalemma of the sarcolemma noted by electron microscopy (figure 3). In addition, these changes developed whether or not the tissue was incubated in oxygenated or anoxic media. Tissue Ca^{2+} only was increased significantly when the IDS was increased. The relationship between the IDS and ATP was particularly striking (figure 11). When ATP fell to very low levels, it invariably was accompanied by a big increase in the IDS.

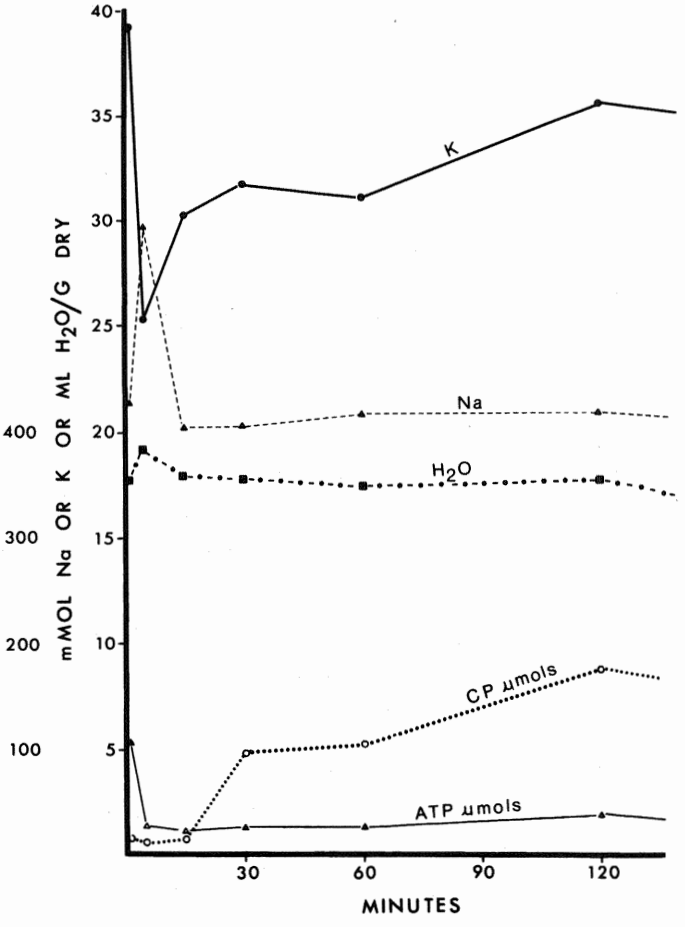

Figure 10. This figure shows the changes in Na^+, K^+, total tissue water (TTW), creatine phosphate (CP), and ATP that occur while slices of control canine left ventricle are being prepared and then incubated. In order to slow ischemic metabolism during the preparation of the slices, the excised left ventricular tissue was cooled to 15–20°C. Thus, at zero time, the CP was low and ADP and AMP were high. When the slices then were placed in oxygenated Kreb's Ringer's phosphate at 37°C, oxidative phosphorylation resumed and the adenylate change was restored; however, as this tissue was warmed, some of the adenine nucleotide pool was lost as nucleosides. Within a few minutes, CP was resynthesized; ATP stayed constant thereafter. There was a transient increase in TTW and Na^+ while K^+, on the other hand, decreased during the first few minutes of incubation. Thereafter, the TTW and Na^+ decreased and K^+ reaccumulated in the $[H_2O]_i$.

Relationship between cold swelling and in vivo ischemic cell injury

As is shown in figure 12, inhibition of active metabolism in myocytes by incubation at 0°C resulted in marked cell swelling, loss of K^+, and gain of Na^+. When metabolism was allowed to resume by the rewarming of slices, then the TTW, K^+ content, and Na^+ content returned quickly towards control. The speed with which

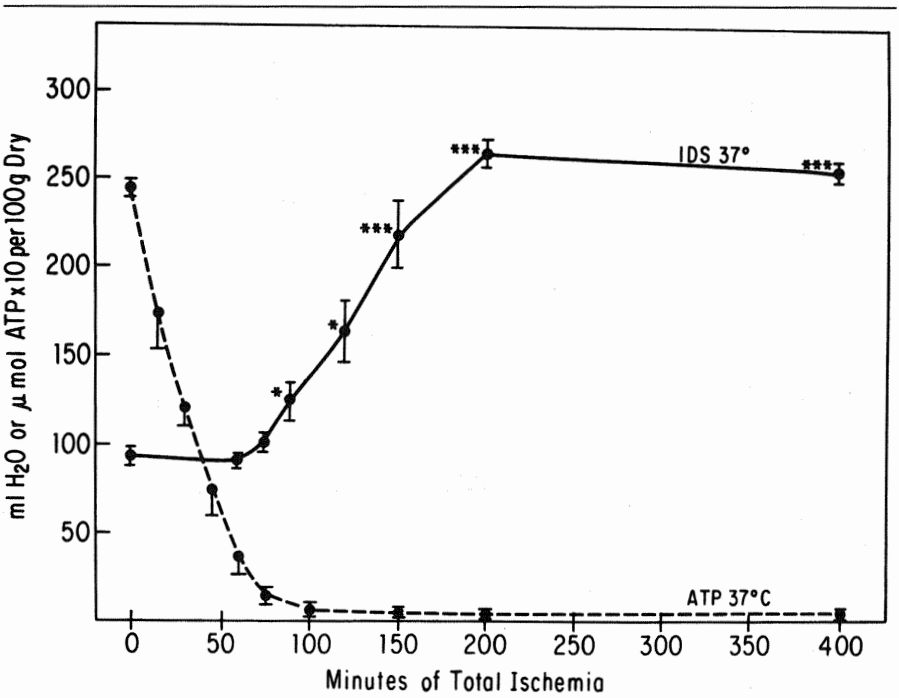

Figure 11. The relationship is shown here between ATP depletion in caine left ventricle subjected to total ischemia at 37°C for 400 minutes and the inulin diffusable space (IDS) in thin freehand slices prepared from this tissue after varying intervals of ischemia. The IDS provides a measure of the integrity of the sarcolemma because inulin is excluded from the $[H_2O]_i$ of healthy myocytes. Note that ATP depletion is virtually complete after 100 minutes of total ischemia and that the IDS assessed in slices of this tissue simultaneously is significantly increased; however, the maximum increase in IDS is noted after 200 minutes of ischemia. Electron micrographs of the sarcolemma of myocytes from this experiment first show focal disruptions in the plasmalemma after 75–100 minutes of ischemia that increase in number and size as the period of ischemia is extended. Thus, good morphologic and functional evidence of sarcolemmal disruption is present in total ischemia and is associated closely with the level of ~P. The same changes are noted in slices prepared from severely ischemic tissue in vivo. However, in in vivo ischemia, the changes occur at roughly twice the speed seen in in vitro total ischemia.

ion gradients are reestablished is shown in figure 13 using ^{86}Rb as a surrogate for K^+. The restoration of cell volume could be inhibited totally by including ouabain, an inhibitor of the Na–K ATPase (figures 12 and 13) in the media, an observation that showed that this ATPase is critical to the recovery of cell volume regulation following cell swelling in myocardium.

Slices prepared from reversibly injured tissue were indistinguishable from control. Thus, the Na–K ATPase still is fully functional in reversibly injured canine left ventricular tissue.

Irreversibly injured tissue exhibited big increases in IDS, loss of Mg^{2+}, failure to

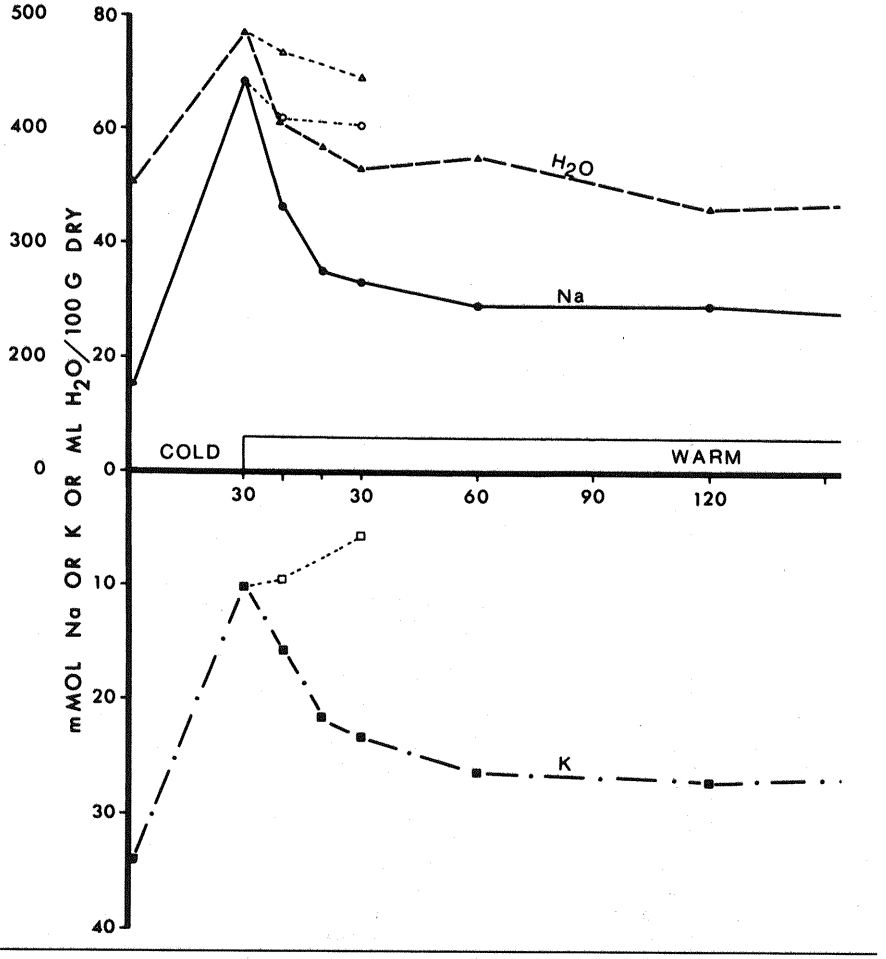

Figure 12. The effects of cold-induced swelling and subsequent warm incubation on slices of normal myocardium is illustrated here. Cold incubation resulted in massive efflux of K^+ and influx of Na^+ and water. These changes were largely reversible by subsequent rewarming in an oxygenated medium (closed circles). Rewarming in the presence of ouabain (open circles) caused additional K^+ efflux and prevented most of the extrusion of Na^+ and water. Reproduced with permission from [19].

accumulate K^+, and failure to exclude Na^+. Although this tissue swelled in the cold, resumption of metabolism by rewarming did not reverse cell swelling. We believe that loss of sarcolemmal integrity explains most of these changes in the irreversibly injured tissue. Thus, the results of our in vitro test of cell volume regulation in tissue injured in vivo failed to show any alterations in cell volume regulation and ion homeostasis until a significant number of myocytes were irreversibly injured. At this point in time, marked alterations in cell volume regulation were easily detectable.

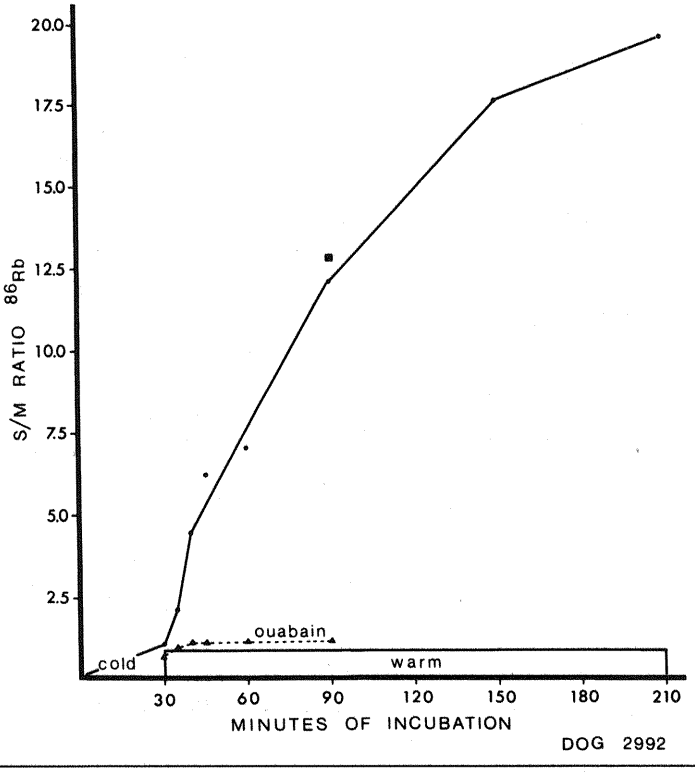

Figure 13. This figure shows the rate at which ^{86}Rb is accumulated in tissue slices of control canine left ventricle that have been swollen by 30 minutes at 0–1°C. The degree of swelling and K^+ loss produced by cessation of respiration by cold was identical to that shown in figure 12. A tracer dose of ^{86}Rb was included in the medium when the slices were rewarmed to 37°C in order to assess the capacity of the tissue to accumulate K^+ ion. Note the speed with which the slice-to-medium ratio (S/M) increased due to Na–K ATPase activity during the first 10 minutes of warm incubation. Accumulation continued for 60 minutes thereafter. Note that ouabain totally inhibited ^{86}Rb, as it did K uptake in figure 12.

Intracellular ion changes during ischemia in intact myocardium as detected by NMR

The development of fluorine-containing Ca^{2+} indicators [45] and extracellular shift reagents [46,47] has allowed changes in cytosolic [Ca^{2+}] and [Na^+] to be measured in intact myocardium using nuclear magnetic resonance. Although the earliest fluorine-containing Ca^{2+} indicator (5F-BAPTA) had a high calcium affinity that buffered calcium transients and decreased contractility, it did permit an evaluation of the time course of changes in cytosolic [Ca^{2+}] during ischemia [48,49]. Furthermore, a newer Ca^{2+} chelator has been developed [50] that has a much lower calcium affinity and therefore has less effect on calcium transients and contractility.

Results with these indicators have shown that there is a significant increase in cytosolic free $[Ca^{2+}]$ during the reversible phase of ischemic injury to a value of 2–4 μM, which is fully reversible upon reperfusion [48]. Similar results have been obtained [51] with the high-calcium affinity indicator and the low-calcium affinity indicator, suggesting that the buffering effect of the indicator was not substantially altering the effect of ischemia on cytosolic $[Ca^{2+}]$. Further studies were performed [52] with the low-affinity indicator using rabbit hearts with the indicator loaded into the sarcoplasmic reticulum (SR); these studies showed that during the reversible phase of ischemic injury, SR $[Ca^{2+}]$ did not change appreciably. Thus, the increase in cytosolic $[Ca^{2+}]$ was not due to release of Ca^{2+} from the SR, but there was no evidence of calcium uptake by the SR despite an increase in cytosolic $[Ca^{2+}]$, which was attributed to the decrease in phosphorylation potential to drive the SR ATPase [52].

Studies of intracellular $[Na^+]$ using shift reagents to separate intracellular from extracellular sodium have shown an early rise in $[Na^+]_i$ during ischemia to more than twice the level in control myocardium [47,53]. This rise in $[Na^+]_i$ during ischemia can be blocked by inhibitors of Na–H exchange [53], suggesting that intracellular acid production is the primary stimulus for sodium entry using the Na–H exchanger and that this sodium influx is greater than sodium efflux by the Na–K ATPase. Inhibition of the Na–H exchanger during ischemia also delays the rise in $[Ca^{2+}]_i$ but does not prevent an eventual rise in $[Ca^{2+}]_i$, suggesting that there are multiple pathways that contribute to the rise in $[Ca^{2+}]_i$ during ischemia but that Na–Ca exchange coupled to Na–H exchange is the first pathway resulting in net calcium influx to be activated during ischemia.

DISCUSSION

The results of the experiments reviewed in this chapter show clearly that extensive changes in cell volume regulation occur in ischemic tissue during the phase of reversible injury. These changes include a rise in $[K^+]_E$ with an associated fall in $[K^+]_i$ and increases in $[H^+]_E$, $[H^+]_i$, $[Mg^{2+}]_i$, $[Na^+]_i$, and $[Ca^{2+}]_i$, and a marked rise in $[P_i]_i$. There is considerable indirect evidence that these changes are accompanied by an increase in intracellular volume. Moreover, most of these major ion and water changes are repaired quickly in vivo or in vitro if oxygenation is restored and ischemia is relieved, the principal exception being the rise in free cytosolic Mg^{2+} concentration, which recovers incompletely during early reperfusion [54] because of the loss of adenine nucleotides that normally chelate much of the intracellular Mg^{2+}. Thus, there is no evidence of significant failure of ion pumps such as the Na–K ATPase during the reversible phase of ischemic injury.

However, volume regulation in reversibly injured reperfused tissue is not restored to its control condition until many hours of reperfusion have passed. The tissue is persistently edematous and contains more K^+ on a dry weight basis than control tissue.

Role of Ca^{2+} in ischemic injury

No significant increase in total myocyte Ca^{2+} content has been detectable in vivo in reversibly injured tissue, either prior to reperfusion or during early reperfusion. This finding is not inconsistent with in vitro studies using fluorine-containing calcium indicators and NMR to estimate cytosolic free $[Ca^{2+}]$, since the modest rise in cytosolic free $[Ca^{2+}]$ would be insignificant relative to the total tissue Ca^{2+} content. The NMR studies show that the rise in cytosolic $[Ca^{2+}]$ remains in the μM range after 20 minutes of total ischemia in isolated perfused hearts and is readily reversible during reperfusion. Although no changes in total tissue Ca^{2+} content were observed in vivo in ischemic or in reperfused living myocardium damaged by ischemia, it seems likely that increases in cytosolic free $[Ca^{2+}]$ occurred. If they did occur, their magnitude must be small or else the tissue Ca^{2+} defect is repaired very quickly when aerobic respiration resumes during reperfusion.

The concept that massive Ca^{2+} entry is deleterious is strongly supported by in vivo studies on irreversible ischemic injury. Moreover, it seems very likely that uncontrolled calcium influx is the lethal event in both catecholamine poisoning and the calcium paradox. However, it is not established that Ca^{2+} entry is the proximate cause of lethality in in vivo ischemic injury. There is evidence that the modest rise in cytosolic $[Ca^{2+}]_i$ during nonlethal ischemic injury contributes to stunning by protease activation, which triggers selective proteolysis of cytoskeletal proteins [55,56]. Whether such a process might contribute to lethal injury is unknown, but there is no clear evidence of massive proteolysis of the cytoskeleton even with prolonged periods of ischemia. Failure of cell volume regulation could also be a primary mechanism of lethal ischemic injury, since osmotic swelling of myocytes subjected to prolonged anoxia can produce sarcolemmal disruption and since there is likely to be substantial cell swelling during early reperfusion of intact ischemic myocardium because of the hypertonicity of the ischemic myocytes at the start of reperfusion. Furthermore, even modest abnormalities in ionic composition could induce hypercontraction of myocytes when oxygen is first reintroduced into the ischemic/reperfused bed. These events could be as critical to the survival of marginal myocytes as an abrupt rise in $[Ca^{2+}]_i$.

SUMMARY

The changes in ion content and H_2O detectable in vivo in the intact canine heart in reversible and irreversible ischemic injury are described in this chapter, with emphasis on the role that Ca^{2+} movements may play in causing ischemic injury. Changes in extracellular ion concentrations and pH revealed by ion-specific electrodes in ischemia are reviewed, as are the contributions of NMR measurements of ionized Ca^{2+} to our understanding of Ca^{2+} ion homeostasis in ischemia.

During the reversible phase of ischemic injury in vivo, there is little evidence of significant failure of ion pumps. Nevertheless, substantial shifts in ions and water occur while the myocardium is ischemic. Moreover, after reperfusion with arterial blood, living reversibly injured myocytes exhibit altered volume regulation that

persists for minutes to hours. Increases in intracellular Ca^{2+} ion are in the μM range during the reversible phase and in the mM range during the irreversible phase of ischemic injury, at which time the so-called calcium overload is clearly present. It is not known whether the overload is an epiphenomenon or a primary cause of lethal injury in ischemia and reperfusion.

REFERENCES

1. Barry WH, Hasin Y, Smith TW. 1985. Sodium pump inhibition, enhanced calcium influx via sodium–calcium exchange, and positive inotropic response in cultured heart cells. Circ Res 56:231–241.
2. Barry WH, Smith TW. 1984. Movement of Ca^{2+} across the sarcolemma: effects of abrupt exposure to zero external Na concentration. J Mol Cell Cardiol 16:155–164.
3. Murphy E, Aiton JF, Horres R, Lieberman M. 1983. Calcium elevation in cultured heart cells: its role in cell injury. Am Physiol Soc 245:C316–C321.
4. Cala PM. 1980. Volume regulation by Amphiuma red blood cells. The membrane potential and its implications regarding the nature of the ion-flux pathways. J Gen Physiol 76:683–708.
5. Jennings RB, Steenbergen C Jr, Kinney RB, Hill ML, Reimer KA. 1983. Comparison of the effect of ischaemia and anoxia on the sarcolemma of the dog heart. Eur Heart J 4(Suppl):123–127.
6. Steenbergen C Jr, Murphy E, Levy L, London RE. 1987. Elevation in cytosolic free calcium concentration early in myocardial ischemia in perfused rat heart. Circ Res 60:700-707.
7. Steenbergen C Jr, Perlman ME, London RE, Murphy E. 1993. Mechanism of preconditioning. Ionic alterations. Circ Res 72:112–115.
8. Jennings RB, Reimer KA. 1979. Biology of experimental, acute myocardial ischaemia and infarction. In Hearse DJ, de Leiris J (eds), Enzymes in Cardiology: Diagnosis and Research. Great Britain/New York: John Wiley & Sons, pp. 21–57.
9. Menick FJ, White FC, Bloor CM. 1971. Coronary collateral circulation: determination of an anatomical anastomotic index of functional collateral flow capacity. Am Heart J 82:503–510.
10. Schaper W, Wusten B. 1979. Collateral circulation. In Schaper W (ed), Pathophysiology of Myocardial Perfusion. Amsterdam: Elsevier/North Holland Biomedical Press, pp. 415–470.
11. Jennings RB, Murry CE, Steenbergen C Jr, Reimer KA. 1990. Development of cell injury in sustained acute ischemia. Circulation 82(Suppl):II-2–II-12.
12. Jennings RB, Reimer KA, Steenbergen C Jr. 1986. Myocardial ischemia revisited. The osmolar load, membrane damage, and reperfusion (editorial). J Mol Cell Cardiol 18:769–780.
13. Jennings RB, Steenbergen C Jr. 1985. Nucleotide metabolism and cellular damage in myocardial ischemia. Annu Rev Physiol 47:727–749.
14. Jennings RB, Kaltenbach JP, Smetters GW. 1957. Enzymatic changes in acute myocardial ischemic injury. Arch Pathol Lab Med 64:10–16.
15. Hill JL, Gettes LS. 1980. Effect of acute coronary artery occlusion on local myocardial extracellular K^+ activity in swine. Circulation 61:768–778.
16. Jennings RB, Reimer KA. 1973. The fate of the ischemic myocardial cell. In Corday E, Swan HJC (eds), Myocardial Infarction. New Perspectives in Diagnosis and Management. Baltimore: Williams and Wilkins, pp. 13–24.
17. Jennings RB, Schaper J, Hill ML, Steenbergen C Jr, Reimer KA. 1985. Effect of reperfusion late in the phase of reversible ischemic injury. Changes in cell volume, electrolytes, metabolites, and ultrastructure. Circ Res 56:262–278.
18. Jennings RB, Reimer KA. 1992. Lethal reperfusion injury: fact or fancy? In Parratt JR (ed), Myocardial Response to Acute Injury. London: Macmillan Press, pp. 17–34.
19. Reimer KA, Jennings RB. 1982. Ion and water shifts, cellular. In Cowley RA, Trump BF (eds), Cellular Injury in Shock, Anoxia and Ishemia. Pathophysiology. Prevention and Treatment. Baltimore: Williams and Wilkins, pp. 132–147.
20. Jennings RB, Crout JR, Smetters GW. 1957. Studies on distribution and localization of potassium in early myocardial ischemic injury. Arch Pathol 63:586–592.
21. Jennings RB, Sommers HM, Kaltenbach JR, West JJ. 1964. Electrolyte alterations in acute myocardial ischemic injury. Circ Res 14:260–269.

22. Basuk WL, Reimer KA, Jennings RB. 1986. Effect of repetitive brief episodes of ischemia on cell volume, electrolytes and ultrastructure. J Am Coll Cardiol 8(Suppl):33A–41A.
23. Jennings RB, Ganote CE, Kloner RA, Whalen DA Jr, Hamilton DG. 1975. Explosive swelling of myocardial cells irreversibly injured by transient ischemia. In Fleckenstein F, Rona G (eds), Pathophysiology and Morphology of Myocardial Cell Alteration. Baltimore: University Park Press, pp. 405–413.
24. Jennings RB, Hawkins HK, Hill ML. 1977. Myocardial cell volume control in ischemic injury. In Lefer A, Kelliher G, Rovetto M (eds), Pathophysiology: Therapeutics of Myocardial Injury. New York: Spectrum Publications pp. 351–365.
25. Jennings RB, Shen AC. 1972. Calcium in experimental myocardial ischemia. In Bajusz E, Rona G (eds), Recent Advances in Studies on Cardiac Structure and Metabolism. Myocardiology. Baltimore: University Park Press, pp. 639–655.
26. Shen AC, Jennings RB. 1972. Myocardial calcium and magnesium in acute ischemic injury. Am J Pathol 67:417–440.
27. Shen AC, Jennings RB. 1972. Kinetics of calcium accumulation in acute myocardial ischemic injury. Am J Pathol 67:441–452.
28. Weiss J, Shine KI. 1982. Extracellular K^+ accumulation during myocardial ischemia in isolated rabbit heart. Am J Physiol 242:H619–H628.
29. Fleet WF, Johnson TA, Graebner CA, Gettes LS. 1985. Effect of serial brief ischemic episodes on extracellular K^+, pH, and activation in the pig. Circulation 72:922–932.
30. Pike MM, Luo CS, Clark MD, Kirk KA, Kitakaze M, Madden MC, Cragoe EJ, Pohost GM. 1993. NMR measurements of Na^+ and cellular energy in ischemic rat heart: role of Na^+–H^+ exchange. Am J Physiol 265:H2017–H2026.
31. Whalen DA Jr, Hamilton DG, Ganote CE, Jennings RB. 1974. Effect of a transient period of ischemia on myocardial cells. I. Effects on cell volume regulation. Am J Pathol 74:381–398.
32. Kloner RA, Ganote CE, Whalen D, Jennings RB. 1974. Effect of a transient period of ischemia on myocardial cells. II. Fine structure during the first few minutes of reflow. Am J Pathol 74:399–422.
33. Herdson PB, Sommers HM, Jennings RB. 1965. A comparative study of the fine structure of normal and ischemic dog myocardium with special reference to early changes following temporary occlusion of a coronary artery. Am J Pathol 46:367–386.
34. Lehninger AL. 1970. Mitochondria and calcium ion transport. Biochem J 119:129–138.
35. Kloner RA, Ganote CE, Jennings RB. 1974. The "no-reflow" phenomenon after temporary coronary occlusion in the dog. J Clin Invest 54:1496–1508.
36. Yellon DM, Jennings RB. 1991. Myocardial Protection: The Pathophysiology of Reperfusion and Reperfusion Injury. New York: Raven Press, pp. 1–214.
37. Fleckenstein A. 1971. Specific inhibitors and promotors of calcium action in the excitation contraction coupling of heart muscle and their role in the prevention or production of myocardial lesions. In Harris P, Opie L (eds), Calcium and the Heart. New York: Academic Press, pp. 135–189.
38. Fleckenstein A, Fleckenstein-Grun G. 1980. Cardiovascular protection by Ca antagonists. Eur Heart J 1(Suppl B):15–21.
39. Fleckenstein A, Janke J, Doring HJ, Leder O. 1975. Key role of Ca in the production of noncoronarogenic myocardial necroses. In Fleckenstein A, Rona G (eds), Recent Advances in Studies on Cardiac Structure and Metabolism. Baltimore: University Press, pp. 21–32.
40. Ganote CE, Nayler WG. 1985. Contracture and the Calcium Paradox (editorial review). J Mol Cell Cardiol 17:733–745.
41. Bolli R. 1990. Mechanism of myocardial "stunning." Circulation 82:723–738.
42. Murry CE, Richard VJ, Jennings RB, Reimer KA. 1991. Myocardial protection is lost before contractile function recovers from ischemic preconditioning. Am J Physiol (Heart Circ Physiol) 260 (29):H796–H804.
43. Murry CE, Richard VJ, Reimer KA, Jennings RB. 1990. Ischemic preconditioning slows energy metabolism and delays ultrastructural damage during sustained ischemia. Circ Res 66:913–931.
44. Swain JL, Sabina RL, Hines JJ, Greenfield JC Jr, Holmes EW. 1984. Repetitive episodes of brief ischemia (12 min) do not produce a cumulative depletion of high energy phosphate compounds. Cardiovasc Res 18:264–269.
45. Metcalfe JC, Hesketh TR, Smith GA. 1985. Free cytosolic Ca^+ measurements with fluorine labelled indicators using 19F NMR. Cell Calcium 6:183–195.
46. Pike MM, Frazer JC, Dedrick DF, Ingwall JS, Allen PD, Springer CS, Smith TW. 1985. 23Na and 39K nuclear magnetic resonance studies of perfused rat hearts. Biophys J 48:159–173.

47. Malloy CR, Buster DC, Margarida M, Castro CA, Geraldes CFGC, Jeffrey FMH, Sherry AD. 1990. Influence of global ischemia on intracellular sodium in the perfused rat heart. Magn Reson Med 15:33–44.
48. Steenbergen C, Murphy E, Levy L, London RE. 1987. Elevation in cytosolic free calcium concentration early in myocardial ischemia in perfused rat heart. Circ Res 60:700–707.
49. Marban E, Kitakaze M, Kusuoka H, Porterfield JK, Yue DT, Chacko VP. 1987. Intracellular free calcium concentration measured with 19F NMR spectroscopy in intact ferret hearts. Proc Natl Acad Sci USA 84:6005–6009.
50. London RE, Rhee CK, Murphy E, Gabel S, Levy LA. 1994. NMR-sensitive fluorinated and fluorescent intracellular calcium ion indicators with high dissociation constants. Am J Physiol 266:C1313–C1322.
51. Murphy E, Steenbergen C, Levy LA, Gabel S, London RE. 1994. Measurement of cytosolic free calcium in perfused rat heart using TF-BAPTA. Am J Physiol 266:C1323–C1329.
52. Chen W, Steenbergen C, Levy LA, Vance J, London RE, Murphy E. 1996. Measurement of free Ca^{2+} in sarcoplasmic reticulum in perfused rabbit heart loaded with 1,2-bis(2-amino-5,6-difluorophenoxy)ethane-N,N,N′,N′-tetraacetic acid by 19F NMR. J Biol Chem 271:7398–7403.
53. Murphy E, Perlman M, London RE, Steenbergen C. 1991. Amiloride delays the ischemia-induced rise in cytosolic free calcium. Circ Res 68:1250–1258.
54. Murphy E, Steenbergen C, Levy LA, Raju B, London RE. 1989. Cytosolic free magnesium levels in ischemic rat heart. J Biol Chem 264:5622–5627.
55. Westfall MV, Solaro RJ. 1992. Alterations in myofibrillar function and protein profiles after complete global ischemia in rat hearts. Circ Res 70:302–313.
56. Matsumura Y, Saeki E, Inoue M, Hori M, Kamada T, Kusuoka H. 1996. Inhomogeneous disappearance of myofilament-related cytoskeletal proteins in stunned myocardium of guinea pig. Circ Res 79:447–454.
57. Reimer KA, Jennings RB. 1992. Myocardial ischemia, hypoxia, and infarction. In Fozzard HA, Jennings RB, Haber E, Katz AM, Morgan HE (eds), The Heart and Cardiovascular System. New York: Raven Press, pp. 1875–1973.
58. Reimer KA, Hill ML, Jennings RB. 1981. Prolonged depletion of ATP and of the adenine nucleotide pool due to delayed resynthesis of adenine nucleotides following reversible myocardial ischemic injury in dogs. J Mol Cell Cardiol 13:229–239.

IONIC MECHANISMS OF REPERFUSION INJURY

MICHAEL J. SHATTOCK

The Rayne Institute, St. Thomas' Hospital

Summary. Contractile and electrical dysfunction seen during early reperfusion can be attributed, to a large extent, to disturbances in ion regulation. Ion regulation is influenced primarily by three major sequalae of reperfusion: 1) the slow recovery of ATP, 2) the thermodynamic redistribution of ions down their electrochemical gradients, and 3) the direct damage induced to ion translocating proteins by the oxidant stress that accompanies the early minutes of reperfusion. All these processes combine to create the unfavorable conditions in which E-C coupling is compromised, leading to stunning and arrhythmias. Disturbances in Na ion distribution may be particularly important, since all three of the above sequalae profoundly affect Na transport. Firstly, the depletion of ATP during ischemia not only may limit Na–K ATPase activity on reperfusion but also may cause the Na–K pump protein to translocate away from the surface membrane. This outcome is likely to limit the ability of the cell to extrude Na during the critical early moments of reperfusion. This inability to extrude Na is then compounded by an increased influx of Na via the Na–H exchanger that occurs as the second sequalae of reperfusion comes into effect—the thermodynamic redistribution of ions. Finally, oxidant stress can inhibit the activity of the remaining Na–K pump by selectively oxidizing key thiol groups on the protein molecule. These metabolic, thermodynamic, and "direct damage" effects of reperfusion thus combine to create Na and Ca overload, contractile dysfunction, and arrhythmias.

INTRODUCTION

Numerous studies have sought to investigate the mechanisms underlying, and possible therapeutic approaches to, ischemic injury in the heart. In the 1970s and 1980s, the concept of pharmacological infarct size reduction was investigated by

S. Mochizuki, N. Takeda, M. Nagano and N. Dhalla (eds.). THE ISCHEMIC HEART.

many laboratories, and many studies have suggested that ischemic injury can be prevented, and infarct size reduced, *in the absence of reflow*. It is now clear, however, that such interventions may delay, rather than prevent, the development of ischemic injury and that, if the myocardium within the area at risk of infarction is to permanently survive, blood flow must be restored. Although attention focused on the ischemic myocardium, little attention was paid to the possible deleterious consequences of reperfusion until the recent advent of safe and effective thrombolytic and angioplasty procedures. The development of these techniques, however, has necessitated a careful reassessment of the contribution of reperfusion per se to cellular damage following a transient ischemic episode.

One of the earliest indications that reperfusion itself can exacerbate tissue injury was the observation of electrical disturbances and ventricular arrhythmias immediately following reflow of an ischemic region of the dog heart [1]. In the 1970s, Hearse and colleagues demonstrated that the readmission of oxygen to the hypoxic heart can lead to membrane disruption and loss of cellular proteins [2–4]. In these studies, the cellular injury induced by reoxygenation was shown to be significantly greater than that which would have occurred if the hypoxia had been maintained, and this finding led to the concept of the *oxygen paradox*. The cellular damage on reoxygenation was shown to be proportional not only to the duration and severity of the preceding hypoxia but also to the pO_2 of the reperfusing medium [4]. Thus, it became clear that it is the readmission of oxygen per se, rather than the restitution of flow, that underlies reperfusion-induced injury. The central role of oxygen in mediating reperfusion-induced injury in the heart has focused attention on the possible role of oxygen-derived free radicals and oxidant stress in cellular damage during early reperfusion.

The literature concerning the ionic changes in ischemia and reperfusion is contradictory and confusing. To a large extent, this confusion has arisen as a consequence of two factors. Firstly, it is only within the last 10 years that it has been possible to measure intracellular ionic activities precisely (using ion-selective microelectrodes or fluorescent probes), and these techniques are inherently difficult to adapt for use in experimental models that are truly ischemic. The second source of confusion arises as a consequence of the first: the lack of a suitable model of ischemia has led many workers to resort to the use of hypoxia and/or metabolic blockade to mimic ischemia. It is increasingly apparent that such approaches, although useful in themselves, do not fully reflect the ischemic situation. For example, it is clear from a number of studies that cellular Ca handling is very different in hypoxia from that in ischemia [5].

IONIC CHANGES DURING ISCHEMIA

It is clear that the ion movements during early reperfusion will, to some extent, depend on the changes in ionic balance that occur in the preceding ischemic period. It is therefore useful to briefly review these changes. During ischemia, extracellular

potassium rises in a triphasic pattern such that, after 30 minutes, potassium levels in the interstitium can reach 25–30 mM [6,7]. Over this time, an intracellular acidification occurs that leads to a progressive extracellular acidification [8]. After approximately 10–15 minutes of zero-flow ischemia, the acidification of the extracellular space exceeds that inside the cell [9]. During ischemia, there is also a progressive rise in inorganic phosphate, and the combination of this and the fall in pH_i has been suggested to underlie the failure of contraction during early ischemia [10–12].

During ischemia, there is a progressive rise in intracellular Na such that, after 30 minutes, $[Na]_i$ can have risen to as high as 25 mM [13,14]. This rise in $[Na]_i$ dissipates the transmembrane Na gradient, which has a profound effect on a number of ion exchange processes that derive their energy from this gradient (such as the Na–Ca exchanger, Na–H exchanger, Na–HCO_3 cotransporter etc).

Allen and coworkers used the Ca-activated photoprotein aequorin to investigate the influence of hypoxia and glycolytic inhibition on intracellular Ca in isolated mammalian ventricular muscle [5,15]. In these studies, hypoxic contractures were induced with little or no associated rise in intracellular Ca, with resting free Ca only increasing slightly at the peak of the contracture. Similar observations have been made by others. Cobbold and Bourne, using aequorin-loaded isolated ventricular myocytes, showed a dissociation between the onset of anoxia-induced contracture and the rise in intracellular Ca [16]. An ion-selective microelectrode study has also demonstrated that after 20 minutes of hypoxia intracellular Ca was not increased despite a rise in $[Na]_i$ over the same time course [17]. The general consensus of the literature indicates that contractile failure and contracture in hypoxia, or metabolic inhibition, is not initiated by a rise in intracellular Ca [18]. This finding contrasts with the recent observations made in ischemic preparations using Ca-sensitive fluorescent probes. Allen et al. have recently reported a novel gas-perfused papillary muscle model of ischemia [19]. Using this approach, they demonstrated that "ischemia" is accompanied by a transient decrease in free Ca followed by a large increase. Similar results have recently been reported by Morgan and Kihara, who demonstrated an ischemia-induced rise in end-diastolic Ca to more than 1 μmole/L and an increase in the Ca transient in aequorin-loaded ferret ventricle. [20]

In 1987, Lee et al. described the use of the fluorescent Ca indicator Indo-1 AM to measure intracellular Ca in isolated perfused hearts [21]. In this study, ischemia produced a marked increase in both peak-systolic and end-diastolic Ca within 30 seconds that reached a plateau after 90 seconds. Lorell et al. have, however, recently demonstrated that Indo-1 loads preferentially into the endothelium and that a large fraction of the fluorescence signal is thus derived from nonmyocyte sources [22]. The problem is that in order for the dye to reach the myocytes, it must, by obligation, pass through the vascular endothelium. Once inside the endothelial cells, the majority of the dye is de-esterified and trapped, and hence little esterified dye passes through to the myocytes. This problem, and related problems with the use of NMR, have recently been discussed by Marban et al. [23].

IONIC CHANGES DURING EARLY REPERFUSION

The ionic disturbances associated with reperfusion can be broadly divided into three categories that can be termed *metabolic*, *thermodynamic*, and "*direct damage*".

Metabolic factors that influence ion movements during early reperfusion

ATP-dependent pumps

The Na–K pump is inhibited during prolonged ischemia due to depletion of ATP and the intracellular acidosis [24]. During reperfusion, the slow reactivation of oxidative phosphorylation and the associated slow recovery of ATP may limit the reactivation of the Na–K pump. Avkiran et al., using a histochemical method, have demonstrated that the recovery of the Na–K ATPase activity is gradual and remains incomplete even after four minutes of reperfusion [5]. The consequence of this slow recovery of Na–K pump function is that intracellular Na may remain elevated during the early phase of reperfusion. Van Echteld showed preischemic Na levels of 10.5 mM, a rise to 25 mM after 30 minutes of ischemia, and an incomplete recovery of Na on reperfusion to a sustained level of 15 mM [14].

While the Ca pump of the sarcolemma is also ATP dependent, its contribution to relaxation is small and therefore its inhibition is not likely to significantly slow relaxation during ATP depletion [26]. The CaATPase of the sarcoplasmic reticulum may be more significantly affected. Using the techniques of rapid rewarming after a period of rapid cooling, we have recently shown that Ca uptake into the SR is slowed in the stunned myocardium while Na–Ca exchange and the CaATPase of the sarcolemma remain unaffected [27]. Although this finding may reflect free radical-mediated damage to the pump protein, ATP depletion in the postischemic heart may contribute to limiting SR Ca uptake on reperfusion.

ATP-dependent changes in the interaction between the cytoskeleton and ion translocating proteins

In 1991, using a kidney cell line, Molitoris et al. demonstrated that ATP depletion following metabolic inhibition resulted in the translocation of the Na–K ATPase from the basolateral to the apical membrane [28]. In these studies, Molitoris et al. showed that the pump molecule is initially strongly associated with the cytoskeleton but that during ATP depletion the pump detaches from the cytoskeleton and is freely mobile in the membrane. Free of its cytoskeletal anchorage, the pump then appears to move around the cell membrane from the basolateral to the apical membranes [28]. We have investigated whether a similar detachment occurs in *hearts* subjected to ischemia and reperfusion. We have used immunohistochemistry and subcellular fractionation (measuring pump protein using immunoblotting, and protein activity using a conventional assay) to assess the distribution of the Na–K pump in rat myocardium during aerobic perfusion, ischemia, and reperfusion. Interestingly, we found that, under control conditions, in contrast to the situation in the kidney, in isolated rat hearts the Na–K pump protein is *not* associated with the cytoskeleton. During ischemia, however, the pump becomes more strongly associated with the cytoskeleton and, through fluorescence immunohistochemistry, can be

seen to translocate away from the surface membrane. From these studies it appears that the Na–K pump may be internalized in the heart during ischameia. On reperfusion, the pump returns to the surface membrane, but its relocalization appears to be patchy and incomplete. Identical results were obtained in cells subjected to metabolic inhibition with FCCP and deoxyglucose. Thus, in addition to ATP depletion limiting ATPase activity, it seems that ATP depletion can physically cause the translocation of the pump away from the surface membrane. This will result in less efficient Na extrusion from the cell during ischemia, and its incomplete recovery during reperfusion may contribute to the slow recovery of $[Na]_i$ measured in NMR studies [14]. The translocation of the pump away from the surface membrane may have additional consequences. If the enzymatic function of the translocated, internalized pump is still intact, then it may continue to consume ATP in a futile cycle. However, if the act of cytoskeletal attachment and internalization of the pump actually inhibits its enzymatic activity, then this act may represent a way in which the cell can minimize ATP consumption during ischemia.

Thermodynamic factors that influence ion movements during early reperfusion

The passive redistribution of ions down their electrochemical gradients may play an important role in reperfusion injury. Intracellular Na, elevated during ischemia [29,30] is likely to play a critical role during early reperfusion, and the concept that the Na–Ca exchange mechanism may initiate reperfusion-induced Ca overload is supported by a number of studies [13,14,31–34].

The role of the Na–H exchange in ischemia–reperfusion-induced ion movements has been described in detail by Lazdunski [35]. Lazdunski has proposed that, during ischemia, intracellular Na rises due to Na pump inhibition, intracellular acidosis inhibits Na–Ca exchange, and the associated extracellular acidosis limits Na–H exchange. On reperfusion, however, the extracellular acidosis is rapidly removed, revealing a large outward transsarcolemmal proton gradient. Na–H exchange is then activated with a resultant transient Na influx in exchange for intracellular protons, and this returns pH_i to normal. Lazdunski suggests that this Na influx causes the rise in Na on reperfusion reported by some authors [13], which in turn promotes cellular Ca overload via Na–Ca exchange. In support of this idea, the reperfusion-induced rise in Na can be prevented by the blocker of the Na–H exchanger amiloride [13], and transient acidotic reperfusion can prevent reperfusion-induced cellular Ca overload, myocardial stunning, and arrhythmias [25,36,37]. In contrast, using ^{23}Na-NMR, Van Echteld et al. showed preischemic Na levels of 10.5 mM, a rise to 25 mM after 30 minutes of ischemia, and no initial rise in intracellular Na on reperfusion but a rapid fall to a sustained level of 15 mM [14]. Poole-Wilson and Tones could not detect an increased efflux of Na on reoxygenation as might be expected if Na–Ca exchange moves Ca into the cell [32]. They suggest that this finding may be due to an associated increased influx of Na through the Na–H exchange mechanism that balances exactly with the increased efflux of Na via Na–Ca exchange [32]. It therefore seems likely that early in reperfusion the efflux of Na

through Na–Ca exchange may closely balance the influx of Na via Na–H exchange [32]. The observation that intracellular Na may transiently rise in some studies [13] but not in others [14] may reflect small changes in conditions that influence which of these exchange processes dominates in the early seconds of reperfusion. The net effect, however, is that on reperfusion Na–Ca exchange is dramatically but transiently stimulated to move Ca into the cell [13,38]. Interventions that alter the Na gradient can thus markedly influence cellular Ca uptake during reperfusion [33]. The mechanical, metabolic, and electrical recovery of reperfused or reoxygenated hearts has been shown to be inversely related to the intracellular Na concentration at the time of reoxygenation [24,34,39].

The washout of intracellular potassium may also play an important role in arrhythmogenesis. In an elegant series of studies, Curtis used a dual perfusion system to regionally elevate potassium in the vascular bed perfusing a region of an isolated rabbit heart [40,41]. Even in the absence of ischemia and reperfusion, regional washout of potassium induced ventricular arrhythmias. Regional washout of potassium is unlikely to induce any permanent injury, and the arrhythmias induced in this model are likely to reflect fully reversible regional changes in excitability and conduction velocity.

Direct damage to ion translocators and ion movements during early reperfusion

One of the most immediate and dramatic consequences of reperfusion following regional ischemia in many animal models is the induction of severe ventricular arrhythmias. Virtually immediately after the restitution of flow to the ischemic bed, the heart shows a burst of ventricular tachycardia that rapidly degenerates into fibrillation. Such reperfusion-induced arrhythmias are extremely reproducible and have been shown to occur with a peak incidence that temporally correlates with the peak in free radical production [42]. More direct evidence linking these two events is provided by studies examining the antiarrhythmic effects of free radical scavenging agents. In 1984, Woodward and Zakariah showed that allopurinol could prevent reperfusion arrhythmias in the isolated rat heart preparation [9]. Since then, many studies, including those of Bernier et al., have demonstrated that a wide variety of anti-free radical agents can reduce the susceptibility of the heart to reperfusion-induced arrhythmias [43].

Further evidence for the direct involvement of free radicals in disturbing the electrical and ionic homeostasis of the heart comes from a series of studies undertaken to investigate whether free radicals and oxidant stress, *in the absence of ischemia and reperfusion*, can cause arrhythmias. The production of radicals under experimental conditions by many enzyme-based generating systems is slow, and hence the onset of electrical changes measured in some studies has been correspondingly delayed. This finding has led some investigators to conclude that free radicals may not play an important role in the initiation of the very rapid electrical changes seen on reperfusion [44,45]. However, using the photoactivation of rose bengal, a very rapid and reproducible burst of oxidant stress can be induced. In aqueous solution, rose

bengal can be elevated to a triplet state by illumination with light of appropriate wavelength (500–600 nm) and, in the presence of oxygen, this triplet decays, producing singlet oxygen (75% of decays) and superoxide (20% of decays) [29]. In a series of studies using this technique, Hearse and colleagues have shown that a rapid burst of oxidant stress can produce changes in the epicardial ECG of rat hearts that develop within seconds and rapidly degenerate into ventricular arrhythmias [46,47].

The evidence implicating oxidant stress in reperfusion-induced arrhythmias in the heart can be considered to be threefold: 1) free radicals are produced during the early moments of reperfusion, 2) anti-free radical interventions are antiarrhythmic, and 3) free radical-generating systems, *in the absence of ischemia and reperfusion*, are arrhythmogenic.

Despite no evidence of permanent damage, hearts reperfused after short periods of reversible ischemia show prolonged contractile dysfunction [48]. This temporary decrease in contractile performance often persists for many hours or days and has been termed *myocardial stunning*. The immediate postischemic contractile performance of the heart following infarction is a major determinant of mortality [49] and may be important in determining the successful outcome of angioplasty or thrombolysis. A number of studies have shown that oxidant stress, in the early moments of reperfusion, may underlie myocardial stunning. Bolli et al. showed that MPG, a free radical scavenger and spin-trapping agent, administered one minute *before* reperfusion can significantly alleviate myocardial contractile depression in the reperfused dog heart [48]. Conversely, when MPG was given one minute *after* reperfusion, myocardial stunning was unaffected. In this study, the early administration of MPG was also shown to produce a parallel reduction in radical generation during reperfusion. This study elegantly demonstrates the role of free radicals and oxidant stress in myocardial stunning and indicates the rapidity of these effects. There appears, therefore, to be a critical "window," in the first minute of reperfusion, when these free radical-mediated events may be manipulated. The rapidity and brevity of this window suggests that the mechanism by which oxidant stress initiates the process of myocardial stunning, as for cardiac arrhythmias, must be fast-acting.

Cellular targets for free radicals and oxidant stress

While many biological molecules may be targets for oxidant stress and free radicals, it is clear that the cell membrane and its associated proteins may be particularly vulnerable. The ability of the cell to control its intracellular ionic environment as well as its ability to maintain a polarized membrane potential and electrical excitability depends on the activity of ion translocating proteins such as channels, pumps, and exchangers. Either direct or indirect disturbance of the activity of these ion translocators must ultimately underlie reperfusion and oxidant stress-induced arrhythmias in the heart. A number of studies have therefore investigated the effects of free radicals and oxidant stress on cellular electrophysiology and the activity of key membrane-bound ion translocating proteins.

Burton et al. used fluorescence techniques to demonstrate directly that free radical-generating systems elevate intracellular Ca in cardiac tissue [50]. Other evidence that intracellular Ca homeostasis is disturbed by oxidant stress was obtained in studies using isolated myocardial preparations and electrophysiological techniques [51–54]. In these studies, the appearance of after-contractions, after-depolarizations, and transient inward currents in cells exposed to oxidant stress suggests that the sarcoplasmic reticulum can be induced to release and reuptake calcium [52,54]. Studies of sarcoplasmic reticulum isolated from stunned myocardium show that intracellular calcium handling may be altered by the process of ischemia and reperfusion [30,55]. However, oscillatory calcium release can be induced in undamaged SR simply by loading the cell with calcium, and therefore, direct damage to the SR is not a prerequisite for abnormal intracellular Ca cycling.

We have investigated the effects of oxidant stress on isolated calcium release channels isolated from sheep heart SR and reconstituted into lipid bilayers [56]. In these studies, rose bengal-induced oxidant stress caused an increase in channel opening and eventually a irreversible loss of channel function. In addition, oxidant stress can inhibit SR CaATPase and hence can limit calcium reaccumulation into the SR [57]. However, even in the presence of caffeine, when SR function should be inhibited, cells still show evidence of profound cellular calcium overload [53]. This finding suggests that although the SR may contribute to the *expression* of cellular calcium overload, the primary event causing this overload may occur at the cell surface membrane. Thus, it seems likely that two factors may be important in mediating the effects of oxidant stress on SR function: first, a cellular calcium overload, mediated by changes in the calcium-regulating properties of the surface membrane, is in itself likely to cause spontaneous SR calcium release and arrhythmias; and second, SR calcium release [56] and reuptake [57] may be directly affected by oxidant stress.

Recent studies by Crompton et al. have shown that oxidant stress may open a Ca-sensitive nonselective pore in the inner mitochondrial membrane that is blocked by cyclosporin-A [58–62]. This pore opening results in massive mitochondrial swelling, dissipation of the transmembrane proton gradient, and disruption of mitochondrial energy production [60]. Since the mitochondria may play a role as a high-capacity cytosolic calcium buffer [26], disruption of mitochondrial function may also contribute to calcium overload and cell injury [58,61].

The importance of the Na–Ca exchange in mediating oxidant stress-induced cellular calcium overload has also been suggested by a number of studies [52,54,63–65]. Inward calcium transport by the exchanger may be facilitated by two important consequences of oxidant stress: 1) the prolongation of the action potential [53,54,66–68] and 2) intracellular sodium loading following increased sodium influx [64] and inhibition of the Na–K pump [69]. In addition to the Na–Ca exchange mechanism, the sarcolemma also contains a CaATPase that removes calcium from the cytosol. This calcium pump plays only a small role in the extrusion of calcium from the cell during normal activity [26,70]. However, Kaneko et al. have shown that the activity of the CaATPase may be inhibited, and thus the ability of the cell

to extrude calcium in the presence of a maintained oxidant stress may be further compromised [57].

The single most important ion translocator in the sarcolemma, the Na–K pump, appears to be particularly sensitive to oxidant stress and free radicals [69]. We have shown that oxidant stress can profoundly inhibit pump function, and this may contribute to cellular Ca overload and arrhythmias. In a recent series of studies, we have demonstrated that the Na–K pump can be reversibly inhibited by modifiers of protein sulphydryl groups [71–73]. It therefore seems likely that free radicals and oxidant stress may modulate protein function by promoting the formation of mixed disulphides (with free thiols such as intracellular glutathione) or the formation of irreversible disulphide bonds within the protein structure. Such protein S-H groups may therefore represent an important target for therapeutic interventions aimed at ischemia/reperfusion injury in the heart.

REFERENCES

1. Tennant R, Wiggers CJ. 1935. The effect of coronary occlusion on myocardial contraction. Am J Physiol 112:351–361.
2. Hearse DJ, Humphrey SM, Chain EB. 1973. Abrupt reoxygenation of the anoxic potassium arrested perfused rat heart: a study of myocardial enzyme release. J Mol Cell Cardiol 5:395–407.
3. Hearse DJ, Humphrey SM, Nayler WG, Slade A, Border D. 1975. Ultrastructural damage associated with reoxygenation of the anoxic myocardium. J Mol Cell Cardiol 7:315–324.
4. Hearse DJ, Humphrey SM, Bullock GR. 1978. The oxygen paradox and the calcium paradox: two facets of the same problem? J Mol Cell Cardiol 10:641–668.
5. Allen DG, Orchard CH. 1983. Intracellular calcium concentration during hypoxia and metabolic inhibition in mammalian ventricular muscle. J Physiol 339:107–122.
6. Kléber AG. 1983. Resting membrane potential, extracellular potassium activity, and intracellular sodium activity during acute global ischemia in isolated perfused guinea pig hearts. Circ Res 52:442–450.
7. Kléber AG. 1984. Extracellular potassium accumulation during acute myocardial ischaemia. J Mol Cell Cardiol 16:389–394.
8. Yan G-X, Kléber AG. 1992. Changes in extracellular and intracellular pH in ischemic rabbit papillary muscle. Circ Res 71(2):460–470.
9. Woodward B, Zakaria M. 1985. Effects of some free radical scavengers on reperfusion-induced arrhythmias in the isolated rat heart. J Mol Cell Cardiol 17:485–593.
10. Fabiato A, Fabiato F. 1978. Effects of pH on the myofilaments and the sarcoplasmic reticulum of skinned cells from cardiac and skeletal muscles. J Physiol 276:233–255.
11. Kentish JC. 1986. The Effects of inorganic phosphate and creatine phosphate on force production in skinned muscles from rat ventricle. J Physiol 370:585–604.
12. Orchard CH, Kentish JC. 1990. Effects of changes of pH on the contractile function of cardiac muscle. Am J Physiol 258:C967–C981.
13. Tani M, Neely JR. 1989. Role of intracellular Na^+ in Ca^{2+} overload and depressed recovery of ventricular function if reperfused ischemic rat heart. Possible involvement of H^+–Na^+ and Na^+–Ca^{2+} exchange. Circ Res 65:1045–1056.
14. Van Echteld CJA, Kirkels JH, Eijgelshoven MHJ, van der Meer P, Ruigrok TJC. 1991. Intracellular sodium during ischaemia and calcium-free perfusion: a ^{23}Na NMR study. J Mol Cell Cardiol 23:297–307.
15. Eisner DA, Allen DG, Orchard CH. 1985. Regulation of resting calcium concentration in cardiac muscle. In Parratt JR (ed), Control and Manipulation of Calcium Movement. London: Raven Press, pp. 65–86.
16. Cobbold PH, Bourne PK. 1984. Aequorin measurements of free calcium in single heart cells. Nature 312:444–446.
17. Guarnieri T. 1989. Direct measurement of $[Ca^{2+}]_i$ in early and late reperfused myocardium. Circulation 80(4, Suppl II):961.

18. Allen DG, Orchard CH. 1987. Myocardial contractile function during ischemia and hypoxia. Circ Res 60:153–168.
19. Allen DG, Lee JA, Smith GL. 1988. The consequences of simulated ischaemia on intracellular Ca^{2+} and tension in isolated ferret ventricular muscle. J Physiol 410:297–323.
20. Kihara Y, Grossman W, Morgan JP. 1989. Direct measurement of changes in intracellular calcium transients during hypoxia, ischemia, and reperfusion of the intact mammalian heart. Circ Res 65:1029–1044.
21. Lee H-C, Smith N, Mohabir R, Clusin WT. 1987. Cytosolic calcium transients from the beating mammalian heart. Proc Nat Acad Sci 84:7793–7797.
22. Lorell BH, Apstein CS, Cunningham MJ, Schoen FJ, Weinberg EO, Peeters GA, Barry WH. 1990. Contribution of endothelial cells to calcium-dependent fluoresence transients in rabbit hearts loaded with Indo 1. Circ Res 67:415–425.
23. Marban E, Kitikaze M, Koretsune Y, Yue DT, Chacko VP, Pike MM. 1990. Quantification of $[Ca^{2+}]_i$ in perfused hearts. Critical evaluation of the 5F-BAPTA and nuclear magnetic resonance method as applied to the study of ischemia and reperfusion. Circ Res 66:1255–1267.
24. Kim M-S, Akera T. 1987. O_2 free radicals: cause of ischemia–reperfusion damage to cardiac Na–K–ATPase. Am J Physiol 252:H252–H257.
25. Avkiran M, Ibuki C, Shimada Y, Haddock PS. 1996. Effects of acidic reperfusion on arrhythmias and Na(+)-K(+)-ATPase activity in regionally ischemic rat hearts. Am J Physiol 270:H957–H964.
26. Bers DM, Bassani JWM, Bassani RA. 1994. Competition and redistribution among calcium transport systems in rabbit cardiac myocytes. Cardiovasc Res 27:1772–1777.
27. Miller JIA, Shattock MJ. 1996. Impaired SR calcium uptake contributes to contractile dysfunction in stunned myocardium. J Mol Cell Cardiol 28(5):A85.
28. Molitoris A, Geerdes A, McIntosh JR. 1991. Dissociation and redistribution of Na^+,K^+–ATPase from its surface membrane actin cytoskeletal complex during cellular ATP depletion. J Clin Invest 88:462–469.
29. Lee PCC, Rodgers MAJ. 1987. Laser flash photokinetic studies of rose bengal sensitized photodynamic interactions of nucleotides and DNA. Photochem Photobiol 45:79–86.
30. Limbruno U, Zucchi R, Ronca-Testoni S, Galbani P, Ronca G, Mariani M. 1989. Sarcoplasmic reticulum function in the "stunned" myocardium. J Mol Cell Cardiol 21:1063–1072.
31. Grinwald PM. 1982. Calcium uptake during post-ischaemic reperfusion in the isolated rat heart. J Mol Cell Cardiol 14:359–365.
32. Poole-Wilson PA, Tones MA. 1988. Sodium exchange during hypoxia and on reoxygenation in the isolated rabbit heart. J Mol Cell Cardiol 20(Suppl II):15–22.
33. Poole-Wilson PA, Harding DP, Bourdillon PDV, Tones MA. 1984. Calcium out of control. J Mol Cell Cardiol 16:175–187.
34. Renlund DG, Gerstenblith G, Lakatta EG, Jacobus WE, Kallman CH, Weisfeldt ML. 1984. Reduction of myocardial post-ischemic injury without altering the ischaemic insult. J Mol Cell Cardiol 16:795–801.
35. Lazdunski M, Frelin C, Vigne P. 1985. The sodium/hydrogen exchange system in cardiac cells: its biochemical and pharmacological properties and its role in regulating internal concentrations of sodium and internal pH. J Mol Cell Cardiol 17:1029–1042.
36. Kitikaze M, Weisenfeldt ML, Marban E. 1986. Acidosis during reperfusion prevents myocardial stunning in ferret heart. Circulation 74:225.
37. Hori M, Kitakaze M, Sato H, Iwakura K, Gotoh K, Kusuoka H, Kitabatake A. 1989. Transient acidosis by staged reperfusion prevents myocardial stunning. Circulation 80(4, Suppl II):2381.
38. Shen AC, Jennings RB. 1972. Myocardial calcium and magnesium in acute ischaemic injury. Am J Pathol 67:416–440.
39. Neubauer S, Ingwall JS. 1989. Predicting ventricular fibrillation in hypoxic myocardium. Circulation 80(4, Suppl II):766.
40. Curtis MJ. 1991. The rabbit dual-perfusion model: a new method for assessing the pathological relevance of individual products of ischaemia and reperfusion: role of potassium in arrhythmogenesis. Cardiovasc Res 25:1010–1022.
41. Curtis MJ, Pugsley MK, Walker MJA. 1993. Endogeneous chemical mediators of ventricular arrythmias in ischaemic heart disease. Cardiovasc Res 27:703–719.
42. Manning AS, Hearse DJ. 1984. Reperfusion-induced arrhythmias: mechanisms and prevention. J Mol Cell Cardiol 16:497–517.
43. Bernier M, Hearse DJ, Manning AS. 1986. Reperfusion-induced arrhythmias and oxygen-derived free-radicals: studies with anti-free radical interventions and free radical generating system in the isolated perfused rat heart. Circ Res 58:331–340.

44. Coetzee WA, Opie LH. 1992. Effects of oxygen free radicals on isolated cardiac myocytes from guinea-pig ventricle: electrophysiological studies. J Mol Cell Cardiol 24:651–663.
45. Parratt JR, Wainwright CL. 1987. Failure of allopurinol and a spin trapping agent N-t-butyl-alpha-phenyl nitrone to modify significantly ischaemia and reperfusion-induced arrhythmias. Br J Pharmacol 91:49–59.
46. Hearse DJ, Kusama Y, Bernier M. 1989. Rapid electrophysiological changes leading to arrhythmias in the aerobic rat heart. Photosensitization studies with rose bengal-derived reactive oxygen intermediates. Circ Res 65:146–153.
47. Kusama Y, Bernier M, Hearse DJ. 1989. Singlet oxygen-induced arrhythmias. Dose and light response studies for photoactivation of rose bengal in the rat heart. Circulation 80:1432–1448.
48. Bolli R, Jeroudi MO, Patel BS, Aruoma OI, Halliwell B, Lai EK, McCay PB. 1989. Marked reduction of free radical generation and contractile dysfunction by antioxidant therapy begun at the time of reperfusion. Circ Res 65:607–622.
49. Pasternak RC, Braunwald E, Sobel BE. 1988. Acute Myocardial Infarction: Heart Disease. Philadelphia: WB Saunders.
50. Burton KP, Morris AC, Massey KD, Buja LM, Hagler HK. 1990. Free radicals alter ionic calcium levels and membrane phospholipids in cultured rat ventricular myocytes. J Mol Cell Cardiol 22:1035–1047.
51. Hayashi H, Miyata H, Watanabe H, Kobayashi A, Yamazaki N. 1989. Effects of hydrogen peroxide on action potentials and intracellular Ca^{2+} concentration of guinea pig heart. Cardiovasc Res 23:767–773.
52. Matsuura H, Shattock MJ. 1991. Membrane potential fluctuations and transient inward currents induced by reactive oxygen intermediates in isolated rabbit ventricular cells. Circ Res 68:319–329.
53. Shattock MJ, Matsuura H, Hearse DJ. 1991. Functional and electrophysiological effects of oxidant stress on isolated ventricular muscle: role for oscillatory calcium release from sarcoplasmic reticulum in arrhythmogenesis? Cardiovasc Res 25:645–651.
54. Shattock MJ, Hearse DJ, Matsuura H. 1990. Ionic currents underlying oxidant stress-induced arrhythmias. In Vereecke J, van Bogaert PP, Verdonck F (eds), Ionic Currents and Ischemia. Leuven: Leuven University Press, pp. 165–189.
55. Krause SM, Jacobus WE, Baker LC. 1989. Alterations in cardiac sarcoplasmic reticulum calcium transport in the post-ischemic "stunned" myocardium. Circ Res 65:526–530.
56. Holmberg SRM, Cumming DVE, Kusama Y, Hearse DJ, Poole-Wilson PA, Shattock MJ, Williams AJ. 1991. Reactive oxygen species modify the structure and function of the cardiac sarcoplasmic reticulum calcium release channel. Cardioscience 2:19–25.
57. Kaneko M, Beamish RE, Dhalla NS. 1989. Depression of heart sarcolemmal Ca-pump activity by oxygen free radicals. Am J Physiol 256:H368–H374.
58. Crompton M, Costi A. 1990. A heart mitochondrial Ca^{2+}-dependent pore of possible relevance to re-perfusion-induced injury. Biochem J 266:33–39.
59. Crompton M, Ellinger H, Costi A. 1988. Inhibition by cyclosporin A of a Ca^{2+} dependent pore in heart mitochondria activated by inorganic phosphate and oxidative stress. Biochem J 255:357–360.
60. Crompton M, McGuinness O, Nazareth W. 1992. The involvement of cyclosporin A binding proteins in regulating and uncoupling mitochondrial energy transduction. Biochim Biophys Acta 1101(2):214.
61. Crompton M. 1990. The role of Ca^{2+} in the function and dysfunction of heart mitochondria. In Langer GA (ed), Calcium and the Heart. New York: Raven Press, pp. 167–198.
62. McGuiness O, Yafei N, Costi A, Crompton M. 1990. The presence of two classes of high-affinity cyclosporin A binding sites in mitochondria. Eur J Biochem 194:671–679.
63. Beresewicz A, Horackova M. 1991. Alterations in electrical and contractile behavior of isolated cardiomyocytes by hydrogen peroxide: possible ionic mechanisms. J Mol Cell Cardiol 23:899–918.
64. Bhatnagar A, Srivastava SK, Szabo G. 1990. Oxidative stress alters specific membrane currents in isolated cardiac myocytes. Circ Res 67:535–549.
65. Matsuura H, Shattock MJ, Hearse DJ. 1991. Calcium overload induced by oxidant stress is dependent on an intact transarcolemmal sodium gradient. J Mol Cell Cardiol 23:S7.
66. Barrington PL. 1990. Effects of free radicals on the electrophysiological function of cardiac membranes. Free Rad Biol Med 9:355–365.
67. Barrington PL, Meier CF, Weglicki WB. 1988. Abnormal electrical activity induced by free radical generating systems in isolated cardiocytes. J Mol Cell Cardiol 20:1163–1178.
68. Tarr M, Valenzeno DP. 1989. Modification of cardiac action potential by photosensitizer-generated reactive oxygen. J Mol Cell Cardiol 21:539–543.

69. Shattock MJ, Matsuura H. 1993. Measurement of Na^+–K^+ pump current in isolated rabbit ventricular myocytes using the whole-cell voltage-clamp technique. Inhibition of the pump by oxidant stress. Circ Res 72:91–101.
70. Barry WH, Bridge JHB. 1993. Intracellular calcium homeostasis in cardiac myocytes. Circulation 87:1806–1815.
71. Haddock PS, Shattock MJ. 1993. Chemical oxidation of sulphydryl groups results in a depression of the Na^+–K^+ pump current in isolated adult guinea pig ventricular myocytes. J Physiol 473:182P.
72. Haddock PS, Shattock MJ, Hearse DJ. 1995. Modulation of cardiac Na^+–K^+ pump current: role of protein and nonprotein sulfhydryl redox status. Am J Physiol 38(1):H297–H319.
73. Shattock MJ, Haddock PS. 1994. Oxidant stress and the heart: modulation of ion transport mechanisms during ischaemia and reperfusion. In Winyard PG, Blake DR (eds), *Immunopharmacology of Free Radical Species*. London: Academic Press.

MECHANISM OF INHIBITION OF Na^+–H^+ EXCHANGER (NHE1) BY ATP DEPLETION: IMPLICATIONS FOR MYOCARDIAL ISCHEMIA

TOSHITARO IKEDA, SHIGEO WAKABAYASHI, and MUNEKAZU SHIGEKAWA

National Cardiovascular Center Research Institute

Summary. Na^+–H^+ exchange activity is metabolic energy dependent and may be inhibited when cell ATP level is reduced during myocardial ischemia. We found that ATP depletion inhibits activity of the cardiac isoform of the Na^+–H^+ exchanger (NHE1) by decreasing its apparent affinity for cytoplasmic H^+, but not its V_{max} value. By using a set of deletion mutants of the regulatory cytoplasmic domain of NHE1, we identified a 26-amino-acid-containing segment required to confer sensitivity to ATP depletion. This segment is localized within the most amino-terminal subdomain of the cytoplasmic domain that is critically important for the maintenance of high pH_i sensitivity of NHE1 under normal physiological conditions, as well as for upregulation of pH_i sensitivity induced by stimulation with growth factors.

INTRODUCTION

Intracellular acidosis occurs during myocardial ischemia. Elevation of cytoplasmic H^+ concentration induces a marked depression of cardiac contractility, which is due presumably to the inhibitory effects of H^+ on various cellular processes, including membrane excitation and activation of contractile proteins [1]. In cardiomyocytes, two mechanisms, i.e., the Na^+–H^+ exchanger and Na^+–HCO_3^- cotransporter, are responsible for extrusion of H^+ or its equivalent from the cytoplasm to recover from acidosis [2,3]. Whereas these two transporters were shown to contribute similarly to the H^+ extrusion in acid-loaded guinea pig ventricular myocytes, the Na^+–H^+ exchanger reportedly contributes more to the acid removal under the influence of the adrenergic hormone that is released abundantly in the ischemic heart [3–5]. A

S. Mochizuki, N. Takeda, M. Nagano and N. Dhalla (eds.). THE ISCHEMIC HEART.

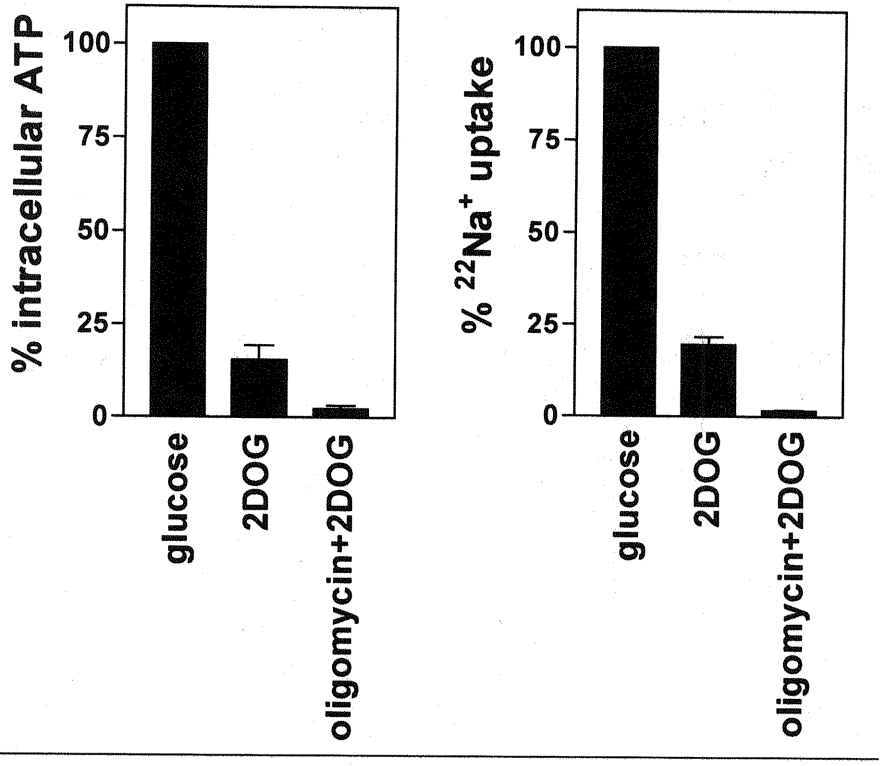

Figure 1. Effects of metabolic inhibitors on cell ATP level and EIPA-sensitive $^{22}Na^+$ uptake in cells expressing NHE1. Wild-type transfectants were preincubated for 30 minutes with either 5 mM glucose, 5 mM 2-deoxyglucose (DOG), or 5 mM DOG plus 2 μg/mL oligomycin.

larger contribution of the Na^+–H^+ exchanger in H^+ extrusion under ischemic conditions seems to be consistent with the well-documented finding that cardiomyocytes are effectively protected from the ischemia–reperfusion-associated sodium overload and cell injury by the Na^+–H^+ exchange inhibitors [6].

A family of mammalian Na^+–H^+ exchangers have recently been cloned [7]. The Na^+–H^+ exchanger isoform expressed in cardiomyocytes (NHE1) is one that is expressed in virtually all cell types and is highly sensitive to inhibition by amiloride and its analogues. The NHE1 molecule consists of two distinct functional domains, i.e., an N-terminal ion transport domain containing 10–12 membrane-spanning segments and a large carboxy-terminal cytoplasmic regulatory domain (see figure 6A for the molecular topology). NHE1 is a phosphorylatable and calmodulin-binding protein and is rapidly activated in response to various extracellular stimuli, including adrenergic hormone, various growth factors and Ca^{2+}-mobilizing vasoactive peptides, and hyperosmotic stress [7–11]. These stimuli enhance NHE1 activity by increasing its affinity for cytoplasmic H^+.

In ischemic myocardium, cellular ionic homeostasis becomes severely disturbed. Previous reports have indicated that Na^+–H^+ exchange activity is metabolic energy dependent and is inhibited when the cellular ATP level is reduced [12]. In this study, we investigated the mechanism by which ATP depletion causes the inhibition of activity of the cardiac isoform of the Na^+–H^+ exchanger.

MATERIALS AND METHODS

Construction of Na^+–H^+ exchanger mutants and their expression in cells

Plasmids carrying various carboxy-terminal truncation mutants and internal deletion mutants lacking aa 516–566 (Δ516–566) and aa 567–635 (Δ567–635) were constructed as described previously [13,14]. The exchanger-deficient PS120 cells (5×10^5 cells/100-mm dish) were transfected with each plasmid, and stable transfectants were maintained and selected as described [13,14].

Determination of $^{22}Na^+$ uptake activity and pH_i

We measured the intracellular pH (pH_i) dependence of 5-(*N*-ethyl-*N*-isopropyl)amiloride (EIPA)-sensitive $^{22}Na^+$ uptake in cells that were pH_i clamped by the K^+–nigericin method [14]. Serum-depleted cells in 24-well dishes were preincubated for 30 minutes at 37°C in Na^+-free choline chloride–KCl medium (20 mM Hepes/Tris [pH 7.4], 140 mM choline chloride–KCl, 2 mM $CaCl_2$, and 1 mM $MgCl_2$) containing 5 μM nigericin and either 5 mM glucose, 5 mM 2-deoxyglucose, or 5 mM 2-deoxyglucose plus 5 μg/mL oligomycin. The KC1 concentration in this medium was varied from 1 to 120 mM, while the total concentration of KC1 plus choline chloride was maintained at 140 mM. For some wells, the uptake medium additionally contained 0.1 mM EIPA. $^{22}Na^+$ uptake was started by adding the choline chloride–KC1 solution containing $^{22}NaCl$ (37 kBq/mL; final concentration, 1 mM), 1 mM ouabain, and 100 μM bumetanide. One minute later, cells were rapidly washed four times with ice-cold phosphate-buffered saline to terminate $^{22}Na^+$ uptake.

In some experiments, EIPA-sensitive $^{22}Na^+$ uptake was measured after cells had been acidified by an NH_4Cl prepulse technique as described [13]. Cells were loaded with NH_4Cl for 30 minutes at 37°C in NaCl standard solution (20 mM Hepes/Tris [pH 7.4], 120 mM NaCl, 5 mM KCl, 2 mM $CaCl_2$, 1 mM $MgCl_2$, and 5 mM glucose) containing 0–30 mM NH_4Cl. When cell ATP was depleted, NH_4^+ loading was performed for 30 minutes in choline chloride standard solution containing 0–50 mM NH_4Cl, 5 mM KCl, and either 5 mM 2-deoxyglucose or 5 mM 2-deoxyglucose plus 2 μg/mL oligomycin in order to avoid intracellular Na^+ accumulation caused by ATP depletion. After NH_4Cl loading, cells were rapidly washed once with choline chloride standard solution and then incubated in the same medium for 40 seconds. $^{22}Na^+$ uptake was started as described above and terminated 40 seconds later. Intracellular pH in cells prepulsed with NH_4Cl was measured by monitoring the distribution of [^{14}C]benzoic acid (74 kBq/mL) under the same

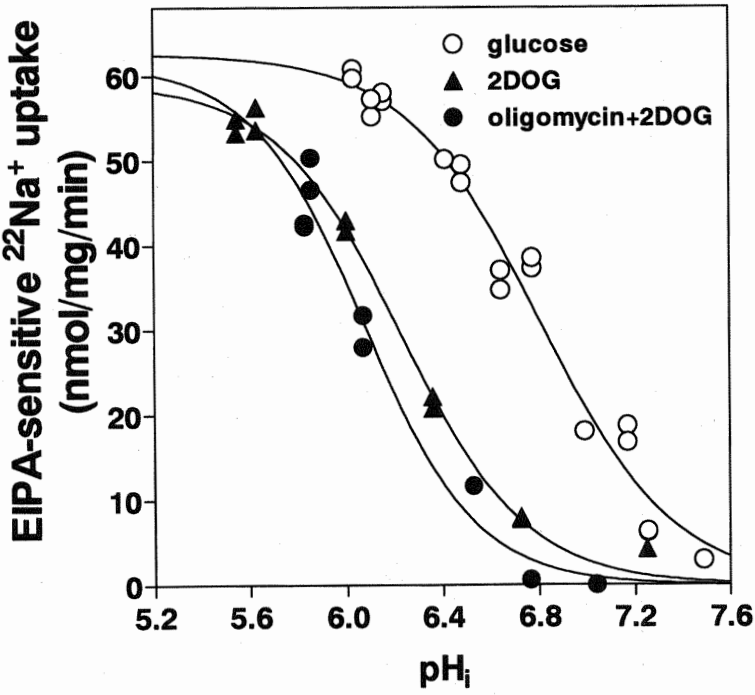

Figure 2. Effect of ATP depletion on pH_i dependence of EIPA-sensitive $^{22}Na^+$ uptake in the wild-type NHE1. Wild-type transfectants were treated as in figure 2 with either glucose, DOG, or DOG plus oligomycin. Then pH_i dependence of $^{22}Na^+$ uptake was measured by the NH_4^+-prepulse method.

conditions as those used for $^{22}Na^+$ uptake measurement, except that the uptake medium contained [^{14}C]benzoic acid and nonradioactive NaCl [13].

RESULTS AND DISCUSSION

The cardiac isoform of the Na^+–H^+ exchanger (NHE1) was expressed in the exchanger-deficient PS120 cells. In figure 1, changes in EIPA-sensitive $^{22}Na^+$ uptake and the ATP level were measured in cells treated for 30 minutes with either 5 mM 2-deoxyglucose or 5 mM 2-deoxyglucose plus 2 μg/mL oligomycin. These treatments reduced cell ATP to 15.3% ± 4.0% and 2.2 ± 1.0% (means ± SD, n = 3) of control, respectively. Reduction of cellular ATP was accompanied by inhibition of NHE1 activity, which is consistent with previous results obtained with other nontransfected cultured cells [12]. When EIPA-sensitive $^{22}Na^+$ uptake into cells treated with either 2-deoxyglucose or 2-deoxyglucose plus oligomycin was measured as a function of the cytoplasmic pH (pH_i), its pH_i dependence was markedly (>0.5 pH unit) shifted to an acidic side as compared to that for nontreated control cells, without any change in the V_{max} value (figure 2). Thus, ATP depletion inhibited NHE1 activity by decreasing its apparent affinity for cytoplasmic H^+, but

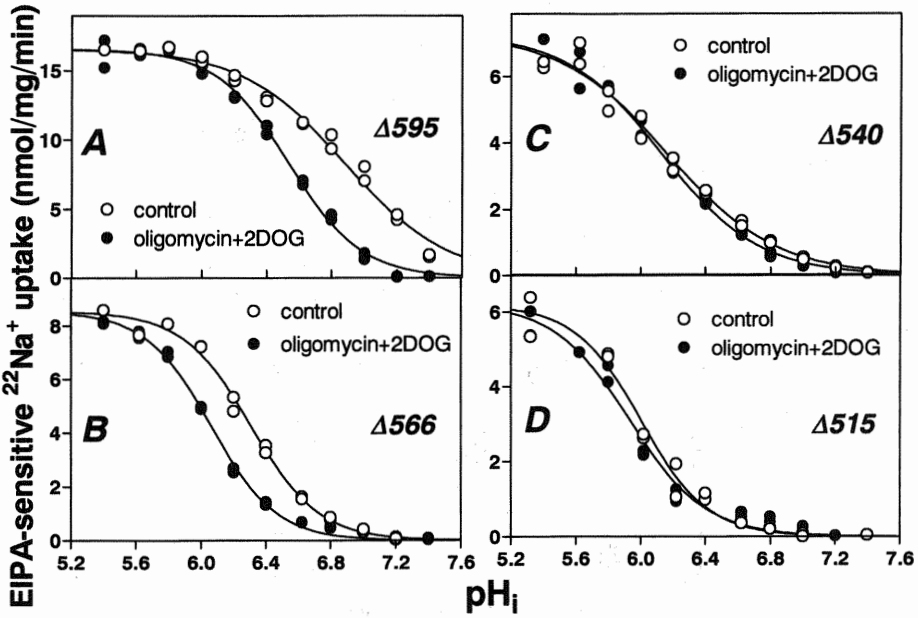

Figure 3. Effect of ATP depletion on pH_i dependence of EIPA-sensitive $^{22}Na^+$ uptake in various deletion mutant transfectants. EIPA-sensitive $^{22}Na^+$ uptake into cells transfected with indicated NHE1 variants were measured under control (○) and ATP depletion (●) conditions by the K^+–nigericin pH-clamped method.

not its V_{max} value. A very similar large acidic shift of pH_i dependence of NHE1 activity was observed, when the entire cytoplasmic domain of NHE1 was truncated (compare pH_i dependences of EIPA-sensitive $^{22}Na^+$ uptake in wild-type and mutant Δ515 transfectants in figure 5). We thus hypothesize that the cytoplasmic domain is required for the maintenance of high pH_i sensitivity of NHE1 and that ATP depletion induces a pK shift in NHE1 through a structural derangement of the cytoplasmic domain in a manner mimicked by complete deletion of this domain.

We determined which segment of the cytoplasmic domain is responsible for the observed inhibition by ATP depletion. In the experiment shown in figure 3, we compared pH_i dependencies of EIPA-sensitive $^{22}Na^+$ uptake in mutants with various carboxy-terminal truncations of the cytoplasmic domain in the presence and absence of the 2-deoxyglucose plus oligomycin-induced ATP depletion. When the cytoplasmic tail (aa 595–815) was truncated (Δ595), the ATP depletion induced an acidic shift of pH_i dependence without a change in V_{max}, as in the wild-type NHE1 (figure 3A). Upon further truncation to aa 567 (Δ566), the sensitivity to ATP depletion was still retained (figure 3B). However, the ATP sensitivity disappeared completely in mutant Δ540 in which 26 amino acids were truncated from Δ566 (figure 3C) or when the remaining cytoplasmic domain was totally removed (Δ515) (figure 3D). The data were consistent with the finding that internal deletion mutant Δ567–635

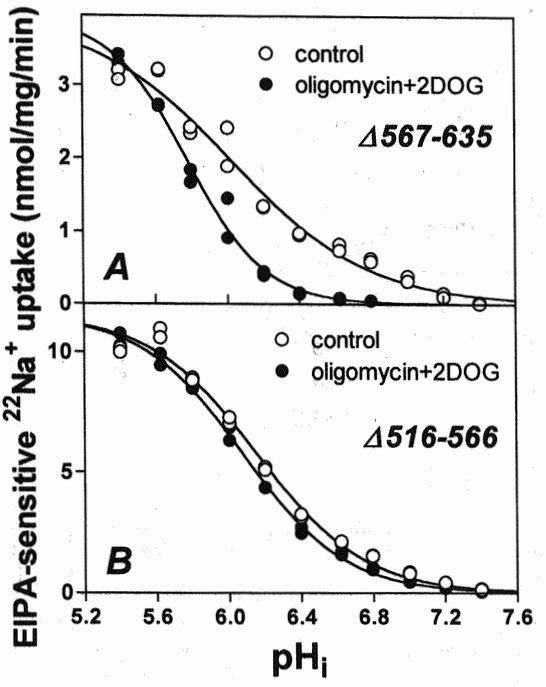

Figure 4. Effect of ATP depletion on pH_i dependences of EIPA-sensitive $^{22}Na^+$ uptake in internal deletion mutant transfectants. EIPA-sensitive $^{22}Na^+$ uptake into cells transfected with indicated internal deletion mutants were measured under control (○) and ATP depletion (●) conditions by the K^+–nigericin pH-clamped method.

containing these 26 amino acids retained the sensitivity to ATP depletion, whereas internal deletion mutant Δ515–566 lacking them were insensitive to ATP depletion (figure 4A and 4B). Thus, a specific sequence within aa 540–566 is required to confer ATP sensitivity to NHE1.

As mentioned above, truncation of the cytoplasmic domain markedly changed the pH_i dependence of NHE1 activity even under metabolically normal conditions. Figure 5 shows the result of an experiment measuring the effect of successive carboxy-terminal truncation of the cytoplasmic domain on NHE1 activity in the absence of ATP depletion. Although truncation of aa 660–815 (subdomain IV in figure 6) did not exert a significant effect on the pH_i sensitivity of NHE1, further truncation of aa 636–659 (Δ635) induced an alkaline shift of the pH_i dependence. This 24-amino-acid segment (subdomain III in figure 6) was characterized previously to be a CaM-binding domain that has an autoinhibitory function against the pH_i dependence of NHE1 [10,11]. On the other hand, aa 596–635 (subdomain II in figure 6) was apparently silent for the pH_i sensitivity (figure 5). Further truncation of aa 516–595 (subdomain I in figure 6), producing mutant Δ515 lacking the entire cytoplasmic domain, resulted in a remarkable acidic shift of pH_i dependence (figure

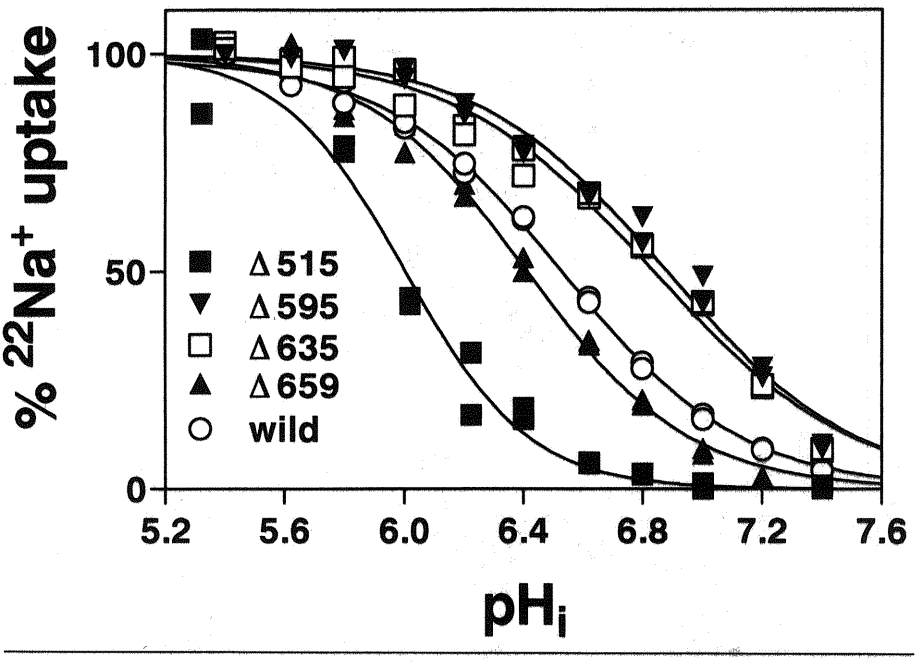

Figure 5. pH_i-dependences of EIPA-sensitive $^{22}Na^+$ uptake in various deletion mutant transfectants in the absence of ATP depletion. EIPA-sensitive $^{22}Na^+$ uptake into cells transfected with indicated NHE1 variants were measured under normal control conditions by the K^+–nigericin pH-clamped method. Data are represented as the $^{22}Na^+$ uptake activity normalized by the V_{max} value.

5), indicating that subdomain I is required for the maintenance of high pH_i sensitivity of NHE1. The cytoplasmic domain of NHE1 is therefore grouped into at least four subdomains in terms of pH_i sensitivity in the absence of ATP depletion (figure 6B).

It is important to note that the pH_i sensitivity (affinity for cytoplasmic H^+) of the wild-type NHE1 in ATP-depleted cells was very low and almost equivalent to that of Δ515, a mutant depleted of subdomain I. We found that the segment of cytoplasmic domain that confers sensitivity to ATP depletion was localized in subdomain I (figures 3 and 4). In our previous study, it was suggested that activation of NHE1 in response to growth factors is mediated via two different regions of the cytoplasmic domain, one being subdomain III involved in Ca^{2+}/CaM-dependent, rapid activation of NHE1 and the other being aa 567–635 involved in the slow and long-lasting activation induced by growth factors [10,11,13]. Since the latter alkalinization by thrombin still occurs in cells expressing mutant Δ595 (Wakabayashi et al., unpublished), aa 566–595 in subdomain I seems to be critical for this effect of growth factors. Available evidence suggests that such an effect of thrombin is mediated via a phohosphorylatable cytosolic factor(s) [9,13]. Thus, the latter may interact with this portion of subdomain I.

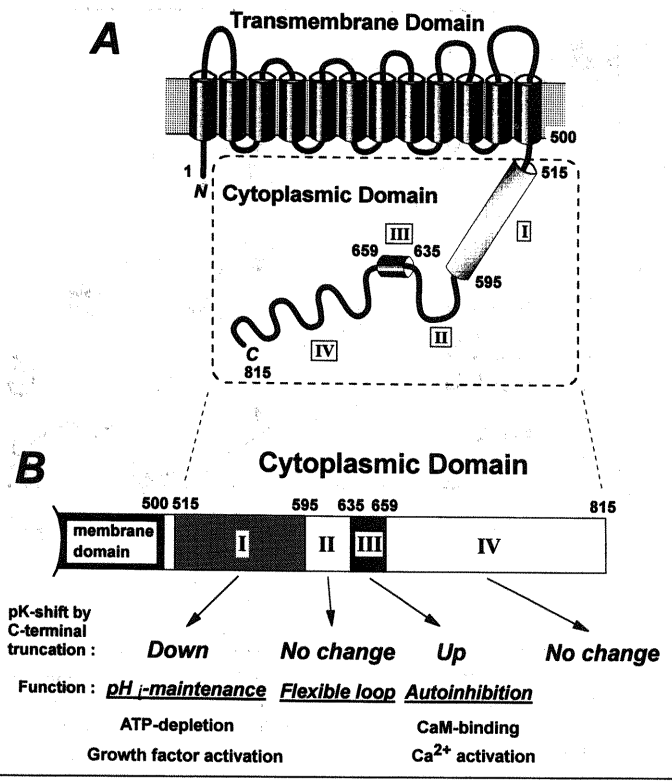

Figure 6. Molecular topology of NHE1 (**A**) and schematic representation of cytoplasmic subdomains (**B**). Observed changes in pH_i sensitivity caused by carboxy-terminal truncation of these subdomains and their proposed functions are shown in the figure.

All these results suggest that subdomain I is critically important for the maintenance of high pH_i sensitivity of NHE1 under normal physiological conditions, as well as upregulation or downregulation of pH_i sensitivity induced by cell ATP depletion and stimulation with growth factors. The pH_i sensitivity of NHE1 is generally thought to be regulated through a change in proton affinity of the H^+-modifier site ("pH-sensor") that is distinct from the H^+-transport site [7]. A change in proton affinity presumably occurs via mechanism(s) involving direct or indirect interactions of the H^+-modifier site with different regions of the cytoplasmic domain, as previously postulated for the activation of NHE1 activity by the CaM-binding autoinhibitory subdomain III [10,11]. However, the relationship between subdomain I and the H^+-modifier site is currently unclear, because the location of the modifier site in the NHE1 molecule is unknown.

It may be that subdomain I has a stimulatory function on the H^+-modifier site, increasing its proton affinity, and that ATP depletion blunts such interaction. The

underlying mechanism for the observd effect of ATP depletion is unclear, although dephosphorylation of the NHE1 protein does not appear to be involved [13,15]. Besides protein dephosphorylation, cell ATP depletion would cause other cellular changes such as reorganization of the cell cytoskeleton, activation of stress-sensitive cellular reactions, and intracellular acidosis. The present finding that a short specific segment of subdomain I is required to confer the ATP sensitivity suggests that a specific unidentified factor interacting with this segment could be involved in the ATP depletion-induced inhibition of NHE1.

REFERENCES

1. Orchard CH, Kentish JC. 1990. Effects of changes in pH on the contractile function of cardiac muscle. Am J Physiol 258:C967–C981.
2. Lazdunsky M, Frelin C, Vigne P. 1985. The sodium/hydrogen exchange system in cardiac cells: its biochemical and pharmacological properties and its role in regulating internal concentrations of sodium and internal pH. J Mol Cell Cardiol 17:1029–1042.
3. Lagadic-Gossmann D, Buckler KJ, Vaughan-Jones RD. 1992. Role of bicarbonate in pH recovery from intracellular acidosis in the guinea-pig ventricular myocytes. J Physiol (Lond) 458:361–384.
4. Lagadic-Gossmann D, Vaughan-Jones RD, Buckler KJ. 1992. Adrenaline and extracellular ATP switch between two modes of acid extrusion in the guinea-pig ventricular myocyte. J Physiol (Lond) 458:385–407.
5. Schömig A, Kurtz T, Richardt G, Schömig E. 1990. The role of catecholamines in ischemia. J Cardiovasc Pharmacol 16:S105–S112.
6. Scholtz W, Albus U. 1995. Potential of selective sodium-hydrogen exchange inhibitors in cardiovascular therapy. Cardiovasc Res 29:184–188.
7. Wakabayashi S, Shigekawa M, Pouyssegur J. 1997. Molecular physiology of vertebrate Na^+/H^+ exchanger. Physiol Rev 77:51–74.
8. Grinstein S, Rotin D, Mason MJ. 1989. Na^+/H^+ exchange and growth factor-induced cytosolic pH changes. Role in cellular proliferation. Biochem Biophys Acta 988:73–97.
9. Sardet C, Counillon L, Franchi A, Pouysségur J. 1990. Growth factors induce phosphorylation of the Na^+/H^+ antiporter, a glycoprotein of 110 kD. Science 247:723–726.
10. Bertrand B, Wakabayashi S, Ikeda T, Pouysségur J, Shigekawa M. 1994. The Na^+/H^+ exchanger isoform 1 (NHE1) is a novel member of the calmodulin-binding proteins. J Biol Chem 269:13703–13709.
11. Wakabayashi S, Bertrand B, Ikeda T, Pouysségur J, Shigekawa M. 1994. Mutation of calmodulin-binding site renders the Na^+/H^+ Exchanger (NHE1) highly H^+-sensitive and Ca^{2+} regulation-defective. J Biol Chem 269:13710–13715.
12. Cassel D, Katz M, Rotman M. 1986. Depletion of cellular ATP inhibits Na^+/H^+ antiport in cultured human cells. Modulation of the regulatory effect of intracellular protons on the antiport activity. J Biol Chem 261:5460–5466.
13. Wakabayashi S, Bertrand B, Shigekawa M, Fafournoux P, Pouysségur J. 1994. Growth factor activation and "H^+-sensing" of the Na^+/H^+ exchanger isoform 1 (NHE1). Evidence for an additional mechanism not requiring direct phosphorylation. J Biol Chem 269:5583–5588.
14. Ikeda T, Schmitt B, Pouysségur J, Wakabayashi S, Shigekawa M. 1997. Identification of cytoplasmic subdomains that control pH-sensing of the Na^+/H^+ exchanger (NHE1): pH-maintenance, ATP-sensitive, and flexible loop domains. J Biochem (Tokyo) 121:295–303.
15. Goss GG, Woodside M, Wakabayashi S, Pouysségur J, Waddell T, Downey GP, Grinstein S. 1994. ATP dependence of NHE-1, the ubiquitous isoform of the Na^+/H^+ antiporter. Analysis of phosphorylation and subcellular localization. J Biol Chem 269:8741–8748.

This Page Intentionally Left Blank

THE SOURCE AND FATE OF PROTONS IN THE REPERFUSED ISCHEMIC HEART

GARY D. LOPASCHUK and ALEXANDER S. CLANACHAN

Cardiovascular Disease Research Group, University of Alberta

Summary. *Metabolic modulation* (i.e., optimizing the energy substrate preference by the heart during and following ischemia) is an exciting new approach to treating ischemic heart disease. However, the relationship between glucose metabolism and alterations in proton production and clearance during and following ischemia remains poorly understood. It is clear, however, that the recovery of mechanical function and cardiac efficiency in the reperfused postischemic heart is influenced by both the source and fate of protons. Inhibition of the *source* of protons during ischemia and/or reperfusion by improving the coupling between glycolysis and glucose oxidation will increase the rate of recovery of pH_i and improve recovery of mechanical function and efficiency. Modulation of the *fate* of protons will also affect pH_i, but the consequences on function and efficiency will depend on the specific pathway by which the protons are cleared.

INTRODUCTION

Myocardial ischemia impairs contractility and, if prolonged, leads to myocardial infarction. Early restoration of blood flow, termed *reperfusion*, is the most effective strategy to minimize the adverse consequences of ischemia. Reperfusion is a common clinical event occurring during cardiac surgery, angioplasty, and thrombolytic therapy. Unfortunately, reperfusion, even in the absence of irreversible cell injury, does not always result in immediate and complete recovery of contractile function. An understanding of the mechanisms underlying the injury associated with ischemia–reperfusion is essential if new therapies are to be developed.

A critical component of ischemia–reperfusion injury is the accumulation of protons intracellularly that leads to a decrease in intracellular pH (pH_i). Numerous

S. Mochizuki, N. Takeda, M. Nagano and N. Dhalla (eds.). THE ISCHEMIC HEART.

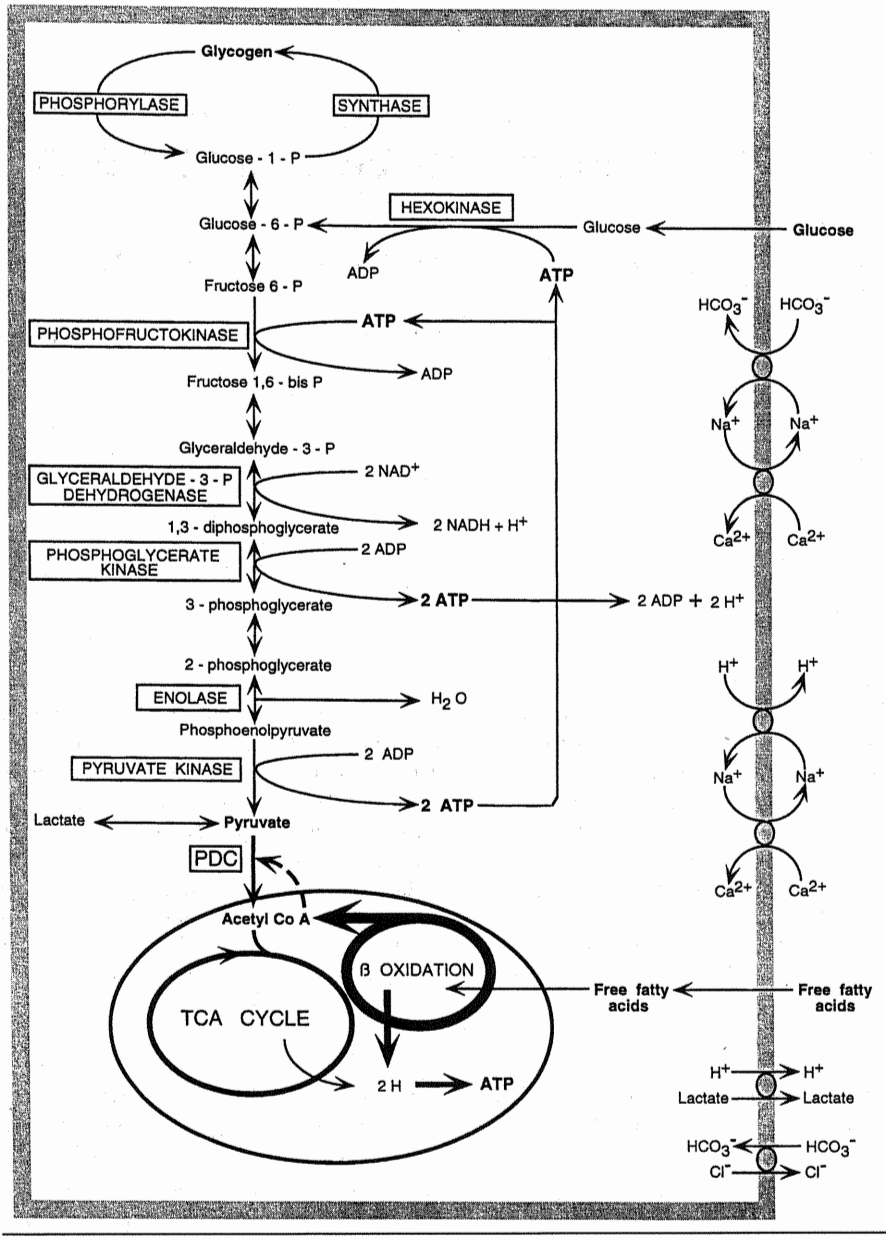

Figure 1. Overview of glucose metabolism in the heart, and how protons are produced and cleared by the heart.

PRODUCTION OF H^+ FROM GLUCOSE METABOLISM

Hydrolysis of ATP derived from glucose:

1. glycolysis + aerobic disposal of pyruvate

$$\text{glucose} \rightarrow 6\ CO_2 + 6\ H_2O$$

2. glycolysis + **no** aerobic disposal of pyruvate

$$\text{glucose} \rightarrow 2\ \text{lactate}^- + 2\ H^+$$

Proton production = 2 x (glycolysis - glucose oxidation)

Proton production:
lessened by inhibition of glycolysis
lessened by stimulation of glucose oxidation

increased by inhibition of glucose oxidation
increased by stimulation of glycolysis

Figure 2. Production of H^+ from glucose metabolism.

studies have shown that an important fate of these protons is clearance by the Na^+–H^+ exchanger, which leads to Na^+ accumulation within the myocyte. Activation of the Na^+–Ca^{2+} exchanger by this high intracellular Na^+ can provoke entry of Ca^{2+}, with all the associated adverse consequences of Ca^{2+} overload.

A considerable research effort has addressed the fate of protons, particularly the pathways by which they are cleared during and following ischemia [1–14]. However, much less attention has been directed at the sources of proton production, particularly proton production during the actual reperfusion period following ischemia. Our previous studies have shown that glucose metabolism is a potential source of proton production during reperfusion [15–23]. During most clinical conditions of reperfusion following ischemia, the heart is exposed to fatty acid levels that are 5–6-fold higher than normal [24,25]. A consequence of this exposure is that rates of glucose oxidation are markedly inhibited, resulting in a significant production of protons due to an uncoupling of glycolysis from glucose oxidation (see figures 1, 2, and 3). We have also shown that overcoming fatty acid inhibition of glucose oxidation during reperfusion, or directly improving the coupling of glycolysis to glucose oxidation, decreases proton production and improves the recovery of mechanical function postischemia [15,17,19–23]. However, the relationship between proton production from glucose metabolism and the actual recovery of pH_i following ischemia has not been established.

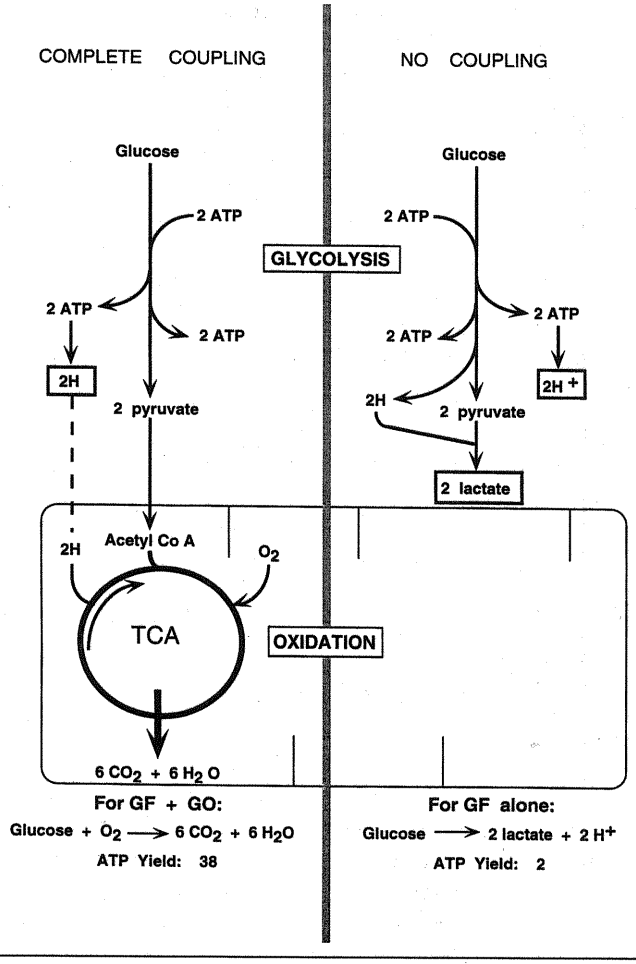

Figure 3. Glycolysis coupled to glucose oxidation and uncoupled from glucose oxidation in the heart.

MYOCARDIAL ISCHEMIA

The pathology of myocardial ischemia is complex and remains to be completely characterized. The mechanisms involved in myocardial injury during reperfusion are also not completely understood, and a considerable research effort has gone into trying to understand these processes. Novel areas of investigation such as preconditioning, apoptosis, NO biochemistry, and oxidative stress have all contributed to our understanding of the sequelae involved in cell injury during ischemia. Although the relative contribution of any particular process to cell injury during and following ischemia has not been unequivocally determined, it is clear that acidosis and Ca^{2+} accumulation are two important contributing factors to myocyte injury. Another

factor that is important to recovery of mechanical function reperfusion is the energy substrates used by the heart. As discussed below, a complex relationship exists between energy substrate metabolism and acidosis in the ischemic and reperfused ischemic heart.

ENERGY SUBSTRATE METABOLISM

Aerobic metabolism

Myocardial ATP production under normal aerobic conditions arises predominantly from the mitochondrial oxidation of acetyl CoA, derived from carbohydrates (primarily glucose and lactate), free fatty acids, and to a lesser extent ketone bodies and amino acids (see figure 1 and reviews [18,26,27,28]). The major source of intramitochondrial acetyl CoA arises from the β-oxidation of fatty acids.

The other main energy substrate, glucose, passes through glycolysis to form pyruvate [26]. Glycolysis produces only 2 moles of ATP per mole of glucose, so its contribution to total myocardial ATP supply is very low (less than 10%). However, glycolysis assumes greater importance during ischemia as ATP is produced without the consumption of oxygen (see below). The pyruvate dehydrogenase (PDH) complex (PDC) is a key rate-limiting enzyme in the oxidation of glucose, and its activity is under phosphorylation control [29]. Pyruvate produced by glycolysis is either converted to acetyl CoA (oxidative metabolism) or is converted to lactate and released from the heart.

Ischemic conditions

During ischemia, when the supply of O_2 becomes limiting for oxidative phosphorylation, both fatty acid and carbohydrate oxidation decrease and ATP production is impaired. Glycolysis and glycogenolysis initially increase in an attempt to compensate for this decrease in ATP supply. Anaerobic glycolysis, while potentially beneficial due to its ability to generate ATP in the absence of O_2, may also be detrimental. During mild ischemia, glycolytic ATP production benefits the heart [30]. However, during severe ischemia, the benefits of glycolytic ATP production are overshadowed by the accumulation within the myocardial cell of glycolytic by-products, particularly H^+ and lactate (figures 1 and 2) [1,31]. While considerable debate has focused on the potential benefits or harm associated with glycolysis uncoupled from glucose oxidation during ischemia, relatively little attention has been paid to the importance of this coupling during the critical period of reperfusion.

Aerobic reperfusion following ischemia

During reperfusion following ischemia, a rapid recovery of mitochondrial oxidative phosphorylation must occur for contractile function to recovery. It has been suggested that a delay in recovery contributes to the impairment in postischemic function (stunning) by limiting the supply of ATP for mechanical activity [32]. However, we recently assessed overall TCA cycle activity during early recovery and found that the relationship between myocardial O_2 consumption (MVO_2) and TCA

cycle activity recovers rapidly with reperfusion, but the relationship between TCA cycle activity and left ventricular (LV) work is impaired [17,21]. This finding suggests that the reduction in cardiac efficiency during reperfusion is due to an alteration in energy utilization rather than in energy production. We showed that the preferential oxidation of fatty acids, as opposed to glucose, is an important contributor to this decreased efficiency [33–37].

During reperfusion, fatty acid oxidation is the predominant source of ATP production, providing 95% to 100% of the heart's energy requirements. High fatty acid oxidation rates during reperfusion are partly due to elevated plasma concentrations of fatty acids known to occur following acute myocardial infarction or cardiac bypass surgery [24,25]—mediated, in part, by catecholamine-induced stimulation of lipolysis—as well to the use of heparin both during surgery and after acute myocardial infarction. These high levels of fatty acids (1–2 mM) are associated with an increased incidence of complications associated with the infarction [25], and numerous experimental studies have also shown that high levels of fatty acids contribute to ischemic injury [28,33,35,38,39,40]. We have demonstrated that high levels of fatty acids also have deleterious effects during the actual period of reperfusion following ischemia [18,33,37,40].

Fatty acid oxidation rates during reperfusion of ischemic hearts are also high due to a "dysregulation" of this pathway [45]. Our Laboratory group has been investigating the molecular mechanisms that control fatty acid oxidation. We demonstrated that malonyl CoA, a potent inhibitor of carnitine palmitoyltransferase (CPT) 1 [41], is a key factor regulating changes in fatty acid oxidation in the postischemic heart [42–46]. This change occurs due to a decrease in malonyl CoA production by acetyl CoA carboxylase (ACC) [45,46]. During reperfusion of hearts following a severe episode of ischemia, a decreased production of malonyl CoA by ACC is seen, resulting in an acceleration of fatty acid oxidation [45]. The rapid change in ACC activity is due to its phosphorylation and inhibition by a novel AMP-activated protein kinase (AMPK) [45,46]. This kinase is allosterically activated by 5′AMP during and following myocardial ischemia [47]. We propose that activation of AMPK is a key determinant of the high rate of fatly acid oxidation in the postischemic heart.

The main consequence of high fatty acid oxidation rates is that glucose oxidation is low during reperfusion [33,37]. These low rates of glucose oxidation, relative to rates of glycolysis, contribute to the poor cardiac efficiency during reperfusion, secondary to the production of protons when the heart is already clearing protons produced during ischemia.

GLUCOSE METABOLISM AND PROTON PRODUCTION

When glucose (from exogenous or endogenous sources) is metabolized by glycolysis followed by oxidation, with the associated synthesis and hydrolysis of ATP, the net production of protons is zero. However, if glycolysis is uncoupled from glucose oxidation (as in the presence of high fatty acids) such that rates of glycolysis exceed

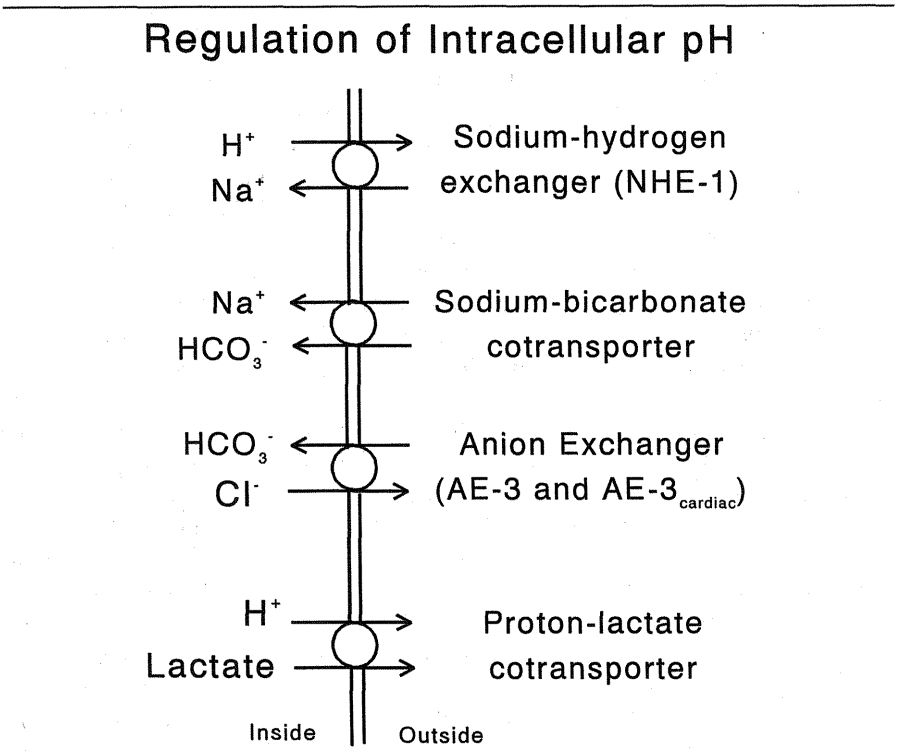

Figure 4. Pathways regulating intracellular pH in the heart.

that of glucose oxidation, there is a net production of two protons per molecule of glucose that passes through glycolysis that is not oxidized [45,48]. In the presence of high levels of fatty acids, which preferentially inhibit glucose oxidation, the uncoupling of glycolysis and glucose oxidation, even in the absence of ischemia, is a significant source of proton production (6 to 10 μmol/min/g dry wt) [20–23]. Importantly, the uncoupling of glycolysis from glucose oxidation, which is enhanced during ischemia, persists during reperfusion. The resulting continued production of protons may slow the recovery of pH_i during the critical early period of reperfusion and may explain the reduction in myocardial efficiency (LV work per mole O_2 consumed) that has been noted during reperfusion, both in vivo [49,50] and in vitro [17,21]. This outcome may occur by a direct action of acidosis on the contractile apparatus and/or indirectly via an increased consumption of ATP for the correction of the associated ionic imbalances. Thus, while a minimal level of glycolytic flux is essential for cell survival, excessive rates of glycolysis can be detrimental. However, no studies to date have directly assessed the actual contribution of proton production from glucose metabolism to rates of recovery of pH_i during reperfusion.

A number of different approaches can be made to alter proton production from glucose metabolism. One approach is to stimulate glucose oxidation during reperfusion by directly activating PDC with dichloroacetate (DCA). DCA increases glucose oxidation, decreases the production of protons from glucose metabolism, and improves function and cardiac efficiency during reperfusion of ischemic hearts [15–17,51,52]. Small clinical trials have shown that DCA has efficacy in the treatment of angina [53] and congestive heart failure [54]. We have also recently shown that DCA can improve the recovery of LV function of infants postsurgery [55]. L-carnitine also improves functional recovery following ischemia, which we have demonstrated occurs secondary to a stimulation of glucose oxidation [56,57]. L-carnitine has been shown in a number of clinical trials to have efficacy in the treatment of angina [58], myocardial infarction [59], and congestive heart failure [60].

Improving coupling between glycolysis and glucose oxidation by inhibiting excessive rates of glycolysis is another approach to decrease proton production. Improved coupling between glycolysis and glucose oxidation is associated with the cardioprotective effects of adenosine [19] and ischemic preconditioning [20]. Several studies have addressed the effects of adenosine on glycolysis during aerobic perfusion, during ischemia, and during reperfusion. Although a stimulation of glycolysis has been suggested [61–63], it now appears that the primary effects of adenosine is inhibition of glycolysis in fatty acid perfused hearts [19,20,22,64]. We showed that adenosine improves the coupling of glycolysis to glucose oxidation, decreases proton production from the hydrolysis of glycolytically derived ATP, and improves cardiac efficiency during reperfusion of ischemic hearts [19,20,22]. The cause of the reduction in glycolysis by adenosine is unclear, but we have shown that it is mediated by an adenosine A_1 receptor mechanism [23].

A third approach to improving the coupling of glucose oxidation to glycolysis is to inhibit fatty acid oxidation. This result can be achieved by inhibition of fatty acid uptake by mitochondria [33,37] or by direct inhibition of β-oxidation [65,66]. Agents that inhibit β-oxidation (ranolazine and trimetazidine) have been shown in a number of clinical trials to have efficacy in the treatment of myocardial ischemia [67–72]. Smaller clinical trials have also shown that CPT 1 inhibitors have efficacy in the treatment of myocardial ischemia (Dr. Roland Vetter, University of Berlin, personal communications). Since all these agents also stimulate glucose oxidation [37,65,66], the combined clinical and experimental data support the concept that pharmacological agents that improve glucose metabolism have potential as "anti-ischemic" agents.

FATE OF PROTONS AND THE REGULATION OF pH_i

Intracellular pH (pH_i) of the cardiac myocyte is closely regulated in order to avoid the dramatic effects of changes in pH_i on ionic conductances, metabolic processes, Ca^{2+} homeostasis, and myofilament Ca^{2+} sensitivity [73]. Numerous studies have clearly shown that intracellular acidosis occurs during ischemia and that when

normal pH is reestablished during reperfusion, there is an associated intracellular accumulation of Na^+ that leads to Ca^{2+} overload with the accompanying deleterious consequences on myocardial function (for reviews, see [12,13]).

Maintenance of pH_i in the normal physiological range requires mechanisms for H^+ extrusion, HCO_3^- (OH^-) influx, or both. Cardiac myocytes possess a number of membrane-located ion transporters that influence pH_i. These include the Na^+–H^+ exchanger (NHE-1) [11–14], the Cl^-–HCO_3^- exchanger [9–11], the H^+–lactate cotransporter [8,14], and the Na^+–HCO_3^- cotransporter (see figure 4). The activities and relative importance of each of these systems may be influenced by 1) their level of expression, 2) individual ionic transmembrane gradients, 3) regulation in response to a number of neurohumoral factors, and 4) drug-induced alteration of activity. While NHE-1 activity is considered to contribute significantly to pH_i regulation [4–7,12,13], experimental data indicate the other transporters also are involved and may even have a greater role in the regulation of pH_i than the NHE-1 [8–11]. The mechanisms for regulating the fate of myocardial protons may assume even greater importance in the etiology of the mechanical dysfunction under conditions of high levels of fatty acid, which enhance proton production due to an impairment of the coupling of glycolysis to glucose oxidation. Moreover, beneficial or detrimental consequences on cardiac function can be anticipated depending on the relative activities of these ionic transporters in the regulation of pH_i and their associated effects on Na^+ accumulation.

Na^+–H^+ exchanger

The NHE-1 exchanger, which facilitates the exchange of one external Na^+ for one internal H^+, has been extensively studied and seems to play a key role in the regulation of pH_i [11–13]. Activation occurs in response to increases in intracellular H^+ concentrations or following stimulation by either α-adrenoceptor [74] or angiotensin II receptor agonists [75]. The activity of the NHE-1 is inhibited by increased extracellular H^+ (acidosis), by analogues of amiloride, including dimethylamiloride (DMA) or ethylisopropylamiloride (EIPA), or by newer investigational agents such as HOE 694 or HOE 642 [4–7]. The contribution of this system to pH_i regulation under normal aerobic conditions and normal pH_i is controversial, since a number of studies indicate that the system does not operate when pH_i is within normal limits. However, extensive data show that the NHE-1 has a critical role in the ischemic and acidotic heart. Efflux of H^+ by the Na^+–H^+ exchanger is rapid and is accompanied by increases in intracellular Na^+. Thus, although activity of this exchanger serves to restore pH_i, this outcome is at the cost of Na^+ accumulation and Ca^{2+} overload. Consequently, inhibition of this exchanger (for example, with DMA or HOE 694 [4–7] or with controlled reperfusion with acidic perfusate) improves recovery of mechanical function of the postischemic heart, but the recovery of pH_i is delayed. There is now considerable interest in the development of inhibitors of this system, e.g., HOE 694, for the clinical management of reperfusion injury. In the presence of NHE-1 inhibitors, the other transport systems assume a greater importance in pH_i regulation.

We have recently confirmed the cardioprotective properties of DMA in our model and have also shown that DMA, when present during ischemia and throughout reperfusion, improves LV efficiency during reperfusion [17,20,21]. In contrast to our studies with adenosine or DCA, glucose metabolism was not markedly altered by DMA. Thus, manipulation of the fate of protons via this efflux pathway influences the recovery of mechanical function independent of proton production from glucose. This finding correlates with the observation that function is improved by inhibitors of NHE-1 without improvements in myocardial ATP levels. Whether NHE-1 inhibitors exert their beneficial effects during ischemia or during the critical early period of reperfusion is still unclear [2,76], as is the effect of these agents on the rate of recovery of pH_i following ischemia in fatty acid perfused hearts.

Na^+–HCO_3^- cotransporter

An Na^+- and HCO_3^--dependent transporter is present in cardiac myocytes that increases pH_i by neutralizing intracellular protons [9,10]. However, as in the case of the NHE-1, activation of this system would also cause Na^+ and hence Ca^{2+} overload. The system is activated by α-adrenoceptor agonists, and these have been shown to accelerate the recovery of pH_i following an acid load. Recent studies have indicated that the system is involved in the regulation of myocardial pH_i [11], but it may possess a lesser role than NHE-1. However, control of pH_i by the Na^+–HCO_3^- cotransporter will assume greater importance in the presence of inhibitors of the NHE-1 (e.g., amiloride).

H^+–lactate cotransporter

Efflux of protons may also occur by the H^+–lactate cotransporter (monocarboxylate carrier), which is stimulated by the high levels of intracellular H^+ and lactate produced by glycolysis [8]. Efflux of protons by this route has the advantage that protons are cleared without the deleterious consequences of Na^+ accumulation. However, a potential adverse effect of efflux of H^+ by this route during reperfusion relates to the loss of lactate, which is a readily available substrate for oxidation by the PDC and TCA cycle. A lower rate of TCA cycle activity may prolong the time that glycolysis is uncoupled from oxidation, thereby contributing to a continued proton production during the critical early period of reperfusion. We have examined the consequences of inhibition of the H^+–lactate cotransporter with α-cyano-4-hydroxycinnamate (CHC, 5 mM) [8,14,76] and have determined that CHC does not improve the recovery of mechanical and metabolic function of the postischemic heart [77]. This finding suggests that this cotransporter does not play a major role in pH_i regulation during ischemia. However, the activity of other transporters may have increased in order to compensate and consequently, this transporter may assume greater importance when proton efflux by other transporters is inhibited. Although the concentration of CHC used in our experiments was chosen in preliminary experiments to have no significant actions on baseline aerobic function, interpretation of the consequences of CHC is complicated by its concomitant

inhibition of the mitochondrial monocarboxylate transporter that would tend to impair pyruvate oxidation and ATP regeneration.

Cl^-–HCO_3^- exchanger (anion exchanger, AE)

The Cl^-–HCO_3^- transporter mediates the transmembrane flux of the anions Cl^- and HCO_3^-. Although extensively studied in a number of cell types, little is known about the role and regulation of the cardiac isoforms AE3 and $AE3_{cardiac}$ [78–81]. AE activity may cause acidification or alkalinization dependent on the concentration gradients of the bicarbonate and chloride anions [11]. The Cl^- gradient (Cl^-_o/Cl_{-i} = 105/50) favors Cl^- influx, HCO_3^- efflux, and hence cytoplasmic acidification. However, indirect evidence suggests that AE systems in contracting hearts may cause alkalinization via HCO_3^- influx [11]. Inhibition of AE either by 4-acetamide-4'-isothiocyanatostilbene-2,2'-disulphonic acid (SITS, 100 μM) or by replacement of extracellular HCO_3^- with HEPES buffer causes a reversible acidification and lowers pH_i of perfused hearts. Similarly, elimination of the Cl^- gradient by extracellular Cl^- substitution also lowers pH_i. These results contrast with those using isolated cells, where slight increases in pH_i have been observed upon removal of HCO_3^-. Thus, under conditions of mechanical work and proton production, AE activity would be expected to be beneficial by reducing intracellular acidosis and the potential for Na^+ accumulation by NHE-1.

Differential effects on pH_i and Na^+

While biochemical characterization of the pH-regulating transporters has been achieved with isolated cells, we anticipate that these transporters may differentially affect recovery of mechanical function during reperfusion following ischemia. As Na^+–K^+ ATPase activity is impaired by reduced ATP availability, Na^+ that enters the myocyte by the Na^+-dependent mechanisms accumulates and, via interactions with the Na^+–Ca^{2+} exchanger, provokes Ca^{2+} accumulation. Control of pH_i by Na^+-independent systems offers the advantage of reducing acidosis without causing adverse effects on Na^+ gradients. The role of these transporters in the regulation of pH_i and mechanical function should therefore be optimally studied under conditions of appropriate rates of proton production and workload.

RELATIONSHIP BETWEEN PROTON PRODUCTION AND CARDIAC EFFICIENCY POSTISCHEMIA

As discussed, during reperfusion of the ischemic heart, a rapid recovery of MVO_2 and TCA cycle activity can occur despite a significant decrease in the recovery of contractile function [17,21]. Our recent studies suggest that the production of H^+ from glucose metabolism is an important contributor to the impaired recovery of mechanical functions and to the decrease in cardiac efficiency, as are the pathways by which H^+ is cleared from the heart during reperfusion [17,21]. Support for this conclusion has also been provided by Hata et al. [82], who demonstrated that inhibition of Na^+–H^+ exchange activity with DMA can decrease the oxygen cost of

contractility in hearts recovering from acidosis. These authors suggest that this finding is the result of a smaller proportion of ATP being used to reestablish Na^+ and Ca^{2+} homeostasis. We have also demonstrated that altering the fate of H^+, as opposed to the source of H^+ production, can also improve cardiac efficiency. Under our experimental conditions, DMA had no significant effects on energy substrate metabolism or overall TCA acetyl-CoA and ATP production [21] in the post-ischemic hearts. Similarly, H^+ production from glucose utilization was also not affected [21]. However, DMA significantly improved both the recovery of cardiac function and cardiac efficiency during reperfusion. These beneficial effects of DMA can be explained by its selective inhibitory effects on Na^+–H^+ exchange, since the concentration used was far below the concentration known to inhibit other ionic transport pathways.

ACKNOWLEDGMENT

GDL is a Senior Scholar of the Alberta Heritage Foundation for Medical Research and a Medical Research Council of Canada Scientist.

REFERENCES

1. Tani M, Neely JR. 1989. Role of intracellular Na^+ and Ca^{2+} overload and depressed recovery of ventricular function of reperfused ischemic rat hearts. Possible involvement of H^+–Na^+ and Na^+–Ca^{2+} exchange. Circulation 65:1045–1056.
2. Meng HP, Pierce GN. 1990. Protective effect of 5-(N,N-dimethyl)amiloride on ischemia–reperfusion injury in hearts. Am J Physiol 258:H1615–H1619.
3. Scholz W, Albus U, Linz W, Martorana P, Lang HJ, Scholekens BA. 1992. Effects of Na+/H+ exchange inhibitors in cardiac ischemia. J Mol Cell Cardiol 24:731–740.
4. Pierce GN, Cole WC, Liu K, Massaeli H, Maddaford TG, Chen YJ, McPherson CD, Jain S, Sontag D. 1993. Modulation of cardiac performance by amiloride and several selected derivatives of amiloride. J Pharmacol Exp Ther 264:1280–1291.
5. Meng HP, Maddaford TG, Pierce GN. 1993. Effect of amiloride and selected analogues on postischemic recovery of cardiac contractile function. Am J Physiol 264:H1831–H1835.
6. Moffat MP, Karmazyn N. 1993. Protective effects of the potent Na/H exchange inhibitor methylisobutyl amiloride against post-ischemic contractile dysfunction in rat and guinea-pig hearts. J Mol Cell Cardiol 25:959–971.
7. Myers ML, Mathur S, Li GH, Karmazyn M. 1995. Sodium–hydrogen exchange inhibitors improve postischemic recovery of function in perfused rabbit heart. Cardiovasc Res 29:209–214.
8. Vandenburg JI, Metcalfe JC, Grace AA. 1993. Mechanisms for pHi recovery after global ischemia in the perfused heart. Circ Res 72:993–1003.
9. Grace AA, Kirschenlor HL, Metcalfe JC, Smith GA, Weissberg PL, Cragoe EJ Jr, Vandenberg JI. 1993. Regulation of intracellular pHi in the perfused heart by external HCO3- and Na(+)-H+ exchange. Am J Physiol 265:H289–H298.
10. Xu P, Spitzer KW. 1994. Na-independent Cl(−)–HCO3- exchange mediates recovery of pHi from alkalosis in guinea pig ventricular myocytes. Am J Physiol 267:H85–H91.
11. Kusuoka H, Marban E, Cingolani HE. 1994. Control of steady-state intracellular pH in intact perfused ferret hearts. J Mol Cell Cardiol 26:821–829.
12. Karmazyn M, Moffat MP. 1993. Role of Na+/H+-exchange in cardiac physiology and pathophysiology: mediation of myocardial reperfusion injury by the pH paradox. Cardiovasc Res 27:915–924.
13. Pierce GN, Czubryt MP. 1993. The contribution of ionic imbalance to ischemia/reperfusion-induced injury. J Mol Cell Cardiol 27:53–63.
14. Khandoudi N, Bernard M, Cozzone P, Feuvray D. 1995. Mechanisms of intracellular pH regulation during postischemic reperfusion of diabetic rat hearts. Diabetes 44:196–202.

15. Lopaschuk GD, Wambolt RB, Barr RL. 1993. An imbalance between glycolysis and glucose oxidation is a possible explanation for the detrimental effects of high levels of fatty acids during aerobic reperfusion of ischemic hearts. J Pharmacol Exp Ther 264:135–144.
16. McVeigh JJ, Lopaschuk GD. 1990. Dichloroacetate stimulation of glucose oxidation improves recovery of ischemic rat hearts. Am J Physiol 259:H1079–H1085.
17. Lui B, El Alaoui-talibi Z, Clanachan AS, Schulz R, Lopaschuk GD. 1996. Uncoupling of contractile function from mitochondrial tricarboxylic acid cycle activity and oxygen consumption during reperfusion of ischemic rat hearts. Am J Physiol 270:HH72–H80.
18. Lopaschuk GD, Belke DB, Gamble J, Itoi T, Schonekess BO. 1994. Regulation of fatty acid oxidation in the mammalian heart in health and disease. Biochim Biophys Acta 1213:263–276.
19. Finegan BA, Lopaschuk GD, Coulson CS, Clanachan AS. 1993. Adenosine alters glucose use during ischemia and reperfusion in isolated rat hearts. Circulation 87:900–908.
20. Finegan BA, Lopaschuk GD, Ghandi M, Clanachan AS. 1995. Ischemic preconditioning inhibits glycolysis and proton production during ischemia and reperfusion in working rat hearts. Am J Physiol 269:H1767–H1775.
21. Liu B, Clanchan AS, Schulz R, Lopaschuk GD. 1996. Cardiac efficiency is improved following ischemia by altering both the source and fate of protons. Circ Res 79:940–948.
22. Finegan BA, Clanachan AS, Coulson CS, Lopaschuk GD. 1992. Adenosine modification of energy substrate use in isolated hearts perfused with fatty acids. Am J Physiol 262:H1501–H1507.
23. Clanachan AS, Lopaschuk GD, Gandhi M, Finegan BA. 1996. Adenosine A1 receptor stimulation during reperfusion inhibits glycolysis and enhances recovery of mechanical function of working rat hearts following ischaemia. Br J Pharmacol 118:355–363.
24. Lopaschuk GD, Collins-Nakai R, Olley PM, Montague TJ, McNeil G, Gayle M, Penkoske P, Finegan BA. 1994. Plasma fatty acid levels in infants and adults after myocardial ischemia. Am Heart J 128:61–67.
25. Oliver MF, Kurien VA, Greenwood TW. 1968. Relation between serum-free-fatty acids and arrhythmias and death after acute myocardial infarction. Lancet 1:710–714.
26. Neely JR, Morgan HE. 1974. Relationship between carbohydrate and lipid metabolism and the energy balance of the heart. Annu Rev Physiol 36:413–459.
27. Opie LH. 1991. Carbohydrates and lipids. In Opie LH (ed), The Heart. Physiology and Metabolism, 2nd ed. New York: Raven Press, pp. 208–246.
28. Saddik M, Lopaschuk GD. 1991. Myocardial triglyceride turnover and contribution to energy substrate utilization in isolated working rat hearts. J Biol Chem 266:8162–8170.
29. Patel MS, Roche TE. 1990. Molecular biology and biochemistry of pyruvate dehydrogenase complexes. FASEB J 4:3224–3233.
30. Owen P, Dennis S, Opie LH. 1990. Glucose flux rate regulates onset of ischemic contracture in globally underperfused rat hearts. Circ Res 66:344–354.
31. Neely JR, Grotyohann LW. 1984. Role of glycolytic products in damage to ischemic myocardium. Dissociation of adenosine trihosphate levels and recovery of function of reperfused ischemic hearts. Circ Res 55:816–824.
32. Zimmer SD, Ugurbil K, Michurski SP, Mohanakrishnan P, Ulstad VK, Foker JE, From AH. 1989. Alterations in oxidative function and respiratory regulation in the post-ischemic myocardium. J Biol Chem 264:12402–12411.
33. Lopaschuk GD, Spafford MA, Davies NJ, Wall SR. 1990. Glucose and palmitate oxidation in isolated working rat hearts reperfused after a period of transient global ischemia. Circ Res 66:546–553.
34. Benzi RH, Lerch R. 1992. Dissociation between contractile function and oxidative metabolism in postischemic myocardium. Attenuation by ruthenium red administered during reperfusion. Circ Res 71:567–576.
35. Liedtke AJ, Nellis S, Neely JR. 1978. Effects of excess free fatty acids on mechanical and metabolic function in normal and ischemic myocardium in swine. Circ Res 43:652–661.
36. Liedtke AJ, Demaison L, Eggleston AM, Cohen LM, Nellis SH. 1988. Changes in substrate metabolism and effects of excess fatty acids in reperfused myocardium. Circ Res 62:535–542.
37. Lopaschuk GD, Wall SR, Olley PM, Davies NJ. 1988. Etomoxir, a carnitine palmitoyltransferase I inhibitor, protects hearts from fatty acid-induced ischemic injury independent of changes in long chain acylcarnitine. Circ Res 63:1036–1043.
38. Opie LH. 1969. Metabolism of the heart in health and disease. II. Am Heart J 77:100–122.
39. Renstrom B, Nellis SH, Liedtke AJ. 1989. Metabolic oxidation of glucose during early myocardial reperfusion. Circ Res 65:1094–1101.

40. Saddik M, Lopaschuk GD. 1992. Myocardial triglyceride turnover during reperfusion of isolated rat hearts subjected to a transient period of global ischemia. J Biol Chem 267:3825–3831.
41. McGarry JD, Woeltje KF, Kuwajima M, Foster DW. 1989. Regulation of ketogenesis and the renaissance of carnitine palmitoyltransferase. Diabetes Metab Rev 5:271–284.
42. Saddik M, Gamble J, Witters LA, Lopaschuk GD. 1993. Acetyl-CoA carboxylase regulation of fatty acid oxidation in the heart. J Biol Chem 268:25836–25845.
43. Lopaschuk GD, Witters LA, Itoi T, Barr R, Barr A. 1994. Acetyl-CoA carboxylase involvement in the rapid maturation of fatty acid oxidation in the newborn rabbit heart. J Biol Chem 269:25871–25878.
44. Lopaschuk GD, Gamble J. 1994. The 1993 Merck Frosst Award. Acetyl-CoA carboxylase: an important regulator of fatty acid oxidation in the heart. Can J Physiol Pharmacol 72:1101–1109.
45. Kudo N, Barr AJ, Barr RL, Desai S, Lopaschuk GD. 1995. High rates of fatty acid oxidation during reperfusion of ischemic hearts are associated with a decrease in malonyl-CoA levels due to an increase in 5′-AMP-activated protein kinase inhibition of acetyl-CoA carboxylase. J Biol Chem 270:17513–17520.
46. Kudo N, Gillespie JG, Kung L, Witters LA, Schulz R, Clanachan AS, Lopaschuk GD. 1996. Characterization of 5′AMP-activated protein kinase activity in the heart and its role in inhibiting acetyl CoA carboxylase during reperfusion following ischemia. Biochim Biophys Acta 1301:67–75.
47. Hardie GD. 1989. Regulation of fatty acid synthesis via phosphorylation of acetyl-CoA carboxylase. Prog Lipid Res 28:117–146.
48. Dennis SC, Gevers W, Opie LH. 1991. Protons in ischemia: where do they come from; where do they go to? J Mol Cell Cardiol 23:1077–1086.
49. Laster SB, Becker LC, Ambrosio G, Jacobus WE. 1989. Reduced aerobic metabolic efficiency in globally "stunned" myocardium. J Mol Cell Cardiol 21:419–426.
50. Furukawa S, Kreiner G, Bavaria JE, Streicher JT, Edmunds LHJ. 1991. Recovery of oxygen utilization efficiency after global myocardial ischemia. Ann Thorac Surg 52:1063–1068.
51. Racy-Burns LA, Burns AH, Summer WR, Shepherd RE. 1989. The effect of dichloroacetate on the isolated no flow arrested rat heart. Life Sci 44:2015–2023.
52. Wahr JA, Childs KF, Bolling SF. 1994. Dichloroacetate enhances myocardial functions and metabolic recovery following global ischemia. J Cardiothorac Vasc Anesth 8:192–197.
53. Wargovich TJ, Macdonald RG, Hill JA, Feldman RL, Stacpoole PW, Pepine CJ. 1988. Myocardial metabolic and hemodynamic effects of dichloroacetate in coronary artery disease. Am J Cardiol 61:65–70.
54. Bershin RM, Wolfe C, Kwasman M, Lau D, Klinski C, Tanaka K, Khorrami P, Henderson GN, de Marco T, Chatterjee K. 1994. Improved hemodynamic function and mechanical efficiency in congestive heart failure with dichloroacetate. J Am Coll Cardiol 23:1617–1624.
55. Collins-Nakai RL, Suarex-Almazor M, Karmy-Jones R, Penkoske P, Teo K, Lopaschuk GD. 1995. Dichloracetic acid (DCA) after open heart surgery in infants and children (abstract). Can J Cardiol 11:106E.
56. Broderick TL, Quinney HA, Barker CC, Lopaschuk GD. 1993. Beneficial effect of carnitine on mechanical recovery of rat hearts reperfused after a transient period of global ischemia is accompanied by a stimulation of glucose oxidation. Circulation 87:972–981.
57. Broderick TL, Quinney HA, Lopaschuk GD. 1992. Carnitine stimulation of glucose oxidation in the fatty acid perfused isolated working rat heart. J Biol Chem 267:3758–3763.
58. Ferrari R, Cucchini F, Visioli O. 1984. The metabolic effects of L-carnitine in angina pectoris. Intern J Cardiol 5:213–216.
59. Iliceto S, Scrutinio D, Bruzzi P, D'ambrosio G, Boni L, Di Biase M, Biasco G, Hugenholtz PG, Rizzon P. 1995. Effects of L-carnitine administration on left ventricular remodeling after acute anterior myocardial infarction: the L-carnitine ecocardiografia digitalizzata infarto miocardico (CEDIM) trial. J Am Coll Cardiol 26:380–387.
60. Ghidini O, Azzurro M, Vita G, Sartori G. 1988. Evaluation of the therapeutic efficacy of L-carnitine in congestive heart failure. Int J Clin Pharmacol Ther Toxicol 26:218–220.
61. Wyatt DA, Edmunds MC, Rubio R, Berne RM, Lasley RD, Mentzer RM Jr. 1989. Adenosine stimulates glycolytic flux in isolated perfused rat hearts by A1-adenosine receptors. Am J Physiol 257:H1952–H1957.
62. Buxton DB, Kjaer Pedersen K, Nguyen A. 1992. Metabolic effects of adenosine in the isolated perfused rat heart. J Mol Cell Cardiol 24:173–181.
63. Janier MF, Vanoverschelde JL, Bergmann SR. 1993. Adenosine protects ischemic and reperfused myocardium by receptor-mediated mechanisms. Am J Physiol 264:H163–H170.

64. Vander Heide RS, Reimer KA, Jennings RB. 1993. Adenosine slows ischaemic metabolism in canine myocardium in vitro: relationship to ischaemic preconditioning. Cardiovasc Res 27:669–673.
65. McCormack JG, Barr RL, Lopaschuk GD. 1996. Ranolazine stimulates glucose oxidation in normoxic, ischemic and reperfused ischemic rat hearts. Circulation 93:135–142.
66. McCormack JG, Baracos VE, Lopaschuk GD. 1996. Effects of ranolazine on oxidative substrate preference in epitrochlearis muscle. J Appl Physiol 81:905–910.
67. Cocco G, Rousseau MF, Bouvy T, Cheron P, Williams G, Detry JM, Pouleur H. 1992. Effects of a new metabolic modulator, ranolazine, on exercise tolerance in angina pectoris patients treated with β-blocker or diltiazem. J Cardiovasc Pharmacol 20:131–138.
68. Bouvy T, Rousseau MF, Cocco G, Cheron P, William GJ, Detry JMR. 1993. Improvement in exercise tolerance and left ventricular filling dynamics in patients with angina pectoris with the novel metabolic modulator, ranolazine. Acta Cardiol 48:98–99.
69. Kober G, Buck T, Sievert H, Vallbracht C. 1992. Myocardial protection during percutaneous transluminal coronary angioplasty: effects of trimetazidine. Eur Heart J 82:1109–1115.
70. Syntex Research brochure for investigational studies.
71. Detry JM, Sellier P, Pennaforte S, Cokkinos D, Dargie H, Mathies P. 1994. Trimetazidine: a new concept in the treatment of angina. Comparison with propranalol in patients with stable angina. Br J Clin Pharmacol 37:279–288.
72. Harpey C, Clauser P, Labrid C, Freyria JL, Poirier JP. 1989. Trimetazidine, a cellular antiischemic agent. Cardiovasc Drug Rev 6:292–312.
73. Puceat M, Vassort G. 1995. Neurohumoral modulation of intracellular pH in the heart. Cardiovasc Res 29:178–183.
74. Puceat M, Clement-Chomienne O, Terzic A, Vassort G. 1993. Alpha 1-adrenoceptor and purinergic agonists modulate Na-HJ-antiport in single cardiac cells. Am J Physiol 264:H310–H319.
75. Matsui H, Barry WH, Livsey C, Spitzer KW. 1995. Angiotension II stimulates sodium–hydrogen exchange in adult rabbit ventricular myocytes. Cardiovasc Res 29:215–221.
76. Wang X, Levi AJ, Halestrap AP. 1994. Kinetics of the sarcolemmal lactate carrier in single heart cells using BCECF to measure pHi. Am J Physiol 267:H1759–1769.
77. Liu B, Clanachan AS, Schulz R, Lopaschuck GD. 1997. Manuscript in preparation.
78. Linn SC, Askew GR, Menon AG, Shull GE. 1995. Conservation of an AE3 Cl-/HCO3- exchanger cardiac-specific exon and promoter region and AE3 mRNA expression patterns in murine and human hearts. Circ Res 76:584–591.
79. Linn SC, Kudrycki KE, Shull GE. 1992. The predicted translation product of a cardiac AE3 mRNA contains an N terminus distinct from that of the brain AE3 Cl-/HCO3- exchanger. Cloning of a cardiac AE3 cDNA, organization of the AE3 gene, and identification of an alternative transcription initiation site. J Biol Chem 267:7927–7935.
80. Puceat M, Korichneva I, Cassoly R, Vassort G. 1995. Identification of band 3-like proteins and Cl-/HCO3- exchange in isolated cardiomyocytes. J Biol Chem 270:1315–1322.
81. Korichneva I, Puceat M, Cassoly R, Vassort G. 1995. Cl-HCO3- exchange in developing neonatal rat cardiac cells. Biochemical differentiation and immunolocalization of band 3-like proteins. Circ Res 77:556–564.
82. Hata K, Takasago T, Saeki A, Nishioka T, Goto Y. 1994. Stunned myocardium after rapid correction of acidosis. Increased oxygen cost of contractility and the role of the Na(+)-H+ exchange system. Circ Res 74:794–805.

This Page Intentionally Left Blank

INTRACELLULAR CALCIUM REGULATION IN CARDIAC CELLS DURING ACIDOSIS

CESARE M.N. TERRACCIANO and KENNETH T. MACLEOD

Imperial College School of Medicine at National Heart & Lung Institute

Summary. The effects of intracellular acidosis on Ca^{2+} regulation mechanisms in enzymatically isolated guinea pig ventricular myocytes were studied. Comparable degrees of acidosis were obtained by NH_4Cl removal or application of lactate. Intracellular pH and $[Ca^{2+}]$ were monitored using the fluorescent indicators 2′-7′-bis-(carboxyethyl)-5(6)-carboxyfluorescein (BCECF) and indo-1. Release of Ca^{2+} from the sarcoplasmic reticulum was produced by rapid cooling or application of caffeine. Using caffeine, we have shown that acidosis affects Na^+–Ca^{2+} exchange-mediated Ca^{2+} extrusion. This effect was not observed when the increase of intracellular Na^+ during acidosis was prevented by blocking the Na^+–H^+ exchange. Using Na^+-free/Ca^{2+}-free solution to study the activity of the SR Ca^{2+} ATPase on cytoplasmic Ca^{2+}, Ca^{2+} extrusion was slower in the presence of lactate but was unchanged after removal of NH_4Cl. Using paired rapid cooling contractures, the relative contributions of the cellular mechanisms to Ca^{2+} extrusion were investigated. In acidosis produced by application of lactate and acetate, the relative role of the SR Ca^{2+} uptake was reduced, probably in favor of Na^+–Ca^{2+} exchange.

INTRODUCTION

The hypothesis that intracellular acidosis could contribute to the contractile failure of the ischemic myocardium was put forward by Katz and Hecht in 1969 [1]. An increase of intracellular lactic acid during ischemia and the depressant action of acidosis on myocardial contractility support this hypotheis. The demonstrations that during ischemia an intracellular acidosis develops rapidly and that simulated ischemia and lactic acidosis produce similar effects on force and on Ca^{2+} handling [2] provide

S. Mochizuki, N. Takeda, M. Nagano and N. Dhalla (eds.). THE ISCHEMIC HEART.

more evidence, although the precise relationship between acidosis induced by ischemia and contractile failure is often not clear [3].

Many groups have shown that acidosis follows cardiac ischemia (e.g., [4–7]) and the severity of acidosis is probably related to the blood flow and the duration of the ischemic condition. Although myocardial acidosis could be a consequence of lactate production due to the increase in anaerobic glycolysis, Gevers [8] pointed out that the production of lactate is only one of many factors responsible for acidosis.

The effect of acidosis on cardiac performance has been known since 1880, when Gaskell [9] showed in the frog heart how perfusion with a solution containing lactic acid 'quickly brings the ventricle to standstill in the position of complete relaxation . . . , the height of each beat is lowered and at the same time the beat assumes a more pointed character.' He showed that alkalosis had the opposite effect. A major factor contributing to the decline of function originally observed by Gaskell is the sensitivity of the myofilaments themselves to pH (e.g., [10–12]). However, acidosis produces a variety of other effects on the ionic balance of the cells that have important functional consequences (see [11,13]). Many of these other effects involve alterations to the mechanisms responsible for Ca^{2+} regulation that bring about two widely observed effects of acidosis: an increase in cytoplasmic diastolic Ca^{2+} [14–20] and changes in the amplitude and duration of the Ca^{2+} transient [16–22].

In this chapter, we will describe recent work that uses well-established single-cell techniques [23–26] to investigate how the major systems involved in the Ca^{2+} balance of the cell alter in response to acidosis.

METHODS

Male Dunkin Hartley guinea pigs (weight, 200–450 g) were killed by cervical dislocation. The heart was rapidly removed and placed in a Krebs–Henseleit (KH) solution at 5°C. Cells were isolated by enzymatic dissociation using a technique described in detail by MacLeod and Harding [27]. Cell shortening was measured using a video-based motion detector as described by Steadman et al. [28].

Intracellular Ca^{2+} and pH measurements

Intracellular $[Ca^{2+}]$ and pH were measured using the ratiometric Ca^{2+}-sensitive fluorescent dye indo-1 and the pH-sensitive fluorescent dye BCECF. The techniques used to measure intracellular pH are described in detail by MacLeod and Harding [27]. In the experiments described here, cells were incubated with 5 μM of the fluorescent dye BCECF AM or Indo-1 AM (Molecular Probes, Inc., Eugene, Oregon, USA) for 20 minutes at room temperature. Once loaded, cells were stored in the dark also at room temperature and used within 6–7 hours.

Fluorescence calibration of indo-1 was performed to compare the results obtained in different experimental conditions—namely, at different pH or in the presence of different substances that might affect the fluorescence of the indicator, following the calibration technique described by Bassani et al. [26]. The value for K_d was

determined in vitro using three series of solutions containing a known amount of free [Ca^{2+}]. 1 μM indo-1 pentapotassium salt (Molecular Probes, Inc., Eugene, Oregon, USA) was added to a solution containing (in mM): KCl, 140; HEPES, 10; $MgCl_2$, 1; and BAPTA, 1. The first group was the control, with pH = 7.2 ± 0.005. The second group of solutions had the same composition, but the pH was set at 7.0 ± 0.005 in order to simulate the change in pH obtained with the NH_4Cl removal technique. The third group was identical to the second (pH 7.0 ± 0.005) but also contained 10 mM lactic acid (Sigma Chemical Co. Ltd, Poole, UK) to resemble the intracellular conditions during extracellular application of 20 mM lactate.

No significant changes of K_d for indo-1 were seen when the pH was reduced from 7.2 to 7.0 (K_d at pH 7.2 = 227 ± 3 nM; K_d at pH 7.0 = 235 ± 7 nM, n = 3). Presumably this reduction in pH is too small to produce a significant shift in K_d. The K_d increased significantly in the presence of 10 mM lactate (K_d at pH 7.0 + lactate = 325 ± 16 nM, n = 3; t test between K_d at pH 7.2 and pH 7.0 + lactate, p = 0.004; between K_d at pH 7.0 and pH 7.0 + lactate, p = 0.007, n = 3).

The values of R_{max}, R_{min}, and b were calculated in vivo as described by Bassani et al. [26] by superfusing the cells either with a solution at pH 7.2 (control) or pH 7.0 (acidosis) or in the presence of 20 mM lactate (pH 7.2). The results for R_{min} obtained in three cells for each group were control = 0.283 ± 0.002; acidosis = 0.284 ± 0.001; lactate = 0.308 ± 0.004. Results for R_{max} were control = 0.878 ± 0.01; acidosis = 0.854 ± 0.04; lactate = 1.053 ± 0.04. Results for b (which equals $S_{f\lambda}/S_{b\lambda}$, where $S_{f\lambda}$ is the fluorescence emitted by the free dye and $S_{b\lambda}$ is the fluorescence emitted by the bound dye measured at a wavelength λ) were control = 2.555 ± 0.25; acidosis = 2.634 ± 0.27; lactate = 3.123 ± 0.18.

No difference was found in R_{max}, R_{min}, and b at pH 7.2 and 7.0. However, in the presence of lactate, a significant increase in R_{max} and R_{min} compared with control was seen (t test between R_{max} in control and 20 mM lactate, p = 0.005; between R_{max} in control and 20 mM lactate, p = 0.013).

It was therefore evident that if the calibration was carried out in vitro, lactate produced an increase of K_d, and, if the calibration was made in vivo, lactate produced an increase in R_{max} and R_{min}. The two findings alter the calculation of [Ca^{2+}] using the formula reported by Grynkiewicz et al. [29], in opposing ways. The result of adding 20 mM lactate to the superfusing solution is that the relationship between indo-1 fluorescence is shifted to the right, implying a larger change in fluorescence for the same change in Ca^{2+} compared with control. Since no significant difference was found in indo-1 fluorescence at pH 7.2 and pH 7.0, in the experiments with NH_4Cl removal, no attempt was made to calculate Ca^{2+} from the indo-1 signal. The fluorescence in control and in acidosis was compared as Δ indo-1 ratio. In lactate, it is necessary to express the fluorescence in terms of [Ca^{2+}], since the changes to K_d, R_{max}, and R_{min} described above affect the fluorescence and so must be considered. Ca^{2+} was calculated from fluorescence using the mean values of the parameter reported above.

Electrophysiology

The electrophysiological experiments were performed using an Axochlamp-2A system (Axon Instruments, Foster City, California, USA). To avoid dialysis of the cells and to minimize the effects of changing the intracellular environment, high-resistance microelectrodes were used. In all the experiments described, borosilicate glass microelectrodes (Clark Electromedical Instruments, GC150F-15, Reading, UK) with resistances between 20 and 30 MΩ were pulled with a micropipette puller (model P-87 Flaming/Brown, Sutter Instruments Co., Novato, California, USA). The microelectrode filling solution contained KCl, 2 M; EGTA; 0.1 mM; HEPES, 5 mM, pH = 7.2. Unless otherwise stated, in the current clamp mode, the cells were stimulated at 0.5 Hz with a 1.0 nA pulse of depolarizing current of 10 ms duration. The voltage clamp protocols varied in different experiments and will be described separately. Current clamp and voltage clamp protocols were controlled with pClamp software (versions 5.5 and 6, Axon Instruments Inc., Foster City, California, USA) and Strathclyde software (kindly provided by Dr John Dempster, Department of Pharmacology, University of Strathclyde, UK).

Acquisition systems and statistical analysis

The data obtained from the video edge-detection system, the epifluorescence apparatus, and the Axoclamp-2A system were simultaneously recorded on a Racal store 7DS tape recorder (Racal Recorders Ltd., Southampton, UK), a Lectromed Multitrace 4 chart recorder (Lectromed Limited, St. Peter, Jersey, Channel Islands, UK), and on computer. The acquisition software program used for cell contraction and epifluorscence experiments and also employed for data analysis was Axotape 2.0 (Axon Instruments Inc., Foster City, California, USA).

To assess statistical differences between means, the Student's *t*-test was performed. Unless otherwise specified, the results are expressed as mean ± standard error of the mean (SEM).

Solutions

The temperature of the superfusing solution was approximately 22°C in all experiments. The rate of superfusion was 2–3 mL/min (the volume of the superfusion chamber was approximately 60 μL).

The composition (in mM) of the normal Tyrode (NT) solution was NaCl, 140; KCl, 6; $MgCl_2$, 1; $CaCl_2$, 2; glucose, 10; HEPES, 10; pH to 7.4 with 2 M NaOH. The composition of the Na^+-free/Ca^{2+}-free solution was LiCl, 140; KOH, 6; MgCl, 1; glucose, 10; HEPES, 10; EGTA, 0.1; pH to 7.4 with 1 M LiOH. When required, NH_4Cl was added as a solid to the superfusing NT solution shortly before use. Different concentrations of DL lactic acid (sodium salt, Sigma Chemical Co., Poole, UK) (5–40 mM) were added to the superfusing solution where needed, and pH was readjusted to 7.4 with NaOH. Na^+–H^+ exchange was inhibited using amiloride (Sigma Chemical Co. Ltd, Poole, U.K.) or ethylisopropyl-amiloride (EIPA; gift from Dr. S.E. Harding) dissolved in NT solution before the experiments.

RESULTS AND DISCUSSION

Although many ways could be used to produce an intracellular acidification (e.g., by acidifying the extracellular medium or by using CO_2), the NH_4Cl overshoot technique and the application of lactate were used. The first could be considered a standard technique in cardiac physiology, and the second has been used because it produces a less transient acidosis and resembles a pathophysiological situation. Moreover, these methods allow us to produce an intracellular acidification without changing the external pH. To quantify the effects of the acidification techniques, a group of experiments were performed to measure the changes in cytoplasmic pH under the same conditions that will be used in the later work on Ca^{2+} regulation. The cytoplasmic pH changes have been measured using the fluorescent indicator BCECF.

NH_4Cl removal technique

The NH_4Cl removal technique is one of the most commonly used methods to produce an intracellular acidosis in experimental conditions. It has been widely used in cardiac physiology to investigate acidosis (e.g., [30–32]). Advantages of its use are 1) changing the concentration and the time of exposure allows an approximate grading of the pH change; 2) the extracellular pH is unaffected; and 3) in the presence of active cytoplasmic pH regulation, the effect on cytoplasmic pH is reversible.

A solution containing 15 mM NH_4Cl was applied for five minutes and then withdrawn. Cytoplasmic pH was measured in five cells using BCECF fluorescence (see figure 1, top panel). During application of NH_4Cl, cytoplasmic pH reached 7.43 $\pm$ 0.03 (n = 5) after 0.576 $\pm$ 0.094 minutes and then started to decline again. After five minutes of NH_4Cl superfusion, cytoplasmic pH was 7.35 $\pm$ 0.02 (n = 5). Removal of NH_4Cl reduced cytoplasmic pH to 7.01 $\pm$ 0.03 (n = 5) in 0.97 $\pm$ 0.027 minutes. The recovery from acidosis was complete in 6.01 $\pm$ 0.4 minutes. These observations allow us to set the time for measurements in the following experiments at one minute after removal of NH_4Cl, when the intracellular acidification reaches its peak.

The NH_4Cl removal technique produces a transient reduction in pH_i, which recovers quickly to control values. Such a situation is unlikely to be present in pathophysiological conditions. In an effort to obtain a more faithful reproduction of the acidosis present during ischemia and to study a less transient change in cytoplasmic pH, lactate was added to the superfusing solution, and its effects on Ca^{2+} regulation were studied.

Superfusion with 20 mM lactate

In the presence of 20 mM lactate, cytoplasmic pH was also recorded using BCECF fluorescence (figure 1, top panel). After five minutes of application, pH changed by 0.16 units (from 7.19 $\pm$ 0.02. to 7.03 $\pm$ 0.008, mean $\pm$ SEM; n = 6). In these conditions, such a change is achieved in approximately 1.5 minutes and maintained

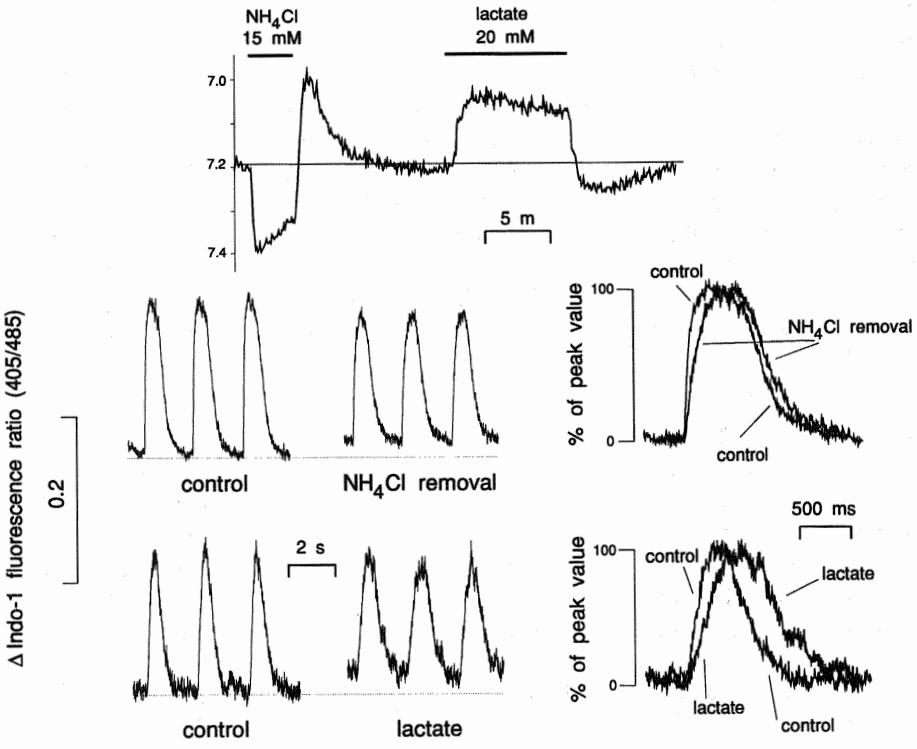

Figure 1. The effects of NH_4Cl and lactate application on intracellular pH and cytoplasmic Ca^{2+}. Top panel shows the effects of the two acidification techniques on intracellular pH measured using BCECF. Comparable levels of intracellular acidosis were achieved with the two techniques, although lactate-induced acidosis was more stable. The figure also shows the effects of acidosis produced by NH_4Cl removal (middle traces) and lactate (bottom traces) on diastolic indo-1 fluorescence and the indo-1 transient. On the right portion of the panels, transient changes of indo-1 fluorescence elicited in control and in acidosis were scaled and superimposed.

for several minutes. During five minutes of superfusion with 20 mM lactate, no large changes in pH were detected [(pH_i at peak) − (pH_i after 5 min in lactate) = 0.008 ± 0.06 pH units; $n = 6$], so the acidosis produced is much less transient than that obtained after removal of NH_4Cl. This difference will be exploited in our experiments investigating Ca^{2+} regulation.

The change in cytoplasmic pH (7.03) obtained with the application of 20 mM lactate is similar to the one obtained with the NH_4Cl removal technique (7.01), allowing us to compare the results recorded with the two different acidification techniques (figure 1, top panel). The main difference between the two acidification techniques is the faster pH recovery phase after acidification produced by NH_4Cl removal. Since the intracellular acidosis produced with this technique is quite transient, it can only be used for measurements over a short time interval, in our

conditions between 60 and 90 seconds after removal of NH_4Cl. The acidosis produced by the application of lactate is more stable because lactate was constantly present in the extracellular space and is mainly transported across the cell membrane with an H^+ via the H^+-monocarboxylate cotransporter. At physiological pH, it is almost completely dissociated, so a new equilibrium is reached with an increase of intracellular lactate and $[H^+]_i$.

Effects of intracellular acidosis on Ca^{2+} transients and diastolic Ca^{2+}

Figure 1 shows the effects of removal of 15 mM NH_4Cl (middle traces) and a five-minute application of lactate (lower traces) on Ca^{2+} transients from cells stimulated at 0.5 Hz.

Using two different acidification techniques, similar changes in Ca^{2+} during twitches were obtained (see table 1). In both the NH_4Cl rebound technique and the lactate application, an increase in the diastolic level of Ca^{2+} was observed. This outcome has been previously shown by different authors in different species and with different kinds of acidosis (e.g., [2,14,18,19,22,33,34]). Although many hypotheses have been forwarded to explain this phenomenon, the source of the increase in diastolic Ca^{2+} is still unclear. Many experiments have been performed to test possible mechanisms responsible in stimulated and resting cardiac tissue. The use of inhibitors of different intracellular and sarcolemmal Ca^{2+} regulation systems, such as the Na^+–K^+ pump, Ca^{2+} channels, mitochondria, SR, Na^+–Ca^{2+} exchange, or Na^+–H^+ exchange [16,19,22] could not prevent the increase in diastolic Ca^{2+} during acidosis. An important factor in influencing the increase in diastolic Ca^{2+} during acidosis is the competition of H^+ with Ca^{2+} for intracellular buffering sites. This factor was suggested by Bers and Ellis [14] and Vaughan-Jones et al. [35], who showed changes in cytoplasmic Ca^{2+} following changes in cytoplasmic pH. More evidence for the role of cytoplasmic buffering in increasing diastolic Ca^{2+} in acidosis is provided by the dependence of such an increase on the rate of stimulation.

Table 1. Effects of acidosis on the indo-1 transient

	NH_4Cl removal	Lactate
Diastolic level	21.2% ± 4.5% (n = 13) increase	10.18% ± 1.7% (n = 15) increase
Indo-1 transient amplitude	Control: 0.206 ± 0.01 Acidosis: 0.146 ± 0.01 n = 15; t-test, $p < 0.001$ (values in indo-1 ratio units)	Control: 894 ± 108 Lactate: 650 ± 88 n = 15; t-test, $p = 0.0038$ (values in nM Ca^{2+})
TTP	Control: 392 ± 47 ms Acidosis: 572 ± 56 ms n = 13; t-test, $p = 0.021$	Control: 350 ± 18 ms Lactate: 659 ± 61 ms n = 15; t-test, $p < 0.0001$
Recovery (T50 and T90: time to 50% and 90% relaxation)	T90 control: 997 ± 30 ms Acidosis: 1083 ± 34 ms n = 9; t-test, $p = 0.034$	T50 control: 281 ± 23 ms Lactate: 446 ± 25 ms n = 15; t-test, $p < 0.0001$

Gambassi et al. [19] showed that the size of diastolic changes in Ca^{2+} in quiescent myocytes was not affected by 1) changing SR function with 5 μM ryanodine, 2) preventing transarcolemmal Ca^{2+} influx by removing Ca^{2+} from the superfusing solution (and adding 0.1 mM EGTA), and 3) blocking the mitochondrial uniporter by 50 μM ruthenium red. In our experiments carried out in the presence of lactate, when the rate of stimulation was reduced from 0.5 Hz to 0.2 Hz, the increase in diastolic Ca^{2+} during application of lactate was smaller. Although competition between Ca^{2+} and H^+ for myofilament binding sites can explain the reduction in cell shortening observed in acidosis, it cannot account completely for the increase in diastolic Ca^{2+}. As suggested by Orchard and Kentish [11], binding site competition would be the explanation if the increase in Ca^{2+} and decrease in force were concurrent. Since the decline in force happens *before* the increase of diastolic Ca^{2+} [11,21,22], other mechanisms should also be considered. Orchard in 1987 [22] showed that, in the presence of caffeine, when the uptake and release of Ca^{2+} from the SR were ineffective, there was a temporal coincidence between the increase in diastolic Ca^{2+} and decrease in tension, suggesting that in the initial stages of acidosis the SR takes up more Ca^{2+} than is available due to the reduction of binding sites in the intracellular space. However, although intracellular buffering is important, part of the increase is attributable to other Ca^{2+} regulation mechanisms involved in E-C coupling.

When NH_4Cl was removed, a reduction in the amplitude of indo-1 transients was seen. This finding is in contrast with previous observations in different species (rat, ferret, rabbit, cat papillary muscles [21]; ferret and rat papillary muscle [22]), where the amplitude of the Ca^{2+} transient was increased. In the latter work, several acidification techniques, including NH_4Cl removal, were used, and a transient but marked increase of aequorin light was always detected during acidosis.

Similar to the removal of NH_4Cl, the acidosis obtained after five minutes of superfusion with lactate resulted in a decrease in the amplitude of the Ca^{2+} transient. This result is also in contrast with other work, where an increase of the amplitude of the Ca^{2+} transient has been described during the application of lactic acid (in ferret muscle [2] and in rat myocytes [18]). In the latter paper, by Cairns et al. [18], this increase was evident when a fura-2 calibration was performed and account was taken of an increase in K_d measured in acidosis. The increase of K_d shifts the Ca^{2+}/fura-2 fluorescence relationship so that the correction of this value in acidosis produces a larger $[Ca^{2+}]$ for the same fluorescence intensity. In Cairns et al., calibration was not done in the presence of lactate and the fluorescence signal was corrected only for the reduction of pH induced by lactate. As shown in Methods section, there is an increase in K_d when the indo-1 calibration is performed in the presence of lactate; calibration in vivo, though, shows increases in R_{max} and R_{min}. Correcting these values counterbalances the shift of the Ca^{2+}/indo-1 fluorescence curve. Moreover, for greater intensities of fluorescence there is an opposite effect, so the curve shifts to the right. This means that for any high level of Ca^{2+}, the indo-1 signal is larger in the presence of lactate. These observations could explain the different results obtained by Cairns et al. Nevertheless, they cannot explain the

difference with experiments (e.g., [22]) where aequorin was used, since changes of pH between 6.6 and 7.4 do not appear to affect the Ca^{2+} sensitivity of this protein [36].

It is unclear whether the different results in guinea pig ventricular myocytes in the experimental conditions described here are species-dependent effects due to a different role of the Ca^{2+} regulation systems in acidosis. During acidosis, almost all mechanisms able to control Ca^{2+} within the cell seem to be affected (for a review, see [11]). In different species and conditions, they could be influenced by acidosis in different ways, producing different changes.

Results reported for twitches suggest that in acidosis the rate of increase of Ca^{2+} in the cytoplasm and the extrusion of Ca^{2+} from the cytoplasm are slower than in control. To investigate the mechanisms responsible for these effects, we have used two techniques to generate SR Ca^{2+} release and to study subsequent Ca^{2+} uptake and efflux.

Rapid cooling contractures (RCCs)

Rapid cooling of skeletal and cardiac muscle produces a contracture; this phenomenon is reversible, since the tissue completely relaxes to control levels upon rewarming. Early studies in skeletal [37] and cardiac muscle [38] hypothesized that the contracture is related to release of Ca^{2+} from the SR. Our techniques to produce RCCs in guinea pig cardiac myocytes have been described in detail elsewhere [20,39].

During an RCC, cytoplasmic [Ca^{2+}] remains high, since mechanisms involved in Ca^{2+} regulation are greatly slowed at low temperatures [40,41]. Rewarming of the preparation to control temperature brings about a rapid relaxation that is explained by reactivation of the mechanisms at higher temperature.

The inhibition of Ca^{2+} regulatory mechanisms during cooling allows separation of the release of Ca^{2+} from its extrusion. Moreover, during such an artificially produced interval in the Ca^{2+} cycling, it is possible to change the experimental conditions to obtain specific inhibition of one or several mechanisms of Ca^{2+} extrusion without affecting release from the SR. Bers and Bridge [40], for example, used this technique to analyze the rewarming phase after an RCC and to study the relative roles of the SR Ca^{2+} ATPase and Na^+–Ca^{2+} exchange in producing relaxation of rabbit ventricular papillary muscles. Similar experiments have been performed here during intracellular acidosis.

Figure 2 shows the effects of rewarming after rapid cooling in both acidification conditions described above. Top traces were produced during superfusion with NT solution. The Ca^{2+} extrusion mechanisms were not affected, and the rate of decline of the fluorescence trace depends on the capability of the cell to extrude Ca^{2+} from the cytoplasm. On the left, the indo-1 fluorescence signal during rewarming after RCCs in control and one minute after removal of NH_4Cl have been superimposed. On the right, Ca^{2+} signals recorded in control conditions and after five minutes in lactate are shown. The rate of decline of the indo-1

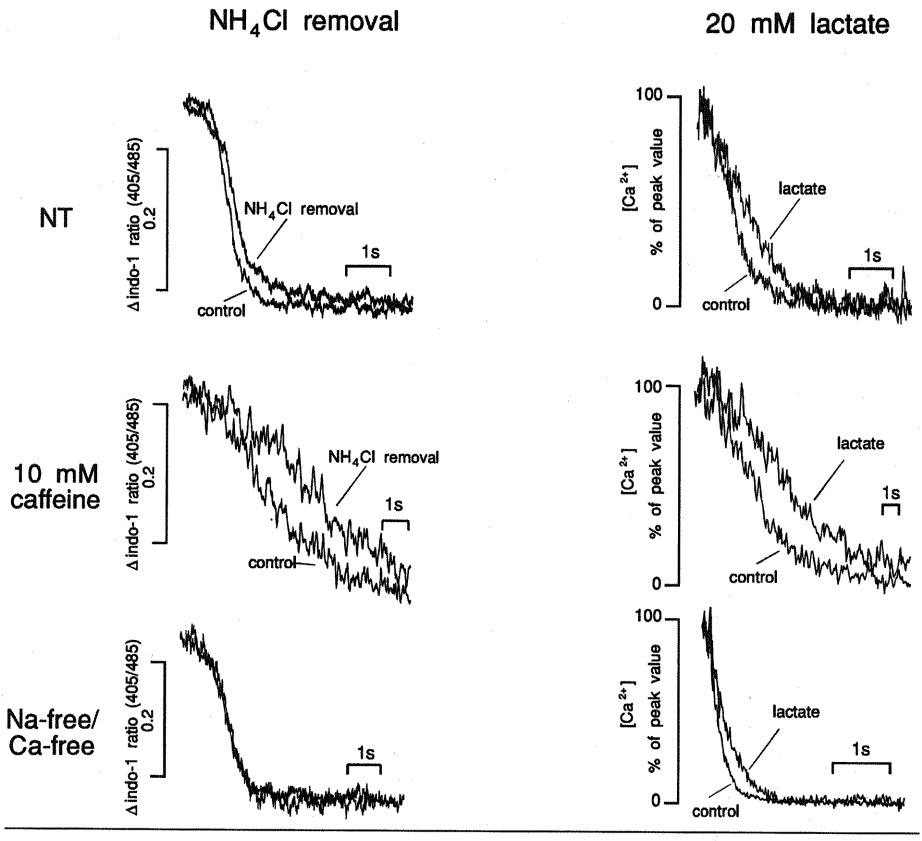

Figure 2. The effects of NH_4Cl removal (left traces) and lactate application (right traces) on the indo-1 fluorescence recovery during rewarming after RCCs are shown. Top traces were elicited during superfusion with NT solution. On the left, the indo-1 fluorescence signal during rewarming after RCCs in control and one minute after removal of NH_4Cl have been superimposed. On the right, traces are shown in control and lactate where Ca^{2+} has been calculated from the calibration parameters described in the Methods section. Middle traces were obtained in the presence of 10 mM caffeine. Bottom traces were acquired the absence of extracellular Ca^{2+} and Na^{2+}.

fluorescence signal during acidosis elicited by NH_4Cl removal or application of lactate was slower than in control (table 2). These results suggest that Ca^{2+} removal from the cytoplasm is affected by acidosis produced either by lactate or by NH_4Cl removal.

In guinea pig ventricular myocytes, the main mechanisms involved in Ca^{2+} extrusion are the SR Ca^{2+} ATPase and Na^+–Ca^{2+} exchange [20]. Together they account for some 95% of relaxation. Since the relaxation after RCCs was slower in acidosis compared with control, these two systems have been investigated separately through use of specific inhibitory conditions. Na^+–Ca^{2+} exchange has been studied using RCCs in the presence of 10 mM caffeine (figure 2, middle traces), and the SR

Table 2. Effects of acidosis on the time to 50% recovery of the indo-1 fluorescence signal during rewarming after RCCs

	NH_4Cl removal	Lactate
NT	Control: 1034 ± 62 ms Acidosis: 1310 ± 27 ms $n = 8$; $p = 0.0034$	Control: 465 ± 55 ms Acidosis: 821 ± 62 ms $n = 16$; $p < 0.0001$
10 mM caffeine	Control: 3948 ± 322 ms Acidosis: 5021 ± 281 ms $n = 8$; $p = 0.0012$	Control: 1852 ± 155 ms Lactate: 2922 ± 289 ms $n = 8$; $p = 0.035$
Na^{+}-free/Ca^{2+}-free	Control: 1879 ± 155 ms Acidosis: 1906 ± 119 ms $n = 13$; p = n.s.	Control: 551 ± 46 ms Acidosis: 772 ± 67 ms $n = 11$; $p = 0.0013$

Ca^{2+} uptake has been investigated by removing the contribution of the exchanger by superfusing the cells with a Na^{+}-free/Ca^{2+}-free solution (figure 2, lower traces). In both groups of experiments, cells were stimulated at 0.5 Hz, and after a 10-second rest, a cooling period in NT solution was applied.

Na^{+}–Ca^{2+} exchange. During the plateau of the RCC, the superfusing solution was changed to a new cold solution containing 10 mM caffeine. When a new plateau of contraction was achieved, the cell was rewarmed using a solution containing 10 mM caffeine but at room temperature. Caffeine application was continued until the decline in indo-1 fluorescence was complete. Rewarming in the presence of caffeine is slower than rewarming performed in the absence of caffeine (note the difference in time scale between the upper and middle traces in figure 2), since the Na^{+}–Ca^{2+} exchanger is likely to be the only mechanism responsible for Ca^{2+} extrusion. The rate of this decline is therefore a good index of the exchanger activity, and it has been used to study this mechanism in acidosis.

The rate of decline in indo-1 fluorescence after a RCC in control and one minute after removal of NH_4Cl, in the presence and absence of 10 mM caffeine, has been measured. Such experiments are illustrated in the middle left traces of figure 2. During acidosis when caffeine was applied, Ca^{2+} extrusion was slower than in control (table 2). Similarly, Ca^{2+} decline during rewarming in the presence of lactate (middle right traces) was 62% ± 14% slower than control if the time-to-50% decline was measured (table 2). These results suggest that acidosis produces a slower extrusion of Ca^{2+} from the cytoplasm via Na^{+}–Ca^{2+} exchange. Three assumptions need to be made to support these findings: 1) Slower mechanisms, such as mitochondria and sarcolemmal Ca^{2+} ATPase, in guinea pig cardiac myocytes account for a constant, small amount of Ca^{2+} removal when SR uptake is ineffective. Bassani et al. [26], using rabbit ventricular myocytes, ascribed approximately 93% of Ca^{2+} extrusion to Na^{+}–Ca^{2+} exchange in the presence of caffeine or thapsigargin. This finding suggests that, in this species, a higher percentage of Ca^{2+} is eliminated from the cytoplasm using the slower mechanisms. Although the rate of activity of mitochondria and sarcolemmal Ca^{2+} ATPase are too slow to affect the twitch

duration (about 37- and 50-fold slower, respectively, than the exchanger at removing Ca^{2+} [42]), they might affect the relaxation after an RCC. 2) Acidosis itself does not affect the relative importance of the slower mechanisms that extrude Ca^{2+} from the cytoplasm. 3) Other factors related to the fluorescence technique, such as Ca^{2+} buffering produced by indo-1, autofluorescence, and sequestration of the dye in noncytoplasmic compartments, are not affected by acidosis.

SR Ca^{2+} ATPase. To assess the role of SR uptake on Ca^{2+} extrusion during acidosis, RCCs were performed in the absence of external Na^+ and Ca^{2+} in control conditions and one minute after removal of NH_4Cl. These experiments are shown in the lower traces in figure 2. The cells were stimulated at 0.5 Hz (not shown). After stimulation was stopped, the cells were superfused with a Na^+-free/Ca^{2+}-free solution at room temperature. After five seconds of rest, rapid cooling was applied and maintained for several seconds. The cooling solution had the same composition as the Na^+-free/Ca^{2+}-free one. Rewarming was then produced by switching back to Na^+-free/Ca^{2+}-free solution at room temperature. The rate of decrease of indo-1 fluorescence was unchanged one minute after removal of NH_4Cl (rate of decline in acidosis was 107% ± 6.1% of control; $n = 13$). Some differences were noted with an identical protocol to the one described above but with the acidosis produced by 20 mM lactate. T50 of the declining phase of the Ca^{2+} signal in lactate was longer than control (table 2). These results show that the Ca^{2+} uptake from the SR is slower when the cell has been superfused for five minutes with 20 mM lactate and suggest that the rate of Ca^{2+} uptake from the SR, the main mechanism of Ca^{2+} removal in these experimental conditions, is affected after five minutes in lactate but is unchanged one minute after removal of NH_4Cl.

To explain this discrepancy, several hypotheses could be forwarded:

1. Since it has been shown that the two acidification techniques produce a similar change in pH, the effect on the SR Ca^{2+} uptake is not pH dependent but is related to lactate itself. The reasons why SR Ca^{2+} uptake changes were not detected after removal of NH_4Cl are unclear. A reduction in the SR Ca^{2+} uptake in acidosis was detected in SR vesicles isolated from embryonic chick ventricular myocardium [16]. However, the experimental conditions and the changes in pH were different (Kohmoto et al. [16] started from pH 7.05 to 6.8 and 6.6, while in these experiments pH changed from 7.2 to 7.0).

2. Rewarming after RCCs in the absence of external Na^+ and Ca^{2+} is a reliable technique to study the SR Ca^{2+} pump only if it is assumed that the minor mechanisms of extrusion, such as mitochondria and the sarcolemmal Ca^{2+} pump, can be ignored. It has been shown that these mechanisms extrude only about 3% of the cytoplasmic Ca^{2+} released during rapid cooling [43] in more physiological conditions. It is not clear whether they could affect the Ca^{2+} extrusion in acidosis. Mitochondria in particular have been found to play an important role in producing the increase in cytoplasmic diastolic Ca^{2+} during acidosis in rat cardiac myocytes

[19]. Whether they could then be affected differently during removal of NH_4Cl or application of lactate is unknown.

3. There could be a time-dependent effect of acidosis. An important difference between the two techniques used to produce intracellular acidosis is that NH_4Cl removal produces a decrease of cytoplasmic pH within one minute. Lactate application produces a slower but more prolonged acidosis. For these reasons, measurements have been performed one minute after NH_4Cl removal and after five minutes in lactate. The different effect on the SR Ca^{2+} uptake could be due to the different duration of the acidosis. The duration of acidosis has already been considered an important factor in producing changes in Ca^{2+} regulation in cardiac muscle. Orchard, in 1987 [22], showed that the amplitude of the Ca^{2+} transient assessed with aequorin in ferret and rat papillary muscles exposed to acidosis has a triphasic time course. Initially, the Ca^{2+} transient is unchanged for a short period, during which force production is reduced. This is followed by a temporary increase and then a reduction to control levels again within few minutes. The same effect was observed after removal of NH_4Cl and in the presence of lactate. A similar triphasic time course was observed by Orchard et al. [33] when spontaneous Ca^{2+} release from the SR during acidosis was studied. In a recent review, Orchard and Cingolani [13] summarized this hypothesis, suggesting the existence of

1. an initial period when a reduction in spontaneous release from the SR could be detected due to an inhibitory effect of pH on the SR,
2. an increase in diastolic cytoplasmic Ca^{2+} that could overcome the pH inhibition and produce an increase in spontaneous release, and
3. a decline in spontaneous activity, presumably due to reduction in cytoplasmic Ca^{2+} as the proton load is removed by pH regulation.

The different phases could be ascribed to the relative speed of action of acidosis on different mechanisms involved in the development of the Ca^{2+} changes. The results obtained after different intervals of acidosis (one minute in NH_4Cl and five minutes in lactate) suggest that the SR Ca^{2+} uptake could be affected in a time-dependent fashion and that this could play a role in determining the phasic changes.

Harrison et al. [17], using rat ventricular myocytes, noted that the increase in the Ca^{2+} transient during acidosis was connected with the increase in $[Na^+]_i$ and that it was abolished by ryanodine. Moreover, they detected an increase in Ca^{2+} stored in the SR (released during application of caffeine) in acidosis. They concluded that a functional SR is required to explain the increase in amplitude of the Ca^{2+} transient initially during acidosis. We have evidence for normal SR Ca^{2+} uptake assessed one minute after removal of NH_4Cl, i.e., during the initial phase of acidosis. The second phase proposed by Orchard and Cingolani could be produced not only by an increased diastolic Ca^{2+} but also from an increased SR Ca^{2+} content that regulates the gain function of Ca^{2+} release [44].

The effect of five minutes of lactate acidosis could be explained by a reduction of SR Ca^{2+} uptake, responsible for a reduction of the SR Ca^{2+} content and therefore for a reduction in the gain of CICR. This suggestion is consistent with the results reported by Fabiato and Fabiato [10] and Kentish and Xiang [45] and could contribute to the third period of the Orchard and Cingolani hypothesis.

It should be noted that we did not observe the temporary increase in the Ca^{2+} transient in the acidotic conditions used. In addition, using fast application of caffeine, we failed to detect an increase in SR Ca^{2+} content in early acidosis induced by NH_4Cl. Since in guinea pig cardiac myocytes the SR Ca^{2+} uptake is slower in comparison with rat and ferret [46], one could suggest that, in this species, an increase of SR Ca^{2+} load during the first part of acidosis does not occur.

Fast application of caffeine

Fast application of caffeine was used during acidosis to study Na^+–Ca^{2+} exchange activity. Although the role of the exchanger in Ca^{2+} extrusion during acidosis has already been studied during the rewarming phase of RCCs in caffeine, the rapid application of caffeine allows the measurement of the transient inward current thought to be carried by the Na^+–Ca^{2+} exchanger. This method is a more direct way of assessing exchanger activity. Both the NH_4Cl removal technique and application of lactate were used. Cells were voltage clamped at their resting membrane potential, and 10 mM caffeine was applied to obtain a reproducible increase in indo-1 fluorescence and transient inward current [20].

NH_4Cl induced acidosis. Figure 3 shows recordings of indo-1 fluorescence and the transient inward current in voltage-clamped cells in control and in acidosis one minute after removal of NH_4Cl. The decline of indo-1 fluorescence in acidosis was significantly slower than in control (T50 in control: 729 ± 28 ms; T50 in acidosis: 858 ± 34 ms; $n = 7$; paired t − test, $p = 0.0045$; T90 in control: 2248 ± 123 ms; T90 in acidosis: 2680 ± 83 ms; $n = 7$; $p = 0.0081$). The amplitude of the transient increase in indo-1 fluorescence was reduced in acidosis by 26.9% ± 6.7% compared with control (amplitude in control: 0.054 ± 0.005 indo-1 ratio units; amplitude in acidosis: 0.039 ± 0.004; $n = 7$; $p = 0.0066$). Although the systolic value (i.e., the maximum level of fluorescence reached on caffeine application) appears reduced in this example, it was not significantly different between the two groups.

The transient inward current simultaneously recorded during acidosis was also affected. Although in the case shown in figure 3 the amplitude of the current was decreased in acidosis, in 11 cells examined, the difference was not significant (current amplitude in control: 315.7 ± 37.5 pA; current amplitude in acidosis: 379.2 ± 56 pA). The T50 was increased by 62% ± 15% (T50 in control: 308 ± 31 ms; T50 in acidosis: 483 ± 55 ms; $n = 11$; $p = 0.003$), again suggesting that the kinetics of Na^+–Ca^{2+} exchange are affected during acidosis.

Lactate-induced acidosis. Figure 4 shows a Ca^{2+} transient and current recorded in control (left panel) and after five minutes in lactate (right panel). When lactate was applied for five minutes, fast application of caffeine elicited a Ca^{2+} transient 19.6%

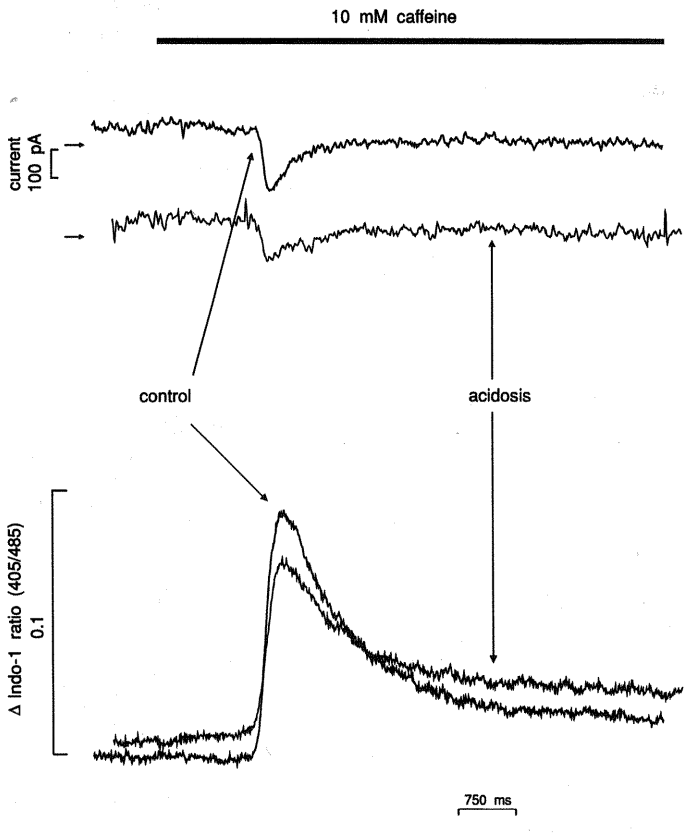

Figure 3. The effects of acidosis elicited by removal of NH_4Cl on the caffeine-induced transient inward current (top traces) and indo-1 fluorescence (bottom traces) are shown. Arrows indicate zero level of current. (From Terracciano and MacLeod [20], with permission of the American Physiological Society.)

± 6% smaller compared with control (amplitude in control: 543.9 ± 54 mM; amplitude in lactate: 416.1 ± 40 nM; $n = 16$; paired t-test, $p = 0.012$). The systolic level of Ca^{2+} was unchanged (control: 568.8 ± 137 nM; lactate: 475.9 ± 41 nM; $n = 16$; $p = 0.7523$), probably because the diastolic level of Ca^{2+} was increased. The rate of the increase of Ca^{2+} in lactate was significantly slower than in control (TTP in control: 569.8 ± 70 ms; TTP in lactate: 753.4 ± 81 ms; $n = 15$; $p = 0.0006$). The time required to produce half of the extrusion of Ca^{2+} from the cytoplasm in lactate was 64.8% ± 10% longer than in control (T50 in control: 795 ± 48 ms; T50 in lactate: 1294.5 ± 101 ms; $n = 16$; $p < 0.0001$). The time constant τ derived from the monoexponential curve fitted on the decay phase of the Ca^{2+} signal was also increased in lactate compared with control (τ in control: 1093 ± 74 ms; τ in lactate:

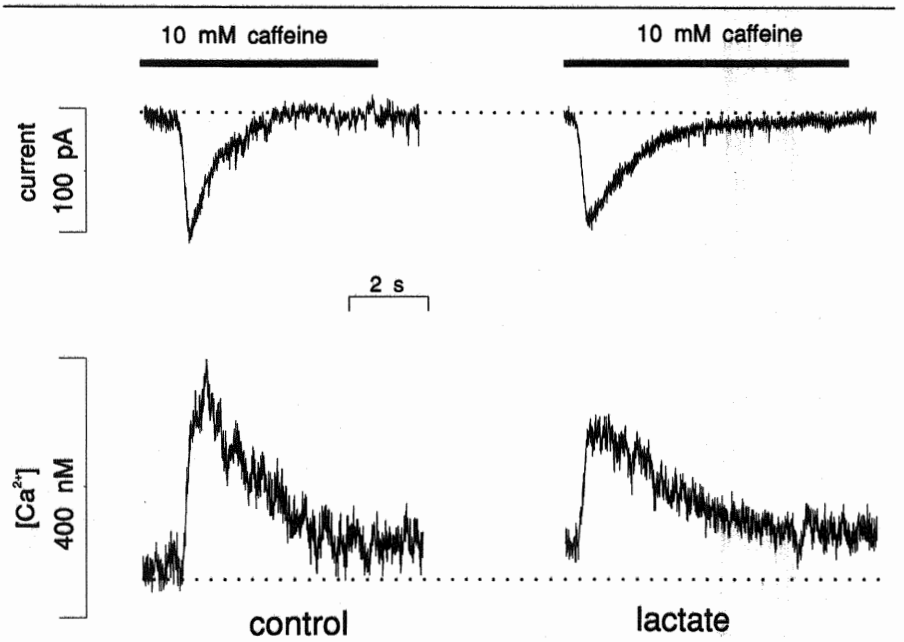

Figure 4. The effects of application of lactate on caffeine-induced transient inward current and cytoplasmic [Ca^{2+}] are shown. Dotted lines indicate level of current and [Ca^{2+}] before application of caffeine in control.

1785 ± 183 ms; $n = 16$; $p = 0.0004$). These results suggest a slower extrusion of Ca^{2+} from the cytoplasm during lactate superfusion.

Figure 4 also shows caffeine-induced inward currents recorded in control and in lactate. The amplitude of the current was not affected by lactate superfusion (amplitude in control: 125 ± 12 pA; amplitude in lactate: 140 ± 27 pA; $n = 18$; $p = 0.479$). The integrated area was also unchanged (area in control: 142 ± 18 pA.s; area in lactate: 190 ± 44 pA.s; $n = 16$; $p = 0.186$). The rate of decay was affected. The time to half decay of the current in lactate was 33.7% ± 9% longer than control (T50 in control: 653 ± 50 ms; T50 in lactate: 890 ± 113 ms; $n = 10$; $p = 0.013$). Similar results were obtained when the decay was analyzed fitting a mono exponential curve. The time constant τ in lactate was 73.3% ± 25% larger than control (τ in control: 0.91 ± 0.1 s; τ in lactate: 1.52 ± 0.27 s; $n = 17$; $p = 0.0104$).

Considerations. Similar results have been obtained in both acidotic conditions when 10 mM caffeine was quickly applied. The main findings are as follows:

1. *The amplitude of the Ca^{2+} transient was smaller in acidosis.* This finding suggests that the releasable Ca^{2+} from the SR is reduced in acidosis compared with control. Nevertheless, there are several difficulties with the interpretation of the indo-1 fluorescence measurements. Firstly, when caffeine is applied, the cytoplasmic [Ca^{2+}]

that is reached could be at a level where the relationship with indo-1 fluorescence is not linear. This outcome could produce an underestimation of the systolic $[Ca^{2+}]$ observed. If, in addition, the diastolic level is increased, the overall measurements will give a reduction in size of the transient. On several occasions, though, the signal was not saturated and a difference in size was still detectable. Secondly, the time-to-peak of the transient in acidosis was slower than in control. In this situation, the same amount of Ca^{2+}, released more slowly from the SR, would produce a smaller amplitude of the transient, since part of it could be reduced effectively by the Na^+–Ca^{2+} exchanger.

2. *The rate of release of Ca^{2+} was reduced in acidosis together with the rate of the increase of the inward current.* It could be speculated that in acidosis, Ca^{2+} is released more slowly from the SR after application of caffeine and therefore is extruded more slowly from the cell via Na^+–Ca^{2+} exchange. Reasons for Ca^{2+} being released from the SR at a slower rate are unclear. It has been shown for skeletal [47] and cardiac [48] ryanodine receptors incorporated in planar bilayers that lower pH inhibits the P_o of the channel. Moreover, when the acidosis was produced in the trans-chamber corresponding to the luminal face, a reduction of the unitary conductance of the channels was found [48]. This result could be responsible for the reduction in the TTP of the Ca^{2+} transients during twitches and during caffeine application. Another explanation is related to the observation that a reduction in SR loading induces a reduction of the rate of release [39]. Since the SR Ca^{2+} content seems to be reduced in acidosis, this finding could explain the reduction in the rate of release independently from a direct effect of pH on ryanodine receptors.

3. *The decline of Ca^{2+} in acidosis was slower than in control.* This result resembles the one obtained after RCCs during rewarming in caffeine.

4. *The transient inward current already ascribed to Na^+–Ca^{2+} decayed more slowly in acidosis.* This result provides more evidence that the kinetics of the exchanger are affected by acidosis. Measuring the current is a more direct way to study Na^+–Ca^{2+} exchange. We have already provided evidence that the current we measure is due to Na^+–Ca^{2+} exchange [20,39]. From the results obtained, it is concluded that Na^+–Ca^{2+} exchange is affected similarly by intracellular acidosis, produced either by NH_4Cl removal or by superfusion with 20 mM lactate.

5. *The amplitude and the area of the transient inward current were unchanged in acidosis.* These results are in contrast to the alteration in size of the caffeine-induced Ca^{2+} transient, which was smaller in acidosis. The actual systolic Ca^{2+} level reached during acidosis was unchanged compared with control. This difference in results between exchange current and the caffeine-induced Ca^{2+} transient may suggest that 1) the amount of Ca^{2+} seen by the exchange does not reflect closely the bulk cytoplasmic Ca^{2+} concentration, 2) Ca^{2+} diffusion is altered in acidosis, and/or 3) Ca^{2+} binding to indo-1 and/or optical characteristics of the dye may change in acidosis, therefore causing a smaller fluorescence transient. While any of the above cannot be ruled out, another explanation for these results is that this method overestimates the exchange current when diastolic $[Ca^{2+}]$ increases. The size of the current generated by caffeine application will be dependent on the systolic level of

Ca^{2+} that is reached. If the systolic level of the Ca^{2+} transient is the same in acidosis as in control, then the absolute size of the exchange current will not be expected to change. From this analysis, when diastolic Ca^{2+} increases during acidosis, the holding current would be expected to be more inward. Nevertheless, no changes in holding current were detected. This outcome could presumably be because this holding current is a mixture of a number of currents (e.g., K^+ current), since in our experiments no attempt was made to inhibit them (with Cs^+, for example). Thus the size of the Na^+–Ca^{2+} exchange current measured in acidosis could be overestimated to an uncertain degree (but related to the increase in diastolic $[Ca^{2+}]$). Although these observations do not affect the main finding that there is a reduction of the kinetics of the exchanger in acidosis, it makes unreliable the estimates of the SR Ca^{2+} content during acidosis.

In conclusion, although more investigations are required to assess the SR Ca^{2+} content, several findings suggest that the kinetics of Na^+–Ca^{2+} exchange are affected in acidosis.

Role of Na^+–H^+ exchange

Several investigators have shown that Na^+–Ca^{2+} exchange is regulated by pH. Philipson et al. [49], using sarcolemmal vesicles isolated from dog ventricles, showed that the exchanger was severely inhibited at pH 6 and stimulated at pH 9. They suggested that this inhibition was due to an intrinsic interaction between H^+ and Na^+–Ca^{2+} exchange. On the other hand, Bountra and Vaughan-Jones [31], using guinea pig papillary muscle and sheep cardiac Purkinje fibers, have reported an increase in intracellular Na^+ during acidosis mediated by an activation of Na^+–H^+ exchange. They showed that after removal of NH_4Cl, the intracellular Na^+ activity in guinea pig tissue increased from 6 to 8 mM. This increase was prevented by application of amiloride, an inhibitor of Na^+–H^+ exchange. $[Na^+]_i$ is an important factor in determining the amount of Ca^{2+} transported by the Na^+–Ca^{2+} exchanger, and so to test whether the kinetics of the exchanger were affected because of the increase in $[Na^+]_i$ or a direct alteration of pH_i, we performed the same inward current measurements during inhibition of the Na^+–H^+ exchanger either with amiloride or EIPA. In this condition, as shown before [15,17,31,50], the increase in $[Na^+]_i$ is prevented, and therefore a direct effect of pH on Na^+–Ca^{2+} exchange could be ascertained.

EIPA was also used, since Na^+–Ca^{2+} exchange is partially affected by amiloride [51]. Moreover, EIPA has been shown in other tissues to be about 100 times more potent and more specific than amiloride for Na^+–H^+ exchange (in rat aortic smooth muscle cells [52]). Since both the drugs are fluorescent, changes in intracellular Ca^{2+} with indo-1 could not be measured. However, the absence of indo-1 loading was a favorable point, since problems associated with it, such as an increase in intracellular Ca^{2+} buffering, were avoided. The experimental protocol was also identical to the previous experiments, but the cells were continuously superfused with 1 mM

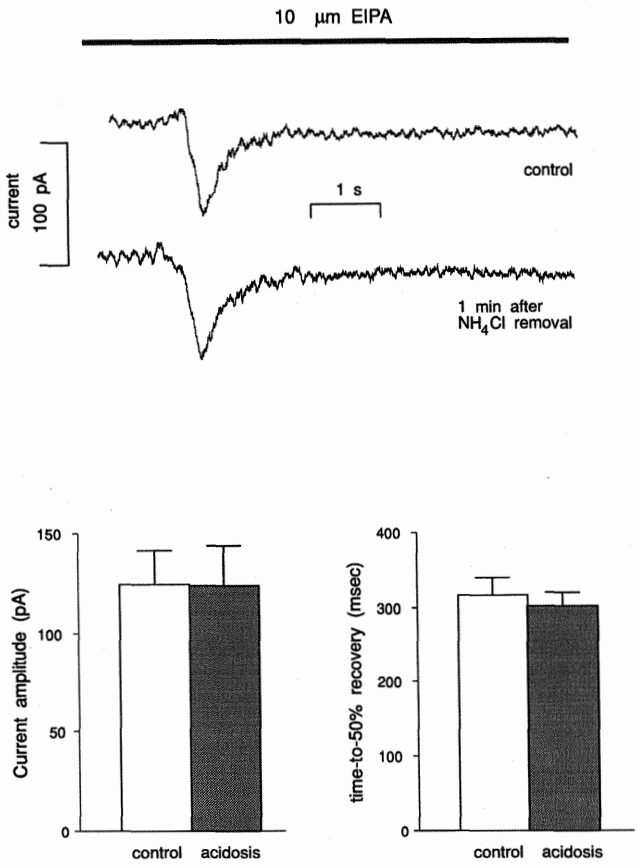

Figure 5. The effects are shown of the inhibition of Na^+–H^+ exchange by EIPA on the caffeine-induced transient inward currents elicited in control and after NH_4Cl removal (top traces). The graphs in the bottom part of the figure show that in the presence of EIPA, no significant difference in current amplitude or recovery was detected between acidosis and control.

amiloride or 10 μM EIPA. The caffeine-induced transient inward current was measured in control and one minute after removal of NH_4Cl.

As expected, the decay of the caffeine-induced transient inward current in amiloride was slower than in control, since Na^+–Ca^{2+} exchange is partially affected by this drug [51] (T50 in control: 250.6 ± 24 ms; T50 in 1 mM amiloride: 374.6 ± 30 ms; $n = 6$; $p = 0.01$). When amiloride was present, no differences in the transient inward current elicited by fast application of caffeine were noted in control and acidosis (current amplitude in control + amiloride: 293.3 ± 29.8 pA; current amplitude in acidosis + amiloride: 294.5 ± 35.1 pA; $n = 12$; $p = 0.979$) (T50 in control + amiloride: 449.4 ± 53.6 ms; T50 in acidosis + amiloride: 434.7 ± 54.3 ms; $n = 11$; $p = 0.849$).

Figure 5 shows that with EIPA used instead of amiloride, no difference in the transient inward current elicited by fast application of caffeine in control and in acidosis was found. The mean change in current amplitude in the presence of 10 μM EIPA in acidosis was 0.4 ± 8% (n = 6). T50 in control + EIPA was 316 ± 24 ms, and T50 in acidosis + EIPA was 315 ± 19 ms (n = 6).

During acidosis, there are two possible ways the efflux of Ca^{2+} via the exchange could be slowed: 1) direct inhibition of the exchange by the increase in intracellular H^+ concentration and/or 2) competitive (allosteric) inhibition of the exchange due to an increase in intracellular Na^+ concentration.

As mentioned above, there is evidence of the direct effect of protons on Na^+–Ca^{2+} exchange in canine cardiac membrane vesicles [49] and in guinea pig ventricular myocytes [53]. Moreover, Doering and Lederer [54], using the giant excised patch technique with guinea pig cardiac myocytes, have shown a direct effect of protons on the exchanger. The authors showed that there is a rapid "primary" blockade of the exchanger produced by protons independent of $[Na^+]$.

On the other hand, an increase in intracellular Na^+ concentration during acidosis has been demonstrated [17,31]. Since the exchanger activity is strictly dependent on $[Na^+]_i$, the slow efflux of Ca^{2+} may be a consequence of increased $[Na^+]_i$. The findings described above are consistent with ones observed in conditions where $[Na^+]_i$ was increased. O'Neill et al. [55] found that the rate constants for decay of caffeine-induced Ca^{2+} transients were significantly slowed when taurine was absent from the cell isolation medium or when ouabain was present in the superfusate. The inclusion of taurine during cell isolation is thought to lower $[Na^+]_i$ [56], and ouabain inhibits the Na^+–K^+ pump, resulting in an increase in $[Na^+]_i$. Thus, their data suggested that a reduction in the rate of decay of the caffeine-induced Ca^{2+} transients could be a consequence of an increase in $[Na^+]_i$.

Finally, the two situations mentioned above could be combined. In 1994, Doering and Lederer [57] developed a model that hypothesized two components to the inhibition of Na^+–Ca^{2+} exchange by protons. In this model, intracellular Na^+ binding to the exchanger enhances the affinity of the exchanger for inhibitory intracellular protons.

In the presence of amiloride or EIPA, the changes in kinetics of the Na^+–Ca^{2+} exchange current were not observed when intracellular pH was lower. The use of these drugs causes a further decrease in cytoplasmic pH after removal of NH_4Cl and a prolongation in the recovery of cytoplasmic pH (e.g., [27,30–32,50,58]). This observation contradicts the hypothesis of a direct effect of H^+ on the Na^+–Ca^{2+} exchanger. Moreover, these compounds have been shown to inhibit the increase in intracellular Na^+ and the resultant increase in active force during acidosis [15,17,31]. It may be suggested that the increase in $[Na^+]_i$ during acidosis is the reason for changes in the kinetics of Na^+–Ca^{2+} exchange, since preventing such an increase abolishes the slower rate of decay of the Na^+–Ca^{2+} exchange current.

Relative contribution of different mechanisms to Ca^{2+} extrusion during acidosis

From the observations so far, it is clear that several mechanisms together contribute to the impairment of Ca^{2+} handling observed during acidosis. An attempt was made to determine their relative role in Ca^{2+} extrusion from the cytoplasm during acidosis using a technique described by Hryshko et al. [59], namely, paired RCCs.

Briefly, during rewarming after an RCC, Ca^{2+} is extruded from the cytoplasm by several mechanisms. Some of these mechanisms take Ca^{2+} out the cell (Na^+–Ca^{2+} exchange and sarcolemmal Ca^{2+} ATPase) and others accumulate it (SR and mitochondria). Since rapid cooling releases Ca^{2+} from the SR, eliciting a second cooling period after the rewarming phase following the first RCC will produce a release of the Ca^{2+} accumulated within the SR during that rewarming phase. This method can therefore be used to measure the ability of the SR to compete with the other mechanisms for Ca^{2+} uptake. If Na^+–Ca^{2+} exchange is inhibited by superfusing the cell with Na^+-free/Ca^{2+}-free solution, the amount of Ca^{2+} released from the SR during the second cooling period will be the total Ca^{2+} minus that extruded by the slow systems (mitochondria and sarcolemmal Ca^{2+} ATPase). Subtracting the second RCC obtained in NT from this will give the approximate percentage of Ca^{2+} extruded by Na^+–Ca^{2+} exchange [59].

Paired RCCs in NT and Na^+-free/Ca^{2+}-free solution were used in control conditions and after five minutes in 20 mM lactate. A five-minute application of acetate was also used to produce a more stable intracellular acidification. Approximately one minute is required for the protocol to be performed. NH_4Cl removal, therefore, is not a reliable acid loading technique, since the acidosis obtained varies within a short time interval. It should be noted that the amplitude of the contracture was used, since the indo-1 fluorescence during the cooling contractures had values close to saturation.

The cells were initially stimulated at 0.5 Hz. Stimulation was stopped, and after a five-second rest, rapid cooling was applied. Cooling was maintained until the contracture developed completely. Rewarming was then applied, and 10 seconds later a second cooling period was elicited. When RCCs in Na^+-free/Ca^{2+}-free solutions were performed, the superfusion in Na^+-free/Ca^{2+}-free solution was started after stopping stimulation and was continued throughout both the cooling periods. In these experiments performed in control conditions, the ratio (second RCC) RCC_2 to (first RCC) RCC_1 was approximately 0.64, suggesting that in these cells the SR took up about 64% of the Ca^{2+} released from the previous RCC. After five minutes in lactate, the ratio RCC_2/RCC_1 was 0.39, suggesting that the percentage of Ca^{2+} taken up by the SR in acidosis is reduced to approximately 39% (figure 6, upper graph). After five minutes in acetate, the ratio $RCC_2/RCC_1 \times 100$ was approximately 52%, significantly lower than that of the control but also significantly higher than lactate. These results suggest that, during rewarming after RCCs, SR Ca^{2+} uptake is reduced in acidosis. These results also suggest a more specific effect of lactate on Ca^{2+} regulation, independent of the accompanying acidosis.

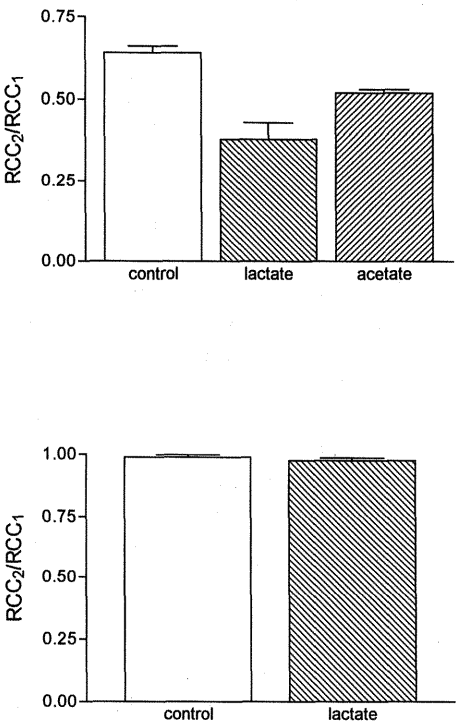

Figure 6. Top graph shows results from paired RCCs in NT. RCC_2/RCC_1 was reduced in lactate and in acetate compared with control (control: 0.641 ± 0.01, $n = 28$; lactate: 0.380 ± 0.05, $n = 14$; acetate: 0.522 ± 0.01, $n = 15$; t-test between control and lactate, $p < 0.0001$; between control and acetate, $p < 0.001$). RCC_2/RCC_1 in lactate was significantly smaller than in acetate ($p = 0.012$). Bottom graph shows results from paired RCC in Na^+-free/Ca^{2+}-free solution. No difference was detected between control conditions and lactate (control: 0.989 ± 0.01, $n = 12$; lactate: 0.975 ± 0.01, $n = 12$; t-test, $p = 0.333$).

To assess the amount of Ca^{2+} extruded via Na^+–Ca^{2+} exchange and the minor mechanisms in acidosis, paired RCCs were performed in Na^+-free/Ca^{2+}-free solution (figure 6, lower graph). No difference was found in control and in lactate (RCC_2 was approximately 96% of RCC_1 in both cases). These results suggest that mitochondria and sarcolemmal Ca^{2+} ATPase account for about 4% of Ca^{2+} extrusion and that their relative role is unchanged after five minutes in lactate.

These findings suggest that after five minutes in lactate, the relative contribution of the SR Ca^{2+} ATPase to the removal of Ca^{2+} from the cytoplasm is reduced. Since the minor systems seem to have an unchanged role, the relative contribution of Na^+–Ca^{2+} exchange is increased. This happens despite an increase in $[Na^+]_i$, which is responsible for slower kinetics of the exchanger. The implications of these results are 1) a possible depletion of Ca^{2+} from the SR in lactate, which could explain the reduction in the size of the caffeine-induced Ca^{2+} transient described

above and which is consistent with other authors [10,45] and 2) an increase in diastolic cytoplasmic Ca^{2+} observed after five minutes in lactate due to slower kinetics of Na^+–Ca^{2+} exchange in conditions when this system is the more important mechanism in Ca^{2+} extrusion from the cytoplasm. Interestingly, when acetate was used to produce intracellular acidosis, the relative contribution of the exchanger to Ca^{2+} extrusion was also increased. However, the value was significantly smaller than the one obtained in lactate, suggesting that, although reduction in intracellular pH can be responsible in part for the effect observed, a portion could be more specifically ascribed to lactate itself.

To accept these results, some assumptions need to be made. The first is that relative changes in cell shortening correspond to relative changes in Ca^{2+} released from the SR, as suggested by Hryshko et al. [59].

Another important assumption regards the effect of pH on the shortening–pCa relationship. It has been shown in skinned multicellular preparations that changes in pH affect myofilament sensitivity to Ca^{2+} (e.g., [10–12]) and therefore the force produced. In addition, it has been reported that the tension–pCa relationship curves at different pH shift in parallel on the pCa axis, without changes in slope [11]. A possible source of misinterpretation of the results in acidosis could be a nonlinear shortening–pCa relationship over the range of [free Ca^{2+}] encountered when the SR is emptied with RCCs or caffeine application. Nevertheless, Orchard and Kentish [11] showed that in *skinned* trabeculae from the guinea pig at pH 7.2 and pH 7.0 for a range of [free Ca^{2+}] up to 3 μM, the relationship between force and [Ca^{2+}] was approximately linear. These results suggest that acidosis does not affect the linearity of the tension–[Ca^{2+}] relationship for [Ca^{2+}] up to 3 μM but does reduce its slope. For the same [Ca^{2+}], a smaller tension would therefore be predicted in acidosis. However, since the paired-RCCs method compares the amplitude of the second RCC with the first at the same pH, the ratio RCC_2/RCC_1 is independent of differences in myofilament sensitivity, and so the technique can be used to assess the *relative* release of Ca^{2+} from the SR compared with the release during a first RCC.

A third important assumption is that the changes in threshold [Ca^{2+}] for the activation of myofilaments during acidosis do not affect the results. It has been shown in myofibrillar preparations that lower pH decreases the threshold [Ca^{2+}] for myofilament activation [10,11]. One possibility is that because in acidosis force does not increase until higher [Ca^{2+}] is reached, one could underestimate the amount of Ca^{2+} released from the SR. From the data reported in Orchard and Kentish [11] at pH 7.2 and pH 7.0, the minimum [Ca^{2+}] required to generate tension was 318 nM and for pH 7.0 was 420 nM, suggesting that the amplitude of the contraction is slightly underestimated in acidosis. However, the diastolic [Ca^{2+}] is increased during acidosis. This could compensate to some extent for an increased threshold [Ca^{2+}] of myofilament activation, reducing the larger difference between diastolic [Ca^{2+}] and level of activation predicted in acidosis. It should be emphasized again that these results were extrapolated from experiments performed in skinned multicellular preparations and that their application in the evaluation of the function of isolated cardiac myocytes could be misleading.

CONCLUSIONS

During intracellular acidosis produced either by NH_4Cl removal or by application of lactate, diastolic $[Ca^{2+}]$ was increased, and Ca^{2+} transient amplitude was reduced and its time course prolonged. Ca^{2+} extrusion from the cytoplasm, studied by measuring the decline of indo-1 fluorescence during rewarming after RCCs, was slower in acidosis compared with control. Ca^{2+} extrusion was still slower in the presence of caffeine, suggesting that Na^+–Ca^{2+} exchange is affected by acidosis. Experiments performed during inhibition of Na^+–H^+ exchange, in order to prevent the increase in intracellular Na^+ during acidosis, showed that $[Na^+]_i$ plays an important role in the slower Ca^{2+} extrusion mediated by Na^+–Ca^{2+} exchange.

RCCs in Na^+-free/Ca^{2+}-free solutions were performed to investigate the SR Ca^{2+} uptake in acidosis. One minute after removal of NH_4Cl, no difference in Ca^{2+} extrusion compared with control was detected. However, after five minutes in lactate, Ca^{2+} extrusion brought about by SR Ca^{2+} ATPase was slower than in control conditions. Several hypotheses have been forwarded to explain these different results.

Finally, using paired RCCs, we have shown that the relative contribution of SR Ca^{2+} uptake to Ca^{2+} extrusion during acidosis produced by lactate or acetate is reduced, presumably in favor of the Na^+–Ca^{2+} exchanger.

REFERENCES

1. Katz AM, Hecht HH. 1969. The early "pump" failure of the ischemic heart. Am J Med 47:497–502.
2. Allen DG, Lee JA, Smith GL. 1989. The consequences of simulated ischaemia on intracellular Ca^{2+} and tension in isolated ferret ventricular muscle. J Physiol 410:297–323.
3. Allen DG, Morris PG, Orchard CH, Pirolo JS. 1985. A nuclear magnetic resonance study of metabolism in the ferret heart during hypoxia and inhibition of glycolysis. J Physiol 361:185–204.
4. McNamara JJ, Soeter JR, Suehiro GT, Anema RJ, Smith GT. 1974. Surface pH changes during and after myocardial ischemia in primates. J Thorac Cardiovasc Surg 67:191–194.
5. Neely JR, Whitmer JT, Rovetto MJ. 1975. Effect of coronary blood flow on glycolytic flux and intracellular pH in isolated rat hearts. Circ Res 37:733–741.
6. Cobbe SM, Poole-Wilson PA. 1980. Tissue acidosis in myocardial hypoxia. J Mol Cell Cardiol 12:761–770.
7. Lange R, Kloner LA, Zierler M, Carlson N, Seiler M, Khuri SF. 1983. Time course of ischemic alterations during normothermic and hypothermic arrest and its reflection by on-line monitoring of tissue pH. J Thorac Cardiovasc Surg 86:418–434.
8. Gevers W. 1977. Generation of protons by metabolic processes in heart cells. J Mol Cell Cardiol 9:867–874.
9. Gaskell WH. 1880. On the tonicity of the heart and blood vessels. J Physiol 3:48–75.
10. Fabiato A, Fabiato F. 1978. Effects of pH on the myofilaments and the sarcoplasmic reticulum of skinned cells from cardiac and skeletal muscle. J Physiol 276:233–255.
11. Orchard CH, Kentish JC. 1990. Effects of changes of pH on the contractile function of cardiac muscle. Am J Physiol 258:C967–C981.
12. Solaro RJ, Lee JA, Kentish JC, Allen DG. 1988. Effects of acidosis on ventricular muscle from adult and neonatal rats. Circ Res 63:779–787.
13. Orchard CH, Cingolani HE. 1994. Acidosis and arrhythmias in cardiac muscle. Cardiovasc Res 28:1312–1319.
14. Bers DM, Ellis D. 1982. Intracellular calcium and sodium activity in sheep heart Purkinje fibres. Effect of changes of external sodium and intracellular pH. Pflugers Arch 393:171–178.
15. Kim D, Smith TW. 1988. Cellular mechanisms underlying calcium–proton interactions in cultured chick ventricular cells. J Physiol 398:391–410.

16. Kohmoto O, Spitzer KW, Movsesian MA, Barry WH. 1990. Effects of intracellular acidosis on $[Ca^{2+}]_i$ transients, transsarcolemmal Ca^{2+} fluxes, and contraction in ventricular myocytes. Circ Res 66:622–632.
17. Harrison SM, Frampton JE, McCall E, Boyett MR, Orchard CH. 1992. Contraction and intracellular Ca^{2+}, Na^+, and H^+ during acidosis in rat ventricular myocytes. Am J Physiol 262:C348–C357.
18. Cairns SP, Westerblad H, Allen DG. 1993. Changes in myoplasmic pH and calcium concentration during exposure to lactate in isolated rat ventricular myocytes. J Physiol 464:561–574.
19. Gambassi G, Hansford RG, Sollott SJ, Hogue BA, Lakatta EG, Capogrossi MC. 1993. Effects of acidosis on resting cytosolic and mytochondrial Ca^{2+} in mammalian myocardium. J Gen Physiol 102:575–597.
20. Terracciano CMN, MacLeod KT. 1994. The effect of acidosis on Na^+/Ca^{2+} exchange and consequences for relaxation in isolated cardiac myocytes from guinea-pig. Am J Physiol 267:H477–H487.
21. Allen DG, Orchard CH. 1983. The effects of changes of pH on intracellular calcium transients in mammalian cardiac muscle. J Physiol 335:555–567.
22. Orchard CH. 1987. The role of the sarcoplasmic reticulum in the response of ferret and rat heart muscle to acidosis. J Physiol 384:431–449.
23. Bridge JHB. 1986. Relationships between sarcoplasmic reticulum and trans-sarcolemmal Ca^{2+} transport revealed by rapidly cooling rabbit ventricular muscle. J Gen Physiol 88:437–473.
24. Bers DM, Bridge JHB, Spitzer KW. 1989. Intracellular Ca^{2+} transients during rapid cooling contractures in guinea-pig ventricular myocytes. J Physiol 417:537–553.
25. Callewaert G, Cleeman L, Morad M. 1989. Caffeine-induced Ca^{2+} release activates Ca^{2+} extrusion via Na^+–Ca^{2+} exchanger in cardiac myocytes. Am J Physiol 257:C147–C152.
26. Bassani JWM, Bassani RA, Bers DM. 1994. Relaxation in rabbit and rat cardiac cells: species-dependent differences in cellular mechanisms. J Physiol 476:279–293.
27. MacLeod KT, Harding SE. 1991. The effects of phorbol ester on contraction, intracellular pH and intracellular Ca^{2+} in isolated mammalian ventricular myocytes. J Physiol 444:481–498.
28. Steadman BW, Moore KB, Spitzer KW, Bridge JH. 1988. A video system for measuring motion in contracting heart cells. IEEE Trans Biomed Eng 35:264–272.
29. Grynkiewicz G, Poenie M, Tsien RY. 1985. A new generation of Ca^{2+} indicators with greatly improved fluorescence properties. J Biol Chem 260:3440–3450.
30. Deitmer JW, Ellis D. 1980. Interactions between the regulation of the intracellular pH and sodium activity of sheep cardiac Purkinje fibres. J Physiol (Lond) 304:471–488.
31. Bountra C, Vaughan-Jones RD. 1989. Effect of intracellular and extracellular pH on contraction in isolated, mammalian cardiac muscle. J Physiol 418:163–187.
32. Bountra C, Powell T, Vaughan-Jones RD. 1990. Comparison of intracellular pH transients in single ventricular myocytes and isolated ventricular muscle of guinea-pig. J Physiol 424:343–365.
33. Orchard CH, Houser SR, Kort AA, Bahinski A, Capogrossi MC, Lakatta EG. 1987. Acidosis facilitates spontaneous sarcoplasmic reticulum Ca^{2+} release in rat myocardium. J Gen Physiol 90:145–165.
34. Fry CH, Poole-Wilson PA. 1981. Effects of acid base changes on excitation–contraction coupling in guinea-pig and rabbit cardiac ventricular muscle. J Physiol 313:141–160.
35. Vaughan-Jones RD, Lederer WJ, Eisner DA. 1983. Ca^{2+} ions can affect intracellular pH in mammalian cardiac muscle. Nature 301:522–524.
36. Cobbold PH, Rink TJ. 1987. Fluorescence and bioluminescence measurement of cytoplasmic free calcium. Biochem J 248:313–328.
37. Konishi M, Kurihara S, Sakai T. 1985. Change in intracellular calcium ion concentration induced by caffeine and rapid cooling in frog skeletal muscle fibres. J Physiol 365:131–146.
38. Kurihara S, Sakai T. 1985. Effects of rapid cooling on mechanical and electrical responses in ventricular muscle of guinea-pig. J Physiol 361:361–378.
39. Terracciano CMN, Naqvi RU, MacLeod KT. 1995. Effects of rest interval on the release of calcium from the sarcoplasmic reticulum in isolated guinea pig ventricular myocytes. Circ Res 77:354–360.
40. Bers DM, Bridge JHB. 1989. Relaxation of rabbit ventricular muscle by Na–Ca exchange and sarcoplasmic reticulum calcium pump: ryanodine and voltage sensitivity. Circ Res 65:334–342.
41. Bers DM. 1991. Excitation–Contraction Coupling and Cardiac Contractile Force. Dordrecht: Kluwer Academic Publishers.
42. Bassani RA, Bassani JWM, Bers DM. 1992. Mitochondrial and sarcolemmal Ca^{2+} transport reduce $[Ca^{2+}]_i$ during caffeine contractures in rabbit cardiac myocytes. J Physiol 453:591–608.
43. Terracciano CMN, Naqvi RU, MacLeod KT. 1993. Effects of hypoxia on sodium/calcium exchange in isolated guinea-pig cardiac myocytes. Biophys J 64:A41.

44. Janczewski AM, Spurgeon HA, Stern MD, Lakatta EG. 1995. Effects of sarcoplasmic reticulum Ca^{2+} load on the gain function of Ca^{2+} release by Ca^{2+} current in cardiac cells. Am J Physiol 268:H916–H920.
45. Kentish JC, Xiang J-Z. 1995. Acidosis inhibits Ca^{2+} loading and Ca-induced Ca-release from the SR in saponin-skinned rat myocardium. Biophys J 68:A181.
46. Bassani RA, Bassani JWM, Bers DM. 1994. Relaxation in ferret ventricular myocytes: unusual interplay among calcium transport systems. J Physiol 476:295–308.
47. Ma J, Fill M, Knudson CM, Campbell KP, Coronado R. 1988. Ryanodine receptor of skeletal muscle is a gap junction-type channel. Science 242:99–102.
48. Rousseau E, Pinkos J. 1990. pH modulates conducting and gating behaviour of single calcium release channels. Pflugers Arch 415:645–647.
49. Philipson KD, Bersohn MM, Nishimoto AY. 1982. Effects of pH on Na^+–Ca^{2+} exchange in canine cardiac sarcolemmal vesicles. Circ Res 50:287–293.
50. Lai Z, Hotokebuchi N, Cragoe EJ Jr, Nishi K. 1994. Effects of 5-(N,N-Hexamethylene)Amiloride on action potentials, intracellular Na, and pH of guinea pig ventricular muscle in vitro. J Cardiovasc Pharmacol 23:259–267.
51. Slaughter RS, Garcia ML, Cragoe EJ, Reeves JP, Kaczorowski GJ. 1988. Inhibition of sodium–calcium exchange in cardiac sarcolemmal membrane vescicles. 1 Mechanism of inhibition by amiloride analogues. Biochemistry 27:2403–2409.
52. Little PJ, Cragoe EJ, Bobik A. 1986. Na–H exchange is a major pathway for Na^+ influx in rat vascular smooth muscle. Am J Physiol (Cell Physiol) 251:C707–C712.
53. Earm YE, Irisawa H. 1986. Effects of pH on the Na–Ca exchange current in single ventricular cells of the guinea-pig. Jpn Heart J 27:153–158.
54. Doering AE, Lederer WJ. 1993. The mechanism by which cytoplasmic protons inhibit the sodium–calcium exchanger in guinea-pig heart cells. J Physiol 466:481–500.
55. O'Neill SC, Valdeolmillos M, Lamont C, Donoso P, Eisner DA. 1991. The contribution of Na–Ca exchange to relaxation in mammalian cardiac muscle. Ann NY Acad Sci 639:444–452.
56. Chapman RA, Rodrigo GC. 1990. Intracellular amino acids and the regulation of $[Na^+]_i$: an effect upon calcium tolerance in isolated guinea-pig ventricular myocytes. J Physiol 426:16P.
57. Doering AE, Lederer WJ. 1994. The action of Na^+ as a cofactor in the inhibition by cytoplasmic protons of the cardiac Na–Ca exchanger in the guinea-pig. J Physiol 480(1):9–20.
58. Grace AA, Kirschenlohr HL, Metcalfe JC, et al. 1993. Regulation of intracellular pH in the perfused heart by external HCO_3^- and Na^+–H^+ exchange. Am J Physiol 265:H289–H298.
59. Hryshko LV, Stiffel V, Bers DM. 1989. Rapid cooling contractures as an index of sarcoplasmic reticulum calcium content in rabbit ventricular myocytes. Am J Physiol 257:H1369–H1377.

INTRACELLULAR pH REGULATION AND MYOCARDIAL ISCHEMIA–REPERFUSION INJURY

DANIELLE FEUVRAY

Laboratoire de Physiologic Cellulaire

Summary. Changes in cellular cation homeostasis figure prominently in the pathogenesis of cellular damage during ischemia and reperfusion. With respect to the functional alterations related to reperfusion of the ischemic heart, it is now recognized that reactivation of the Na^+–H^+ exchange (NHE) following ischemia-induced acidosis plays a key role in the development of such alterations. Na^+-coupled acid extrusion via Na^+-linked HCO_3^- influx also contributes to the recovery of pH_i after ischemia. In this context, the diabetic rat heart appears to be an interesting model, since a significant decrease in NHE activity has been shown to be associated with this pathological state. In diabetic myocytes, the acid efflux carried by NHE following an acid load was markedly decreased (for example, a 42% reduction at pH_i 6.9 when compared to normal). On the contrary, acid efflux carried by the Na^+-linked HCO_3^- influx remained nearly identical in both normal and diabetic cells. As a consequence, the marked decrease in total acid efflux from the diabetic myocytes essentially results from the significant decrease in NHE activity. This depressed NHE activity may afford some protection against ischemia–reperfusion injury. A protection was indeed observed in perfused hearts isolated from diabetic rats, in which there was a markedly improved recovery of contractility following ischemia, comparable to that obtained with a pharmacological block of NHE, as compared to normal hearts. This outcome was associated with a markedly slower pH_i recovery.

INTRODUCTION

The maintenance of a steady-state intracellular pH (pH_i) range (7.1–7.2) is of paramount importance for myocyte contractility. The mechanisms employed by cells to maintain their pH within that range include a combination of both

S. Mochizuki, N. Takeda, M. Nagano and N. Dhalla (eds.). THE ISCHEMIC HEART.

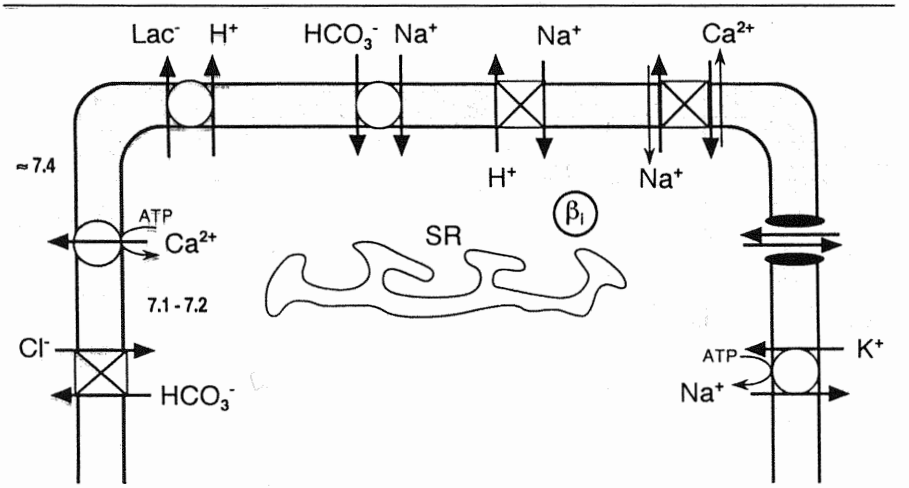

Figure 1. Mechanisms of regulation of intracellular pH (pH_i) in cardiac muscle cells. β_i is the intrinsic H^+ buffering power. The usual mode of operation of ion transporters is shown by the directions of the arrows. Na^+–H^+ is the sodium–proton exchanger; Na^+–HCO_3^- is the sodium-linked bicarbonate influx or sodium–bicarbonate symporter; Lac^-–H^+ is the lactate–proton cotransporter; Cl^-–HCO_3^- is the sodium-independent chloride–bicarbonate exchanger.

intracellular buffering of H^+ ions [1] and specific plasma membrane carriers that extrude excess acid (or alkali) from the cell [2]. Theses various sarcolemmal transport mechanisms include the Na^+–H^+ exchange, a Na^+-linked HCO_3^- influx, a lactate–H^+ cotransport, and the Na^+-independent Cl^-–HCO_3^- exchange. Na^+–H^+ exchange, Na^+, HCO_3^--dependent transport, and lactate–H^+ cotransport are all activated by an intracellular acidification [3,4] and are then responsible for acid (-equivalent) efflux, whereas Cl^-–HCO_3^- exchange acts as an acidifying mechanism by extruding HCO_3^- ions [2,3] (figure 1).

INTRACELLULAR pH DURING ISCHEMIA

Excessive stimulation of glycolytic flux and lack of washout during ischemia leads to proton accumulation [5]. Ischemic acidosis is thought to be predominantly due to a retention of protons from glycolytic ATP turnover [6]. In this context, the diabetic heart provides an interesting model for experimentation. Indeed, myocardial metabolic changes associated with diabetes [7] may very well influence the source and fate of H^+ ions, especially during and following ischemia.

Although the pH_i values of working hearts from streptozotocin (STZ)-induced diabetic rats have been shown to be identical to those of normal hearts in control perfusion conditions, a somewhat slower fall in pH_i is observed in diabetic hearts submitted to a zero-flow ischemic period [8]. This finding may reflect a reduced rate of anaerobic glycolysis, since diabetes has been shown to induce phosphofructokinase inhibition [9]. In addition, tissue lactate levels in our study that used

unpaced hearts [8] were relatively low at the end of the ischemia in the diabetic group, as compared to normal. However, the mean pH_i value reached after a 30-minute period of zero-flow ischemia did not differ significantly from that of normal hearts. The observation of nearly identical kinetics of pH_i decrease during a zero-flow ischemic period in normal and diabetic hearts under similar perfusion conditions may indicate that despite important diabetes-induced myocardial metabolic change [7,10], the intracellular intrinsic H^+ buffering power (β_i) remains unchanged. Intrinsic cardiac buffering capacity was estimated to be increased at lower pH_i, such as it occurs during ischemia [11]. Indeed, our most recent experiments in single ventricular myocytes, in which the intracellular intrinsic H^+ buffering power, β_i, was estimated, clearly show no change in β_i is diabetic myocardial cells as compared to normal myocardial cells [12].

Alternatively, similar kinetics of pH_i decrease with ischemia in both groups of hearts may also be in favor of similar activity of membrane pH_i regulatory mechanisms during the ischemic period. Most likely, there is good experimental evidence indicating that the activity of at least some of these regulatory mechanisms may be rapidly affected during global ischemia. Myocardial ischemia is in fact associated with a decline of both pH_i and external pH [13], and extracellular pH is an important modulator of acid extrusion in the heart [14]. In view of the direct inhibition of Na^+–H^+ exchange by decreased external pH [15], activation of this ionic exchange probably occurs essentially at the beginning of an ischemic episode, and especially when the heart is reperfused at a physiological pH. On the other hand, little is at present known of the modulation of the Na^+-linked HCO_3^- influx, especially of its possible sensitivity to external pH.

Removal of H^+ ions during ischemia might also occur via a lactate–H^+ cotransport [16]. However, the sarcolemmal L-lactate carrier, whose kinetics have been determined in single heart cells from rat and guinea pig hearts [17], may also be rapidly inhibited during ichemia. Inhibition may occur through either reduced transmembrane lactate or pH gradient or both [17]. In this regard, at least the transmembrane lactate gradient should be reduced during ischemia in diabetic hearts in comparison to normal hearts, in relation to the significant decrease in glycolytic flux [7,18].

INTRACELLULAR pH REGULATION DURING POSTISCHEMIC REPERFUSION

Acid efflux from mammalian cardiac cells relies upon a common ion (i.e., Na^+) through the activities of both the Na^+–H^+ exchanger and an Na^+- and HCO_3^--dependent alkalinizing transporter (figure 1). Activation of both systems will promote Na^+ influx into the cell and may thus have indirect consequences on cardiac function. Intracellular pH regulation via the degree of activation of specific sarcolemmal regulatory mechanisms may thus play a major role in the recovery of myocardial pH_i from ischemia and in the recovery of myocardial contractility. Our initial work [8], which compared pH_i data from streptozotocin-induced diabetic rat hearts with reduced activity of the Na^+–H^+ exchange process [19,20] versus normal

hearts with pharmacological block of the exchanger, has provided support for a critical role of the Na^+–H^+ exchanger in the early stage of reperfusion.

Upon reperfusion following ischemia, pH_i recovery occurred more slowly in the diabetics compared to normal hearts. This outcome was observed despite the absence of any significant difference in coronary flow rate on reperfusion between the two groups of hearts. The possibility of a decrease in proton washout to explain the slow kinetics of recovery can therefore be excluded. The most plausible explanation appeared to be the depressed activity of the Na^+–H^+ exchange process previously shown in papillary muscle cells of rats with similar STZ-induced diabetes [19]. Moreover, when the Na^+–H^+ exchange process was pharmacologically inhibited by the presence of amiloride in normal hearts, a slow pH_i recovery was observed. In addition, the higher functional recovery on reperfusion, as assessed by the recoveries of aortic flow and stroke volume, was observed for those hearts with slower pH_i recovery. These data, together with those from studies showing that inhibition of the antiporter could reduce Na^+ accumulation during reperfusion [21,22], have revealed the determinant role of the Na^+–H^+ exchanger in the modulation of the cardiac response to reperfusion.

Specific sarcolemmal transport mechanisms other than the Na^+–H^+ exchanger may also participate in pH_i recovery after ischemia. HCO_3^--activated acid efflux [23] as well as lactate–H^+ cotransport [16] are likely candidates. Their possible contribution was recently examined in hearts of both normal and STZ-induced diabetic rats [4]. Our study showed that an HCO_3^--dependent mechanism contributes to pH_i recovery after ischemia in hearts from diabetic rats, as well as in hearts from normal rats (figure 2). In addition, when the Na^+–H^+ exchanger was pharmacologically blocked in nominally HCO_3^- free solution, a rapid rise in pH_i still occurred at the very beginning of reperfusion, during the first 2–3 minutes (figure 2). This was, however, less abrupt in diabetic hearts. This early rise in pH_i, which could be reduced by supplying external lactate and inhibited by α-cyano-4-hydroxycinnamate in the two groups of hearts, suggests that a coupled H^+–lactate efflux may be a major mechanism for acid extrusion in the initial stage of reperfusion. This mechanism may be less stimulated in diabetic hearts exhibiting a less abrupt initial pH_i recovery, simply because the tissue lactate accumulated at the end of ischemia was found to be significantly lower in those diabetic hearts than in normal hearts.

Upon reperfusion of normal hearts in the presence of HCO_3^- buffer, full activation of both the Na^+–H^+ exchanger and the Na^+-linked HCO_3^- influx would favor Na^+ overloading and consequently Ca^{2+} overload via Na^+–Ca^{2+} exchanger (figure 1; see [24] for review). This outcome may then account for the low recovery of function observed in hearts from normal rats (figure 3). By contrast, a more rapid and higher functional recovery was observed in diabetic hearts. In this respect, it is worth nothing that our most recent experiments, performed on isolated myocytes, showed that the activity of the Na^+-linked HCO_3^- influx is unaffected by diabetes (Le Prigent et al., personal communication). Therefore, the slower pH_i recovery and the better function recovery on reperfusion in diabetic hearts are likely associated with the significant decrease in Na^+–H^+ exchange activity.

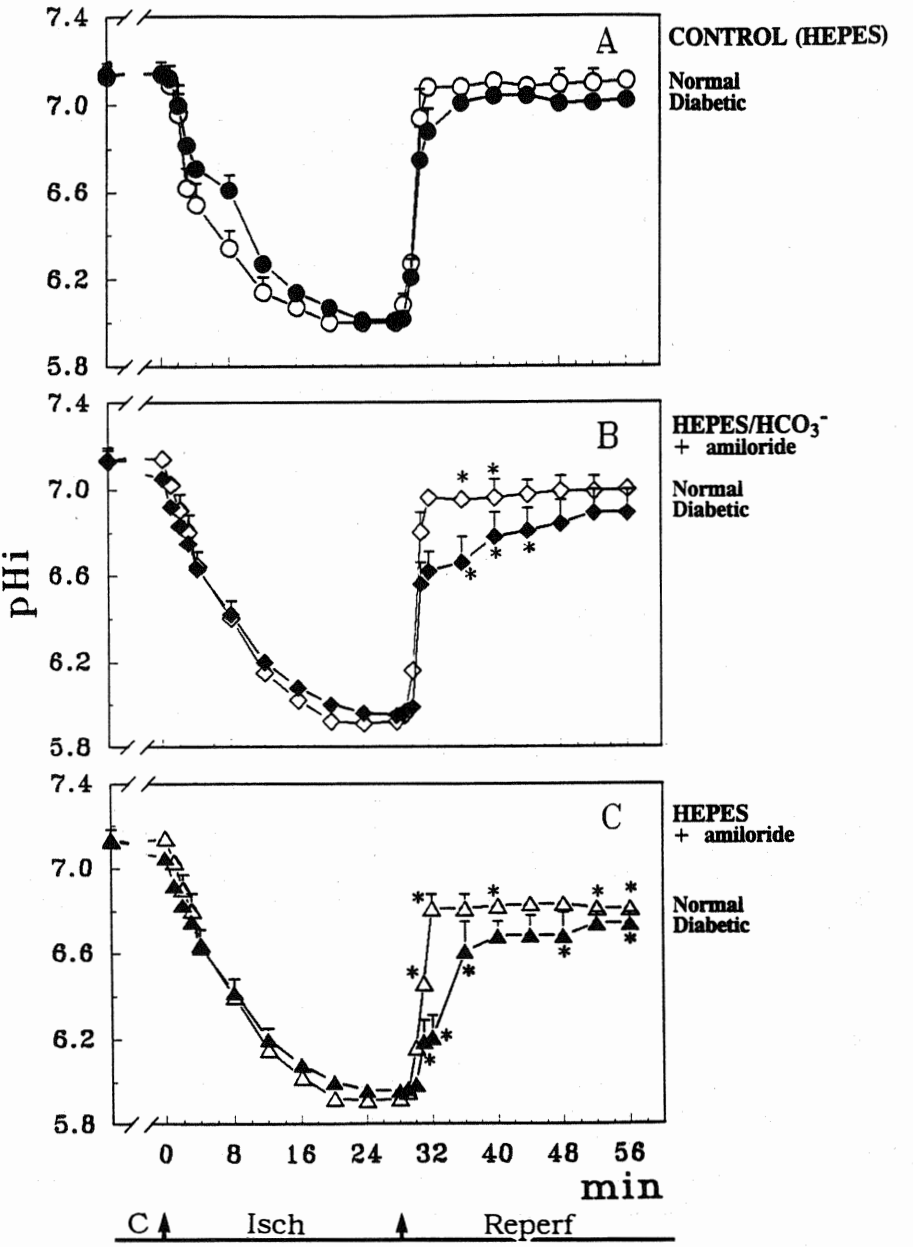

Figure 2. Time courses of changes in pH_i during zero-flow ischemia (28 min at 37°C) and reperfusion of normal and diabetic hearts. Ischemia was induced at zero time. (**A**) Hearts were perfused with a N-2-hydroxyethylpiperazine-N′-2-ethanesulphonic acid (HEPES)-buffered solution. (**B**) Hearts were perfused in the presence of amiloride and received HEPES-buffered solution until switching to HCO_3/CO_2 buffer at the beginning of reperfusion. (**C**) Hearts were perfused with HEPES-buffered solution in the presence of amiloride. *, $p < 0.05$ vs. the corresponding control normal or diabetic hearts. (Reprinted with permission from [4].)

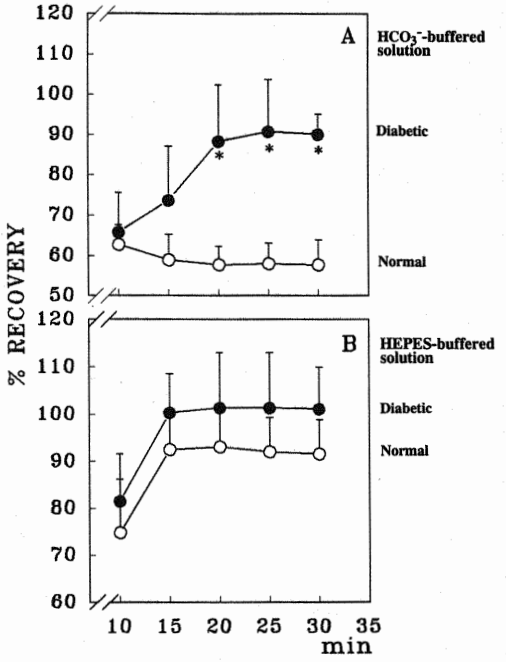

Figure 3. Time courses of functional recovery with reperfusion of normal and diabetic hearts. The percentage of recovery of ventricular function was calculated from the products of heart rate and developed pressure obtained before and after ischemia. Hearts were perfused with either an HCO_3^--buffered solution or a HEPES-buffered solution. $n = 7$ hearts in each group. ★, $p < 0.05$ vs. normal hearts. (Reprinted with permission from [4].)

CONCLUSION

Changes in cellular cation homeostasis figure prominently in the pathogenesis of cellular damage during ischemia and reperfusion. With respect to the functional alterations related to reperfusion of the ischemic heart, reactivation of Na^+-dependent pH_i regulatory mechanisms, following ischemia-induced acidosis, plays a key role in the development of such alterations. In particular, our studies examining pH_i regulation following an ischemic insult in diabetic hearts have made it possible to highlight the critical role played by the Na^+–H^+ exchanger in the modulation of the cardiac response to reperfusion. However, neurohormonal regulation of cardiac pH_i during ischemia and reperfusion has, so far, not been investigated. This regulation could be another important aspect to explore in future studies.

ACKNOWLEDGMENTS

The valuable assistance of Mrs. Françoise James in the preparation of this manuscript is gratefully acknowledged.

REFERENCES

1. Roos A, Boron WF. 1981. Intracellular pH. Physiol Rev 61:296–434.
2. Vaughan-Jones RD. 1988. Regulation of intracellular pH in cardiac muscle. In Bock G, Marsh J (eds), Proton Passage Across Cell Membranes. Ciba Foundation Symposium, vol. 39. Chichester: Wiley, pp. 23–46.
3. Pucéat M, Vassort G. 1995. Neurohumoral modulation of intracellular pH in the heart. Cardiovasc Res 29:178–183.
4. Khandoudi N, Bernard M, Cozzone P, Feuvray D. 1995. Mechanisms of intracellular pH regulation during postischemic reperfusion of diabetic rat hearts. Diabetes 44:196–202.
5. Neely JR, Grotyohann LW. 1984. Role of glycolytic products in damage to ischemic myocardium. Circ Res 55:816–824.
6. Dennis SC, Gevers W, Opie LH. 1990. Protons in ischemia: where do they come from; where do they go to? J Mol Cell Cardiol 23:1077–1086.
7. Feuvray D. 1996. Response to ischemia and reperfusion by the diabetic heart. In Karmazyn M (ed), Myocardial Ischemia: Mechanisms, Reperfusion, Protection. Basel: Birkhäuser Verlag, pp. 409–421.
8. Khandoudi N, Bernard M, Cozzone P, Feuvray D. 1990. Intracellular pH and role of Na^+/H^+ exchange during ischaemia and reperfusion of normal and diabetic rat heart. Cardiovasc Res 24:873–878.
9. Randle PJ, Newsholme EA, Garland PB. 1964. Regulation of glucose uptake by muscle. Effects of fatty acid, ketone bodies and pyruvate, and of alloxan diabetes and starvation, on the uptake and metabolic fate of glucose in rat heart and diaphragm muscle. Biochem J 93:652–665.
10. Wall SR, Lopaschuck GD. 1989. Glucose oxidation rates in fatty acid-perfused isolated working heart from diabetic rats. Biochim Biophys Acta 1006:97–103.
11. Wolfe CL, Gilbert HF, Brindle KM, Radda GK. 1988. Determination of buffering capacity of rat myocardium during ischemia. Biochim Biophys Acta 971:9–20.
12. Le Prigent K, Lagadic-Gossmann D, Feuvray D. 1997. Modulation by pH_0 and intracellular Ca^{2+} of Na^+–H^+ exchange in diabetic rat isolated ventricular Myocites. Circ Res 80:253–260.
13. Neely JR, Whitmer JT, Rovetto MJ. 1975. Effect of coronary blood fow on glycolytic flux and intracellular pH in isolated rat hearts. Circ Res 36:733–741.
14. Vauheel B, de Hemptinne A, Leusen I. 1986. Influence of surface pH on intracellular pH regulation in cardiac and skeletal muscle. Am J Physiol 250:C748–C760.
15. Vaughan-Jones RD, Wu M-L. 1990. Extracellular H^+ inactivation of Na^+–H^+ exchanger in the sheep cardiac Purkinje fibre. J Physiol (Lond) 428:441–466.
16. Poole RC, Halestrap AP. 1993. Transport of lactate and other monocarboxylates across mammalian plasma membranes. Am J Physiol 264:C761–C782.
17. Wang X, Levi AJ, Halestrap AP. 1994. Kinetics of the sarcolemmal lactate carrier in single heart cells using BCECF to measure pH_i. Am J Physiol 267:H1759–H1769.
18. Feuvray D, Idell-Wenger JA, Neely NR. 1979. Effects of ischemia on rat myocardial function and metabolism in diabetes. Circ Res 44:322–329.
19. Lagadic-Gossmann D, Chesnais JM, Feuvray D. 1988. Intracellular pH regulation in papillary muscle from streptozotocin diabetic rats: an ion-sensitive microelectrode study. Pflügers Arch 412:613–617.
20. Pierce GN, Ramjiawan B, Dhalla NS, Ferrari R. 1990. Na^+–H^+ exchange in cardiac sarcolemmal vesicles isolated from diabetic rats. Am J Physiol 258:H255–H261.
21. Tani M, Neely JR. 1989. Role of intracellular Na^+ in Ca^{2+} overload in depressed recovery of ventricular function of reperfused ischemic rat hearts. Circ Res 65:1045–1056.
22. Meng H-P, Pierce GN. 1990. Protective effects of 5-(N,N-dimethyl) amiloride on ischemia–reperfusion injury in hearts. Am J Physiol 258:H1615–H1619.
23. Lagadic-Gossmann D, Buckler KJ, Vaughan-Jones RD. 1992. Role of bicarbonate in pH recovery from intracellular acidosis in the guinea-pig ventricular myocyte. J Physiol (Lond) 458:361–384.
24. Pierce GN, Czubryt. 1995. The contribution of ionic imbalance to ischemia/reperfusion-induced injury. J Mol Cell Cardiol 27:53–63.

This Page Intentionally Left Blank

REGULATION OF $[Na^+]_i$ AND $[Ca^{2+}]_i$ DURING MYOCARDIAL ISCHEMIA AND REPERFUSION IN A SINGLE-CELL MODEL

HIDEHARU HAYASHI, HIROSHI SATOH, HIDEKI KATOH, TAKURO NAKAMURA, SHIHO SUGIYAMA, and HAJIME TERADA

Hamamatsu University School of Medicine

Summary. To study the regulation of $[Na^+]_i$ and $[Ca^{2+}]_i$ during metabolic inhibition (MI) by the perfusion of 3.3 mM amytal and 5 μM CCCP, $[Na^+]_i$ and $[Ca^{2+}]_i$ were measured simultaneously using guinea pig ventricular myocytes that were dual-loaded with SBFI/AM and fluo-3/AM. It was suggested that 1) $[Na^+]_i$ increased during MI by both the activated Na^+ influx via Na^+–H^+ exchange and the suppressed Na^+ extrusion via the Na^+–K^+ pump, 2) Na^+–Ca^{2+} exchange was inhibited during MI, causing the dissociation between $[Na^+]_i$ and $[Ca^{2+}]_i$, 3) Na^+–Ca^{2+} exchange could be reactivated by energy repletion, resulting in an increase of $[Ca^{2+}]_i$ and 4) cell contracture during MI was related to rigor due to energy depletion, while cell contracture after energy repletion was likely to be related to Ca^{2+} overload. We also investigated the regulation of $[Na^+]_i$, $[Ca^{2+}]_i$, and pH_i during simulated ischemia (MI with extracellular acidosis) and reperfusion. Na^+–H^+ exchange was active during simulated ischemia. After reperfusion, Na^+–H^+ exchange was activated further as pH_i was recovered, resulting in an additional $[Na^+]_i$ elevation.

INTRODUCTION

Myocardial ischemia has profound effects on the function and viability of cardiac myocytes. Although reperfusion is necessary for the functional recovery, it is not always beneficial to damaged myocardium. Among several mechanisms implicated in ischemia–reperfusion injury, an abnormal handling of intracellular Ca^{2+} is supposed to be a final pathway of cell injury. However, the mechanisms of Ca^{2+} overload and the causal relationship between Ca^{2+} overload and cell injury in ischemia–reperfusion remain poorly defined [1]. Recent studies have indicated that intracellular Na^+ concentration ($[Na^+]_i$) increases during hypoxia–ischemia and that

S. Mochizuki, N. Takeda, M. Nagano and N. Dhalla (eds.). THE ISCHEMIC HEART.

several Na^+ transport pathways, such as Na^+–H^+ exchange [2], the fast Na^+ channel [3], and the Na^+–K^+ pump [4], are implicated in the increase of $[Na^+]_i$. The elevated $[Na^+]_i$ leads, via Na^+–Ca^{2+} exchange, to the subsequent increase in intracellular Ca^{2+} concentration ($[Ca^{2+}]_i$), causing inotropic or toxic effect [5]. However, it has been demonstrated in cardiac myocytes that the activity of Na^+–Ca^{2+} exchange is dependent on both cellular ATP [6] and pH levels [7]. Therefore, it remains controversial whether the level of $[Ca^{2+}]_i$ is linked to that of $[Na^+]_i$ during hypoxia–ischemia and whether the increase in $[Ca^{2+}]_i$ is a cause of cell contracture. If the interaction of $[Na^+]_i$ and $[Ca^{2+}]_i$ could be monitored in isolated myocytes, it becomes possible to assess the regulating factor for Na^+–Ca^{2+} exchange activity at the cell level and their contribution to cell injury.

We have developed a new method for the simultaneous measurement of $[Na^+]_i$ and $[Ca^{2+}]_i$ in isolated myocytes using sodium-binding benzofuran isophthalate (SBFI) and fluo-3 coupled with digital imaging fluorescence microscopy [8–10]. This technique can provide a great advantage in the investigation of the relationship between these ion concentrations. In the study reported in this chapter, we monitored the relationships among $[Na^+]_i$, $[Ca^{2+}]_i$, and cell shape during metabolic inhibition (MI) and energy repletion (RE) [11]. The aim of the study was to clarify 1) the mechanisms for the increase in $[Na^+]_i$ during MI, 2) the relationship between $[Na^+]_i$ and $[Ca^{2+}]_i$ during MI and ER, and 3) the relationship between $[Ca^{2+}]_i$ and cell injury during MI and ER. We also investigated the regulation of $[Na^+]_i$, $[Ca^{2+}]_i$, and intracellular pH (pH_i) during simulated ischemia (MI with extracellular acidosis) and reperfusion.

MATERIALS AND METHODS

Guinea pig ventricular myocytes were loaded with SBFI/AM (5 μM) and fluo-3/AM (10 μM) and were perfused with the solution equilibrated with 95% O_2–5% CO_2 (pH 7.4) at room temperature. As shown in figure 1, the cells were illuminated by ultraviolet light via an epifluorescence illuminator from a 100-W xenon lamp. Video images were obtained using a Nikon fluor (×20) objective and a silicon-intensified target camera (Hamamatsu Photonics Inc.), with the output digitized by ARGUS (Hamamatsu Photonics Inc.). The exciting wavelengths were 340 and 380 nm for SBFI and 500 nm for fluo-3. After passing the filters, the exciting light was reflected by dichroic mirrors (400 nm half-pass wavelength for SBFI, and 520 nm half-pass wavelength for fluo-3). Images of fluorescence intensities were obtained sequentially at 510 nm for SBFI, and 540 nm for fluo-3, after background subtraction. We used in vivo calibration of SBFI using gramicidin as an ionophore [12]. $[Ca^{2+}]_i$ was expressed as the percent change of fluorescence intensity of fluo-3 against the control level (corrected $F500/F_0500$) [11]. In measurement of pH_i, the cells were loaded with BCECF/AM (0.5 μM) [13,14]. The fluorescent signal was obtained with excitation wave lengths at 490 and 450 nm and an emission wave length at 505–560 nm.

For metabolic inhibition (MI), the perfusate contained 3.3 mM amytal and 5 μM carbonyl cyanide m-chlorophenylhydrazone (CCCP) in the absence of glucose [15].

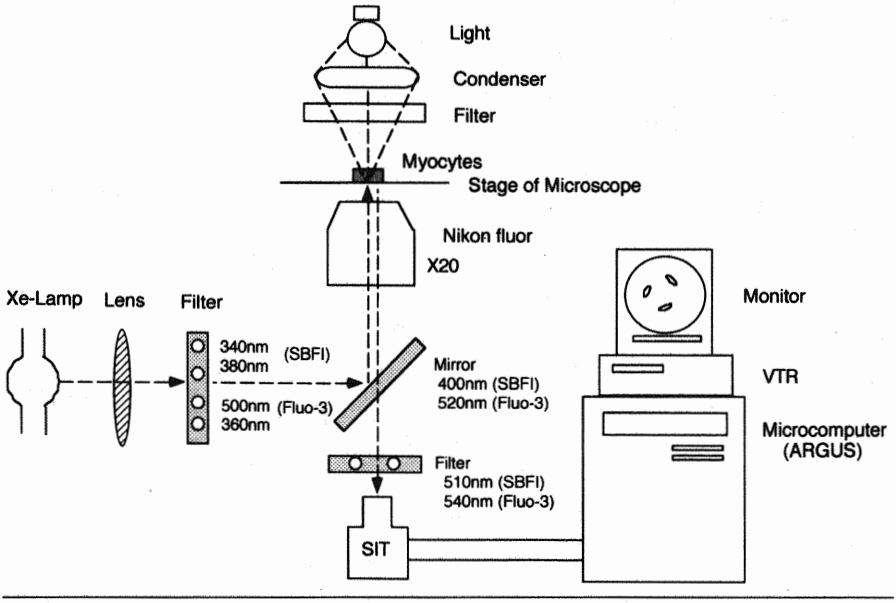

Figure 1. Schematic diagram of apparatus. SIT: a silicon-intensified target camera. Details are in the text.

For energy repletion (ER), 10 mM glucose was applied for 30 minutes in the presence of metabolic inhibitors after 20 minutes of MI. Simulated ischemia was made by MI with extracellular acidosis (pH 6.6), and reperfusion was simulated by the washout of metabolic inhibitors with the solution containing 10 mM glucose at pH 7.4.

REGULATION OF $[Na^+]_i$ AND $[Ca^{2+}]_i$ DURING METABOLIC INHIBITION

Regulation of $[Na^+]_i$

Most myocytes changed from an elongated rod-shaped form to contracted (60%–90% of the initial length) and hypercontracted forms (less than 60% of the initial length) during MI. The time at which cells had contracted varied between 25 and 50 minutes (36.6 ± 1.4 min, n = 29). The intervals at which cell shape changed from contracted to hypercontracted forms were also variable, ranging between 1 and 15 minutes (5.7 ± 0.4 min, n = 24).

During the early phase of MI, three possible Na^+ transport pathways have been implicated to account for the increase in $[Na^+]_i$: 1) increased Na^+ influx via Na^+–H^+ exchange activated by glycolysis-induced intracellular acidosis, 2) Na^+ influx via the fast Na^+ channel, and 3) decreased Na^+ extrusion via the Na^+–K^+ pump. Figure 2 shows the time courses of the changes in $[Na^+]_i$ during 30 minutes perfusion of metabolic inhibitors in the absence of glucose (0G MI), or during 30 minutes of MI in the presence of 1 μM hexamethylene amiloride (HMA), a specific inhibitor of

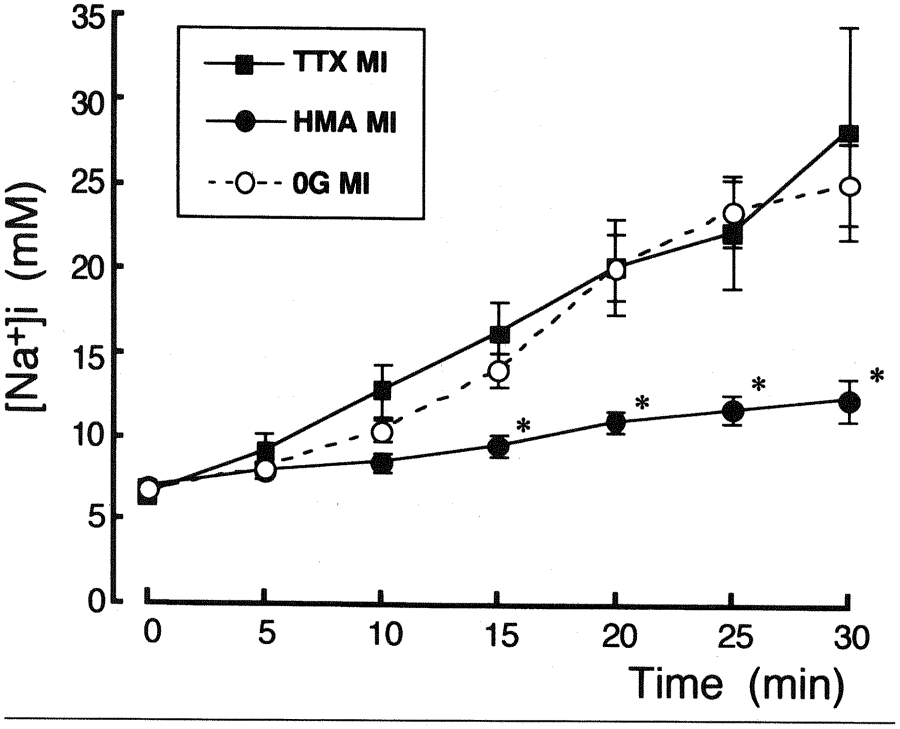

Figure 2. Na^+ influx pathways during metabolic inhibition (MI). MI was achieved by applying 3.3 mM amytal and 5 μM CCCP in the glucose-free Krebs solution. The time courses of $[Na^+]_i$ during 30 minutes perfusion of metabolic inhibitors in the absence of glucose (○: 0G MI; $n = 20$), or in the presence of 10 μM tetrodotoxin (■: TTX; $n = 19$) or 1 μM hexamethylene amiloride (●: HMA: $n = 15$). Drugs were present at least 10 minutes before MI and during the entire period of MI. Cells that remained rod-shaped during this period were used for the comparisons. Values are mean ± SE. *, $p < 0.01$ vs. 0G MI by two way ANOVA [11].

Na^+–H^+ exchange [16], or 10 μM tetrodotoxin (TTX), an inhibitor of the fast Na^+ channel. Cells were preincubated with these agents for at least 10 minutes before MI. There were no changes in $[Na^+]_i$ during this period. During MI, the application of HMA suppressed the increase in $[Na^+]_i$ significantly, whereas TTX had no effect. The rise of $[Na^+]_i$ by the perfusion of metabolic inhibitors was also suppressed by the addition of glucose (data not shown). The values of $[Na^+]_i$ at 30 minutes were 25.0 ± 2.4 mM in MI only, 12.3 ± 1.3 mM in the presence of HMA, and 28.1 ± 6.3 mM in the presence of TTX, respectively [11].

Previous studies proposed that stimulation of Na^+–H^+ exchange could be main pathway for the Na^+ loading during MI [2]. The involvement of Na^+–H^+ exchange was supported by our observation that HMA prevented the increase in $[Na^+]_i$ during the early phase of MI. The involvement of the Na^+ channel is unlikely in our study, because we used resting, unstimulated myocytes. In fact, 10 μM TTX

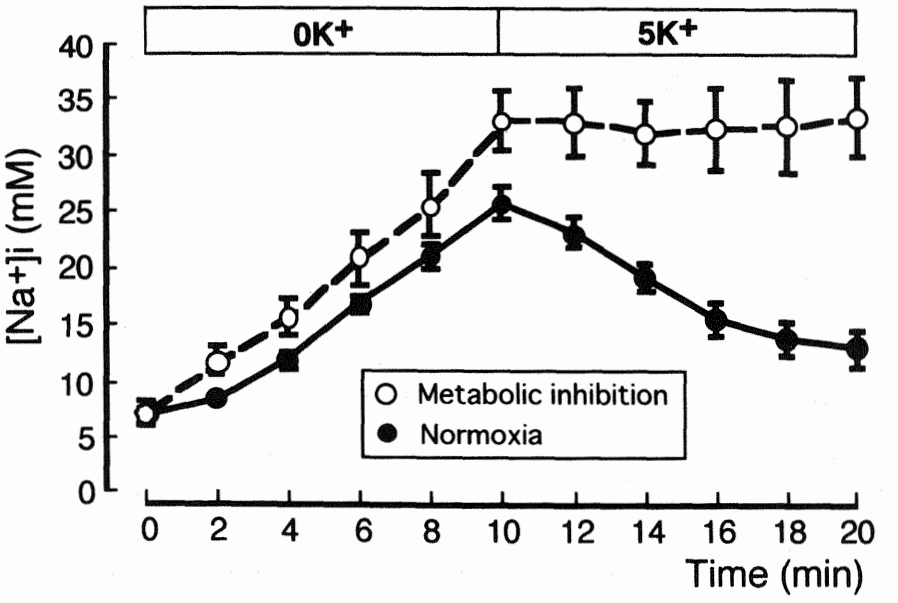

Figure 3. Effects of the reactivation of the Na^+–K^+ pump on the changes in $[Na^+]_i$ during MI. The values of $[Na^+]_i$ when myocytes were perfused for 10 minutes with the solution which K^+ and Ca^{2+} were simultaneously omitted during normoxic perfusion (●; $n = 19$) and during MI (○; $n = 28$). Five mM K^+ was reintroduced (5K^+ in the figure) to reactivate the Na^+–K^+ pump. Values are mean ± SE [19].

could not suppress the increase in $[Na^+]_i$ during the early phase of MI [17]. However, Haigney et al. [18] reported that 1 μM R56865, a compound that blocks noninactivating components of the Na^+ current, blunted the rise in $[Na^+]_i$ during hypoxia, mainly after rigor onset in rat myocytes. Further studies must be performed to determine the possible contribution of the fast Na^+ channel, especially in beating myocytes.

Figure 3 shows the changes in $[Na^+]_i$ when myocytes were exposed to a K^+-free solution, which would inhibit the Na^+–K^+ pump. To prevent immediate Ca^{2+} loading of myocytes exposed to a K^+-free solution [8], Ca^{2+} was removed and 1 mM EGTA was added from the beginning of MI. $[Na^+]_i$ increased from 6.7 ± 0.2 mM to 25.9 ± 1.4 mM ($p < 0.01$) during normoxic perfusion, and from 6.7 ± 0.5 mM to 33.3 ± 2.7 mM ($p < 0.01$) during MI. The readmission of 5 mM K^+ (5 K^+), which reactivates the Na^+–K^+ pump, could partly reverse $[Na^+]_i$ during normoxic perfusion, but could not reverse $[Na^+]_i$ during MI. It was suggested that the Na^+–K^+ pump was significantly inhibited after 10 minutes of MI [19].

It has been reported that when rat myocytes were incubated with 3 mM amytal and 2 μM CCCP, ATP_i fell dramatically and reached minimum by five minutes [15]. Assuming that normoxic cellular ATP_i was 8 mM and that ATP_i fell to

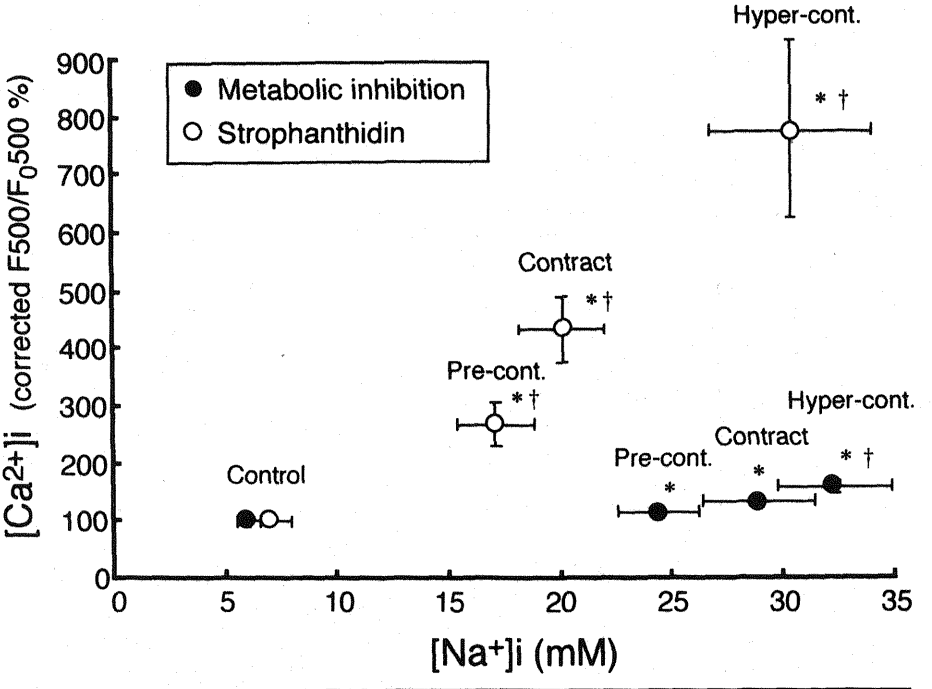

Figure 4. Relationships among cell shape, $[Na^+]_i$, and $[Ca^{2+}]_i$. The relationships among cell shape, $[Na^+]_i$, and $[Ca^{2+}]_i$ were compared between during MI (●; $n = 31$) and during 500 μM strophanthidin perfusion (○; $n = 20$). Control: rod-shaped cells before the perfusion. Pre-cont.: rod shaped cells 1–5 minutes before contracture. Conntract: contracted cells. Hyper-cont.: hypercontacted cells. Values are mean ± SE. *, $p < 0.01$ vs. control in $[Na^+]_i$, †, $p < 0.01$ vs. control in $[Ca^{2+}]_i$ by one-way ANOVA [11].

approximately 2.5% of the normoxic level after MI [15], the calculated ATP_i level would be 0.2 mM. This value is comparable to the reported Michaelis constant for the Na^+–K^+ pump (0.1 mM) [1]. It is, therefore, possible that ATP_i depletion during MI could cause the time-dependent inhibition of the Na^+–K^+ pump, resulting in a gradual increase in $[Na^+]_i$. We cannot exclude the possibility that the Na^+–K^+ pump was inhibited by the decline of pH_i, since the Na^+–K^+ pump activity has been reported to be dependent on pH [20].

In summary, it was indicated that $[Na^+]_i$ during metabolic inhibition in resting myocytes increases by the increased Na^+ influx via Na^+–H^+ exchange and the decreased Na^+ extrusion via the Na^+–K^+ pump.

Effects of metabolic inhibition on $[Na^+]_i$, $[Ca^{2+}]_i$, and cell shape

Next, we investigated the relationships among $[Na^+]_i$, $[Ca^{2+}]_i$, and cell shape during MI and compared with those during strophanthidin perfusion, as illustrated in figure 4. During the perfusion of 500 μM strophanthidin [9], both $[Na^+]_i$ and $[Ca^{2+}]_i$

increased significantly in precontracted cells (rod-shaped), and then spontaneous Ca^{2+} oscillations were observed in contracted cells. The increases in $[Na^+]_i$ and $[Ca^{2+}]_i$ became greater as cell shape changed from a quiescent rod-shaped form to contracted and hypercontracted forms. The values of $[Na^+]_i$ and $[Ca^{2+}]_i$ were 17.1 ± 1.7 mM, 268% ± 38% of the control in precontracted cells; 20.1 ± 1.9 mM, 434% ± 57% of the control when cells contracted; and 30.4 ± 3.6 mM, 774% ± 149% of the control when cells hypercontracted, respectively [9].

On the other hand, there was no increase in $[Ca^{2+}]_i$ in precontracted cells and contracted cells during MI, though $[Na^+]_i$ increased significantly. When cells hypercontracted, $[Ca^{2+}]_i$ increased significantly. The values of $[Na^+]_i$ and $[Ca^{2+}]_i$ were 23.5 ± 1.6 mM, 104% ± 4% of the control in precontracted cells; 28.1 ± 2.4 mM, 117% ± 5% of the control when cells contracted; and 31.5 ± 2.5 mM, 134% ± 7% of the control when cells hypercontracted, respectively. The $[Ca^{2+}]_i$ levels during MI were much lower than those during strophanthidin perfusion ($p < 0.01$) [11]. These data suggested that although $[Na^+]_i$ and $[Ca^{2+}]_i$ increased significantly during MI, the distinct increase in $[Ca^{2+}]_i$ occurred after myocytes had hypercontracted, and that there was a dissociation in the relationship between $[Na^+]_i$ and $[Ca^{2+}]_i$.

Many investigators have reported the activity of the Na^+–Ca^{2+} exchange during hypoxia from various viewpoints, such as Na^+–Ca^{2+} exchange current [6] and the changes in $[Ca^{2+}]_i$ [4]. In this study, we estimated the activity of Na^+–Ca^{2+} exchange from the relationship between $[Na^+]_i$ and $[Ca^{2+}]_i$ in intact ventricular myocytes and suggested that the activity was suppressed during MI. Miura and Kimura [21] revealed that the increase in $[Na^+]_i$ would shift the reversal potential of Na^+–Ca^{2+} exchange toward more negative membrane potentials. Though this shift would thereby promote Ca^{2+} influx by the exchanger, which would lead to an increase in $[Ca^{2+}]_i$, there was no significant increase in $[Ca^{2+}]_i$ during MI in this study. The ATP dependence of the Na^+–Ca^{2+} exchange has been reported in cardiac vesicles [22], giant excised cardiac sarcolemmal patches [6], and cardiac myocytes [23]. Doering and Lederer [7] also showed that protons inhibit Na^+–Ca^{2+} exchange. It is, therefore, likely that the dissociation between $[Na^+]_i$ and $[Ca^{2+}]_i$ during MI was related to the inhibition of Ca^{2+} entry via Na^+–Ca^{2+} exchange by both ATP depletion and intracellular acidosis.

Figure 5 summarizes the effects of various agents on the changes in the percent of rod-shaped cells, $[Na^+]_i$, and $[Ca^{2+}]_i$ during 50 minutes of MI. The perfusion of 1 μM HMA completely abolished the increase in $[Na^+]_i$ but did not affect the increase in $[Ca^{2+}]_i$ nor the percent of rod-shaped cells. This finding implies that the increase in $[Ca^{2+}]_i$ was independent of the increase in $[Na^+]_i$. In other words, Ca^{2+} influx via Na^+–Ca^{2+} exchange (or reduced Ca^{2+} extrusion via the exchange) was not responsible for the increase in $[Ca^{2+}]_i$. Therefore, the increase in $[Ca^{2+}]_i$ could be related to the depression of other regulatory mechanisms of $[Ca^{2+}]_i$, such as sarcolemmal Ca^{2+}–ATPase and/or SR Ca^{2+} uptake. When Ca^{2+}-free solution (with 1 mM EGTA) was perfused, $[Ca^{2+}]_i$ was significantly lower than that in MI, but the decrease of the percent of rod-shaped cells was not attenuated. The increase in

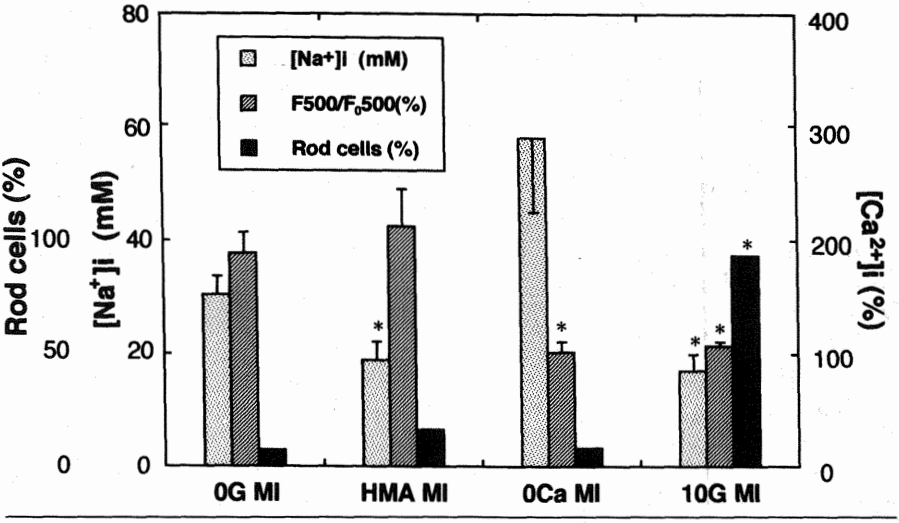

Figure 5. Contributing factors for the changes in cell shape, $[Na^+]_i$, and $[Ca^{2+}]_i$ during MI. MI was achieved by applying 3.3 mM amytal and 5 μM CCCP for 50 minutes in glucose-free Krebs solution (0G MI). The effects of 50 minutes perfusion of 1 μM hexamethylene amiloride (HMA), Ca^{2+}-free solution (0Ca), or 10 mM glucose (10G) on the increases in $[Na^+]_i$ and $[Ca^{2+}]_i$ cexpressed as corrected $F500/F_0500$) and on the percent of rod-shaped cells by metabolic inhibitors were examined. Values are mean ± SE and compared with those in 0G MI. *, $p < 0.01$ by one-way ANOVA, or $p < 0.05$ by chi-squared test [11].

$[Na^+]_i$ was obviously greater than that in MI, presumably as a result of increased sarcolemmal Na^+ permeability [24]. These data suggested that the increase in $[Na^+]_i$ or $[Ca^{2+}]_i$ was not a necessary prerequisite for cell contracture during MI. Under the conditions that oxidative phosphorylation is inhibited by metabolic inhibitors, glycolysis and glucose uptake are accelerated. When glucose was perfused with metabolic inhibitors, cells could remain viable using glycolytic energy [14]. After 50 minutes perfusion of metabolic inhibitors in the presence of 10 mM glucose (10G MI), only 2 of 28 myocytes developed contracture. The increases in $[Na^+]_i$ and $[Ca^{2+}]_i$ were much less than those during MI.

We showed that cell contracture during MI was not related to Ca^{2+} overload but was related to rigor due to energy depletion. In fact, the contracture developed before significant increase in $[Ca^{2+}]_i$ occurred and was not protected by the perfusion of Ca^{2+}-free solution [25,26]. In contrast, the presence of 10 mM glucose was effective for the preservation of rod-shaped cells [14]. In this study, we did not measure cellular ATP levels. Precise information about the ATP levels in individual myocytes is necessary to appreciate the contribution of ATP levels to the changes in ionic concentrations or those in cell morphology. Bowers et al. [27] estimated cytosolic ATP level using firefly luciferase microinjected into isolated myocytes and demonstrated that cell shortening during MI coincided with an abrupt fall in cytosolic ATP.

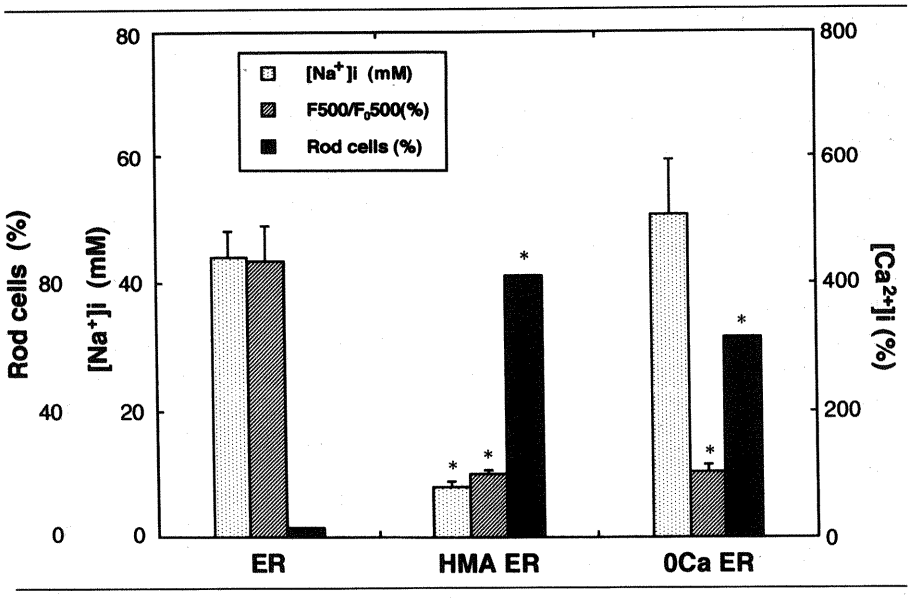

Figure 6. Effects of energy repletion (ER) on the changes is cell shape, $[Na^+]_i$, and $[Ca^{2+}]_i$. After 20 minutes of MI, 10 mM glucose was applied for 390 minutes (ER). The effects of the perfusion of 1 μM HMA or Ca^{2+}-free solution (0Ca) on the increases in $[Na^+]_i$ and $[Ca^{2+}]_i$ (expressed as corrected $F500/F_0500$) and on the percent of rod-shaped cells were examined. Drugs were present at least 10 minutes before MI and during entire periods of MI and ER. Values are mean ± SE and compared with those in ER only. *, $p < 0.01$ by one-way ANOVA, or $p < 0.05$ by chi-squared test [11].

It was concluded that energy depletion could be a main cause for both the cell contracture and the changes in ionic concentrations during MI.

EFFECTS OF ENERGY REPLETION ON $[Na^+]_I$, $[Ca^{2+}]_I$, AND CELL SHAPE

Figure 4 showed that there was a dissociation in the relationship between $[Na^+]_i$ and $[Ca^{2+}]_i$ during MI compared with that during strophanthidin perfusion. If the energy depletion was a cause for the dissociation, energy repletion could cancel it. After 20 minutes of MI, 10 mM glucose was applied for 30 minutes in presence of metabolic inhibitors (energy repletion: ER). After 20 minutes of MI, $[Na^+]_i$ increased from 6.4 ± 0.3 mM to 16.0 ± 1.2 mM, whereas $[Ca^{2+}]_i$ was kept at the low level. After ER, $[Na^+]_i$ continued to increase, reaching 42.6 ± 4.8 mM at 50 minutes (figure 6, left column). $[Ca^{2+}]_i$ showed a marked progressive increase to 442% ± 72% of the control at 50 minutes ($p < 0.01$ v.s. in MI). Furthermore, these changes were accompanied by morphological changes from the rod-shaped form to contracted and hypercontracted forms. The percent of rod-shaped cells decreased significantly at 50 minutes (figure 6, left column). It was suggested that ER could, at least in part, eliminate the dissociation between $[Na^+]_i$ and $[Ca^{2+}]_i$ [11].

The addition of 10 mM glucose after 20 minutes of MI resulted in progressive increase in $[Ca^{2+}]_i$. Since the pH_i levels were similar before and after the addition of

glucose (data not shown), ER by glycolysis was thought to be a main cause for the reactivation of the Ca^{2+} entry via Na^+–Ca^{2+} exchange. Haworth and Gokner [23] have described that, since the calculated Km of Na^+–Ca^{2+} exchange for ATP was no more than 10% of the normal ATP level, the exchanger would not be limited by ATP as long as it kept 25% of the original level.

Next, we sought to examine the contribution of $[Na^+]_i$ and extracellular Ca^{2+} to the increase in $[Ca^{2+}]_i$ and cell shape after ER. Figure 6 also summarizes alterations in the percent of rod-shaped cells, $[Na^+]_i$, and $[Ca^{2+}]_i$ after ER in the presence of 1 μM HMA or Ca^{2+}-free solution. Cells were perfused with HMA or Ca^{2+}-free solution during the overall period of MI and ER (50 min). HMA suppressed the decrease of the percent of rod-shaped cells and the increases in both $[Na^+]_i$ and $[Ca^{2+}]_i$ after ER. In the Ca^{2+}-free perfusion (0 Ca), although $[Na^+]_i$ increased further, both the decrease in the percent of rod-shaped cells and the increase in $[Ca^{2+}]_i$ were suppressed. Since the suppression of the increase in $[Na^+]_i$ (by HMA) and the removal of external Ca^{2+} could nearly eliminate the increase in $[Ca^{2+}]_i$ and cell contracture, it was suggested that the increase in $[Ca^{2+}]_i$ after ER was dependent on the increased Ca^{2+} influx (or decreased Ca^{2+} efflux) via Na^+–Ca^{2+} exchange and that cell contracture was, at least in part, related to the increase in $[Ca^{2+}]_i$. Previous studies have also demonstrated that the manipulation of $[Na^+]_i$ during ischemia could influence postischemic Ca^{2+} overload and myocardial dysfunction, suggesting the contribution of Na^+–Ca^{2+} exchange [28,29].

In this study, cell contracture after ER was associated with the increase in $[Ca^{2+}]_i$, and it is now accepted that Ca^{2+} overload precipitates many kinds of processes that cause cell damage, including uncoupling of mitochondrial oxidative phosphorylation, activation of phospholipases, production of free fatty acid and lysophospholipids, and activation of Ca^{2+}–ATPase [30]. In some cells, however, contracture developed with little or no increase in $[Ca^{2+}]_i$. We have previously demonstrated that $[Ca^{2+}]_i$ elevation prior to cell contracture after the washout of cyanide was significantly lower than that during the perfusion of strophanthidin [31]. Furthermore, some investigators have suggested that the partial ATP restoration [32] or pH_i recovery [33] by itself could be a cause for cell injury on reperfusion or reoxygenation.

REGULATION OF $[Na^+]_i$ AND $[Ca^{2+}]_i$ DURING SIMULATED ISCHEMIA AND REPERFUSION

We have already shown that the decrease in pH_i during MI led to the activation of Na^+–H^+ exchange that caused the increase in $[Na^+]_i$. However, it has been reported that extracellular acidosis inhibits the activity of Na^+–H^+ exchange by reducing the transsarcolemmal H^+ gradient [34]. Furthermore, the changes in $[Na^+]_i$ after reperfusion is still controversial. According to the hypothesis of Dennis et al. [16], accelerating Na^+–H^+ exchange on reperfusion induces an increase in $[Na^+]_i$, which leads to a displacement of the equilibrium of Na^+–Ca^{2+} exchange in favor of the rise in $[Ca^{2+}]_i$. Tani and Neely [29] measured myocardial Na^+ content with biochemical method and showed that $[Na^+]_i$ rose continuously during ischemia and rapidly increased further after reperfusion in rat heart.

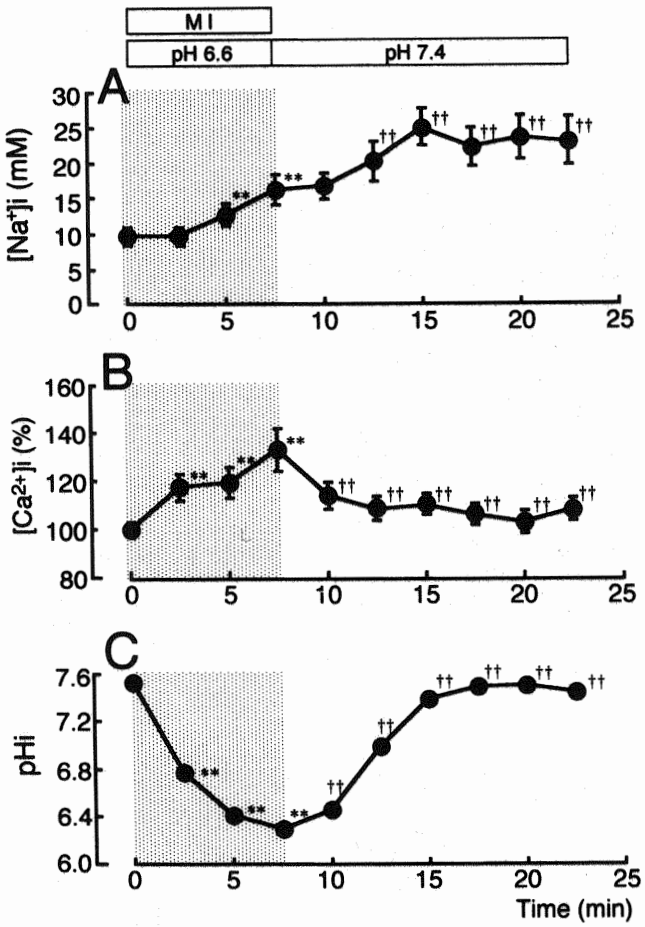

Figure 7. Effects of simulated ischemia and reperfusion on $[Na^+]_i$, $[Ca^{2+}]_i$, and pH_i. Simulated ischemia was achieved by applying 3.3 mM amytal and 5 μM CCCP in a glucose-free HEPES solution (pH 6.6) for 7.5 minutes, and reperfusion was done by the washout of metabolic inhibitors with a solution that contained 10 mM glucose (pH 7.4). (**A**) The values of $[Na^+]_i$ ($n = 22$); (**B**) the values of $[Ca^{2+}]_i$, expressed as corrected $F500/F_0500$ ($n = 22$); (**C**) pH_i ($n = 6$). Values are mean ± SE. **, $p < 0.01$ vs. control; ††, $p < 0.01$ vs. ischemia 7.5 minutes.

We, therefore, investigated the regulation of intracellular ion concentrations during MI with extracellular acidosis of pH 6.6 (simulated ischemia) and the washout of metabolic inhibitors with the solution containing 10 mM glucose at pH 7.4 (simulated reperfusion). Figure 7 shows the changes in $[Na^+]_i$, $[Ca^{2+}]_i$, and pH_i during 7.5 minutes of simulated ischemia and the subsequent reperfusion. $[Na^+]_i$ and $[Ca^{2+}]_i$ were measured simultaneously in 22 cells. The pH_i was measured separately in six other cells. $[Na^+]_i$ increased from 9.8 ± 1.3 mM to 16.2 ± 2.1 mM ($p < 0.01$) after 7.5 minutes of simulated ischemia and increased further to 25.0 ± 2.6 mM at

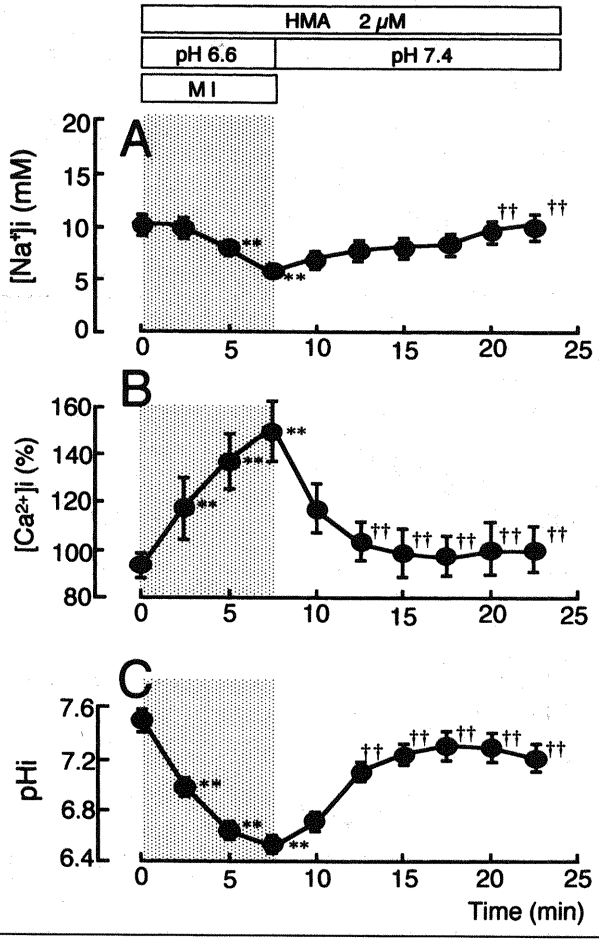

Figure 8. Effects of HMA on $[Na^+]_i$, $[Ca^{2+}]_i$, and pH_i during simulated ischemia–reperfusion. Myocytes were preincubated for 10 minutes with a HEPES solution that contained 10 mM glucose and 2 μM HMA (pH 7.4). Data were shown after cells were subjected to simulated ischemia–reperfusion. (**A**) The values of $[Na^+]_i$ (n = 11), (**B**) $[Ca^{2+}]_i$, expressed as corrected $F500/F_0500$ (n = 11), (**C**) pH_i (n = 8). **, $p < 0.01$ vs. control; ††, $p < 0.01$ vs. ischemia 7.5 minutes.

7.5 minutes after reperfusion. $[Ca^{2+}]_i$ increased to 133% ± 9% of the control at 7.5 minutes of simulated ischemia and decreased to the control level after reperfusion. The pH_i decreased from 7.55 ± 0.01 to 6.30 ± 0.01 at 7.5 minutes of simulated ischemia and recovered to the control level within 7.5 minutes after reperfusion. There were no changes in cell shape in all 22 cells during simulated ischemia and after reperfusion.

To study the role of Na^+–H^+ exchange, 11 cells were preincubated with the control solution (pH 7.4), which contained HMA (2 μM), for 10 minutes. Figure 8

shows the changes in $[Na^+]_i$, $[Ca^{2+}]_i$, and pH_i during the same protocol of simulated ischemia and reperfusion in the continued presence of HMA. $[Na^+]_i$ decreased slightly, but not significantly, during the control period. During simulated ischemia, $[Na^+]_i$ decreased from 10.0 ± 0.5 mM to 5.8 ± 0.6 mM ($p < 0.01$), while $[Ca^{2+}]_i$ increased to 153% ± 13% of the control level ($p < 0.01$) at 7.5 minutes of simulated ischemia. There was no statistical difference between the values of $[Ca^{2+}]_i$ at 7.5 minutes after simulated ischemia with and without HMA (153% ± 13% vs. 133% ± 9%). There was no significant increases in $[Na^+]_i$ shortly after reperfusion in the presence of HMA. The pH_i decreased from 7.44 ± 0.07 to 6.51 ± 0.05 during simulated ischemia, but recovered incompletely after reperfusion.

It has been reported that extracellular acidosis inhibits the activity of Na^+–H^+ exchange by reducing the transsarcolemmal H^+ gradient [34]. However, the Na^+ influx via Na^+–H^+ exchange was thought to be active under our experimental condition of simulated ischemia because the pH_i also largely decreased (to ~6.3) and HMA inhibited the increase in $[Na^+]_i$. It was also suggested that the increase in $[Ca^{2+}]_i$ during simulated ischemia might not be related to the increase in $[Na^+]_i$, and that the recovery of pH_i after reperfusion was partially dependent on Na^+–H^+ exchange.

As shown in figure 7, $[Na^+]_i$ continued to increase during the initial few minutes after reperfusion, with a time course similar to the recovery of pH_i. Since the extracellular pH level was returned to 7.4 immediately after reperfusion, the H^+ gradient was expected to increase transiently, causing a massive Na^+ influx via Na^+–H^+ exchange [2]. Because the pH of the solution was switched to the physiological value after reperfusion, the transsarcolemmal H^+ gradient during reperfusion should have become steeper than that during simulated ischemia. It is, therefore, likely that the Na^+–H^+ exchange is more activated during reperfusion than during simulated ischemia, which could cause a further increase in $[Na^+]_i$. Our results contrast to those recently reported by Ladilov et al. [35], who showed that $[Na^+]_i$ fell rapidly without transient increase on reperfusion after anoxic incubation with pH 6.6 in isolated rat myocytes. The reason behind the different results are unknown, but Ladilov et al. reoxygenated the cells after rigor shortening occurred and both the $[Na^+]_i$ and $[Ca^{2+}]_i$ extremely increased (near saturation of fluorescent ratios).

CONCLUSION

We investigated the relationship between intracellular ion concentrations during metabolic inhibition–energy repletion or during simulated ischemia–reperfusion using a single-cell model (figure 9). During myocardial ischemia, $[Na^+]_i$ increases by both the activated Na^+ influx via Na^+–H^+ exchange and the suppressed Na^+ extrusion via the Na^+–K^+ pump. However, Na^+–Ca^{2+} exchange is inhibited by energy depletion and intracellular acidosis, causing the dissociation between $[Na^+]_i$ and $[Ca^{2+}]_i$. Therefore, the increase in $[Ca^{2+}]_i$ is not related to the increase in $[Na^+]_i$ and could be related to the depression of other $[Ca^{2+}]_i$ regulatory mechanisms such as sarcolemmal Ca^{2+}–ATPase and SR Ca^{2+} uptake. After reperfusion, Na^+–H^+

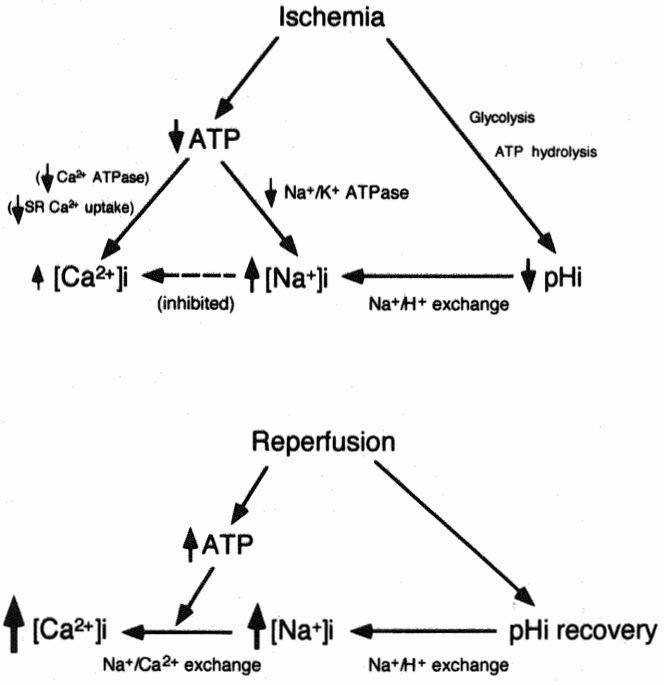

Figure 9. Summary of ion interaction during myocardial ischemia and reperfusion. Details are in the text.

exchange is activated further as pH_i is recovered, resulting in an additional $[Na^+]_i$ elevation. Na^+–Ca^{2+} exchange could be reactivated by reperfusion, resulting in a significant increase in $[Ca^{2+}]_i$. It was also suggested that cell contracture during ischemia is related to rigor due to energy depletion, while cell contracture after reperfusion is likely to be related to Ca^{2+} overload.

REFERENCES

1. Allen DG, Orchard CH. 1987. Myocardial contractile function during ischemia and hypoxia. Circ Res 60:153–168.
2. Lazdunski M, Frelin C, Vigne P. 1985. The sodium/hydrogen exchange system in cardiac cells: its biochemical and pharmacological properties and its role in regulating internal concentrations of sodium and internal pH. J Mol Cell Cardiol 17:1029–1042.
3. January CT, Fozzard HA. 1984. The effects of membrane potential, extracellular potassium, and tetrodotoxin on the intracellular sodium ion activity of sheep cardiac muscle. Circ Res 54:652–664.
4. Guarnieri T. 1987. Intracellular sodium–calcium dissociation in early contractile failure in hypoxic ferret papillary muscle. J Physiol (Lond) 388:449–465.
5. Sheu SS, Fozzard HA. 1982. Transmembrane Na^+ and Ca^{2+} electrochemical gradients in cardiac muscle and their relationship to force development. J Gen Physiol 80:325–351.
6. Collins A, Somlyo AV, Hilgemann DW. 1992. The giant cardiac membrane patch method: stimulation of outward Na^+–Ca^{2+} exchange current by Mg ATP. J Physiol (Lond) 454:27–57.
7. Doering AE, Lederer WJ. 1993. The mechanism by which cytoplasmic protons inhibit the sodium–calcium exchanger in guinea-pig heart cells. J Physiol (Lond) 466:481–499.

8. Hayashi H, Satoh H, Noda N, Terada H, Kobayashi A, Hirano M, Yamashita Y, Yamazaki N. 1994. Simultaneous measurement of intracellular Na^+ and Ca^{2+} during K^+-free perfusion in isolated myocytes. Am J Physiol 266 (Cell Physiol 35):C416–C422.
9. Satoh H, Hayashi H, Noda N, Terada H, Kobayashi A, Hirano M, Yamashita Y, Yamazaki N. 1994. Regulation of $[Na^+]i$ and $[Ca^{2+}]i$ in guinea pig myocytes: dual loading of fluorescent indicators SBFI and fluo 3. Am J Physiol 266 (Heart Circ Physiol 35):H568–H576.
10. Hayashi H, Miyata H. 1994. Fluorescence imaging of intracellular Ca^{2+}. J Pharmacol Toxicol Methods 31:1–10.
11. Satoh H, Hayashi H, Katoh H, Terada H, Kobayashi A. 1995. Na^+/H^+ and Na^+/Ca^{2+} exchange in regulation of $[Na^+]i$ and $[Ca^{2+}]i$ during metabolic inhibition. Am J Physiol 268 (Heart Circ Physiol 37):H1239–H1248.
12. Satoh H, Hayashi H, Noda N, Terada H, Kobayashi A, Hirano M, Yamashita Y, Yamazaki N. 1991. Quantification of intracellular free sodium ions by using a new fluorescent indicator, sodium-binding benzofuran isophthalate in guinea pig myocytes. Biochem Biophys Res Commun 175:611–616.
13. Miyata H, Hayashi H, Suzuki S, Noda N, Kobayashi A, Fujiwake H, Hirano M, Yamazaki N. 1989. Dual-loading of the fluorescent indicators fura-2 and 2,7-biscarboxyethyl-5(6)carboxyfluorescein (BCECF) in isolated myocytes. Biochem Biophys Res Commun 163:500–505.
14. Hayashi H, Miyata H, Noda N, Kobayashi A, Hirano M, Kawai T, Yamazaki N. 1992. Intracellular Ca^{2+} concentration and pHi during metabolic inhibition. Am J Physiol 262 (Cell Physiol 31):C628–C634.
15. Li Q, Hohl CM, Altshuld RA, Stokes BT. 1989. Energy depletion–repletion and calcium transients in single cardiomyocytes. Am J Physiol 257 (Cell Physiol 26):C427–C434.
16. Dennis SC, Coetzee WA, Cragoe EJ Jr, Opie LH. 1990. Effects of proton buffering and of amiloride derivatives on reperfusion arrhythmias in isolated rat hearts. Circ Res 66:1156–1159.
17. MacLeod KT. 1989. Effects of hypoxia and metabolic inhibition on the intracellular sodium activity of mammalian ventricular muscle. J Physiol (Lond) 416:455–468.
18. Haigney MCP, Miyata H, Lakatta EG, Stern MD,Silvermann HS. 1992. Dependence of hypoxic cellular calcium loading on Na^+–Ca^{2+} exchange. Circ Res 71:547–557.
19. Katoh H, Satoh H, Nakamura T, Terada H, Hayashi H. 1994. The role of Na^+/H^+ exchange and the Na^+/K^+ pump in the regulation of $[Na^+]_i$ during metabolic inhibition in guinea pig myocytes. Biochem Biophys Res Commun 203:93–98.
20. Russell JM, Boron WF, Brodwick MS. 1983. Intracellular pH and Na fluxes in barnacle muscle with evidence for reversal of the ionic mechanism of intracellular pH regulation. J Gen Physiol, 82:47–78.
21. Miura Y, Kimura J. 1989. Sodium–calcium exchange current: dependence on internal Ca and Na and competitive binding of external Na and Ca. J Gen Physiol 93:1129–1145.
22. Caroni P, Carafoli E. 1983. The regulation of the Na^+–Ca^{2+} exchange of heart sarcolemma. Eur J Biochem 132:451–460.
23. Howorth RA, Gokner AB. 1992. ATP dependence of calcium uptake by the Na–Ca exchanger of adult heart cells. Circ Res 71:210–217.
24. Rodrigo GC, Chapman RA. 1991. The calcium paradox in isolated guinea-pig ventricular myocytes: effects of membrane potential and intracellular sodium. J Physiol (Long) 434:627–645.
25. Allshire A, Piper M, Cuthbertson KSR, Cobbold PH. 1987. Cytosolic free Ca^{2+} in single rat heart cells during anoxia and reoxygenation. Biochem J 244:381–385.
26. Li Q, Altshuld RA, Stokes BT. 1988. Myocyte deenergization and intracellular free calcium dynamics. Am J Physiol 255 (Cell Physiol 24): C162–C168.
27. Bowers KC, Allshire AP, Cobbold PH. 1992. Bioluminescent measurement in single cardiomyocytes of sudden cytosolic ATP depletion coincident with rigor. J Mol Cell Cardiol 24:213–218.
28. Anderson SE, Murphy E, Steenbergen C, London RE, Cala PM. 1990. Na–H exchange in myocardium: effects of hypoxia and acidification on Na and Ca. Am J Physiol 259 (Cell Physiol 28):C940–C948.
29. Tani M, Neely JR. 1989. Role of intracellular Na^+ in Ca^{2+} overload and depressed recovery of ventricular function of reperfused ischemic rat heart. Circ Res 65:1045–1056.
30. Cheung JY, Bonventre JV, Malis CD, Leaf A. 1986. Calcium and ischemic injury. N Engl J Med 314:1670–1676.
31. Hayashi H, Miyata H, Kobayashi A, Yamazaki N. 1990. Heterogeneity in cellular response and intracellular distribution of Ca^{2+} concentration during metabolic inhibition. Cardiovasc Res 24:605–608.

32. Nichols CG, Lederer WJ. 1990. The role of ATP in energy-deprivation contractures in unloaded rat ventricular myocytes. Can J Physiol Pharmacol 68:183–194.
33. Bond JM, Chacon E, Herman B, Lemasters J. 1993. Intracellular pH and Ca^{2+} homeostasis in the pH paradox of reperfusion injury to neonatal rat cardiac myocytes. Am J Physiol 265 (Cell Physiol 34):C129–C137.
34. Vaughan-Jones RD, Wu Ml. 1990. Extracellular H^+ inactivation of Na^+–H^+ exchange in the sheep cardiac Purkinje fibre. J Physiol (Lond) 428:441–456.
35. Ladilov YV, Siegmund B, Piper HM. 1995. Protection of reoxygenated cardiomyocytes against hypercontracture by inhibition of Na^+/H^+ exchange. Am J Physiol (Heart Circ Physiol 37):H1531–H1539.

ATP-SENSITIVE POTASSIUM CHANNELS AND MYOCARDIAL ISCHEMIA

CANWEN JIANG*, PHILIP A. POOLE-WILSON**, and SEIBU MOCHIZUKI***

* *Genzyme Corporation*
** *Imperial College School of Medicine at National Heart and Lung Institute*
*** *Jikei University School of Medicine*

Summary. The K_{ATP} channel plays an important role in mediating a variety of pathophysiological responses during myocardium ischemia and exhibits cardioprotective effects. As a consequence of the recent cloning of the subunits of the K_{ATP} channel, efforts are being made to understand its properties, regulation, and physiological role in coupling the metabolic state of a cell to excitability. Advances are anticipated in the understanding of the cellular and molecular mechanisms underlying the role of the K_{ATP} channel during myocardial ischemia. The modulators of the K_{ATP} channel are of great value as therapeutic agents for the treatment of ischemic heart disease. Newly identified tissue-selective K_{ATP} channel openers may result in important advances in the treatment of cardiovascular disease.

INTRODUCTION

ATP-sensitive potassium (K_{ATP}) channels are found in cardiac, smooth, and skeletal muscle, in β-pancreatic cells, and in neurons [1]. The K_{ATP} channels are characterized by an inhibition of channel opening when the ATP concentration at the cytoplasmic cell surface is increased [2], and they thereby couple cellular metabolism to changes in transmembrane electric activity. In β-pancreatic cells, K_{ATP} channels regulate insulin secretion. The insulin secretins, namely, sulfonylureas, stimulate insulin secretion by inhibiting the activity of K_{ATP} channels and subsequently depolarizing the cell membrane and activating voltage-operated Ca^{2+} channels [1]. In cardiac muscle, activation of K_{ATP} channels requires a decrease in intracellular ATP to submillimolar concentrations. The channel remains closed and is not involved in the regulation of cardiac action potential in physiological conditions. In

S. Mochizuki, N. Takeda, M. Nagano and N. Dhalla (eds.). THE ISCHEMIC HEART.

contrast, the K_{ATP} channels help control the resting membrane potential in vascular smooth muscle. They are involved in mediating endothelium-dependent and -independent coronary artery relaxation and constriction. During hypoxia, metabolic inhibition, and ischemia, activation of the K_{ATP} channel significantly shortens the action potential duration and reduces the cell excitability. This alteration of cell contractility minimizes ATP consumption and promotes cell survival, should the ischemia be transient. In addition, activation of the K_{ATP} channel in vascular smooth muscle during the onset of ischemia results in coronary artery relaxation, which increases coronary blood flow. Since the recent successful cloning the K_{ATP} channel in a number of tissues, the molecular and cellular mechanisms underlying the regulation of the channel are being revealed. These advances will certainly enhance the understanding of the pathophysiology of myocardial ischemia. Furthermore, a number of K_{ATP} channel modulators have been shown to affect ischemia-related arrhythmias and to mimic cardioprotective ischemic preconditioning. The therapeutical potential of the K_{ATP} channel modulators for the treatment of various cardiovascular diseases has been intensively explored over several years. Successful identification of tissue-selective K_{ATP} channel openers has greatly improved the prospects for their clinical utilization. This chapter describes the properties and regulation of the K_{ATP} channel in the cardiovascular system, and the basic aspects of its physiological, pathophysiological, and therapeutical significance. The important and complex role of the K_{ATP} channel in mediating responses to ischemia and the therapeutical potential of the K_{ATP} channel modulators for the treatment of ischemic heart disease are emphasized.

PROPERTIES AND REGULATION OF K_{ATP} CHANNELS IN CARDIAC AND VASCULAR SMOOTH MUSCLE

The K_{ATP} channel is found in high density in cardiac muscle. Assuming that all K_{ATP} channels are identical and noninteracting, the number of channels per cell is estimated at 2000–50,000 in cardiac myocytes, and the density is between 0.5 and 10 channels/μm^2 [3,4]. The conductance of the K_{ATP} channel is 10, 63, and 80 pS for 5.4, 50, and 100 mM K^+, respectively, at the outer surface of the cell membrane [2]. In vascular smooth muscle cells, the single channel conductance is 135–148 pS [5,6]. The K_{ATP} channels discriminate strongly against external Na^+, and in physiological solutions containing 140 mM Na^+, the reversal potential approximates the K^+ equilibrium potential of −90 mV in cardiac myocytes [2] and vascular smooth muscle [5]. As a member of the inward rectifier channel family, the K_{ATP} channels display a weak inward rectification, allowing substantial outward current to flow at positive potentials [2,7]. Recently, it has been demonstrated that intrinsic rectifying factors may correspond to one or more of the polyamines in the metabolic pathway from ornithine to spermine [8]. The kinetics of the K_{ATP} channel are shown to include at least one open state and two closed states.

In cardiac myocytes, ATP inhibits the activity of the K_{ATP} channels in a concentration-dependent manner. ATP is only effective when applied to the intracellular membrane surface, and the inhibition is independent of membrane potential

[2,9]. Through the use of different methods, different sensitivities of the channel to ATP have been reported. In whole-cell or open-cell attached patches, the threshold concentration of ATP in the internal solution for the appearance of K_{ATP} current is found to lie between 1 and 2 mM [3,10]. Under these conditions, 500 μM ATP induces half maximal inhibition. However, with inside-out patches, half maximal inhibition is obtained with 100 μM ATP [2,10], possibly due to the channel protein being modified by excising the patch membrane. The alternative explanation is that, in inside-out patches, other intracellular modulators of the K_{ATP} channels such as ADP can be washed away [11]. The principal effect of ATP on the channel kinetics is to reduce both the mean open time of the channel and the number of openings per burst [10]. Nonhydrolyzable ATP analogues such as adenosine 5′-O-3′-triphosphate are about as effective as ATP itself in inhibiting the K_{ATP} channel in both cardiac and vascular smooth muscle cells [1]. A number of purines such as guanosine triphosphate have been shown to reduce K_{ATP} channel activity [10], possibly binding to a separate site that is closely related to the ATP binding site [2]. However, it should be noted that adenine nucleotides are considerably less effective than ATP in inhibiting the channel. Furthermore, alterations of every part of the ATP molecule reduce its ability to close the channel. These observations suggest that the nucleotide binding site has specificity for ATP [1].

In most inside-out patches, channel activity decays rapidly after patch excision if ATP is not present (a process called *rundown*). Channel activity reappears after the channel has been blocked again for a few minutes (the *refreshment effect*). This action of ATP requires the presence of Mg^{2+}, and nonhydrolyzable ATP analogues do not mimic the refreshment effect, suggesting that the presence of low concentrations of ATP and Mg^{2+} at the intracellular site of the membrane is essential to maintain the channel in an active state [1].

The most important intracellular modulator of the K_{ATP} channel other than ATP is ADP. ADP has an inhibitory effect on the fully activated K_{ATP} channels, producing a 50% inhibition at a concentration of 0.8–2 mM in cardiac myocytes [2], and the inhibition is Mg^{2+} dependent [13]. Activation is favored when channel activity has substantially declined. In relatively stable patches, the dose–response curve for ADP resembles a parabola, with low concentrations increasing, and high concentrations decreasing, channel activity [1]. ADP shifts the ATP concentration–response curve to higher concentrations, suggesting that ADP relieves ATP binding competitively to the same site as ATP [14]. Indeed, the effects of the changes in the cytosolic ADP:ATP ratio on channel activity are more pronounced than the changes in the ATP concentrations [14].

Phosphorylation and dephosphorylation of proteins are key mechanisms in signal transduction pathways that control a wide variety of cellular events. Phosphorylation of transmembrane ion channels can significantly alter channel proterties. The possible role of phosphorylation in the elucidation of the requirement of Mg^{2+}–ATP to maintain the activity of the K_{ATP} channel is unclear. However, protein kinase C is capable of regulating the activity of K_{ATP} channels in cardiac myocytes, possibly by changing the apparent stoichiometry of ATP binding, and the effect can be reversed

by the activity of an endogenous membrane-associated type 2A protein phosphatase. When cytosolic ATP is below 100 μM, protein kinase C inhibits K_{ATP} channel activity, while at physiological levels of ATP (millimolar), protein kinase C activates the channel. In vascular smooth muscle cells, phosphorylation of K_{ATP} channels by protein kinase C may be one of the end effectors of muscarinic receptor stimulation. Coupling of acetylcholine to muscarinic receptors can lead to activation of protein kinase C, which in return phosphorylates and inhibits K_{ATP} channels. It is possible that K_{ATP} channels in vascular smooth muscle cells are the target for a variety of extracellular stimuli that act via protein kineses [15].

INHIBITORS AND OPENERS OF K_{ATP} CHANNELS

The K_{ATP} channel can be inhibited by quinine and tetraethylammonium [10]. Cations such as Ba^{2+} block the K_{ATP} channel in cardiac myocytes [16]. In vascular smooth muscle cells, the current carried by the K_{ATP} channel and the hyperpolarization of the resting potential caused by the activation of the channel are inhibited by Ba^{2+} [5,17]. A group of sulfonylureas, represented by glyburide, inhibit the K_{ATP} channels in a variety of tissues, including cardiac and vascular smooth muscle [1,18]. In cardiac and vascular smooth muscle, glyburide at micromolar concentrations markedly inhibits the activity of the K_{ATP} channels [1,5]. This inhibition is specific, since the same concentrations of glyburide do not block either voltage-dependent or Ca^{2+}-activated K^+ channels and Ca^{2+} channels [1].

A group of benzopyran derivatives, represented by lemakalim (the active enantiomer of the racemate cromakalim), and other agents such as diazoxide have been demonstrated to open the K_{ATP} channels [18]. In vascular smooth muscle, lemakalim activates the K_{ATP} channels and hyperpolarizes the cell membrane. The hyperpolarization results in the closure of Ca^{2+} channels and reduction in intracellular free Ca^{2+} concentration. The vascular smooth muscle cells then relax, and blood vessels undergo dilation. In human [19] and animal [18] cardiac myocytes, lemakalim and other openers activate the K_{ATP} channels. The concentration of drugs activating the cardiac K_{ATP} channel depends on the level of intracellular ATP. With physiological concentrations of intracellular ATP, more than 100 μM of lemakalim or nicorandil is required to open cardiac K_{ATP} channels. The activation of the K_{ATP} channels leads to hyperpolarization of the cell membrane and shortening of cardiac action potential. The effects of these K_{ATP} channel openers are inhibited by sulfonylureas.

MOLECULAR STRUCTURE OF K_{ATP} CHANNELS

The properties of the K_{ATP} channel suggest that it belongs to the superfamily of the inwardly rectifying K^+ channels. However, no inward rectifier clone, when expressed alone, has the biophysical and pharmacological signatures of native K_{ATP} channels. A fully functional K_{ATP} channel is composed of at least a pore-forming rectifier channel and a sulfonylurea receptor protein. The proposed transmembrane topology of classical rectifier channel subunits consists of cytoplasmic N and C termini, six transmembrane domains, and a conserved hydrophobic P or H5 loop between the fifth and sixth

transmembrane domains. The recently cloned rectifier channels including the subunit forming the K_{ATP} channel are assumed to have only two transmembrane domains with each subunit, although they retain the H5 loop that is responsible for K^+ selectivity [20]. There is a proposed ATP-binding domain in the kidney K_{ATP} channel, but this domain shows no ATP sensitivity [21]. The sulfonylurea receptor belongs to the family of ATP-binding cassette membrane proteins, including the cystic fibrosis transmembrane conductance regulator [22]. While the cystic fibrosis transmembrane conductance regulator functions as a Cl^- channel that is defective in cystic fibrosis, expression of the sulfonylurea receptor alone does not result in the formation of a functional K_{ATP} channel. Coexpression of the suflonylurea receptor and an inward rectifier channel is required for a functional K_{ATP} channel with the biophysical and pharmacological properties of the native K_{ATP} channels [23]. The sulfonylurea receptor processes two nucleotide-binding domains and therefore contributes to the regulation of the K_{ATP} channel complex by ATP. Naturally, the inhibition of the K_{ATP} channel by sulfonylureas is conferred to the K_{ATP} channels by the receptor.

PHYSIOLOGICAL ROLE OF K_{ATP} CHANNELS IN CARDIAC AND CORONARY ARTERIAL SMOOTH MUSCLE

The K_{ATP} channels provide a linkage between the membrane excitability and the metabolic state of cardiac cells. During hypoxia, metabolic inhibition, and ischemia, activation of K_{ATP} channels significantly shortens the action potential duration and thereby alters the excitation–contraction coupling. Activation of K_{ATP} channels requires a decrease in intracellular ATP to submillimolar concentrations, suggesting that the channels are in a closed state in normal physiological conditions. Though glyburide has been reported to cause cardiac action-potential shortening in the absence of K_{ATP} channel openers [24], other studies have not observed any effect of glyburide at concentrations sufficient to abolish channel opening by lemakalim or by depletion of intracellular ATP [19]. Since the density of the K_{ATP} channel in the membrane of cardiac myocytes is extremely high, it is possible that less than 1% of the available conductance will be sufficient to shorten the cardiac action potential and influence the excitation–contraction coupling [25,26]. There is good evidence that measurable cardiac action-potential shortening will occur if intracellular ATP falls even slightly below a normal physiological level [26].

In vascular smooth muscle cells, the K_{ATP} channel has been shown to be active at physiological concentrations of extracellular Ca^{2+} and intracellular ATP [27]. This finding indicates that the K_{ATP} channels may aid in the control of the resting membrane potential of vascular smooth muscle cells. Calcitonin gene-related peptide, an important regulator of coronary artery tone, has been shown to activate the K_{ATP} channel in intact vascular smooth muscle cells with physiological levels of intracellular ATP [5,17,28,29]. The K_{ATP} channel is involved in mediating endothelium-dependent coronary artery dilation and constriction, another important mechanism controlling the coronary artery tone. There is evidence that the endothelium-dependent relaxation in response to acetylcholine is partially mediated by the K_{ATP} channels in rabbit coronary arteries [30]. Furthermore, endothelin-1

induces a potent contraction, and the closure of the K_{ATP} channels, which are active at resting conditions, may be partially responsible for the endothelin-1-induced contraction [31]. Therefore, in coronary arteries, the K_{ATP} channel mediates various physiological responses and plays an important role in the regulation of coronary artery tone.

ACTIVATION OF THE K_{ATP} CHANNEL DURING ISCHEMIA

Under most physiological conditions, intracellular ATP in cardiac myocytes is at about a 2-mM concentration, and the K_{ATP} channels remain closed. During ischemia or metabolic inhibition, intracellular ATP declines and the K_{ATP} channels are activated. At the onset of ischemia, however, several studies have shown that, although intracellular ATP does fall, a more substantial fall to below the concentration believed to activate the K_{ATP} channels does not occur, even after several minutes of ischemia have elapsed. The discrepancy between the rate and magnitude of the decline of the intracellular ATP and the rapid activation of the K_{ATP} channel at the onset of ischemia may be attributable to different mechanisms. Some studies suggest that glycolytically derived ATP from sources near the sarcolemma may be more important than mitochondrially derived ATP in regulating the K_{ATP} channels [32]. This possibility depends on the concept of subcellular compartmentation of energy sources. Thus, the intracellular ATP near the channel may fall markedly while cytoplasmic ATP remains relative constant [32]. Other authors argue that if gradients for intracellular ATP exist within the cell, then they must be very small and of little consequence [33]. The alternative explanation is that the slight reduction in ATP and increase in ADP alter the ATP:ADP ratio, which is more important than the slight decrease in ATP alone in activating the cardiac K_{ATP} channels. In addition, cellular acidosis, which occurs in the ischemic cardiac myocytes, increases the sensitivity of the cardiac K_{ATP} channel to the small decrease in intracellular ATP. Lactate, generated during ischemia, can directly activate K_{ATP} channels in cardiac myocytes [34], although it is not clear whether the activation of the cardiac K_{ATP} channel by lactate is due to a direct interaction between lactate and the channel or secondary to the decrease in pH. Furthermore, extracellular adenosine released from ischemic cardiac myocytes promotes the activation of the K_{ATP} channels via activation of G-proteins [35]. These combined events result in the activation of the K_{ATP} channel and consequently generate a large outward current that dramatically shortens the cardiac action potential. The alteration of cardiac action potential leads to a decline in the Ca^{2+} current entering the cell and the contractility of the cardiac myocytes. The reduction in the Ca^{2+} current prevents Ca^{2+} overload, which is linked to cell necrosis. Massive release of K^+ from the ischemic myocardium due to the activation of K_{ATP} channels and their accumulation in extracellular space result in depolarization, which in combination with shortening of action potential duration significantly reduces the cell contractility [36]. The decline in cell contractility minimizes ATP consumption and promotes cell survival, should the ischemia be transient [37]. It has been demonstrated that pretreatment of

myocardium with K_{ATP} channel inhibitors such as sulfonylureas compromises recovery of mechanical activity after reperfusion. In contrast, K_{ATP} channel openers improve the recovery of ischemic myocardium and reduce the infarct size in ischemic hearts in vivo [38].

In coronary smooth muscle cells, the effects of hypoxia rather than ischemia have been intensively investigated. Hypoxia can cause either coronary artery relaxation or contraction depending on the species and the degree of hypoxia. The release of endothelium-derived relaxing factor, endothelium-derived hyperpolarizing factor, and prostaglandins has been demonstrated to mediate hypoxia-induced coronary artery dilation [35,39]. It is possible that K_{ATP} channels may partially mediate the endothelium-dependent relaxation in response to hypoxia [30,35]. There is experimental evidence that activation of the K_{ATP} channels may mediate hypoxic or ischemic dilation of coronary arteries in perfused heart preparations [40]. During partial myocardial ischemia, the intracellular ATP concentration of coronary artery smooth muscle cells declines due to aerobic metabolism. Activation of the K_{ATP} channels hyperpolarizes the cell membrane, and hyperpolarization in turn closes Ca^{2+} channels. Consequently, coronary arteries dilate [40]. However, it should be noted that adenosine directly activates K_{ATP} channels in cardiac and coronary arterial smooth muscle cells [35,41,42]. Adenosine and other metabolites released from hypoxic or ischemic myocardium may partially account for the hypoxic coronary artery dilation [35,43]. The relaxation of coronary arteries in response to hypoxia or ischemia increases blood supply to the myocardium.

K_{ATP} CHANNELS AND ISCHEMIA-RELATED ARRHYTHMIAS

Acute myocardial ischemia frequently results in lethal ventricular arrhythmias. During early ischemia, the cardiac action potential shortens and extracellular K^+ accumulates as a result of net K^+ loss from the myocardium [36,44]. The accumulated extracellular K^+ causes depolarization of cardiac myocytes and increases automaticity. The shortening of refractoriness and the slowing of conduction are the most important electrophysiological basis for arrhythmogenesis. Although the precise mechanism is not understood, ischemia-induced ventricular arrhythmias are related to wavelet reentry. Since the activation of K_{ATP} channels is responsible for the shortening of the action potential and the net loss of K^+ from ischemic myocardium [36,44], the K_{ATP} channel may play a role in ischemia-related arrhythmogenesis. Thus, inhibition of the K_{ATP} channels and consequent prevention of action-potential shortening and extracellular K^+ accumulation should be antiarrhythmic. In some experimental models, sulfonylureas have been demonstrated to be effective in reducing ischemia-related arrhythmias. In isolated rat hearts, the incidence rate of ventricular fibrillation is significantly decreased by glyburide and other sulfonylureas [45]. Furthermore, there is experimental evidence that K_{ATP} channel openers increase the incidence rate of reentry arrhythmias because the action-potential shortening in acute ischemia is enhanced [46]. However, other studies have failed to show any effects of glyburide on ischemia- or reperfusion-

induced arrhythmias in rats [47]. This discrepancy reflects the complexity of the pathogenesis of ischemia-related arrhythmias. In addition to its direct electrophysiological role, activation of the K_{ATP} channels has profound effects on cellular events during myocardial ischemia. For example, Ca^{2+} entry and overload are known to be arrhythmogenic [48]. Activation of the K_{ATP} channels could hyperpolarize the cell and decrease excitability, which in return reduces Ca^{2+} entry. The reduction of Ca^{2+} overload could decrease the incidence of arrhythmias. Thus, K_{ATP} channel openers may act as potent antiarrhythmic agents. For example, arrhythmias due to early afterdepolarization are suppressed by K_{ATP} channel openers. Furthermore, the decrease in cell excitability due to the activation of K_{ATP} channels preserves high-energy phosphates and prevents irreversible cell injury. K_{ATP} channel openers postpone the time to ischemic contracture. Because of the complexity of ischemia-related arrhythmias, whether K_{ATP} channel modulation is proarrhythmic or antiarrhythmic strongly depends on the timing and the nature of the electrophysiological mechanisms underlying the arrhythmias [49].

CARDIOPROTECTIVE PRECONDITIONING AND K_{ATP} CHANNELS

In 1986, investigators reported that four five-minute periods of coronary artery occlusion interspersed with five-minute periods of reperfusion prior to a more prolonged ischemia resulted in a marked reduction in infarct size in dog hearts [50]. The ischemic preconditioning was defined as an adaptive response to a brief ischemic insult that protects cardiac myocytes from a subsequent, prolonged period of ischemia. This phenomenon has been demonstrated in all species tested, and a number of mechanisms have been proposed to underlie the cardioprotective mechanism. Adenosine, acetylcholine, and bradykinin have been shown to mimic ischemic preconditioning. These endogenous mediators may exhibit their cardiac protection via activation of protein kinase C [51]. A large number of pharmacological studies from Dr. Gross's laboratory and others established the linkage between the activation of K_{ATP} channels and ischemic preconditioning [52]. In canine hearts, intravenous administration of glyburide, either before or immediately following a five-minute period of ischemic preconditioning, completely abolishes its cardioprotective efforts. The dose of glyburide used has no effect on infarct size in nonpreconditioned dogs, suggesting a role for the K_{ATP} channel in ischemic preconditioning. These results are supported by experiments using nonsulfonylurea K_{ATP} channel inhibitors such as 5-hydroxydecanoate. When glyburide is administered intracoronarily only during the five-minute period of preconditioning or only during the first five minutes of the prolonged 60-minute occlusion period, in both instances ischemic preconditioning is completely abolished [53]. These experiments demonstrate that activation of K_{ATP} channels is not only necessary to trigger the ischemic preconditioning responses but also to maintain the protective effects over an indefinite period of time [52]. Clinical studies have shown that glyburide inhibits an ischemic preconditioning-like effect produced by consecutive two-minute periods of coronary angioplasty separated by five minutes of reperfusion in patients

with coronary artery disease [54]. These results are consistent with findings in various animal models. Further evidence indicating the involvement of the K_{ATP} channel in ischemic preconditioning is generated in experiments using K_{ATP} channel openers. Several in vivo studies have demonstrated that the K_{ATP} channel openers can mimic the cardioprotective effects. In anesthetized dogs, nonhypotensive doses of nicorandil and other openers administered prior to or during a 60-minute occlusion period significantly reduce myocardial infarct size. Four five-minute intracoronary infusions of K_{ATP} channel openers with intermittent five-minute drug-free periods mimic the effects of four five-minute periods of ischemia separated by five-minute periods of reperfusion to reduce infarct size in anesthetized dogs. In pigs, which have a sparse collateral circulation as compared to dogs, similar results have been obtained [52]. However, it should be noted that in small animal species, namely, rabbit and rat, contradictory results have been reported in the literature [52].

The role of K_{ATP} channels in ischemic preconditioning has been utilized to elucidate the cardioprotective effects of adenosine and other mediators. Pharmacological experiments in dogs in vivo have shown that K_{ATP} channel inhibitors such as glyburide block the action of adenosine and acetylcholine, which mimic ischemic preconditioning [52]. Since adenosine directly activates the K_{ATP} channel in coronary artery smooth muscle in vitro and in vivo, and since acetylcholine-induced endothelium-dependent vasodilation is partially mediated by the K_{ATP} channel [30,35], these results are not surprising. The mechanisms by which activation of the K_{ATP} channel produces a cardioprotective effect, however, are not fully understood. Although pharmacological experiments have demonstrated the role of the K_{ATP} channels in ischemic preconditioning, efforts should be made to investigate the cellular and molecular mechanisms.

DEVELOPMENT OF K_{ATP} CHANNEL MODULATORS

The sulfonylureas that specifically inhibit the K_{ATP} channel in β-pancreatic cells are well-established drugs for the treatment of non-insulin-dependent diabetes mellitus. The inhibition of the K_{ATP} channels and consequent prevention of action-potential shortening and extracellular K^+ accumulation should be antiarrhythmic during myocardial ischemia. However, whether K_{ATP} channel modulation is proarrhythmic or antiarrhythmic strongly depends on the timing and the nature of the electrophysiological mechanisms underlying the arrhythmias [49]. The complexity of ischemia-related arrhythmias discourages the use of K_{ATP} channel modulators as antiarrhythmic drugs.

Because of their potent peripheral vasodilating effects, one possible clinical application of the K_{ATP} channel openers is in the treatment of hypertension. However, preclinical and clinical studies have not shown any advantage of the first generation of K_{ATP} channel openers over established antihypertensive drugs such as Ca^{2+} channel blockers and angiotensin-converting enzyme inhibitors. The side effects, such as reflex tachycardia and cardiac hypertrophy, also limit their clinical potential [55]. In addition, the possible use of K_{ATP} channel openers (represented by

nicorandil) as antianginal drugs has been intensively explored. Nicorandil has been shown to be effective in the treatment of stable angina pectoris, with comparable efficacy to the three major established groups of antianginals (nitrates, β-blockers, and Ca^{2+} antagonists). Nicorandil does not adversely affect the patient's lipid status, and tolerance does not develop [56]. However, the possible use of K_{ATP} channel openers in the treatment of both hypertension and angina is threatened by the fact that the first generation of K_{ATP} channel openers do not have tissue selectivity and open K_{ATP} channels in an indiscriminant manner. Drug discovery efforts aimed at the identification of new K_{ATP} channel openers with tissue selectivity have dominated the field of ion channel modulator research over the past decade.

K_{ATP} channel openers can protect the ischemic myocardium at concentrations that cause very little cardiodepression, which gives them a great potential advantage over Ca^{2+} blockers (55). However, hypotension due to the vasodilator effect of the first generation of K_{ATP} channel openers may cause underperfusion of the myocardium already at risk and may thus compromise the cardioprotective effects of these agents against ischemia. Efforts to find K_{ATP} channel openers with reduced vasodilator effects have resulted in the identification of new compounds with favorable pharmacological profiles. These newly identified compounds exhibit cardioprotective effects in several models of myocardial ischemia without significant change in hemodynamic variables. In addition, compounds that selectively cause smooth muscle dilation without significant effect on cardiac action potential have been obtained by simple modifications of existing structures [55].

REFERENCES

1. Ashcroft FM. 1988. Adenosine 5′-triphosphate-sensitive potassium channels. Annu Rev Neurosci 11:97–118.
2. Moma A. 1983. ATP-regulated K^+ channels in cardiac muscle. Nature 305:147–148.
3. Noma A, Shibasaki T. 1985. Membrane current through adenosine-triphosphate-regulated potassium channels in guinea-pig ventricular cells. J Physiol 363:463–480.
4. Nichols CG, Lederer WJ. 1990. The regulation of ATP-sensitive K^+ channel activity in intact and permeabilized rat ventricular myocytes. J Physiol 423:91–110.
5. Standen NB, Quayle JM, Davies NW, Brayden JE, Huang Y, Nelson MT. 1989. Hyperpolarizing vasodilators activate ATP-sensitive K^+ channels in arterial smooth muscle. Science 245:177–180.
6. Silberberg SD, Van Breemen C. 1990. An ATP, calcium and voltage sensitive potassium channel in porcine coronary artery smooth muscle cells. Biochem Biophys Res Commun 172:517–522.
7. Nichols CG, Lederer WJ. 1991. Adenosine triphosphate-sensitive potassium channels in the cardiovascular system. Am J Physiol 261:H1675–H1686.
8. Loptin AN, Makhina EN, Nichols CG. 1994. Potassium channel block by cytoplasmic polyamines as the mechanism of intrinsic rectification. Nature 372:366–369.
9. Sturgess NC, Ashford ML, Carrington CA, Hales CN. 1986. Single channel recordings of potassium currents in an insulin-secreting cell line. J Endocrinol 109:201–207.
10. Kakei M, Noma A, Shibasaki T. 1985. Properties of adenosine-triphosphate-regulated potassium channels in guinea-pig ventricular cells. J Physiol 363:441–462.
11. Rorsman P, Trube G. 1990. Biophysics and physiology of ATP-regulated K^+ channels. In Cook N (ed), Potassium Channels. Chichester, UK: Ellis Horwood Limited, pp. 96–116.
12. Tung RT, Kurachi Y. 1991. On the mechanism of nucleotide diphosphate activation of the ATP-sensitive K^+ channel in ventricular cell of guinea-pig. J Physiol 437:239–256.
13. Findlay I, Dunne MJ. 1986. ATP maintains ATP-inhibited K^+ channels in an operational state. Pflugers Arch 407:238–240.

14. Kakei M, Kelly RP, Ashcroft SJ, Ashcroft FM. 1986. The ATP-sensitivity of K^+ channels in rat pancreatic B-cells is modulated by ADP. FEBS Lett 208:63–66.
15. Light P. 1996. Regulation of ATP-sensitive potassium channels by phosphorylation. Biochim Biophys Acta 1286:65–73.
16. Kakei M, Noma A. 1984. Adenosine-5′-triphosphate-sensitive single potassium channel in the atrioventricular node cell of the rabbit heart. J Physiol 352:265–284.
17. Nelson MT, Huang Y, Brayden JE, Hescheler J, Standen NB. 1990. Arterial dilations in response to calcitonin gene-related peptide involve activation of K^+ channels. Nature 344:770–773.
18. Weston AH, Edwards G. 1992. Recent progress in potassium channel opener pharmacology. Biochem Pharmacol 43:47–54.
19. Jiang C, Mochizuki S, Poole-Wilson PA, Harding SE, Macleod KT. 1994. Effect of lemakalim on action potentials, intracellular calcium, and contraction in guinea pig and human cardiac myocytes. Cardiovasc Res 28:851–857.
20. Ho K, Nichols CG, Lederer WJ, Lytton J, Vassiley PM, Kanazirska MV, Hebert SC. 1993. Cloning and expression of an inwardly rectifying ATP-regulated potassium channel. Nature 362:31–38.
21. Nichols CG, Makhina EN, Pearson WL, Sha Q, Lopatin AN. 1996. Inward rectification and implications for cardiac excitability. Circ Res 78:1–7.
22. Aguilar-Bryan L, Nichols CG, Wechsler SW, Clement JP IV, Boyd AE III, Gonzalez G, Herrera-Sosa H, Nguy K, Nelson DA. 1995. Cloning of the beta cell high-affinity sulfonylurea receptor: a regulator of insulin secretion. Science 268:423–426.
23. Inagaki N, Gonoi T, Clement JP IV, Namba N, Inazawa J, Gonzalez G, Aguilar-Bryan L, Seino S, Bryan J. 1995. Reconstitution of IK_{ATP}: an inward rectifier subunit plus the sulfonylurea receptor. Science 270:1166–1170.
24. Faivre JF, Findlay I. 1990. Action potential duration and activation of ATP-sensitive potassium current in isolated guinea-pig ventricular myocytes. Biochim Biophys Acta 1029:167–172.
25. Findlay I. 1988. Effects of ADP upon the ATP-sensitive K^+ channel in rat ventricular myocytes. J Memb Biol 101:83–92.
26. Nichols CG, Ripoll C, Lederer WJ. 1991. ATP-sensitive potassium channel modulation of the guinea pig ventricular action potential and contraction. Circ Rec 68:280–287.
27. Clapp LH, Curney AM. 1992. ATP-sensitive K^+ channels regulate resting potential of pulmonary arterial smooth muscle cells. Am J Physiol 262:H916–H920.
28. De Weille JR, Fosset M, Mourre C, Schmid-Antomarchi H, Bernardi H, Lazdunski M. 1989. Pharmacology and regulation of ATP-sensitive K^+ channels. Pflugers Arch 414(Suppl 1):S80–S87.
29. Jiang C. 1993. The Regulatory Role of Adenosine 5'-Triphosphate-Sensitive Potassium Channels in Mammalian Cardiac Muscle and Coronary Smooth Muscle. Ph.D. thesis, Imperial College of Science, Technology, and Medicine, School of Medicine at the National Heart and Lung Institute, University of London, 1993.
30. Jiang C, Poole-Wilson PA, Collins P. 1991. Comparison of rabbit coronary arterial relaxation induced by acetylcholine and lemakalim: activation of ATP sensitive potassium channels. Cardiovasc Res 25:930–935.
31. Miyoshi Y, Nakaya Y, Wakatsuki T, Nakaya S, Fujino K, Saito K, Inoue I. 1992. Endothelin blocks ATP-sensitive K^+ channels and depolarizes smooth muscle cells of porcine coronary artery. Circ Res 70:612–615.
32. Weiss J, Hiltbrand B. 1985. Functional compartmentation of glycolytic versus oxidative metabolism in isolated rabbit heart. J Clin Invest 75:436–447.
33. Elliott AC, Smith GL, Allen DG. 1989. Simultaneous measurements of action potential duration and intracellular ATP in isolated ferret hearts exposed to cyanide. Circ Res 64:583–591.
34. Keung EC, Li Q. 1991. Lactate activates ATP-sensitive potassium channels in guinea pig ventricular myocytes. J Clin Invest 88:1772–1777.
35. Jiang C, Collins P. 1994. Inhibition of hypoxia-induced relaxation of rabbit isolated coronary arteries by NG-monomethyl-L-arginine but not glibenclamide. Br J Pharmacol 111:711–716.
36. Jiang C, Crake T, Poole-Wilson PA. 1991. Inhibition by barium and glibenclamide of the net loss of $^{86}Rb^+$ from rabbit myocardium during hypoxia. Cardiovasc Res 25:414–420.
37. Escande D, Henry P. 1993. Potassium channels as pharmacological targets in cardiovascular medicine. Eur Heart J 14(Suppl B):2–9.
38. Auchampach JA, Maruyama M, Cavero I, Gross GJ. 1991. The new K^+ channel opener Aprikalim (RP 52891) reduces experimental infarct size in dogs in the absence of hemodynamic changes. J Pharmacol Exp Ther 259:961–967.

39. Edwards G, Weston AH. 1990. Potassium channel openers and vascular smooth muscle relaxation. Pharmacol Ther 48:237–258.
40. Daut J, Maier-Rudolph W, Beckerath N, Mehrke G, Gunter K, Goedel-Meinen L. 1990. Hypoxic dilation of coronary arteries is mediated by ATP-sensitive potassium channels. Science 247:1341–1342.
41. Kirsch GE, Codina J, Birnbaumer L, Brown AM. 1990. Coupling of ATP-sensitive K^+ channels to A1 receptors by G proteins in rat ventricular myocytes. Am J Physiol 259:H820–H826.
42. Belloni FL, Hintze TH. 1991. Glibenclamide attenuates adenosine-induced bradycardia and coronary vasodilatation. Am J Physiol 261:H720–H727.
43. Wei HM, Kang YH, Merrill GF. 1989. Canine coronary vasodepressor responses to hypoxia are abolished by 8-phenyltheophylline. Am J Physiol 257:H1043–H1048.
44. Venkatesh N, Lamp ST, Weiss JN. 1991. Sulfonylureas, ATP-sensitive K^+ channels, and cellular K^+ loss during hypoxia, ischemia, and metabolic inhibition in mammalian ventricle. Circ Res 69:623–637.
45. Kantor PF, Coetzee WA, Carmeliet EE, Dennis SC, Opie LH. 1990. Reduction of ischemic K^+ loss and arrhythmias in rat hearts. Effect of glibenclamide, a sulonylurea. Circ Res 66:478–485.
46. Cole WC, McPherson CD, Sontag D. 1991 ATP regulated K^+ channels protect the myocardium against ischemia/reperfusion damage. Circ Res 69:571–581.
47. Adams D, Crome R, Lad N, Manning AS, Mackenzie I. 1990. Failure of the ATP-dependent K^+ channel inhibitor, glibenclamide, to reduce reperfusion-induced or ischemic arrhythmias in rat hearts. Br J Pharmacol 100(Suppl):438p.
48. Curtis MJ, Walker MJA. 1986. The mechanism of action of the optical enantiomers of verapamil against ischemia-induced arrhythmias in the conscious rat. Br J Pharmacol 89:137–147.
49. Wilde AAM. 1993. Role of ATP-sensitive K^+ channel current in ischemic arrhythmias. Cardiovasc Drugs Ther 7:521–526.
50. Murry CE, Jennings RB, Reimer KA. 1986. Preconditioning with ischemia: a delay of lethal cell injury in ischemic myocardium. Circulation 74:1124–1136.
51. Liu Y, Ytrehus K, Downey JM. 1994. Evidence that translocation of protein kinase C is a key event during ischemic preconditioning of rabbit myocardium. J Mol Cell Cardiol 26:661–668.
52. Gross GJ. 1995. ATP-sensitive potassium channels and myocardial preconditioning. Basic Res Cardiol 90:85–88.
53. Auchampach JA, Grover GJ, Gross GJ. 1992. Blockade of ischemic preconditioning in dogs by the novel ATP-dependent potassium channel antagonist sodium 5-hydroxydecanoate. Cardiovasc Res 26:1054–1062.
54. Tomai F, Crea F, Caspardone A, Versaci F, Depaulis R, Penta de Peppo A, Chiaririe L, Gioffre' PA. 1994. Ischemic preconditioning during coronary angioplasty is prevented by glibenclamide, a selective ATP-sensitive K^+ channel blocker. Circulation 90:700–705.
55. Atwal KS. 1994. Pharmacology and structure-activity relationships for K_{ATP} modulators: tissue-selective K_{ATP} openers. J Cardiovasc Pharmacol 24:S12–S17.
56. Knight C, Purcell H, Fox K. 1995. Potassium channel openers: clinical application in ischemic heart disease—overview of clinical efficacy of nicorandil. Cardiovasc Drugs Ther 9:229–236.

II. PRECONDITIONING AND PROTECTION OF ISCHEMIA–REPERFUSION INJURY

This Page Intentionally Left Blank

EARLY AND DELAYED PROTECTION AGAINST VENTRICULAR ARRHYTHMIAS INDUCED BY PRECONDITIONING

AGNES VEGH*, ADRIENN KIS*, JULIUS GY PAPP*, and JAMES R. PARRATT**

* *Albert Szent-Györgyi Medical University*
** *University of Strathclyde*

Summary. Ischemic preconditioning, induced by brief periods of coronary artery occlusion, results not only in a reduction in myocardial ischemic damage but also in suppression of those life-threatening ventricular arrhythmias that result from a subsequent, more prolonged ischemia–reperfusion insult. Although this protection is marked, the antiarrhythmic effect is transient and the protection wanes with time (e.g., 60 minutes after the preconditioning stimulus, the antiarrhythmic effect is almost lost). Protection against ventricular arrhythmias can also result from brief periods of cardiac pacing, which leads to both immediate and delayed protection, e.g., a marked reduction in the incidence of ischemia-induced ventricular fibrillation, five minutes after pacing and also 24 hours later. This delayed protection against arrhythmias is less marked 48 and 72 hours after the pacing stimulus but can be reinstated, and lasts for a more prolonged period, if dogs are repaced at a time when protection from the initial pacing stimulus begins to wane. Whether it is possible to protect the heart in the longer term by pacing is unknown but is under investigation. Although the precise mechanisms of both the early and delayed protection are not yet fully understood, there is some evidence that endogenous protective mediators derived from coronary vascular endothelium, such as bradykinin, nitric oxide, and prostanoids (most likely prostacyclin), are involved in both phases of this antiarrhythmic protection. These may then trigger the induction, during the late phase, of protective proteins.

INTRODUCTION

One of the most important consequences of the abrupt reduction in coronary blood flow that results from coronary artery occlusion, both in humans and in experimental animals, is the occurrence of those life-threatening ventricular arrhythmias that

S. Mochizuki, N. Takeda, M. Nagano and N. Dhalla (eds.). THE ISCHEMIC HEART.

are, in the clinical situation, responsible for sudden cardiac death [1–3]. Severe myocardial ischemia, infarction, and sudden cardiac death are leading causes of cardiovascular mortality in modern societies. Protecting the myocardium from ischemic injury is thus a major aim in the reduction of morbidity and mortality from ischemic heart disease. Despite advances in drug therapy and interventional cardiology (e.g., early thrombolysis, percutaneous coronary angioplasty) and surgery (coronary bypass surgery), further research is required to explore new strategies that might ultimately provide practical therapeutic interventions.

There has been much recent interest in experimental cardiology in the observation that the heart (and indeed other organs) is able to protect itself against fatal, severe injury if it has been previously subjected to a similar, sublethal stress. Ischemic preconditioning is one form of such cardioprotective adaptation, first described by Murry and colleagues in 1986 [4]. Ischemic preconditioning can be defined as *the increased tolerance of the heart that can be induced by brief periods of ischemia and reperfusion.* There is evidence that ischemic preconditioning offers an extremely powerful protection against ischemic damage [4] and against occlusion and reperfusion-induced ventricular arrhythmias [5–7] and that it also enhances the recovery of contractile function during reperfusion of the ischemic myocardium [8]. The protection achieved by preconditioning exceeds the effectiveness of any known pharmacological intervention [9,10] and may represent an important clinically accessible component of myocardial protection. Although the precise mechanisms of this phenomenon are not fully understood, much of the evidence suggests that endogenous myocardial protective substances are involved [11].

The purpose of this chapter is to outline the evidence for the antiarrhythmic effects of preconditioning and to discuss the possible mechanisms of this protection with particular reference to studies made in a canine model of ischemia and reperfusion.

THE ANTIARRHYTHMIC EFFECTS OF ISCHEMIC PRECONDITIONING: HISTORICAL BACKGROUND

Before the "preconditioning era," there were several published observations demonstrating the reduction, by brief periods of ischemia, of the severity of ventricular arrhythmias resulting from a subsequent period of ischemia. For example, as early as 1950, Harris [12] showed that dogs are more likely to survive a coronary artery occlusion if this is performed in two stages. Much later, Gülker and his colleagues investigated the effect of multiple coronary artery occlusions on the ventricular fibrillation threshold [13]. They showed that the decrease in the ventricular fibrillation threshold became increasingly less marked, and the duration increasingly shorter, during repeated occlusions, and that the last (fifth) occlusion resulted in no significant decrease in fibrillation threshold at all. Later, Barber [14] not only confirmed that brief periods of ischemia result in less severe ischemic changes (i.e., epicardial ST-segment elevation) [15–17] but also reduced the number of ventricular premature beats that occurred during the second, and subsequent, occlusions of the same short duration. None of these studies was designed, however, to explore

the possibility that ventricular arrhythmias arising during a *prolonged* ischemic insult could be modified if that insult had been preceded by one or more shorter periods of ischemia—in other words, to test the hypothesis that ischemic preconditioning results not only in a reduction in myocardial ischemic damage but also in a suppression of ventricular arrhythmias.

The first report that ischemic preconditioning might protect the myocardium against reperfusion-induced ventricular arrhythmias came from the studies of Shiki and Hearse [5]. In anesthetized rats, they showed that the incidence and severity of ventricular arrhythmias following the release of short periods of coronary artery occlusion of the same duration (five minutes) was markedly attenuated if the recovery period between the repeated occlusions was 10 or 20 minutes. This antiarrhythmic effect was, however, greatly attenuated if the second occlusion–reperfusion insult was performed hours or even days after the first occlusion. This study was, in effect, similar to that of Barber [14] except that reperfusion arrhythmias were examined and that very much longer "rest" (reperfusion) periods were used. Neither of these studies provided evidence relevant to the important question of whether brief ischemic episodes also protect the heart against those ventricular arrhythmias that occur during a longer period of ischemia–reperfusion. Shiki and Hearse [5] also failed to observe the reappearance of protection against arrhythmias 24 hours after the initial preconditioning stimulus, i.e., the late, or delayed, second window of protection that has since aroused such considerable interest. Perhaps the explanation for this is that the preconditioning stimulus (a single five-minute coronary artery occlusion) was too weak.

THE ANTIARRHYTHMIC EFFECTS OF ISCHEMIC PRECONDITIONING

The first demonstration that short periods of sublethal ischemic stress are protective against those ventricular arrhythmias that occur during a subsequent longer period of ischemia–reperfusion was provided by a collaborative study, performed in parallel in Glasgow and in Szeged, using two different species [18,19]. Komori, working in the Glasgow department, examined in an anesthetized rat model whether brief periods of ischemia reduced the severity of arrhythmias during a subsequent, more prolonged period of coronary artery occlusion. He found that the number of ventricular premature beats and both the incidence and duration of ventricular tachycardia (VT) during a 30-minute occlusion were markedly suppressed if that prolonged occlusion had been preceded 10 minutes earlier by a single three-minute occlusion [7,19]. A single one-minute preconditioning occlusion was not effective, whereas a five-minute occlusion in this model [20] resulted in a high incidence of ventricular arrhythmias following reperfusion of the ischemic myocardium. It seemed from these results that in anesthetized rats, a single three-minute preconditioning occlusion is optimal for triggering protection against those ventricular arrhythmias that occur during a subsequent 30-minute period of ischemia, commencing shortly (10 minutes) after this preconditioning stimulus (table 1). This protection was, however, much less pronounced if the time interval between the single preconditioning

Table 1. The number of ventricular premature beats (VPBs), the incidence and duration of ventricular tachycardia (VT), and the incidence of ventricular fibrillation (VF) in rats following preconditioning

Duration of preconditioning occlusion (min)	*n*	Number of VPBs	Incidence of VT (%)	Duration of VT (s)	Incidence of VF (%)
0 (Control)	12	1236 ± 262	100	95.6 ± 28.7	42
1	8	1230 ± 370	100	109.8 ± 30.9	50
3	10	200 ± 60[a]	70	12.6 ± 3.8[a]	10
5	10	394 ± 152[b]	60[b]	55.1 ± 20.3	30

[a] $p < 0.01$ cp. nonpreconditioned animals.
[b] $p < 0.05$ cp. nonpreconditioned animals.
Note: Rats were subjected to a 30-minute occlusion of the left coronary artery. In the preconditioned rats, this was preceded 10 minutes earlier by a preconditioning occlusion of 1, 3, or 5 minutes. Preconditioning periods of 3 or 5 minutes significantly reduced the arrhythmias occurring during a longer occlusion. Values are mean (±SEM).

occlusion and the prolonged occlusion was increased from 10 minutes to 30 minutes and was entirely lost if the reperfusion period was further increased to one hour [7].

This marked antiarrhythmic effect of ischemic preconditioning was also confirmed in a large animal arrhythmia model, which had been used for many years in the Szeged department. In mongrel dogs, anesthetized with a mixture of chloralose and urethane, we showed that if a prolonged, 25-minute occlusion of the anterior descending branch of the left coronary artery (LAD) was preceded, 20 minutes earlier, by one or two brief (five-minute) occlusions of that same artery, the severity of the arrhythmias during the prolonged occlusion was markedly reduced [6,7]. This pronounced antiarrhythmic effect of preconditioning is illustrated in figure 1. Usually these early postocclusion ventricular arrhythmias (e.g., ventricular premature beats) occur in two phases: phase 1a and phase 1b (figure 1) [21]. However, when this prolonged occlusion was preceded 20 minutes earlier by two five-minute periods of occlusion, separated by a 20-minute reperfusion interval, the number of premature ectopic beats was markedly suppressed over the entire 25-minute occlusion period. This was real protection, i.e., there was an absolute reduction in the number of ectopic beats and there was no shift in the distribution of these to a later time. This was demonstrated in experiments in which the occlusion time was prolonged from 25 minutes to 60 minutes [7].

There is considerable evidence that the severity of ventricular arrhythmias during coronary artery occlusion depends, among other factors, upon the site of occlusion, the area at risk, the anesthetic used, the weight of the dogs (heart: body weight ratio), the extent of the preexisting coronary collateral circulation, the electrolyte balance, and the degree of cardiac sympathetic drive. The influence of these various factors has been discussed recently [22,23]. In the chloralose-urethane anesthetized canine model, occlusion of the LAD proximal to the first main diagonal branch produces severe myocardial ischemia and results in an area at risk of infarction of about 40%–43% of the mass of the left ventricle (including the septum), a great

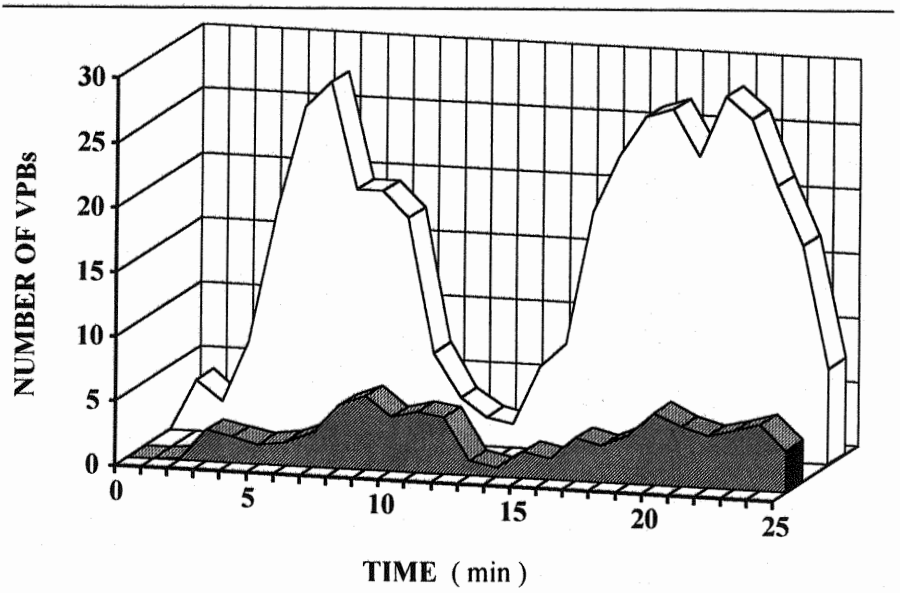

Figure 1. Distribution of ventricular premature beats (VPBs) at one-minute intervals over a 25-minute occlusion period of the left anterior descending (LAD) coronary artery, in control dogs (open histograms) and in dogs subjected to preconditioning by two five-minute occlusions of the LAD (hatched histograms). VPBs over a 25-minute occlusion of a coronary artery occur in two phases: phase Ia and phase Ib. When this prolonged occlusion is preceded by two brief (five-minute) occlusions of that same artery, there is a marked reduction in the number of VPBs throughout the entire occlusion period.

number of ventricular premature ectopic beats (VPBs; more than 400 during a 25-minute occlusion), and a high incidence (90%–100%) of ventricular tachycardia (VT), with many episodes of VT (more than nine per dog; see figure 2). In 40%–50% of these dogs, ventricular fibrillation (VF) results. Clearly, this is a very severe arrhythmia model. Further, the subsequent reperfusion of the ischemic myocardium results in ventricular fibrillation in all the dogs (figure 2). All these severe ventricular arrhythmias were reduced dramatically when the heart was previously subjected to short periods of ischemia. For example, the incidence and number of episodes of VT during occlusion were significantly less in these preconditioned dogs. However, the most striking feature of this protection was the absence of VF during occlusion and the increased survival from the combined ischemia–reperfusion insult (figure 2).

There is no doubt that ischemic preconditioning also reduces the severity of arrhythmias in rat hearts subjected to coronary artery occlusion both in vivo [7,18,19,24] and in vitro [25–27]. Some studies using a canine model of preconditioning have shown a similar reduction in arrhythmia severity [6,7,28], but some investigators [29,30] have been unable to confirm this marked antiarrhythmic effect. There is only one example of preconditioning inducing protection against

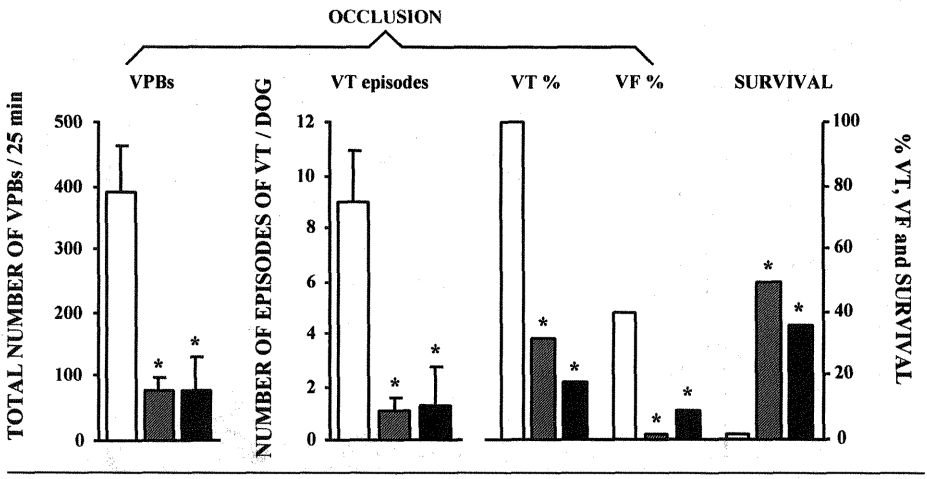

Figure 2. The incidence and severity of ventricular arrhythmias during a 25-minute occlusion of the anterior descending branch of the left coronary artery, and survival following reperfusion at the end of the occlusion period, in control dogs (open columns) and in dogs subjected to preconditioning, either by two (hatched columns) or four five-minute (solid columns) coronary artery occlusions. The severity of these ventricular arrhythmias during such a prolonged occlusion is markedly reduced when the dogs had been previously preconditioned, either by two or four brief periods of occlusion of that same artery. *, $p < 0.05$ cp. control dogs.

arrhythmias in anesthetized pigs [31]. Most of the laboratories using a pig model for assessing ischemic injury as a primary endpoint failed to demonstrate such an antiarrhythmic protection [32].

A number of possible explanations for these discrepancies have been previously discussed in detail [22,23], and this is not the place to repeat them. Apart from the variability in the protocols used by the different groups, one difference of some potential importance is the fact that multiple preconditioning occlusions (usually four five-minute episodes with short reperfusion intervals), or longer periods of ischemia (10 minutes), were used in those studies that aimed primarily to examine the effects of preconditioning on infarct size [4]. We surmised that these protocols might have detrimental effects on arrhythmias during a subsequent prolonged occlusion. Certainly, it would be difficult in our model to use a preconditioning occlusion of as long as 10 minutes because reperfusion after such a long preconditioning occlusion would certainly result in immediate ventricular fibrillation. Indeed, Li and his colleagues [28] showed, also in dogs, that whereas a single five-minute preconditioning occlusion reduced the incidence of ventricular fibrillation, a greater number of preconditioning occlusions (12 × 5 minutes) resulted in a high mortality during the subsequent prolonged occlusion.

It seemed of interest to determine in our model, which has consistently demonstrated an antiarrhythmic effect of preconditioning, whether multiple occlusions still protect the myocardium against ischemia-induced life-threatening ventricular

arrhythmias in a similar way to that achieved by one or two such occlusions. In a series of experiments, we preconditioned dogs with four five-minute periods of LAD occlusion interspersed with five-minute reperfusion periods, and five minutes later subjected the heart to a 25-minute coronary artery occlusion. Figure 2 shows that four five-minute periods of coronary artery occlusion resulted in a similar protection against ventricular arrhythmias to that which occurred in dogs preconditioned by only two such occlusions. Thus, in our hands, increasing the number of preconditioning occlusions (at least up to four) with short reperfusion intervals (five instead of 20 minutes) still maintained the antiarrhythmic effect during a prolonged occlusion. This finding might mean that other factors, such as the anesthesia used, the risk zone, sympathetic drive, etc., are particularly important in the generation of these early ventricular arrhythmias. Certainly, there seems little point in attempting to examine possible antiarrhythmic effects of preconditioning in an inappropriate model in which coronary artery occlusion results in only a few premature beats (a mean of less than 50 over a 60-minute occlusion period) [29] even under control conditions. This outcome probably reflects the depressant effects of barbiturate anesthesia on the myocardium.

There was clear evidence from our studies that preconditioning reduces the severity of myocardial ischemia. This result was demonstrated by the measurement of epicardial ST-segment elevation and the degree of inhomogeneity of electrical activation, within the ischemic area [6,7]. Preconditioning by an increased number of occlusions also confirmed this antiischemic effect of preconditioning. Thus, when dogs were preconditioned by four, rather than only two, five-minute periods of coronary artery occlusion and, five minutes later, subjected to a 25-minute occlusion, there was marked epicardial ST-segment elevation, particularly during the first five-minute preconditioning occlusion. The following preconditioning occlusions and the prolonged occlusion resulted in significantly less pronounced epicardial ST-segment elevation (figure 3) and less marked changes in the degree of inhomogeneity (figure 4). These changes were significantly less marked than those seen in control dogs. This modification of ischemia severity occurred without a significant change in collateral blood flow, since the reduction in peripheral coronary perfusion pressure, measured in a small branch of the LAD distal to the occlusion site, was the same during each coronary artery occlusion (figure 5). This finding might indicate that the anti-ischemic, and perhaps also the antiarrhythmic, effects of ischemic preconditioning are not dependent upon changes in collateral blood flow. This question was particularly important to clarify in our experiments because there has been some debate as to whether species with a variable coronary collateral circulation, such as dogs, can be preconditioned in such a way as to reduce ventricular arrhythmias induced by ischemia. However, there is no evidence that coronary blood flow is higher when the artery is occluded a second time, i.e., that an increase in collateral (overlap) blood flow is responsible for the decreased injury seen at sites immediately below surface electrodes [14,28], or that there is any significant change in peripheral coronary pressure (an index of collateral perfusion) during successive coronary artery occlusions (figure 5). Even Murry and colleagues

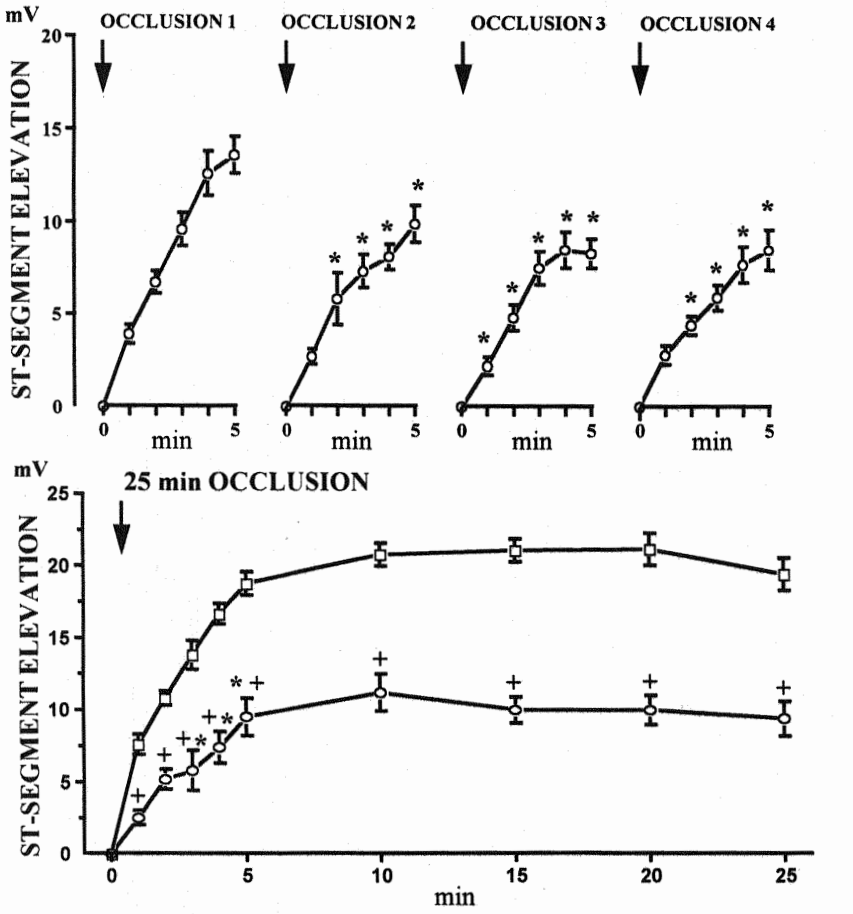

Figure 3. Changes in epicardial ST-segment elevation in anaesthetized control dogs (open squares), and in dogs preconditioned by four five-minute occlusions and then, five minutes later, subjected to a 25-minute occlusion of the left anterior descending coronary artery (open circles). This figure shows that the most marked epicardial ST-segment elevation occurs during the first five-minute preconditioning occlusion. The following preconditioning occlusions, and the prolonged occlusion, result in a significantly less pronounced ST-segment elevation. This increase in epicardial ST-segment during prolonged occlusion is significantly less marked than in control dogs during the same occlusion period. *, $p < 0.05$ cp. first preconditioning occlusion; +, $p < 0.05$ cp. control group.

in their initial study demonstrated that the reduction in infarct size was apparent at any level of collateral circulation [4]. Further, the protective effects of preconditioning, including arrhythmia suppression, are present in those species with very little coronary collateral development (e.g., rats).

The antiarrhythmic effect of ischemic preconditioning has thus been demonstrated in at least two species (rats and dogs). This protection is *marked* (reduction in

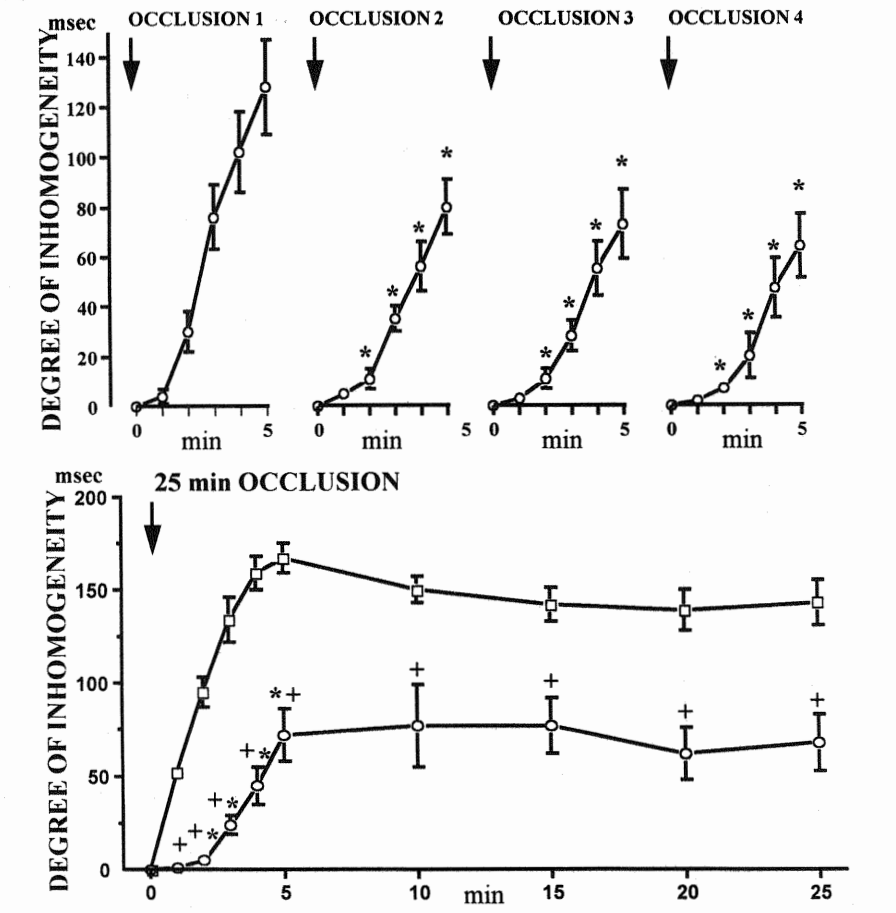

Figure 4. Changes in the degree of inhomogeneity of electrical activation in anaesthetized control dogs subjected to a 25-minute coronary artery occlusion (open squares), and in dogs preconditioned by four five-minute occlusions and then, five minutes later, subjected to a 25-minute occlusion of the left anterior descending coronary artery (open circles). The most pronounced increase in the degree of inhomogeneity is seen during the first five-minute preconditioning occlusion. The following preconditioning occlusions, and the prolonged occlusion itself, result in significantly less marked changes in the degree of inhomogeneity. The increase in the degree of inhomogeneity is also significantly less marked during the prolonged occlusion in the preconditioned dogs than in the control dogs. *, $p < 0.05$ cp. first preconditioning occlusion; +, $p < 0.05$ cp. control group.

the severity of arrhythmias) and *real* (absolute reduction in the number and incidence of ventricular arrhythmias without shifting to a later time period). However, this marked antiarrhythmic effect of preconditioning is transient; the protection wanes with time. For example, if the time interval between the preconditioning occlusions and the prolonged occlusion is increased from 20 minutes to 60 minutes, the antiarrhythmic effect is markedly attenuated (figure 6). The number of VPBs

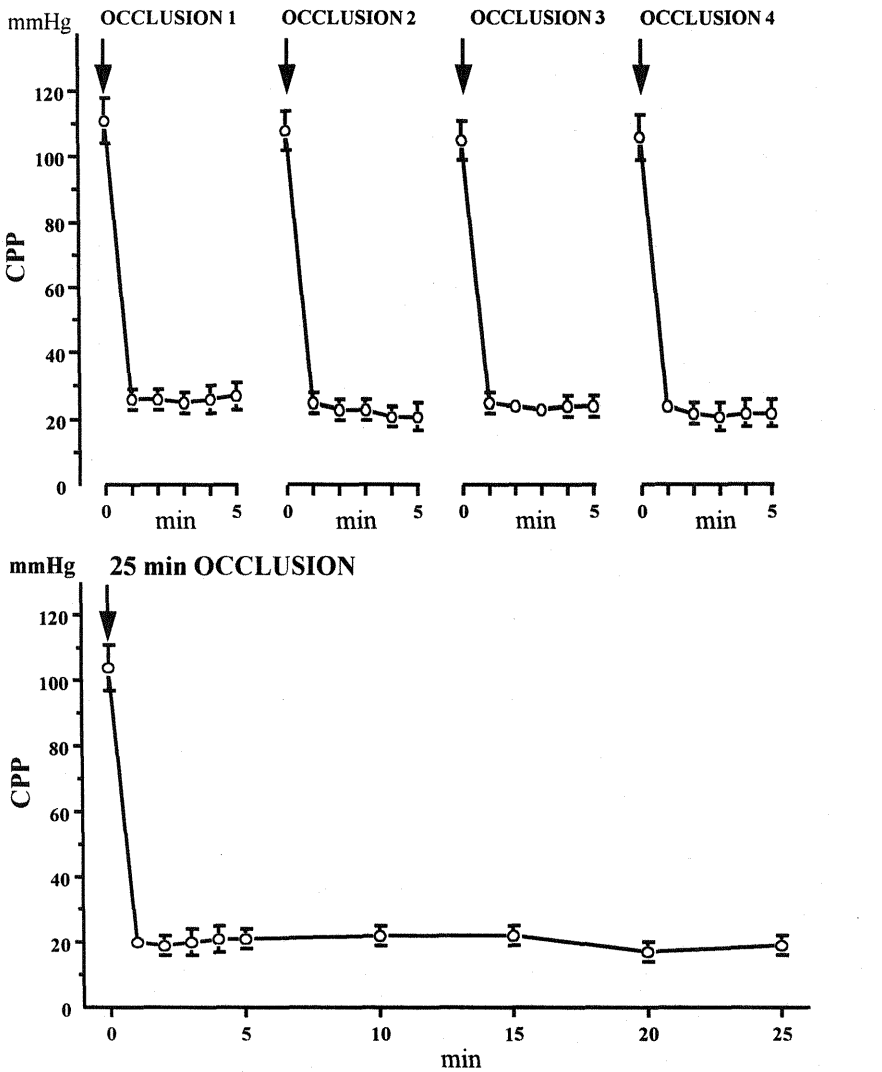

Figure 5. Changes in peripheral coronary perfusion pressure (CPP; mmHg) during brief (five-minute) and prolonged (25-minute) occlusions, measured in a small branch of the left anterior descending coronary artery distal to the occlusion site. The reduction in peripheral CPP is the same during repeated occlusions of the LAD, suggesting there is no collateral vessel recruitment.

and the incidence and number of episodes of VT during coronary artery occlusion are similar to those in control dogs and, although the incidence of VF during occlusion is still reduced, nearly all the dogs fibrillated on reperfusion. Survival, as in control dogs, is either not observed at all or is much reduced.

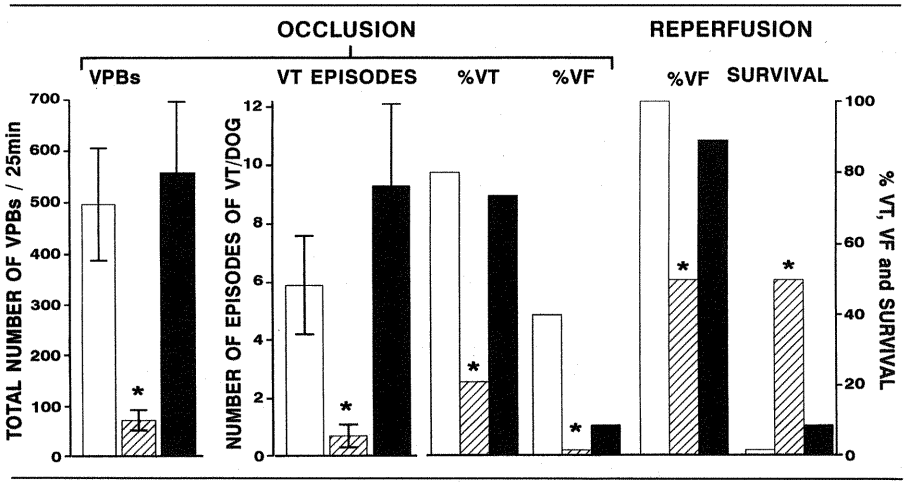

Figure 6. The transient nature of protection afforded by ischemic preconditioning (by brief coronary artery occlusions) against ventricular arrhythmias in anesthetized dogs. The protection is lost if the time between the preconditioning occlusions and the prolonged occlusion is increased from 20 minutes to 60 minutes. The figure shows the number of ventricular premature beats (VPBs), the number of episodes of ventricular tachycardia (VT), and the incidences of VT and ventricular fibrillation (VF) during a 25-minute occlusion of the left anterior descending coronary artery and during subsequent reperfusion. There is a reduction in the number of VPBs and VT episodes and in the incidences of both VT and VF (and an increased survival) in those dogs that were preconditioned by two five-minute occlusions (striped columns), provided that the reperfusion time was 20 minutes, but not if the reperfusion time was increased to one hour (solid columns). *, $p < 0.05$ cp. control nonpreconditioned dogs (open columns).

PRECONDITIONING BY RAPID CARDIAC PACING

In most studies concerned with suppression of ischemia- and reperfusion-induced ventricular arrhythmias, the preconditioning stimulus has been complete occlusion of a major branch of a coronary artery (or global ischemia in isolated hearts). The question as to whether it is possible to induce preconditioning of the myocardium by means other than short coronary artery occlusion was initially investigated by rapid cardiac pacing. In 1991 we reported that rapid (overdrive) ventricular pacing reduces the consequences of subsequent periods of regional ischemia in anesthetized dogs [33]. Thus, the epicardial ST-segment elevation, the changes in the degree of inhomogeneity of electrical activation within the ischemic area, and ventricular arrhythmias that normally occur during a 25-minute LAD occlusion were markedly reduced when the dogs were subjected to two brief (two-minute) periods of rapid right ventricular pacing (300 beats/min) two minutes prior to the occlusion. In conscious rabbits, overdrive pacing also reduced changes in left ventricular end-diastolic pressure and endocardial ST-segment elevation induced by subsequent periods of overdrive pacing [34]. Perhaps these were the first attempts to induce preconditioning of the myocardium by means other than by short coronary artery occlusions. Since then it has become well established that preconditioning can be

induced by stimuli other than complete occlusion of a coronary artery. Thus, similar infarct size limitation can be achieved by partial coronary artery occlusion [35,36], by hypoxia [37], by increasing stretch in the left ventricular wall via acute volume overload [38], by transient ischemia in adjacent myocardial regions [39], and even following ischemia in organs other than the heart (preconditioning at a distance; [40,41]). However, none of these studies was designed to investigate, as a primary endpoint, the effects of these various preconditioning stimuli on ventricular arrhythmias.

We do not understand precisely why cardiac pacing protects the heart against the effects of a subsequent coronary artery occlusion. One possibility is that these short periods of cardiac overdrive pacing result in transient ischemia, especially in the endocardial regions of the left ventricular wall, because subendocardial perfusion pressure would be drastically reduced due to the combination of reduced coronary artery diastolic perfusion pressure and a markedly elevated left ventricular end-diastolic pressure [42]. Evidence for subendocardial ischemia was obtained in experiments in which we recorded the electrocardiogram from the endocardium of the *left* ventricle during *right* ventricular pacing [43]. Immediately following cessation of pacing, there were transient electrographic changes (4–5 mV ST-segment elevation) indicative of myocardial ischemia. This ischemia was limited to the endocardium, since there was no evidence for ST-segment changes in the epicardial surface of the left ventricle at this time [43].

A similar marked protection was seen against occlusion and reperfusion arrhythmias if the heart was paced at a lower frequency (220 beats/min) but for a longer period (four times for five minutes) [43,44]. In these experiments, dogs were paced four times for five minutes at a rate of 220 beats/min, using a bipolar pacing electrode introduced into the right ventricle. This procedure was followed, at various time intervals after cessation of pacing, by a 25-minute coronary artery occlusion and then by reperfusion. Such cardiac pacing markedly reduced the severity of ventricular arrhythmias during coronary artery occlusion when this was induced five minutes later. These results are illustrated in figure 7. In contrast to the control group, in which 43% of the dogs fibrillated during occlusion and all the dogs died following reperfusion, no dog in the paced group died during occlusion and 55% of the dogs survived reperfusion. However, as with the antiarhythmic effects of classical preconditioning, the protection was lost if the time between the pacing stimulus and the commencement of the prolonged coronary artery occlusion was increased. When dogs were preconditioned by cardiac pacing, the duration of the protection was much shorter than when preconditioning was induced by brief coronary artery occlusions, suggesting that the duration of the protection may depend on the *intensity* of the proceeding ischemic stimulus. Thus, when the artery was occluded five minutes after the end of the pacing stimulus, there was marked antiarrhythmic protection (figure 7). However, this protection was attenuated if the interval between the pacing period and the occlusion was increased to 15 minutes, and protection was almost lost when this interval was increased to one or six hours (figure 8).

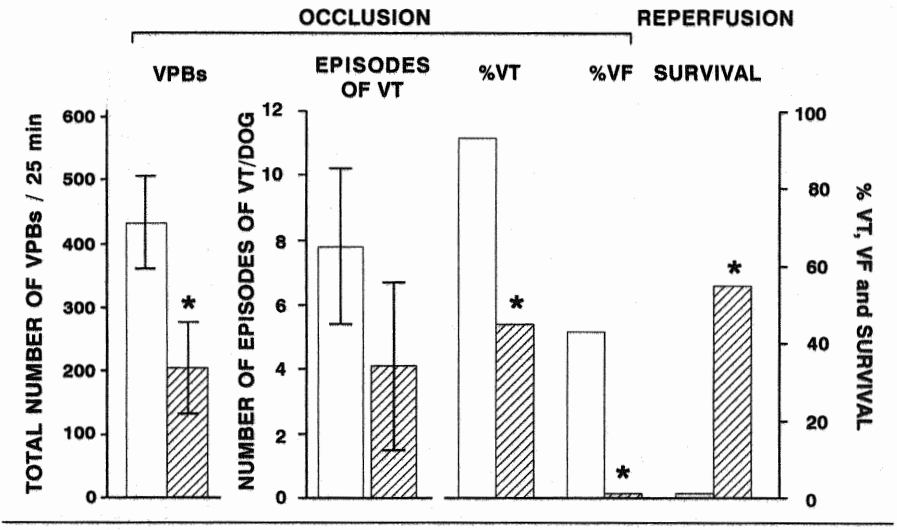

Figure 7. The severity of ventricular arrhythmias during a 25-minute coronary artery occlusion in control dogs (open columns) and in dogs subjected to right ventricular pacing five minutes previously (striped columns). Cardiac pacing (four times for five minutes at a rate of 220 beats/min) five minutes before occlusion of the left anterior descending coronary artery markedly reduces the number of ventricular premature beats (VPBs), the number of episodes of ventricular tachycardia (VT), and the incidences of VT and ventricular fibrillation (VF) during occlusion, and also increases survival from the combined ischemia–reperfusion insult. *, $p < 0.05$ cp. control, nonpaced dogs.

On the basis of these results, we conclude that preconditioning induced either by short coronary artery occlusions or by cardiac pacing results in a marked antiarrhythmic effect against those ventricular arrhythmias that occur during a subsequent, more prolonged ischemia–reperfusion insult.

DELAYED ANTIARRHYTHMIC EFFECTS OF CARDIAC PACING

As outlined above, one of the disappointments of classical ischemic preconditioning is that the protection is relatively short-lived. In most experiments, the protection is lost as the time interval between the preconditioning stimulus and the prolonged ischemic insult is increased to one or two hours; the protection induced by cardiac pacing disappears in an even shorter time. A very important step in preconditioning research was the discovery that the protection afforded by short coronary artery occlusions returned several hours later [45,46]. Two groups, in Japan and in the United Kingdom, showed that brief periods of coronary artery occlusion resulted in *both early protection* against myocardial necrosis, disappearing within two hours, *and delayed protection*, with a time course of many hours. This phenomenon is now known as late or delayed myocardial protection or the *second window* [47].

A similar delayed protection against ischemia-induced ventricular arrhythmias, resulting from cardiac pacing, has been observed in our canine mode ([43,48,49]; see

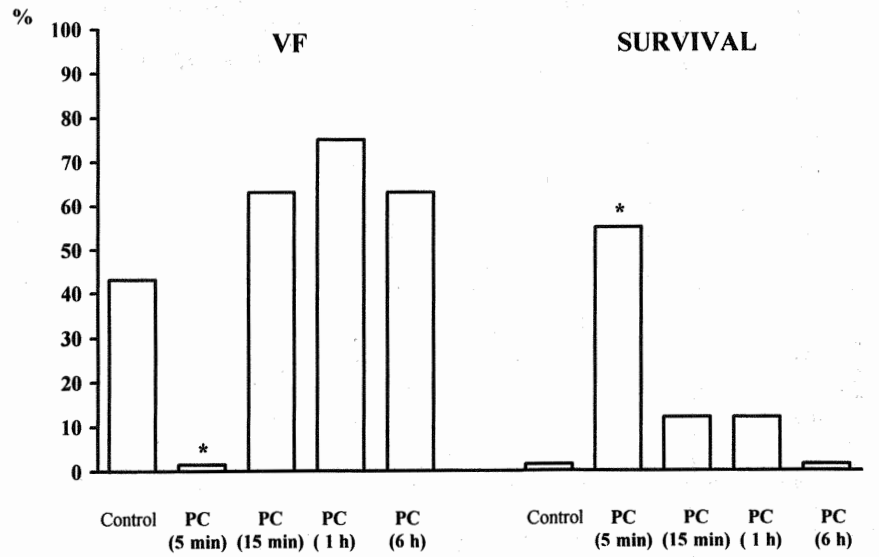

Figure 8. The incidence of ventricular fibrillation during a 25-minute occlusion of the left anterior descending coronary artery, and the overall survival from the combined ischemia–reperfusion insult, in control dogs and in dogs subjected to preconditioning by cardiac pacing at different times prior to the coronary occlusion. The incidence of ventricular fibrillation during occlusion is markedly reduced five minutes after cessation of pacing. This protection is attenuated, or abolished, if the time between the last pacing period and the occlusion is increased to 15 minutes, one hour, or six hours. Survival from the ischemia–reperfusion episode is markedly increased five minutes, but not 15 minutes, one hour, or six hours after pacing. *, $p < 0.05$ cp. control dogs.

figure 9). The total number of VPBs, the incidence and number of episodes of VT, and the incidence of ventricular fibrillation during coronary artery occlusion were all reduced in dogs paced 24 hours previously. Further, 50% of these dogs survived the combined ischemia–reperfusion insult; in contrast, there were few survivors in the sham-operated control dogs. This delayed protection against ventricular fibrillation was not observed when the time between the pacing stimulus and the occlusion was extended to 48 or 72 hours (figure 10), although these was still evidence of protection against VPBs and VT.

Recently we have tried to widen this time window of protection by repeating the preconditioning pacing stimulus at a time when the antiarrhythmic effect of the previous pacing had already waned [50]. In these experiments, we paced dogs, under light pentobarbitone anesthesia, on day 1 but instead of occluding the coronary artery on day 3, when we had determined that the antiarrhythmic protection would be virtually lost, we repeated the pacing stimulus at this time. Forty-eight hours after this second pacing stimulus (on day 5), we reanesthetized the dogs and occluded the left anterior descending coronary artery for 25 minutes. Repeated pacing during the period when the protection had faded resulted in a more prolonged protection

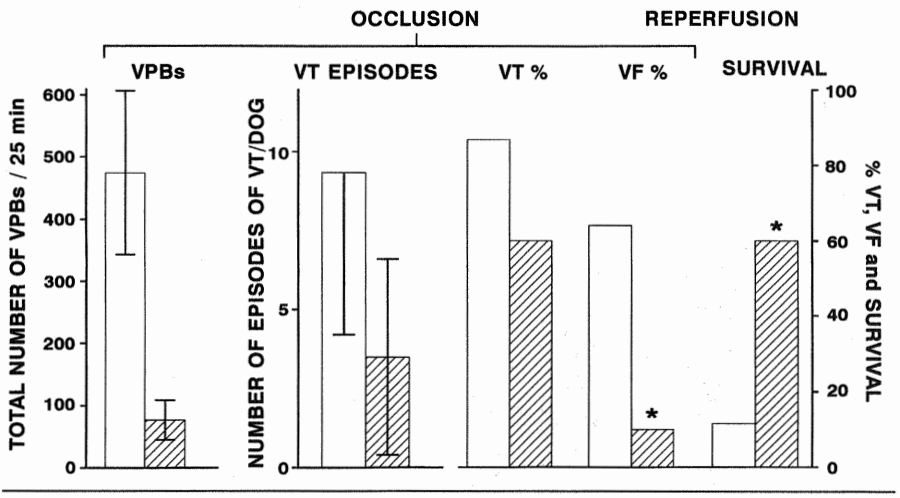

Figure 9. The incidence and severity of ventricular arrhythmias during a 25-minute coronary artery (LAD) occlusion in control dogs (open columns) and in dogs subjected to right ventricular pacing 20–24 hours previously (striped columns). Cardiac pacing markedly reduced the number of ventricular premature beats (VPBs), the number of episodes of ventricular tachycardia (VT), and the incidences of VT and ventricular fibrillation (VF) in these dogs when they were subjected to a 25-minute occlusion 20–24 hours later. Sixty percent of these dogs survived the combined ischemia–reperfusion insult; in contrast, there were few survivors in the control group. *, $p < 0.05$ cp. control, non-paced dogs.

against severe ventricular arrhythmias (VT and VF) than when dogs were paced only once, i.e., 48 hours after the first pacing [50]. Thus, at this time no dog in the repeatedly paced group died during occlusion, in contrast to a high mortality (from VF) in both the sham-operated controls and in those dogs paced only once. Further, 50% of the dogs subjected to repeated pacing survived the combined ischemia–reperfusion insult (figure 11). *It seems from these results that repeated pacing widens the time window of protection against these life-threatening ventricular arrhythmias.*

AN HYPOTHESIS FOR THE MECHANISM OF THE ANTIARRHYTHMIC EFFECT OF ISCHEMIC PRECONDITIONING

It is well accepted that cardiac adapatation induced by preconditioning is a general phenomenon; i.e., the hearts of all species so far studied can be preconditioned. Whereas the phenomenon is well described, little is known at present concerning the mechanisms involved in this protection. A number of possibilities that have been suggested to explain this marked cardioprotection have been reviewed elsewhere [51]. The most likely of these involve alterations in the generation and release of endogenous substances from either ischemic cardiac myocytes, endothelial cells, or both. These mediators may either be protective or potentially injurious [10,11,52]. It is very likely that several mediators, both protective and injurious, are released during the early phase of ischemia, that is, in response to the transient ischemic

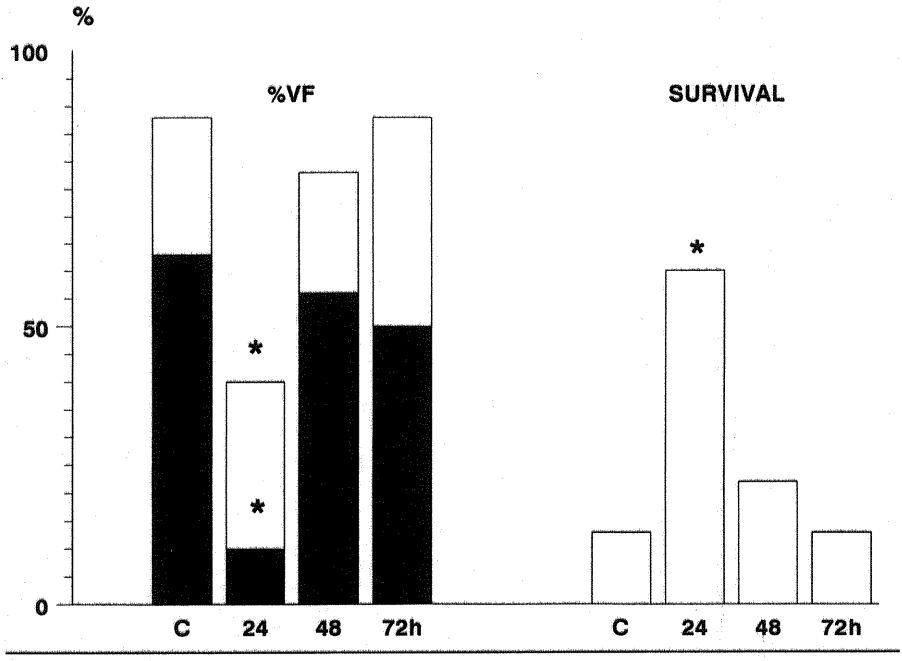

Figure 10. Delayed antiarrhythmic protection induced by cardiac pacing. This figure illustrates the incidence of ventricular fibrillation during a 25-minute occlusion of the left anterior descending coronary artery (solid columns) and following reperfusion (open columns), as well as the overall survival from the combined ischemia–reperfusion insult, in control dogs and in dogs subjected to preconditioning by cardiac pacing at different times prior to the coronary occlusion. The most marked suppression of occlusion and reperfusion ventricular fibrillation occurred 24 hours after cardiac pacing. This delayed protection was not observed if the time between the pacing stimulus and the occlusion was increased to 48 or 72 hours. *, $p < 0.05$ cp. sham-operated controls.

injury such as would occur during a preconditioning stimulus. A strong case can be made for the hypothesis that, after preconditioning, there is an increased liberation of protective substances such as adenosine, nitric oxide, and bradykinin, and a reduced release of potentially injurious substances such as endothelin and noradrenaline. It is also very likely that more than one protective mediator is released to compensate for the harmful consequences of ischemic stress. These mediators, acting at different receptors, might induce protection in different parallel ways, or there might he a final, common pathway. Some believe that this pathway involves the translocation of protein kinase C (PKC) from the cytosol to the sarcolemmal and nuclear membranes. This subject has been recently reviewed in depth [53].

The role of adenosine, as originally proposed by Downey and colleagues [54], with the subsequent involvement of PKC activation, in mediating the infarct size limitation associated with ischemic preconditioning seems clear in most species except rats (reviewed recently by Miura [55]). However, there is no evidence that adenosine plays any role in the antiarrhythmic effect of ischemic preconditioning

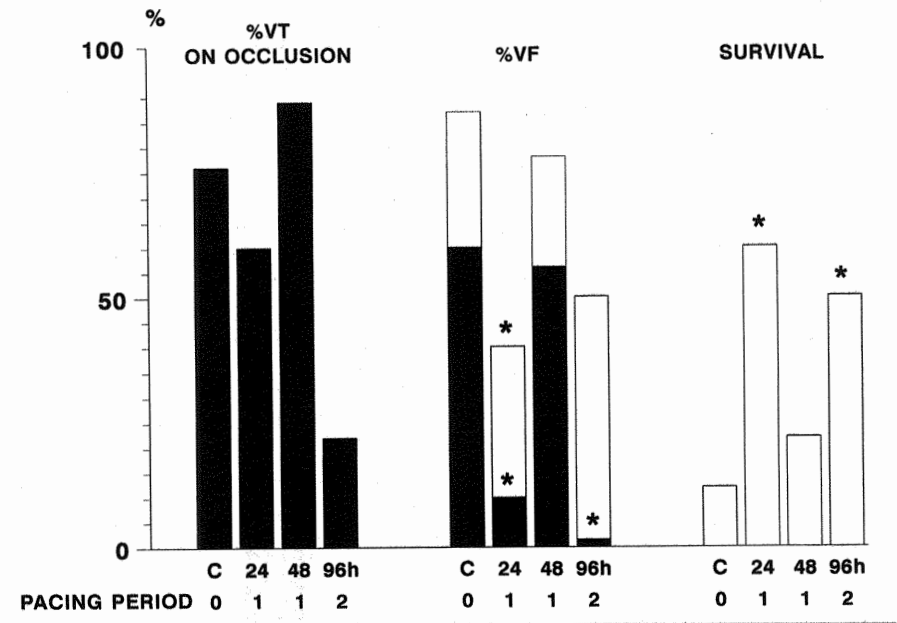

Figure 11. Delayed antiarrhythmic protection induced by repeated pacing. The incidences of ventricular tachycardia (VT) and ventricular fibrillation (VF) during occlusion (solid columns) and following reperfusion (open columns) are shown, as well as survival from the combined ischemia–reperfusion insult, in control dogs, in dogs paced 24 or 48 hours before coronary artery occlusion, and in dogs subjected to repeated pacing both 48 hours before coronary artery occlusion and again 48 hours after this first pacing stimulus. Repeated pacing at a time when the protection from the initial pacing stimulus had faded resulted in more prolonged protection against VT and VF and an increased survival (at 96h) compared to when dogs were paced only once 48 hours before the occlusion. *, $p < 0.05$ cp. sham-operated controls.

either in rats [56] or dogs [57], despite the fact that in both these species adenosine can act as an endogenous antiarrhythmic substance [58].

The hypothesis that other endogenous protective substances, particularly those derived from the coronary vascular and endocardial endothelium, are involved in the antiarrhythmic effects of ischemic preconditioning comes mainly from studies performed in the canine model described above. This hypothesis [59] is outlined in figure 12. It assumes that the target organ for preconditioning is the coronary vascular endothelium and that mediators, derived from such endothelial cells, modify arrhythmogenesis by direct communication, via diffusable mediators, with cardiac myocytes. In brief, the evidence, which has been recently summarized in some depth [60], is as follows:

1. Evidence from coronary endothelial denudation using a detergent. Although this approach is not possible in the *in vivo* canine heart, studies using rat isolated perfused hearts in which the coronary vascular endothelium had been removed

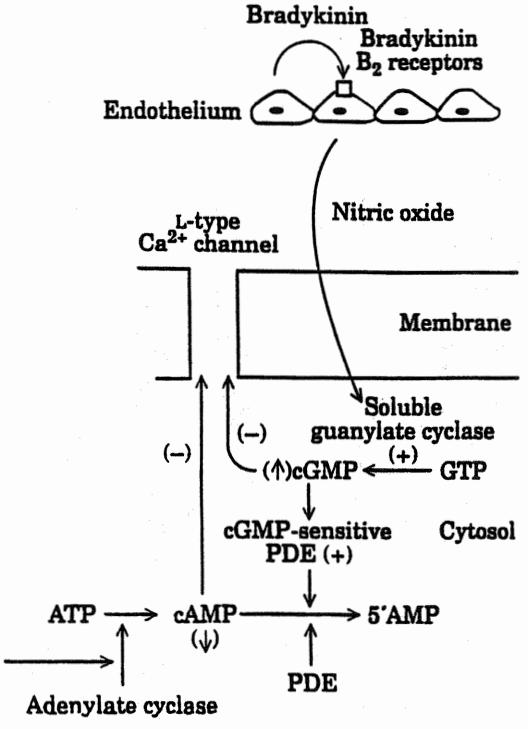

Figure 12. Role of endothelium-derived endogenous protective mediators in ischemic preconditioning—an hypothesis. Bradykinin is released, probably from endothelial cells (which have the mechanisms for generating and releasing kinins), and then acts on B2 receptors on the endothelial surface to increase the calcium transient within these cells and to activate the L-arginine nitric oxide pathway. Nitric oxide then "talks" to the cardiac myocyte, stimulates soluble guanylyl cyclase, and elevates cyclic GMP. This stimulates cGMP-sensitive phosphodiesterase (thus reducing cAMP levels), inhibits calcium entry through L-type calcium channels, and depresses myocardial contractility. From [59], with permission.

revealed that coronary artery occlusion resulted in a higher incidence, and greater severity, of arrhythmias than in control, endothelium-intact hearts [61]. For example, in Sprague–Dawley rats there was a mean of 2724 ± 434 ventricular premature beats over the 20-minute occlusion period in endothelium-denuded hearts compared with only 255 ± 39 beats in hearts in which the coronary vascular endothelium was intact. The incidence and duration of ventricular tachycardia during the occlusion period were also much greater in endothelium-denuded hearts (100% and 711 ± 186 seconds compared to 75% and 14.5 ± 5.4 seconds) [61]. These results suggest that, following coronary occlusion, protective substances are released from the coronary vascular endothelium that modify arrhythmia severity.

2. Substances normally derived from vascular endothelial cells (for example, bradykinin and prostacyclin), when infused locally into a side branch of the coronary

artery to be occluded or directly into the artery itself, are profoundly antiarrhythmic [62,63]. In the case of bradykinin, this protection is mediated through nitric oxide generation, since it is markedly attenuated in the presence of an inhibitor of the L-arginine nitric oxide pathway [64].

There is also some evidence that the amount of prostacyclin released under conditions of coronary artery occlusion is related to the number of ventricular premature beats that occurs up to that sampling time [65].

3. Potentiation of mediator release also suppresses early ischemia-induced ventricular arrhythmias. For example, nafazatrom, which inhibits prostacyclin breakdown, is antiarrhythmic in the canine model [66]. We have yet to examine whether treatment with angiotensin-converting enzyme (ACE) inhibitors modifies early ischemia-induced arrhythmias in the canine model that we have used to demonstrate the antiarrhythmic effects of ischemic preconditioning. Whether this is true in other models, and in humans, remains uncertain but has been recently reviewed [67].

4. Evidence for the release of protective mediators during preconditioning comes from studies in which their generation by endothelial cells, or their effects at receptor level, have been inhibited. Thus, blockade of bradykinin B_2 receptors with icatibant increases the severity of arrhythmias following coronary artery occlusion [68,69] (figure 13), as well as markedly attenuating the protective effects of ischemic preconditioning. This finding suggests that *bradykinin* is a key mediator in protection against ischemia-induced arrhythmias.

The situation regarding *prostacyclin* is more complicated because it is not possible to selectively inhibit its generation without influencing the release of a variety of cyclooxygenase products that influence coronary vascular dynamics and arrhythmogenesis. There is some evidence in the canine model that the nonspecific inhibition of all cyclooxygenase products markedly attenuates the antiarrhythmic effects of preconditioning [6] and that the dual inhibition of both the cyclooxygenase *and* L-arginine nitric oxide pathways completely prevents this protection [70]. The effects of prostacyclin on arrhythmogenesis during coronary artery occlusion have been extensively reviewed [71,72].

The role of *nitric oxide* in modulating arrhythmia severity during ischemia and preconditioning has been analyzed in two ways. First, the antiarrhythmic effects of preconditioning are attenuated following inhibition of the L-arginine nitric oxide pathway [73]. Second, the local intracoronary administration of methylene blue (which inhibits the effect of nitric oxide on soluble guanylyl cyclase) completely abolishes the antiarrhythmic effect of preconditioning [74]. This outcome is illustrated in figure 14.

The above evidence suggests that endothelial-derived substances protect against the consequences of ischemia by suppressing life-threatening ventricular arrhythmias and that preconditioning in some way stimulates this release. This conclusion would provide a partial explanation why, when there is coronary vascular endothelial dysfunction (as in hypertension, atherosclerosis, ventricular hypertrophy and

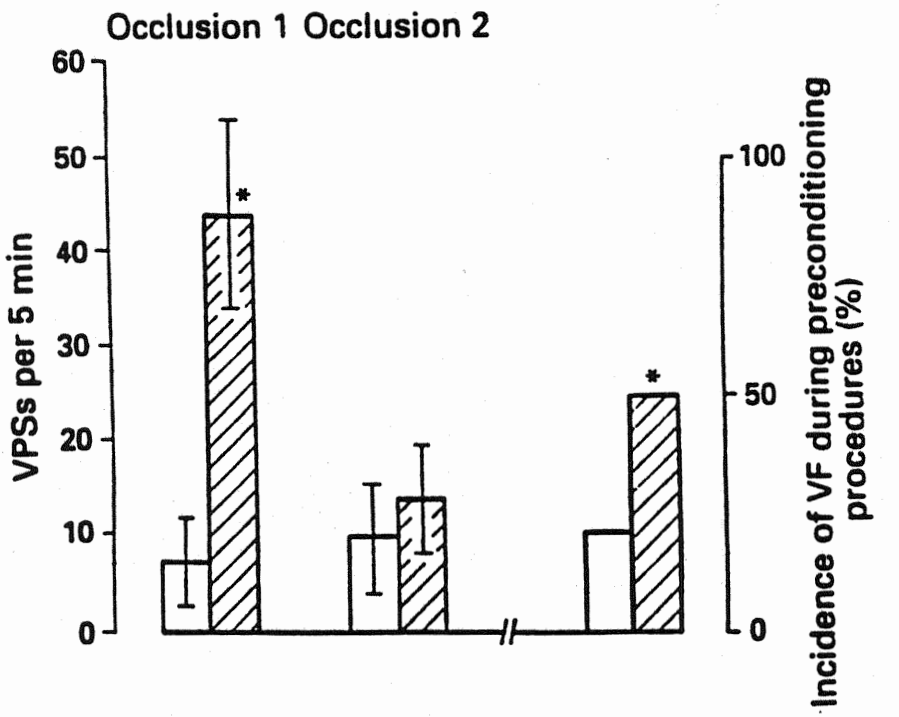

Figure 13. Ventricular premature beats during two five-minute preconditioning coronary artery occlusion periods in dogs in the absence (open columns) and presence (hatched columns) of the bradykinin B2 antagonist icatibant. On the right is shown the incidence of ventricular fibrillation that occurred during the preconditioning procedure in the two groups of dogs. Arrhythmia severity is increased during the preconditioning stimulus in the presence of icatibant. From [68], with permission.

ischemic heart disease), arrhythmia severity might be increased, although the precise relationship between endothelial dysfunction and arrhythmia severity in patients is almost impossible to document. Certainly, in spontaneously hypertensive rats, where there is evidence of endothelial dysfunction, there is an increased arrhythmia severity following coronary artery occlusion [75].

POSSIBLE MECHANISMS OF DELAYED MYOCARDIAL PROTECTION AFFORDED BY RAPID CARDIAC PACING

We know much less about the mechanisms involved in the delayed protection against ischemia-induced arrhythmias described above than we do regarding the protective effects of "classical" ischemic preconditiong. The possible mechanisms of this second window of protection in reducing myocardial necrosis have been recently reviewed [76]. They include the induction of heat-shock (stress) proteins, an increase in antioxidant activity, the induction of nitric oxide synthase (iNOS),

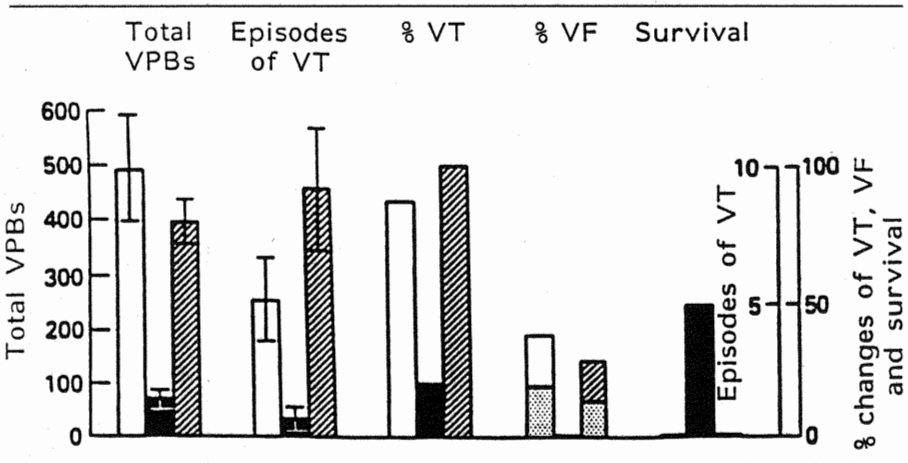

Figure 14. The effect of infusing methylene blue (by intracoronary infusion and given during both preconditioning and the prolonged occlusion in a total dose of 325 mg; shaded columns) on the protective effects of ischemic preconditioning (solid columns) in anesthetized mongrel dogs. The control data are seen in the initial open columns. Shown are the total number of ventricular premature beats (VPBs) during the 25-minute occlusion period, the number of episodes and incidence of ventricular tachycardia (VT), the incidence of ventricular fibrillation (VF), and survival from the combined ischemia–reperfusion insult. The incidence of VF is given both as the total incidence throughout the 25-minute occlusion period and during the first five minutes (stippled column). Reproduced from [74], with permission.

and the role of adenosine-mediated protein kinase C translocation and the influence this has on nuclear transcription events through activation of other kinase signal cascades.

There are only two series of experiments that shed light on the mechanisms of the delayed antiarrhythmic effect of cardiac pacing outlined above. These show that protection is abolished by prior treatment with dexamethasone [49] or by prior administration of icatibant [77]. These results again suggest that mediators normally derived from endothelial cells are also involved in this delayed protection. One possible explanation for the reversal of the protection by dexamethasone is prevention of the induction of nitric oxide synthase and cyclooxygenase-2, although, of course, dexamethasone has many other actions. The induction of these enzymes has also been suggested as a possible mechanism for the delayed antiarrhythmic effects of bacterial endotoxin (and the nontoxic monophosphoryl derivative of the lipid A component of the endotoxin molecule) that have been recently described [78–80]. These protective effects of endotoxin are cytokine mediated [81].

ACKNOWLEDGMENTS

The work described in this chapter has been variously supported, since 1989, by the Royal Society, the Wellcome Trust, the British Council (in collaboration with the Hungarian Committee for Technical Development) and by the Hungarian State

Government (OTKA). The collaboration has also been stimulated by a Scientific Network Grant from the European Union (CIPA-CT-924009). We particularly acknowledge the collaboration of many individuals within the Szeged and Glasgow departments, especially Professor Laszlo Szekeres, Drs. Brain Furman and Nigel Pyne and, in Strasbourg, Professor Jean-Claude Stoclet. It is a pleasure also to acknowledge the significant help of Mrs Margaret Laird in the preparation of this manuscript.

REFERENCES

1. Parratt JR. 1982. Early Arrhythmias Resulting from Myocardial Ischaemia. London: Macmillan.
2. Goldstein S, Bayes-de-Luna A, Soldevila JE. 1994. Sudden Cardiac Death. New York: Futura.
3. Zehender M, Meinertz T, Just H. 1994. Myocardial Ischaemia and Arrhythmia. Darmstadt: Steinkopf.
4. Murry CE, Jennings RB, Reimer KA. 1986. Preconditioning with ischemia: a delay of lethal cell injury in ischemic myocardium. Circulation 74:1124–1136.
5. Shiki K, Hearse DJ. 1987. Preconditioning of ischemic myocardium: reperfusion-induced arrhythmias. Am J Physiol 253:H1470–H1476.
6. Vegh A, Szekeres L, Parratt JR. 1990. Protective effect of preconditioning of the ischaemic myocardium involves cyclooxygenase products. Cardiovasc Res 12:1020–1022.
7. Vegh A, Komori S, Szekeres L, Parratt JR. 1992. Antiarrhythmic effects of preconditioning in anaesthetised dogs and rats. Cardiovasc Res 26:487–495.
8. Cave AC, Hearse DJ. 1992. Ischaemic preconditioning and contractile function: studies with normothermic and hypothermic global ischaemia. J Mol Cell Cardiol 24:1113–1123.
9. Schott RJ, Rohmann S, Braun ER, Schaper W. 1990. Ischemic preconditioning reduces infarct size in swine myocardium. Circulation Res 66:1133–1142.
10. Parratt JR. 1995. Possibilities for the pharmacological exploitation of ischaemic preconditioning. J Mol Cell Cardiol 27:991–1000.
11. Parratt JR. 1993. Endogenous myocardial protective (antiarrhythmic) substances. Cardiovasc Res 27:693–702.
12. Harris AG. 1950. Delayed development of ventricular ectopic rhythms following experimental coronary occlusion. Circulation 1:1318–1326.
13. Gülker H, Kramer B, Stephan K, Meesmann W. 1977. Changes in ventricular fibrillation threshold during repeated short-term coronary occlusion and release. Basic Res Cardiol 72:547–562.
14. Barber MJ. 1983. Effect of time interval between repeated brief coronary artery occlusions on arrhythmias, electrical activity and myocardial blood flow. J Am Coll Cardiol 2:699–705.
15. Maroko PR, Kjekshus JK, Sobel BE, Watanabe T, Covell JW, Ross J, Braunwald E. 1971. Factors influencing infarct size following experimental coronary artery occlusions. Circulation 43:67–74.
16. Marshall RJ, Parratt JR. 1977. The haemodynamic and metabolic effects of MG8926, a prospective antidysrhythmic and antianginal agent. Br J Pharmacol 59:311–322.
17. Marshall RJ, Parratt JR. 1979. The effects of disopyramide phosphate on early post-coronary artery ligation dysrhythmias, and on epicardial ST-segment elevation, in anaesthetised dogs. Br J Pharmacol 66:241–250.
18. Komori S, Parratt JR, Szekeres L, Vegh A. 1990. Preconditioning reduces the severity of ischaemia and reperfusion-induced arrhythmias in both anaesthetised rats and dogs. J Physiol 423:16P.
19. Komori S, Fukimaki S, Ijili H, Asakawa T, Watanabe Y, Tamura Y, Parratt JR. 1990. Inhibitory effect of ischemic preconditioning on ischemic arrhythmias using a rat coronary artery ligation model. Jpn J Electrocardiol 10:774–782.
20. Kane KA, Parratt JR, Williams FM. 1984. An investigation into the characteristics of reperfusion-induced arrhythmias in the anaesthetised rat and their susceptibility to antiarrhythmic agents. Br J Pharmacol 82:349–357.
21. Meesmann W. 1982. Early arrhythmias and primary ventricular fibrillation after acute myocardial ischaemia in relation to pre-existing coronary collaterals. In Parratt JR (ed), Early Arrhythmias Resulting from Myocardial Ischaemia. London: Macmillan, pp. 93–112.
22. Parratt JR, Vegh A, Kaszala K, Papp JGy. 1996. Suppression of life-threatening ventricular arrhythmias by brief periods of ischaemia and by cardiac pacing with particular reference to delayed

myocardial protection. In Marber MS, Yellon DM (eds), Ischaemia: Preconditioning and Adaptation. BIOS Scientific Publishers, pp. 85–111.
23. Vegh A, Parratt JR. 1996. Ischaemic preconditioning markedly reduces the severity of ischaemia and reperfusion-induced arrhythmias: role of endogenous myocardial protective substances. In Wainwright CL, Parratt JR (eds), Myocardial Preconditioning. Berlin: Springer, pp. 35–60.
24. Li Y, Kloner RA. 1992. Cardioprotective effects of ischaemic preconditioning is not mediated by prostanoids. Cardiovasc Res 26:226–231.
25. Lawson CS, Coltart DJ, Hearse DJ. 1993. Dose-dependency and temporal characteristics of protection by ischaemic preconditioning against ischaemia-induced arrhythmias in rat hearts. J Mol Cell Cardiol 25:1391–1402.
26. Lawson CS, Avkiran M, Shattock MJ, Coltart DJ, Hearse DJ. 1993. Preconditioning and reperfusion arrhythmias in the isolated rat heart: true protection or temporal shift in vulnerability? Cardiovasc Res 27:2274–2281.
27. Piacentini L, Wainwright CL, Parratt JR. 1993. The antiarrhythmic effect of ischaemic preconditioning in isolated rat hearts involves a pertussis toxin sensitive mechanism. Cardiovasc Res 27:674–680.
28. Li Y, Vasquez JA, Gallagher KP, Lucchesi BR. 1990. Myocardial protection with preconditioning. Circulation 82:609–619.
29. Przyklenk K, Kloner RA. 1995. Preconditioning: a balanced perspective. Br Heart J 74:575–577.
30. Vander Heide RS, Schwartz LM, Jennings RB, Reimer KA. 1995. Effect of catecholamine depletion on myocardial infarct size in dogs: role of catecholamines in ischemic preconditioning. Cardiovasc Res 30:656–662.
31. Wainwright CL, Parratt JR. 1990. Electrocardiographic and haemodynamic effects of myocardial preconditioning in pigs. J Mol Cell Cardiol 22(Suppl III):PF65.
32. Ovize M, Aupetit JF, Rioufol G, Laufona J, Andre-Fouet X, Minaire Y, Faucon G. 1995. Preconditioning reduces infarct size but accelerates time to ventricular fibrillation in ischemic pig heart. Am J Physiol 269:H72–H79.
33. Vegh A, Szekeres L, Parratt JR. 1991. Transient ischaemia induced by rapid cardiac pacing results in myocardial preconditioning. Cardiovasc Res 25:1051–1053.
34. Szekeres L, Papp JGy, Szilvassy Z, Udvary E, Vegh A. 1993. Moderate stress by cardiac pacing may induce both short term and long term cardioprotection. Cardiovasc Res 27:593–596.
35. Koning MMG, Simonis L, De Zeeuw S, Nieukoop S, Post S, Verdouw PD. 1994. Ischaemic preconditioning by partial occlusion without intermittent reperfusion. Cardiovasc Res 28:1146–1151.
36. Ovize M, Przyklenk K, Kloner RA. 1992. Partial coronary stenosis is sufficient and complete reperfusion is mandatory for preconditioning the canine heart. Circulation Res 71:1165–1173.
37. Shizukuda Y, Maller RT, Lee SC, Downey HF. 1992. Hypoxic preconditioning of ischaemic canine myocardium. Cardiovasc Res 26:534–542.
38. Ovize M, Kloner RA, Przyklenk K. 1994. Stretch preconditions canine myocardium. Am J Physiol 266:H137–H146.
39. Przyklenk K, Bauer B, Ovize M, Kloner RA, Whittaker P. 1993. Regional ischaemic "preconditioning" protects remote virgin myocardium from subsequent sustained coronary occlusion. Circulation 87:893–899.
40. McClanahan TB, Nao BS, Wolke LJ, Martin BJ, Metz TE, Gallagher KP. 1993. Brief renal occlusion and reperfusion reduces myocardial infarct size in rabbits. FASEB J 7:A176.
41. Gho BC, Shoemaker RG, Van der Lee C, Sharma HS, Verdouw PD. 1994. Myocardial infarct size limitation in rat by transient renal ischaemia. Circulation 90:4-2,I-476.
42. Marshall RJ, Parratt JR. 1980. The early consequences of myocardial ischaemia and their modification. J Physiol (Paris) 76:699–715.
43. Kaszala K, Vegh A, Papp JGy, Parratt JR. 1996. Time-course of the protection against ischaemia and reperfusion-induced ventricular arrhythmias resulting from brief periods of cardiac pacing. J Mol Cell Cardiol 28:2085–2095.
44. Kaszala K, Vegh A, Papp JGy, Parratt JR. 1995. The role of bradykinin in pacing-induced preconditioning. J Mol Cell Cardiol 28:A14.
45. Kuzuya T, Hoshida S, Yamashita N, Fuji H, Oe H, Hori M, Kamada T, Tada M. 1993. Delayed effects of sublethal ischemia on the acquisition of tolerance to ischemia. Circulation Res 72:1293–1299.
46. Marber MS, Latchman DS, Walker JM, Yellon DM. 1993. Cardiac stress protein elevation 24 hours

after brief ischemia or heat stress is associated with resistance to myocardial infarction. Circulation 88:1264–1272.
47. Yellon DM, Baxter GF. 1995. A "second window of protection" or delayed preconditioning phenomenon: future horizons for myocardial protection? J Mol Cell Cardiol 27:1023–1034.
48. Vegh A, Papp JGy, Kaszala K, Parratt JR. 1994. Cardiac pacing in anaesthetised dogs preconditions the heart against arrhythmias when ischaemia induced 24 h later. J Physiol (Lond) P480.
49. Vegh A, Papp JGy, Parratt JR. 1994. Prevention by dexamethasone of the marked antiarrhythmic effects of preconditioning induced 20 h after rapid cardiac pacing. Br J Pharmacol 113:1081–1082.
50. Kis A, Vegh A, Papp JGy, Parratt JR. 1996. Repeated pacing widens the time window of delayed protection against ventricular arrhythmias in dogs (abstract 229). J Mol Cell Cardiol 28:A59.
51. Parratt JR. 1994. Protection of the heart by ischaemic preconditioning: mechanisms and possibilities for pharmacological exploitation. Trends Pharmacol Sci 15:19–25.
52. Curtis MJ, Pugsley MK, Walker MJA. 1993. Endogenous chemical mediators of ventricular arrhythmias in ischaemic heart disease. Cardiovasc Res 27:703–719.
53. Cohen MV, Liu Y, Downey JM. 1996. Activation of protein kinase C is critical to the production of preconditioning. In Wainwright CL, Parratt JR (eds), Myocardial Preconditioning. Berlin: Springer, pp. 189–206.
54. Liu GS, Thornton J, Van Winkle DM, Stanley AWH, Olson RA, Downey JM. 1991. Protection against infarction afforded by preconditioning is madiated by A_1 adenosine receptors in rabbit heart. Circulation 84:350–356.
55. Miura T. 1996. Preconditioning against myocardial infarction—its features and adenosine-mediated mechanism. In Wainwright CL, Parratt JR (eds), Myocardial Preconditioning. Berlin: Springer, pp. 1–17.
56. Piacentini L, Wainwright CL, Parratt JR. 1992. The antiarrhythmic effect of preconditioning in rat isolated hearts does not involve A_1 receptors. Br J Pharmacol 107:137P.
57. Vegh A, Papp JGy, Parratt JR. 1995. Pronounced antiarrhythmic effects of preconditioning in anaesthetised dogs: is adenosine involved? J Mol Cell Cardiol 27:349–356.
58. Boachie-Ansah G, Kane KA, Parratt JR. 1993. Is adenosine an endogenous myocardial protective (antiarrhythmic) substance under conditions of ischaemia. Cardiovasc Res 27:77–83.
59. Parratt JR, Vegh A. 1996. Endothelial cells, nitric oxide and ischaemic preconditioning. Basic Res Cardiol 91:27–30.
60. Parratt JR, Vegh A, Zeitlin IJ, Ahmad M, Oldroyd K, Kaszala K, Papp JGy. 1997. Bradykinin and endothelial-myocyte interactions in ischaemic preconditioning: a review. Am J Cardiol 80:124–131A.
61. Fatehi-Hassanabad Z, Furman BL, Parratt JR. 1996. The effect of the endothelium on coronary artery occlusion-induced arrhythmias in rat isolated perfused hearts. J Physiol 494:112–113P.
62. Vegh A, Szekeres L, Parratt JR. 1991. Local coronary infusions of bradykinin profoundly reduce the severity of ischaemia-induced arrhythmias in anaesthetised dogs. Br J Pharmacol 104:294–295.
63. Coker SJ, Parratt JR. 1983. Prostacyclin—antiarrhythmic or arrhythmogenic? Comparison of the effects of intravenous and intracoronary prostacyclin and ZK36374 during coronary artery occlusion and reperfusion in anaesthetised greyhounds. J Cardiovasc Pharmacol 5:557–567.
64. Vegh A, Papp JGy, Szekeres L, Parratt JR. 1993. Prevention by an inhibitor of the L-arginine nitric oxide pathway of the antiarrhythmic effects of bradykinin in anaesthetised dogs. Br J Pharmacol 110:18–19.
65. Coker SJ, Parratt JR, Ledingham IMcA, Zeitlin IJ. 1981. Thromboxane and prostacyclin release from ischaemic myocardium in relation to arrhythmias. Nature 291:323–324.
66. Coker SJ, Parratt JR. 1984. The effects of nafazatrom on arrhythmias and prostanoid release during coronary artery occlusion and reperfusion in anaesthetised greyhounds. J Mol Cell Cardiol 16:43–52.
67. Pahor M, Ganbassi G, Carbonia P. 1994. Antiarrhythmic effects of ACE inhibitors: a matter of faith or reality. Cardiovasc Res 28:173–182.
68. Vegh A, Papp JGy, Parratt JR. 1994. Attenuation of the anti-arrhythmic effects of ischaemic preconditioning by blockade of bradykinin B_2 receptors. Br J Pharmacol 113:1167–1172.
69. Parratt JR, Vegh A, Papp JGy. 1995. Bradykinin as an endogenous myocardial protective substance with particular reference to ischemic preconditioning—a brief review of the evidence. Can J Physiol Pharmacol 73:837–842.
70. Kis A, Vegh A, Papp JGy, Parratt JR. 1997. Dual blockade of the cyclooxygenase and L-arginine nitric oxide pathways prevents the antiarrhythmic effect of preconditioning. Exp Clin Cordiol 2:112–118.
71. Parratt JR. 1989. Eicosanoids and arrhythmogenesis. In Vaughan-Williams EM (ed), Handbook of Experimental Pharmacology. Vol. 89, Antiarrhythmic Drugs. Berlin: Springer, pp. 569–589.

72. Parratt JR. 1987. Modification of the thromboxane/prostacyclin balance as an approach to antiarrhythmic therapy during myocardial ischaemia and reperfusion; the concept of endogenous antiarrhythmic substances. In Dhalla NS, Innes IR, Beamish RE (eds), Myocardial Ischaemia. Boston: Martinus Nijhoff, pp. 21–35.
73. Vegh A, Szekeres L, Parratt JR. 1992. Preconditioning of the ischaemic myocardium; involvement of the L-arginine nitric oxide pathway. Br J Pharmacol 107:648–652.
74. Vegh A, Papp JGy, Szekeres L, Parratt JR. 1992. The local intracoronary administration of methylene blue prevents the pronounced antiarrhythmic effect of ischaemic preconditioning. Br J Pharmacol 107:910–911.
75. Kolar F, Parratt JR. 1997. Antiarrhythmic effect of ischaemic preconditioning in hearts of spontaneously hypertensive rats. Exp Clin Cardiol 2:124–127.
76. Yellon DM, Baxter GF. 1995. A "second window of protection" or delayed preconditioning phenomenon: future horizons for myocardial protection? J Mol Cell Cardiol 27:1023–1034.
77. Vegh A, Kaszala K, Papp JGy, Parratt JR. 1995. Delayed myocardial protection by pacing-induced preconditioning: a possible role for bradykinin. Br J Pharmacol 116:288P.
78. Wu S, Furman BL, Parratt JR. 1994. Attenuation by dexamethasone of endotoxin protection against ischaemia-induced ventricular arrhythmias. Br J Pharmacol 113:1083–1084.
79. Wu Song, Furman BL, Parratt JR. 1996. Delayed protection by bacterial lipopolysaccharide (endotoxin) against ischaemia-induced myocardial damage and arrhythmias. Br J Pharmacol 118:2157–2163.
80. Vegh A, Papp JGy, Parratt JR, Elliott GT. 1996. Pretreatment with monophosphoryl lipid-A (MPL-C) reduces ischaemia-induced ventricular arrhythmias (abstract 217). J Mol Cell Cardiol 28:A56.
81. Stein B, Frank P, Schmitz W, Scholz H, Thoenes M. 1996. Endotoxin and cytokines induce direct cardioprotective effects in mammalian cardiomyocytes via induction of nitric oxide synthase. J Mol Cell Cardiol 28:1631–1639.

This Page Intentionally Left Blank

EFFECTS OF ISCHEMIC PRECONDITIONING ON Na^+–Ca^{2+} EXCHANGER ACTIVITY AND ION REGULATION IN ISOLATED PERFUSED RAT HEARTS

SHINGO SEKI, HIROYUKI OKUMURA, TAKEHIKO IZUMI, FUMIKO OKAZAKI, SATOSHI TAKEDA, MASAYUKI TANIGUCHI, IKUO TANIGUCHI, and SEIBU MOCHIZUKI

Jikei University School of Medicine

Summary. We investigated the effects of ischemic preconditioning (IP) on the incidence of reperfusion-induced ventricular fibrillation (VF), intracellular ion regulation, and Na^+–Ca^{2+} exchanger activity using isolated perfused rat hearts. The hearts perfused in a working-heart mode were exposed to sustained global ischemia for 15 minutes and were reperfused for 20 minutes. For preconditioning, the hearts were exposed to two short periods (3 or 5 minutes) of ischemia and reperfusion prior to induction of sustained ischemia. The incidence of VF decreased from 90% in the control hearts to 20% in the preconditioned hearts ($p < 0.05$). Treatment with an Na^+–Ca^{2+} exchanger blocker, Ni^{2+} (0.5 μM), reduced the antiarrhythmic effect of IP. Thus, 70% of the preconditioned hearts treated with Ni^{2+} developed VF on reperfusion. To investigate the effect of IP on changes in intracellular ion levels, rat hearts perfused in Langendorff's mode were exposed to low-flow ischemia for 15 minutes and were reperfused for 15 minutes. Intracellular pH (pH_i) and Ca^{2+} concentrations ($[Ca^{2+}]_i$) were measured ratiometrically using the fluorescent ion indicators 2′,7′-bis(2-carboxylethyl)-5(6)-carboxyfluorescein (BCECF) or fura-2 with the simultaneous measurement of left ventricular pressure. IP limited the development of intracellular acidosis and prevented the rise in diastolic $[Ca^{2+}]_i$ during sustained ischemia. Ni^{2+} treatment reversed this effect of IP on diastolic $[Ca^{2+}]_i$. During exposure to an Na^+ free extracellular medium, which reversed the Na^+–Ca^{2+} exchanger mode, IP significantly suppressed the peak amplitude (65.2% ± 7.8% of control, $p < 0.005$) and prolonged the time to peak (16.7 ± 0.9 seconds vs. 12.8 ± 1.5 seconds, $p < 0.05$) of the diastolic $[Ca^{2+}]_i$ increase. Results indicated that the Na^+–Ca^{2+} exchanger may be important in ion regulation during IP.

S. Mochizuki, N. Takeda, M. Nagano and N. Dhalla (eds.). THE ISCHEMIC HEART.

INTRODUCTION

It is well established that ischemic preconditioning provides cardioprotective effects during the subsequent ischemia and reperfusion, reducing infarct size [1–3], improving contractile function on reperfusion [4,5], and suppressing reperfusion arrhythmias [6]. Several mechanisms have been proposed to explain these effects of preconditioning, including the preservation of myocardial high-energy stores [7], stimulation of the adenosine A_1 receptor [8], activation of ATP-sensitive K^+ channels [9], and the translocation and activation of protein kinase C [10].

In addition, alterations in some ionic states, such as reductions in intracellular acidosis or in Ca^{2+} overload, have been reported as consequences of preconditioning. Intracellular Ca^{2+} overload is one of the most important factors contributing to cell injury [11]. Using the fluorescent indicator fura-2 in rat hearts perfused in Langendorff's mode, we previously demonstrated an increase in diastolic $[Ca^{2+}]_i$ during the early phase of ischemia [12]. Moreover, Steenbergen et al., who used nuclear magnetic resonance, reported that ischemic preconditioning suppressed the accumulation of intracellular H^+, Na^+, and Ca^{2+} during sustained ischemia [5]. These authors hypothesized that these changes in ion levels were mediated by the Na^+–H^+ exchanger and the Na^+–Ca^{2+} exchanger. Although a stimulation of Ca^{2+} influx via the Na^+–Ca^{2+} exchanger has been emphasized in ischemia and reperfusion, the involvement of this exchanger in ischemic preconditioning remains unclear.

We analyzed the effect of preconditioning on the incidence of reperfusion-induced ventricular arrhythmias using the working rat heart model in the presence or absence of the Na^+–Ca^{2+} exchanger blocker nickel chloride (Ni^{2+}). We also investigated the effect of preconditioning on changes in intracellular Ca^{2+} or pH during ischemia and reperfusion using an isolated Langendorff's perfused rat heart and the fluorescent ion indicators fura-2 or 2′,7′-bis(2-carboxylethyl)-5(6)-carboxyfluorescein (BCECF). Finally, we determined the changes in sarcolemmal Na^+–Ca^{2+} exchanger activity before and after preconditioning and evaluated the possible role of this exchanger in ion regulation during preconditioning.

METHODS

Isolated rat heart preparation

Adult male Sprague–Dawley rats (300–350 g) were anesthetized with pentobarbital sodium (50 mg/kg ip), and the hearts were removed promptly. The hearts then were perfused in a working-heart mode using Krebs–Henseleit bicarbonate buffer [13]. The perfusate contained 118 mM NaCl, 4.7 mM KCl, 25 mM $NaHCO_3$, 2.5 mM $CaCl_2$, 1.2 mM $MgSO_4$, 0.5 mM EDTA, 1.2 mM KH_2PO_4, and 11 mM glucose (pH 7.4, 37°C) and was gassed with 95% O_2, 5% CO_2.

Whole-heart ischemia was induced by clamping the bypass to activate the one-way ball valve and cut the backflow of the perfusate from the aorta to the coronary artery during diastole [13]. During ischemia the hearts were paced electrically at 300 beats/min. This procedure reduced the coronary flow to less than 10% of the

control value. At reperfusion, both clamping and pacing were released. The electrocardiogram was monitored via a carbon electrode attached to the surface of the heart.

To investigate the effects of preconditioning on changes in the intracellular ionic state, hearts were perfused using the Langendorff's mode with *N*-2-hydroxy-ethylpiperazine-*N'*-2-ethanesulfonic acid (HEPES)-buffered Tyrode solution that contained 140 mM NaCl, 6 mM KCl, 1 mM $MgCl_2$, 2 mM $CaCl_2$, 10 mM HEPES, and 10 mM glucose, gassed with 100% O_2 (pH 7.4, 37°C). Coronary flow was maintained at 13–14 mL/min using a peristaltic pump. Short ischemia and sustained ischemia were induced by reducing the perfusion flow to 10% of the control value without concurrent pacing. Left ventricular pressure (LVP) was measured with a polygraph system (Nihon Kohden Co., Tokyo, Japan) by inserting the catheter through the pulmonary vein and left atrium into the left ventricle.

Measurement of intracellular ion levels

Prior to the experiments, the hearts were loaded with fluorescent indicators by simple perfusion for 30 or 15 minutes with HEPES-buffer containing 4 μM fura-2/AM for measurement of Ca^{2+} [14,15] or 2 μM BCECF/AM for pH determination [16]. The fluorescent indicators first had been dissolved in dimethyl sulfoxide containing pluronic F-127 (25% w/v). After loading, the hearts were washed with normal Tyrode solution for another 15 minutes.

An optic-fiber and analysis system [15] (Nihon Bunkou Co., Tokyo; CAF-110, CA-200DP) was used for fluorescence measurement. Excitation light from a xenon arc-lamp (UV) was focused onto the ingoing leg of the fiber attached to the surface of the left ventricle. The fluorescent (emission) light was collected through the outgoing leg of the fiber. Intracellular levels of Ca^{2+} ($[Ca^{2+}]_i$) were determined using the ratio of fura-2 emission at 500 nm after excitation with UV light at 340 nm and 380 nm. This value was used as a qualitative index of the free cytosolic Ca^{2+} concentration and was independent of the fura-2 concentration. The fluorescence signals obtained by this method showed high signal-to-noise ratio. To measure intracellular pH (pH_i), we monitored the ratio of BCECF emission at 540 nm after excitation at 450 nm and 500 nm. To calibrate BCECF fluorescence, the hearts were exposed to a high $[K^+]_o$ solution that contained skinning agent, 10^{-5} M nigericin, thus clamping the pH_i with the perfusate pH [16]. The hearts were then perfused with three different calibration solutions (pH: 7.4, 7.0, and 6.6). A fluorescence versus pH curve was obtained, and pH_i values were determined. Before loading, we measured the background fluorescence of an unloaded heart (which is due primarily to NADH [17]) to confirm that it was minimal. Throughout the experiment, fura-2 or BCECF fluorescence and hemodynamic parameters were monitored simultaneously.

Protocol

The study consisted of three experimental groups (figure 1). In the control group, the hearts were perfused aerobically before they were exposed to sustained global

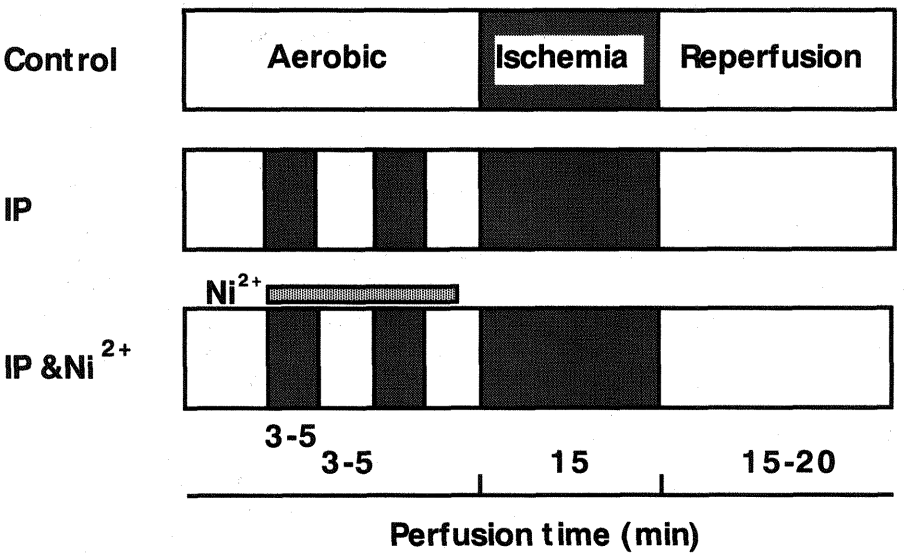

Figure 1. Experimental protocol. Hearts were exposed to sustained global ischemia for 15 minutes and were reperfused for 15 or 20 minutes. Top: control. Middle: ischemic preconditioning (IP). Before sustained ischemia, the hearts were exposed to two short periods (3 or 5 minutes) of ischemia and reperfusion. Bottom: ischemic preconditioning with Ni^{2+} (0.5 μM) treatment (IP&Ni^{2+}).

ischemia for 15 minutes and were reperfused for another 15 minutes in Langendorff's mode or for 20 minutes in the working-heart mode. The preconditioning group received two short periods (3 or 5 minutes) of ischemia and reperfusion prior to the induction of sustained global ischemia. The third group underwent the same protocol as the preconditioning group, but the hearts were treated with the Na^+–Ca^{2+} exchanger blocker 0.5 μM Ni^{2+} during preconditioning.

Statistical analysis

Data are presented as mean ± SE. Student's *t*-test was used to evaluate the significance of the differences between groups. Fisher's exact probability test was used to analyze the incidence of ventricular arrhythmias. A p level less than 0.05 was considered statistically significant.

RESULTS

Incidence of reperfusion-induced ventricular arrhythmias

The mean coronary flow in all groups at preischemic perfusion in the working-heart mode was 15.0 ± 1.2 mL/min. In the control group without any preconditioning, ischemia and reperfusion led to ventricular fibrillation (VF) in 90% of the hearts (figure 2). This effect was sustained throughout the period of reperfusion. For preconditioning, the hearts were subjected to two five-minute periods of ischemia,

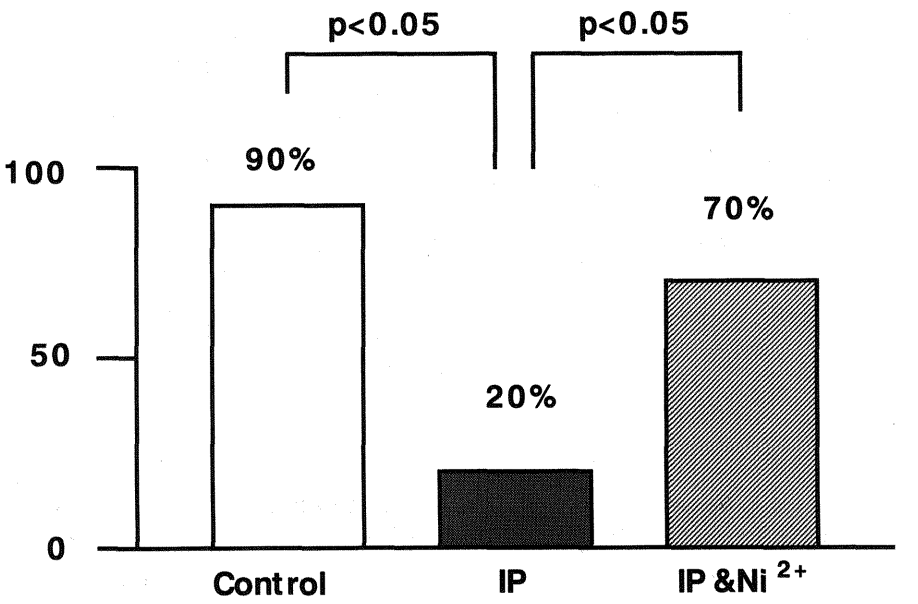

Figure 2. Incidence of ventricular fibrillation induced by reperfusion (n = 10, each group). Open bar: control hearts. IP: hearts exposed to ischemic preconditioning by two short (five-minute) periods of ischemia and reperfusion prior to sustained ischemia. IP&Ni^{2+}: hearts exposed to ischemic preconditioning and treated with Ni^{2+} (0.5 μM).

separated by five minutes of reperfusion. After this treatment, only 20% of the hearts developed VF in response to sustained ischemia and reperfusion ($p < 0.05$ vs. control). Ni^{2+} treatment reduced the antiarrhythmic effect of preconditioning. As a result, 70% of the Ni^{2+}-treated hearts developed VF on reperfusion ($p < 0.05$ vs. control).

Changes in intracellular ion levels during sustained ischemia

To determine the effect of preconditioning on intracellular pH (pH_i), hearts perfused in Langendorff's mode were subjected to preconditioning of two ischemic periods of three minutes each, separated by three minutes of reperfusion. In the control hearts, the pH_i declined significantly from 6.9 ± 0.1 to 6.4 ± 0.1 during sustained ischemia ($p < 0.05$ vs. preischemic value) and recovered after reperfusion (figure 3). Preconditioning limited the severity of intracellular acidosis induced by sustained ischemia (pH_i = 6.6 ± 0.1, $p < 0.05$ vs. control). The difference in pH_i between the control and the preconditioned group was statistically significant at 10 and 12 minutes of ischemia.

We also investigated the effects of preconditioning on the intracellular levels of Ca^{2+} as determined by the fluorescence ratio and on left ventricular pressure (LVP) during ischemia and reperfusion. Figure 4 shows the typical results obtained with

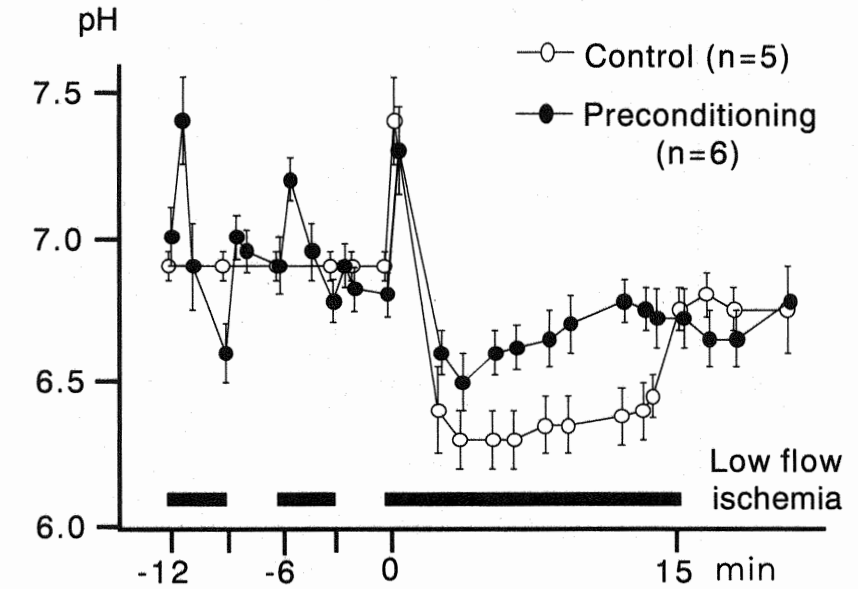

Figure 3. Effect of preconditioning on intracellular pH (pH_i). Time course of changes in pH_i during aerobic perfusion or preconditioning, sustained ischemia (15 minutes), and reperfusion. For ischemic preconditioning, two short (three-minute) periods of ischemia and reperfusion were performed before sustained ischemia. ○: control hearts. ●: preconditioned hearts.

individual hearts. During preischemic perfusion in Langendorff's mode, the mean LVP in the control heart was 98.7 ± 12.5 mmHg. The LVP decreased rapidly during ischemia but recovered partially after reperfusion (figure 4). Preconditioning with two three-minute periods of ischemia accelerated the recovery of LVP compared with the control heart.

In the control heart, the diastolic $[Ca^{2+}]_i$ was elevated during sustained ischemia and returned to the preischemic value after reperfusion (figure 4). In the preconditioned heart, in contrast, the diastolic $[Ca^{2+}]_i$ rose during the short ischemic periods, but the rise during sustained ischemia was prevented. These results are consistent with those previously reported by Steenbergen et al. [5]. Ni^{2+} treatment abolished the effect of preconditioning on diastolic $[Ca^{2+}]_i$.

Changes in diastolic $[Ca^{2+}]_i$ observed in individual hearts were confirmed by evaluating the pooled data from five hearts in each group. These analyses demonstrated that preconditioning significantly suppressed the $[Ca^{2+}]_i$ increase during sustained ischemia and that Ni^{2+} treatment reversed the effect of preconditioning (data not shown).

Effect of preconditioning on the activity of the Na^+–Ca^{2+} exchanger

To determine the activity of the Na^+–Ca^{2+} exchanger, hearts from the control group and the preconditioned group were each exposed for 20 seconds to an Na^+-free extracellular medium, in which Na^+ was replaced by trisaminomethane.

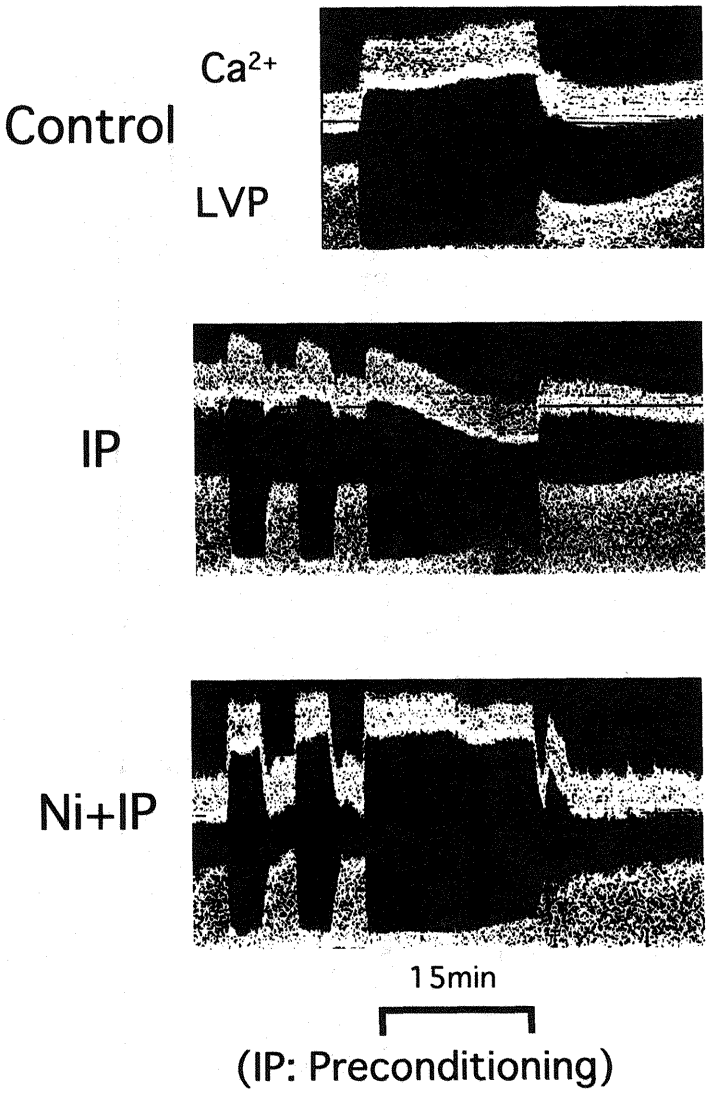

Figure 4. Effect of preconditioning on intracellular Ca^{2+} ($[Ca^{2+}]_i$) and left ventricular pressure (LVP). Original traces. Top: control. Middle: ischemic preconditioning (IP) by two short (three-minute) periods of ischemia and reperfusion prior to sustained ischemia. Bottom: ischemic preconditioning with Ni^{2+} (0.5 μM) treatment (Ni + IP). For each panel, the upper trace indicates $[Ca^{2+}]_i$ (expressed as fluorescence ratio), and the lower trace indicates LVP (mmHg).

This procedure affects the Na^+ gradient between the extracellular and the intracellular space and activates the reverse mode of the Na^+–Ca^{2+} exchanger [18]. Consequently, Na^+ leaves the cell and Ca^{2+} enters the cytosol via the exchanger. When the heart is returned to perfusion with normal Tyrode's solution, the Na^+

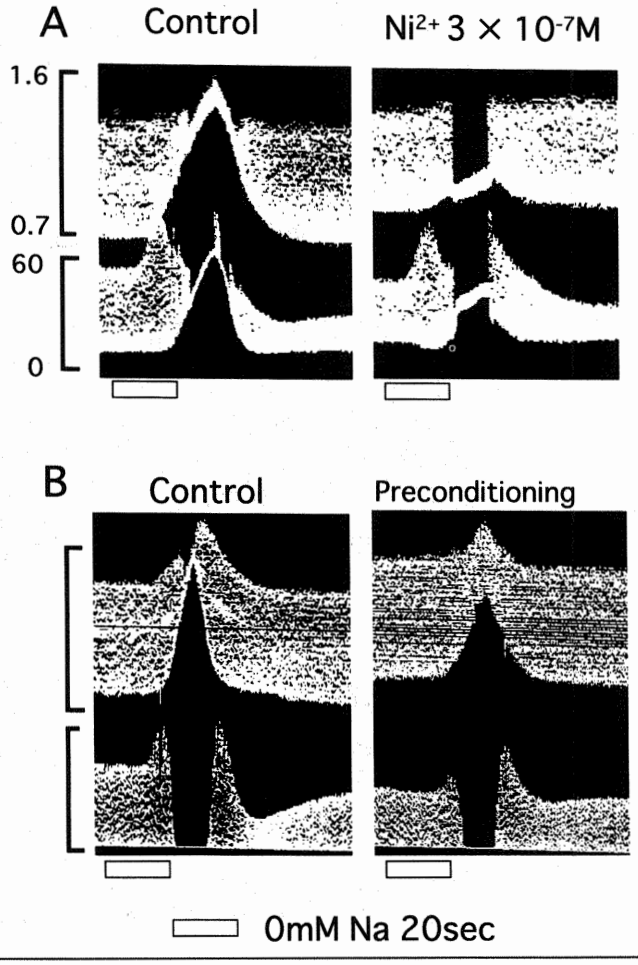

Figure 5. Effect of Ni^{2+} (0.3 μM) treatment or preconditioning on intracellular Ca^{2+} ($[Ca^{2+}]_i$) during exposure to Na^+-free medium. Original traces. (**A**) Left: control; right: Ni^{2+} treatment without ischemic preconditioning. (**B**) Left: control; right: after ischemic preconditioning. For each panel, the upper trace indicates $[Ca^{2+}]_i$, and the lower trace indicates left ventricular pressure (mmHg). For ischemic preconditioning, two short (three-minute) periods of ischemia and reperfusion were performed.

gradient returns to its basal condition, and Ca^{2+} is removed partially by the forward mode of the exchanger.

To evaluate the activity of the reverse mode, we measured the peak amplitude and the time-to-peak of the rise in diastolic $[Ca^{2+}]_i$. The decay time of diastolic $[Ca^{2+}]_i$ was also measured to evaluate the exchanger's forward mode. These parameters were reproducible for more than 20 minutes under aerobic perfusion.

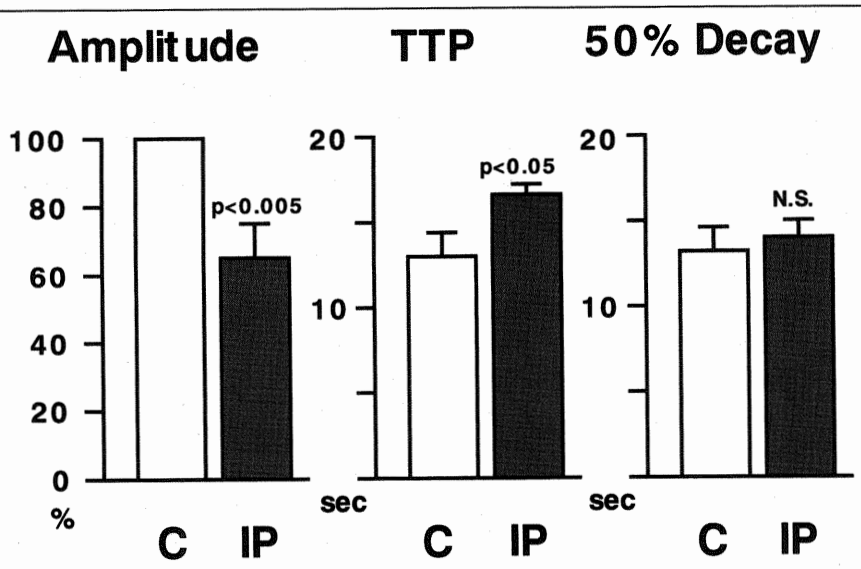

Figure 6. Effect of ischemic preconditioning on changes in diastolic $[Ca^{2+}]_i$ during exposure to Na^+-free medium (n = 8). Open bar: control hearts (C). Solid bar: preconditioned hearts (IP). Amplitude (% change): peak amplitude. TTP (sec): time to peak. 50% Decay (sec): time from peak to 50% decay. For ischemic preconditioning, two short (three-minute) periods of ischemia and reperfusion were performed.

Figure 5 shows a typical original trace of $[Ca^{2+}]_i$ and LVP obtained from individual hearts during exposure to Na^+-free medium. The absence of Na^+ resulted in a transient elevation of the diastolic $[Ca^{2+}]_i$ and a cessation of contraction. Pretreatment with Ni^{2+} (0.3 μM) markedly suppressed the increase in $[Ca^{2+}]_i$ induced by exposure to Na^+-free medium (figure 5A). This result confirmed that the increase in Ca^{2+} level was due primarily to the activation of the reverse mode of the Na^+–Ca^{2+} exchanger.

Preconditioning with short periods of ischemia significantly lowered the peak amplitude of the diastolic $[Ca^{2+}]_i$ increase compared with the control heart. The time-to-peak of the Ca^{2+} transient was prolonged after preconditioning (figure 5B). These results suggest that the preconditioning may suppress the reverse mode of the Na^+–Ca^{2+} exchanger.

These conclusions were confirmed when the pooled data of the changes in diastolic $[Ca^{2+}]_i$ were analyzed (n = 8; see figure 6). Thus, preconditioning significantly reduced the peak amplitude (65.2% ± 7.8% of the control; $p < 0.005$) and prolonged the time-to-peak (16.7 ± 0.9 sec vs. 12.8 ± 1.5 sec in the control; $p < 0.05$) of the increase in diastolic $[Ca^{2+}]_i$. However, no difference in the 50% decay time of diastolic $[Ca^{2+}]_i$ was observed between the control and the preconditioning group (13.2 ± 1.5 sec vs. 14.0 ± 1.2 sec). Thus, preconditioning did not affect the activity of the forward mode of the Na^+–Ca^{2+} exchanger.

DISCUSSION

The present study investigated the effects of ischemic preconditioning on reperfusion-induced ventricular arrhythmias and attempted to elucidate the mechanisms involved. Our analyses led to three major findings. First, ischemic preconditioning suppressed the incidence of reperfusion-induced ventricular fibrillation. This effect was attenuated by Ni^{2+} treatment. Second, ischemic preconditioning suppressed the rise in diastolic $[Ca^{2+}]_i$ during sustained ischemia. Again, Ni^{2+} treatment reversed this effect. Third, preconditioning suppressed the response of diastolic $[Ca^{2+}]_i$ to exposure to Na^+-free extracellular medium.

Our results support previous findings that preconditioning has a variety of beneficial effects. Similarly, Shiki and Hearse previously demonstrated the antiarrhythmic effects of preconditioning in isolated perfused rat hearts [6]. In those studies, brief periods of regional ischemia rendered the myocardium more resistant to subsequent episodes of ischemia and to reperfusion-induced arrhythmias.

The results of many investigations have suggested a strong correlation between an elevated $[Ca^{2+}]_i$ and myocardial damage [11,19,20]. It has been proposed that during ischemia and reperfusion, Ca^{2+} influx via the reverse mode of the Na^+–Ca^{2+} exchanger contributes to an overload of intracellular Ca^{2+} [5,21]. According to this model, sustained ischemia causes intracellular acidosis and leads to the accumulation of intracellular Na^+ ($[Na^+]_i$) by inhibiting Na^+–K^+ ATPase and activating the Na^+–H^+ exchanger. The rise in $[Na^+]_i$ could result in Ca^{2+} overload by inducing the reverse mode of the Na^+–Ca^{2+} exchanger. Alternatively, the increase in $[Na^+]_i$ may have caused an overload of Ca^{2+} by suppressing the extrusion of Ca^{2+} via the forward mode of the Na^+–Ca^{2+} exchanger [22].

In the study reported here, preconditioning prevented the elevation of the diastolic $[Ca^{2+}]_i$ level during sustained ischemia. It is possible that in the preconditioned heart, a decrease in H^+ production may have lessened the Na^+–H^+ exchanger-dependent accumulation of $[Na^+]_i$ during ischemia. This in turn, would reduce the rise in $[Ca^{2+}]_i$ via the Na^+–Ca^{2+} exchanger. However, Ni^{2+}, which blocks both the reverse and the forward mode of the Na^+–Ca^{2+} exchanger, abolished the effect of preconditioning on diastolic $[Ca^{2+}]_i$ during sustained ischemia. Moreover, preconditioning suppressed only the reverse mode and not the forward mode of the Na^+–Ca^{2+} exchanger when the hearts were exposed to an Na^+-free extracellular medium. These observations suggest that preconditioning suppressed the influx of Ca^{2+} via the reverse mode of the Na^+–Ca^{2+} exchanger while maintaining Ca^{2+} extrusion via the forward mode of this exchanger. Treatment with Ni^{2+} may inhibit not only the influx of Ca^{2+} but also Ca^{2+} extrusion. Thus, preconditioning may exert its protective effect primarily by maintaining the function of the forward mode of the Na^+–Ca^{2+} exchanger rather than by suppressing the reverse mode. However, to elucidate the exact mechanism, future studies should investigate the effects of more selective inhibitors of the Na^+–Ca^{2+} exchanger during ischemia.

We did not detect a significant cytosolic Ca^{2+} overload following reperfusion in nonpreconditioned hearts. Activation of the reverse mode of the Na^+–Ca^{2+}

exchanger is thought to play a dominant role in Ca^{2+} overload upon reperfusion. If indeed diastolic $[Ca^{2+}]_i$ in this model was elevated not only during sustained ischemia but also during reperfusion, preconditioning might reduce the Ca^{2+} overload by inhibiting Ca^{2+} influx via the reverse mode of the Na^+–Ca^{2+} exchanger.

We also evaluated the activity of the Na^+–Ca^{2+} exchanger by exposing the hearts to Na^+-free extracellular medium. Baartscheer et al. recently reported that the increase in $[Ca^{2+}]_i$ during this procedure was due to an influx from the extracellular space as well as to the release of intracellular Ca^{2+} stores from organelles, such as the sarcoplasmic reticulum (SR) in cardiac myocytes [23]. In the present study, the Na^+–Ca^{2+} exchanger blocker Ni^{2+} markedly suppressed the increase in $[Ca^{2+}]_i$. In addition to blocking the Na^+–Ca^{2+} exchanger, Ni^{2+} may also act as a blocker of L-type Ca^{2+} channels. This possibility seems unlikely, however, because pretreatment with verapamil, a blocker of the L-type Ca^{2+} channel, did not affect the increase in $[Ca^{2+}]_i$ induced by exposure to Na^+-free medium (data not shown). Therefore, exposure to Na^+-free medium could be used to measure the activity of the reverse mode of the Na^+–Ca^{2+} exchanger, at least qualitatively. We cannot completely exclude the idea that Ca^{2+} uptake by the SR contributed to the decay of $[Ca^{2+}]_i$. Such a contribution seems unlikely, however, because pretreatment with thapsigargin, an inhibitor of the SR Ca^{2+} ATPase, did not affect the decay time (data not shown). This matter remains to be further elucidated.

The present study employed the fluorescent indicator fura-2 to determine the levels of $[Ca^{2+}]_i$. It is possible that a portion of the fura-2 signals may have arisen from nonmyocytes or from sources other than the cytosol. However, consistent with a previous report [14], we found no significant contribution of the endothelial cells to the fura-2 fluorescence in this model. Moreover, Lee et al. observed that very little of the Mn^{2+}-quenchable fluorescence would be due to mitochondria trapping [19]. The use of fluorescent indicators is therefore suitable for the measurement of $[Ca^{2+}]_i$ in the beating heart.

In summary, we found that blockade of the Na^+–Ca^{2+} exchanger using Ni^{2+} reduced the antiarrhythmic effect of preconditioning during reperfusion. Ni^{2+} reversed the reduction of Ca^{2+} overload caused by preconditioning, and that preconditioning suppressed the activity of the reverse mode of the Na^+–Ca^{2+} exchanger but did not affect the forward mode. These data suggest that the regulation of ion levels by the Na^+–Ca^{2+} exchanger may be involved in ischemic preconditioning.

REFERENCES

1. Murry CE, Richard VJ, Reimer KA, Jennings RB. 1990. Ischemic preconditioning slows energy metabolism and delays ultrastructural damage during a sustained ischemic episode. Circ Res 66:913–931.
2. Li GC, Vasquez JA, Gallagher KP, Lucchesi BR. 1990. Myocardial protection with preconditioning. Circulation 82:609–619.
3. Schott RJ, Rohmann S, Braun ER, Schaper W. 1990. Ischemic preconditioning reduces infarct size in swine myocardium. Circ Res 66:1133–1142.
4. Cohen MV, Liu GS, Downey JM. 1991. Preconditioning causes improved wall motion as well as smaller infarcts after transient coronary occlusion in rabbits. Circulation 84:341–349.

5. Steenbergen C, Perlman ME, London RE, Murphy E. 1993. Mechanism of preconditioning. Ionic alterations. Circ Res 72:112–125.
6. Shiki K, Hearse DJ. 1987. Preconditioning of ischemic myocardium: reperfusion-induced arrhythmias. Am J Physiol (Heart Circ Physiol) 253:H1470–H1476.
7. Kida M, Fujiwara H, Ishida M, Kawai C, Ohura M, Miura I, Yabuuchi Y. 1991. Ischemic preconditioning preserves creatine phosphate and intracellular pH. Circulation 84:2495–2503.
8. Liu GS, Thornton J, Van Winkle DM, Stanley AWH, Olsson RA, Downey JM. 1991. Protection against infarction afforded by preconditioning is mediated by A_1 adenosine receptors in rabbit heart. Circulation 84:350–356.
9. Gross GJ, Auchampach JA. 1992. Blockade of ATP-sensitive potassium channels prevents myocardial preconditioning in dogs. Circ Res 70:223–233.
10. Ytrehus K, Liu Y, Downey JM. 1994. Preconditioning protects ischemic rabbit heart by protein kinase C activation. Am J Physiol (Heart Circ Physiol) 266:H1145–H1152.
11. Barry WH. 1991. Calcium and ischemic injury. Trends Cardiovasc Med 1:162–166.
12. Seki S, Miyoshi K, Ishiki M, Taniguchi M, Mochizuki S. 1996. Ca^{2+}-dependent fluorescence transients and contractility during low-flow ischemia and reperfusion in rat hearts containing fura-2. Jpn Circ J 60:515.
13. Neely JR, Rovetto MJ, Whitmer JT, Morgan HE. 1973. Effects of ischemia on function and metabolism of isolated working rat heart. Am J Physiol 225:651–658.
14. Field ML, Azzawi A, Styles P, Henderson C, Seymour A-ML, Radda GK. 1994. Intracellular Ca^{2+} transients in isolated perfused rat heart: measurement using the fluorescent indicator Fura-2/AM. Cell Calcium 16:87–100.
15. Liu X, Engelman RM, Rousou JA, Flack JE, Deaton DW, Das DK. 1994. Normothermic cardioplegia prevents intracellular calcium accumulation during cardioplegic arrest and reperfusion. Circulation 90:II-316–II-320.
16. Mohabir R, Lee H-C, Kurz RW, Clusin WT. 1991. Effects of ischemia and hypercarbic acidosis on myocyte calcium transients, contraction, and pH_i in perfused rabbit hearts. Circ Res 69:1525–1537.
17. Camacho SA, Figueredo VM, Brandes R, Weiner MW. 1993. Ca^{2+}-dependent fluorescence transients and phosphate metabolism during low-flow ischemia in rat hearts. Am J Physiol 265:H114–H122.
18. Mochizuki S, MacLeod KT. 1992. The effects of hypoxia on cytosolic Ca^{2+} during low Na^+ exposure in isolated cardiac myocytes from guinea-pig. J Physiol (Lond) 446:334.
19. Lee HC, Smith N, Mohabir R, Clusin WT. 1987. Cytosolic calcium transients from the beating mammalian heart. Proc Natl Acad Sci USA 84:7793–7797.
20. Kihara Y, Grossman W, Morgan JE. 1989. Direct measurement of changes in intracellular calcium transients during hypoxia, ischemia and reperfusion in intact mammalian heart. Circ Res 65:1029–1044.
21. Tani M, Neely JR. 1989. Role of intracellular Na^+ in Ca^{2+} overload and depressed recovery of ventricular function of reperfused ischemic rat hearts. Possible involvement of H^+–Na^+ exchange and Na^+–Ca^{2+} exchange. Circ Res 65:1045–1056.
22. Seki S, MacLeod KT. 1995. Effects of anoxia on intracellular Ca^{2+} and contraction in isolated guinea pig cardiac myocytes. Am J Physiol 268:H1045–H1052.
23. Baartscheer A, Schumacher CA, Opthof T, Fiolet JWT. 1996. The origin of increased cytoplasmic calcium upon reversal of the Na^+/Ca^{2+} exchanger in isolated rat ventricular myocytes. J Mol Cell Cardiol 28:1963–1973.

LONG-TERM BUT NOT SHORT-TERM CARDIOPROTECTION CAN BE INDUCED BY PRECONDITIONING IN HYPERCHOLESTEROLEMIA

LÁSZLÓ SZEKERES, P. FERDINANDY, I. NAGY, and Z. SZILVÁSSY

Albert Szent-Györgyi Medical University

Summary. Preconditioning of the heart by single or multiple noninjurious ischemic stimuli may induce both short-term (up to 2 hours) and long-term (3 to 24–48 hours) cardiac protection against the consequences of a subsequent severe stress. Up to now, however, both short-term and long-term protection has been demonstrated only in normal, metabolically healthy animals.

Therefore, the aim of the study reported in this chapter was to test whether short-term and long-term (delayed) cardiac protection could be induced under conditions of experimental atherosclerosis in hypercholesterolemic rabbits that had been fed a cholesterol-rich diet over two months. Repeated brief periods of rapid ventricular pacing were used to induce delayed protection of the heart. Moderation of postpacing right intracavitary ST-segment elevation and of left ventricular end-diastolic pressure (both produced by ventricular overpacing at 500 beats/min for 15 minutes) was found both in normal animals and in those fed a cholesterol-rich diet. However, the short-lived protection induced by a single preconditioning pacing was present only in healthy, normal animals. The cardioprotective effect of short-term preconditioning appeared in parallel with an attenuation of the ischemia-induced increase in cardiac cAMP content measured by radioimmunoassay. The same parallel could be observed in delayed cardioprotection in both normal and hypercholesterolemic rabbits. An increase in cardiac cGMP content was characteristic of short-term but not of long-term protection. These results suggest that the delayed cardiac protection evoked by multiple brief, rapid pacings operates even in hypercholesterolemia-induced experimental atherosclerosis but that the short-term protection evoked by a single pacing period is lost in hypercholesterolemic rabbits.

S. Mochizuki, N. Takeda, M. Nagano and N. Dhalla (eds.). THE ISCHEMIC HEART.

INTRODUCTION

The heart can be protected against the harmful effects of a severe stress not only by drugs but also by cardiac adaptation to stress. The basis of the adaptation phenomenon is that a minor, reversible stress to the heart (and, according to recent findings, to other organs as well) may induce adaptation to stresses, which in turn might prevent or moderate the pathologic consequences of a later, more severe stress.

Depending on the intensity of the adaptation-inducing, reversible, preconditioning stress, two types of adaptive processes can be induced:

1. Preconditioning by brief periods of ischemia results in short-term cardioprotection (less than two hours) that is, however, powerful against ischemic cell injury leading to necrosis, against life-threatening ventricular arrhythmias, and against contractile dysfunction. This type of protection has been reviewed recently by Parratt [1].
2. In 1983, we described a delayed form of cardiac adaptation (DCA) to stress that prevented or moderated stress-induced ischemic, morphologic, or metabolic changes, ventricular arrhythmias, or contractile dysfunction *days* after a more intensive but still noninjurious stress, e.g., a low dose of prostacyclin (PgI_2) and its stable analogues [2,3], brief periods of rapid cardiac pacing [4], or repeated low doses of isoprenaline [5]. These types of interventions are termed *preparatory* or *preconditioning* stress or stimuli.

All preconditioning stimuli used to induce DCA activate the adenylate cyclase–cAMP pathway. PgI_2 and its analogues act via the PgI_2 receptor [6], whereas pacing [4] or brief coronary artery occlusion [7] may liberate both PgI_2 and catecholamines. The latter activate the adenylate cyclase–cAMP pathway via β-adrenoceptors. The above-mentioned repeated application of low isoprenaline doses evoking DCA and delayed cardioprotection also works by stimulating the adenylate cyclase–cAMP pathway through its action on the β-adrenoceptors.

In order to estimate the degree of protection. standardized and reproducible test stimuli were used that produced reversible changes in different cardiac parameters. These test (challenging) stresses were occlusion of the left anterior descending (LAD) coronary artery (in dogs), a brief period of rapid cardiac pacing (in rabbits), or as described recently, joint administration of a low dose of α- and β-adrenoceptor agonists [8]. Responses to the test stimuli, both before and at different times after the preconditioning treatment, were then compared.

Preconditioning-induced changes appeared as a limitation of the infarct size or as a reduction of the severity of arrhythmias, both due to coronary artery occlusion [1], or further as a diminution of ischemic and hemodynamic changes due to brief overload by rapid pacing [3,6].

The protective effects of DCA were maximal 24–48 hours after preconditioning and could be prolonged at will by administration of a low-maintenance dose every third day [9]. The literature on DCA and on delayed effects has been reviewed by Szekeres [6] and by Parratt and Szekeres [10].

Cardiac protection, either short-term (SCP) or delayed (DCP), has so far been produced in normal, healthy animals only. Therefore, the objective of the experiments reported here was to investigate whether SCP or DCP could be induced under pathological conditions, e.g., in hypercholesterolemia-induced experimental atherosclerosis in rabbits, generated by feeding the animals a cholesterol-rich diet (1.5% cholesterol-enriched chow versus normal chow) for two months.

METHODS

Adult male New Zealand White rabbits weighing 2.5–3 kg were used in this study. One animal per cage was housed in air-conditioned animal rooms at 21°C with 60%–70% humidity and a 12-hour light/dark daily cycle. All animals had free access to normal laboratory chow and tap water. At least a one-week adaptation period was allowed before surgery.

Superficial anesthesia of the rabbits was performed with 15 mg/kg diazepam (Richter Gedeon Pharmaceuticals, Hungary) injected into the ear vein. For local pain relief, 10 mg/kg lidocaine (EGIS Pharmaceuticals, Hungary) was given subcutaneously. Then, under aseptic conditions, a bipolar French-4 electrode catheter (Cordis, Germany) was introduced via the right jugular vein into the apex of the right ventricle. The correct position of the electrode catheter was established by analysis of the intracavital electrogram recorded from the implanted electrode catheter, which thus could serve for both recording and ventricular stimulation. The electrocardiogram (ECG) was monitored through bipolar chest-lead electrodes. For measuring intraventricular pressure, a polyethylene cannula, attached to an electromanometer (Hugo Sachs Electronic, Germany) through a Statham P23Db transducer (Gould, France) was inserted into the left ventricular cavity via the right external carotid artery. For intravenous injection of substances, another polyethylene catheter was inserted into the left jugular vein. In 12 instrumented, conscious rabbits, the following parameters of cardiac function were determined: ST-segment elevation in the right endocardial electrogram, an indicator of myocardial ischemia; changes in the ventricular effective refractory period (VERP); and the left ventricular end-diastolic pressure (LVEDP), indicative of the adequacy of the left ventricular pump function. In addition, in a separate set of experiments, cardiac cAMP and cGMP content was determined by means of radioimmunoassay (RIA) using Amersham RIA kits [11].

All these values were determined at rest (R), i.e., before and after delivery of a challenging or test stress (P) consisting of high-rate (500 beats/min) right ventricular pacing for 15 minutes. The test stimulus produced the following transitory changes: 1) elevation of the ST segment in the intracavitary electrogram, 2) increase of LVEDP, and 3) shortening of VERP. Details of the methods used were described earlier [4,11].

The following experimental protocol was used on the seventh day after surgery:

1. Baseline (resting = R) VERP and LVEDP values were determined.
2. In the controls, ST-segment elevation and pre-(R) and postpacing (P) LVEDP and VERP values were determined after delivery of a test stimulus.

3. To assess the changes due to short-term cardioprotection, the effect of a *single preconditioning pacing* (i.e., 500 beats/min for five minutes) on the test-pacing-induced changes was estimated. Single-pacing preconditioning was carried out 24 hours after the preceding, control test stimulus and 30 minutes before the next test pacing.
4. In order to estimate changes due to delayed (long-term) cardio-protective adaptation, the effect of *multiple preconditioning pacing* (i.e., successive five-minute pacings at 500 beats/min with 30-minute intervals over a period of two days) on the test pacing-induced changes was estimated. Twenty-four hours after completing delivery of multiple-pacing preconditioning, the test pacing was applied.
5. Six rabbits continued to be fed ordinary laboratory chow (normal group); the other six were fed a cholesterol-rich (1.5%) diet. Both diets lasted eight weeks.

   Serum cholesterol measured [11] before and after the eight-week period remained unchanged in the normal diet group (2.1 ± 0.39 vs. 1.9 ± 0.26 mmol/L) but increased in the cholesterol-fed group (from 2.0 ± 0.29 to 24.7 ± 3.6 mmol/L). In this group, 55% lipid accumulation [11] was found in the thoracic aorta and LAD coronary artery.
6. Cardiac cAMP and cGMP levels were estimated in two groups of 36 rabbits each, one group on each diet. Within these groups, the animals were divided into six subgroups with six animals in each subgroup. The first subgroup was used to estimate the nonpaced baseline values of the cyclic nucleotide content (CNC), the second to measure CNC 30 minutes after a single preconditioning pacing at rest, the third to estimate CNC immediately after test pacing, the fourth to estimate CNC immediately after a second test pacing delivered 30 minutes after the first one, the fifth to determine CNC 24 hours after termination of the preconditioning protocol with multiple pacings at rest, and the sixth with the same protocol but immediately after the test pacing.

Statistical analysis

Data were expressed as mean ± SEM. Analysis of variance was used for repeated measurements, followed by a modified t-test for paired data according to the Bonferroni method as suggested by Wallenstein et al. [12]. Differences were considered statistically significant when p was less than or equal to 0.05.

All experiments performed in this study were in accordance with the recommendations of the declaration of Helsinki regarding the use and care of laboratory animals and with the permission of the Ethical Committee for the Protection of Animals in Research (Albert Szent-Györgyi Medical University, Szeged, Hungary).

RESULTS

ST segment

Test-pacing-induced elevation of the ST segment was more expressed in hypercholesterolemic than in metabolically healthy, normal rabbits. A single precondition-

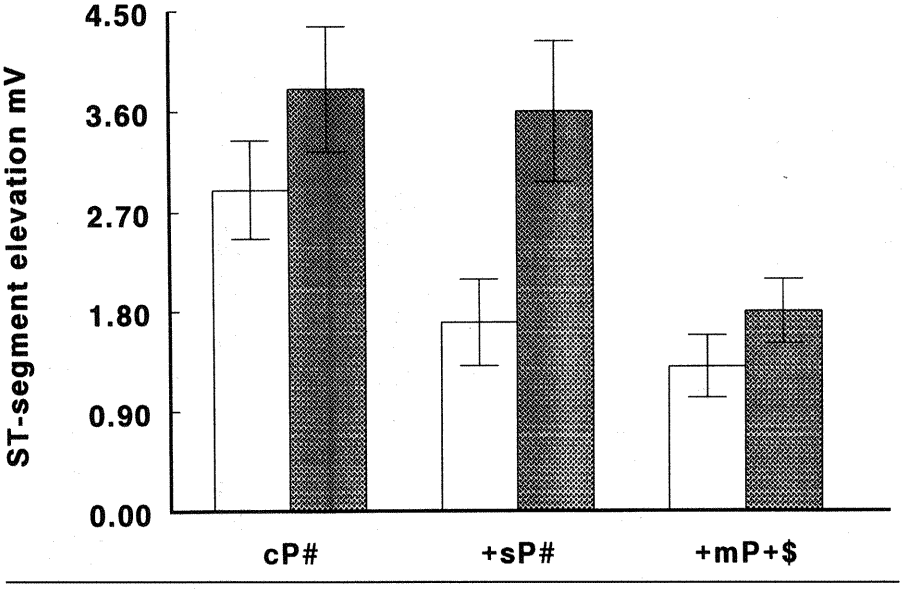

Figure 1. Test pacing (500 beats/min over 15 minutes) induced elevation of the ST segment in the endocardial electrogram of normal and hypercholesterolemic conscious rabbits, before and after preconditioning due to a single or to serial (multiple) pacings. Ordinate: ST-segment elevation mV. Open bar: normal, metabolically healthy group; shaded bar: hypercholesterolemic group. c: nonpaced control; P: values measured immediately after test pacing; s: single preconditioning pacing; m: multiple preconditioning pacing. Significant differences ($p < 0.05$) were observed for prepacing vs. postpacing (*), atherosclerotic vs. normal (#), preconditioned vs. nonpreconditioned (+), and single preconditioning vs. multiple preconditioning ($).

ing pacing was able to moderate significantly the pacing-induced ST-segment elevation in normal but not in hypercholesterolemic animals. On the other hand, in both normal and hypercholesterolemic animals, long-term protection induced by multiple preconditioning pacing appeared as a significant reduction of ST-segment elevation produced by test pacing (figure 1).

Left ventricular end-diastolic pressure

LVEDP was higher in the hypercholesterolemic than in the normal, healthy rabbits in the nonpreconditioned and in the single-pacing preconditioned group. Test pacing significantly enhanced LVEDP in both normal and hypercholesterolemic animals in the control (nonpreconditioned) group. Single preconditioning pacing was able to moderate the test-pacing-induced elevation of LVEDP in normal but not in hypercholesterolemic animals. However, multiple preconditioning pacing significantly moderated test-pacing-induced LVEDP elevation in both normal and hypercholesterolemic rabbits (figure 2).

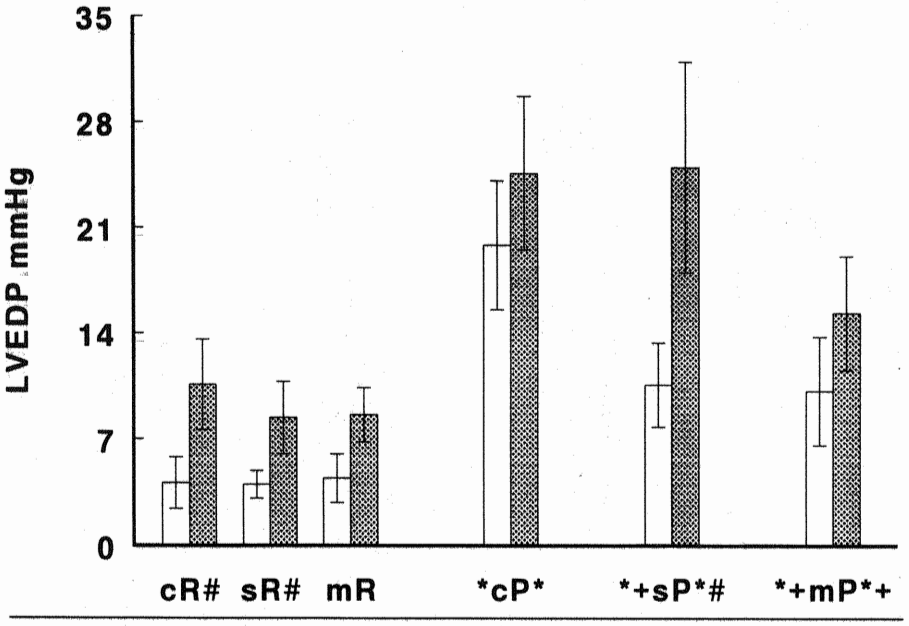

Figure 2. Baseline values and test-pacing-induced elevation of the left ventricular end-diastolic pressure (LVEDP) in normal and hypercholesterolemic conscious rabbits, before and after preconditioning due to a single or to serial (multiple) pacings. Ordinate: LVEDP mmHg. R: rest (baseline values). All other signs and symbols as in figure 1.

Ventricular effective refractory period

In the nonpaced, resting state, VERP was not affected by single preconditioning pacing; however, it was significantly prolonged by multiple preconditioning pacing in both normal and hypercholesterolemic animals. Test pacing significantly shortened VERP in both normal and hypercholesterolemic rabbits, whereas single preconditioning pacing failed to prolong it, and multiple preconditioning pacing prolonged it in both normal and hypercholesterolemic animals above values observed in the nonpreconditioned, resting state (figure 3).

Changes in cardiac cAMP level

In the resting state, the cAMP level was only slightly increased—more in the hypercholesterolemic than in the normal group. Test pacing markedly increased the cAMP levels in both groups. Single preconditioning pacing significantly reduced the elevated cAMP level to near the low resting values, but only in the normal healthy rabbits; no effect was observed in the hypercholesterolemic animals. On the other hand, multiple preconditioning pacing was able to prevent test-pacing-induced marked elevation of the cardiac cAMP level in both normal and hypercholesterolemic animals (figure 4).

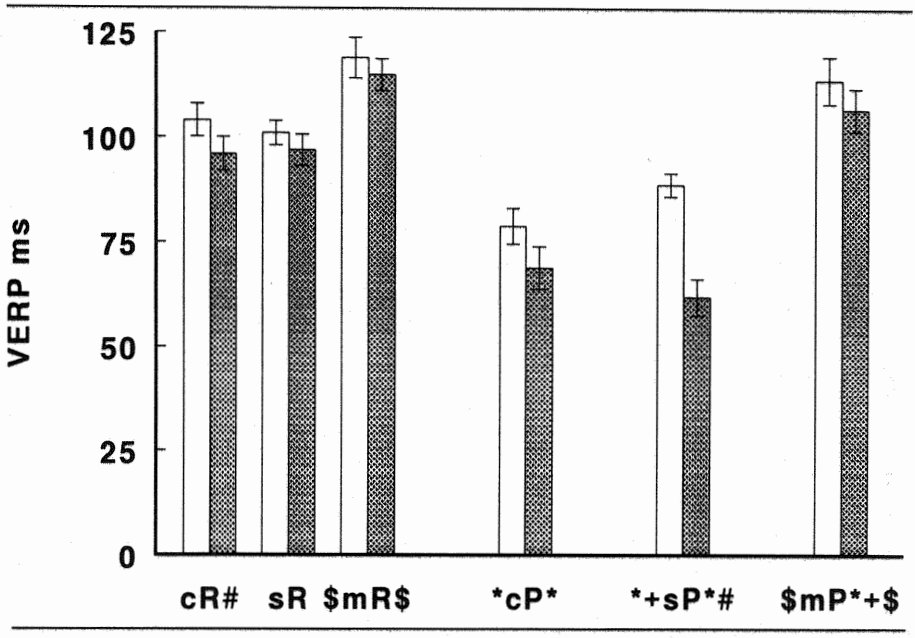

Figure 3. Baseline values and test-pacing-induced shortening of the ventricular effective refractory period (VERP) in normal and hypercholesterolemic conscious rabbits, before and after preconditioning due to a single or to serial (multiple) pacings. Ordinate: VERP msec. All other signs and symbols as in figures 1 and 2.

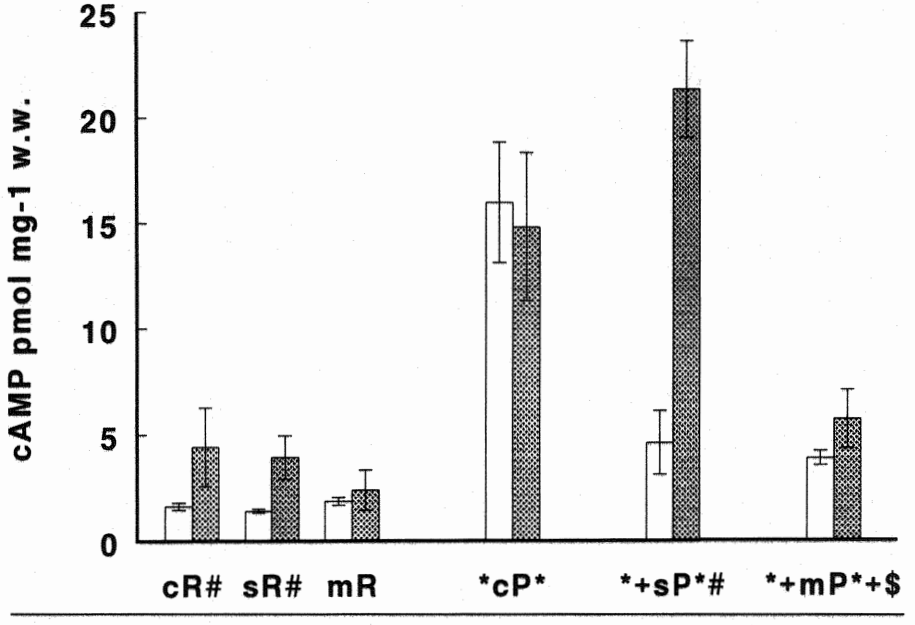

Figure 4. Baseline values and test-pacing-induced elevation of the cardiac cAMP level in normal and hypercholesterolemic conscious rabbits, before and after preconditioning due to a single or to serial (multiple) pacings. Ordinate: cardiac cAMP-level pmol/mg wet weight. All other signs and symbols as in figures 1 and 2.

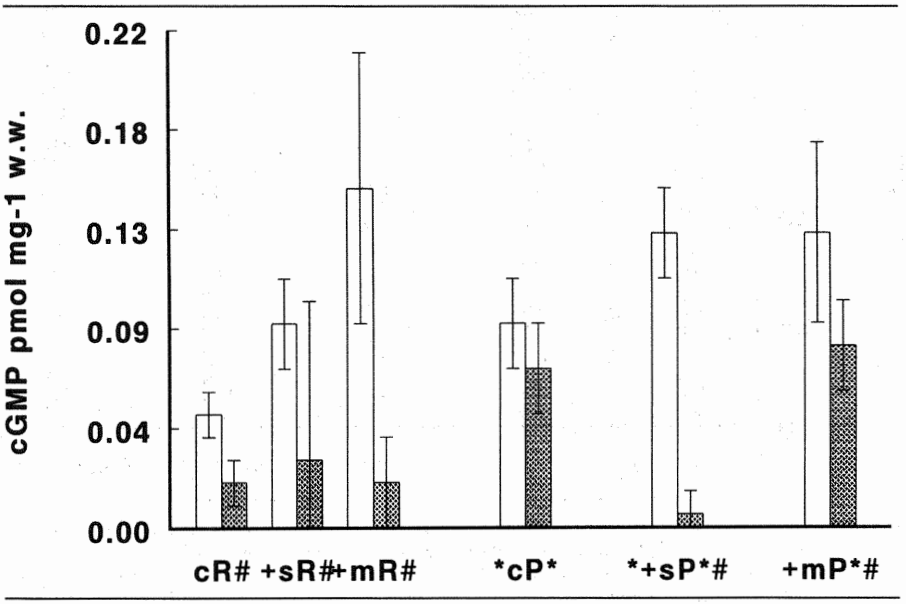

Figure 5. Baseline values and test-pacing-induced elevation of the cardiac cGMP level in normal and hypercholesterolemic conscious rabbits, before and after preconditioning due to a single or to serial (multiple) pacings. Ordinate: cardiac cGMP-level pmol/mg wet weight. All other signs and symbols as in figures 1 and 2.

Changes in cardiac cGMP level

In the resting state, the cGMP level increased after single preconditioning pacing and even more after multiple preconditioning pacing, but only in the normal healthy group. No such change occurred in hypercholesterolemic animals. Pacing induced rather inconsistent changes in both groups (figure 5).

DISCUSSION

These experiments compared the changes due to single- or multiple-pacing-induced preconditioning in the baseline values and after frequency loading (by test pacing) in some basic cardiac parameters, such as ST-segment elevation in the endocardial electrogram, LVEDP, and VERP, in normal, metabolically healthy rabbits as compared to hypercholesterolemic rabbits. In addition, in order to shed light at least partially on the possible mechanism, the role of the second messengers cAMP and cGMP was also investigated by estimating their cardiac level at the different experimental conditions applied in the study.

It was interesting to find that the baseline values of LVEDP were not affected by either single- or multiple-pacing-induced preconditioning—an outcome similar to VERP, which, however, was slightly but significantly prolonged by multiple-pacing-induced preconditioning. ST-segment changes were within the normal

margin of error. Accordingly, baseline values of the cardiac cAMP level were not affected either by a single- or multiple-pacing-induced preconditioning. The baseline values of LVEDP and cAMP were somewhat higher and those of VERP somewhat lower in the hypercholesterolemic group than in the normal, healthy group. Entirely different changes occurred in the baseline values of the cardiac cGMP level. Single preconditioning pacing caused a significant increase as compared to the nonpreconditioned control values, and this increase was even more expressed after multiple-pacing-induced preconditioning in the healthy normal group; however, much lower values, not affected by preconditioning, were observed in the hypercholesterolemic group.

In conclusion, we were unable to demonstrate any protective effect of preconditioning at the level of the baseline values except for the above-mentioned slight prolongation of VERP after multiple-pacing-induced preconditioning.

A loading of the heart (by test pacing) is needed in order to demonstrate the cardioprotective effect of either single- or multiple-pacing-induced preconditioning. Test pacing evoked a marked elevation of the ST segment, an increase in LVEDP and cAMP, and a shortening of VERP in the nonpreconditioned healthy animals and in the hypercholesterolemic animals as well.

Short-term cardioprotection induced by single preconditioning pacing protected against test-pacing-induced ST-segment elevation, increase in LVEDP, shortening of VERP, and increase of cardiac cAMP-level in the normal, healthy animals only.

Delayed, prolonged cardioprotection induced by multiple-pacing preconditioning protected against the above changes both in normal and in hypercholesterolemic animals.

The fact that moderation of a test-pacing-induced increase in the cardiac cAMP level parallels the protective action of both single-pacing and multiple-pacing preconditioning suggests that the adenylate cyclase–cAMP pathway may play a major role in the mechanism of this protection, whereas a similar role of cGMP is unlikely to occur since no parallel was observed in animals subjected to test pacing.

Our results also show a fundamental difference in the mechanisms of short-term and long-term cardioprotection. It was suggested earlier that short-term cardioprotection is mainly based on the liberation of endogenous protective substances [1], whereas the induction of some key enzymes regulating transmembrane ion transport and breakdown of excess amounts cAMP [6] is mainly responsible for long-term cardio-protection.

SUMMARY AND CONCLUSIONS

1. Preconditioning either by single pacing or by multiple pacing did not produce changes significantly different from those observed in nonpreconditioned controls in the baseline values of LVEDP, cAMP, and VERP. VERP, however, was significantly longer after multiple pacing. In contrast, baseline values of cGMP were enhanced by preconditioning.

2. The baseline values of LVEDP and cAMP were significantly higher and those of cGMP and VERP lower in hypercholesterolemic animals than in normal animals.
3. Increasing the cardiac workload by test pacing enhanced changes in LVEDP, cAMP, and VERP in the nonpreconditioned normal and hypercholesterolemic animals.
4. Short-term cardioprotection induced by single-pacing preconditioning protected against test-pacing-induced ST-segment elevation, increase in LVEDP, shortening of VERP, and increase of cardiac cAMP level in normal healthy animals only.
5. Delayed, prolonged cardioprotection induced by multiple-pacing preconditioning protected against the above changes both in normal and in hypercholesterolemic, atherosclerotic animals.

ACKNOWLEDGMENT

This work was supported by a grant-in-aid (No: T019951) from the Hungarian National Science Foundation (OTKA)

REFERENCES

1. Parratt JR. 1994. Protection of the heart by ischaemic preconditioning: mechanisms and possibilities for pharmacological evaluation. Trends Pharmacol Sci 15:19–25.
2. Szekeres L, Krassói I, Udvary É. 1983. Delayed antiischemic effect of PgI2 and of a new stable PgI2 analogue 7-oxo-prostacyclin-Na in experimental model angina in dogs. J Mol Cell Cardiol 15(Suppl I):394.
3. Szekeres L, Koltai M, Pataricza J, Takáts I, Udvary É. 1984. On the late antiischaemic action of the stable PgI2 analogue: 7-oxo-PgI2-Na and its possible mode of action. Biomed Biochim Acta 43:135–142.
4. Szekeres L, Papp JGy, Szilvássy Z, Udvary É, Végh Á. 1993. Moderate stress by cardiac pacing may induce both short term and long term cardioprotection. Cardiovasc Res 27:593–596.
5. Kovanecz I, Szekeres L, Papp JGy. 1996. Long term ischaemic preconditioning of the heart induced by repeated beta-adrenergic stress. Abstracts of the 5th Joint Meeting of Hungarian, Italian and Polish Pharmacological Societies, June 20–22, 1996, Pécs, Hungary.
6. Szekeres L. 1996. On the mechanism and possible therapeutic application of delayed cardiac adaptation to stress. Can J Cardiol 12:177–185.
7. Kuzuya T, Hoshida S, Yamashita N, Fuji H, Oe H, Hori M, Kamada T, Tada M. 1993. Delayed effects of sublethal ischemia on the acquisition of tolerance to ischemia. Circulation Res 72:1293–1299.
8. Kovanecz I, Papp JGy, Szekeres L. 1997. Increased cardiac workload by adrenoceptor agonists for the estimation of potential anti-ischaemic activity in a conscious rabbit model. J Pharmacol Toxicol Methods 37:149–159.
9. Krause EG, Szekeres L. 1995. On the mechanism and possible therapeutic application of delayed adaptation of the heart to stress situations. Mol Cell Biochem 147:115–122.
10. Parratt JR, Szekeres L. 1995. Delayed protection of the heart against ischaemia. Trends Pharmacol Sci 16:351–355.
11. Szilvássy Z, Ferdinándy P, Bor P, Jakab I, Lonovics J, Koltai M. 1994. Ventricular overdrive pacing-induced anti-ischemic effect: a conscious rabbit model of preconditioning. Am J Physiol 266 (Heart Circ Physiol 35): H2033–H2041.
12. Wallenstein S, Zucker CL, Fleiss JL. 1980. Some statistical methods useful in circulation research. Circ Res 47:1–9.

CONTRIBUTION OF ENDOGENOUS CATECHOLAMINES TO PRECONDITIONING: IS IT THROUGH FACILITATION OF ADENOSINE PRODUCTION?

KATSUO SUZUKI, AKIHITO TSUCHIDA, and TETSUJI MIURA

Sapporo Medical University School of Medicine

Summary. Studies using adrenoceptor blockers have reported very contradictory results and do not allow us to draw a clear conclusion about the role of adrenoceptors in infarct size limitation by preconditioning. However, reserpinization consistently abolished the protection of preconditioning in our studies and in those of others, indicating the contribution of endogenous catecholamines. Our findings using microdialysis suggest that the role of catecholamines in preconditioning is not through modulating production of adenosine, a key trigger of the preconditioning mechanism. In light of the negative data from adrenoceptor blockers on preconditioning in the rabbit, it is speculated that the contribution of endogenous catecholamines, at least in this species, may be through a non-receptor-mediated mechanism such as free radicals.

INTRODUCTION

Exposing the myocardium to a sublethal episode of brief ischemia enhances its tolerance to ischemic infarction in various animal models. Numerous studies on this phenomenon, termed *ischemic preconditioning*, have indicated that the protective mechanism of preconditioning is triggered by activation of several classes of receptors, i.e., adenosine [1], bradykinin B_2 [2,3], and opioid receptors [4,5]. Of these receptors, the role of the adenosine receptor in preconditioning has been the most well characterized. A copious amount of adenosine is produced during ischemia and stimulates adenosine receptors in the myocardium [6,7]. It has been shown that adenosine receptors (probably A_1 and A_3 receptors) need to be activated for triggering the mechanism of preconditioning in the heart [1,8], and occupancy of the

S. Mochizuki, N. Takeda, M. Nagano and N. Dhalla (eds.). THE ISCHEMIC HEART.

adenosine receptors is necessary also for maintaining the anti-infarct tolerance of cardiac myocytes during sustained ischemia [9]. Furthermore, the level of interstitial adenosine during preconditioning ischemia is thought to be a determinant of the extent of cardioprotection [10]. In contrast, the role of adrenergic receptors in preconditioning has not yet been clarified, though the sympathetic nerve system is expected to be activated upon coronary occlusion for preconditioning [11,12]. However, previous studies indicate a close interrelationship between the adrenergic system and adenosine receptor-mediated regulation of the myocyte function [6,7]. For example, while elevation of sympathetic tone increases the myocardial oxygen demand and thus adenosine metabolism, activation of the A_1 receptor counteracts and suppresses the adenylate cyclase activity stimulated by the β-adrenoceptor. This chapter will briefly discuss the relationship between adrenoceptor and adenosine and a possible role of endogenous catecholamines in the infarct size-limiting effect of ischemic preconditioning.

ADRENOCEPTOR AND ADENOSINE

Coronary artery occlusion elicits activation of the sympathetic nerves, and released norepinephrine increase myocardial oxygen demand, which presumably promotes adenosine release from the myocytes via an increase in cytosolic free ADP [6,13]. Furthermore, it has been shown that adenosine release during ischemia and hypoxia is significantly enhanced by β-receptor stimulation in isolated hearts [6,14,15], although the increase of adenosine is a transient phenomenon. α_1-Adrenoceptor has also been proposed by Kitakaze et al. [16] to contribute to adenosine production. They reported that adenosine release into the coronary vein in the ischemic myocardium was suppressed by α_1-adrenoceptor blockade but not by β-blockade in the dog heart *in situ*. When these results are taken together, it is conceivable that adrenoceptors (α-and/or β-receptors) activated by endogenous catecholamines may enhance adenosine production and thus facilitate adenosine receptor activation during preconditioning. However, alteration of *interstitial* adenosine during preconditioning has not been analyzed in light of adrenoceptor activity.

EFFECT OF ADRENOCEPTOR BLOCKADE ON PRECONDITIONING: ANY SPECIES DIFFERENCES?

Although the role of adrenergic receptors in preconditioning has been the subject of many investigations, the reported effects of adrenoceptor blockers on the infarct size-limiting effect of preconditioning are contradictory in the literature. Kitakaze et al. [17] reported that the infarct size-limiting effect of preconditioning was abolished by prazosin in a dog model of infarction. In contrast, cardioprotection of preconditioning in rabbits and rats was not blocked by BE2254 (an α_1-blocker) [18], phenoxybenzamine [19], phentolamine [20], prazosin [21], or a combination of prazosin plus metoprolol [22],—results that argue against the requisite role of adrenoceptor activity in preconditioning. However, experiments *in vivo* using receptor blockers always suffer from the possibility of insufficiency in the dose of blockers. Actually, in a preliminary study using rabbits, very large doses of bunazosin

attenuated the effect of preconditioning on infarct size [23]. Unfortunately, the effects of α-adrenoceptor agonists on infarct size are also discrepant in the literature. Although a preconditioning-like infarct size limitation by intracoronary injection of methoxamine was reported in dogs by Kitakaze et al. [17], their findings could not be reproduced in a recent study by Sebbag et al. [24]. The reason for the different outcomes can hardly be explained by the slight differences in methodology of these two studies. However, the differences in effects of α-blockers on preconditioning in the dog, rabbit, and rat [17–23] suggest that there may be species differences in the role of the α-adrenoceptor, at least in the mechanism of preconditioning: the α-adrenoceptor may be important for preconditioning in the dog but not in the rabbit or rat. It is interesting to note that the adrenoceptor is not the only class of receptors for which the role in preconditioning is different between animal species. A crucial role of adenosine in triggering the mechanism of preconditioning has been indicated from the studies using rabbits [1], dogs [25,26], and pigs [27], though the data in the rat model of infarction rather dispute the involvement of the adenosine receptor in preconditioning in this species [19,28,29].

EFFECT OF CATECHOLAMINE DEPLETION ON PRECONDITIONING AND ADENOSINE IN THE HEART

In addition to adrenoceptor blockers, sympathectomy is a useful method to obtain an insight into the role of the endogenous adrenergic system. Toombs et al. [30] first reported that reserpine pretreatment abolished preconditioning protection, supporting the importance of endogenous catecholamines. However, the mechanism for the effect of reserpinization has not been investigated, and the anesthetic agents used by Toombs et al. (ketamine/xylazine) could have modified the results, as was the case in studies concerning the ATP-sensitive potassium channel in preconditioning [22,31,32]. Accordingly, we assessed the effect of reserpinization on preconditioning in pentobarbital-anesthetized rabbits and also examined the possibility that the effect of reserpine is through suppression of ischemia-induced buildup of adenosine in the cardiac interstitium.

Effect of reserpine on the infarct size-limiting effect of preconditioning

In our series of experiments, rabbits were reserpinized by intraperitoneal injection of 3 mg/kg and 5 mg/kg of reserpine at 48 hours and 24 hours, respectively, before induction of myocardial infarction. This protocol of reserpinization reduced the myocardial norepinephrine content from the control value of 2248 ± 28 ng/g of tissue to 11 ± 3 ng/g. The effect of reserpine treatment on plasma norepinephrine is shown in table 1. In the control rabbits, plasma norepinephrine was 0.162 ± 0.043 ng/mL under the baseline condition, and it increased by approximately 40% after five minutes of coronary occlusion. By contrast, in 3 of 6 reserpinized rabbits, baseline norepinephrine was not detectable, and the levels of norepinephrine after coronary occlusion were approximately 10% of the values in the untreated controls. In untreated rabbits anesthetized with pentobarbital, infarct size after 45 minutes of coronary artery occlusion followed by three-hour reperfusion was 60.8% ± 2.2% of

Table 1. Plasma norepinephrine before and after coronary occlusion

Rabbit	Baseline	Ischemia 5′
Control		
SZ-50	0.085	0.150
SZ-53	0.093	0.148
SZ-60	0.218	0.308
SZ-62	0.253	0.305
Mean	0.162	0.228[a]
SE	0.043	0.091
Reserpine-treated		
SZ-51	ND	0.022
SZ-52	ND	0.014
SZ-54	0.055	0.083
SZ-63	ND	0.015
SZ-64	0.037	0.065
SZ-65	0.015	0.024
Mean		0.037[b]
SE		0.012

[a] $p < 0.05$ vs. baseline.
[b] $p < 0.05$ vs. control.
Note: Values are ng/mL. ND: not detectable.

Table 2. Summary of infarct size data

Group	*N*	Heart weight (g)	Risk area (cm^3)	Infarct area (cm^3)	%IS/AR
Control	14	6.9 ± 0.3	0.74 ± 0.11	0.46 ± 0.08	60.8 ± 2.2
PC	11	7.2 ± 0.5	0.71 ± 0.13	0.20 ± 0.05	28.9 ± 6.1[a]
Res	10	6.7 ± 0.4	0.63 ± 0.09[a]	0.24 ± 0.04	37.3 ± 2.7[a]
Res-PC	9	6.0 ± 0.3	0.79 ± 0.13	0.34 ± 0.06	43.1 ± 2.8[a]

[a] $p < 0.05$ vs. control.
%IS/AR: infarct size as percent of area at risk.

the area at risk, and preconditioning with five-minute ischemia and five-minute reperfusion before the 45-minute coronary occlusion limited infarct size to 28.9% ± 6.1% (table 2). However, in reserpinized rabbits, preconditioning failed to protect the heart from infarction: infarct size was 43.1% ± 2.8% in preconditioned hearts and 37.3% ± 2.7% in nonpreconditioned hearts. Figure 1 shows that reserpine blocked the downward shift of the infarct-size–risk-area-size relationship by preconditioning. These results are concordant with the findings by Toombs et al. [30], who employed a different anesthesia. However, infarct size was slightly limited by reserpine alone in our study, which was not observed in the study by Toombs et al. [30]. These differences are most likely due to the difference in the kind of anesthetics (ketamine/xylazine vs. pentobarbital). This explanation is supported by recent findings in *pentobarbital-anesthetized dogs* that reserpine had a very modest infarct size-limiting effect and achieved inhibition of protection afforded by

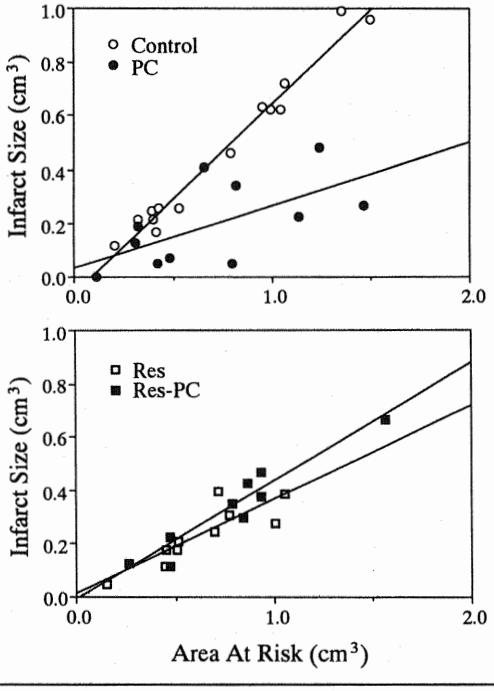

Figure 1. Scatter-plot of infarct size against the size of area at risk. Upper panel: the control group (Control) versus the group that received preconditioning with five-minute ischemia/five-minute reperfusion (PC). Lower panel: the group that received reserpinization (Res) versus the group that received reserpinization plus preconditioning (Res-PC). There were significant correlations between infarct size and risk area size in all four study groups. The slope of the regression line in the PC group was significantly smaller than that in the Control group, indicating myocardial salvage by preconditioning ($Y = 0.26X + 0.01$ vs. $Y = 0.70X - 0.07$, $p < 0.05$) In contrast, there was no significant difference in the regression lines between the Res and the Res-PC group, indicating that preconditioning failed to protect reserpinized hearts from infarction ($Y = 0.35X + 0.02$ vs. $Y = 0.44X - 0.01$, p = NS).

preconditioning [33]. Taken together, the effect of reserpine on preconditioning in our studies and earlier ones [30,33] suggests that endogenous catecholamines play a role in the cardioprotective mechanism of preconditioning.

In contrast with reserpine, surgical sympathectomy of the heart did not make the heart refractory to preconditioning in a study by Ardell et al. [34]. This difference, associated with different methods of sympathetics denervation, cannot be easily explained, but preservation of circulating catecholamines and myocardial epinephrine in surgically denervated rabbits might be responsible.

Effect of reserpinization on the interstitial adenosine level during ischemia

Since earlier studies suggest that adenosine production in ischemic myocardium may be accelerated by α- and/or β-adrenoceptor activation [6,13–16], we hypothesized

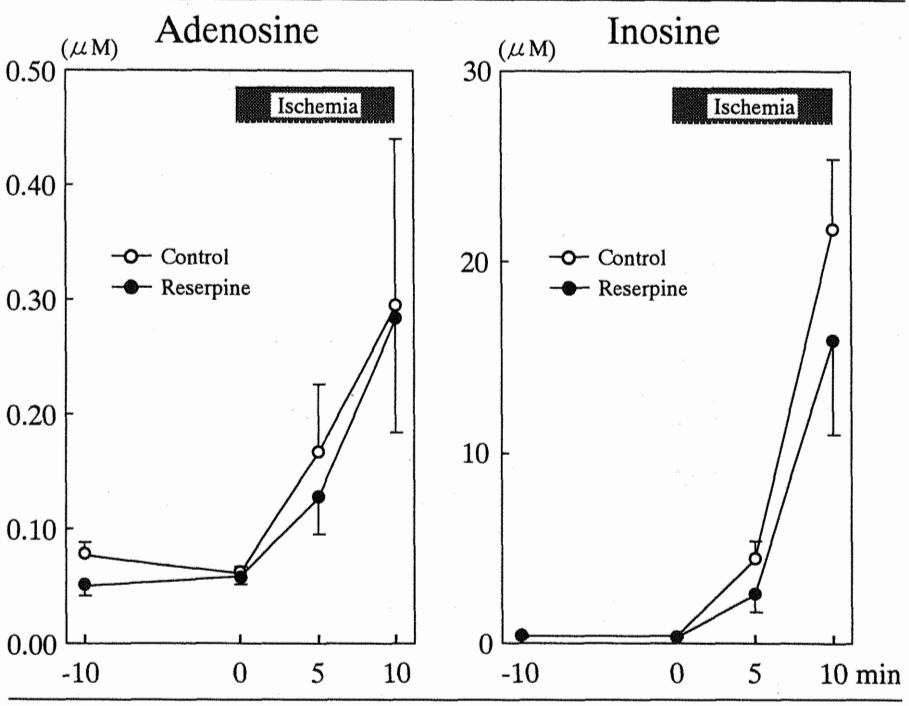

Figure 2. Time course of dialysate adenosine and inosine levels during myocardial ischemia. A microdialysis probe was inserted in the midmyocardium of the left marginal artery's territory in an open-chest anesthetized rabbit. After a stabilization period of two hours, two baseline samples were collected every 10 minutes and then the left marginal artery was occluded by the snare. Dialysates from the ischemic region were sampled every five mintes. Adenosine (left panel), inosine (right panel), and hypoxanthine (data not shown) levels were determined by HPLC. Open circles and closed circles depict the untreated and reserpinized rabbits, respectively.

that refractoriness of the reserpinized heart to ischemic preconditioning may be due to failure of the interstitial adenosine level to reach a threshold for triggering the cardioprotective mechanism. To examine this hypothesis, the time course of the interstitial adenosine level was assessed by using an *in vivo* microdialysis technique in untreated and reserpinized rabbits. The microdialysis probe and HPLC system for purine assay used in this laboratory was described previously [35]. Figure 2 shows the time course of adenosine and inosine in the dialysate samples from the ischemic myocardium in pentobarbital-anesthetized rabbits. The adenosine level increased from 0.060 ± 0.006 μM to 0.165 ± 0.061 μM after five-minute ischemia and to 0.293 ± 0.146 μM after 10-minute ischemia in untreated controls. In reserpinized rabbits, the increase in adenosine after the onset of ischemia was less (from 0.058 ± 0.007 μM to 0.126 ± 0.032 μM after five-minute ischemia and to 0.282 ± 0.099 μM after 10-minute ischemia) than that in the controls. However, this difference in adenosine and also the difference in inosine levels (figure 2) were statistically insignificant. Furthermore, it should also be noted that interstitial

adenosine level in reserpinized rabbits is estimated to be approximately 0.6 μM after five-minute ischemia, since *in vitro* recovery of adenosine in our dialysis system is approximately 20%. This value of adenosine is well above K_D (i.e., in the nanomolar range) of adenosine receptors in the myocytes [36]. These findings argue against the contribution of endogenous catecholamines to preconditioning through regulation of the interstitial adenosine level.

WHY ARE RESERPINIZED HEARTS REFRACTORY TO PRECONDITIONING?

Since the effect of reserpinization on interstitial adenosine in the ischemic myocardium was not large enough to explain the effect of this agent on preconditioning against infarction, it remains unclear why reserpine pretreatment makes the myocardium refractory to preconditioning protection. However, a few possibilities could be considered. First, depletion of endogenous catecholamines may result in the reduction of free radicals generated during preconditiong. Recent studies suggest that free radicals participate in triggering the preconditioning mechanism [37,38], possibly through activation of protein kinase C [38] and/or opening of ATP-sensitive potassium channels [39,40]. While there are several potential sources of free radicals in the myocytes and endothelial cells [41], studies by Rump and Klaus [42,43] indicated the importance of auto-oxidation of endogenous catecholamines. In their study, myocardial injury during coronary occlusion was attenuated by superoxide dismutase (SOD), a free radical scavenger, in nonreserpinized hearts, but not in hearts with depleted stores of catecholamines [42]. Furthermore, deleterious effects of *exogenous* norepinephrine on ischemic injury in reserpinized hearts was also completely prevented by SOD [43]. Thus, depletion of endogenous catecholamines by reserpine many eliminate some of the free radicals generated during preconditioning ischemia–reperfusion, which could mimic the effect of SOD or other free radial scavengers on preconditioning [37,38]. Secondly, protein kinase C activity in the heart may be modified by reserpinization. The importance of this kinase in the maintenance of ischemic tolerance against infarction has been supported by a number of studies showing that several classes of protein kinase C inhibitors given before sustained ischemia abolished protection afforded by preconditioning [44–47]. Although there are no current data indicating suppression of any protein kinase C isoforms in the reserpinized myocardium, activities of protein kinase C-α and -β in the brain [48], and protein kinase C-θ in the skeletal muscle [49] were shown to be reduced after reserpine treatment. Thirdly, we cannot totally exclude a nonspecific toxic effect of reserpine on the myocardium. However, it is unlikely that reserpine exerted such a toxic effect in our rabbit experiments and in a study by Vander Heide at al. [33], since reserpinization alone actually reduced infarct size slightly in these studies.

REFERENCES

1. Downey JM, Miura T. 1994. The role of adenosine in ischemic preconditioning. In Hori M, Maruyama M, Reneman RS (eds), Cardiac Adaptation and Failure. Tokyo: Springer-Verlag, pp. 147–166.

2. Wall TM, Sheely R, Harmtman JC. 1994. Role of bradykinin in myocardial preconditioning. J Pharmacol Exp Ther 270:681–689.
3. Goto M, Liu Y, Yang XM, Ardell JL, Cohen MV, Downey JM. 1995. Role of bradykinin in protection of ischemic preconditioning in rabbit hearts. Circ Res 77:611–621.
4. Chien GL, Van Winkle DM. 1996. Naloxone blockade of myocardial ischemic preconditioning is stereoselective. J Mol Cell Cardiol 28:1895–1900.
5. Miki T, Sato H, Cohen MV, Downey JM. 1996. Opioid receptor contributes to ischemic preconditioning through protein kinase C activation in rabbits (abstract). Circulation 94(Suppl I):I392–I393.
6. Olsson RA, Pearson JD. 1991. Cardiopurinoceptors. Physiol Rev 70:761–845.
7. Mubagwa K, Mullane K, Flameng W. 1996. Role of adenosine in the heart and circulation. Cardiovasc Res 32:797–813.
8. Liu GS, Richards GS, Olsson RA, Mullane K, Walsh RS, Downey JM. 1994. Evidence that the adenosine A_3 receptor may mediate the protection afforded by preconditioning in the isolated rabbit heart. Cardiovasc Res 28:1057–1061.
9. Thornton JD, Thornton CS, Downey JM. 1993. Effect of adenosine receptor blockade: preventing protective preconditioning depends on time of initiation. Am J Physiol 265:H504–H508.
10. Miura T, Ogawa T, Iwamoto T, Shimamoto K, Iimura O. 1992. Dipyridamole potentiates the myocardial infarct size-limiting effect of preconditioning. Circulation 86:979–985.
11. Malliani A, Schwartz PJ, Zanchetti A. 1969. A sympathetic reflex elicited by experimental coronary occlusion. Am J Physiol 217:703–709.
12. Schomig A, Haass M, Richard G. 1991. Catecholamine release and arrhythmias in acute myocardial ischemia. Eur Heart J 12(Suppl F):38–47.
13. Bunger R, Mallet RT, Hartman DA. 1998. Redox manipulation of free cardiac adenylates and purine nucleoside release. Reciprocity between cytosolic phosphorylation potential and reduction-oxidation state or free AMP in perfused working heart. In de Jong JW (ed), Myocardial Energy Metabolism. Dordrecht: Martinus Nijihoff, pp. 67–81.
14. Deussen A, Schrader J. 1991. Cardiac adenosine production is linked to myocardial PO_2. J Mol Cell Cardiol 23:495–504.
15. Fenton RA, Dobson JG Jr. 1993. Hypoxia enhances isoproterenol-induced increase in heart interstitial adenosine, depressing β-adrenergic contractile responses. Circ Res 72:571–578.
16. Kitakaze M, Hori M, Tamai J, et al. 1987. α_1-Adrenoceptor activity regulates release of adenosine from the ischemic myocardium in dogs. Circ Res 60:631–639.
17. Kitakaze M, Hori M, Morioka T, et al. 1994. α_1-Adrenoceptor activation mediates the infarct size-limiting effect of ischemic preconditioning through augmentation of 5′-nucleotidase activity. J Clin Invest 93:2197–2205.
18. Thornton JD, Daly JF, Cohen MV, Yang X-G, Downey JM. 1993. Catecholamines can induce adenosine receptor-mediated protection of the myocardium but do not participate in ischemic preconditioning in the rabbit. Circ Res 73:649–655.
19. Bugge E, Ytrehus K. 1995. Ischaemic preconditioning is protein kinase C dependent but not through stimulation of alpha adrenergic or adenosine receptors in the isolated rat heart. Cardiovasc Res 29:401–406.
20. Van Winkle DM, Haessler R, Wolff RA, Kuzume K, Anselone CG, Davis RF. 1994. α-Adrenergic cardioprotection involves adenosine, but ischemic preconditioning does not involve α-adrenergic activation (abstract). FASEB J 8:A569.
21. Tsuchida A, Miura T, Miki T, Sakamoto J, Iimura O. 1994. Role of α_1-adrenergic receptor and protein kinase C in infarct size limitation by ischemic preconditioning in rat heart (abstract). Circulation 90(Suppl I):I–647.
22. Miura T, Goto M, Miki T, Sakamoto J, Shimamoto K, Iimura O. 1995. Glibenclamide, a blocker of ATP-sensitive potassium channels, abolishes infarct size limitation by preconditioning in rabbits anesthetized with xylazine/pentobarbital but not with pentobarbital alone. J Cardiovasc Pharmacol 25:531–538.
23. Kariya T, Minatoguchi S, Ohno T, et al. 1995. Selective α_1-antagonist, Bunazosin, can dose-dependently block infarct size limiting effect of ischemic preconditioning in rabbits (abstract). J Mol Cell Cardiol 27:A519.
24. Sebbag L, Katsuragawa M, Verbinski S, Jennings RB, Reimer KA. 1993. Intracoronary administration of the α_1-receptor agonist, methoxamine, does not reproduce the infarct-limiting effect of ischemic preconditioning in dogs. Cardiovasc Res 32:830–838.

25. Grover GJ, Sleph PG, Czwonczyk S. 1992. Role of ATP-sensitive potassium channels in mediating preconditioning in the dog heart and their possible interaction with adenosine A_1-receptors. Circulation 86:1310–1316.
26. Yao Z, Gross GJ. 1994. A comparison of adenosine-induced cardioprotection and ischemic preconditioning in dogs. Efficacy, time course, and role of K_{ATP} channels. Circulation 89:1229–1236.
27. Van Winkle DM, Chien GL, Wolff RA, Soifer BE, Kuzume K, Davis RF. 1994. Cardioprotection provided by adenosine receptor activation is abolished by blockade of the K_{ATP} channel. Am J Physiol 266:H829–H839.
28. Liu Y, Downey JM. 1992. Ischemic preconditioning protects against infarction in rat heart. Am J Physiol 263:H1107–H1112.
29. Li Y, Kloner RA. 1993. The cardioprotective effects of ischemic preconditioning are not medicated by adenosine receptors in rat hearts. Circulation 87:1642–1648.
30. Toombs CF, Wlitse AL, Shebuski RJ. 1993. Ischemic preconditioning fails to limit infarct size in reserpinized rabbit myocardium. Implication of norepinephrine release in the preconditioning effect. Circulation 88:2351–2358.
31. Thornton JD, Thornton CS, Sterling DJ, Downey JM. 1993. Blockade of ATP-sensitive potassium channels increases infarct size but does not prevent preconditioning in rabbit hearts. Circ Res 72:44–49.
32. Toombs CF, Moore TL, Shebuski RJ. 1993. Limitation of infarct size in the rabbit by ischaemic preconditioning is reversible with glibenclamide. Cardiovas Res 27:617–622.
33. Vander Heide RS, Schwartz LM, Jennings RB, Reimer KA. 1995. Effect of catecholamine depletion on myocardial infarct size in dogs: role of catecholamines in ischemic preconditioning. Cardiovasc Res 30:656–662.
34. Ardell JL, Yang X-M, Barron RA, Downey JM, Cohen MV. 1996. Endogenous myocardial norepinephrine is not essential for ischemic preconditioning in rabbit heart. Am J Physiol 270:H1078–H1084.
35. Miura T, Suzuki K, Shimamoto K, Iimura O. 1996. Suppression of the degradation of adenine nucleotides during ischemia may not be sufficient mechanism for infarct size limitation by preconditioning. Basic Res Cardiol 91:452–432.
36. Olah ME, Stiles GL. 1992. Adenosine receptors. Annu Rev Physiol 54:211–215.
37. Tanaka M, Fujiwara H, Yamasaki K, Sasayama S. 1994. Superoxide dismutase and N_2-mercaptopropionyl glycine attenuate infarct size limitation effect of ischemic preconditioning in the rabbit. Cardiovasc Res 28:980–986.
38. Baines CP, Goto M, Downey JM. 1996. Oxygen free radical release during ischemic preconditioning triggers protection in rabbit myocardium via activation of protein kinase C. Circulation 94(Suppl I):I–424.
39. Tokube K, Kiyosue T, Arita M. 1996. Opening of cardiac K_{ATP} channel by oxygen free radicals produced by xanthine oxidase reaction. Am J Physiol 271:H478–H489.
40. Ichinari K, Kakei M, Matsuoka T, Nakashima H, Tanaka H. 1996. Direct activation of the ATP-sensitive potassium channel by oxygen free radicals in guinea-pig ventricular cells: its potentiation by MgADP. J Mol Cell Cardiol 28:1867–1877.
41. Downey JM, Yellon DM. 1992. Do free radicals contribute to myocardial cell death during ischemia–reperfusion? In Yellon DM, Jennings RB, (ed), Myocardial Protection: The Pathophysiology of Reperfusion and Reperfusion Injury. New York: Raven Press, pp. 35–57.
42. Rump AFE, Rosen R, Klaus W. 1993. Cardioprotection by superoxide dismutase: A catecholamine-dependent process? Anesth Analg 76:239–246.
43. Rump AFE, Klaus W. 1994. Evidence for norepinephrine cardiotoxicity mediated by superoxide anion radicals in isolated rabbit hearts. Naunyn-Schmiedebergs Arch Pharmacol 349:295–300.
44. Ytrehus K, Liu Y, Downey JM. 1994. Preconditioning protects ischemic rabbit heart by protein kinase C activation. Am J Physiol 266:H1145–H1152.
45. Speechly-Dick ME, Mocanu MM, Yellon DM. 1994. Protein kinase C. Its role in ischemic preconditioning in the rat. Circ Res 75:586–590.
46. Liu Y, Cohen MV, Downey JM. 1994. Chelerythrine, a highly selective protein kinase C inhibitor, blocks the anti-infarct effect of ischemic preconditioning in rabbit hearts. Cardiovasc Drugs Ther 8:881–882.
47. Sakamoto J, Miura T, Goto M, Iimura O. 1995. Limitation of myocardial infarct size by adenosine A_1 receptor activation is abolished by protein kinase C inhibitors in the rabbit. Cardiovasc Res 29:682–688.

48. Komachi H, Yanagisawa K, Shirasaki Y, Miyatake T. 1994. Protein kinase C subspecies in hippocampus and striatum of reserpinized rat brain. Brain Res 634:127–130.
49. Hilgenberg L, Yearwood S, Milstein S, Miles K. 1996. Neural influence on protein kinase C isoform expression in skeletal muscle. J Neurosci 16:4994–5003.

HYPOXIC PRECONDITIONING OF ISOLATED CARDIOMYOCYTES OF ADULT RAT

MICHIKO NOJIRI, KOUICHI TANONAKA, KEN-ICHI YABE, and SATOSHI TAKEO

Tokyo University of Pharmacy and Life Science

Summary. The present study was undertaken to examine whether or not cytoprotective effects of hypoxic preconditioning were detectable in isolated, quiescent cardiomyocytes of adult rats. The cardiomyocytes were incubated for 120 minutes under hypoxic conditions (sustained hypoxia), followed by 15-minute reoxygenation. Sustained hypoxia decreased the number of viable cells (from 99% to 70% of the initial cell), which consisted of rod- and square-shaped cardiomyocytes. It also decreased the number of rod-shaped cardiomyocytes (from 90% to 40% of the initial cell) and simultaneously increased the number of square-shaped cells (from 10% to 30% of the initial cell). Fifteen-minute reoxygenation resulted in a further decrease in the numbers of viable cells (less than 50% of the initial cell) and square-shaped cells (10% of the initial cell), whereas it did not change the number of rod-shaped cells. Hypoxia–reoxygenation also induced a release of purine nucleosides and bases (ATP metabolites) into the incubation medium. When the cardiomyocytes were subjected to 20 minutes of hypoxic incubation, followed by 30 minutes of normoxic incubation (hypoxic preconditioning), sustained hypoxia-induced decreases in the numbers of viable cells and rod-shaped cells were attenuated (80% and 60% of the initial cell, respectively). The intervention also attenuated sustained hypoxia-induced increase in the number of square-shaped cells (18% of the initial cell). The number of rod-shaped cells subjected to hypoxic preconditioning at the end of 15-minute reoxygenation was similar to that at the end of sustained hypoxia, whereas the number of square-shaped cells decreased to 10% of the initial cells, which was similar to that of square-shaped cells without hypoxic preconditioning. The intervention also suppressed the release of ATP metabolites during hypoxia–reoxygenation. The cardioprotective effect of hypoxic preconditioning was abolished by the presence of 10 μM polymyxin B, an inhibitor of protein kinase C (PKC) during hypoxic preconditioning. Treatment of nonpreconditioned cardiomyocytes with 1000 pM phorbol 12-myristate

13-acetate, a PKC stimulator, for 50 minutes prior to sustained hypoxia mimicked cytoprotection induced by hypoxic preconditioning. The results show that hypoxic preconditioning is detectable in isolated, quiescent cardiomyocytes of adult rats, and the mechanism may be related to activation of PKC.

INTRODUCTION

A brief period of ischemia and subsequent reperfusion has been shown to attenuate the detrimental consequence of ischemia–reperfusion. This phenomenon is termed *ischemic preconditioning* [1]. Ischemic preconditioning delays cellular injury, slows energy metabolism, and reduces the incidence of ventricular arrhythmias during subsequent sustained ischemia–reperfusion in in vivo and in situ animals and in isolated perfused hearts [2–5]. The mechanism underlying the ischemic preconditioning, however, still remains unclear. It is of interest to determine whether preconditioning can be demonstrated in isolated cardiomyocytes. If so, it would be suggested that preconditioning does not rely on cells other than cardiomyocytes, since isolated cardiomyocytes are free of neuronal and humonal factors and are uncontaminated with other types of cells such as endothelial and smooth muscle cells. Generally, cardiomyocytes of adult animals are considered to be hardly preconditioned by hypoxic or ischemic intervention. Recently, several investigators have reported that isolated rabbit cardiomyocytes were preconditioned [6–8]. Although there are several experiments using rabbit isolated cardiomyocytes, ischemic or hypoxic preconditioning of cardiomyocytes of adult rats has been poorly demonstrated. Zhou et al. [9] have recently shown that preconditioning of isolated rat cardiomyocytes contributes to "second windows" of cytoprotection against oxidative stress. However, the method and benefit of ischemic or hypoxic preconditioning of cardiomyocytes are not well established. The purpose of the study reported in this chapter was to determine whether or not hypoxic preconditioning can be demonstrated in isolated, quiescent cardiomyocytes of adult rats.

MATERIALS AND METHODS

This study was designed according to the Guidelines of Experimental Animal Care issued by the Prime Minister's Office of Japan. The experimental protocol of this study was approved by the University Committee of Animal Use and Welfare.

Experimental animals

Male Sprague–Dawley rats (Charles River Japan, Astugi, Japan) weighing 250–270 g were used in the study. The rats were conditioned at 23 ± 1°C with a constant humidity of 55 ± 5% and a cycle of 12 hours light and 12 hours dark. The animals had free access to food and tap water.

Isolation of calcium-tolerant cardiomyocytes of adult rats

Calcium-tolerant ventricular cardiomyocytes of adult rats were prepared according to a method described previously [10]. After anesthesia with intraperitoneal injection of 50 mg/kg pentobarbital, rat hearts were rapidly excised and then mounted on the

aortic cannula of a Langendorff apparatus. The perfusion buffer contained the following composition (mM): NaCl 130, KCl 4.8, KH_2PO_4 1.2, $MgSO_4$ 1.2, $CaCl_2$ 1.25, sodium pyruvate 5, glucose 11, and 2-[4-(2-hydroxyethyl)-1-piperazinyl]ethanesulfonic acid (HEPES) 10 (pH 7.4). The buffer was equilibrated with 100% oxygen gas. The hearts were perfused for five minutes with calcium-free perfusion buffer to wash out calcium in the vascular and extracellular space and then further perfused for 20 minutes in a recirculating manner with calcium-free buffer supplemented with 12.5 μM $CaCl_2$, 0.05% collagenase, and 0.1% bovine serum albumin (BSA). After perfusion with the buffer containing collagenase, the ventricular tissue was chopped in a calcium-free perfusion buffer containing 1% BSA. The chopped tissue was incubated for three minutes in the buffer containing collagenase. The suspended solution was filtered through a mesh. The filtered suspension was centrifuged at 22 × g for one minute. The sediments were resuspended in a calcium-free buffer containing 1% BSA. The calcium concentration for suspension of cells was gradually elevated up to 1 mM. The cells were centrifuged at 22 × g for one minute to sediment viable cells, that is, calcium-tolerant cardiomyocytes. The resultant cell suspension in a minimal essential medium (MEM) containing 1 mM $CaCl_2$ was plated to laminin-coated dishes, and then the cells were incubated at 37°C for 60 minutes. The dishes were then rinsed with MEM to remove floating, dead cells. By this method, approximately 2 million cardiomyocytes were isolated in the present study.

Hypoxia and reoxygenation

Cardiomyocytes (0.8 to 1.0 × 10^5 cells per dish) were placed on the bottom of culture dishes in an air-tight sealed chamber. The chamber had two gas pathways, namely, an inlet and an outlet. There was a glass ball at the top of the gas outlet that could prevent outflow of gas temporarily. Sustained hypoxia was induced by incubating the cardiomyocytes in glucose-free HEPES solution (pH 7.4) with 0.1% BSA (hypoxic medium) for 120 minutes at 37°C in the chamber, which was filled with an atmosphere of 100% nitrogen gas. After sustained hypoxia, the cardiomyocytes were reoxygenated for 15 minutes by exchanging nitrogen gas with 100% oxygen gas in the chamber and adding glucose into the incubation medium at a final concentration of 11 mM [10]. The pO_2 of the medium in the apparatus was less than 25 mmHg under hypoxic conditions and more than 650 mmHg under normoxic conditions when determined by a blood gas analyzer (model 288; Ciba-Corning, Medfield, Massachusetts, USA).

Hypoxic preconditioning

To determine optimal duration for hypoxic preconditioning, cardiomyocytes in MEM were incubated under hypoxic conditions in the chamber described above for different time intervals ranging from 10 to 30 minutes and were then postincubated for 30 minutes under oxygenated conditions (10- to 30-minute hypoxic preconditioning). After 10- to 30-minute hypoxic preconditioning, the cardiomyocytes were subjected to hypoxia–reoxygenation.

Treatment with agents

To elucidate the mechanism underlying the cytoprotective effects of hypoxic preconditioning, cardiomyocytes were incubated with appropriate concentrations of polymyxin B, a protein kinase C (PKC) inhibitor, or phorbol 12-myristate 13-acetate (PMA), a PKC stimulator, only for 50 minutes prior to sustained hypoxia. The cardiomyocytes were subjected to 20-minute hypoxic preconditioning in the presence of 1 to 10 μM polymyxin B and then to hypoxia–reoxygenation. In another set of experiments, the cardiomyocytes were incubated for 50 minutes in the presence of 10 to 1000 pM PMA under normoxic conditions and then were subjected to hypoxia–reoxygenation.

Morphological examination

After an appropriate period of incubation, the cardiomyocytes were fixed with 2% glutaraldehyde, and then their morphological appearances in the same area as that counted prior to sustained hypoxic incubation were examined with a microscope (IMT-2; Olympus Inc., Tokyo, Japan). Three types of isolated cardiomyocytes, that is, rod-, square-, and round-shaped cells, were classified. The ratios of cell length to cell width were more than 3 for the rod-shaped cardiomyocyte (rod cell), and less then 3 for the square-shaped cell (square cell). The round-shaped cell (round cell) was apparently rounded. The rod and square cells were considered to be viable, whereas the round cells were considered to be dead. This criterion was based on the results of trypan blue staining, that is, rod and square cells did not stain blue but round cells stained blue in the presence of the dye. Therefore, in this study, *number of viable cells* means the number of rod and square cells.

Determination of ATP metabolites released into medium

After hypoxia–reoxygenation or 135-minute normoxia, the incubation medium was collected, and purine nucleosides and bases released from cardiomyocytes (ATP metabolites) were analyzed by HPLC (L-6000 series, Hitachi, Tokyo, Japan) according to the method described previously [11]. The ATP metabolites were separated through a Cosmosil $5C_{18}$-AR column (Nacarai Tesque, Kyoto, Japan) by elution with 250 mM $NH_4H_2PO_4$ containing 3.5% CH_3CN (pH 6.0), at a constant flow rate of 1.0 mL/min. Absorbance at 254 nm was monitored with a UV-detector.

Statistics

The results are expressed as the mean ± SEM. Statistical significance was estimated by analysis of variance (ANOVA) followed by Dunnett's or Bonferroni's multiple comparison. Differences with a probability of 5% or less were considered to be statistically significant ($p < 0.05$).

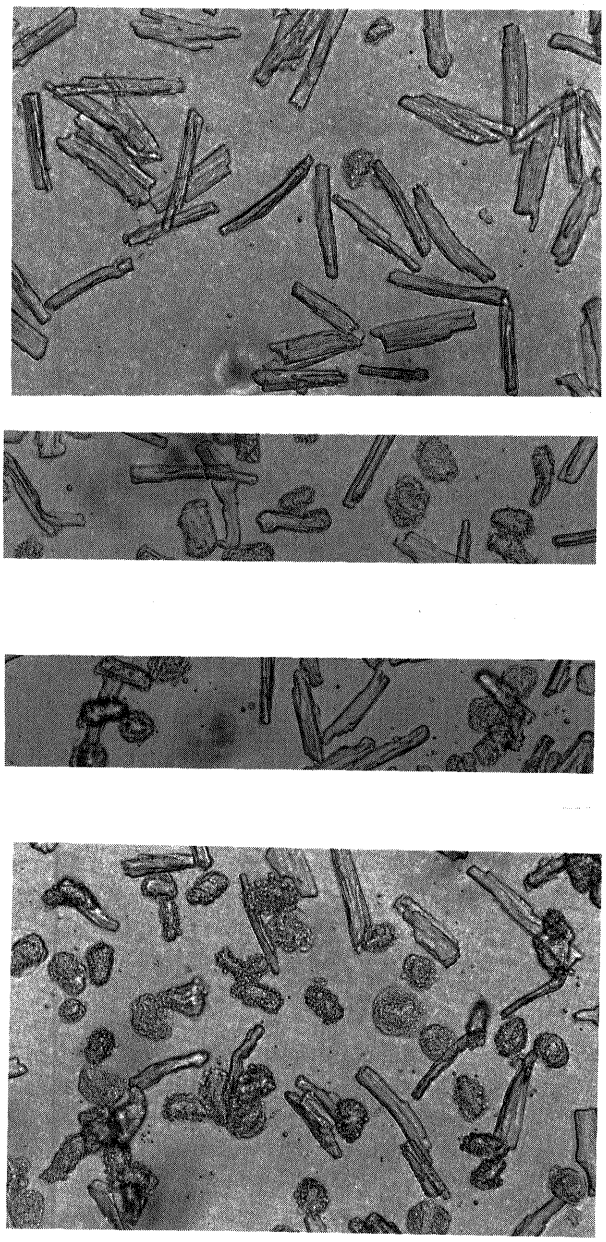

Figure 1. Photographs of cardiomyocytes prior to 120-minute hypoxia (at 0 minutes, upper panel), at the end of 120-minute hypoxia (at 120 minutes, middle panel), and at the end of 15-minute reoxygenation (at 135 minutes, lower panel). Rod- and square-shaped cardiomyocytes were attached to the bottom, coated with laminin in a culture dish, whereas round-shaped cardiomyocytes were not attached to the bottom of the culture dish. The horizontal bar at the bottom represents 50 μm.

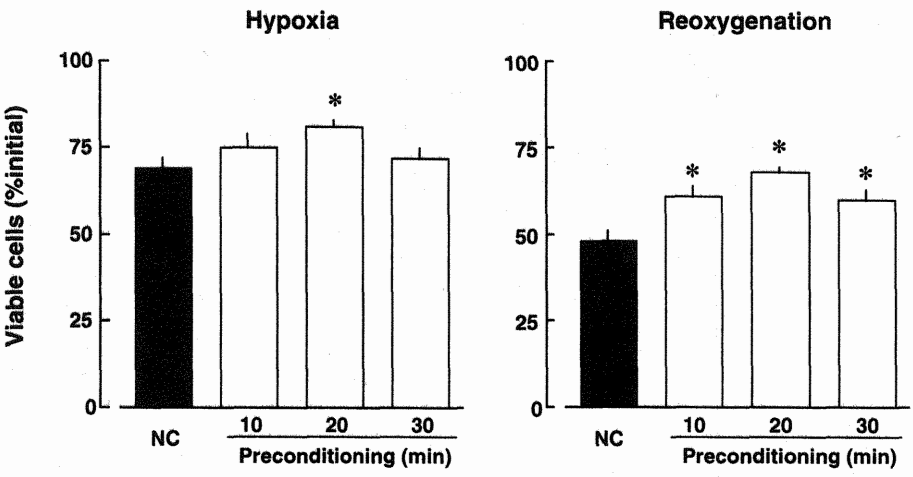

Figure 2. The numbers of viable cardiomyocytes (trypan blue-unstained cells) without (NC; closed columns) and with (PC; open columns) an exposure to 10- to 30-minute hypoxic preconditioning and those after 120-minute hypoxia (left panel) and subsequent reoxygenation (right panel). Values are expressed as percentages of cells in each group to their initial cell numbers. Each value represents the mean ± SEM of five experiments. *, significantly different from nonpreconditioning group ($p < 0.05$).

RESULTS

Hypoxia–reoxygenation

Figure 1 shows photographs of cardiomyocytes at the onset of sustained hypoxia (upper panel), at the end of sustained hypoxia (middle panel), and at the end of reoxygenation (lower panel). After isolation of calcium-tolerant, quiescent cardiomyocytes, the numbers of rod and square cells attached to the bottom of the culture dishes were 92% and 8%, respectively, whereas the round cells were less than 1%. The number of viable cells—that is, rod and square cells—at the end of sustained hypoxia was approximately 70% of the initial viable cells (left panel in figure 2). After reoxygenation, the number of viable cells further decreased to less than 50% of the initial viable cells (right panel in figure 2). The numbers of rod and square cells at the end of sustained hypoxia were 38% and 32% of the initial viable cells, respectively (figure 3). At the end of hypoxia–reoxygenation, the number of square cells decreased to 10% of the initial viable cells (right panel in figure 3), whereas the number of rod cells was similar to that at the end of sustained hypoxia (left panel in figure 3). The number of surviving cardiomyocytes subjected to 120-minute normoxia in the absence of glucose followed by 15-minute normoxia in the presence of glucose (135-minute normoxia) was 97% ± 3% of the initial viable cells. Hypoxia–reoxygenation also induced the release of ATP metabolites from cardiomyocytes into incubation medium (figure 4). ATP metabolites detected in the present study were mostly inosine and hypoxanthine. Incubation of rod and square cells under 135-minute normoxic conditions did not release ATP metabolites (figure 4).

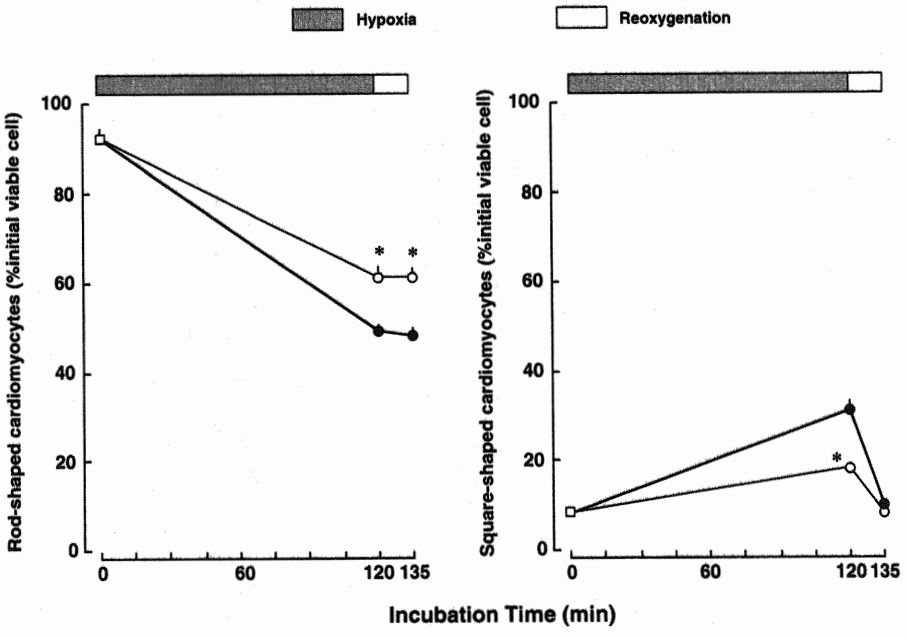

Figure 3. The time course of changes in the number of rod-shaped (left panel) and square-shaped (right panel) cardiomyocytes during 120-minute hypoxia–15-minute reoxygenation. Open circles represent the number of rod- or square-shaped cells after 20-minute hypoxic preconditioning followed by 120-minute hypoxia–15-minute reoxygenation. Closed circles represent the number of rod- or square-shaped cells after 50-minute normoxia followed by 120-minute hypoxia–15-minute reoxygenation. Open squares represent the numbers of rod- and square-shaped cells prior to 120-minute hypoxia. Hatched and open columns represent the numbers of these cells subjected to hypoxic and normoxic incubation, respectively. Values are expressed as percentages of cells in each group to their initial viable cell numbers. Each value represents the mean ± SEM of five experiments. *, significantly different from the nonpreconditioning (closed circles) group ($p < 0.05$).

Hypoxic preconditioning

When the cardiomyocytes were exposed to 20 minutes of hypoxia followed by a 30-minute reoxygenation prior to sustained hypoxia (20-minute hypoxic preconditioning), the number of viable cells at the end of sustained hypoxia was significantly higher than that of nonpreconditioned cells (more than 80% of the initial viable cells; left panel in figure 2). Hypoxia–reoxygenation-induced decrease in the number of viable cells was significantly attenuated by the intervention of 10- to 30-minute hypoxic preconditioning (right panel in figure 2).

When the cardiomyocytes were subjected to 20-minute hypoxic preconditioning, the sustained hypoxia-induced decrease in the number of rod cells was significantly attenuated (left panel in figure 3). The sustained hypoxia-induced increase in the number of square cells was also attenuated by 20-minute hypoxic preconditioning (18% of the initial viable cells; right panel in figure 3). At the end of reoxygenation, the number of rod cells in the 20-minute hypoxic preconditioning group was

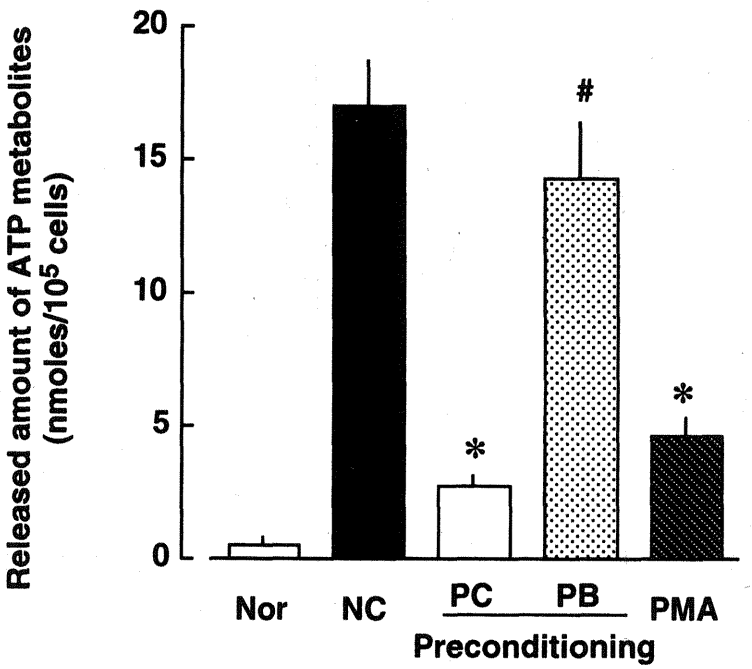

Figure 4. Released amounts of ATP metabolites from cardiomyocytes into incubation medium during 120-minute hypoxia–15-minute reoxygenation. Nor (open column) represents the group of cardiomyocytes subjected to 135-minute normoxia. NC represents the group of cardiomyocytes subjected to 120-minute hypoxia–15-minute reoxygenation alone. PC represents the group for cardiomyocytes subjected to hypoxic preconditioning and then to 120-minute hypoxia–15-minute reoxygenation. PB represents the group for cardiomyocytes subjected to hypoxic preconditioning in the presence of 10 μM polymyxin B and then to 120-minute hypoxia–15-minute reoxygenation. PMA represents the group for cardiomyocytes incubated for 50 minutes in the presence of 1000 pM PMA and then subjected to 120-minute hypoxia–15-minute reoxygenation. Each value represents the mean ± S.E.M. of five experiments. #Significantly different from PC and *significantly different from NC ($p < 0.05$).

similar to that at the end of sustained hypoxia, whereas the number of square cells decreased to 10% of the initial viable cell despite the intervention of hypoxic preconditioning (figure 3). Ten- to 30-minute hypoxic preconditioning *per se* did not alter the morphological appearance of viable cells. In addition, the release of ATP metabolites induced by hypoxia–reoxygenation was suppressed by the intervention of 20-minute hypoxic preconditioning. The amount of ATP metabolites released from 20-minute hypoxic preconditioned cardiomyocytes was 15% of that from nonpreconditioned cells (figure 4).

Effects of polymyxin B and PMA

When the cardiomyocytes were subjected to 20-minute hypoxic preconditioning in the presence of 1, 3, and 10 μM polymyxin B, the numbers of viable cells at the end

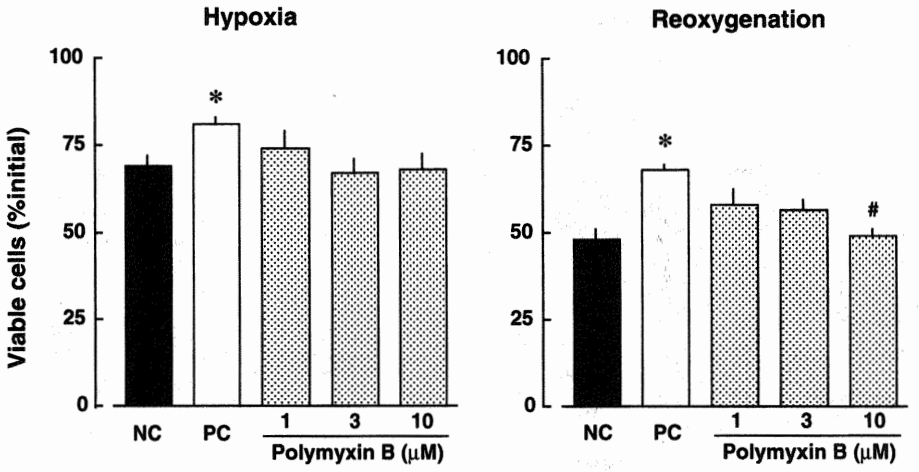

Figure 5. Effects of various concentrations of polymixin B on preconditioned cardiomyocytes after 120-minute hypoxia (left panel) and 120-minute hypoxia–15-minute reoxygenation (right panel). Cardiomyocytes were exposed to hypoxic preconditioning in the absence (PC, open column) and presence of 1 to 10 μM polymixin B (hatched columns) followed by 120-minute hypoxia or 120-minute hypoxia–15-minute reoxygenation. NC represents the number of cardiomyocytes incubated for 50 minutes under normoxic conditions followed by 120-minute hypoxia–15-minute reoxygenation. Values are expressed as percentages of cells in each group to their initial viable cell numbers. Each value represents the mean ± S.E.M. of five experiments. *Significantly different from NC group and #significantly different from PC group ($p < 0.05$).

of sustained hypoxia were 75%, 69%, and 70% of the initial viable cells, respectively (left panel in figure 5). At the end of reoxygenation, the numbers of viable cells in these groups were 57%, 55%, and 50% of the initial viable cells, respectively (right panel in figure 5). Treatment of cardiomyocytes with 10 μM polymyxin B abolished 20-minute hypoxic preconditioning-induced suppression of the release of ATP metabolites during hypoxia–reoxygenation (figure 4). Treatment with 10 μM polymyxin B during either 20-minute hypoxic preconditioning or 50-minute normoxia did not affect the morphological changes in cardiomyocytes. It did not induce the release of ATP metabolites into the medium during 135-minute subsequent normoxia either.

When the cardiomyocytes were incubated in the presence of 10 to 1000 pM PMA for 50 minutes under normoxic conditions and then subjected to sustained hypoxia and reoxygenation, the numbers of viable cells at the end of sustained hypoxia were similar to the number of viable cells untreated with PMA (left panel in figure 6). After hypoxia–reoxygenation, the numbers of viable cells pretreated with 10, 100, and 1000 pM PMA were 47%, 52%, and 68% of the initial viable cells, respectively (right panel in figure 6). Treatment with 1000 pM PMA suppressed the hypoxia–reoxygenation-induced release of ATP metabolites into the medium (figure 4).

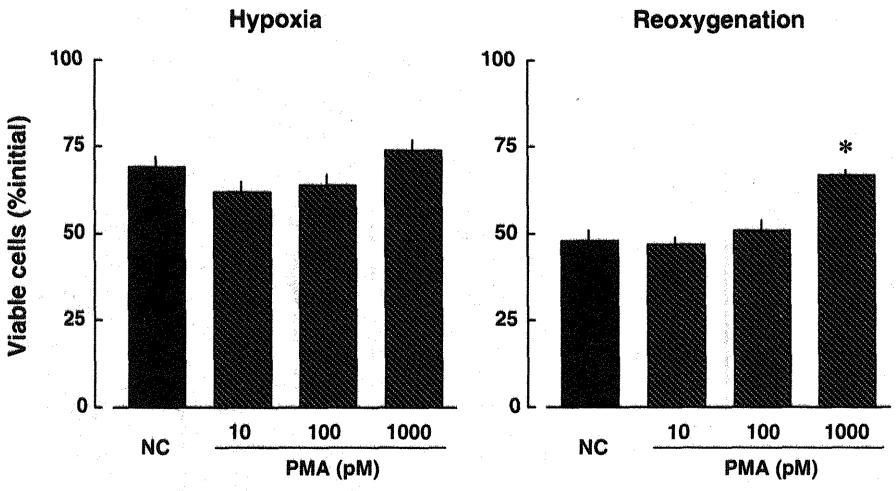

Figure 6. Effects of treatment with various concentrations of phorbol 12-myristate 13-acetate (PMA) on cardiomyocytes subjected to 120-minute hypoxia (left panel) and 120-minute hypoxia–15-minute reoxygenation (right panel). Cardiomyocytes were incubated for 50 minutes in the absence (NC, closed column) and presence of 1 to 1000 pM PMA (closed, striped columns) under normoxic conditions and then subjected to 120-minute hypoxia or 120-minute hypoxia–15-minute reoxygenation. Values are expressed as percentages of cells in each group to their initial cell numbers. Each value represents the mean ± S.E.M. of five experiments. *Significantly different from NC ($p < 0.05$).

Treatment with 1000 pM PMA during 50-minute normoxia neither affected the morphological appearances in cardiomyocytes nor induced the release of ATP metabolites into the medium during 135-minute subsequent normoxia.

DISCUSSION

In the study reported here, we observed that sustained hypoxia induced a decrease in the numbers of viable cells and rod cells and an increase in the number of square cells, and that reoxygenation induced a further decrease in the number of viable cells. From the results on the effects of different periods of hypoxic preconditioning, it was found that 20-minute hypoxic preconditioning was optimal to exert cytoprotective effects. Since there were no changes in the number of rod cells after reoxygenation regardless of the presence or absence of hypoxic preconditioning, the decrease in the number of viable cells observed after reoxygenation is attributed to the loss of square cells. In another word, the cytoprotective effect induced by hypoxic preconditioning is due to prevention or attenuation of sustained hypoxia-induced increase in square cells.

We also observed that hypoxia–reoxygenation induced a release of ATP metabolites into the incubation medium. ATP metabolites have been shown to be released from hypoxic–reoxygenated rabbit or ischemic–reperfused rat hearts, which is considered to be a marker of an increase in transmembrane flux of substrates across the

sarcolemma [12–15]. The intervention of hypoxic preconditioning suppressed the hypoxia–reoxygenation-induced release of ATP metabolites into the incubation medium. The results suggest that the intervention is capable of suppressing the hypoxia–reoxygenation-induced increase in transmembrane flux of ATP metabolites. In in vitro experiments, a release of creatine kinase or lactate dehydrogenase from myocardial tissue and cardiomyocytes is regarded as an index of the increase in transmembrane flux [9,10,16,17]. We failed to detect the activities of these enzymes in the present study, possibly due to the limitation of detectable activities of the enzymes released into the incubation medium. In contrast, it is possible to detect and quantify the released amount of ATP metabolites from small numbers of cardiomyocytes during hypoxia–reoxygenation with the aid of an HPLC apparatus [12]. Takeo et al. [12,16] showed that the released amount of ATP metabolites from perfused hearts was closedly and inversely related to the degree of posthypoxic contractile recovery. They also showed that the posthypoxic recovery was enhanced by the supplementation of exogenous adenosine, inosine, or hypoxanthine [13]. Generally, a decrease in the release of ATP metabolites from myocardium is attributable to a reduction in the rate of ATP breakdown [18–20]. The reduced rate of ATP breakdown could induce a preservation of high-energy phosphates in hypoxic and ischemic tissue, that is, energy-sparing effects. However, several reports [21–23] showed that the hypoxia–reoxygenation-induced release of ATP metabolites was suppressed by treatment with antiarrhythmic agents or *dl*- and *d*-propranolol, whereas the content of high-energy phosphates of the hearts after ischemia did not differ regardless of treatment with or without those agents. These results suggest that suppression of the release of ATP metabolites during reoxygenation is independent of energy-sparing effects. The findings also suggest that ATP salvage synthesis plays an important role in the posthypoxic contractile recovery of the heart. Thus, attenuation of hypoxia–reoxygenation-induced loss of ATP metabolites may contribute to the cytoprotective effects of hypoxic preconditioning.

Several investigators suggests that one of the mechanisms underlying the cardioprotective effects of ischemic or pharmacological preconditioning in animals is the activation of PKC [24–29]. Thus, we examined the involvement of PKC in the effects of hypoxic preconditioning. We found that the presence of 10 μM polymyxin B, a PKC inhibitor [28,30], during 20-minute hypoxic preconditioning decreased the number of rod cells at the end of sustained hypoxia. The presence of polymyxin B also induced a considerable amount of the ATP metabolites released into the incubation medium during hypoxia–reoxygenation. In the present study, the effects of hypoxic preconditioning were abolished by treatment with the PKC inhibitor polymyxin B. However, the specificity of polymyxin B as a PKC inhibitor is not high. Thus, we examined the effect of PKC activation, using PMA [24,31,32] and found that the PKC stimulator induced a cytoprotection of cardiomyocytes like the hypoxic preconditioning. Our results suggest that the cardioprotective mechanism of hypoxic preconditioning in rat cardiomyocytes can be, at least in part, attributed to activation of PKC.

In conclusion, the present study demonstrated that hypoxic preconditioning directly protected isolated, quiescent cardiomyocytes of adult rats against hypoxia–reoxygenation injury and suggested that one of the possible mechanisms underlying the cytoprotective effect of hypoxic preconditioning may be mediated by activation of PKC.

REFERENCES

1. Murry CE, Jennings RB, Reimer KA. 1986. Preconditioning with ischemia: a delay of lethal cell injury in ischemic myocardium. Circulation 74:1124–1136.
2. Shiki K, Hearse DJ. 1987. Preconditioning of ischemic myocardium: reperfusion induced arrhythmias. Am J Physiol 253:H1470–H1476.
3. Murry CE, Richard VJ, Reimer KA, Jennings RB. 1990. Ischemic preconditioning slows energy metabolism and delays ultrastructural damage during sustained ischemic episode. Circ Res 66:913–931.
4. Hagar JM, Hale SL, Kloner RA. 1991. Effect of preconditioning ischemia on reperfusion arrhythmias after coronary artery occlusion and reperfusion in the rat. Circ Res 68:61–68.
5. Liu GS, Richards SC, Olsson RA, Mullane K, Walsh RS, Downey JM. 1994. Evidence that the adenosine A_3 receptor may mediate the protection afforded by preconditioning in the isolated rabbit heart. Cardiovasc Res 28:1057–1061.
6. Armstrong S, Ganote CE. 1994. Adenosine receptor specificity in preconditioning of isolated rabbit cardiomyocytes: evidence of A_3 receptor involovement. Cardiovasc Res 28:1049–1056.
7. Armstrong S, Downey JM, Ganote CE. 1994. Preconditioning of isolated rabbit cardiomyocytes: induction by metabolic stress and blockade by the adenosine antagonist SPT and calphostin C, a protein kinase inhibitor. Cardiovasc Res 28:72–77.
8. Gottlieb RA, Gruol DL, Zhu JY, Engler RL. 1996. Preconditioning in rabbit cardiomyocytes. Role of pH, vacuolar proton ATPase, and apoptosis. J Clin Invest 97:2391–2398.
9. Zhou X, Zhai X, Ashraf M. 1996. Direct evidence that initial oxidative stress triggered by preconditioning contributes to second window of protection by endogenous antioxidant enzyme in myocytes. Circulation 93:1177–1184.
10. Hayashi M, Nasa Y, Tanonaka K, Sasaki H, Miyake R, Hayashi J, Takeo S. 1995. The effects of long-term treatment with eicosapentaenoic acid and docosahexaenoic acid on hypoxia/reoxygenation injury of isolated cardiac cells in adult rats. J Mol Cell Cardiol 27:2031–2041.
11. Liu J, Tanonaka K, Sanbe A, Yamamoto K, Takeo S. 1993. Beneficial effects of quinidine on post-ischemic contractile failure of isolated rat hearts. J Mol Cell Cardiol 25:1249–1263.
12. Takeo S, Tanonaka K, Miyake K, Fukumoto T. 1988. Role of ATP metabolites in induction of incomplete recovery of cardiac contractile force after hypoxia. Can J Cardiol 4:193–200.
13. Takeo S, Tanonaka K, Miyake K, Fukumoto T. 1988. Adenine nucleotide metabolites are beneficial for recovery of cardiac contractile force after hypoxia. J Mol Cell Cardiol 20:187–199.
14. Tanonaka K, Matsumoto M, Minematsu R, Miyake K, Murai R, Takeo S. 1989. Beneficial effect of amosulalol and phentolamine on post-hypoxic recovery of contractile force and energy metabolism in rabbit hearts. Br J Pharmacol 97:513–523.
15. Liu J, Tanonaka K, Ohtsuka Y, Sakai Y, Takeo S. 1993. Improvement of ischemia/reperfusion-induced contractile dysfunction of perfused hearts by class Ic antiarrhythmic agents. J Pharmacol Exp Ther 266:1247–1254.
16. Takeo S, Tanonaka K, Tazuma Y, Fukao N, Yoshikawa C, Fukumoto T, Tanaka T. 1988. Diltiazem and verapamil reduce the loss of adenine nucleotide metabolism from hypoxic hearts. J Mol Cell Cardiol 20:187–199.
17. Tanonaka K, Maruyama Y, Takeo S. 1991. Beraprost, a prostacyclin mimetic agent, is beneficial for post-hypoxic recovery of cardiac function and metabolites in isolated rabbit hearts. Br J Pharmacol 104:779–786.
18. Schrader J, Haddy F, Gerlach E. 1977. Release of adenosine, inosine and hypoxanthine from the isolated guinea pig heart during hypoxia. Pflugers Arch 369:1–6.
19. Vary TC, Angelakos ET, Schaffer SW. 1979. Relationship between adenine nucleotide metabolism and irreversible ischemic tissue damage in isolated perfused rat heart. Circ Res 45:218–225.
20. Takeo S, Sakanashi M. 1983. Possible mechanisms for reoxygenation-induced recovery of myocardial high-energy phosphates after hypoxia. J Mol Cell Cardiol 15:577–594.

21. Takeo S, Tanonaka K, Shimizu K, Hirai K, Miyake K, Minematsu R. 1989. Beneficial effects of lidocaine and disopyramide on oxygen-deficiency-induced contractile failure and metabolic disturbance in isolated rabbit hearts. J Pharmacol Exp Ther 248:306–314.
22. Takeo S, Yamada H, Tanonaka K, Hayashi M, Sunagawa N. 1990. Possible involvement of membrane-stabilizing action in beneficial effect of beta adrenoceptor blocking agents on hypoxic and posthypoxic myocardium. J Pharmacol Exp Ther 254:847–856.
23. Fujioka H, Yoshihara S, Tanaka T, Fukumoto T, Kuroiwa A, Tanonaka K, Hayashi M, Takeo S. 1991. Enhancement of post-hypoxic contractile and metabolic recovery of perfused rat hearts by dl-propranolol: possible involvement of non-beta-receptor mediated activity. J Mol Cell Cardiol 23:949–962.
24. Armstrong S, Ganote CE. 1994. Preconditioning of isolated rabbit cardiomyocytes: effects of glycolytic blockade, phorbol esters, and ischaemia. Cardiovasc Res 28:1700–1706.
25. Speechly-Dick ME, Mocanu MM, Yellon DM. 1994. Protein kinase C: its role in ischemic preconditioning in the rat. Circ Res 75:586–590.
26. Ytrehus K, Liu Y, Downey JM. 1994. Preconditioning protects ischemic rabbit heart by protein kinase C activation. Am J Physiol 266:H1145–H1152.
27. Li Y, Kloner RA. 1995. Does protein kinase C play a role in ischemic preconditioning in rat hearts? Am J Physiol 268:H426–H431.
28. Liu Y, Tsuchida A, Cohen MV, Downey JM. 1995. Pretreatment with angiotensin II activates protein kinase C and limits myocardial infarction in isolated rabbit hearts. J Mol Cell Cardiol 27:883–892.
29. Mitchell MB, Meng X, Ao L, Brown JM, Harken AH, Banerjee A. 1995. Preconditioning of isolated rat heart is mediated by protein kinase C. Circ Res 76:73–81.
30. Goto M, Liu Y, Yang X-M, Ardell JL, Cohen MV, Downey JM. 1995. Role of bradykinin in protection of ischemic preconditioning in rabbit hearts. Circ Res 77:611–621.
31. Armstrong S, Ganote CE. 1995. In vitro ischaemic preconditioning of isolated rabbit cardiomyocytes: effects of selective adenosine receptor blockade and calphostin C. Cardiovasc Res 29:647–652.
32. Armstrong SC, Hoover DB, Delacey MH, Ganote CE. 1996. Translocation of PKC, protein phosphatase inhibition and preconditioning of rabbit cardiomyocytes. J Mol Cell Cardiol 28:1479–1492.

This Page Intentionally Left Blank

PHARMACOLOGICAL MODIFICATION OF ISCHEMIC PRECONDITIONING DURING PERCUTANEOUS TRANSLUMINAL CORONARY ANGIOPLASTY

TETSUYA UEDA*, KAZUHIKO HASHIMURA*, YASUHIKO MATSU-URA*, YOJI KATO*, TAKENORI YASUDA*, ISAO MORI*, and YOSHIYUKI KIJIMA**

* *Ishinkai Yao General Hospital*
** *Higashi-osaka Municipal Hospital*

Summary. In the progression of repetitive balloon inflations during percutaneous transluminal coronary angioplasty (PTCA), the heart becomes more tolerant to ischemia. The study reported here analyzed the effects of theophylline and nicorandil on this intriguing phenomenon. Twenty-one patients with stable angina pectoris due to a significant stenosis at the left anterior descending artery were subjected to PTCA. The balloon was inflated twice for two minutes each with a three-minute reperfusion period. Theophylline, an adenosine receptor antagonist, was intravenously administered (0.6 mg/kg/hr) to six patients during PTCA (theophylline group). Nicorandil, a hybrid between nitrate and an ATP-sensitive potassium channel opener, was intravenously administered (6 mg/hr) to nine patients during PTCA (nicorandil group). The rest of the patients served as controls (ischemic preconditioning group, $n = 6$). Cardiac adaptation to the second ischemia was observed in the ischemic preconditioning group, judging from lactate metabolism and electrocardiography. In both the theophylline and nicorandil groups, the difference between the two ischemic events was abolished. In the nicorandil group, the severity of the first ischemia was less than that of the ischemic preconditioning group. In conclusion, signal transduction through the adenosine receptor and opening of the ATP-sensitive potassium channels might play key roles, interactively or independently, in the cardioprotection observed in the process of PTCA.

INTRODUCTION

Ischemic preconditioning of the heart was first described as the infarct size-limiting effect at the level of animal experiments [1]: brief repetitive episodes of ischemia reduce the size of myocardial infarction caused by the subsequent ischemia. In humans, cardiac adaptation to ischemia was documented during percutaneous

S. Mochizuki, N. Takeda, M. Nagano and N. Dhalla (eds.). THE ISCHEMIC HEART.

transluminal coronary angioplasty (PTCA), judged by lactate metabolism and electrocardiography [2]. A number of hypotheses have been proposed for the mechanism by which the heart becomes more tolerant to ischemia [3].

One promising candidate to mediate this phenomenon is adenosine, known as an endogenous cardioprotective substance [4,5]. Reports have appeared that support a crucial role of adenosine in ischemic preconditioning in animals [6–8] and also in humans [9,10]. Another candidate is the opening of the ATP-sensitive potassium channels [11]. Ischemic preconditioning during PTCA was abolished by glibenclamide, an ATP-sensitive potassium channel blocker [12], suggesting a crucial role of the ATP-sensitive potassium channel in this cardioprotection. The study reported here aimed to determine 1) whether or not theophylline, a nonselective adenosine receptor antagonist, affects cardioprotection during PTCA; and 2) whether or not nicorandil, a hybrid between nitrate and ATP-sensitive potassium channel opener [13], affords cardioprotection during PTCA.

METHODS

Twenty-one patients with stable angina pectoris due to an isolated organic stenosis at the left anterior descending artery were subjected to PTCA. Angiographical delay of coronary flow across the stenotic site was not found before PTCA. Collateral vessels were not found before and after PTCA. A history of myocardial infarction was not found in any patients. All medications were discontinued for at least 15 hours prior to the PTCA except for long-acting nitrates, calcium channel blockers, and aspirin.

A PTCA balloon was inflated twice for two minutes each with a three-minute reperfusion period as described previously [14]. Patients were divided into three groups: an ischemic preconditioning group ($n = 6$), a theophylline group ($n = 6$), and a nicorandil group ($n = 9$). For the ischemic preconditioning and theophylline groups, 2 mg of isosorbide dinitrate was intracoronarily injected prior to the first balloon inflation. In the theophylline group, 250 mg of theophylline (as the ethylenediamine salt, aminophylline) was infused for 20 minutes followed by continuous infusion (0.6 mg/kg/hr) prior to moving to the catheterization laboratory. During the theophylline administration, no patients complained of theophylline-related symptoms, including headache, nausea, and palpitation. Plasma concentration of theophylline at the end of PTCA was within its therapeutic range, i.e., 10 to 20 μg/mL. For the nicorandil group, 2 mg of nicorandil was injected intravenously at one hour prior to PTCA, followed by continuous infusion (6 mg/hr). Nicorandil was purchased from Chugai Pharmaceutical Co. (Tokyo, Japan). The stenotic sites were successfully dilated to less than 50% stenosis in all cases. Written informed consent was obtained from each patient.

Electrocardiography and lactate metabolism were used to evaluate the severity of ischemia [14]. ΣST was defined as the sum of ST elevation in precordial leads except for V_1. For the lactate measurements, blood was sampled immediately before and at 30 seconds after each ischemic event, simultaneously from the great cardiac

vein (through a 5-Fr NIH catheter) and from the ascending aorta. Lactate extraction ratio (LER) was calculated according to the following equation:

$$\text{LER (\%)} = 100 \times [\text{arterial lactate concentration (mg/dL)} - \text{coronary venous lactate concentration (mg/dL)}]/\text{arterial lactate concentration (mg/dL)}$$

For each ischemic event, ΔLER was defined as the difference between LER before and after each inflation, i.e.,

$$\Delta\text{LER-1} = \text{LER}_{\text{pre-1}} - \text{LER}_{\text{post-1}}$$

$$\Delta\text{LER-2} = \text{LER}_{\text{pre-2}} - \text{LER}_{\text{post-2}}$$

All data were reported as mean ± standard deviation (SD). LER and ΣST between groups and within each group were compared using two-way ANOVA with repeated measures followed by Bonferroni's *t*-test. ΣST-2/ΣST-1, ΔLER-2/ΔLER-1, and hemodynamic parameters between groups were compared using the unpaired Student's *t*-test. When p was less than 0.05, the difference was considered statistically significant.

RESULTS

No significant differences were found among the ischemic preconditioning, theophylline, and nicorandil groups with regard to hemodynamic parameters prior to PTCA (table 1). LER was obtained at four different timings, i.e., immediately before and at 30 seconds after each ischemic event ($\text{LER}_{\text{pre-1}}$, $\text{LER}_{\text{post-1}}$, $\text{LER}_{\text{pre-2}}$, and $\text{LER}_{\text{post-2}}$). In the three groups, LER prior to the second inflation ($\text{LER}_{\text{pre-2}}$) was similar to that prior to the first inflation ($\text{LER}_{\text{pre-1}}$), indicating that the first ischemia completely recovered during the three-minute reperfusion. For the ischemic preconditioning group, $\text{LER}_{\text{post-1}}$ was more negative than $\text{LER}_{\text{post-2}}$ (−144.5% ± 100.9% vs. −65.4% ± 89.7%, $p < 0.05$). ΣST during the first inflation (ΣST-1) was greater than that during the second inflation (ΣST-2) (2.05 ± 1.56 mV vs. 1.08 ± 0.69 mV, $p < 0.05$). These results indicate that heart became more tolerant to the second ischemia, a finding consistent with the previous report [2].

In both the theophylline and nicorandil groups, $\text{LER}_{\text{post-1}}$ was at a similar level to $\text{LER}_{\text{post-2}}$ (−91.6% ± 56.6% vs. −101.7% ± 27.3% for the theophylline group, −45.1% ± 41.6% vs. −43.5% ± 51.1% for the nicorandil group). ΣST-1 was also similar to ΣST-2 (1.73 ± 0.40 mV vs. 1.84 ± 0.40 mV for the theophylline group, 1.38 ± 0.80 mV vs. 1.46 ± 0.89 mV for the nicorandil group). The ratio of ΔLER-2 to ΔLER-1 in the ischemic preconditioning group (0.49 ± 0.28) was less than that of the theophylline group (1.20 ± 0.34, $p < 0.01$) and of the nicorandil group (1.06 ± 0.38, $p < 0.01$). The ratio of ΣST-2 to ΣST-1 in the ischemic preconditioning group (0.65 ± 0.25) was less than that of the theophylline group (1.07 ± 0.13, $p < 0.01$) and of the nicorandil group (1.06 ± 0.12, $p < 0.01$). These results

Table 1. Effects of theophylline and nicorandil on ischemic preconditioning [14,17]

	Ischemic preconditioning group (n = 6)	Theophylline group (n = 6)	Nicorandil group (n = 9)
Age (years)	58.5 ± 9.7	66.3 ± 12.5	68.3 ± 10.6
Gender (M/F)	6/0	4/2	7/2
Systolic blood pressure (mmHg)[a]	123 ± 28	125 ± 12	136 ± 24
Heart rate (beats/min)	68 ± 8	70 ± 13	66 ± 9
Rate-pressure product (mmHg/min)[b]	8292 ± 1502	8814 ± 2080	8915 ± 2138
LER_{pre-1} (%)[c]	43.7 ± 11.1	22.8 ± 16.2	31.5 ± 7.7
LER_{post-1} (%)	−144.5 ± 100.9[e]	−91.6 ± 56.6	−45.1 ± 41.6[i]
LER_{pre-2} (%)	35.9 ± 6.8	20.7 ± 15.9	37.1 ± 6.3
LER_{post-2} (%)	−65.4 ± 89.7	−101.7 ± 27.3	−43.5 ± 51.1
ΔLER-2/ΔLER-1	0.49 ± 0.28	1.20 ± 0.34[g]	1.06 ± 0.38[j]
ΣST-1 (mv)[d]	2.05 ± 1.56[f]	1.73 ± 0.40	1.38 ± 0.80
ΣST-2 (mV)	1.08 ± 0.69	1.84 ± 0.40	1.46 ± 0.89
ΣST-2/ΣST-1	0.65 ± 0.25	1.07 ± 0.13[h]	1.06 ± 0.12[k]

[a] Systolic arterial pressure and heart rate were measured noninvasively at the left brachial artery immediately before PTCA.
[b] Systolic arterial pressure multiplied by heart rate, as an indicator of the cardiac oxygen consumption.
[c] Lactate extraction ratio (LER) was calculated at four different timings, i.e., before and after the first ischemia (pre-1 and post-1) and the second ischemia (pre-2 and post-2). ΔLER was defined as difference between LER before and after each inflation ($\Delta LER\text{-}1 = LER_{pre-1} - LER_{post-1}$; $\Delta LER\text{-}2 = LER_{pre-2} - LER_{post-2}$).
[d] ΣST-1, during the first ischemia; and ΣST-2, during the second ischemia.
[e] $p < 0.05$ vs. LER_{post-2} of the ischemic preconditioning group.
[f] $p < 0.05$ vs. ΣST-2 of the ischemic preconditioning group.
[g] $p < 0.01$ vs. ΔLER-2/ΔLER-1 of the ischemic preconditioning group.
[h] $p < 0.01$ vs. ΣST-2/ΣST-1 of the ischemic preconditioning group.
[i] $p < 0.01$ vs. LER_{post-1} of the ischemic preconditioning group.
[j] $p < 0.01$ vs. ΔLER-2/ΔLER-1 of the ischemic preconditioning group.
[k] $p < 0.01$ vs. ΣST-2/ΣST-1 of the ischemic preconditioning group.

indicate that both theophylline and nicorandil abolished the difference between the two ischemic events.

LER_{post-1} of the nicorandil group was more positive than that of the ischemic preconditioning group (−45.1 ± 41.6 vs. −144.5 ± 100.9, $p < 0.01$). No significant difference was found in LER_{post-2} between the ischemic preconditioning and nicorandil groups. These results indicate that nicorandil affords cardioprotection without preceding ischemia.

DISCUSSION

In this chapter, we described the pharmacological modification of ischemic preconditioning during PTCA. Two pharmacological tools were employed: 1) theophylline, a nonselective adenosine receptor antagonist; and 2) nicorandil, a hybrid between nitrate and ATP-sensitive potassium channel opener. Nicorandil is the sole tool to open the ATP-sensitive potassium channels in clinical settings. We found both drugs abolished the difference between the first and second ischemic events. Subsequently, one needs to think about whether these drugs *trigger* or *block* the preconditioning effect during PTCA.

In the ischemic preconditioning group, the first ischemia was more severe than the second one. Nicorandil attenuated the severity of the first ischemia to trigger the preconditioning effect (see LER_{post-1} in table 1). This pharmacological preconditioning by nicorandil might be mediated by its pharmacological action as either nitrate or ATP-sensitive potassium channel opener [13]. In the ischemic preconditioning group, isosorbide dinitrate was intracoronarily injected immediately before the first inflation, indicating that this classical nitrate did not abolish the difference between the two ischemic events. Thus, we would believe that the opening of the ATP-sensitive potassium channels by nicorandil might be a crucial step for the cardioprotection during PTCA.

Our data using theophylline are compatible with the speculation that theophylline antagonizes the adenosine receptor to block the cardioprotection during PTCA [14]. Data from other groups [10,15] also support this adenosine hypothesis.

One of the signal transduction pathways through the adenosine receptor is the G-protein-mediated opening of the ATP-sensitive potassium channels [16]. We would propose a coupling of the adenosine receptor with the ATP-sensitive potassium channels during PTCA in humans. The ATP-sensitive potassium channels may be opened by other factors than adenosine, including acidic pH, intracellular lactate, and an increased ratio of ADP to ATP. The crosstalk between the two distinct mechanisms needs to be investigated further.

ACKNOWLEDGMENTS

We thank Mitsuaki Chujo, Ph.D (Chugai Pharmaceutical Co.) for his critical comments on this chapter.

REFERENCES

1. Murry CE, Jennings RB, Reimer KA. 1986. Preconditioning with ischemia: a delay of lethal cell injury in ischemic myocardium. Circulation 74:1124–1136.
2. Deutsch E, Berger M, Kussmaul WG, Hirshfeld JW, Hermann HC, Laskey WK. 1990. Adaptation to ischemia during percutaneous transluminal coronary angioplasty: clinical, hemodynamic, and metabolic features. Circulation 82:2044–2051.
3. Murry CE, Jennings RB, Reimer KA. 1991. New insights into potential mechanisms of ischemic preconditioning. Circulation 84:442–445.
4. Ely SW, Berne RM. 1992. Protective effects of adenosine in myocardial ischemia. Circulation 85:893–904.
5. Berne RM. 1980. The role of adenosine in the regulation of coronary blood flow. Circ Res 47:807–813.
6. Liu GS, Thornton JD, Van Winkle DM, Stanley AWH, Olsson RA, Downey JM. 1991. Protection against infarction afforded by preconditioning is mediated by A1 adenosine receptors in rabbit heart. Circulation 84:350–356.
7. Tuchida A, Miura T, Miki T, Shimamoto K, Iimura O. 1992. Role of adenosine receptor activation in myocardial infarct size limitation by ischaemic preconditioning. Cardiovasc Res 26:456–461.
8. Kitakaze M, Hori M, Takashima S, Sato H, Inoue M, Kamada T. 1993. Ischemic preconditioning increases adenosine release and 5′-nucleotidase activity during myocardial ischemia and reperfusion in dogs. Circulation 87:208–215.
9. Okazaki Y, Kodama K, Sato H, Kitakaze M, Hirayama A, Mishima M, Hori M, Inoue M. 1993. Attenuation of increased regional myocardial oxygen consumption during exercise as a major cause of warm-up phenomenon. J Am Coll Cardiol 21:1597–1604.
10. Tomai F, Crea F, Gaspardone A, Versaci F, Paulis RD, De Paulis R, Polisca P, Chiariello L, Gioffré PA. 1996. Effects of A_1 adenosine receptor blockade by bamiphylline on ischaemic preconditioning during coronary angioplasty. Eur Heart J 17:846–853.

11. Gross GS, Auchambach JA. 1992. Blockade of ATP-sensitive potassium channels prevents myocardial preconditioning in dogs. Circ Res 70:223–233.
12. Tomai F, Crea F, Gaspardone A, Versaci F, Paulis RD, de Peppo AP, Chiariello L, Gioffré PA. 1994. Ischemic preconditioning during coronary angioplasty is prevented by glibenclamide, a selective ATP-sensitive K channel blocker. Circulation 90:700–705.
13. Taira N. 1989. Nicorandil as a hybrid between nitrates and potassium channel opener. Am J Cardiol 63:18J–24J.
14. Hashimura K, Kijima Y, Matsu-ura Y, Ueda T, Kato Y, Mori I, Minamino T, Kitakaze M, Hori M. 1997. Effect of theophylline on adaptation of the heart to myocardial ischemia during percutaneous transluminal coronary angioplasty in patients with stable angina pectoris. Am J Cardiol 79:475–477.
15. Kerensky RA, Kutcher MA, Braden GA, Applegate RJ, Solis GA, Little WC. 1995. The effects of intracoronary adenosine on preconditioning during coronary angioplasty. Clin Cardiol 18:91–96.
16. Kirsch GE, Codina J, Birnbaumer L, Brown AM. 1990. Coupling of ATP-sensitive K^+ channels to A_1 receptors by G proteins in rat ventricular myocytes. Am J Physiol 259:H820–H826.
17. Kijima Y, Hashimura K, Matsu-ura Y, Kato Y, Ueda T, Yasuda T, Mori I. 1996. Nicorandil pharmacologically preconditions human heart to ischemia during coronary balloon angioplasty. J Mol Cell Cardiol 28:A319.

PROTECTION AGAINST INJURY DURIN GMYOCARDIAL ISCHEMIA AND REPERFUSION: CONCEPTS AND STRATEGIES

DAVID J. HEARSE

The Rayne Institute, St. Thomas' Hospital

Summary. Myocardial ischemia remains the largest single factor contributing to death in the Western hemisphere. It arises in many guises, such as regional ischemia in evolving myocardial infarction and induced whole heart ischemia in cardiac surgery and transplantation. Ischemia initiates a sequence of progressively more severe cellular events that, unless interrupted by early reperfusion, will culminate in cell death and tissue necrosis. Early reperfusion is not always possible, and therefore attempts have been made to develop procedures to slow the rate of progression of ischemic injury so that less irreversible injury occurs and more tissue is available for salvage at the time of reperfusion. Developing and successfully applying such protective interventions requires a detailed knowledge of the complex temporal, spatial, cellular, and molecular characteristics of the ischemic process. Further complications are added by the possibility that reperfusion, although an absolute prerequisite for the survival of ischemic tissue, may not be without hazard. Reperfusion injury may subtract from the obvious benefit of the restoration of coronary flow and, as such, merits consideration as a possible target in the development of myocardial protective strategies. In addition to the conventional pharmacological approach to cardioprotection, there is intense interest in exploiting the ability of the heart to use adaptive processes, such as preconditioning and the expression of stress proteins, to control the ravages of ischemia. Myocardial protection has achieved great success in cardiac surgery through the development of cardioplegic solutions but is yet to make a major impact on the control of injury during evolving infarction.

INTRODUCTION

The objectives of this chapter are to: 1) discuss the origins and the nature of ischemic injury, 2) identify factors influencing the evolution of injury, 3) consider

S. Mochizuki, N. Takeda, M. Nagano and N. Dhalla (eds.). THE ISCHEMIC HEART.

various cellular targets for ischemic injury, 4) assess the overall importance of reperfusion injury, 5) discuss conceptual approaches to cardioprotection, and 6) identify new ideas and approaches in the realm of myocardial protection.

In the human heart, myocardial ischemia may take many forms. It may exist for periods as short as a few seconds or minutes, it may last for hours, or it may persist for years. In terms of discussing interventions to combat myocardial ischemia, this chapter will focus on: 1) *regional* ischemia, as occurs during evolving myocardial infarction, and 2) whole heart of *global* ischemia, as occurs during cardiac surgery and transplantation.

THE COMPLEXITY OF ISCHEMIC INJURY

Understanding and successfully manipulating myocardial ischemic injury requires a consideration of the temporal, spatial, cellular, and molecular characteristics of ischemia.

The temporal characteristics of myocardial ischemia and the need for early reperfusion

Myocardial ischemia initiates a continuum of progressively more severe cellular changes that, unless interrupted by early reperfusion, inevitably culminate in cell death and tissue necrosis. Following the total or partial occlusion of a coronary artery, metabolic and functional changes are initiated within seconds. These changes, which become progressively more severe with time, are initially of a reversible nature. However, with increasing durations of ischemia, they become more severe, and eventually irreversible injury occurs. From this point on, the cells are destined for tissue necrosis. From this it follows that, the longer the duration of elapsed ischemia, the fewer will be the number of reversibly injured cells and the smaller will be the amount of tissue potentially available for salvage and return to normal contractile function.

Time is of the essence. Successful and complete salvage of ischemic tissue *can only be achieved by early reperfusion* at a time when tissue injury is restricted to the reversible phase. Under such conditions (depending upon the duration and severity of preceding ischemia), cardiac function normally returns within a relatively short time. With longer durations of ischemia, recovery may take some time (myocardial stunning), but, so long as the injury is still reversible, a full recovery will eventually occur. Reperfusion of irreversibly injured tissue, by definition, cannot evoke a recovery of cardiac function and may even be detrimental (see Reperfusion Injury below).

The spatial characteristics of ischemic injury and the anatomy of cell death

Within the heart, ischemic injury does not evolve in a uniform manner. Regional differences in metabolism and energy requirements render the endocardium most vulnerable to injury. For this reason, myocardial injury and tissue necrosis usually originate in the endocardium and, with time, migrate as a wave front of cell death

towards to the epicardial surface. Thus, the classical dog heart study of Reimer and Jennings [1] charted the temporal evolution of necrotic injury transmurally across the canine heart over a period of 40 minutes to 96 hours of regional ischemia. This study illustrated beautifully not only the spatial nature of ischemic injury but also its temporal characteristics—both of which must be taken fully into account in the application and assessment of any intervention designed to beneficially modify the ischemic process.

DEFINING STRATEGIES FOR PROTECTING THE ISCHEMIC HEART

It is apparent from the preceding sections that there are two key objectives that must be implemented in any attempt to prevent the deterioration of ischemic injury to tissue necrosis. Firstly, since *early reperfusion is an absolute prerequisite for the survival of ischemic tissue*, every attempt must be made to reverse ischemic injury by reperfusing the affected tissue at the earliest possible opportunity. Secondly, if early reperfusion is not possible, attempts should be made to *slow the rate of the evolution of ischemic injury* so as to delay, for as long as possible, the onset of irreversible injury. In this way, more cells will remain in a reversible state of injury for a longer period of time, and more tissue will be able to recover when reperfusion is eventually achieved.

In the case of regional ischemia and evolving myocardial infarction, reperfusion may occasionally occur spontaneously; however, most reperfusion requires intervention using thrombolytic or surgical procedures. Such procedures may take considerable time to implement, and this fact underlines the potential importance of slowing the rate of development of ischemic injury until reperfusion can be affected. With global ischemia in cardiac surgery, reperfusion can be instituted at will; however, the extended ischemic times required for complex surgical procedures requires that injury-slowing procedures be applied to prevent infarction during the course of surgery. As will be discussed later, the use of interventions to slow the rate of development of ischemic injury has been highly successful in open heart surgery and cardiac transplantation. Developing such interventions to successfully manipulate the rate of ischemic injury requires a detailed knowledge of the many factors that influence the evolution of injury.

Factors influencing the rate of evolution of ischemic injury

A host of complex, interacting factors are known to influence the rate at which tissue injury occurs in the ischemic heart. These factors conspire together to result in highly variable rates of injury both within and between hearts—even in the face of an identical ischemic insult. Some of the major factors influencing the rate of evolution of injury are: 1) the extent (if any) of residual coronary or noncoronary collateral flow, 2) various diseases that may coexist with the ischemia such as hypertrophy, diabetes, and hypertension, 3) heart rate, metabolic rate and tissue temperature, 4) variations in the metabolic response to ischemia (particularly in relation to patterns of substrate metabolism), 5) nutritional and hormonal status, 6)

the presence of a variety of cardioactive drugs, 7) previous ischemia and various adaptive processes, and 8) the age, sex, and species of the tissue. Variable combinations of all of the above factors means that *there is no universal time after which ischemic tissue becomes irreversibly injured.* This important generalization, together with the vital role played by collateral flow in determining the rate of evolution of ischemic injury, is clearly illustrated in the classic study by Schaper et al. [2], which demonstrated how the evolution of necrosis within an area of regional ischemia occurs extremely rapidly in animals that have little or no collateral flow (such as the rat and rabbit), while it occurs slowly in animals that have collaterals (such as the dog). In animals such as the guinea pig, necrosis does not occur because the coronary vessels are is totally collateralized. Thus, 90 minutes following the occlusion of a coronary artery, the extent of necrosis within the zone of ischemia may range between 0% and 100%.

DEVELOPING INTERVENTIONS TO MANIPULATE THE RATE OF ISCHEMIC INJURY PRIOR TO REPERFUSION

When early reperfusion is not possible, attempts should be made to slow the rate of ischemic injury using interventions that do not rely upon the restitution of flow. Successful development of such interventions requires a detailed knowledge of the molecular characteristics of the cascade of metabolic and cellular changes that are induced by ischemia. Armed with this knowledge, it should be possible to identify key detrimental changes that might act as targets for selective intervention. There are, of course, a multitude of changes that occur following the onset of myocardial ischemia [3], and the nature and sequence of these changes may vary greatly from heart to heart. In order to successfully slow such a process, it is necessary to target metabolic changes that are occurring during the early (reversible) phase of ischemia. Such an approach has been subject of many studies aimed ameliorating the potentially devastating consequences of ischemia.

Molecular targets for anti-ischemic intervention

There have been many studies with hundreds of different interventions, and these interventions all have been suggested to possess the ability to slow the progression of myocardial ischemic injury. In general, one or more of the following approaches have been adopted: 1) limiting the accumulation of protons and toxic metabolites during the ischemic process, 2) modifying the extent of nutrient and energy depletion, 3) minimizing cellular sodium and calcium overload, 4) modifying the regulation of various enzymes and proteins, 5) combating loss of potassium, cofactors, and trace elements, 6) limiting damage to nuclear material, 7) combating the activation of lytic enzymes and attack by leukocytes, and 8) countering cell swelling and membrane disruption. Thus, using a variety of species and experimental models, both in vivo and in vitro, agents such as calcium antagonists, buffers, osmotic agents, substrates, extracellular high-energy phosphates, and magnesium have all been shown to reduce the degree of ischemic injury and, upon reperfusion, to enhance

the recovery of function. Investigators who have made the effort to undertake dose–response studies [4] for such interventions have reaped rewards in that optimal concentrations of a single intervention can often be shown to confer a remarkable degree of protection. As will be discussed later, the concept of injury slowing by anti-ischemic interventions has been very successfully applied to cardiac preservation during open hearts surgery and transplantation.

Cellular targets for injury

Cardiologists might be criticized for being preoccupied with protecting the myocyte (possibly as a consequence of the ease of measuring the biological and physiological activity of this cell type) while ignoring the consequence of ischemia on other cellular constituents of the heart. For understanding and effectively controlling ischemic injury, it is vital to remember that the heart is composed of a multitude of interacting cell types in addition to the myocyte. These include cells of the endothelium, vascular smooth muscle, conducting tissue, connective tissue, and even the blood-borne elements carried through the heart. Each of these would be expected to be vulnerable to ischemic injury, and therefore, the rational development of any anti-ischemic intervention should ideally attempt to target and protect as many of these cell types as possible. Unfortunately, this obvious requirement has rarely been considered; furthermore, little attention has been given to the real possibility that interventions conferring cellular protection to one cell type (for example, the ability of potassium to protect the myocyte) might, in high concentrations, prove detrimental to other cell type (such as the endothelium).

Recently, increasing attention has focused on the possibility that the microcirculation (and in particular the endothelium) might be particularly vulnerable to injury during ischemia and reperfusion [5]. Indeed, the possibility is now emerging that the microcirculation might be the primary determinant of the survival of the heart as a whole. Realization of such a possibility should open many new avenues in the protection of the heart against ischemic injury.

IS IT INSUFFICIENT TO CONSIDER ONLY ISCHEMIA? CELLULAR EVENTS DURING REPERFUSION

Despite many thousands of experiments and a multitude of putative anti-ischemic interventions, few (if any) interventions facilitate a complete recovery from ischemic injury. This has led investigators to question whether the failure of heart to recover during reperfusion necessarily only reflects the severity of the ischemic injury. This concern has been supported by an increasing number of experimental studies that have indicated that interventions given *only at the time of reperfusion* may improve ischemic recovery. A survey of the literature reveals that there are now many interventions that appear to be able to improve the rate or extent of postischemic function recovery (or to limit the size of an infarct measured at the end of reperfusion) when administered only at the time of reperfusion.

Successful reperfusion interventions include: 1) the modification of extracellular potassium, calcium, sodium, or magnesium, 2) the manipulation of substrate avail-

ability and utilization with agents such as glutamate, aspartate, or pyruvate, 3) the control of free radicals and oxidant stress with agents such as superoxide dismutase, catalase, vitamin E, vitamin C, and allopurinol, 4) the manipulation of physical factors such as oxygen tension, temperature, osmolarity, and pH, 5) the control of blood-borne elements such as leukocytes and platelets, and 6) the administration of vasoactive agents such as adenosine, nitrates, and dipyridamol as a means of enhancing coronary flow and its distribution. Success in improving the outcome of reperfusion with interventions administered only at the time of reperfusion has led investigators to suggest that some component of reperfusion injury may be damaging and, as such, may subtract from the obvious benefit of the restoration of flow.

Reperfusion-induced injury

Although reperfusion is an absolute prerequisite for tissue survival, the possibility exists that reperfusion may increase injury *over and above that sustained during ischemia.* Certainly, there is convincing evidence that reperfusion is able to precipitate a number of unfavorable cellular changes, and the term *reperfusion injury* has fallen into common usage [6,7]. However, the existence and importance of reperfusion injury (and hence the need for intervention) has become highly controversial, with some investigators denying its existence while other claim that it is an important determinant of tissue survival. Some of the confusion and controversy relating to the existence and importance of reperfusion injury can be resolved if the phenomenon is divided into *reversible* reperfusion injury and *irreversible* (or lethal) reperfusion injury.

Reversible reperfusion injury is defined as transient (but nonetheless potentially detrimental) injury, induced by the act of reperfusion, from which the heart can eventually recover. A classic example of such injury is myocardial stunning [8,9], the prolonged contractile dysfunction that persists after reperfusion despite the absence of necrosis. It may take several hours or days for the heart to recover from this contractile deficit, but so long as sufficient time is allowed, a full recovery will eventually occur.

Although reversible, myocardial stunning represents a significant clinical problem that may be a factor in precipitating left ventricular failure with its attendant morbidity and mortality. It is thought to be particularly important during reperfusion in cardiac surgery and transplantation, and it may also occur following angina, successful thrombolysis, and exercise-induced ischemia. As a consequence, there has been much interest in the mechanism(s) underlying stunning and in interventions that might attenuate the phenomenon.

A variety of possible mechanisms have been suggested to be responsible for myocardial stunning, including: 1) an impaired resynthesis of adenosine triphosphate 2) functional sympathetic denervation, 3) heterogeneous reperfusion, 4) loss of creatine kinase activity, 5) damage to myocardial collagen, 6) free radicals and oxidant stress, and 7) perturbations of calcium homeostasis. It is now becoming clear that the last two of these mechanisms (possibly working in concert) are most likely

to be the most important contributors to myocardial stunning [10]. The contribution of free radicals and oxidant stress to myocardial stunning and the fact that injury is occurring during reperfusion are clearly illustrated in the important study by Bolli and colleagues [11] in which an antioxidant intervention was given to the dog heart *only at the time of reperfusion*, resulting in a dramatic attenuation of stunning.

A second example of reversible reperfusion injury is the transient burst of various arrhythmias that frequently occurs during the early moments of reperfusion. These arrhythmias may include ventricular fibrillation (a complication frequently encountered during reperfusion in cardiac surgery). Although potentially lethal, these arrhythmias are reversible in the sense that they may terminate spontaneously, can be electrically converted, or can be prevented with drugs. Again, as with myocardial stunning, there have been many studies of the mechanism(s) underlying the genesis of arrhythmias during ischemia and reperfusion. In the case of reperfusion arrhythmias, it would appear that the most likely mechanisms, as with stunning, involve free radical-induced oxidant stress and (possibly as a consequence) disturbances of ionic homeostasis [10]. As with stunning, reperfusion arrhythmias can be effectively prevented through the administration of a variety of antioxidant interventions or through the manipulation of ion composition or pH during the early minutes of reperfusion.

Lethal reperfusion injury: does it exist?

The existence of this lethal, irreversible reperfusion injury (which some believe to be capable of killing cells that were viable in the moments before reperfusion) is particularly controversial. This author is of the opinion that, at the present time, these is little or no conclusive evidence for the existence of this particular form of reperfusion injury [6]. This is not to deny its existence but simply to highlight the fact that definitive experiments to demonstrate its existence and quantitative importance have yet to be reported.

DEFINING THE GOALS AND CONCEPTS FOR CARDIAC PROTECTION DURING ISCHEMIA AND REPERFUSION

From the preceding sections, it should be apparent that the primary goals for achieving cardiac protection during ischemia must be: 1) restoration of flow to the tissue as soon as possible 2) the use of interventions to slow the rate of development of ischemic injury until such a time as reperfusion can be affected, and 3) minimization of the severity of reperfusion injury so as to facilitate as rapid a recovery of function as possible.

A number of conceptual approaches can be identified to help facilitate the achievement of these goals. These include: 1) the application of anti-ischemic agents to slow tissue injury, 2) the use of reperfusion interventions to accelerate recovery from reperfusion injury, and 3) the exploitation of endogenous (adaptive) responses.

The use of interventions to slow the evolution of ischemic injury

A large portfolio of potential anti-ischemic interventions (designed to target various deleterious ischemia-induced cellular changes) has now been established. Although, when used on their own, many interventions have been reported to significantly reduce ischemic injury, it is perhaps naive to expect a single intervention to achieve extensive or long-lasting protection during severe ischemia. For this reason, a polypharmacological approach to anti-ischemic therapy would seem appropriate. Although, for a variety of reasons, this approach has rarely been attempted in the context of regional ischemia and evolving myocardial infarction, polypharmacology has formed the cornerstone of the very successful development of anti-ischemic cardioplegic interventions for use during cardiac surgery and transplantation. As reviewed elsewhere [12], three basic approaches have been combined and exploited by surgeons so as to greatly enhance the ability of human heart to withstand extended periods of severe global ischemia. These are: 1) the use of cardioplegic agents such as potassium to rapidly arrest the heart during ischemia and thereby conserve energy for tissue protection and subsequent recovery, 2) the inclusion in cardioplegic solutions of agents such as buffers, substrates, and drugs to combat as many deleterious ischemia-induced changes as possible, and 3) the combination of chemical cardioplegia with hypothermia so as to further slow the rate of cellular reactions that contribute to ischemia-induced injury. As mentioned above, this approach has been particularly successful both in the context of cardiac surgery and cardiac transplantation, where human hearts, which would fail to recover after less than one hour of unmodified global ischemia, now routinely withstand up to four hours of ischemic arrest with good postischemic functional recovery.

Using interventions to minimize reperfusion injury and enhance the rate of postischemic recovery

As mentioned previously (particularly in the realm of cardiac surgery), it would appear to be appropriate to advocate the use of reperfusion solutions to ameliorate any unfavorable components of the reperfusion process. In this way, it should be possible to use agents such as: 1) antioxidants to attenuate stunning—an approach that would seem preferable to overriding stunning through the administration of inotropic agnets such as calcium or catecholamines with their attendant risk of increasing heart rate and arrhythmogenesis, 2) vasoactive drugs to improve the extent and quality of reperfusion by manipulating vascular responses during reperfusion, and 3) ion and pH regulation to promote the rapid reestablishment of ionic homeostasis.

EXPLOITING ENDOGENOUS RESPONSES: AN ADDITIONAL WEAPON FOR CARDIOPROTECTION?

The final, and perhaps most challenging, conceptual approach to protecting the myocardium during ischemia and reperfusion arises from the recognition that the heart has an inherent ability to protect itself against the ravages of ischemia. This

protection can be achieved by exploiting a variety of endogenous adaptive responses, two of which are currently attracting considerable attention [13,14]. These are: 1) the ability of the heart to express stress proteins and 2) the phenomenon of ischemic preconditioning. Although not the subject of the chapter, it is now known that the heart responds to a variety of stresses (for example, transient heart shock) by the expression of a spectrum of stress-response proteins. These proteins, which are maximally expressed some 24 hours after the initial stress, have been shown to be responsible for a substantial enhancement of the ability of the heart to resist ischemic injury. The nature of the mechanisms underlying this powerful adaptive response are currently under investigation and might lead to the development of mimetics capable of affording additional protection to the ischemic heart. Likewise, the phenomenon of ischemic preconditioning is an adaptive response whereby the resistance of the heart to injury during ischemia and reperfusion can be *temporarily* enhanced by prior (less than two hours) exposure to one or more *brief* (less than five minutes) episodes of ischemia and reperfusion. Myocardial preconditioning has been shown to protect against tissue necrosis (measured as a limitation of infarct size following reperfusion), to improve postischemic recovery of contractile function (probably as a secondary consequence to the reduction or infarct size), and, in some species, to exert a profound protective effect against both ischemia- and reperfusion-induced arrhythmias. The brief periods of ischemia that precondition the heart can be substituted by a number of pharmacological and biochemical mimetics. Thus, brief exposure to adenosine, norepinephrine, bradykinin, and a variety of other receptor agonists can produce striking protection. Such studies are greatly aiding in the resolution of the mechanisms underlying this important adaptive phenomenon. Once the mechanism of preconditioning is definitively established, it may be possible to develop pharmacological agents that exploit the adaptive response for sustained periods of time. However, the extent to which such interventions (or indeed ischemic preconditioning itself) can be additive to other forms of cardioprotection remains to be resolved.

REFERENCES

1. Reimer KA, Jennings RB. 1979. The "wavefront phenomenon" of myocardial ischemic death: II Transmural progression of necrosis within the framework of ischemic bed size (myocardium at risk) and collateral flow. Lab Invest 40:633–644.
2. Schaper W. 1984. Experimental infarcts and the microcirculation. In Hearse DJ, Yellon DM (eds), Therapeutic Approaches to Myocardial Infarct Size Limitation. New York: Raven Press, pp. 79–90.
3. Hearse DJ. 1979. Cellular damage during myocardial ischemia: metabolic changes leading to enzyme leakage. In Hearse DJ, de Leiris J (eds), Enzymes in Cardiology: Diagnosis and Research. London: John Wiley, pp. 1–19.
4. Hearse DJ, Stewart DA, Braimbridge MV. 1978. Myocardial protection during ischemic cardiac arrest: the importance of magnesium in cardioplegic infusates. J Thorac Cardiovasc Surg 75:877–885.
5. Hearse DJ, Maxwell L, Saldanha C, Gavin JB. 1993. The myocardial vasculature during ischemia and reperfusion: a target for injury and protection. J Mol Cell Cardiol 25:759–800.
6. Hearse DJ. 1991. Ischemia, reperfusion and the determinants of tissue injury. Cardiovasc Drugs Ther 4:767–776.
7. Hearse DJ. 1992. Myocardial injury during ischemia and reperfusion: concepts and controversies. In Yellon DM, Jennings RB (eds), Myocardial Protection: The Pathophysiology of Reperfusion and Reperfusion Injury. New York: Raven Press, pp. 13–32.

8. Bolli R. 1990. Mechanism of myocardial stunning. Circulation 82:723–738.
9. Hearse DJ, Bolli R. 1992. Reperfusion-induced injury: manifestations, mechanisms and clinical relevance. Cardiovasc Res 26:101–108.
10. Hearse DJ. 1991. Stunning: a radical re-view. Cardiovasc Drugs Ther 5:853–876.
11. Bolli R, Patel BS, Jeroudi MO, Lai EK, McCay PB. 1988. Demonstration of free radical generation in stunned myocardium of intact dogs with the use of the spin trap α-phenyl N-tert-butyl nitrone. J Clin Invest 82:476–485.
12. Hearse DJ, Braimbridge MV, Jynge P. 1981. Protection of the Ischemic Myocardium: Cardioplegia. New York: Raven Press.
13. Yellon DM, Latchman DS. 1992. Stress proteins and myocardial protection during ischemia and reperfusion. In Yellon DM, Jennings RB (eds), Myocardial Protection: The Pathophysiology of Reperfusion and Reperfusion Injury. New York: Raven Press, pp. 185–195.
14. Przyklenk K, Kloner RA, Yellon DM. 1994. Ischemic Preconditioning: The Concept of Endogenous Cardioprotection. Boston: Kluwer.

MECHANISMS OF CARDIOPROTECTIVE EFFECTS OF PROPRANOLOL AGAINST REPERFUSION INJURY

BRUCE KOWALUK, NEELAM KHAPER, CLAUDIO RIGATTO, VINCE PALACE, and PAWAN K. SINGAL

St. Boniface General Hospital Research Centre and University of Manitoba

Summary. Oxygen-derived free radicals are known to play a critical role in reperfusion injury, and antioxidants have been shown to protect against ischemia–reperfusion (I–R) injury. The study reported in this chapter was designed to examine the mechanism of propranolol protection, a nonspecific beta-adrenergic blocking drug, against acute I–R injury. Isolated rat hearts subjected to 60-minute global ischemia and 40-minute reperfusion showed a significant rise in the resting tension associated with a poor recovery of the contractile function. Hearts perfused with the buffer containing propranolol displayed almost complete recovery of contractile force and a significant decrease in resting tension. Antioxidant enzyme activities, superoxide dismutase (SOD), glutathione peroxidase (GSHPx), and catalase (CAT) were no different in control and propranolol-exposed hearts. Atenolol, a β1-specific blocker, offered no significant protection against I–R-induced contractile dysfunction. Perfusion with atenolol resulted in a decrease in catalase and an increase in GSHPx activities. Lipid peroxidation in the I–R hearts was significantly reduced by propranolol. It is suggested that propranolol protection under acute conditions may not involve β-blockade or changes in endogenous antioxidant enzymes. Rather, it may be secondary to the membrane-stabilizing and/or direct antioxidant effects of the drug. Protection by a chronic treatment has been earlier suggested to involve an increase in endogenous antioxidant reserve. Thus, propranolol protection, under acute as well as chronic treatments, appears to involve antioxidant effects with different characteristics.

INTRODUCTION

Numerous studies in the past have provided considerable evidence that a sustained period of ischemia (I) can lead to irreversible myocardial damage. It has also been

S. Mochizuki, N. Takeda, M. Nagano and N. Dhalla (eds.). THE ISCHEMIC HEART.

fairly well established that reperfusion (R) of ischemic myocardium, though required, can exacerbate this damage. Some of the suggested mechanisms for this injury include the development of acidosis [1], alterations in membrane fluidity [2], increased intracellular calcium [3], and depletion of energy stores [4–7]. An imbalance between oxygen free radicals and antioxidants has also been implicated in the pathogenesis of this injury [8–12]. Different interventions have been shown to reduce myocardial injury [5,13–15]. Specifically, administration of exogenous antioxidants has been demonstrated to ameliorate the damage due to oxidative stress [11,13,16].

Propranolol, a nonspecific β-adrenergic blocking drug, has been shown to reduce the consequences of myocardial ischemia and subsequent reperfusion [5,14,17–19]. In addition to its β-blocking effect, propranolol also has inherent antioxidant activity and some poorly defined membrane-stabilizing properties [14,18,20]. Previous studies done in our laboratory have shown that chronic treatment of rats with propranolol results in a significant increase in antioxidant enzyme activity associated with a decrease in lipid peroxidation. In the same study, it was also demonstrated that the hearts of these chronically treated rats, when subjected to ischemia–reperfusion (I–R), exhibited improved recovery of function [19].

In the study reported here, we analyzed whether propranolol protection against I–R injury under acute conditions was associated with changes in antioxidant enzyme activities, lipid peroxidation, β-adrenoreceptor blockade, and/or membrane stabilization. Atenolol, a β_1-specific adrenergic blocking agent, was also used for comparison.

METHODS

Ischemia–reperfusion

Male Sprague–Dawley rats weighing 380 ± 45 g and maintained on a standard diet were sacrificed by decapitation. Hearts were removed, rinsed in the perfusion buffer, and attached via the ascending aorta to a steel cannula for retrograde perfusion according to the Langendorff method. The hearts were paced at 3 Hz with a stimulus duration of 5 ms. Hearts were perfused at 8 mL/min at 37°C with a modified Krebs–Henseleit buffer consisting of the following (mM): NaCl 120; $NaHCO_3$ 25.4; KCl 4.8; KH_2PO_4 1.2; $MgSO_4$ 0.86; $CaCl_2$ 1.25; and glucose 11.0 (pH 7.4). The buffer was continuously gassed with 95% O_2 and 5% CO_2. A preload tension of 2 g was applied to all the hearts to achieve an optimal (95% of L max) force–tension relationship [21]. Global ischemia was induced by clamping the aortic flow, and reperfusion was done by removing the clamp. Hearts were allowed a period of stabilization before being subjected to 60 minutes of global ischemia and 40 minutes of reperfusion. Myocardial contractile force and resting tension were continuously monitored by a Grass force transducer (FT03) attached by a hook to the apex of the heart. The signal generated was digitized and recorded by Axotape for analysis. In order to study the effects of the drug, propranolol (3.4 μM) was added to the perfusion medium prior to I–R. Atenolol, a β_1-adrenergic blocking

agent, was used for comparison at a concentration of 3.8 μM. Following I–R, control as well as propranolol- or atenolol-exposed hearts were removed from the perfusion apparatus and homogenized to determine the activities of endogenous antioxidant enzymes and the extent of lipid peroxidation.

Antioxidant enzymes

Superoxide dismutase (SOD) activity

SOD in the hearts was determined by the method previously described [22]. Hearts were homogenized in (1:10 wt/v) 50 mmol/L Tris-HCl, pH 8.20, containing 1 mmol/L diethylenetriamine pentaacetic acid. After centrifugation at 20,000 × g for 20 minutes, the supernatant was aspirated and assayed for total SOD activity by following the inhibition of pyrogallol autooxidation. Pyrogallol (24 mmol/L) was prepared in 10 mmol/L HCl and kept at 4°C prior to use. Catalase, 30 μmol/L stock solution, was prepared in an alkaline buffer (pH 9.0). Aliquots of supernatant (150 μg protein) were added to Tris HCl buffer containing 25 μL pyrogallol and 10 μL catalase. The final assay volume of 3 mL was made up with the same buffer. Changes in absorbance at 420 nm were recorded at one-minute intervals for five minutes. SOD activity was determined from a standard curve of the percent inhibition of pyrogallol autooxidation developed with commercially available SOD. Data are expressed as SOD units/mg protein as compared to the standard.

Glutathione peroxidase (GSHPx) activity

GSHPx activity was determined in the whole heart homogenate by the method previously described [23]. Hearts were homogenized in (1:10 wt:vol) 75 mmol/L phosphate buffer pH 7.0. The homogenate was centrifuged at 20,000 × g for 20 minutes, and the supernatant was aspirated and assayed for GSHPx activity. GSHPx activity was assayed in a 3-mL cuvette containing 2.0 mL of 75 mmol/L phosphate buffer, pH 7.0. The following solutions were then added: 50 μL of 60 mmol/L glutathione, 100 μL glutathione reductase solution (30 units/mL), 50 μL of 0.12 mol/L NaN_3, 100 μL of Na_2 EDTA, 100 μL of 3.0 mmol/L NADPH, and 100 μL cytosolic fraction. The reaction was started by adding 100 μL of 7.5 mmol/L H_2O_2, and the conversion of NADPH to NADP was monitored by recording the change of absorbance at 340 nM at one-minute intervals for five minutes. GSHPx activity was expressed as nanomoles of NADPH oxidized to NADP/min/mg protein with a molar extinction coefficient for NADPH at 340 nm of 6.22×10^6.

Catalase activity

Catalase activity in the hearts was determined using the method previously described [24]. Hearts were homogenized in (1:10 wt:vol) 50 mmol/L potassium phosphate buffer, pH 7.4. The homogenate was centrifuged at 20,000 × g for 20 minutes. Then 50 μL of supernatant was added to a 3-mL cuvette that contained 2.95 mL of 19 mmol/L hydrogen peroxide in 50 mmol/L potassium phosphate buffer, pH 7.4. Changes in absorbance at 240 nM were continuously followed for five minutes.

Catalase activity was expressed as μmoles H_2O_2 consumed/min/mg protein using a standard curve constructed by assaying commercially available catalase in the same manner.

Lipid peroxidation

Lipid peroxide content in hearts was determined by measuring the thiobarbituric acid reactive substances (TBARS) by the method described previously [25]. Hearts were homogenized in (10% wt/vol) 0.2 mol/L Tris 0.16 mol/L KCl buffer, pH 7.4, and incubated at 37°C for one hour. A 2-mL aliquot was collected from the incubation mixture and pipetted into a Corning culture tube. This was followed by the addition of 2.0 mL of 40% trichloroacetic acid (TCA) and 1.0 mL of 0.2% thiobarbituric acid (TBA). Then 100 μL of 2% butylated hydroxytoluene was added to the TBA reagent mixture to minimize peroxidation during the assay procedure. Next, tubes were boiled for 15 minutes and cooled on ice for five minutes. Then 2 mL of 70% TCA was added and the contents were again vortexed briefly. Tubes were allowed to stand for 20 minutes and then were centrifuged at 800 × g for 20 minutes. The developed color was read at 532 nm on a Zeiss spectrophotometer. A standard curve was constructed with commercially available malondialdehyde and used in the final determination of TBARS.

Protein and statistical analysis

Proteins were determined by the method previously described [26]. Data were expressed as the mean ± SEM. The data were evaluated with a one-way analysis of variance (ANOVA) followed by Bonferroni test. Values of $p < 0.05$ were considered significant.

RESULTS

Cardiac function

Myocardial-developed force and resting tension were recorded, and these data are shown in figures 1 and 2. Isolated hearts maintained on K-H solution showed normal function. In hearts subjected to 60 minutes of global ischemia, developed force declined to zero. Upon reperfusion for 40 minutes, there was marginal (5%–15%) recovery of force in control hearts as compared to preischemic values. Propranolol-supplemented hearts, on the other hand, showed complete recovery of contractile force immediately following reperfusion (figure 1). Developed force in these hearts at 40 minutes of reperfusion was about 80%. Atenolol, a specific β_1-blocker, did not cause any significant improvement in the recovery of the contractile force upon reperfusion (figure 1).

The resting (or diastolic) tension response to ischemia and reperfusion is shown in figure 2. Global ischemia in control hearts resulted in a significant increase (>350%) in the resting tension, and upon reperfusion there was some recovery. However, the resting tension at the end of 40 minutes of reperfusion was significantly greater (>150%). Propranolol-treated hearts exhibited significantly less rise in

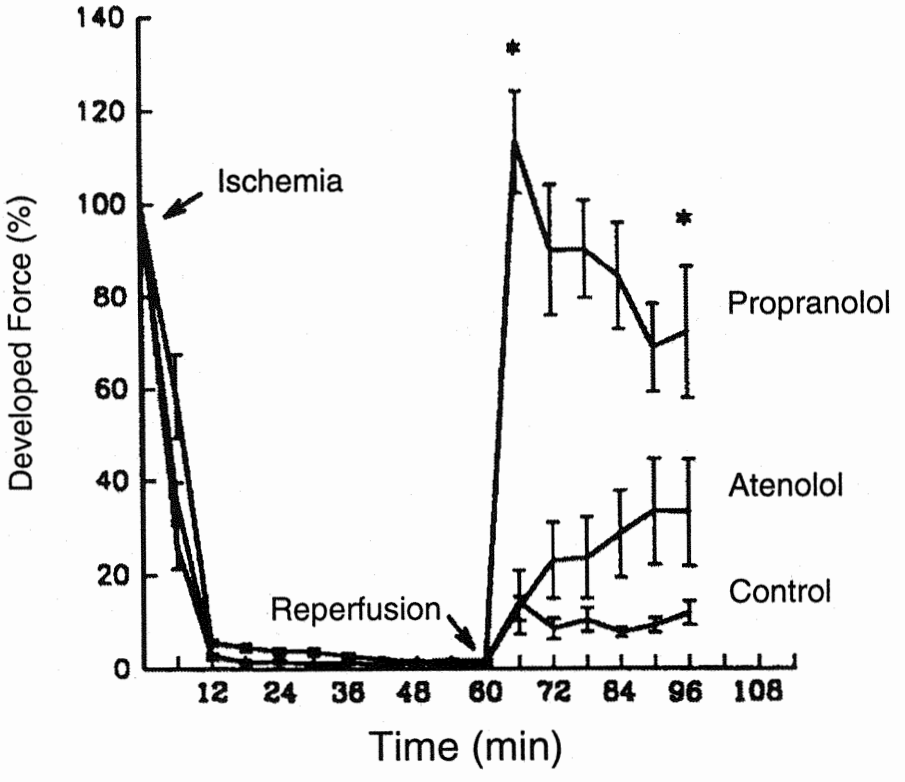

Figure 1. Recovery of force at different times of reperfusion in rat hearts subjected to 60 minutes of global ischemia and 40 minutes of reperfusion with and without the addition of propranolol or atenolol. Data are expressed as mean ± SEM of 7–9 experiments. *, statistically significant ($p < 0.05$) as compared to control heart.

the resting tension, which was completely recovered by the end of 40 minutes of reperfusion. Atenolol-treated hearts showed a significant rise in resting tension during ischemia and demonstrated some restoration during reperfusion, but never to the control levels (figure 2). These changes in the atenolol-treated hearts were quite similar to those seen in control hearts.

Antioxidants

At the end of I–R, control as well as drug-exposed hearts were analyzed for antioxidant enzymes, SOD, catalase, and GSHPx activities, and these data are shown in figure 3. There was no significant difference in any of the enzyme activities between the control and propranolol-exposed hearts. Catalase activity was significantly decreased in the atenolol-exposed hearts as compared to the controls (figure 3). Atenolol-exposed hearts also displayed a significant increase in glutathione peroxidase activity as compared to the controls (figure 3).

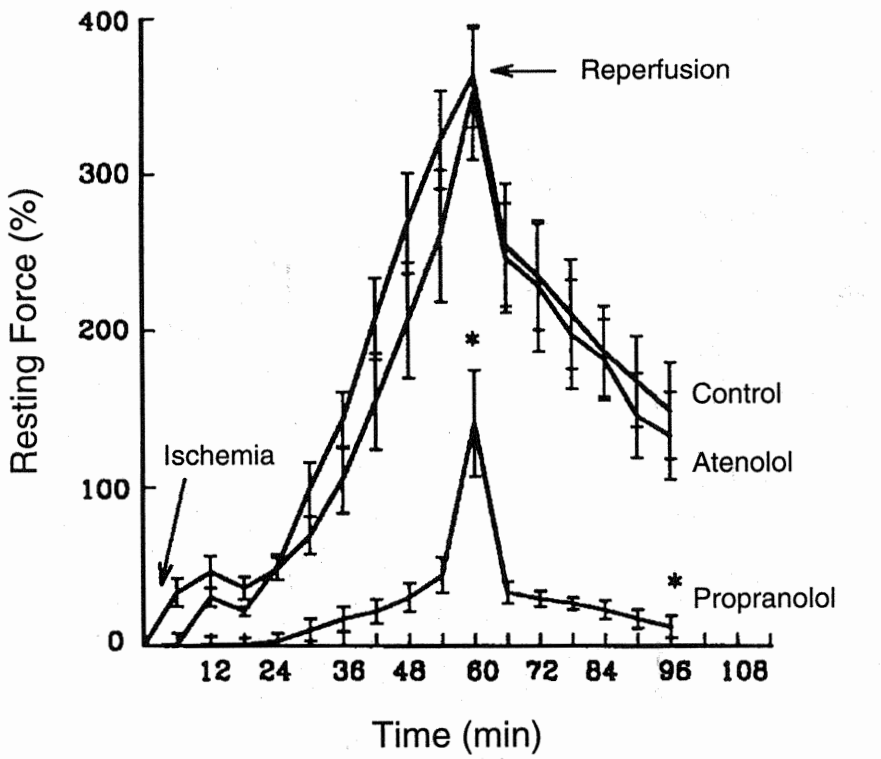

Figure 2. Change in resting tension in rat hearts subjected to 60 minutes of global ischemia and 40 minutes of reperfusion with and without propranolol or atenolol. Data expressed as mean ± SEM of 7–9 experiments. *, statistically significant ($p < 0.05$) as compared to control heart.

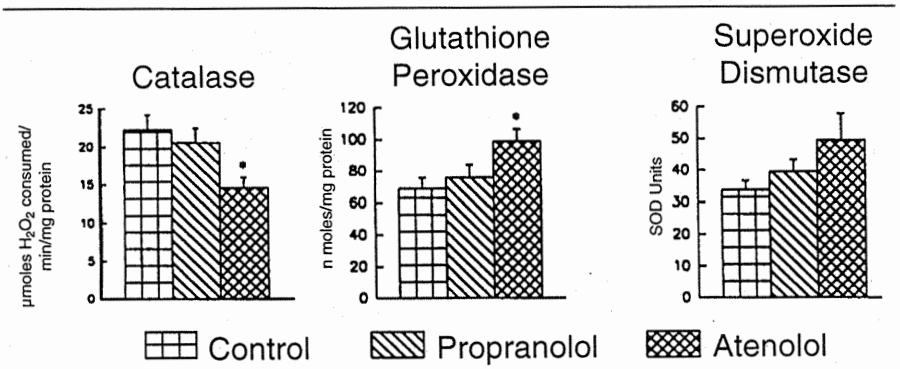

Figure 3. Effects of addition of propranolol or atenolol in the perfusion medium on antioxidant enzyme activities in rat hearts subjected to 60 minutes of global ischemia and 40 minutes of reperfusion. Data expressed as mean ± SEM of 6–8 hearts. *, statistically significant ($p < 0.05$) as compared to control hearts.

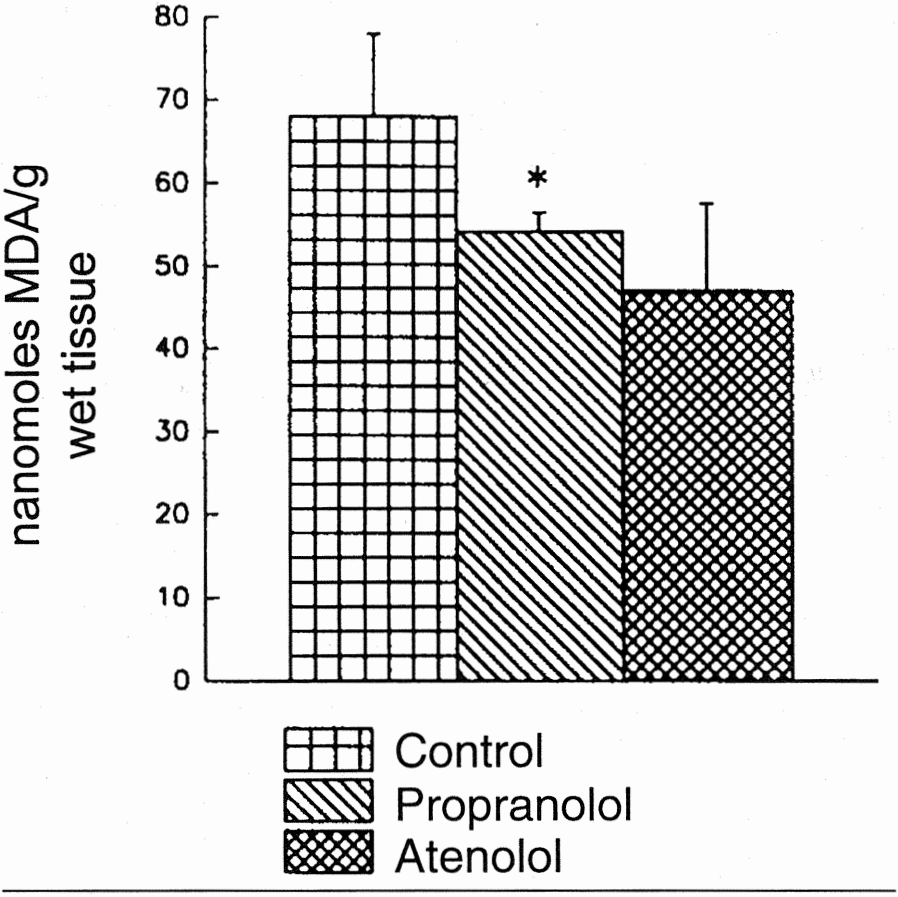

Figure 4. Effects of propranolol or atenolol on malondialdehyde content in rat hearts subjected to 60 minutes of global ischemia and 40 minutes of reperfusion. Data expressed as mean ± SEM of 6–8 hearts. *, statistically significant ($p < 0.05$) as compared to control hearts.

Lipid peroxidation

The extent of lipid peroxidation, as assessed by malondialdehyde (MDA), was studied in the propranolol- and atenolol-exposed hearts at the end of I–R. The MDA level in the control hearts was 68 ± 10 nmol/g wet wt. Levels of MDA from propranolol-treated hearts exposed to I–R were significantly less as compared to the control values (figure 4). Atenolol also resulted in a decline in the MDA levels at the end of I–R, but due to a large scatter, these differences were not significant.

DISCUSSION

Data in the present study clearly showed that propranolol offers significant protection against I–R injury in rat hearts, as has also been reported in previous studies

[19]. In the present study, this protection was manifested by improved contractile force and an attenuated increase in resting tension upon reperfusion of the heart, without any change in any of endogenous antioxidant enzyme activities. Since atenolol, a β_1-specific blocker, did not offer any protection when administered in similar concentrations, it is suggested that β-blockade per se may not play an important role in propranolol protection. Propranolol, a cationic amphiphile and more lipophilic than atenolol, is more able to infiltrate the membrane lipid bilayer, thereby stabilizing its structure and modulating the oxidative stress injury [14,20]. In this regard, atenolol has been reported to offer only partial protection against hypoxia reoxygenation injury, whereas propranolol treatment resulted in maintenance of cell structure and prevented lipid peroxide formation [14]. This finding suggests that, in acute conditions, the protection may indeed be due to membrane stabilizing and/or antioxidant properties of the drug [14]. From a molecular perspective, structural analogues of the naphthalene moiety found in propranolol have been shown to have protective activity of up to 60% of propranolol, suggesting that this structure may have true antioxidant activity [14].

A reduction in lipid peroxidation with propranolol, in the I–R hearts, correlated with an improvement in contractile function. A decrease in lipid peroxidation with propranolol has also been reported by others [14,18,27,28]. Based on our findings as well as on data reported in literature, it is hypothesized that the direct antioxidant and/or membrane-stabilizing property of propranolol may have a significant role in the protection against oxidative stress injury. The molecular basis of injury due to oxidative stress are not made clear by this study, but these may involve modification of proteins as well as lipids.

A chronic treatment of rabbits with propranolol resulted in protection against hypoxic as well as ischemic injury even after β-blockade had dissipated [17,29]. In our previous studies, hearts from rats chronically treated with propranolol showed improved recovery of force compared to the untreated hearts when subjected to global I–R [19]. In the same study, it was reported that adding propranolol or atenolol in the perfusion medium prior to I–R and continued until the end of reperfusion resulted in improved recovery of function only in the propranolol-perfused hearts. This protective effect was suggested to be due to an increase in antioxidant enzyme activity in animals chronically treated with propranolol [19]. Since the hearts from propranolol treated animals showed a potent response to epinephrine in ex vivo conditions, the role of β-blockade in protection against I–R was also ruled out. However, in the present study, propranolol did not change any of the antioxidant enzyme activities, suggesting that antioxidant enzyme changes are not involved in protection against acute I–R challenge. Atenolol did cause some increase in GSHPx and decrease in catalase, but offered no protection. Since catalase and GSHPx hydrolyze H_2O_2, it can be concluded that these opposite changes in these potent antioxidants may have canceled out each other.

Based on the data from our previous and present studies on propranolol effects, it is proposed that in chronic conditions, the maintenance of antioxidant reserve by increasing endogenous antioxidant enzyme activities secondary to β-blockade or

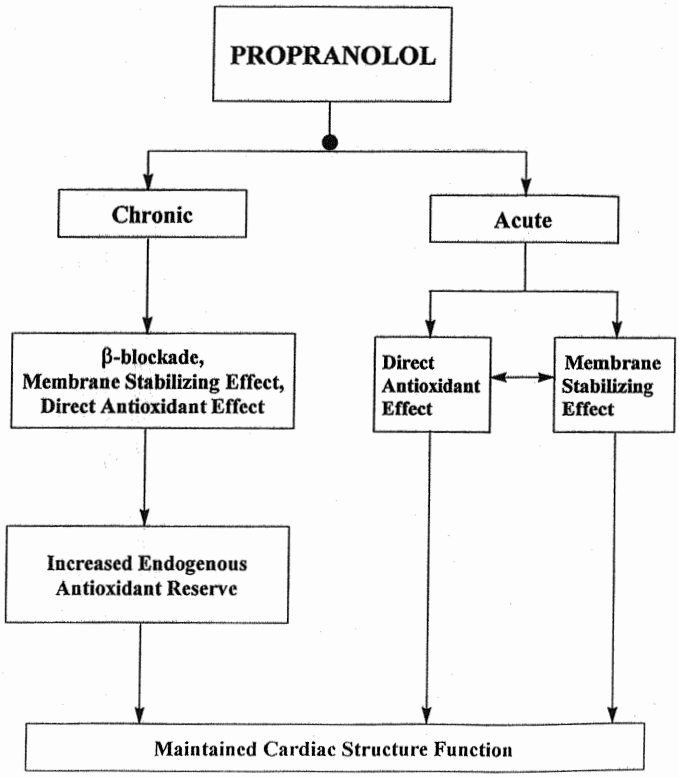

Figure 5. Proposed scheme for the propranolol-induced protection against I–R injury.

membrane-stabilizing or even direct antioxidant effects of the drug protects cardiac structure and function against I–R injury. Under acute conditions, however, the membrane-stabilizing property and/or the direct antioxidant property of propranolol are responsible for maintaining the cardiac function. This proposed hypothesis is presented in figure 5. Direct β-blockade due to propranolol during I–R does not appear to have a role in protection in either acute or chronic conditions. However, under chronic conditions, β-blockade may have an indirect role by influencing the antioxidant enzyme reserve.

ACKNOWLEDGMENTS

This research was supported by a grant from the Medical Research Council (MRC) of Canada. PKS is supported by the MRC; BK and CR were supported by the Heart and Stroke Foundation of Manitoba, and NK by a student fellowship from the University of Manitoba.

REFERENCES

1. Garlick PB, Radda GK, Seeley PJ. 1979. Studies on acidosis in the ischemic heart by phosphorus nuclear magnetic resonance. Biochem J 184:547–554.
2. Steenbergen RCS, Hill M, Jennings RB. 1989. Volume regulation and plasma membrane injury in aerobic, anaerobic and ischemic myocardium *in vitro*. Effects of osmotic cell swelling on plasma membrane integrity. Circ Res 57:864–875.
3. Bourdillon PDV, Poole-Wilson PA. 1981. The effects of ischemia and reperfusion on calcium exchange and mechanical function in isolated rabbit myocardium. Cardiovasc Res 15:121–130.
4. Weglicki WB, Mak IT, Dickeas BF, Kramer JH. 1987. Models of injury of cardiovascular membranes by amphiphiles and free radicals. In Dhalla NS, Innes IR, Beamish RE (eds), Myocardial Ischemia. Boston: Martinus Nijhoff, pp. 113–122.
5. Ziegelhoffer A, Das PK, Sharma GP, Singal PK, Dhalla NS. 1979. Propranolol effects on myocardial ultrastructure and high energy phosphates in anesthetized dogs subjected to ischemia and reperfusion. Can J Physiol Pharmacol 57:979–986.
6. Edoute Y, Sanan D, Lochner A, Graney D, Kotez JCN. 1981. Effects of propranolol on myocardial ultrastructure, mitochondrial function and high energy phosphates of isolated working rat hearts with coronary artery ligation. J Mol Cell Cardiol 13:619–639.
7. Hearse DJ. 1979. Oxygen deprivation and early myocardial contractile failure: a reassessment of the possible role of adenosine triphosphate. Am J Cardiol 44:1115–1121.
8. Bolli R. 1991. Oxygen derived free radicals and myocardial reperfusion injury. An overview. Cardiovasc Drug Ther 5:249–268.
9. Ferrari R, Ceconi C, Curello S, Guarnieri C, Caldarera CM, Albertini A, Visioli O. 1985. Oxygen mediated myocardial damage during ischemia and reperfusion. Role of the cellular defenses against oxygen toxicity. J Mol Cell Cardiol 17:937–945.
10. Zweier JL, Flaherty JT, Weisfeldt ML. 1987. Direct measurement of free radical generation following reperfusion of ischemic myocardium. Proc Natl Acad Sci USA 84:1404–1407.
11. Dhaliwal M, Kirshenbaum LA, Randhawa AK, Singal PK. 1991. Correlation between antioxidant changes during hypoxia recovery on reoxygenation. Am J Physiol 261 (Heart Circ Physiol 30):H632–H638.
12. Kaul N, Siveski-Iliskovic N, Hill M, Slezak J, Singal PK. 1993. Free radicals and the heart. J Pharmacol Toxicol Methods 30:55–67.
13. Jolly SR, Kane WJ, Bailie MB, Abrams GD, Lucchesi BR. 1984. Canine myocardial reperfusion injury. Its reduction by the combined administration of superoxide dismutase and catalase. Circ Res 54:277–285.
14. Mak IT, Weglicki WB. 1988. Protection by β-blocking agents against free-radical mediated sarcolemmal lipid peroxidation. Circ Res 63:262–266.
15. Nayler WG, Gordon M, Stephens DJ, Sturrock WG. 1985. The protective effect of prazosin on the ischemic and reperfused myocardium. J Mol Cell Cardiol 17:685–699.
16. Tamura Y, Chi L, Driscoll EM, Hoff PT, Freeman BA, Gallagher PK, Lucchesi BR. 1988. Superoxide dismutase conjugated to polyethylene glycol provides sustained protection against myocardial ischemia/reperfusion injury in canine heart. Circ Res 63:944–959.
17. Nayler WG, Ferrari R, Williams A. 1980. Protective effect of pretreatment with verapamil, Nifedipine and propranolol on mitochondrial function in the ischemic and reperfused myocardium. Am J Cardiol 46:242–248.
18. Mak IT, Kramer JH, Freedman AM, Tse SYH, Weglicki WB. 1990. Oxygen radical mediated injury of myocyte-protection by propranolol. J Mol Cell Cardiol 22:687–695.
19. Singal PK, Singh N, Seneviratne CK, Rigato C, Kowaluk B. 1995. Propranolol protection against ischemic injury: An antioxidant effect. J Mol Cell Cardiol A277:27.
20. Connally ME, Kersting F, Dollery CT. 1976. The clinical pharmacology of beta-adrenoreceptor-blocking drugs. Prog Cardiovasc Dis 19:203–234.
21. Slezak J, Tribulova N, Pristacova J, Uhrik B, Thomas T, Khaper N, Kaul N, Singal PK. 1995. Hydrogen peroxide changes in ischemic and reperfused heart: cytochemistry biochemical and X-ray microanalysis. Am J Pathol 147:772–781.
22. Marklund SL. 1985. Pyrogallol autooxidation. In Greenwald RN (ed), Handbook of Methods for Oxygen Radical Research. Boca Raton, FL: CRC Press, pp. 243–247.
23. Paglia DE, Valentine WN. 1967. Studies on the quantitative and qualitative characterization of erythrocyte glutathione peroxidase. J Lab Clin Med 70:158–169.

24. Claiborne A. 1985. Catalase activity. In Greenwald RA (ed), Handbook of Methods for Oxygen Radical Research. Boca Raton, FL: CRC Press, pp. 283–284.
25. Siveski-Iliskovic N, Kaul N, Singal PK. 1994. Probucol promotes endogenous antioxidants and provides protection against adriamycin-induced cardiomyopathy in rats. Circulation 89:2829–2835.
26. Lowry OH, Rosenbrough NJ, Farr AL, Randall RJ. 1951. Protein measurement with the folin phenol reagent. J Biol Chem 193:265–275.
27. Mak IT, Arroyo CM, Weglicki WB. 1989. Inhibition of sarcolemmal carbon-centred free radical formation by propranolol. Circ Res 65:1154–1156.
28. Sugawara H, Tobisi K, Onodera S. 1994. Absence of antioxidant effects of nifedipine and diltiazem on myocardial membrane lipid peroxidation in contrast with those of nisoldipine and propranolol. Biochem Pharmacol 47(5):887–892.
29. Nayler WG, Yepez CE, Fassold E, Ferrari R. 1978. Prolonged protective effect of propranolol on hypoxic heart muscle. Am J Cardiology 42:217–225.

This Page Intentionally Left Blank

MANGANESE SUPEROXIDE DISMUTASE INDUCED BY EXTRACELLULAR STRESS ENHANCES MYOCARDIAL TOLERANCE TO ISCHEMIA–REPERFUSION

TSUNEHIKO KUZUYA, MASASHI NISHIDA, SHIRO HOSHIDA, NOBUSHIGE YAMASHITA, MASATSUGU HORI, and MICHIHIKO TADA

Osaka University Medical School

Summary. In this chapter, we describe our recent findings showing that an intrinsic radical scavenger, manganese superoxide dismutase (Mn-SOD), is induced in cardiac myocytes in response to various external stresses, such as ischemic (hypoxic) preconditioning, heat shock, and α1-adrenergic stimulation. The induction of Mn-SOD is well correlated with the acquisition of tolerance to ischemia–reperfusion injury of the myocardium. Because inhibition of Mn-SOD induction abolishes the tolerance to ischemia–reperfusion, Mn-SOD plays a pivotal role as a rescue protein in cardiac myocytes, and the induction of Mn-SOD could be an adaptation mechanism against ischemic heart disease.

INTRODUCTION

Oxygen radicals have been proposed as one of the culprits that cause myocardial injury during ischemia–reperfusion. In the late 1980s, several groups successfully detected the presence of oxygen radical species in myocardial tissue soon after reperfusion following ischemia [1,2] and at later phases of reperfusion [3]. Oxygen radicals were produced in myocardial tissue after reperfusion, and the production of oxygen radicals was augmented during the course of extended cardiac injury after reperfusion. Therefore, many studies were designed to scavenge radical species to prevent reperfusion injury to the myocardium [4]. Exogenous radical scavengers, such as superoxide dismutase (SOD) and catalase, successfully reduced reperfusion injury in in vivo models. Recent studies have shown, however, that the heart is not merely threatened by oxygen radicals but also has its own intrinsic radical scavenging system, which includes Mn-SOD, Cu,Zn-SOD, catalase, and the glutathione redox

S. Mochizuki, N. Takeda, M. Nagano and N. Dhalla (eds.). THE ISCHEMIC HEART.

system. These enzymes were revealed to be induced by exogenous stimuli such as endotoxin, cytokines, and hyperthermia [5–8]. Among these enzymes, Mn-SOD is located in the cardiac mitochondria and is supposed to play a major role in scavenging superoxide generated by the electron transport system on the front line. Therefore, we tried to examine whether or not the induction of mitochondrial Mn-SOD is responsible for the acquisition of tolerance to ischemia–reperfusion of the heart by scavenging superoxide generated in mitochondria.

INDUCTION OF Mn-SOD AFTER ISCHEMIC PRECONDITIONING

Firstly, we examined the relationship between the tolerance of myocardium to ischemia and Mn-SOD induction in a preconditioning model of canine LAD occlusion–reperfusion [9]. Mn-SOD protein was measured by enzyme-linked immunosorbent assay soon, 3 hours, 12 hours, and 24 hours after repeated ischemia. Mn-SOD content in the subendocardium increased gradually, with a peak observed 24 hours after sublethal ischemia (60% increase). At this peak point, myocardial Mn-SOD activity, simultaneously measured by the nitroblue tetrazolium method, had also increased by about 80% of normal control. In the experiment reported here, we could not seen any differences in activity of other antioxidant enzymes, including Cu,Zn-SOD, catalase, and glutathione peroxidase. Next, we demonstrated that such an ischemic preconditioning protocol results in a delayed protective response against myocardial necrosis after a subsequent prolonged ischemia in the dog [10]. Immediately after, or 3, 12, and 24 hours after four five-minute occlusions of LAD, dogs were subjected to 90 minutes of occlusion followed by five-hour reperfusion. When the second ischemia was applied immediately after the first sublethal ischemia, the percent risk area infarcted was markedly decreased to 14% compared with the necrotic area in control animals. However, the reduction of myocardial infarction disappeared when the time interval between sublethal and sustained ischemia was 3 and 12 hours. Interestingly, the size of myocardial infarction was again reduced when the prolonged ischemia–reperfusion was applied 24 hours after ischemic preconditioning. The time course of the reappearance of tolerance to ischemia–reperfusion was identical with that of Mn-SOD induction in the preconditioned myocardium.

To investigate the role of enhancement of cardiac SOD activity in protection against ischemia–reperfusion injury, we examined whether the preconditioning phenomenon could be mimicked in cultured rat myocytes by exposing them to hypoxia (7 mmHg) and reoxygenation (143 mmHg) before exposure to sustained hypoxia–reoxygenation (hypoxic preconditioning) [11]. In control cells, which were subjected to normoxia instead of hypoxia for the first hour, Mn-SOD content and activity showed a slight decrease during the following 36 hours. On the other hand, in the cells exposed to hypoxia, both the activity and content of Mn-SOD increased markedly, with a peak at 24 hours after reoxygenation from hypoxia. We also examined the expression of Mn-SOD mRNA after hypoxia–reoxygenation by Northern hybridization using a rat Mn-SOD cDNA probe. Mn-SOD mRNA gives

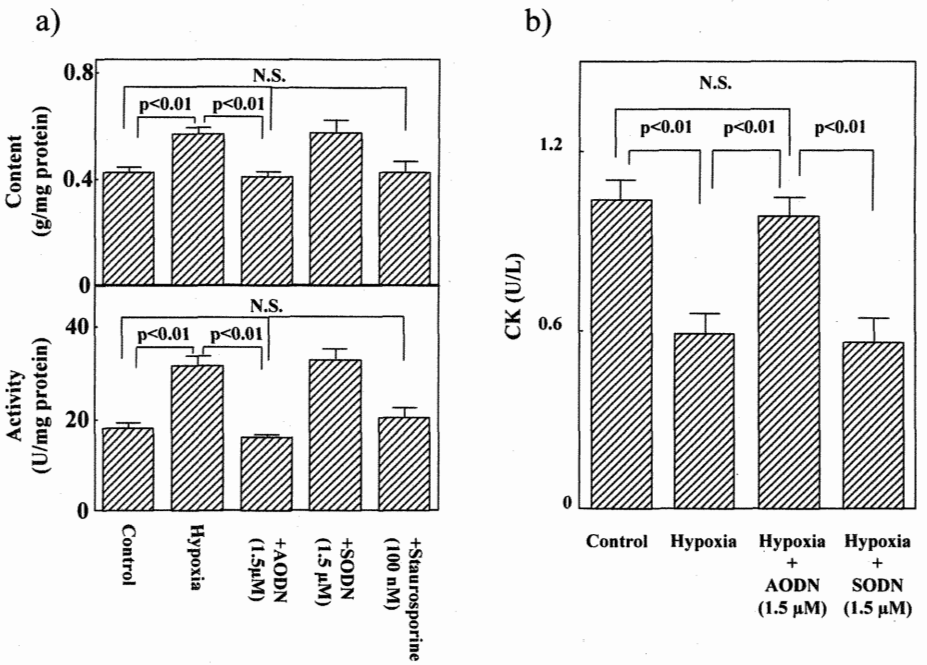

Figure 1. (**a**) Cardiac myocytes were exposed to hypoxia (one hour) and reoxygenation (24 hours). Mn-SOD content (upper panel) and activity (lower panel) in the cells were examined. Antisense oligodeoxyribonucleotides (AODN) to Mn-SOD mRNA were applied to some cultures 24 hours before the experiments. (**b**) Twenty-Four hours after exposure to hypoxia–reoxygenation, cardiac myocytes were exposed to prolonged hypoxia for three hours and reoxygenated for one hour. Myocyte injury was assessed by creatine kinase (CK) release into culture medium.

two bands at 4.0 kb and 1.0 kb. The basal expression of Mn-SOD mRNA observed before hypoxia increased after reoxygenation and reached its peak 30 minutes after reoxygenation (180% of control level, when it was normalized to actin signal). Nextly, we examined myocyte injury by assessing CK release from the cultures after exposure to prolonged hypoxia (three hours) and reoxygenation (one hour). When myocyte cultures were preexposed to hypoxic preconditioning as above, CK release from myocyte cultures after exposure to prolonged hypoxia was markedly reduced when the second hypoxia was applied 24 hours after the first hypoxia, compared with cells without hypoxic preconditioning. The time course of this increase in myocardial tolerance to hypoxia after exposure to brief preceding hypoxia was apparently similar to that of Mn-SOD induction.

Having confirmed that the simulation of ischemia–reperfusion by hypoxia–reoxygenation mimics the acquisition of tolerance to ischemia in vivo, we examined the cause–effect relationship between Mn-SOD induction and tolerance to hypoxia in the culture model using antisense oligodeoxyribonucleotides to Mn-SOD mRNA. Induction of Mn-SOD content and activity after exposure to hypoxia was

abolished completely when antisense oligonucleotides to Mn-SOD mRNA were added to myocyte cultures (figure 1a). Oligonucleotides having sense sequence did not attenuate the induction of Mn-SOD. Staurosporine, a protein kinase C inhibitor, also attenuated the induction of Mn-SOD in myocyte cultures after exposure to brief hypoxia. As we confirmed that antisense oligodeoxyribonucleotides to Mn-SOD mRNA inhibited the induction of Mn-SOD protein, we examined the effect of the oligonucleotides on CK release from myocytes after exposure to prolonged hypoxia–reoxygenation. Cardiac myocytes were exposed to one hour of hypoxia, with or without antisense oligonucleotides to Mn-SOD, 24 hours prior to the exposure to prolonged hypoxia (figure 1b). CK release from myocyte cultures was attenuated by 51% when the cells were exposed to brief hypoxia in comparison to the cells without exposure to preceding brief hypoxia. However, antisense oligonucleotides to Mn-SOD abolished the expected decrease in CK release from myocytes with hypoxic preconditioning. Sense oligonucleotides did not change CK release from preconditioned myocytes. These results indicate that Mn-SOD induction in cardiac myocytes after exposure to brief hypoxia is the mechanism of the acquisition of tolerance to lethal hypoxia in cardiac myocytes.

INDUCTION OF MN-SOD AFTER HEAT STRESS [12]

Heat shock is also known to increase the tolerance of myocardium to ischemic stress by inducing heat-shock proteins (HSPs) [8,13]. Therefore, a heat shock model of cultured myocytes could be a model to examine the relationship between HSPs and Mn-SOD induction in the acquisition of tolerance to ischemia–reperfusion. We examined the expression of Mn-SOD and HSP72 in rat neonatal cardiac myocytes by exposing them to heat shock at 42°C for one hour (figure 2a). Mn-SOD mRNA exhibited transient expression that peaked at 30 minutes after heat shock. HSP72 mRNA expression probed with PCR fragment of mouse cDNA was also increased dramatically at 30 minutes after heat shock. As we confirmed that heat shock induces both Mn-SOD and HSP72 in myocardial cells, we used antisense oligonucleotides to separate the effect of heat-shock protein and Mn-SOD on the acquisition of tolerance to ischemia. Antisense oligonucleotides to Mn-SOD were added to myocyte cultures during heat shock and following normothermic incubation for 24 hours. Twenty-four hours after heat shock at 42°C for one hour, Mn-SOD content increased significantly. This increase in Mn-SOD content was abolished by the addition of 1.5 μM of antisense oligonucleotides. HSP72 protein was induced in the myocytes 24 hours after heat shock. The increase in HSP72 was not inhibited by the addition of antisense oligonucleotides to Mn-SOD at the dose that abolished Mn-SOD induction. These results indicate that the antisense oligonucleotides used in this experiments inhibited only Mn-SOD induction, not that of HSP72. Although several constructs were examined at a variety of doses, antisense oligonucleotides against HSP72 mRNA could not inhibit the induction of HSP72 protein.

Therefore, we used the Mn-SOD antisense oligonucleotides to separate the effect of Mn-SOD induction and HSP72 induction. To examine whether Mn-SOD and

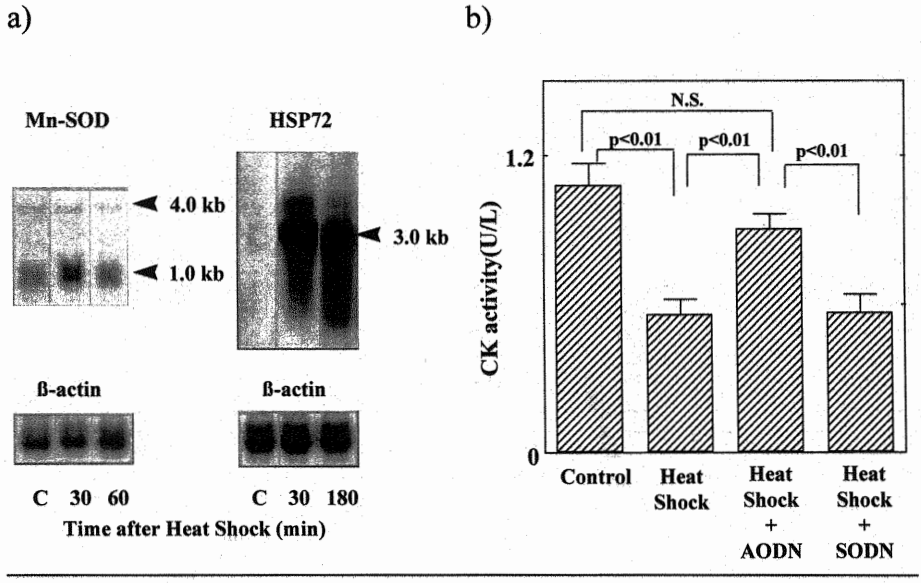

Figure 2. (**A**) Cardiac myocytes were exposed to heat shock at 42°C for one hour. Total RNA was isolated from myocytes, and expression of Mn-SOD (left panel) and HSP72 (right panel) mRNA was detected by Northern blot analysis. (**B**) Twenty-four hours after exposure to heat shock, myocytes were exposed to hypoxia (three hours) followed by reoxygenation (one hour). CK release from cultured cells was measured thereafter. In some experiments, AODNs to Mn-SOD mRNA, which specifically inhibited the induction of Mn-SOD protein but not that of HSP72, were applied to myocyte cultures.

HSP72 play roles in the acquisition of tolerance to hypoxia after heat stress, we tested the effect of Mn-SOD antisense oligonucleotides on CK release from myocytes after hypoxia–reoxygenation (figure 2b). Heat stress for one hour at 42°C increased the tolerance of myocytes to hypoxia 24 hours after heat shock, i.e., CK release from myocytes after three hours of hypoxia followed by one hour of reoxygenation decreased by 50% compared with control cells without heat stress. Antisense oligonucleotides to Mn-SOD, which inhibited Mn-SOD induction after heat stress but not HSP72 induction, attenuated significantly the decrease in CK release. Sense oligonucleotides used as controls did not alter CK release from heat-stressed myocytes. These results indicate that Mn-SOD is induced after heat stress together with HSP72 and plays a pivotal role in the acquisition of the tolerance to ischemia after heat shock. The role of Mn-SOD in cardioprotection might be distinct from that of HSP72, because inhibition of Mn-SOD alone by antisense oligonucleotides abolished the tolerance of myocytes to hypoxia–reoxygenation.

MN-SOD INDUCTION AFTER α1-ADRENERGIC STIMULATION

Finally, we examined the mechanism by which the effect of preconditioning is connected to the induction of Mn-SOD. Recent studies have revealed that cardiac

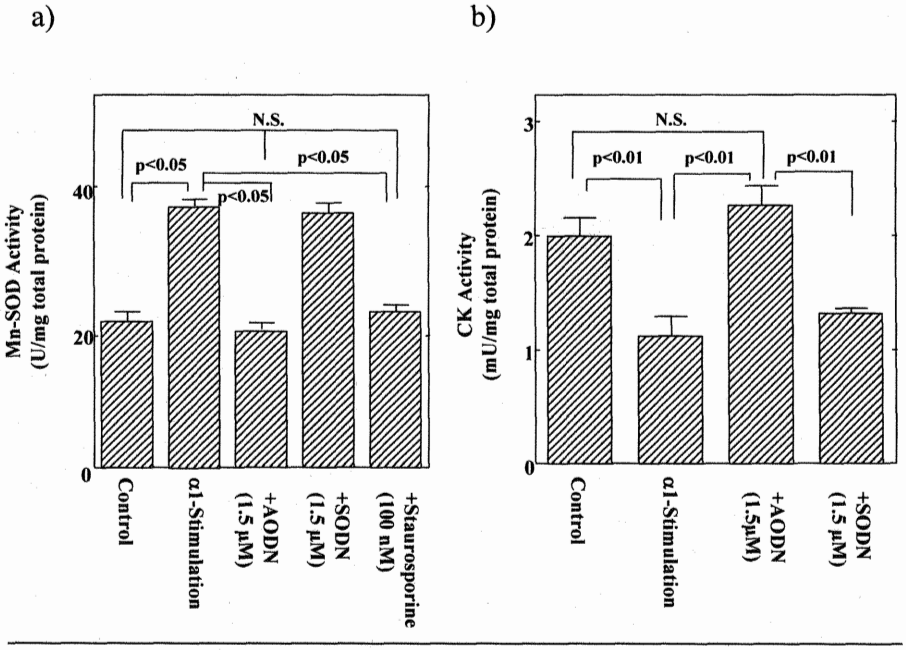

Figure 3. (**A**) Cardiac myocytes were exposed to 0.2μM norepinephrine in the presence of 2μM propranolol, and 2μM yohimbine. Twenty-four hours after stimulation, Mn-SOD activity in cultures was examined. AODNs, SODNs to Mn-SOD mRNA, and staurosporine were added to some cultures. (**B**) Hypoxia (three hours) followed by reoxygenation (one hour) was applied to myocyte cultures after α1-adrenergic stimulation. CK release into culture medium was assessed.

myocytes respond to various stresses, such as ischemia, heat shock, and adrenergic stimulation, and acquire an intrinsic cardioprotective capacity from them. In this preconditioning phenomenon of hearts, the mechanism is well examined regarding the α1-adrenergic stimulation pathway conducted through adenosine, K-channel, or protein kinase C to the final effectors. Therefore, we hypothesized that the induction of Mn-SOD in cardiac myocytes in our experimental models could be conducted through an α1-adrenergic receptor-mediated mechanism via protein kinase C [14]. We stimulated cultured rat neonatal cardiac myocytes with norepinephrine in the absence or presence of adrenergic receptor blockades. Twenty-four hours after norepinephrine was added to the myocyte cultures, Mn-SOD activity in culture dish increased dose dependently up to 0.2μM and declined thereafter. Although the total protein content in the cell also increased after norepinephrine stimulation, the increase in Mn-SOD was shown to be specifically larger than the nonspecific increase in proteins by dividing Mn-SOD activity by the total protein amount. Mn-SOD mRNA expression after the addition of norepinephrine showed that Mn-SOD transcription was augmented 30 minutes after stimulation. To confirm the receptor specificity of this phenomenon, we examined the effect of adrenergic receptor antagonists and an agonist on Mn-SOD induction. The aug-

mented Mn-SOD activity in myocytes by the addition of norepinephrine (0.2 μM) was not attenuated by an α2-adrenergic blocker, yohimbine (2 μM), and an α-adrenergic blocker, propranolol (2 μM). However, an α1-adrenergic blocker, prazosine (2 μM), abolished the increase in Mn-SOD activity induced by norepinephrine. An α1-adrenergic agonist, methoxamine (20 μM), also increased Mn-SOD activity in the myocytes 24 hours after the addition. These results indicate that the induction of Mn-SOD after norepinephrine was conducted through α1-adrenergic stimulation. Mn-SOD activity that had increased via α1-adrenergic stimulation was attenuated by the addition of antisense oligonucleotides to Mn-SOD mRNA. A protein kinase C inhibitor, staurosporine (100 nM), also attenuated the increase in Mn-SOD activity (figure 3a). Finally, we examined whether or not Mn-SOD induced by α1-adrenergic stimulation could increase the tolerance of the myocytes to hypoxia–reoxygenation. Cardiac myocytes were exposed to α1-adrenergic stimulation for 24 hours, and then hypoxia (three hours) followed by reoxygenation (one hour) was applied to the cells. CK release from the myocytes was significantly attenuated by α1-adrenergic stimulation. However, antisense oligonucleotides to Mn-SOD, which inhibited the induction of Mn-SOD by norepinephrine, abolished the expected decrease in CK release from hypoxia–reoxygenated myocytes (figure 3b).

REFERENCES

1. Garlick PB, Davies MJ, Hearse DJ, Slater TF. 1987. Direct detection of free radicals in the reperfused rat heart using electron spin resonance. Circ Res 61:757–760.
2. Zweier JL, Flaherty JT, Weisfeldt ML. 1987. Direct measurement of free radical generation following reperfusion of ischemic myocardium. Proc Natl Acad Sci USA 84:1404–1407.
3. Kuzuya T, Hoshida S, Kim Y, Nishida M, Fuji H, Kitabatake A, Tada M, Kamada T. 1990. Detection of oxygen-derived free radical generation in the canine postischemic heart during late phase of reperfusion. Circ Res 66:1160–1165.
4. Opie LH. 1989. Reperfusion injury and its pharmacologic modification. Circulation 80:1049–1062.
5. Brown JM, White CW, Terada LS, Grosso MA, Shanley PF, Mulvin DW, Banerjee A, Whitman GJ, Harken AH, Repine JE. 1990. Interleukin 1 pretreatment decreases ischemia/reperfusion injury. Proc Natl Acad Sci USA 87:5026–5030.
6. Eddy LJ, Goeddel DV, Wong GH. 1992. Tumor necrosis factor-alpha pretreatment is protective in a rat model of myocardial ischemia–reperfusion injury. Biochem Biophys Res Commun 184:1056–1059.
7. Murry CE, Jennings RB, Reimer KA. 1986. Preconditioning with ischemia: a delay of lethal cell injury in ischemic myocardium. Circulation 74:1124–1136.
8. Yellon DM, Pasini E, Cargnoni A, Marber MS, Latchman DS, Ferrari R. 1992. The protective role of heat stress in the ischaemic and reperfused rabbit myocardium. J Mol Cell Cardiol 24:895–907.
9. Hoshida S, Kuzuya T, Fuji H, Yamashita N, Oe H, Hori M, Suzuki K, Taniguchi N, Tada M. 1993. Sublethal ischemia alters myocardial antioxidant activity in canine heart. Am J Physiol 264:H33–H39.
10. Kuzuya T, Hoshida S, Yamashita N, Fuji H, Oe H, Hori M, Kamada T, Tada M. 1993. Delayed effects of sublethal ischemia on the acquisition of tolerance to ischemia. Circ Res 72:1293–1299.
11. Yamashita N, Nishida M, Hoshida S, Kuzuya T, Hori M, Taniguchi N, Kamada T, Tada M. 1994. Induction of manganese superoxide dismutase in rat cardiac myocytes increases tolerance to hypoxia 24 hours after preconditioning. J Clin Invest 94:2193–2199.
12. Yamashita N, Hoshida S, Nishida M, Igarashi J, Taniguchi N, Tada M, Kuzuya T, Hori M. 1997. Heat shock-induced manganese superoxide dismutase enhances the tolerance of cardiac myocytes to hypoxia-reoxygenation injury. J Mol Cell Cardiol 29:1805–1813.

13. Hutter MM, Sievers RE, Barbosa V, Wolfe CL. 1994. Heat-shock protein induction in rat hearts. A direct correlation between the amount of heat-shock protein induced and the degree of myocardial protection. Circulation 89:355–360.
14. Yamashita N, Nishida M, Hoshida S, Igarashi J, Hori M, Kuzuya T, Tada M. 1996. α1-adrenergic stimulation induced tolerance of cardiac myocytes to hypoxia through induction and activation of manganese superoxide dismutase. Am J Physiol 271:H1356–H1362.

THIOCTIC ACID PREVENTS OXIDATIVEDAMAGE IN ISOLATED CARDIAC MYOCYTES

HANS-GEORG OLBRICH*, P. GRABISCH*, T. DICKFELD*, I. HENKE*, and E. MUTSCHLER**

* *Medizinische Klinik IV, Kardiologie*
** *Johann Wolfgang Goethe-Universität*

Summary. Thioctic acid and its reduced form, dihydrolipoic acid, may protect myocardium against ischemia–reperfusion damage. It is unknown whether or not thioctic acid exerts its protective action by any direct effect on heart muscle cells. The in vitro study reported here aimed to investigate the effect of thioctic acid against oxidative damage in singlet oxygen-challenged isolated cardiac myocytes. Cardiac myocytes were isolated from adult rat hearts by collagenase perfusion. Singlet oxygen was generated by photoexcitation of rose bengal (0.1 μM). Exposure to singlet oxygen induced irreversible hypercontracture in 70% to 80% of rod-shaped cardiomyocytes accompanied by a significant increase in the production of thiobarbituric acid reactive substances as an indicator for lipid peroxidation. Pretreatment of the cardiomyocytes with thioctic acid (1 mM) significantly increased the number of surviving cardiomyocytes after exposure to singlet oxygen to 52.6% ± 9.6% vs. 22.2% ± 6.3% ($p < 0.5$) and reduced the amount of thiobarbituric acid reactive substances to 385 ± 42 vs. 635 ± 90 nmol/g protein ($p < 0.5$). The data suggest a cardioprotective effect of thioctic acid, which is possibly due to its antioxidative action.

INTRODUCTION

Membrane phospholipid peroxidation induced by free oxygen radicals is regarded as a major mechanism of injury in a variety of diseases [1]. Among these, reactive oxygen species have been shown to play a central role in mediating reperfusion-induced injury following a period of ischemia in the heart [2,3].

In recent years, increasing attention has been paid to the therapeutic use of thioctic acid in a variety of diseases in which free radical peroxidation of membrane

S. Mochizuki, N. Takeda, M. Nagano and N. Dhalla (eds.). THE ISCHEMIC HEART.

phospholipids is of pathogenetic significance [4]. Thioctic acid is a naturally occurring compound that is physiologically involved as a cofactor for oxidative decarboxylation of pyruvate alpha-ketoglutarate dehydrogenase reactions, which are essential processes in metabolism. Recent investigations showed that thioctic acid and its reduced form, dihydrolipoic acid, may protect myocardium against ischemia–reperfusion damage [5,6]. It is postulated that this protective action largely depends on the presence of high concentrations of vitamin E [6,7].

Thus, far, it is unknown whether or not thioctic acid exerts any direct effect on heart muscle cells. Therefore, the study reported here aimed to examine the direct cardioprotective potential of thioctic acid against oxidative damage using the in vitro model of isolated cardiomyocytes. We applied a simple oxidation system in which a rapid and reproducible burst of oxidant stress is induced by the photoactivation of rose bengal. In aqueous solution, rose bengal can be elevated to a triplet state by illumination with light of appropriate wave length (500–600 nm). In the presence of oxygen, this triplet state decays producing singlet oxygen (75% of decays) and superoxide (20% of decays) [8].

METHODS

Isolation of cardiomyocytes

Single cardiomyocytes were isolated from adult rat hearts according to the method described by Piper et al. [9], with some minor modifications as described previously [10]. Hearts of male Wistar rats (body weight 250–300 g) were isolated and perfused via the aorta using an oxygenated modified Krebs–Ringer–Hepes (KRH) buffer (pH 7.3, 37°C; flow rate: 10 mL/min) of the following composition: 125 mM NaCl, 2.6 mM KCl, 1.2 mM KH_2PO_4, 1.2 mM $MgSO_4 \times 7\ H_2O$, 5.5 mM glucose, and 10 mM Hepes. After five minutes perfusion, the hearts were perfused for another 25 minutes with a KRH buffer supplemented with 25 μM $CaCl_2$, 0.06% collagenase (Wako, Neuss, Germany), and 0.1% fatty acid-free bovine serum albumin (BSA) (Sigma Chemie, Deisenhofen, Germany). After dispersion of the cells, and a stepwise increase of $CaCl_2$ to 0.5 mM, aliquots of the cell suspension were layered on a 10-cm-high column with a KRH buffer containing 2% BSA (Serva Feinbiochemica, Heidelberg, Germany) and a final concentration of 1 mM $CaCl_2$. Myocytes were allowed to settle for 10 minutes and the supernatant was removed. The remaining cell suspension was resuspended with KRH buffer (supplemented with 1 mM $CaCl_2$, pH 7,4), and aliquots were divided into plastic test tubes. The protein content of the myocyte suspension was determined according the method described by Lowry et al. [11]. The protein content of the cell suspension amounted to 5.43 ± 0.51 mg/mL (19 separate preparations). All experiments were carried out at room temperature (20°C). This investigation conforms with the Guide for the Care and Use of Laboratory Animals published by the U.S. National Institutes of Health (NIH publication No. 85-23, revised 1985).

Reactive oxygen species

Reactive oxygen species were generated by photoexcitation of the light-sensitive dye rose bengal, producing singlet oxygen as described previously by Ver Donck et al. [12]. Thirty minutes prior to photoexcitation, rose bengal (0.1 μM) alone or in combination with thioctic acid was added to the KHR incubation medium. A fiber optic cable connected to a cold light source (150 W Xenophot lamp KL 1500, Schott, Mainz, Germany) was positioned in the test tube 2 cm above the surface of the cell suspension, and the tube was wrapped with a reflecting foil. The cell suspension was then illuminated for a fixed period of 80 or 120 seconds. For the determination of the number of rod-shaped cells and for the formation of thiobarbituric acid-reactive substances (TBARS), aliquots of the suspension were removed immediately before and 15 minutes after termination of the illumination.

Cell count and morphological evaluation

About 90% of the cardiomyocytes in the cell suspension in KRH displayed a rod-shaped morphology. The number of calcium-tolerant rod-shaped cardiomyocytes was determined by counting aliquots of the cell suspension using an improved Neubauer counting chamber (Fischer, Frankfurt am Main, Germany). For this purpose, five squares of the Neubauer counting chamber were evaluated at a magnification of 100 ×, and the number of rod-shaped cells (around 50 cells) was counted. The volume of one square amounts to 0.1 μL. Therefore, the number of rod-shaped cells per milliliter suspension proves to be as follows:

$$\text{Counted cells} \times 2 \times 10^3 = \text{cells/mL}$$

Singlet-oxygen-induced cell damage was assessed on the basis of shape changes from elongated rod-shaped to hypercontracted rounded cells (figure 1). Such shape changes of isolated cardiomyocytes are regarded as resulting from intolerance to physiological calcium concentrations due to membrane injury [13].

Assessment of lipid peroxidation

The accumulation of secondary lipid peroxidation products reacting with thiobarbituric acid was measured spectrophotometrically according to a method described by Wong et al. [14]. Plasma lipoperoxides were hydrolyzed by boiling in dilute phosphoric acid (0.44 M H_3PO_4). The hydrolysis products, consisting of malondialdehyde (MDA) and other aldehydes, were reacted with thiobarbituric acid (42 mM) to form thiobarbituric acid-reactive substances (TBARS). Plasma proteins were precipitated with methanol–NaOH (0.09 M) and removed from the medium by centrifugation (9.500 × g). The amount of thiobarbituric acid-reactive substances was then quantified spectrophotometrically by absorbance at 532 nm. Lipoperoxide concentrations were calculated by reference to a calibration curve prepared by means of tetramethoxypropan (TMP), which liberates stoichiometric amounts of MDA when hydrolyzed in the presence of thiobarbituric acid [15].

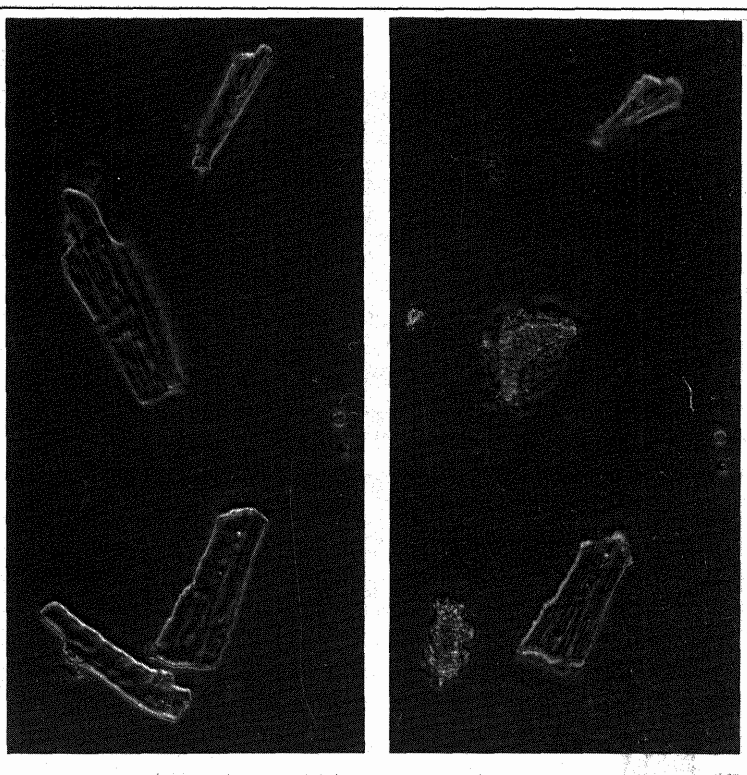

Figure 1. Rose bengal–560 nm light-induced shape changes of cardiomyocytes from elongated rod-shaped to hypercontracted rounded cells. Left: Before illumination; right: 15 minutes after illumination (80 seconds). Magnification × 400.

Drugs

Rose bengal was purchased from Sigma Chemie (Deisenhofen, Germany). Thioctic acid was a gift from Woerwag Pharma (Stuttgart, Germany). Both compounds were dissolved in KRH buffer supplemented with 1 mM $CaCl_2$ and further diluted in the same buffer to their final concentrations.

Experimental protocol

To investigate the effect of thioctic acid against rose bengal–light-induced cell damage, each analytical run for morphologic evaluation of the cardiomyocytes and determination of TBARS consisted of duplicate assays of the following probes: untreated cells, cells incubated with rose bengal for 30 minutes in the dark, cells incubated with rose bengal 15 minutes after illumination, cells incubated with rose bengal and thioctic acid for 30 minutes in the dark, and cells incubated with rose bengal and thioctic acid 15 minutes after illumination. In the case of TBARS determination, each experiment included the duplicate assay of TMP working

standard solutions. According to this protocol, the examination of one drug concentration afforded one separate preparation.

Statistical analysis

Each measurement was done in duplicate. The data are presented as the mean ± SEM of n separate preparations (animals). Statistical analysis of the data was carried out by employing analysis of variance and the two-sided Mann–Whithney–U-test [16]. A p value of less than 0.05 was considered statistically significant.

RESULTS

Effect of photoexcitation of rose bengal

Photoexcitation of rose bengal (0.1 μM) resulted in a sharp and rapid loss of rod-shaped cells and a 10-fold increase in the production of TBARS, indicating lipid peroxidation (figure 2). Both effects slightly depended on the duration of illumination.

Control experiments

After addition of rose bengal (0.1 μM) to the cell suspension followed by 30 minutes of incubation in the dark, the number of rod-shaped cells remained constant (figure 2). Illumination of the cardiomyocyte suspension in the absence of rose bengal did not influence the number of rod-shaped cells either (data not shown).

Effect of thioctic acid

In spite of using a fixed exposure time to illumination, the cardiomyocytes showed a variability in sensitivity to rose bengal–light. Therefore, each experiment included a control consisting of incubation solely with rose bengal. Coincubation with thioctic acid in addition to rose bengal for 30 minutes prior to photoexcitation improved the number of surviving rod-shaped myocytes in a concentration-dependent manner (figure 3, table 1). A significant protection was observed with 1.0 mM thioctic acid: the number of rod-shaped myocytes was doubled in comparison to rose bengal alone. Concomitantly, the production of TBARS (figure 4) was reduced by about 40%, thus indicating a diminished lipid peroxidation in the presence of 1.0 mM thioctic acid. At lower concentrations (10 and 100 μM) thioctic acid was not effective, whereas above 1.0 mM, i.e., with 10 mM thioctic acid, significant deterioration in the number of rod-shaped cells as compared to rose bengal alone was observed in spite of a constant reduction in the production of TBARS.

DISCUSSION

In the present study, the influence of thioctic acid on singlet-oxygen-induced damage in isolated rat cardiomyocytes was examined. The value of isolated heart muscle cells for structural and functional studies has been widely recognized for more than ten years [17]. The advantage of single-cell preparations is the homoge-

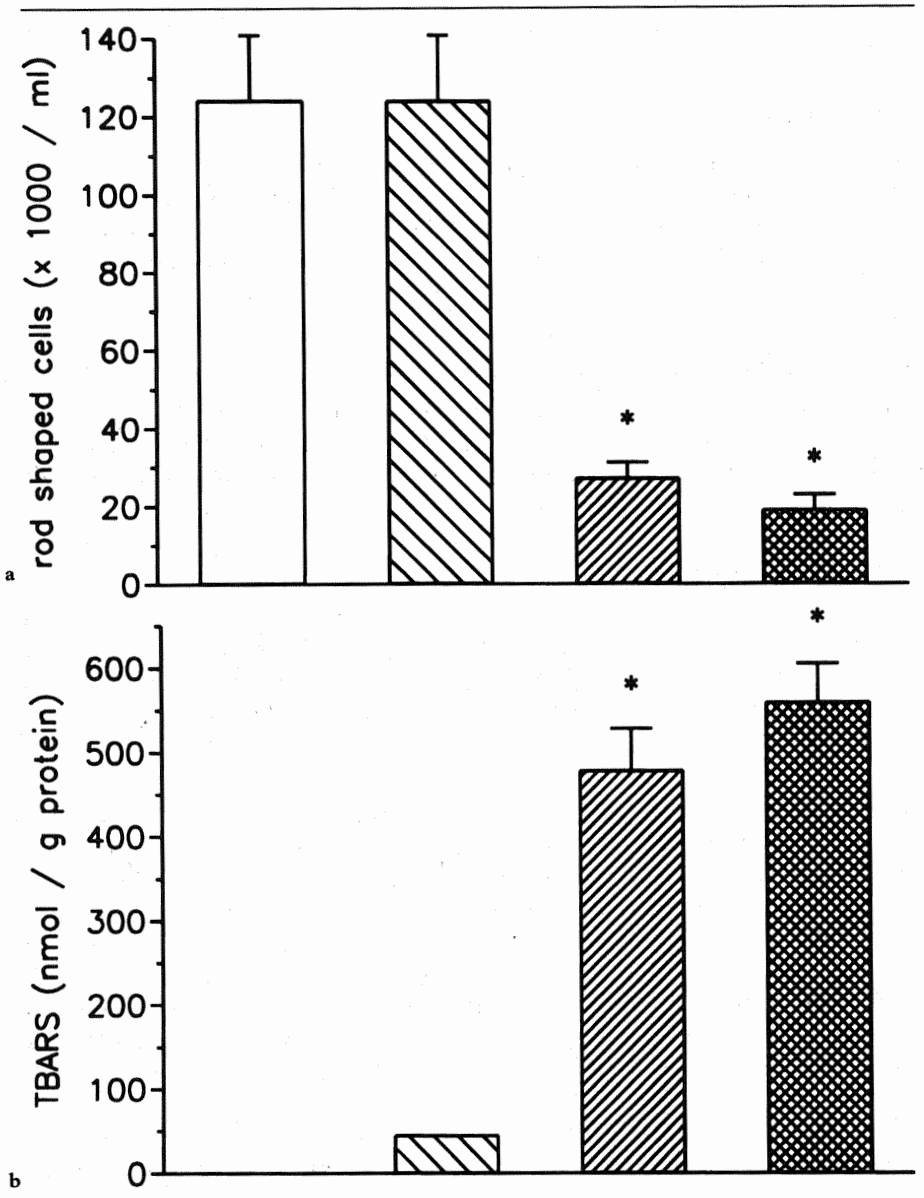

Figure 2. The effect of rose bengal–light on the number of rod-shaped cardiomyocytes (above) and formation of thiobarbituric acid-reactive substances (TBARS) (below). ••: after isolation procedure; ••: during incubation with rose bengal (0.1 μM) in the dark; ••: after 80-second illumination; ••: after 120-second illumination. $n = 6$ separate preparations; *p, $p < 0.005$ vs. incubation with rose bengal in dark.

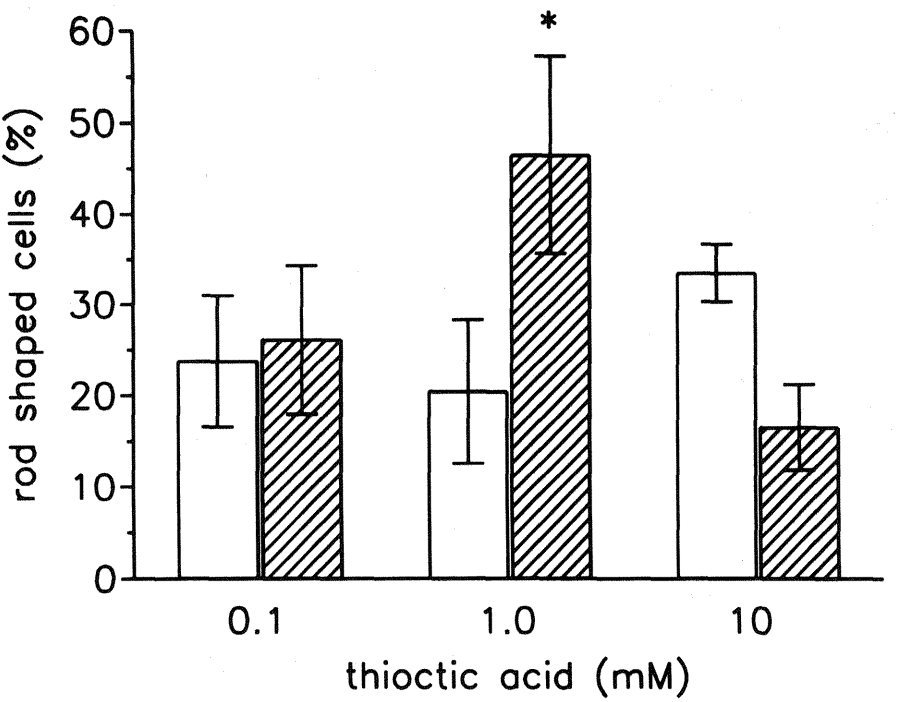

Figure 3. The effect of tioctic acid on singlet-oxygen-induced loss of rod-shaped cardiomyocytes (due to hypercontracture). Singlet oxygen was generated by illumination of rose bengal (see Methods). Percentage of rod-shaped cells 15 minutes after illumination (80 seconds) in the presence of rose bengal (0.1 μM) alone (••) or in combination with various concentrations of thioctic acid (••). n = 5 to 7 separate preparations; *β, p = 0.036 vs. rose bengal alone.

Table 1. Effect of thioctic acid on the number of rod-shaped cells and content of thiobarbituric acid reactive substances in suspensions of cardiomyocytes after exposure to rose bengal–light (see Methods)

		Rose bengal alone		Rose bengal + TA		
TA (mM)		Rod-shaped cells (cells × 10^3/mL)	TBARS (nmol/g protein)	Rod-shaped cells (cells × 10^3/mL)	TBARS (nmol/g protein)	n
0.1	a	75.68 ± 11.81	35.0 ± 12.2	76.83 ± 10.30	39.9 ± 12.3	6
	b	21.67 ± 9.19	435.4 ± 76.4	23.67 ± 9.67	454.1 ± 69.9	
1.0	a	81.33 ± 6.50	69.6 ± 16.2	78.00 ± 8.54	66.0 ± 21.2	6
	b	18.33 ± 7.79	635.3 ± 110.2	40.50 ± 11.86*	384.7 ± 51.4*	
10	a	101.33 ± 10.91	88.4 ± 41.8	92.50 ± 15.67	90.6 ± 37.1	3
	b	50.00 ± 16.17	268.8 ± 65.5	20.33 ± 4.84	152.0 ± 55.5	

*p = 0.036 vs. rose bengal alone.
TA: thioctic acid; TBARS: thiobarbituric acid-reactive substances; a: incubation in the dark; b: after illumination; n: number of separate preparations.

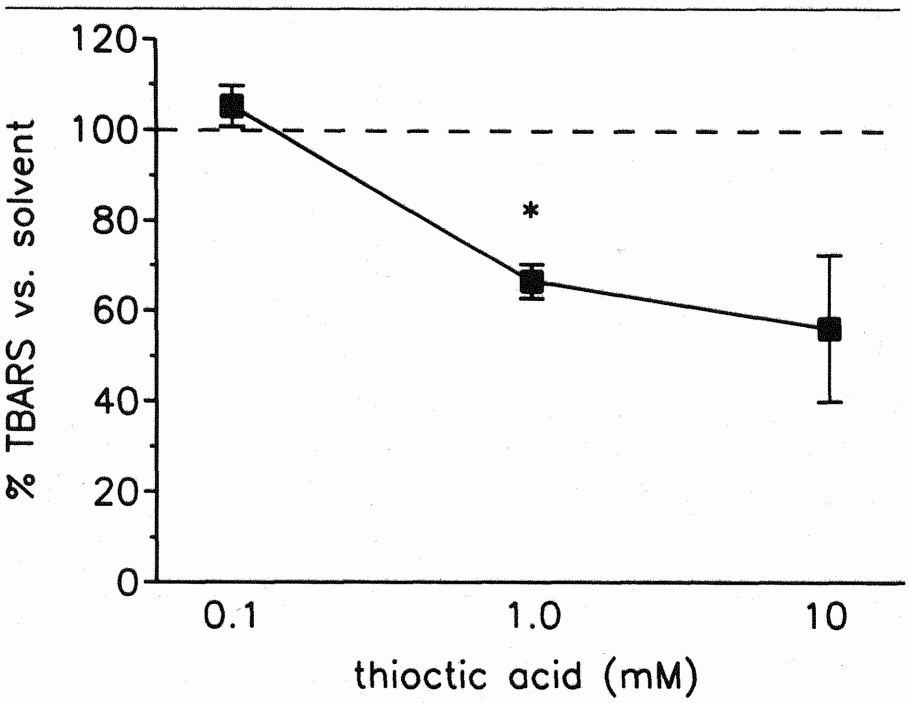

Figure 4. Relative amount of TBARS in the presence of thioctic acid in addition to rose bengal (squares) in relation to incubation with rose bengal alone (=100%). n = 3 to 6 separate preparations; *p, p = 0.036 vs. rose bengal alone.

neity of the cell population, which makes it possible to evaluate the characteristics of individual cells in the absence of external influences, i.e., interactions between myocytes and microvasculature, regional differences in blood flow, influences of neighboring tissues, and neuronal, mechanical, and hormonal modulation [17–19]. In addition, since a large number of cells are obtained from one organ, a multitude of experiments can be carried out, thereby saving on experimental animals. On the other hand, experimental methods using isolated cells are not devoid of shortcomings [19]. The proteolytic enzymes used during isolation may have altered some of the sarcolemmal components and may therefore influence certain cell functions. Also, removing cells from their natural habitat creates an experimental condition that may profoundly differ from the in vivo situation, e.g., the bathing medium of isolated cells represents an infinite space in contrast to the limited extracellular space in intact myocardium. This difference may result in extra- and intracellular concentrations of ions and metabolites that are not the same as those found in multicellular preparations. Therefore, discrepancies between in vivo and in vitro situations are inevitable; however, they do not necessarily invalidate the model.

The deleterious effect of singlet oxygen generated by rose bengal–photoexcitation on isolated cardiac myocytes associated with the occurrence of TBARS indicative

for lipid peroxidation, as seen in the present study, corresponds to previous findings from Ver Donck et al. [12]. The photoexcitation of the light-sensitive dye rose bengal is known as an efficient generator of singlet molecular oxygen [20,21]. This active oxygen species is generated from active quenching of the lowest photoexcited dye triplet state by molecular oxygen [22] and forms endoperoxides in unsaturated lipids by additional reactions with isolated double bonds [23,24].

The present data indicate a protective effect of thioctic acid against singlet-oxygen-induced hypercontracture in isolated cardiac myocytes that showed a dose-dependent behavior. Preincubation with 1 mM thioctic acid increased the number of rod-shaped myocytes and reduced the production of TBARS following photoexcitation of rose bengal. The reduction of TBARS suggests that the protective effect of thioctic acid can be attributed to its antioxidative action. The efficacy of 1 mM thioctic acid corresponds well to concentrations that have been shown to exert antioxidative activity by other investigators [25,26]. The protection could have been due to absorption of light by thioctic acid responsible for activation of rose bengal. This seems unlikely, however, because the maximum light absorption for thioctic acid lies below 400 nm (335 nm, data not shown). At 10 mM, however, thioctic acid obviously lost its protective activity and adversely appeared to increase the singlet-oxygen-induced myocyte damage. In contrast, concomitantly the amount of TBARS remained low, indicating a separation of the protective effect from prevention of lipid peroxidation. An explanation for this phenomenon may come from interactions of thioctic acid with cellular membranes. Hofmann et al. [27] reported that the R- and S-enantiomers of the racemic mixture of thioctic acid exerted different activities. At higher concentrations, the S-enantiomer lost its positive effect on membrane fluidity, indicating that, when exceeding an optimal concentration, the site of membrane interaction no longer allows a favorable high equilibrium between sulfhydryl groups and disulfides. This finding may provide a possible explanation for the deleterious effect of 10 mM thioctic acid in our study.

Several mechanisms may have contributed to the protective effect of thioctic acid:

1. Thioctic acid has been shown to quench singlet oxygen in a chemical reaction with a high quenching constant [26,28].
2. Thioctic acid is readily taken up by mammalian cells and reduced intracellularly to dihydrolipoic acid [29], yet the exact mechanism of reduction is unknown. The redox couple dihydrolipoic acid–thioctic acid has a strong redox potential of −0.32 V [30], which enables it to reduce the oxidized forms of other antioxidants like ascorbate and glutathion, which in turn recycle vitamin E [31,32]—the major chain-breaking antioxidant that protects membranes from lipid peroxidation [33].
3. Lipid peroxidation of membranes causes oxidation of sulfhydryl groups, forming disulfides [34]. A loss of sulfhydryl groups is paralleled by a substantial decrease in membrane fluidity [35]. The redox couple dihydrolipoic acid–thioctic acid was shown to restore the availability of sulfhydryl groups and to increase mem-

brane fluidity [27]. This direct interaction of thioctic acid with biomembranes may also contribute to its protective activity.

In conclusion, the data of the in vitro study reported here may provide a rationale for further investigations to test the usefulness of thioctic acid in therapeutic situations such as ischemia–reperfusion injury during open heart surgery.

ACKNOWLEDGMENT

The authors are grateful to Professor G. Zimmer for his helpful discussions during the preparation of this chapter.

REFERENCES

1. Marx JL. 1987. Oxygen free radicals linked to many diseases. Science 235:529–531.
2. Hearse DJ, Humphrey SM, Bullock GR. 1978. The oxygen paradox and the calcium paradox: two facets of the same problem? J Mol Cell Cardiol 10:641–668.
3. Garlick PB, Davies MJ, Hearse DJ, Slater TF. 1987. Detection of free radicals in the reperfused rat heart using electron spin resonance spectroscopy. Circ Res 61:757–760.
4. Borbe HO, Ulrich H (eds). 1989. Thioctsäure. Frankfurt: pmi Verlag GmbH.
5. Serbinova E, Khwaja S, Reznick AZ, Packer L. 1992. Thioctic acid protects against ischemia–reperfusion injury in the isolated perfused Langendorff heart. Free Radical Res Commun 17:49–59.
6. Haramaki N, Packer L, Assadnazari H, Zimmer G. 1993. Cardiac recovery during post-ischemic reperfusion is improved by combination of vitamin E with dihydrolipoic acid. Biochem Biophys Res Commun 196:1101–1107.
7. Scholich H, Murphy ME, Sies H. 1989. Antioxidant activity of dihydrolipoate against microsomal lipid peroxidation and its dependence on alpha-tocopherol. Biochim Biophys Acta 1001:256–261.
8. Lee PCC, Rodgers MAJ. 1987. Laser flash photokinetic studies of rose bengal sensitized photodynamic interactions of nucleotides and DNA. Photochem Photobiol 45:79–86.
9. Piper HM, Probst I, Schwartz P, Hütter JF, Spiekermann PG. 1982. Culturing of calcium stable adult cardiac myocytes. J Mol Cell Cardiol 14:397–412.
10. Ver Donck L, Pauwels PJ, Vandeplassche G, Borgers M. 1986. Isolated rat cardiac myocytes as an experimental model to study calcium overload: the effect of calcium entry blockers. Life Sci 38:765–772.
11. Lowry OH, Rosenborogh NJ, Farr AL, Randall RJ. 1951. Protein measurement with the folin–phenol reagent. J Biol Chem 193:265–267.
12. Ver Donck L, Van Reempts J, Vandeplassche G, Borgers M. 1988. A new method to study activated oxygen species induced damage in cardiomyocytes and protection by Ca^{2+}-antagonists. J Mol Cell Cardiol 20:811–823.
13. Slade AM, Severs NJ, Powell T, Twist VW. 1983. Isolated calcium-tolerant myocytes and the calcium paradox: an ultrastructural comparison. Eur Heart J 4(Suppl H):113–122.
14. Wong SHY, Knight JA, Hopfer SM, Zaharia O, Leach CN Jr, Sunderman FW Jr. 1987. Lipoperoxides in plasma as measured by liquid-chromatographic separation of malondialdehyde-thiobarbituric acid adduct. Clin Chem 33:214–220.
15. Gutteridge JM. 1975. The use of standards for malondialdehyde. Anal Biochem 69:518–526.
16. Sachs L. 1992. Angewandte Statistik, 7th ed. Berlin: Springer Verlag.
17. Dow JW, Harding NGL, Powell T. 1981. Isolated cardiac myocytes. (I) Preparation of adult myocytes and their homology with intact tissue. Cardiovasc Res 15:483–514.
18. Piper HM, Schwartz P, Spahr R, Hütter JF, Spiekermann PG. 1984. Absence of reoxygenation damage in isolated heart cells after anoxic injury. Pflügers Arch 401:71–76.
19. Borgers M, Ver Donck L, Vandeplassche G. 1988. Pathophysiology of cardiomyocytes. Ann N Y Acad Sci 522:433–453.
20. Pooler JP, Valenzo DP. 1981. Dye-sensitized photodynamic inactivation of cells. Med Phys 8:614–628.
21. Gandin E, Lion Y, Van de Vorst A. 1983. Quantum yield of singlet oxygen production by xanthene derivatives. Photochem Photobiol 37:271–278.

22. Foote CS. 1976. Photo-sensitized oxidation and singlet oxygen: consequences in biological systems. In Pryor WD (ed), Free Radicals in Biology, vol II. New York: Academic Press, pp. 85–134.
23. Halliwel B, Gutteridge JMC. 1985. Free Radicals in Biology and Medicine. Oxford: Clarendon Press.
24. Rawls HR, Van Santen PJ. 1970. A possible role for singlet oxygen in the initiation of fatty acid autoxidation. J Am Oil Chem Soc 47:121–125.
25. Suzuki YJ, Tsuchiya M, Packer L. 1991. Thioctic acid and dihydrolipoic acid are novel antioxidants which interact with reactive oxygen species. Free Rad Res Commun 15:255–263.
26. Devasagayam TPA, Subramanian M, Pradhan DS, Sies H. 1993. Prevention of singlet oxygen-induced DNA damage by lipoate. Chem Biol Interactions 86:79–92.
27. Hofmann M, Mainka M, Tritschler H, Fuchs J, Zimmer G. 1995. Decrease of red cell membrane fluidity and -SH groups due to hyperglycemic conditions is counteracted by alpha-lipoic acid. Arch Biochem Biophys 324:85–92.
28. Kaiser S, Di Mascio P, Sies H. 1989. Lipoat und Singulettsauerstoff. In Borbe HO, Ulrich H (eds), Thioctsäure. Frankfurt: pmi Verlag GmbH, pp. 69–76.
29. Handelman GJ, Han D, Tritschler H, Packer L. 1994. Alpha-liponic acid reduction by mammalian cells to the dithiol form and release into the culture medium. Biochem Pharmacol 47:1725–1730.
30. Jocelyn PC. 1967. The standard redox potential of cysteine–cystine from the thiol–disulphide exchange reaction with glutathione and lipoic acid. Eur J Biochem 2:327–331.
31. Bast A, Haenen GRMM. 1990. Regulation of lipid peroxidation of glutathion and lipoic acid: involvement of liver microsomal vitamin E free radical reductase. In Emerit I, Packer L, Auclair C (eds), Antioxidants in Therapy and Preventive Medicine. New York: Plenum Press, pp. 111–116.
32. Kagan VE, Shvedova A, Serbinova E, Khan S, Swanson C, Powell R, Packer L. 1992. Dihydrolipoic acid—a universal antioxidant both in the membrane and in the aqueous phase. Biochem Pharmacol 44:1637–1649.
33. Burton GW, Ingold KU. 1981. Autoantioxidation of biological molecules: 1. The antioxidant activity of vitamine E and related chain breaking phenolic antioxidants in vitro. J Am Chem Soc 103:6472–6477.
34. Yagi T, Hatefi Y. 1984. Thiols in oxidative phosphorylation: inhibition and energy-potentiated uncoupling by monothiol and dithiol modifiers. Biochemistry 24:2449–2455.
35. Zimmer G, Freisleben HJ. 1988. Membrane fluidity determinations from viscosimetry. In Aloia RC, Curtain CC, Gordon LM (eds), Advances in Membrane Fluidity, vol 1. Methods for Studying Membrane Fluidity. New York: Alan R Liss, pp. 297–318.

This Page Intentionally Left Blank

TRANSFECTION OF HEAT-SHOCK PROTEIN 70 ENHANCES MYOCARDIAL TOLERANCE TO ISCHEMIA: EVIDENCE FOR A ROLE OF HSP70 IN ISCHEMIA–REPERFUSION INJURY

YOSHIKI SAWA, KEN SUZUKI, YASUFUMI KANEDA, KEISHI KADOBA, HONG-ZHI BAI, KOJI KAGISAKI, RYUICHI MORISHITA, and HIKARU MATSUDA

Osaka University

Summary. The enhancement of myocardial tolerance mediated by heat-shock protein 70 (HSP70) can be utilized for further advancement in myocardial protection in clinical settings. Recently, we have developed a novel in vivo gene transfection method for the entire heart. We investigated the possibility of enhancing myocardial tolerance to ischemia–reperfusion injury by introducing the HSP70 gene into the whole heart by means of in vivo gene transfection with HVJ (Hemagglutinating virus of Japan)–liposome procedure. HVJ–liposome, either with the human HSP70 gene (H group; $n = 5$) or without the gene (C group; $n = 5$), was infused into rat hearts via the coronary arteries. The hearts obtained from nontreated rats (N group; $n = 5$) were also examined. Western blotting analysis clearly showed overexpression of HSP70 in the H group. Recovery rate of left ventricular developed pressure, rate–pressure product, and coronary flow after ischemia–reperfusion injury (37°C, 30 minutes) were significantly higher for the H group than for either the C or N group ($p < 0.05$). CK leakage for the first five minutes of reperfusion was lower in the H group than in the C and N groups ($p < 0.05$). HSP70 was overexpressed in rat hearts as a result of in vivo gene transfection with HVJ–liposome. Higher myocardial tolerance to ischemia–reperfusion injury was observed in the HSP70-overexpressing heart as compared to the control and even the nontreated hearts. Our results demonstrate the protective effect of gene-transfection-induced HSP70 against ischemia–reperfusion injury in the myocardium, suggesting the possibility of clinical application of gene therapy with HSP70 to ischemia–reperfusion injury.

INTRODUCTION

Heat-shock protein (HSP) is a self-preservation protein that is induced in order to maintain cell homeostasis against various forms of stress, such as heat stress [1–3]. In

S. Mochizuki, N. Takeda, M. Nagano and N. Dhalla (eds.). THE ISCHEMIC HEART.

HSP families, HSP70 is induced in the myocardium under various forms of stress, such as whole-body heat shock [4–11], brief ischemia [12–14], warm blood cardioplegia [15], administration of certain drugs [16–18], hemodynamic overload [19], or myocardial stretch [20]. These HSP70-overexpressing hearts show enhanced myocardial tolerance to ischemia–reperfusion injury. However, previous experiments using these induction methods for HSP70 could not provide sufficient evidence that HSP70 enhances tolerance to ischemia in the myocardium, because such methods are liable to increase catalase activities [5,9,16,21,22] or to generate some other cytoprotective proteins such as superoxide dismutase [15,16] and other HSP families [12,16,19,23,24]. To establish direct evidence of improvement in myocardial tolerance with HSP70, a method to alter genetic information, such as transgenic or gene transfection, should be used.

Current studies reported that transgenic mice overexpressing HSP70 showed a significant increase in myocardial tolerance to ischemia–reperfusion injury, indicating a direct effect of HSP70 on myocardial ischemia–reperfusion injury [25,26]. In a transgenic model, however, the heart is genetically altered to overexpress HSP70 inborn, so it may adapt itself to such a situation and thus develop a character different from that of the natural heart. Therefore, this model may be unsuitable for investigating the effect of the induction of HSP70 acquired in clinical settings. Moreover, the transgenic technique itself reportedly presents serious difficulties for clinical application.

Intravenous injection [27,28] or direct injection [29–32] methods for gene delivery to the heart have been previously reported. However, a method for transfection to the entire heart, one that can overexpress proteins in the entire heart and enhance cardiac function, has not yet been established. We have recently developed and reported on a novel gene transfection method for the entire heart, mediated by the Hemagglutinating virus of Japan (HVJ)–liposome [33]. Therefore, it is felt that gene transfection of HSP70 with our method may provide both direct evidence and the possibility for clinical application of HSP70 to myocardial ischemia–reperfusion injury.

The objective of the study reported here was to investigate whether HSP70 induced by this gene transfection method enhances myocardial tolerance to ischemia–reperfusion injury.

METHODS

Animal care

All studies were performed with the approval of the Ethical Committee for Animal Research, Osaka University Medical School.

Construction of cDNA of HSP70

The multicloning sites of expression vector pcDNA3 (Invitrogen corporation, cytomegalovirus promoter) was restricted by EcoR1/BamH1. A full-length human HSP70 cDNA (5725 bps), kindly provided by Dr. Sue Fox (Department of Bio-

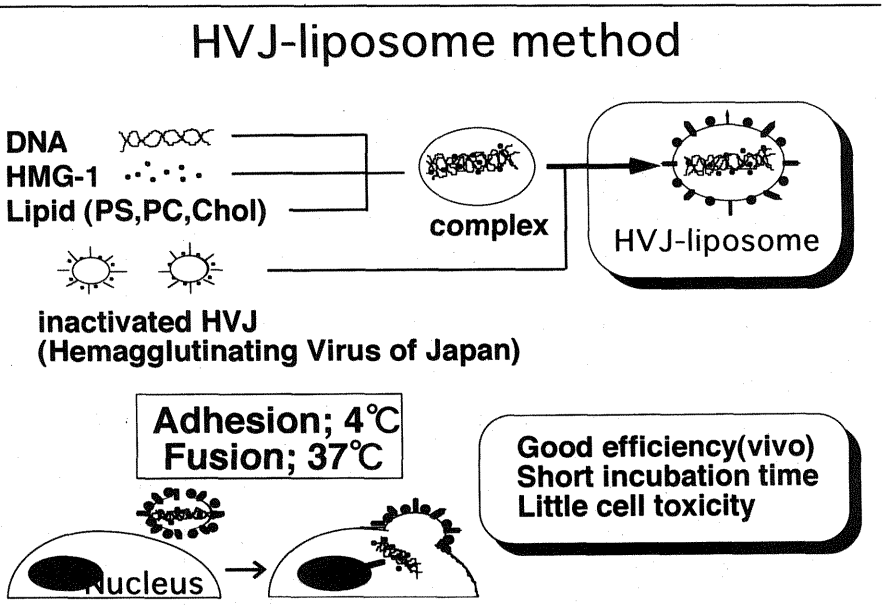

Figure 1. Scheme of HVJ–liposome method. Dry lipid [phosphatidylserine (PS), phosphatidylcholine (PC), and cholesterol (Chol)] were mixed with high-mobility-group (HMG) 1 nuclear protein, prepared by vortexing, sonication, and shaking, and then mixed with inactivated HVJ.

chemistry, Molecular Biology and Cell biology, Northwestern University, USA), was restricted by EcoR1/BamH1 and inserted into the previously restricted pcDNA3.

Preparation of HVJ–liposome (figure 1)

The preparation of HVJ–liposome has been previously described [34–43]. Briefly, dry lipid (phosphatidylserine, phosphatidylcholine, and cholesterol) were mixed at a weight ratio of 1:4.8:2. The lipid mixture (10 mg) was deposited on the side of a flask by removing tetrahydrofuran in a rotary evaporator. High-mobility-group (HMG) 1 nuclear protein was purified from calf thymus. A DNA–HMG1 complex (200 μg:64 μg) was then formed by incubation at 20°C for one hour. The dried lipid was hydrated in 200 μL of a balanced salt solution (BSS; 137 mM NaCl, 5.4 mM KCl, 10 mM Tris-HCl, pH 7.6) containing the DNA–HMG1 complex. A liposome–DNA–HMG1 complex suspension was prepared by vortexing, sonication for three seconds, and shaking for 30 minutes to form liposomes. Purified HVJ (Z strain) was inactivated by ultraviolet irradiation (110 erg/mm^2/second) for three minutes just before use. The liposome suspension (0.5 mL, containing 10 mg of lipids) was mixed with HVJ (30,000 hemagglutinating units) in a total volume of 2 mL of BSS for fusion into HVJ–liposomes. The mixture was incubated at 4°C for 10 minutes and then at 37°C for 30 minutes under gentle shaking. Free HVJ was

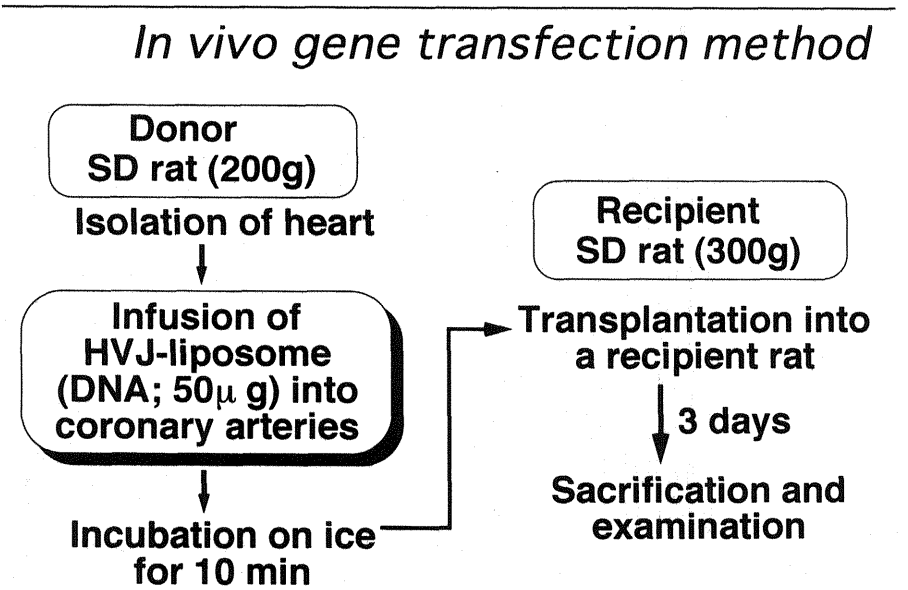

Figure 2. In vivo gene transfection method into myocardium. The hearts of Sprague–Dawley rats were arrested with cold crystalloid cardioplegic solution and isolated. HVJ–liposome solution was delivered into the coronary arteries through the canula during cardiac arrest. The hearts were then heterotopically transplanted into the abdomens of recipient rats of the same strain. Rats were sacrificed under ether anesthesia on the third day after transfection.

removed from the HVJ–liposomes by sucrose density gradient centrifusion. The top layer of the sucrose gradient containing the HVJ–liposome solution was collected for use.

Gene transfection through coronary arteries (figure 2)

Under anesthesia with sodium pentobarbital (50 mg/kg, intraperitoneal injection) and anticoagulation with heparin (200 USP units, intraperitoneal injection), the hearts of Sprague–Dawley rats (weight: 200–220 g) were transfected with gene as described before [28]. Briefly, the rat hearts were arrested with cold crystalloid cardioplegic solution and isolated. A canula for coronary infusion was inserted through the aorta. A total of 1 mL of HVJ–liposome solution, either with cDNA of HSP70 (H group; $n = 5$) or without (C group; $n = 5$) was delivered into the coronary arteries through the canula during cardiac arrest. The hearts were then heterotopically transplanted into the abdomens of recipient rats of the same strain (weight: 300 g) under general anesthesia according to the methods described before. Rats were sacrificed under ether anesthesia on day 3 after transfection, thus allowing the introduced gene to express proteins and to decrease HSP70 intrinsically induced by transfection procedure.

Nontreated rats

Nontreated rats were sacrificed under ether anesthesia, and the hearts (N group; $n = 5$) were also examined without transplantation.

Western blotting analysis

The hearts from the three groups were immediately frozen in liquid nitrogen and homogenized with tissue homogenizer in phosphate buffered saline (137 mmol/L NaCl, 2.7 mmol/L KCl, 1.5 mmol/L KH_2PO_4, 8.0 mmol/L $NaHPO_4$) containing 2 mmol/L of phenylmethanesulfonyl fluoride and centrifuged at 3000 rpm at 4°C for 10 minutes. The supernatant was centrifuged once at 15,000 rpm at 4°C and again at 30,000 rpm at 4°C. Protein concentrations were determined with the bicinchoninic acid method (BCA Protein Assay Reagent, Pierce). Equal amount of proteins were denatured in Laemmli's sample buffer, boiled for five minutes, and loaded onto a sodium dodecylsulphate 7.5% polyacrylamide gel electrophoresis system and subjected to 200 V until the dye front reached the lower margin of the gel. Following one-dimensional electrophoresis, the proteins were transferred onto a 0.2-micron PVDF membrane (BIO-RAD) at 300 mA for one hour. Blots were incubated in Tris-buffered saline-Tween 20 (TBST; 20 mmol/L Tris-HCl, pH 7.5, 150 mmol/L NaCl, 0.05% Tween 20) containing 2% skim milk to block nonspecific binding sites on the membrane. The membrane was immunoreacted overnight at 4°C with a 1:1000 dilution of antihuman HSP70 monoclonal antibody (SPA-810, Stress Gen Biotechnologies Corp.) in TBST containing 1% skim milk. Following further repeated washing in TBST containing 2% skim milk, the blots were incubated for one hour at 25°C in a 1:1000 dilution of alkaline phosphatase-conjugated goat antimouse IgG (Cappel) in TBST containing 1% skim milk. The membrane was then washed in TBST containing 2% skim milk and incubated with 50 mg/mL of 5-bromo-4-chloro-3-indolyl phosphate to which 75 mg/mL of nitro blue tetrazolium in carbonate buffer was added for coloring.

Myocardial tolerance to ischemia–reperfusion injury

Rats from three groups were anesthetized by ether inhalation and anticoagulated by intravenous injection of 200 USP units of heparin. Rat hearts were quickly excised, immersed in cold perfusion buffer, and perfused retrogradely through aortic cannula by using the Langendorff apparatus with a modified Krebs–Henseleit buffer (120 mmol/L NaCl, 4.5 mmol/L KCl, 20 mmol/L $NaHCO_3$, 1.2 mmol/L KH_2PO_4, 1.2 mmol/L $MgCl_2$, 2.5 mmol/L $CaCl_2$, and 10 mmol/L glucose; gassed with 95% O_2 + 5% CO_2 obtain pH 7.4 at 37°C) with pressure equal to 1 mH_2O. The temperature of the hearts was maintained at 37°C with a water-jacketed chamber. A thin-wall latex balloon was inserted into the left ventricle through the left atrium to measure the left ventricular pressure. After 30 minutes of stabilization, the heart rate (HR), left ventricular (LV) systolic pressure, and coronary flow (CF) were measured with the LV end-diastolic pressure stabilized at 10 mmHg. The hearts were then exposed to global ischemia for 30 minutes at 37°C, followed by

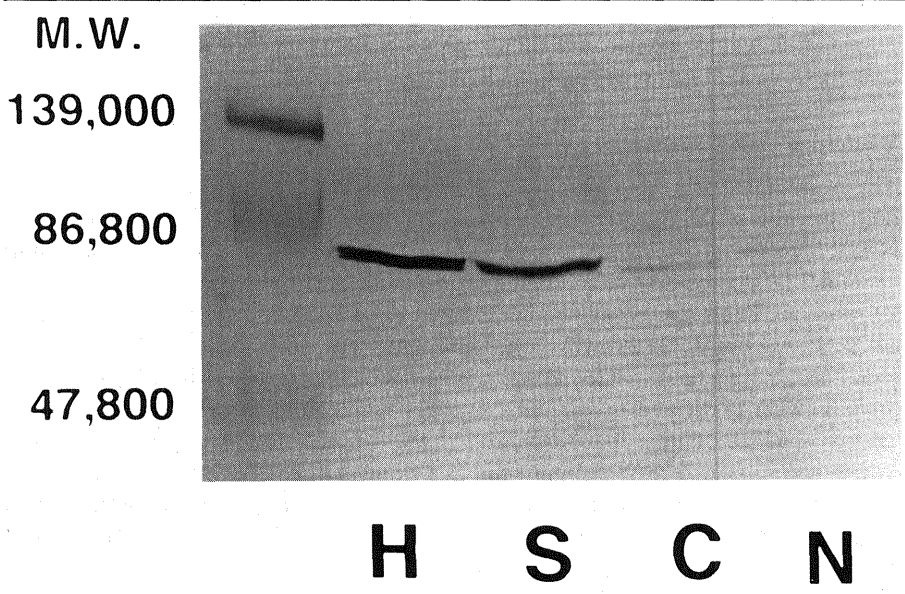

Figure 3. Western blotting analysis for HSP70. Stronger expression of HSP70 was observed in the H group than in the C and N groups. MW: molecular weight.

reperfusion with 37°C Krebs–Henseleit buffer solution. The reperfusate during the first five minutes was collected to measure CK leakage. After 30 minutes of reperfusion, HR, LV pressure, and CF were measured at 10 mmHg of LV end-diastolic pressure.

Statistical analysis

All values were expressed as mean ± SEM. Statistical analysis was performed with the Bonferrioni/Dunn (Dunn's procedure as a multiple comparison procedure) method (Statview Software, Macintosh). A value of p less than 0.05 was considered statistically significant.

RESULTS

Fifteen rats were divided into three groups and examined for the effect of HSP70 introduced by gene transfection on ischemia–reperfusion injury. Five rat hearts in the H group were infused through coronary arteries with HVJ–liposome solution containing cDNA of human HSP70. Another five rat hearts infused with HVJ–liposome solution without gene (C group) and another five hearts isolated from nontreated rats (N group) were examined and compared to the H group. The expression of HSP70 was evaluated with Western blotting analysis using a monoclonal antibody to human HSP70. The myocardial tolerance to ischemia–reperfusion injury was assessed with the Langendorff perfusion model.

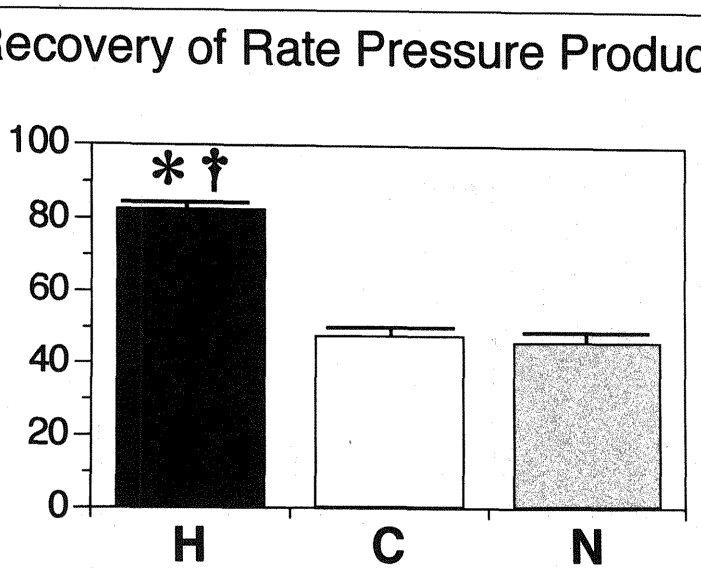

Figure 4. Percent recovery of rate–pressure product. Better recovery of rate–pressure product was shown in the H group than in the C and N groups. *, $p < 0.05$ vs. the C group; †, $p < 0.05$ vs. the N group. All values were expressed as mean ± SEM.

Western blotting analysis

Western blotting analysis clearly showed stronger expression of HSP70 in the H group than in the C and N groups (figure 3). In the C and N groups, only thin bands were observed, which were considered to represent rat constitutive HSP70.

Myocardial tolerance to ischemia–reperfusion injury

Assessment of the H group with the Langendorff perfusion model showed enhanced recovery of myocardial function as well as attenuated myocardial damage after ischemia–reperfusion injury. There was no significant difference in heart rates among any of the groups. The recovery rate of the rate–pressure product (RPP) was significantly ($p < 0.05$) higher for the H group (82.2% ± 2.4%) than for the C (46.0% ± 4.8%) and N (47.8% ± 6.1%) groups when LV end-diastolic pressure was maintained at 10 mmHg (figure 4). The recovery rate of the left ventricular developed pressure (LVDP) was also significantly ($p < 0.05$) higher for the H group (94.2% ± 2.1%) than for the C (50.2% ± 3.3%) and N (50.6% ± 10.5%) groups. Finally, the recovery rate of the coronary flow was significantly ($p < 0.05$) higher for the H (91.4% ± 2.8%) group than for the C (63.6% ± 5.2%) and N (61.4% ± 7.9%) groups (figure 5). In addition, CK leakage during the first five minutes of reperfusion was significantly ($p < 0.05$) lower in the H (110.4 ± 12.3 IU) group than that in the C (222.6 ± 52.4 IU) and N (210.0 ± 24.8 IU) groups (figure 6). The C and N groups showed no significant differences in the recovery rate of RPP, LVDP, and coronary flow, nor in CK leakage.

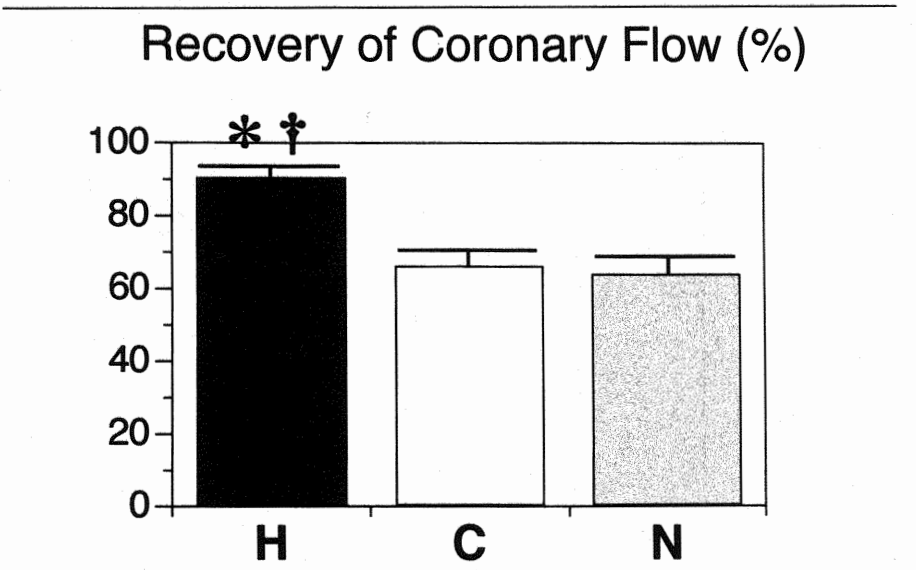

Figure 5. Percent recovery of coronary flow. Better recoveries of coronary flow were shown in the H group than in the C and N groups. *, $p < 0.05$ vs. the C group; †, $p < 0.05$ vs. the N group. All values were expressed as mean ± SEM.

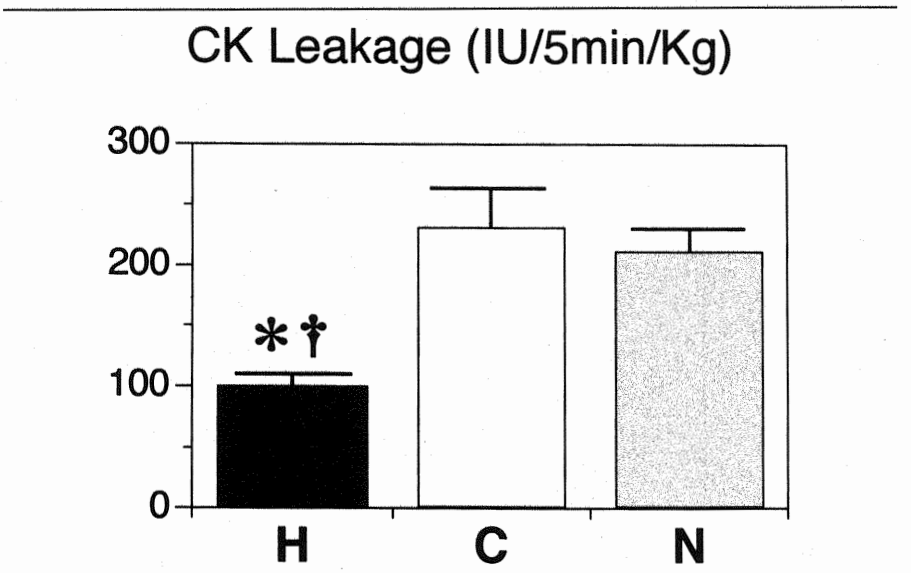

Figure 6. CK leakage for the first five minutes of reperfusion. CK leakage in reperfusion was lower in the H group than in the C and N groups. *, $p < 0.05$ vs. the C group; †, $p < 0.05$ vs. the N group. All values were expressed as mean ± SEM.

DISCUSSION

The contribution of HSP70 itself to the improvement in myocardial tolerance had not been proved in previous in vivo experiments [4–20] because of the difficulty in isolating the effect of HSP70 alone. The enhancement of tolerance to different types of stress mediated by overexpressed HSP70 induced by in vitro gene transfection has been reported in various cells, such as in the case of thermal stress in fibroblasts [34] or in rat-derived cell line H9c [35], in metabolic stress in mouse 10 T1/2 cell [36], and in ischemia in rat embryonic heart-derived cell line H9c(2-1) [37]. However, none of these cells are adult cardiac myocytes, and these experiments in vitro have different conditions from those in vivo. In addition, no reports have been published on an in vivo transfection method for the whole heart [33]. In this study, we have demonstrated that our gene transfection method can induce an overexpression of HSP70 in the entire heart and enhance the ischemic tolerance of the heart. An investigation using this method, as well as a study using transgenic mice overexpressing HSP70 [25,26], could thus provide evidence of the enhancement of myocardial tolerance mediated by HSP70 itself. However, the conditions for models with transgenic mice and with gene transfection seem to be different. Our results demonstrate the protective effect of HSP70 under different conditions from those in studies with transgenic mice [25,26].

Recent developments in cardiac protection have improved the outcomes of cardiac surgery and cardiac preservation. However, even the latest myocardial protection techniques are still limited in their effectiveness, and further modifications appear to be needed. Enhancement of the self-preservation capacity of the myocardium appears to be quite useful for the establishment of further advanced myocardial protection. Therefore, the enhancement of myocardial tolerance mediated by overexpressed HSP70 may be a candidate for further advancement in myocardial protection in clinical settings. To apply HSP70 in clinical settings, previously described methods for inducing HSP70 [4–20] involve some difficulties. Whole-body heat stress [4–11] appears to involve risks of causing some harmful effects in other organs, such as the cerebral system. Drugs such as adriamycin or heavy metals [16–18] are also thought to produce injurious side effects. Furthermore, these methods are seriously limited in their capacity to induce HSP70 and in the duration of induction. Warm (42°C) blood cardioplegia has been reported as a new approach for myocardial preservation in cardiac surgery [15]. This method seems to have more potential for clinical application, but also seems to have serious limitations in terms of HSP70 inducing capacity and duration. In contrast, our gene transfection method with the viral envelope (HVJ–liposome) can overexpress HSP70 without myocardial damage, virus infection, or side effects on other organs [33]. Furthermore, the duration of overexpression of HSP70 is much longer than that obtained with the method described above [33]. Therefore, our method is seen to have a major potential for clinical application in cases of myocardial protection, cardiac preservation, or transplantation. Our transfection method still needs further investigation for clinical application, such as determination of the optimal amount

and duration of HSP70 overexpression, reducing the incubation time after transfection, or minimizing the side effects of the overexpression of proteins.

To conclude, we have demonstrated that HSP70 was overexpressed in rat hearts with in vivo gene transfection mediated by HVJ–liposome and that myocardial tolerance to ischemia–reperfusion injury was enhanced in the HSP70-overexpressing heart. These results demonstrate the role of HSP70 in preventing myocardial ischemia–reperfusion injury, thus suggesting the possibility of clinical application of gene therapy with HSP70 to ischemia–reperfusion injury of the heart.

ACKNOWLEDGMENT

We would like to express our gratitude to Dr. Sue Fox (Department of Biochemistry, Molecular Biology and Cell Biology, Northwestern University, USA) who kindly provided us with a full-length human HSP70 cDNA.

REFERENCES

1. Lindquist S, Craig EA. 1988. The heat-shock proteins. Annu Rev Genet 22:631–677.
2. Schlesinger MJ. 1990. Heat shock proteins. J Biol Chem 265:12111–12114.
3. Black SC, Lucchesi BR. 1993. Heat shock proteins and the ischemic heart. An endogenous protective mechanism. Circulation 87:1048–1050.
4. Currie RW. 1987. Effect of ischemia and perfusion temperature on synthesis of stress-induced (heat shock) proteins in isolated and perfused rat hearts. J Mol Cell Cardiol 19:795–808.
5. Karmmazyn M, Mailer K, Currie RW. 1990. Acquisition and decay of heat-shock-enhanced postischemic ventricular recovery. Am J Physiol H424–H431.
6. Currie RW, Tanguay RM, Kingma JG. 1993. Heat shock response and limitation of tissue necrosis during occlusion/reperfusion in rabbit hearts. Circulation 87:963–971.
7. Yellon DM, Pasini E, Cargnoni A, Marber MS, Latchman DS, Ferrari R. 1992. The protective role of heat stress in the ischemic and reperfused rabbit myocardium. Mol Cell Cardiol 24:895–907.
8. Walker DM, Pasini E, Kucukoglu S, Marber MS, Iliodromitis E, Ferrari R, Yellon DM. 1993. Heat stress limits infarct size in the isolated perfused rabbit heart. Cardiovasc Res 27:962–967.
9. Steare SE, Yellon DM. 1993. The protective effect of heat stress against reperfusion arrhythmias in the rat. J Mol Cell Cardiol 25:1471–1481.
10. Donnely TJ, Sievers RE, Vissern FLJ, Welch WJ, Wolfe CL. 1992. Heat shock protein induction in rat hearts. A role for improved myocardial salvage after ischemia and reperfusion? Circulation 85:769–778.
11. Hutter MM, Sievers RE, Barbosa V, Wolfe CL. 1994. Heat shock protein induction in rat heart. A direct correlation between the amount of heat-shock protein induced and the degree of myocardial protection. Circulation 89:355–360.
12. Marber MS, Latchman DS, Walker JM, Yellon DM. 1993. Cardiac stress protein elevation 24 hours after brief ischemia or heat stress is associated with resistance to myocardial infarction. Circulation 88:1264–1272.
13. Sun JZ, Tang XL, Knowlton AA, Park SW, Qiu Y, Bolli R. 1995. Late preconditioning against myocardial stunning. An endogenous protective mechanism that confer resistance to postischemic dysfunction 24 h after brief ischemia in conscious pigs. J Clin Invest 95:388–403.
14. Knowlton AA, Brecher P, Apstein CS. 1991. Rapid expression of heat shock protein in the rabbit after brief cardiac ischemia. J Clin Invest 87:139–147.
15. Liu X, Engelman RM, Moraru II, Rousou JA, Flack JE, Deaton DW, Maulik N, Das DK. 1992. Heat shock. A new approach for myocardial preservation in cardiac surgery. Circulation 86:358–363.
16. Maulik N, Wei Z, Liu X, Engelman RM, Rousou JA, Das DK. 1994. Improved postischemic ventricular functional recovery by amphetamine is linked with its ability to induce heat shock. Mol Cell Biochem 137:17–24.
17. Huber SA. 1992. Heat-shock protein induction in adriamycin and picornavirus-infected cardiocytes. Lab Invest 67:218–224.

18. Low-Friedrich I, Schoeppe W. 1991. Effects of calcium channel blockers on stress protein synthesis in cardiac myocytes. J Cardiovasc Pharm 17:800–806.
19. Delcayre C, Samuel JL, Marotte F, Best-Belpome M, Mercadier JJ, Rappaport L. 1988. Synthesis of stress proteins in rat cardiac myocytes 2–4 days after imposition of hemodynamic overload. J Clin Invest 82:460–468.
20. Knowlton AA, Eberli FR, Brecher P, Romo GM, Owen A, Apstein CS. 1991. A single myocardial stretch or decreased systolic fiber shortening stimulates the expression of heat shock protein 70 in the isolated, erythrocyte-perfused rabbit heart. J Clin Invest 88:2018–2025.
21. Currie RW, Karmazyn M. 1990. Improved post-ischemic ventricular recovery in the absence of changes in energy metabolism in working rat heart following heat-shock. J Mol Cell Cardiol 22:631–636.
22. Currie RW, Karmazyn M, Klog M, Mailer K. 1988. Heat-shock response is associated with enhanced postischemic ventricular recovery. Circ Res 63:543–549.
23. Currie RW, Tanguay RM. 1991. Analysis of RNA for transcripts for catalase and SP71 in rat hearts after in vivo hyperthermia. Biochem Cell Biol 69:375–382.
24. Wall SR, Fliss H, Korecky B. 1993. Role of catalase in myocardial protection against ischemia in heat shocked rats. Mol Cell Biochem 129:187–194.
25. Marber MS, Mestril R, Chi SH, Sayen R, Yellon DM, Dillmann WH. 1995. Overexpression of the rat inducible 70-kD heat stress protein in a transgenic mouse increases the resistance of the heart to ischemic injury. J Clin Invest 95:1446–1456.
26. Plumier JCL, Ross BM, Currie RW, Angelidis CE, Kazlaris H, Kollias G, Pagoulatos GN. 1995. Transgenic mice expressing the human heat shock protein 70 have improved post-ischemic myocardial recovery. J Clin Invest 95:1854–1860.
27. Stratford-Perricaudet LD, Makeh I, Perricaudet M, Briand P. 1992. Widespread long-term gene transfer to mouse skeletal muscles and heart. J Clin Invest 90:626–630.
28. Zhu N, Liggitt D, Liu Y, Debs R. 1993. Systemic gene expression after intravenous DNA delivery into adult mice. Science 261:209–211.
29. Kass-Eisler A, Falck-Pedersen E, Alvira M, Rivera J, Buttrick PM, Wittenberg BA, Cipriani L, Leinwand LA. 1993. Quantitative determination of adenovirus-mediated gene delivery to rat cardiac myocytes in vitro and in vivo. Proc Natl Acad Sci USA 90:11498–11502.
30. Lin H, Parmacek MS, Morle G, Bolling S, Leiden JM. 1990. Expression of recombinant genes in myocardium in vivo after direct injection of DNA. Circulation 82:2217–2221.
31. Buttrick PM, Kass A, Kitsis RN, Kaplan ML, Leinwand LA. 1992. Behavior of genes directly injected into the rat heart in vivo. Circ Res 70:193–198.
32. French BA, Mazur W, Geske RS, Bolli R. 1994. Direct in vivo gene transfer into porcine myocardium using replication-deficient adenoviral vectors. Circulation 90:2414–2424.
33. Sawa Y, Suzuki K, Bai HZ, Shirakura R, Morishita R, Kaneda Y, Matsuda H. In press. Efficiency of in-vivo gene transfection into transplanted rat heart by coronary infusion of HVJ–liposome. Circulation.

This Page Intentionally Left Blank

CALCIUM BUT NOT AMILORIDE IMPROVES THE MECHANICAL FUNCTION OF REPERFUSED ONE-WEEK-OLD RABBIT HEARTS

SHINJI TERAMACHI, TOSHIYUKI ITOI, and ZENSHIRO ONOUCHI

Kyoto Prefectural University of Medicine

Summary. It is hypothesized that intracellular Ca^{2+} overload is a cause of prolonged post-ischemic ventricular dysfunction. We studied the effects of amiloride and of increasing extracellular Ca^{2+} concentration on the functional recovery of isolated reperfused immature rabbits.

Isolated working hearts from one-week-old rabbits were subjected to a 40-minute period of global ischemia followed by 30 minutes of aerobic reperfusion. Contractile function was 45% of the preischemic level in hearts reperfused with buffer containing 1.75 mM Ca^{2+} (group 1). No significant difference in recovery of mechanical function was seen between hearts in which 300 μM amiloride was added five minutes before the onset of ischemia (group 2) and in hearts of group 1. When Ca^{2+} was increased to 2.5 mM during reperfusion (group 3), mechanical function was significantly recovered to 128% of the preischemic level. There were no significant differences in efflux of both lactate and creatine phosphokinase among the three groups.

Therefore, we conclude that, unlike the adult heart, increasing Ca^{2+} during reperfusion may be beneficial for reperfused one-week-old rabbit hearts rather than adding amiloride five minutes before ischemia.

INTRODUCTION

Myocardial protection of neonatal hearts in the setting of open heart surgery to correct congenital heart defects remains a fundamental clinical problem. The rates of contractile dysfunction from open heart surgery are higher in neonates than adults, and these rates have been attributed, in part, to inadequate myocardial protection during ischemia [1,2]. Despite poor clinical outcomes, experimental studies have

S. Mochizuki, N. Takeda, M. Nagano and N. Dhalla (eds.). THE ISCHEMIC HEART.

primarily shown that the immature heart is more resistant to myocardial ischemia [3,4]. The reasons for the discrepancy between the clinical situation and these experimental studies remain unclear.

At the level of the myocyte, many differences exist between the immature and mature heart. One major difference includes a greater reliance of the immature heart on extracellular Ca^{2+} for excitation–contraction coupling [5,6]. In the adult heart, an accumulation of intracellular Ca^{2+} contributes to the depression of the mechanical function during reperfusion following ischemia, with high extracellular Ca^{2+} contributing to the accumulation of intracellular Ca^{2+} [7–9]. Although high extracellular Ca^{2+} is speculated to be a contributing factor to reperfusion injury in the mature heart, it is widely used postsurgery in infants. Itoi and Lopaschuk (1996) have demonstrated that increase of Ca^{2+} improved postischemic functional recovery in isolated immature rabbit hearts [10]. However, whether high Ca^{2+} concentration ($[Ca^{2+}]$) is detrimental or beneficial for functional recovery of ischemic immature hearts remains to be clarified.

Several findings have revealed that Ca^{2+} entry occurs through the Na^+–Ca^{2+} exchanger during reperfusion following ischemia [11]. H^+ ions increased in ischemic myocardium are exchanged with Na^+ via the Na^+–H^+ exchanger, resulting in an accumulation of intracellular Na^+ [11–14]. This excess of intracellular Na^+ allows the entry of a massive amount of Ca^{2+} through the Na^+–Ca^{2+} exchanger. It has been shown in the mature heart that amiloride, widely used to inhibit Na^+–H^+ exchanger activity, improved contractile function of myocardium after reperfusion, with reduction of Na^+ and Ca^{2+} [15–17].

The purpose of the study reported here was to reveal, in the immature heart, whether or not the interaction between the Na^+–H^+ exchanger and the Na^+–Ca^{2+} exchanger contributes to the depression of contractile function during reperfusion. Thus, we studied the effect of amiloride on reperfused one-week-old rabbit hearts. Furthermore, we attempted to characterize the role of extracellular $[Ca^{2+}]$ in the reperfusion recovery of mechanical function in immature hearts from one-week-old rabbits.

METHODS

Heart perfusion

All studies were performed on one-week-old Japanese white rabbits that were separated from the doe in the evening of the day before experimentation. Rabbits were cared for according to the Rules and Regulations of Animal Research of Kyoto Prefectural University of Medicine.

Rabbits were anesthetized with an overdose of pentobarbital–Na (25 mg/100 g). When the rabbit completely lacked sensation, the thoracic cavity was quickly opened, and the heart was excised without the pericardium and placed in Krebs–Henseleit buffer. Hearts were cannulated via the aorta and a retrograde (Langendorff) perfusion was begun with Krebs–Henseleit buffer, pH 7.4, gassed with 95% O_2–5% CO_2. The buffer contained 11 mM glucose and 1.75 mM Ca^{2+}.

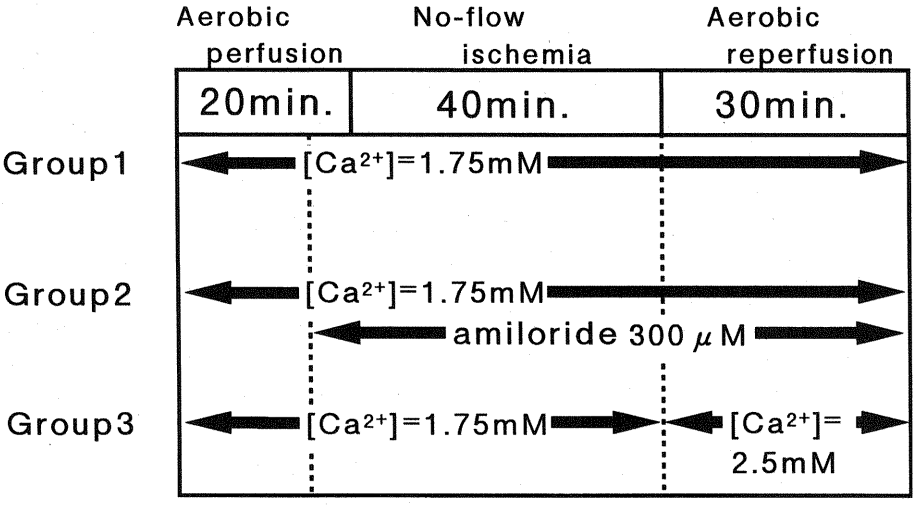

Figure 1. Outline of perfusion protocols. The initial perfusion was started with the modified Krebs–Henseleit buffer containing 1.75 mM Ca^{2+} for 20 minutes and followed by 40-minute ischemia at room temperature (25°C). In group 1 (n = 8), hearts were reperfused with 1.75 mM [Ca^{2+}] perfusate. In group 2 (n = 7), was added 300 μM amiloride to the hearts five minutes before the onset of ischemia. [Ca^{2+}] was added to hearts in group 3 (n = 8) during the reperfusion period.

The elapsed time between opening the thoracic cavity and initiating the retrograde perfusion never exceeded 30 seconds. After the left atrial cannulation, the heart was switched to the left ventricular working mode by initiating perfusion via the left atrial cannula at a constant 8-mmHg left atrial preload and a 30-mmHg hydrostatic aortic afterload. Heart rate and aortic peak systolic pressure were continuously measured using a pressure transducer in line with the aortic outflow line. Mechanical function was expressed as heart rate × aortic peak systolic pressure (double product). The perfusate for the working mode was Krebs–Henseleit buffer containing 118 mM NaCl, 4.7 mM KCl, 1.2 mM KH_2PO_4, 1.2 mM $MgSO_4$, 1.2 mM Palmitate, 5.5 mM glucose, 3% bovine serum albumin, and 1.75 mM $CaCl_2$. The exact concentration of free Ca^{2+} ions varied between 1.25 mM and 1.32 mM because about 25% of total Ca^{2+} ions combined with albumin. Palmitate was prebound to albumin, since palmitate is difficult to dissolve in buffer [18]. We chose 1.2 mM palmitate because of the high concentrations of free fatty acids seen in the clinical setting of cardiac surgery in infants [19]. The buffer was continuously equilibrated with 95% O_2:5% CO_2 (pH ~ 7.4, 37°C).

Perfusion protocol

Hearts were subjected to an initial 20-minute aerobic perfusion followed by 40 minutes of global no-flow ischemia at a room temperature of 25°C and 30 minutes of aerobic reperfusion. Figure 1 shows the three experimental groups used in this

study. Group 1 ($n = 8$) consisted of hearts perfused with 1.75 mM Ca^{2+} throughout the protocol. Group 2 ($n = 7$) hearts were perfused under the same conditions as Group 1, except 300 μM amiloride was present. In this case, amiloride was added to the circulating perfusate five minutes before the onset of ischemia. Group 3 ($n = 8$) consisted of hearts perfused with 1.75 mM Ca^{2+} prior to and during ischemia, followed by reperfusion with 2.5 mM Ca^{2+}.

Measurement of lactate and creatine phosphokinase (CPK)

We measured lactate concentration and CPK activity of buffer from the coronary sinus to compare the myocardial damage after ischemia of the three groups. We sampled this buffer at 20 minutes of initial perfusion (preischemia) and at 1 minute, 5 minutes, and 30 minutes of reperfusion. We measured the concentration of lactate with a measuring kit (Determiner LA, Kyowa Medex Co., Ltd., Tokyo, Japan) and the activity of CPK with a measuring kit (Unimate CK, Japan Roche Co., Ltd., Tokyo, Japan).

Statistical analysis

One-way analysis of variance was used to determine the statistical difference among the three groups. Significant difference between two groups was determined by Student's *t*-test with Scheffe's correction for repeated comparison. When the analyses compared two paired groups, we used paired *t*-test to detect significant differences.

A value of p less than 0.05 was considered significant. All data are presented as mean ± SEM.

RESULTS

Effects of addition of amiloride and 2.5 mM Ca^{2+} on reperfusion recovery of ischemic one-week-old rabbit hearts

No significant differences were found among the three groups in body weight and heart weight of one-week-old rabbits on the day of the experiment (table 1).

When the one-week-old isolated hearts were subjected to 40-minute global ischemia, the mechanical function recovered 59% of preischemic level at 10 minutes after initial reperfusion and leveled off by the end of a 30-minute reperfusion (45% recovery of preischemic level; see figure 2). The depression of functional recovery

Table 1. Body weights and heart weights of each group

	Body weight (g)	Heart weight (g)
Group 1 ($n = 8$)	137.5 ± 7.0	1.03 ± 0.11
Group 2 ($n = 7$)	125.7 ± 5.1	1.00 ± 0.05
Group 3 ($n = 8$)	140.0 ± 9.5	1.03 ± 0.08

Values are the mean ± SEM of hearts in each group.

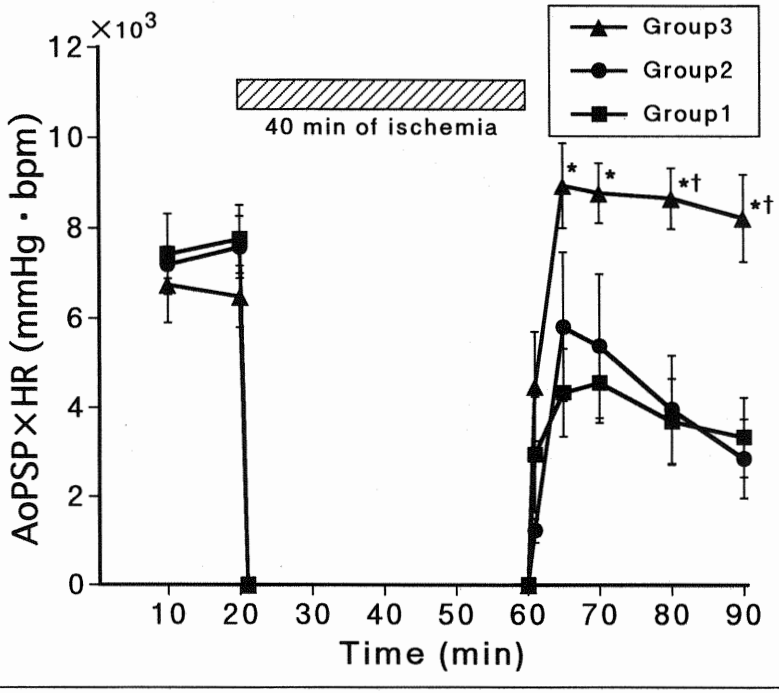

Figure 2. Mechanical heart functions of isolated working hearts from immature rabbits. HR × AoPSP (= double product) was measured in hearts as described in the Methods section. A 40-minute period of global ischemia at room temperature was produced by clamping all inflow and outflow lines. Following ischemia, flow was reinitiated for a 30-minute period of aerobic reperfusion. Hearts were divided into three groups: group 1 (n = 8) hearts were perfused with 1.75 mM [Ca^{2+}] throughout the entire perfusion; for group 2 (n = 7), 300 μM amiloride was added in the perfusate five minutes before the onset of ischemia, and hearts were perfused with 1.75 mM [Ca^{2+}] throughout the entire perfusion; and in group 3 (n = 8), perfusate [Ca^{2+}] was increased to 2.5 mM at the initiation of ischemic period. All data are presented as the mean ± SEM. HR: heart rate; AoPSP: aortic peak systolic pressure. *, significantly different from group 1; †, significantly different from group 2.

in these hearts reflects both the decrease in heart rate and the peak systolic pressure (table 2). Existence of 300 μM amiloride (hearts in group 2) improved neither heart rates nor aortic peak systolic pressure of hearts in group 1 (table 2), and the mechanical function represented by the double product was not enhanced by the addition of amiloride in comparison with the function of hearts in group 1 (figure 2).

When [Ca^{2+}] in perfusate was raised to 2.5 mM during the reperfusion period, complete recovery of heart function to preischemic levels was obtained (figure 2). This was due to a significant increase in aortic peak systolic pressure (table 2). It should be noticed that mechanical function was significantly enhanced, even at the earliest time period of five minutes of reperfusion. This finding was in contrast to

Table 2. Effect of 40-minute ischemia on mechanical function of isolated working hearts from one-week-old rabbits

Perfusion condition	Heart rate (beats/min)	Aortic peak systolic pressure (mmHg)
Preischemia		
Group 1	206.5 ± 17.2	37.9 ± 3.0
Group 2	188.6 ± 12.6	39.9 ± 1.6
Group 3	197.8 ± 15.0	32.8 ± 2.5
Reperfusion		
1 min		
Group 1	118.3 ± 27.6	19.3 ± 4.9
Group 2	108.0 ± 24.1	11.7 ± 1.0
Group 3	109.3 ± 20.7	37.1 ± 5.1[a,b]
30 min		
Group 1	152.5 ± 26.0	20.3 ± 3.8
Group 2	136.3 ± 24.7	18.7 ± 4.1
Group 3	204.3 ± 13.3	39.1 ± 3.0[a,b]

[a] Significantly different from group 1 hearts.
[b] Significantly different from group 2 hearts.
Hearts were perfused as described in the Methods section. Group 1 (n = 8) hearts were perfused with 1.75 mM Ca^{2+}. Group 2 (n = 7) was similar to group 1, except that 300 μM amiloride was added five minutes before the onset of ischemia. Group 3 was similar to group 1, except that 2.5 mM Ca^{2+} was present during reperfusion. Values are mean ± SEM.

the mature rat heart, in which increasing [Ca^{2+}] is detrimental to the ischemic heart. Adult rat hearts perfused with 2.5 mM Ca^{2+} have a marked depression of mechanical function following 30 minutes of ischemia [20], whereas hearts perfused with 1.25 mM Ca^{2+} will recover to a greater extent even when subjected to 35 minutes of ischemia [21].

CPK and lactate efflux from ischemic one-week-old rabbit hearts

Increases of CPK efflux from hearts after 40 minutes of global ischemia were significant but did not exceed the double numbers of preischemic levels in each experimental group (table 3). Furthermore, the levels of CPK concentrations were the same among the three groups. These data showed that the intervention of 40-minute ischemia against isolated one-week-old rabbit hearts created ischemic damage on the myocardium, thus decreasing the contractile function at the reperfusion period.

Lactate efflux from isolated one-week-old rabbit hearts at one minute of reperfusion was obvious in each group (table 4). These values of efflux at one minute of reperfusion represent total lactate, which was accumulated in the extracellular space during ischemia and was metabolized from glucose during reperfusion. While the levels of lactate efflux, which represent production via glycolysis, decreased promptly until five minutes of reperfusion and leveled off at 30 minutes of reperfusion, the lactate efflux at five minutes and 30 minutes of reperfusion was still higher than the efflux levels in the preischemic hearts of each group (table 4).

Table 3. Levels of CPK efflux (U/I) from isolated working hearts from one-week-old rabbits

		Reperfusion		
	Preischemia	1 min	5 min	30 min
Group 1	75.4 ± 15.3	95.1 ± 19.1[a]	96.1 ± 17.9	109.3 ± 20.8[a]
Group 2	56.9 ± 13.3	125.7 ± 45.5	85.9 ± 26.9	82.3 ± 18.9[a]
Group 3	107.5 ± 23.8	155.1 ± 39.1[a]	125.1 ± 29.7[a]	130.0 ± 26.2[a]

[a] Significantly different from comparable preischemic hearts.
Hearts were perfused as described in the Methods section. Group 1 (n = 8) hearts were perfused with 1.75 mM Ca^{2+}. Group 2 (n = 7) was similar to group 1, except that 300 μM amiloride was added five minutes before the onset of ischemia. Group 3 (n = 8) was similar to group 1, except that 2.5 mM Ca^{2+} was present during reperfusion. Values are mean ± SEM.

Table 4. Levels of lactate efflux (mg/dL) from isolated working hearts from one-week-old rabbits

		Reperfusion		
	Preischemia	1 min	5 min	30 min
Group 1	1.24 ± 0.36	5.11 ± 1.25[a]	2.43 ± 0.43[a]	2.35 ± 0.44[a]
Group 2	0.90 ± 0.10	11.23 ± 1.99[a]	3.84 ± 1.28[b]	2.40 ± 0.34[a,b]
Group 3	1.06 ± 0.20	7.28 ± 1.17[a]	2.06 ± 0.29[a,b]	2.03 ± 0.27[a,b]

[a] Significantly different from comparable preischemic.
[b] Significantly different from comparable hearts after one-minute reperfusion.
Hearts were perfused as described in the Methods section. Group 1 (n = 8) hearts were perfused with 1.75 mM Ca^{2+}. Group 2 (n = 7) was similar to group 1, except that 300 μM amiloride was added five minutes before the onset of ischemia. Group 3 (n = 8) was similar to group 1, except that 2.5 mM Ca^{2+} was present during reperfusion. Values are mean ± SEM.

Neither adding amiloride nor raising Ca^{2+} concentration resulted in a significant difference in lactate efflux from the control group (group 1).

DISCUSSION

Reperfusion of the ischemia-subjected heart results in impaired contractile force, known as *stunning*. Several findings support the hypothesis that intracellular calcium overload during reperfusion causes stunning [22–24]. Intracellular Ca^{2+} concentration ($[Ca^{2+}]_i$) increases with Ca^{2+} inflow via the Na^+–Ca^{2+} exchanger during the early reperfusion period. The Na^+–Ca^{2+} exchanger is activated toward an increase of $[Ca^{2+}]_i$ by a high concentration of intracellular Na^+ [11,22,23].

The Na^+ entry through the Na^+–H^+ exchanger associated with intracellular pH recovery may contribute to a rise in concentration of intracellular Na^+ [25,26]. This excess of intracellular Na^+ allows the entry of a massive amount of Ca^{2+} through the Na^+–Ca^{2+} exchanger. The early excessive $[Ca^{2+}]_i$ levels may damage intracellular organelles involved with contraction and thereby produce prolonged mechanical dysfunction after short-term ischemia. It has been reported that administration of Na^+–H^+ exchanger inhibitor (amiloride) in ischemic and reperfusion periods was beneficial for functional recovery of reperfused mature hearts [15–17].

Intracellular pH recovery just after ischemia in immature heart is principally mediated by lactate efflux and HCO_3^-–Cl^- exchange rather than Na^+–H^+ exchange. Nakanishi et al. have demonstrated that the HCO_3^--dependent mechanism (HCO_3^-–Cl^- exchanger) is much more active for H^+ extrusion in immature myocardium than in mature hearts [27]. They also showed that the intracellular acidosis of newborn myocytes with added NH_4Cl is more greatly corrected by HCO_3^-–Cl^- exchange than by Na^+–H^+ exchange. If this is the case, it is reasonable to assume that increase of intracellular Na^+ would barely occur in the immature heart at reperfusion period. This assumption might be supported by the finding that neither Ca^{2+} nor Na^+ accumulate to any degree during reperfusion of ischemic hearts from two-week-old rabbits [28]. Our study showed that amiloride had no influence on the functional recovery of reperfused immature hearts from one-week-old rabbits (figure 2). This finding indicated that an increase of Na^+ via the Na^+–H^+ exchanger might not play an important role in contractile depression of the reperfused immature heart.

Lactate extrusion is another important system to control the intracellular pH. There was good lactate efflux in the early reperfusion period of the three groups, and there was no significant difference among the three groups, suggesting that amiloride did not change lactate efflux for acid extrusion. High calcium concentration in perfusate also had no influence on lactate efflux. It is likely that the intracellular acidosis in the immature heart is markedly corrected not only by the HCO_3^-–Cl^- exchange but also by lactate efflux during ischemia and the early reperfusion period.

This study demonstrates that increasing the perfusate [Ca^{2+}] from 1.75 mM to 2.5 mM is beneficial to the mechanical functional recovery of reperfused immature hearts. This effect of Ca^{2+} in the immature rabbit hearts differs from that observed in mature hearts. High extracellular Ca^{2+} during reperfusion of adult hearts contributes to functional impairment in the postischemic myocardium by contributing to cytosolic Ca^{2+} overload [7–9]. The reason for the different effects of Ca^{2+} between mature and immature hearts is not clear but may be related to a number of differences at the level of the myocyte.

The newborn heart, in contrast to the adult heart, requires extracellular Ca^{2+} for excitation–contraction coupling. Morphometric and biochemical studies showed that the amount of sarcoplasmic reticulum (SR) is higher in adult than in neonatal animals [29,30] and that Ca^{2+}–ATPase content, Ca^{2+} uptake capacity, and Ca^{2+}-dependent ATPase activity are low in fetal cardiac muscle [30–32]. A recent study revealed that the cardiac ryanodine receptor (calcium release channel) mRNA level increased gradually from fetus to adult [33]. These findings suggest that the amount of Ca^{2+} released into the cytoplasm from SR with contraction is lower in immature hearts than in mature hearts. Riva and Hearse demonstrated that the immature rat heart requires a higher extracellular [Ca^{2+}] for stable contraction than the adult heart [6]. The Na^+–Ca^{2+} exchange activity of sarcolemma from immature hearts is similar to that seen in mature hearts and may contribute substantially in controlling both Ca^{2+} influx and efflux before complete maturation of the SR system [34–36].

It is hypothesized that increase of glucose oxidation is relevant for contractile recovery for reperfused ischemic hearts [4,10,20]. Increase of Ca^{2+} during reperfusion resulted in enhancement of carbohydrate oxidation and ATP production [10]. In our study, lactate efflux from reperfused hearts was high even at 30 minutes of reperfusion. However, we could not determine whether or not there were any changes in glucose oxidation among the three groups because there were no significant differences in lactate efflux.

The issue of high Ca^{2+} in the reperfused immature heart is still controversial. Pearl et al. have demonstrated, in a piglet heart, a beneficial effect of normocalcemic cardioplegia compared to low-calcemic cardioplegia [37]. In contrast, Aoki et al. [38] and Caspi et al. [39] suggested that decreasing $[Ca^{2+}]$ below normal levels in the cardioplegic solution helps preserve left ventricular function during reperfusion. If the hearts were reperfused with 5.0 mM Ca^{2+}, severe ventricular arrhythmia occurred at five minutes of reperfusion, although contractile function showed high levels like those in the reperfused hearts with 2.5 mM Ca^{2+} (data not shown). These data suggest that intracellular calcium overload may be detrimental not only for reperfused mature hearts but also for immature hearts. However, the immature heart may have a higher tolerance against intracellular calcium overload than mature hearts. Further experiments are needed to determine the optimal $[Ca^{2+}]$ to be used both during and following cardioplegic arrest in the newborn heart, when improved myocardial protection in the clinical setting could be achieved.

CONCLUSION

We have shown in this study that in one-week-old rabbit hearts subjected to global ischemia, amiloride did not improve contractile function during reperfusion, but increasing perfusate $[Ca^{2+}]$ during reperfusion from 1.75 mM to 2.5 mM enhanced the function. Thus, unlike the adult heart, it may be beneficial for functional recovery of the reperfused immature heart to increase $[Ca^{2+}]$ rather than to inhibit the Na^+–H^+ exchanger.

ACKNOWLEDGMENT

We thank MERCK Research Laboratories for kindly providing amiloride. This work was supported by Research Grant No. 07457599 from the Japanese Ministry of Education, Science and Culture.

REFERENCES

1. Sawa Y, Matsuda H, Shimazaki Y, Hirose H, Kadoba K, Takami H, Nakada T, Kawashima Y. 1987. Ultrastructual assessmant of the infant myocardium receiving crystalloid cardioplegia. Circulation 76(Suppl V):V141–V155.
2. del Nido PJ, Mickle DAG, Wilson GJ, Benson LN, Weisel RD, Coles JG, Trusler GA, Williams WG. 1988. Inadequate myocardial protection with cold cardioplegic arrest during repair of tetralogy of Fallot. J Thorac Cardiovasc Surg 95:223–229.
3. Avrikan M, Hearse DJ. 1989. Protection of the myocardium during global ischemia: is crystalloid cardioplegia effective in the immature myocardium? J Thorac Cardiovasc Surg 97:220–228.
4. Itoi T, Huang L, Lopaschuk GD. 1993. Glucose use in neonatal rabbit hearts reperfused after global ischemia. Am J Physiol 265 (Heart Circ Physiol 34):H427–H433.

5. Jarmakani JM, Nakanish T, George BL, Bers D. 1982. Effect of extracellular calcium on myocardial mechanical function in the neonatal rabbit. Dev Pharmacol Ther 5:1–13.
6. Riva E, Hearse DJ. 1991. Isolated, perfused neonatal rat heart preparation for studies of calcium and functional stability. Ann Thorac Surg 52:987–992.
7. Kuroda H, Ishiguro S, Mori T. 1986. Optimal calcium concentration in the initial perfusate for post-ischemic myocardial performance (calcium concentration during reperfusion). J Mol Cell Cardiol 18:625–633.
8. du Toit E, Opie LH. 1992. Modulation of severity of reperfusion stunning in the isolated rat heart by agents altering calcium flux at onset of reperfusion. Circ Res 70:965–967.
9. Jeremy RW, Koretsune Y, Marban E, Becker LC. 1992. Relation between glycolysis and calcium homeostasis in post-ischemic myocardium. Circ Res 70:1180–1190.
10. Itoi T, Lopaschuk GD. 1996. Calcium improves mechanical function and carbohydrate metabolism following ischemia in isolated bi-ventricular working hearts from immature rabbits. J Mol Cell Cardiol 28:1501–1514.
11. Tani M. 1990. Mechanisms of Ca^{2+} overload in reperfused ischemic myocardium. Annu Rev Physiol 52:543–559.
12. Crespo LM, Granthan CJ, Cannell MB. 1990. Kinetics, stoichiometry and role of the Na–Ca exchange mechanism in isolated cardiac myocytes. Nature 345:618–621.
13. Reuter H. 1991. Ins and outs of Ca^{2+} transport. Nature 349:567–568.
14. Steenbergen C, Murphy E, Watts JA, London RE. 1990. Correlation between cytosolic free calcium, contracture, ATP, and irreversible ischemic injury in perfused rat heart. Circ Res 66:135–146.
15. Mochizuki S, Seki S, Ejima M, Onodera T, Taniguchi M, Ishikawa S. 1993. Na^+/H^+ exchanger and reperfusion-induced ventricular arrhythmias in isolated perfused heart: possible role of amiloride. Mol Cell Biochem 119:151–157.
16. Murphy E, Perlman M, London RE, Steenbergan C. 1991. Amiloride delays the ischemia-induced rise in cytosolic free calcium. Circ Res 68:1250–1258.
17. Karmazyn M. 1988. Amiloride enhances postischemic ventricular recovery: possible role of Na^+–H^+ exchange. Am J Physiol 255 (Heart Circ Physiol 24):H608–H615.
18. Saddik M, Lopaschuk GD. 1991. Myocardial triglyceride turnover and contribution to energy substrate utilization in isolated working rat hearts. J Biol Chem 266:8162–8170.
19. Lopaschuk GD, Collins-Nakai R, Olley PM, Montague TJ, McNeil G, Gayle M, Penkoske P, Finegan BA. 1994. Plasma fatty acid levels in infants and adults following myocardial ischemia. Am Heart J 128:61–67.
20. McVeigh JJ, Lopaschuk GD. 1990. Dichloroacetate stimulation of glucose oxidation improves recovery of ischemic rat hearts. Am J Physiol 259 (Heart Circ Physiol 28):H1079–H1015.
21. Broderick TL, Quinney HA, Lopaschuk GD. 1993. Beneficial effect of carnitine on mechanical recovery of rat hearts reperfused after a transient period of global ischemia is accompanied by a stimulation of glucose oxidation. Circulation 87:972–981.
22. Kusuoka H, Marban E. 1992. Cellular mechanisms of myocardial stunning. Annu Rev Physiol 54:243–256.
23. Braunwald E, Kloner RA. 1982. The stunned myocardium: prolonged, postischemic ventricular dysfunction. Circulation 66:1146–1149.
24. Bolli R. 1990. Mechanism of myocardial "stunning". Circulation 82:723–738.
25. Fliegel L, Dyck JRB. 1995. Molecular biology of the cardiac sodium/hydrogen exchanger. Cardiovasc Res 29:155–159.
26. Vandenberg JI, Metcalfe JC, Grace AA. 1993. Mechanism of pH_i recovery after global ischemia in the perfused heart. Circ Res 72:993–1003.
27. Nakanishi T, Gu H, Seguchi M, Cragoe Jr EJ, Momma K. 1992. HCO_3^--dependent intracellular pH regulation in the premature myocardium. Circ Res 71:1314–1323.
28. Pridjian AK, Levitsky S, Krukenkamp I, Silverman NA, Feinberg H. 1987. Developmental change in reperfusion injury. A comparison of intracellular cation accumulation in the newborn, neonatal, and adult heart. J Thorac Cardiovasc Surg 93:428–433.
29. Maylie JG. 1984. Excitation–contraction coupling in neonatal and adult myocardium of cat. Am J Physiol 242 (Heart Circ Physiol 11):H834–H843.
30. Nakanishi T, Jarmakani JM. 1984. Developmental changes in myocardial mechanical function and subcellular organelles. Am J Physiol 246 (Heart Circ Physiol 15):H615–H625.
31. Mahony L, Jones LR. 1986. Developmental changes in cardiac sarcoplasmic reticulum in sheep. J Biol Chem 261:15257–15265.

32. Pegg W, Michalak M. 1987. Differentiation of sarcoplasmic reticulum during cardiac myogenesis. Am J Physiol 252 (Heart Circ Physiol 21):H22–H31.
33. Arai M, Otsu K, MacLennan DH, Periasamy M. 1992. Regulation of sarcoplasmic reticulum gene expression during cardiac and skeletal muscle development. Am J Physiol 262 (Cell Physiol 31):C614–C620.
34. Boucek RJ Jr, Shelton ME, Artman M, London E, Pettus R. 1985. Myocellular calcium regulation by the sarcolemmal membrane in the adult and immature rabbit heart. Basic Res Cardiol 80:316–325.
35. Artman M. 1992. Sarcolemmal Na^+–Ca^{2+} exchange activity and exchanger immunoreactivity in developing rabbit hearts. Am J Physiol 263 (Heart Circ Physiol 32):H1506–1513.
36. Wetzel GT, Chen F, Klitzner TS. 1993. Ca^{2+} channel kinetics in acutely isolated fetal, neonatal, and adult rabbit cardiac myocytes. Circ Res 72:1065–1074.
37. Pearl JM, Laks H, Drinkwater DC, Meneshian A, Sun B, Gates RM, Chang P. 1993. Normocalcemic blood or crystalloid cardioplegia provide better neonatal myocardial protection than does low-calcium cardioplegia. J Thorac Cardiovasc Surg 105:201–206.
38. Aoki M, Nomura F, Kawata H, Mayer E. 1993. Effect of calcium and preischemic hypothermia on recovery of myocardial function after cardioplegic ischemia in neonatal lambs. J Thorac Cardiovasc Surg 105:207–213.
39. Caspi J, Herman SL, Coles JG, Benson LN, Radde I, Augustine J, Hamilton F, Caltellarin S, Kumar R, Wilson GJ. 1990. Effect of low perfusate Ca^{2+} concentration on newborn myocardial function after ischemia. Circulation 82(Suppl IV):IV371–IV379.

This Page Intentionally Left Blank

EFFECTS OF BIBR-277, AN ANGIOTENSIN-II TYPE-1 RECEPTOR ANTAGONIST, ON ISCHEMIC MYOCARDIAL STUNNING IN DOGS

TOHRU NAKAI, KUMI SATOH, ATSUKO YAMAMOTO, KATSUJI HOSHI, and KAZUO ICHIHARA

Hokkaido College of Pharmacy

Summary. BIBR-277, an angiotensin-II type-1 receptor antagonist, improved the recovery of contractile function of the stunned myocardium. Enalapril also lessened the contractile dysfunction during reperfusion in the stunned myocardium. These drugs may act to reduce ischemic damage by removing the systemic and coronary vasoconstrictive effects of angiotensin II.

INTRODUCTION

The renin–angiotensin system plays an important role in the regulation of cardiovascular function as well as water balance [1] and is activated following acute myocardial infarction in both humans [2] and experimental animals [3]. Angiotensin II may compensate for the decrease in blood pressure due to failure of cardiac contractile function and also increases cell proliferation to repair the injured cells [4]. However, angiotensin II also increases coronary vascular resistance and myocardial necrosis [5]. Angiotensin-converting enzyme inhibitors are a successful treatment for patients with hypertension and congestive heart failure [6,7]. This group of drugs also protects the myocardium from ischemia–reperfusion injury [8].

To abolish the deleterious effect of angiotensin II on the ischemic–reperfused heart, an angiotensin receptor antagonist, rather than angiotensin-converting enzyme inhibitors, may be more useful both because angiotensin-converting enzyme inhibitors block kininase II and increase the level of bradykinin [9] and because localized angiotensin II may be formed by the chymase, which is not affected by angiotensin-converting enzyme inhibitors [10]. Several angiotensin-II

S. Mochizuki, N. Takeda, M. Nagano and N. Dhalla (eds.). THE ISCHEMIC HEART.

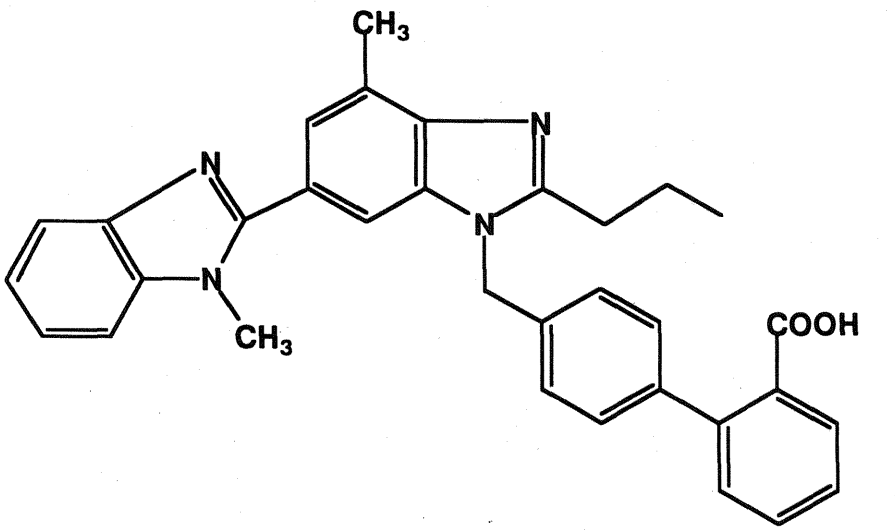

Figure 1. Chemical structure of BIBR-277.

type-1 receptor-selective antagonists are now available. The chemical structure of BIBR-277, 4′-[(1,4′-dimethyl-2′-propyl-[2,6′-bi-1H-enzimidazole]-1′-yl)methyl]-[1,1′-biphenyl]-2-carboxylic acid, is shown in figure 1 [11,12]. BIBR-277 potentially interacts with angiotensin type-1 receptors, but not with type-2 receptors [11]. We will have more direct information about the involvement of the renin–angiotensin system in cardiovascular disease when we use angiotensin receptor antagonists instead of angiotensin-converting enzyme inhibitors. In the study reported here, we examined the effect of BIBR-277 on dysfunction of myocardial contraction after reperfusion following ischemia, that is, ischemic stunning in dogs. The effects of enalapril were also determined and compared with those of BIBR-277.

METHODS

Animal preparation

Healthy mongrel dogs of either sex weighing 7–30 kg were anesthetized with sodium pentobarbital (30 mg/kg, i.v.) and ventilated with room air. Left thoracotomy was performed between the fourth and fifth ribs, and the left ventricle was exposed. After the heart had been suspended in a pericardial cradle, the main trunk of the left anterior descending coronary artery (LAD) was dissected free from the distal end to the first diagonal branch, and was loosely encircled with a silk thread ligature. The coronary flow as measured using a magnetic flow probe positioned at the LAD proximal to the ligature. A pair of ultrasonic crystals was implanted in a circumferential plane at the LAD region. The segment shortening function (%SS) was calculated according to the equation

$$\%SS = \{(DL - SL)/DL\} \times 100,$$

where DL is the diastolic segment length and SL is the systolic segment length. Arterial blood pressure was measured via a cannula introduced from the left femoral artery and advanced to a point near the aortic arch. Heart rate was counted from the R-wave of the electrocardiogram limb lead II.

After control observation had been completed, either saline, or 0.3, 1, or 3 mg/kg of BIBR-277, or 1 mg/kg of enalapril was injected from the left femoral vein over a period of 30 seconds. The ligature around the LAD was tied 10 minutes after the injection and then released 20 minutes after the ligation. Hemodynamic parameters were measured for a further 60 minutes.

Assay of cardiac angiotensin II

An additional 15 dogs were used for the assay of cardiac immunoreactive angiotensin II. After 20 minutes of LAD ligation, the nonischemic and ischemic myocardial samples were removed from the left circumflex region and the LAD region, respectively. Either saline solution, BIBR-277 at a dose of 3 mg/kg, or enalapril at 1 mg/kg was injected i.v. 10 minutes before LAD ligation. The myocardial samples were quickly frozen with liquid nitrogen and stored at −85°C until the assay was performed. Extraction of the myocardium for determination of angiotensin II contents was performed according to the method of Sirett et al. [13]. Briefly, tissue samples were homogenized with ice-cold 80% ethanol containing 0.1 nM phenylmethylsulphonylfluoride, and centrifuged. The pellet was resuspended and rehomogenized with the ethanol, and recentrifuged. The supernatants obtained from the first and second centrifugation were combined and boiled for 15 minutes. After cooling, an equal volume of ice-cold chloroform was added to the supernatant. The upper aqueous solution was collected after shaking vigorously and was then dried in a vacuum centrifuge evaporator. The residue was dissolved with distilled water and was used for determination of cardiac angiotensin II by means of the [^{125}I] angiotensin II radioimmunoassay kit (Nichols Institute, Netherlands).

Statistical analysis

The data are expressed as mean ± SE. The significance of differences between groups was evaluated by one-way analysis of variance (ANOVA) followed by Dunnett's *t*-test. A value less than 0.05 was considered statistically significant.

RESULTS

Hemodynamic changes

BIBR-277 experiment

Changes in systolic and diastolic blood pressures, heart rate, and coronary flow during ischemia and reperfusion in the BIBR-277 group are illustrated in figure 2. In the saline group, ischemia decreased systolic and diastolic blood pressures, and

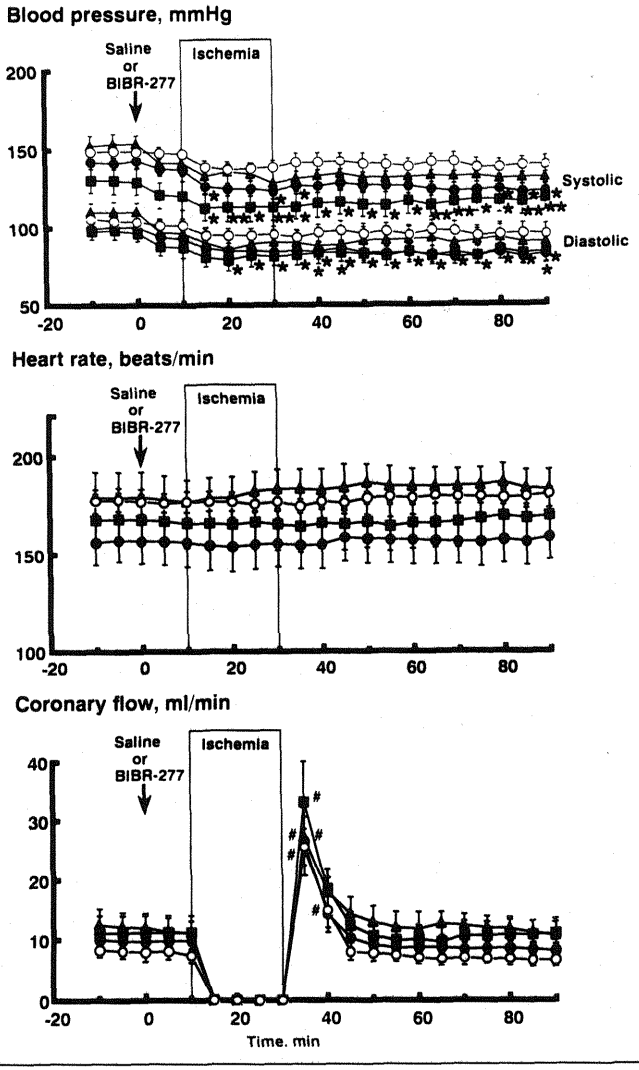

Figure 2. The effect of BIBR-277 on changes in blood pressures, heart rate, and coronary flow during ischemia and reperfusion. After 10 minutes of control measurement, either saline (○) or BIBR-277 (0.3 mg/kg; ▲, 1 mg/kg; ■ or 3 mg/kg; ●) was injected i.v. The left anterior descending coronary artery was ligated 10 minutes after the injection. After 20 minutes of coronary ligation, the ligated coronary artery was released so that the ischemic myocardium was reperfused. To avoid complexity, symbols indicating significant difference within a group are not shown. *, $p < 0.05$ and **, $p < 0.01$, vs. the corresponding value in the saline group. #, $p < 0.05$ vs. the value obtained before injection (0 minutes) in each group.

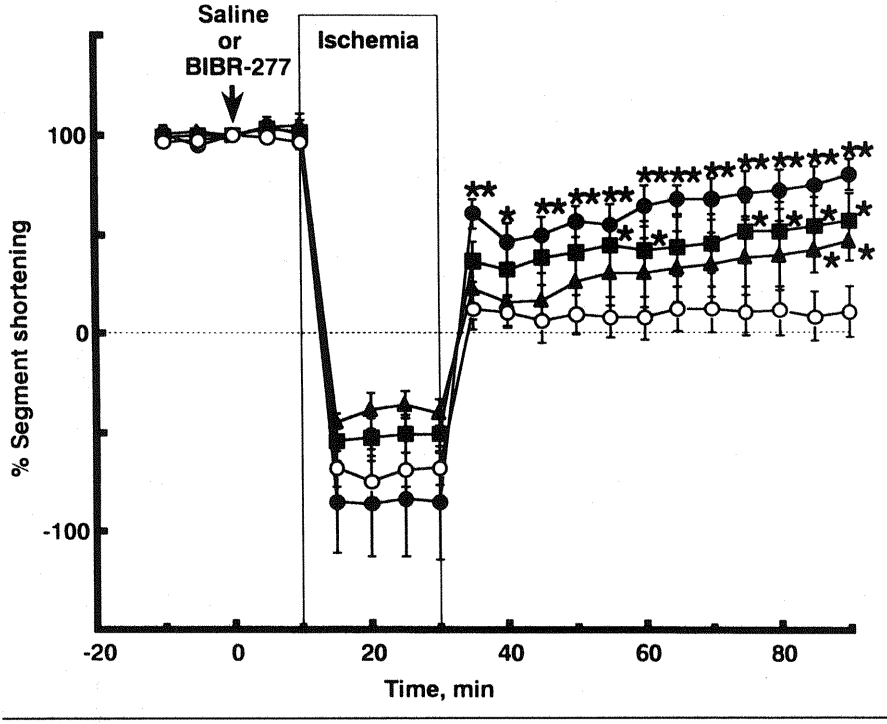

Figure 3. The effect of BIBR-277 on changes in the percent of segment shortening (%SS) during ischemia and reperfusion. Changes in %SS are expressed as percentage of the value just before the injection. Symbols and experimental protocol are the same as those in figure 2. *, $p < 0.05$, and **, $p < 0.01$ vs. the corresponding value in the saline group.

reperfusion returned the pressures to their preischemic levels. Heart rate did not change throughout the experiment. Coronary flow decreased to 0 mL/min during ischemia and returned beyond the preischemic level during reperfusion, indicating the reactive hyperemia. The coronary flow measured 5 and 10 minutes after reperfusion was significantly higher than that before ischemia. In the BIBR-277 groups, systolic and diastolic blood pressures significantly decreased 10 minutes after BIBR-277 injection and decreased further during ischemia. The decreased levels of blood pressure were sustained even after reperfusion. The response of blood pressure to BIBR-277 at the different dosages was similar. Changes in heart rate and coronary flow during ischemia and reperfusion were not modified by BIBR-277.

Changes in %SS during ischemia and reperfusion in the saline and BIBR-277 groups are shown in figure 3. In the saline group, %SS significantly decreased and became below 0%, indicating bulging. Reperfusion returned the %SS that had been decreased by ischemia toward the preischemic level, but the recovery was incom-

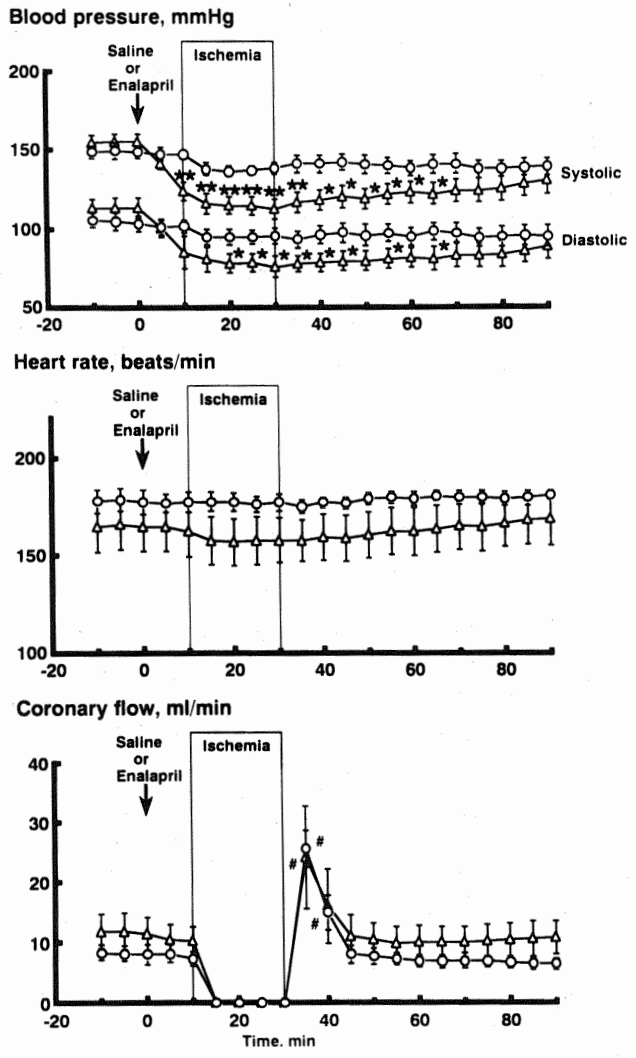

Figure 4. The effect of enalapril on changes in blood pressures, heart rate, and coronary flow during ischemia and reperfusion. Enalapril (1 mg/kg; △) was injected at 0 minutes. The experimental protocol is the same as that in figure 2. Data obtained in saline group (○) are cited from figure 2. *, $p < 0.05$, and **, $p < 0.01$ vs. the corresponding value in the saline group. #, $p < 0.05$ vs. the value obtained before injection (0 minutes) in each group.

plete. BIBR-277 itself did not change the %SS before ischemia. In the BIBR-277 group, ischemia also showed the ventricular bulging to the same extent as in the saline group. BIBR-277 potentiated the recovery of %SS during reperfusion in a dose-dependent manner.

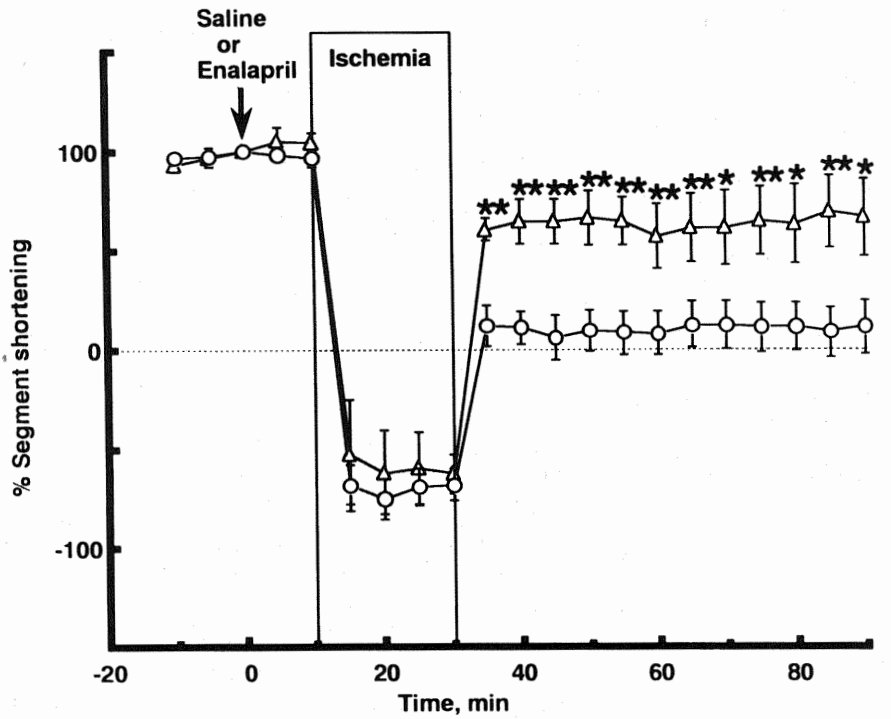

Figure 5. The effect of enalapril on changes in the %SS during ischemia and reperfusion. Symbols and experimental protocol are the same as those in figure 4. To avoid complexity, symbols indicating significant difference within a group are not shown. *, $p < 0.05$ and **, $p < 0.01$, vs. the corresponding value in the saline group.

Enalapril experiment

Hemodynamic changes during ischemia and reperfusion in the enalapril group are illustrated in figure 4. Hemodynamic changes in the saline group were similar to those in the BIBR-277 experiment. In the enalapril group, systolic and diastolic blood pressures significantly decreased 10 minutes after enalapril injection. The decreased levels of blood pressure were sustained during ischemia and reperfusion. Changes in heart rate and coronary flow during ischemia–reperfusion were not modified by enalapril, although the coronary flow during reperfusion appeared to be high in the enalapril group as compared with that in saline group. Enalapril did not modify the %SS before and during ischemia. However, it significantly enhanced the recovery of %SS during reperfusion (figure 5). The recovery of %SS with enalapril was between the levels seen with 1 mg/kg and 3 mg/kg of BIBR-277.

Table 1. The myocardial angiotensin II contents in the nonischemic and ischemic regions 20 minutes after coronary ligation

Treatment	*n*	Nonischemic region	Ischemic region
Saline	5	7.18 ± 1.52	7.38 ± 2.41
BIBR-277	5	9.85 ± 1.58	8.54 ± 2.32
Enalapril	5	5.58 ± 1.85	5.92 ± 1.33

All data are the means ± SE and are expressed as pg/g wet tissue. Saline, BIBR-277 (3 mg/kg), or enalapril (1 mg/kg) was injected i.v. 10 minutes before the onset of ischemia. Ischemia was initiated by ligation of the left anterior descending coronary artery for 20 minutes, and then the heart sample was removed from the circumflex (nonischemic) and LAD (ischemic) regions. *n* = number of animals.

Myocardial angiotensin II contents

Myocardial angiotensin II contents in the nonischemic and ischemic regions are summarized in table 1. The content in the BIBR-277 group appeared to be higher, while that in the enalapril group appeared to be lower than that in the saline group, although the difference was not statistically significant. Ischemia did not change the myocardial contents of angiotensin II in any of the three groups.

DISCUSSION

Although angiotensin II may be needed by the heart in pathophysiological conditions, it also constricts the arterial vessels (including the coronary arteries), enhances cardiac contractility, and increases norepinephrine release [14–16]. These effects may worsen myocardial damage, particularly in the ischemic heart. In the present study, both BIBR-277 and enalapril improved myocardial contractile function during reperfusion following ischemia. These drugs decreased the arterial blood pressure without reflex tachycardia, resulting in a reduction of myocardial oxygen demand. This effect may be partly responsible for the improvement of myocardial contraction during reperfusion following ischemia. In a study of isolated perfused rat hearts, Yoshiyama et al. [17] have reported that pretreatment of the rat with TCV-116, another angiotensin type-1 receptor antagonist, and delapril, an angiotensin-converting enzyme inhibitor, improves postischemic cardiac function and decreases creatine kinase release during reperfusion. Our results obtained in dogs in vivo support these findings. These data suggest that angiotensin II may worsen ischemic myocardial injury during ischemia and reperfusion. It is well known that exogenous angiotensin II accelerates ischemia–reperfusion injury and produces cardiac necrosis [17–19]. In addition, angiotensin II increases myocardial cytosolic Ca^{2+} through activation of phosphatidylinositol turnover [20]. An increase of cytosolic Ca^{2+} makes ischemic myocardial damage worse. Ischemia produces an increase in angiotensin II in the myocardium [21,22]. We measured the tissue content of angiotensin II in the 20-minute ischemic myocardium (table 1) but failed to detect any significant increase in angiotensin II during ischemia. It may be difficult to detect the ischemic changes of angiotensin II content in the myocardial tissue because the angiotensin II

released during ischemia may quickly move into the venous blood and disappear from the tissue. Although a significant difference was not observed, angiotensin II content in the myocardium appeared to increase in the presence of BIBR-277 and to decrease in the presence of enalapril. The former change could be due to the decrease in the apparent numbers of angiotensin II receptors, and the latter to the converting enzyme inhibition.

There are two pathways of the angiotensin-II generating system—one dependent on angiotensin-converting enzyme and the other independent of it. We conducted the experiment reported here because the formation of local angiotensin II during ischemia occurs via the converting-enzyme-independent pathway. However, both angiotensin-II receptor antagonists and converting-enzyme inhibitors showed cardioprotective effects. Our results indicate that local angiotensin II formed through the converting-enzyme-independent pathway may not be a major determinant in the mechanisms of myocardial ischemia injury.

ACKNOWLEDGMENT

BIBR-277 was kindly supplied by Nippon Boehringer Ingelheim Co. Ltd.

REFERENCES

1. Valloton MB. 1987. The renin–angiotensin system. Trends Pharmacol Sci 8:69–74.
2. Mcalpine HM, Cobbe SM. 1988. Neuroendocrine change in acute myocardial infarction. Am J Med 84(Suppl 3A):61–66.
3. Liang C, Gavras H, Black J, Sherman LG, Hood WB. 1982. Renin–angiotensin system inhibition in acute myocardial infarction in dogs. Effects on systemic hemodynamics, mycoardial blood flow, segmental myocardial function and infarct size. Circulation 66:1249–1255.
4. Katoh Y, Komuro I, Shibasaki Y, Yamaguchi H, Yazaki Y. 1989. Angiotensin II induces hypertrophy and oncogene expression in cultured rat heart myocytes. Circulation 80(Suppl II):II–450.
5. Gavras H, Kremer D, Brown JJ. 1975. Angiotensin and norepinephrine induced myocardial lesions; experimental and clinical studies in rabbits and man. Am Heart J 89:321–332.
6. Packer M. 1987. Converting enzyme inhibition in the management of severe chronic congestive heart failure: physiologic concept. J Cardiovasc Pharmacol 10(Suppl 7):S83–S87.
7. Robertoson JIS, Tillman DM. 1987. Converting enzyme inhibitors in the treatment of hypertension. J Cardiovasc Pharmacol 10(Suppl 7):S43–S48.
8. Ertl G. 1988. Angiotensin converting enzyme inhibitors and ischaemic heart disease. Eur Heart J 9:716–727.
9. Okunishi H, Miyazaki M, Okamura T, Toda N. 1987. Different distribution of two types of angiotensin-generating enzymes in the aortic wall. Biochem Biophys Res Commun 149:1186–1192.
10. Kinoshita A, Uratu H, Bunpus FM, Husain A. 1991. Multiple determinants for the high substrate specificity of an angiotensin II-forming chymase from human heart. J Biol Chem 266:19192–19197.
11. Wienen W, Hauel N, Van Meel JCA, Narr B, Ries U, Entzeroth M. 1993. Pharmacological characterization of the novel nonpeptide angiotensin II receptor antagonist, BIBR 277. Br J Pharmacol 110:245–252.
12. Izumi H, Nakai T, Kano S, Hoshi K, Ichihara K. 1996. Effects of BIBR-277, an angiotensin II type 1 receptor antagonist, on stunned myocardium in dogs. Coronary Artery Dis 7:775–779.
13. Sirett NE, Bray JJ, Hubbard JI. 1981. Localization of immunoreactive angiotensin II in the hippocampus and striatum of rat brain. Brain Res 217:405–411.
14. Koch-Weser J. 1964. Myocardial actions of angiotensin. Circ Res 14:337–344.
15. Blumberg AL, Ackerly JA, Peach MJ. 1975. Differentiation of neurogenic and myocardial angiotensin II receptors in isolated rabbit atria. Circ Res 36:719–726.
16. Miwa K, Toda N. 1984. Regional differences in the response to vasoconstrictor agents of dog and monkey isolated coronary arteries. Br J Pharmacol 82:295–301.

17. Yoshiyama M, Kim S, Yamagishi H, Omura T, Tani T, Yanagi S, Toda I, Teragaki M, Akioka K, Takeuchi K, Takeda T. 1994. Cardioprotective effect of the angiotensin II type 1 receptor antagonist TCV-116 on ischemia–reperfusion injury. Am Heart J 128:1–6.
18. Gavras H, Brown JJ, Lever AF, Macadam RF, Robertson JIS. 1971. Acute renal failure, tubular necrosis, and myocardial infarction induced in the rabbit by intravenous angiotensin II. Lancet 2:19–22.
19. Tan L-B, Jalil JE, Pick R, Janicki JS, Weber KT. 1991. Cardiac myocyte necrosis induced by angiotensin II. Circ Res 69:1185–1195.
20. Brown K. 1989. Angiotensin receptors are implicated in the mechanism of mass action. Trends Pharmacol Sci 10:87–89.
21. Gondo M, Maruta H, Arakawa K. 1989. Direct formation of angiotensin II without renin or converting enzyme in the ischemic dog heart. Jpn Heart J 30:219–229.
22. Noda K, Sasaguri M, Ideishi M, Ikeda M, Arakawa K. 1993. Role of locally formed angiotensin II and bradykinin in the reduction of myocardial infarct size in dogs. Cardiovasc Res 27:334–340.

REPERFUSION 12 HOURS AFTER CORONARY OCCLUSION SALVAGES MYOCARDIUM IN DOGS: STUDIES IN A SINGLE-HEART MODEL

AKIO KIMURA, KINJI ISHIKAWA, IWAO OGAWA, HIRONARI KOKA, SHOJI NAKAI, MASAHIKO INAGAKI, MASARU MIYATAKA, TAKAYA HASEGAWA, and RYO KATORI

Kinki University School of Medicine

Summary. In our single-heart model, half permanently occluded and half reperfused, reperfusion 12 hours after coronary artery occlusion salvaged myocardium in dogs. This finding may be one of the reasons why late reperfusion is beneficial in patients with acute myocardial infaction.

INTRODUCTION

Coronary thrombolysis, when followed by successful reperfusion in acute myocardial infarction, reduces mortality [1]. This beneficial effect is accomplished by a myocardial salvage and a limitation of infarct size when reperfusion is performed within six hours after onset of chest pain [2]. The guideline of coronary thrombolysis for acute myocardial infarction proposed by a joint committee of the American College of Cardiology and the American Heart Association in 1990 [3] showed that coronary thrombolysis is usually indicated and considered useful/effective (class I) in patients within six hours of pain onset. Several studies have shown that coronary thrombolysis within six hours salvages myocardium and limits infarct size [4], and is thus effective in improving left ventricular function [5] and reducing mortality [1]. However, no demonstrable myocardial salvage is evident when coronary thrombolysis is performed more than six hours after pain onset. Reperfusion therapy performed beyond this time window is usually called *late reperfusion therapy* [6]. The Fibrinolytic Therapy Trialists' (FTT) Collaborative Group [7] summarized several large clinical trials and found that fibrinolytic therapy performed within 7–12 hours after pain onset significantly reduces mortality. Many

S. Mochizuki, N. Takeda, M. Nagano and N. Dhalla (eds.). THE ISCHEMIC HEART.

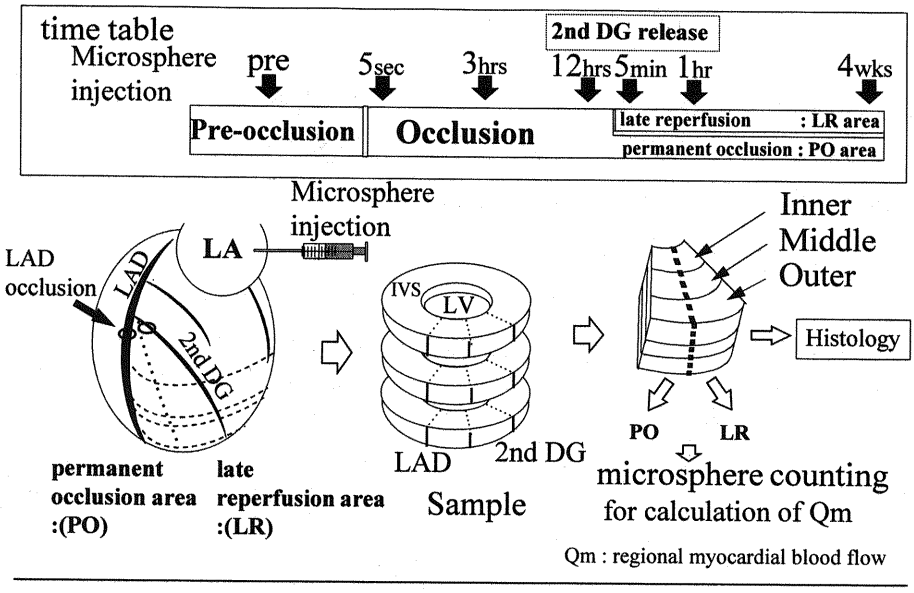

Figure 1. Experimental protocol.

other studies have also indicated that late reperfusion therapy reduces left ventricular remodeling and improves prognosis [8–10]. However, the mechanisms that cause these beneficial effects of late reperfusion therapy performed beyond the time window for myocardial salvage have not been well explained.

Reimer et al. [11] have performed a series of studies indicating that myocardial necrosis develops as a wavefront, appearing at the inner layer in the center of the risk area and gradually extending to the outer layer and also laterally. Accordingly, myocardium at the epicardium will remain viable for considerably longer than that at the endocardium. Provided that reperfusion is achieved before all myocardium at the outer layer becomes necrotic, myocardial salvage will result. The purpose of the study reported in this chapter is to determine whether late reperfusion will cause myocardial salvage, especially at the outer layer.

MATERIALS AND METHODS

The details of this experiment will be described in their original form in a separate report. Briefly, in 11 open-chest mongrel dogs, the left anterior descending coronary artery (LAD) was occluded with a silk suture after the ramification of the second diagonal branch. This second diagonal branch was occluded with a rubber band (figure 1). Twelve hours after occlusion of both arteries, the rubber band was removed to reperfuse the second diagonal branch, but the suture of LAD was not removed. In this model, we can compare the extent of necrosis at the permanently occluded area and at the area with late reperfusion in a single heart. Dogs were bred

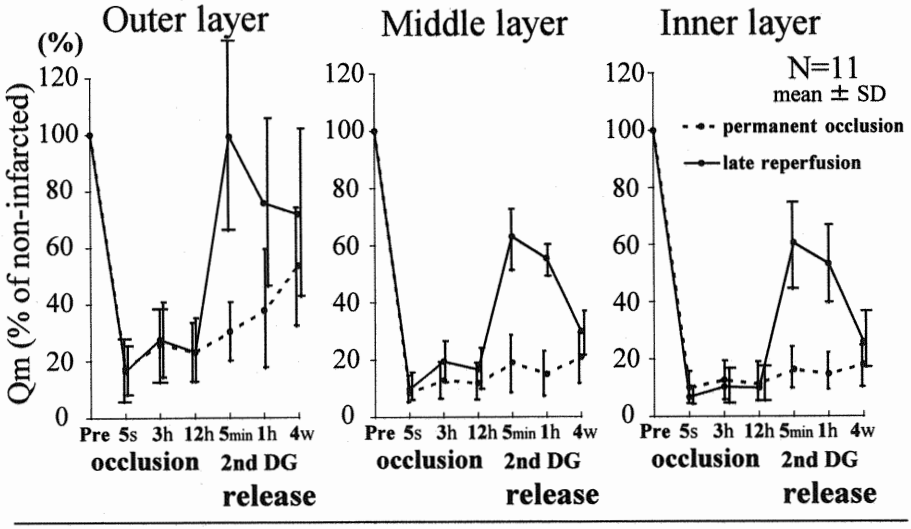

Figure 2. Regional myocardial blood flow (Qm: % of noninfarcted) in the risk areas.

for four weeks, and then the heart was removed. In order to measure regional myocardial blood flow (Qm), a nonradioactive colored microsphere was injected into the left atrium before or after occlusion and also after reperfusion of the second diagonal branch. Qm was calculated as the percent of noninfarcted myocardium, as was described previously as an index of flow change [12]:

$$Qm = \frac{[Q/Qc]\ \text{infarcted}}{[Q/Qc]\ \text{noninfarcted}} \times 100(\%),$$

where Q is the Qm of interest and Qc is the Qm of preocclusion.

After the heart was removed, a transverse section was made between the occluded portion and the apex. This section was dipped in the TTC to identify the necrosis. The ratio of necrosis to the full thickness of the section was measured as the transmurality of the necrosis. This section was then stained with PAS in preparation for microscopic analysis by multiple photo scanning. The amount of viable myocardium in each photograph was counted by a point-counting system with a grid of 100 cross points [13]. Also, the extent of fibrosis in each photograph was graded macroscopically from 0 to 5, where 0 indicates no fibrosis and 5 indicates totally fibrotic myocardium. The averages of myocardium score and the extent of fibrosis from the multiple photographs were calculated at the areas of permanent occlusion and late reperfusion.

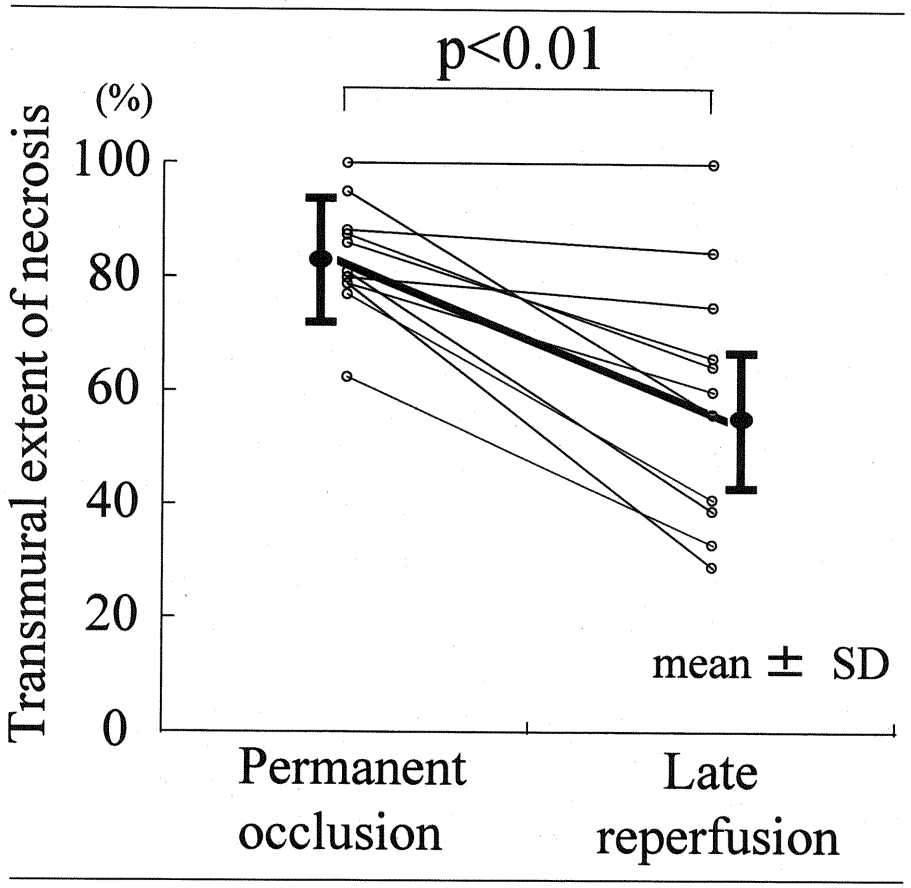

Figure 3. Transmural extent of necrosis by TTC.

RESULTS

Complete data will appear in the separate report. Briefly, the change of Qm during occlusion and after reperfusion is shown in figure 2. During occlusion, Qm was reduced markedly; there were no differences in Qm at the areas of permanent occlusion and late reperfusion. After reperfusion of the second diagonal branch, there was a transient increase of Qm in this area. At four weeks, Qm at the permanent occlusion had increased considerably, and the differences in Qm between the two areas had disappeared. The transmural extent of necrosis was less at the late reperfusion area than at the permanent occlusion area (figure 3). There were more viable myocardium and less fibrosis at the late reperfusion area compared with the area of permanent occlusion (figures 4 and 5).

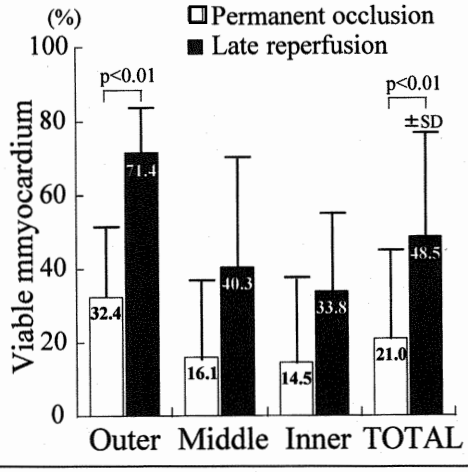

Figure 4. Viable myocardium.

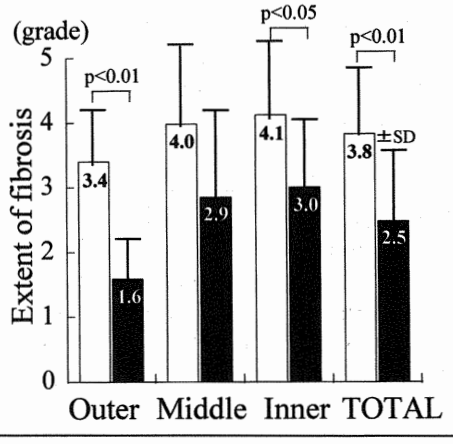

Figure 5. Extent of fibrosis.

DISCUSSION

This study showed that reperfusion 12 hours after coronary occlusion reduces the transmural extent of necrosis, increases the amount of viable myocardium, and reduces the extent of fibrosis at the risk area. These results indicate that late reperfusion salvaged myocardium. The present study is unique in that permanent occlusion and late reperfusion were created in a single heart, thus allowing a comparison of the extent of necrosis in a paired sample in spite of individual variations of necrosis based on coronary anatomy. Also, this study is unique in that

Qm during occlusion was measured, so all data were analyzed knowing that the flow reduction was equal between the two areas.

The previous study conducted in our laboratory demonstrated that the extent of fibrosis was less in a group of dogs where reperfusion was made 12 hours after occlusion than the corresponding fibrosis in permanent occlusion dogs [14]. The present result, together with our previous study [14], is in conflict with many experimental results that failed to show any myocardial salvage by late reperfusion [15–17]. The classic study reported by Reimer et al. [15] concluded that as much as 33% of the myocardium will be salvaged when reperfused three hours after occlusion, while only 16% will be salvaged at six hours in dogs. The trivial amount of myocardial salvage obtained by late reperfusion will be unable to be detected in the clinical studies. In our previous study, Qm at the epicardial rim is preserved at a surprisingly high level after coronary occlusion in dogs [18]. During occlusion, m of the myocardium within 0.5 mm of the epicardial surface remained at 74.8 ± 8.8% of preocclusion levels in dogs. This mechanism can explain why the outer layer at the infarcted myocardium remains viable. It is not difficult to assume that a myocardial layer exists beneath this viable myocardium—a layer that can be salvaged by late reperfusion.

Hochman and Choo [16] have reported that late reperfusion prevented ventricular remodeling and dilatation rather than salvaging the myocardium in rats. Their study has been quoted repeatedly as conclusive evidence that late reperfusion does not exert myocardial salvage. However, when the effect of late reperfusion can be evaluated in a heart where necrosis develops early in some area of the heart and late in other areas, a time difference exists within the heart in the development of necrosis, and reperfusion done during this time lag can salvage the myocardium where necrosis develops late. The rat heart is known to have very small native collaterals, and Qm after occlusion is as low as 6.1% [19]. Accordingly, necrosis will develop at the risk area rapidly, allowing little time for myocardial salvage in rats. Thus, the conclusion of Hochman and Choo, which is based on rats, does not offer an appropriate concept of acute myocardial infarction from which to evaluate the effect of late reperfusion.

CLINICAL IMPLICATIONS

The precise mechanisms that offer beneficial effects from late reperfusion have not been well explained. Limitation of infarct expansion and remodeling are postulated as two of the important mechanisms [20]. The present study showed that late reperfusion caused myocardial salvage in dogs. The human heart has fewer collaterals than dogs, and thus myocardial salvage by late reperfusion, as demonstrated in our dog experiment, cannot be extrapolated as a whole to human patients. However, since it is also known that the human heart has more collaterals than the rat heart [21], more myocardial salvage will be expected in humans than in rats. A limited amount of myocardial salvage by late reperfusion may not be detected in clinical examinations. However, no matter how limited the amount of myocardial salvage

is, the myocardium salvaged will elicit contractile force and play an important role to oppose infarct expansion, to reduce ventricular remodeling, and to improve prognosis.

REFERENCES

1. Katori R, Ishikawa K, Kanamasa K, Morishita M, Ohno M, Ogawa I, Namikawa H, Okayama A. 1987. Improved prognosis after coronary thrombolysis with urokinase in acute myocardial infarction. Jpn Heart J 28:863–872.
2. Kennedy JW, Martin GV, Davis KB, Maynard C, Stadius M, Sheehan FH, Ritchie JL. 1988. The Western Washington Intravenous Streptokinase in Acute Myocardial Infarction randomized trial. Circulation 77:345–352.
3. Gunnar RG, Bourdillon PDV, Dixon DW, Fuster V, Karp RB, Kennedy JW, Klocke FJ, Passamani ER, Pitt B, Rapaport E, Reeves TJ, Russell RO Jr, Sobel BE, Winters WL Jr. 1990. ACC/AHA guidelines for the early management of patients with acute myocardial infarction. Circulation 82:664–707.
4. Serruys PW, Simoons ML, Suryapranata H, Vermeer F, Wijns W, Brand M, BÄR F, Zwaan C, Krauss XH, Remme WJ, Res J, Verheugt FWA, Domburg R, Lubsen J, Hugenholtz PG. 1986. Preservation of global and regional left ventricular function after early thrombolysis in acute myocardial infarction. J Am Coll Cardiol 7:729–742.
5. Ishikawa K, Oda A, Kanamasa K, Morishita M, Ono M, Ogawa I, Shimizu M, Koka H, Katori R. 1988. Effect of coronary thrombolysis on left ventricular ejection fraction in patients with acute myocardial infarction. Jpn Circ J 52:1141–1148.
6. Topol EJ, Califf RM, Vandormael M, Grines CL, George BS, Sanz ML, Wall T, O'Brien M, Schwaiger M, Aguirre FV, Young S, Popma JJ, Sigmon KN, Lee KL, Ellis SG, the Thrombolysis and Angioplasty in Myocardial Infarction-6 study group. 1992. A randomized trial of late reperfusion therapy for acute myocardial infarction. Circulation 85:2090–2099.
7. Fibrinolytic Therapy Trialists' (FTT) Collaborative Group. 1994. Indications for fibrinolytic therapy in suspected acute myocardial infarction: collaborative overview of early mortality and major morbidity results from all randomized trials of more than 1000 patients. Lancet 343:311–322.
8. Richard V, Murry CE, Reimer KA. 1995. Healing of myocardial infarcts in dogs. Effects of late reperfusion. Circulation 92:1891–1901.
9. LATE Study Group. 1993. Late assessment of thrombolytic efficacy (LATE) study with alteplase 6–24 hours after onset of acute myocardial infarction. Lancet 342:759–766.
10. Topol EJ, Califf RM, Vandormael M, Grines CL, George BS, Sanz ML, Wall T, O'Brien M, Schwaiger M, Aguirre FV, Young S, Popma JJ, Sigmon KN, Lee KL, Ellis SG, TAMI-6 Study Group. 1992. A randomized trial of late reperfusion therapy for acute myocardial infarction. Circulation 85: 2090–2099.
11. Reimer KA, Heide RSV, Richard VJ. 1993. Reperfusion in acute myocardial infarction: effect of timing and modulating factors in experimental models. Am J Cardiol 72:13G–21G.
12. Nakai S, Ishikawa K, Ogawa I, Koka H, Kamata N, Akiyama H, Katori R. 1995. New collateral flow increasing early after coronary occlusion prevented myocardial necrosis in dogs. Heart Vessels 10:171–177.
13. Baandrup U, Olsen EGJ. 1981. Critical analysis of endomyocardial biopsies from patients suspected of having cardiomyopathy. Br Heart J 45:475–486.
14. Kamata N. 1996. Effect of reperfusion 12 hours after coronary occlusion on myocardial salvage in dogs. Acta Medica Kinki Univ 21:193–203.
15. Reimer KA, Lowe JE, Rasmussen MM. Jennings RB, 1977. The wavefront phenomenon of ischemic cell death. 1. Myocardial infarct size vs duration of coronary occlusion in dogs. Circulation 56:786–794.
16. Hochman JS, Choo H. 1987. Limitation of myocardial infarct expansion by reperfusion independent of myocardial salvage. Circulation 75:299–306.
17. Hale SL, Kloner RA. 1988. Left ventricular topographic alterations in the completely healed rat infarct caused by early and late coronary artery reperfusion. Am Heart J 116:1508–1513.
18. Ishikawa K, Kamata N, Nakai S, Akiyama H, Koka H, Ogawa I, Katori R. 1994. Preservation of high regional blood flow at epicardial rim after coronary occlusion in dogs. Am J Physiol 267 (Heart Circ Physiol 36):H528–H534.

19. Maxwell MP, Hearse DJ, Yellon DM. 1987. Species variation in the coronary collateral circulation during regional myocardial ischemia: a critical determinant of the rate of evolution and extent of myocardial infarction. Cardiovasc Res 21:737–746.
20. Tiefenbrunn AJ, Sobel BE. 1992. Timing of coronary recanalization. Paradigms, paradoxes, and pertinence. Circulation 85:2311–2315.
21. Weisman HF. Healy B. 1987. Myocardial infarct expansion, infarct extension, and reinfarction: pathophysiologic concepts. Prog Cardiovasc Dis 30:73–110.

ECTO-5′-NUCLEOTIDASE AND CARDIOPROTECTION

MASAFUMI KITAKAZE, TETSUO MINAMINO, KOICHI NODE, HIROHARU FUNAYA, YASUNORI UEDA, HIROSHI ASANUMA, TSUNEHIKO KUZUYA, and MASATSUGU HORI

Osaka University School of Medicine

Summary. When brief periods of ischemia precede sustained ischemia, infarct size is markedly limited, a phenomenon known as *ischemic preconditioning*. The main target for the recent basic research on ischemic preconditioning is to seek how adenosine relates to the infarct size-limiting effect. One possibility is that ischemic preconditioning augments release of adenosine during ischemia and reperfusion. To test this idea, we examined whether ischemic preconditioning activates the enzyme responsible for adenosine release, i.e., 5′-nucleotidase, and tested the cause–effect relationship between activation of 5′-nucleotidase and the infarct size-limiting effect. We found that activation of ecto-5′-nucleotidase plays a crucial role for attenuation of infarct size. Ischemic preconditioning increased ecto-5′-nucleotidase activity and adenosine release during reperfusion. An inhibitor of ecto-5′-nucleotidase blunted the infarct size-limiting effect of ischemic preconditioning. Furthermore, activation of ecto-5′-nucleotidase was attributable to the activation of protein kinase C via α_1-adrenoceptor stimulation, because both prazosin and GF109203X (an inhibitor of protein kinase C) blunted the activation of ecto-5′-nucleotidase and thereby attenuated the infarct size-limiting effect. We found the phosphorylation of ecto-5′-nucleotidase due to activation of protein kinase C either by the treatment with phorbol ester or by ischemic preconditioning, suggesting that phosphorylation of this enzyme due to protein kinase C may play a key role for activation of ecto-5′-nucleotidase. We also found that transfection of ecto-5′-nucleotidase in the rat neonatal cardiomyocytes exerts potent cytoprotection against hypoxia and reoxygenation injury. Taken together, we propose potential mechanisms for cardioprotection attributable to activation of ecto-5′-nucleotidase in ischemic preconditioning.

INTRODUCTION

When brief periods of ischemia precede sustained ischemia, infarct size is markedly limited, a phenomenon known as *ischemic preconditioning* [1,2]. The precise mecha-

S. Mochizuki, N. Takeda, M. Nagano and N. Dhalla (eds.). THE ISCHEMIC HEART.

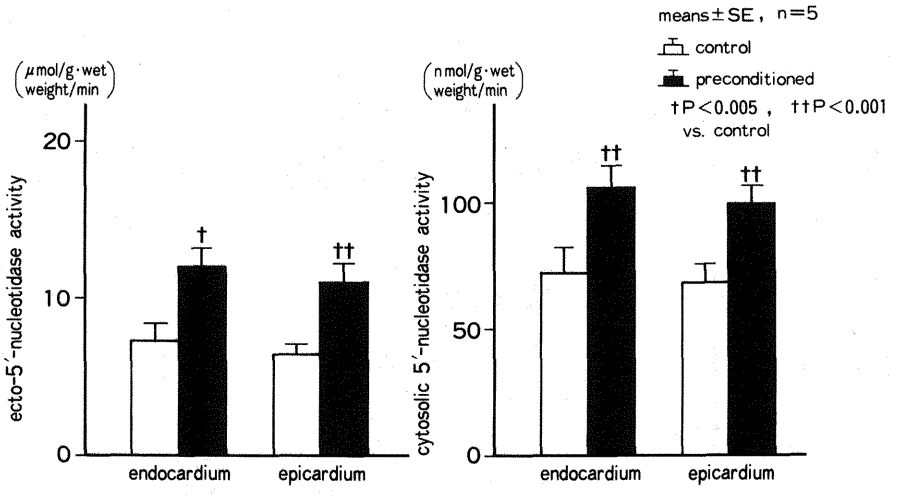

Figure 1. The bar graphs showing ecto- and cytosolic 5′-nucleotidase activity in the control and ischemic preconditioned myocardium. Both ecto- and cytosolic 5′-nucleotidase activities were increased by ischemic preconditioning [11].

nisms underlying this phenomenon have been investigated [3,4] because identification of the primary mediator of ischemic preconditioning may contribute to the development of potential treatment of acute myocardial infarction. Several lines of evidence suggest that beneficial effects of ischemic preconditioning are observed in the clinical settings [5,6]. Recently, Liu et al. [7] experimentally demonstrated that an exposure to 8-sulfophenyltheophylline blunts the infarct size-limiting effect of ischemic preconditioning and that brief periods of exposures to adenosine, instead of transient ischemia, mimic ischemic preconditioning. Thornton et al. [8] showed that adenosine A_1 receptor activation is responsible for the infarct size-limiting effect of ischemic preconditioning. Indeed, it has been clarified that adenosine contributes to the reduction of infarct size [9,10]. One possibility that may link adenosine with cardioprotection in ischemic preconditioning is that release of adenosine during ischemia and reperfusion is enhanced by ischemic preconditioning. Here, we discuss this possibility, showing the activity of the enzymes responsible for adenosine release, i.e., ecto-5′-nucleotidase, with and without ischemic preconditioning, and test the cause–effect relationship between activation of ecto-5′-nucleotidase and cardioprotection.

ADENOSINE RELEASE AND 5′-NUCLEOTIDASE ACTIVITY IN ISCHEMIC PRECONDITIONING

First, we tested whether the ischemic preconditioning procedure increases ecto-5′-nucleotidase activity and adenosine release during reperfusion [11,12]. In anesthetized open-chest dogs, after intravenous administration of heparin (500 units/kg),

we cannulated and perfused the left anterior descending (LAD) coronary artery with blood from the left carotid artery through an extracorporeal bypass tube. Coronary blood flow and coronary perfusion pressure in the perfused area was measured. A small-caliber (1 mm), short (7 cm) collecting tube was introduced into a small coronary vein near the center of the perfused area to sample coronary venous blood for measurements of adenosine concentration. After the bypass tube to the LAD coronary artery was occluded four times for five minutes, both ecto- and cytosolic 5′-nucleotidase activity was increased (figure 1). Adenosine concentration in the coronary venous blood was higher in the group with ischemic preconditioning compared with the untreated control group.

Is the activation of ecto-5′-nucleotidase directly linked with enhanced release of adenosine during ischemia and reperfusion? Adenosine is produced simply by the enzymatic reactions: the dephosphorylation of 5′-AMP by 5′-nucleotidase and the hydrolysis of S-adenosylhomocysteine (SAH) by SAH-hydrolase. Although adenosine is produced through the latter pathway in the normoxic hearts [13], 5′-nucleotidase is related to adenosine production during ischemia and hypoxia [14,17]. This idea is supported by the fact that α,β-methyleneadenosine 5′-diphosphate (AOPCP, an inhibitor of ecto-5′-nucleotidase; 80 μg/kg/min) potently reduces adenosine production in the ischemic myocardium [12]. Furthermore, the extents of decrease in reactive hyperemic flow following a brief period of coronary occlusion were comparably reduced under the treatment with either AOPCP or 8-sulfophenyltheophylline (an adenosine-receptor antagonist), suggesting that adenosine production during ischemia is attributable to ecto-5′-nucleotidase [18]. On the other hand, accumulation of 5′-AMP seems to be the other factor that regulates adenosine production. Cytosolic 5′-AMP concentration crucially depends on the duration and severity of ischemia and culminates up to 1×10^{-2}–10^{-4} M. Considering that production of adenosine is 1×10^{-6}–10^{-8} M, even considerable changes in AMP concentration would not affect adenosine production during ischemia.

On the other hand, there is a report indicating that increases in adenosine concentration in the interstitial space are not augmented during sustained ischemia in the ischemic preconditioning group [19]. We also observed differences in the interstitial and coronary venous adenosine levels during sustained ischemia in the ischemic preconditioning group in our experiment. One possible explanation for this difference is that we measured adenosine concentrations in coronary and venous blood, where adenosine level is largely affected by endothelial cells. In turn, the interstitial adenosine levels might be affected by myocardial ecto-5′-nucleotidase. Indeed, we found that, ischemic preconditioning may activate ecto-5′-nucleotidase differently at the endothelial cells and cardiomyocytes. Second, it is possible that even if the adenosine concentration in the microenvironment surrounding ecto-5′-nucleotidase on the myocardial cellular membrane is increased by activated ecto-5′-nucleotidase, the alteration of interstitial volume determined by myocardial cellular swelling and the rate of washout due to the lymphatic stream may change the interstitial adenosine concentration. In any of these possible situations, the temporal and topical increases in the adenosine concentration surrounding ecto-5′-

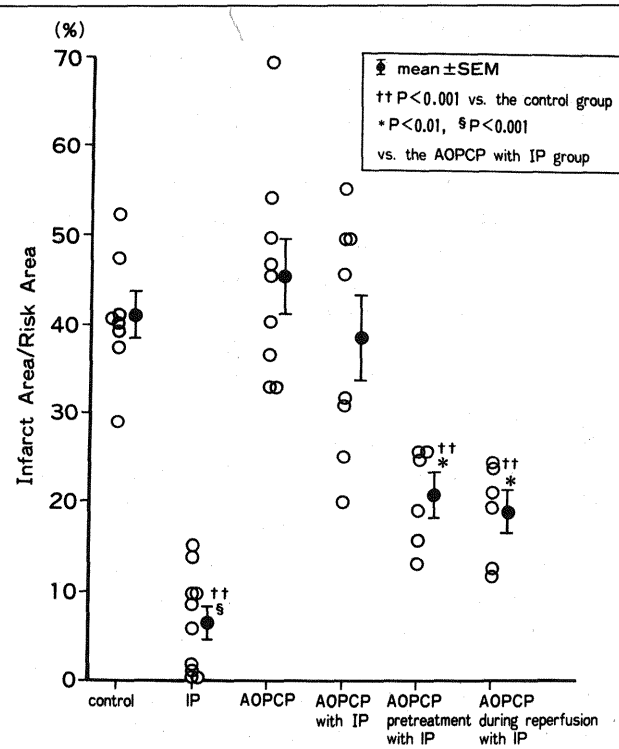

Figure 2. Infarct size in the control group, the ischemic preconditioning group, the AOPCP treatment group, the AOPCP treatment with IP group, the AOPCP pretreatment with IP group, and the AOPCP during reperfusion with IP group. Infarct size was markedly decreased by ischemic preconditioning. The infarct size-limiting effect of ischemic preconditioning was completely abolished by administration of AOPCP. Administration of AOPCP during the ischemic preconditioning procedure or during reperfusion following sustained ischemia attenuated ($p < 0.001$) infarct size compared with infarct size in the control group. On the other hand, infarct size of the AOPCP pretreatment with IP group and the AOPCP during reperfusion with IP group were larger ($p < 0.01$) than that in the ischemic preconditioning group [12].

nucleotidase may be able to directly activate the adenosine receptors located at the same cellular membrane. This hypothesis may not contradict Van Wylen's observation. This close juxtaposition may explain how ecto-5′-nucleotidase activates the adenosine receptors. Indeed, the regulatory systems, including the ATP receptors, G proteins, ecto-5′-nucleotidase and K_{ATP} channels, are closely linked to each other and present in a single patch of no more than 1 μm^2 [20].

ROLE OF ACTIVATION OF 5′-NUCLEOTIDASE IN SALVAGE OF MYOCARDIAL NECROSIS IN ISCHEMIC PRECONDITIONING

To test the cause-and-effect relationship between activation of 5′-nucleotidase and the infarct size-limiting effect in ischemic preconditioning, we examined whether

AOPCP blunted the infarct size limiting-effect of ischemic preconditioning [12]. AOPCP was administered into the LAD coronary artery five minutes prior to the ischemic preconditioning (IP) procedures and was continued for 60 minutes of reperfusion except for the coronary occlusion period (the AOPCP treatment with IP group). In the other dogs, AOPCP was administered into the LAD coronary artery 40 minutes prior to ischemia and was continued for 60 minutes of reperfusion except for the coronary occlusion period (the AOPCP treatment group). To discriminate the role of increases in 5′-nucleotidase activity during the ischemic preconditioning procedure (the AOPCP pretreatment with the IP group) or during reperfusion (the AOPCP during reperfusion with the IP group) on the infarct size-limiting effect, we infused AOPCP only during the ischemic preconditioning procedure or only during reperfusion up to 60 minutes in the ischemic preconditioned dogs. There were no significant differences in risk area and collateral flow during ischemia between the six groups. Figure 2 depicts infarct size in the six groups. Ischemic preconditioning markedly attenuated infarct size, and AOPCP completely abolished the infarct size-limiting effect of ischemic preconditioning. In the AOPCP pretreatment with IP and in the AOPCP during reperfusion with IP groups, infarct size was partially attenuated compared with the AOPCP treatment with IP group and the AOPCP treatment group. The infarct sizes in these two groups were smaller than those of the control and AOPCP groups and larger than those in the ischemic preconditioning group. These results indicate that increased 5′-nucleotidase activity during ischemic preconditioning procedures and during early reperfusion synergistically contributes to the infarct size-limiting effect of ischemic preconditioning.

To prove the role of ecto-5′-nucleotidase directly, we transfected the cDNA of ecto-5′-nucleotidase using the lipofectin method. In the rat neonatal cardiomyocytes, we transfected cDNA of ecto-5′-nucleotidase, and we found that the activity of ecto-5′-nucleotidase increases 2–3-fold compared with the control cardiomyocytes. The transfected cardiomyocytes exert potent cardioprotection against injury from hypoxia (180 minutes) and reoxygenation (60 minutes); the extent of injury assessed by LDH release decreased to almost half compared with the control. Therefore, we believe that the activation of ecto-5′-nucleotidase directly exerts cardioprotection against ischemia and reperfusion injury.

ROLE OF ACTIVATION OF PROTEIN KINASE C VIA α_1-ADRENOCEPTORS IN ACTIVATION OF ECTO-5′-NUCLEOTIDASE AND THE SALVAGE OF MYOCARDIAL NECROSIS IN ISCHEMIC PRECONDITIONING

According to the data of Downey's group [21], protein kinase C is tightly linked to ischemic preconditioning. We have reported that activation of protein kinase C increases ecto-5′-nucleotidase activity in the rat cardiomyocytes (figure 3 [22]). Since protein kinase C is activated by ischemic preconditioning [23], ischemic preconditioning may increase ecto-5′-nucleotidase activity via protein kinase C activation. We also observed that activation of ecto-5′-nucleotidase due to ischemic preconditioning is blunted by GF109203X, an inhibitor of protein kinase C, in

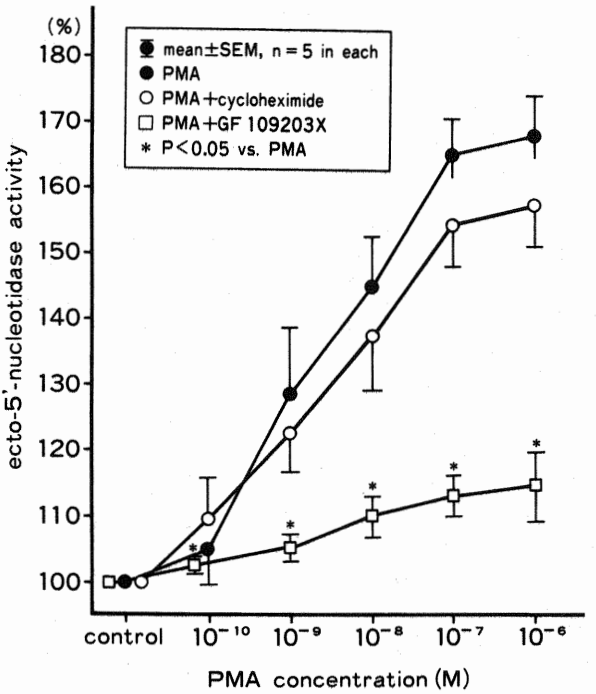

Figure 3. The dose–response relation between phorbol 12-myristate 13-acetate (PMA) and ecto-5′-nucleotidase activity with and without either GF109203X (an inhibitor of protein kinase C) and cycloheximide (an inhibitor of protein synthesis) in rat cardiomyocytes. Ecto-5′-nucleotidase activity in the control conditions were 6.44 ± 0.89, 5.96 ± 0.78, and 5.81 ± 0.44 nmol/mg protein/min in the PMA, PMA with GF109203X, and PMA with cycloheximide groups, respectively [22].

canine hearts. Furthermore, inhibition of protein kinase C by GF109203X blunted the infarct size-limiting effect of ischemic preconditioning (figure 4). We have also shown that ecto-5′-nucleotidase is phosphorylated in the preconditioned myocardium. Therefore, we speculate that phosphorylation of ecto-5′-nucleotidase due to protein kinase C may change the characteristics of the active site of ecto-5′-nucleotidase or induce a conformational change in the structure of 5′-nucleotidase.

The next question is how protein kinase C is activated during ischemic preconditioning. Since ischemic preconditioning increases release of norepinephrine from the presynaptic vesicles, we tested the role of α_1-adrenoceptor activation in cardioprotection in ischemic preconditioning [24]. In open-chest dogs, constant infusion of prazosin (4 μg/kg/min) into the LAD coronary artery was begun five minutes prior to ischemic preconditioning and continued through the first 60 minutes of the reperfusion period, except during coronary occlusion (the prazosin with IP group). In the other dogs, prazosin was infused into the LAD coronary artery beginning 40 minutes prior to ischemia without ischemic preconditioning and

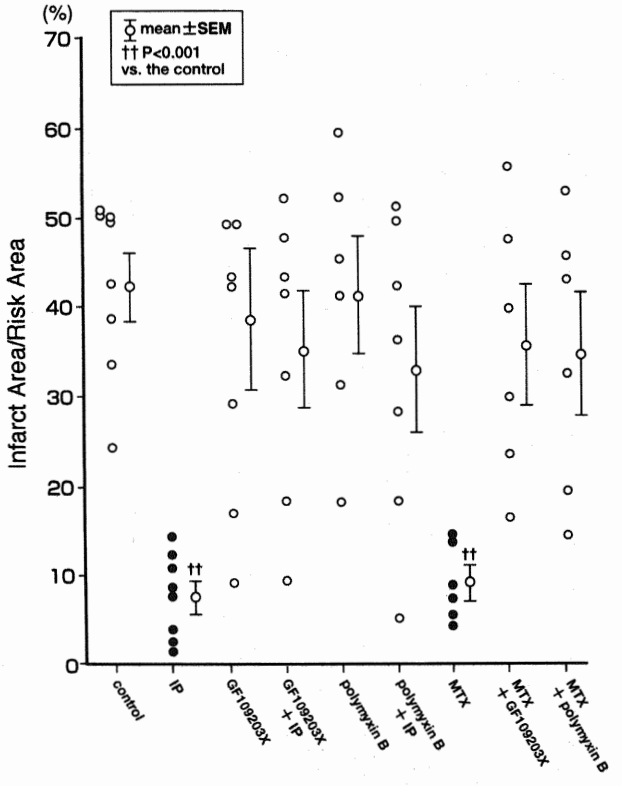

Figure 4. Infarct size in the control group, the ischemic preconditioning group, the prazosin with IP group, the GF109203X group, the IP with GF109203X group, the polymyxin B group, the IP with polymyxin B group, the methoxamine group, the methoxamine with GF109203X group, and the methoxamine with GF109203X group, Infarct size was decreased in the ischemic preconditioning group. The infarct size-limiting effect of ischemic preconditioning was abolished by GF109203X and polymyxin B. On the other hand, methoxamine mimicked the infarct size-limiting effect of ischemic preconditioning, which was blunted by GF109203X and polymyxin B [23].

continued for 60 minutes of reperfusion, except during coronary occlusion (the prazosin group). To test whether α_1-adrenoceptor stimulation mimics the infarct size-limiting effect of ischemic preconditioning, we administered methoxamine into the LAD (40 μg/kg/min, four cycles for five minutes with five-minute intervals; the methoxamine group). Following methoxamine exposure, 90 minutes of coronary occlusion and six hours of reperfusion were imposed. Furthermore, to examine the role of increased ecto-5′-nucleotidase activity due to exposures of methoxamine, we concomitantly infused AOPCP five minutes prior to ischemic preconditioning and continued for 60 minutes of reperfusion, except during 90 minutes of coronary occlusion to animals treated with methoxamine (the methoxamine with AOPCP group). In another group, we determined the effect of AOPCP on infarct size (the

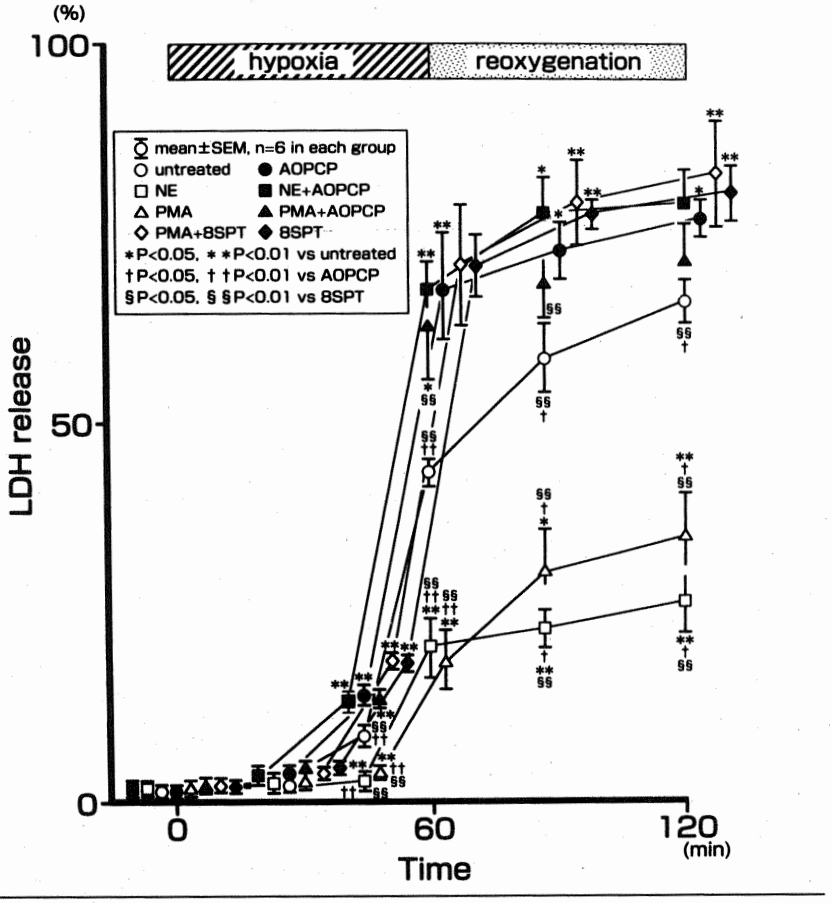

Figure 5. Sequential changes in cellular viability assessed by LDH release in the untreated, the methoxamine pretreatment, the PMA pretreatment, the methoxamine pretreatment and AOPCP treatment, the PMA pretreatment and AOPCP treatment, and the AOPCP treatment groups during 60 minutes of hypoxia and 60 minutes of reoxygenation of the rat cardiomyocytes. The extent of LDH release due to hypoxia and reoxygenation was significantly smaller in the methoxamine- and PMA-treated groups than the untreated group, which was blunted by AOPCP [26].

AOPCP group). In this group, AOPCP was administered prior to 40 minutes of coronary occlusion and during one hour of reperfusion following 90 minutes of coronary occlusion.

Ischemic preconditioning increased both ecto- and cytosolic 5′-nucleotidase activity in the myocardium. Prazosin administration without ischemic preconditioning decreased ecto- and cytosolic 5′-nucleotidase activity and blunted the increases in ecto- and cytosolic 5′-nucleotidase activity due to ischemic preconditioning. Methoxamine increased both ecto- and cytosolic 5′-nucleotidase activity to the levels obtained by ischemic preconditioning. We further observed that prazosin

completely abolishes the infarct size-limiting effect of ischemic preconditioning. With the methoxamine administration, infarct size was attenuated to the level seen with ischemic preconditioning. However, the infarct size-limiting effect due to exposure of methoxamine was blunted by AOPCP, and no difference in infarct size existed between the methoxamine with AOPCP and the AOPCP groups. This observation is consistent with previous studies. It has been reported that α_1-adrenoceptor activation is intimately involved in the attenuation of the severity of ischemia and reperfusion [16] and ischemic preconditioning [25]. We also observed that transient exposures to methoxamine or 12-myristate 13-acetate increased ecto-5′-nucleotidase activity and mediated cardioprotection against hypoxia and reoxygenation in rat cardiomyocytes (figure 5 [26]). Therefore, these results may lead us to the hypothesis that α_1-adrenoceptor stimulation mediates the cardioprotection seen in ischemic preconditioning, which is attributable to activation of ecto-5′-nucleotidase.

CLINICAL RELEVANCE

The finding in the present study suggests two clinical applications for treatment of acute myocardial infarction. One strategy to limit infarct size is to find a method to increase 5′-nucleotidase activity. As we observed, protein kinase C activation may increase 5′-nucleotidase activity and may attenuate contractile dysfunction and infarct size. Another possibility is to enhance adenosine release. Administration of adenosine and potentiators of adenosine production, e.g., acadesine, dilazep, or dipyridamole, may limit infarct size. Both strategies merit clinical investigation, although a further understanding of the basic process involved in ischemic preconditioning is necessary.

REFERENCES

1. Murry CE, Jennings RB, Reimer KA. 1986. Preconditioning with ischemia: a delay of lethal cell injury in ischemic myocardium. Circulation 74:1124–1136.
2. Li GC, Vasquez JA, Gallagher KP, Lucchesi BR. 1990. Myocardial protection with preconditioning. Circulation 82:609–619.
3. Murry CE, Richard VJ, Reimer KA, Jennings RB. 1990. Ischemic preconditioning slows energy metabolism and delays ultrastructural damage during a sustained ischemic episode. Circ Res 66:913–931.
4. Steenbergen CM, Perlman R, London E, Murphy E. 1993. Mechanism of preconditioning lonic alterations. Circ Res 72:112–125.
5. Deutsch E, Berger M, Kussmaul WG, Hirshfeld KW Jr, Herrmann HC, Laskey W. 1990. Adaptation in ischemia during percutaneous transmural coronary angioplasty. Clinical, hemodynamic, and metabolic features. Circulation 82:2044–2051.
6. Okazaki Y, Kodama K, Sato H, Kitakaze M, Hirayama A, Mishima M, Hori M, Inoue M. 1993. Attenuation of increased regional oxygen consumption during exercise as a major cause of warm-up phenomenon. J Am Coll Cardiol 21:1597–1604.
7. Liu GS, Thornton J, Van Winkle DM, Stanley AWH, Olsson RA, Downey JM. 1991. Protection against infarction afforded by preconditioning is mediated by A_1 adenosine receptors in rabbit heart. Circulation 84:350–356.
8. Thornton JD, Liu GS, Olsson RA, Downey JM. 1992. Intravenous pretreatment with A_1-selective adenosine analogue protects the heart against infarction. Circulation 85:659–665.
9. Miura T, Ogawa T, Iwamoto T, Shimamoto K, Iimura O. 1992. Dipyridamole potentiates the myocardial infarct size-limiting effect of ischemic preconditioning. Circulation 86:979–985.

10. Olafsson B, Forman MB, Puett DW, Pou A, Cates CU, Friesinger GC, Virmani R. 1987. Reduction of reperfusion injury in the canine preparation by intracoronary adenosine: importance of the endothelium and the no-reflow phenomenon. Circulation 76:1135–1145.
11. Kitakaze M, Hori M, Takashima S, Sato H, Inoue M, Kamada T. 1993. Ischemic preconditioning increases adenosine release and 5′-nucleotidase activity during myocardial ischemia and reperfusion in dogs. Implication for myocardial salvage. Circulation 87:208–215.
12. Kitakaze M, Hori M, Morioka T, Minamino T, Takashima S, Sato H, Shinozaki Y, Chujo M, Mori H, Inoue M, Kamada T. 1994. The infarct size-limiting effect of ischemic preconditioning is blunted by inhibition of 5′-nucleotidase activity and attenuation of adenosine release. Circulation 89:1237–1246.
13. Lloyd HGE, Schrader J. 1987. The importance of the transmethylation pathway for adenosine metabolism in the hearts. In Gerlach E, Becker BF (eds), Topics and Perspectives in Adenosine Research. Berlin/Heidelberg: Springer-Verlag, pp. 199–207.
14. Sparks NV Jr, Bardengeuer H. 1986. Regulation of adenosine formation by the heart. Circ Res 58:193–201.
15. Hori M, Kitakaze M. 1991. Adenosine, the heart, and coronary circulation. Hypertension 18:565–574.
16. Kitakaze M, Hori M, Kamada T. 1993. Role of adenosine and its interaction with alpha adrenoceptor activity in ischemic and reperfusion injury of the myocardium. Cardiovasc Res 27:18–27.
17. Imai S, Nakazawa M, Imai M, Jin H. 1986. 5′-Nucleotidase inhibitors and the myocardial reactive hyperemia and adenosine content. In Gerlach E, Becker BF (eds), Topics and Perspectives in Adenosine Research. Berlin/Heidelberg: Springer-Verlag, pp. 416–424.
18. Kitakaze M, Hori M, Takashima S, Iwai K, Sato H, Inoue M, Kitabatake A, Kamada T. 1992. Superoxide dismutase enhances ischemia-induced reactive hyperemic flow and adenosine release in dogs: a role of 5′-nucleotidase activity. Circ Res 71:558–566.
19. Van Wylen DGL. 1994. Effects of ischemic preconditioning on interstitial purine metabolite and lactate accumulation during myocardial ischemia. Circulation 89:2283–2289.
20. Al-Awqati Q. 1995. Regulation of ion channels by ABC transporter that secrete ATP. Science 269:805–806.
21. Tsuchida A, Liu Y, Liu GS, Cohen MV, Downey JM. 1994. Alpha1-adrenergic agonists precondition rabbit ischemic myocardium independent of adenosine by direct activation of protein kinase activation. Circ Res 75:576–585.
22. Kitakaze M, Hori M, Morioka T, Minamino T, Takashima S, Okazaki Y, Node K, Komamura K, Iwakura K, Inoue M, Kamada T. 1995. α_1-Adrenoceptor activation increases ectosolic 5′-nucleotidase activity and adenosine release in rat cardiomyocytes by activing protein kinase C. Circulation 91:2226–2234.
23. Kitakaze M, Node K, Minamino T, Komamura K, Funaya H, Shinozaki Y, Chujo M, Mori H, Inoue M, Hori M, Kamada T. 1996. The role of activation of protein kinase C in the infarct size-limiting effect of ischemic preconditioning through activation of ecto-5′-nucleotidase. Circulation 93:781–791.
24. Kitakaze M, Hori M, Morioka T, Minamino T, Takashima S, Sato H, Shinozaki Y, Chujo M, Mori H, Inoue M, Kamada T. 1994. $Alpha_1$-adrenoceptor activation mediates the infarct size-limiting effect of ischemic preconditioning through augmentation of 5′-nucleotidase activity. J Clin Invest 93:2197–2205.
25. Banerjee A, Locke-Winter C, Rogers KB, Mitchell MB, Brew EC, Cairns CB, Bensard DD, Harken AH. 1993. Preconditioning against myocardial dysfunction after ischemia and reperfusion by a-adrenergic mechanism. Circ Res 73:656–670.
26. Kitakaze M, Minamino T, Node K, Komamura K, Inoue M, Hori M, Kamada T. 1996. Activation of ecto-5′-nucleotidase by protein kinase C attenuates irreversible cellular injury due to hypoxia and reoxygenation in rat cardiomyocytes. J Mol Cell Cardiol 28:1945–1955.

LIMITATION OF STUNNING IN DOG MYOCARDIUM BY THE NUCLEOSIDE–NUCLEOTIDE MIXTURE OG-VI

SEIICHIRO KANO*, YASUNAGA OKAZAKI*, TOHRU NAKAI*, KUMI SATOH*, KATSUJI HOSHI*, HIDEAKI KOHRI**, and KAZUO ICHIHARA*****

* *Hokkaido College of Pharmacy*
** *Nutrition Research Institute*
*** *Kochi Medical School*
**** *Asahikawa Medical College*

Summary. OG-VI improves mechanical and metabolic function in the stunned myocardium because it provides substrates for the adenine nucleotide biosynthesis. This solution can be used as an energy ameliorant for therapy of patients with ischemic heart disease.

INTRODUCTION

Ischemia or ischemia–reperfusion induces myocardial cell damage. Reperfusion following ischemia does not completely restore the myocardial mechanical function and the tissue level of adenosine triphosphate (ATP). In particular, myocardial contractile dysfunction caused during reperfusion after a brief period of ischemia is known as *myocardial stunning* [1]. Creatine phosphate (CrP) plays an important role in the energy transport process [2,3]. ATP synthesized via mitochondrial respiration transfers its high-energy phosphate to creatine in the mitochondria. The CrP resulting from the phosphate transfer moves to cytosol, and then gives the high-energy phosphate back to adenosine diphosphate (ADP) at the compartment including contractile elements in order to resynthesize ATP. Because the CrP content, which has been lowered by brief ischemia, is completely restored or restored beyond the preischemic level during reperfusion [3], mitochondria can produce ATP after reperfusion following brief ischemia. One of the major causes of ischemia-induced myocardial injury is the loss of adenine nucleotides from the myocardial cells during ischemia and/or reperfusion following ischemia [4,5]. Loss of adenine nucleotides in the cell during ischemia may cause a lack of ADP near the contractile elements, leading to failure in transferring the high-energy phosphate of CrP to ADP. A low

S. Mochizuki, N. Takeda, M. Nagano and N. Dhalla (eds.). THE ISCHEMIC HEART.

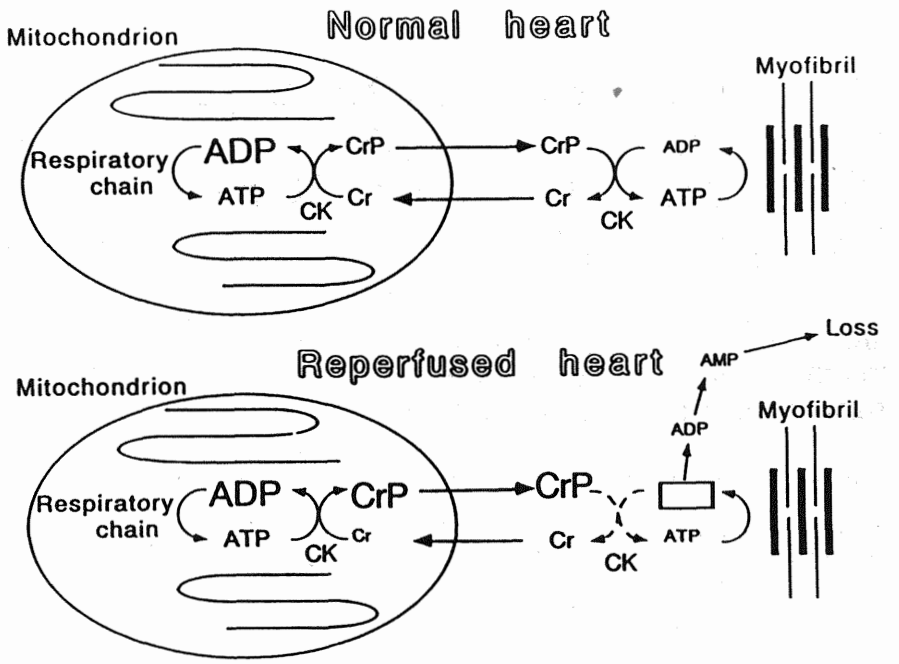

Figure 1. Energy transport system in the normal and ischemia–reperfused heart. Because loss of adenine nucleotide from the ADP store near the myofibrils occurs during ischemia, the high-energy phosphates that are delivered by creatine phosphate (CrP) cannot be accepted during reperfusion.

free-ADP concentration limits the regeneration of ATP at the myofibrillar level and may be responsible for the depression of contractility [6]. The concept for this energy transport system is schematically shown in figure 1 [7]. Therefore, we are looking for some substances that can fill the ADP stores and restore the myocardial mechanical function during ischemia and reperfusion. We [7] have found several substances that succeed in preventing myocardial stunning and have named this kind of drug *energy ameliorants*.

OG-VI is a solution composed of 30 mM inosine, 30 mM sodium 5′-guanylate, 30 mM cytidine, 22.5 mM uridine, and 7.5 mM thymidine [8]. It was first expected to provide substrates for the salvage pathway of mononucleotides that serve as the basis of high-molecular nucleic acid synthesis and to improve the function of the liver that had been injured by surgical stress [8–10]. The nucleotides produced from OG-VI may be utilized as precursors of not only nucleic acids but also high-energy phosphates. Because OG-VI is a mixture of nucleosides and nucleotides, it may replenish the cytosolic ADP store with adenine nucleotides, leading to improvement of myocardial contractile function of the reperfused heart [11–13]. The aim of the study reported here, therefore, was to examine whether OG-VI can be a candidate for one of the energy ameliorants.

METHODS

Animal preparation

Healthy mongrel dogs of either sex were anesthetized with sodium pentobarbital (30 mg/kg, i.v.) and ventilated with room air. Left thoracotomy was performed between the fourth and fifth ribs, and the left ventricle was exposed. After the heart had been suspended in a pericardial cradle, the main trunk of the left anterior descending coronary artery (LAD) was dissected free, from the distal end to the first diagonal branch, and was loosely encircled with a silk thread ligature. To measure mean left ventricular end-systolic and end-diastolic pressure (LVESP and LVEDP, respectively) and the first derivative of left ventricular pressure (LV dP/dT), a polyethylene tube connected to a pressure transducer was inserted into the left ventricular chamber through the cardiac apex. LAD flow was measured using a magnetic flow probe positioned in the LAD proximal to the ligature. A pair of ultrasonic crystals was implanted in a circumferential plane at the LAD region. The two crystals of each pair were separated by about 1 cm. The percentage of segment shortening (%SS) was calculated using the equation

$$\%SS = \left[(DL - SL)/DL\right] \times 100,$$

where DL is the diastolic segment length and SL the systolic segment length. DL was determined at the beginning of the rising phase of positive LV dP/dT (onset of isovolumic contraction), and SL was determined at the peak negative LV dP/dT. Arterial blood pressure was measured via a cannula introduced from the left femoral artery and advanced to a point near the aortic arch. Heart rate was monitored from the pulse pressure of arterial pressure.

Biochemical assay

The frozen subendocardial tissue samples were pulverized in a mortar and pestle, precooled in liquid nitrogen, and extracted with three volumes of 6% prechloric acid. The tissue levels of adenosine triphosphate (ATP), adenosine diphosphate (ADP), adenosine monophosphate (AMP), glucose 6 phosphate (G6P), fructose 6 phosphate (F6P), fructose 1,6 diphosphate (FDP), pyruvate, and lactate were determined in the neutralized perchloric acid extract, according to standard enzymatic procedures.

Experimental protocol

After a 20–30-minute postsurgical stabilization period, each experiment was performed. The infusion of OG-VI solution or the related solution was started 30 minutes before LAD ligation and was continued until the experiment was completed. The heart was made ischemic for 20 minutes and reperfused for 30 minutes. OG-VI solution was made by dissolving 30 mM inosine, 30 mM cytidine, 30 mM sodium 5′-guanylate, 22.5 mM uridine, and 7.5 mM thymidine in 0.45% sodium chloride solution to adjust the osmotic pressure. Total nucleoside–nucleotide

concentration of OG-VI was 120 mM. The present study consists of four parts of the experiment, as follows:

1. effects of OG-VI on stunned myocardium;
2. effects of the constituents of OG-VI on stunned myocardium;
3. effects of OG-VI with DPCPX, a selective adenosine A_1 receptor antagonist, on stunned myocardium; and
4. effects of OG-VI on ischemic myocardial metabolism.

In the first experiment, either saline or OG-VI (24 and 12 μmol/kg/min) was infused at 0.1 mL/kg/min from the left femoral vein at random. In the second experiment, either saline, OG-VI (12 μmol/kg/min), an inosine and sodium 5′-guanylate mixture (IG; 6 μmol/kg/min), a cytidine, uridine and thymidine mixture (CUT; 6 μmol/kg/min), or AICAr (3 μmol/kg/min) was infused at 0.1 mL/kg/min). In the third experiment, 1 mg/kg of 8-cyclopentyl-1,3-dipropylxanthine (DPCPX), a selective adenosine A_1-receptor antagonist, was intravenously injected 15 minutes before starting the saline and 1.2 μmol/kg/min of OG-VI infusions. In the fourth experiment, the three-minute ischemic myocardial sample was taken from the ischemic region of the left ventricle for biochemical assay. Infusion of saline or OG-VI (12 μmol/kg/min and 1.2 μmol/kg/min, respectively) was begun 30 minutes before the onset of ischemia.

Statistical analysis

All values are expressed as means ± SEM. The significance of differences between groups in hemodynamics and energy and carbohydrate metabolites was evaluated using two-way analysis of variance (ANOVA) followed by the Tukey-Kramer multiple test. Differences were considered statistically significant when p was less than 0.05.

RESULTS

Many hemodynamic parameters were measured in the present study. Only the changes in segment shortening function (%SS) are described here (experiments 1–3). The values of %SS were normalized to preinfusion values of %SS in each experiment.

Effects of OG-VI on stunned myocardium (figure 2)

In both the saline and OG-VI groups, %SS decreased markedly during ischemia. The decreased %SS returned towards preligation levels after reperfusion, but the recovery of %SS was incomplete. OG-VI at either dosage significantly enhanced the recovery of %SS during reperfusion as compared with saline.

Effects of the constituents of OG-VI on stunned myocardium (figure 3)

In this section, saline, OG-VI, an inosine and sodium 5′-guanylate mixture (IG), a cytidine, uridine and thymidine mixture (CUT), or AICAr was infused. Although

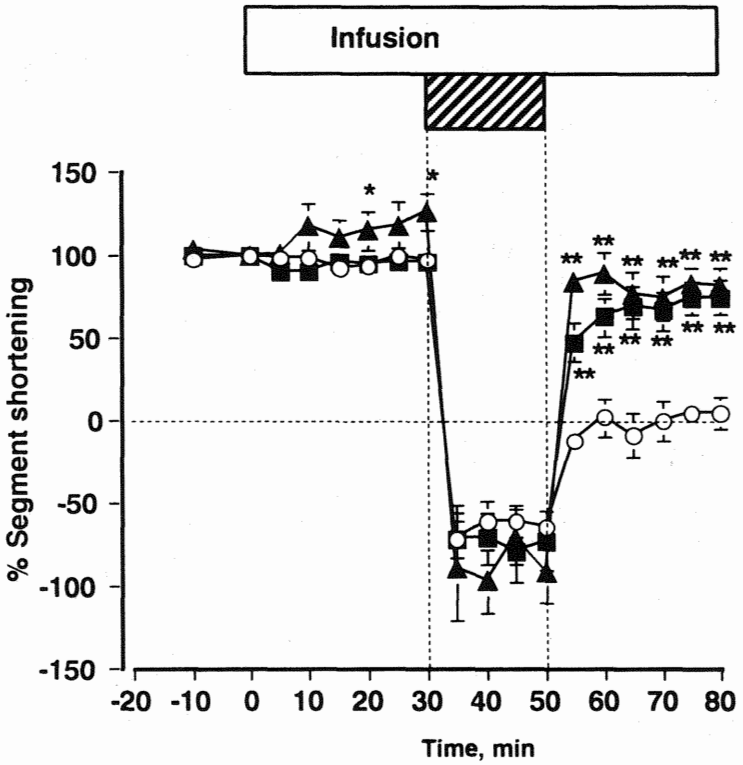

Figure 2. Effects of OG-VI on segment shortening function (%SS) of the ischemic–reperfused area. Either saline (○), 12 μmol/kg/min OG-VI (■), or 24 μmol/kg/min OG-VI (▲) was infused from the left femoral vein. Ischemia was induced by ligating the left anterior descending coronary artery (LAD) 30 minutes after the onset of infusion. The values of %SS were normalized to the preinfusion values of %SS (at 0 min; % control). All values are mean ± SEM. Symbols indicating statistical significance are shown only the difference vs. saline group to avoid complexity. *, $p < 0.05$, and **, $p < 0.01$ compared with saline-infused group at the corresponding time.

OG-VI does not contain AICAr, it was used as a reference drug. In all five groups, including the slaine group, %SS significantly decreased and became below zero during ischemia. In the AICAr group, the decrease in %SS due to ischemia was less than that in the saline group, although a statistical significance was observed only at 20 minutes postischemia. In the IG group, the decrease in %SS during ischemia also appeared to be less than those in the OG-VI and CUT groups. However, the ischemic %SS measurements were not statistically different from each other. The %SS values that had decreased due to ischemia returned towards their respective preischemic levels after reperfusion, although the recovery of the %SS was incomplete. Infusion of OG-VI and IG significantly expedited recovery of the %SS during reperfusion as compared with infusion of saline. Infusion of AICAr also significantly

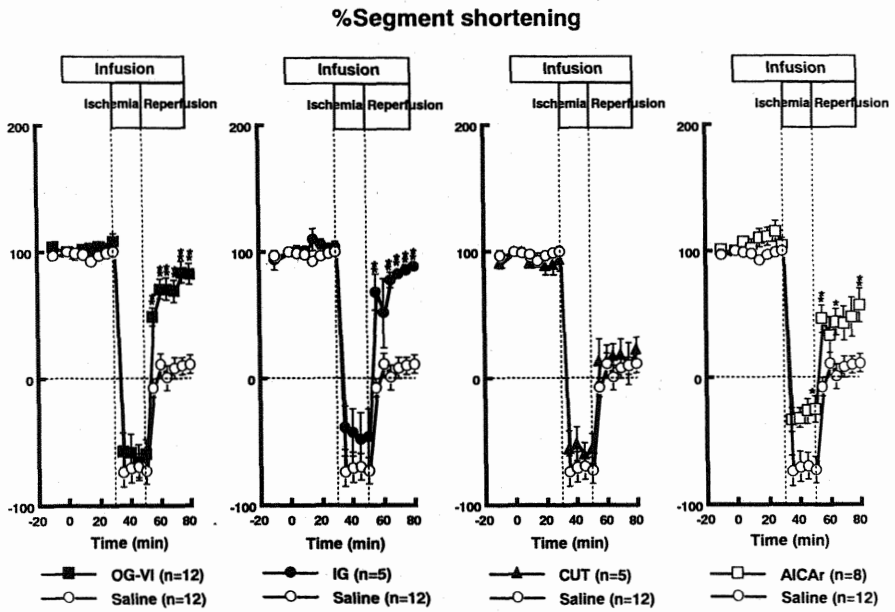

Figure 3. Effects of OG-VI and its constituents on %SS of the ischemic–reperfused area. Either saline (○), 12 μmol/kg/min OG-VI (■), 6 μmol/kg/min IG component (●), 6 μmol/kg/min CUT component (▲), or 3 μmol/kg/min AICAr (□) solution was infused. Protocol is the same as that in figure 2. ⋆, $p < 0.05$, and ⋆⋆, $p < 0.01$ as compared with saline group at the corresponding time.

enhanced the recovery of %SS during reperfusion at 5, 15, and 30 minutes of reperfusion. However, infusion of CUT did not potentiate the recovery of %SS during reperfusion.

Effects of OG-VI with DPCPX, a selective adenosine A_1-receptor antagonist on stunned myocardium (figure 4)

DPCPX itself did not affect these parameters of hemodynamics. Ischemia significantly decreased %SS in all groups. The %SS decreased below zero during ischemia, and that in the animals pretreated with DPCPX appeared to be lower than that without the drug. Recovery of the %SS during reperfusion in the presence of DPCPX was less than that in the absence of DPCPX. However, the protective effect of OG-VI was still observed in the presence of DPCPX. The %SS with OG-VI improved to the same extent as OG-VI increased %SS during reperfusion without DPCPX.

Effects of OG-VI on ischemic myocardial metabolism (table 1)

Because the effects of OG-VI on metabolic changes in 30-minute reperfused hearts were controversial, we examined those in three-minute postischemic hearts in this

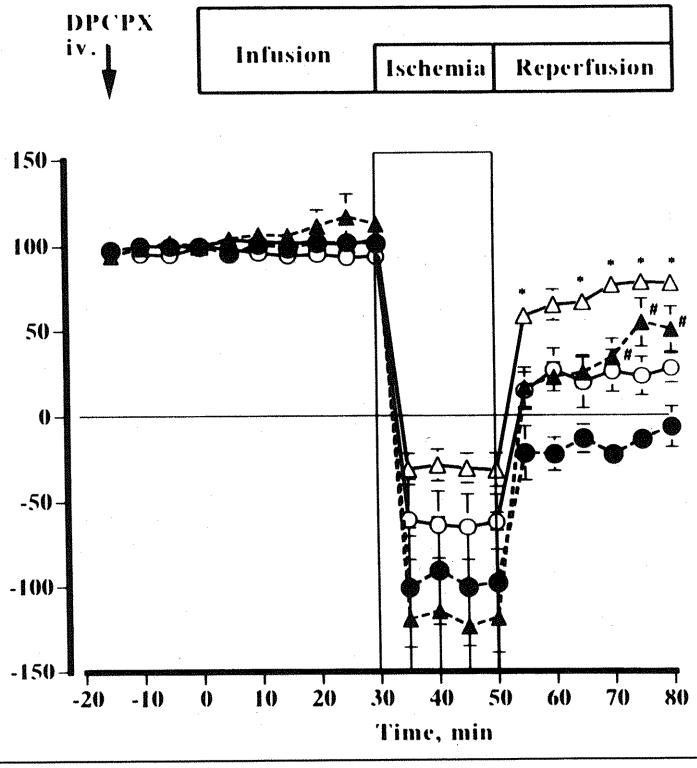

Figure 4. Effects of pretreatment with DPCPX on changes in %SS of the ischemia–reperfused area caused by OG-VI infusion. Either saline (○) or 1.2 μmol/kg/min OG-VI (△) was infused. A selective adenosine A_1-receptor antagonist, 8-cyclopentyl-1,3-dipropylxanthine (DPCPX) of 1 mg/kg, was injected i.v. 15 minutes before starting the saline (●) and OG-VI (▲) infusion. Protocol is the same as that in figure 2. *, $p < 0.05$ vs. saline group at the corresponding time; #, $p < 0.05$ vs. saline + DPCPX group at the corresponding time.

section of the experiment. In the saline group, ischemia significantly decreased the levels of ATP and FDP, whereas it significantly increased the levels of AMP, G6P, F6P, and lactate. The levels of ADP and pyruvate did not change during ischemia. In the OG-VI groups, ischemia also significantly decreased the level of ATP, and increased the levels of G6P and F6P. However, the ischemia-induced alterations of ATP, G6P, and F6P were significantly attenuated by OG-VI infusion. OG-VI significantly preserved the total adenine nucleotide level that should have been decreased by ischemia. The ratio of ([G6P] + [F6P])/[FDP] in the OG-VI group at either dose was significantly lower than that in the saline group. The accumulation of lactate in the ischemic myocardium also appeared to be reduced by OG-VI infusion, but insignificantly.

Table 1. The levels of energy and carbohydrate metabolites in the nonischemic and ischemic heart

	Saline		OG-VI, 1.2 μmol/kg/min		OG-VI, 12 μmol/kg/min	
	Nonischemia (n = 6)	Ischemia (n = 8)	Nonischemia (n = 6)	Ischemia (n = 8)	Nonischemia (n = 5)	Ischemia (n = 8)
ATP	5.26 ± 0.17	3.91 ± 0.14[a]	5.43 ± 0.19	4.48 ± 0.15[a,c]	5.32 ± 0.31	4.62 ± 0.11[b,d]
ADP	1.05 ± 0.12	1.43 ± 0.14	0.99 ± 0.08	1.74 ± 0.12[a]	1.19 ± 0.07	1.49 ± 0.20
AMP	0.17 ± 0.02	0.25 ± 0.02[b]	0.16 ± 0.02	0.21 ± 0.02	0.26 ± 0.04	0.23 ± 0.04
TAN	6.48 ± 0.25	5.59 ± 0.20[b]	6.58 ± 0.15	6.42 ± 0.11[c]	6.77 ± 0.22	6.33 ± 0.24[c]
G6P	0.23 ± 0.03	0.87 ± 0.10[a]	0.32 ± 0.08	0.65 ± 0.09[b]	0.37 ± 0.07	0.56 ± 0.09[c]
F6P	0.03 ± 0.01	0.20 ± 0.02[a]	0.06 ± 0.02	0.15 ± 0.02[a]	0.07 ± 0.01	0.13 ± 0.01[b,c]
FDP	0.13 ± 0.01	0.05 ± 0.01[a]	0.16 ± 0.03	0.09 ± 0.01[c]	0.25 ± 0.06	0.10 ± 0.03[b]
HP ratio	2.08 ± 0.29	23.06 ± 4.10[a]	2.48 ± 0.55	9.89 ± 2.07[a,c]	2.02 ± 0.38	10.15 ± 2.28[a,c]
Pyruvate	0.10 ± 0.03	0.15 ± 0.02	0.20 ± 0.02	0.14 ± 0.01[b]	0.11 ± 0.02	0.14 ± 0.03
Lactate	2.17 ± 0.33	10.15 ± 0.37[a]	1.94 ± 0.37	8.14 ± 1.05[a]	2.87 ± 0.82	8.76 ± 0.92[a]

[a] $p < 0.01$ compared with nonischemia in each group.
[b] $p < 0.05$ compared with nonischemia in each group.
[c] $p < 0.05$ compared with ischemia in the saline group.
[d] $p < 0.01$ compared with ischemia in the saline group.
Data are the mean ± SE and are expressed as μmol/g wet tissue, except for HP ratio. Ischemia was induced by ligating the left anterior descending coronary artery for three minutes. Infusion of either saline or OG-VI was started 30 minutes before the onset of ischemia. ATP: adenosine triphosphate; ADP: adenosine diphosphate; AMP: adenosine monophosphate; TAN: total adenine nucleotides; G6P: glucose 6 phosphate; F6P: fructose 6 phosphate; FDP: fructose 1,6 diphosphate; HP ratio: hexose phosphate ratio (([G6P] + [F6P])/[FDP]).

DISCUSSION

Myocardial mechanical dysfunction during reperfusion after brief ischemia is termed *stunning* [1]. The proposed hypotheses to explain the mechanical dysfunction of stunned myocardium are as follows: failure of ATP resynthesis resulting from damage of mitochondrial function [14], loss of total adenine nucleotides in the cells [15], cytosolic Ca^{2+} overload [16], and formation of oxygen-derived free radicals [17]. Ichihara and colleagues [3,7] and Greenfield and Swain [6] have demonstrated that a main cause of myocardial stunning is loss of total adenine nucleotides in the cells. Because the CrP level is restored to more than the preischemic level after reperfusion following brief ischemia, the mitochondria are presumably able to resynthesize high-energy phosphates even when the ATP level and cardiac mechanical function are not restored [3,7]. On the basis of our concept (figure 1), in the reperfused heart, lack of ADP near the contractile elements is the most important factor involved in the myocardial stunning.

The present study clearly showed that OG-VI helped reverse myocardial dysfunction during reperfusion after brief ischemia. In addition, OG-VI significantly preserved adenine nucleotides in an early stage of ischemia. Because OG-VI is a mixture of nucleosides and nucleotides, it may replenish the cytosolic ADP store with adenine nucleotides, leading to improvement of myocardial contractile function of the reperfused heart.

IG solution also produced a significant improvement of myocardial stunning in the present study. Inosine may play an important role in enhancement of myocardial contractile function in stunned myocardium. However, IG did not show a signifi-

cant recovery of ATP and total adenine nucleotides in the reperfused myocardium following ischemia [12]; inosine alone was ineffective in counteracting myocardial stunning [21]. Purine and pyrimidine nucleosides and nucleotides themselves play an important role in regulation of purine and pyrimidine metabolism through their positive or negative feedback regulation [18]. We believe that keeping the balance of purine and pyrimidine nucleotide metabolism is very important in order to improve both the myocardial metabolic and contractile dysfunction during reperfusion following ischemia.

Some investigators have reported that AICAr, an intermediate in purine biosynthesis, is the most effective substrate in restoring myocardial ATP levels [19]. However, a significant recovery of %SS in the OG-VI group as compared with that in the saline group was observed during whole reperfusion period, whereas that in the AICAr group was observed only at 5-, 15-, and 30-minute reperfusion.

Because adenosine dilates the coronary arteries and because ischemic preconditioning is mediated by adenosine receptors [20], adenosine receptor activation may protect the myocardium against ischemic injury. Although pretreatment with DPCPX lessened the myocardial contractile function during reperfusion after ischemia, the protective effect of OG-VI on the stunned myocardium was still observed. Therefore, the beneficial effect of OG-VI may not be due to activation of adenosine receptors with OG-VI or its metabolites.

ACKNOWLEDGMENT

This work was supported by a Grant-in-Aid for General Scientific Research of the Ministry of Education, Science and Culture of Japan (no. 06454613).

REFERENCES

1. Braunwald E, Kloner RA. 1982. The stunned myocardium: prolonged, postischemic ventricular dysfunction. Circulation 66:1146–1149.
2. Kuprianov VV, Steinschneider AY, Ruuge EK, Smirnov VN, Saks VA. 1983. ^{31}P-NMR spectrum of phosphocreatine: deuterium-induced splitting of the signal. Biochem Biophys Res Commun 114:1117–1125.
3. Ichihara K, Abiko Y. 1984. Rebound recovery of myocardial creatine phosphate with reperfusion after ischemia. Am Heart J 108:1594–1597.
4. Reibel DK, Rovetto MJ. 1979. Myocardial adenosine salvage rates and restoration of ATP content following ischemia. Am J Physiol 237:H247–H252.
5. Vary TC, Angelakos ET, Schaffer SW. 1979. Metabolism and irreversible ischemic tissue damage in isolated perfused rat heart. Circ Res 45:218–225.
6. Greenfield RA, Swain JL. 1987. Disruption of myofibrillar energy use: dual mechanisms that may contribute to postischemic dysfunction in stunned myocardium. Circ Res 60:283–289.
7. Nakai T, Kano S, Satoh K, Hoshi K, Ichihara K. 1996. Effects of adenine nucleotide analogues on myocardial dysfunction during reperfusion after ischemia in dogs. J Cardiovasc Pharmacol 28:264–270.
8. Ogoshi S, Iwasa M, Mizobuchi S, Iwasa Y, Martiz A, Tamiya T. 1990. Effect of a nucleoside and nucleotide mixture on protein metabolism in rats given total parenteral nutrition after 70% hepatectomy. In Tanaka T, Okada A (eds), Nutritional Support in Organ Failure. Amsterdam: Elsevier Science, pp. 309–317.
9. Ogoshi S, Mizobuchi S, Iwasa M, Tamiya T. 1989. Effect of a nucleoside–nucleotide mixture on protein metabolism in rats after seventy percent hepatectomy. Nutrition 5:173–178.

10. Ogoshi S, Iwasa M, Kitagawa S, Ohmori Y, Mizobuchi S, Iwasa Y, Tamiya T. 1988. Effects of total parenteral nutrition with nucleoside and nucleotide mixture on D-galactosamine-induced liver injury in rats. J Parenter Enter Nutr 12:53–57.
11. Satoh K, Nakai T, Hoshi K, Ichihara K. 1993. Limitation of stunning in dog myocardium by nucleoside and nucleotide mixture, OG-VI. Coronary Artery Dis 4:1007–1012.
12. Kano S, Nakai T, Kohri H, Ichihara K. 1995. Effects of OG-VI, a nucleoside/nucleotide mixture, and its constituents on myocardial stunning in dogs. Coronary Artery Dis 6:811–818.
13. Okazaki Y, Kano S, Ogoshi S, Ichihara K. 1997. Effects of OG-VI, a nucleoside/nucleotide mixture, on ischemic myocardial metabolism in dogs. Coronary Artery Dis 8:39–43.
14. Jennings RB, Ganote CE. 1976. Mitochondrial structure and function in acute myocardial ischemic injury. Circ Res 38(Suppl I):I80–I91.
15. Swain JL, Hines JJ, Sabina RL, Holmes EW. 1982. Accelerated repleteion of ATP and GTP pools in postischemic canine myocardium using a precursor of purine de novo synthesis. Circ Res 51:102–105.
16. Bolli R, Jeroudi MO, Patel BS, Aruoma OI, Halliwell B, Lai EK, MacCay PB. 1989. Marked reduction of free radical generation and contractile dysfunction by antioxidant therapy begun at the time of reperfusion. Circ Res 65:607–622.
17. Bolli R. 1990. Mechanism of myocardial stunning. Circulation 82:723–738.
18. Martin DW Jr. 1980. Metabolism of purine and pyrimidine nucleotides. In Harper HA, Rodwell VW, Mayes PA (eds), Review of Physiological Chemistry. Los Altos: Lange Medical Publications, pp. 440–459.
19. Sabina RL, Kernstine KH, Boyd RL, Holmes EW, Swain JL. 1982. Metabolism of 5-amino-4-imidazolecarboxamide riboside in cardiac and skeletal muscle. J Biol Chem 257:10178–10183.
20. Miura K, Kano S, Nakai T, Satoh K, Ichihara K. 1987. Inhibitory effects of glibenclamide and pertussis toxin on the attenuation of ischemia-induced myocardial acidosis following ischemic preconditioning in dogs. Jpn Circ J 61:709–714.
21. Kano S, Satoh K, Hoshi K, Ichihara K. In Press. Effects of OG-VI, a neucleoside/neucleotide mixture, on stunned Myocardium in dogs: Is the adenosine A_1 receptor involved? Coronary Artery Dis 9.

DECREASE IN MYOCARDIAL ISCHEMIC TOLERANCE WITH AGING IN FISCHER 344 RATS

MASATO TANI, KEN SHINMURA, HIROSHI HASEGAWA, YUKAKO SUGANUMA, and YOKO HAYASHI

Keio University School of Medicine

Summary. Some animal studies indicate that ischemic tolerance is decreased in the senescent myocardium. However, the results of cardiac operations in the elderly are compatible with those performed in middle-aged people. It is important to determine whether ischemic tolerance may be decreased in middle age. Hearts from young adult (12 weeks old) or the middle-aged (50 weeks old) Fischer 344 rats were subjected to 15, 20, or 25 minutes of global ischemia followed by reperfusion. The recovery of left ventricular function and high-energy phosphates was significantly lower in the hearts of middle-aged rats than in those of the young adult rats after any period of global ischemia. The increase in left ventricular end-diastolic pressure was also greater in the middle-aged rats, although there were no differences in these indexes in the two age groups before the induction of ischemia. The incidence of reperfusion-induced ventricular fibrillation was significantly higher and the release of creatine kinase in the coronary effluent during reperfusion significantly greater in the middle-aged rats than in the young adult rats. Results indicate that rat hearts are more vulnerable to ischemia, even in middle age.

INTRODUCTION

The indications for cardiac procedures including surgery and coronary angioplasty have been expanded in recent years, resulting in an increased number of elderly patients being considered as candidates for these procedures. Temporary ischemia and reperfusion are inevitable during these procedures, although the elderly reportedly sustain a greater morbidity and mortality rate after an acute myocardial infarction than younger patients [1]. It is important to determine whether the myocardial susceptibility to injury during the index episode of ischemia–reperfusion

S. Mochizuki, N. Takeda, M. Nagano and N. Dhalla (eds.). THE ISCHEMIC HEART.

may increase with age. Several groups of investigators have reported that the hearts of senescent animals (rats aged 72–100 weeks, rabbits aged 28–38 months, sheep aged 7.1 years) were less tolerant to ischemia–reperfusion as compared with those of young adults (rats aged 12–24 weeks, rabbits aged 18–25 weeks, sheep aged 0.75 years) [2–6]. Despite the increased incidence of complicating noncardiac conditions and previous episodes of myocardial damage in elderly patients, the results of cardiac procedures performed in the elderly are reported to be as acceptable as those performed in the middle-aged [7–11]. We suspect that the myocardium may be vulnerable to ischemia–reperfusion injury even before senescence, that is, in middle-age.

To test the hypothesis that the myocardium is vulnerable to ischemia–reperfusion injury during middle age, we conducted the study reported here in Fischer 344 rats. This strain of rats has been extensively investigated as a model of aging [2,12–14] and provides a homogeneous population that allows study of precisely defined ages [12]. In addition, significant coronary, vascular, or valvular abnormalities do not occur in this strain with aging [12]. We compared the recovery of cardiac function and metabolites, the release of CK in the coronary effluent, and the incidence of reperfusion-induced ventricular tachyarrhythmias in hearts obtained from young adult and middle-aged rats.

MATERIALS AND METHODS

Hearts from young adult male (12 weeks old) or middle-aged male (50 weeks old) Fischer 344 rats were evaluated. The body mass of the young adults ranged from 200 to 220 g, while that of middle-aged rats ranged from 330 to 380 g. Hearts were perfused by the Langendorff technique with Krebs–Henseleit bicarbonate buffer (37°C) gassed with O_2:CO_2 (95%:5%). The buffer contained 118 mmol/L NaCl, 25 mmol/L $NaHCO_3$, 4.7 mmol/L KCl, 1.2 mmol/L $MgSO_4$, 1.2 mmol/L KH_2PO_4, 1.75 mmol/L $CaCl_2$, 0.5 mmol/L EDTA, 11 mmol/L glucose, and 5 mmol/L pyruvate.

Perfusion protocol

The hearts of 32 animals in each age group were subjected to 10 minutes of recirculating perfusion followed by 15, 20, or 25 minutes of sustained global ischemia and 30 minutes of reperfusion. The hearts were then frozen with Wollenberger clamps that had been cooled in liquid nitrogen. They were stored in liquid nitrogen for the assay of metabolites before ischemia and after each period of ischemia followed by 30 minutes of reperfusion (n = 8, respectively).

Analysis of left ventricular (LV) function

LV pressure was recorded with a plastic catheter tipped with a latex balloon that was placed into the left ventricle through the left atrium. The LV end-diastolic pressure (LVEDP) was adjusted to 9 mmHg by filling the balloon with fluid. Global ischemia was sustained for 25 minutes or less, since our preliminary study showed that the

no-reflow phenomenon was minimal when the ischemic period lasted less than 25 minutes. LV function was measured before sustained global ischemia was induced in hearts to obtain the preischemic values. Pacing was turned off during sustained global ischemia to avoid inducing too high an incidence of ventricular tachyarrhythmias during reperfusion [15]. Pacing was turned on after 25 minutes of reperfusion to obtain measurements of postischemic recovery of LV function.

Analysis of ventricular tachycardia (VT) and fibrillation (VF)

An epicardial electrocardiogram (ECG) was recorded throughout the experiment. Three platinum electrodes were attached directly to the left atrium, the right ventricle, and the apex of the left ventricle. The surface ECGs were analyzed to determine the incidence of VT and/or VF according to the criteria of the Lambeth Conventions [16]. The heart was considered to be in VF if individual QRS deflections could no longer be distinguished from one another and a rate could no longer be measured on the ECG. VT was defined as the occurrence of six or more consecutive premature ventricular complexes.

Analysis of cardiac metabolites

Neutralized perchloric acid extracts were obtained from frozen hearts and assayed for ATP, creatine phosphate, and lactate using standard enzymatic procedures [17].

Analysis of creatine kinase (CK) release

The coronary effluent obtained during 30 minutes of reperfusion was stored from reperfused hearts as an index of myocardial injury in each age group ($n = 8$ in each group). CK activity was measured by the adenosine diphosphate-dependent dephosphorylation of creatine phosphate [18].

Statistical analysis

Data are presented as mean ± SE. Statistical comparisons among groups or among time points in each group were performed by two-way analysis of variance followed by Tukey's test. A chi-squared followed by Fisher's exact test was used to determine differences in the incidence of VT or VF during reperfusion. A level of p less than 0.05 was considered statistically significant.

RESULTS

Recovery of LV function

There were no significant differences in the indexes of LV function measured before the induction of sustained global ischemia in the hearts from the two age groups (figure 1). Hearts stopped beating within three minutes of the onset of ischemia; the intraventricular pressure increased significantly 10 to 20 minutes after the onset of ischemia in both age groups. The increase in intraventricular pressure at the end of 15, 20, or 25 minutes of ischemia was significantly greater in the hearts from the

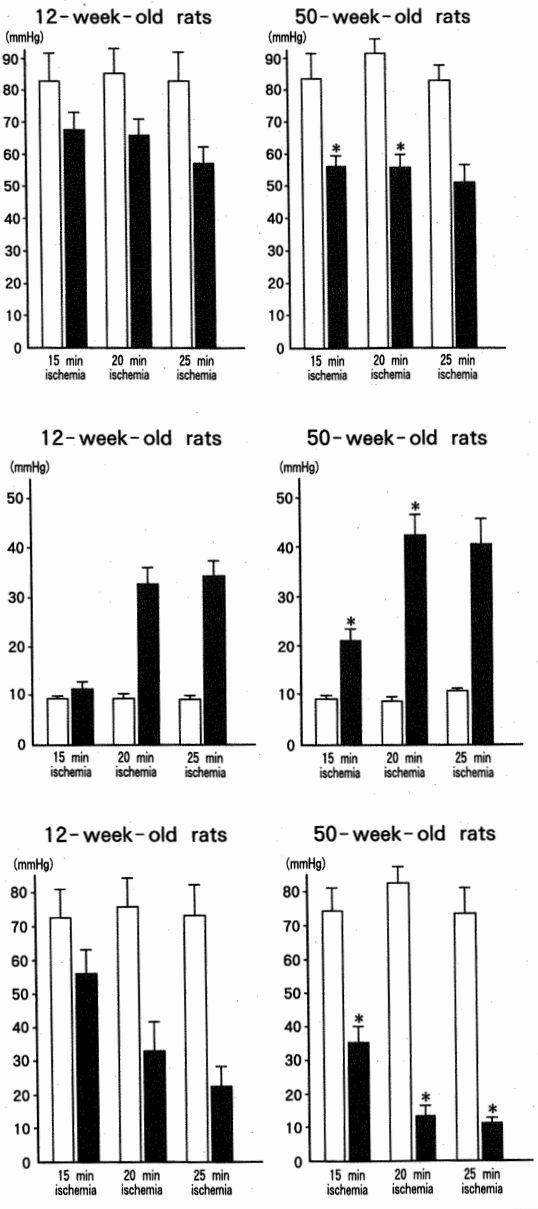

Figure 1. Left ventricular function. Left ventricular systolic pressure (LVSP; top panels), left ventricular end-disastolic pressure (LVEDP; middle panels), and left ventricular developed pressure (LVDP = LVSP − LVEDP; bottom panels) before and after each period of ischemia followed by 30 minutes of reperfusion in the hearts of rats aged 12 and 50 weeks. □: measured before ischemia; ■: after each period of ischemia followed by reperfusion. ★, $p < 0.05$ vs. corresponding values in hearts from rats aged 12 weeks.

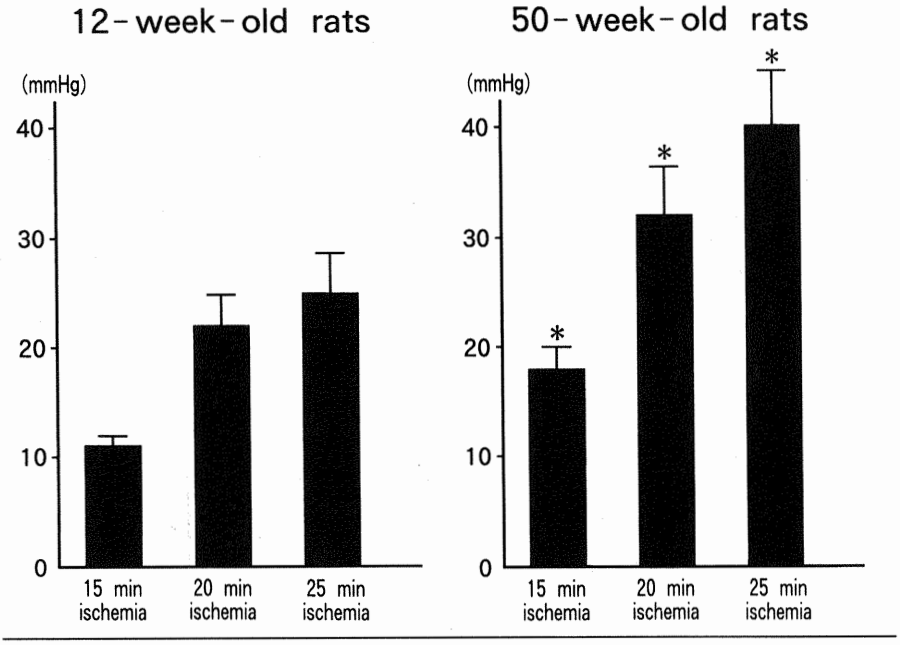

Figure 2. Increase in intraventricular pressure during ischemia. Intraventricular pressure was recorded at the end of each period of ischemia. *, $p < 0.05$ vs. corresponding values in hearts from rats aged 12 weeks.

middle-aged rats as compared with those from the young adult rats (figure 2). The recovery of LV systolic pressure tended to be lower after any period of ischemia followed by reperfusion in the hearts from middle-aged rats as compared with those from young adult rats (figure 1, top panels), although a statistically significant difference was seen only after 15 minutes of ischemia. The recovery of LV developed pressure was significantly lower after any period of ischemia followed by reperfusion in the hearts from the middle-aged rats due to a marked increase in LV end-diastolic pressure (figure 1, middle and bottom panels and figure 2), although the difference after 25 minutes of ischemia did not achieve statistical significance.

The extent of recovery of LV peak positive and peak negative *dP/dt* (the first derivative of LV pressure) was significantly lower after any period of ischemia followed by reperfusion in the hearts from the middle-aged rats as compared with that after each period of ischemia and reperfusion in the hearts from the young adult rats (figure 3).

Myocardial energy metabolites

Concentrations of myocardial energy metabolites after control normoxic perfusion (before ischemia) did not differ significantly between the hearts of the two age groups (figure 4). The recovery of ATP and creatine phosphate during 30 minutes

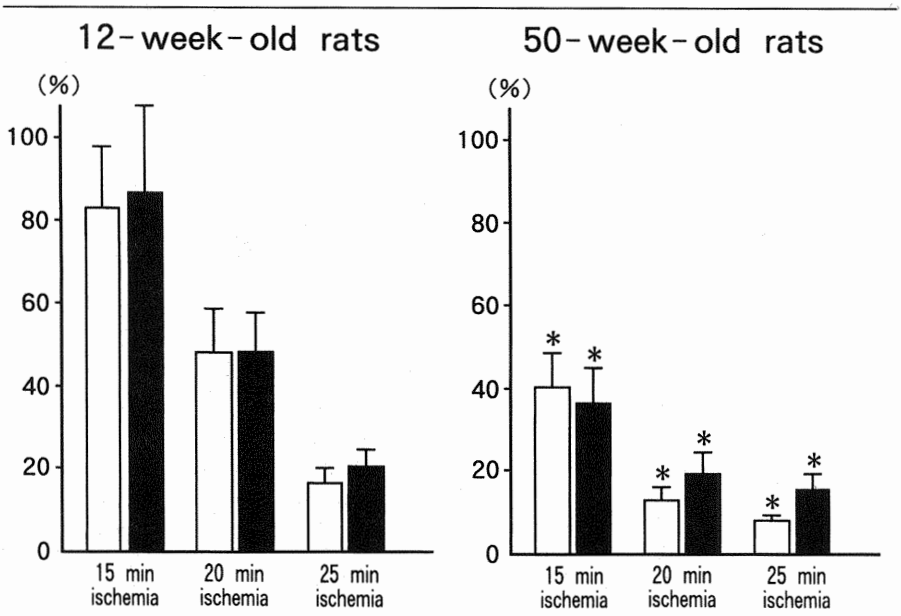

Figure 3. Percent recovery of the first derivative of left ventricular pressure. Percent recovery was calculated by dividing the value obtained after reperfusion by that before each period of ischemia. □: percent recovery of peak positive *dP/dt* after each period of ischemia; ■: percent recovery of peak negative *dP/dt*. ⋆, $p < 0.05$ vs. corresponding value in hearts from rats aged 12 weeks.

of reperfusion after any periods of ischemia was better in the hearts from young adult rats than each value in the hearts of the middle-aged rats. The lactate levels before the induction of ischemia or after each period of ischemia followed by reperfusion did not differ between the two age groups.

Reperfusion-induced VT and VF

In the hearts from the middle-aged rats, the incidence of reperfusion-induced VT or VF during reperfusion after 20 minutes of ischemia was higher than in the young adult rat hearts (figure 5), although the incidence did not differ after 15 or 25 minutes of ischemia.

Release of CK in the coronary effluent during reperfusion

The release of CK into the coronary effluent collected from the reperfused hearts revealed that the myocardial damage was more severe in the hearts of the middle-aged rats as compared with those from the young adult rats after any period of ischemia (figure 6).

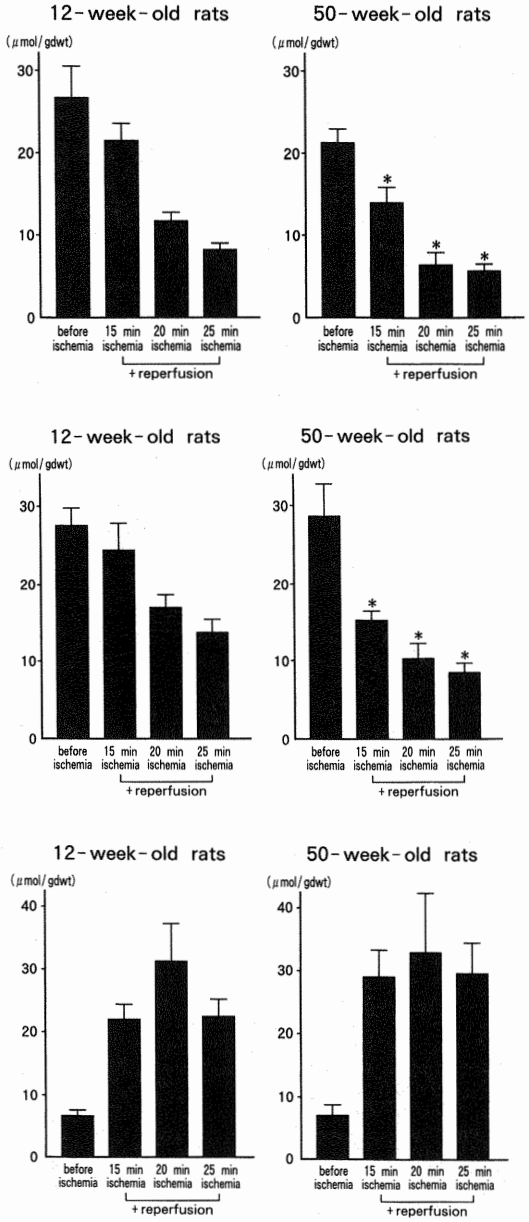

Figure 4. Myocardial energy metabolite contents. Myocardial contents of adenosine triphosphate (ATP; top panels), creatine phosphate (middle panels), and lactate (bottom panels) were measured using some hearts frozen before ischemia or after each period of ischemia followed by reperfusion. *, $p < 0.05$ vs. corresponding values in hearts from rats aged 12 weeks.

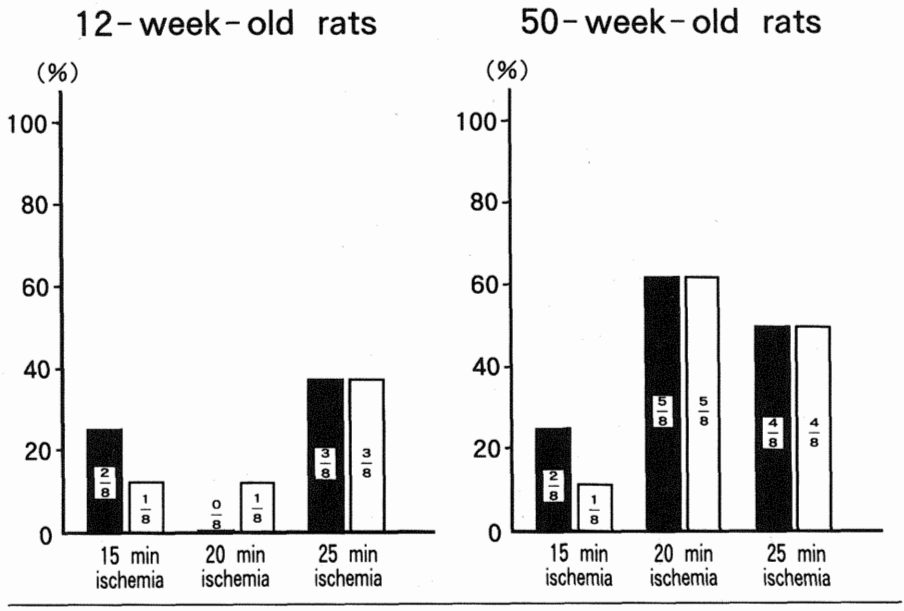

Figure 5. Incidence of reperfusion-induced ventricular tachycardia (VT)/fibrillation (VF). ■: VF; □: VT. *, $p < 0.05$ vs. corresponding value in hearts from rats aged 12 weeks.

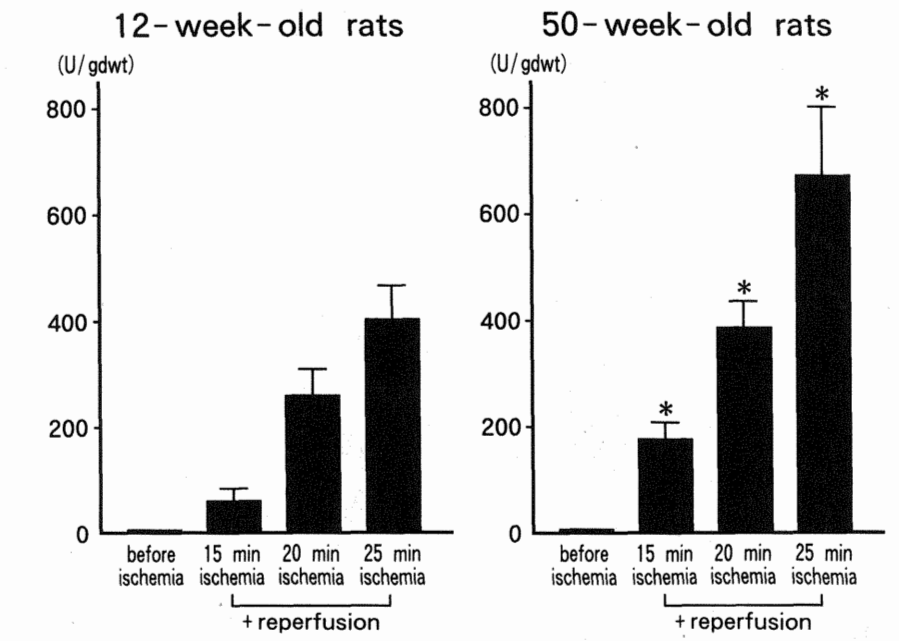

Figure 6. Release of creatine kinase in the coronary effluent during reperfusion. Creatine kinase (CK) release was measured in the coronary effluent collected from each heart. *, $p < 0.05$ vs. corresponding values in hearts from rats aged 12 weeks.

DISCUSSION

Our results indicated that rat myocardium became less tolerant to ischemia–reperfusion in middle age, before the animals reached senescence. The recovery of cardiac function and the myocardial concentration of high-energy phosphates were significantly lower in the hearts from the middle-aged rats than in those from the young adult rats. The depressed recovery of ventricular function and metabolites in the hearts from the middle-aged rats was associated with the increase in CK release in the coronary effluent and higher incidence of ventricular tachyarrhythmias during reperfusion.

Ischemic tolerance in the middle-aged rat hearts

Hearts from senescent animals that correspond in age to the eighth or ninth decade in humans (for example, rats aged 75 to 100 weeks) have been reported to be less tolerant to ischemia–reperfusion injury than the hearts of young animals (for example, rats aged 12 to 24 weeks) [2–6]. The concentration of ATP or creatine phosphate in the normoxically perfused myocardium is reportedly lower in the senescent than the young adults [19]. Therefore, a lower initial value of ATP at the onset of ischemia would lead to a persistent deficiency of ATP early in the ischemic period. If true, a deficiency of ATP may be responsible, at least in part, for the decrease in ischemic tolerance in the senescent myocardium, since this deficiency of ATP accelerates ischemic contracture, causing a worsening of myocardial damage [20,21]. We found that elevation of intraventricular pressure was greater at the end of any period of ischemia in the hearts from the middle-aged rats than in those from the young adult rats. However, we did not detect any significant differences in the hearts from the two age groups in the levels of high-energy phosphates before the induction of ischemia, although the ATP level was slightly, but not significantly, lower in the hearts from the older rats.

The recovery of high-energy phosphates during reperfusion was lower in the hearts from the middle-aged rats, which may be one cause of the decreased recovery of contractile function in that group. Utilization of hypoxanthine, a degradation product of adenine nucleotide that is shunted through the salvage pathway, increased in the aged myocardium [19] during normoxic perfusion, although no further metabolic increases were observed during reperfusion. Therefore, the production of ATP via a de novo pathway would be depressed in the hearts of older rats, in that energy consumption would be lower due to the poorer recovery of contractile function. Snoeckx et al. [4] reported that the poorer recovery of creatine phosphate in the hypertrophied myocardium of the aged spontaneously hypertensive rat (SHR) could be attributable to hypoperfusion of the subendocarium. We did not find any significant increase in the lactate level in the hearts of the middle-aged rats, which would suggest abscence of severe hypoxia.

The myocardial activity of superoxide dismutase, an antioxidant enzyme, reportedly decreases with age in the Fischer 344 rat, while that of catalase and of glutathione peroxidase was unchanged [22]. A decrease in the capacity for scaveng-

ing oxygen-free radicals could lead to a reduction in ischemic tolerance with age, although the extracellular administration either of superoxide dismutase with catalase or of substrates for the glutathione redox pathway had little effect on the recovery of cardiac function in the rat [23].

Ataka et al. [5] showed that the elevation of intracellular [Ca^{2+}] was greater in hearts from aged rabbits (28–38 months old) as compared with that from young animals (18–25 weeks old). Damage to intracellular organelles such as mitochondria or sarcoplasmic reticulum that regulate intracellular [Ca^{2+}] may increase with age [3,24]. We and other authors [25–28] have proposed the hypothesis that the H^+ that accumulates during ischemia was exchanged for extracellular Na^+ via the Na^+–H^+ exchanger, resulting in an increase in intracellular [Na^+] and in the activation of the reverse mode of Na^+–Ca^{2+} exchange. The kinetic property of these exchangers may be altered with age, although the intracellular pH decreased to the same extent in the myocardium from mature or aged rabbits [5].

Clinical implications

A greater morbidity and mortality rate after acute myocardial infarction has been reported in the elderly [1]. However, similar outcomes have been reported in middle-aged and senescent patients after cardiac operations such as coronary artery bypass grafting or open heart surgery for valvular heart diseases, despite the fact that ischemic insult cannot be avoided during these operations [7–11]. The differences between these clinical studies may be due to the fact that the former study was performed retrospectively, at least in part, with pooled data from unselected patients under uncontrolled conditions, whereas many of the latter studies were conducted propsectively in patients under preoperatively controlled conditions. Previous experiments have shown that the senescent myocardium is susceptible to injury during ischemia–reperfusion as compared with the myocardium from younger animals. It can be inferred that the myocardium becomes vulnerable to ischemic insult by middle age and that there is no difference in ischemic tolerance in the heart of middle-aged or elderly subjects. Our experimental results support this idea. Approaches are needed to protect myocardium that has become vulnerable to ischemia–reperfusion injury with aging [29].

REFERENCES

1. Grines CL, DeMaria AN. 1990. Optimal utilization of thrombolytic therapy for acute myocardial infarction: concepts and controversies. J Am Coll Cardiol 16:223–231.
2. Lesnefsky EJ, Gallo DS, Ye J, Whittingham TS, Lust WD. 1994. Aging increased ischemia–reperfusion injury in the isolated, buffer-perfused heart. J Lab Clin Med 124:843–851.
3. Frolkis VV, Frolkis RA, Mkhitarian LS, Fraifeld VE. 1991. Age-dependent effects of ischemia and reperfusion on cardiac function and Ca^{2+} transport in myocardium. Gerontology 37:233–239.
4. Snoeckx LHEH, Van der Vusse GJ, Coumans WA, Willemsen PHM, Reneman RS. 1993. Differences in ischaemia tolerance between hypertrophied hearts of adult and aged spontaneously hypertensive rats. Cardiovasc Res 27:874–881.
5. Ataka K, Chen D, Levitsky S, Jimenez E, Feinberg H. 1992. Effect of aging on intracellular Ca^{2+}, pH_i, and contractility during ischemia and reperfusion. Circulation 86(Suppl II):II-371–II-376.
6. Misare BD, Krukenkamp IB, Levitsky S. 1992. Age-dependent sensitivity to unprotected cardiac ischemia: the senescent myocardium. J Thorac Cardioasc Surg 103:60–65.

7. Edmunds LH Jr, Stephenson LW, Edie RN, Ratcliffe MB. 1988. Open-heart surgery in octogenarians. N Engl J Med 319:131–136.
8. Christakis GT, Ivanov J, Weisel RD, Birnhaum PL, David TE, Salerno TA. 1989. The changing pattern of coronary artery bypass surgery. Circulation 80(Suppl I):I-151–I-161.
9. Horvath KA, DiSesa VJ, Peigh PS, Couper GS, Collins JJ Jr, Cohn LH. 1990. Favorable results of coronary artery bypass grafting in patients older than 75 years. J Thorac Cardiovasc Surg 99:92–96.
10. Levinson JR, Atkins CW, Buckley MJ, Newell JB, Palacios IF, Block PC, Fifer MA. 1989. Octogenarians with aortic stenosis. Outcome after aortic valve replacement. Circulation 80(Suppl I):I-49–I-56.
11. Fremes SE, Goldman BS, Ivanov J, Weisel RD, David TE, Salerno T. 1989. Valvular surgery in the elderly. Circulation 80(Suppl I):I-77–I-90.
12. Coleman GL, Barthold SW, Osbaldiston GW, Foster SJ, Jonas AM. 1977. Pathological changes during aging in barrier-reared Fischer 344 male rats. J Gerontol 32:258–278.
13. Solleveld HA, Boorman GA. 1986. Spontaneous renal lesions in five rat strains. Toxicol Pathol 14:168–174.
14. Goodman DG, Ward JM, Squire RA, Chu KC, Linhart MS. 1979. Neoplastic and nonneoplastic lesions in aging F344 rats. Toxicol Appl Pharmacol 48:237–248.
15. Bernier M, Curtis MJ, Hearse DJ. 1989. Ischemia-induced and reperfusion-induced arrhythmias: importance of heart rate. Am J Physiol 256:H21–H31.
16. The Lambeth Conventions 1988. Guidelines for the study of arrhythmias in ischemia, infarction and reperfusion. Cardiovasc Res 22:447–455.
17. Bergmeyer HU. 1963. Methods in Enzymatic Analysis. New York: Academic Press, pp. 1464–1468, 1777–1779, 2101–2110, 2129–2131.
18. Hughes BP. 1962. A method for the estimation of serum creatine kinase and its use in comparing creatine kinase and aldolase activity in normal and pathological sera. Clin Chim Acta 7:519.
19. Finelli C, Guarnieri C, Muscari C, Ventura C, Caldarera CM. 1993. Incorporation of [^{14}C]hypoxanthine into cardiac adenine nucleotides: effect of aging and post-ischemic reperfusion. Biochim Biophys Acta 1180:262–266.
20. Tani M, Hasegawa H, Suganuma Y, Shinmura K, Nakamura Y. 1996. Protection of ischemic myocardium by inhibition of contracture in isolated rat hearts. Am J Physiol 271:H2515–H2519.
21. Koretsune Y, Marban E. 1990. Mechanism of ischemic contracture in ferret hearts: relative roles of $[Ca^{2+}]_i$ elevation and ATP depletion. Am J Physiol 258:H9–H16.
22. Rao G, Xia E, Richardson A. 1990. Effect of age on the expression of antioxidant enzymes in male Fischer 344 rats. Mech Ageing Dev 53:49–60.
23. Tani M. 1990. Effects of anti-free radical agents on Na^+, Ca^{2+} and function in reperfused rat hearts. Am J Physiol 259:H137–H143.
24. Narayanan N. 1981. Differential alterations in ATP-supported calcium transport activities of sarcoplasmic reticulum and sarcolemma of aging myocardium. Biochim Biophys Acta 678:442–459.
25. Tani M. 1990. Mechanisms of Ca^{2+} overload in reperfused ischemic myocardium. Annu Rev Physiol 52:543–559.
26. Lazdunski M, Frelin C, Vigne P. 1985. The sodium/hydrogen exchange system in cardiac cells. Its biochemical and pharmacological properties and its role in regulating internal concentrations of sodium and internal pH. J Mol Cell Cardiol 17:1029–1042.
27. Tani M, Neely JR. 1989. Na^+ accumulation increases Ca^{2+} overload and impairs function in anoxic rat heart. J Mol Cell Cardiol 22:57–72.
28. Tani M, Neely JR. 1989. Role of intracellular Na^+ in Ca^{2+} overload and depressed recovery of ventricular function of reperfused ischemic rat hearts: possible involvement of H^+/Na^+ and Na^+/Ca^{2+} exchange. Circ Res 65:1045–1056.
29. Tani M, Suganuma Y, Hasegawa H, Shinmura K, Hayashi Y, Guo X, Nakamura Y. 1997. Changes in ischemic tolerance and effect of preconditioning in middle-aged rat heart. Circulation 95:2559–2566.

This Page Intentionally Left Blank

UNDERPERFUSION INJURY IN DIABETIC RAT HEARTS: EFFECTS OF NOREPINEPHRINE AND/OR INSULIN ON STIFFNESS INCREASE AND ABNORMAL ENERGY METABOLISM

MAKIE HIGUCHI*, KANAKO MIYAGI, and MATAO SAKANASHI****

* *Osaka University Medical School*
** *University of the Ryukyus*

Summary. Diabetic hearts were more susceptible than nondiabetic hearts to flow reduction and readily exhibited an increase in left ventricular diastolic stiffness in isolated rat hearts. Norepinephrine during underperfusion exacerbated the injury and improved the reperfusion injury, particularly in diabetic hearts, while the positive inotropic response was decreased by the progression of diabetes. The increase in stiffness correlated closely with ATP depletion and lactate accumulation in the subendocardium, which was metabolically more susceptible than the subepicardium. The correlation curves, however, were not coincidental: the critical ATP level was significantly higher in diabetic hearts. The markedly high glycogen content in diabetic hearts probably helps delay the start of underperfusion injury. The degree of injury depended on the degree and duration of underperfusion with norepinephrine and on the severity of diabetes. In vivo and ex vivo insulin prevented the injury.

INTRODUCTION

Ischemic incidence and damage are probably increased in organs with diabetes mellitus (DM) as an underlying disease. Diabetics have an increased incidence of congestive heart failure and a resultant increase in mortality despite smaller infarct areas following ischemia than nondiabetics [1]; during exercise the same is true even in young men with no evidence of cardiovascular disease [2]. This cardiac dysfunction may be due to deterioration of microcirculation caused by abnormalities in vascular sensitivity and reactivity of ligands [3–10], to abnormalities in excitation conduction systems [11], or to abnormalities in the myocardium, e.g., changes in myocardial metabolism [12], tissue antioxidant status [13], sarcolemmal enzyme activity [14,15], or contractile protein itself [11].

S. Mochizuki, N. Takeda, M. Nagano and N. Dhalla (eds.). THE ISCHEMIC HEART.

However, comparisons of the degree of ischemic injury and the extent of recovery in cardiac function during reperfusion in DM and non-DM hearts have shown conflicting results; DM hearts were reported to be more sensitive [4,16] or more resistant [17] to ischemia, or were comparable to non-DM hearts [18]. These discrepancies may be explained, at least in part, by differences in the duration and degree of ischemia, the preparations, the parameters monitored, and/or evaluation time.

During severe ischemia, the active glycolytic pathway, in particular, could be important for preserving the integrity of the cellular membrane and preventing ischemic contracture [19–23]. In DM hearts, however, greater limitations of glucose uptake and glycolysis [12,24–29], a lower activity of pyruvate dehydrogenase [30], a higher tissue glycogen [28,31], an accelerated polyol pathway, and an increase in long chain fatty acid intermediate metabolites [12] were observed, and thus abnormal myocardial energy metabolism during underperfusion is inferred. In addition, partial ischemia (low-flow perfusion) that precedes complete ischemia or presents in the area adjacent to infarct is particularly important in preventing ischemic progress; circulation and metabolism under partial ischemia are organ specific. The inner rather than the outer layer of the left ventricular (LV) free wall is more vulnerable to ischemic injury in the metabolic and morphological aspects [32–34].

Therefore, we examined whether DM hearts are more susceptible than non-DM hearts to flow reduction and to physiologically active substances and whether they readily exhibit an increase in LV diastolic stiffness in isolated underperfused rat hearts. To investigate the relationship of abnormal energy metabolism with the mechanical dysfunction, the tissue substrate content in the LV subendocardium and subepicardium was measured and analyzed separately [35–38].

METHODS

Animals and treatment

As described in our previous reports [35–38], eight-week-old male Sprague–Dawley rats were used. Diabetes mellitus (DM) was induced by a single intravenous (i.v.) injection of 50 or 60 mg/kg streptozotocin (STZ, Sigma, St. Louis. USA) dissolved in physiological saline. The non-DM (normal) group received the vehicle only. The diabetic state was assessed by confirming that blood glucose in the evening was greater than 300 mg/dL three days after the injection of STZ, and the in vivo insulin-treated DM group received a subcutaneous injection of insulin (4 U/rat; Lente, Novo, Denmark) every evening for 5–6 days. The rats were fed ad libitum and sacrificed 8, 11, 13, and 45 days after the injection of STZ or vehicle.

Heart perfusion protocol and measurement of mechanical performance

The animals were anesthetized with ether, and venous blood samples were obtained for measurement of plasma glucose by an enzymatic method and glycosylated hemoglobin by affinity chromatography.

After thoracotomy, the hearts were rapidly excised and perfused with a

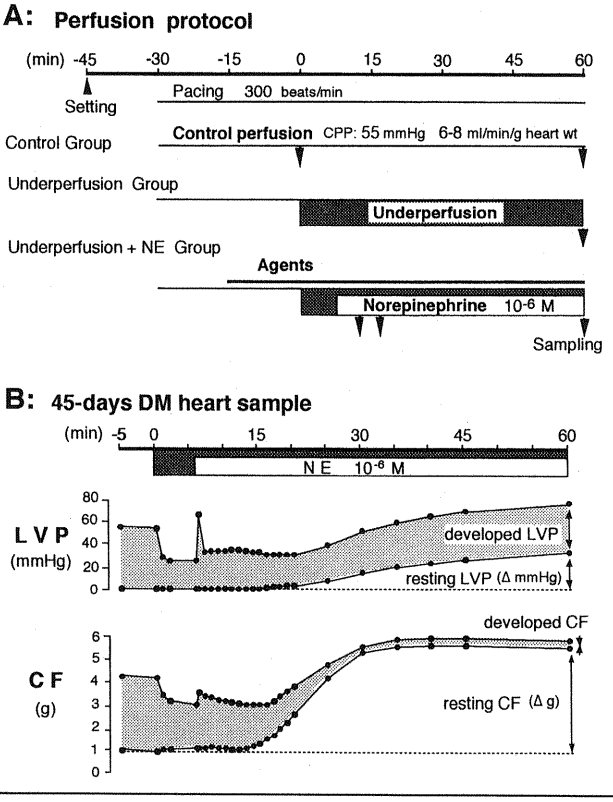

Figure 1. (**A**) Perfusion protocol. Langendorff rat hearts with a balloon in the left ventricle (LV) were paced at 300 beats/min and perfused with Krebs–Henseleit solution (11 mM or 27.5 mM glucose) at 36°C throughout the experiments. Flow rate was adjusted to provide a coronary perfusion pressure (CPP) of about 55 mmHg (control perfusion), using a microtube pump. The hearts were exposed to underperfusion by reducing the flow rate, and five minutes after the start of underperfusion, the perfusate was changed to that containing norepinephrine (NE 10^{-6} M). Insulin was infused 15 minutes before and during underperfusion. After 30 and 90 minutes of control perfusion and after 13, 17, 30, and 60 minutes of underperfusion with or without NE, the hearts were quickly frozen in liquid nitrogen, as indicated by arrows, to measure tissue substrates. (**B**) Sample records of the LV pressure (LVP) and the contractile force (CF) during underperfusion with NE in a 45-day diabetic (DM) rat heart (lower).

Langendorff apparatus. The perfusate was Krebs–Henseleit solution (pH 7.4, 36°C) containing 1.25 mM $CaCl_2$ and 11 mM or 27.5 mM glucose, gassed with 95% O_2–5% CO_2. Mean coronary perfusion pressure (CPP) was measured through a side tube of the cannula inserted into the aorta. Heart rate (HR) was measured with a cardiotachometer (AT-601G, Nihon Kohden, Tokyo, Japan). Coronary flow rate (CFR) was measured by collecting drops of venous effluent from the heart.

Figure 1A shows the perfusion protocol. CFR was gradually increased by a microtube pump (Minipuls 2, Gilson, Middleton, U.S.A.) to provide a CPP of

about 55 mmHg. The hearts were then paced at 300 beats/min by an electronic stimulator (SEN-3301, Nihon Kohden) throughout the experiments. The paced hearts were divided into three groups: control, underperfusion, and underperfusion with norepinephrine (NE, Sankyo, Tokyo, Japan). In the control group, the hearts were perfused at a flow rate adjusted to provide a CPP of about 55 mmHg (control perfusion) for 30 or 90 minutes. In the underperfusion group, after 30-minute control perfusion, the hearts were exposed to 60-minute underperfusion. In the underperfusion with NE group, after 30-minute control perfusion, the hearts were exposed to 13, 17, 30, or 60-minute underperfusion by reducing the flow rate to 0.4–6 mL/min/g heart weight, and five minutes after the start of underperfusion, the perfusate was changed to that containing 10^{-6} M NE. At the end of each perfusion, the hearts were quickly frozen in liquid nitrogen for subsequent measurement of tissue substrates. In the ex-vivo insulin-treated underperfusion with NE subgroup, insulin (2 mU/min/g heart weight, Novo, Actrapid) was infused 15 minutes before and during underperfusion by an infusion pump (SP-60, Nipro, Osaka, Japan).

Figure 1B shows a sample record. To detect changes in the contractile responses of the left ventricle, the isometric tension along the longitudinal direction of the whole heart, as contractile force (CF), and the isovolumic pressure, as left ventricular pressure (LVP), were monitored simultaneously. To monitor CF, a force-displacement transducer (TB-611T and AP-621G, Nihon Kohden) was attached by a thread with a hook to the ventricular apex. To monitor LVP, a fluid-filled balloon connected to a pressure transducer (TP-101T and AP-620G, Nihon Kohden) was placed in the left ventricle. Diastolic force (resting tension) in the CF and the LV diastolic pressure were expressed in terms of resting CF and resting LVP, respectively. The resting CF and resting LVP during the control perfusion before the infusion of agents were adjusted to 1 g and 0 mmHg, respectively, and differences (Δg and ΔmmHg) from the normal perfusion levels just before underperfusion were measured to detect changes in LV stiffness. CF and LVP developed from the diastolic to the systolic tension and pressure were measured as developed CF and developed LVP, respectively, and the $\pm dF/dt$ and the $\pm dP/dt$ were derived with differentiators (ED-601G, Nihon Kohden) respectively.

Reperfusion was induced by the flow returning to the preundeperfusion level.

At the end of each perfusion, the hearts were quickly frozen in liquid nitrogen for subsequent measurement of tissue substrates.

Determination of myocardial energy metabolites

The energy metabolites in the LV subendocardium and subepicardium were determined and analyzed separately. The LV free walls of the frozen hearts were dissected into inner and outer halves, which corresponded to the subendocardial and subepicardial portions, respectively. The solidly frozen tissue was weighed (wet weight) and after five-hour lyophilization, the dried tissue was again weighed (dry weight). The tissue water content was estimated from the wet and dry weights. The dried tissue was extracted with 0.6 M perchloric acid. The mixture was centrifuged at 12,000 g for 15 minutes at 2°C, and the supernatant was used to determine tissue

metabolites. Creatine phosphate and inorganic phosphate were determined by the method of Fiske and Subbarow, as modified by Furchgott and DeGubareff [39]. ATP was determined by the firefly luminescence method, using ATP Monitoring Reagent (BioOrbit Oy, Turku, Finland) and a Lumiphotometer (TD-4000, Laboscience, Tokyo, Japan). Lactate was determined by an enzymatic method, using Lactate Test BMY (Boehringer Mannheim Germany). The approximate tissue lactate concentration was estimated from the water and lactate content. Tissue glycogen was determined by the enzymatic method of Keppler and Decker [40] with a starch measuring reagent "Starch" (Boehringer Mannheim), as described in detail in our previous paper [38].

Measurement of regional myocardial flow rate

Tissue flow distribution was determined by the dye microspheres method with Dye-trak (Triton, San Diego, U.S.A.). Blue and yellow microspheres (diameter, 15 μm) were injected into the coronary perfusion line just before and after 60-minute underperfusion, respectively. The LV free wall was dissected into the subendocardium and the subepicardium. Multiple dye microspheres in the dried tissue were collected, and the dyes were dissolved in N,N-dimethylformamide (Nacalai Kyoto, Japan) and determined with a UV-VIS recording spectrophotometer (UV-2200A, Shimadzu Kyoto, Japan).

Statistics

The data were analyzed statistically by Student's t-test, or analysis of variance (ANOVA) for multiple comparisons.

RESULTS AND DISCUSSION

Effects of norepinephrine on cardiac dysfunctions during underperfusion and reperfusion in diabetic rat hearts

In non-DM hearts, myocardial ischemia is followed by a release of catecholamines [41], and catecholamines improve or aggravate myocardial metabolism and contractile function, depending on the degree of coronary blood flow [42]. In DM hearts, exercise-induced global LV dysfunction [2] and a decrease in catecholamine-induced calcium uptake through the myocardial sarcolemma [43] have been observed. This reduced myocardial response to catecholamine may bear relevance to the increased incidence of heart failure in DM. On the other hand, reports that norepinephrine (NE) induces augmented vasconstriction in the arterial bed in DM [4,6,10] indicate that altered DM vascular reactivity may play a role in the onset of cardiac dysfunction and ischemic heart disease in DM.

The first purpose of our investigations is, therefore, to clarify whether DM hearts are more vulenerable than non-DM hearts to underperfusion and to reperfusion. The second purpose is to examine the effects of NE during underperfusion on the underperfusion and reperfusion injuries in non-DM hearts and in DM hearts with or without insulin in vivo treatment [35].

Figure 2 shows the increases in LV diastolic stiffness (increases in resting CF and

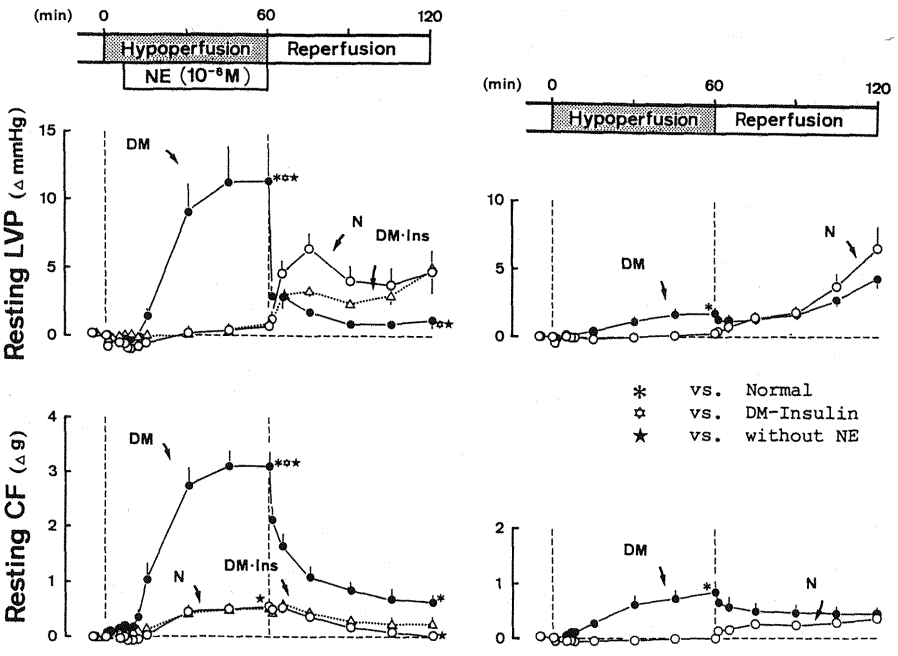

Figure 2. Changes in resting LVP and resting CF in isolated nondiabetic (N: open circles), streptozotocin (60 mg/kg i.v.)-induced eight-day diabetic (DM: solid circles) and in vivo insulin (4 U/day s.c.)-treated diabetic rat hearts (DM-Ins: open triangles) during underperfusion (1 mL/min) with or without norepinephrine (NE 10^{-6} M), and during reperfusion with the preunderperfusion flow level. Vertical lines indicate SEM. Significant difference ($p < 0.05$) from nondiabetic group (asterisk), from insulin-treated diabetic group (star of David), and from the group without norepinephrine (star) at the end of 60-minute underperfusion and at the end of 60-minute reperfusion. Other details as in legend to figure 1.

resting LVP) during underperfusion (1 mL/min, 60 minutes) and reperfusion (60 minutes) in STZ (60 mg/kg i.v.)-induced eight-day DM and non-DM hearts, and the effects of NE (10^{-6} M) and in vivo insulin (4 U/day/rat s.c.) treatment on the injuries. The 60-minute underperfusion without NE caused a slight but significant increase in LV stiffness only in DM hearts, a smaller transmural lactate accumulation in DM hearts, and similar ATP decreases in both heart groups. NE during underperfusion caused deterioration of these cardiac dysfunctions in both groups, particularly in DM hearts. The 60-minute reperfusion caused partial recovery in LV stiffness and cardiac movement in DM heart with NE, while it caused more marked increases in LV stiffness in non-DM hearts and DM hearts without NE than underperfusion. Coronary perfusion pressure recovered the control levels in DM hearts and reached levels above preunderperfusion in non-DM hearts. Both groups showed similar partial recovery of ATP. NE during underperfusion improved the mechanical dysfunction during reperfusion in DM hearts, but there was a smaller

recovery in ATP than in hearts without NE. The partial recovery of ATP may result from the loss of adenine nucleotides and/or the disorder of high-energy transfer via creatine kinase, because creatine phosphate recovered to above the preunderperfusion levels. Insulin in vivo treatment in DM restored the cardiac functions to the non-DM levels.

Severe regional myocardial ischemia in vivo causes a decrease in myocardial contractility in the ischemic area and an elevation of LVEDP [42,44]. This elevation may be due to an increased LVED volume resulting from heart failure or to increased LV stiffness, i.e., a depressed LV compliance. In the present experiment using isolated perfused hearts with a balloon in the LV, an elevated resting LVP probably indicates an increase in LV stiffness because of the constant LVED volume. This finding probably indicates that DM hearts increase the diastolic stiffness of the LV wall during underperfusion, which is augmented by NE. This conclusion is consistent with the report [16] in which an elevated LVEDP, despite no increase in LVED volume, has been observed in in vivo DM canine hearts with regional ischemia. DM hearts are thus more vulnerable to underperfusion than non-DM hearts. Our previous study in anesthetized non-DM dogs [42] suggests that catecholamines at high concentrations probably further aggravate the impaired cardiac function under severe ischemia. The present results also confirm the deleterious effects of NE during underperfusion on cardiac function in both groups, and, moreover, make it clear that DM hearts are more susceptible than non-DM hearts to NE during underperfusion. This finding may in part account for the higher incidence of heart failure following acute myocardial ischemia in DM.

The impaired myocardial energy metabolism and sarcolemma integrity may be partly responsible for the higher degree of ischemic contracture in DM than in non-DM hearts. The smaller lactate accumulation may indicate a larger limitation of glycolytic energy production in DM hearts. A limitation of glucose availability in DM hearts [12,25,26] in turn contributes to the lower lactate content [31]. It is inferred that the depletion of ATP produced by glycolysis damages the integrity of the cellular membrane [20], and decreases in sarcolemmal Na^+, K^+-ATPase [14] and Ca^{2+} pump activities [15] have been observed in DM hearts. Therefore, it is supposed that Ca^{2+} accumulation in the underperfused myocardium is augmented in DM hearts and facilitated by NE. The metabolic derangements were probably augmented by an imbalance between supply and demand of myocardial oxygen, e.g., perfusion obstructed by the elevated extravascular pressure and the elevated diastolic tension. In fact, the metabolic changes in the isolated underperfused hearts were more pronounced in the inner layer of the LV wall than in the outer layer, as observed in in vivo canine hearts [34].

An enhanced LV diastolic stiffness during reperfusion indicates that non-DM hearts rather than DM hearts seem to be more susceptible to reperfusion injury, which cannot be explained by decrease in ATP alone. This conclusion is in agreement with the report in which the increase in Ca^{2+} uptake during reperfusion of ischemic DM hearts was obviously less than that of non-DM hearts and the reduced Ca^{2+} uptake was highly correlated with the improved recovery of LV

function in DM hearts [17]. A decrease in catecholamine-induced Ca^{2+} uptake through the DM myocardial sarcolemma under normal perfusion was also observed [43,45]. Thus, the better function in DM hearts may result from less Ca^{2+} uptake and/or less LV stiffness. Myocardial edema, which also enhances LV diastolic stiffness [46], was observed during reperfusion, and the level tended to be lower in DM hearts. The erectile properties of the myocardium (effects of CPP and CPF on diastolic stiffness) are greater at larger LVEDP and in ischemia-injured hearts [47]. In non-DM hearts, sympathetic stimulation causes coronary vasodilation, and vasodilation induced by adenosine is more marked and reactive hyperemic responses of coronary arterial bed after ischemia are larger than in DM hearts [6]. NE infusion after coronary ligation results in the absence of edema in nonischemic areas of DM hearts despite an increase of edema in non-DM hearts [4]. Reduced vasodilation in the coronary arterial bed in DM [9] and enhanced vasoconstrictive reactivity to catecholamines in experimental DM rat coronary artery [6] and hindquarters [3,10] have been observed. Thus, we also infer that the reperfusion in DM hearts causes less extensive myocardial edema than in non-DM hearts, which may in part be responsible for the better cardiac movement during reperfusion. Higher myocardial edema under reperfusion in non-DM hearts might result in the higher CPP and the swelling of the hearts that is responsible for the lower resting CF.

In conclusion, the DM heart is more vulnerable to underperfusion, while the non-DM heart is more vulnerable to reperfusion injury. Norepinephrine exacerbates the underperfusion injury and imporved the reperfusion injury, particularly in DM hearts, and insulin in vivo treatment restores the injuries to the non-DM levels.

Correlation of LV stiffness increase and abnormal myocardial energy metabolism at 60-minute underperfusion with NE

In non-DM hearts, ATP depletion and the consequent changes play a crucial role in ischemic injury [48,49]. In underperfused DM hearts, ATP supply from ischemia-induced acceleration of glycolysis [50,51] may be insufficient because glucose uptake in DM hearts is limited [12,24]. The myocardial responses to various degrees of flow deficiency, especially in the presence of NE, could be different in non-DM and DM hearts.

Therefore, the differences between non-DM and STZ (60 mg/kg i.v.)-induced 11-day DM rat hearts were examined with reference to the effects of various low-flow rates (0.4–6 mL/min/g heart weight, 60 minutes) with NE (10^{-6} M) on the mechanical and regional energy-metabolic functions and with reference to the diastolic state related to tissue energy metabolite content [36].

Figure 3 shows an increase in LV stiffness (increases in resting CF and resting LVP) at 60-minute underperfusion with NE, depending on a decrease in coronary flow rate. In simultaneously monitoring LVP and CF in isolated hearts, a slight but distinct increase in LV stiffness was detected at an elevated resting CF, and a large increase in LV stiffness correlated quantitatively with the elevation of the resting LVP. LV stiffness increased in relation to flow-rate decrease at flows below 1 and 6 mL/min/g heart weight with NE in non-DM and DM hearts, respectively. The

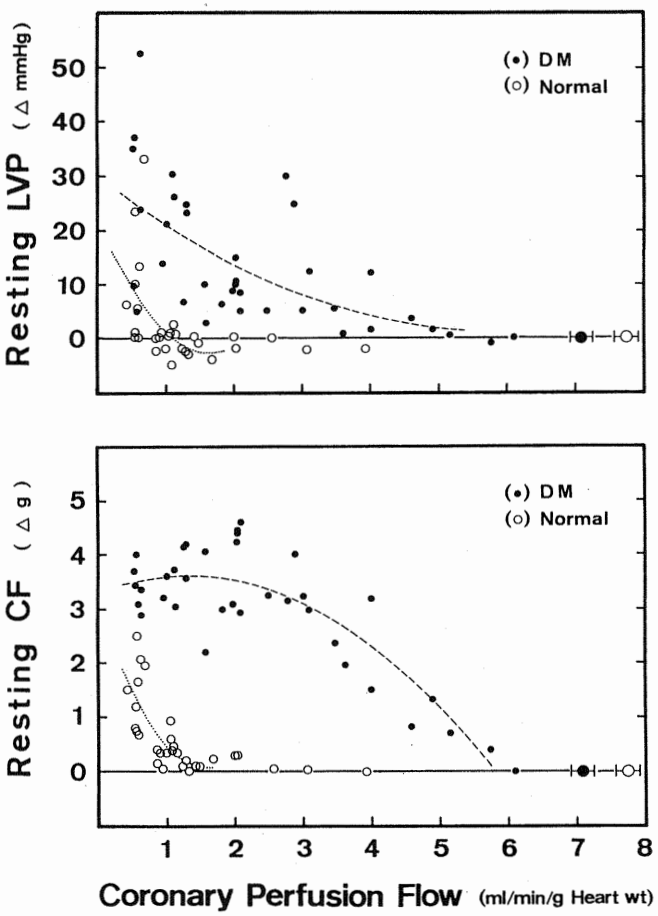

Figure 3. Relationships between changes in resting LVP (upper) and resting CF (lower) vs. 60-minute underperfusion (0.4–6 mL/min/g heart weight) with norepinephrine (NE 10^{-6} M) in nondiabetic (Normal: open circles) and streptozotocin (60 mg/kg i.v.)-induced 11-day diabetic rat hearts (DM: solid circles). Coronary perfusion flow was decreased to arbitrary low-flow rate. Values on ordinate represent changes in the parameters at each 60-minute low-flow with NE from each value just before underperfusion. Data are derived from individual hearts. Large-sized open and solid circles with vertical and horizontal bars show mean ± SEM of each parameter just before underperfusion without norepinephrine in nondiabetic and diabetic hearts, respectively. Other details as in legend to figure 1.

results indicate that DM hearts are more susceptible to flow reduction with NE and suffer from LV stiffness elevation under moderate ischemia.

Figure 4 shows the decreases in the subendocardial and subepicardial ATP contents at 60-minute underperfusion with NE depending on a decrease in coronary flow rate. ATP content in both layers of both groups decreased linearly in

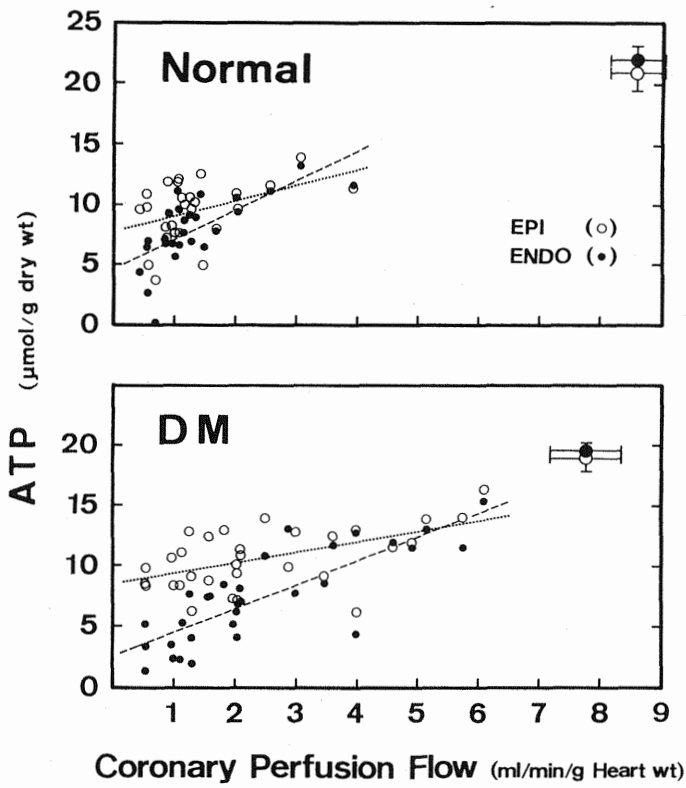

Figure 4. Relationships between ATP content in the left ventricular inner (subendocardium, ENDO: solid circles) and outer layers (subepicardium, EPI: open circles) vs. 60-minute underperfusion with norepinephrine (NE 10^{-6}M) in nondiabetic (Normal, upper) and diabetic rat hearts (DM, lower). Data are derived from individual hearts. Large-sized open (EPI) and solid circles (ENDO) with vertical and horizontal bars show mean ± SEM of ATP content just before underperfusion without NE. Other details as in legends to figures 1 and 3.

relation to flow decrease. The decrease was more pronounced in the inner than in the outer layer of both groups, with marked increase in LV stiffness, and the decrease in the inner layer was obviously greater in the DM hearts. The results indicate that the subendocardium of the isolated perfused heart is metabolically more susceptible to underperfusion with NE injury, particularly in the DM hearts.

Figure 5 shows the relationship between an increase in LV stiffness and subendocardial ATP depletion or lactate accumulation at 60-minute underperfusion with NE. The increase in LV stiffness correlated closely with the subendocardial ATP depletion and lactate increase in both groups, but the correlation curves for the non-DM and DM hearts were not coincident. A distinct increase in LV stiffness was observed at a level of subendocardial ATP content below about 5 μmol/g dry

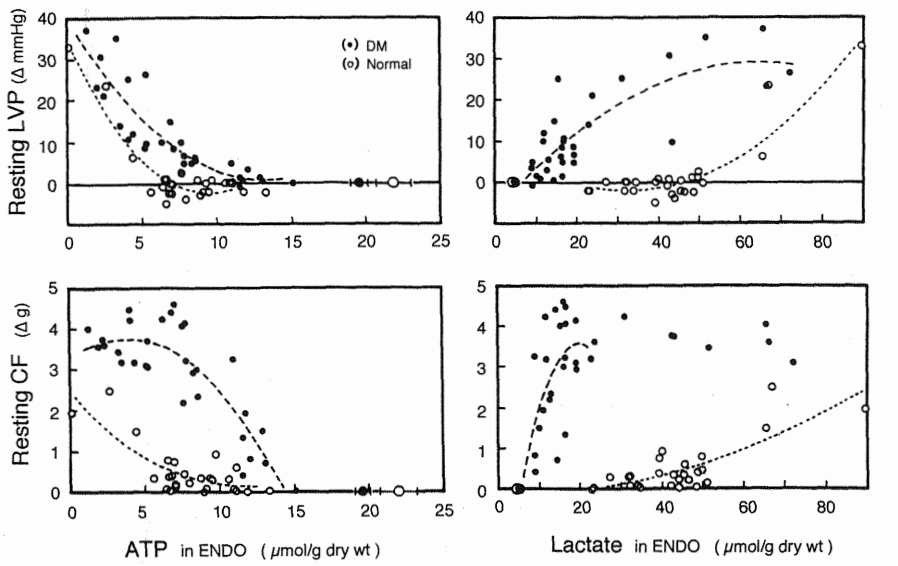

Figure 5. Relationships between changes in resting LVP (upper) and resting CF (lower) vs. subendocardial ATP (left) and lactate content (right) in nondiabetic (Normal: open circles) and diabetic rat hearts (DM: solid circles). Large-sized open and solid circles with vertical and horizontal bars show mean ± SEM of each parameter just before underperfusion without NE in nondiabetic and diabetic hearts, respectively. Other details as in legends to figures 1, 3, and 4.

weight in the non-DM hearts and at a level below 13 μmol/g dry weight in the DM hearts. This finding indicates that LV stiffness in the DM hearts is more susceptible to a decrease in subendocardial total ATP than is the stiffness in the non-DM hearts. Therefore, the difference in the LV stiffness between the non-DM and DM hearts cannot be explained by the total ATP level or by lactate level itself in the tissue. The greater limitation of glycolytic energy production [12,24,28,29], disorder of the intracellular ATP distribution, and/or greater damage to the integrity of the cellular membrane and intracellular ion homeostasis [14,15] may be involved in the marked increase in LV stiffness in the DM hearts.

In conclusion, the DM heart is more susceptible than the non-DM heart to flow reduction with NE and readily exhibits an increase in LV diastolic stiffness and abnormal energy metabolism, particularly in the subendocardium. In each DM or non-DM heart group, the increase in LV stiffness correlates closely with the subendocardial ATP depletion and lactate accumulation. The critical ATP level causing an increase in LV stiffness, however, is higher in the DM heart, and the critical lactate level is lower; therefore, the critical levels of total ATP and lactate in the tissue of the non-DM heart cannot refer to those in the DM heart without insulin.

Protective effect of ex vivo insulin on underperfused diabetic rat hearts

Ischemia leads to stimulation of glycolysis depending on the degree of tissue perfusion and cardiac work [50]. The active glycolytic pathway could be important in maintaining the cellular ATP level to preserve cellular membranes and myocardial integrity [23]. When ATP is simultaneously broken down, an increased rate of glycolysis results in tissue acidosis [52], which inhibits glycolysis [53]. Thus, glucose availability during ischemia, i.e., acceleration or inhibition of glycolysis, is closely associated with improvement or exacerbation of ischemic injury [23]. Insulin enhances glucose utilization in both non-DM [54] and DM hearts [24]: hence, insulin plus glucose therapy has been used to protect against ischemic myocardial injury [55,56]. However, the efficacy of such intravenous infusion to patients with [57] or without DM [58] has been controversial. The efficacy in experimental studies using isolated hearts is also dependent on the ischemic conditions [51,59]. The diverse results may result in part at least from the dual effect on glycolysis: direct acceleration and indirect inhibition.

In our studies [35,36], DM rather than non-DM hearts were more susceptible to flow reduction. A greater limitation of glucose availability in DM hearts [12] may be involved in the discrepancy. The preventive effect of ex vivo insulin on underperfusion with NE injury was greater in the DM hearts than in the non-DM hearts [37]. Ischemia plus insulin-induced accumulation of a high tissue level of lactate inhibits glycolysis [51,60]; a high concentration of tissue lactate may limit the beneficial effect of insulin. Rovetto et al. [60] suggest that insulin and 22 mM glucose may be more harmful than beneficial in severely ischemic tissue. The more favorable effect in DM hearts may result from the lower tissue lactate level; the acceleration of glucose transport by insulin is slower and the increase in glucose uptake is smaller in DM than in non-DM hearts [24,27,54]. In the DM hearts, high glucose plus insulin under severe ischemia may, however, cause a high tissue lactate level.

Figure 6 shows the relationship between an increase in LV stiffness (an increase in resting CF) and a decrease in the subendocardial ATP content at 60-minute underperfusion (0.6 mL/min/g heart weight) with NE (10^{-6} M) in isolated non-DM and STZ (60 mg/kg i.v.)-induced 13-day DM hearts. The effect of ex vivo insulin (2 mU/min/g heart weight) on the underperfusion with NE injury and the influence of tissue lactate concentration on the effect were invesigated under normal (11 mM) and high (27.5 mM) perfusate glucose. In DM hearts during underperfusion with NE under 11 mM glucose, insulin increased the water content in the subendocardium and tended to decrease the subendocardial lactate accumulation (13.0 → 7.5 mM); insulin partially improved the abnormal myocardial energy metabolism and significantly reduced the increase in LV stiffness. In DM hearts under 27.5 mM glucose, the underperfusion injury was similar to that under 11 mM glucose' but insulin maintained the high tissue lactate level (16.0 → 15.2 mM) and improved the underperfusion injury only to the non-DM heart level. In non-DM hearts under 11 mM glucose, the underperfusion injury was smaller than in DM

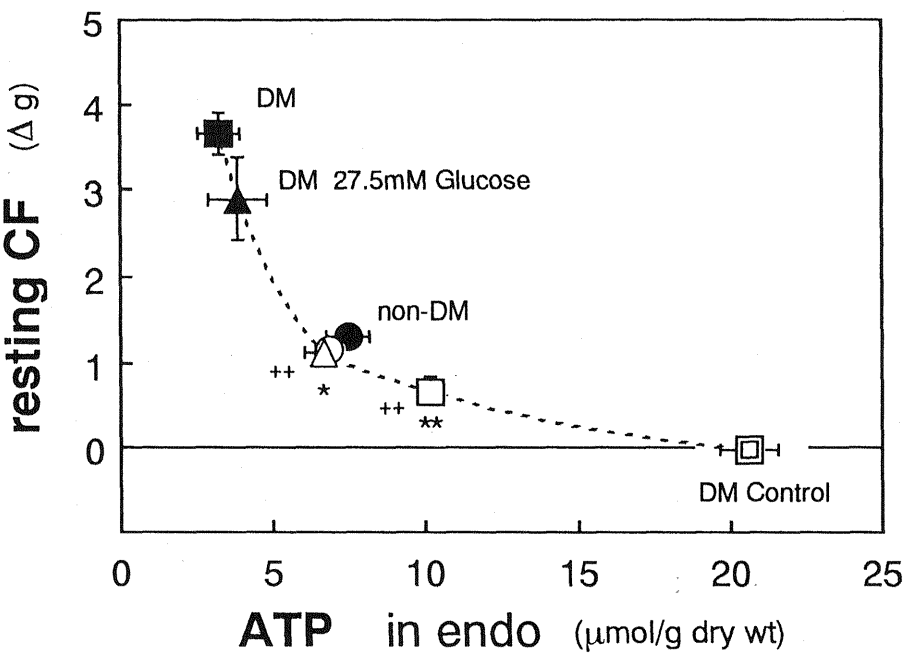

Figure 6. Relationship between an increase in resting CF and a decrease in subendocardial ATP content. Double square shows the value during control perfusion in the streptozotocin (60 mg/kg i.v.)-induced 13-day diabetic (DM) rat hearts. Solid circle, square, and triangle show the values at 60-minute underperfusion (0.6 mL/min/g heart weight) with norepinephrine (NE 10^{-6} M) in the nondiabetic (non-DM) and diabetic (DM) groups under 11 mM and 27.5 mM perfusate glucose, respectively. Open circle, square, and triangle show the values in the respective ex vivo insulin (2 mU/min/g heart weight)-treated groups. Vertical and horizontal lines are SEM. *, $p < 0.05$; **, $p < 0.01$ in ATP content; $^{++}$, $p < 0.01$ in resting CF vs. each group without insulin. In insulin-treated DM groups, the values of ATP content and resting CF under 11 mM perfusate glucose are higher ($p < 0.01$) and lower ($p < 0.05$), respectively, than those under 27.5 mM glucose. Other details as in legend to figure 1.

hearts; insulin tended to increase the tissue lactate further (11.0 → 12.9 mM) and did not improve the smaller injury.

The present results indicate that acute intracoronary application of insulin in DM hearts improves the underperfusion with NE injury to a level above that of non-DM hearts, but does not improve a less severe injury in non-DM hearts. The beneficial effect of insulin on the injury decreases under high perfusate glucose and is probably influenced by the tissue lactate level.

In DM hearts, daily subcutaneous administration of insulin before isolation of the hearts restored the altered cardiac metabolism and function during underperfusion with [35] or without [61] NE to the non-DM heart level. In the present experiments [37], ex vivo application of insulin into the isolated hearts during underperfusion with NE again alleviated the dysfunctions in the DM hearts; also the

improved functions were better than the non-DM heart levels during underperfusion with NE. The results suggest that acute intracoronary infusion of insulin during ischemia, even in uncontrolled DM hearts, may permit an improvement of ischemic injury.

The subendocardial lactate concentration during ischemia with insulin was 7.5 ± 0.6 mM, which was sufficient to stimulate glycolysis [53,60]. Thus, insulin in DM hearts caused an increase in ATP content without any further increase in lactate content, and ATP increase may be attributed to transmural acceleration of glucose utilization by insulin. At least two conceivable mechanisms may account for the results. One could be that extrusion of lactate from tissue to the perfusion fluid increased because of an increase in the water content of the subendocardium and cardiac movement improved by insulin. The other possibility could be that metabolism of pyruvate, produced by glycolysis, to acetyl CoA rather than lactate was accelerated, since there is a report that low pyruvate dehydrogenase activity in diabetic hearts is stimulated by insulin [30].

The metabolic effects of insulin probably contributed to the improvement in diastolic dysfunction. In the present experiments, the tissue ATP content during ischemia with insulin in DM hearts, 10.2 ± 0.3 μmol/g dry weight in the subendocardium and 13.2 ± 0.6 μmol/g dry weight in the subepicardium, was probably sufficient to attenuate the increase in LV stiffness during ischemia. In non-DM hearts, the ATP level required to prevent ischemic contracture was about 8 μmol/g dry weight of whole ventricle [51] and about 5 μmol/g dry weight of subendocardium (figure 5) [36]. If the ATP content was over the critical level in the presence of insulin, ischemic contracture could not be evoked. Insulin probably improved the mechanical changes, at least in part, by improving myocardial energy metabolism.

The effect of insulin on activation of enzymes associated with intracellular ion homeostasis was not examined in the present study, but it may also contribute to the improvement of diastolic dysfunction. In DM hearts, the enzyme levels, sarcolemmal Na^+, K^+–ATPase activity [14], and sarcolemmal and sarcoplasmic reticular Ca^{2+}–ATPase activities [15] are decreased; these enzyme activities have been found to be increased by in vitro insulin [62,63].

In non-DM hearts, insulin did not improve the less severe ischemic injury. Insulin increases glucose transport through the plasma membrane more efficiently than glucose itself [64]. However, insulin has a slight or no effect on the rate of glucose utilization when glucose is the sole substrate present and is maximally used, e.g., during a high workload [65] or during ischemia [54,55]. In addition, the lactate content in the subepicardium during underperfusion with NE was significantly higher in non-DM hearts than in DM hearts. This possibly implies that non-DM hearts utilized glucose more and minimized the effect of insulin. According to results of studies with experimental conditions similar to ours [53,60], the high lactate concentration in the subendocardium of non-DM hearts (12.9 ± 0.9 mM) does not markedly accelerate glycolysis. Thus, in the present non-DM hearts, insulin probably failed to increase the tissue ATP content and to improve the increase in LV stiffness.

In conclusion, acute intracoronary application of insulin to the severely ischemic myocardium is probably beneficial in the DM heart: an increase in LV stiffness is prevented, together with a partial but sufficient recovery from tissue ATP depletion. The addition of insulin in the non-DM heart, on the other hand, is probably hardly effective in less severe ischemic injury.

Glycogen depletion and LV stiffness increase in underperfused diabetic rat hearts: participation of the degree and duration of underperfusion and/or diabetes

In non-DM hearts, preservation of the glycogen store is beneficial for the ischemic myocardium on the condition that it does not result in high tissue levels of lactate [66–69]. In addition, the rate of glycolytic flux from glucose correlates best with prevention or delay of ischemic contracture [23]. As compared with non-DM hearts, DM hearts show increased cardiac glycogen [70–72], hypersensitivity of glycogen phosphorylase activation by epinephrine [7], and less lactate production during underperfusion with NE [36]. Therefore, the high glycogen content in DM hearts may have some protective effects against cardiac dysfunction during underperfusion with NE. However, decreases in glucose utilization [28,29] and functional and ultrastructural alterations [8], depending on the duration of DM, have also been observed.

In our previous studies in isolated perfused rat hearts [35,36], we showed DM hearts to be more susceptible than non-DM hearts to flow reduction and to exhibit an increase in LV diastolic stiffness readily; norepinephrine (NE) exacerbated this effect, particularly in the DM hearts. The results of that study were obtained after more than 30 minutes of underperfusion. During short-term underperfusion, however, DM hearts showed slightly more mechanical movement than non-DM hearts.

In the present study, therefore, we examined the relationship between cardiac dysfunction, particularly the increase in LV stiffness, and glycogen level during underperfusion (2 mL/min/g heart weight) with NE (10^{-6} M) in non-DM and DM rat hearts with different durations of DM, i.e., with different glycogen content. We noted that the start of the underperfusion injury was delayed in the hearts with longer duration of diabetes, (i.e., in those with higher glycogen content), although the degree of injury during the long-term underperfusion accompanied by glycogen depletion depended on the duration of DM [38].

Characterization of diabetic state

Characteristics of the 45-day non-DM rats and the STZ (50 mg/kg i.v.) -induced eight-day and 45-day DM rats used in the isolated heart experiments were as follows (mean ± S.E.): body weight, 458 ± 8, 259 ± 5, and 237 ± 7 g; heart weight, 1.28 ± 0.02, 0.88 ± 0.01, and 0.88 ± 0.02 g; plasma glucose, 174 ± 7, 523 ± 11' and 525 ± 13 mg/dL; and glycosylated hemoglobin, 3.66 ± 0.19, 6.61 ± 0.13, and 11.94 ± 0.42%, respectively. There were significant differences ($p < 0.01$) between the non-DM and DM groups in the parameters, but not between the two DM groups in any of the parameters, except for glycosylated hemoglobin ($p < 0.01$).

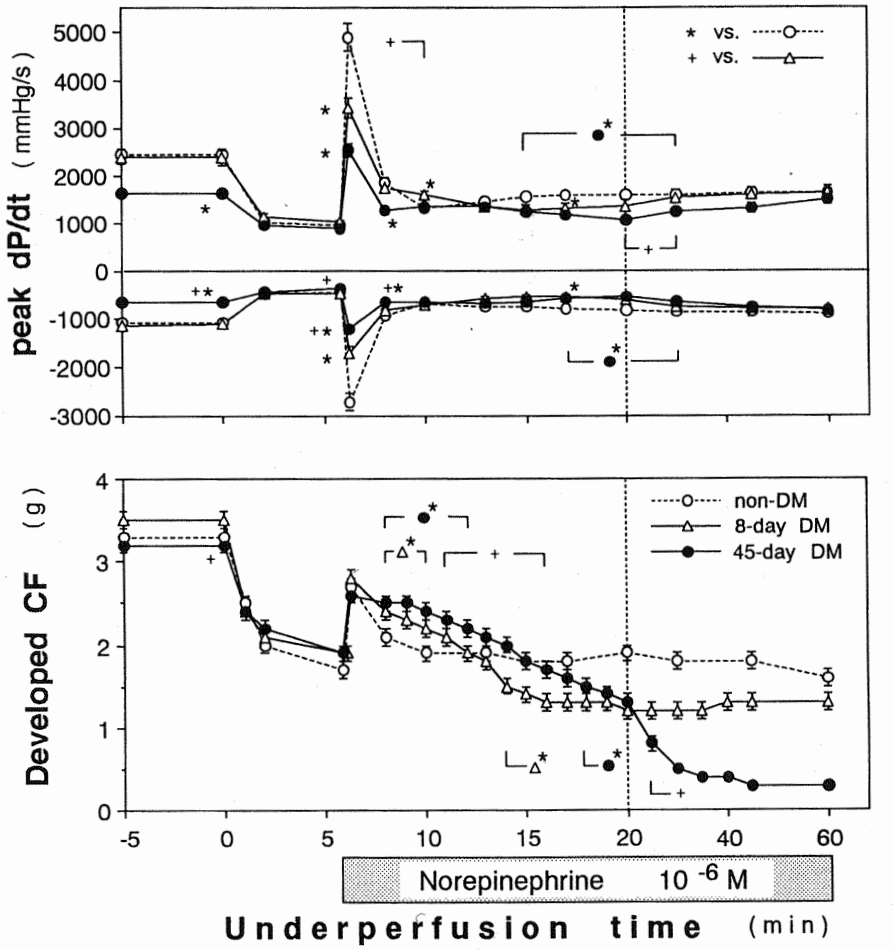

Figure 7. Developed CF and peak LV diastolic (−) and systolic (+) *dP/dt* during underperfusion (2 mL/min/g heart weight) with norepinephrine (NE, 10^{-6} M) in 45-day nondiabetic (non-DM: open circles) and streptozotocin (50 mg/kg i.v.)-induced eight-day (open triangles) and 45-day diabetic rat hearts (solid circles). Vertical lines indicate SEM. *, $p < 0.05$ vs. 45-day non-DM group; +, $p < 0.05$ vs. eight-day DM group. Other details as in legend to figure 1.

Contractile dysfunction during underperfusion with NE

Figure 7 shows the changes in the LV peak systolic and diastolic *dP/dt*, and the developed CF. With the induction of underperfusion, the values for the parameters decreased rapidly. The peak systolic and diastolic *dP/dt* values in the 45-day DM group did not exceed values in the other two groups throughout the perfusion. NE infusion during underperfusion induced transient marked increases in the values for the parameters. The maximal responses to NE for the peak systolic and diastolic

dP/dt decreased signficantly with the duration of DM. Following the marked augmentation in the developed CF, there was a moderate increase, the duration of which was greatest in the following order: 45-day DM > eight-day DM > non-DM hearts. It was greater in the 45-day DM hearts than in the eight-day DM hearts until around 20 minutes after the onset of underperfusion. After 20 minutes of underperfusion with NE, the developed CF decreased with the progression of DM.

DM is likely to change cardiac functions, and the changes probably depend on the severity of DM, the degree and duration of ischemia, and sympathetic activity. The present model of experimental DM indicates that, in 45-day DM hearts, significant depression is induced in the LV contractile function during control perfusion, while this outcome does not occur in eight-day DM hearts. On the other hand, during underperfusion, the response to NE, i.e., the marked positive inotropic effect induced by β-adrenoceptors just after administration and almost completely inhibited by propranolol, was already significantly depressed in eight-day DM hearts. The responses of LV contractile and diastolic velocities to NE decreased with the progression of DM. The present results regarding the depression in mechanical function of DM hearts agreee with a previous finding [8]. More precise study of the causes of the depression is necessary, but it appears that, rather than there being a deficiency in high-energy phosphate compound, changes in contractile proteins [11], impairment of β-adrenoceptor, and/or cyclic AMP levels [7], or dysfunction in Ca^{2+} mobilization during stimulation–contraction coupling [43] could be involved in this depression.

Diastolic state during underperfusion with NE

Figure 8 shows the increases in LV diastolic stiffness (increases in resting LVP and resting CF). In the non-DM hearts during underperfusion with NE, the LV stiffness showed only slight increases. For about 5–10 minutes following the peak response immediately after the infusion of NE during underperfusion, the LV contraction, as shown by the developed LVP and the developed CF values, was greater in DM hearts, the extent depending on the duration of DM. During this period, the diastolic tension did not rise markedly, and the decreases in diastolic velocity did not differ among the three groups. The diastolic tension started to rise 12–13 minutes after the onset of underperfusion with NE in eight-day DM hearts and about 17 minutes after the onset of underperfusion in 45-day DM hearts, the extent of the rise being less in 45-day DM hearts until about 20 minutes after the onset of underperfusion. These results indicate that, except for the marked β-adrenoceptor response immediately after the infusion of NE, the cardiac movement during underperfusion with NE is greater in DM hearts than in non-DM hearts whenever LV stiffness does not increase. Until about 20 minutes after the onset of underperfusion with NE, the LV stiffness was less and the cardiac contraction was greater in 45-day than in eight-day DM hearts. After 20 minutes of underperfusion with NE, the diastolic pressure and tension increased with the progression of DM, i.e., the increase in LV stiffness was more marked and CPP started to rise gradually in the 45-day DM hearts.

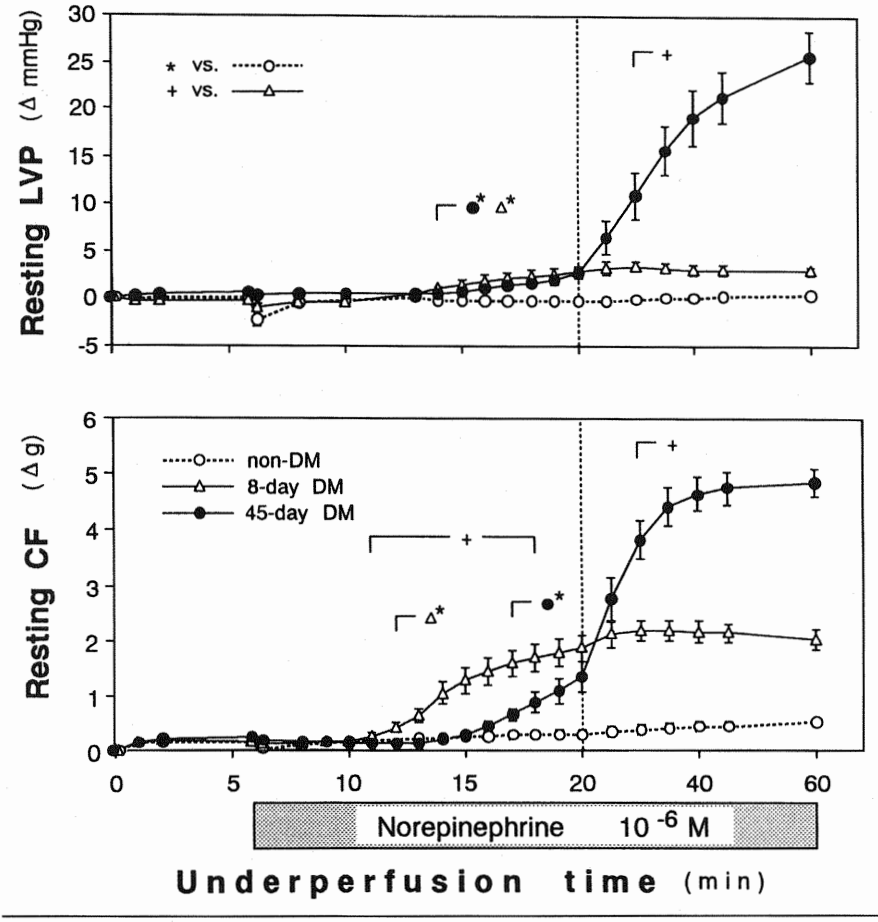

Figure 8. Resting CF and resting LVP during underperfusion with NE in 45-day nondiabetic (non-DM: open circles), eight-day (open triangles), and 45-day diabetic rat hearts (solid circles). Vertical lines indicate SEM. *, $p < 0.05$ vs. 45-day non-DM group; $^{+}$, $p < 0.05$ vs. eight-day DM group. Other details as in legends to figures 1 and 7.

Myocardial glycogen during underperfusion with NE

Figure 9 shows the changes in the subendocardial content of glycogen and glucose. During control perfusion, glycogen levels in non-DM, eight-day, and 45-day DM hearts were 85 ± 7, 120 ± 6, and 206 ± 11 μmol/g dry weight, respectively, in the subendocardium. About 13 minutes after the onset of underperfusion with NE, the glycogen level in the eight-day DM hearts had decreased to half (58 ± 3 μmol/g dry weight) when the diastolic tension began to increase (figure 8). In the 45-day DM hearts, glycogen decreased more markedly, with a marked increase in tissue glucose and without greater lactate accumulation (figure 10), but these glycogen levels were

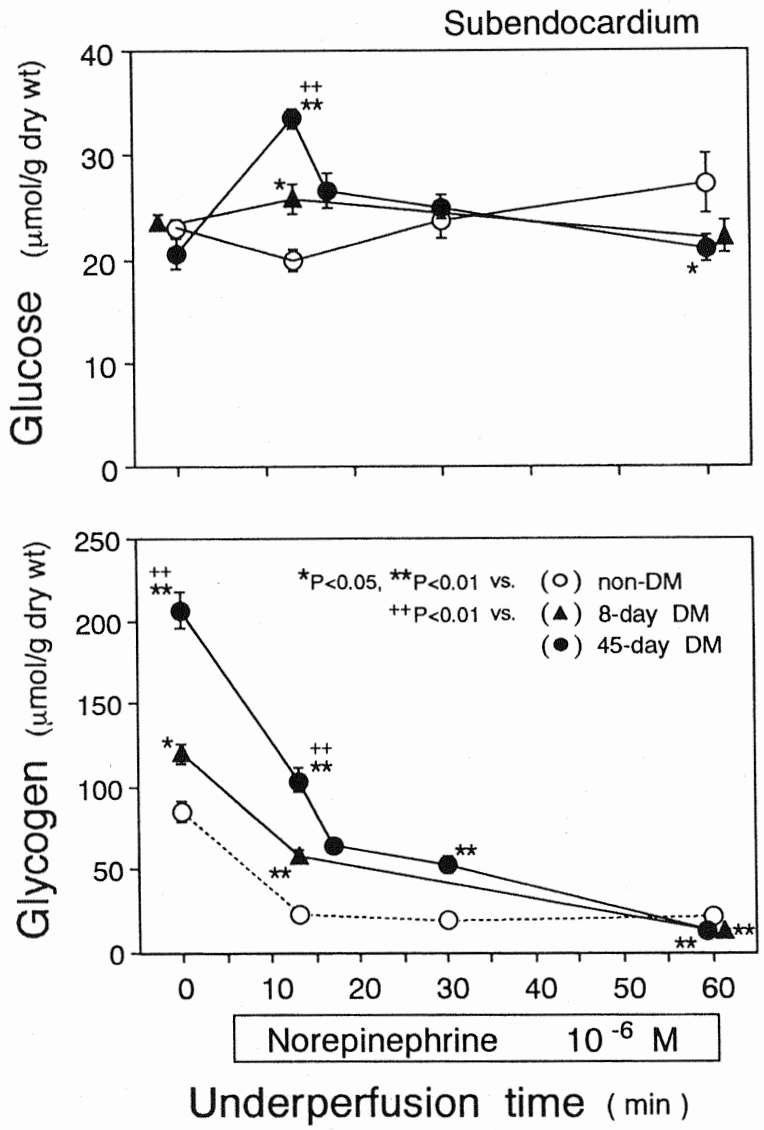

Figure 9. Subendocardial glycogen and glucose content just before underperfusion (0 minutes), and after 13, 17, 30, and 60 minutes of underperfusion with NE in the 45-day nondiabetic (non-DM: open circles), the eight-day (solid triangles), and the 45-day diabetic rat hearts (solid circles). Vertical lines indicate S.E. Other details as in legends to figures 1 and 7.

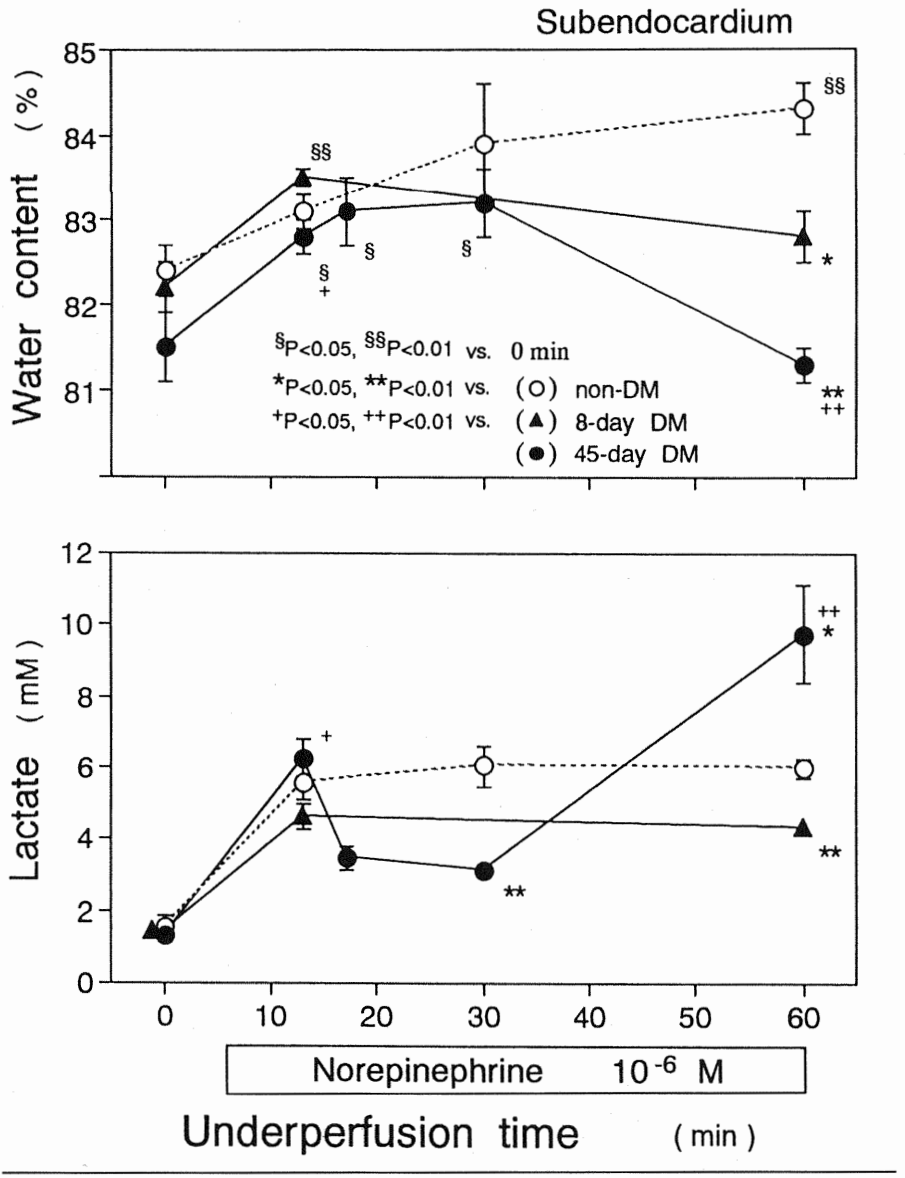

Figure 10. Lactate concentration and water content in the subendocardium just before underperfusion (0 minutes), and after 13, 17, 30, and 60 minutes of underperfusion with NE in 45-day nondiabetic (non-DM: open circles), eight-day (solid triangles), and 45-days diabetic rat hearts (solid circles). Vertical lines indicate S.E. §, $p < 0.05$, and §§, $p < 0.01$ vs. respective value of water content at 0 minutes in each group. Other details as in legends to figures 1 and 7.

still higher (104 ± 7 μmol/g dry weight) than those in the eight-day DM hearts, and the diastolic tension did not increase (figure 8). About 17 minutes after the onset of underperfusion, the glycogen decreased to the 13-minute level of the eight-day DM hearts (64 ± 2 μmol/g dry weight), and the diastolic tension began to increase (figure 8). After 60 minutes of underperfusion with NE, the glycogen levels were markedly low in both DM hearts (less than 20 μmol/g dry weight), and diastolic tension had increased twice as much in 45-day DM as in eight-day DM hearts and was related to the decreased subendocardial ATP level. The results indicate that the markedly high glycogen content in DM hearts probably helps delay the start of the increase in LV stiffness during underperfusion with NE. Ultimately, however, the degree of the injury depends on the duration, i.e., the severity, of the DM.

Myocardial water and lactate content during underperfusion with NE

Figure 10 shows the changes in the subendocardial water content and lactate concentration. During normal perfusion, water content was greater in the subepicardium than in the subendocardium in the non-DM and 45-day DM hearts, and there was no significant difference between the layers during underperfusion with NE. The subendocardial water content in the non-DM hearts increased with increasing underperfusion time. The content in both the DM hearts also increased during 30-minute underperfusion with NE. However, 60 minutes after the onset of underperfusion, the water content had decreased to the control perfusion level in each group; the subendocardial water content showed significant differences among the groups, in inverse proportion to the increase in LV stiffness, indicating that tissue water content is not involved in the increase of stiffness (figure 8). The tissue lactate concentrations were almost the same in the three groups during control perfusion and increased similarly after 13 minutes of underperfusion with NE. The concentrations in the subendocardium and the subepicardium of the 45-day DM hearts were then slightly decreased 17–30 minute after the onset of underperfusion with NE; 60 minutes after the onset of underperfusion with NE, the subendocardial concentration alone increased again markedly, this being related to the increase in LV stiffness (figure 8).

Myocardial energy metabolism during underperfusion with NE

Figure 11 shows the regional energy metabolism in the LV free wall. During control perfusion, the subendocardium and the subepicardium did not differ in their tissue content of high-energy phosphates. However, during underperfusion with NE, the metabolic changes were more marked in the subendocardium. The subendocardial ATP content decreased depending on the duration of underperfusion with NE. The ATP content 13–30 minutes after the onset of underperfusion with NE, when the diastolic tension had begun to increase only in the DM hearts, was similar in the three groups. After 60-minute underperfusion with NE, however, marked decreases in ATP relating to increases in LV stiffness (figure 8) were observed in the DM hearts.

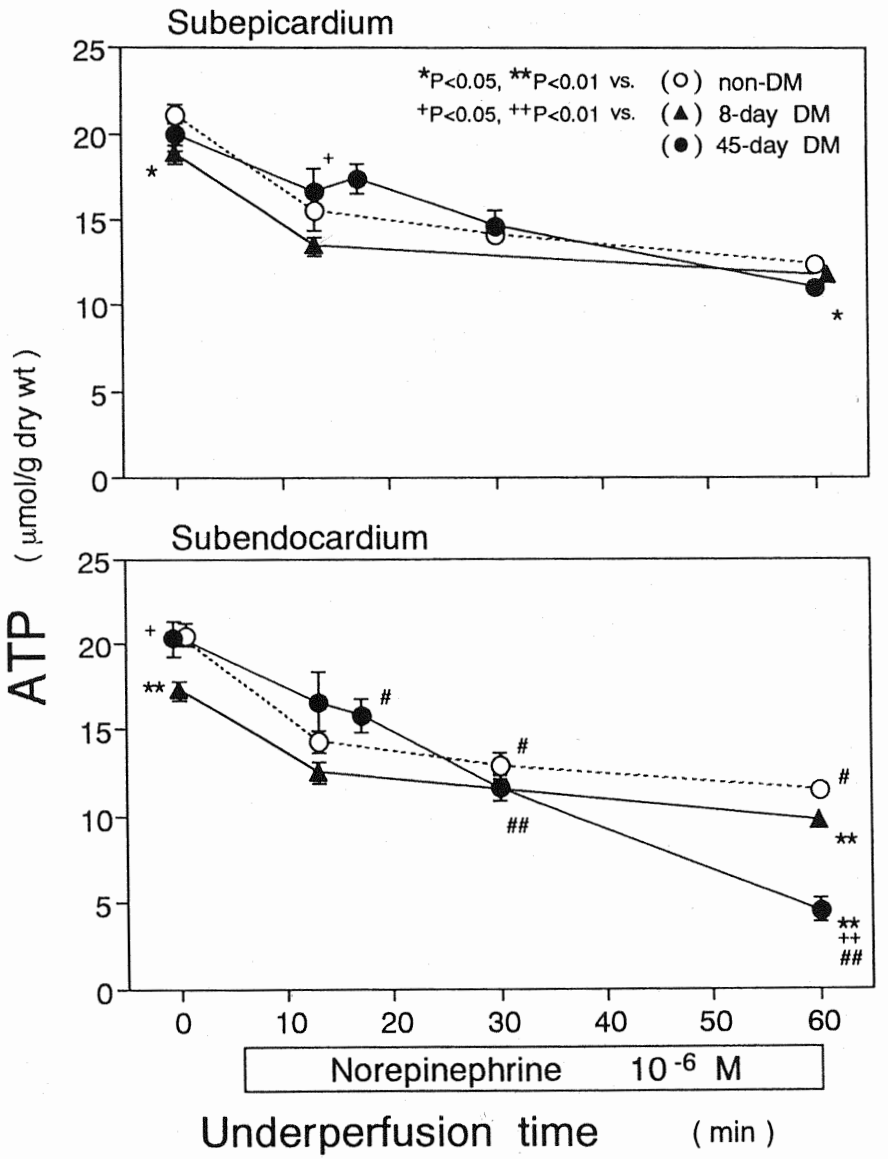

Figure 11. ATP content in the subendocardocardium and subepicardium just before underperfusion (0 minutes), and after 13, 17, 30, and 60 minutes of underperfusion with NE in 45-day nondiabetic (non-DM: open circles), eight-day (solid triangles), and 45-day diabetic rat hearts (solid circles). Vertical lines indicate S.E. $^{\#}$, $p < 0.05$, and $^{\#\#}$, $p < 0.01$ vs. respective subepicardium. Other details as in legends to figures 1 and 7.

The glycogen content increased markedly, depending on the duration of DM, whereas during underperfusion the glycogen decreased gradually. The decrease after 13-minute underperfusion with NE was more marked in 45-day DM than eight-day DM hearts and was accompanied by a marked increase in tissue glucose. These results are compatible with previous findings showing that increased glycogen is used during underperfusion and that the DM-related hypersensitivity of glycogen phosphorylase activation by epinephrine is due to a DM-related increase in free intracellular Ca^{2+} concentration rather than to changes in cyclic AMP [7,73]. In non-DM hearts, beneficial effects of preserving a glycogen store in ischemic injury have been reported [66–69]; however, the marked increase in lactate induced by glycogenolysis during ischemia is harmful for postischemic cardiac function [74]. In our studies, myocardial lactate during underperfusion with NE in the absence [36] or presence [37] of insulin increases less in DM hearts than in non-DM hearts. A decrease in glycogen level unaccompanied by marked lactate accumulation has also been observed in DM hearts during ischemia [75]. The present results are consistent with those reports. After 13-minute underperfusion with NE, the glycogen level was still higher in 45-day DM than in eight-day DM hearts; the critical glycogen level when the diastolic tension began to rise was about 60 μmol/g dry weight in both DM hearts. During 30-minute underperfusion with NE, the marked glycogen degradation was not accompanied by a reciprocal increase in tissue lactate, and the tissue ATP levels were preserved at above 12 μmol/g dry weight in all groups. Thus, at least during underperfusion with NE, the markedly high glycogen content that is manifested with the progression of DM probably helps delay the initiation of the increase in LV stiffness; this beneficial effect may be due to maintenance of the availability of the glycolytic substrates required for ATP production.

After about 20 minutes of underperfusion with NE, however, both the increase in LV stiffness and the extent of abnormal myocardial energy metabolism were exacerbated with the progression of DM. The subendocardium of the LV free wall was metabolically more susceptible than the subepicardium to injury by 60-minute underperfusion with NE; and the increase in LV stiffness correlated closely with the ATP depletion in the subendocardium. The present results confirm our previous report (figure 5) [36], in which we also observed that the correlation curves for non-DM and DM hearts were not coincident. The subendocardial ATP levels relating to a distinct increase in LV stiffness were higher in the DM than the non-DM hearts. The present results also indicate that in the same heart group the decrease in the subendocardial ATP level correlates with the increase in LV stiffness during underperfusion with NE, although the differences between the non-DM and DM hearts in the degree and the onset time of increase in LV stiffness during underperfusion with NE cannot be explained simply by the tissue total ATP level. The greater limitation of glucose availability [28,29] and damage to the integrity of the cellular membrane and intracellular ion homeostasis [14,15] with the progression of DM may be involved in the increase in stiffness in the DM hearts, since these hearts would have consumed almost all the glycogen reserves as the underperfusion with NE proceeded. This idea is supported by the results of our previous studies, in

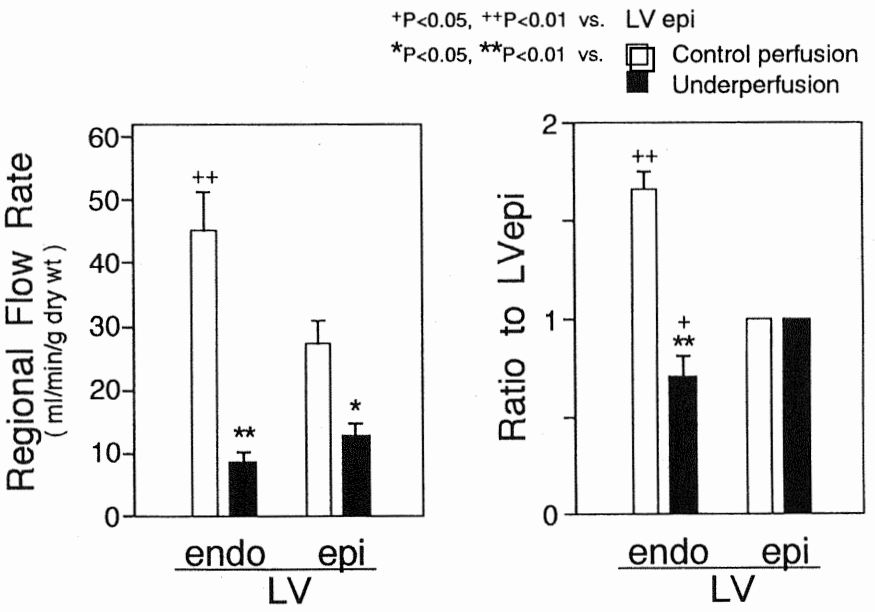

Figure 12. Flow distribution in the subendocardium (endo) and subepicardium (epi) of the left ventricular free wall (LV), just before (control perfusion: open bar) and 60 minutes after the start of underperfusion (2 mL/min/g heart weight: solid bar) with norepinephrine (10^{-6} M) in 45-day diabetic rat hearts. Tissue flow was determined by the dye microspheres method. Vertical lines are S.E. $^{+}$, $p < 0.05$, and $^{++}$, $p < 0.01$ vs. respective subepicardium. Other details as in legends to figures 1 and 7.

which an increase in the stiffness of DM hearts was improved to the non-DM heart level by both in vivo [35] and ex vivo [37] administration of insulin. The creatine phosphate: inorganic phosphate ratio, which reflects the state of myocardial oxidative metabolism, decreased to less than one-sixth of the control perfusion levels within 13 minutes of underperfusion with NE in all groups, and after 60-minute underperfusion with NE the ratio in the 45-day DM hearts decreased further, reflecting a marked increase in inorganic phosphate and decrease in creatine phosphate. This marked impairment of oxidative metabolism may be also involved in the exacerbation of the cardiac stiffness.

Regional myocardial flow distribution in isolated underperfused diabetic rat heart

Figure 12 shows that the regional myocardial flow distribution during control perfusion is greater in the LV inner layer (subendocardium) than in the outer layer (subepicardium) of the isolated 45-day DM rat heart. When the distribution of low flow rates was examined 60 minutes after the start of underperfusion with an NE-containing fluid, the flow rate in the inner layer of the LV free wall was significantly lower than that in its outer layer. This reflects the abnormal regional myocardial energy metabolism very well.

In conclusion, the myocardial content of glycogen increases depending on the duration of DM. The markedly high glycogen content in the DM heart is probably utilized during underperfusion and helps delay the initiation of the increase in cardiac stiffness; the high glycogen content has preventive effects against the injury incurred in short-term underperfusion with NE. After the glycogen depletion, however, the underperfusion with NE injury is exacerbated by the progression of DM.

REFERENCES

1. Jaffe AS, Spadaro JJ, Schechtman K, Roberts R, Geltman EM, Sobel BE. 1984. Increased congestive heart failure after myocardial infarction of modest extent in patients with diabetes mellitus. Am Heart J 108:31–37.
2. Vered Z, Battler A, Segal P, Liberman D, Yerushalmi Y, Berezin M, Neufeld HN. 1984. Exercise-induced left ventricular dysfunction in young men with asymptomatic diabetes mellitus (diabetic cardiomyopathy). Am J Cardiol 54:633–637.
3. Brody MJ, Dixon RL. 1964. Vascular reactivity in experimental diabetes mellitus. Circ Res 14:494–501.
4. Palik I, Koltai MZ, Kolonics I, Wagner M, Pogátsa G. 1982. Effects of coronary occlusion and norepinephrine on the myocardium of alloxan-diabetic dogs. Basic Res Cardiol 77:499–506.
5. Gøtzsche O. 1983. The adrenergic β-receptor adenylate cyclase system in heart and lymphocytes from streptozotocin-diabetic rats. In vivo and in vitro evidence for a desensitized myocardial β-receptor. Diabetes 32:1110–1116.
6. Koltai MZ, Jermendy G, Kiss V, Wagner M, Pogátsa G. 1984. The effects of sympathetic stimulation and adenosine on coronary circulation and heart function in diabetes mellitus. Acta Physiol Hung 63:119–125.
7. Miller TB Jr. 1984. Phosphorylase activation hypersensitivity in hearts of diabetic rats. Am J Physiol 246:E134–E140.
8. Jackson CV, McGrath GM, Tahiliani AG, Vadlamudi RVSV, McNeill JH. 1985. A functional and ultrastructural analysis of experimental diabetic rat myocardium. Diabetes 34:876–883.
9. Gebremedhin D, Koltai MZ, Pogátsa G, Magyar K, Hadhazy P. 1988. Influence of experimental diabetes on the mechanical responses of canine coronary arteries: role of endothelium. Cardiovasc Res 22:537–544.
10. Friedman JJ. 1989. Vascular sensitivity and reactivity to norepinephrine in diabetes mellitus. Am J Physiol 256:H1134–H1138.
11. Garber DW, Neely JR. 1983. Decreased myocardial function and myosin ATPase in hearts from diabetic rats. Am J Physiol 244:H586–H591.
12. Feuvray D, Idell-Wenger JA, Neely JR. 1979. Effects of ischemia on rat myocardial function and metabolism in diabetes. Circ Res 44:322–329.
13. Wohaieb SA, Godin DV. 1987. Alterations in free radical tissue-defense mechanisms in streptozocin-induced diabetes in rat: effects of insulin treatment. Diabetes 36:1014–1018.
14. Pierce GN, Dhalla NS. 1983. Sarcolemmal Na^+,K^+-ATPase activity in diabetic rat heart. Am J Physiol 245:C241–C247.
15. Heyliger CE, Prakash A, McNeill JH. 1987. Alterations in cardiac sarcolemmal Ca^{2+} pump activity during diabetes mellitus. Am J Physiol 252:H540–H544.
16. Haider B, Ahmed SS, Moschos CB, Oldewurtel HA, Regan TJ. 1977. Myocardial function and coronary blood flow response to acute ischemia in chronic canine diabetes. Circ Res 40:577–583.
17. Tani M, Neely JR. 1988. Hearts from diabetic rats are more resistant to in vitro ischemia: possible role of altered Ca^{2+} metabolism. Circ Res 62:931–940.
18. Vogel WM, Apstein CS. 1988. Effects of alloxan-induced diabetes on ischemia–reperfusion injury in rabbit hearts. Circ Res 62:975–982.
19. McDonald TF, MacLeod DP. 1973. Metabolism and the electrical activity of anoxic ventricular muscle. J Physiol 229:559–582.
20. Bricknell OL, Daries PS, Opie LH. 1981. A relationship between adenosine triphosphate, glycolysis and ischaemic contracture in the isolated rat heart. J Mol Cell Cardiol 13:941–945.
21. Lipasti JA, Nevalainen TJ, Alanen KA, Tolvanen MA. 1984. Anaerobic glycolysis and the development of ischemic contracture in isolated rat heart. Cardiovasc Res 18:145–148.

22. Weiss JN, Lamp ST. 1987. Glycolysis preferentially inhibits ATP-sensitive K^+ channels in isolated guinea pig cardiac myocytes. Science 238:67–69.
23. Owen P, Dennis S, Opie LH. 1990. Glucose flux rate regulates onset of ischemic contracture in globally underperfused rat hearts. Circ Res 66:344–354.
24. Morgan HE, Cadenas E, Regen DM, Park CR. 1961. Regulation of glucose uptake in muscle. II. Rate-limiting steps and effects of insulin and anoxia in heart muscle from diabetic rats. J Biol Chem 236:262–268.
25. Hearse DJ, Stewart DA, Chain EB. 1975. Diabetes and the survival and recovery of the anoxic myocardium. J Mol Cell Cardiol 7:397–415.
26. Ingebretsen CG, Moreau P, Hawelu-Johnson C, Ingebretsen WR Jr. 1980. Performance of diabetic rat hearts: effects of anoxia and increased work. Am J Physiol 239:H614–H620.
27. Denton RM, Brownsey RW, Belsham GJ. 1981. A partial veiw of the mechanism of insulin action. Diabetologia 21:347–362.
28. Chen V, Ianuzzo CD, Fong BC, Spitzer JJ. 1984. The effects of acute and chronic diabetes on myocardial metabolism in rats. Diabetes 33:1078–1084.
29. Whitfield CF, Osevala MA. 1984. Hexose transport modification of rat hearts during development of chronic diabetes. J Mol Cell Cardiol 16:1091–1099.
30. Ohlen J, Siess EA, Löffler G, Wieland OH. 1978. The effect of insulin on pyruvate dehydrogenase interconversion in heart muscle of alloxan-diabetic rats. Diabetologia 14:135–139.
31. Penpargkul S, Schaible T, Yipintsoi T, Scheuer J. 1980. The effect of diabetes on performance and metabolism of rat hearts. Circ Res 47:911–921.
32. Takenaka F, Higuchi M. 1974. High-energy phosphate contents of subepicardium and subendocardium in the rat treated with isoproterenol and some other drugs. J Mol Cell Cardiol 6:123–135.
33. Edoute Y, Van Der Merwe E, Sanan D, Kotze JCN, Steinmann C, Lochner A. 1983. Normothermic ischemic cardiac arrest of the isolated working rat heart. Effects of time and reperfusion on myocardial ultrastructure, mitochondrial oxidative function, and mechanical recovery. Circ Res 53:663–678.
34. Higuchi M. 1989. Participation of the vasodilating property of nipradilol in improving ischemic derangement of myocardial energy metabolism. J Cardiovasc Pharmacol 14:157–165.
35. Higuchi M, Ikema S, Matsuzaki T, Hirayama K, Sakanashi M. 1991. Effects of norepinephrine on hypoperfusion–reperfusion injuries in hearts isolated from normal and diabetic rats. J Mol Cell Cardiol 23:137–148.
36. Higuchi M, Ikema S, Sakanashi M. 1992. Correlation of contractile dysfunction and abnormal tissue energy metabolism during hypoperfusion with norepinephrine in isolated rat hearts: differences between normal and diabetic hearts. J Mol Cell Cardiol 24:1125–1141.
37. Higuchi M, Uezu K, Sakanashi M. 1993. Ex vivo effect of insulin on normal and diabetic rat hearts hypoperfused with norepinephrine. Eur J Pharmacol 242:293–300.
38. Higuchi M, Miyagi K, Nakasone J, Sakanashi M. 1995. Role of high glycogen in underperfused diabetic rat hearts with added norepinephrine. J Cardiovasc Pharmacol 26:899–907.
39. Furchgott RF, DeGubareff T. 1956. The determination of inorganic phosphate and creatine phosphate in tissue extracts. J Biol Chem 223:377–388.
40. Keppler D, Decker K. 1984. 1.2 Glycogen. In Bergmeyer HU (ed), Methods of Enzymatic Analysis (Metabolites 1: Carbohydrates, vol. 6), 3rd ed. Weinheim: Verlag Chemie, pp. 11–18.
41. Schömig A, Dart AM, Dietz R, Mayer E, Kubler W. 1984. Release of endogenous catecholamines in the ischemic myocardium of the rat: Part A: Locally mediated release. Circ Res 55:689–701.
42. Higuchi M, Asakawa T. 1985. Effects of nitroglycerin on regional myocardial function in the underperfused canine heart. J Cardiovasc Pharmacol 7:1087–1095.
43. Gøtzsche O. 1985. Abnormal myocardial calcium uptake in streptozocin-diabetic rats. Evidence for a direct insulin effect on catecholamine senitivity. Diabetes 34:287–290.
44. Barry WH, Brooker JZ, Alderman EL, Harrison DC. 1974. Changes in diastolic stiffness and tone of the left ventricle during angina pectoris. Circulation 49:255–263.
45. Bielefeld DR, Pace CS, Boshell BR. 1983. Altered sensitivity of chronic diabetic rat heart to calcium. Am J Physiol 245:E560–E567.
46. Cross CR, Rieben PA, Salisbury PF. 1961. Influence of coronary perfusion and myocardial edema on pressure–volume diagram of left ventricle. Am J Physiol 201:102–108.
47. Vogel WM, Apstein CS, Briggs LL, Gaasch WH, Ahn J. 1982. Acute alterations in left ventricular diastolic chamber stiffness: role of the "erectile" effect of coronary arterial pressure and flow in normal and damaged hearts. Circ Res 51:465–478.

48. Hearse DJ, Garlick PB, Humphrey SM. 1977. Ischemic contracture of the myocardium: mechanisms and prevention. Am J Cardiol 39:986–993.
49. Jennings RB, Reimer KA, Hill ML, Mayer SE. 1981. Total ischemia in dog hearts, in vitro 1. Comparison of high energy phosphate production, utilization, and depletion, and of adenine nucleotide catabolism in total ischemia in vitro vs. severe ischemia in vivo. Circ Res 49:892–900.
50. Kübler W, Spieckermann PG. 1970. Regulation of glycolysis in the ischemic and anoxic myocardium. J Mol Cell Cardiol 1:351–377.
51. Apstein CS, Gravino FN, Haudenschild CC. 1983. Determinants of a protective effect of glucose and insulin on the ischemic myocardium. Effects on contractile function, diastolic compliance, metabolism, and ultrastructure during ischemia and reperfusion. Circ Res 52:515–526.
52. Dennis SC, Gevers W, Opie LH. 1991. Protons in ischemia: where do they come from; where do they go to? J Mol Cell Cardiol 23:1077–1086.
53. Rovetto MJ, Lamberton WF, Neely JR. 1975. Mechanisms of glycolytic inhibition in ischemic rat hearts. Circ Res 37:742–751.
54. Morgan HE, Henderson MJ, Regen DM, Park CR. 1961. Regulation of glucose uptake in muscle. I The effects of insulin and anoxia on glucose transport and phosphorylation in the isolated, perfused heart of normal rats. J Biol Chem 236:253–261.
55. Brachfeld N. 1973. The glucose–insulin–potassium (GIK) regimen in the treatment of myocardial ischemia. Circulation 48:459–462.
56. Farah AF, Alousi AA. 1981. The actions of insulin on cardiac contractility. Life Sci 29:975–1000.
57. Gwilt DJ, Petri M, Lamp P, Nattrass M, Pentecost BL. 1984. Effect of intravenous insulin infusion on mortality among diabetic patients after myocardial infarction. Br Heart J 51:626–630.
58. Kostis JB, George J, Hayase K, Moreyra AE, Kuo PT. 1979. Effect of glucose–insulin–potassium solution on the exercise performance of patients with coronary artery disease. Am Heart J 98:351–360.
59. Eberli FR, Weinberg EO, Grice WN, Horowitz GL, Apstein CS. 1991. Protective effect of increased glycolytic substrate against systolic and diastolic dysfunction and increased coronary resistance from prolonged global underperfusion and reperfusion in isolated rabbit hearts perfused with erythrocyte suspensions. Circ Res 68:466–481.
60. Rovetto MJ, Whitmer JT, Neely JR. 1973. Comparison of the effects of anoxia and whole heart ischemia on carbohydrate utilization in isolated working rat hearts. Circ Res 32:699–711.
61. Mochizuki S, Ishikawa S, Abe M. 1984. Insulin treatment and myocardial function in isolated perfused heart from diabetic rat. Jpn Circ J 48:255–265.
62. Ku DD, Sellers BM. 1982. Effects of streptozotocin diabetes and insulin treatment on myocardial sodium pump and contractility of the rat heart. J Pharmacol Exp Ther 222:395–400.
63. Gupta MP, Lee S, Dhalla NS. 1989. Activation of heart sarcoplasmic reticulum Ca^{2+}-stimulated adenosine triphosphate by insulin. J Pharmacol Exp Ther 249:623–630.
64. Zaninetti D, Greco-Perotto R, Jeanrenaud B. 1988. Heart glucose transport and transporters in rat heart: regulation by insulin, workload and glucose. Diabetologia 31:108–113.
65. Taegtmeyer H, Hems R, Krebs HA. 1980. Utilization of energy-providing substrates in the isolated working rat heart. Biochem J 186:701–711.
66. Hoekenga DE, Brainard JR, Hutson JY. 1988. Rates of glycolysis and glycogenolysis during ischemia in glucose–insulin–potassium-treated perfused hearts: a ^{13}C, ^{31}P nuclear magnetic resonance study. Circ Res 62:1065–1074.
67. Lagerstrom CF, Walker WE, Taegtmeyer H. 1988. Failure of glycogen depletion to improve left ventricular function of the rabbit heart after hypothermic ischemic arrest. Circ Res 63:81–86.
68. Schneider CA, Taegtmeyer H. 1991. Fasting in vivo delays myocardial cell damage after brief periods of ischemia in the isolated working rat heart. Circ Res 68:1045–1050.
69. Elliott AC, Smith GL, Eisner DA, Allen DG. 1992. Metabolic changes during ischemia and their role in contractile failure in isolated ferret hearts. J Physiol 454:467–490.
70. Bhimji S, Godin DV, McNeill JH. 1986. Coronary artery ligation and reperfusion in alloxan-diabetic rabbits: ultrastructural and haemodynamic changes. Br J Exp Pathol 67:851–863.
71. Eto M, Watanabe K, Sekiguchi M, Iwashima Y, Morikawa A, Oshima E, Ishii K. 1987. Metabolic and morphological changes of the heart in Chinese hamsters (CHAD strain) with spontaneous long-term diabetes. Diabetes Res Clin Pract 3:297–305.
72. Maulik MG, Seth SD, Manchanda SC, Singh U, Maulik SK. 1991. Isoproterenol fails to produce myocardial necrosis in streptozotocin-induced diabetic rats. Ind J Exp Biol 29:837–840.
73. Wolleben CD, Jaspers SR, Miller TB Jr. 1987. Use of adult rat cardiomyocytes to study cardiac glycogen metabolism. Am J Physiol 252:E673–E678.

74. Neely JR, Grotyohann LW. 1984. Role of glycolytic products in damage to ischemic myocardium. Dissociation of adenosine triphosphate levels and recovery of function of reperfused ischemic hearts. Circ Res 55:816–824.
75. Kilgour RD, Riggs CE Jr. 1987. Glycogenolysis and lactogenesis in the ischemic diabetic rat heart. Diabetes Res 4:27–29.

DO KETONE BODIES CONTRIBUTE TO PROTECTION AGAINST DAMAGE CAUSED BY BOTHMYOCARDIAL ISCHEMIA AND REPERFUSION INJURY?

KIYOTAKA SATO, TAKASHI MASUDA, SHINICHIROU YAMAMOTO, NARIHISA MATSUYAMA, SHINYA KAWABATA, and TOHRU IZUMI

Kitasato University School of Medicine

Summary. Effects of ketone bodies on cardiac performance and mitochondrial energetics were investigated in experimental myocardial ischemia, with a special focus on the following reperfusion injury.

Twenty-one isolated rat hearts were classified into three categories by perfusion mode after ischemia: seven hearts were exposed to 10 minutes of myocardial ischemia followed by 30 minutes of coronary reperfusion with normal Krebs–Henseleit (K–H) buffer without using ketone bodies (K(−)group), and the other seven hearts were exposed to the same ischemia and reperfused with K–H buffer containing 5 mM ketone bodies (Ke group). These were compared with seven normal hearts that were exposed to neither ischemia nor reperfusion (control group). Cardiac performance was assessed by several indices: max *dp/dt*, cardiac output, cardiac work, and cardiac efficiency. Mitochondrial energetics were estimated by using mitochondrial redox state, its potentiality, and cytosolic ΔGATP hydrolysis energy.

As a result, the Ke group demonstrated a more rapid improvement of LV contractility than the K(−) group after reperfusion. From the standpoint of energetics, the ketone bodies seemed to economically augment the mitochondrial metabolism because the mitochondrial redox state, cytosolic ΔGATP hydrolysis energy, and concentration of phosphocreatine were remarkably increased.

Thus, it was concluded that, in myocardial ischemia, ketone bodies function as a substrate to produce mitochondrial energy, and through this function, work to protect the myocardium against both transient ischemia and the following reperfusion injury.

INTRODUCTION

In recent years, powerful interventional therapies have been widely employed to treat ischemic heart disease, including its acute phase. Due to rapid advances in these

S. Mochizuki, N. Takeda, M. Nagano and N. Dhalla (eds.). THE ISCHEMIC HEART.

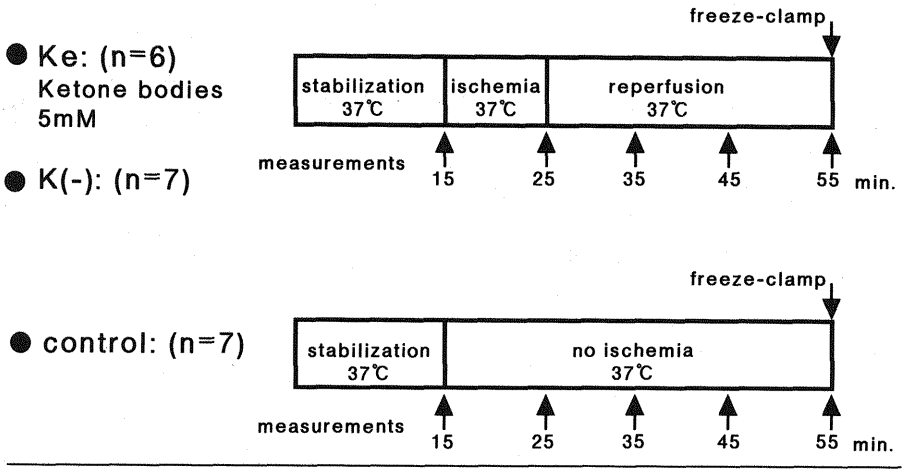

Figure 1. Experimental protocol.

therapies, the question of how to protect the myocardium from reperfusion injury has become an urgent clinical and experimental focus. Analysis of this problem at the molecular level has resulted in a new concept of apoptosis in the myocardium, with emphasis on a primary preventive method: how to lower the energy cost at the cellular level in myocardial ischemia. We have previously demonstrated that ketone bodies are able to function cytologically in a manner similar to insulin, namely, they take up glucose into the cardiocyte [1]. Additionally, it has already been shown that ketone bodies can serve as metabolic substrates during an abnormal metabolic state, such as ketoacidosis in the myocardium and even in the brain [2]. Thus, the study reported here aimed to clarify the effects of ketone bodies on myocardial energy metabolism in ischemic hearts, with special reference to the protective activities of ketone bodies against myocardial ischemia.

MATERIALS AND METHODS

Using 300–350 g male Wistar rats, a working heart perfusion system with a prelod of 10 cm H_2O and an 80-mmHg afterload was made according to the method of Neely et al. [3]. The experimental protocol is shown in figure 1. After a 15-minute stabilization period, total ischemia was induced for 10 minutes by blocking the perfusate, after which reperfusion was performed for 30 minutes. Physiological parameters were recorded every 10 minutes, beginning before the initiation of ischemia. The hearts were divided into three groups: a Ke group (n = 7), in which 5-mM ketone bodies (4 mM D-β-hydroxybutyrate and 1 mM acetoacetate) were mixed with a modified Krebs–Henseleit bicarbonate buffer before the ischemia; a K(−) group (n = 7), in which the perfusion was performed without the admixture of ketone bodies; and a control group (n = 7), in which the perfusion was

$$\text{Cytosolic } \frac{[\Sigma ATP]}{[\Sigma ADP]\,[\Sigma Pi]} = \frac{[\Sigma DHAP]\,[\Sigma PYR]}{[\Sigma 3PG]\,[\Sigma LACT]} \times \frac{K_{G+G}}{K_{LDH} \times K_{TPI}}$$

$$\Delta G_{ATPHydr} = \Delta G^{O} + RT \ln \frac{[\Sigma ADP]\,[\Sigma Pi]}{[\Sigma ATP]}$$

$$\text{Mitochondrial } \frac{[NAD^{+}]}{[NADH]} = \frac{[\Sigma \alpha KG]\,[NH_3^{+}]\,[H^{+}]}{[\Sigma Glutamate] \times K_{GLDH}}$$

$$Eh_{NAD^{+}/NADH} = E^{O}_{NAD^{+}/NADH} + \frac{RT}{nF} \ln \frac{[NAD^{+}]}{[NADH]} \times \frac{10^{-7}}{[H^{+}]}$$

Figure 2. Calculation of cytosolic phosphorylation potential and mitochondrial energy parameters.

performed without inducing ischemia. After 30 minutes of reperfusion, the hearts were freeze-clamped, excess perfusate removed under liquid N_2, and the frozen tissue deproteinized with cold $HClO_4$ [4].

The myocardium obtained was dissolved in perchloric acid (PCA), and the tissue contents of ATP, phosphocreatine (PCr), DHAP, pyruvate, lactate, 3-phosphogly cerate (3-PG), glutamate, α-ketoglutarate, and ammonia were measured suing standard techniques of enzymatic analysis [4,5]. Total tissue bicarbonate and CO_2 content were estimated using phosphoenolpyruvate carboxylase (EC 4.1.1.31) [6]. The cytosolic phosphorylation potential, ΔGATP hydrolysis energy, mitochondrial redox state (NAD^+/NADH), and redox potential ($Eh_{NAD^+/NADH}$) were calculated from the various enzyme equilibriums (figure 2) [1]. We have already shown that ΔGATP hydrolysis energy is equal to mitochondrial membrane potential energy ($\Delta G_{QH^2/NAD^+}$), and that membrane potential energy can be calculated as the sum of the energy of the electrotransport chain ($\Delta G_{Q/QH^2}$) and the redox energy of NADH ($\Delta G_{NAD^+/NADH}$) (figure 3) [1]. We also calculated the energy of the electrotransport chain by using this formula.

RESULTS

Physiological parameters

The left ventricular (LV) peak positive *dP/dt* showed a significantly higher value in the Ke group than in the other two groups immediately after reperfusion. In the 10-minute period immediately after perfusion, this value was significantly lower in the K(−) group, by approximately 15%, compared with the control group. Moreover, when the LV peak positive *dp/dt* was compared before and after the ischemia, there

$$\Delta G_{ATPHydr} \doteq \Delta G_{QH_2 / NAD^+}$$

$$= \Delta G \text{ of } Q / QH_2 - NAD^+ / NADH$$

$$= -nF\,(Eh_{Q/QH_2} - Eh_{NAD^+/NADH})$$

Figure 3. Mitochondrial redox state. Findicates the Faraday constant: 96.458KJ/mol/V. *n* indicates sign and valence of the ion: $n = 2$.

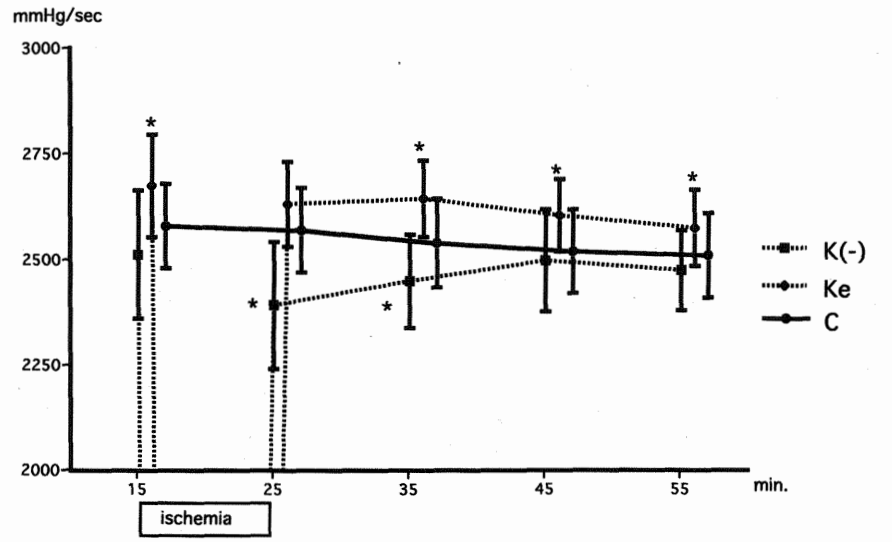

Figure 4. Left ventricular peak positive *dP/dt*. * indicates significant differences from control group ($p < 0.05$).

was a significant reduction in the K(−) group up to 10 minutes after ischemia compared to the value before ischemia; no difference in values before or after ischemia was observed in the Ke group (figure 4).

There were no significant differences in coronary flow between the three groups before ischemia, but in two groups, namely, the Ke and K(−) groups, the value was significantly increased, by approximately 10%, from the control group in the first minute of reperfusion. Furthermore, in the Ke group, an increase of approximately 15% in coronary flow, compared to the control group, continued through the 30-minute reperfusion period. When comparing the values before and after ischemia,

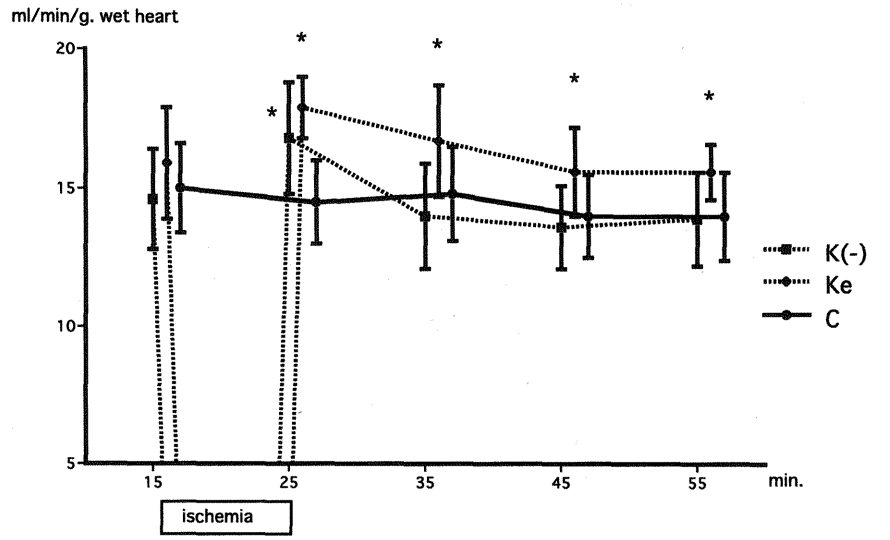

Figure 5. Coronary flow. * indicates significant differences from control group ($p < 0.05$).

the Ke and K(−) groups showed an approximately 10% increase in the first minute of reperfusion, compared to coronary flow before ischemia (figure 5).

Cardiac output was significantly greater in the Ke group than in the other two groups before ischemia. In the first minute of reperfusion, this value in the K(−) group decreased significantly, by approximately 40%, compared to that of the control group, but no significant difference was observed between the control group and the Ke group. However, there was no significant difference among the three groups in cardiac output after 10 minutes of reperfusion (figure 6).

In determinations of cardiac efficiency, the Ke group had significantly higher values than the other two groups, both before ischemia and after reperfusion. Only in the K(−) group was a significantly lower value found, approximately 15%, compared to the control group immediately after reperfusion (figure 7).

Intracellular metabolite concentrations

The pH and the ATP and α-ketoglutarate concentrations in the myocardial cells did not differ significantly among the three groups. Intracellular phosphocreatine (PCr) concentrations were 11.4 μmol/mL in the control group, 8.5 μmol/mL in the K(−) group, and 10.7 μmol/mL in the Ke group. This value in the K(−) group was significantly lower than that of the control group, but no such significant difference between the control group and the Ke group was found. Increases were seen in the K(−) group in DHAP, pyruvate, and glutamate concentratios,

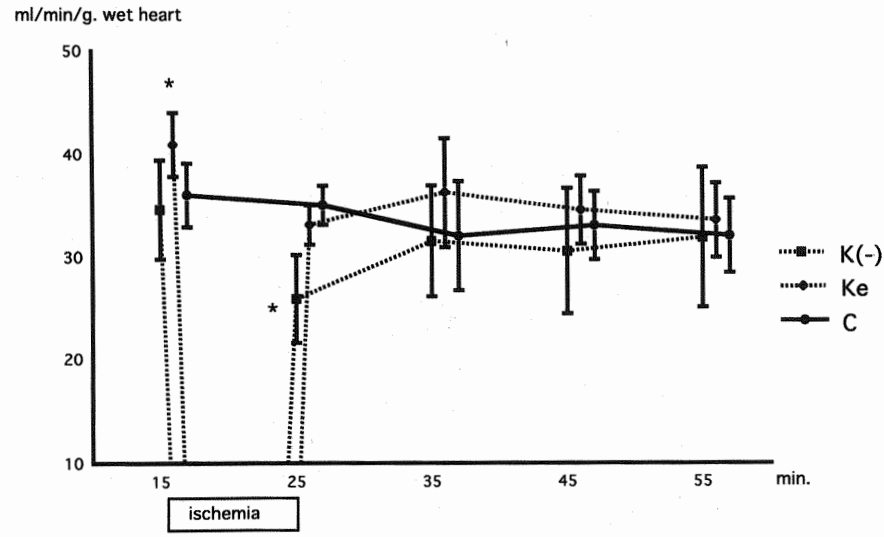

Figure 6. Cardiac output. * indicates significant differences from control group ($p < 0.05$).

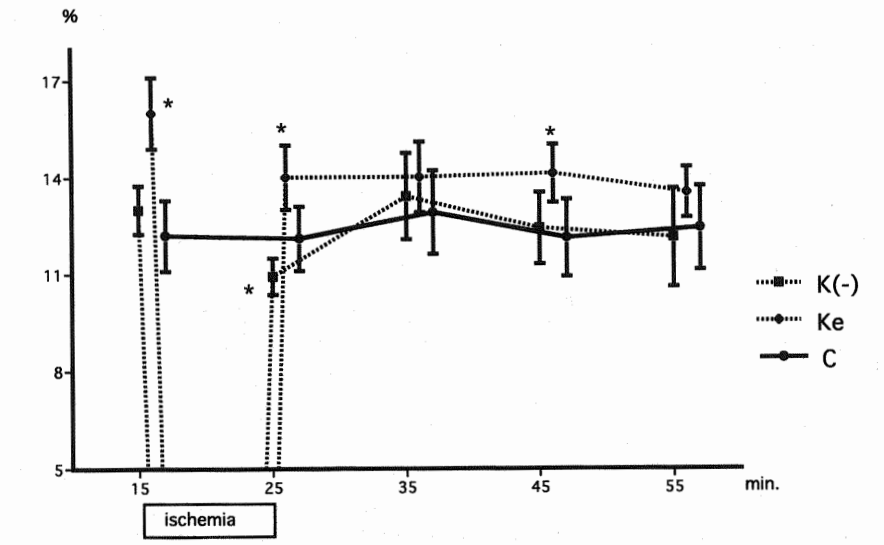

Figure 7. Cardiac efficiency. * indicates significant differences from control group ($p < 0.05$).

Table 1. Metabolites in working perfused rat hearts

	Control	K(−)	Ketone
pH	7.19 ± 0.29	7.17 ± 0.23	7.18 ± 0.25
ATP	8.92 ± 0.45	8.42 ± 0.51	8.88 ± 0.66
P-Cr	11.40 ± 1.05	8.51 ± 1.25[a]	10.70 ± 1.77
DHAP	0.055 ± 0.018	0.100 ± 0.011[a]	0.106 ± 0.030[a]
Pyruvate	0.059 ± 0.004	0.075 ± 0.003[a]	0.037 ± 0.012[a]
Lactate	1.09 ± 0.43	1.59 ± 0.45	0.85 ± 0.77[a]
3-PG	0.105 ± 0.007	0.055 ± 0.007[a]	0.081 ± 0.05[a]
Glutamate	3.28 ± 0.49	15.28 ± 0.89[a]	12.07 ± 0.18[a]
αKG	0.062 ± 0.007	0.053 ± 0.008	0.044 ± 0.004
Ammonia	0.301 ± 0.024	0.291 ± 0.025	0.630 ± 0.025[a]

[a] Significant differences from control group ($p < 0.05$).
Values are mean ± SD in mmol/mL of total intracellular water.

Table 2. Cytosolic phosphorylation potential and mitochondrial energy parameters

	Control	K(−)	Ketone
$\Delta G_{ATPHydr}$ (kJ/mol)	−56.4 ± 0.6	−56.0 ± 0.4	−58.2 ± 0.4[a]
$Eh_{NAD^+/NADH}$ (mV)	−280.8 ± 2.5	−291.1 ± 2.1[a]	−297.1 ± 3.2[a]
Eh_{Q/QH_2} (mV)	11.4 ± 0.9	1.1 ± 0.6[a]	5.4 ± 0.5[a]

[a] Significant differences from control group ($p < 0.05$).
Values are mean ± SD.

and the 3-phosphology cerate (3-PG) concentration was decreased. In the Ke group, increases were found in DHAP, glutamate, and ammonia concentrations, and decreases were found in pyruvate, lactate, and 3-PG concentrations (table 1).

Redox state

Cytosolic phosphorylation potential and mitochondrial energy parameters calculated from intracellular metabolite concentrations are shown in table 2. The ΔGATP hydrolysis energy was 56 kJ/mol in the control group, 56 kJ/mol in the K(−) group, and approximately 58 kJ/mol in the Ke group; the Ke group had a significantly higher value than the other two groups. The mitochondrial redox potential of NADH ($Eh_{NAD^+/NADH}$) was 280 mV in the control group, 291 mV in the K(−) group, and 297 mV in the Ke group; significantly higher values were observed in the K(−) and Ke groups. The mitochondrial electrotransport chain potential (Eh_{Q/QH^2}) was 11.4 mV in the control group, 1.1 mV in the K(−) group, and 5.4 mV in the Ke group; significantly lower values were shown in the K(−) and Ke groups.

DISCUSSION

The chemiosmotic hypothesis is widely considered to be the mechanism of oxidative phosphorylation in ATP synthesis in the mitochondria [7,8], i.e., the

mechanism by which the oxidation–reduction energy in the electrotransport chain is used in the phosphate bonding of ATP. However, many of the details of this oxidative phosphorylation mechaism are unknown. We have shown that the total mobilization energy of the cellular activity by which ATP synthase is able to produce ATP, i.e., ΔGATP hydrolysis energy, is equal to the mitochondrial membrane potential energy ($\Delta G_{QH^2/NAD^+}$), and that this membrane potential energy can be calculated as the sum of the energy of the electrotransport chain ($\Delta G_{Q/QH_2}$) and the redox energy of NADH ($\Delta G_{NAD^+/NADH}$) (figure 3) [1]. On the other hand, in the stunned myocardium resulting from acute ischemia, several factors contribute to mitochondrial respiration, and it has been reported that calcium receptivity and mitochondrial membrane permeability of ATP [9–12] are changed, but the details have not yet been elucidated.

In the present study, ΔGATP hydrolysis energy did not differ between the control group and the K(−) group, but this value was significantly higher in the K(+) group than in the others. This evidence is compatible with the findings, from the viewpoint of energy supply, that the physiological parameters in the K(−) group, in which the ischemia was provoked, were maintained at the same level as in the control group, and that the left ventricular contractility in the K(+) group was greater than in the others. On the other hand, the state of mitochondrial oxidation, which is a source of this energy supply, differed among the three groups. In the K(−) group, a reductive tendency in the energy utilization of the electrotransport chain ($\Delta G_{Q/QH_2}$) was recognized, and the NADH redox potential ($Eh_{NAD^+/NADH}$) was elevated in comparison with the others. In the Ke group, a reduction in the energy utilization was also confirmed, but this tendency was slighter than that in the K(−) group. Though the redox potential of NADH ($Eh_{NAD^+/NADH}$) indicated a higher value than in the other groups, the mitochondrial membrane potential remained at a high level. As previously reported, ketone bodies can supply electrons to succinyl CoA of the TCA cycle in the myocardium and incrase the redox potential of NADH ($Eh_{NAD^+/NADH}$) [1]. In the present ischemia plus reperfusion experiment, ketone bodies seemed to function as metabolic substrates and to contribute to stabilize the mitochondrial membrane potential. This result supports the hypothesis that the ketone bodies may work protectively for the myocardium against damage caused by ischemia and the following reperfusion injury, even in clinical medicine.

Through the present studies, we obtained the following conclusions:

1. Ketone bodies are able to augment cardiac performance in comparison with the control group after ischemia plus reperfusion.
2. Concerning metabolism, they increased the mitochondrial NADH redox potential and elevated mobilization energy.
3. Consequently, it is expected that, in myocardial ischemia, ketone bodies function as a substrate to produce mitochondrial energy, and through this function, they work protectively for the myocardium against both transient ischemia and the following reperfusion injury.

ACKNOWLEDGMENT

This work was partially funded by the Grants-in-Aid for Scientific Research from the Ministry of Education, Japan.

REFERENCES

1. Sato K, Kashiwaya Y, Keno CA, Tsuchiya N, King T, Radda GK, Chance B, Clark K, Veech RL. 1995. Insulin, ketone bodies, and mitochondrial energy transduction. FASEB J 9:651–658.
2. Smith EL, Hill RL, R, LJ, Handler P, White A. 1985. The ketone bodies and ketosis. In Principles of Biochemistry, vol. 7. New York: Mc-Graw-Hill, pp. 389–391.
3. Neely JR, Liebermeister H, Battersby EJ, Morgan HE. 1967. Effect of pressure development on oxygen consumption by isolated rat heart. Am J Physiol 212:804–814.
4. Masuda T, Dobson GP, Veech RL. 1990. The Gibbs–Donnan near-equilibrium system of heart. J Biol Chem 265:20321–20334.
5. Yoshihiro Kashiwaya, Kiyotaka Sato, Naotaka Tsuchiya, Todd King, Richard L. Veech, Janet Passoneau. 1994. Control of Glucose Utilization in Working Perfused Rat Heart. J Biol Chem 269:25502–25514.
6. Dobson GP, Veech RL, Hoeger U, Passonneau JV. 1991. Enzymatic determination of total CO_2 in freeze-clamped animal tissues and plasma. Anal Biochem 195:232–237.
7. Mitchell P. 1996. Chemiosmotic coupling in oxidative and photosynthetic phosphorylation. Biol Rev Cambridge Philosophic Soc 41:445–502.
8. Mitchell P, Moyle J. 1967. Chemiosmotic hypothesis of oxidative phosphorylation. Nature 213:137–139.
9. Xu KY, Zweier JL, Becker LC. 1995. Functional coupling between glycolysis and sarcoplasmic reticulum Ca^{2+} transport. Circ Res 77:88–97.
10. Tani M, Neely JR. 1989. Role of intracellular Na^+ in Ca^{2+} overload and depressed recovery of ventricular function of reperfused ischemic rat hearts. Possible involvement of H^+–Na^+ and Na^+–Ca^{2+} exchange. Circ Res 65:1045–1056.
11. Schaefer S, Carr LJ, Prussel E, Ramasamy R. 1995. Effects of glycogen depletion on ischemic injury in isolated rat hearts: insights into preconditioning. Am J Physiol 268:H935–H944.
12. de Albuquerque CP, Gerstenblith G, Weiss RG. 1994. Importance of metabolic inhibition and cellular pH in mediating preconditioning contractile and metabolic effects in rat hearts. Circ Res 74:139–150.

This Page Intentionally Left Blank

EFFECT OF BASIC FIBROBLAST GROWTH FACTOR ON THE REGIONAL MYOCARDIAL BLOOD FLOW OF ACUTELY INFARCTEDMYOCARDIUM IN EXPERIMENTAL ANIMALS

KINJI ISHIKAWA

Kinki University School of Medicine

Summary. Basic fibroblast growth factor (bFGF) was injected into the myocardium of acutely infarcted rats and dogs to elucidate any change of the regional myocardial blood flow for four weeks. The regional myocardial blood flow was increased at the infarcted myocardium and salvaged myocardium in dogs but not in rats. This study showed that the effect of bFGF in acutely infarcted myocardium has a species difference.

INTRODUCTION

Basic fibroblast growth factor (bFGF) is one of the potent growth factors that promote angiogenesis. Yanagisawa-Miwa et al. [1] reported in 1992 that bFGF caused a marked increase of capillaries and arterioles accompanied by a better left ventricular ejection fraction and a smaller infarct size in acutely infarcted dogs. Several attempts were made thereafter to augment neovascularization in the acutely infarcted myocardium with bFGF and to use bFGF to improve collateral supply and salvage myocardium in experimental animals. Most of these reports confirmed the Yanagisawa–Miwa finding [1] that bFGF promote angiogenesis [2–9] and limits infarct size [9,10] in dogs [4,8,9], pigs [2,3,5,6,10], and rabbits [11]. However, only a limited number of experiments were performed to measure the change of regional myocardial blood flow (Qm) at the infarcted myocardium elicited by bFGF [4,6,8,12–14]. Although several studies have confirmed an increased Qm at maximal vasodilatation induced by chromonar [4,8,12], only one report [6] showed an increased Qm at the resting state in the chronic myocardial ischemia. To elucidate the myocardial salvage by bFGF in an abrupt coronary occlusion model [1–3,9], the

S. Mochizuki, N. Takeda, M. Nagano and N. Dhalla (eds.). THE ISCHEMIC HEART.

Table 1 Experimental protocols and the results

Exp No.	Animal	bFGF Dose	bFGF Route	Infarct size	Regional myocardial flow
1	Dog	30 μg	intracoronary bolus	~	~
2	Dog	300 μg	intramyocardial shot	↓	↑↑
3	Rat	10 μg	iv 24hrs	~	~
4	Rat	100 μg	intramyocardial shot	~	~

~: no effect ↓: reduced ↑↑: increased markedly

substantial increase of Qm at the early phase of coronary occlusion must be clarified. The purpose of the study reported here was to elucidate whether there is any increase of Qm immediately after coronary occlusion in dogs and rats.

MATERIALS AND METHODS

Four experiments [13–16] were performed in dogs and rats, each with a different dosage of bFGF (table 1). All experiments were performed with open-chest animals under general anesthesia. The coronary artery was occluded by suture. All animals were maintained under normal conditions for four weeks thereafter. Recombinant human bFGF (Kaken Pharmaceutical Co., Tokyo, Japan) was used in these experiments.

Experiment 1 [13]

bFGF (30 μg) was injected as a bolus into the left circumflex artery after occlusion of the left anterior descending artery (LAD) in eight dogs (bFGF group), while in 11 dogs, bFGF was not injected (control group).

Experiment 2 [15]

In eight dogs, bFGF (300 μg) dissolved in 1.75 mL of physiological saline was injected in the midwall of the LAD area divided in five places, while saline was similarly injected in 12 dogs as a control. The LAD was occluded approximately one minute after these intramyocardial injections.

Experiment 3 [14]

In seven Sprague–Dawley (SD) rats, bFGF (10 μg) dissolved in 12 mL of physiological saline was continuously infused over 24 hours into the jugular vein initiated immediately after coronary occlusion, while in 12 SD rats, physiological saline alone was similarly infused as a control.

Experiment 4 [16]

In 11 SD rats, bFGF (10 μg) dissolved in 0.04 mL of physiological saline was injected into the myocardial wall of the occluded coronary artery divided in three places, while in 15 SD rats, physiological saline alone was similarly injected as a control.

Calculation of regional myocardial blood flow (Qm)

Nonradioactive colored microspheres [17] were injected in all dogs and rats at preocclusion, after occlusion and four weeks later to calculate the Qm. Qm was expressed as the percent of Qm at preocclusion, and this value was expressed as a ratio to the Qm value of normal noninfarcted myocardium (Qm % of noninfarcted) as follows:

$$\text{Qm}\left(\%\text{ of noninfarcted}\right) = \frac{\left[\text{Q/Q preocclusion}\right]\text{ infarcted}}{\left[\text{Q/Q preocclusion}\right]\text{ noninfarcted}} \times 100.$$

Histological analysis

A histological speciemen of each infarcted myocardium was photographed at ×100, and the amount of viable myocardium was assessed by a point-counting system [18] with a grid of 100 cross points. In a totally necrotic area, the myocardium score is near zero, and in normal myocardium, near 100. Using these photographs, the extent of fibrosis was scored visually as 0, 1, 2, 3, 4, 5, where 0 indicates fibrosis not present and 5 indicates all fibrotic.

Infarct size

In experiments 3 [14] and 4 [16], the rat heart was sliced at a thickness of 1 mm from base to apex. The total wall areas of the normal, infarcted, and border zones were measured to calculate infarct size.

RESULTS

The overview of the results of the four experiments is shown in table 1. In experiment 1 in dogs, the Qm at the infarcted myocardium showed no difference between the control and bFGF groups [13]. The amount of viable myocardium and extent of fibrosis at the infarcted myocardium also showed no difference between the two groups.

In experiment 2 [15], the Qm was remarkably decreased immediately (Five seconds) after coronary occlusion to 22 ± 3% (±SE) in the control group and to 14 ± 3% (% of noninfarcted) at the bFGF group at the inner layer (figure 1). The Qm at four weeks increased considerably in both groups, and the Qm in the bFGF group was significantly greater than that of the control group (control vs. bFGF: 39

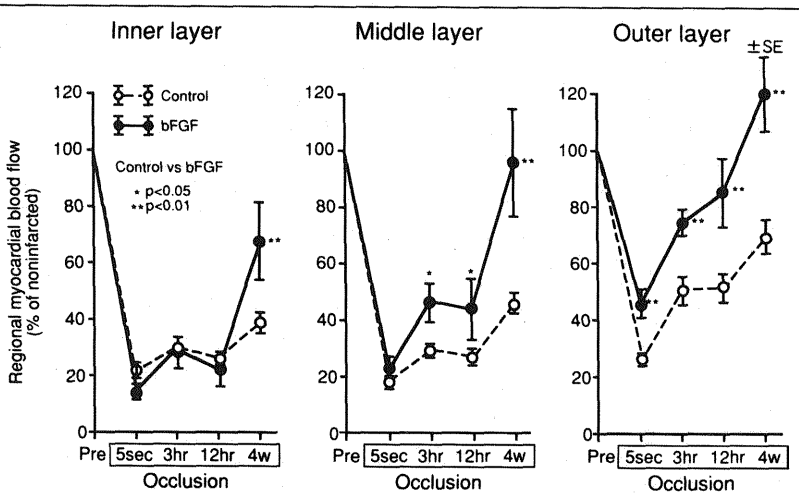

Figure 1. Increase of regional myocardial blood flow (Qm) at the infarcted myocardium by bFGF in experiment 2 [15].

± 4% vs. 68 ± 14%, $p < 0.01$) at the inner layer. At the middle layer, the Qm immediately after occlusion was not different between groups (control vs. bFGF: 18 ± 2% vs. 23 ± 4%). Three hours after occlusion, the Qm in the bFGF group was significantly greater than that of the control group. The Qm at four weeks was also significantly greater in the bFGF group (control vs. bFGF: 46 ± 4% vs. 96 ± 19%, $p < 0.01$). At the outer layer, the Qm immediately (five seconds) after occlusion was significantly greater in the bFGF group (control vs. bFGF: 26 ± 2% vs. 46 ± 5%, $p < 0.01$). This difference was maintained at four weeks (Qm at four weeks, control vs. bFGF: 70 ± 6% vs. 121 ± 13%, $p < 0.01$). The absolute value of the Qm four weeks after occlusion was slightly greater in the bFGF group, but this difference was not significant (Qm at the outer layer, control vs. bFGF: 1.30 ± 0.21 mL/min/g vs. 1.88 ± 0.34 mL/min/g). Figure 2 shows the amount of viable myocardium and the extent of fibrosis at the infarcted area in both groups. There was more abundant viable myocardium at the middle and outer layers and less fibrosis at all three layers in the bFGF group than in the control group.

In the two experiments using rats [14,16], the Qm at the infarcted myocardium and at the border zone showed no difference between the control and bFGF groups. The myocardium score and extent of fibrosis showed no group differences in either experiment. The infarct size was not significantly different between the control and bFGF groups in experiments 3 [14] and 4 [16] (experiment 3: control vs. bFGF 18.6 ± 6.5% vs. 19.2 ± 9.3%; experiment 4: control vs. bFGF 19.1 ± 1.8% vs. 17.5 ± 2.6%).

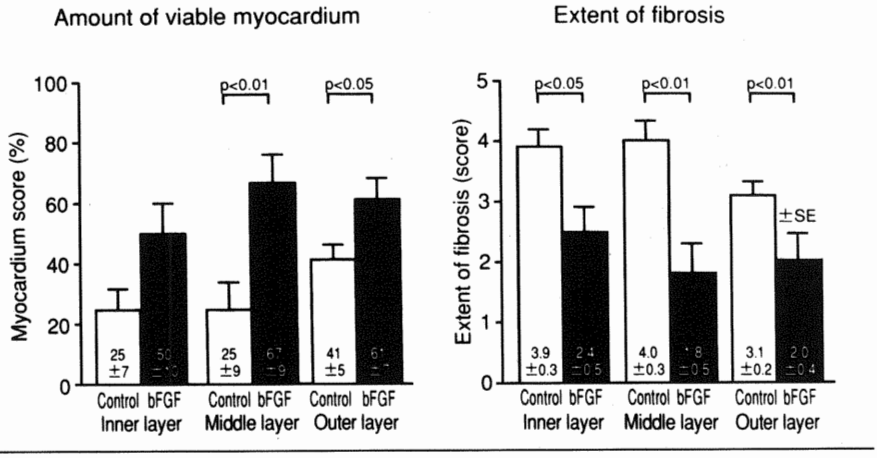

Figure 2. The amount of viable myocardium and the extent of fibrosis at the infarcted area in experiment 2 [15].

DISCUSSION

Increases of Qm immediately after and at four weeks at the infarcted myocardium were observed in the bFGF-treated dogs in experiment 2 [15]. This increase in Qm caused by the intramyocardial injection of bFGF might explain the observed increase of viable myocardium and reduction of fibrosis at the infarcted area in the bFGF group.

Experiment 2 [15] is unique in that the Qm increased immediately (five seconds) after coronary occlusion in dogs. The acute effects of bFGF administration have been studied [4,8,19], and vasodilator hypotensive effects were demonstrated [4,8,19]. Unger et al. [4] observed an 80% increase in coronary blood flow at the nonischemic myocardium following an intracoronary injection of bFGF (110 μg), reaching a maximal effect eight minutes after administration and declining to baseline after 2.5 hours. The present experiment 2 [15] showed that bFGF elicited an acute coronary flow increase by vasodilator effect at the occluded area. The significant increase in Qm four weeks after occlusion in experiment 2 may correspond to the increased neovascularization by bFGF.

Another new finding of experiment 2 [15] is that the Qm at resting state was increased by bFGF. Many investigators have studied Qm days or weeks after coronary occlusion and found an increase of maximal Qm following maximal coronary vasodilatation induced by chromonar [4,8,12] or by pacing [10]. In the present study, the Qm four weeks after coronary occlusion was increased by bFGF at the resting state. The present finding coincides with that of Lopez et al. [6], who reported that the Qm was higher at rest in bFGF-treated pigs.

In our experiment 1 [13], the Qm was not increased in the bFGF group when bFGF (30 μg) was injected as a bolus into the contralateral coronary artery in dogs, while in experiment 2 [15], bFGF (300 μg) was injected into the myocardial wall. Lopez et al. [6] injected bFGF intramyocardially at 10 μg or 100 μg and found a dose-related increase in the Qm. The dosage in our experiment 1 [13] may not have been sufficient to increase the Qm.

In the two present rat experiments, bFGF caused no change in the Qm nor did it salvage myocardium. Recombinant human bFGF has been shown to exert angiogenic effects on hind limb [20], mesentric-window assay [21], aortic smooth muscle [22], and cerebral cortex [23] in rats. It was reported that bFGF causes angiogenic effect on these tissues but may not on rat hearts, where native collaterals are scanty [24]. However, this suggestion may not be accurate, because bFGF caused angiogenic effects in pigs [3,5,6], where the native collaterals are less than in rats [24]. All the experiments reported in pigs used an ameroid constrictor to cause gradual coronary occlusion [3,5,6]. bFGF may exert an angiogenic action provided that the coronary artery is occluded gradually by ameroid in animals with poor collaterals. A model with gradual coronary occlusion may be necessary to elucidate the effects of bFGF in rat hearts.

The present study showed a considerable increase of the Qm in experiment 2 [15] accompanied by remarkable myocardial salvage at the infarcted area in bFGF-treated dogs. It is important to establish whether the increase in the Qm is enough to explain the myocardial salvage. Reimer et al. [25] studied the effect of complete reperfusion on myocardial salvage by the removal of ligated sutures. They concluded that the average effect of reperfusion in dogs is to limit the transmural extent of the infarct by about 40% at 90 minutes and 10% to 35% at three hours. It is questionable whether a partial increase and not the complete normalization of the Qm in the present bFGF group might have produced such a great increase of viable myocardium and reduction of fibrosis at the infarcted area. Furthermore, at the inner or middle layers where increases of the Qm are less prominent compared with the outer layer, there were considerable increases of viable myocardium and reductions of fibrosis (figure 2). These results indicate that the increase of the Qm immediately after occlusion seen at the outer layer may play a part in the salvage of myocardium, but at the same time, another mechanism to salvage myocardium must be present. Uchida et al. [9] suggested that bFGF may provide direct myocyte protection against ischemia in the salvage of infarcted myocardium. Araki et al. [26] demonstrated that the removal of FGF from the medium of human umbilical vein endothelial cells in culture resulted in the death of the cells. They concluded that the process of active death of vascular endothelial cells is inhibited by growth factor. Yamada et al. [27] studied the atrophic changes of the thalamus in a focal infarction model in rats. They demonstrated that an intracisternal injection of bFGF prevented retrograde degeneration of thalamic neurons. Other studies [28,29] indicated that bFGF support the survival of central neurons in vitro. MacMillan et al. [30] studied necrosis of CA1 pyramidal neurons by carotid artery occlusion in the gerbil and reported that an intraventricular infusion of acidic FGF resulted in the attenuation of the severity of

ischemic neuronal necrosis. These studies suggest that bFGF has the ability to prolong cell survival under hypoxic or ischemic conditions [10,31], and this may be another mechanism by which bFGF salvages myocardium.

In conclusion, the present experiments demonstrated that bFGF, when given in a sufficient dose in an appropriate acute infarction model, increases regional myocardial blood flow by direct vasodilator action immediately after occlusion and gradually protects ischemic myocardium by angiogenesis.

ACKNOWLEDGMENT

This study was supported in part by a Grant-in-Aid for Scientific Research from the Ministry of Education, Science and Culture, Japan.

REFERENCES

1. Yanagisawa-Miwa A, Uchida Y, Nakamura F, Tomaru T, Kido H, Kamijo T, Sugimoto T, Kaji K, Utsuyama M, Kurashima C, Ito H. 1992. Salvage of infarcted myocardium by angiogenic action of basic fibroblast growth factor. Science 257:1401–1403.
2. Banai S, Shou M, Jaklitsch MT, Ferrara N, Epstein SE, Unger EF. 1992. Enhancement of coronary collateral blood flow by intracoronary injection of vascular endothelial growth factor (abstract). J Am Coll Cardiol 19:191A.
3. Battler A, Scheinowitz M, Bor A, Hasdai D, Vered Z, Segni ED, Varda-Bloom N, Nass D, Engelberg S, Eldar M, Belkin M, Savion N. 1993. Intracoronary injection of basic fibroblast growth factor enhances angiogenesis in infarcted swine myocardium. J Am Coll Cardiol 22:2001–2006.
4. Unger EF, Banai S, Shou M, Lazarous DF, Jaklitsch MT, Scheinowitz M, Correa R, Klingbell C, Epstein SE. 1994. Basic fibroblast growth factor enhances myocardial collateral flow in a canine model. Am J Physiol 266:H1588–H1595.
5. Sellke FW, Wang SY, Friedman M, Harada K, Edelman ER, Grossman W, Simons M. 1994. Basic FGF enhances endothelium-dependent relaxation of the collateral-perfused coronary microcirculation. Am J Physiol 267:H1303–H1311.
6. Lopez JJ, Starebier A, Edelman ER, Hibberd MG, Caputo RP, Carrozza JP, Prasad PV, Douglas PS, Sellke FW, Simons M. 1995. Local bFGF treatment results in angiographic collateral development, dose related increase in coronary flow and myocardial function in chronic myocardial ischemia (abstract),. Circulation 92(Suppl I):I–67.
7. Barrios V, Cuevas B, Carceller F, Asin E, Jiménez JJ, Navarro J, Garcia-Segovia J, Moya JL, Minguez I, Cuevas P. 1995. Angiogenesis in the rat heart induced by local delivery of basic fibroblast growth factor. Eur Heart J 16(Suppl):171.
8. Lazarous DF, Scheinowitz M, Shou M, Hodge E, Rajanayagam S, Hunsberger S, Robison WG Jr., Stiber JA, Correa R, Epstein SE, Unger EF. 1995. Effects of chronic systemic administration of basic fibroblast growth factor on collateral development in the canine heart. Circulation 91:145–153.
9. Uchida Y, Yanagisawa-Miwa A, Nakamura F, Yamada K, Tomaru T, Kimura K, Morita T. 1995. Angiogenic therapy of acute myocardial infarction by intrapericardial injection of basic fibroblast growth factor and heparin sulfate: an experimental study. Am Heart J 130:1182–1188.
10. Harada K, Grossman W, Friedman M, Edelman ER, Prasad PV, Keighley CS, Manning WJ, Sellke FW, Simons M. 1994. Basic fibroblast growth factor improves myocardial function in chronically ischemic porcine hearts. J Clin Invest 94:623–630.
11. Landau C, Jacobs AK, Haudenschild CC. 1995. Intrapericardial basic fibroblast growth factor induces myocardial angiogenesis in a rabbit model of chronic ischemia. Am Heart J 129:924–931.
12. Lazarous DF, Shou M, Scheinowitz M, Hodge E, Thirumurti V, Kitsiou AN, Stiber JA, Lobo AD, Hunsberger S, Guetta E, Epstein SE, Unger EF. 1996. Comparative effects of basic fibroblast growth factor and vascular endothelial growth factor on coronary collateral development and the arterial response to injury. Circulation 94:1074–1082.
13. Miyataka M, Ishikawa K, Ogawa I, Koka H, Nakai S, Kino H, Inagaki M, Kimura A, Katori R. 1996. Contralateral arterial bolus injection of 30 micrograms of basic fibroblast growth factor failed

to augment myocardial blood flow in infarcted myocardium in dogs. Acta Med Kinki Univ 21:53–58.
14. Inagaki M, Ishikawa K, Ogawa I, Koka H, Nakai S, Kino H, Kimura A, Miyataka M, Katori R. 1996. Regional blood flow in infarcted myocardium of basic fibroblast growth factor-treated rats. Acta Med Kinki Univ 21:59–63.
15. Miyataka M, Ishikawa K, Ogawa I, Koka H, Nakai S, Kino H, Inagaki M, Kimura A, Hasegawa T, Kitayama K, Katori R. 1996. Intramyocardial injection of basic fibroblast growth factor (bFGF) at infarcted myocardium increased regional myocardial blood flow and salvaged myocardium in dogs (abstract). J Mol Cell Cardiol 28:A320.
16. Inagaki M, Ishikawa K, Ogawa I, Koka H, Nakai S, Kino H, Kimura A, Miyataka M, Hasegawa T, Kitayama K, Katori R. 1996. Effect of basic fibroblast growth factor on the regional myocardial blood flow of the acutely infarcted myocardium in rats (abstract). J Mol Cell Cardiol 28:A320.
17. Ishikawa K, Kamata N, Nakai S, Akiyama H, Koka H, Ogawa I, Katori R. 1994. Preservation of high regional blood flow at epicardial rim after coronary occlusion in dogs. Am J Physiol 267:H528–H534.
18. Baandrup U, Olsen EGJ. 1981. Critical analysis of endomyocardial biopsies from patients suspected of having cardiomyopathy. I: Morphological and morphometric aspects. Br Heart J 45:475–486.
19. Cuevas P, Carceller F, Ortega S, Zazo M, Nieto I, Giménez-Gallego G. 1991. Hypotensive activity of fibroblast growth factor. Science 254:1208–1210.
20. Chleboun JO, Martins RN, Mitchell CA, Chirila TV. 1992. bFGF enhances the development of the collateral circulation after acute arterial occlusion. Biochem Biophys Res Commun 185:510–516.
21. Norrby K. 1994. Basic fibroblast growth factor and de novo mammalian angiogenesis. Microvasc Res 48:96–113.
22. van Neck JW, Medina JJ, Onnekink C, van der Ven PFM, Bloemers HPJ, Schwartz SM. 1993. Basic fibroblast growth factor has a differential effect on myoD conversion of cultured aortic smooth muscle cells from newborn and adult rats. Am J Pathol 143:269–282.
23. Cuevas P, Giménez-Gallego G, Carceller F, Cuevas B, Crespo A. 1993. Single topical application of human recombinant basic fibroblast growth factor (rbFGF) promotes neovascularization in rat cerebral cortex. Surg Neurol 39:380–384.
24. Maxwell MP, Hearse DJ, Yellon DM. 1987. Species variation in the coronary collateral circulation during regional myocardial ischaemia: a critical determinant of the rate of evolution and extent of myocardial infarction. Cardiovasc Res 21:737–746.
25. Reimer KA, Heide RSV, Richard VJ. 1993. Reperfusion in acute myocardial infarction: effect of timing and modulating factors in experimental models. Am J Cardiol 72:13G–21G.
26. Araki S, Shimada Y, Kaji K, Hayashi H. 1990. Apoptosis of vascular endothelial cells by fibroblast growth factor deprivation. Biochem Biophys Res Commun 168:1194–1200.
27. Yamada K, Kinoshita A, Kohmura E, Sakaguchi T, Taguchi J, Kataoka K, Hayakawa T. 1991. Basic fibroblast growth factor prevents thalamic degeneration after cortical infarction. J Cereb Blood Flow Metab 11:472–478.
28. Morrison RS, Sharma R, DeVellis J, Bradshaw RA. 1986. Basic fibroblast growth factor supports the survival of cerebral cortical neurons in primary culture. Proc Natl Acad Sci USA 83:7537–7541.
29. Walicke PA. 1988. Basic and acidic fibroblast growth factor have trophic effects on neurons from multiple CNS regions. J Neurosci 8:2618–2627.
30. MacMillan V, Walton-Roche K, Davis J. 1993. Acidic fibroblast growth factor infusion reduces ischemic CA1 hippocampal damage in the gerbil. Can J Neurol Sci 20:37–40.
31. Casscells W. 1995. Growth factor therapies for vascular injury and ischemia. Circulation 91:2699–2702.

INTRAMYOCARDIAL INJECTION OF BASIC FIBROBLAST GROWTH FACTOR INCREASED REGIONAL MYOCARDIAL BLOOD FLOW ANDSALVAGED INFARCTED MYOCARDIUM IN DOGS

MASARU MIYATAKA, KINJI ISHIKAWA, IWAO OGAWA, HIRONARI KOKA,SHOJI NAKAI, HIROFUMI KINO, MASAHIKO INAGAKI, AKIO KIMURA, TAKAYA HASEGAWA, KOJI KITAYAMA, and RYO KATORI

Kinki University School of Medicine

Summary. We studied whether basic fibroblast growth factor (bFGF) might increase regional Myocardial blood flow (Qm) at the infarcted myocardium. In eight dogs, bFGF 300 μg was injected into the myocardium supplied by the left anterior descending coronary artery (LAD), and the artery was ligated. In 12 dogs, saline was injected (control group). Nonradioactive colored microspheres were used to determine Qm. The amount of viable myocardium and the extent of fibrosis in the infarcted area four weeks after occlusion were measured histologically. In the outer layer, the Qm values immediately after and four weeks after occlusion were 26 ± 2% and 70 ± 6%, respectively, in the control group, and 46 ± 5% and 121 ± 13%, respectively, in the bFGF group. The Qm at both times in the bFGF group was significantly higher than the corresponding control group values ($p < 0.01$). The Qm at four weeks in the inner and middle layers also significantly increased in the bFGF group. There was more viable myocardium (control vs. bFGF group: 41 ± 5% vs. 61 ± 7%, $p < 0.05$) and less fibrosis (3.1 ± 0.2 vs. 2.0 ± 0.4, $p < 0.01$) at the outer layer in the bFGF group. bFGF caused a marked increase of the Qm, an increase of viable myocardium, and a decrease of fibrosis at the infarcted myocardium. We conclude bFGF was effective in limiting infarct size in acute myocardial infarction.

INTRODUCTION

In 1992, Yanagisawa-Miwa et al. [1] performed a provocative study in dogs showing that basic fibroblast growth factor (bFGF) 10 μg injected into the circumflex coronary artery twice after ligation of the left anterior descending coronary artery (LAD) reduced the myocardial infarct size, preserved good left ventricular function, and promoted abundant collateral development. Although they did not measure the

S. Mochizuki, N. Takeda, M. Nagano and N. Dhalla (eds.). THE ISCHEMIC HEART.

regional myocardial blood flow (Qm) at the infarcted myocardium, their results suggested that bFGF can be a useful therapeutic measure to augment the myocardial supply in coronary artery disease. Several investigators measured Qm at the infarcted myocardium treated by bFGF [2–4], and some reported an increased response of Qm [2,3], while others reported that the duration of this increase was limited (to four weeks) [4]. In the study reported here, we clarify the effect of bFGF on the Qm and provide a brief review of the effect of bFGF on acutely ischemic myocardium in experimental animals.

MATERIALS AND METHODS

The details of this study will be presented in a separate paper. Briefly, the LAD of dogs was occluded by suture. In the bFGF group, human recombinant bFGF (Kaken Pharmaceutical Co., Tokyo, Japan) dissolved in 1.75 mL of physiological saline was injected in the LAD area in eight dogs, while saline was similarly injected in 12 dogs as a control. The LAD was occluded approximately one minute after these intramyocardial injections. The dogs were maintained as usual for four weeks. To measure the Qm, nonradioactive colored microspheres were injected into the left atrium [5].

After sacrifice of the dogs by pentobarbital, the myocardium surrounded by the LAD and second diagonal artery was removed to calculate the Qm and for histological analysis. The Qm was expressed as a ratio to the value of normal noninfarcted myocardium (Qm; % of noninfarcted) as an index of myocardial blood flow as follows:

$$Q_m = [Q/Q \text{ preocclusion}]\text{infarcted}/[Q/Q \text{ preocclusion}]\text{ noninfarcted} \times 100\ (\%)$$

Histological specimens of the infarcted myocardium were photographed at ×100, the amount of viable myocardium was counted with a point-counting system with a grid of 100 cross points. In totally necrotic areas, the myocardium score is near zero, and in normal myocardium near 100. Using these photographs, the extent of fibrosis was scored visually as 0, 1, 2, 3, 4, or 5, where 0 indicates fibrosis not present and 5 indicates all fibrosis.

RESULTS

The results will be presented in detail in the separate paper. Briefly, the Qm was markedly reduced immediately (five seconds) after coronary occlusion, especially at the inner layer, in both groups (figure 1). At the outer layer, the Qm immediately after occlusion in the bFGF group was approximately twice the value of the control group. The Qm at four weeks in the bFGF group was significantly greater than in the control group (figure 1). Myocardial fibrosis was significantly less in the bFGF group than in the control group at all three layers (figure 2). The amount of viable myocardium (myocardium score) was significantly greater in the bFGF group compared with the control group at the middle and outer layers (figure 2).

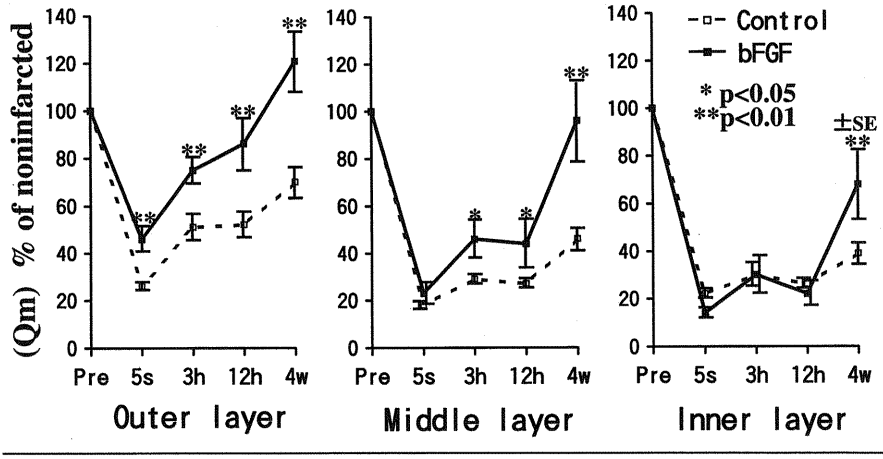

Figure 1. Changes in the regional myocardial blood flow (Qm) after coronary occlusion at the infarcted myocardium in the control and bFGF groups. bFGF: basic fibroblast growth factor.

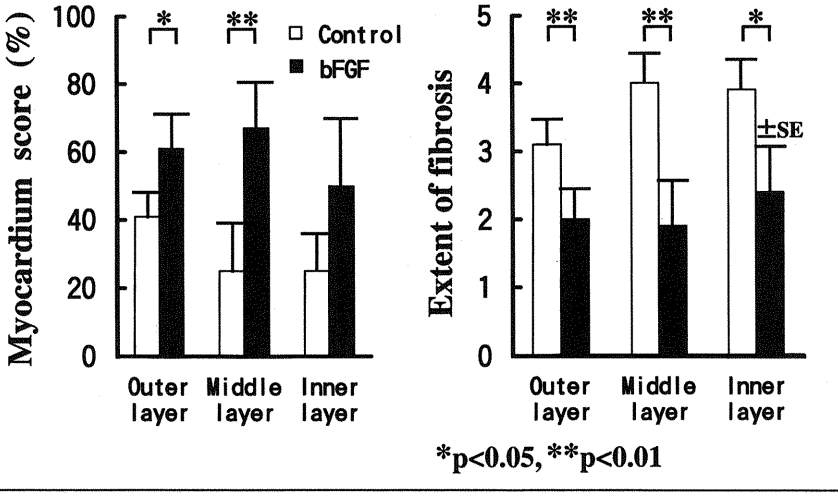

Figure 2. The amount of viable myocardium and the extent of fibrosis at the infarcted myocardium in the two groups.

DISCUSSION

We injected human recombinant bFGF into the myocardium just prior to coronary occlusion in dogs and found that the regional myocardial blood flow (Qm) at the infarcted myocardium after coronary occlusion was significantly greater than that of control (saline-injected) dogs. The extent of fibrosis was reduced and the amount of viable myocardium was more abundant in the infarcted myocardium of the bFGF group, indicating that bFGF effectively reduced the infarct size.

The angiogenic action of bFGF has been studied extensively in dogs [1,2,4,6–8], pigs [3,9–11], rabbits [12], and rats [13] using angiography [1,6,12], microscopy [4,6,9,11,12], and flow measurements by microsphere techniques [3,4,7,8,10,13]. Our previous study in dogs [8] failed to show any increase of Qm by 30 μg bFGF injected intracoronarily. In the present study, we used a larger dose and found a significant increase in Qm. Some studies have reported no increase of microvessels after the direct application of acidic FGF in dogs [14]. However, many studies found a profound increase of microvessels after the application of bFGF, especially at the outer layers in dogs [6] or rabbits [12], or at the border zone in dogs [1]. In contrast, the present study revealed a uniform increase in the Qm at the inner, middle, and outer layers four weeks after coronary occlusion.

In the present study, we injected bFGF in a single dose at the middle layer of the infarcted area. The distribution and deposition of exogenous bFGF in a single dose have been well studied. bFGF administered into the perivascular space is distributed in the extravascular space without transendothelial transport and binds to the basement membrane and heparan sulfate proteoglycan complexes in the intercellular matrix; such bound bFGF could act as a reservoir for the slow release of bFGF [15]. Unger et al. [2] injected a daily dose of bFGF (110 μg) intracoronarily into the collateral-dependent zone for 28 days in dogs with ameroid constrictors on the left circumflex coronary artery. They measured Qm as a ratio to the normal zone during maximal coronary vasodilation and found a significant increase of this ratio at the epicardium as well as endocardium. A subsequent study performed in their laboratory [4] showed that an increase of the flow ratio during maximal coronary vasodilation persisted for three weeks after the left atrial injection of bFGF. At four weeks, control dogs showed a similar response of flow, and no significant difference was present between bFGF-treated and control dogs. In our abrupt coronary occlusion intramyocardial bFGF injection model, the Qm exceeded that of control dogs at the resting level. This change is consistent with the report by Lopez et al. [3] of Qm values of 0.59 ± 0.09 in the control and 1.01 ± 0.13 mL/min/g in bFGF-treated pigs at rest. These increases might correspond to the marked increase of microvessels in bFGF-treated animals [1,4,6,9,11,12].

Yanagisawa-Miwa et al. [1] reported that the ratio of infarct weight to left ventricular wall weight was reduced from 19.9 ± 2.4% to 5.5 ± 1.4% by bFGF. Their subsequent study [6] showed an infarct weight reduced from 24 ± 5.2% to 10 ± 1.8%. Harada et al. [10] also found a fourfold reduction in the left ventricular infarct size in bFGF-treated ameroid-constrictor pigs. In the present study, the extent of fibrosis was reduced markedly in all three layers in the infarcted myocardium. Viable myocardium in the infarcted myocardium also showed a marked increase by bFGF treatment. These changes are compatible with the previous reports in dogs [1,6] and pigs [10].

The change of Qm early after coronary occlusion is particularly important in the understanding of myocardial salvage [16]. bFGF has vasodilatory hypotensive effects that are mediated, in part, through the activation of nitric oxide synthase (NOS) and the subsequent generation of NO [17]. A bolus injection of bFGF into the circum-

flex coronary artery elicited an 80% increase in coronary flow, reaching a maximal effect eight minutes after the administration and declining to baseline after 2.5 hours [2]. This finding may well explain the present significant increase of Qm at five seconds after occlusion at the outer layer and at three hours after occlusion at the middle and outer layers. These immediate increases in Qm produced by bFGF might explain the marked reduction in infarct size in the present study. However, it is difficult to explain the marked myocardial salvage in the bFGF group by partial normalization of the Qm early after infarction in this group. This finding indicates that the beneficial effect observed is partially attributed to a flow increase produced by bFGF; however, at the same time, another mechanism to salvage myocardium by bFGF must be present.

Uchida et al. raised three possibilities for this mechanism: increased flow through the native artery, opening of latent collateral vessels by its vasodilating effect, and direct myocyte protection against ischemia [6]. Casscells summarized the recently proposed concepts regarding growth factor therapies for ischemia, noting the ability of bFGF to prolong cell survival under hypoxic or ischemic conditions [18]. These biological effects on myocytes elicited by bFGF may also contribute to the reduction of myocardial infarct size.

CONCLUSION

This study showed that bFGF increased the regional myocardial blood flow (Qm) and reduced infarct size. The limitation of infarct size might be due to augmented myocardial flow and cellular protection elicited by bFGF.

REFERENCES

1. Yanagisawa-Miwa A, Uchida Y, Nakamura F, Tomaru T, Kido H, Kamijo T, Sugimoto T, Kaji K, Utsuyama M, Kurashima C, Ito H. 1992. Salvage of infarcted myocardium by angiogenic action of basic fibroblast growth factor. Science 257:1401–1403.
2. Unger EF, Banai S, Shou M, Lazarous DF, Jaklitsch MT, Scheinowitz M, Correa R, Klingbeil C, Epstein SE. 1994. Basic fibroblast growth factor enhances myocardial collateral flow in a canine model. Am J Physiol 266:H1588–H1595.
3. Lopez JJ, Starebier A, Edelman ER, Hibberd MG, Caputo RP, Carrozza JP, Prasad PV, Douglas PS, Sellke FW, Simons M. 1995. Local bFGF treatment results in angiographic collateral development, dose related increase in coronary flow and myocardial function in chronic myocardial ischemia (abstract). Circulation 92:I-67.
4. Lazarous DF, Scheinowitz M, Shou M, Hodge E, Rajanayagam MAS, Hunsberger S, Robison WG Jr, Stiber JA, Correa R, Epstein SE, Unger EF. 1995. Effects of chronic systemic administration of basic fibroblast growth factor on collateral development in the canine heart. Circulation 91:145–153.
5. Ishikawa K, Kamata N, Nakai S, Akiyama H, Koka H, Ogawa I, Katori R. 1994. Preservation of high regional blood flow at epicardial rim after coronary occlusion in dogs. Am J Physiol 267:H528–H534.
6. Uchida Y, Yanagisawa-Miwa A, Nakamura F, Yamada K, Tomaru T, Kimura K, Morita T. 1995. Angiogenic therapy of acute myocardial infarction by intrapericardial injection of basic fibroblast growth factor and heparin sulfate: An experimental study. Am Heart J 130:1182–1188.
7. Unger EF, Banai S, Shou M, Jaklitsch MT, Epstein SE. 1991. Intracoronary injection of basic fibroblast growth factor enhances collateral blood flow in the canine myocardium (abstract). Circulation 84:II-96.
8. Miyataka M, Ishikawa K, Ogawa I, Koka H, Nakai S, Kino H, Inagaki M, Kimura A, Katori R. 1996. Contralateral arterial bolus injection of 30 micrograms of basic fibroblast growth factor failed

to augment myocardial blood flow in infarcted myocardium in dogs. Acta Med Kinki Univ 21:53–58.
9. Battler A, Scheinowitz M, Bor A, Hasdai D, Vered Z, Di Segni E, Varda-Bloom N, Nass D, Engelberg S, Eldar M, Belkin M, Savion N. 1993. Intracoronary injection of basic fibroblast growth factor enhances angiogenesis in infarcted swine myocardium. J Am Coll Cardiol 22:2001–2006.
10. Harada K, Grossman W, Friedman M, Edelman ER, Prasad PV, Keighley CS, Manning WJ, Sellke FW, Simons M. 1994. Basic fibroblast growth factor improves myocardial function in chronically ischemic porcine hearts. J Clin Invest 94:623–630.
11. Sellke FW, Wang SY, Friedman M, Harada K, Edelman ER, Grossman W, Simons M. 1994. Basic FGF enhances endothelium-dependent relaxation of the collateral-perfused coronary microcirculation. Am J Physiol 267:H1303–H1311.
12. Landau C, Jacobs AK, Haudenschild CC. 1995. Intrapericardial basic fibroblast growth factor induces myocardial angiogenesis in a rabbit model of chronic ischemia. Am Heart J 129:924–931.
13. Inagaki M, Ishikawa K, Ogawa I, Koka H, Nakai S, Kino H, Kimura A, Miyataka M, Katori R. 1996. Regional blood flow in infarcted myocardium of basic fibroblast growth factor-treated rats. Acta Med Kinki Univ 21:59–63.
14. Banai S, Jaklitsch MT, Casscells W, Shou M, Shrivastav S, Correa R, Epstein SE, Unger EF. 1991. Effects of acidic fibroblast growth factor on normal and ischemic myocardium. Circ Res 69:76–85.
15. Edelman ER, Nugent MA, Karnovsky MJ. 1993. Perivascular and intravenous administration of basic fibroblast growth factor: Vascular and solid organ deposition. Proc Natl Acad Sci USA 90:1513–1517.
16. Reimer KA, Lowe JE, Rasmussen MM, Jennings RB. 1977. The wavefront phenomenon of ischemic cell death. 1. Myocardial infarct size vs duration of coronary occlusion in dogs. Circulation 56:786–793.
17. Kostyk SK, Kourembanas S, Wheeler EL, Medeiros D, McQuillan LP, D'Amore PA, Braunhut SJ. 1995. Basic fibroblast growth factor increases nitric oxide synthase production in bovine endothelial cells. Am J Physiol 269:H1583–H1589.
18. Casscells W. 1995. Growth factor therapies for vascular injury and ischemia. Circulation 91:2699–2702.

EFFECT OF BASIC FIBROBLAST GROWTH FACTOR ON THE REGIONAL MYOCARDIAL BLOOD FLOW IN ACUTELY INFARCTED MYOCARDIUM IN RATS

MASAHIKO INAGAKI, KINJI ISHIKAWA, IWAO OGAWA, AKIO KIMURA, MASARU MIYATAKA, TAKAYA HASEGAWA, KOJI KITAYAMA, and RYO KATORI

Osaka University Medical School

Summary. This study showed that intramyocardial injection of basic fibroblast growth factor (bFGF) 100 μg neither enhances angiogenesis nor salvages myocardium in the acutely infarcted myocardium in rats. Although enhanced angiogenesis and myocardial salvage by bFGF has been shown in dogs and pigs, further experimental studies are necessary before applying bFGF in clinical practice.

INTRODUCTION

Basic fibroblast growth factor (bFGF) is one of the potent growth factors promoting angiogenesis [1]. Yanagisawa-Miwa et al. [2] reported that bFGF given to dogs with acutely infarcted myocardium promoted angiogenesis in the infarcted myocardium, preserved better left ventricular function, and limited the infarct size. Since dogs have abundant native collaterals, bFGF may exert significant effects on angiogenesis, increased regional myocardial blood flow, and limited infarct size. The human heart has fewer native collaterals than dogs. Therefore, the effect of bFGF must be evaluated in experimental animals with fewer native collaterals. The present study measured regional myocardial blood flow (Qm) of the infarcted myocardium and investigated whether bFGF increased Qm and limited infarct size in rats, where native collaterals are known to be scanty [3].

MATERIALS AND METHODS

The study protocol was almost the same as that used in our previous report [4], except that in the present study, bFGF 100 μg dissolved in 0.04 mL of saline was

S. Mochizuki, N. Takeda, M. Nagano and N. Dhalla (eds.). THE ISCHEMIC HEART.

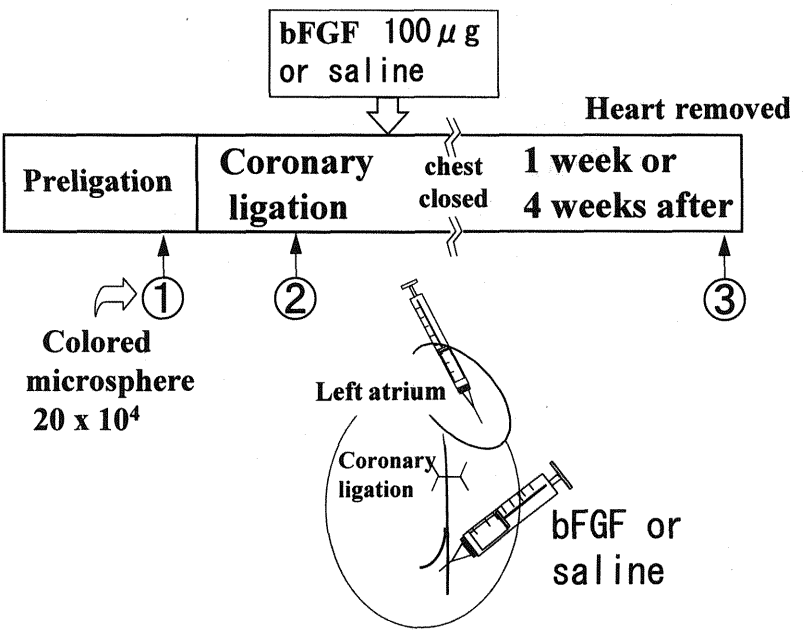

Figure 1. Schematic representation of the experiment.

injected into a risk area just after coronary occlusion. The details of the study protocol will be presented in a separate paper. Briefly, the left coronary artery was occluded by sutures in 33 Sprague–Dawley (SD) rats under anesthesia. In 15 SD rats, saline 0.04 mL (control group) was injected into the risk area; in the other 18 SD rats, bFGF 100 μg dissolved in 0.04 mL of saline was similarly injected (bFGF group) (figure 1). The control group was maintained for four weeks. In the bFGF group, 11 SD rats were maintained for four weeks, while the other seven SD rats were maintained for one week to elucidate the time course change. Four weeks (or one week) after occlusion, the heart was removed. Nonradioactive colored microspheres were injected into the left atrium to measure regional myocardial blood flow (Qm) as described previously [4,5]. The following equation was used in these calculations:

$$Q_m = \frac{[Q/Qc]\text{infarcted}}{[Q/Qc]\text{noninfarcted}} \times 100\ (\%),$$

where Q is Qm of interest and Qc is Qm at preocclusion.

The removed heart was sliced at a thickness of 1 mm from apex to base. The total area of the infarcted portion (infarct size) was measured as the percent of total left ventricle to calculate infarct size. One slice at the midportion of the infarct was used

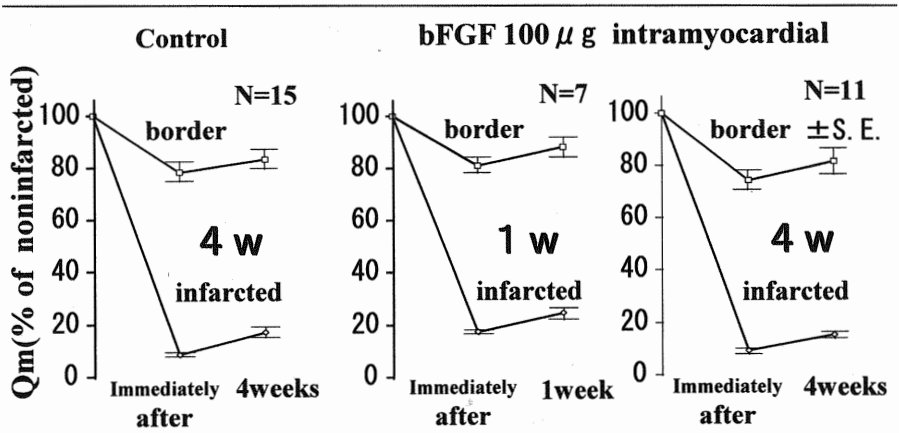

Figure 2. Regional myocardial blood flow (Qm) at the infarcted area and border zone in the three groups.

for histological analysis. Multiple microscopic photographs were obtained from this slice. The amount of viable myocardium (myocardium score) was calculated from each photograph using the point-counting method [6] with a grid of 100 cross points. A myocardial score near 100 indicates the tissue is noninfarcted, while almost zero indicates a totally necrotic area. The extent of fibrosis was determined macroscopically on each photograph; if there is no fibrosis, the score is 0, and when totally fibrotic, the score is 5.

RESULTS

Qm in the three groups is shown in figure 2. There was a marked reduction in Qm after coronary occlusion at the infarcted area, and a slight reduction at the border zone. There was no difference in these values among the three groups. At four weeks or one week after occlusion, Qm increased slightly at the infarcted area as well as at the border zone, and again there is no difference among the three groups. Figure 3 showed the myocardial score and the extent of fibrosis in the three groups. There are no differences in these indices among the three groups.

DISCUSSION

We found that when bFGF 100 μg was injected into the myocardium, there was no change in Qm and no myocardial salvage or infarct size limitation in rats. This finding is in accordance with our previous report [4] in which we injected 10 μg of bFGF intravenously over 24 hours after coronary occlusion in rats.

In a separate experiment in dogs [7], we found that intracoronary injection of bFGF 30 μg was not effective, but 300 μg injected into the risk area prior to coronary occlusion caused a marked increase in Qm, an increase in viable myocardium, and decreased fibrosis at the infarcted myocardium in dogs [8]. This finding

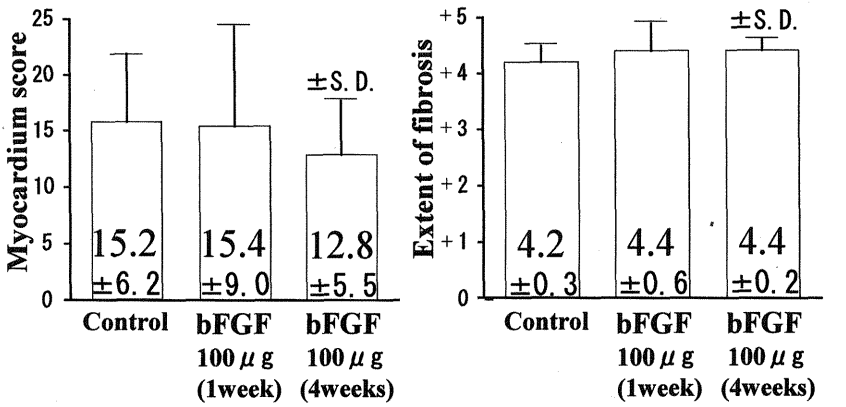

Figure 3. Amount of viable myocardium and extent of fibrosis at the infarcted area in the three groups.

suggests that the effect of bFGF is dose dependent. However, 100μg of bFGF in rats is a sufficiently greater dose than 300μg in dogs, and higher doses of bFGF cannot be expected to cause any additional effect. The other difference from our dog experiment [8] is that bFGF was given after occlusion of the coronary artery. When given prior to occlusion, angiogenic effects may be elicited in rats.

We used human recombinant type bFGF for this experiment. If we could use bFGF of rats, there might be pronounced angiogenesis. However, it is known that this growth factor is homologous. Augmented angiogenesis in the extremities of rats has been induced by human recombinant bFGF [9]. Again, a species difference of bFGF is not likely to be the reason that we could not demonstrate angiogenesis in rats. However, bFGF may have organ specificity, that is, bFGF may elicite angiogenesis in the extremities but not in the myocardium.

Rats have fewer native collaterals than dogs [3]. This difference might be a reason why there was no effect of bFGF on the infarcted myocardium. However, in pigs, where native collaterals are more scanty than in rats [3], bFGF caused a significant increase in Qm and myocardial salvage by bFGF. In the ischemic model in pigs, an ameroid constrictor was used to cause gradual occlusion of the coronary arteries [10]. If we could apply a device to cause gradual coronary occlusion in rats, bFGF might induce angiogenesis as in pigs.

The present study indicated that the effects of bFGF on the ischemic myocardium is modified by many factors, including the dosage of bFGF, timing of injection, species differences, and organ specificities, and may even be modified by the nature of the ischemic myocardium. These questions must be answered before application of bFGF in clinical practice.

REFERENCES

1. Horrigan MCG, MacIsaac AI, Nicolini FA, Vince DG, Lee P, Ellis SG, Topol EJ. 1996. Reduction in myocardial infarct size by basic fibroblast growth factor after temporary coronary occlusion in a canine model. Circulation 94:1927–1933.
2. Yanagisawa-Miwa A, Uchida Y, Nakamura F, Tomaru T, Kido H, Kamijo T, Sugimoto T, Kaji K, Utsuyama M, Kurashima C, Ito H. 1992. Salvage of infarcted myocardium by angiogenic action of basic fibroblast growth factor. Science 257:1401–1403.
3. Maxwell MP, Hearse DJ, Yellon DM. 1987. Species variation in the coronary collateral circulation during regional myocardial ischaemia: a critical determinant of the rate of evolution and extent of myocardial infarction. Cardiovasc Res 21:737–746.
4. Inagaki M, Ishikawa K, Ogawa I, Koka H, Nakai S, Kino H, Kimura A, Miyataka M, Katori R. 1996. Regional blood flow in infarcted myocardium of basic fibroblast growth factor-treated rats. Acta Med Kinki Univ 21:59–63.
5. Ishikawa K, Kamata N, Nakai S, Akiyama H, Koka H, Ogawa I, Katori, R. 1994. Preservation of high regional blood flow at epicardial rim after coronary occlusion in dogs. Am J Physiol 267:H528–H534.
6. Baandrup U, Olsen EGJ. 1981. Critical analysis of endomyocardial biopsies from patients suspected of having cardiomyopathy. I: Morphological and morphometric aspects. Br Heart J 45:475–486.
7. Miyataka M, Ishikawa K, Ogawa I, Koka H, Nakai S, Kino H, Inagaki M, Kimura A, Katori R. 1996. Contralateral arterial bolus injection of 30 micrograms of basic fibroblast growth factor failed to augment myocardial blood flow in infarcted myocardium in dogs. Acta Med Kinki Univ 21:53–58.
8. Miyataka M, Ishikawa K, Katori R. 1998. Basic fibroblast growth factor increased regional myocardial blood flow and limited infarct size of acutely infarcted myocardium in dogs. Angiology in press.
9. Yang HT, Deschenes MR, Ogilvie RW, Terjung RL. 1996. Basic fibroblast growth factor increases collateral blood flow in rats with femoral arterial ligation. Circ Res 79:62–69.
10. Sellke FW, Wang SY, Friedman M, Harada K, Edelman ER, Grossman W, Simons M. 1994. Basic FGF enhances endothelium-dependent relaxation of the collateral-perfused coronary microcirculation. Am J Physiol 267:H1303–H1311.

This Page Intentionally Left Blank

GENE THERAPY FOR MYOCARDIAL INFARCTION

RYUICHI MORISHITA, MOTOKUNI AOKI, HIDETSUGU MATSUSHITA, YASUFUMI KANEDA, JITSUO HIGAKI, and TOSHIO OGIHARA

Osaka University Medical School

Summary. The lack of efficient treatment for myocardial infarction remains an unresolved problem in the field of cardiovascular disease. Gene therapy may be a potential therapeutic strategy for the treatment of myocardial infarction. However, current methods of in vivo gene transfer into the heart are limited by their low efficiency and/or potential toxicity. In this chapter, we discussed the advantage of an efficient technique of gene and oligodeoxynucleotides (ODNs) transfer into the intact heart in vivo using the Sendai virus (HVJ: Hemagglutinating Virus of Japan)—liposome method. The potential gene therapy strategy for myocardial infarction is also discussed.

IN VIVO GENE TRANSFER INTO HEART

Recent progress in molecular biology has led to the development of gene therapy [1,2], as a new treatment strategy for cardiovascular diseases. Targeted diseases range from single gene deficiency diseases to more complex diseases in adults such as restenosis after angioplasty. We have previously reported a potential efficient therapy using antisense strategy against cell-cycle regulatory genes for the treatment of restenosis after angioplasty [3–6]. We and other investigators have also reported successful gene therapy using functional transgenes in animal models of restenosis [3–12]. Another apparent major target of gene therapy is cardiac diseases, including myocardial infarction and cardiomyopathy. Nevertheless, there is no report of successful gene therapy in the heart in vivo, because it is very difficult to transfect efficiently into cardiac myocytes in vivo as well as in vitro. Development of in vivo transfer techniques of genes whose product can correct a critical process may

S. Mochizuki, N. Takeda, M. Nagano and N. Dhalla (eds.). THE ISCHEMIC HEART.

provide an approach to treating this disease. Lin et al. [13], followed by other investigators [14–18], demonstrated in vivo gene transfer into the heart using direct injection of "naked" DNA. However, this approach is relatively inefficient, resulting in gene transduction in less than 1% of the cells in the area of DNA injection [13], and is therefore apparently far from the realm of gene therapy. To overcome these problems, some investigators have recently focused on the adenoviral gene transfer method [19–22]. The adenoviral vector seems to be very efficient when applied via direct injection or coronary infusion [19–22], but there are some theoretical disadvantages [23,24]. In addition to efficiency, the safety of the gene transfer method is also an important issue. Taking all these concerns into consideration, the current methods have several theoretical disadvantages.

Based upon these previous studies, we reasoned that the establishment of alternative efficient approaches to gene transfer into the heart is necessary for the understanding and treatment of cardiovascular diseases. Recently, we have developed the HVJ–liposome-mediated transfer method for in vivo gene transfer into adult rat liver, kidney, and blood vessels [3–7,25–27]. This method is easy to manipulate and highly efficient, and there is no limitation on the size of the vector DNA. Moreover, the HVJ method has little toxicity—direct in vivo injection into the liver or kidney did not show any acute or long-term impairment of hepatic or renal function [3–7,25–27]. In the present study, we modified this method for successful in vivo gene transfer into the heart as follows: 1) direct injection and 2) coronary infusion.

Initially, we performed direct injection of HVJ–liposome complex into rat heart in vivo. Direct injection of HVJ–liposome complex containing β-galactosidase vector resulted in positive staining for β-galactosidase at three days after transfection (figure 1), whereas direct injection of control vector without β-galactosidase gene failed to result in any positive staining (figure 1). The percentage of positively stained cells around the injection site was very high (nearly 80%), but the stained region was limited to around the injection site. Moreover, luciferase activity was significantly higher in hearts transfected with luciferase vector by HVJ–liposome method than in hearts transfected by direct injection of "naked" plasmid DNA ($p < 0.01$). Unfortunately, we found significant injury and fibrosis at the injection site (data not shown). In some rats, accumulation of macrophages and neutrophils was observed at the injection site. However, no significant damage induced by the HVJ–liposome complex could be detected.

On the other hand, in cardiovascular disease, antisense strategy has also been a center of interest since we and others have reported gene therapy using the antisense strategy for restenosis after angioplasty [3–6]. However, little is known about application of antisense strategy to cardiac diseases such as myocardial infarction due to the lack of a suitable delivery method of antisense oligodeoxynucleotides (ODNs) into heart in vivo. Therefore, we employed the HVJ–liposome method to establish nontoxic and effective antisense ODN delivery technique into heart in vivo. To address this issue, we also examined the application of HVJ–liposome-mediated method for in vivo ODN transfer into adult rat heart.

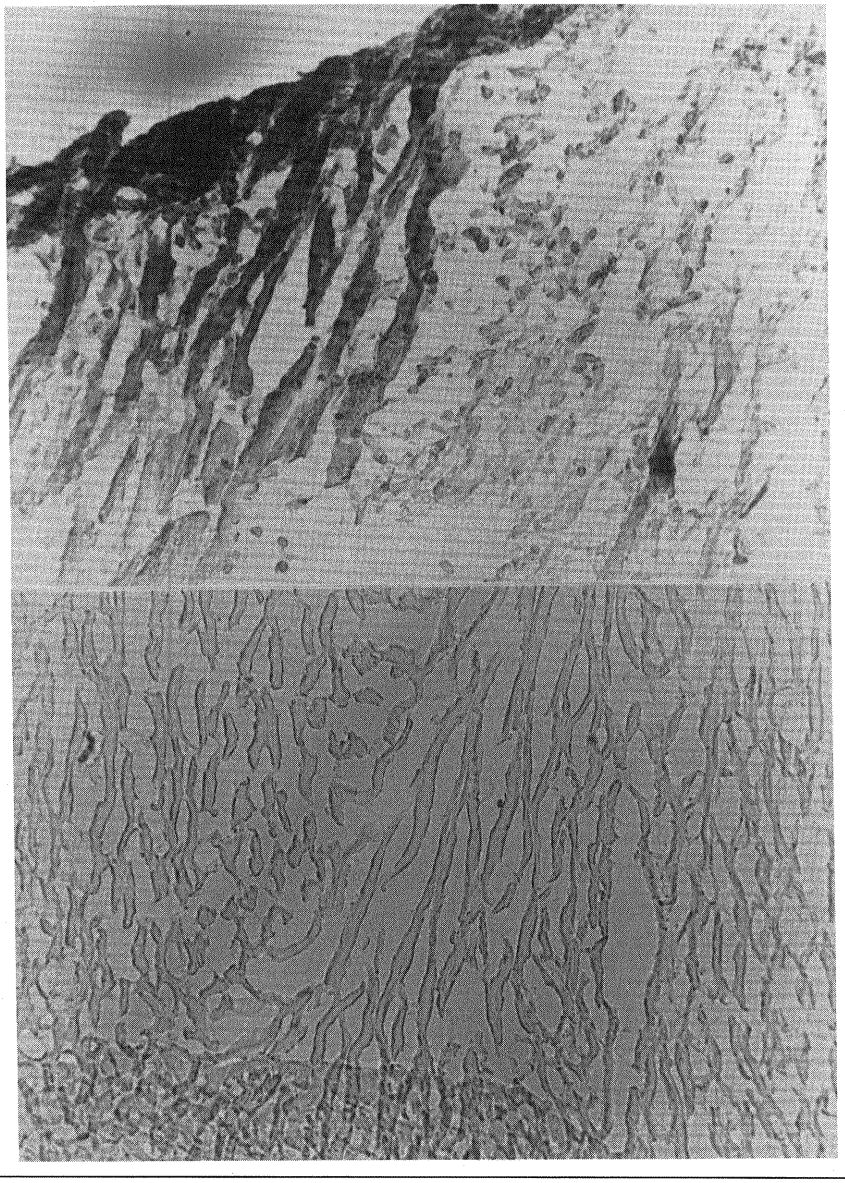

Figure 1. Direct injection of the HVJ–liposome complex containing β-galactosidase or control vector plasmid into rat heart in vivo (×200). Upper panel: Transfection of HVJ–liposome complex containing β-galactosidase vector (10 μg/mL). Lower panel: Transfection of HVJ–liposome complex containing control vector (10 μg/mL).

In this study, we compared the effectiveness of HVJ–liposome method with direct transfer in in vivo transfer into heart by direct needle injection. To investigate the cellular fate and localization of ODNs, FITC-labeled antisense ODNs were transfected. As shown in figure 2, fluorescence in hearts transfected by direct transfer rapidly disappeared within three days, whereas fluorescence in hearts transfected by the HVJ–liposome method was sustained in the nuclei and was widely distributed. Moreover, even after seven days, the fluorescence still remained in the nuclei, and myocytes showing fluorescence were widespread within a 5 mm area around the injection site. Marked enhancement of ODN stability was also confirmed by the measurement of fluorescence. Transfection of FITC-labeled ODNs by the HVJ–liposome method (1 μM) resulted in a significant increase in fluorescence of the lower heart as compared to direct transfer (10 μM, "naked") at four days after transfection (data not shown). Interestingly, fluorescence could also be detected in the upper part of the heart transfected with the HVJ–liposome method ($p < 0.05$), whereas no fluorescence was detected in hearts transfected with "naked" FITC-labeled antisense ODNs. Although fluorescence could not be detected at seven days after transfection by direct transfer, transfection of FITC-labeled antisense ODNs by the HVJ–liposome method resulted in a sustained fluorescence at least up to seven days after transfection.

Unfortunately, severe damage from inflammation and neutrophil accumulation in the myocardium was observed on hematoxylin–eosin staining, even in rats injected with vehicle (BSS solution alone), similar to transfer of the β-galactosidase gene. Although the needle injection itself caused severe damage to the myocardium, there was no evidence of inflammation attributable to the HVJ–liposome vector. Moreover, we also evaluated the effect of direct injection of the HVJ–liposome complex on the ECG. ECG in rats transfected with the HVJ complex showed no change between before and after transfection via direct injection (figure 3). These in vivo results were consistent with in vitro data. Our in vitro data demonstrated a nuclear staining pattern that was visualized within 10 minutes after transfection by the HVJ–liposome method. Nuclear fluorescence could be seen in approximately 90% of viable cells (figure 4). Although the fluorescence in the hearts transfected by direct transfer disappeared within three days, the fluorescence in the hearts transfected by the HVJ–liposome technique was sustained in the nuclei for at least seven days (data not shown).

The HVJ–liposome method utilizes fusion between the lipid membrane and the cell membrane [29]. HVJ has two surface glycoproteins—HN-protein, which is associated with the attachment between the HVJ–liposome complex containing ODNs and myocytes, and F-protein, which causes fusion between the lipid membrane and the cell membrane, resulting in rapid release of ODNs or transgenes in liposomes into the cytoplasm. Although in the ordinary pathway without vector, ODNs are trapped in endosomes, resulting in lysosomal degradation, in the pathway utilizing the HVJ–liposome vector the endocytosis step is skipped.

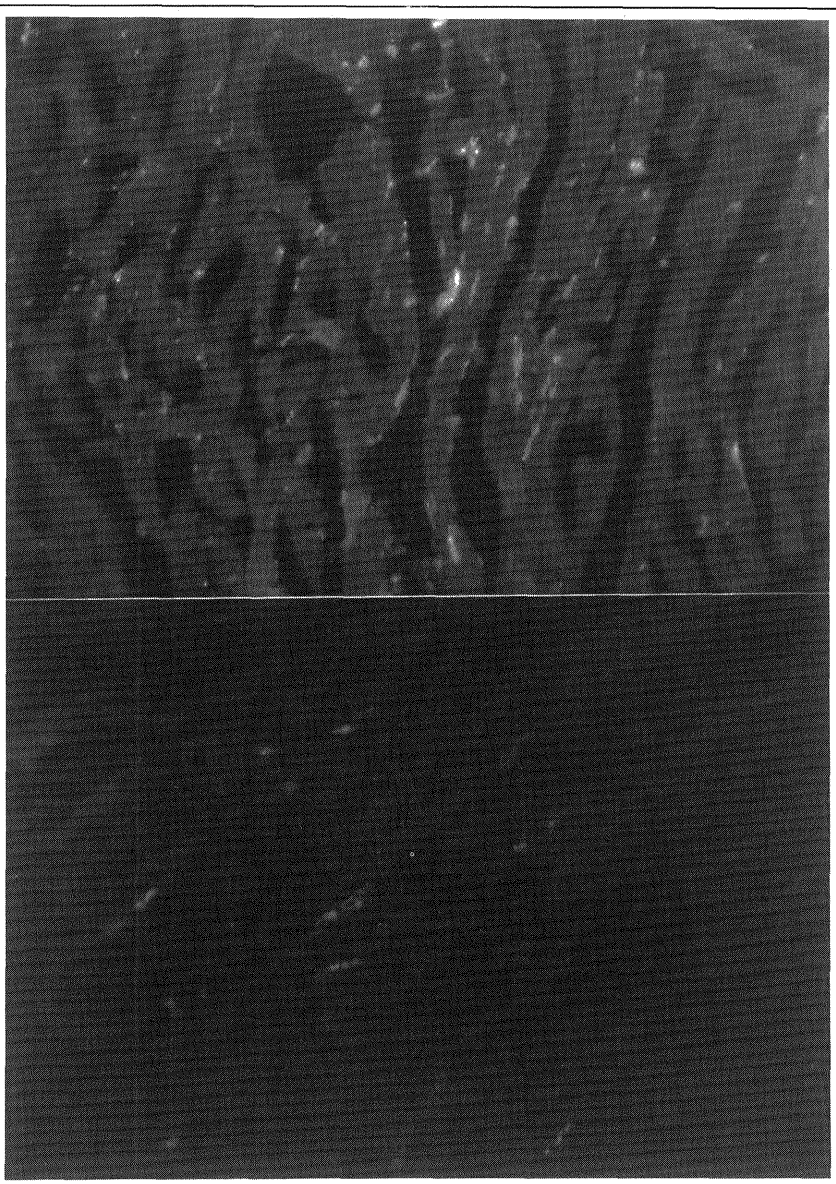

Figure 2. Time course of fluorescence in heart of rats transfected with FITC-labeled ODNs by the HVJ–liposome method or direct transfection. Upper panel: three days after transfection using the HVJ–liposome method (1 μM) around the injection site (×200). Lower panel: three days after transfection without vector (10 μM) around injection site (×200).

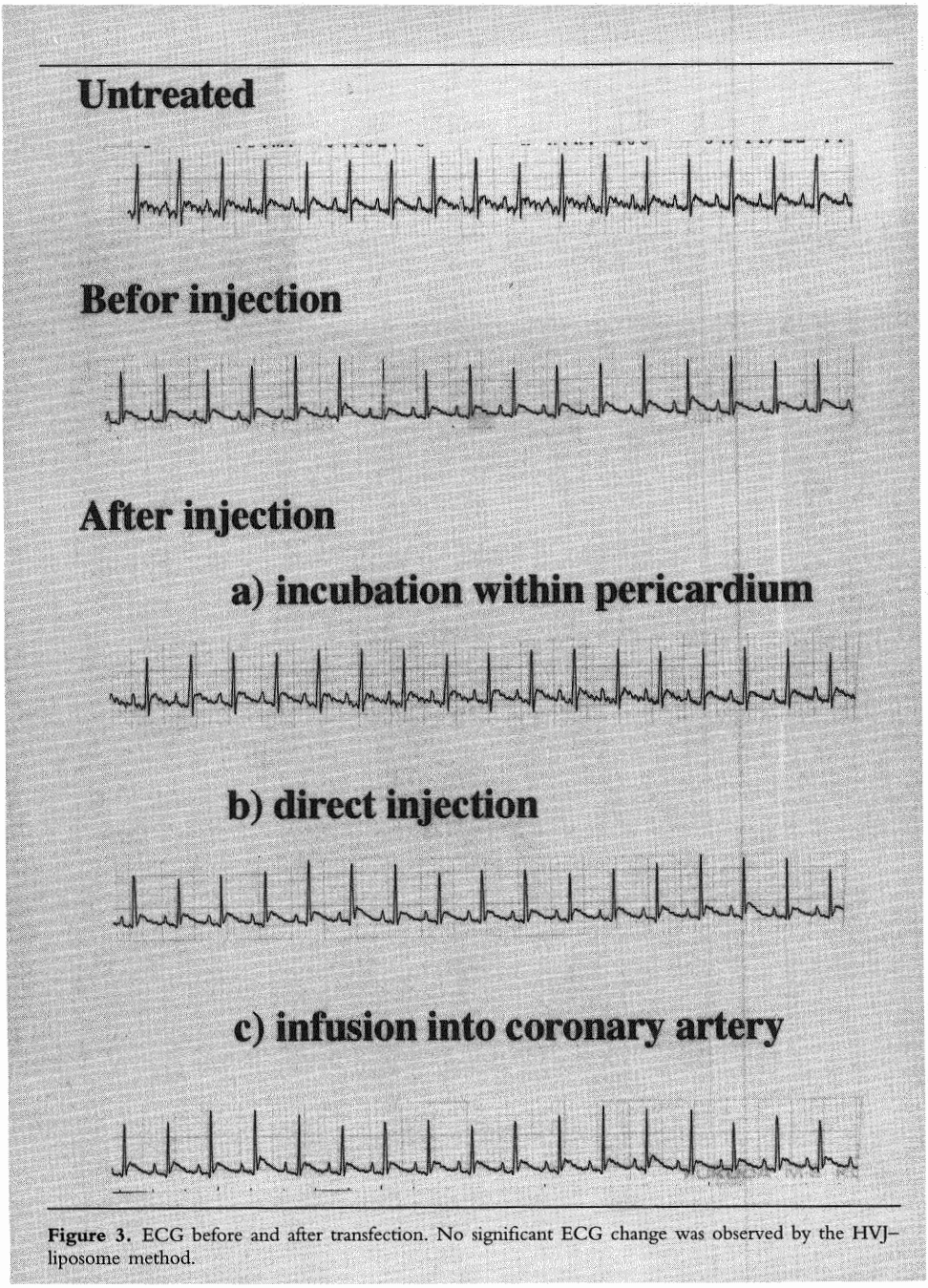

Figure 3. ECG before and after transfection. No significant ECG change was observed by the HVJ–liposome method.

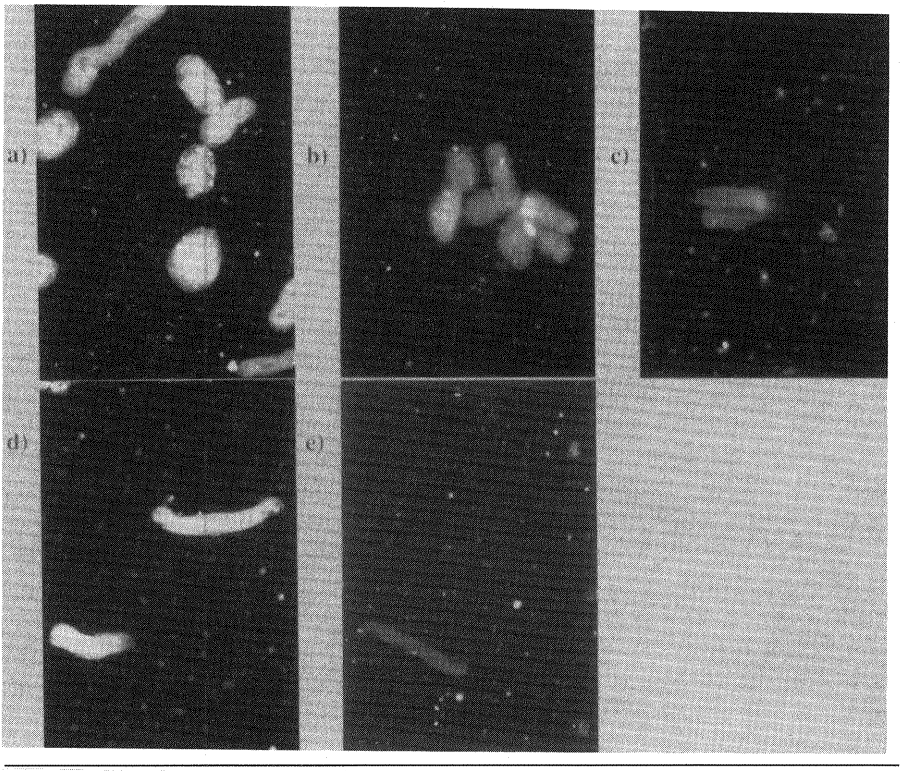

Figure 4. In vitro transfer of ODN to cultured myocytes (×200). (**a**) 24 hours after transfection using the HVJ-liposome method (1 μM); (**b**) three days after transfection using the HVJ–liposome method (1 μM); (**c**) seven days after transfection using the HVJ–liposome method (1 μM); (**d**) 24 hours after transfection without vector (10 μM); (**e**) three days after transfection without vector (10 μM).

GENE THERAPY FOR MYOCARDIAL INFARCTION

Currently, there are several different strategies for the treatment of myocardial infarction, as shown in table 1. Neovascularization therapy using recombinant peptide has been demonstrated by Miwa et al. and others [29,30]. Gene therapy using angiogenic growth factors that cause neovascularization greater than that with recombinant peptides has been considered. One gene therapy for myocardial infarction converts fibroblasts to muscles by myo D, resulting in the enhancement of contractility. Other ideas include 1) replication of dead myocytes by genetically modified cardiac myocytes and 2) prevention of myocardial infarction by NFkB decoy ODN, as discussed below.

Replacement of genetically grafted cardiac myocytes

Cell grafting has also emerged as an accepted approach for the delivery of therapeutic agents to patients. More recently, the use of genetically modified cells for the

delivery of recombinant molecules has also emerged as a powerful tool for ex vivo gene therapy. For the application of ex vivo gene therapy to cardiac diseases, myoblast grafting has been reported [31–33]. Koh et al. previously reported the differentiation and long-term survival of C2C12 myoblast grafts in the heart that were introduced by direct injection [32], and that myoblasts transfected with transforming growth factor-β promote vascular endothelial cell DNA synthesis [33]. Therefore, we initially examined the potential of cell grafting into intact heart. Cardiac myocytes transfected with FITC-labeled ODNs demonstrated fluorescence in the host heart in vivo. It is easy to study the kinetics of grafts in the host heart using FITC-labeled ODN transfected grafts as presented in this study. Moreover, the HVJ–liposome method is also useful for prolongation of the half-life and enhancement of the effects of ODNs transfected ex vivo (figure 5), consistent with the direct injection data (unpublished observation).

Of importance, survival of myocyte grafts in noninfarcted and border-zone areas was observed, but not in the infarcted area. Probably grafts in infarcted areas cannot survive due to the absence of blood supply. If recanalization occurred, graft survival might increase. Interestingly, a previous report described the formation of gap junctions between the injected cultured rat neonatal myocytes and the native cardiac myocytes in the intact heart [33]. Therefore, targeted expression of recombinant molecules in intracardiac grafts could induce a beneficial response in the myocardium. For example, grafts expressing angiogenic factors (as exemplified by basic and acidic fibroblast growth factor, TGF-β, and vascular endothelial growth factor) might induce neovascularization in a paracrine manner. A more exciting application of intracardiac myocyte grafting lies in the potential replacement of diseased myocardium. It is well known that ventricular cardiac myocytes in the adult mammal have no capacity to reenter the cell cycle. Therefore, myocyte death due to infarction is consequently irreversible. Our present finding that adult myocyte grafts can survive in the host heart raises the possibility that damaged myocardium could be replaced by implanted cardiac myocytes, potentially resulting in a direct contribution to the cardiac work force. Alternatively, cardiac myocyte grafts transfected with antisense ODNs targeting unknown genes that maintain myocytes in the differentiated stage outside the cell cycle might induce the replication of cardiac myocytes, resulting in rapid healing in myocardial infarction.

Prevention of myocardial infarction by NFkB decoy

As discussed above, the application of DNA technology such as antisense strategy to regulate the transcription of disease-related genes in vivo has important therapeutic potential. Moreover, recently the transfection of *cis*-element double-stranded (ds) ODSs (= decoy) as a new, powerful tool in a new class of antigene strategies to study transcriptional regulation has been reported [34–36]. We have also considered decoy strategy as a powerful strategy for gene therapy [7,37]. Transfection of ds ODNs corresponding to the *cis* sequence will result in the attenuation of the authentic *cis–trans* interaction, leading to the removal of the *trans* factors from the

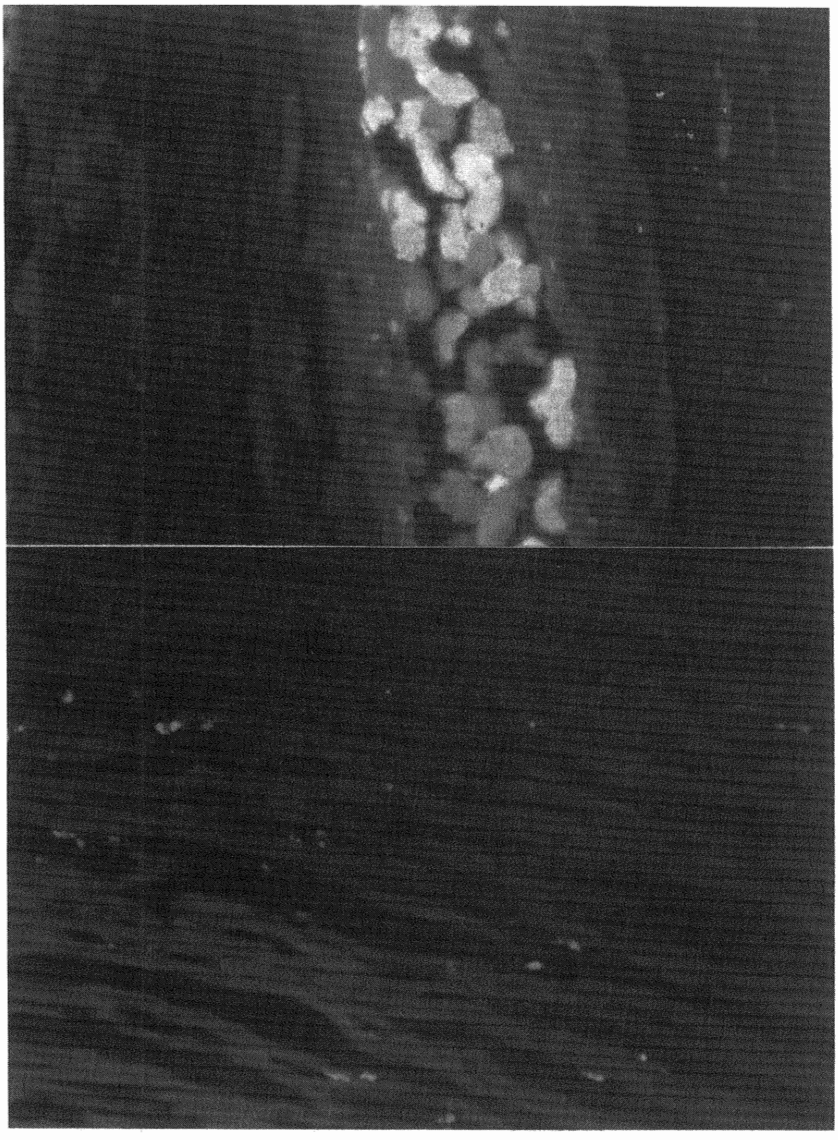

Figure 5. Time course of fluorescence in hearts of rats grafted with cardiac myocytes transfected with FITC-labeled ODNs ex vivo by the HVJ–liposome method or direct transfection. Upper panel: 24 hours after transfection using the HVJ–liposome method (1 μM) (×200). Lower panel: 24 hours after transfection without vector (10 μM)(×200).

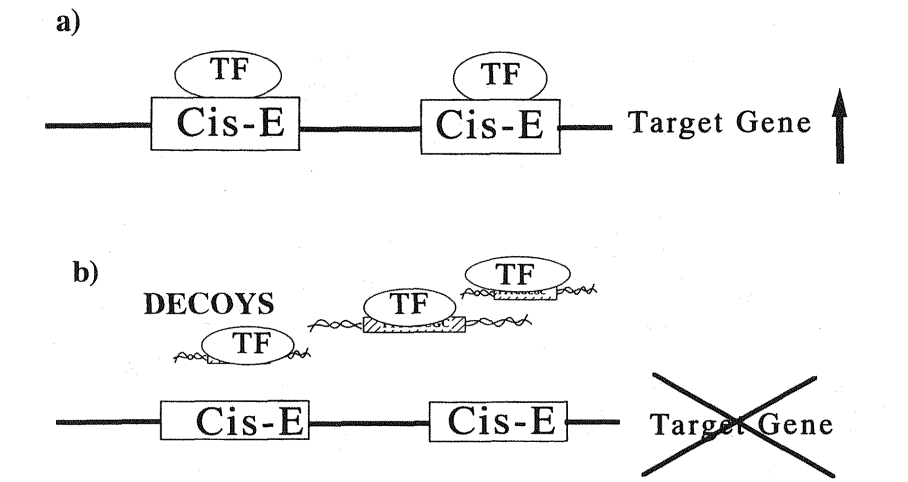

Figure 6. Scheme of "decoy" strategy. TF: transcriptional factor; cis-E: *cis*-element. (**a**) In the basal state, TF is bound to the *cis*-element, resulting in continuous activation of target gene expression; (**b**) TF decoy *cis*-element dsODNs bind to TF, resulting in prevention of TF interaction and transactivation of TF-promoting target gene expression.

endogenous *cis*-element, with subsequent modulation of gene expression (figure 6). Therefore, the decoy approach may enable us to treat diseases by modulation of endogenous transcriptional regulation. For example, the transcriptional factor NFkB plays a pivotal role in the coordinated transactivation of cytokine and adhesion molecule genes, e.g., IL-6, IL-8 and VCAM, to name a few [38,43]. Activation of these genes has been postulated to be involved in numerous diseases, such as myocardial damage after ischemic reperfusion [44–46]. We hypothesized that synthetic double-stranded (ds) DNA with high affinity for NFkB may be introduced in vivo as a decoy *cis*-element to bind the transcriptional factor and to block the activation of genes mediating such diseases, resulting in an effective therapy for treating diseases. Currently, few studies have reported an application of the decoy ODN strategy as in vivo gene therapy.

To establish effective decoy ODN transfer in rat MI model, we initially evaluated cellular localization of FITC-labeled ODNs. Transfection of FITC-labeled ODNs via infusion into rat coronary artery resulted in widely distributed fluorescence in microvascular endothelial cells and myocytes across the endothelium. Next, we applied the NFkB decoy strategy to a rat MI model. After reperfusion, the protein level of IL-8 was elevated in infarcted myocardium as detected by ELISA (data not shown), consistent with previous reports on increases in mRNA and protein expressions of cytokines and adhesion molecules. We initially transfected NFkB decoy ODN into the coronary artery before LAD occlusion. Transfection of NFkB decoy ODN into rat coronary artery prior to LAD occlusion markedly reduced the

area of myocardial infarction at 24 hours after reperfusion, whereas no difference was observed between scrambled decoy ODN-treated and untransfected rats. Finally, we examined the therapeutic efficacy of this strategy via intracoronary administration immediately after reperfusion, similar to the clinical situation. NFkB decoy ODNs, introduced in vivo by the HVJ–liposome complex, inhibited myocardial infarction, in contrast to rats treated with HVJ–liposome containing scrambled control decoy or vehicle. The specificity of the NFkB decoy in the inhibition of cytokine and adhesion molecule expression was confirmed by in vitro experiments using human and rat coronary artery endothelial cells.

Here, we report a novel therapeutic strategy to prevent myocardial infarction utilizing in vivo transfer of a decoy *cis*-element to bind the critical transcriptiond factor NFkB and thereby to block the coordinated transactivation of several cytokine and adhesion molecule genes necessary for disease processes. Since NFkB has been postulated to play an important role in the pathogenesis of numerous disease, e.g., cancer and arthritis, the development of the NFkB decoy strategy may provide a useful therapeutic tool for treating these diseases.

FUTURE DIRECTION OF GENE THERAPY IN MYOCARDIAL INFARCTION

Gene therapy in the field of cardiovascular disease would be useful for the treatment of many diseases, including the prevention of restenosis after angioplasty, myocardial infarction, and rejection in heart transplantation. For example, the gene transfer of angiogenic factors such as bFGF and VEGF may salvage infarcted myocardium beyond that achieved by recombinant neovasculization therapy. An alternative potential strategy for myocardial infarction gene therapy is to convert fibroblasts to skeletal muscle cells by transfection of Myo D gene in order to achieve sufficient contraction, as discussed above. To achieve gene therapy in the heart, it is important to establish an efficient technique of gene and/or ODN transfection into cardiac myocytes in vivo.

The first federally approved human gene therapy protocol started on September 14, 1990, for adenosine deaminase (ADA)-deficient patients [1,2]. Six years since the first approval, more than 30 active clinical studies of gene therapy are under investigation. In the cardiopulmonary field, five protocols (LDL receptor to hepatocytes by using retroviral method, CFTR to lung using both adenoviral and cationic liposomal approaches, vascular endothelial growth factor to ASO and restenosis, and E2F decoy to restenosis after CABG) have been approved. Their objectives are generally to evaluate 1) the in vivo efficacy of gene transfer method, 2) the safety of the gene transfer method, and 3) the possible therapeutic efficacy. Although there are still many unresolved issues, human gene therapy for cardiovascular disease is now a reality. Consequently, it is time to take a hard look at practical issues that will determine the real clinical potential. These include 1) further innovations in gene transfer methods, 2) well-defined disease targets, 3) cell-specific targeting strategies, and 4) effective and safe delivery systems. The treatment of human diseases by gene therapy has moved from the theoretical to the practical

realm. Since the first human trial in 1990, [1,2], gene therapy has expanded to include many diseases such as cancer and immunodeficiency. At this stage, the approval of NIH and FDA has been limited to somatic gene therapy.

As gene therapy becomes a therapeutic reality, the following must be addressed: 1) *safety*, 2) *persistence of gene expression and duration of treatment*, and 3) *regulation*. In the future, we must find ideal and suitable promoters that can be regulated but still express sufficient amounts of the product (e.g., a "cut-off" system) for effective gene therapy.

REFERENCES

1. Anderson WF. 1992. Human gene therapy. Science 256:808–813.
2. Miller AD. 1992. Human gene therapy comes of age. Nature 357:455–460.
3. Morishita R, Gibbons GH, Ellison KE, Nakajima M, Zhang L, Kaneda Y, Ogihara T, Dzau VJ. 1993. Single intraluminal delivery of antisense cdc 2 kinase and PCNA oligonucleotides results in chronic inhibition of neointimal hyperplasia. Proc Natl Acad Sci USA 90:8474–8479.
4. Morishita R, Gibbons GH, Ellison KE, Nakajima M, Leyen HVL, Zhang L, Kaneda Y, Ogihara T, Dzau VJ. 1994. Intimal hyperplasia after vascular injury is inhibited by antisense cdk 2 kinase oligonucleotides. J Clin Invest ••:1458–1464.
5. Morishita R, Gibbons GH, Kaneda Y, Ogihara T, Dzau VJ. 1994. Pharmacokinetics of antisense oligonucleotides (cyclin B1 and cdc 2 kinase) in the vessel wall: enhanced therapeutic utility for restenosis by HVJ-liposome method. Gene 149:13–19.
6. Leyen HVL, Gibbons GH, Morishita R, Lewis NP, Zhang L, Nakajima M, Kaneda Y, Cooke JP, Dzau VJ. 1995. Gene therapy inhibiting neointimal vascular lesion: in vivo transfer of ecnitric oxide synthase gene. Proc Natl Acad Sci USA 92:1137–1141.
7. Morishita R, Gibbons GH, Horiuchi M, Ellison KE, Nakajima M, Zhang L, Kaneda Y, Ogihara T, Dzau VJ. 1995. A novel molecular strategy using cis element "decoy" of E2F binding site inhibits smooth muscle proliferation in vivo. Proc Natl Acad Sci USA 92:5855–5859.
8. Ohno T, Gordon D, San H, Pompili VJ, Imperiale MJ, Nabel GJ, Nabel EG. 1994. Gene therapy for vascular smooth muscle cell proliferation after arterial injury. Science 265:781–784.
9. Seltzer J, Chang M, Barr E, Parmacek MS, Leiden JM. 1994. Inhibition of vascular smooth muscle cell proliferation in vitro and in vivo by a replication-defective adenovirus encoding a non-phosphorylatable retinoblastoma gene product. Circulation 90:I–90.
10. Simons M, Edelman ER, DeKeyser J-L, Langer R, Rosenberg RD. 1992. Antisense c-myb oligonucleotides inhibit intimal arterial smooth muscle cell accumulation in vivo. Nature 359: 67–80.
11. Shi Y, Fard A, Galeo A, Hutchinson HG, Vermami P, Dodge GR, Hall DJ, Shaheen F, Zalewski A. 1994. Transcatheter delivery of c-myc antisense oligomers reduces neointimal formation in a porcine model of coronary artery balloon injury. Circulation 90:944–951.
12. Lin H, Parmacek MS, Morle G, Bolling S, Leiden JM. 1990. Expression of recombinant genes in myocardium in vivo after direct injection of DNA. Circulation 82:2217–2221.
13. Buttric PM, Kass A, Kitsis RN, Kaplan MR, Lainwand LA. 1992. Behavior of genes directly injected into the rat heart in vivo. Circ Res 70:193–198.
14. Rudiger von Harsdorf, Schott RJ, Shen Y-T, Vatner SF, Mahdavi V, Nadal-Ginard B. 1993. Gene injection into canine myocardium as a useful model for studying gene expression in the heart of large mammals. Circ Res 72:688–695.
15. Gal D, Weir L, Leclerc G, Pickering JG, Hogan J, Isner JM. 1993. Direct myocardial transfection in two animal models evaluation of parameters affecting gene expression and percutaneous gene delivery. Lab Invest 68:18–25.
16. Kitsis RN, Buttrick PM, McNally EM, Kaplan ML, Leinwand LA. 1991. Hormonal modulation of a gene injected into rat heart in vivo. Proc Natl Acad Sci USA 88:4138–4142.
17. Acsadi G, Jiao S, Jani A, Duke D, Williams P, Chong W, Wolff JA. 1991. Direct gene transfer and expression into rat heart in vivo. New Biologist 3:71–81.
18. Schneider MD, French BA. 1993. The advent of adenovirus gene therapy for cardiovascular disease. Circulation 88:1937–1942.

19. Kirshenbaum LA, MacLellan WR, Mazur W, French BA, Schneider MD. 1993. Highly efficient gene transfer into adult ventricular myocytes by recombinant adenovirus. J Clin Invest 92: 381–387.
20. Guzman RJ, Lemarchand P, Crystal RG, Epstein SE, Finkel T. 1993. Efficient gene transfer into myocardium by direct injection of adenovirus vectors. Circ Res 73:1202–1207.
21. French BA, Mazur W, Geske RS, Bolli R. 1994. Direct in vivo gene transfer into porcine myocardium using replication-deficient adenoviral vectors. Circulation 90:2414–2424.
22. Barr E, Carroll JC, Kalynych AM, Tripathy SK, Kozarski, Wilson JM, Leiden JM. 1994. Efficient catheter-mediated gene transfer into the heart using replication-defective adenovirus. Gene Ther 1:51–58.
23. Dzau VJ, Morishita R, Gibbons GH. 1993. Gene therapy in the cardiovascular diseases. Trends Biotechnol 11:205–210.
24. Morishita R, Gibbons GH, Dzau VJ. 1993. Gene therapy as potential treatment for cardiovascular diseases. In Singh BN (ed), Cardiovascular Pharmacology and Therapeutics. New York: Livingstone pp. 51–61.
25. Kaneda Y, Iwai K, Uchida T. 1989. Increased expression of DNA cointroduced with nuclear protein in adult rat liver. Science 243:375–378.
26. Kaneda Y, Iwai K, Uchida T. 1989. Introduction and expression of the human insulin gene in adult rat liver. J Biol Chem 264:12126–12129.
27. Tomita N, Higaki J, Morishita R, Kato K, Mikami H, Kaneda Y, Ogihara T. 1992. Direct in vivo gene introduction into rat kidney. Biochem Biophys Res Commun 186:129–134.
28. Nakanishi M, Uchida T, Sugawa H, Ishiura M, Okada Y. 1985. Efficient introduction of contents of liposomes into cell using HVJ (Sendai virus). Exp Cell Res 159:399–409.
29. Yanagisawa-Miwa A, Uchida Y, Nakamura F, Tomaru T, Kido H, Kamijo T, Sugimoto T, Kaji K, Utsuyama M, Kurashima C, Itoh H. 1992. Salvage of infarcted myocardium by angiogenic action of basic fibroblast growth factor. Science 257:1401–1403.
30. Harada K, Lopez JJ, Friedman M, Prasad PV, Hibberd M, Sellke FW, Simons M. 1994. Vascular endothelial growth factor improves myocardial function in chronically ischemic porcine hearts (abstract). Circulation 90:I–427.
31. Koh GY, Klug MG, Soonpaa MH, Field LJ. 1993. Differentiation and long-term survival of C2C12 myoblast grafts in heart. J Clin Invest 92:1548–1554.
32. Koh GY, Kim SJ, Klug MG, Park K, Soonpaa MH, Field LJ. 1995. Targeted expression of transforming growth factor-b1 in intracardiac grafts promotes vascular endothelial cell DNA synthesis. J Clin Invest 95:114–121.
33. Soonpaa MH, Koh GY, Klug MG, Field LJ. 1994. Formation of nascent intercalated disks between grafted fetal cardiomyocytes and host myocardium. Science 264:98–101.
34. Bielinska A, Shivdasani RA, Zhang L, Nabel GJ. 1990. Regulation of gene expression with double-stranded phosphorothioate oligonucleotides. Science 250:997–1000.
35. Sullenger BA, Gallardo HF, Ungers GE, Giboa E. 1990. Overexpression of TAR sequence renders cells resistant to human immunodeficiency virus replication. Cell 63:601–608.
36. Yamada T, Horiuchi M, Morishita R, Zhang L, Pratt RE, Dzau VJ. In press. In vivo identification of a negative regulatory element in the mouse renin gene using direct gene transfer. J Clin Invest.
37. Morishita R, Higaki J, Tomita N, Aoki M, Moriguchi A, Tamura K, Murakami K, Kaneda Y, Ogihara T. 1996. Role of transcriptional cis-elements, angiotensinogen gene-activating element, of angiotensinogen gene in blood pressure regulation. Hypertension 27:502–507.
38. Lenardo MJ, Baltimore D. 1989. NF-kappa B: a pleitropic mediator of inducible and tissue-specific gene control. Cell 58:227–229.
39. Libermann TA, Baltimore D. 1990. Activation of interleukin-6 gene expression through the NF-kappa B transcription factor. Mol Cell Biol 10:2327–2334.
40. Satriano J, Schlondorff. 1994. Activation of attenuattion of transcriptional factor NF-kB in mouse glomerular cells in response to tumor necrosis factor-, immunoglobulin G, and adenosine 3′:5′-cyclic monophosphate. J Clin Invest 94:1629–1636.
41. Neish AS, Williams AJ, Palmer HJ, Whitley MZ, Collins T. 1992. Functional analysis of the human vascular cell adhesion molecule 1 promoter. J Exp Med 176:1583–1593.
42. Brennan DC, Jevnikar AM, Takei F, Reubin-Kelley VE. 1990. Mesangial cell accessory functions: mediation by intracellular adhesion molecule-1. Kidney Int 38:1039–1046.
43. Sedor JR, Konieczkowski M, Huang S, Gronich JH, Nakazato Y, Gordon G, King CH. 1993. Cytokines, mesangial cell activation and glomerular injury. Kidney Int 39:S65–S70.

44. Herskowitz A, Choi S, Ansari AA, Wesselngh S. 1995. Cytokine mRNA expression in postischemic/reperfused myocardium. Am J Pathol 146:419–428.
45. Kukielka GL, Smith CW, LaRosa GJ, Manning AM, Mendoza LH, Daly TJ, Hughes BJ, Youker KA, Hawkins HK, Michael LH, Rot A, Entman ML. 1995. Interleukin-8 gene induction in the myocardium after ischemia and reperfusion in vivo. J Clin Invest 95:89–103.
46. Kukielka GL, Entman ML. ••. Adhesion molecule-dependent cardiovascular injury. In Poste G, Metcalf B (eds), Cellular Adhesion: Molecular Definition to Therapeutic Potential. New York: Plenum, pp. 187–212.

ADENOVIRAL VECTORS AS EXPERIMENTAL AND THERAPEUTIC TOOLS

ANTHONY ROSENZWEIG and TAKASHI MATSUI

Massachusetts General Hospital

Summary. Adenoviral-mediated gene transfer to the cardiovascular system is of interest both for gene therapy applications and for the development of genetic overexpression models for pathophysiologic studies in vitro and in vivo. Recombinant adenoviral vectors (Ad) are particularly appealing tools for gene transfer to the cardiovascular system because of their high efficiency and ability to transduce nonreplicating cells, such as vascular endothelial and smooth muscle cells, as well as cardiocytes in vitro and in vivo. The disadvantages of these vectors currently limit their clinical application and include the transience of expression and the immune response they evoke. Efforts are underway in many laboratories to improve the adenoviral vector system by deleting immunogenic viral genes or by combining gene transfer with transient immunosuppression. In the meantime, however, the ability of current adenoviral vectors to transduce cardiovascular cells and tissues can be exploited to help elucidate the role of specific molecules in the pathophysiology of cardiovascular diseases. In this way, appropriate molecular strategies can be developed for use as improved vectors become available. In addtion, such experiments can also advance efforts toward human gene therapy by providing insights into vector–host interactions, which can help guide vector development.

INTRODUCTION

Adenoviral-mediated gene transfer using recombinant replication-deficient vectors has been achieved in a wide variety of mammalian cell types both in vitro and in vivo. Recombinant adenoviral vectors offer several significant advantages over other approaches to gene transfer, particularly for the vascular endothelial cells that compose the lining of the cardiovascular system. The viruses can be prepared at

S. Mochizuki, N. Takeda, M. Nagano and N. Dhalla (eds.). THE ISCHEMIC HEART.

extremely high titre, infect nonreplicating cells, and confer high-efficiency and high-level transduction [1–7]. Multiple reports have demonstrated the feasibility of this method of gene transfer to the vascular wall in both quiescent and injured blood vessels [5,6], as well as in the myocardium [8,9]. Cardiovascular gene transfer using recombinant adenoviral vectors appears to offer the potential of genetic manipulation of specific molecules either for gene therapy or for the development of experimental models in vitro or in vivo. However, current in vivo or clinical applications of these vectors are limited by a significant host immune and inflammatory response, which appears to be the predominant mechanism accounting for the transience of transgene expression. We will now review 1) the construction of adenoviral vectors, 2) the nature of the host response, 3) experimental applications of current adenoviral vectors, and 4) approaches to improved adenoviral vector systems.

ADENOVIRAL VECTORS

Adenoviruses comprise a large family of linear, double-stranded DNA viruses that commonly cause transient illnesses in humans, including conjunctivitis, upper respiratory illness, and acute gastroenteritis. Adenoviral DNA does not generally integrate into the host genome, and adenoviruses have not been associated with any human malignancy. Adenoviral illnesses are self-limited in the normal host due to a vigorous immune response to the virus. This fact probably underlies at least in part both the favorable biosafety profile of using these viruses as vectors as well as the major limitation to their clinical application. Transcription of most viral gene products depends on the presence of a series of transcription factors encoded in *Early region 1* (*E1*) [10–13]. Therefore, by substituting an exogenous cDNA for *E1*, it was initially thought that two goals would be simultaneously accomplished: expression of the exogenous cDNA and blockade of viral gene expression. While the former hypothesis has been repeatedly validated, the latter appears to be only partly true. As discussed below, expression of other viral genes can still take place either because their dependence on *E1* is incomplete or because the absence of *E1* is complemented by other transcription factors found in the host cell.

Although other approaches are possible, exogenous cDNA are most commonly substituted for *E1* through homologous recombination in the human kidney epithelial 293 cell line [14] by cotransfection of a "shuttle vector" containing the exogenous cDNA and 2 to 3 kb of adenoviral sequences along with a source of the remaining viral genome. The immortalized 293 cell line contains approximately 11% of the adenoviral genome (including *E1*) integrated into the host chromosomes [15], and therefore provides in *trans* the *E1* transcription factors needed to efficiently propagate the *E1*-deleted recombinants generated. Recombinants are identified first as plaques on the lawn of viable 293 cells. Once isolated, plaques are further propagated in 293 cells and screened for their ability to confer expression of the exogenous cDNA. Positive isolates should be further plaque-purified and checked for contamination with *E1*-containing (wild-type) adenoviruses. High-titre stocks

can then be prepared through propagation in 293 cells and density gradient purification [14].

THE HOST RESPONSE

The normal host is capable of a vigorous humoral and cellular immune response to adenoviral transduction. The humoral response probably plays a significant role in undermining the efficacy of repeated administration of adenoviral vectors. The cellular response predominates in the response to infected tissues and can ultimately result in destruction of transduced cells, thereby eliminating viral transgene expression [16]. The infiltrating effector cells are predominantly MHC Class I-restricted cytotoxic T lymphocytes [17–19]. The severity and extent of this immune response appears to vary significantly. Certain target sites elicit a more vigorous response. Moreover, different species [20] or even strains of the same species [21] have significantly different degrees of cellular immune response to adenoviral vectors and consequently differing durations of transgene expression. At least part of the immune response appears directed at viral antigens expressed after infection of the host cell, despite *E1* deletion. Further blocking of viral gene expression (for example, through mutation of the adenoviral DNA polymerase complex) results in substantially less host immune response and greater duration of transgene expression [22–24].

CURRENT APPLICATIONS

The issues above present substantial hurdles to the clinical application of recombinant adenoviral vectors. However, these vectors remain powerful tools for mediating somatic gene transfer and appear particularly well suited for the cardiovascular system. The predominant cells of the cardiovascular system are either postmitotic and do not replicate at all (such as cardiocytes) or replicate at extremely low levels under normal circumstances (such as vascular endothelial or smooth muscle cells). Adenoviral vectors (unlike, for example, retroviruses) are capable of infecting and transducing such nondividing cell populations with an efficacy (efficiency and level of expression) that makes feasible experiments that could not be performed otherwise.

For example, to define the role of specific adhesion molecules in the recruitment of leukocyte populations in atherogenesis, our laboratory has generated recombinant adenoviral vectors carrying the cDNAs for these molecules. Such vectors can then be used to effectively transduce human vascular endothelial cells in culture to study the adhesion biology of specific leukocyte subsets in simulated physiological flow systems. For such applications, it is essential that virtually all the endothelial cells studied express the molecule of interest, a goal that is impractical without adenoviral vectors but readily achievable with them. Using this approach, our laboratory has demonstrated that the atherogenesis-associated adhesion molecule, vascular cell adhesion molecule-1 (VCAM-1), is sufficient by itself to support adhesion of memory T cells to otherwise unactivated vascular endothelium, under simulated physiological laminar flow conditions [25]. Memory T cells are the predominant lymphocyte

population present in atherosclerotic plaque [26], and this finding supports the hypothesis that VCAM-1 plays an active role in their recruitment into the vessel wall.

As another example, our laboratory has recently used adenoviral gene transfer to study the role of the sarcoplasmic reticulum (SR) ATPase (SERCA2a) in primary cardiocyte cultures. Overexpression of SERCA2a resulted in increased peak intracellular calcium and an acceleration of the relaxation phase, as well as enhancement of myocyte shortening [27]. Studying such issues in transiently transfected cardiocytes is precluded by the extremely low efficiency of traditional transfection techniques in this cell population and the difficulties of identifying transfected cells for study while they remain viable. Using adenoviral vectors, essentially all the cells express the transgene, and so the level of expression can be easily titrated by adjusting the multiplicity of infection (MOI = plaque-forming units of virus per host cell) used [27]. Since SR ATPase activity is reduced in experimental and human heart failure, such recombinant vectors should facilitate studies of the role of this protein in the pathogenesis of heart failure models.

Translation of such in vitro results to in vivo models requires confronting the host response to the virus itself. How big a problem this poses will depend very much on the specific model to be studied. For example, adenoviral gene transfer has been used successfully by several groups to study models of vascular gene transfer in the rat carotid injury model [28,29]. This usage may, in part, reflect the independent observation that vascular gene transfer to rat vessels elicits a less dramatic host response than vascular gene transfer to rabbit vessels [20]. For systems not as amenable, other options include working in an immunoincompetent [30] or transiently immunosuppressed host [31], which can effectively remove the host immune response as a factor.

FUTURE VECTOR SYSTEMS

Both in vivo experiments and clinical applications would be greatly facilitated by improvements in the adenoviral vector system. The discovery that incorporating a temperature-sensitive mutation in the adenoviral DNA polymerase in addition to *E1* deletion significantly reduces the host immune response and prolongs transgene expression [22–24] provides an important proof of principle. However, the practical application of these so-called "second generation" adenoviral vectors is currently limited by the temperature-sensitive nature of the employed mutation. This temperature-sensitive mutation provides an incomplete block at physiological temperatures [23]. Moreover, the viruses grow slowly and generate lower titres at the permissive temperature. Obviously, complete deletion of this and potentially other loci would be more satisfactory but will require that the deletions be complemented in *trans* by new producer cell lines or helper virus. Recently, adenoviral vectors that have been deleted of almost all viral genes have been developed by using a helper virus strategy [32]. However, production of these vectors, which requires separation from the helper virus on a density gradient, will need to be improved before

winning widespread application. Other avenues being explored include transient immunosuppression of the host or regimens designed to make the host tolerant specifically to the adenoviral vector. It may also be possible to identify the features of the adenovirus that enhance gene transfer and to use these to augment the efficacy of other gene transfer approaches [33,34].

CONCLUSION

Adenoviral vectors remain attractive vehicles for somatic gene transfer to cells and tissues of the cardiovascular system. However, it is likely that therapeutic applications of gene transfer technology to the cardiovascular system will require both improvement in current vectors based on biological insights into their host interactions and a better understanding of cardiovascular pathophysiology. Both goals can be furthered by experimental application of currently available vectors to the cardiovascular system.

ACKNOWLEDGMENTS

The authors gratefully acknowledge support from the NIH (HL54202 to AR), the D.Y. and Joan Fu Fund for Cardiovascular Research (AR), the Merrill Lynch Research Fund (AR), and Bristol-Myers Squibb (to the CVRC).

REFERENCES

1. Akli S, Caillaud C, Vigne E, Stratford-Perricaudet LD, Poenaru L, Perricaudet M, Kahn A, Peschanski MR. 1993. Transfer of a foreign gene into the brain using adenovirus vectors. Nature Genet 3:224–228.
2. Berkner KL. 1988. Development of adenovirus vectors for the expression of heterologous genes. Biotechniques 6:616–629.
3. Jaffe HA, Danel C, Longenecker G, Metzger M, Setoguchi Y, Rosenfeld MA, Gant TW, Thorgeirsson SS, Stratford-Perricaudet LD, Perricaudet M, et al. 1992. Adenovirus-mediated in vivo gene transfer and expression in normal rat liver. Nature Genet 1:372–378.
4. Le Gal La Salle G, Robert JJ, Berrard S, Ridoux X, Stratford-Perricaudet LD, Perricaudet M, Mallet J. 1993. An adenovirus vector for gene transfer into neurons and glia in the brain. Science 259:988–990.
5. Lee SW, Trapnell BC, Rade JJ, Virmani R, Dichek DA. 1993. In vivo adenoviral vector-mediated gene transfer into balloon-injured rat carotid arteries. Circ Res 73:797–807.
6. Lemarchand P, Jones M, Yamada I, Crystal RG. 1993. In vivo gene transfer and expression in normal uninjured blood vessels using replication-deficient recombinant adenovirus vectors. Circ Res 72:1132–1138.
7. Willard JE, Landau C, Glamann DB, Burns D, Jessen ME, Pirwitz MJ, Gerard RD, Meidell RS. 1994. Genetic modification of the vessel wall: comparison of surgical and catheter-based techniques for delivery of recombinant adenovirus. Circulation 89:2190–2197.
8. Guzman RJ, Lemarchand P, Crystal RG, Epstein SE, Finkel T. 1993. Efficient gene transfer into myocardium by direct injection of adenovirus vectors. Circ Res 73:1202–1207.
9. Stratford-Perricaudet LD, Makeh I, Perricaudet M, Briand P. 1992. Widespread long-term gene transfer to mouse skeletal muscles and heart. J Clin Invest 90:626–630.
10. Jones N, Shenk T. 1979. An adenovirus type 5 early gene function regulates expression of other early viral genes. Proc Natl Acad Sci USA 76:3665–3669.
11. Jones N, Shenk T. 1979. Isolation of adenovirus type 5 host range deletion mutants defective for transformation of rat embryo cells. Cell 17:683–689.
12. Shenk T, Jones N, Colby W, Fowlkes D. 1980. Functional analysis of adenovirus-5 host-range deletion mutants defective for transformation of rat embryo cells. Cold Spring Harb Symp Quant Biol 1:367–375.

13. Galos RS, Williams J, Shenk T, Jones N. 1980. Physical location of host-range mutations of adenovirus type 5; deletion and marker-rescue mapping. Virology 104:510–513.
14. Graham FL, Prevec L. 1991. Manipulation of adenovirus vectors. In Murray EJ (ed), Gene Transfer and Expression Protocols, vol. 7. Clifton, NJ: Humana Press, pp. 109–128.
15. Graham FL. 1987. Growth of 293 cells in suspension culture. J Gen Virol 68:937–940.
16. Yang Y, Nunes FA, Berencsi K, Furth EE, Gonczol E, Wilson JM. 1994. Cellular immunity to viral antigens limits E1-deleted adenoviruses for gene therapy. Proc Natl Acad Sci USA 91:4407–4411.
17. Yang Y, Ertl HC, Wilson JM. 1994. MHC class I-restricted cytotoxic T lymphocytes to viral antigens destroy hepatocytes in mice infected with E1-deleted recombinant adenoviruses. Immunity 1:433–442.
18. Yang Y, Xiang Z, Ertl HC, Wilson JM. 1995. Upregulation of class I major histocompatibility complex antigens by interferon gamma is necessary for T-cell-mediated elimination of recombinant adenovirus-infected hepatocytes in vivo. Proc Natl Acad Sci USA 92:7257–7261.
19. Yang Y, Wilson JM. 1995. Clearance of adenovirus-infected hepatocytes by MHC class I-restricted CD4+ CTLs in vivo. J Immunol 155:2564–2570.
20. Newman KD, Dunn PF, Owens JW, Schulick AH, Virmani R, Sukhova G, Libby P, Dichek DA. 1995. Adenovirus-mediated gene transfer into normal rabbit arteries results in prolonged vascular cell activation, inflammation, and neointimal hyperplasia. J Clin Invest 96:2955–2965.
21. Barr D, Tubb J, Ferguson D, Scaria A, Lieber A, Wilson C, Perkins J, Kay MA. 1995. Strain related variations in adenovirally mediated transgene expression from mouse hepatocytes in vivo: comparisons between immunocompetent and immunodeficient inbred strains. Gene Ther 2:151–155.
22. Yang Y, Nunes FA, Berencsi K, Gonczol E, Engelhardt JF, Wilson JM. 1994. Inactivation of E2a in recombinant adenoviruses improves the prospect for gene therapy in cystic fibrosis. Nature Genet 7:362–369.
23. Engelhardt JF, Ye X, Doranz B, Wilson JM. 1994. Ablation of E2A in recombinant adenoviruses improves transgene persistence and decreases inflammatory response in mouse liver. Proc Natl Acad Sci USA 91:6196–6200.
24. Engelhardt JF, Litzky L, Wilson JM. 1994. Prolonged transgene expression in cotton rat lung with recombinant adenoviruses defective in E2a. Human Gene Ther 5:1217–1229.
25. Gerszten R, Luscinskas F, Ding H, et al. In press. Adhesion of memory lymphocytes to VCAM-1-transduced human vascular endothelial cells under simulated physiological flow conditions in vitro. Circ Res.
26. Stemme S, Holm J, Hansson GK. 1992. T lymphocytes in human atherosclerotic plaques are memory cells expressing CD45RO and the integrin VLA-1. Arterioscler Thromb 12:206–211.
27. Hajjar R, Kang J, Gwathmey J, Rosenzweig A. In press. Physiological effects of adenoviral gene transfer of sarcoplasmic reticulum calcium ATPase in isolated rat myocytes. Circulation.
28. Guzman RJ, Hirschowitz EA, Brody SL, Crystal RG, Epstein SE, Finkel T. 1994. In vivo suppression of injury-induced vascular smooth muscle cell accumulation using adenovirus-mediated transfer of the herpes simplex virus thymidine kinase gene. Proc Natl Acad Sci USA 91:10732–10736.
29. Chang MW, Barr E, Seltzer J, Jiang YQ, Nabel GJ, Parmacek MS, Leiden JM. 1995. Cytostatic gene therapy for vascular proliferative disorders with a constitutively active from of the retinoblastoma gene product. Science 267:518–522.
30. Quinones MJ, Leor J, Kloner RA, Ito M, Patterson M, Witke WF, Kedes L. 1996. Avoidance of immune response prolongs expression of genes delivered to the adult rat myocardium by replication-defective adenovirus. Circulation 94:1394–1401.
31. Kay MA, Holterman AX, Meuse L, Gown A, Ochs HD, Linley PS, Wilson CB. 1995. Long-term hepatic adenovirus-mediated gene expression in mice following CTLA4Ig administration. Nature Genet 11:191–197.
32. Fisher KJ, Choi H, Burda J, Chen SJ, Wilson JM. 1996. Recombinant adenovirus deleted of all viral genes for gene therapy of cystic fibrosis. Virology 217:11–22.
33. Curiel DT, Agarwal S, Wagner E, Cotten M. 1991. Adenovirus enhancement of transferrin-polylysine-mediated gene delivery. Proc Natl Acad Sci USA 88:8850–8854.
34. Curiel DT. 1994. High-efficiency gene transfer employing adenovirus-polylysine-DNA complexes. Nat Immunity 13:141–164.

PREVENTION OF TRANSPLANTATION-ASSOCIATED ARTERIOSCLEROSIS BY ANTIADHESION THERAPY

MITSUAKI ISOBE and JUN-ICHI SUZUKI

Shinshu University School of Medicine

Summary. Although it seems highly likely that an immunological response against the transplanted coronary endothelium is an important facet of the etiology of graft coronary arteriopathy, important questions regarding the molecular targets and the relative role of the cellular and humoral response remain unanswered. Graft coronary arteriopathy also serves as a model for the study of other forms of coronary arterial disease. Extensive research into this condition will help provide insight into aspects of this disease, as well as those of ordinary coronary atherosclerosis and restenosis after coronary angioplasty.

INTRODUCTION

Heart transplantation is now widely accepted as a way of treating patients with end-stage heart failure. Over the last 20 years, the incidence of allograft rejection has been greatly reduced by immunosuppression with cyclosporine, corticosteroids, azathioprine, and antilymphocyte serum [1]. However, graft coronary arteriopathy remains a major limitation for extended survival following cardiac transplantation [2–4]. At least 40% of transplanted hearts develop angiographically detectable graft coronary disease within five years after transplantation [5,6]. In general, there is about 4% mortality per year over 11 years after heart transplantation. This fall of survival is almost a straight line from year 1 through year 12 and projected out would represent a maximum survival of approximately 20 years for the entire population. Graft coronary arteriopathy is responsible for more than one third of these deaths [1]. Therefore, graft coronary arteriopathy is one of the most serious complications of cardiac transplantation. A fundamental understanding of the patho-

S. Mochizuki, N. Takeda, M. Nagano and N. Dhalla (eds.). THE ISCHEMIC HEART.

physiology of graft coronary arteriosclerosis should yield insights permitting preventive or regression therapies appropriate for this particular process.

CHANGES IN SMOOTH MUSCLE HEAVY CHAIN ISOFORMS

It is already known that the major pathological features of graft coronary arteriopathy are diffuse and circumferential thickening of intima of the vessel wall [7–9]. The main component of the intimal thickening is smooth muscle and endothelial cells as well as varying number of infiltrating cells. We have found that this proliferation of smooth muscle cells accompanies phenotypic transformation of vascular smooth muscle myosin heavy chain [10].

In our models of experimental heart transplantation, graft coronary arteriopathy develops in rats and monkeys under suboptimal immunosuppression with FK506 and humanized anti-LFA-1 monoclonal antibody, respectively. Nagai et al. used immunohistochemistry to analyze phenotypes of the vascular smooth muscle heavy chain isoforms of thickened intima and found a reduction in SM2, the differentiated form of vascular smooth muscle myosin, and an increase in SMemb, the undifferentiated form [11,12]. The expression of α smooth muscle actin and SM2 in rats is demonstrated in figure 1. In our rat model, intimal thickening was observed as early as 14 days after transplantation, and developed progressively. Expression of SM2 decreased in parallel with the development of thickening of the imtima suggesting an increase in SMemb expression. These changes in phenotypic transformation are similar to those observed in other forms of coronary arterial disease [13].

ROLES OF ADHESION MOLECULES IN THE GRAFT ARTERIOPATHY

The role of cell adhesion molecules in the development of atherosclerosis has been investigated in detail. The adherence of blood monocytes and lymphocytes to endothelial cells lining large arteries is one of the earliest detectable events in atherosclerosis in animal models and human tissues [14,15]. Cybulsky et al. [16] identified a leukocyte adhesion molecule in the rabbit, which appears to be directed to mononuclear leukocytes and is expressed selectively by arterial endothelial cells covering early foam cell lesions of both dietary and Watanabe heritable hyperlipidemic rabbits. This molecule was revealed to be rabbit VCAM-1. Recent pathological studies using human atherosclerotic plaques showed induction of ICAM-1 and E-selectin as well as VCAM-1 [17–22]. These investigations revealed the immunological aspects of atherogenesis.

Adhesion molecules had been identified as key molecules in eliciting an immune response to allografted hearts. We have already reported that a short-term administration of monoclonal antibodies to ICAM-1 and LFA-1 results in the induction of immunological tolerance to transplanted heart allografts in a murine model [23,24]. However, the role of these adhesion molecules in graft arteriosclerosis is obscure to date. Russell et al. reported that long-term administration of anti-ICAM-1 plus anti-LFA-1 monoclonal antibodies with basic immunosuppression with anti-CD4 and anti-CD8 antibodies could suppress neointimal formation at days 30 and 60 in their

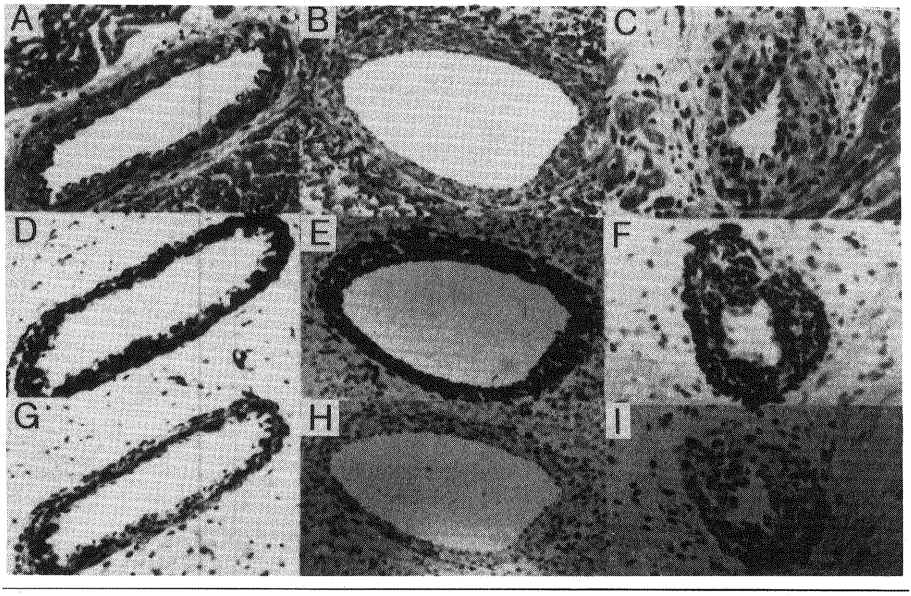

Figure 1. Microscopic findings of rat coronary arteries. Sections stained with hematoxylin-eosin (**A, B, C**), anti-α-smooth muscle actin (α-SMA) antibody (**D, E, F**), and anti-SM2 antibody (**G, H, I**). Both α-SMA and SM2 are expressed in the medial layer of native heart (A, D, G). The allograft harvested on day 14 with FK506 treatment (B, E, H) does not show intimal thickening; however, SM2 expression was reduced. The allograft harvested on day 35 (C, H, I) shows intimal thickening, and SM2 expression is also reduced in the medial layer and thickened intima.

mouse model of heart transplantation [25]. We analyzed the induction phenomenon of cell adhesion molecules in the thickened intima and evaluated the effects of short-term administration of monoclonal antibodies to cell adhesion molecules on the prevention of graft coronary arteriopathy [26]. The effect was compared with nonspecific immunosuppression by FK506.

CARDIAC TRANSPLANTATION AND IMMUNOSUPPRESSION

We employed a murine model of heterotopic heart transplantation. Donor hearts were transplanted into recipients using a microsurgical technique [27–29]. BALB/c hearts were transplanted into C3H/He recipients as allografts. Recipients received 50 μg/day each of anti-ICAM-1 [30] and anti-LFA-1 [31] monoclonal antibodies for three consecutive days starting immediately after transplantation. The graft beat was checked daily by palpation. The complete cessation of graft beat was interpreted as rejection. We have shown that all cardiac allografts are accepted indefinitely by this regimen of treatment [23]. Other mice received daily injection of FK506, 0.1 or 1 mg/kg/day, starting on the day of transplantation and lasting for 60 days after transplantation. The majority of mice treated with these amounts of FK506 accepted cardiac allograft over 60 days; however, some mice treated with 1 mg/kg of FK506

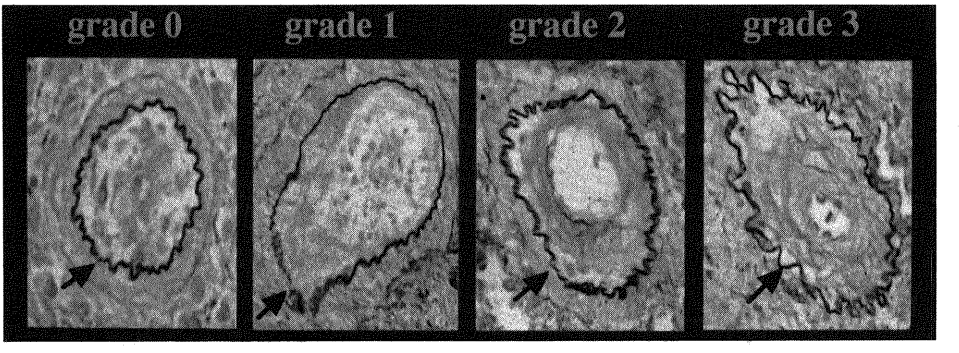

Figure 2. Sections of mouse coronary arteries in cardiac allografts with Elastica van Gieson staining are demonstrated. Method for semiquantitative analysis of intimal thickening is shown. Arrows indicate inner elastic lamina.

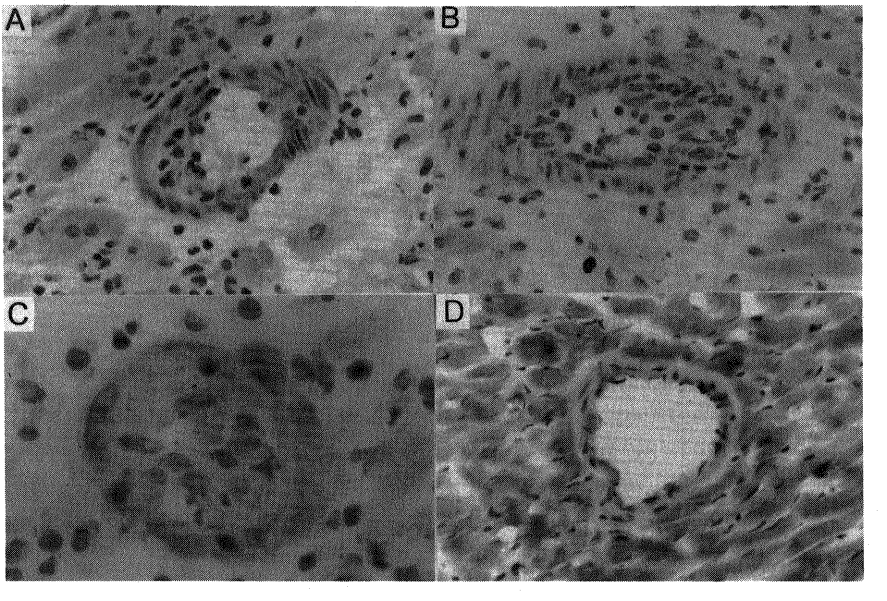

Figure 3. Sections of mouse coronary arteries in cardiac allografts at 60 days after transplantation stained with hematoxylin-eosin are shown. Allografts treated with 1 mg/kg (**A**) or 0.1 mg/kg (**B**, **C**) of FK506 show mild to severe intimal thickening. However, an allograft treated with a five-day course of anti-ICAM-1 and anti-LFA-1 (**D**) does not show intimal thickening.

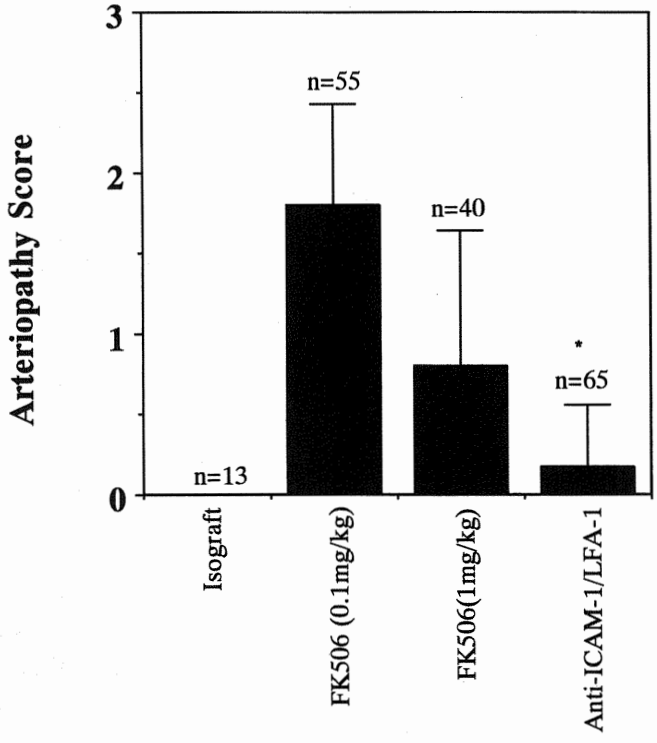

Figure 4. Comparisons of intimal thickening. Intimal thickening in coronary arteries of mice with anti-ICAM-1 and anti-LFA-1 treatment is significantly reduced as compared with that of mice treated with either low or high dose of FK506. *, both $p < 0.05$.

died, probably due to toxicity of the immunosuppressant. All mice were sacrificed at 60 days for histological examinations.

INTIMAL THICKENING IN A MOUSE MODEL OF CARDIAC TRANSPLANTATION

As shown in figure 2, degrees of intimal thickening were semiquantified by Elastica van Gieson stained sections. Almost all allografts treated with FK506 at 60 days showed various degrees of intimal thickening. Some vessels were almost occluded. The thickness was more severe in mice treated with 0.1 mg/kg of FK506 than in mice with 1 mg/kg of FK506. In contrast, coronary arteries of mice treated with a short-term course of anti-ICAM-1 and anti-LFA-1 monoclonal antibodies revealed much less thickening (figure 3). Figure 4 shows comparisons of the intimal thickening score among the three groups. Monoclonal antibody treatment significantly reduced the severity of intimal thickening.

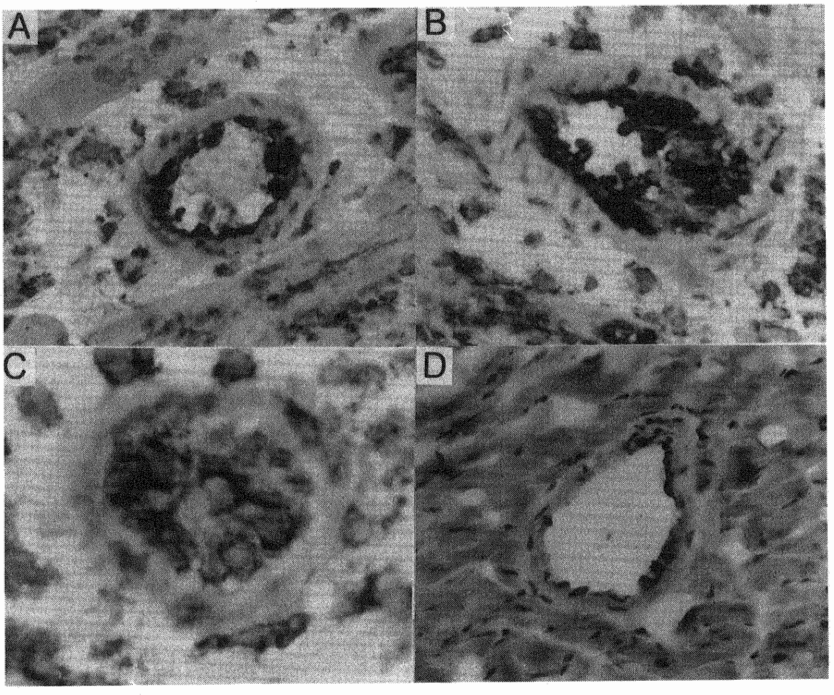

Figure 5. Sections of mouse coronary arteries in cardiac allografts at 60 days after transplantation stained with anti-ICAM-1 monoclonal antibody are shown. Allografts treated with 1 mg/kg (**A**) or 0.1 mg/kg (**B, C**) of FK506 show increased ICAM-1 expression in mildly to severely thickened intima. However, an allograft treated with a five-day course of anti-ICAM-1 and anti-LFA-1 (**D**) does not show increased expression of ICAM-1.

EXPRESSION OF ADHESION MOLECULES AND GROWTH FACTORS

In normal endothelium of murine heart tissues, VCAM-1 expression is usually faint or absent [32,33], and ICAM-1 expression is weak [34]. Thickened intima in mice treated with 0.1 or 1 mg/kg of FK506 showed marked induction of both ICAM-1 and VCAM-1 expression, as demonstrated in figures 5 and 6, respectively. This enhanced expression of adhesion molecules was reduced in the mice treated with anti-ICAM-1 and anti-VCAM-1 monoclonal antibodies. We have already reported that circulating antibodies to ICAM-1 or LFA-1 disappear by 14 days after the cessation of antibody administration (M. Isobe et al., paper in submission). Therefore, the reduction observed at 60 days after surgery is not due to direct effects of antibodies to cell adhesion molecules.

Growth factors are shown to be critical in eliciting coronary atherosclerosis. The cytokines and the growth factors promote macrophage recruitment and proliferation of smooth muscle cells, both of which are mediated by cell adhesion molecules [35]. PDGF-B mRNA expression was analyzed by in situ reverse transcriptase polymerase

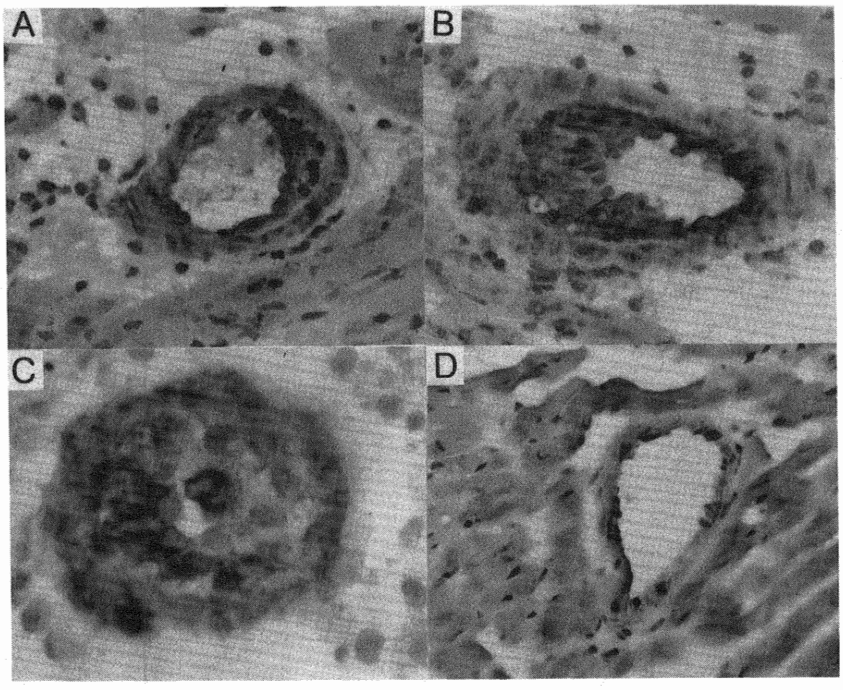

Figure 6. Sections of mouse coronary arteries in cardiac allografts at 60 days after transplantation stained with anti-VCAM-1 monoclonal antibody are shown. Allografts treated with 1 mg/kg (**A**) or 0.1 mg/kg (**B**, **C**) of FK506 show increased VCAM-1 expression in mildly to severely thickened intima. However, an allograft treated with a five-day course of anti-ICAM-1 and anti-LFA-1 (**D**) does not show increased expression of VCAM-1.

chain reaction (RT-PCR). The method of using this technique to detect mRNA in situ has been described elsewhere [36–38]. Normal endothelium and endothelium in mice treated with monoclonal antibodies to ICAM-1 and LFA-1 did not show PDGF-B transcription. However, enhanced transcription of this molecule was observed in the thickened intima in mice treated with FK506 (figure 7).

INVOLVEMENT OF CELL CYCLE REGULATORY GENES

It is now clear that cell growth is dependent on the coordinated actions of cell cycle regulatory genes [39]. Activation and phosphorylation of the cell cycle regulatory genes cyclin A and cdk (cyclin-dependent kinase) 2 kinase are critical to the process of cell growth and proliferation [40]. The cdk 2 kinase plays an important role in transition through the G1/S phase, which is important in the process of cell proliferation [41,42]. Morishita et al. reported that intimal hyperplasia after vascular balloon injury was inhibited by antisense cdk 2 kinase oligonucleotide [43] using hemagglutinating virus of Japan–liposome method [44]. However, involvement of

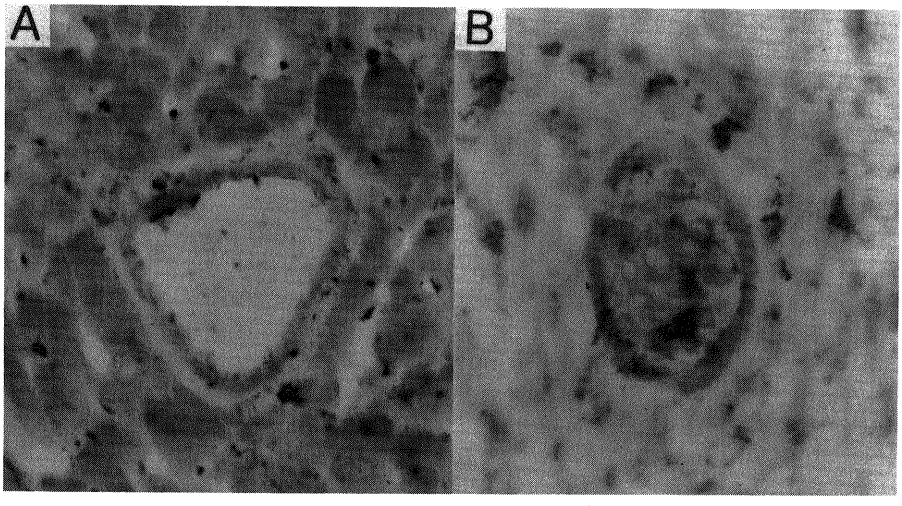

Figure 7. Expression of PDGF-B mRNA detected with in situ RT-PCR in a mouse treated with anti-ICAM-1 and anti-LFA-1 (**A**) or a low dose of FK506 (**B**). PDGF-B mRNA expression is shown in the thickened intima of coronary artery in an FK506-treated mouse (B) but not in an antibody-treated mouse (A).

these cell cycle regulatory genes has not been investigated in the transplanted cardiac allografts.

We hypothesized that cdk 2 kinase plays a critical role in the development of intimal thickening after cardiac transplantation. To evaluate this assumption, in situ RT-PCR was employed for the detection of cdk 2 kinase mRNA-positive cells in the graft coronary arteries. The cdk 2 kinase mRNA-expressing cells were observed in the occluded arteries of mice treated with a low dose of FK506, while cdk 2 kinase mRNA was almost nonexistent in the arteries of the transplanted grafts in the mice treated with antibodies to ICAM-1 and LFA-1 (data not shown). These observations lead to the possibility that graft coronary arteriopathy could be effectively prevented by gene therapy targeting these cell cycle regulatory genes. This possibility is currently under investigation in our laboratory (J. Suzuki et al. Nature Med. 3:900, 1997).

DISCUSSION

Graft arteriopathy remains a serious complication following cardiac transplantation and is a major determinant of cardiac recipient survival. Although transplant graft coronary arteriopathy has many distinctive features, it shares several characteristics with coronary atherosclerosis in nontransplanted hearts and more closely with postangioplasty restenosis and vein graft atherosclerosis and therefore can act as a model for the study of these conditions (table 1).

Table 1. Characteristics of graft coronary arteriopathy as compared with atherosclerosis and coronary restenosis

	Graft arteriopathy	Atherosclerosis	Restenosis
Histology	Intimal thickening	Eccentric plaque formation Complicated lesion	Intimal thickening Elastic recoil
Distribution	Large to small Diffuse	Large Segmental	Local
Calcification	None	Frequent	None
Course	Months to years	Years	Weeks to months
Angina pain	Absent	Frequent	Frequent
Risk factors	Unknown	DM, tobacco, hyperlipidemia, hypertension, etc.	Unknown
Treatment	Retransplantation	CABG, PTCA	PTCA, new device
Prevention	Unknown	Management of risk factors	Unknown

Although the exact cause or causes of the disease remain unknown, several factors appear to be implicated, both nonimmunological and immunological [45]. Many hypotheses regarding the pathogenesis of this disease have emerged over the years. Some authors have attributed its development to cytomegalovirus infection [46,47]. Also, cyclosporine and prednisone, agents at the foundation of modern immunosuppressive therapy, can alter lipid metabolism in manners that might potentiate atherogenesis. Furthermore, involvement of the immunological process has been discussed based on the presence of the infiltration of T cells [48] and enhanced expression of HLA class II antigens ICAM-1, VCAM-1, and E-selectin [32,49,50]. Since the process of inflammatory cell emigration into tissues involves the expression of adhesion molecules on the endothelium, there is evidence that transendothelial migration and positioning might further contribute to smooth muscle cell proliferation. Several studies have demonstrated that the expression of ICAM-1 and VACM-1 in the vascular endothelium increased in parallel to the severity of cellular rejection and in response to therapy [51].

Our data from a murine model of graft coronary arteriosclerosis revealed the involvement of certain cell adhesion molecules. Also, we demonstrated that FK506 inhibited intimal thickening development in a dose-dependent manner. Similar effects of cyclosporine have also been shown [52].

In this study we reported that a five-day course of monoclonal antibodies to ICAM-1 and LFA-1 prevents arterial intimal thickening for a prolonged period of time over 60 days. This study is unique because it reveals that the mechanism of prevention of graft arteriopathy must differ essentially between the tolerance induced by short-term monoclonal antibody therapy without other immunosuppression and continuous administration of basic immunosuppression with or without anti-ICAM-1 and anti-LFA-1 treatment, which has been reported by other investigators [25]. Although the mechanism of this effectiveness remains uncertain, the tolerance induced by short-term monoclonal antibody therapy alleviates the subse-

quent cytokine-mediated upregulation of adhesion molecules that triggers the immune system, leading to the proliferation of smooth muscle cells.

ACKNOWLEDGMENT

This study has been performed in collaboration with Professor Ryozo Nagai of Gunma University, Professor Yoshio Yazaki of The University of Tokyo, Dr. Ryuichi Morishita, Professor Toshio Ogihara, Dr. Yoshiki Sawa, and Professor Hikaru Matsuda of Osaka University. The authors acknowledge Professor Morie Sekiguchi of Shinshu University for his invaluable discussions. The monoclonal antibodies are kind gifts from Professor Ko Okumura of Juntendo University. We would like to thank Mrs. Misako Tomioka for her excellent technical assistance. This investigation was supported in part by grants-in-aid from the Ministry of Welfare and Health of Japan and from the Ministry of Science, Culture, Sports and Education, grants from Ono Medical Research Foundation, a Grant-in-Aid of the Japan Medical Association, and a Japan Heart Foundation-Pfizer Pharmaceuticals Grant for Research on Coronary Artery Disease.

REFERENCES

1. Hosenpud JD, Novick RJ, Bennett LE, Keck BM, Fiol B, Daily OP. 1996. The Registry of the International Society for Heart and Lung Transplantation: thirteenth official report—1996. J Heart Lung Transplant 15:655–674.
2. Uretsky BF, Murali S, Reddy PS, Rabin B, Lee A, Griffith BP, Hardesty RL, Trento A, Bahnson HT. 1987. Development of coronary artery disease in cardiac transplant patients receiving immunosuppressive therapy with cyclosporine and prednisone. Circulation 76:827–834.
3. Johnson DE, Alderman EL, Schroeder JS, Gao SZ, Hunt S, DeCampli WM, Stinson E, Billingham M. 1991. Transplant coronary artery disease: histopathologic correlations with angiographic morphology. J Am Coll Cardiol 17:449–457.
4. Botas J, Pinto FJ, Chenzbraun A, Liang D, Schroeder JS, Oesterle SN, Alderman EL, Popp RL, Yeung AC. 1995. Influence of preexistent donor coronary artery disease on the progression of transplant vasculopathy. An intravascular ultrasound study. Circulation 92:1126–1132.
5. Gao SZ, Schroeder JS, Alderman EL, Hunt SA, Silverman JF, Wiederhold V, Stinson EB. 1987. Clinical and laboratory correlates of accelerated coronary artery disease in the cardiac transplant patient. Circulation 75:V56–V61.
6. Gao SZ, Alderman EL, Schroeder JS, Silverman JF, Hunt SA. 1988. Accelerated coronary vascular disease in the heart transplant patient: coronary arteriographic findings. J Am Coll Cardiol 12:334–340.
7. Billingham ME. 1989. Graft coronary disease: the lesions and the patients. Transplant Proc 21:3665–3666.
8. Billingham ME. 1990. Cardiac transplantation. In Sale GE (ed), The Pathology of Organ Transplantation. Boston, MA: Butterworth, pp. 133–152.
9. Hosenpud JD. 1993. Immune mechanism of cardiac allograft vasculopathy: an update. Transplant Immunol 1:231–241.
10. Suzuki J, Isobe M, Aikawa M, Kawauchi M, Shiojima I, Kobayashi N, Tojo A, Kimura K, Nishikawa T, Sakai T, Sekiguchi M, Yazaki Y, Nagai R. 1996. Nonmuscle and smooth muscle myosin heavy chain expression in rejected cardiac allografts—a study in rat and monkey models. Circulation 94:1118–1124.
11. Nagai R, Kuro-o M, Babij P, Periasamy M. 1989. Identification of two types of smooth muscle myosin heavy chain isoforms by cDNA cloning and immunoblot analysis. J Biol Chem 264:9734–9737.
12. Kuro-o M, Nagai R, Tsuchimochi H, Katoh H, Yazaki Y, Ohkubo A, Takaku F. 1989. Developmentally regulated expression of vascular smooth muscle myosin heavy chain isoforms. J Biol Chem 264:18272–18275.

13. Aikawa M, Sivam PN, Kuro-o M, Kimura K, Nakahara K, Takewaki S, Ueda M, Yamaguchi H, Yazaki Y, Periasamy M, et al. 1993. Human smooth muscle myosin heavy chain isoforms as molecular markers for vascular development and atherosclerosis. Circ Res 73:1000–1012.
14. Ross R. 1993. The pathogenesis of atherosclerosis: a perspective for the 1990s. Nature 362:801–809.
15. Munro JM, Cotran RS. 1988. The pathogenesis of atherosclerosis: atherogenesis and inflammation. Lab Invest 58:249–261.
16. Cybulsky MI, Gimbrone MA Jr. 1991. Endothelial expression of a mononuclear leukocyte adhesion molecule during atherogenesis. Science 251:788–791.
17. van der Wal AC, Das PK, Tigges AJ, Becker AE. 1992. Adhesion molecules on the endothelium and mononuclear cells in human atherosclerotic lesions. Am J Pathol 141:1427–1433.
18. Poston RN, Haskard DO, Coucher JR, Gall NP, Johnson-Tidey RR. 1992. Expression of intercellular adhesion molecule-1 in atherosclerotic plaques. Am J Pathol 140:665–673.
19. O'Brien KD, Allen MD, McDonald TO, Chait A, Harlan JM, Fishbein D, McCarty J, Ferguson M, Hudkins K, Benjamin CD, et al. 1993. Vascular cell adhesion molecule-1 is expressed in human coronary atherosclerotic plaques. Implications for the mode of progression of advanced coronary atherosclerosis. J Clin Invest 92:945–951.
20. Davies MJ, Gordon JL, Gearing AJ, Pigott R, Woolf N, Katz D, Kyriakopoulos A. 1993. The expression of the adhesion molecules ICAM-1, VCAM-1, PECAM, and E-selectin in human atherosclerosis. J Pathol 171:223–229.
21. Gurtner GC, Davis V, Li H, McCoy MJ, Sharpe A, Cybulsky MI. 1995. Targeted disruption of the murine VCAM-1 gene: essential role of VCAM-1 in chorioallantoic fusion and placentation. Gene Dev 9:1–14.
22. O'Brien KD, McDonald TO, Chait A, Allen MD, Alpers CE. 1996. Neovascular expression of E-selectin, intercellular adhesion molecule-1, and vascular cell adhesion molecule-1 in human atherosclerosis and their relation to intimal leukocyte content. Circulation 93:672–682.
23. Isobe M, Yagita H, Okumura K, Ihara A. 1992. Specific acceptance of cardiac allograft after treatment with anti-ICAM-1 and anti-LFA-1. Science 255:1125–1127.
24. Isobe M, Ihara A. 1993. Tolerance induction against cardiac allograft by anti-ICAM-1 and anti-LFA-1 treatment: T cells respond to in vitro allostimulation. Transplant Proc 25:1079–1080.
25. Russell PS, Chase CM, Winn HJ, Colvin RB. 1994. Coronary atherosclerosis in transplanted mouse hearts. I. Time course and immunogenetic and immunopathological considerations. Am J Pathol 144:260–274.
26. Suzuki J, Isobe M, Yamazaki S, Horie S, Okubo Y, Sekiguchi M. 1997. Short-term blockade of ICAM-1 and LFA-1 prevents cardiac allograft arteriopathy in mice. J Heart Lung Transplant 10:1141–1148.
27. Ono K, Lindsey ES. 1969. Improved technique of heart transplantation in rats. J Thorac Cardiovasc Surg 57:225–229.
28. Isobe M, Haber E, Khaw BA. 1991. Early detection of rejection and assessment of cyclosporine therapy by indium-111 antimyosin imaging in mouse heart allografts. Circulation 84:1246–1255.
29. Isobe M, Narula J, Strauss HW, Khaw BA, Haber E. 1992. Imaging the rejecting heart: in vivo detection of MHC class II antigen induction. Circulation 85:738–746.
30. Takei F. 1985. Inhibition of mixed lymphocyte response by a rat monoclonal antibody to a novel murine lymphocyte activation antigen (MALA-2). J Immunol 134:1403–1407.
31. Nishimura T, Yagi H, Yagita H, Uchiyama Y, Hashimoto Y. 1985. Lymphokine-activated cell-associated antigen involved in broadreactive killer cell-mediated cytotoxicity. Cell Immunol 94:122–132.
32. Taylor PM, Rose ML, Yacoub MH, Pigott R. 1992. Induction of vascular adhesion molecules during rejection of human cardiac allografts. Transplantation 54:451–457.
33. Isobe M, Suzuki J, Yagita H, Okumura K, Yamazaki S, Nagai R, Yazaki Y, Sekiguchi M. 1994. Immunosuppression to cardiac allografts and soluble antigens by anti-vascular cellular adhesion molecule-1 and anti-very late antigen-4 monoclonal antibodies. J Immunol 153:5810–5818.
34. Ohtani H, Strauss HW, Southern JF, Miyasaka M, Tamatani T, Sekiguchi M, Isobe M. 1995. Intercellular adhesion molecule-1 induction: a sensitive and quantitative marker for cardiac allograft rejection. J Am Coll Cardiol 26:793–799.
35. Ross R, Masuda J, Raines EW, Gown AM, Katsuda S, Sasahara M, Malden LT, Masuko H, Sato H. 1990. Localization of PDGF-B protein in macrophages in all phases of atherogenesis. Science 248:1009–1012.
36. Nuovo GJ, Gallery F, MacConnell P, Braun A. 1994. In situ detection of polymerase chain reaction-amplified HIV-1 nucleic acids and tumor necrosis factor-a RNA in the central nervous system. Am J Pathol 144:659–666.

37. Horie S, Okubo Y, Suzuki J, Isobe M. 1996. An emaciated man with eosinophilic pneumonia. Lancet 348:166.
38. Suzuki J, Isobe M, Ando A, Kasajima T, Sekiguchi M. 1997. In situ detection of cytokine mRNA in mice cardiac allograft rejection. Transplant Proc 29:1512.
39. Pagano M, Pepperkok R, Verde F, Ansorge W, Draetta G. 1992. Cyclin A is required at two points in the human cell cycle. EMBO J 11:961–971.
40. Pagano M, Draetta G, Jansen DP. 1992. Association of cdk2 kinase with the transcription factor E2F during S phase. Science 255:1144–1147.
41. Tsai LH, Harlow E, Meyerson M. 1991. Isolation of the human cdk2 gene that encodes the cyclin A- and adenovirus E1A-associated p33 kinase. Nature 353:174–177.
42. Koff A, Ohtsuki M, Polyak K, Roberts JM, Massague J. 1993. Negative regulation of G1 in mammalian cells: inhibition of cyclin E-dependent kinase by TGF-beta. Science 260:536–539.
43. Morishita R, Gibbons GH, Ellison KE, Nakajima M, von der Leyen H, Zhang L, Kaneda Y, Ogihara T, Dzau VJ. 1994. Intimal hyperplasia after vascular injury is inhibited by antisense cdk 2 kinase oligonucleotides. J Clin Invest 93:1458–1464.
44. Kaneda Y, Iwai K, Uchida T. 1989. Increased ecpression of DNA co-introduced with nuclear protein in adult rat liver. Science 243:375–378.
45. Johnson MR. 1992. Transplant coronary disease: nonimmunologic risk factors. J Heart Lung Transplant 11:S124–S132.
46. Grattan MT, Moreno CC, Starnes VA, Oyer PE, Stinson EB, Shumway NE. 1989. Cytomegalovirus infection is associated with cardiac allograft rejection and atherosclerosis. JAMA 261:3561–3566.
47. Loebe M, Schuler S, Zais O, Warnecke H, Fleck E, Hetzer R. 1990. Role of cytomegalovirus infection in the development of coronary artery disease in the transplanted heart. J Heart Transplant 9:707–711.
48. Salomon RN, Hughes CC, Schoen FJ, Payne DD, Pober JS, Libby P. 1991. Human coronary transplantation-associated arteriosclerosis. Evidence for a chronic immune reaction to activated graft endothelial cells. Am J Pathol 138:791–798.
49. Page C, Rose M, Yacoub M, Pigott R. 1992. Antigenic heterogeneity of vascular endothelium. Am J Pathol 141:673–683.
50. Tanio JW, Basu CB, Albelda SM, Eisen HJ. 1994. Differential expression of the cell adhesion molecules ICAM-1, VCAM-1, and E-selectin in normal and posttransplantation myocardium. Cell adhesion molecule expression in human cardiac allografts. Circulation 89:1760–1768.
51. Jang Y, Lincoff AM, Plow EF, Topol EJ. 1994. Cell adhesion molecules in coronary artery disease. J Am Coll Cardiol 24:1591–1601.
52. Koskinen PK, Lemstrom KB, Hayry PJ. 1995. How cyclosporine modifies histological and molecular events in the vascular wall during chronic rejection of rat cardiac allografts. Am J Pathol 146:972–980.

INDEX

This Page Intentionally Left Blank